UNCLASSIFIED

AD NUMBER

AD-221 596

NEW LIMITATION CHANGE

TO **DISTRIBUTION STATEMENT - A**

Approved for public release;
distribution is unlimited.

LIMITATION CODE: 1

FROM **NO PRIOR DISTRIBUTION STATEMENT**

AUTHORITY

OSVD; AUG 2, 1960

19990308152

THIS PAGE IS UNCLASSIFIED

SUMMARY TECHNICAL REPORT OF DIVISION 10, NDRC

VOLUME 1

AD-221 596

MILITARY PROBLEMS WITH AEROSOLS AND NONPERSISTENT GASES

OFFICE OF SCIENTIFIC RESEARCH AND DEVELOPMENT
VANNEVAR BUSH, DIRECTOR

NATIONAL DEFENSE RESEARCH COMMITTEE
JAMES B. CONANT, CHAIRMAN

DIVISION 10
W. A. NOYES, JR., CHIEF

WASHINGTON, D. C., 1946

Reproduced From
Best Available Copy

19980615 152

UNCLASSIFIED

SUMMARY TECHNICAL REPORT
OF THE
NATIONAL DEFENSE RESEARCH COMMITTEE

This document contains information affecting the national defense of the United States within the meaning of the Espionage Act, 50 U. S. C., 31 and 32, as amended. Its transmission or the revelation of its contents in any manner to an unauthorized person is prohibited by law.

This volume is classified in accordance with security regulations of the War and Navy Departments because certain chapters contain materials which was at the date of printing. Other chapters may have had a lower classification or none. The reader is advised to consult the War and Navy agencies listed on the reverse of this page for the current classification of any material.

[redacted]

UNCLASSIFIED

Military Problems with Aerosols and Nonpersistent

22960

none

Noyes, W. A.; Pierce, W. C.; McCabe, W. L. and others
Office of Scientific Research and Development, Washington, D. C. Vol-1

~~Incl.~~ U.S. Eng. 725 pp tables, diagrs, graphs

The work performed on gas masks, micrometeorology and the behavior of chemical warfare gas clouds, aerosols, and new munitions for smoke and toxic gases, and other nonrelated problems ;such as insect control and the preparation of fluorine, is discussed. Work on the gas masks was conducted for the most part to increase their filtration and absorptionproperties. The general properties, stability, formation, measurement of particles, filtration, testing, and smoke screens are discussed in connection with aerosols. Topics such as the atomization of liquids, thermal generator munitions, munitions for the dispersal of solid particles, and plasticized white phosphorus are taken up in relation to new munitions for smoke and toxic gases.

Copies of this report obtainable from Air Documents Division; Attn: MCIDXD

Ordnance and Armament (22)
Chemicals and Incendiaries (11)
8-22-11

Chemical warfare - Gases (23102); Gas masks (44029); Gases, Liquefied (44507.5)

Air Documents Division, T-2
ATSC, Wright Field
RC-880 F 22960

UNCLASSIFIED

Manuscript and illustrations for this volume were prepared for publication by the Summary Reports Group of the Columbia University Division of War Research under contract OEMsr-1131 with the Office of Scientific Research and Development. This volume was printed and bound by the Columbia University Press.

Distribution of the Summary Technical Report of NDRC has been made by the War and Navy Departments. Inquiries concerning the availability and distribution of the Summary Technical Report volumes and microfilmed and other reference material should be addressed to the War Department Library, Room 1A–522, The Pentagon, Washington 25, D. C., or to the Office of Naval Research, Navy Department, Attention: Reports and Documents Section, Washington 25, D. C.

Copy No.

067

This volume, like the seventy others of the Summary Technical Report of NDRC, has been written, edited, and printed under great pressure. Inevitably there are errors which have slipped past Division readers and proofreaders. There may be errors of fact not known at time of printing. The author has not been able to follow through his writing to the final page proof.

Please report errors to:

JOINT RESEARCH AND DEVELOPMENT BOARD
PROGRAMS DIVISION (STR ERRATA)
WASHINGTON 25, D. C.

A master errata sheet will be compiled from these reports and sent to recipients of the volume. Your help will make this book more useful to other readers and will be of great value in preparing any revisions.

UNCLASSIFIED

UNCLASSIFIED

SUMMARY TECHNICAL REPORT OF DIVISION 10, NDRC

VOLUME 1

MILITARY PROBLEMS WITH AEROSOLS AND NONPERSISTENT GASES

OFFICE OF SCIENTIFIC RESEARCH AND DEVELOPMENT
VANNEVAR BUSH, DIRECTOR

NATIONAL DEFENSE RESEARCH COMMITTEE
JAMES B. CONANT, CHAIRMAN

DIVISION 10
W. A. NOYES, JR., CHIEF

WASHINGTON, D. C., 1946

UNCLASSIFIED

UNCLASSIFIED

NATIONAL DEFENSE RESEARCH COMMITTEE

James B. Conant, *Chairman*

Richard C. Tolman, *Vice Chairman*

Roger Adams	Army Representative [1]
Frank B. Jewett	Navy Representative [2]
Karl T. Compton	Commissioner of Patents [3]

Irvin Stewart, *Executive Secretary*

[1] *Army representatives in order of service:*

Maj. Gen. G. V. Strong
Maj. Gen. R. C. Moore
Maj. Gen. C. C. Williams
Brig. Gen. W. A. Wood, Jr.
Col. E. A. Routheau
Col. L. A. Denson
Col. P. R. Faymonville
Brig. Gen. E. A. Regnier
Col. M. M. Irvine

[2] *Navy representatives in order of service:*

Rear Adm. H. G. Bowen
Capt. Lybrand P. Smith
Rear Adm. J. A. Furer
Rear Adm. A. H. Van Keuren
Commodore H. A. Schade

[3] *Commissioners of Patents in order of service:*

Conway P. Coe
Casper W. Ooms

NOTES ON THE ORGANIZATION OF NDRC

The duties of the National Defense Research Committee were (1) to recommend to the Director of OSRD suitable projects and research programs on the instrumentalities of warfare, together with contract facilities for carrying out these projects and programs, and (2) to administer the technical and scientific work of the contracts. More specifically, NDRC functioned by initiating research projects on requests from the Army or the Navy, or on requests from an allied government transmitted through the Liaison Office of OSRD, or on its own considered initiative as a result of the experience of its members. Proposals prepared by the Division, Panel, or Committee for research contracts for performance of the work involved in such projects were first reviewed by NDRC, and if approved, recommended to the Director of OSRD. Upon approval of a proposal by the Director, a contract permitting maximum flexibility of scientific effort was arranged. The business aspects of the contract, including such matters as materials, clearances, vouchers, patents, priorities, legal matters, and administration of patent matters were handled by the Executive Secretary of OSRD.

Originally NDRC administered its work through five divisions, each headed by one of the NDRC members. These were:

Division A — Armor and Ordnance
Division B — Bombs, Fuels, Gases, & Chemical Problems
Division C — Communication and Transportation
Division D — Detection, Controls, and Instruments
Division E — Patents and Inventions

In a reorganization in the fall of 1942, twenty-three administrative divisions, panels, or committees were created, each with a chief selected on the basis of his outstanding work in the particular field. The NDRC members then became a reviewing and advisory group to the Director of OSRD. The final organization was as follows:

Division 1 — Ballistic Research
Division 2 — Effects of Impact and Explosion
Division 3 — Rocket Ordnance
Division 4 — Ordnance Accessories
Division 5 — New Missiles
Division 6 — Sub-Surface Warfare
Division 7 — Fire Control
Division 8 — Explosives
Division 9 — Chemistry
Division 10 — Absorbents and Aerosols
Division 11 — Chemical Engineering
Division 12 — Transportation
Division 13 — Electrical Communication
Division 14 — Radar
Division 15 — Radio Coordination
Division 16 — Optics and Camouflage
Division 17 — Physics
Division 18 — War Metallurgy
Division 19 — Miscellaneous
Applied Mathematics Panel
Applied Psychology Panel
Committee on Propagation
Tropical Deterioration Administrative Committee

UNCLASSIFIED

UNCLASSIFIED

NDRC FOREWORD

As events of the years preceding 1940 revealed more and more clearly the seriousness of the world situation, many scientists in this country came to realize the need of organizing scientific research for service in a national emergency. Recommendations which they made to the White House were given careful and sympathetic attention, and as a result the National Defense Research Committee [NDRC] was formed by Executive Order of the President in the summer of 1940. The members of NDRC, appointed by the President, were instructed to supplement the work of the Army and the Navy in the development of the instrumentalities of war. A year later, upon the establishment of the Office of Scientific Research and Development [OSRD], NDRC became one of its units.

The Summary Technical Report of NDRC is a conscientious effort on the part of NDRC to summarize and evaluate its work and to present it in a useful and permanent form. It comprises some seventy volumes broken into groups corresponding to the NDRC Divisions, Panels, and Committees.

The Summary Technical Report of each Division, Panel, or Committee is an integral survey of the work of that group. The first volume of each group's report contains a summary of the report, stating the problems presented and the philosophy of attacking them, and summarizing the results of the research, development, and training activities undertaken. Some volumes may be "state of the art" treatises covering subjects to which various research groups have contributed information. Others may contain descriptions of devices developed in the laboratories. A master index of all these divisional, panel, and committee reports which together constitute the Summary Technical Report of NDRC is contained in a separate volume, which also includes the index of a microfilm record of pertinent technical laboratory reports and reference material.

Some of the NDRC-sponsored researches which had been declassified by the end of 1945 were of sufficient popular interest that it was found desirable to report them in the form of monographs, such as the series on radar by Division 14 and the monograph on sampling inspection by the Applied Mathematics Panel. Since the material treated in them is not duplicated in the Summary Technical Report of NDRC, the monographs are an important part of the story of these aspects of NDRC research.

In contrast to the information on radar, which is of widespread interest and much of which is released to the public, the research on subsurface warfare is largely classified and is of general interest to a more restricted group. As a consequence, the report of Division 6 is found almost entirely in its Summary Technical Report, which runs to over twenty volumes. The extent of the work of a Division cannot therefore be judged solely by the number of volumes devoted to it in the Summary Technical Report of NDRC: account must be taken of the monographs and available reports published elsewhere.

The varied activities of Division 10, under the leadership of W. A. Noyes, Jr., included the study and development of gas mask filters and absorbents, screening smokes, chemical warfare munitions, offensive chemical warfare dispersal of insecticides, and many problems related to these fields. Perhaps one of the most notable achievements of NDRC was the Division's development of smoke generators which were used for screening strategic targets in all theaters of war.

The Division's contributions not only greatly aided the Allied war effort and saved both military and civilian lives, but will continue to benefit mankind in peacetime. The Summary Technical Report of Division 10, prepared under the direction of the Division Chief and authorized by him for publication, presents the methods and results of the widely varied research and development programs carried out by the very able personnel of the Division and its contractors. For their invaluable achievements, we join the Nation in expressing our grateful appreciation.

Vannevar Bush, Director
Office of Scientific Research and Development

J. B. Conant, Chairman
National Defense Research Committee

UNCLASSIFIED

FOREWORD

In presenting the Summary Technical Report of Division 10 of the National Defense Research Committee, the Chief of the Division desires especially to thank those who have contributed of their time and energy to its preparation. In particular, Dr. W. C. Pierce has accepted full responsibility for obtaining the manuscript from the various authors and for editing it into final form for publication. This task has been a long and arduous one which has maintained Dr. Pierce's contacts with defense work for many months after the close of the war. He deserves special thanks for his efforts. However, his efforts would have been fruitless without the active cooperation of all of those who prepared the various chapters. The names of these men are too numerous to mention in this foreword, but they deserve our real gratitude for putting in clear, concise form the results of nearly six years of effort on military research. Without the work they have done, the task of reviewing and utilizing the vast amount of information accumulated would have been superhuman for those who might engage in this work in the future.

Division 10 was formed from Section B–5 and B–6 of old Division B of the National Defense Research Committee. At the time of its formation, the Chiefs of these two Sections were Dr. W. H. Rodebush, of the University of Illinois, and Dr. D. M. Yost, of the California Institute of Technology. These two men deserve much credit for organizing the scientific work which later was incorporated in Division 10.

Finally, it should be stated that the work of the Division was in a very real sense a cooperative venture. The Summary Technical Report makes no attempt to allocate credit either to individuals or to contractors. From a purely scientific point of view, this is best. From the standpoint of feeling of satisfaction which may be gained by individuals who have contributed to a worthy cause, the personal credit side is emphasized in the volume entitled "Chemistry in World War II." In that volume, an effort is made, inadequate as that effort may be, to give the names of those who have done the work.

Finally, the Division Chief feels that in addition to those who have edited and written this volume, his sincere thanks are due to all of those who contributed to the work in the laboratory and in the field. Without the efforts of these people, the work of the Division could not have been carried out.

W. A. Noyes, Jr.
Chief, Division 10

PREFACE

DURING WORLD WAR II, Division 10, in common with other Divisions of NDRC, issued voluminous reports. These were widely distributed, but even so, there are few complete files available today. A future worker could, by access to a complete file, reconstruct quite accurately the picture as of today. This would, however, be very tedious and time consuming because of the large volume of reports and because these reports were written for current use and often dealt with fragmentary phases of the work; quite often the conclusions were changed during the progress of the work.

The purpose of this volume is:

1. To summarize the work done during World War II.

2. To present final conclusions drawn from this work, from a critical point of view.

3. To suggest further work which according to the judgment of today might be profitable.

In compiling this volume an account is given of most of the activities of the Division, as enumerated in the Non-Technical Summary, above. One major activity of the Division, namely the field testing of gases, is largely omitted because this work was performed jointly with CWS and is adequately reported in the publications from San José, Dugway Proving Ground, and Project Coordination Staff. An account of NDRC participation in these activities is given in the History.

The technical work of Division 10 and its predecessors Sections B5 and B6 was described in a series of different reports, each of which had different circulations and were intended for different purposes. Complete files of the more important series, the NDRC and OSRD reports, are reproduced in the microfilms. Since other series of reports were of an ephemeral nature they were not completely reproduced, but copies are available in the Division files. The following reports were issued:

1. *OSRD.* These are formal reports, each presumably covering some completed phase of work. Distribution was through the OSRD office and, in general, these reports were not circulated to individual contractors. Serial numbers were chronological, without reference to the Division from which the report originated. A list of titles of OSRD reports from Division 10 is given in the Bibliography.

2. *B6 NDRC Reports.* This series, designated by roman numerals, was started in 1941 as a means of disseminating information among the contractors of the Section. Much of the material in these reports is also given in the OSRD reports. The B6 series was discontinued with the formation of Division 10. A list of titles is given in the Bibliography.

3. *Division 10 Informal Reports.* This series was a continuation of the B6 series, for interchange of information among the Division contractors. A separate series was published for each of the sections of Division 10, each with its own serial number. Designations are 10.1-1, etc. The series was continued to the end of the war. A list of titles is given in the Bibliography.

4. *Contractor's Reports.* At the conclusion of a contract a final report was required. In addition some contractors submitted special reports upon request, or periodically. These reports are to be found only in the Division files. In a few instances they are included in the microfilms.

5. *Monthly Summary Report.* This was a monthly report of the "news letter" type designed for distribution only among the contractors of Sections 10.1 and 10.5. It started January 15, 1943, and continued until April 15, 1945. While all of the material given in this series was more formally reported in the OSRD series, the MSR has been included in the microfilms.

6. *Munitions Development Laboratory [MDL] Monthly Progress Reports.* This series was published from January 1944 to June 1945, for rapid dissemination of information concerning developments in the MDL. It is included in the microfilms.

7. *Bimonthly Report of the Division Chief.* Bimonthly the Division Chief prepared a summarizing report of activities, which was given a limited distribution in the upper echelon of OSRD and to the Services. Since all of the material of these reports is given firsthand elsewhere, they are not included in the microfilms.

ACKNOWLEDGMENTS

The reports in this volume were for the most part written after the end of the war, by the men who had actively participated in the program. These authors, whose names appear in the various chapters, made personal sacrifices of time and energy to write the reports at a time when their major interests lay in

other activities. The editor desires to acknowledge his indebtedness to all authors for the competent and authoritative summaries they have prepared. Particular mention should be made of the assistance rendered by Dr. David Sinclair, of the Johns Manville Corporation, for serving as editor and advisor in the manuscript of the aerosol section, and by Dr. Jack G. Roof of the University of Oregon who served as editor and advisor for the section on Micrometeorology.

W. Conway Pierce
Editor

CONTENTS

CHAPTER		PAGE
	Summary	1
	PART I	
	THE GAS MASK	
1	U. S. Gas Masks	7
2	Testing of Gas Mask Charcoal and Canisters	12
3	Manufacture of Activated Charcoal	23
4	Impregnation of Charcoal	40
5	Surveillance of Impregnated Charcoal	88
6	Adsorption and Pore Size Measurements on Charcoals and Whetlerites	97
7	Mechanism of Chemical Removal of Gases	150
8	The Adsorption Wave	169
9	Canister Design	183
10	The Aerosol Filter	190
11	Performance of U. S. and Foreign Gas Canisters	194
12	Protection against Carbon Monoxide	203
13	Criticisms and Recommendations	207
	PART II	
	MICROMETEOROLOGY AND THE BEHAVIOR OF CHEMICAL WARFARE GAS CLOUDS	
14	General Meteorological Principles	213
15	Micrometeorological Instruments	239
16	Behavior of Gas Clouds	260
17	Field Sampling Methods for Nonpersistent Gases	284
	PART III	
	AEROSOLS	
18	General Properties of Aerosols	297
19	Stability of Aerosols and Behavior of Aerosol Particles	301
20	Formation of Aerosols	314
21	Optical Properties of Aerosols	318
22	Measurement of Particle Size and Size Distribution	334
23	Filtration of Aerosols	354
24	Methods of Testing Smoke Filters	360
25	Smoke Screens	375
26	Travel and Persistence of Aerosol Clouds	380
27	Theory of Obscuration	389

PART IV
NEW MUNITIONS FOR SMOKE AND TOXIC GASES

CHAPTER		PAGE
28	Introduction	395
29	Atomization of Liquids	398
30	Thermal Generator Munitions	411
31	Fuel Blocks for Thermal Generator Munitions	459
32	New Screening Smoke Mixtures	485
33	Exhaust Smoke Generator for Airplane Engines	507
34	Munitions for Dispersal of Liquid Droplets	524
35	Munitions for the Dispersal of Solid Particles	534
36	Dispersion of Herbicides	546
37	Plasticized White Phosphorus	551

PART V
MISCELLANEOUS TOPICS

38	Insect Control — The Development of Equipment for the Dispersal of DDT	577
39	Inorganic Toxic Gases	604
40	The Preparation of Fluorine	610
41	The Stabilization of Cyanogen Chloride	613
42	Stabilization and Flame Inhibition of Hydrogen Cyanide	618
43	Wind-Tunnel Studies of Fog Dispersal, Gas Diffusion, and Flow over Mountainous Terrain	621
44	Radioactive Tracers	640
	Glossary	645
	Bibliography	647
	OSRD Personnel	696
	Contract Numbers	698
	Project Numbers	704
	Index	707

SUMMARY

By *W. A. Noyes, Jr.*

DIVISION 10 WAS FORMED from two sections which had been established in 1940 for studying the broad problems of aerosols and of gas mask absorbents respectively. By the end of the war, the activities of the Division had broadened to cover many subjects, some of which were totally unrelated to either of those assigned by the Services at the beginning. For the purposes of discussion, the work of the Division may be subdivided under the following headings:

1. Gas mask filters.
2. Screening smokes.
3. Chemical warfare munitions (including smoke munitions).
4. Gas mask absorbents.
5. Offensive chemical warfare and related problems.

Certain miscellaneous activities do not fall under one or another of the above headings.

The work on the gas mask filter was necessitated by the threat of toxic aerosols set up by munitions. The U. S. Army gas mask filter of 1940 was satisfactory for many toxic smokes of the type first used by the Germans during World War I, but this filter proved to be vulnerable under certain climatic conditions particularly at high humidities. Moreover, solid agents of exceedingly high toxicity are known, and the possibility of their use made desirable an improvement in the protection afforded by the filter.

The activities of the Division centered around improvement in the filter testing methods and improvement in the filter itself. The use of radioactive tracers permitted quantitative measurements of filter penetration to be made, but optical methods were much better for penetrometers to be used in control of canister production. Several improvements were made in optical penetrometers and the devices in use by the Army and the Navy at the close of the war, had their origins in the work of Division 10.

The theory of filtration developed by Section B-5 indicated clearly that the fibers of a satisfactory filter must have diameters of the same order of magnitude as those of the particles to be removed. Since such particles may be only a few tenths of a micron in diameter, filter fibers of that size were demanded.

While synthetic fibers were produced on a small scale by Division 10 contracts, the naturally occurring material of high availability and with the right fiber diameter is asbestos. The incorporation of asbestos in alpha cellulose paper together with methods of providing adequate tensile strength were the achievements of Division 10. Army and Navy gas mask canisters during the last two years of the war were equipped with paper filters developed under Division 10 contracts.

The screening of strategic targets was one of the early important problems brought to the attention of Section B-5. A critical examination of the theory of screening was carried out on several contracts with the result that a white smoke with particles of such diameter as to give maximum scatter of wave lengths in the neighborhood of 5000 Angstrom units was shown to be best. Methods of producing such smokes were devised in the laboratory and carried forward to a practical scale by various contracts. Smoke generators using high boiling petroleum fractions were developed and used in large numbers by the Armed Services. This is one of the notable achievements of the NDRC in the war effort.

The tactical use of smoke demands a different type of screening material than the strategic use. White phosphorus was the principal material used in bursting munitions, but it had the serious disadvantage of short burning time and of "pillaring". These disadvantages were overcome by producing a white phosphorus plasticized with synthetic rubber.

The offensive use of chemical warfare had been confined mainly to the standard agents of the last

war in bursting munitions and in spray tanks. Division 10 was assigned the problem of developing new devices particularly for those agents which are destroyed by heat and which may have toxicities considerably higher than those known previously such as mustard gas and phosgene. A thermal generator for setting up aerosol clouds of mustard gas was developed and showed promise in the tests carried out by the Chemical Warfare Service, although bombs based on this principle were not manufactured in quantity during the war. For thermolabile solids which are exceedingly toxic, a bomb was devised using gas pressure without burster. The main difficulty in using this type of agent is concerned with proper micronization of the solid material and the prevention of agglomeration at the time the bomb is burst. Satisfactory progress was made on these matters, but the impression is gained that the problem is far from solved.

The gas mask absorbent in use by the United States Army in 1940 showed good protection against most agents when dry, but was vulnerable toward certain agents such as arsine and cyanogen chloride when wet. The work of Division 10 on gas mask absorbents concerned improvement in testing methods and improvement in the impregnation of charcoal. Related studies resulted in removal of soda lime from the canister filling, since this material is inert toward gases other than phosgene and hydrogen cyanide, the testing of gas mask absorbents by introduction of a simulated breathing machine, the improvement in indicator solutions, and the full demonstration that absorbents should be tested in canisters rather than in tubes.

The incorporation of silver and chromium along with copper for impregnating the charcoal was the main contribution of Division 10 to gas mask absorbents. This impregnation gives well-balanced protection against non-persistent agents under all conditions of humidity and temperature which might be encountered in the field. There is some instability in storage, and certain types of charcoal are better than others in this respect. Nevertheless, it was shown that for ordinary conditions of use, this type of impregnated charcoal is adequate.

The contributions of the Division on offensive chemical warfare other than munitions, were concerned with improvement in field sampling devices, development of meteorological instruments, and aid to the Armed Services in carrying out an extensive program of field experimentation with chemical warfare munitions and agents. The results of this program were imparted to the Armed Services and aided materially in changing the doctrine for the use of chemical warfare agents. Many men were involved at several different field stations in this country and overseas.

The work of the Division on the dispersal of insecticides involved a demonstration that there is an optimum particle size which is materially greater than that of a good screening smoke. Since most insecticides such as DDT cannot be volatilized without decomposition, the production of a satisfactory aerosol must be based on principles different from those used in screening smoke generators. It was shown that a frothing mixture made by oil solutions of DDT and water heated to the proper temperature in a rapid stream, produced products of controlled size several microns in diameter. It was demonstrated that particles of this size are most effective either for mosquitoes on the wing or for larvicide control. Several generators for setting up such aerosols from the ground were developed and exhaust smoke generators for planes and for a jeep could be adapted to dispersion of DDT aerosols. The plane devices were adopted by TVA and by UNRRA and were used to some extent by the Armed Services.

Some of the problems not related to any of the above subjects may be mentioned in passing:

1. The dissipation of fog over airfield runways was deemed to be of vital importance due to plane losses in the United Kingdom. The British system of gasoline burners was expensive and probably could not have been used under conditions of high wind velocity. Various methods of setting up heated air curtains were studied by Division 10 and plans for installations on several Pacific islands were provided. A method of high-intensity sound precipitation of fogs was also studied, but while some favorable results were obtained, it is probable that this method would not have been practicable in actual use.

2. The purification of certain inorganic compounds to be used by Division 16 in infrared viewing devices was undertaken by one contract in Division 10. Extraordinarily high degrees of purity are essential for compounds to be used in this connection, and the work of Division 10 did show that some of these impurities are more important than others.

3. In some Pacific islands, such peculiar air currents are encountered that the location of airfields must recognize this situation. Since it is impossible for detailed measurements of these air currents to



be made in actual practice, the Air Forces requested Division 10 to make model studies in a wind tunnel. This was done, and the results were of interest to the Air Forces in determining the locations for airfields.

4. Since the Chemical Warfare Service requested a study of the vulnerability of the gas mask canister to be made, it was essential that new types of compounds be synthesized. Many new compounds were made, but most of them involved fluorine in one form or another. Consequently, attention was directed to improvement in fluorine generators and to methods of synthesis using elemental fluorine. These extensive investigations did not disclose any new war gases of unusual promise, but they did serve to eliminate certain ones from consideration.

5. Cyanogen chloride as a war gas has some advantages over phosgene, particularly in that protection against it by most gas mask canisters is very poor indeed. In humid, tropical climates, the Japanese canisters gave almost zero protection. Since cyanogen chloride is not stable in ordinary steel containers for long periods of time, a careful investigation of means of increasing the stability was made. Many of the factors affecting the rate of polymerization were studied, and although the final stabilizer was proposed by Division 9, the contributions of Division 10 to this subject were considerable.

6. Hydrogen cyanide is a quick-acting lethal agent of great promise, but it is inflammable, and, when used in most munitions, it is destroyed by a fair fraction of the bursts. Means of preventing inflammation of this agent were studied by Division 10, and it was found that the incorporation of small percentages of certain hydrocarbons improved stability upon detonation markedly. It is believed, however, that the final solution of this problem has not yet been found.

7. The oxygen rebreather developed by the Naval Research Laboratory using KO_2 had one serious disadvantage due to the accumulations of nitrogen in the circulating system. The elimination of this nitrogen was the subject of a series of studies made by Division 10. A small, supplementary bellows which would flush out a small fraction of the gases during each breathing cycle was proposed and shown to be satisfactory, although it was not adopted.

8. At one time, it was proposed that the dissemination of herbicides over enemy territory might destroy crops and aid materially in shortening the war. Means of disseminating these compounds were studied by Division 10 and a proposal was made which probably would have been adopted by the Army had the war lasted much longer.

9. Smoke signals, particularly with colored smokes, were used either for target identification, for air attacks or for markers during submarine tests. Division 10 designed smoke floats and bombs for both of these purposes.

10. The standard smoke pot used by the Army contained a mixture of hexachloroethane, zinc oxide, and some reducing agent, such as finely divided aluminum. Manufacture of these mixtures is dangerous, and the smoke from such pots is extremely toxic due to the zinc. Division 10 developed an oil smoke pot in which the oil is vaporized in a suitably designed Venturi by the hot gases from a burning fuel block. This smoke pot would have been in production had the war lasted a few months longer.

PART I

THE GAS MASK

In the period 1941 to 1945 there was very close cooperation between the National Defense Research Committee [NDRC] and the Services on all matters pertaining to the gas mask. Problems of research and development were attacked jointly, often with interchange of personnel. It is, therefore, not possible or desirable to confine this report to that work which was done by the NDRC. Rather, for completeness, a résumé of the entire field of gas mask development is given in Part I and consequently, no attempt is made to allocate credit, either to the various branches of the Services or to NDRC.

Chapter 1

U. S. GAS MASKS

By *W. Conway Pierce*

1.1 INTRODUCTION

THE DEVELOPMENT of a military gas mask began with the first gas attack [1] which was made by the Germans on April 21, 1915, in which they released a cloud of chlorine for travel downwind. By May 3, 1915, British troops had been issued cotton cloth pads soaked in a solution of sodium thiosulfate and sodium carbonate, which provided a measure of protection. From April 1915 to the end of World War I, the race between offense and defense was close. In the offense, the use of chlorine was followed in turn by phosgene [CG], chloropicrin [PS], mustard gas [H], lacrimators, and irritant smokes. Concurrently, gas protection went through the stages of an impregnated pad, a series of helmets of impregnated cloth, and finally a box respirator. This respirator was the progenitor of today's mask, consisting of a canister filled with chemicals for air purification and a facepiece. The efficiency of charcoal as an air purifier was recognized early and by April 1916, British troops were using a canister which contained charcoal, soda lime, and permanganate particles.

When the United States entered World War I, an intensive research and development program was started on gas masks. The general design of the U. S. mask that grew out of this work was much like the British. The mask consisted of four major components: a facepiece, canister, hosetube, and carrier. While crude according to present standards, it gave adequate protection against the attainable field concentrations of that time. The facepiece was constructed of rubberized cloth and gave protection both to the eyes and to the respiratory tract. Breathing was through the mouth by means of a hard rubber bit held in the teeth, and nose-breathing was prevented by a clip to close the nostrils. The mask was very uncomfortable. It was, however, perhaps even safer than modern masks, because there was no possible danger from leaks at the face seal. The canister contained about 680 ml of a 60-40 mixture of activated coconut charcoal with soda lime granules. Protection was poor against cyanogen chloride [CK] and arsine [SA], particularly when the charcoal was humidified, but neither of these gases was used during the war. Excellent protection was afforded against the gases then in use, such as CG, PS, H, and diphosgene. Smoke protection was very poor, but was apparently adequate because there are no records of mask failure caused by smoke penetration. The carrier was a knapsack slung on the chest when in use, but otherwise carried by a shoulder strap.

Following World War I, a continuing program of gas mask research and development was maintained at Edgewood Arsenal. Although budgets were small and staffs limited, extensive progress was made and the masks in use at the start of World War II were much superior to those of 1918. Comfort was increased by use of Tissot-type facepieces which permit nasal breathing. Smoke protection was much better, with the use of a carbon-impregnated filter paper through which all inspired air was passed. Gas protection was increased by an improved design of canister and by the impregnation of the charcoal with cupric oxide which acts as an oxidizing and basic medium for retention of acid or reducing gases. Nevertheless, there were at the start of the war two serious defects: (1) gas protection was poor against CK, SA, and certain other gases when the charcoal had become partially saturated with water vapor by equilibration with air of high humidity, and (2) the smoke protection could be broken down by prolonged exposure to a smoke which contained liquid droplets. Both of these, as well as other problems, were solved during the 1940 to 1945 period.

1.2 GAS MASKS OF WORLD WAR II

Army Service gas masks [1–3,6] of 1940 to 1945 were of various types.

Service, Old Style, M2A1-1XA1-IV [a]

As improvements were made, one or the other of the components was altered and Service masks were issued with MIA1, MIA2, M2A1, and M2A2 facepieces, MIXA1 and M9A2 canisters, and MIII, MIIIA1, MIV, MIVA1 carriers. The mask was characterized by a flat-type carrier mounted beneath the left armpit, a Tissot-type facepiece connected by a long hosetube to the canister, and a large oval canister. The complete assembly weighed about 5½ lb. The MIA1 and MIA2 facepieces were made of stockinette covered rubber sheets, assembled with a seam beneath the chin. The eyelenses were of flat safety glass. All other facepieces were molded in one piece from natural, reclaimed, or synthetic rubber, and had curved plastic eyelenses. Several different types of head harness and outlet valves were used in the various models. All types of facepieces had Tissot tubes to direct incoming air across the eyelenses to prevent fogging.

Service, Lightweight, M3-10A1-6

The Service mask was developed in 1943 to replace the old-style Service mask. The name "lightweight" is somewhat misleading. As originally designed, the weight was about 3½ lb but, before starting production, protective capes and ointment were added to the carrier, so that the resulting weight was 5½ lb, the same as that of the old mask. The lightweight Service mask may have M2A1, M2A2, M3, or M4 facepieces and M10 or M10A1 canisters.

The differences between the old style and lightweight Service masks are chiefly in the canister and carrier. The latter is designed for use in various positions, namely, chest, side, or back. The hosetube is shortened from 27 to 18 in. The M10 and M10A1 canisters are cylindrical, measuring 3 7/16 in. in diameter by 5½ in. long. They differ only in the volumes of charcoal, which are respectively 275 and 340 ml. The M3 and M4 facepieces are equipped with nosecups to keep exhaled air from contact with the eyelenses as an aid in prevention of fogging.

[a] The model numbers for the gas mask assembly refer respectively to facepiece, canister, and carrier. Designations are not given for the minor constituents such as hosetube, outlet valve, and head harness. Prior to 1942, model numbers of standard items were in roman numerals, but items standardized thereafter were given arabic model numbers. Thus, the MIXA1 canister was revised in 1943 to M9A2. Revisions of a basic model are denoted by the letter A followed by an arabic number.

Combat or Assault M5-11-7

The combat mask was developed in 1943 to provide a lightweight compact mask without a hosetube for use by assault troops. Objectives in this development were:

1. Light weight.
2. Waterproof carrier, so that mask is not soaked by immersion during an amphibian operation.
3. Compactness.
4. Elimination of hosetube.

It was not required that this mask be as rugged as the Service mask.

The mask, when developed, exceeded the proposed requirements in many respects. After various tests, it was decided to mount the canister on the left cheek as in the British light mask, and to make the canister interchangeable with the British mask. The M11 canister departs from previous practice in that the air flow is axial through a flat bed. The carrier M7 is constructed of rubberized cloth and is made so that the flap has a watertight seal which will withstand immersion for hours. The complete assembly without capes or ointment weighs about 3 lb.

Diaphragm

Diaphragm masks are the same as Service masks in all parts except the facepiece, which contains a diaphragm for voice transmission. The diaphragm mask is classed as a limited standard.

Optical

Optical masks are made in two styles. Facepiece M2 is designed for use with the other components of a Service mask. Its distinguishing feature is the addition of plane-adjustable eyepieces, and a diaphragm for voice transmission. Facepiece M1 is a special unit requiring its own canister, carrier, et cetera. It is provided with optical eyelenses and a diaphragm. The canister is mounted on a clip at the rear of the head harness and is connected by two 8⅞-in. hosetubes to the air inlet of the facepiece. It is about the same size as an M10 canister and gives about the same protection. This model is no longer used by the Army.

Training M2-1-1

Optional parts of the training mask are M2A1, M2A2 facepieces and M1A1 canister. This mask was developed as a compact, lightweight, inexpensive mask for use in training, and was never intended for combat duty. Features are a standard Service facepiece with a small cylindrical canister directly attached at the air inlet of the facepiece so that the

canister is suspended beneath the chin. The carrier is a small canvas or duck sack which is attached to the belt or carried by a shoulder strap. The complete assembly weighs about 2 lb.

Because of its light weight and compactness the training mask was used in 1942 and 1943 as a Service mask in some theaters, but this practice was discontinued after the introduction of the M3-10A1-6 mask. The weakness of the training mask is in the slight protection afforded by the canister and in the interference which the swinging canister causes in strenuous exercise.

Combat Mask — Chin Type

In the spring of 1945, a reconversion program was organized to make use of natural rubber facepieces from old-style Service masks which had been replaced by the M3-10A1-6 assembly. At this time, no rubber was available for the manufacture of new face blanks, and it was believed that old rubber facepieces were superior to new ones made from neoprene, the only material available at the time. Part of the available old facepieces were converted to lightweight Service masks, and the remainder to a chin-type mask using the M11 canister. This was done by fitting the facepiece with a metal adapter so that an M11 canister could be mounted beneath the chin. This model had serious disadvantages but was considered serviceable. New face blanks for this mask were not planned and production was limited to conversion of old face blanks.

Navy

The Navy mask of World War II was like the old-type optical mask (with the canister mounted on the head harness) except that curved plastic eyelenses were used. The earlier canisters contained about 275 ml charcoal, but later this was changed to about 360 ml, thereby increasing the protection.

1.3 GAS MASK CANISTERS

The canisters used in World War II are described below. Typical performance data for new canisters are given in Table 1.

MIXA1

This is a radial-flow canister weighing about 1,000 g. The outer body is of corrugated sheet metal, rectangular in cross section but with rounded lateral edges. The adsorbent [b] is held in an inner chemical container made of perforated metal sheet. Air enters the outer container through an inlet valve at the bottom and flows radially through the charcoal bed to a central inner tube which is attached to an elbow nozzle mounted on the top of the can. A thin felt bag covers the inner tube and serves as a dust filter. The outer body measures about $3\frac{1}{8}$ x $4\frac{3}{4}$ x $6\frac{1}{2}$ in.

The filling is of two types: (1) Type D mixture of copper impregnated charcoal and soda lime in the proportions 80 to 20, and (2) copper or copper-silver impregnated charcoal. The mesh size is 6-20 U. S. screen. The volume of adsorbent is about 650 ml. The aerosol filter consists of 10 plies of carbon impregnated paper wrapped about the outer surface of the chemical container. This paper is made by aspiration of soot from a smoky flame through a porous texture paper. Fine carbon filaments are trapped in the coarse network of the paper and serve as a filter for removal of aerosols.

M9A2

This canister is identical in construction with the MIXA1 but differs in the filter and adsorbent. To facilitate identification, it is marked by a yellow top. The filter is asbestos impregnated paper, depending upon the fine asbestos fibers for filtration. The adsorbent is Type ASC charcoal (copper-silver-chromium). The gas protection is the best of any known canister, because of the large volume of adsorbent. The design is not efficient for utilization of the charcoal because penetration occurs through sections where the layer depth is least and not all the adsorbent is effective.

M10

This canister is cylindrical, measuring $3\frac{7}{16}$ in. in diameter by $5\frac{1}{2}$ in. in height. The general principle is like that of the MIXA1 with radial air flow. The filter is asbestos impregnated paper. The adsorbent is 275 ml, 12-30 mesh, Type ASC whetlerite. The weight is about 465 g.

---

[b] Throughout this section of the book there is some confusion in usage of the words *adsorbent* and *absorbent*. Strictly speaking, an adsorbent removes gas by physical adsorption on the surface while an absorbent removes gas by chemical reaction. The distinction is difficult to make in many instances since removal by chemical reaction in the gas mask canister is preceded by adsorption on the charcoal surface. Consequently, most of the authors speak of adsorption and adsorbents; the Chemical Warfare Service, on the other hand, prefers the terms absorbent and absorption.

TABLE 1. Gas mask canister data.*

Model	Filling type	Volume	Layer depth cm	Weight in grams of gas† retained at break						
				CK 80–80	CK 0–80	AC 0–80	AC 80–80	CG	SA 80–80	PS 80–80
M1XA1	A or D	650	2.5	<0.5	2	8	3	50	<0.5	7
M9A2	ASC	650	2.5	15.0	20	15	15	50	>12.0	7
M1	A	220	1.6	<0.2	1	3	1	10	<0.2	4
M1A1	ASC	220	1.6	1.0	4	4	4	10	>5.0	4
M10	ASC	275	1.6	3.0	7	7	7	15	>12.0	7
M10A1	ASC	340	1.8	10.0	15	10	10	25	>12.0	10
M11	ASC	250	2.8	3.0	7	7	7	15	>12.0	7

* These are average values for production canisters tested at high flow rate to a break of physiological significance. The CG life is about the same for dry and humidified charcoal.

† See Chapter 2 for conditions of the tests and meaning of the symbols.

M10A1

The outer size and general construction are the same as the M10, the only difference being in the size of the chemical container, which holds 340 ml ASC whetlerite. As shown by data in Table 1, the gas protection is much greater than that of the M10. The weight is about 500 g. After introduction of the M10A1 model, no more M10 canisters were manufactured.

M1

The M1 training canister was the first of the cylindrical radial-flow models to be developed. It was designed for attachment directly to the facepiece. Construction is exactly like the M10, the only difference being in the length, which is 4⅜ in. The adsorbent is about 210 ml Type A whetlerite. The filter is carbon impregnated paper. In 1943 the M1 was replaced by the M1A1.

M1A1

This canister is identical with the M1, except that the filling is ASC whetlerite and the filter is asbestos impregnated paper.

M11

The design of the assault mask was made possible by the development of this lightweight axial-flow canister, the development of which depended upon perfecting an asbestos-bearing paper which could be folded to give a large area in a small space. The paper used now contains 5 to 10% asbestos fibers which are incorporated with the wood pulp in the paper manufacture and which provide the network of fine strands responsible for filtration. A method for folding a single sheet of area 500 to 600 sq cm to give a fluted filter of low resistance which is mounted at the influent side of the canister has been developed. Above the filter there is a charcoal bed 2.8 cm in depth by 10 cm in diameter. The volume is 250 ml. Prior to May 1945, M11 canisters had steel parts and weighed about 350 g, but production of aluminum body canisters weighing about 250 g was started later. The reduction in weight makes the assault mask much more comfortable to wear, because this side-mounted canister exerts a marked torque on the left cheek.

The M11 canister is more efficiently designed than the M10 and gives equal or slightly better protection with 25 ml less charcoal. It is, however, not nearly so rugged as the M10 or M10A1 canisters and must be replaced far more frequently. For the purpose originally designed, that is, for use by assault troops, it is excellent. Only field experience in gas warfare will show whether the assault mask is better than the Service mask for use under all conditions.

1.4 PROGRESS IN 1940 TO 1945 PERIOD [4, 5]

The improvements effected in gas protection during World War II are summarized below.

1. High-quality domestic charcoals were developed from both coal and wood. These can now be produced in any desired amount and are more economical and better than the coconut charcoal used prior to the war. The cost of production was lowered to less than 30 cents per pound for some types of activated charcoal.

2. An improved impregnated charcoal known as Type ASC was developed and was produced exclusively after the spring of 1943. It was made by impregnating with a copper-silver-chromium solution and drying at 150 to 200 C. This adsorbent gave a much better balanced protection than the previously used Type A whetlerite. Protection was about the

same as that of Type A whetlerite for CG, H, and PS, but was much better against AC, CK, and SA, particularly when the charcoal was equilibrated with moist air. Canisters filled with ASC whetlerite provided good protection against all known war gases, both wet and dry. For a comparison, see the performance data of MIXA1 and M9A2 canisters in Table 1.

3. It was shown that carbon-impregnated filter paper broke down rapidly when exposed to a smoke containing droplets of liquid, such as an oil-screening smoke. This was attributed to action of the liquid droplets on the fine carbon filaments which were necessary for filtration. Processes were developed for impregnating paper with asbestos fibers, which gave very efficient filters that did not break down on exposure to liquid smokes. The filters used on M1A1, M9A2, M10, and M10A1 canisters were of this type.

4. An asbestos-bearing, thick-sheet paper suitable for making folded filters of the German type was developed. It was made by suitably incorporating asbestos with wood fiber during the mixing of pulp in the paper mill. When a sheet 500 to 600 cm^2 in area after suitable folding was made into a filter, the pressure drop was low and the efficiency of filtration was very high. This type of filter, used on the M11 canister, was the best of any U. S. design.

5. Two different methods were developed for folding the single-sheet type of canister filter: one, like the German, by a special machine; the other by hand operation. Both types produced excellent filters.

6. Methods were developed for waterproofing canisters of various masks so that accidental immersion during a landing operation would not spoil a canister. All these devices had the weakness that some time was required to prepare a waterproofed mask for use. A waterproofing treatment for canister filters was effective in preventing the entrance of water into the adsorbent section when the canister was subjected to a brief immersion.

7. A good facepiece canister mask of the combat type was developed for use by troops requiring the utmost mobility. This mask was compact and light, weighing only 1.6 lb without the carrier. The waterproof carrier protected the mask very well, even from prolonged immersion while wading ashore, yet provided instant accessibility to the mask.

8. It was shown that with modern impregnated charcoal the use of soda lime as an additional adsorbent is neither necessary nor desirable. Consequently, the use of soda lime in the canister was discontinued in 1942.

9. Improved methods were developed for testing charcoal, canisters, and filters.

10. Extensive studies were made of the humidification of canisters in field use and the effect of humidification on performance. Numerous field and laboratory surveillance tests were made to determine the useful field life of canisters.

11. Theoretical studies of the nature of the adsorption wave, the factors important in canister design, the structure of activated charcoal, and the state of the impregnant on the charcoal have made possible a much better understanding of the factors which influence gas protection.

12. Improvements were made in components of the facepiece, such as the eyelens and outlet valve. A nosecup was designed to reduce fogging of the eyelens in cold climates. Synthetic rubber was used to make facepieces of satisfactory performance except at low temperatures.

1.5 STATUS IN 1945

It was generally believed that the gas protection of U. S. troops was the best of any nation's armies. The supply of lightweight and combat Service masks was large enough to provide several masks for each man in active theaters. All these masks had ASC-filled canisters with asbestos-type filters. The U. S. facepieces compared favorably in comfort and vision with those of other nations.

Although adequate protection was offered, it was felt that further improvements could and should be made. All the existing masks were very uncomfortable for prolonged wear, particularly in tropical climates. Vision was far from perfect for any of the facepieces. All masks were, as carried, too bulky and heavy. Facepieces and hosetubes were subject to penetration by mustard gas and were difficult to decontaminate. Detailed comments on these and other features of the masks are given in Chapter 13, together with recommendations for further research and developments.

Chapter 2

TESTING OF GAS MASK CHARCOAL AND CANISTERS

By *W. Conway Pierce*

2.1 THEORY OF GAS PENETRATION TESTS

WHEN A GAS-AIR MIXTURE is passed through a layer of adsorbent, the total amount of gas taken up before the *break point* — a point at which penetration is noted — will depend upon two factors: the activity and the capacity [1] of the adsorbent toward the gas used, with other conditions such as concentration and flow rate being kept constant. By activity is meant a rate function of gas adsorption. It is an inverse function of the depth of layer which will just permit instantaneous penetration. Capacity is defined as the weight of gas restrained per unit volume of adsorbent (footnote b, Chapter 1) when saturation is reached at a given partial pressure of gas.

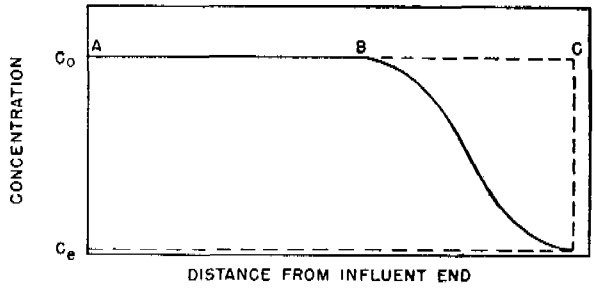


FIGURE 1. Distribution of gas concentration in tube of adsorbent which is partially saturated.

The effects of activity and capacity on gas life (time to the break point) are shown in Figures 1 and 2. For an idealized case Figure 1 illustrates the distribution of gas concentration along a long tube of adsorbent at the time a break is reached. C_o is the influent concentration, and C_e the effluent. In the region AB the adsorbent is saturated or in equilibrium with gas at a partial pressure C_o. In the region BC the adsorbent is progressively less saturated as the effluent end is approached. The total amount of gas restrained at the break time is determined mainly by the length of the saturated region AB and the capacity N_0 of the adsorbent. The length of the saturated region in turn depends upon the activity, or the length of the unsaturated region BC. This length depends upon the probability that a gas molecule will collide with the adsorbent surface and, after collision, be retained. The probability of striking the surface is a function of velocity, particle size, temperature, and other factors. A more complete discussion of these is given in Chapter 8.

Figure 2 illustrates the effects of activity and capacity on break times for layers of varied depths of

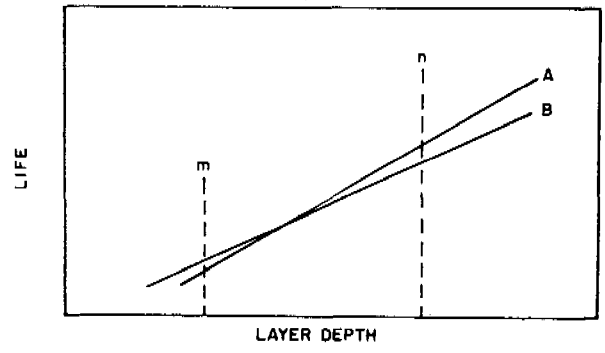


Figure 2. Life-thickness curve, showing effect of layer depth of adsorbent upon gas life. Adsorbents A and B have different activities and capacities. The intercept in the x-axis gives the critical depth and the slope gives the increase in life per centimeter of length of bed, which is related to the capacity, N_0 of the adsorbent.

two adsorbents with different characteristics. Curves such as these are experimentally obtained by determining and plotting gas lives for various layer depths. At bed depth m adsorbent B will have the longer life, but at bed depth n adsorbent A has the longer life. Adsorbent A has greater capacity but lower activity than B.

Because of the separate effects of activity and capacity on the test life, it is not possible to obtain a reliable index of adsorbent quality from a single test unless the test is made under the conditions at which

the adsorbent is to be used. Therefore, while tube tests were used formerly as the basis for charcoal specifications, it is customary now to base the specification tests upon performance in the canister for which the charcoal is procured, and to make the canister test at conditions simulating actual use.

2.2 TEST GASES

At the present time, both British and Americans evaluate adsorbent quality in terms of the canister protection afforded against five standard agents: AC, CK, CG, PS, and SA. In addition, there is a tube test used to determine the extent of activation of the charcoal. The U. S. test for this is known as the *accelerated PS test*, and the British test is called the *volume activity* [VA]. The latter is essentially a measurement of adsorptive power for carbon tetrachloride [2] under specific conditions.[a]

The choice of the test gases used is based in part upon the expected hazards in gas warfare and in part on long established custom. CG, AC, and CK certainly represent probable hazards. CG, moreover, can be considered as typical for the gases which hydrolize to give halogen acids. AC and CK are perhaps typical of cyanide-containing gases. The use of PS in testing dates back to 1918, when it was an important war gas. Now it is not considered a good war gas but is retained in testing because it is the only one of the standard agents removed by physical adsorption. SA does not seem to represent an actual hazard, since to date no good methods have been discovered for setting up high field concentrations. Its use in testing also dates back to 1918, when it was found to penetrate the existing canisters readily and was considered as a potential hazard. Considerable thought has been given to use of additional test gases to evaluate U. S. adsorbents. Extensive surveys have been made of charcoal protection for many different types of gases, but to date no new agent of high toxicity and ability to penetrate a canister has come to light, except agents of types represented in the CG and AC tests.

It is noted that the list of standard test gases does not include the persistent agents such as mustard and the nitrogen mustards. These are omitted for two reasons: (1) adsorbent tests with persistent agents are experimentally very difficult because of the low vapor pressures (which limit the gas concentration) and the long lives obtained, and (2) experience has shown that the persistent agents, which have high boiling points, are very effectively removed from air by physical adsorption on charcoal. Any canister which will protect against PS will protect against a dosage of mustard vapor many times greater than is needed for penetration of the facepiece (by solution in the rubber). Consequently, such tests are not made a part of charcoal specifications and are performed only occasionally.[14]

Each of the agents CG, CK, PS, and SA evaluates a different characteristic of the absorbent. (See Chapter 7.) The dry CG life depends upon the amount and state of the copper oxide impregnant. The wet SA life is a function of the silver impregnant; the CK life depends upon the state and amount of hexavalent chromium present as a Cu-Cr compound; and the PS life depends on the adsorptive power of the charcoal. All gas lives are highly dependent upon the quality of the activated charcoal used as the base for the impregnant.

2.3 TEST CONDITIONS

Humidity

Prior to 1941 all gas tests were made either at 0-0 or 0-50 RH.[b] About this time, work was begun on the development of impregnants to improve SA and CK protection, and emphasis began to be placed on tests of moist samples. Partly by chance, and partly by design, the practice of equilibrating test samples with air at 80% RH was begun and this figure soon became standard for wet tests. In retrospect, it is seen that the 80% RH was a good choice, because for most charcoals the water adsorption isotherms are somewhat flat in the region of 70 to 90% RH (see Chapter 6). Consequently, if equilibration is done at 80% RH, an exact humidity control is not important, because a 5 to 10% variation will not greatly affect the amount of water taken up. Further, it now seems that canisters which have been in use in tropical climates have water contents approximately equal to that picked up on 80% equilibration.

Several different humidity conditions are now used

[a] An empirical correlation [3] between VA values and PS lives can be obtained by the relation VA × 2.5 = PS life. This is not exact but is sufficiently accurate to give the proper order of magnitude for the PS life.

[b] The first figure represents the humidity of the air with which charcoal is equilibrated prior to testing, and the second, the humidity of the test air. Thus 80-50 would denote a sample equilibrated with 80% RH air and tested with air at 50% RH (relative humidity).

in research and specification control testing. They are 0-0 (PS tube test), 0-50, 0-80, 80-80, and 80-50. The last is used only when hydrolysis of the gas in air causes difficulty at high humidity. 0-0 canister tests are not used chiefly because of the difficulty in drying large volumes of air.

TABLE 1. Canister test conditions.

Gas	Humidity charcoal	Humidity air	Concentration mg/l	Flow rate lpm
CG	AR	50	20	32-steady
PS	AR	50	50	32-steady
AC	AR	50	10	32-steady
CK	E-80	80	4	50-breather
SA	E-80	80	10	50-breather

In the present routine whetlerite inspection tests, the conditions listed in Table 1 are used. The symbol AR appearing in the table designates normally dry charcoal "as received." In this case, the moisture content is less than 2% by weight. If necessary, the charcoal is dried at 150 C. E-80 indicates that the charcoal is equilibrated at 80% relative humidity before testing. CG is tested at 0-50 because performance is usually better at 80-50. AC gives about the same life at 0-80 or 80-80. CK and SA are tested at 80-80 because protection is lower at this condition than at 0-80.

HUMIDIFIERS

Humidification of charcoal for testing is a laborious task, because the adsorption of water vapor from an air stream is not so rapid a process as removal of most other gases. Rather, when humidified air is blown through a layer of charcoal, only a small fraction of the water is removed. At 80% RH and an air flow of 10 liters per minute (lpm), it may require as much as 2 to 4 days to equilibrate an M10A1 canister.

In order to care for the large numbers of samples required in inspection testing, a special humidifier was designed at Edgewood Arsenal to handle 50 canisters simultaneously, and several units were constructed by the Carrier Corporation. Operation was very satisfactory and reliable; a single machine can, on continuous duty, equilibrate over 100 canisters per day.

A number of designs for laboratory equilibrators have been developed. All operate on the same principle, that is, streams of dry and saturated air are mixed in the ratios to provide the desired humidity, then blown to a distributor manifold to which sample containers are attached. These outfits give satisfactory operation but lack the convenience and automatic control of the large Carrier unit.

The rate of equilibration varies from one charcoal to another. It is customary, therefore, to continue the passage of moist air through a sample until the weight becomes constant. Most types of charcoal can be equilibrated in less than eight hours on the Carrier equilibrator.

It is, fortunately, unnecessary to humidify samples at constant temperature. Adsorption isotherms made at various temperatures (see Chapter 6) have shown that the amount of water taken up by a sample depends upon the relative humidity of the air stream and not on the specific moisture content. All test samples are equilibrated, therefore, at room temperature.

FLOW RATE [5]

For many years it was conventional to make canister tests at a 32-lpm flow with occasional engineering tests at 64 lpm or higher. The 32-lpm flow rate was established in 1918 as an average breathing rate for men at moderately heavy exercise. During World War I most tests were, for convenience, made at steady flow. Some experimental machines to simulate intermittent breathing were designed and tested. The results of these tests are not available today, but in the light of present knowledge it is deduced that in tests of 1918 canisters there was little difference in steady and intermittent flow lives.[c] Probably it was because of such findings that intermittent flow testing did not become established at that time.

In 1942 it was found that man-tests under conditions of heavy exercise gave gas lives much shorter than the standard 32-lpm lives for thin-bed canisters such as the M1 and M10. Further investigation showed that the peak flow rates of men at heavy exercise were of the order of 150 to 200 lpm, with minute volumes of the order of 50 to 60 lpm. At these flow rates, the adsorbent bed depth of M1 and M10 canisters is so near the critical depth that penetration occurs within a few minutes, and only a small fraction of the adsorbent is saturated at the break time. These studies led to the development of breather pumps[4] for use in canister testing, to simulate human

[c] The basis for this deduction is that in the deep-bed 1918 canister the unsaturated zone was probably but a fraction of the total bed depth. Consequently, in intermittent flow tests the increased flow rate did not markedly affect the amount of charcoal which was saturated at the break time. It is only in thin-bed canisters that large effects are produced by an increase in flow rate.

SE[redacted]

breathing. Experimentally, it was found that a motor-driven reciprocating pump would give canister lives in good agreement with those from man-tests when the pump was operated at a speed to give a volume of 50 lpm. This pump, as first constructed, gave a sine-wave type of flow curve somewhat different from the flow curve of human breathing. Consideration was at first given to the idea of constructing a cam-driven pump which would duplicate the average human breathing rate curve,[15] but when it was found that the sine-wave pump gave test lives in agreement with man-tests the cam-drive design was abandoned. Subsequent experience with breather pump tests confirms the conclusion that it is not necessary to make the flow curve for the pump conform to the curve for human subjects.

When the breather pump was officially adopted for canister testing, the previously used 50 lpm flow rate was retained. This was a desirable choice, since this flow rate is also used in British tests, which are made at standard flow rates of 16 and 50 lpm. It is recognized that a 50-lpm flow does not represent the maximum value for men at heavy exercise, for whom values as high as 80-90 lpm, with peak flow near 250 lpm, have been reported; but it is thought that this rate is as high as any rate of sustained breathing likely to be found.

The peak instantaneous flow rate for a 50-lpm sine-wave pump is about 155 lpm. In the British 50-lpm test, the peak is 100 lpm, the test being performed by an interrupted steady-flow, off-and-on 50% of the time. In a number of comparisons, it has been found that if indicators are identical, the British test agrees with the U. S. test. Only in exceptional instances, where the thickness of adsorbent layer is near the critical depth, might it be expected that the British and U. S. tests would disagree. Then the U. S. test, because of the higher peak flow, might give considerably shorter lives.

At the present time, whetlerite inspection tests are made by 32-lpm steady flow for PS, CG, and AC, and by 50-lpm intermittent flow for CK and SA. This use of both types developed at the time the breather pump was adopted, because of equipment shortage. Since this plan has worked out satisfactorily for inspection testing, there is no reason for changing the CG and AC tests to the higher flow rate. The CK test suffices to disclose any whetlerite of low activity, and the 32-lpm tests for CG and AC provide indications of the gas capacity and the quality of the impregnant.

The flow rate used in charcoal tube tests was for many years standardized at 500 ml per min per sq cm or a linear velocity of 500 cm per min. (An exception was in the accelerated PS tube test which was made at 1,000 cm per min linear flow.) The origin of this rate is not known, but probably it was started in 1918 for the purpose of correlating tube and canister tests, since the linear flow in the 1918 canister was at about 500 cm per min for a total flow of 32 lpm.

In research tube testing, there is no *a priori* reason to employ any standard flow rate. However, a value of 500 cm per min is today most widely used because the apparatus was originally designed for this rate, and flowmeters are calibrated for this value.

Indicators

When a layer of adsorbent is traversed by a gas-air stream the initial concentration distribution through the absorbent may be represented by the curve of Figure 3A. Some gas penetrates instantly because

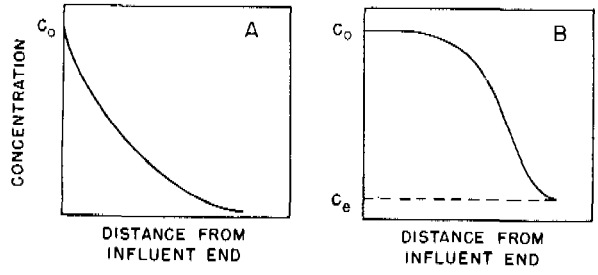


Figure 3. Distribution of gas concentration in tube of adsorbent. (A) condition at start of exposure, (B) condition at break point.

the distribution along the adsorbent layer is exponential with distance, but the penetrating concentration is much lower than the usual "break" concentration except when very thin layers are used. As the test continues, the adsorbent at the influent side becomes saturated and the unsaturated region moves progressively toward the effluent end of the bed. The situation at time t_b is as shown in Figure 3B. When the effluent concentration reaches the break concentration C_b, the adsorbent is considered to be exhausted and the time required for penetration to reach C_b is taken as the test life t_b. From these considerations one can see that the choice of test indicator has an important role in defining the adsorbent life.[11, 12] If the indicator is exceedingly sensitive, penetration may be observed at zero time. On the other hand, if the indicator is insensitive, penetration may

not be indicated until the effluent concentration becomes large, when most of the bed is saturated.

In practice, an effort is made to select an indicator of such sensitivity that it will show a break when the concentration of gas that penetrates is of physiological significance, that is, when the gas becomes noticeable by causing lacrimation or choking or when it approaches a concentration which may be dangerous if breathed for a short time. For gases such as CG or CK, which are detectable by smell or lacrimation at low concentrations, the indicator break point should coincide with human detection. In case of gases which are detected with difficulty, such as SA and AC, the indicator break point is fixed below the concentrations or dosages which are thought to be dangerous.

A list of the break point conditions in use at the present time is given in Table 2, with source references for each. It will be noted that the SA indicator

TABLE 2. Break point concentrations of test indicators.

Agent	Break point concentrations mg/l	Physiological significance	Source
CG	0.007 ± 0.001	lacrimatory	TDMR 753
	0.009 ± 0.002	coughing	NDRC 10.1–3
AC	0.004	?	EATR 251
SA	10 mg total	dangerous	TDMR 456
			NDRC 10.1–3
PS	0.01 ± 0.003	odor	TDMR 456
CK	0.008	lacrimatory	NDRC 10.1–24

responds to a total penetration of 10 mg, while all others are expressed on a gas concentration basis. This differentiation is made because the effects of SA are thought to be cumulative, while for the other gases there is a detoxification threshold below which the gas may be breathed without danger.

It is apparent from the data of Table 2 that the test indicators show a break before the point is reached at which a lethal dosage penetrates. Some measurements have been made of the dosage required to cause penetration of Japanese, German, and U. S. canisters in lethal amounts [13] for continued gas exposure and for gas exposure followed by desorption. These studies show that for U. S. canisters there is a considerable safety factor after penetration becomes detectable before it becomes dangerous. For gases such as CK, which are harassing, the penetration will cause discomfort or perhaps panic at just about the time of the chemical break.

Descriptions of the indicators now used are given in the references of Table 2. These indicators are solutions which contain a chemical that will react with the test gas, together with some substance which will show a color change. Effectively, there is a titration of the indicator chemical by the test gas. Thus, it is necessary to employ a measured volume of indicator solution and to obtain the color change within a prescribed time interval, usually 2 or 3 minutes. In a test, there is a series of indicator breaks at constantly diminishing time intervals until the point is reached at which a fresh solution will give a color change within the prescribed interval. Sometimes it is not easy to establish just where this point is reached, which causes some uncertainty in the test life. Normally, however, the effluent concentration rises quite rapidly near the break point, and this point can be located quite accurately.

Either physical or chemical break indicators may be employed in testing. In research work physical methods are preferred because they are generally more objective than chemical tests, which usually depend upon color changes in a solution. Further advantages of physical methods are that they give an instantaneous rather than a cumulative concentration value, and that physical method readings can usually be recorded automatically. Disadvantages are in their nonspecificity and in the complicated and expensive equipment required. Almost any type of physical measurement which applies to a binary system of known components may be applied. Among those instruments which have found wide applicability in adsorbent testing and gas detection are gas interferometers, ultraviolet, visible, and infrared absorption photometers, bridges for measuring the conductivity of solutions containing the gas or heat conductivity from hot-wire meters, and *p*H measurements on solutions. Each of these methods has special fields of applicability.

CONCENTRATION OF TEST GAS

In World War I it was customary to test at a volume concentration of 1,000 ppm except when this made service times too long; in such cases, concentrations of 5,000 or 10,000 ppm were used. The British still make many of their canister tests at a concentration of 1 per 100 (1% by volume), but present U. S. practice is to express concentration as milligrams gas per liter and to use a round number instead of working on a volume basis. Many tests are made at 4 mg per l, particularly in research. When a higher concentration is needed to obtain lives of con-

venient length, the values are usually 10, 20, or 50 mg per l.

The choice of test gas concentration is usually made on the basis of the life obtained. In canister tests it is convenient to have lives of 25 to 50 min. Longer lives are too time consuming and shorter ones are subject to too much error because of uncertainty in fixing the exact break point. Whenever possible, it is desirable to make gas tests at low concentrations (near 4 mg per l) which correspond fairly well with average field concentrations, where values of 10 to 50 mg per l are attained usually for only short periods. Testing at high concentrations has two disadvantages: (1) often a high concentration will cause large heat effects which tend to dry the canister and may also affect protection because of the temperature rise of the adsorbent; (2) if the test gas is removed by adsorption alone, a test at high concentration may indicate a misleading amount of protection because the adsorbent at the influent side is saturated at a high partial pressure of gas. For example, it was found that in a test of non-impregnated charcoal with CK at high concentration (27 mg per l) a dosage of about 135 mg per min per l was required for penetration. When the gas concentration was reduced to 0.27 mg per l, the protection was reduced to a dosage of 13. At the high concentration, the influent layers held a large amount of gas. In the 0.27 mg per l test, the influent layers held little gas because of the low partial pressure, and the protection obtained was low. When the test gas is destroyed by chemical action, there is not such a great difference in the amount of protection afforded at high and low concentrations. U.S. ASC-filled canisters will restrain about the same weight of AC, CK, or CG at 4 or 20 mg per l.

Temperature

In general, little has been done about temperature control in tube and canister testing. Customarily, such tests are made at the prevailing room temperature, because for most of the test gases, minor variations in temperature do not cause large effect. Moreover, control of external temperature would not greatly affect temperatures within the canister because heat conductivity in the charcoal bed is low.

The only control test made at constant temperature is the SA tube test (now obsolete). In this test it has been found that a thermostatically controlled water jacket around the test tube will aid in attaining reproducible results.

2.4 TUBE TESTS

A tube test [6–9] is made by blowing a gas-air mixture through an adsorbent bed (of predetermined thickness) in a small tube until penetration occurs. Tests of this type are much more convenient and economical than canister tests which require large air flows and large quantities of gas and charcoal. Originally, during World War I, there was probably fair correlation [10] between tube test lives and canister tests on the same adsorbent, because at that time the canister construction was like that of a large tube, with axial flow through a thick bed of adsorbent. Later, as canisters were made with thin beds and low linear flow rates, a good correlation between tube and canister tests lives no longer existed. The use of tube tests for charcoal and whetlerite specifications was discontinued in 1943, except for the PS test, and today all gas protection specifications are based upon performance in the canister for which the adsorbent is procured. Tube tests are still widely used in research studies because of their convenience, speed, and the small quantity of sample required. Properly interpreted, they yield much useful information.

The equipment required for tube testing is simple. A gas-air mixture is prepared by introducing a metered gas stream, or a gas-laden air stream from a bubbler tube, into a metered air stream. After passing through a mixing chamber the gas-air mixture is forced into a manifold to which the test samples are attached. The test tubes are uniform-bore glass cylinders, usually about 2 cm in diameter and contain near the lower end a flat, perforated plate acting as a support for the layer of adsorbent. The test sample is loaded into the tube by gravity fall from a vibrator hopper, which gives a slow and uniform feed rate. The customary bed depth is 5 cm, which requires only about 15 ml of the sample. Flow is downward through the sample to avoid disturbance of the packing. The lower or effluent end of the tube is connected to a container for the indicator solution.

The standard tube test line of 1945 is designed for very efficient and uniform operation. Many conveniences have been developed to aid in keeping the desired gas concentration and uniform flow rates. The most recent models are of all glass construction with few rubber joints to become contaminated or develop leaks. Eight samples can be tested simultaneously. Complete descriptions are given in CWS Pamphlet Number 2.

SECRET

Gas for the test line is supplied either from a cylinder (under pressure), by bubbling a dry air stream through a tube of the liquefied agent, or from a gasometer. The latter is the least convenient method and is used today only for arsine. CG is usually supplied from a cylinder, CK and AC are vaporized from a liquid or supplied from a pressure cylinder. PS is always vaporized from the liquid because of the high boiling point.

PS Test

Since 1918, one of the specification tests for activated charcoal has been the chloropicrin life, which is assumed to represent the adsorptive power of the charcoal for a non-reactive gas. This test is run on a 10 cm layer of charcoal in a tube with an inside diameter of approximately 1.4 cm at a rate of flow of 1 l per min per sq cm of cross sectional area (1,000 cm per min linear flow). The gas concentration is 47 mg per l. Humidity conditions are 0-0. The break-point indicator is a starch-potassium iodide solution through which the effluent gas is passed after pyrolysis in a heated quartz tube.

Despite its long established usage, the PS test does not provide a good criterion for evaluating activated charcoal. The following objections may be cited:

1. The PS life does not correlate with the protection that charcoal will afford for other non-persistent gases after impregnation. Following the discovery of the ASC process for whetlerization (Chapter 4) it was found that some of the charcoals with highest PS lives gave the poorest 80-80 CK protection. It is now known that the performance of impregnated charcoal is to some degree correlated with the presence of large pores which provide channels for gas molecules to penetrate rapidly into the granule and that this characteristic is not related to the PS life.

2. The PS test is carried out at high relative gas pressure, which corresponds to a point near saturation on the adsorption isotherm (see Chapter 6). The amount of gas taken up is not a measure of the surface available for adsorption but rather is a measure of the total volume of pores in the sizes that are filled with liquid at saturation. Of more importance is a knowledge of the amount of gas which is held at low partial pressures.

3. The retentivity, or amount of gas held very tightly by adsorption, is not related to the PS life.

It is believed that the PS test should be discontinued and some other test for the adsorptive power of charcoal should be substituted. Apparently it is desirable to work at a low relative pressure of gas corresponding to a low point on the isotherm where capillary condensation does not occur. This cannot be done conveniently with PS because the lives obtained would be too long. It has been suggested that a life test with ethyl chloride might be used and studies are now being made of the correlation of ethyl chloride lives with degree of activation and retentivity of charcoal. If such a test is used, the gas should be non-reactive, of low boiling point, and easily detected by chemical methods. Ethyl chloride satisfies these conditions nicely.

Modified Tube Tests

Frequent reference is made in Chemical Warfare Service [CWS] and National Defense Research Committee [NDRC] reports to "modified tube tests." These are tube tests made with layer depths and (sometimes) flow rates other than the standard conditions, for the purpose of correlating the service times with those for a specific canister. Such a correlation is purely empirical, because flow rates are not the same as in radial-flow canisters, but for a given type of charcoal it is possible to select a bed depth which will yield a tube life in fair agreement with an M10 or M10A1 canister. The only use for such tests is in experimental impregnation programs when there is not sufficient sample for regular canister tests.

2.5 CANISTER TESTS

Types

As stated previously, canister tests in use today are of two types: steady flow at 32 lpm and intermittent flow at 50 lpm with a peak rate near 155 lpm. In addition, in research and investigation of enemy canisters intermittent flow tests are used at various other rates, the more common of which are 25 and 16 lpm.

The basis for using these low flow rate tests is that the usual 50-lpm test gives the protection afforded for men at heavy exercise. In the field, it is probable that most people exposed to a gas attack may be occupying a fixed position and not exercising heavily during the period of the attack. Such an inference can be drawn from the reports of gas officers in World War I. Consequently, it is desirable to know what protection an enemy canister will afford under optimum defensive conditions. Often the protection at low flow rates may be excellent, because of high ca-

pacity, when penetration occurs very quickly at high flow rates.

The general principles of canister testing are like those of tube testing; a gas-air stream is passed through the canister until tests of the effluent stream show penetration of gas at a predetermined concentration. In one important respect, canister tests used during World War II differ from tube tests. The gas is *pulled* through a canister by suction applied at the nozzle, while in tube tests gas is forced through the adsorbent bed by pressure. The difference is one of experimental convenience only.

In steady-flow test outfits there is suction flow throughout the system, but the standard arrangement used in breather machine testing employs a combination of pressure and suction. In this arrangement the gas-air mixture is prepared in a pressure system and blown to the canister chamber where it envelops the canister at atmospheric pressure. This has two advantages: (1) changes may be made in the flow rate through the canister without changing the gas-air flow rate, which would require readjustment of all controls; (2) man tests may be made when desired by disconnecting the pump and attaching a gas mask facepiece through which the subject breathes.

Details of steady and intermittent flow tests are given in current editions of CWS Pamphlet Number 2. The most recent one describes the newest model intermittent flow machines, which accommodate two canisters for simultaneous testing. These differ from the single canister model only in having two canister containers attached to a common gas manifold. It is necessary to double the rate of gas supply. The breather pump for two canisters has two cylinders with the pistons operated 180° out of phase, so that gas is drawn half of the time from each canister.

Desorption Tests

If a gas is removed by physical adsorption there is a definite vapor pressure of the adsorbate over the charcoal and passage of air through an exposed canister will lead to desorption of the gas. This may be serious in case of a gas of high volatility which is not destroyed by chemical reaction with water or with the impregnant in the canister. For example, Type A whetlerite will desorb CK readily. Exposure to a small dosage followed by passage of air will cause penetration in amounts sufficient to cause discomfort. The danger of desorption from U. S. canisters with ASC whetlerite is small for any of the known toxic agents; all of those which have high volatility react with the impregnant and are destroyed (CG, CK, AC, and SA), while the agents of low volatility are so firmly held by physical adsorption that exposure to a large dosage is necessary before desorption will occur in dangerous concentrations.

Numerous desorption tests [13] have been made of CK and AC from German and Japanese canisters. A known dosage of gas is put into the canister by carrying on the test for a predetermined time. Then the gas is cut off while passage of pure air is continued at the usual test rate. A portion of the effluent air is passed through an absorbing solution and at regular intervals samples are titrated by a suitable reagent. In this way, data are obtained for the concentration of gas penetrating as a function of time. Data for such tests are shown in Chapter 10.

2.6 MAN TESTS

It is frequently desirable to determine canister performance by man tests. Extensive use was made of such tests in World War I, but in World War II they were made rarely. In World War I, large gas chambers were arranged so that canisters could be mounted in the gas atmosphere for testing while the subject remained outside the chamber and breathed through a gas mask hosetube. The present intermittent-flow canister test machine is designed to permit man tests without necessarily constructing special chambers. For such a test the pump is disconnected and the subject breathes through a facepiece attached at the effluent connection to the canister.

Man tests may be made with or without chemical indicators. If indicators are used, the subject is protected by an auxiliary canister which adsorbs gas penetrating from the test canister. Often it is desired to check or confirm chemical indicator break points. Then the protective canister is removed and the gas is detected by its odor or lacrimatory effects. Such tests should never be made with SA, which is odorless,[d] or with AC, which is insidious in its effects, but can be made with CG and CK, both of which are readily detected. Much useful information has been gained from a limited use of man tests. Any new or unexpected performance from an experimental model canister should be confirmed by a man test; occasion-

[d] As ordinarily made there is a pronounced odor associated with SA, but apparently this material (probably a carbide) is removed by charcoal; and the gas which penetrates a canister has no odor.

ally, it is desirable to recheck standard machine tests by man tests with the subjects at heavy exercise.

2.7 MINICAN TESTS

The name "minican tests" has been applied to special tube tests carried out under canister conditions; that is, with depth of layer and linear flow rate made the same as in the canister. This type of test has not been widely used, because results are always questionable, but on occasion it has provided useful information. Examples are tests of enemy canisters when only one was available and tests of collective protector canisters.

For an axial flow canister, a minican test is merely a tube test with proper flow rate and depth of layer. The minicans simulating radial flow canisters must, however, provide for a variation in flow rate from influent to effluent sides, since the flow rate in an annular layer of adsorbent varies inversely as the radius. A fair approximation for canisters such as the M10 has been obtained by use of a funnel-shaped layer with the areas at top and bottom proportional respectively to the outer and inner areas of the canister.

Sources of potential error in minican tests are the possibility of wall leakage because the surface-volume ratio is so much greater than in an actual canister, and the possibility of temperature effects vastly different from those in the canister.

2.8 FIELD TESTS OF CANISTERS

In connection with field experiments on the travel of gas clouds, numerous tests have been made of the actual protection afforded by canisters under various conditions. Such tests contribute no information that could not be obtained in the laboratory by reproducing the field concentration-time conditions, but they do provide vivid illustrations of the possibility for breaking canisters.

Two types of field canister tests have been carried out, with live goats and with breather pumps. The pumps are specially designed to operate at low power consumption. A rubber bellows is driven by a small motor to give a flow of about 16 lpm with 24 to 30 c. Effluent gas from the canister is passed either through a recording meter or through an absorbing solution which is later titrated. The entire apparatus is housed in a gas-tight box to avoid leakage effects while operating in a high gas concentration.

2.9 LAYER DEPTH STUDIES

A very useful tube test, known as a layer depth test, was used to some extent in 1918 but much more extensively during World War II. Measurements were made of tube test lives at varied depths of layer and the resulting lives plotted as in Figure 2. From the slope of the curves, the capacity N_0 is computed. The intercept of the linear or nearly linear portion with the depth axis is known as the critical depth λc. There is no quantitative correlation of N_0 and λc with canister performance, but qualitatively the relation is very good. In a thin bed canister λc is the important factor, and in a thick bed N_0 is most important.

Layer depth studies were most useful in research for studying impregnation methods, aging, and mechanisms of gas removal. They are also useful in evaluating and interpreting canister performance because a knowledge of N_0 gives an efficiency ratio for the canister. This efficiency ratio is defined by the equation

$$\text{Efficiency} = \frac{\text{mg of gas restrained}}{N_0 \text{ (in mg per ml)} \times \text{volume}}.$$

2.10 OTHER TESTS

In addition to the gas tests of adsorbents already discussed, numerous other tests are used in the manufacture and development of adsorbents and gas mask canisters. These are not discussed in detail because complete directions are given in CWS specifications, but they are listed.

Heat of Wetting

Until recently one of the basic charcoal tests has been the heat of wetting, that is, the heat evolved per unit mass or unit volume of charcoal when immersed in benzene. To some extent the heat of wetting is a measure of the degree of activation, but it may also depend upon the pore volume.

Formerly it was believed that heat of wetting was measured by the tightness with which an adsorbate is held on charcoal,[9] but recently there has been doubt as to the interpretation of heat of wetting data, and this test has been dropped from charcoal specifications.

Hardness

The standard hardness test is an empirical measure of the amount lost when a specified sample is shaken in a sieve with steel balls (CWS Pamphlet

Number 2, Part II, Section L). The purpose of the test is to prevent the use of soft charcoal which may break into dust after loading into the canister, but it does not accurately evaluate the desired quality in a charcoal and some other testing method might be better. No improved method is available, however, and until it is, the present test will be retained.

Screen Analysis

Because the pressure drop and gas protection afforded by a given volume of charcoal depend upon the size and size distribution of particles, all charcoal is procured under rigid screen analysis specifications. These are based upon U. S. standard screen sizes. Charcoal for M1, 10, 10A1, and 11 canisters is 12-30 mesh. The usual distribution is near 20% (12-16), 50% (16-20), 30% (20-30) by weight, but considerable deviation is permitted among the three sizes.

Apparent Density

The apparent density is the mass in grams per milliliter of charcoal as loaded by slow gravity fall into a glass cylinder.

Rough Handling

An essential property of a gas mask canister is its ability to withstand jolting and impacts in normal usage without becoming deformed, losing adsorbent, or developing a high resistance. Empirical rough-handling tests of various types have been used for different types of canisters. All subject the test canister to very drastic treatment, after which the resistance must not exceed a specified amount and the gas life must not be below a stated minimum. All these rough-handling tests, while admittedly empirical, are based upon treatment which the canister might receive in combat use. All employ the principles of impact and of vibration.

Filter Tests

Filter tests are described in Chapter 24.

2.11 DEFICIENCIES IN TEST METHODS

Although adequate for specification testing and the usual demands of research programs, the charcoal testing methods now used have some deficiencies. The most important of these are:

1. Tube tests, as previously indicated, show poor correlation with the lives of thin-bed canisters. This may be illustrated by data from a surveillance program for an extruded coconut charcoal whetlerized by the ASC process (see Chapter 5 for a discussion of surveillance).

Table 3. Comparison of tube and canister lives.

Storage condition	5 cm tube life	M10 canister life
Freshly prepared	180–200	46
75 days, dry, 25 C	188–201	30
75 days, wet, 25 C	88–122	0–2
75 days, wet, 50 C	142–159	0–2
75 days, dry, 50 C	177–204	20

2. Minican tests cannot be relied on for exact indications of canister lives. They do, however, agree much better than the standard tube tests. The chief weakness in the minican test is the danger of wall leakage, particularly for thin-bed canisters, because the wall-volume ratio is much greater for small volumes than for the canister.

3. Mesh distribution must be very carefully controlled in all tests, whether tube or canister. Changes in mesh size distribution affect the critical depth λc which is particularly important in tests of thin depths of adsorbent. Further, there is often a difference in the degree of activation of large and small particles.

4. The reproducibility of breather pump canister tests is not so good as desired. Greatest difficulty is encountered in the CK 80-80 test, which in many of the research studies is the most critical test. In general, canisters of poor to ordinary quality give quite reproducible lives, provided loading is carefully done with well mixed samples. Fortunately, most of inspection testing is confined to samples giving M10A1 CK 80-80 lives of about 30 to 50 min. But with long lives ranging from 70 to 100 min, quite erratic test results are often obtained. The following reasons are suggested to account for poor test precision.

a. The break occurs very slowly and it is difficult to fix the point at which the penetrating concentration of gas is sufficient to change the indicator solution within the specified time interval.

b. Because the break occurs slowly, the effect of leakage or channeling caused by variations in packing the adsorbent may affect the apparent life markedly. In a long-life sample a good fraction of the adsorbent lies in the saturated region. Any leakage of gas through this region causes more rapid penetration.

c. A slight variation in the water content of the

charcoal may exert considerable influence on the life of a slowly breaking sample. As gas is taken up in the saturated zone, water is driven off, and as the sample dries the critical depth progressively decreases.

d. The CK indicator has a temperature coefficient. The effect of this may become more pronounced as the life increases, particularly if the break occurs slowly and it is difficult to fix the exact time at which the break occurs.

5. The PS test is not a good criterion of charcoal quality, as discussed above.

SECRET

Chapter 3

MANUFACTURE OF ACTIVATED CHARCOAL

By *Warren L. McCabe*

3.1 INTRODUCTION

WHEN GAS WARFARE was introduced in 1915, it was immediately necessary to find a suitable defense against this weapon. This means of defense was a canister containing activated carbon through which the soldier breathed. Activated carbon, now treated with catalysts to destroy non-adsorbable toxics, is at present the universal filling for military gas mask canisters.

Although a number of carbonaceous raw materials were used in World War I to make gas mask charcoal, the most satisfactory product was manufactured from coconut shells. For the physical adsorption of high molecular weight toxics, coconut chars are satisfactory but have two deficiencies: (1) the raw materials are obtainable only in tropical regions and must be transported over long distances; (2) the usual coconut char does not possess the proper pore structure to function satisfactorily as a base for the metallic catalysts necessary to destroy chemically, especially under conditions of high humidity, those toxics which are not adsorbed physically. It is known now that the second deficiency can be corrected by proper processing, but it is still undesirable to rely on a charcoal made from an uncertain supply of a foreign raw material if a satisfactory product can be made from domestic substances. During the last few years, therefore, considerable work has been done to develop from plentiful domestic raw materials a relatively inexpensive carbon which is both an active adsorbent and a suitable catalyst base and which is hard and strong enough to withstand rough handling in the canister without disintegrating.

The effort has yielded satisfactory results. Carbons of excellent quality and moderate cost are being produced in large quantity. They are impregnated with a whetlerizing solution and heat treated to produce a canister filling which provides balanced protection against all toxic agents appearing practicable as field agents. They function satisfactorily under wide variations of humidity and temperature. The main raw materials are waste wood and bituminous coal, both of which are available in nearly unlimited quantities. Other raw materials, including some of synthetic rather than natural origins, yield reasonably satisfactory products, but are not used in commercial processes.

Most of the important practical developments have come from empirical trial and error experiments conducted for the most part by charcoal manufacturing companies, rather than from scientific research. The manufacture of high grade gas mask carbons is an art rather than a science. Nevertheless, a fairly comprehensive understanding of what constitutes a good charcoal has been attained, and the important factors in the manufacturing process have been identified.

Although the present state of charcoal manufacture is satisfactory, and the quality of the product is high enough to discourage the use of gas as a military weapon, the modern adsorbent has not been tested in an enemy gas attack, and until the product has met the test of actual combat, there is a definite chance that it may be deficient. Reliance must be placed on the resources of science to correct such a deficiency, if it appears. Primarily this chapter summarizes the present scientific and practical knowledge that can be drawn upon to solve future problems which might arise in the manufacture of charcoal for gas mask use.

3.2 GENERAL METHODS OF MANUFACTURE OF GAS MASK CARBON

The manufacture of gas mask charcoal is a typical industrial process. In common with all such operations, a charcoal plant receives raw materials and converts them by physical and chemical operations to products which function differently from the raw materials. The activated product from the modern manufacturing process possesses an internal pore

structure of an extent and character that renders the charcoal a remarkably active adsorbent for high molecular weight air-borne molecules. In its early use, the action of the material as a physical adsorbent was its important characteristic. Since World War I, activated charcoal has been used as the raw material for the process of whetlerization, in which the carbon is impregnated with metallic catalysts which are intimately incorporated with the granule and which are active in destroying those low molecular weight toxics that are not adsorbed physically.

Whetlerization processes are described in Chapter 4. This chapter treats only of the manufacture of charcoal suitable for whetlerization.

Charcoal making processes are of two main types, which are differentiated by the method of activation. The first method is activation by hot gases, usually containing steam, and the second method is activation by chemicals.

The manufacture of gas-activated carbon usually includes the following steps:

1. Crushing, grinding, and briquetting a carbonaceous raw material.
2. Crushing the briquettes and sizing the crushed material.
3. Devolatilization of the crushed material.
4. Gas activation by hot gases, usually containing steam.
5. Screening the activated material to meet size specifications.

Not all processes include all the steps, nor do they operate the steps in the same order. Certain processes have additional steps. For example, in the manufacture of charcoal from compressed wood, a high temperature calcination treatment is used between the carbonization and activation steps.

The manufacture of charcoal by chemical activation is a more specialized process that has but little in common with gas activation. It is described later in this chapter.

In the preparation of charcoal by gas activation, the preliminary crushing and grinding is usually necessary to establish the preliminary structure for the system of macropores (see Chapter 6), which are necessary in the final product to give, under high humidity conditions, a good CK life. The briquetting step in the process is necessary to construct a structure that will withstand subsequent crushing and processing and remain strong and hard enough for practical use in a canister.

The briquettes are crushed to form a convenient size of granule for carbonization and activation. In at least one process, the final size of the finished granules is established by carefully sizing the crushed, briquetted material before carbonization and activation.

Most raw materials contain quantities of water, hydrocarbons, oxygen compounds, and other volatile matter that must be removed before an active carbon can be prepared. A devolatilization process is required, which consists of a low temperature carbonization. The devolatilization must be conducted in such a manner that the volatile matter will be disengaged from the residue without puffing or caking the particle and ruining its density and strength.

Activation is the term applied to the step of developing adsorptive rate and capacity in a carbonized and devolatilized material. During this step, additional devolatilization is accomplished, and the pore system is completed.

Final screening to meet definite size specification is necessary. If the average particle size is too large, the rate of reaction between charcoal and toxic will be reduced and the canister life, especially in thin beds, will be too low. If the particle size is too small, or the range of sizes too great, the resistance to breathing will be excessive. Ideally, regular geometric particles of a single uniform size are desired, but practical manufacturing operations require that a reasonably wide spectrum of sizes be allowed, and because of crushing the particles are irregular in shape.

The details of actual processes, and the results of investigation of carbonization and activation are discussed in detail in later sections of this chapter. Because problems concerning the selection of raw materials have been of serious moment during the history of activated carbon, the next section is devoted to a discussion of the raw materials used in the manufacture of gas mask carbon.

3.3 RAW MATERIALS

In the past, there has been an opinion that suitable gas mask carbon could only be manufactured from specialized and highly organized plant structures. Much attention was given to the morphological characteristics of the shells, pits, and like materials that were used in the early gas mask charcoal processes. During the last few years, however, a wide variety of raw materials has been used to prepare gas mask charcoals, and there seem to be no definite requirements on raw materials save that they must be car-

bonaceous and that they must not have been heated to such a high temperature that they have become inert.

The main problem in manufacturing a suitable gas mask carbon is to obtain one that not only has satisfactory physical adsorption properties as measured by the PS life test, for example, but also to obtain a product that can be converted into an ASC whetlerite that has a satisfactory canister performance and stability against CK under humid conditions.

The raw materials now being used to manufacture charcoals are as follows.

Bituminous coal of the Pittsburgh seam is the raw material for the largest single production. Coals from the Emerald and Black Diamond mines are used. Charcoal from these coals meets all present specifications including those for the aging of ASC whetlerites under conditions of high humidity and high temperature. The charcoal is of unusually high retentivity. Its apparent density is also high and is in the range of 0.48 to 0.52 g per ml before whetlerization. This charcoal is low in moisture pick-up and high in ash as compared with other charcoals. Its only deficiency is weight, which makes it unattractive for use in the lightweight canister. The process was developed and and is being operated by the Pittsburgh Coke and Chemical Company, Pittsburgh, Pennsylvania [PCC].

The standard low density charcoal is prepared from briquetted waste sawdust from Douglas fir. The briquettes or Prest-o-logs are carbonized under pressure and activated by steam. These charcoals have a lower density than those from bituminous coal, are somewhat less satisfactory with respect to retentivity and aging, but meet all present specifications, and are more satisfactory than the PCC char in lightweight canisters. The charcoal is produced by the Crown-Zellerbach Company of Seattle, Washington.

Satisfactory charcoals are being made in smaller quantities from pecan shells,[25] English walnut shells,[23] black walnut shells,[53, 19] and peach pits.[53, 19] The manufacture of charcoal from such materials is rather small because of the limited supply of raw materials. These chars are produced by the Barnebey-Cheney Engineering Company, Columbus, Ohio.

Hardwood sawdust, activated chemically by zinc chloride using recently developed techniques, yields charcoals that meet present specifications. These materials have the unusually low apparent density of about 0.3 before whetlerization. They have low retentivities and require expensive equipment and plants for their manufacture, and therefore they are not in procurement. Standby plants were available for operation, had the product been needed.

The standard charcoals made in England are prepared from mixtures of British coals. The coals are blended in such a fashion that the carbonization process can be conducted without undue swelling and coking.[14] Because British practice does not include whetlerization, it is not known whether the British coal mixture would give a satisfactory whetlerite.

Coconut charcoals prepared in relatively small quantities by laboratory methods yielded a charcoal that is satisfactory in initial ASC performance. These have not been commercialized and their characteristics in aging are unknown.

Small experimental quantities of a relatively low density coal have been prepared by mixing Pittsburgh seam coal with sawdust and processing the mixture in the PCC process. The materials had moderate density and satisfactory canister lives, but were deficient in hardness.[26]

Several other and unusual raw materials have been used to prepare charcoals of promising quality. In no case have the products been completely evaluated in canister lives and aging characteristics. They have been developed to a point, however, where it is quite probable that satisfactory materials could be prepared from them, but they are of interest only from a theoretical point of view as showing the wide variety of raw materials that can be used to make a satisfactory adsorbent. The Godfrey L. Cabot Company has prepared, from carbon black and a starch and tar binder, charcoals giving satisfactory ASC whetlerites as measured by tube tests. Charcoals made by carbonizing Saran (a vinylidene hydrochloride polymer) have satisfactory characteristics as base charcoals. They whetlerize moderately well after steam activation. Both of these products are of interest largely because they demonstrate that reasonably good adsorbents can be made from materials of synthetic origin rather than of plant structure.

Considerable development work was done in the Kimberley-Clark Company, Neenah, Wisconsin, on a charcoal made by mixing 50 to 75% by weight of crude lignin precipitated from waste sulfite liquor with 25 to 50% of poplar wood flour. Char from this raw material was evaluated by tube tests and found to yield satisfactory ASC whetlerite. The lignin contributed substantially to the yield of carbon and did not function only as a binder. The aging characteristics of the material are not known.

A charcoal manufactured by the Colorado Fuel and Iron Company [56] from western bituminous coal gave satisfactory activated carbon (good PS life) but one that could not be whetlerized to a satisfactory product. The material was made by carbonizing and steam activating lump coal without previous briquetting. Its aging characteristics are not known. Newer information on the factors controlling whetlerizability suggest that this coal also might yield a satisfactory product if it were crushed and briquetted before carbonization.

The older product obtained by the zinc chloride activation of hardwood was an excellent adsorbent and could be treated to form a superior Type A whetlerite. The material was deficient, however, as a raw material for ASC whetlerite, and plants manufacturing the product were shut down when ASC whetlerite was adopted. During research and development, intermediate products, satisfactory in initial ASC lives but deficient in aging against CK under humid conditions, were made by this process.

Several other raw materials yield satisfactory activated carbons which meet the specifications for unimpregnated charcoal but do not form satisfactory ASC whetlerites. Coquito nuts,[23] apricot pits,[24, 17] Masonite,[46] high density carbonized hardwood,[50] Cliffs-Dow Char,[38] NRL–MPGO from Activated Carbon Incorporated,[35] and the pitch coke obtained from the low pressure carbonization of coal [45] all yielded materials which could be activated to a satisfactory PS life and hardness, but either have yielded unsatisfactory ASC whetlerites or have not been evaluated as an ASC whetlerite.

Several materials, which yielded activated carbons having PS lives between 20 and 40 min, have not been evaluated with respect to ASC lives because of their low quality as absorbents. The materials are: Morrell char, which is made of a mix of wood char, coke and tar binder; [46] carbons from lignocellulose; [29] ordinary hardwood char; [27] low temperature coke freeze from bituminous coal; [45] anthracite coal; [32] chlorinated anthracite coal; [3] Seabury carbon (Delco-Remy).[49]

A number of other carbonaceous materials yielded on activation products that have PS lives below 20. Some of these materials are: gas coke; [34] various woods treated with hydrofluoric acid; [48] scrub oak; [48] semi-anthracite; [45] and a mixture of wood charcoal and pitch.[48]

Conclusions

The raw materials listed above are typical of those that have been tried in the past and those used at present. The following conclusions can be drawn:

1. Because charcoals of the highest grade as measured by complete evaluation of all important properties can be made from waste wood and bituminous coal, there is no necessity to consider the use of esoteric raw materials of special character, of limited availability, or of foreign origin.

2. From a fundamental point of view, the fact that satisfactory adsorbents and reasonably satisfactory whetlerites have been obtained from materials such as waste sulfite liquor, carbon black, and Saran, make it unnecessary to manufacture charcoals from naturally occurring raw materials. Morphological structure is not necessary. Even the degraded type of vegetable structure left in bituminous coal is probably of little importance in the use of coal as a raw material. Indeed, the first step in the processing of the coal is to grind it to 300-mesh size and thus largely destroy any structure that it might have.

3. Many of the materials that were found to yield mediocre or poor charcoals were evaluated before present knowledge of the fundamentals of charcoal processing was available. A number of the above materials could probably be used by proper briquetting, carbonizing, and activating techniques if there were any reason for using them.

4. A complete and final answer concerning the applicability of a given raw material for the manufacture of gas mask carbon can only be given by preparing several large batches of the carbon and testing each batch thoroughly in canisters against the known agents, by preparing ASC whetlerites and determining the aging characteristics and retentivities of the whetlerites, and by obtaining hardness and rough-handling data on the finished whetlerite. No single test is definitive in the evaluation of a gas mask charcoal.

5. Unless future emergencies show that some very unusual characteristic, not at present identified, is necessary for a satisfactory gas mask carbon, there appears to be no reason to use raw materials other than waste wood or bituminous coal.

3.4 BRIEF DESCRIPTION OF COMMERCIAL MANUFACTURING PROCESSES FOR GAS ACTIVATED CARBONS

Complete descriptions of the processes being used to manufacture gas mask charcoal are given in a

Chemical Warfare Service [CWS] report.[16] The following descriptions are for the purpose of making the present chapter complete.

3.4.1 Process of Pittsburgh Coke and Chemical Company[a]

This process was the major one used in World War II and produced more gas-mask carbon than all others combined. It is used in two large plants operated by the PCC. The process is of interest, first, because the production of a gas-mask charcoal from a very large supply of common raw material has been reduced to its simplest terms through its use, and, second, the product obtained has unusual qualities not possessed by other charcoals. The material is especially noteworthy for the stability of ASC whetlerite prepared from it.

The raw material is Pittsburgh seam bituminous coal. The two coals that have been used in practice are Emerald seam coal and Black Diamond seam coal. Other analogous coals can be used. These two coals are very much alike and contain 35 to 38% volatile matter and 6 to 8% ash. The raw material is broken to a size between four and ten mesh U. S. standard screen, and is stored in an elevated bin holding some 70 tons of coal. From the bin, it is fed by gravity to impact mill pulverizers in which the size is reduced until at least 65% of the material passes through a 300-mesh screen. During early operations, the coal was mixed with a coal tar pitch to aid in briquetting. Present practice omits the pitch and uses a small amount of steam intermixed with the pulverized coal to moisten it and to heat it sufficiently for briquetting. The ground coal is charged into large Kraft paper bags. Each bag contains several pounds of coal. The bag is placed in the dies of the briquetting press where it is briquetted at a pressure of 10,000 to 15,000 psi. The cylindrical briquettes, after being discharged from the hydraulic press, are passed through a series of crushers in which the material is broken to the proper size mesh distribution. The size of the final product is controlled during this screening operation. The fines, amounting to about 25% of the total material to the screens, are returned to the impact mill to be rebriquetted. The oversize material of the screens is recycled in closed circuit to the grinder. The intermediate material has a size range between 10 and 22 mesh U. S. standard. The size reduction obtained during the further processing steps reduces the material to a 12- to 30-mesh size which passes standard CWS specifications.

The sized material is elevated to a feed bin and weighed into the carbonizers or bakers. Each carbonizer or baker consists of two parallel tubes mounted together in a gas-fired furnace. The tubes are ½-in. plate steel. They are each about 60 ft long and 3 ft in diameter. The crushed charge passes in series through two bakers and emerges from the second baker at a temperature of about 1000 F. The temperatures are not measured in the bakers themselves, but in the gas space external to the tubes. These temperatures increase from 600 F at the feed end to about 1050 F at the discharge end. The time of baking is about 4¼ hours.

In both bakers, a small current of steam is passed to sweep out volatile matter. A certain amount of fortuitous air leakage also occurs and this leakage is probably important for the carbonization step.

The baked material, which still contains some 12% volatile matter, is discharged into wheelbarrows and charged by hand into the activators.

The activators are operated in batch. There are approximately 30 activators in each of the two plants. Each activator is a cast chrome-steel tube 15 ft 6 in. long by 14¾ in. in diameter. The charge is heated externally by coke-oven gas. The activators are mounted in pairs. The activators are charged from the front by blowing the charge from hopper carts with compressed air. A lid with a 4-in. central hole makes a loose rolling fit with the wall end of the activator and is held in place by a flange which fits over the lip of the activator cylinder. Steam, in an unknown amount, is superheated by passing it through a chrome-steel pipe positioned in the furnace and is admitted to the back of the activators. Both the gas formed by activation and the excess steam issue from the 4-in. opening in the lid in the front of the activator. The combustible gases burn in the atmosphere. The temperature in the furnace is 1760 F and the charcoal temperature is 1740 F. Temperature control is manual.

The charge to an activator is 225 lb; approximately 113 lb of activated product is obtained after an activation time of 285 min. The activators are emptied by removing the lid in the front and raking the charge out over the lip into wheelbarrows.

[a] The information in this section was obtained through various visits of NDRC and CWS personnel to the PCC plants.

Neither steam nor combustion gases are cut off during the discharge or charge operations.

One feature of the activation process is the size separation that occurs in the activators. The large particles tend to rise to the top of the bed and are usually more thoroughly activated than those which remain submerged.

The activated product cools in air and is given a final screening to insure proper size. The fines accumulated during this screening are very small in amount.

The yields are as follows: From 100 lb of coal 80 lb of primary char after baking and 37 lb of activated char are obtained. The block density of the briquettes is 1.2. The apparent density of the crushed briquetted material is about 0.60. The apparent density of the baked material is about 0.58 and the density of the activated product is about 0.50.

The process is practiced in two plants; one at Neville Island, Pittsburgh, Pennsylvania, and the other at Carnegie, Pennsylvania. The processes in the two plants differ in minor respects but both operations are essentially as described.

3.4.2 The Prest-o-log Process [30]

This process successfully manufactures a satisfactory grade of gas-mask charcoal from waste wood. It is essentially the same as a process that was being developed at the end of World War I. Many practical difficulties were overcome before satisfactory operation. Considerable effort was necessary both in plant and pilot plant before a satisfactory product was obtained. The process produces a carbon of relatively low apparent density which makes it attractive for use in lightweight canisters. It is not as satisfactory from the point of view of initial gas life, retentivity, nor stability as the product from the PCC process.

The problem of attaining a high density briquette from waste sawdust has been solved in a novel fashion by the development of a mechanical means for compacting sawdust to a briquette. The product of the briquetting operation is known as Prest-o-logs. The Prest-o-logs used in the Seattle plant are made by the Weyerhaeuser Company, and the logs are delivered to the pilot plant ready for processing. The Prest-o-logs are about 13 in. long, and are 4⅛ in. in diameter. Each log is sawed into six 2-in. briquettes by means of gangsaws. The briquettes are charged into two carbonizing furnaces which consist essentially of tubes 60 feet long mounted in furnaces. Each furnace contains four vertical banks of seven tubes each. Holes are provided for gas escape at 4-in. intervals along the entire length of each tube. The essential feature of the carbonization process is the use of pressure constantly applied to the briquettes during carbonization. Extensive and detailed pilot plant work done on the process [29, 31] shows that the pressure is essential during the period of the exothermic reaction in order to maintain proper density in the carbonized product. Between each briquette is placed a cast iron spacer ½ in. thick. Pilot plant work demonstrated that these spacers are necessary to transfer heat to the center of the briquette and thus eliminate soft centers.

The pressure is applied by a hydraulically operated plunger. The total net pressure over the entire tube is 160 psi. Discharge of the carbonized briquettes at the end of the tube is accomplished by means of a hydraulically operated gate. An ingenious control system allows the operator at the end of the tube to charge fresh briquettes periodically at the entrance and discharge carbonized briquettes at the exit. The iron spacers are separated from the discharged briquettes, returned by a conveyor, and reused. The gases formed by the carbonization issue through the ¼-in. holes drilled in the carbonizing tubes and burn in the space surrounding the tubes. The heat requirement for the carbonization is more than met by the heat of combustion of the gases formed, and city gas is required only during the starting-up period.

The primary charge is crushed in two steps. The first stage is accomplished in a Robinson sawtoothed crusher and gives a discharge consisting of particles approximately ½ to ⅛ in. in diameter. The second stage is a Robinson gyratory crusher. The product is screened over Rotex screens to give three fractions. The first fraction is larger than 6 mesh and is returned to the feed of the second press; the second fraction is 6-20 mesh and is used for further processing; the third fraction is fine material which is wasted. The percentage of fines is about 22%. Because there is no possible way of recycling fines, they are completely lost from further processing.

After size separation the char is calcined. The calciner is a rotary kiln like those used in cement manufacture. It is 77 ft long and 8 ft 9 in. inside diameter. It is lined with 12 in. of refractory and insulation. The calciner is divided into three sections. The first

section, or preheater, is 39 ft long and is separated by a bridge wall from a second, or calcination, section which is 26 ft long. The third division is a cooling section 13 ft long. The calciner rotates at about ½ rpm. The temperature of the charcoal at the feed end is about 800 F, and at the bridge wall about 1400 F. Air inlet pipes supply air to burn the combustible gases formed by the calcinators in the kiln. In the calcining section, the charcoal temperature is about 1700 F at the entrance and 1900 to 2100 F as the end where the material passes to the cooling section. Electrical heating is used in the calciner section. The current is applied in two circuits through commutator rings and the charcoal itself acts as an electric conductor. The heat required to bring the carbon to 2000 F is obtained in part from the electric energy supplied through the electrodes and in part from the heat of combustion of gases formed by the continued devolatilization of the charcoal.

The purpose of the calcination step is to develop strength and density in the particle and to complete the devolatilization. Pilot plant work showed that a satisfactory product can be prepared by this process without the calcination step but that very careful carbonization is necessary if this step is omitted. Also, the maximum PS life cannot be obtained without calcination.[30, 32] The carbonization step is considerably easier to operate if followed by calcination and to some extent deficiencies in carbonization can be eliminated in calcination.

The activator is a continuous rotary kiln. It is 60 ft long, 8 ft 8 in. inside diameter, and has a 12-in. refractory and installation lining. It rotates at ¾ rpm. The activating section is 48 ft long and the unlined cooling section is 9 ft long. Both measurements are taken on the inside. The heat required for the activation process is obtained first, by burning the combustible gases generated during activation, and second, by electrical heat supplied through electrodes in the furnace walls. Steam is blown through nozzles placed in the wall of the activator. The steam pipes are connected to manifolds outside the wall of the activator and the manifolds brought to the automatic valve which emits steam to the activator bed. The steam in each set of inlet tubes is on during one-fourth of each revolution. The flow of steam is automatically shut off when the steam ports are not covered by the charcoal bed. Air pipes connected to an air manifold pass through the activator wall into the center of the activator to provide air for the combustion and volatile matter. The product of the activator is given a final screening. Fines amounting to 14% are wasted.

The overall yield of the process is between 6 and 8%. The losses are distributed approximately as follows: in the saws, 14½%; in the charring furnace, about 71%; grinding loss 22%; calcination loss 24%; activation loss 36%; and loss in the final grinding, 16%. Loss in each step is based on the weight of material charged to that step.

The material is in the calcinating tubes about 130 min, in the calciner about 36 hr, and in the activator about 24 hr. Pilot plant work shows [29, 31] that these long times of carbonization, calcination, and activation are unnecessary.

3.4.3 Miscellaneous Processes for Manufacture of Gas-Activated Charcoal

Several charcoal processes have been developed through the laboratory or pilot plant stage but have not been used commercially. There is but little likelihood that any of these processes will ever be used to make gas mask carbon, but they will be described briefly because of the information they provide on the general problem of charcoal manufacture.

Manufactured Charcoal from Carbon Black [22]

This process was carried through the pilot plant scale by the Godfrey L. Cabot Company, Boston, Massachusetts.

Channel black, made by burning natural gas with a deficiency of air under steel channels, is the main raw material for the process. The size of the particles is 50 to 100 A. The carbon black is mixed with approximately an equal weight of Barrett coal tar pitch and wet with 20% casein solution, which acts as a mixing agent. The mixture has a consistency about equal to that of axle grease. The mix is pelleted at a pressure of 50,000 to 100,000 psi. The pellets are ⅜ in. diameter by ⅜ in. long.

The pellets are broken to 8-10 mesh before carbonization. About 45% of the material is fines, which are reprocessed.

The broken pellets are carbonized by being passed through a gas fired furnace. The charge is heated to 1400 F and cooled to room temperature. The charge is at or near 1400 F for about 45 min. The material shrinks during carbonization and has an apparent density of 0.80 after the process.

The carbonized raw char is steam activated in a continuous horizontal tube, 7 ft long. The temper-

ature of activation is 1600 F maximum, and the time is 8 hr. The feed rate is 2 lb per hr and the steam rate was 4 to 12 lb per hr. The overall yield of the process is approximately 35% of the weight of the pellets. The product contains practically no ash.

The product of this process was found to be convertible to ASC whetlerite that gave reasonably well balanced protection against SA, CK, and AC.[6] The PS life of the unwhetlerized char was in the range 50 to 60 min. The evaluation was largely by tube tests and no aging data are available. The estimated cost of charcoal from this process, including an eighteen month write-off, was 30 cents per pound.

The process did not go into commercial use because by the time the pilot plant work was done, the PCC process, which gives a cheaper and better product, was in operation.

Manufacture of Charcoal from Waste Sulfite Liquor and Wood Flour

The Kimberley-Clark Company of Neenah, Wisconsin, completed a pilot plant investigation and preliminary plant design for a process to make gas-mask carbon from a mixture of wood flour and liquor precipitated from waste sulfite. Again, a satisfactory product was obtained (with a possible exception of aging characteristics) but the cost-quality relationship was inferior to that shown by the PCC process, so the plant was not constructed.

The essential steps in the process [1] are: waste sulfite liquor, which has a *p*H of 2.5 to 3.0, is neutralized with caustic soda, and the *p*H raised to 11.5 to 12.0. The alkaline material is cooked in a digester at 75 psi and 320 F for 2 hr. The cooked liquor is pumped into a wood precipitating tank and concentrated sulfuric acid added until the *p*H is 3.5 to 4.0. Lignin is precipitated from the solution. On addition of cold water the lignin hardens and can be broken into pieces approximately 1/16 x 1/8 in. The lumps are washed twice with water and dried to a moisture content of 5%.

The crude mix for carbon manufacture consists of lignin, oak or birch wood flour of 60-80 mesh size, and recycled fines. The lignin and fines are ground to −200 mesh. The minimum proportion of lignin to produce a carbon of satisfactory density and hardness is 50 to 66% of the total of lignin and wood flour. Sodium carbonate, an activation catalyst, is added in amount equal to 0.5% of the weight of the mixture to the material in the blender.

The final mix is pelleted at sufficient pressure to produce a density of 1.16 to 1.22. The pellets are of 5/8-in. diameter, and are made in a commercial 10-ton pelleting machine. A pelleting lubricant, such as Sterotex, is used.

A typical mix has the following raw materials:

Material	Per cent
Lignin (200 mesh)	66
Oak or birch flour (−60 mesh)	22
Recycled fines (−200 mesh)	12
	100

Sterotex, 1% of above
Na_2CO_3, 0.5% of above

The pellets are carbonized in batch, without preliminary crushing, in a rotary retort. The temperature is increased at a uniform rate to a maximum of 1030 F. Two exothermic reactions, one at 510 F and one at 800 F, are encountered during the heating. The carbonizing time is 5 hr. The hot carbonized material is discharged into air-tight containers and cooled. The primary carbon pellets are strong, hard, and retain their original cylindrical shape. They are considerably smaller than the uncarbonized pellets.

The carbonized pellets are crushed and screened to 10 to 18 mesh. The fines, which are approximately 25% by weight of the pellets, are recycled. The apparent density of the carbonized material is 0.5.

Activation is conducted in a rotary batch retort heated by producer gas. The material activates rapidly with steam and activation requires only 60 min. A total of 1 lb of steam per pound of primary carbon is used.

The yield of carbonized material from the pellets is 56% and the yield from the activation step is 43 to 45%. The overall yield is 21 to 22% based on starting material.

Considerable performance data on the product from the process are available, including tube and M10 canister tests on ASC whetlerite made from the charcoal.[36] The PS service life of the base carbon was 50 to 55 min, and the apparent density was 0.41. ASC whetlerite characteristics were excellent in comparison with other charcoals available at the date the tests were made. Aging data and M10A1 canister data are not available as the process was eliminated from consideration before the determination of such data was customary.

The cost of the process is excessive in comparison with that of the PCC process. For example, 25 lb of caustic soda and 25 lb of sulfuric acid are required for 17.5 lb of lignin, and the total cost of the lignin

SECRET

alone is 7½ cents per lb on a basis of a two-year depreciation period. The pelleting process is expensive in comparison with the briquetting of coal. Costs of carbonizing and activating are comparable in the two processes, but costs of raw material alone in the Kimberley-Clark process are 20 cents per lb of carbon and the total cost, including an 18-month write-off, was estimated to be about 50 cents per lb. The actual price of PCC carbon is approximately 20 cents per lb.

Saran

The preparation of activated carbon from Saran has been achieved in the laboratory. The cost of the raw material precludes its ever being used and no work has been done beyond the laboratory stage. The results obtained on the material are of some interest theoretically, because they demonstrate that activated carbon can be made from a completely synthetic raw material which has no morphological structure.

The Saran charcoals were prepared from a copolymer of 15% vinyl chloride and 85% vinylidene chloride.[18] A controlled carbonization, in which HCl is driven off and nearly pure carbon left behind, yields a product that has PS lives of 40 min or more, without steam activation. During carbonization from 20 to 40% of the HCl is removed between 125 and 150 C, and the remainder by heating to 400 C. Some carbon is also driven off. Saran charcoals obtained by carbonization only are not satisfactory bases for ASC whetlerite. Steam activation increases the PS life of the charcoal to a 65 min level, and the steam activated material can be used to prepare reasonably satisfactory but not outstanding ASC whetlerites.[37]

No practical use for Saran charcoals has appeared, and because of the limited supply of raw material and the high cost of the product their further development and commercial manufacture cannot be justified.

Coconut Charcoal

The older types of coconut char, which were made by carbonizing the shells in lump form and steam activating the carbonized char, do not form satisfactory ASC whetlerites. Pore distribution analyses (see Chapter 6) show that such materials are deficient in macro pores. Preliminary laboratory results [42] have been obtained showing that coconut chars can be much improved by either of the following processes.

The first process consists in sizing pit-carbonized coconut shells, slow carbonization of the sized material to 1500 F, and activation at 1700 F. The activated product, when whetlerized with an ASC solution containing 4.25% CrO_3 produced a whetlerite comparing favorably with a U. S. Grade I, Seattle wood whetlerite.

The second process consisted in pulverizing the shells, briquetting hot with 20% by weight of pitch binder, sizing, carbonizing one hour at 1000 F, and activating at 1700 F. When whetlerized with the same solution, the product compared favorably with U. S. Grade I coal char made in the PCC process.

Coconut chars of the above type will probably not compete with the better products manufactured from domestic materials, and there is no reason for developing the above process further.

3.4.4 The Manufacture of Gas Mask Charcoal — Conclusion

Consideration of the various processes used to prepare gas-activated charcoals that were or could be used leads to the following conclusions.

1. Just as scarce unusual raw materials are unnecessary, so are tricky, complicated processes unessential for manufacturing a high-grade modern absorbent. Essentially the most successful processes consist in building a briquette of finely ground particles and of a particle density of about 1.2, carbonizing the briquetted material under such conditions that the strength and density of the material are not destroyed, and steam-activating the carbonized materials.

2. Although the above method is quite generally applicable, the optimum conditions for each raw material must be found by laborious trial-and-error experiments. Also, different raw materials, although yielding satisfactory products when treated in the optimum manner, yield products of varying characteristics and quality.

3. The success of any process in producing uniform charcoal of good quality depends upon careful selection and standardization of the raw material and careful operation and control of all process steps.

4. The manufacture of charcoal is inherently a high-temperature process from the point of view of metallic construction materials. Steam activation requires a temperature of 900 C to 1000 C, if a reasonable plant capacity is desired, and only the better high-chromium alloys withstand such temperatures. This problem is discussed in Section 3.5.

5. The mechanical characteristics of the char are important and must be determined by experiment. The strength of the final particle seems to be determined in the original briquetting operation, but even a strong briquette can be weakened to disintegration during carbonization and activation.

6. Expensive processing of raw material before briquetting is unnecessary, because ground bituminous coal and waste wood sawdust provide excellent raw materials without such processing.

3.5 FUNDAMENTALS OF MANUFACTURE OF CHARCOAL BY STEAM ACTIVATION PROCESSES

From the foregoing review of present and potential processes for the manufacture of steam-activated charcoal, it is apparent that there are three key steps: (1) crushing and briquetting; (2) carbonization; and (3) activation. It is the purpose of this section to present the current knowledge of each of the steps generally taken. The method to be followed is to present the scientific and fundamental background of these operations and to correlate such knowledge with practice.

3.5.1 Crushing and Briquetting

A method for evaluating fundamentally the effects of process variables in charcoal making is to follow changes in the pore structures during the various steps in the manufacturing process. The methods used to determine pore structures and the definitions of sub-micro, micro, and macro pores [21] are discussed in Chapter 6. It is pointed out there that a charcoal that will give balanced protection has a balanced pore structure, and the relative proportions of micro and various sizes of macro pores is important in establishing the characteristics of the final whetlerite prepared from the material. If a final char is deficient in macro pores of the proper sizes, it will not yield a satisfactory whetlerite, especially if the product is evaluated in terms of its wet CK life in thin-bed canisters. If the charcoal is deficient in micro pores it will not be satisfactory as a physical adsorbent. The sub-micro pores seem to have no value.

Large macro pores are built into the charcoal particle before carbonization and activation.[20,21] Certain materials such as walnut shells and peach pits possess a morphological structure that insures an adequate system of macro pores. In general, however, to rely upon a natural structure for such pores is to limit seriously the raw materials that can be used for charcoal manufacture. The performance of charcoals described in Section 3.4, in which the morphological structure of the raw material either never existed or was destroyed before carbonization, shows that the equivalent of the proper morphological structure can be obtained artificially by grinding the raw material and briquetting the fine powder so obtained.

Pore distribution studies of PCC coal charcoal show that the crushing and briquetting operation creates large spaces between the primary particles and that these spaces fall in the large macro pore range. The macro pores formed by briquetting are in the range of about 50 to 700 microns.[20] It is doubtful that they function in a manner to yield a good ASC whetlerite, but they are available as feeder pores from which smaller macro pores can be developed during carbonization and activation. They also facilitate the escape of volatile matter during carbonization and provide channels throughout the charcoal particle during activation. Too large a volume of such large pores is disadvantageous because they represent a waste of charcoal volume if they are present in excess.

It is well known that monolithic graphitic carbon cannot be satisfactorily activated. It is also probable that if such material has been too thoroughly graphitized by excessive heating, an active carbon cannot be made from it even after crushing and briquetting.

An important problem in forming a briquette from a finely ground raw material is that of obtaining strength and rigidity in the briquette. To meet this requirement, various binders are usually used. The most important material used for this is ordinary petroleum pitch. Other materials are starch and lignin. Most binders do not contribute an appreciable part of the final product. Lignin, however, as shown by the Kimberley-Clark process, does break down and add activated carbon to the final product. Experience with the PCC process has shown that by heating the carbon with steam it is possible to briquette the material without binder and the use of pitch for this purpose in the PCC process has been discontinued.

The obtaining of a suitable briquette and the choice of binder and the proportion of binder to char can only be worked out by empirical experiment. No method of predicting the answer to such problems has been found. Attempts to obtain a satisfactory carbon from uncrushed Emerald mine bituminous coal failed.[10]

An increase in briquetting pressure over the range 10,000 to 80,000 psi was accompanied by an increase in particle density from 1.02 to 1.16, and a decrease in macro pore volume of 0.23 to 0.11 cc per cc granule.[20, 21]

Increased briquetting pressures are in the main beneficial, but on a diminishing return basis. Pressures up to 20,000 psi tend to improve hardness and strength, and the gas lives are somewhat improved. Pressures in excess of 20,000 psi have but little effect.

Experiments on the use of very small primary coal particles (1 to 2 microns mean diameter) yielded products having slightly better 80-80 CK canister lives than those made from the usual size of crushed coal particles (1 to 159 microns). The charcoal from the micronized coal (1 to 2 microns) yields a superior secondary whetlerite after a leaching of the primary whetlerite and a second whetlerization.[43]

3.5.2 Carbonization

The function of carbonization is primarily that of removing the bulk of the volatile matter present in most raw materials without destroying the density and strength of the particle. During carbonization certain changes are brought about in the pore distribution. All the volumes of sub-micro, micro, and macro pores increase.[20] The increase in micro pore volume does not, however, bring about an increase in the adsorbing qualities of the char.

The most difficult problem in carbonization is usually the prevention of coking, which results in a porous, puffed-out particle full of large voids. Many materials on carbonization pass through a soft or plastic stage and, if the volatile matter is evolved during such a stage, coking can readily result.

Two techniques useful in preventing coking have been developed. In the carbonization of wood the application of pressure to the wood briquette, as practiced in the Seattle process and as studied on the pilot plant basis by National Defense Research Committee [NDRC], allows the retention of the density of the briquette by applying direct pressure while it is in the plastic stage. It has been found by experiment that the pressure is unnecessary except at a temperature of about 400 F. If pressure is maintained during that stage, the resultant crude char can be further processed to obtain a satisfactory product. In the usual distillation of wood, coking occurs and the primary char obtained possesses too low a density to yield a satisfactory product.

The second technique of carbonization is applicable to coal. It is difficult to carbonize crushed coal briquettes in the absence of oxygen.[10] When carbonization is attempted in a stream of nitrogen, for example, a long carefully conducted carbonization is necessary to obtain material suitable for activation. If, however, air is present during the carbonization, the process can be conducted with considerable rapidity and a satisfactory carbonized char obtained in a total time less than one hour.[41]

A small amount of air can reduce the coking tendency of a coal significantly even if the oxygen absorbed by the coal is negligible.[9] The manufacturing process normally conducted allows a certain amount of air to be fortuitously drawn into the bakers. Also the partially carbonized char is exposed to the air during transfer from one baker to the next.

A deliberate supply of controlled air reduces the coking tendency and allows an easier and shorter carbonization.[41] The critical time at which air is required is during the softening and coking period which occurs at about 600 F. If air is present during this temperature interval an exothermic reaction occurs, which reduces the fuel consumption and which accelerates the carbonization process.

Certain definite indications were obtained showing that the yield versus quality relationship of the final carbon can be improved by air carbonization.[41] An increase of approximately 15% in the CK life of the product was found in some cases. Since this increase is near the limit of precision of the canister test and can also be obtained by variations in whetlerization, this result is not too clearcut.

Carbonization in the presence of air at a maximum temperature of about 1000 F often yields a carbonized product that has considerable PS life, sometimes as much as twenty minutes.[b] A carbonization carried to a higher temperature, 1800 F, for example, gives a product which shows no PS life. There is evidence that shrinkage occurring between the temperatures of 1000 and 1800 F may account for this difference.[20]

Not all raw materials are equally difficult to carbonize. Peach pits,[40] walnut shells, and coconut shells [2] can be carbonized with relative ease without coking. It is doubtful that air has any beneficial effect in such cases. The carbonization of sawdust-lignin mixtures was quite easy. Bituminous coal represents material which is most difficult to carbonize, but the use of air, as described in the preceding

[b] A good charcoal has a PS life of 45-60 min.

paragraph, simplifies the problem of obtaining satisfactory materials for activation by carbonizing briquetted coal.

3.5.3 Activation

The final definitive step in preparing a charcoal by non-chemical means is that of activation. The activation process cannot produce a satisfactory material if the earlier steps are not conducted properly. With the exception of materials such as Saran, however, carbonized chars have little or no activity, and gas activation is required to develop their inherent properties.

As far as the process is concerned, activation is simple. It consists essentially in bringing carbonized char into intimate contact with hot activating gases. Although oxidizing gases such as carbon dioxide, chlorine, and sulfur, can be used for activation, only one active agent (superheated steam) is used in practice. The purpose of the activation process is to create the final desired pore structure in the granule, and also to develop the proper kind of surface in the pores. During activation the particle loses weight, both from the inside and the outside, and both the size and density of the particle decrease significantly.

3.5.4 Process Variables — Steam Activation

The important requirements for a satisfactory commercial activator are: (1) the energy requirement must be provided; (2) uniformity of contact between gas and particles must be obtained; and (3) the proper time of treatment must be provided.

The reaction of carbon and steam is highly endothermic. Approximately 4000 Btu must be supplied for each pound of each carbon gasified. Heat requirements in a small experimental unit can be easily supplied by means of the hot walls of an externally heated container. In a large unit, however, the supplying of heat to the charge is a serious problem. Unless regenerators are used, the supply of heat by means of the hot gases themselves is not practicable. The radiation from the hot gas to the particle is not rapid enough to supply the heat at an appropriate rate unless the gases are at a temperature well above the activation temperature to be used. For example, if the active temperature to be used is 1700 to 1800 F, the hot gases, even when supplied in large quantity as in the Jiggler process (see Section 3.6.1), must be at temperatures above 2500 F. In retort activation, in which the flow of gases is very much less than in Jiggler activation, it is not practicable to supply all of the heat requirement by means of the gases themselves. In general, heat must be transferred through the retort wall. Furthermore, in order that all particles in the activating bed can be reached by heat, the thickness of the bed is limited. Other methods of supplying heat to the charge are the use of electrical heat such as used in the Seattle process, and the supply of heat by burning, in direct contact with the charcoal particles, the gases formed by activation supplemented by external fuel.

Uniformity of activation is important. The uniformity problem has two aspects: (1) activating conditions must be the same throughout the activator; and (2) the individual particles must be activated under uniform conditions. Activators are usually horizontal rotary furnaces in which the particles are brought into contact with the activating gas by continually circulating in the activator. Such activators do not give perfect uniformity;[37] larger particles tend to activate more quickly than the smaller. Satisfactory uniformity of activation can also be obtained by using long continued low-temperature activation processes in which the partially activated material is continually withdrawn in the bottom of the activator and returned to the top.[16] The Jiggler method of activation provides maximum uniformity of contact between gas and char.

In practice, fortunately, a reasonable lack of uniformity in the activated char can be tolerated, but at the expense of a somewhat lowered yield. The development of the activity of the char, both as an adsorbent and as a catalyst base, occurs rapidly during the early stages, but the extent of development of the desired properties becomes constant during the later stages and the characteristics of the final carbon are relatively independent of the amount gasified over a range of 10 to 15% of final yield. Therefore, if certain particles activate somewhat more slowly than others, they tend to reach approximately the same peak if the process is continued long enough, but the yield is lower by 5 to 10% than that obtainable under uniform conditions.[12]

Although steam is the activating agent used in most industrial processes, carbon dioxide can also be used, and is usually present in activators in which steam is used because some CO_2 and much CO is formed during the activating process. In some cases, for example in the Prest-o-log process, the carbon

SECRET

monoxide is allowed to burn in the activator to supply a portion of the heat of activation. Also, if steam-enriched flue gases are used, CO_2 will be present. The activation of carbon by CO_2 alone is slower than with steam under corresponding conditions. In addition, the quality of the product as measured by its capacity for physical adsorption tends to be somewhat less.[28] The presence of 10% or more of CO_2 in the activating gas does no harm and can be tolerated without difficulty.

3.5.5 Temperature Control

The temperature of the char in the activator should be measured and, for best results, maintained under reasonably close control. The accurate measurement of char temperature is not a simple matter because of the effects of rotation and non-uniformity of the char bed both in depth and in length. Also the particles absorb heat rapidly. There is doubt that the activating temperature in one plant can be correlated with that in a different plant. For best results, the temperature measuring device (usually a thermocouple) should be immersed well into a dense bed of carbon.

The effect on product quality of variation in activation temperature over a range of 100 to 150 F is not great. The main effect of temperature is upon rate of gasification, and the control of temperature is essentially a control of rate. The optimum temperature of activation depends upon the char, and usually lies in the range of 1500 to 1800 F. The temperature of activation should not be more than 75 F above or below the optimum. As a rule, if uniformity of contact between gas and char is obtained, the relationship between yield and quality is relatively insensitive to temperature, total gas flow, gas composition, and gas velocity.[27] Large variations in these factors do, however, influence quality.[55]

Close temperature control in itself is of no avail if the time of treatment varies among the particles, or if some particles are in a different gas environment from others. To obtain controlled uniformity of activation all particles must be activated at the same temperature, for the same time, and in contact with gas of the same velocity and analysis.

Activating temperatures are at just about the metallurgical limit, and high-chromium alloys are the best material of construction for externally heated activators. Internally heated activators can be constructed of refractory-lined steel shells.

3.5.6 Changes During Activation

The activation process modifies the crude char in a number of ways. Formerly, the process of activation was considered essentially as a selective oxidation of hydrocarbonlike materials which were retained by adsorption in the pores of the char after carbonization. In this simple explanation, activation was considered to be a cleaning or purging process by which existing pores were purged of high molecular weight materials that were occupying the active centers of the char, and therefore when these materials had been oxidized the existing activating centers were uncovered and made useful.

There is an element of truth in this assumption, but there is reason to believe that it is not the main part of the activating process. It is true that there is a widespread existing pore structure in char after carbonization and before activation. Pores of the sub-micro, micro, and macro size range are present.[21] It is also reasonable to assume that the surface of these pores is contaminated with debris resulting from the cracking of hydrocarbons and analogous processes. During the early part of the activating process, such debris is removed and the existing pore structure uncovered. Charcoal at this stage, however, is not well activated, and has but little more adsorptive capacity than before activation. In fact, in some cases, chars obtained by long continued carbonization have fair PS lives which are destroyed during the initial stages of steam activation. The essential purpose of steam activation is now considered to be a development of a proper pore system in the micro and macro range. The development of the required system is a continuation of the pore development originally set up in the briquetting step.[21]

The final activated char, when studied by X-ray methods,[17] seems to consist of a number of small packets. The sizes of the packets are of the order of 10 to 20 A.[55, 18] The packets themselves are constructed of layers of carbon laid down in a crystal structure essentially graphite, except that the distance from corner to corner of the hexagon rings and the interplanar ends are larger than those of a true graphite. The adsorptive characteristics of the packets may result from the fact that the departure of the crystal parameters from those of graphite distort the force fields in such a way that residual forces are available for attracting foreign molecules.

When carbons are given a prolonged heating at a

temperature of 1000 C or more, the lattice dimensions tend to approach those of graphite and the carbon has little or no adsorptive power.[17]

The sequence of events during activation has been followed by determining, as a function of extent of activation, such properties of the char as apparent densities,[5, 8] heats of wetting,[44, 5, 8] particle densities,[5] ultimate analysis,[44, 5] tube[5] and canister lives[39, 8] of the whetlerites against various toxic agents, water absorption,[8] and development of pore structure as shown by pore analyses[20] and surface areas as shown by nitrogen adsorption.[13]

If the char that has been carbonized at a lower temperature than that of activation is placed in a hot activator, the first stage of the process is thermodevolatilization, which is accompanied by a shrinkage of the particle and an increase in particle density. Generally, the devolatilization is completed before appreciable activation is accomplished.[44]

The percentages of hydrogen and oxygen in the carbonized material depend primarily on the temperature at which the char is heated, and these percentages are higher as this temperature is lowered. Accordingly, when the char is placed in the hot activator, the percentages of hydrogen- and oxygen-drop parallel rapidly with the devolatilization and reach concentrations characteristic of the activator temperature.[44] The important observation was made in the activation of coal charcoal that once the devolatilization is completed the only change in the ultimate analysis of the char during the activation proper is the increase in ash content.[44] The hydrogen content remains surprisingly constant. This observation strongly indicates that the essential process of activation is not one of a selective oxidation of hydrocarbonlike materials, otherwise it could be expected that the percentage of hydrogen would steadily decrease during the activation proper.

Tube and canister lives of the char and the whetlerites made from it increase rapidly during the first stages of the activation, but level off later. The various lives do not reach their peaks at the same time. If the activation is carried well beyond the normal yield, most gas lives tend to fall off because of the loss of carbon and the enlargement of pores to such a size that they are no longer useful. The final result is the production of ash. Sometimes, subsequent to this, the particle disintegrates. There is, therefore, an optimum yield or extent of activation. If the material is underactivated, the yield is high but the gas lives are well below their peaks. If the material is activated too far, gas lives are at a maximum, but the yield is lower than necessary.

3.5.7 Internal versus External Weight Loss

During activation, a very substantial weight loss occurs. For most charcoals a loss of approximately 40 to 60% of the original weight is necessary before the material is completely activated. The loss in weight occurs in two ways. First, the outside of the particle can be burned completely and a smaller granule obtained. Such external weight loss is entirely deleterious and represents nothing but a loss in yield. Second, the interior of the particle loses mass and it is this loss that accompanies the activation process itself.[55] The internal loss is useful and the ratio of the internal loss to the total loss is one measure of the efficiency of an activation process. In general, the ratio of internal loss to total loss varies from about 0.2 to approximately 0.5.

There is no apparent difference between extent of activation of the interior of a granule and that at the surface, provided the granules are in the usual gas mask absorbent size.[44] English work showed that, in the activation of very large particles several inches in diameter, the outside surface is more quickly activated than the inside, assuming, however, that all particles are subject to precisely the same environment. If conditions in the activator are such that particles of one size are hotter or are more thoroughly in contact with steam, these particles will be activated before the remaining particles. In penetrating to the center of the particles, the gas utilizes the macro pores existing in the primary char. After penetration, the activating gas enlarges existing pores, removes by gasification any inactive pore lining material, uncovers active centers, and develops small pores that may or may not be present in the original char. There is considerable evidence to support the hypothesis that many of the small, final pores exist in the carbonized char as small voids hidden among the crystallites, and that many of these pores are rendered accessible by the attack of the activating gas during the process.[55] The fact that the block density, as measured by helium, of the char increases during activation supports such an hypothesis. The development of such hidden voids probably occurs during carbonization, although in naturally occurring materials it is possible that such voids are in the original raw material.

SECRET

3.5.8 Rate of Activation

The rate of activation is most easily determined by measuring the weight rate of loss during activation. Many such data are available. It has been shown, first, that the rate has a high temperature coefficient and shows an Arrhenius constant of 47,500 cal per mole.[55] This implies a rapid increase in rate with increase in temperature and demonstrates that the rate of the activation is not controlled by diffusion of activating gas either to the outside surface of the granule or through the pores. The rate of activation under constant conditions of temperature, steam supply, and steam velocity is constant with time. This indicates that the effective area taking part in the oxidation is constant, and implies that the basic pore structure of the particle has been largely established before pore activation occurs.

The rate is influenced by the composition of the gas in contact with the particle. Actual activation processes in practice may require 6 hours or many days, depending upon the temperature, the rate of supply of activating gas, and steam content. In the Jiggler process, in which large quantities of activating gas are in intimate contact with the char, activations can be conducted in a few minutes.

The gases formed by the activation contain CO, CO_2, and undecomposed steam. The fraction of the steam decomposed varies from 10 to 50% depending upon the temperature and the rate of steam supply. The ratio of CO to CO_2 is approximately that expected from the water-gas equilibrium, provided the reaction is not catalyzed by the ash.[55] In the activation of coal char by the PCC process, the percentage of CO was considerably higher than that called for by the water-gas reaction, probably because of the influence of the high ash content of this charcoal.[52]

Effect of Rate of Activation on Quality

Certain chars, such as bituminous coal chars, can be activated very rapidly, and still yield very satisfactory products. Other chars, such as the Prest-o-log char, must be activated more slowly if optimum results are to be obtained. The effective rate of activation in a given case can only be found experimentally.

3.6 ACTIVATION METHODS

In present commercial plants, charcoal is activated either in horizontal, rotary retorts or in large, vertical shelf furnaces. The retorts may be supplied either in batch or continuously. The PCC process utilizes batch retorts as described above. The Carlisle process utilizes continuous retorts as does a process operated by the Atlas Company of Los Angeles, California.[19] The Barnebey-Cheney Company utilizes large shelf activators through which the charcoal is repeatedly passed for many days until the required activity is developed.

3.6.1 The Jiggler Process

Considerable pilot plant and laboratory work was done on a method of activation that utilizes an upward stream of gas sufficient to agitate or suspend the particles being activated.[47, 51, 54, 33] This method has been known as either the *Jiggler method* or the *boiling bed method* depending upon whether the particles were suspended or merely agitated. The process was not used industrially because satisfactory results were being obtained in existing industrial activators and ample activation capacity was available when the pilot plant work on the Jiggler was completed.

The Jiggler method gives an extremely rapid activation and can be used in preparing very large quantities of char in a small unit, provided the char is of a type that can take a high rate without destroying quality. The process yields the most uniform activation obtainable by any activation process and represents a standard of comparison on this factor. Tentative commercial designs of this equipment are available in case its use is ever desired.

The boiling bed variant of this type of activator utilizes a lower flow rate of steam and causes an agitated bed type of process. The action of the carbon particles in the boiling bed method as compared with that in the Jiggler is analogous to the relationship of a liquid to a gas.

The heat requirement for the Jiggler process can be supplied from the activator walls by utilizing the walls as heat storage between activations. The heat supply required by the boiling bed furnace is obtainable by using a reverberatory roof to radiate heat directly to the rather shallow high density bed of particles characteristic of this method.

3.6.2 Air Treatment of Activated Charcoal

Air is an unsatisfactory agent for the primary activation of charcoal. The reaction between carbon and air is the usual exothermic combustion reaction, and the effect is to burn the outside of the particle to ash rather than to develop the internal pore structure.

Air or air-steam mixtures can be used, however, to improve charcoal already activated.[4] Air-steam treatment at temperatures of 750 to 1060 F, followed by steam devolatilization at 1800 F brought about a 50% increase in the CK (80-80) M10A1 canister life of the whetlerite. The loss in volume caused by the process was 17%. The method has not been evaluated for industrial use.

3.6.3 Chemical Activation of Charcoal

The second main method of preparing activated carbon is by utilizing chemicals as activating agents. Ordinarily, the raw material for the chemical activation is cellulose, ligno-cellulose, or for practical manufacture, waste wood. The essentials of the chemical method are as follows:

The waste wood, usually finely ground, is brought into intimate contact with the activating chemical at a moderate temperature. During the mixing process, the raw material darkens and becomes semiplastic. The reacted mix is then heat-treated to fix the carbon and to bring about the activation proper. Next, the activating chemical is leached out of the carbon. Crushing and sizing can be done at any stage in which the material has the appropriate hardness. Further heat treatment after leaching of the chemical may or may not be practiced.

Of the many chemicals that have been used in the past as activating agents, phosphoric acid and zinc chloride are the two to be preferred. All commercial carbon made by the chemical activation method utilizes zinc chloride. The remainder of this discussion is concerned with the zinc chloride process.

Zinc chloride activated carbons were introduced by the Germans during World War I, and continued development of the process was conducted in the United States in the period between wars. At the time of the national emergency of 1940, zinc chloride activated carbons were considered the highest grade activated carbons obtainable for gas mask purposes. This supposed high quality was a result of the tests used at that time in evaluating gas mask charcoal. The 1940 tests emphasized physical adsorption and the tube lives of Type A whetlerite under dry conditions against AC, CG, and SA. Heat of wetting was also considered of considerable importance. Against such tests the zinc chloride carbons obtained at that time were superior to any other charcoal available. Coal char had not appeared, as yet, upon the scene.

When emphasis was placed on the canister testing of ASC whetlerite against CK, especially under wet conditions, it was found that the old style zinc chloride carbons were definitely defective. These carbons did not take well to ASC whetlerization and ASC whetlerites made from them did not possess satisfactory initial gas lives. Furthermore, when the initial canister lives were corrected by improvements in the processing, it was then found that these carbons were highly unstable as ASC whetlerites and deteriorated rapidly in storage as absorbents for CK under high humidity conditions. Intensive work was done to modify the processing of zinc chloride char to meet these deficiencies. In the main, results were satisfactory and the objective of the work was reached. However, because of the large production and low cost of the coal chars, zinc chloride carbons have not been put into procurement during the last few years. Their main interest under present conditions is because of the fact that the newer products have an unusually low density of 0.30. Large plants constructed when zinc chloride chars were the standard of performance are in stand-by condition, and if necessary large quantities of this char can be made.

Manufacture of Zinc Chloride Chars by the National Carbon Company Process [15]

The present method of manufacturing zinc chloride chars of suitable quality is as follows. Virginia hardwood, milled through 12 mesh, is used as the raw material. The activating solution consists of 65% zinc chloride in water, with 0.25% excess hydrochloric acid to prevent hydrolysis of the zinc. The mix is made from 110 parts of zinc chloride solution, 100 parts of sawdust, and 86 parts of recycled fines. The mix is processed by batches in an agitated, steam-heated mixer. The maximum steam pressure in the mixer jacket is 900 psi gauge. It is important that the reaction be conducted over a definite time-temperature schedule. The maximum temperature of the mix should not rise above 131 C. The temperature at the end of the mix period should be 129 C. The mixing time is 60 min to the maximum temperature and 67 min total to discharge. The mixers are dough-mixers that can be tilted and discharged by dumping. The mix, after reaction, is dumped directly to the feed of an extrusion machine and immediately extruded through a 7-in. auger. The extruded plug is sliced longitudinally into 1-in. thick slabs.

The extruded slabs are dried in open trays at a temperature of 200 C ± 25 C. The time is 8 hr. Dur-

ing this operation, the charge loses 26% of its weight, and becomes hard enough for crushing.

The dried plugs are crushed in closed circuit and screened to obtain a product through a 9-mesh screen and on 20-mesh screens. The oversized particles from the screens are returned to the crushers and the undersized particles are returned as fines to subsequent mixes. The granules are of proper size to give the desired size distribution in the final product at the end of the process.

A more essential step, namely primary calcination, is conducted next. The char is heated in the absence of air in a rotary calciner at a temperature of 700 C for 45 min. At this stage of the process, the charcoal is completely activated. It still contains, however, most of the zinc chloride added in the mixer. To remove the zinc chloride, the char is thoroughly washed by dilute hydrochloric acid and water. About 80 to 85% of the zinc chloride is recovered in the washing and used again in the mixers.

The final step is a secondary calcination at a temperature of 1050 C in a rotary calciner. The time of passage is 60 min.

Notes on the Zinc Chloride Process [15]

The reaction of the mixer appears to be the critical step in the process and a number of the deficiencies of the earlier chars were eventually traced to inadequate control during the mixing operation. It is important that the reaction be carried to a point where the temperature in the mixer drops from its peak. This drop in temperature is probably associated with a drop in the boiling point elevation of the zinc chloride in the mix.[55] The mix obtained by proper control of the mix reaction is called a "reactive mix." Such chars have lower kindling temperatures and considerably higher canister lives than chars obtained from so-called non-reactive mixes, which result from improper mixing technique. The maximum temperature of 130 $\pm$ 2 C also appears to be very critical.

The drying operation is necessary to solidify the extruded mass and to develop enough hardness to allow crushing and sizing. The temperature of this step does not appear to be critical.

The primary calcination at 700 C is conducted at this temperature rather than at lower temperatures. The recalcination at 1050 C allows increased initial CK lives and also improves the stability of the char when made into an ASC whetlerite. If the secondary calcination is less than 1050 C, the resulting char will be unstable.

Mechanism of Chemical Activation [55, 15]

Considerable work was done in the study of the chemical mechanism of activation of carbon by zinc chloride. The opinion of investigators in this field is that at the end of the mixing operation the reaction between the zinc chloride and wood produced a suspension of chemically modified but relatively carbohydrate-free lignin particles in a peptized colloidal solution of carbohydrates derived from cellulose.[55] The zinc chloride attacks the cellulose portion of the ligno-cellulose preferentially to the lignin. During later processing, especially in the 700 C calcination, the peptized carbohydrates and lignin both degenerate to carbon. The zinc chloride decomposes to zinc oxide and HCl. The products from the decomposition of the peptized cellulose are highly aromatic and under the heat treatment the lignin residues, together with the carbon precipitated from the decomposed cellulose, form the final carbon particle and yield a structure that exhibits a desirable macro and micro pore structure. The character of the surface depends on the final calcining temperature.

The zinc chloride process is the most effective process with respect to the utilization of the carbon content of the raw material. The total yield of char from this process is approximately 35%. This represents approximately 60 to 70% of the carbon in the original char. This carbon recovery is higher than that obtained in the Carlisle process (approximately 10 to 15%); (1) because of the recycling of fines which is not practicable in the Carlisle process, and (2) because of the absence of carbonization and gas activation steps. It is larger than the corresponding recovery obtainable in the PCC process (approximately 45%) because in the latter process carbonization and gas activation destroy much of the original carbon content of the coal.

Counterbalancing the excellent yield of the zinc chloride process is the fact that the process is complex and requires acid resisting equipment because of the acidity of the solutions used, and high temperature calciners to obtain satisfactory stability. The process is, therefore, inherently expensive.

The activation obtained in the zinc chloride process is internal rather than external, whereas gas activation is the reverse.

SECRET

Chapter 4

IMPREGNATION OF CHARCOAL

By *R. J. Grabenstetter* and *F. E. Blacet*

4.1 GENERAL CONSIDERATIONS

4.1.1 Introduction

THE IMPREGNATION of gas mask charcoals to increase their capacity to absorb toxic gases has been practiced since the inception of gas warfare in World War I. The charcoal used in early German gas masks was found to be impregnated with either alkali or hexamethylene tetramine.[96] This use of charcoal impregnants by the Germans stimulated Allied investigation of the subject.

It was discovered early that ammonia greatly increased the SA absorptive powers of activated charcoal. The name *Larsonite* was given to ammonia impregnated charcoal. It was prepared either by soaking charcoal in aqueous ammonium hydroxide or by passing gaseous ammonia through the charcoal, followed by heating to 100 C under a 28-in. vacuum for 4 to 5 hr.

Perhaps the most important development in the field of charcoal impregnation made during World War I was the use of copper as an impregnant. As compared with an unimpregnated charcoal, copper-impregnated materials, when tested dry, had at least double the protection against CG and similar gases; triple the protection against AC; and more than ten times the protection against SA. The copper-impregnated charcoal produced at the close of World War I was called *whetlerite*, after J. C. Whetzel and E. W. Fuller who were instrumental in its development. The impregnated gas mask charcoal in production in 1940 was designated Type A whetlerite, although produced by an entirely different process, and contained the copper in a different form from any of the materials earlier called whetlerites.

In the sections of this chapter which follow, a general survey of the field of impregnation of activated charcoals up to May 1945 is presented. The various aspects of charcoal impregnation appear in the following order:

1. Copper and copper-silver impregnations of charcoals. Types A and AS whetlerites, and others.
2. Hexamine- and thiocyanate-impregnation of whetlerites.
3. General studies of charcoal impregnation.
4. Development of copper-silver-chromium impregnation of charcoals. Types ASC whetlerite.
5. Development of copper-silver-molybdenum and copper-silver-vanadium impregnations. Types ASM and ASV whetlerites.
6. Organic base impregnations of charcoal.
7. Absorbent resins as substitutes for activated charcoal.

4.1.2 Copper and Copper-Silver Impregnations of Charcoals — Types A and AS Whetlerites, and Others

IMPREGNATED CHARCOALS DEVELOPED DURING WORLD WAR I

Five types of copper-impregnated charcoals were developed during World War I.[96] These were whetlerites A and B, Rankinite, Rankinite A, and Copper Carbonite.

Whetlerites A and B. Whetlerite A was prepared by precipitating hydrated copper oxide on charcoal by the action of hot caustic on a slurry of copper sulfate solution and charcoal. Whetlerite B was prepared by treating the charcoal first with a copper sulfate solution, and then with finely divided metallic iron or zinc, resulting in the deposition of metallic copper on the charcoal. After impregnation, the materials were dried at 350 C in either trays or rotating driers. Rotating driers with a limited air flow (½ lb of air per lb of charcoal per hour) gave the best results. Whetlerite A has a distinct brown color, whereas the best grades of whetlerite B are a dark, rich red, indicating that both cuprous copper and metallic copper are present, a larger proportion of metallic copper occurring in the latter. Whetlerites A and B were considered equally effective.

The development of these materials began in Feb-

ruary 1918. An experimental plant was built in the latter part of May of that year, and by July the process had reached the stage where plans were made for the manufacture of 70,000 lb per day. Semi plant-scale production was started in September, and at the time of the Armistice, impregnated charcoal was going into some canisters.

Whetlerites A and B are quite different from the adsorbent now designated as Type A whetlerite. The treatment given whetlerites A and B results in reduction of copper compounds to cuprous oxide and copper, either through heat treatment at elevated temperatures (in the case of whetlerite A) or by reduction with metallic iron or zinc at the time of impregnation (in the case of whetlerite B). On the other hand, Type A whetlerite is made by depositing copper ammine carbonate in the pores of the charcoal, and decomposing it to CuO by heat treatment at 150 C. Reduction of the CuO does not occur under these conditions.

Rankinite and Rankinite A. Rankinite is activated charcoal impregnated with copper salts and a small amount of silver nitrate. It is similar to Type AS whetlerite only in the metallic elements used in its preparation. Rankinite was prepared by impregnating charcoal with copper sulfate or nitrate and a small amount of silver nitrate, and drying at 250 C. Rankinite A differed from Rankinite in being subjected to an additional calcination at 400 C or higher, which resulted in reduction of the copper compounds to cuprous oxide and copper. The silver nitrate increased the SA protection appreciably, although Rankinite and Rankinite A were still not good SA absorbents under 80-80 conditions. It is now believed that this deficiency was due to the pore structure of the charcoal.

Copper Carbonite. Copper Carbonite is the name applied to a carbon absorbent made by briquetting carbon fines, copper oxide, and a binder. The briquetted material was roasted, screened, and activated. It had good PS and CG activities.

There was some investigation of the application of copper compounds to charcoal by spraying, followed by heat treatment. Tests indicated that these materials were as good as the other copperized charcoals and whetlerites being produced at the time.

Impregnated Charcoals Developed Since World War I

The copper impregnating technique was developed further in the period 1919–1940.[102, 103] At the beginning of World War II, Type A whetlerite was the standard copper-impregnated charcoal in use for canister fillings. It was chiefly used in the Type D mixture which contained 20% soda lime and 80% Type A whetlerite.

Preparation

Type A whetlerite was made by impregnating activated charcoal with a solution containing 8 to 10% copper, 12 to 15% ammonia, and 8 to 10% carbon dioxide. The impregnated material was drained and dried at 150 to 175 C for about 3 hr, or long enough to reduce the moisture and ammonia contents to specified limits. In large-scale production, the whetlerizing solution was made by dissolving copper scrap in an aqueous solution of ammonium carbonate containing excess ammonia. An air stream was used to agitate the solution and to provide oxygen for the oxidation of the copper. Gaseous carbon dioxide and ammonia were introduced into the solution until the proper concentrations were attained. The solution was removed from contact with the copper when the desired concentration was reached. Air agitation was continued until all the cuprous copper in solution was oxidized.

Small laboratory batches of whetlerizing solution are prepared from basic copper carbonate, ammonium carbonate or bicarbonate, and ammonium hydroxide.

Performance in Canisters

Typical canister service lives for Type A whetlerite and other types of adsorbents are shown in Table 1. The material known as Type D mixture, containing 20% soda lime granules and 80% Type A whetlerite, was the specified canister filling prior to the middle of 1942. Service lives of this material also can be found in Table 1. It is evident that the addition of soda lime to Type A whetlerite is not justified by the performance of the mixture.

Nature of the Impregnant

In an effort to determine the nature of the copper compound left in the charcoal after heat treatment, portions of the whetlerizing solution were evaporated to dryness in evaporating dishes at various rates and under various conditions.[2] The results indicated that the nature of the copper compounds was profoundly affected by the conditions of evaporation and dehydration-decomposition.

Circumstances which allow ammonia to escape faster than carbon dioxide or water (such as rapid

TABLE 1. Service times of standard canisters with different fillings.[105]
(Lives in minutes.)*

Type of canister	Base charcoal	Filling	CG AR–50	g H_2O in canister	CK AR–80	g H_2O in canister	AC	g H_2O in canister	SA AR–80	g H_2O in canister	Water Content: As issued g H_2O per canister	Water Content: Average after 6 wks (5–9 hr wear) g H_2O per can.	Water Content: Saturation val. at 80% RH g H_2O per can.	Water Content: Per cent of saturation at 80% RH reached after 6 wks
MIXA1	National	Type A whet.	76	5	12	7	49	8	>60	58	7	42	154	27
MIXA1	National	Type A whet.	101	154	5	68	36	63	½	155				
MIXA1	National	Type D mixture	54	6	8	5	40	2	>60	6	5	40	134	30
MIXA1	National	Type D mixture	134	87	3	69	22	75	15	67				
MIXA1	Barnebey-Cheney	Type A whet.	62	6	12	5	44	5	>60	63	6	41	107	38
MIXA1	Barnebey-Cheney	Type A whet.	73	106	5	72	31	63	1½	105				
MIXA1	Barnebey-Cheney	Type D mixture	65	5	8	5	35	5	>60	6	4	42	100	42
MIXA1	Barnebey-Cheney	Type D mixture	77	98	3	74	24	67	15	67				
MIXA1	PCI	Type AS whet.	68	7	23	5	52	5	>60	62	6	43	102	42
MIXA1	PCI	Type AS whet.	102	74	9	77	41	65	>60	105				
MIXA2	PCI	Type ASC whet.	87	6	105	6	83	6	>60	66	6	45	101	44
MIXA2	PCI	Type ASC whet.	116	99	76	97	90	41	>60	103				
MIXA2	PCI	Type ASC whet.	101	105	68	102	76	97						
M10	PCI	Type A whet.	38	12	7	14	21	18	42	32	14	26	33	79
M10	PCI	Type AS whet.	38	35	3	31	14	38	>60	39				
M10	Barnebey-Cheney	Type AS whet.	31	22	6	21	25	21	>60	49	20	40	57	70
M10	Barnebey-Cheney	Type AS whet.	35	57	2	51	13	42	>60	57				
M10	PCI	Type ASC whet.†	36	6	28	3	31	4	>60	35	42	27	40	67
M10	PCI	Type ASC whet.	21	43	19	27	30	40	>60	40				
M10	PCI	Type ASC whet.	31	40	18	38	30	4	>60	33				
M10	PCI	Type ASC whet.‡	36	3	39	2	30	33	>60	33				
M10	PCI	Type ASC whet.	35	38	30	20	27	40	>60	37	3	24	40	60
M10	PCI	Type ASC whet.	38	40	15	35								

* Test conditions prevailing in determination of service times:
CG: 50 lpm Breather Machine 10 mg/l concentration.
CK: 50 lpm Breather Machine 4 mg/l concentration.
AC: 50 lpm Breather Machine 4 mg/l concentration.
SA: 50 lpm Breather Machine 4 mg/l concentration.

† Prepared at Edgewood Arsenal.

‡ Prepared at Northwestern University.

heating, or heating in an atmosphere saturated with water vapor) result in the formation of basic copper carbonate, which decomposes to copper oxide only at temperatures above the 150 C generally applied to Type A whetlerite. The presence of appreciable amounts of basic copper carbonate in the whetlerite results in reduced SA and AC absorption. Relatively slow drying at 150 C in a moderate air stream results in the formation first of a complex copper ammine carbonate which subsequently decomposes into finely divided copper oxide with evolution of ammonia and carbon dioxide.

Copper ammine carbonate can be reduced to a mixture of cuprous oxide and copper by treatment at high temperatures.

The best samples of Type A whetlerite produced in the laboratory were made by drying the drained impregnated charcoal in thin layers in trays at room temperature for several hours before oven-drying at 150 C. Convection ovens which allowed a plentiful air flow, and other ovens which were equipped to permit a plentiful flow of preheated air through the sample, produced the best whetlerites. The good samples showed no evidence of reduction of cupric oxide to cuprous oxide and copper.

Copper is not selectively adsorbed by activated charcoal during impregnation. Whetlerizing solution is sorbed into the pores of the charcoal and held mechanically until the water evaporates from the solution. Copper ammine carbonate is deposited in the pores and by proper heat treatment copper oxide is formed.

Type AS Whetlerite

In the search for a charcoal impregnant capable of producing an adsorbent with high SA effectiveness under 80-80 conditions, the effect of using silver nitrate with Type A whetlerizing solution was again investigated[3,4] in 1941. The adsorbent developed (Type AS whetlerite), containing copper and silver, bears some resemblance to the Rankinite of World War I. However, it showed a good SA protection under 80-80 conditions, in contrast to Rankinite. It must be remembered that great advances had been made in activated charcoal production in the period between 1919 and 1940, and it appears that the lack of SA 80-80 protection exhibited by Rankinite might be caused in some measure by the properties of the charcoal itself.

Preparation of Type AS Whetlerite. The conditions for preparing Type AS whetlerite are identical with those of Type A whetlerite. The addition of from 0.1% to 0.5% of silver (as nitrate) to a Type A whetlerizing solution results in a good Type AS solution. Some types of the early zinc-chloride activated, extruded charcoals did not produce an adsorbent with satisfactory SA 80-80 protection when impregnated with Type AS whetlerizing solution. The reason for this is not certain, but seems to have been the result of pore size distribution and the nature of the surface of the extruded rods. This fault was corrected by changing the manufacturing process. At present, all samples of activated charcoal otherwise acceptable for use as gas mask charcoal can be converted to a Type AS whetlerite without trouble. In impregnations effected by stirring charcoal and impregnant until saturation is achieved, it was found that the charcoal remote from the point of entry of the solution did not acquire enough silver to achieve a good SA 80-80 protection. Rapid mixing corrected this condition. Experiments showed that silver could be introduced as satisfactorily by spraying a finished Type A whetlerite as by incorporation with the original whetlerizing solution.[8, 104]

Plant Production

A study of the whetlerizing techniques used at the various plants producing Type A whetlerite showed that the equipment could be used without change for the manufacture of Type AS whetlerite.[9] Since silver requirements are different for different charcoals, the following table of requirements for Type AS solution was compiled:

0.2% $AgNO_3$ in Type AS solution for Barnebey-Cheney nut charcoals

0.1% $AgNO_3$ in Type AS solution for PCI coal charcoals

0.5% $AgNO_3$ in Type AS solution for National, zinc-chloride activated wood charcoals

The National charcoals adsorbed silver from solution so rapidly that the larger concentrations were necessary to get some silver on all particles. Rapid mixing also helped and was recommended in plants using these charcoals.

In view of the possible formation of explosive silver azides in whetlerizing solutions, an investigation was undertaken to determine the conditions under which such compounds might be produced. It was found that a solution containing copper, silver, and ammonia could not be made to yield explosive compounds, although ammoniacal silver solutions containing no copper form an explosive residue when

treated with sodium hydroxide.[10] It was concluded that Type AS whetlerizing solution constitutes no explosion hazard in plants using it.

4.1.3 Summary of Preparative Conditions for Types A and AS Whetlerites

Numerous studies in Types A and AS whetlerites have brought forth the following conclusions.[4–6, 103]

1. Type AS whetlerizing solution should contain 8 to 10% Cu, 12 to 15% NH_3, 8 to 10% CO_2, and 0.1 to 0.5% Ag.
2. Solution-charcoal contact time should be at least 5 min.
3. Method of drainage is not important.
4. Temperature of impregnation may vary between 25 C and 70 C. Above 70 C large amounts of basic copper carbonate are found in the whetlerite.
5. Air drying before heating is not essential.
6. Oven-heating in trays at 150 C for 3 hr produces a good product. A moderate flow of air through the oven is desirable to sweep away NH_3, CO_2 and H_2O vapor. Rotating kiln-type driers provided with a preheated air flow can be used to prepare excellent Type A whetlerites. This type of drier is desirable but not essential.
7. In Type AS solution 0.1% is usually sufficient for good SA protection. Up to 0.5% Ag may be necessary for some types of charcoal.
8. Rapid mixing of solution and charcoal is desirable since silver is removed rapidly from the solution by adsorption on the charcoal.

4.1.4 Studies of Whetlerizing Solutions

Adsorption of Constituents from Whetlerizing Solutions

The adsorption of constituents from a whetlerizing solution was studied as a function of concentration.[6] The concentration ranges covered were 0.5% to 10% copper; 0.7% to 15% ammonia; and 0.7% to 13% carbon dioxide. At low concentrations the adsorption of copper is positive but becomes negative at higher concentrations. (Negative adsorption indicates that the solvent is adsorbed to a greater extent than the solute, resulting in an increase in the concentration of the solute in solution.) The adsorption of ammonia is positive and of carbon dioxide negative over the entire range studied.

A continuous impregnation was run in which the type of charcoal and the concentration of whetlerizing solution were kept constant. The procedure involved the saving of the solution and drainings after impregnation, and adding fresh solution to restore the original volume. Successive equal volumes of charcoal were impregnated by recovered and replenished solution until analyses showed the concentration of the constituents of the solution to be essentially invariant from batch to batch. This procedure corresponded to continuous impregnation wherein the amount of impregnated charcoal being withdrawn from the impregnation is balanced by a flow of fresh solution and charcoal into the tank. The solution in the tank some time after the start of the process attains an equilibrium concentration slightly different from the original solution. This concentration remains constant for any particular set of conditions, and will change if the type of charcoal or the concentration of feed solution is changed. For the particular experiments mentioned above, equal volumes of charcoal and replenished solution were used at each step. The original and equilibrium concentrations are as follows:

Solution	Density	%Cu	%NH_3	%CO_2
Original Type A	1.211	9.67	14.90	12.66
Equilibrium	1.277	10.04	14.44	13.06

When a Type AS solution is used for continuous impregnation, the silver concentration of the original solution must be increased slightly over the concentration found adequate for a one-step impregnation. The required concentration is determined by the nature of the charcoal being impregnated. The concentration used in industrial production is usually between 0.2 and 0.5% silver.[9]

Silver adsorption was studied by a radioactive tracer technique.[7] A solution containing 0.01% silver was used. The adsorption was found to take place at a measurable rate, and was a function of the silver concentration. Over a 1,000-fold concentration range the data fitted a Freundlich isotherm of the form

$$\frac{X^n}{M} = kc,$$

where X = weight of material adsorbed,
M = weight of adsorbent,
c = equilibrium concentration,
n and k = constants to be determined in each case.

In the experiments performed, using CWSN-44 and CWSC-11 charcoals, from 73% to 90% of the

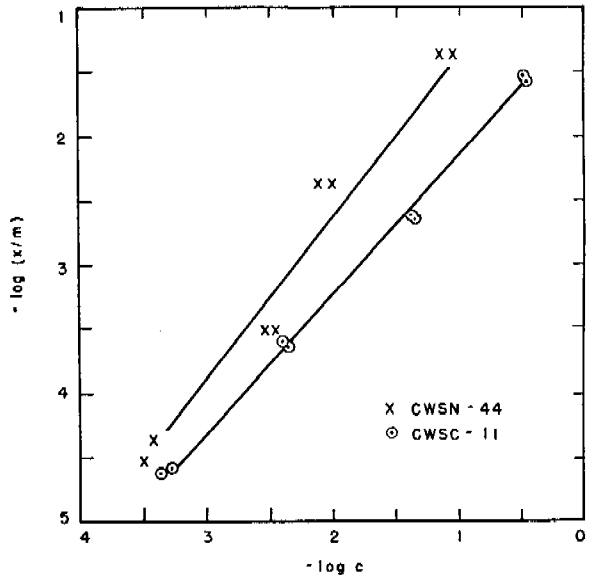


FIGURE 1. Removal of silver from solution by charcoal.

silver was removed from the solution in 30 min. The data are shown in Figures 1 and 2.

In general, the extruded charcoals activated by the zinc chloride process, like CWSN-44 and CWSN-P5, required more silver to give good SA performance than did gas activated charcoals such as the PCI briquetted coals, Seattle pressure carbonized wood charcoals, and nut shell charcoals.

RESULTS OF X-RAY STUDIES OF TYPES A AND AS WHETLERITES

X-ray studies on Types A and AS whetlerites indicate that the copper is present as copper oxide spreads uniformly throughout the grain.[11] There is a direct correlation between the activity of the whetlerite toward AC, and the absence of crystallinity of the impregnants, indicating that the more finely divided or amorphous the copper oxide, the greater the tendency to react with AC. The presence of silver or ammonium nitrate seems to assist in the formation of finely divided copper oxide. The silver appears to be present as finely divided metal.

In the case of some coconut charcoals the solids deposited by impregnation are found in concentric shells in the charcoal granule. These rings appear to be analogous to growth rings in coconut shells. In coconut shell charcoals, about half of the silver deposited by impregnation is on the outside of the granules. Spraying results in the depositing of all the silver on the outer surfaces of the charcoal granules.

Whetlerites dried at low temperatures (25 to 105 C), incompletely dried at higher temperatures, or prepared from whetlerizing solutions having a low ammonia to copper ratio, are likely to contain complex copper ammine carbonate or basic copper carbonate. Neither material reacts with AC when moist.

Heat treatment at 200 to 500 C converts cupric oxide to cuprous oxide and copper. The AC lives of adsorbents thus treated are low, but the SA lives are not appreciably affected. In fact, the presence of some cuprous oxide seems to accompany higher SA protection in Type A whetlerites. Upon equilibration at 80% RII cuprous oxide in whetlerite is converted to cupric oxide. After finely divided cupric oxide is formed in the charcoal, it is quite stable and is not appreciably affected by long heating at 150 C, or wetting by water and redrying in the standard way.

VAPOR PRESSURE OF WHETLERIZING SOLUTIONS

The vapor pressures of the volatile constituents in whetlerizing solutions have been measured.[13, 14] The data indicate that the complex ion present in preponderance is $Cu(NH_3)_4^{++}$, although other complex ions may be present to a much smaller extent. For solutions of high ionic strength the reaction

$$NH_3 + HCO_3^{-} \rightleftarrows NH_4^{+} + CO_3^{--}$$

was found to have an equilibrium constant of 2.1

$$\frac{(NH_4^{+})\ (CO_3^{--})}{(NH_3)\ (HCO_3^{-})} = k = 2.1 \left(\begin{array}{l} \text{Concentration in} \\ \text{moles per 1,000 g} \\ \text{of water} \end{array} \right).$$

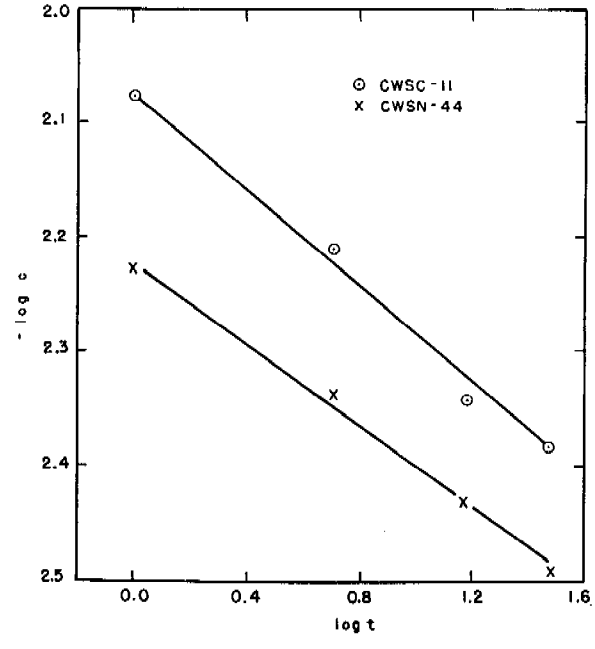


FIGURE 2. Removal of silver from solution by charcoal.

The ammonia pressure may be calculated from Henry's law: $p = k(NH_3)$; $k = 16.8$ when pressure is expressed in mm of Hg at 25 C.

The pressures of CO_2 are low and only a rough correspondence between calculated and observed values was found.

Variations in the vapor pressure of water were in agreement with Raoult's law. Vapor pressure curves for the components of Type A solution over all possible concentration ranges, and curves showing the variation in vapor pressure of the constituents with temperature in the range 15 to 70 C (calculated from the Clausius-Clapeyron equation) are given in the original report.[13, 14] Similar curves for Type ASC solution appear in a later section of this chapter.

Heats of Solution of Volatile Constituents

The average heats of solution of the volatile constituents in Type A solution are:

Heat of solution, kg-cal per mole		
NH_3	CO_2	H_2O
9.1	15.9	11.0

The values for Type AS solution were not measured but should not vary appreciably from the above.

Gases Evolved During Drying of Type A Whetlerites

A study was made of the composition of the gases evolved from whetlerites during drying.[12] For this study, a 5-g sample of charcoal was whetlerized in the usual way and dried in an oven at 150 C with an air stream of 110 ml per min passing through the sample. The gases were collected and analyzed. Ammonia was driven off most rapidly, followed by carbon dioxide and water. The evolution of water lagged predominantly in the early stages, and that of carbon dioxide in the latter stages of drying. Gas evolution was most rapid during the period of drying corresponding to a temperature increase in the charcoal bed from 72 to 85 C. The data are presented in Figures 3 and 4. Figure 3 shows the time versus temperature curves for the charcoal and for the effluent air. Figure 4 shows the percentage evolved of each gas as a function of time and of temperature. Additional data are given in Table 2.

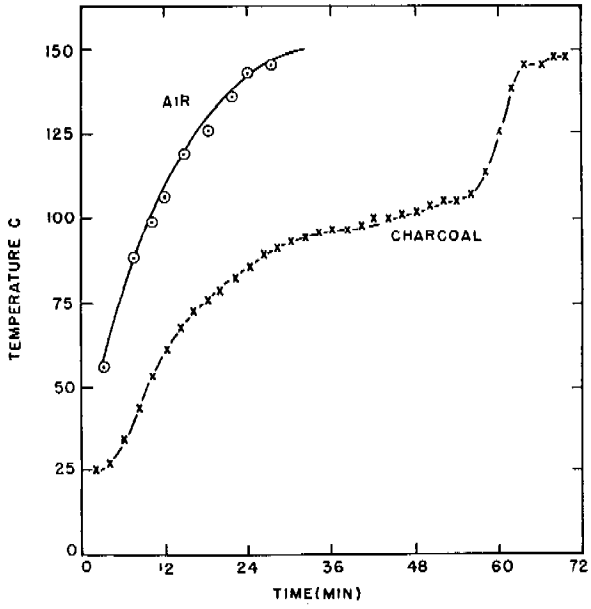


Figure 3. Temperature-time relation in the drying of impregnated charcoal.

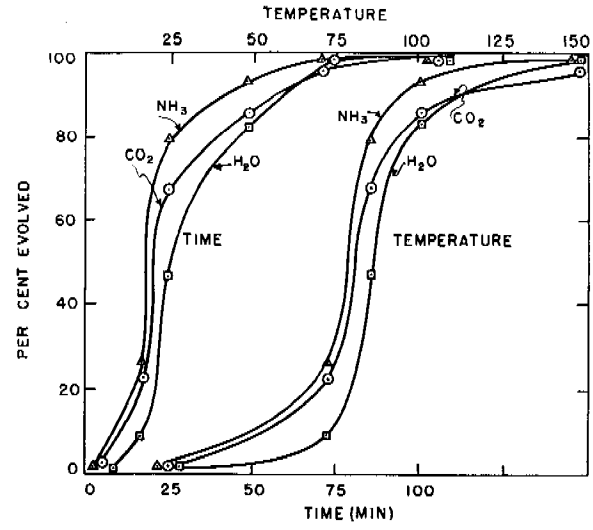


Figure 4. Gas evolution during the drying of charcoal.

4.1.5 Reactions of Types A and AS Whetlerites with Absorbed Gases

Performance data of Types A and AS whetlerites are given in Table 1. It can be seen that the SA 80-80 protection afforded by Type A in the M10A1 canister is negligible, while that afforded by Type AS is entirely adequate.

Adsorption of SA

SA removal is apparently a catalytic oxidation of SA by atmospheric oxygen to As_2O_3 and perhaps to As_2O_5. The product of adsorption of SA is deposited in a shell around the outside of the charcoal granule. It can be extracted with alcohol as As_2O_3 from both Type A and AS whetlerites. Sixty-five per cent of the total As_2O_3 can be extracted easily; the remainder

slowly and with difficulty. The action of cupric oxide is apparently catalytic when the whetlerite is dry. Silver alone acts as a catalyst, but is not so effective as when mixed with cupric oxide. Exhaustion of the adsorbent occurs through deposition of As_2O_3 or As_2O_5 on the active surface, effectively screening it from further contact with SA. Hence SA is an effective poison for AC adsorption, since it also depends on contact with cupric oxide for removal (see below).

TABLE 2. The drying of Type A whetlerite.

Period	I	II	III	IV	V
Total time of drying, min	16	24	48	70	100
Length of period, min	16	8	24	22	30
Temperature range within period, degrees C	22–72	72–85	85–100	100–150	150
Per cent of total amount of each constituent during period					
NH_3	26	53	16	6	1
CO_2	23	45	17	11	4
H_2O	9	38	37	15	1
Cumulative per cent of each constituent evolved					
NH_3	26	79	93	99	100
CO_2	23	68	85	96	100
H_2O	9	47	84	99	100
Average pressure of each constituent during period, mm Hg					
NH_3	64	56		12	
CO_2	18	17		7	
H_2O	118	342		152	
Air	540	325		569	

ADSORPTION OF AC

Types A and AS whetlerites have practically the same protection against AC, when used as a canister filling. The mechanisms of removal appear to be identical. The reactions postulated are:[16–18]

$$2HCN + CuO \longrightarrow Cu(CN)_2 + H_2O,$$

and $$Cu(CN)_2 \longrightarrow CuCN + \tfrac{1}{2}(CN)_2.$$

Cyanogen is present in the effluent air stream near the break point.

A more complete discussion of the mechanism of gas removal can be found in Chapter 7.

ADSORPTION OF BASIC VAPORS

Copper-impregnated charcoals such as Types A and AS whetlerites have greater ethylene imine protection than do unimpregnated charcoals.[36–39] However, impregnated charcoals allow a much more rapid penetration after the break point. A comparison of several basic gases tested against CWSE-1-TE1, a coconut charcoal converted to Type A whetlerite at Edgewood Arsenal, is given in Table 3.

TABLE 3. Protection afforded by Type A whetlerite against basic gases. 5-cm tube test, flow rate 500 ml/cm²/min.

Gas	Conc. mg/l	Per cent R H	Breaktime, min
EN*	3.17	50	110
Diethylene amine	3	50	180
Piperidine	3	50	171
Trimethylene imine	3	50	161

*Ethylene imine.

With the exception of ammonia, basic gases are well adsorbed. As the number of carbon atoms in the methylene imine series increases, the whetlerite protection for the compounds increases, corresponding to the decrease in vapor pressure of the materials.

CWSE1TE1 can be poisoned toward EN by H_2O, AC, and CO_2. Also, the protection decreases with increasing temperature, indicating a straight adsorption mechanism as the principal one. At 25 C the protection is adequate below 70% RH, but is inadequate at higher humidities.

Type A whetlerite, broken by EN, is not regenerated on standing. It is possible that some of the EN is held by formation of a copper coordination complex, but it appears likely that some is held also by adsorption (capillary condensation) since it can be desorbed to some extent by passing air through the charcoal. EN is adsorbed by whetlerite from air-free systems as well as in the presence of air, showing that atmospheric oxygen is not involved in the adsorption mechanism.

ADSORPTION OF OTHER VAPORS

Adsorbed organic vapors and certain reactive gases such as H_2S, Cl_2, and CK reduce the AC and SA lives of Types A and AS whetlerites. This effect is referred to as *poisoning*. In some cases, it is due to simply plugging the pores or covering the reactants or catalysts with an inactive layer or film, rendering the active part of the charcoal unavailable to the toxic gas. This effect may be observed with hydrocarbons and water. Active gases such as H_2S and Cl_2 react with CuO, thus rendering it inactive toward SA or poisoning it as an SA catalyst:

$$CuO + H_2S \longrightarrow CuS + H_2O;$$

$$2CuO + 2Cl_2 + (H_2O) \longrightarrow CuCl_2 + Cu(ClO)_2.$$

Silver is similarly affected by some active gases and particularly by AC.

Protection of Types A and AS whetlerites against CG is adequate either wet or dry. Apparently CG is hydrolyzed very rapidly even by the small amount of residual water on dry whetlerites. Copper oxide serves to retain the hydrochloric acid formed by hydrolysis. Wet, unimpregnated charcoals also have very high CG capacity, the large amounts of moisture apparently retaining HCl effectively.

Many gases are restrained by simple adsorption, particularly those with high boiling points and low vapor pressures at normal temperatures. PS and H are examples of this type. Long protection is afforded, but eventual desorption may occur in canisters exposed to larger dosages.

Tests have been carried out using a large number of different types of gases. The results are shown in Table 4.[19, 20] It will be noticed that NH_3 and CO penetrate almost instantaneously. All the other gases tested were well retained by the whetlerite. Only methyl isocyanide showed a rapid, wet penetration, and it was not instantaneous.

TABLE 4. Absorption of various gases by Type A whetlerite. Test conditions: 5-cm layer equilibrated at RH given in column 2, flow rate 500 $cm^3/cm^2/min$ at concentration indicated.

Gas	Percentage relative humidity	Gas concentration, mg/l	Breaktime, min
SO_2	95	5.2	38
SO_2	50	5.2	65
SO_2	0	5.2	36
Nickel carbonyl	50	5.2	120*
CO	50	...	1
Methyl isocyanide	50	2.8	114
	95	2.8	11
Methyl sulfonyl chloride	50	3–5	140
	95	...	120
Ammonia	95	3–5	5
	95	3–5†	3
Ethylene imine	0	3.17	80
	52	3.17	100
	100	3.17	59
Trimethylene imine	52	3.22	160
Pentamethylene	52	3.28	181

* Showed a CO break in 1 min.
† On E-1 broken with N-hexane.

4.1.6 Type D Mixture

It was found during World War I that dry activated charcoal did not retain CG well, particularly when the charcoal had a low capacity for pure adsorption. Exposure of a canister to high concentrations of CG followed by a long wearing of the gas mask resulted in redistribution and desorption of CG and the production of uncomfortable or dangerous concentrations of gas in the effluent. Humidifying the charcoal resulted in the hydrolysis of CG and the production of uncomfortable, although not dangerous, concentrations of hydrogen chloride in the effluent.

By using a layer of soda lime on the effluent side of the charcoal bed, or dry mixing about 20% by weight of granular soda lime with the charcoal, the retentivity of the canister for CG and HCl was increased, thus producing a satisfactory absorbent for CG.

The use of soda lime was carried over from World War I and was included in the specification for canisters filled with copper-impregnated charcoal. The results in Table 1 indicated that soda lime admixed with Type A or AS whetlerite served no useful purpose. A complete study of the use of soda lime was made in 1942.[21] The results were as follows:

1. Type D mixture (20% soda lime, 80% Type A whetlerite) gives greater CG protection when the whetlerite is of poor quality. High quality whetlerite gives protection as good as, or better than, the mixture.

2. Soda lime mixtures give somewhat better protection than Type A whetlerite against gases which liberate H_2F_2 on adsorption. However, the protection given by Type A whetlerite is very large.

3. Type D mixture is inferior to Type A whetlerite for protection against CK, SA, PS and all other gases with which soda lime does not react. The decrease in protection caused by the addition of 20% of soda lime to Type A whetlerite may be more than 20% in cases where the bed depth of the canister is close to the critical bed depth of the gas being adsorbed.

4. Use of soda lime in the MIXA1 canister is not objectionable since the canister over-protects for all gases except CK at high humidity; in the M10 or M1 canister soda lime is a disadvantage.

Since the development of Type ASC whetlerite, the use of soda lime is no longer a consideration and has been dropped from the specifications.

4.2 HEXAMINE AND THIOCYANATE IMPREGNATIONS OF WHETLERITES

4.2.1 Introduction

As indicated in Table 1, the protection afforded by Type A and Type AS whetlerites against CK and

AC is considerably below the desired level. The best gas mask adsorbents for these agents prepared prior to 1940 were made by a secondary impregnation of Type A whetlerite with a basic solution of sodium thiocyanate or hexamethylenetetramine (hexamine). These materials when used in canisters, that were standard before 1940, absorbed 43 to 176% [94] more CK and 11 to 71% more AC than the Type A whetlerite and Type D mixtures in use previously. The protection toward PS, CG, and SA was equivalent to that of Type A whetlerite and Type D mixture and in each case SA life was practically zero for the humidified canister.

Hexamine and thiocyanate impregnated materials possessed the following disadvantages:

1. Deterioration on storage.
2. Evolution of uncomfortable concentrations of ammonia during use.
3. Necessity for a secondary impregnation for application of the hexamine or thiocyanate. Both of these impregnants are destroyed at the temperature necessary to prepare a good quality Type A whetlerite.

One of the problems under consideration in the period 1941 to 1945 was the improvement of this type of adsorbent with respect to (1) the CK protection after storage, (2) humid SA protection, and (3) the diminution of evolved ammonia.

4.2.2 Hexamethylenetetramine (Hexamine) Impregnations

Hexamethylenetetramine $[(CH_2)_6N_4]$ was used as a charcoal impregnant in German gas masks during World War I. It was believed that it was added to improve CG protection. It was found later that CK protection also was improved by the use of this compound. In 1927, a procedure [97] for the plant impregnation of hexamine charcoals was published by workers at Edgewood Arsenal. Later publications [98–100] summarized the work on this particular type of impregnation. Inasmuch as sodium thiocyanate was considered superior to hexamine, little work was done on hexamine between 1936 and 1942. The work done in this period was concerned mainly with thiocyanate impregnated materials.

Methods of Application of Hexamine

In 1942, the investigation of hexamine was reopened and further experiments were performed.[22, 23] These indicated that hexamine could be added to Type A or AS whetlerite as a secondary impregnant. This procedure is troublesome but is to be preferred to addition to the original solution since the heat treatment necessary to produce a Type A whetlerite of high quality causes extensive decomposition of the hexamine. It was found that sodium hydroxide should be added with the hexamine to reduce the rate of deterioration of the adsorbent. Absence of sodium hydroxide favors higher initial lives but results in a rapid decrease of CK protection during storage (see Table 5). More than 2% of hexamine in the secondary impregnating solution results in evolution of intolerable concentrations of ammonia in use. Optimum concentrations of the secondary impregnating solution were found to be 2% hexamine and 5% sodium hydroxide.

Impregnation is performed by soaking dry charcoal or whetlerite in an aqueous solution of hexamine (containing other desired constituents). In laboratory preparations, the material is soaked for 30 min, drained for 30 min, and oven-dried in a ½-in. layer on a wire screen tray at about 45 to 50 C for 12 to 20 hr. An air stream at a linear velocity of 25 cm per min is passed through the layer of drying whetlerites.

Effect of *p*H on Hexamine Impregnants

Addition of acid to a hexamine impregnating solution decreases the initial CK and AC lives of the adsorbent, as is shown in Table 5.

Table 5. Effect of *p*H on hexamine impregnation of CWSC–11 Type A whetlerite. Test conditions: 5-cm bed depth; 500 cm³ per cm² per min flow rate; gas concentration: CK = 2.5 mg per l; SA = 4 mg per l; AC = 3 mg per l.

Composition of impregnating solution	Tube test service lives, min 80–80 conditions		
2% hexamine	SA	CK	AC
+5% NaOH	..	48	..
+0.5 NaOH	13	67	34
+0.005 NaOH	35	67	35
+0.0	29	67	31
+0.001 NH_2SO_4	36	71	31
+0.1 NH_2SO_4	60	57	13
+3.0 NH_2SO_4	10	0	2
+0.1 NCH_3COOH	58	62	21

Effect of Added Salts on Hexamine Impregnation

Salts of the ammine-forming metals Cu, Cd, Co, Ni, and Zn, were added to the whetlerite with the hexamine in an effort to decrease the evolution of

ammonia from hexamine-impregnated whetlerite. When enough metal was added to decrease the ammonia evolution appreciably, the odor of formaldehyde[b] became noticeable and in most cases was more objectionable than the odor of ammonia. In every case where such metals were added, the CK life was reduced, the degree of reduction depending upon the amount of metal added. Cadmium and zinc diminish CK life to a smaller extent than do cobalt, nickel, and copper. However, cadmium seriously decreases AC protection.

A sample of hexamine whetlerite containing cadmium and emitting a strong odor of formaldehyde was sprayed with sodium hydroxide until the odor was no longer that of formaldehyde but became that of ammonia. It is possible to liberate either of the hydrolytic products of hexamine from the absorbent by controlling the conditions in this way. Probably it would require a very delicate balance of *p*H and metal ion concentration to produce an absorbent having satisfactory canister performance.

X-ray Studies of Hexamine Impregnations

X-ray studies of these materials have revealed that hexamine is precipitated on the charcoal in a different crystalline form from that obtained by the evaporation of a water solution. When standard Type A whetlerite is treated with hexamine in a solution containing cobalt or nickel nitrate, an X-ray pattern characteristic of the copper nitrate hexamine complex appears. The standard pattern for this material was made from a precipitate formed by the addition of copper nitrate to a water solution of hexamine. When hexamine is added in the presence of cadmium nitrate, an altogether different reaction occurs, the products of which have not yet been identified. Some of the copper of the whetlerite apparently is reduced, but it is not dissolved and reprecipitated as a hexamine complex, as is the case when hexamine is applied to Type A whetlerite in the presence of cobalt and nickel nitrates.

CK Surveillance of Hexamine Impregnated Adsorbents

The CK protection of a base charcoal impregnated with hexamine was better than that of a Type A whetlerite similarly treated. After aging in sealed containers at 80% RH and 45 C for 243 days, the CK life of the hexamine impregnated charcoal was better than that of the hexamine impregnated whetlerite. Typical results are shown in Table 6.

Table 6. CK surveillance of hexamine impregnated adsorbents. Tube test conditions: 5-cm bed depth, 500 cm³ per cm² per min flow rate, conc. of CK = 2.5 mg per l.

Adsorbent	CK 80–80 tube lives, min Initial	after 243 days
CWSC–11 charcoal + 2% hexamine + 5% NaOH	49	41
CWSC–11 Type A whetlerite + 2% hexamine + 5% NaOH	33	22
CWSC–11 Type A whetlerite + 1% hexamine + 5% NaOH	28	11
CWSC–11 charcoal + 4% hexamine	70	8
CWSC–11 Type A whetlerite + 4% hexamine	90	3

Hexamine impregnation of charcoal or Type A whetlerite produces an adsorbent with fairly good CK protection but the difficulties encountered in overcoming ammonia evolution and deterioration on aging render it of little value. In case of extreme emergency it might prove to be useful.

4.2.3 Thiocyanate Impregnations

Sodium thiocyanate impregnated whetlerite (or Type E 6 impregnated charcoal as it is officially designated) was developed in an effort to produce an adsorbent superior to hexamine impregnated whetlerite.

In 1926, during a search for new impregnants, it was discovered that the CK protection of charcoal could be improved markedly by impregnating the charcoal with ammonium thiocyanate, alone or in combination with sodium carbonate.[99] In 1933 and 1934 this impregnation was further improved [99] by using a solution of sodium thiocyanate together with sodium hydroxide to impregnate Type A whetlerite. The adsorbent had improved protection for both CK and AC. Designated as Type E 6 impregnated charcoal, it was also found to be more stable than Type A whetlerite impregnated with hexamine and sodium hydroxide.

Application of Thiocyanate to Type A Whetlerite

The material as originally specified was produced by soaking Type A whetlerite in a solution containing 5% sodium hydroxide and 0.5% sodium thiocyanate, draining, and drying to less than 5% moisture in any convenient type of drier at any temperature up to 150 C.

[b] Formaldehyde is formed in decomposition of the hexamine.

Adsorbents prepared by the above method and used as canister fillings evolved an odor of ammonia strong enough to be objectionable to sensitive observers. During storage, these canisters continued to evolve ammonia, and a decrease in CK and AC life was noted. This decrease was much greater during tropical storage than during normal storage at Edgewood Arsenal.

A program was initiated [23] to provide a process of manufacture which would yield a product substantially free from the odor of ammonia. The work proved that insufficient drying was mainly responsible for the ammonia odor of the whetlerite. An adsorbent free from this odor was produced by oven-drying the impregnated material in trays at 80 to 100 C for 20 hr with free circulation of air around the trays. This drying procedure was sufficient to reduce the moisture content to 1.0% or less and to remove the excess ammonia present in the impregnated charcoal. For this study, the same type of secondary impregnating solution was used as had been used previously and techniques of impregnation and drainage were similar. The moisture content had to be reduced to 1% before drying was considered complete.

A study of the preparation [26] of E 6 impregnated charcoal showed that the amount of sodium hydroxide used in the secondary impregnation could be reduced from 5% to 1% and still yield a good product.

Effect of Storage on Thiocyanate Impregnated Type A Whetlerite

The E 6 impregnated charcoal showed a tendency to adsorb a slightly larger quantity of moisture than Type D fillings under conditions of tropical storage. In tropical storage E 6 impregnated charcoal slowly lost adsorptive capacity for AC and CK. However, the decrease is not appreciably different from that of the Type D filling then in use. These effects are compared in Table 7.

Table 7. Changes in absorptive capacity after two years storage in Panama and storage in simulated tropical conditions at Edgewood Arsenal.

Test gas	E 6 impregnated charcoal	Type D filling
PS	47% decrease	36% decrease
CG	79% increase	29% increase
SA	19% decrease	2% decrease
CK	75% decrease	69% decrease
AC	22% increase	17% increase
Moisture content after 2 years surveillance	15.0 to 17.6%	11.0 to 14.1%
Water content before surveillance	1.5%	3.4%

The development of E 6 impregnated charcoal was at this stage in 1940, when further work during the period 1940 to 1945 was done in an attempt to prepare samples in which deterioration of the AC and CK protection in tropical storage would be small.

Decrease in the CK life of an E 6 impregnated charcoal is accompanied by a decrease in the thiocyanate content and an equivalent increase of the sulfate content of the adsorbent. Investigation showed that the thiocyanate of the impregnated charcoal is present in two forms, one of which was easily extractable with hot water and the other not.[24] The extractable form is apparently the part of the thiocyanate that is oxidized during storage. Samples stored at elevated temperatures in a vacuum also show this effect. It appears that atmospheric oxygen is not essential for this reaction. Adsorbed or chemisorbed oxygen is probably responsible for that oxidation of thiocyanate which occurs *in vacuo*.

The CK life falls off as the extractable thiocyanate is oxidized to sulfate, until the life reaches a constant level about twice as great as the CK life of untreated Type A whetlerite. This *residual* life has been attributed to the unextractable thiocyanate. The data in Table 8 show this effect.

Table 8. Correlation of CK life with extractable thiocyanate content of E 6 impregnated charcoal heated at 100 to 110 C in air. Tube test conditions: 5-cm layer, 500 cm³ per cm² per min flow rate, 50% RH, 25 C. Adsorbent dry when tested.

Heating time, hr	CK life min	Extractable S as SO_4^{--}: extractable S as SCN^-	% Unextractable SCN
0	71	..	..
2	69	0.089	32
4½	56	0.46	34
8	52	0.93	34
24	48	3.74	32
67	46	>20	..
Type A whetlerite	27	..	..

The CK life approaches a constant value as the extractable thiocyanate approaches complete oxidation.

Application of Thiocyanate to Type A Whetlerite

Type AS whetlerite was impregnated with thiocyanate. Optimum drying conditions appeared to be 6 hr at 100 C, oven-drying. The initial SA and AC lives were slightly lower than those of Types A or

AS whetlerites but not seriously so. The use of sodium hydroxide was found to decrease the amount of unextractable thiocyanate. The rate of oxidation of extractable thiocyanate to sulfate was not affected by the presence of sodium hydroxide. In addition, it was found that the 80-80 CK protection was superior both initially and after aging for those samples with the lower sodium hydroxide contents.

E 6 impregnated charcoals produced by the above method have approximately as good canister protection for SA, AC, and CG as the Type A whetlerite. CK protection is satisfactory but not outstanding under 80-80 conditions. Silver nitrate sprayed on E 6 impregnated charcoal increases SA protection but decreases CK protection.

Using a radioactive tracer technique,[25] some research was done to determine the solubility of silver thiocyanate in whetlerizing solutions and to determine the adsorption of Ag^+ and SCN^- from whetlerizing solution. No precipitation of AgSCN takes place in a whetlerizing solution containing 0.1% of AgSCN. The Ag^+ and SCN^- are adsorbed completely and fairly rapidly by charcoal.

Since the development of the ASC process the study of both hexamine and thiocyanate impregnations has ceased. Thiocyanate appears to be more useful than the hexamine in whetlerite impregnation. Full manufacturing directives can be quickly compiled from data available.

4.3 GENERAL STUDIES OF CHARCOAL IMPREGNATION

4.3.1 Introduction

It has been known for many years that the adsorptive and catalytic properties of charcoals are dependent upon the nature of the pores in the charcoal and upon the chemical materials other than carbon which are present in the charcoal. Each operation used in the preparation of activated charcoal (for example, carbonization and activation) has an effect on the nature of the pores. The raw material used determines the materials other than carbon which may be found in activated charcoal. The impurities may be altered by impregnation, thus increasing the kind and amounts of chemical materials present, or by leaching, to reduce the kinds and amounts. Ordinarily impregnation is used to add to the charcoal a material which it does not contain initially and which promotes the adsorption of a specific toxic agent.

4.3.2 Catalytic Reactions and Types of Catalysts

Impregnants either react directly with the gas being absorbed or act as catalysts for reactions of the gas with oxygen, water, and so forth.

Although not all of the mechanisms for the absorption of toxic gases by gas mask charcoals have been proved, the reactions that are most likely to occur after physical adsorption are oxidation, decomposition, hydration, hydrolysis, and perhaps reduction. In many cases, more than one reaction may occur. Various catalytic reactions and the catalysts best suited to them are listed in Table 9.[28] This is a generalized table and has been built up from data on many different catalyst carriers under various conditions of use. The elements listed are used in many different forms, for example, pure metal, alloy, oxide, halide, molybdates, and phosphate.

TABLE 9. Catalysts frequently used (in order of efficiency).

Periodic group	Oxidation catalysts
VIII	Pt, Rb, Ir, Ni, Fe, Co
V	V, Nb, Ta, Bi
VI	W, Cr, Mo, U
VII	Mn
I	Cu, Li, D, Na, Ag
IV	Si, Th, Ph, Sn
II	Zn, Hg, Cd
	Decomposition catalysts
VIII	Fe, Ni, Pt, Pd, Os, Rh, Ir
I	Cu, Au, Ag, Na
II	Zn, Ca, Mg
III	Al
IV	Ti, Th, Sn, Zr
VI	Mo, Cr, W, U
	Hydration catalysts
III	Al
IV	Th, Ti, Ce, Si
II	Zn, Cd, Hg, Ca, Mg
I	Ag, Au, Cu
VI	Mo, W, Cr
VIII	Fe, Co, Ni
	Reduction catalysts
VIII	Ni, Fe, Co, Pd, Pt
II	Mg, Zn, Hg, Cd
I	Cu, Ag, Au
VI	Mo, Cr, W
VII	Mn

4.3.3 Charcoal as a Catalyst Carrier

Charcoal has been used as a carrier for many types of catalysts and in many types of reactions. A few of these are listed below:

1. *Synthetic reactions.* Example:

$$CH_3CH_2OH + CH_2 = CH_2 \xrightarrow{\text{catalyst}} C_4H_9OH.$$

Catalyst = bone charcoal containing $Fe_2O_3 + Al_2O_3$ promoted by Yb, La, or Zr.

$$CO + 3H_2 \xrightarrow{\text{catalyst}} CH_4 + H_2O$$

Catalyst = charcoal + Ni, Mn, and Al catalysts.

2. *Decomposition reactions.* Example:

$$H_2O_2 \xrightarrow{\text{catalyst}} H_2O + \tfrac{1}{2}O_2$$

Catalyst = MnO_2 on charcoal.

3. *Oxidation reactions.* Example:

$$O_2 + As_2O_3 \xrightarrow{\text{catalyst}} As_2O_5$$

Catalyst = CuO on activated charcoal. This reaction may have prompted the first use of copper oxide as an SA catalyst.

4. *Reduction reactions.* Example: Reduction of oxygen-containing organic compounds by H_2 over activated charcoal impregnated with Fe, Cr, or Ni.

5. *Hydration and dehydration.* Example: Hydration of ethylenic hydrocarbons to alcohols at 150 C over CuO + WO_3 on activated charcoal.

6. *Hydrogenation and dehydrogenation.* Example: Hydrogenation of fats over Ni on activated charcoal.

7. *Desulfurization.* Example: Desulfurization of crude oil by the use of colloidal molybdenum and copper chromite on activated charcoal.

8. *Chlorination, et cetera.* Example:

$$CO + Cl_2 \xrightarrow{\text{catalyst}} COCl_2$$

Catalyst = $SbCl_5$ on activated charcoal.

Thus a large variety of reactions are catalyzed by the use of the proper impregnant on activated charcoal.

In addition to being a good catalyst carrier, charcoal has the ability to adsorb gases which have relatively low vapor pressures at room temperature and which do not undergo catalytic reaction on impregnated charcoal. Therefore, protection can be expected for the large bulk of toxic materials not specifically considered in selecting the impregnant.

4.3.4 Possible Reactions in the Adsorption of Gases on Gas Mask Charcoal

Since activated charcoal contains a certain amount of adsorbed oxygen, probably present as chemisorbed oxygen, the following reduction reaction is a possibility in some cases:

(carbon + chemisorbed oxygen) + reducible substance + catalyst ⟶ CO_2 + reduced substance.

Carbon + chemisorbed oxygen may be considered as incipient carbon monoxide and should function as a good reducing agent in the presence of reducible material.

Copper oxide when dry, and a mixture of metallic silver and copper oxide when moist have proved to be good catalysts for SA absorption. The reaction involves oxidation of the SA and possibly decomposition prior to the oxidation. Both copper and silver act as oxidation and decomposition catalysts (see Table 9).

Hydration and hydrolysis are possible steps in the absorption of gases like CG and CK.

The impregnants that have proved to be most active toward CK and AC are copper combined with chromate, molybdate, or vanadate. The state of the impregnant after heat treatment is not known definitely, except that chromium must be present with copper in the hexavalent state to form an active catalyst for the destruction of CK. The copper molybdate and copper vanadate impregnants require a drastic heat treatment in preparation. The catalyst may be present as a compound of copper with molybdenum or vanadium, or as a mixture of copper oxide with molybdenum or vanadium oxide. X-ray analysis has not been helpful because the catalyst is either amorphous or, if crystalline, is too finely divided to produce a characteristic X-ray scattering pattern.

Since catalysts have such manifold functions, it is difficult to determine from the nature or kind of catalyst what reaction or reactions are occurring in the presence of the catalyst. Hence, it is difficult also to select a material that will catalyze the removal of a certain toxic gas. In the case of certain acid-base and similar reactions, catalysis is probably not involved and an impregnant can be selected on the basis of the properties of the toxic gas involved and the reaction desired.

As a consequence of the factors enumerated in the foregoing discussion, a large number of compounds were tried as charcoal impregnants and promoters for whetlerites, alone and in various combinations. In Table 10, all the materials tested as impregnants for charcoal and Type A whetlerite are listed with a comment indicating the quality of the absorbent compared to Type A whetlerite. No comment indicates negligible or nonexistent activity toward SA, AC, and CK when tested under conditions stated in the table. Tube tests were employed to evaluate all exploratory impregnations. Whenever promising activity was indicated, further work was carried out to test the value of the impregnant.

TABLE 10. Summary of exploratory impregnations.

Compound	Reference	Comment†
Part A.* Compounds† and mixtures used as impregnants for activated charcoal.		
Acetamide; CH_3CONH_2	109	
$AlCl_3$	33	
Ammonia catalyst	108	
Aniline; $C_6H_5NH_2$	107	
Na_3AsO_3	109	
$BaBr_2$	109	Slight CK activity, AR–80
Beeswax in C_6H_6	108	
Beeswax in CCl_4	108	
$Bi(NO_3)_3$	109	
Na BO_3	109	
NH_4 Br	33	
$NaBrO_3$	33	
HBr	33	
$CdCO_3$	108	
$CdCO_3 + H_2O_2$	108	
$Cd(NO_3)_2$	109	
$Cd(NO_3)_2 + Zn(NO_3)_2$	108	
$CdCl_2$, $CdBr_2$, CdI_2	33	
$(NH_4)_2CO_3$	109	
NH_4Cl	33	
KCl	108	
$KClO_3$	33, 108	
Chloramine T	33	
$K_2Cr_2O_7$	48, 50	
$K_2Cr_2O_7 + AgNO_3$	109	SA activity, 0–50 and 80–80
$[Ag(NH_3)_2]_2CrO_4$	109	SA activity, 0–50 and 80–80
$CuCr_2O_7$ (acid solution)	109	SA, 0–50; CK 0–50
CrO_3 in Type A solution	48	SA, 0–50; AC and CK 0–50; 80–80
$CrO_3 + AgNO_3$ in NH_4OH	48	SA, 0–50 and 80–80
Cu-Cr-Ni-Ag in NH_4OH and $(NH_4)_2CO_3$	48	Like ASC; good SA, AC, and CK 0–50, and 80–80
$(NH_4)_2Cr_2O_7$	108	
$Cr(NO_3)_3$	108	
$Cr(NH_3)_6(C_2H_3O_2)_3$	107	
Cu-Cr-Ag-Mo-W-V	40, 41	Like ASC
$CuCl_2$	33	
$CuCl_2 + 2KCl(K_2CuCl_4)$	33	
$Cu(ClO_4)_2$	33	
$Cu(OH)_2$	107	
$Cu(NH_3)_4(OH)_2$	107	
$Cu(NO_3)_2$	107, 108	
$Cu(NO_3)_2 + Mn(NO_3)_2$	109, 107	
$Cu(NO_3)_2 + NH_4OH + KI$	108	
CuCN in Cu^- (excess)	109	
$CuSO_4 + Fe_2(SO_4)_3 + (NH_4)_2SO_4$	108	
$Cu(C_2H_3O_2)_2$	107	
$Cu(NH_3)_4SO_4$	107	
Cu(ethylene diamine)$_4$ CO_3	107	
$Cu(C_2H_3O_2)_2 + Mn(C_2H_3O_2)_2 + NH_4C_2H_3O_2$	107	
Cu-Ag-Fe	109	SA and AC activity, 0–50 and 80–80
Cu-Ni-Zn whetlerite (carbonates)	109	Like Type A whetlerite
Fehling's solution + dextrose	107	
$CoCl_2$	33	
$Co(NO_3)_2$	77, 107	CO oxidation catalyst
$CoCO_3 + MnSO_4 + (NH_4)_2CO_3$	108	
$Co(NH_3)_4CO_3 + Cd(NH_3)_4CO_3$	108	
$CoCO_3 + NH_4OH + NH_4NO_3$	108	
$CoCO_3 + H_2O_2$	77, 108	CO odixation catalyst
$CoCO_3 + ZnCO_3$	108	
Co-Ni-Cd (ammine carbonates)	108	
Co-Ni-Cd-Zn (ammine carbonates)	108	
KCNO	107, 109	
Formamide	109	
$AuCl_3$	108	SA activity, 0–50 and 80–80
Hydrazine sulfate	109	
Hydroxylamine hydrochloride	109	
$H_2S + ZnCl_2$	109	
HIO_3	33, 107, 108	SA activity, 0–50 and 80–80
$NaIO_3$	33	
KIO_3	33, 108	
KI (Aq)	108	SA activity, 0–50, 80–80
$KI + I_2$ (Aq)	108	
$NH_4I + NaOH + NaSCN$	108	
$Pb(C_2H_3O_2)_2$	108, 109	
$LiNO_3$	108	
LiCl	108	
$Mg(C_2H_3O_2)_2 + Cu(NH_3)_4 \cdot (C_2H_3O_2)_2 + NH_4C_2H_3O_2$	107	
$MnSO_4 + CoCO_3 + (NH_4)_2CO_3$	108	
$KMnO_4$	108	
HgI_2 in C_2H_5OH	108	SA activity, 0–50 and 80–80
$HgI_2 + KI$	33, 108	SA activity, 0–50 and 80–80
$HgCl_2$	33	SA activity, 0–50 and 80–80
$HgBr_2 + NH_4Br$	33	SA activity, 0–50 and 80–80
$Ni(NH_3)_4CO_3$	107	Like Type A whetlerite
$NiCO_3$, saturated	108	
$NiNO_3 + H_2O_2$	108	
Ni-Cu-Ag-Cr	48	Like ASC whetlerite
KNO_2	109	CK activity, 0–50
$NaNO_2$	109	CK activity, 0–50
$Ag(NH_3)_2NO_2$	109	SA activity, 0–50 and 80–80
$HNO_3 + (NH_4)_2HPO_4$	109	
K_2OsBr_6 + Type A solution	3	
OsO_4 + Type A solution	3	
OsO_2 + Type A solution	3	
$(NH_4)_2S_2O_8$	109	
$(NH_4)_2S_2O_8$ + Type AS solution	109	
H_3PO_4	109	
$H_3PO_4 + FeCl_3$	109	
$Na_2HPO_4 + AgNO_3$	109	SA activity, 0–50, 80–80, CK, 0–50
$(NH_4)_2HPO_4 + HNO_3$	109	
$[Ag(NH_3)_2]_2HPO_4$	109	SA activity, 0–50 and 80–80
$AgNO_3$	3, 104, 108, 109	SA activity, 0–50, 80–80‡
Tannic acid	108	

TABLE 10 (*continued*)

Compound	Reference	Comment†	Compound	Reference	Comment§
Part A. (*continued*)					
Thioacetamide	109		$Ag(NH_3)_2VO_3$	109	SA activity, 0–50 and 80–80
Thiosemicarbazide	109	CK activity, 0–50			
$Na_2S_2O_3$; $AgNO_3$ Double impregnation	109	SA activity, 0–50 and 80–80	$Zn(NH_3)_4CO_3$	41, 108, 109	AC activity, 0–50
			$ZnCO_3$ + $CoCO_3$ in excess NH_4OH	108	
$NaSCN + NH_4I + NaOH$	108		Zn halides	33	
$NaSCN + I_2 + KI + NaOH$	108		$ZnCl_2 + H_2S$ (two step)	109	
$Ag(NH_3)_2$ SCN	109	SA activity, 0–50 and 80–80	$Zn(NO_3)_2$	109	
			$Zn(NO_3)_2 + AgNO_3$ (acid)	109	SA activity, 0–50 and 80–80
$SnCl_2$	108				
$SnCl_4$	33		$Zn(NH_3)_4SO_4$	109	
$[Ag(NH_3)_2]_2WO_4$	109	SA activity, 0–50 and 80–80	$ZnSO_4 + MnSO_4$	108	
			$Zn(NH_3)_4CO_3 + AgNO_3 + MoO_3$ in excess NH_4OH and $(NH_4)_2CO_3$	109	SA and AC activity, 0–50 and 80–80, CK activity, 0–50
NH_4VO_3 + Type AS solution	40, 109	Slight SA, AC, and CK activity, 0–50 and 80–80			
			Zn-Cd-Ni (ammoniacal carbonate solution)	108	
Part B. Compounds used in secondary impregnation of Type A whetlerites					
$Al(NO_3)_3$	3		$Mg(NO_3)_2 + NaOH$	3	
$Al(NO_3)_3 + NaOH$	3		$MnCO_3$	3	
$K_2H_2Sb_2O_7$	3		$Mn(NO_3)_2$	3	
$K_2H_2AsO_4 + NaOH$	3		$Hg(NO_3)_2$	3, 32	
$Ba(NO_3)_2$	3		MoO_3	3, 40, 41	
$Ba(NO_3)_2 + NaOH$	3		$MoO_3 + NaOH$	3	
$Bi(NO_3)_3 + NH_4NO_3$	3		$KMnO_4$	3	
$Bi(NO_3)_3 + 5\% HNO_3$	3		$NiCO_3 \cdot 2Ni(OH)_2$	3	
$K_2B_4O_7$	3		$Ni(NO_3)_2$	3	
$CdCO_3$	3		NH_4NO_3	3	Improves SA 0–50
$Cd(NO_3)_2$	3		OsO_4	3	
$Ca(NO_3)_2 + NH_4NO_3$	3		$AgNO_3$	3, 107	SA activity, 0–50 and 80–80
$Ca(NO_3)_2 + NaOH$	3				
$Ce(NO_3)_3$	3, 107		$Sr(NO_3)_2$	3	
$Ce(NO_3)_2 + NH_4NO_3$	3		$Sr(NO_3)_2 + NaOH$	3	
Cr_2O_3	3		NaSCN	3	SA-dry AC, CK 0–50, and 80–80
CrO_3	107				
$K_2Cr_2O_7 + NaOH$	3				
$CoCO_3$	3		$NaSnO_3$	3	
$Co(NO_3)_2$	3		$Th(NO_3)_4$	3	
$Cu(C_2H_3O_2)_2$	3		Na_2WO_4	3	
$AuCl_3$	3	SA activity, 0–50 and 80–80	$[Ag(NH_3)_2]_2WO_4$	109	SA 0–50, 80–80 CK 0–50
			$UO_2(NO_3)_2$	3	
$Fe(NO_3)_3$	3		$UO_2(NO_3)_2 + NH_4NO_3$	3	
$Pb(NO_3)_2$	3		NH_4VO_3	3	
$Pb(NO_3)_2 + NH_4NO_3$	3		$NH_4VO_3 + NH_4NO_3$	3	
$LiNO_3$	3				
$Mg(NO_3)_2$	3				

* Compounds are listed alphabetically with respect to element being investigated.
† No comment indicates poorer performance than is given by Type A whetlerite for SA, AC, and CK.
‡ Silver, in the form of any soluble salt or complex, produces an absorbent having SA activity 0–50 and 80–80.
§ No comment indicates poorer performance than is given by Type A whetlerite for SA. Not tested against AC or CK.

4.3.5 Charcoal Impregnants for the Absorption of CK

Clues to new CK absorbents resulted from an examination of the properties and reactions of CK. The work showed that: [29, 30]

1. CK has an oxidation potential similar to that of oxygen.

2. CK reacts with water and ammonia thus:

$$2CNCl + H_2O \longrightarrow 2CNO^- + 2H^+ + 2Cl^-$$
$$CNCl + NH_3 \longrightarrow NCNH_2 + H^+ + Cl^-$$

3. CK reacts readily with aniline, hexamethylenetetramine, and other amines.

4. Many substances containing sulfur are either oxidized by or form addition compounds with CK.

5. Polymerization of CK is catalyzed by many substances, such as Cl_2 and acids.

6. Phenol-formaldehyde resins impregnated with

tetraethylenepentamine had better CK lives than whetlerite.

7. CK reacts most readily with compounds containing nitrogen or sulfur with free electron pairs.

8. Hopcalite oxidizes CK at temperatures above 40 C.

9. The CK life of Type A whetlerite increases with increase in temperatures.

10. The CK life of unimpregnated activated charcoal decreases with increase in temperatures. This fact, together with item No. 9, shows that Type A whetlerite either reacts with or catalyzes a reaction of CK. The CK activity of Type A whetlerite is very low at room temperature.

11. CK containing radioactive carbon exhibited radioactivity in the effluent gases after absorption by Type A whetlerite.

12. Approximate free energy calculations show that for the reaction,

$$CNCl + 2H_2O = Cl^- + 4H^+ + CO_2 + \tfrac{1}{2}N_2 + 3e,\ E^\circ = -0.7 \text{ v.}$$

Therefore, oxidizing agents should be capable of oxidizing CK.

13. Mixtures of the oxides of Cu, Mn, Ni, V, and Mo in various combinations promoted the destruction of CK by activated charcoal.

The work on the use of metallic oxides led to the development of Types ASM, ASV, and ASC whetlerites. In early experiments, charcoal impregnated simultaneously with Cu, Mn, Ni, and V and heat-treated in a manner that was designed to convert the impregnants to oxides produced a good CK absorbent. Later work [31] showed that a Type A or AS solution in which vanadate, molybdate, tungstate, or chromate is dissolved, produces an excellent impregnant. Molybdenum, vanadium, or tungsten in combination with Type A solution as an impregnant requires a high-temperature heat treatment, (300 to 350 C) either in a vacuum or in the absence of atmospheric oxygen, to produce a satisfactory absorbent. On the contrary, chromium requires a low-temperature heat treatment (150 to 180 C) in a system that is swept out continuously by an air stream. The early experiments with molybdenum and vanadium did not produce an absorbent with satisfactory activity under humid conditions. This is now attributed to the type of activated charcoal employed, since present charcoals can be impregnated with these metals to produce an absorbent satisfactory both dry and humidified.

4.3.6 Charcoal Impregnants for the Absorption of SA

As indicated by research performed during World War I, silver has proved to be the best SA catalyst investigated.[4, 7–9, 101] American work has favored copper-silver combinations, while British practice has been to use a straight silver impregnant applied either by impregnation or spraying, keeping the charcoal humidified to maintain a satisfactory CG protection. Silver is easily incorporated with charcoal or whetlerite, is not subject to deterioration in storage, and only a small amount is required for optimum protection. In addition it does not interfere appreciably with the original desirable properties of the charcoal or whetlerite to which it is added.

The other effective SA reactants found were gold chloride, mercuric halides, potassium iodide or iodine in potassium iodide, ammonium iodide, and iodic acid. None of these had all the desirable properties exhibited by silver.

Impregnation by Mercury

A study was made of mercury,[32] halogen, and halogen salt impregnation. Mercury, as the bromide or chloride, can be added easily to whetlerites as a secondary impregnant and absorbents with good SA 80-80 protection are produced. However, the hazard of mercury poisoning from mercury vapor contained in the effluent air stream is too great to permit its use. The concentration of mercury in the effluent varied from 2.3 to 18.0×10^{-4} mg per l when air was passed through a 5-cm bed of the material contained in a tube with a 3 sq cm cross section at a rate of one l per min. In industry, the incidence of chronic mercury poisoning increases rapidly as the mercury content of the air rises above 2×10^{-4} mg per l.[35]

X-ray evidence indicates that the mercury is present in the charcoal entirely as metallic mercury.

Iodic Acid Impregnation

Iodic acid impregnated charcoal also exhibited good SA 80-80 activity. However, this material aged badly and had a very low SA 80-80 life after standing 30 days at room temperature. Iodic acid gave best results in a whetlerite containing copper and nickel in the mole ratio 9/1. NH_4I also showed some SA activity but was not tested after aging.

4.3.7 Impregnations from Solvents other than Water

Results of the use of nonaqueous solvents in impregnation [3] were uniformly unpromising. The samples were no better than Type A whetlerite (regarding SA protection) and usually were poorer. With liquid ammonia as a solvent, $Cu(NO_3)_2$, $Mg(NO_3)_2$, $Cu(CH_3CoO)_2$, $Pb(NO_3)_2$, $Zn(NO_3)_2$, $Hg(NO_3)_2$, $Co(NO_3)_2$, $Ni(NO_3)_2$ and $AgNO_3$ were used as impregnants. Only $AgNO_3$ yielded absorbents with good SA 80-80 lives.

Impregnations with copper nitrate in acetic acid and copper acetyl acetonate in chloroform gave fair SA 80-80 lives. Nickel carbonyl in benzene gave poor SA lives.

4.3.8 Impregnations from the Vapor Phase

Impregnations from the vapor phase were also unsuccessful. The following substances were added to charcoal in the presence of a hydrogen stream at 1 to 2 mm pressure: Te, Zn, Cd, As, Sb, Pb, Mg, Se, and $FeCl_3$ and these were put on *in vacuo*: $BiCl_3$, $Ni(CO)_4$,[106] nickel dimethylglyoxime, $SnCl_4$, OsO_4, Zn, Se, $HgCl_2$, copper acetyl acetonate, TeO_2, and $TiCl_4$. Only $HgCl_2$ and TeO_2 showed any SA activity. Both were much less effective than Type A whetlerite.

4.4 MOLYBDENUM AND VANADIUM IMPREGNATION

4.4.1 Introduction

The development of copper-silver-molybdenum [ASM] and copper-silver-vanadium [ASV] impregnations for activated charcoal was initiated by the discovery that the CK activity of charcoal could be increased by the use of certain metallic oxides as impregnants.[30] The first of this type of absorbent was prepared by impregnation of charcoal with solutions of the nitrates of metals such as Cu, Ni, and Mn, or Co, Ni, and Mn, together with small amounts of V, Cr, Hg, or Fe. The impregnated charcoal was heated at 400 C in a vacuum or in the absence of oxygen to decompose the nitrates to oxides.

Thus prepared, many metal oxides increase the absorption of CK by charcoal at elevated temperatures, but only those mentioned in the preceding paragraph are effective at 25 C. Further experiments showed that combinations of copper and molybdenum or copper and vanadium were the best impregnants (excepting ASC) and that the other metals were of questionable value for the removal of CK. The combination of copper and tungsten also has some CK activity when used as an impregnant, but has not been developed because it is decidedly inferior to copper and molybdenum or vanadium.

The use of nitrates as impregnants was avoided by the addition of molybdenum, vanadium, or tungsten to a Type AS solution as molybdate, vanadate, or tungsten, respectively. These materials are readily soluble in Type AS solution. The resulting impregnated charcoal retains its SA and CK protection as in the Type AS whetlerite but has in addition much superior CK and AC protection.

The original samples prepared by impregnation with nitrate solution of Cu, Ni, Mn, and V, or with Type AS solution containing molybdate had poor CK 80-80 protection. This has been since attributed to the type of charcoal used in the preparation of the samples. In certain zinc chloride activated, extruded charcoals of the type used in early experiments, the pore size distribution was unfavorable to CK protection. Any charcoal now available, which is otherwise acceptable as gas mask charcoal, can be made into a satisfactory Type ASM whetlerite (as the copper-silver-molybdenum impregnated charcoal is designated).

4.4.2 Effect of Temperature of Heat Treatment

The effect of variation in heat treatment temperature on tube test lives of Type ASM whetlerite is shown in Table 11A. This table brings out clearly the variations caused by the differences in the base charcoals used.

Vanadium impregnations resulted in poor absorbents under similar conditions of heat treatment. SA and AC lives were equivalent to those of the molybdenum-impregnated absorbents but the CK 80-80 lives were poorer. Tungsten absorbents were still less satisfactory than vanadium absorbents in this respect.

Zinc can be used in place of copper in the ASM impregnation. The CK lives of such absorbents are considerably lower, however, than those of the copper containing materials. Some typical results are shown in Table 11.

The use of zinc in place of copper results in rather

TABLE 11A. Performance of Cu-Ag-Mo* impregnated charcoals.

Charcoal	Heat treatment temp C	Tube test lives,† min					
		SA		AC		CK	
		AR–50	80–80	AR–50	80–80	AR–50	80–80
PCI–1	150	93	103	62	40	51	30
PCI–1	200	134	125	83	56	110	36
PCI–1	250	148	151	31	36	80	45
PCI–1	300	156	158	32	46	99	66
PCI–1	350	143	165	35	38	99	77
PCI–1	400	132	155	26	..	66	53
C–11	200	128	109	15	59	55	20
C–11	350	135	141	25	28	67	32
N–44	200	162	136	95	97	29	8
N–44	350	138	192	26	50	68	25
N–P5	200	134	85	34	34	68	8
N–P5	350	112	101	34	68	125	5

* Made from a solution containing 10% Cu, 15% NH_3, 10% CO_2, 1% $AgNO_3$, and 2.5% MoO_3.
† Layer depth=5 cm; flow rate 500 cm^3 per cm^2 per min. Concentration: SA = 4 mg per l; AC 3 mg per l; CK = 2.5 mg per l.

TABLE 11B. Zinc-silver-molybdenum impregnated charcoals.

Charcoal	Heat treatment temp C	Tube test lives,* min					
		SA		AC		CK	
		AR–50	80–80	AR–50	80–80	AR–50	80–80
PCI–P58	150	67	108	33	37	30	11
PCI–P58	250	85	105	..	43	30	5
PCI–P58	350	..	118	26	50	34	12
PCI–P58	450	77	125	..	45	29	5

* Tube Tests: 5 cm layer; Flow rate, 500 cm^3 per cm^2 per min. Concentration SA = 4 mg per l, AC = 3 mg per l, CK = 2.5 mg per l. Impregnating solution contained 5% Zn, 8% NH_3, 5% CO_2, 1.7% Mo, 0.6% Ag.

TABLE 12. Impregnation with mixed Cu, Ag, Mo, Cr, V, and W. (Tube test conditions as in Table 8.)

Charcoal	Heat treatment temp C	Tube test lives, min					
		SA		AC		CK	
		AR–50	80–80	AR–50	80–80	AR–50	80–80
PCI–P58	150	163	154	89	93	88	19
PCI–P58	400	187	219	50	60	135	8

poor performance on all tests, although the SA and AC lives are high enough to be useful. The CK life, however, is very short.

A mixed impregnation of activated charcoal was made with a solution containing 8% copper, 1% silver nitrate, and 0.6% each of molybdenum, chromium, vanadium, and tungsten in the form of molybdate, chromate, vanadate, and tungstate, respectively. The resulting absorbent when heated at 150 C had approximately the absorptive properties to be expected of a sample containing only chromium, silver nitrate, and copper. The CK 80-80 protection after heating at 400 C in a manner designed to activate the molybdenum, vanadium, and tungsten was negligible. The results are shown in Table 12.

It is evident that the SA 80-80 and CK AR-50 lives of the high-temperature sample are quite long. The mixture of oxides of Mo, Cr, V, and Ni acts as a good SA catalyst in the presence of silver and copper. However, this mixture is not so efficient a catalyst for CK as is an equivalent amount of molybdenum in the presence of copper. Vanadium and tungsten are very easily poisoned by moisture under some conditions of preparation.

4.4.3 Effect of Organic Acids

An investigation of the variables involved in the preparation of Type ASM whetlerite [42] showed that the addition of some organic acids to the impregnating solution resulted in a superior whetlerite. The series of organic acids used is shown in Table 13.

TABLE 13. Effect of the addition of organic acids to ASM impregnating solutions.*

Acid added	Tube test life, CK 80–80, min
None	44
Adipic	51
Fumaric	62
Maleic	70
l-Malic	51
Succinic	59
Tartaric	81
Citric	59
Formic	47
Glycolic	68
Phenylacetic	29
Salicylic	50
Sebacic	32

* Solution composition: 10% Cu, 15.8% NH_3, 10% CO_2, 2% Mo, and 5% organic acid. Heat treatment: 130 C for 45 min followed by 315 C for 3½ hours. No air present during high temperature treatment.

Almost every organic acid used resulted in an increased CK life. Tartaric acid was definitely superior to the others since it had approximately double the CK protection of ASM whetlerite without added acid. The solution containing tartaric acid is designated as ASMT impregnating solution and hereafter is referred to as such.

4.4.4 Optimum Concentrations of Components of ASMT Impregnating Solution

A study of ASMT impregnation revealed the following information:

1. CK life is practically independent of the copper concentration in the impregnating solution above 7.5 g of copper per 100 ml of solution. The data are inconclusive at lower copper concentrations. The optimum concentration is approximately 10% copper (12.5 g of copper per 100 ml of solution).

2. A concentration of approximately 5 g of molybdenum per 100 cc of solution (3.9%) is the optimum. Satisfactory CK results have been obtained between 3 and 6 g per 100 cc.

3. The optimum tartaric acid concentration is approximately 6.2% (8 g per 100 ml of solution) for a solution containing 3.9% of molybdenum. For lower molybdenum contents a lowered tartaric acid content is advisable. Increase in tartaric acid concentration is accompanied by a decrease in AC life.

4. The optimum ammonia content is approximately 10% (13.3 g of NH_3 per 100 ml of solution). A large excess of ammonia tends to decrease CK life.

5. The optimum carbon dioxide content is approximately 9%. For maximum CK and AC lives, the CO_2 content should be kept at a low level.

6. The optimum silver content is 0.18% (0.35 g of $AgNO_3$ per 100 ml of solution). Apparently quantities of this magnitude show no effect on CK or AC lives.

The optimum concentrations are summarized in Table 14.

TABLE 14. Optimum concentrations of constituents in ASMT impregnating solution.

Constituent	Added as	g of constituent per 100 ml of solution	% by weight of constituent
Mo	$(NH_4)_2MoO_4$	5.0	3.9 Mo
Cu	$CuCO_3 \cdot Cu(OH)_2$	12.5	9.7 Cu
Tartaric acid	Tartaric acid	8.0	6.2 T.A.
Ag	$AgNO_3$	0.35	0.2 Ag
CO_2	$(NH_4)_2CO_3 \cdot H_2O$	5.3	total CO_2 9.2 CO_2
	$CuCO_3 \cdot Cu(OH)_2$	5.7	
NH_3	NH_4OH	8.0	10.3 NH_3
	$(NH_4)_2CO_3 \cdot H_2O$	4.1	
	$(NH_4)_2MoO_4$	1.2	

Specific gravity = 1.29 g per ml at 25 C.

One liter of solution is prepared as follows:

$(NH_4)_2MoO_4$ (54% Mo)	93 g
$(NH_4)_2CO_3 \cdot H_2O$	136 g
NH_4OH, 28% solution	320 ml
$CuCO_3 \cdot Cu(OH)_2$ (55% Cu)	255 g
Tartaric acid	80 g
$AgNO_3$	3.5 g

Half the molybdate is dissolved in water, half in NH_4OH. Powdered $(NH_4)_2CO_3 \cdot H_2O$ is added to the aqueous molybdate solution and stirred until completely dissolved. The ammoniacal molybdate solution is then added and if any undissolved materials are present the stirring is continued until solution is complete. Then the basic copper carbonate is added and dissolved. This is followed by the tartaric acid and finally 35 ml of a 10% $AgNO_3$ solution. The resulting solution is diluted to 1 liter.

4.4.5 Laboratory Preparation of ASMT Whetlerite [42]

Impregnation and draining in the usual manner are satisfactory for ASMT. If oven-drying is employed, a two-step process is best. This consists of a preliminary tray-drying at 135 C for 6 hours, followed by a final drying in loosely stoppered Erlenmeyer flasks for a short time at 300 to 305 C. The

second drying can be discontinued as soon as the charcoal reaches 300 to 305 C. The materials should be removed from the oven and allowed to cool in the flasks without free exposure to air.

Wetting the charcoal between preliminary and final drying lowered the AC and CK lives appreciably. Passage of ammonia through the sample at this stage had no effect on the CK and AC lives. This indicates that the removal of excess water is desirable before high temperatures are reached, and removal of ammonia is not important for development of CK and AC protection. A study previously mentioned has shown that as a whetlerite dries at 150 degrees, ammonia, carbon dioxide, and water are removed in that order.

TABLE 15. Comparison of ASMT samples prepared in rotary and static oven driers.

Method of drying	Maximum temp C	Tube test lives, min CK 80–80	AC 0–50
Oven dried, 2 step	303	105	59
" " "	303	107	56
" " "	303	90	42
Rotary drier, 1 step	320	126	48
" " "	320	119	59
" " "	332	118	47

The procedure for drying ASMT whetlerites in rotary driers [43] differs in that the impregnated charcoal is heated as rapidly as possible to the maximum temperature and allowed to cool in the oven to a temperature low enough to preclude combustion when the sample is exposed to air. This procedure produces samples as good as and in some cases better than multistep procedures. Representative results of this type of drying procedure compared to oven-drying are shown in Table 15.

Rotary driers, when available, are to be preferred since samples can be produced faster and more conveniently, and also are of higher quality with respect to CK life.

The flow of various gases through the rotary drier while drying ASMT whetlerites had measurable effects. Results of the experiments are shown in Table 16.

Use of gas flow through the drier in general produced a sample with lower CK protection than samples dried with no gas flow. Water vapor was the only gas passed through the drier which produced a sample with approximately the same CK protection as no-flow samples. The type of gas used in the production of the whetlerite may be classified with respect to decreasing CK protection of the product as no flow, water vapor, nitrogen, carbon dioxide, carbon monoxide, and air. This order, after water vapor, is not conclusive. Absence of gas flow is clearly superior, with regard to the CK protection of the sample produced, to flow of any gas with the possible exception of steam.

On the other hand, AC protection is depressed to the greatest extent by materials such as CO and water vapor and is least affected by air flow. There may be a correlation between oxidizing power of the gas used in drying and the AC protection of the whetlerite. Water vapor and hot carbon would produce

TABLE 16. Effect of gas flow during drying on the quality of ASMT whetlerite.

Gas used	Linear flow rate cm/min	Max temp of whetlerite C	Time to reach 300 C min	Temp at which flow was stopped, C	Tube test lives, min CK 80–80	AC 0–50
Air	16	310	155	127	107	65
Air	16	309	33	130	89	57
Air	55	319	30	143	98	55
Air	3	300	38	Continuous	86	48
Air	3	334	34	Continuous	93	44
N_2	32	303	90	154	88	51
N_2	32	301	35	158	89	44
N_2	32	304	35	Continuous	95	36
CO_2	48	307	98	Continuous	83	36
CO_2	48	327	33	Continuous	95	..
CO*	16	310	45	310	80	35
CO*	16	321	98	Continuous	106	24
None	..	320	95	Continuous	126	48
None	..	320	50	Continuous	119	59
None	..	332	33	Continuous	118	47

* Preheated to 350 C.

SECRET

TABLE 17. Aging of ASC, ASM and ASMT, whetlerites, sealed and equilibrated.

Base charcoal	Type	Aging conditions		Tube test lives, min CK 80–80
		Temp C	Time	
PCI 1042	ASC	Freshly equilibrated		73
PCI 1042	ASC	85	13 hr	9
PCI 1042	ASC	60	2 days	11
PCI 1042	ASC	60	8 days	8
PCI 1042	ASC	25	16 days	40
PCI 1042	ASC	25	26 days	14
PCI 343	ASC	Freshly equilibrated		122
PCI 343	ASC	85	6 hr	11
PCI 343	ASC	60	1 day	70
PCI 343	ASC	60	2 days	38
PCI 343	ASC	60	4 days	14
PCI 343	ASC	60	8 days	..
PCI 343	ASM	Freshly equilibrated		71
PCI 343	ASM	80	1 day	39
PCI 343	ASM	60	2 days	55
PCI 343	ASM	60	4 days	58
PCI 343	ASM	60	12 days	39
PCI 343	ASMT	Freshly equilibrated		91
PCI 343	Tartaric acid added	85	2 days	78
PCI 343	ASMT	85	9 days	81
PCI 343	ASMT	60	7 days	84

carbon monoxide, thus explaining why carbon monoxide and water vapor have the same effect on AC protection. It appears that reducing conditions favor high CK protection and low AC protection, and oxidizing conditions favor the reverse. High temperatures favor high CK lives and low AC lives. The optimum temperature is 310 to 320 C. A compromise had to be made between CK life and AC life and a temperature was chosen to give satisfactory protection for both toxic agents.

4.4.6 Aging Characteristics of ASMT and ASC Whetlerites

ASMT whetlerite has excellent aging qualities when stored equilibrated in sealed containers. Under these conditions ASC whetlerite deteriorates very rapidly. On the other hand, ASMT whetlerites deteriorate in open containers as much as do ASC whetlerites. Both retain a satisfactory protection under these conditions for a relatively long time.

Comparisons of the aging rates of ASC and ASMT are found in Tables 17 and 18. From these data it is evident that ASMT is superior when stored moist in closed containers. The use of tartaric acid with ASM solution enhanced the aging properties of ASM whetlerite. This difference disappears, however, when the absorbents are stored in open trays at high relative humidity and high temperature.

Under the conditions of aging shown in Table 18, the CK lives of the materials are almost identical after 24 days of aging, although a higher initial life was characteristic of the ASMT materials. One ASMT material, prepared in an atmosphere of water vapor, retained its life at a high level all through the aging period. This effect may be worthy of more investigation.

It is probable that aging in contact with an excess of air more nearly approaches field conditions than sealed aging since diurnal temperature variation, body movement, and occasional wearing of the mask cause some fresh air to enter the canister periodically.

AC lives of ASMT are usually improved by equilibration at 80% RH. Cyanogen is never observed in the effluent gases when AC is absorbed by ASMT as it is when a Type A or AS whetlerite is used. Both AC and CK are irreversibly absorbed by ASMT whetlerite indicating a chemical change following adsorption rather than physical absorption as the major factor in the functioning of the whetlerite.

TABLE 18. Comparison of ASC and ASMT aged in open trays in air at 110 F and 80 per cent RH.

Base charcoal	Type of whetlerite	Original life	CK 80–80 Tube test lives	
			Aged 19 days	Aged 24 days
PCI 1042	ASC	101	55	42
BC 3	ASC	36	28	29
PCI 1042	ASC	70	68	64
PCI 1042	ASC	88	69	69
PCI 343	ASMT	93	44	64
PCI 343	ASMT	101	54	68
PCI 343	ASMT	114	96	62
PCI 343	ASMT	131	143	125

4.4.7 Pilot Plant Experiments

A pilot scale preparation of ASMT whetlerite was attempted in the pilot plant at Northwestern University,[44] which had been used in the development of the plant scale production of ASC whetlerite.

The purpose of the investigation was to determine whether existing plant equipment could be used in the production of ASMT whetlerite without major changes in design. The rotary drier had been designed for the preparation of material requiring high air flow and relatively low temperature (150 C). ASMT production required rapid heating to relatively high temperatures and no air flow. In fact a leak-tight system is desirable. The ASMT produced was in-

ferior by far to laboratory produced samples. A comparison of the ASMT and ASC whetlerites produced in the pilot plant is shown in Table 19.

TABLE 19. A comparison of ASC and ASMT whetlerites produced in the Northwestern University whetlerization pilot plant.

Base charcoal	M10 canister lives,* CK 80–80	
	ASMT	ASC
PCI-Drum Q	11	30–35
PCI-Drum Q	20	30–35
PCI-Drum NB	11	30–35
PCI-Drum NM	23	30–35
PCI-Drum NN	17	22
National Drum NI	3	0–3
National Drum X	0	0–3

* Canister tests in M10 ⅝-inch canister: CK concentration, 4 mg per l, SIP indicator. Flow rate 50 lpm, breather machine.

In general, the ASMT whetlerites produced had an initial CK life about two-thirds as great as those obtained by ASC impregnation of the same base charcoal. Dry AC tube lives of the ASMT whetlerites were about three-quarters as great as the corresponding ASC materials, and seemed to be relatively independent of drying conditions. There seemed to be no correlation between CK and AC lives.

The quality of the ASMT was markedly affected by the retention time in the drier. Best results were obtained by a very rapid passage through the drier. The optimum charge temperature was approximately 500 F (260 C), although this was not a critical factor.

In order to obtain a satisfactory product and to facilitate temperature control, it was necessary to exclude rigorously all air from the drier. Leakage occurred in some runs causing a sudden rapid rise in temperature. This was attributed to ignition of the charge although there was little evidence of burning.

Unless predrying or backfeeding was employed, the wet feed stock caused caking near the inlet and made cleaning necessary after about 40 hours of operation. This situation was not encountered frequently in the processing of ASC whetlerite. Mixing previously dried product with the feed stock (referred to as backfeeding) was a satisfactory method for the prevention of caking. It is not clear whether such practice is harmful to the quality of the product. Backfeeding is practiced in some ASC whetlerization plants and apparently has no harmful effect if a fairly high quality material is used as backfeed. As far as is known the result is equivalent to a mechanical mixing of the backfeed and product after processing.

For reasons not clearly defined at present, some National Carbon Company zinc chloride activated charcoals which were suitable for ASC production proved to be unsuited for conversion to ASMT whetlerites. A very inferior product resulted from all such attempts in the pilot drier.

It was concluded that the adaptation of existing plants to ASMT production would involve a major change in equipment in order to exclude air and allow very rapid heating and short retention time. These changes were considered not expedient.

4.4.8 Simultaneous Impregnation with Molybdenum and Chromium

In an effort to combine the advantages of ASC and ASM whetlerites in one absorbent, a study of ASCM impregnation was made.[45] It was found to offer no advantages over ASC or ASMT, since preparation at high temperature resulted in a material having the properties of ASMT whetlerite, and preparation at low temperatures resulted in an absorbent similar to ASC whetlerite. A secondary impregnation of ASMT whetlerite with $(NH_4)_2CrO_4$ and heat treating at 150 C produced a material with very large initial CK 80-80 protection, but it had the same aging properties as ASC. Since the preparative procedure was more complicated than that of ASC, it was not considered worthy of further investigation. The study was abandoned when it became clear that the mixed impregnation had no outstanding advantages.

4.4.9 Impregnations with Vanadium

The development of ASV and ASVT whetlerites was similar to that of ASMT whetlerite. The efficacy of vanadium in combination with copper as a charcoal impregnant capable of enhancing the CK absorption of the charcoal was discovered at the same time that the properties of molybdenum as an impregnant were discovered. The preparation of the vanadium absorbent [46] closely resembles that of the molybdenum absorbent.

4.4.10 Impregnating Solution

The initial CK 80-80 protection of copper-silver-vanadium impregnated charcoal (or Type ASV whetlerite, as it is designated) is greatly increased by addition of tartaric acid to the impregnating solution, just as in the case of the ASM whetlerite. The optimum concentrations of the components of the impregnating solution are found in Table 20.

TABLE 20. Optimum concentrations of components of the impregnating solution.

Compound	Amount of compound for 1 liter	Grams of constituent per 100 ml of solution	% of constituent by weight
NH_4VO_3	82 g	3.6 V	2.9 V
$CuCO_3 \cdot Cu(OH)_2$	225 g	12.5 Cu	10.0 Cu
NH_4OH (28% aqueous solution)	320 ml	13.3 NH_3	10.6 NH_3
$(NH_4)_2CO_3 \cdot H_2O$	136 g	11.0 CO_2	8.8 CO_2
Tartaric acid	80 g	8.0 T.A.	6.4 T.A.
$AgNO_3$	3.5 g	2.2 Ag	0.18 Ag

The solution is prepared by mixing the vanadate and basic copper carbonate to a paste with a small amount of water. Ammonium hydroxide is then added to dissolve the paste. To this is added ammonium carbonate, 35 ml of a 10% solution of silver nitrate, and finally the tartaric acid (slowly, to avoid loss of CO_2). The solution is diluted to 1 liter with water.

4.4.11 Preparation of ASVT Whetlerite

Impregnation and draining are carried out in the usual manner. The drying procedure requires a laboratory rotary drier [43] which can be efficiently sealed to prevent air leakage into the drum. A small exit port is necessary to allow water vapor, ammonia, and carbon dioxide to escape during drying without allowing appreciable back diffusion of air.

The optimum drying temperature is 300 to 350 C, although a satisfactory product can be made at a temperature as low as 225 C. The rate of heating is not a critical factor. Good products can be obtained by either slow or rapid heating rates. Exposure of the whetlerite to small amounts of air during drying seriously decreases CK protection. The sample also must be cooled in the absence of air. Use of a stream of N_2 during cooling produces excellent results.

Both CK and AC protection pass through a maximum as tartaric acid content of the ASVT impregnating solution increases. The optimum concentration is approximately 6% tartaric acid. In contrast to ASMT whetlerite, this is independent of vanadium content.

A few representative tube test results are given in Table 21.

AC protection is considerably increased by moisture equilibration. Cyanogen never occurs in the effluent gas stream from this type of absorbent when AC is absorbed. Both CK and AC are adsorbed irreversibly and cannot be desorbed.

The lives shown above are initial lives and are rather high compared to ASMT results. The material

TABLE 21. Performance of ASVT whetlerites.

Treatment of sample	Tube test lives*	
	CK 80–80	AC 0–50
Rotary drier heated to 250 C	138	68
Rotary drier heated 1 hr at 250 C	145	58
Rotary drier heated to 300 C	148	54
Rotary drier heated 1 hr at 300 C	157	47
Rotary drier heated rapidly to 300 C	152	52
Rotary drier heated to 300 C	159	40
Oven dried 3½ hr in flask at 300 C	100	42

* 5-cm bed depth; Flow rate 500 cm per min; 2.5 mg CK per liter.

is approximately as stable as ASMT when stored equilibrated in sealed containers. It is less stable, however, when stored in open or semi-open containers such as might be encountered in a canister under field conditions. Some aging results are shown in Table 22.

TABLE 22. Aging of equilibrated Type ASVT whetlerite under various conditions.

Aging conditions			Tube test life
Temp C	Time, days	Container	CK 80–80
..	none	.....	139
85	2	Stoppered bottle	68
60	10	Stoppered bottle	56
60	30	Stoppered bottle	53
50	10	Stoppered bottle	62
50	30	Stoppered bottle	60
50	10	Open basket	31
50	30	Open basket	8
50	10	Open bottle	38
50	30	Open bottle	11
25	80	Stoppered bottle	100

This material is definitely less stable than Type ASMT or Type ASC whetlerites under conditions of open storage.

In general it has been observed that when Type ASVT whetlerite is stored in tightly stoppered bottles the aging is slow or virtually ceases after the first rapid decrease in CK life. The amount of initial decrease is practically independent of the temperature of storage. This can be explained, if the aging is the

result of oxidation, by the removal of all oxygen from the container. The increased aging in open containers is in agreement with this hypothesis.[46] With open containers, and with bottles fitted with Bunsen valves (to allow the internal pressure to remain at atmospheric pressure) ASVT whetlerites aged to a CK protection equivalent to that of base charcoal in from 10 to 30 days at 50 C.

Two mechanisms have been suggested for this aging: (1) oxidation of V^{+4} to V^{+5}; (2) oxidation of Cu_2O to CuO. No definite analytical data to support these mechanisms is available.

AC protection of Type ASVT whetlerite is satisfactory when the material is equilibrated but is poor when dry. The AC tube life when tested under 80-80 conditions is 80 to 95 min. No cyanogen can be detected in the effluent. Samples exposed to air at high temperatures (thereby almost completely destroying CK protection) gave AC tube test lives of 140 min when tested at 0-50 conditions. This suggests an oxidation mechanism operative in both equilibration and high-temperature air treatment which results in improved AC protection. A life of 140 min is longer than can be accounted for by any known chemical reaction with the impregnant and is probably due to a catalyzed reaction. Perhaps a copper-vanadium compound in the oxidized state is an efficient catalyst for the oxidation of AC. In this connection it is interesting to note that a sample prepared with both molybdenum and vanadium in the impregnating solution (Type ASMV whetlerite) ran 250 min before a trace of AC was transmitted. Cyanogen was detected after 160 min. However, the sample was not an outstanding CK absorbent.

Because of the rapid deterioration of Type ASVT whetlerite when stored in unsealed containers, it was considered an unsuitable filling for present canisters.

In the foregoing discussion no comment has been made concerning the general absorption characteristics of ASMT and ASVT for toxic agents other than CK and AC. In general, the materials absorb CG, SA, PS, H, and other typical toxic agents satisfactorily. CO is not absorbed.

4.5 DEVELOPMENT OF COPPER–SILVER–CHROMIUM IMPREGNANTS

4.5.1 Introduction

The superior properties of mixtures of copper, silver, and chromium as charcoal impregnants for the absorption of CK and AC were first recognized in 1942.[48] Impregnation of charcoal with chromium, and in one case with copper and chromium, had been attempted earlier, but through improper preparation or lack of testing facilities for CK and AC the advantages of this impregnant were not appreciated.

Activated charcoal impregnated with copper and either molybdenum or vanadium, when properly heat-treated, has the ability to adsorb from an air stream, and destroy, rather large quantities of CK and AC. In turn, molybdenum acts more efficiently than tungsten in the removal of CK and AC. From a comparison of the relative positions in the periodic table of tungsten, molybdenum, and chromium with the abilities of these impregnants to affect the absorption of CK, it is indicated that chromium would be more useful than either molybdenum or tungsten. Broadly speaking, such was found to be the case. Although heat treatment conditions required for the preparation of copper-chromium impregnated charcoals are quite different from those used in preparing copper-molybdenum or copper-tungsten impregnated charcoals, the CK-destroying properties are equal to or better than the best molybdenum-containing absorbents.

The first samples of ASC whetlerite were prepared in the laboratory by impregnating activated charcoal with a Type AS solution to which had been added 1.5% chromium in the form of $(NH_4)_2Cr_2O_7$. These products were dried in the same manner as Type AS whetlerites (in wire screen trays in a convection-type oven at 150 C for three hr). The resulting absorbents had good AC and CK lives, superior to those of any previous samples, but inferior to the present Type ASC whetlerites. Later work showed that practically any chromate salt could be used. The material chosen as most convenient for both laboratory and plant operations was chromic anhydride, CrO_3. The material is very easily soluble in the impregnating solutions used, readily available, and relatively cheap.

4.5.2 Optimum Concentrations of Constituents of Type ASC Whetlerizing Solution. Copper and Chromium Concentrations

Experimental results on the variation of AC and CK lives with variation in the copper and chromium concentrations of the whetlerizing solution are given in Figures 5 through 9. The work was evaluated at different times by different kinds of tube and canister tests. Early work was evaluated entirely by means of tube tests which cannot be correlated quantitatively

with canister tests. However, the results of both kinds of tests indicate approximately the same optimum concentrations. The best method of expressing test results, which was perfected at a later date, is by means of layer depth studies leading to an evaluation of N_0 and λ_c. Knowing these values permits the estimate of the service life of the absorbent in any particular canister (see Chapter 8).

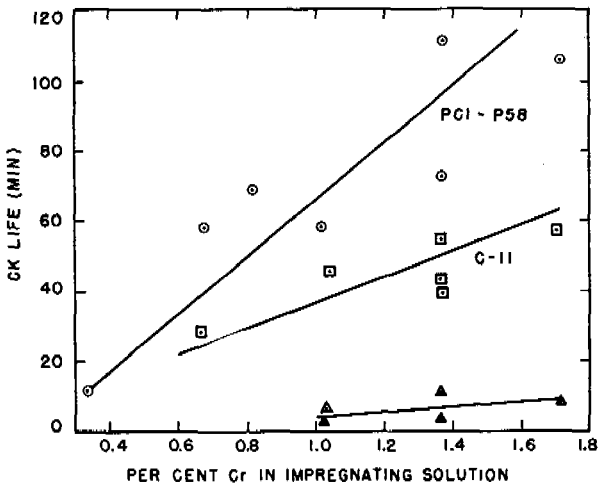


FIGURE 5. Effect of variation in Cr concentration (of whetlerizing solutions) on the AC and CK lives of canisters.

Figure 5 shows the variation of CK 80-80 life with the chromium content of the whetlerizing solution for three different charcoals, using a constant copper and silver content (10% and 0.1% respectively). These charcoals represent approximately the range available, from poorest to best. The three charcoals show an increase in CK life with chromium content, the rate of increase depending upon the charcoal. Curves might flatten out at high chromium content, but they were plotted as straight lines over the entire range studied since the experimental error is great enough to hide any leveling off at the higher concentrations. The reason for this great difference among charcoals is not fully understood, although recent work indicates that pore size distribution in the charcoal is the controlling factor.[49] Figure 6 shows some M10A1 canister results concerning the dependence of CK and AC lives upon hexavalent chromium content of the whetlerite at two different copper contents. The canister results in Figure 6 indicate the same general trend for CK as the tube test results in Figure 5. The AC life also is dependent upon the chromium content of the whetlerite.[50] In the 5-cm tube test (thick beds), the effect is very small or nonexistent, whereas in canister tests (thin beds) the effect is important, as is clearly shown in Figure 6. This indicates that the activity toward AC is being affected by change in chromium content to a greater extent than the capacity for AC absorption.

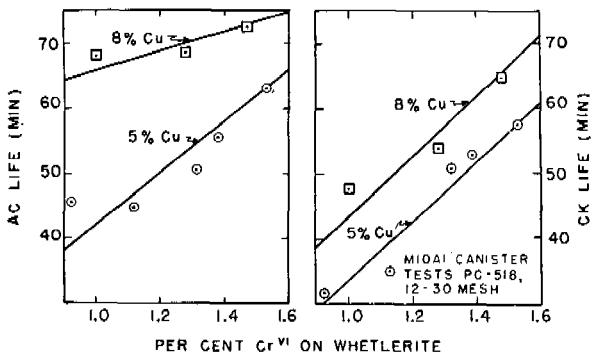


FIGURE 6. Effect of hexavalent Cr and copper content of whetlerite on CK and AC lives. Gas lives are for M10A1 canisters, loaded PCC whetlerite.

The variation of CK life with the copper content of the ASC solution at constant chromium content is shown in Figure 7. The data indicate a leveling off of the curve at about 8% copper. The effect of copper

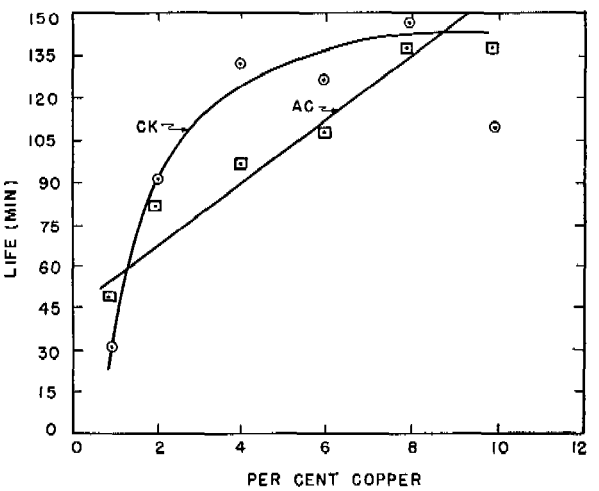


FIGURE 7. Effect on CK life of ASC solution with constant Cr and varying Cu content.

is also shown in Figure 6. There, in the case of AC, the curve representing a copper concentration of 8% has a much smaller slope than that representing 5% copper, thus showing a much greater dependence of AC protection on chromium content at low copper concentration than at high. The CK curves, on the other hand, show the same slope at both copper

levels. However, for both cases, at a given chromium concentration, protection is at a higher level for the higher copper concentration.

Figures 8 and 9 present similar data [51] for the variation of N_0 and λ_c for CK 80-80 with chromium and copper concentrations. Here the data lead to much the same conclusions as the tube and canister tests, except that here the question of thick and thin beds does not enter into the interpretation of the data and choice of optimum conditions.

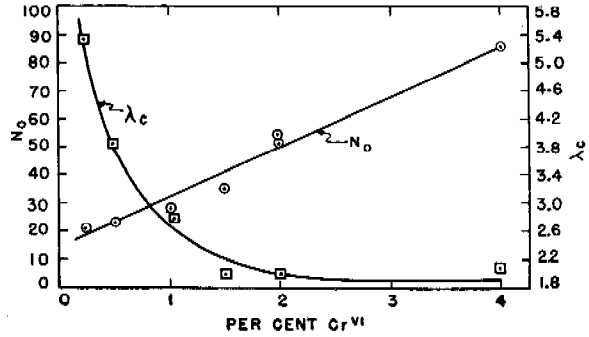


FIGURE 8. Effect of Cr^{VI} content upon critical depth, λ_c, and capacity, N_0, of impregnated charcoal, Type ASC.

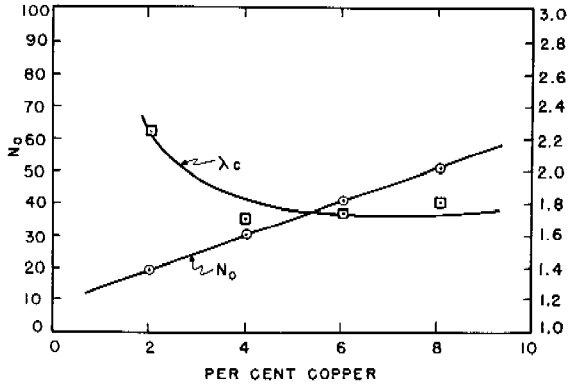


FIGURE 9. Effect of Cu content upon critical depth, λ_c, and capacity, N_0, of impregnated charcoal, Type ASC.

The solution composition chosen as optimum contains 8% copper, 2% hexavalent chromium, and 0.2% silver. (The silver concentration had no effect on the CK and AC lives in this low range and was retained on the basis of the data on Type AS whetlerite. Two per cent silver was sufficient in every case with the charcoals in general use.) The 8% copper concentration, which was chosen to provide AC protection at the desired level, limited the chromium concentration to 2%, because with this amount of copper present at higher chromium concentrations, a heavy crystalline precipitate of $Cu(NH_4)_4CrO_4$ forms at laboratory temperatures (25 C). The heats of solution and reaction warm the solution during preparation resulting in considerably higher solubility of the chromate. The precipitate forms when the concentrated solution is allowed to cool to room temperature. Use of 5% copper allows the inclusion of more chromium, but results in a lower level of protection at any given chromium concentration for both CK and AC, as shown in Figure 6. It is feasible to use higher chromium concentrations at 8% copper if the solution is heated. Similarly the normal ASC solution containing 8% copper and 2% chromium will produce a precipitate if allowed to cool much below room temperature. From a practical point of view the advantage (in increased AC and CK lives) of using more than 2% chromium is more than offset by the trouble encountered due to deposition of solids in the equipment.

Ammonia and Carbon Dioxide Concentration

The ammonia and carbon dioxide concentrations are fixed at that level which keeps the copper in stable solution as $Cu(NH_4)_4CO_3$ and $Cu(NH_4)_4CrO_4$. Variations in the carbon dioxide and ammonia concentrations do not affect the properties of the final whetlerite as long as they do not fall low enough to permit formation of solid basic copper carbonate, chromate (or possibly hydroxide). The solutions have been found to be satisfactory when the concentrations of copper, ammonia, and carbon dioxide are approximately in the ratios of 1:1.5:1. Slight variations in this ratio have no apparent effect.

The commonly used ASC solutions are listed below.

Solution	Symbol	%Cu	%NH_3	%CO_2	%Cr	%Ag
Edgewood ASC	ASC	8.0	12.0	8.0	2.0	0.2
Modified ASC	ASC-1	5.0	8.0	5.0	2.0	0.2

ASC-1 solution is now seldom used, but was used extensively during the period of development.

Functions of the Metallic Constituents

The function of each metallic constituent is brought out in Table 23.

It is apparent that both copper and chromium must be present to produce CK activity. Copper alone, as in Type A whetlerite, produces a whetlerite having dry SA protection, dry AC protection and some wet AC protection, and CK protection equivalent to that of the base charcoal or less. The CG protection of coppered charcoals is usually quite good, wet or dry. Silver alone produces a whetlerite having

TABLE 23. Function of the metallic constituents in ASC solution on charcoal CWS PCI–P58.

Solution composition			Service lives*							
			SA		AC		CK		NH_3	CG
% Cu	% Cr	% Ag	0–50	80–80	0–50	80–80	0–50	80–80	AR–50†	AR–50
10	1.37	0.	126	4	90	124	140	141	30	54
0	1.37	0.	33	0	16	15	38	8	12	46
0	1.37	0.5	70	123	17	15	37	8	14	42
10	1.37	0.1	128	105	87	118	137	111	19	54
10	0.	0.	120	4	80	..	23	0	..	..

* 5-cm tube tests. † AR = moisture content as received.

TABLE 24. Materials for a 1-kilo batch of ASC solution.

Compound	Assumed formula	Purity (by analysis)	Amount used
Basic copper carbonate	$CuCO_3 \cdot Cu(OH)_2$	55.6% Cu, 2.0% CO_2	114 g
Aqueous ammonia	NH_4OH	28% (25.2% by vol.) NH_3	284 cc
Ammonium carbonate	$(NH_4)_2CO_3$	34.2% NH_3, 54.3% CO_2	142 g
Chromic anhydride	CrO_3	52% Cr	34.6 g
Silver nitrate	$AgNO_3$	63.5% Ag	3.2 g
Water			390 cc
		Total	1,000 g
		Sp gr	1.12

SA protection, when wet, but having no protection for any other test gas not absorbed by activated charcoal. Use of both silver and copper in the whetlerite results in good SA protection wet or dry; the properties of this absorbent for other gases are similar to those of Type A whetlerite. To produce an absorbent with good CK activity wet or dry requires both copper and hexavalent chromium on the charcoal. The necessity for the presence of hexavalent chromium as such has been illustrated by numerous experiments in which the change in the hexavalent chromium content of the whetlerite during aging has been related to the CK life of the aged material.[52] Magnetic susceptibility measurements on aging whetlerites[53] also indicate that the CK life is dependent on the presence of hexavalent chromium. Direct impregnations with trivalent chromium (which never exhibits any CK activity) also point toward the same conclusion. However, hexavalent chromium in the absence of copper seems to have no effect on CK protection.

PREPARATION OF ASC SOLUTIONS

The solution used in the laboratory usually contains chromic anhydride and silver nitrate. Plant practice is to prepare a copper ammine carbonate solution by dissolving copper scrap in an aqueous solution of ammonia and carbon dioxide agitated by an air stream which also serves to oxidize the copper. As the copper goes into solution, gaseous ammonia and carbon dioxide are added to bring the composition up to the desired level. When the copper, ammonia, and carbon dioxide reach the proper concentration, the solution is removed from contact with the copper, air is bubbled in until all the cuprous copper in the solution is oxidized, and the required quantities of chromic anhydride and silver nitrate are added.

All calculations for the amounts of material to be added to the solutions should be based upon actual analyses of the compounds used, since the basic copper carbonate and ammonium carbonate are rarely of formula composition. An example of the purity and composition of the materials used in making up an ASC solution is given in Table 24.

A small amount of ammonium hydroxide is reserved for dissolving the silver nitrate. The remainder is mixed with the water and chromic anhydride is added. The resulting solution of ammonium chromate in excess ammonia is used to dissolve the basic copper carbonate and ammonium carbonate. The solution is stirred until all materials are in solution. The solution of silver nitrate in ammonium hydroxide is added last. This order of solution avoids the liberation of carbon dioxide which occurs if the acid chromic anhydride is added to either of the carbonates before being neutralized.

Impregnation with ASC Solution

Laboratory impregnation is carried out as follows: The charcoal, prepared by sieving to the proper mesh distribution, is placed in a beaker and an approximately equal volume of solution is poured over it with stirring. The stirring is continued for a minute or two until the foaming has ceased and the charcoal is completely wet. The charcoal is then allowed to remain in the solution for about 30 min. Although there is some evidence that the charcoal is completely impregnated after about 7 min, the 30-min period is used to allow a safety factor for any unknown variations in the charcoal. After impregnation the "slurry" of solution and charcoal is poured into a cylindrical wire screen basket with a conical bottom, and allowed to drain. The basket is shaken vertically until only a few drops of solution are removed each time the basket is raised. By this method it is possible to obtain reproducible solution-charcoal ratios of between 1.0 and 1.2 g of solution per g of charcoal, which is an optimum for good whetlerite performance. The ratio should lie in this range for reproducible performance of the whetlerite. The drained material is then dried in a rotating drum drier.[54]

The laboratory rotating drum drier consists of a metal drum, 15 in. long and 8 in. in diameter, fitted with interior lifts to keep the charcoal moving while drying. The drum is mounted inside a well-insulated electric oven, and is rotated at a rate of 3 rpm by a small electric motor mounted outside the oven. The charcoal is heated by heaters installed within the oven, and by a stream of heated air which is blown through the rotating drum. Adequately baffled exit ports are provided to carry off the air and gases evolved during drying. The optimum operating conditions for this drier are as follows:

Volume of charge	1,200 ml (wet impregnated charcoal)
Air flow	75 lpm (linear flow of approximately 94 in. per min through drum)
Maximum charge temp	180 C (±10 C)
Time at maximum temp	30 min
Influent air temp	185–195 C

The charge volume 1,200 ml corresponds to a loading of about 10% of the volume of the drum. Larger loading ratios require greater air flow through the drum to produce a high quality material. However, use of air flows greater than 75 lpm in drums of this design results in loss of product through the air vents.

The drier is provided with two temperature controlling devices. A Fenwell Thermoswitch controls one 500-watt heater and is activated by the air temperature outside the rotating drum. It is adjusted to turn the heater off at a temperature approximately 30 degrees below the maximum charge temperature. The other device, a Capacitrol, is connected to a thermocouple in the charcoal bed, indicating the charge temperature and controlling another 500-watt heater. The lag at 180 C is approximately ±5 C. Hence at maximum temperature the charge temperature variation is from 175 to 185 C. Having two heaters allows a rapid heating of the charge; by controlling one heater at a temperature 30 degrees below the maximum, slower final approach to the maximum temperature and smaller variation at the maximum temperature are obtained. The maximum temperature is not critical in the range between 150 and 200 C. However, at 150 C a long heating period is required to reduce the ammonia content of the whetlerite to the specification value, while at 200 C and higher there is danger of ignition of the whetlerite. The compromise maximum of 180 C for 30 min seems to be optimum. The total time of a run is about two hours, since it takes the 1,200-ml charge about 90 min to come to maximum temperature.

Vapor Pressure of the ASC Solution [55]

The vapor pressures of NH_3, CO_2, and H_2O over Types A and ASC solutions were measured at 25 and 50 C. The data for ASC are presented in Figures 10 through 18. Because the data are valuable from the point of view of plant design, the complete set of curves is presented. Variations of the vapor pressures of all components when any one is varied are shown.

Assuming that the Clausius-Clapeyron equation holds within the range of temperatures studied and for an additional 10 degrees below and 20 degrees above, the effect of temperature on the partial pressures of ammonia and carbon dioxide has been calculated. The effect of temperature on the partial pressure of ammonia in Type ASC solution is shown in Figures 19 through 22. Similar data for the carbon dioxide pressures are shown in Figures 23 through 26.

The effect of adding chromium to Type AS solution (producing Type ASC) is to lower the ammonia pressure and to raise the carbon dioxide pressure, as

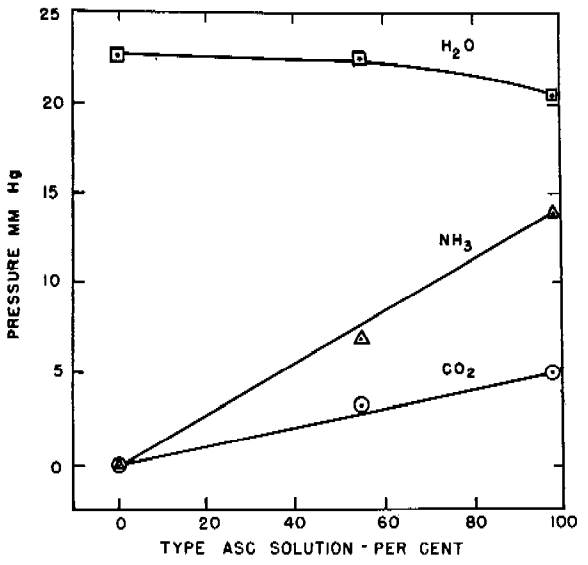


FIGURE 10. Effect of concentration of ASC-1 solution (at 25 C) on vapor pressure (partial pressure) of H_2O, NH_3, and CO_2. (ASC-1 solution is diluted with water to the indicated concentrations; the 100% values are for undiluted solution.)

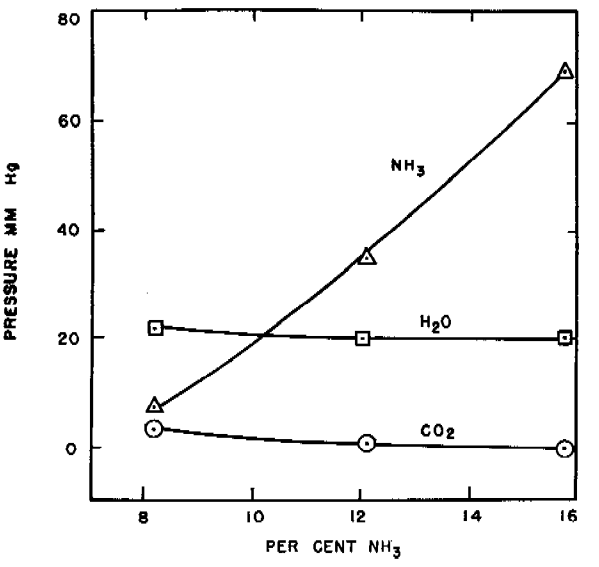


FIGURE 12. Effect of varying ammonia content (8 to 16%) of ASC solutions at 25 C on partial pressure of H_2O, NH_3, and CO_2.

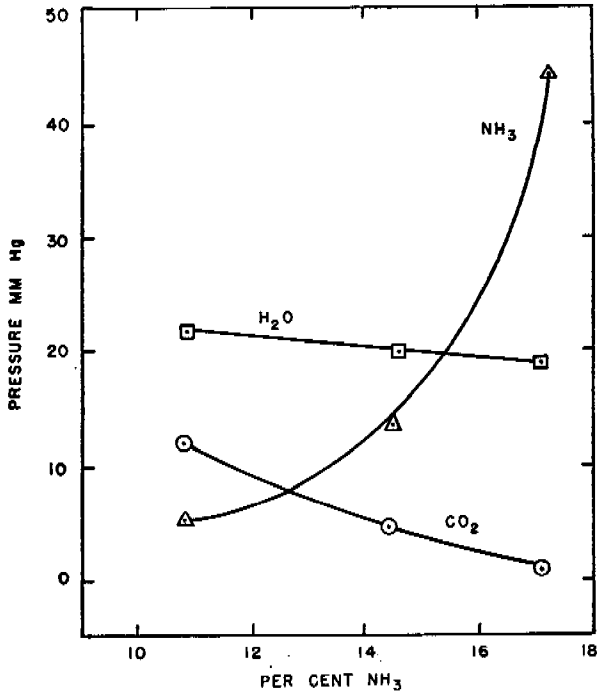


FIGURE 11. Effect of varying ammonia content (10 to 17%) ASC solutions at 25 C on partial pressure of H_2O, NH_3, and CO_2.

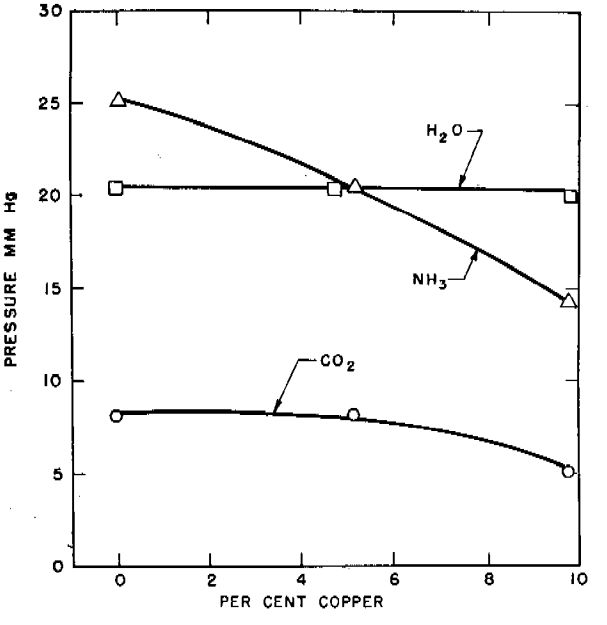


FIGURE 13. Effect of varying copper content (0 to 10%) of ASC solutions at 25 C on partial pressure of H_2O, NH_3, and CO_2.

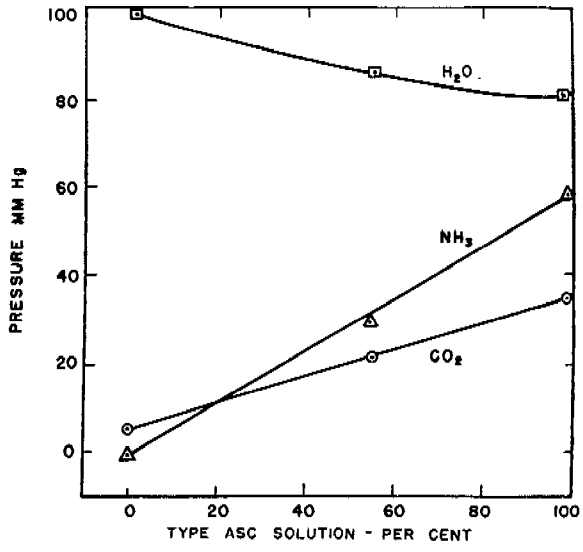


FIGURE 14. Effect of the concentration of ASC–1 solution (at 50 C) on the partial pressures of H_2O, NH_3, and CO_2. (ASC–1 solution diluted with water; the 100% values are for undiluted solution.)

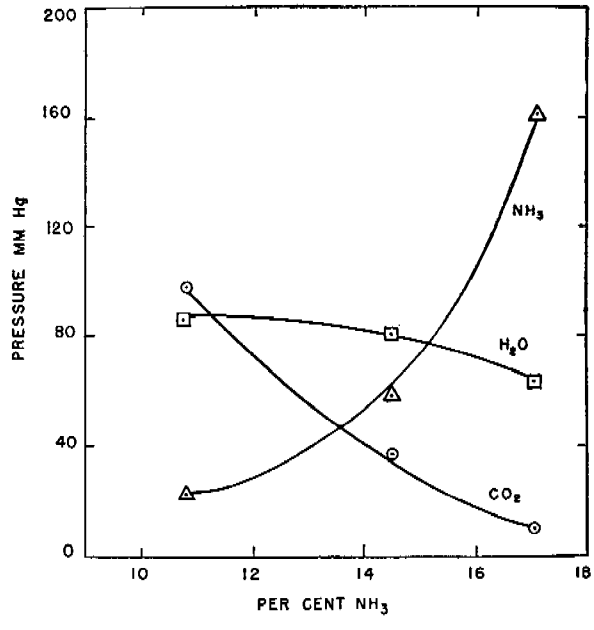


FIGURE 15. Effect of varying ammonia content (11 to 17%) of ASC solutions at 50 C on partial pressure of H_2O, NH_3, and CO_2.

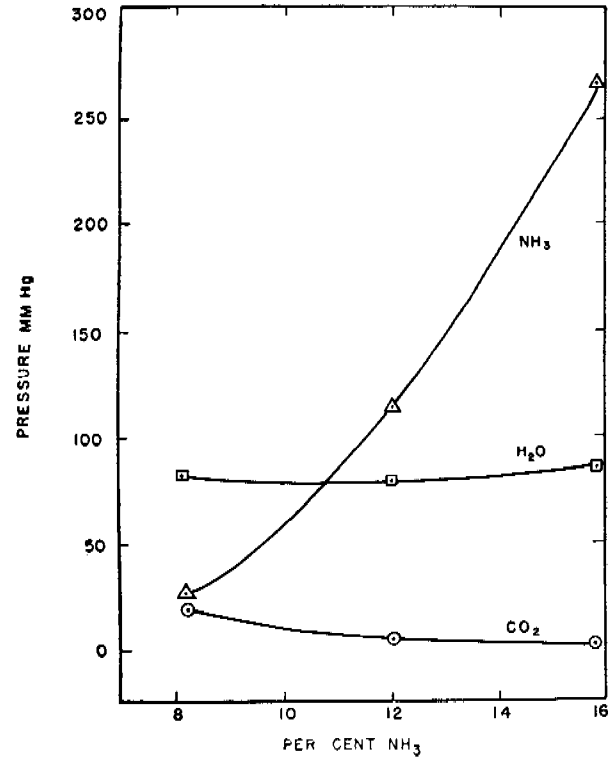


FIGURE 16. Effect of varying ammonia content (8 to 16%) of ASC solutions at 50 C on partial pressure of NH_3, H_2O, and CO_2.

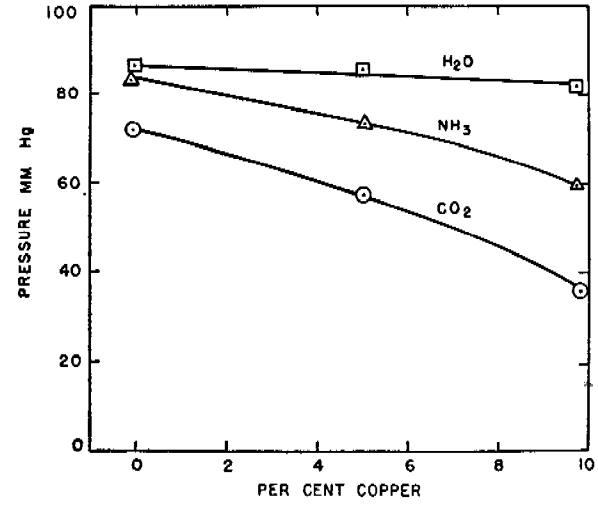


FIGURE 17. Effect of varying copper content (0 to 10%) of ASC solutions at 50 C on partial pressure of NH_3, H_2O, and CO_2.

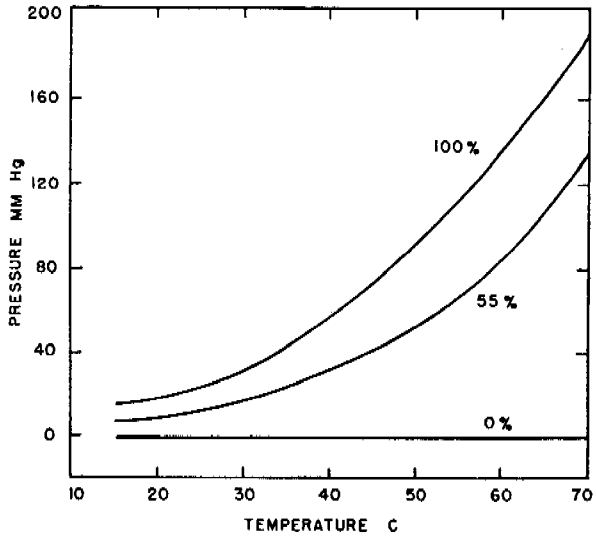


FIGURE 18. Effect of temperature (C) on ammonia pressure of Type A solution and 55% Type A solution (diluted with water).

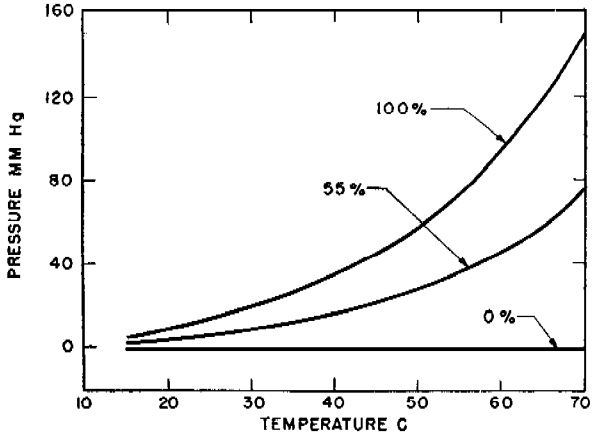


FIGURE 19. Effect of temperature (C) on ammonia pressure of Type ASC solution and 55% Type ASC solution (diluted with water).

would be expected from the addition of any acidic component.

HEATS OF SOLUTION

The integrated form of the Clausius-Clapeyron equation is

$$\ln p = \frac{\Delta H}{RT} + C,$$

where C is the constant of integration, and ΔH is the heat of solution of the vapor. Assuming that plots of $\ln p$ versus $1/T$ are straight lines, and determining the vapor pressures of ammonia and carbon dioxide

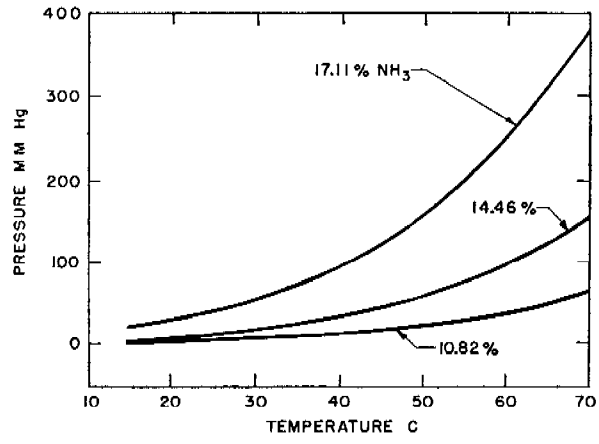


FIGURE 20. Effect of temperature on ammonia pressure of three dilutions of Type ASC solutions (NH_3 variable).

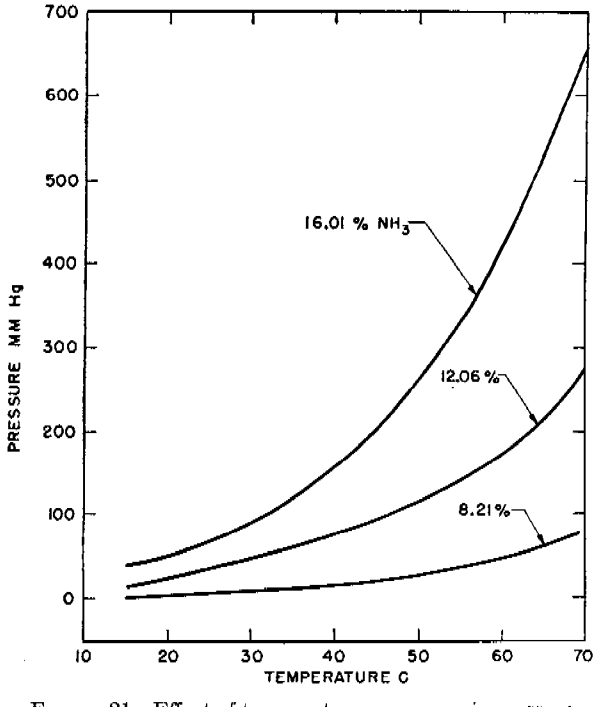


FIGURE 21. Effect of temperature on ammonia pressure of Type ASC solution with different solutions (NH_3 variable).

for the solution at 25 and 50 C, values of ΔH were obtained. The average values are given in Table 25.

TABLE 25. Average heat of solution of the volatile constituents of whetlerizing solutions.

Solution	NH_3	CO_2	H_2O
Type A	9.1	15.9	11.0
Type ASC	10.2	15.6	10.7

As might have been predicted from the vapor

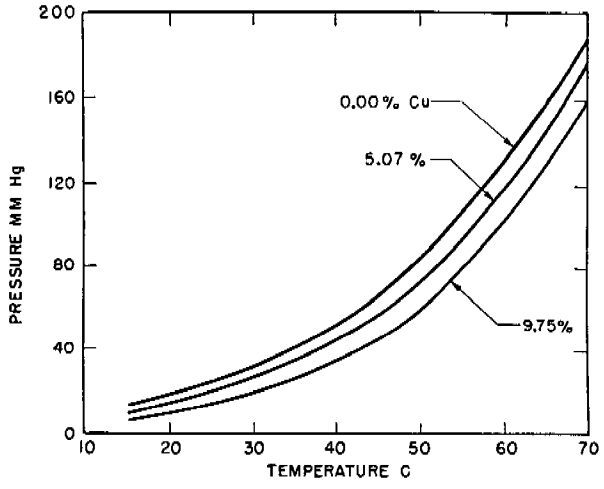


FIGURE 22. Effect of temperature on ammonia pressure of Type ASC solutions (Cu variable).

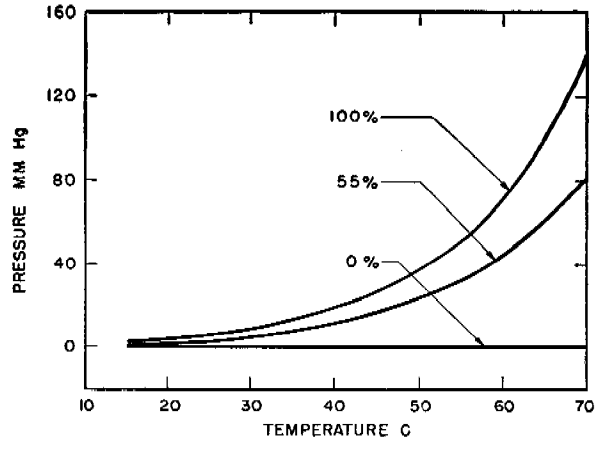


FIGURE 23. Effect of temperature on CO_2 pressure of Type ASC solution and of 55% Type ASC solution diluted with water.

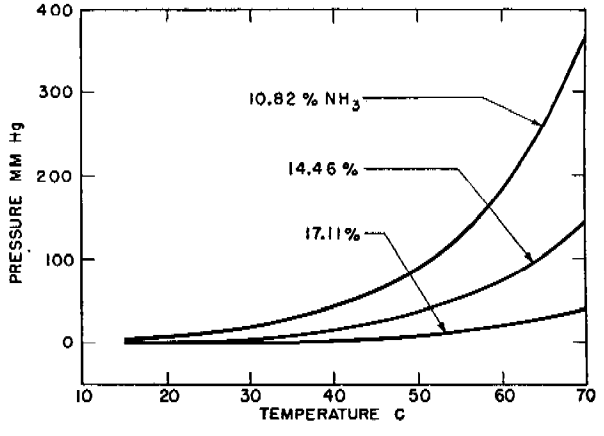


FIGURE 24. Effect of temperature on CO_2 pressure of three dilutions of Type ASC solutions (NH_3 variable).

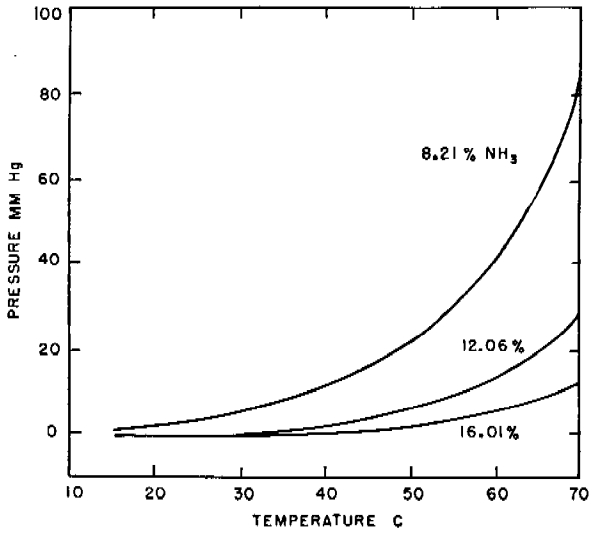


FIGURE 25. Effect of temperature on CO_2 pressure of three dilutions of Type ASC solutions (NH_3 variable).

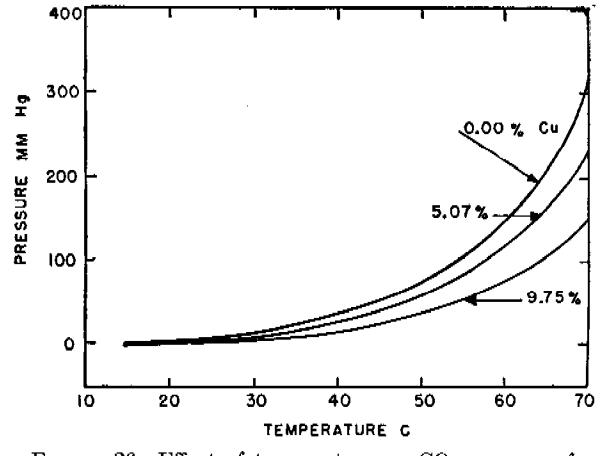


FIGURE 26. Effect of temperature on CO_2 pressure of three dilutions of Type ASC solutions (Cu variable).

pressure data or from a consideration of the types of solutions involved, the heat of solution of ammonia increased while that of carbon dioxide and water decreased as a result of the addition of chromic anhydride to Type A whetlerizing solution.

These vapor pressure data should be useful in the calculation of the composition of the gases leaving the make-up tanks during the air-blowing procedure now used in the industrial whetlerizing plants. In addition, the composition of the gas leaving the recovery tower can be calculated or approximated for known concentrations of recovery tower solution. The efficiency of such recovery processes might be improved or new systems designed on the basis of such data.

Mechanism of Sorption of Chromium from ASC Solution by Charcoal

The impregnation of charcoal with whetlerizing solution apparently involves only a sorption of the solution into the pores of the charcoal. Little or no reaction occurs during the relatively short time that the charcoal is in contact with the solution.[56] The data indicate that most of the chromium present in ASC whetlerite is not taken up by selective adsorption from solution during impregnation, but remains after evaporation of the water from the solution contained in the pores of the charcoal. The adsorption of chromium from ASC solution is a very slow process which is accompanied by some reduction to the trivalent state. The trivalent chromium returns to the solution, and after a few days standing, is precipitated as a complex basic carbonate, a gelatinous mixed precipitate of the following composition: Cr_2O_3, 32.8%; CuO, 6.8%; CO_2, 20.8%; SiO_2, 6.8%; NH_3, 8.8%; H_2O, 22.4%. The silica found in the precipitate was apparently leached from the charcoal by the action of the impregnating solution over a period of several days. Coal base charcoals in particular have a large silica content.

The mechanism for the formation of the precipitate may be postulated as follows:

1. Charcoal + ASC solution ⟶ hexavalent chromium adsorbed on charcoal
2. Cr^{+6} adsorbed on charcoal ⟶ Cr^{+3} adsorbed on charcoal
3. Cr^{+3} adsorbed on charcoal ⟶ Cr^{+3} in solution + charcoal
4. Cr^{+3} in solution ⟶ Cr^{+3} precipitated.

Data showing the rate of adsorption of chromium on CWS PCI-P58, 12 to 20 mesh, is shown in Table 26.

Table 26. Adsorption of chromium from ASC solutions by charcoal CWS PCI-P58.

Time, min	$\%Cr^{+6}$ in solution
0.0	1.06
9.0	1.05
14.0	1.03
31.5	0.983
67.5	0.937
120.	0.917
748.	0.690
3027. (2 days)	0.467

The time intervals involved in the experiment show that very little chromium is adsorbed from the solution in the normal impregnation process since the time of contact is only thirty min. During this period only about 0.08% of chromium is adsorbed from the solution. It is evident that mechanical holding of the solution in the pores and voids accounts for practically all of the chromium found on a whetlerite.

When an aqueous solution of ammonium chromate is allowed to remain in contact with charcoal for several days, the chromium is adsorbed and partially reduced to trivalent chromium which remains on the charcoal. No trivalent chromium appears in the solution, as in the case of ASC solution. On charcoal the chromium is believed to be reactive with, or catalytic toward, the decomposition of CK when in the hexavalent state. Little direct evidence is available to prove this point, because the state of the impregnant on charcoal frequently is so different from the ordinary state of the material that the usual X-ray diffraction experiments give little but the halos or fogs which indicate a very finely divided or amorphous condition. Analytical results, correlated with the change in CK life of ASC whetlerite on aging, indicate clearly that hexavalent chromium is involved in the removal of CK. In an effort to study the state of the impregnant without the drastic treatment involved in analytical procedures, magnetic susceptibility measurements were made on a Gouy balance.[53] The large differences between the magnetic susceptibilities of compounds of copper and compounds of chromium suggested that the valence state of the impregnant might be determined by this means. The results indicated that:

1. CuO on charcoal in a Type A whetlerite has a much higher susceptibility than it has normally. This may be caused by the fact that it is very finely divided, or that it is adsorbed molecularly and the carbon-copper oxide forces act as a diluting effect, increasing the susceptibility of the copper oxide. Large changes in the susceptibility of iron, cobalt, nickel, and manganese salts have been observed when they are adsorbed on charcoal, and these changes seem to be due to surface complex formation with the charcoal.

2. The chromium on Type ASC charcoal changes to the trivalent form upon aging or absorption of CK. Previous work using analytical methods had pointed toward this conclusion. Furthermore, the magnetic measurements strongly indicated that after reduction the chromium is present as $Cr_2O_3 \cdot 4H_2O$. The magnetic susceptibility of CrO_3 is small while that of Cr_2O_3 is very large. The change observed on exposing ASC whetlerite to CK was greater than

could be accounted for by the formation of anhydrous Cr_2O_3. Because there is more than enough water present to allow the formation of the hydrate, and since it forms readily, its presence is a reasonable explanation of the high final susceptibility.

Hexavalent chromium may be present on the charcoal as basic copper chromate ($CuCrO_4 \cdot 2CuO$) or copper dichromate ($CuCr_2O_7$). Both of these compounds exist as the dihydrate at room temperature. The basic chromate is the most probable compound under the conditions of deposition of the materials on the charcoal. The hydrates are:

$CuCrO_4 \cdot 2CuO \cdot 2H_2O$ (loses water at 260 C), basic copper chromate dihydrate.

$CuCr_2O_7 \cdot 2H_2O$ (loses water at 100 C), copper dichromate dihydrate.

Although these materials, when on charcoal, may be sufficiently altered in their properties so that they lose water at a lower temperature than normal, it is possible that hydrates may exist even after being heated to 180 C, as is done in whetlerite preparation.

There is some semi-quantitative data available that can be interpreted as favoring the existence of the basic copper chromate as the material active in the removal of CK. As shown in Figure 7, when an impregnating solution contains about 2% chromium, the CK life increases as the copper concentration of the solution is increased up to approximately 8% of copper, with no further increase at higher copper concentrations. Thus, when the copper-to-chromium ratio reaches a value of about 4 to 1 there is no further increase in CK life. This implies that the copper-chromium compound or complex responsible for the CK activity of the whetlerite might contain copper and chromium in that ratio. In basic copper chromate ($CuCrO_4 \cdot 2CuO$) the ratio is $3Cu/Cr = 194/52$ or 3.7 grams of copper per gram of chromium.

If basic copper chromate is the material in ASC whetlerite which is active in the removal of CK, then any hexavalent chromium above that necessary for the formation of basic copper chromate would not be expected to increase the CK life. Therefore, it is indicated that the total amount of chromium on a whetlerite is no measure of the CK reactivity that can be expected of the whetlerite. For example, an ASC whetlerite treated with hexavalent chromium in secondary impregnations was found by analysis to contain a very large amount of hexavalent chromium. This material was found to have an unsatisfactory CK life. Although both copper and chromium were present, the copper-chromium complex apparently was rendered inactive by the layer of hexavalent chromium put on by the secondary impregnation.

4.5.3 Mechanism of Removal of SA, AC, and CK by Type ASC Whetlerite

A brief description of the mechanism of removal of the common test gases is given in the following paragraphs. A more detailed discussion of removal mechanisms is to be found in Chapter 7.

SA

SA is removed by catalytic oxidation of SA to As_2O_3. The catalyst is predominantly silver, the action of which is apparently enhanced by the presence of copper and chromium.

CK

The following reactions have been postulated for the removal of CK.[78]

1. $5CNCl + 5H_2O \longrightarrow 5HOCN + 5HCl$
2. $2HCl + CuO \longrightarrow CuCl_2 + H_2O$
3. $3HCl + Cr^{+6} \longrightarrow {}^3/_2Cl_2 + Cr^{+3} + 3H^+$

Hexavalent chromium in combination with copper apparently functions as a hydrolysis catalyst. The HCl produced by hydrolysis reacts with CuO until all the available CuO is used. Then the HCl reacts with the chromates present resulting in the destruction of the catalyst. Five moles of CK react with 1 mole of hexavalent chromium as indicated above.

AC

The following mechanism is postulated:

1. $2HCN + CuO \longrightarrow Cu(CN)_2 + H_2O$
2. $2Cu(CN)_2 \longrightarrow Cu_2(CN)_2 + (CN)_2$
3. $(CN)_2 + Cr^{+6} \longrightarrow Cr^{+6} - (CN)_2$ Complex

The first two steps are identical with the mechanism postulated for the reaction of Type A impregnant with AC. The third reaction accounts for the absence of $(CN)_2$ in the effluent from the absorption of AC by Type ASC whetlerite. Apparently no reduction of Cr^{+6} is directly involved.

VARIATION OF ASC WHETLERITE QUALITY WITH CHARCOAL

The reactivity of ASC whetlerites toward CK at 80-80 conditions varies with the base charcoal. Indications are that this variation is a function of the pore size distribution in the charcoal,[49] but the exact

relationship between the pore size distribution and the CK activity has not been developed. Apparently the manner in which water is absorbed by the charcoal and in which the pores are filled is an important factor.[57] Using CWS PCI-1042 and CWSN-S5 charcoals (12 to 16 mesh), a study was made of the effect of water content on the SA, AC, and CK lives of the corresponding whetlerites. The PCI whetlerite was found to give ample protection for all three test gases up to and including equilibration at 97 to 100% RH. The SA and AC lives were almost independent of the moisture content of the whetlerite, while the CK lives decreased approximately linearly from 130 min at zero water content to 46 min at the maximum (33.3% water).

The N-S5 whetlerite gave adequate AC protection over the entire range. The SA lives dropped steadily above 35% RH, and became zero at 85% RH. The CK lives dropped rapidly above 30% RH, and became zero at 60% (35.2% water absorbed). Five-centimeter tube test conditions were used in both cases.

Thus when the two whetlerites have absorbed about the same amount of water (although at different humidities), one has an adequate CK and SA life and the other does not. The fact that the N-S5 has absorbed enough water to bring the reactivity to zero at 60% RH while the PCI-1042 never absorbs enough to do this even at 97 to 100% RH seems to indicate that the pore structure involved is the determining factor (see Chapter 6).

Deterioration of ASC Whetlerites

The greatest disadvantage of ASC whetlerite is its tendency to lose CK reactivity on standing equilibrated in a tightly closed container. Under these conditions a reduction of the hexavalent chromium takes place [58, 52] which results in poor CK performance. There is also some loss of AC life under the same conditions, but this effect is not as serious, particularly under field conditions. ASC whetlerite stored dry in a sealed system shows negligible aging. Equilibrated and stored in air, CO_2, NH_3, O_2, or N_2, it shows deterioration in every case. The deterioration was greatest in CO_2, least in NH_3, and intermediate in air, O_2 and N_2.

It is believed that the variation in the rate of aging in the presence of NH_3 and CO_2 is attributable to their effect on the *p*H, since in reactions involving chromate ion the concentration of hydrogen ion is important. If true, the reduction of the hydrogen ion concentration effected by the NH_3 atmosphere would be expected to reduce the rate of aging. Because the data show that such reduction in rate does occur, this possibility should be borne in mind when considering aging reactions. However, the rate of aging even in ammonia was not negligible. Attempts to use the control of *p*H as a means of eliminating aging have not been successful. Spraying the whetlerite with sodium hydroxide, or inclusion of sodium hydroxide in the impregnating solution were not effective enough to be useful.

ASC whetlerite, AS whetlerite, and base charcoal when equilibrated and stored in closed containers for two to four days at 50 C completely removed all of the oxygen from an approximately equal volume of air. The rate of adsorption of the oxygen decreased as the amount of water on a particular sample of whetlerite or charcoal decreased. It was also noticed that unimpregnated charcoals, if stored equilibrated in sealed containers at about 50 C for three weeks, became unsuitable for conversion to ASC whetlerites.[59] Some base charcoals, after aging, produced whetlerites with CK 80-80 tube lives 50% as large as those of the un-aged charcoal, while others gave lives of less than 10% of the un-aged material. The effect was evident whether the aged material was dried by evacuation before whetlerization, or whetlerized in the equilibrated condition. The fresh material produced whetlerite of the same CK life whether the material was equilibrated before impregnation or not. Heating the aged, wet charcoal at 100 C for three hours, or soaking the material for six hours in ASC solution, produced in most cases a whetlerite that had a CK life approximately equal to that produced from the original material. Only certain zinc chloride activated charcoals, which ordinarily showed excessive aging when converted to ASC whetlerite, failed to respond to these treatments. Tube tests of the whetlerites prepared from aged charcoals frequently showed a large number of breaks before the true breakpoint was reached, in some cases running to as many as 12 breaks. This indicates that the activity of the whetlerite is low, resulting in a slow removal of CK and, with the particular bed depth used (5 cm), resulted in a slow leakage of CK through the tube prior to the true breakpoint (when the concentration of CK in the effluent increases rapidly).

On the basis of the foregoing data, certain speculations as to the nature of the aging process may be made. For both base charcoal and whetlerite, the first step in aging is the same, that is, formation of a layer of adsorbed water. The character of this layer

is dependent on the nature of the charcoal surface prior to water adsorption, which in turn is dependent upon the source of the material and the process used in the activation of the charcoal.

In view of the fact that some oxygen is probably present on the charcoal surface before the water is adsorbed, there are at least two processes by which the chromium compound in ASC whetlerite can be rendered inactive as a catalyst or a reactant:

1. Reaction of the carbon-oxygen-water surface complex with hexavalent chromium, destroying the catalyst or reactant by reduction.

2. Destruction of the active copper-chromium compound or mixture by a reaction (with water or carbon dioxide) not involving the reduction of chromium.

The first postulate seems to be the most likely. It has been observed that ASC whetlerites which contain water do not deteriorate as rapidly when stored in containers which do not seal them from contact with the atmosphere (canisters, for example), as they do when stored in tightly sealed containers. If it be assumed that the carbon-water-oxygen surface complex is more easily oxidized by atmospheric oxygen than by the hexavalent chromium present, then the above observation and the absorption of oxygen from the air in storage containers are explained readily.

The aging of base charcoals appears to proceed also by formation of a surface complex. When base charcoals are allowed to age in a sealed container, they remove oxygen from the air. The adsorbed oxygen may form an extensive layer or layers of surface complex. (The charcoal must be equilibrated before the rapid oxygen adsorption takes place.) The complex thus formed may react with ASC impregnant put on the charcoal to form a layer of trivalent chromium on the charcoal surface, thus rendering the surface inactive.

Another possibility is that the surface becomes strongly hydrophobic when the carbon-oxygen-water surface complex forms. It is known that the carbon-oxygen surface complex formed on charcoals at about 400 C is more hydrophilic than the oxygen complexes formed at lower temperatures.[60] It is possible that the complex formed under the conditions of aging may cause the surface to be hydrophobic enough to prevent the whetlerizing solution from entering the fine pores of the charcoal.

Extensive studies of the aging of ASC whetlerites under field conditions and simulated field conditions have been carried out[61] (see Chapter 5). The results show that for field service under fairly rigorous conditions of temperature and humidity (85 F and above, 70 to 90% RH), an ASC whetlerite prepared from a PCI or a Seattle-wood charcoal and used in an M10A1 canister and carrier is satisfactory from the standpoint of CK protection. With respect to SA, AC, or CG, some deterioration of the whetlerite has been found in laboratory tests (sealed and equilibrated), but under field conditions in the M10A1 canister this has been negligible.

ASC whetlerites, when aged, lose activity more rapidly than capacity. Hence canisters with high flow rates or thin beds show more pronounced aging effects than do canisters with low flow rates or thick bed depths. The M-11 assault canister presents a problem from this point of view because of its short bed depth, and because it is carried in an air-tight carrier which, in hot humid climates, provides excellent conditions for the deterioration of ASC whetlerite, particularly after having been partially humidified by being worn for some time.

Pilot Plant Production of ASC Whetlerite[65]

The best operating conditions for plant production of ASC whetlerite were determined in pilot plant studies. The product was evaluated on the basis of CK 80-80 lives, and the ammonia content of the finished whetlerite. It was found that when these properties were satisfactory, other properties were also satisfactory.

The most critical step in the production of ASC whetlerite is drying. The impregnation step can be varied over wide ranges without having an appreciable effect on the quality of the product.

A complete description of the pilot plant equipment can be found in an OSRD report.[66] The plant consisted essentially of two parts, the impregnator and the drier. The impregnator consisted of a sheet iron tank with a 4-ft screw (2½ in. in diam and 2-in. pitch) leading from the bottom at an angle from the horizontal that could be varied between 20 and 40 degrees. The liquid level in the lower trough could be adjusted to cover up to one-half of the screw length by means of a variable overflow pipe. Screw speed was adjustable to four values (5.8, 4.5, 3.5, and 2.8 rpm). Charcoal was introduced from a tank storage hopper by means of calibrated orifices. With PCI activated, charcoal orifices from $^{15}/_{64}$ to $^{18}/_{64}$ in. in diameter permitted a flow of charcoal of 0.15 to 0.30 lb per min. Impregnating solution flow

was maintained constant by gravity through an overflow Weir meter. Both solution and charcoal entered the tank at the same point where they were thoroughly mixed by an electric stirrer to assure uniformity of impregnation. The impregnator could be adjusted to deliver a wet feed stock containing from 0.75 to 1.1 lb of solution per lb of dry charcoal. The screw delivered the wet feed stock either to a storage crock from which it was transferred to the drier by hand, or to the drier storage hopper from which it was introduced into the drier by means of a screw mechanism, at a controlled rate.

The drier was constructed from three sections of standard 8-in. steel pipe. It was 10 ft long, externally heated by four 60-ft sections of straight 14-gauge Chromel A resistance wire wound directly over two insulating layers of asbestos tape. A coil was wound on each end-section, and the remaining two 60-ft lengths wound on the middle section of the drier. Electric contact was furnished by five commutator rings. The exterior surface of the drum was lagged with 1 in. of 85% magnesia pipe covering. Temperatures of the walls and charge were taken from built-in thermocouples. The heaters were separately controlled to provide a definite heating schedule for the charge as it passed through the drum. The complete drier was mounted on a supporting framework, fabricated from standard steel forms. It was rotated by a pair of idling and a pair of motor-driven grooved pipe-rolls. The slope of the drum was varied by means of a hinge-and-jack system. The drum was constructed to receive a blower at either the feed or discharge end, so that the air flow could be either countercurrent or parallel, and an electric heater was provided to heat the air when desired. The discharge was arranged so that the product could be collected in the absence of air, although in normal operation the product was discharged directly into cans in free contact with the air.

Using the pilot plant, the optimum operating conditions discussed in following paragraphs were determined with respect to CK protection.

Charge Temperature. With plentiful air flow, a maximum charge temperature up to 400 F (205 C) has no deleterious effect on CK life. Above 400 F, and up to ignition temperature, the evidence is inconclusive, but indications are that some reduction of CK life takes place.

Ignition temperature varies for each charcoal, as is shown in Table 27.[81]

With a limited air flow, the CK life reaches a maximum at a temperature well below ignition temperature, although the life is lower than the maximum life reached with plentiful air flow. Ammonia content also is dependent on maximum temperature at any given flow rate. For standard conditions (air flow rate of about 1.5 linear fps), the ammonia content of the whetlerite was about 0.2% at 370 to 390 F.

TABLE 27. Ignition temperature of whetlerites made from various charcoals.

Material	Ignition temperature	
	F	C
PCI activated charcoal B1196	>542	>283
National Carbon charcoal CWSN196B1X	>542	>283
PCI–ASC containing 1% NaOH, run WR–7811	440	227
PCI–ASC BD1063	438	226
Barnebey-Cheney nutshell ASC, drum A116	435	224
PCI–ASC, run WR–52	428	220
Seattle ASC, drum B–825	420	216
National Carbon ASC CWSN196B1X ASC	385	196
PCI E–11 1.5% pyridine, run WR 40	375	190
Seattle E–11, 0.8% pyridine, drum B837	375	190
Seattle E–11, 2.0% pyridine, drum B846	343	173

Temperature Schedule. Extremely rapid increase in temperature during heating is detrimental to CK life. A moderate heating rate is desirable so that the whetlerite reaches maximum temperature in 40 to 60 min. The retention time (time in the drier) has no visible effect as long as the whetlerite is not heated too rapidly. A total time of about 30 min at maximum temperature is desirable, which in turn results in a retention of from 70 to 90 min. Proper control of the feed-end heater, speed of rotation, and pitch of the drum results in the desired rate of heating and retention time.

Air Flow. Air flows less than 0.8 linear fps countercurrent through the drier, or 3 fps parallel-flow, resulted in inferior CK life. The effect is caused by the influence of the vapors in contact with the drying whetlerite. The air acts as a diluent, reducing the rate of whatever deleterious reactions take place in the presence of high concentrations of vapors of H_2O, CO_2, and NH_3. Parallel flow is the most objectionable because the dried whetlerite is in contact with the moist saturated air, whereas in countercurrent flow the dried whetlerite comes in contact only with fresh, dry air. The most convenient flow rate was found to be approximately 1.5 linear fps (80 F basis), or 90 fpm, in good agreement with laboratory driers which operate at a flow of 94 linear fpm.

All data point toward the conclusion that during

the drying operation (especially at the higher temperatures), the whetlerite must not be exposed to high concentrations of H_2O, CO_2, or NH_3 vapors. It is not known which gas is the most harmful.

Flue Gas Atmosphere. A large proportion of excess air is necessary if flue gas is used in the drier. Low CO_2 and H_2O vapor concentrations cannot be maintained in the drier if undiluted flue gas is used as a drying agent, and lowered CK life results.

Back Feeding. In order to obtain a free-flowing feed stock, dried product is sometimes mixed with the wet feed stock. No material effect on the product was observed when up to 50% of the dried product was used as feedback. Other experiments using a different material as feedback resulted in a product approximately equivalent to that obtained by mechanically mixing the feedback material with the product obtained without using any feedback in the drier feed stock. This indicates that the whetlerite is not improved by a second passage through the drier in company with some wet material.[67] Therefore, inferior feedback stock is not desirable.

It was found that 30% or more of dry feedback gave a dry, free-flowing feed material, whereas 20% feedback resulted in a rather cohesive material. With the drier used in pilot plant productions, 20% was sufficient to prevent caking. Other driers of different heating characteristics may have different requirements.

Variation of the feed rate, liquid content of the feed stock, or drier loading had no effect on the quality of the product.

4.5.4 Evolution of Ammonia by Type ASC Whetlerites

Type ASC whetlerites require careful temperature control during drying to avoid de-activation of the catalyst by overheating. Type A whetlerites can be heated to much higher temperatures without deleterious effects. Consequently, when the plant production of Type ASC whetlerite using Type A plant equipment was started in 1943, some trouble was encountered in temperature control and frequent overheating resulted. When it became definitely established that good quality Type ASC whetlerite could be produced at lower temperatures, many lots of insufficiently heated whetlerite were produced. These materials had a relatively high ammonia content, and evolved ammonia vapor when moist. Use of such whetlerite in canister fillings in the tropics (where the whetlerite soon absorbed appreciable amounts of water from atmosphere) resulted in the evolution of large amounts of ammonia with consequent discomfort to the person using the canister.

As soon as the situation was realized, measures were taken to prevent the production of such whetlerites, and a specification test was devised to detect samples which evolve obnoxious amounts of ammonia when equilibrated at 80% RH. Samples which cannot meet this specification are rejected.

The preparation of whetlerites containing large quantities of ammonia is prevented by careful control of the drying temperature (at about 380 F, ± 10 degrees), and use of an adequate air flow through the drier. Such treatment results in a whetlerite which contains approximately 0.15% total ammonia, and which when equilibrated and used in a canister will evolve less than 10 to 20 γ per l [a] of ammonia at normal breathing rates.

The intensity of the odor of ammonia, and its effect on an observer varies with the sensitivity of the observer and with his conditioning. If the observer expects to find the odor of ammonia, he may be able to detect it at concentrations less than 10 γ per l, but will not find concentrations as high as 25 to 30 γ per l unendurable. On the other hand, unprepared observers have a higher threshold for the odor, but will usually find the odor intolerable at a lower concentration than the prepared observers. Therefore, in tropical field tests of Type ASC whetlerite which contained rather high concentrations of ammonia, troops who were prepared for the odor of ammonia while wearing their gas masks rarely found a canister which evolved intolerable concentrations.

Extensive tests of recently produced Type ASC whetlerite which meets ammonia evolution specifications have shown that in tropical regions an odor of ammonia will usually develop in a canister that has been worn long enough to moisten the whetlerite appreciably, but the odor is slight and does not become completely intolerable.

Leaching and Rewhetlerization

In an effort to determine the cause of the variation observed in plant whetlerites made from apparently uniform, high quality charcoals, a study was made of variations in whetlerizing techniques. In some cases the primary whetlerite was leached with hydro-

[a] Normally the odor of ammonia cannot be detected at concentrations less than 10 to 12 γ per l (1 γ = 0.001 mg).

TABLE 28. The effect of rewhetlerization on the performance of whetlerites.

% Cu in rewhetlerizing solution*	% Cu	% Cr	% Cr^{+6}	$\frac{Cr^{+6}}{Cr}$	Service life CK 80–80 M10A1 min	% H_2O equilibrium 80% RH
Original lot AD3–749	5.94	1.52	0.78	0.51	56, 50, 50	24.7
2.5	7.57	2.63	1.86	0.71	91, 82	24.7
2.5	6.32	2.80	1.73	0.62	69, 66	25.5
5.0	6.48	2.89	1.87	0.65	111, 90	23.0
5.0	7.78	2.63	1.75	0.87	107, 96	23.4
8.0	9.33	2.18	1.70	0.78	98, 81	22.6
8.0	9.76	2.22	1.70	0.77	98, 77	22.9

* 1.8 per cent Cr present in all rewhetlerizing solutions.

TABLE 29. The effect of multiple whetlerization on CG life.

Sample	Description	M10A1 canister lives, min			% H_2O equilibrium 80% RH
		CG		PS	
		80–80	0–50	80–50 (tube life)	
PC 518	PCI charcoal not whetlerized	44, 46	9, 10	31, 35	29.2
6727	PC 518 whetlerite	53, 52	55, 55	28, 22	26.2
6728	6727 rewhetlerite	38, 45	51, 44	(45, 43)*	21.4
6739	6728 rewhetlerite	30	38	.. ..	24.3

* Unlikely result.

chloric acid, ammonia, and water, then rewhetlerized. With other samples of whetlerite, a simple rewhetlerization with ASC-1 solution without any previous leaching treatment resulted in phenomenal increases in the CK M10A1 canister lives.[69] A series of experiments was made in which the solution used for rewhetlerization contained from 2.5 to 8% copper, and 1.8% chromium. The results are given in Table 28.

It can be seen that the CK canister life has been approximately doubled by the use of ASC-1 solution (5% Cu), resulting from a combination of increased hexavalent chromium and increased copper on the whetlerite. It will be noticed that using an 8% copper solution resulted in a slightly lower CK life, although the lives are not low enough to be significant.

Life-thickness curves for the original and rewhetlerized product show that rewhetlerization resulted in an increase in capacity without changing the critical layer depth appreciably.

A study was made of the rewhetlerization of various grades of whetlerite from various sources. In many cases Grade II whetlerite (CK M10A1 canister life of less than 35 min) produced a Grade I whetlerite having at least twice the life of the original material. Grade II PCI whetlerites are usually more responsive to this treatment than a material like a Barnebey-Cheney whetlerite because the base charcoals are capable of producing a better whetlerite. The second whetlerization simply realizes the full possibilities of the charcoal.

It was noticed that CG protection seemed to drop on rewhetlerization although not seriously. A second rewhetlerization lowered the CG life even more. These results are shown in Table 29.

These tests were made at 50-lpm intermittent flow. At 32-lpm steady flow, there is an increase in the CG AR-50 lives on rewhetlerization; (40, 42 before rewhetlerization; 60, 64 after). This indicates that an increase in capacity and a decrease in activity for CG has occurred. The PS data are too scanty to allow any conclusions.

Leaching of whetlerite is carried out as follows: The whetlerite is boiled with an equal volume of 1/1 HCl (approximately 6*N*) for 10 min, then washed free of acid with water, treated again with acid, washed with water, and the process repeated with 6*N* NH_4OH. After being washed until neutral, the material is drained and dried at 150 C in the laboratory rotary drier.

After leaching, the charcoals are whetlerized as usual. The results of leaching on a Grade II and a mediocre Grade I are shown in Table 30. The results of various studies on the treatment of activated charcoal with different solutions prior to whetlerization are shown in Table 31. Various types of oxidizing agents were used. It appears that leaching and

SECRET

TABLE 30. Effect of leaching on the performance of rewhetlerized charcoal.

Sample	Description	CK 80-80	CG 80-50	CG 0-50	AC 80-80	% H_2O equilibrium	Whetlerite analysis % Cr	% Cr^6	Cu	% Ag
BD 1518	Grade II PCI	27, 27	44	..	54	..	1.50	0.70	9.48	0.28
6731	Above rewhetlerized ASC–1 solution	64, 63	..	..	68, 71	24.4	1.97	1.81	5.07	0.25
BD 1518L	BD 1518 leached	...	..	..	..	..	0.06	0.02	0.50	0.14
6730	Above rewhetlerized EASC solution	68, 78	51, 45	..	69, 70	24.5	1.67	1.36	7.80	0.38
AD3 1549	Grade I PCI	39, 30	52, 50	49, 45	57, 57	26.1	1.56	0.89	5.70	0.20
6737	Above rewhetlerized ASC–1 solution	75, 65	49, 49	36, 31	103, 74	25.4	2.17	1.73	6.74	0.16
Above leached	.....	..	..	..	..	..	0.03	0.00	0.00	0.15
6732	Above rewhetlerized EASC solution	66, 70	..	..	68, 70	25.6	1.69	1.48	7.15	0.14

TABLE 31. Studies of the leaching process.

Sample	Treatment	% H_2O Pickup	Cr	Cr^6	$\frac{Cr^6}{Cr}$	Cu	Ag	M10A1 canister lives CK 80–80	M10A1 canister lives CG 80–50
TNW 6741R–A	PC518 whetlerized EASC solution	24.8	1.74	1.06	0.61	7.27	0.43	58, 60, 61	..
TNW 6741R–B	Product A leached	..	0.14	0.001	...	0.00	0.23	....	..
TNW 6741R–C	Product B whetlerized with ASC solution	25.2	1.61	1.40	0.869	7.19	0.57	76, 78, 78	..
TNW 6741R–D	PC518 (Activated charcoal) leached and dried as Product B, then whetlerized with ASC solution	26.4	1.54	1.21	0.786	6.08	0.29	66, 69, 71	..
TNW 6751R	PC518 boiled with 1/1 HCl and 2% CrO_3 (char basis), washed, dried, and whetlerized with ASC	24.7	1.51	1.18	0.782	9.04	0.24	61, 55, 59	56
TNW 6752R	PC518 boiled with 2*N* H_2SO_4 and 2% CrO_3; washed, dried and whetlerized ASC	25.1	1.58	1.10	0.692	6.79	..	56, 57	52
TNW 6758R	PC518 soaked in 1/1 HNO_3 for 15 minutes, washed, dried and whetlerized with ASC	25.2	1.48	1.25	0.845	6.07	0.16	74, 55, 66	41
TNW 6762R	TNW 6758R repeated	24.0	1.51	1.14	0.755	7.21	..	54, 71, 60	45
TNW 6763R	PC518 soaked 30 min in ASC solution, washed, boiled with 1/1 HCl, washed, boiled with 1/1 NH_4OH, washed, dried and whetlerized with ASC	23.2	1.65	1.16	0.703	8.79	..	53, 56, 53	54

rewhetlerization are slightly more effective than whetlerization alone, but not sufficiently so to justify the additional treatment.

The results on the use of oxidizing agents prior to whetlerization are not conclusive. Better results were obtained by double whetlerizations than by a whetlerization preceded by any other treatment.

In every case where production PCI whetlerites were leached and rewhetlerized, a very striking increase in CK 80-80 M10A1 canister life occurred. However, laboratory-prepared samples given the same treatment did not show as great an improvement, apparently because they were prepared under controlled conditions which initially came closer to realizing the full possibilities of the charcoal. It would appear that faulty plant operation was the cause of many mediocre or poor whetlerites. Admittedly the leaching and rewhetlerization process in itself does result in improvement, but the amount of improvement caused by this treatment does not account for the remarkable difference in CK 80-80 protection between some plant whetlerites and the leached and rewhetlerized materials prepared from them. Present plant practice usually produces excellent products, ordinarily as good as those prepared by laboratory procedures.

TABLE 32. Results of spraying or soaking Types A or AS whetlerites in chromium solutions.

Charcoal	Treatment	SA 80–80	AC 80–80	CK 80–80	% H_2O equilibrium
PCI–P58	Type AS sprayed with 3.4% aqueous CrO_3	45	123	82	23.1
PCI–P58	Type AS soaked with 3.4% aqueous CrO_3	32	139	116	25.0
PCI–P58	Type AS soaked in $(NH_4)_2\ CrO_4$, aqueous	...	139	204	...
PCI–P58	Type AS soaked in $(NH_4)_2\ CrO_4$ aqueous in excess NH_3	83	99	138	...
PCI–P58	Type AS soaked in ASC solution	161	136	172	...

CONVERSION OF TYPES A AND AS WHETLERITES TO TYPE ASC

In the early work on ASC whetlerite, it was found that a Type A whetlerite prepared from PCI charcoal could be converted to an ASC whetlerite having the good qualities of one prepared directly from the base charcoal in one step.[50] Spraying or soaking the Type A whetlerite with an aqueous solution of CrO_3 or with a solution of $(NH_4)_2\ CrO_4$ in excess ammonia resulted in a product with CK activity. Best results were obtained by soaking in an ammoniacal solution. Later results [82] indicate that even better results are achieved by the use of a solution containing carbonate. This behavior suggests again that the chromium and copper must be in chemical combination in order to be active, since both an ammoniacal and a carbonic solution favor the solution of copper from the Type A whetlerite, allowing it to combine with the chromate present in the solution before being redeposited upon the surface of the charcoal. In Table 32 are shown some tube test results obtained in experiments of this kind.[50]

It will be noticed that the best results on the basis of tube tests were obtained by use of an ASC solution. Later work on the solution used for conversions has shown that a solution containing 8% NH_3, 5% CO_2, 3.5% CrO_3, and 0.4% $AgNO_3$ produces the best results.[82] Presence of soluble copper, in addition to hexavalent chromium, is essential to the development of CK life; the solution described dissolves enough from the Type A whetlerite to produce a good product. An excess of copper tends to reduce PS life.

Not all Types A and AS whetlerites which are available in quantity can be converted to a satisfactory ASC whetlerite. These materials were produced from base charcoals made before the effects of pore structure of charcoal on its suitability for an ASC whetlerite were known. It is not possible to produce a Grade I whetlerite from base charcoal of some types, and it is equally impossible to convert Types A and AS whetlerites made from such base material into Grade I ASC. Various studies on this problem [68, 79, 80, 82] have shown that few of the converted whetlerites are Grade I because of: (1) failure in PS protection by PCI-converted whetlerites; (2) failure in SA protection by Atlas and Barnebey-Cheney Type A whetlerites (converted); (3) failure in CK protection by Barnebey-Cheney Type AS whetlerites (converted).

Type ASC whetlerites of borderline quality may be obtained by reimpregnation of existing stocks of Type A and AS whetlerites, with the probability of getting very little Grade I whetlerite, especially from Barnebey-Cheney charcoals.

It was thought that an additional activation treatment might possibly improve the qualities of certain Type A and AS whetlerites which could not be converted to ASC whetlerite. Experiments on reactivation have shown that such procedure is not fruitful. Reactivation seems to injure PCI and Atlas Type A whetlerites, and to have no effect on Barnebey-Cheney Type AS whetlerites.

At this time it does not appear that reworking charcoals is a useful process. Grade II whetlerites that can be improved by reimpregnation are used as backfeed to an extent governed by the quality of the product obtained. The materials that cannot be improved by any treatment are too poor to be used as backfeed. Because the only materials that can be treated by the reimpregnation process find a use elsewhere, there seems to be little advantage in developing the process further.

4.6 ORGANIC BASE IMPREGNATIONS OF CHARCOAL

4.6.1 Reactions of Certain Organic Bases with CK

The general reaction of CK with primary and secondary amines is as follows: [62]

$$RNH_2 + CNCl \longrightarrow HCl + RNH\text{-}CN \quad \left(\begin{matrix}\text{substituted}\\ \text{cyanamides}\end{matrix}\right)$$
$$R_2NH + CNCl \longrightarrow HCl + R_2N\text{-}CN$$

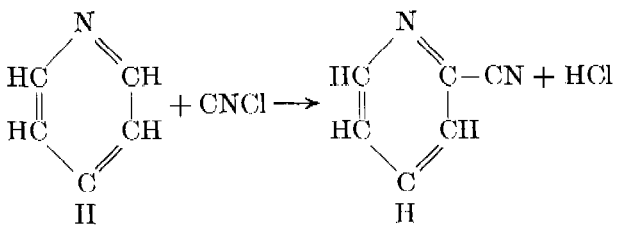
TABLE 33. Organic bases used as specific charcoal impregnants for CK.

Diethylene triamine	N-ethyl morpholine
Triethylene tetramine	N-aminoethyl morpholine
Tetraethylene pentamine	N-hydroxyethyl morpholine
Ethylene diamine	Piperidine
Diethanol diamine	Piperazine hexahydrate
Monoethanol amine	Ammonium nicotinate
Diethanol amine	Nicotine
Triethanol amine	Pyridine
Ethyl monoethanol amine	β-picoline
Ethyl diethanol amine	γ-picoline
Dipropyl amine	β-γ picoline, commercial mixture
Diisopropanol amine	Aniline
Dibenzyl amine	Imidazole
Benzyl ethyl amine	N-ethyl acetamide
Diisoamyl amine	Amino guanidine
Morpholine	Isoquinoline

The HCl formed reacts with excess amine to form the amine hydrochloride.

The reaction takes place readily and was the basis for the use of amines as specific charcoal impregnants for the absorption of CK. Extensive research has been carried out on a large number of organic bases in exploratory impregnations. Many of them have proven to be capable of yielding an absorbent with a rather large capacity for CK. A list of the organic impregnants which removed CK is shown in Table 33.[62, 63, 89] No attempt has been made to show the test lives of these materials because test conditions varied with the source of the experimental work. All materials shown produced an absorbent much better than the original unimpregnated charcoal.

Of these materials, the most useful appeared to be pyridine, the picolines, and N-ethyl morpholine. The reaction of CK with pyridine, and β- and γ-picoline is analogous to the reaction with a primary or secondary amine, except that it is the hydrogen atom on the carbon atom adjacent to the nuclear nitrogen which reacts thus:



α-picoline (α-methyl pyridine) is not active as a charcoal impregnant for CK because there is no reactive hydrogen on one of the carbon atoms adjacent to the nitrogen. Replacement of one α hydrogen by a methyl group apparently renders the other hydrogen inactive.

A number of the materials which produce good CK absorbent are unsatisfactory for use in a gas mask absorbent, due to desorption or decomposition, both of which result in an objectionable odor in the effluent air stream. Pyridine and the picolines when used in small quantities do not have these disadvantages and produce a useful absorbent.

4.6.2 Quality of Pyridine or Picoline Impregnated Charcoals

Pyridine or picoline impregnated charcoals are extremely active, having a critical layer depth of approximately one cm but they have a fairly low absorptive capacity. The absorptive capacity N_0 for a pyridine impregnated charcoal is of the order of 30 mg of CK per ml of absorbent. PCI-ASC whetlerite has an N_0 of from 80 to 190 mg of CK per ml of absorbent, depending on the base charcoal and the quality of the impregnation.[101] M10A1 canister CK lives are of the order of 25 min for the pyridine impregnated charcoals compared to a life of 60 to 70 min for a good ASC. A comparison of the properties of these materials is shown in Table 34.

Pyridine and picoline impregnated charcoals show very little, if any, aging effects.

Either pyridine or picoline can be used as an additional impregnant for Type A, AS, ASC, or ASM whetlerite. The properties of the original absorbent are usually retained practically unchanged, with the added advantage of a greater resistance to aging. Type A and AS, in addition, gain from the treatment some measure of CK protection although it is smaller than that of ASM or ASC. (The pyridine or picoline containing materials are designated by adding P or Pi, respectively, to the usual designation for the particular type of whetlerite in question.)

TABLE 34. Comparison of various types of whetlerites with pyridine and picoline containing absorbent PCI charcoal.

Impregnation	Comment	λc	N_0 g/ml abs.	CK 80–80 life 2.5-cm tube
None	initial life	2.91	9.7	4
3% pyridine, aqueous solution	initial life	2.15	23.4	11
AS solution	initial life	3.57	11.1	4
AS + 3% pyridine	initial life	3.48	30.5	6
ASC	initial life	1.90	83.7	32
ASC	aged 281 hr	2.93	63.2	8
ASC	aged 480 hr	3.65	54.0	5
ASC	aged 954 hr	4.48	34.5	3
ASC + 1% pyridine	initial life	1.69	68.5	33
ASC + 1% pyridine	aged 280 hr	1.73	48.5	21
ASC + 1% pyridine	aged 480 hr	2.15	55.4	22
ASC + 3% pyridine	initial life	1.58	38.5	18
ASC + 3% pyridine	aged 290 hr	1.97	36.5	18
ASC + 3% pyridine	aged 479 hr	2.03	23.3	14
ASC + 3% pyridine	aged 1440 hr	2.18	33.1	12
ASC + 3% pyridine	aged 1922 hr	2.36	31.4	9
ASC + 3% pyridine	aged 2401 hr	2.39	27.4	10
ASC + 3% picoline	initial life	2.13	69.0	23
ASC + 3% picoline	aged 247 hr	2.45	63.9	18
ASC + 3% picoline	aged 440 hr	2.67	61.9	17

The ability to confer great resistance to aging upon ASC whetlerites is the principal reason for the interest in these organic bases. The initial life of an ASCP whetlerite is very slightly different from those of an ASC, and in the M10A1 canister tests is usually slightly lower than that of the corresponding ASC.

The organic bases can be added directly to the original impregnating solution, and the impregnated charcoal is processed in approximately the same way as the usual ASC whetlerite, except that a lower maximum temperature is recommended.

The following conclusions are the results of numerous studies [47, 64] on these impregnants:

1. The method of introducing pyridine or picoline into the whetlerite does not affect the degree to which aging is retarded. The material may be added directly to the impregnating solution or adsorbed by the charcoal or whetlerite from a vapor-laden air stream.

2. The addition of pyridine to ASC whetlerite by vapor treatment does not result in an appreciable reduction of hexavalent chromium. There is some indication that addition of pyridine to the whetlerizing solution results in a lower hexavalent chromium content in the finished whetlerite than is found in a normal ASC.

3. Mixing pyridine-saturated whetlerite with untreated whetlerite is a convenient method of preparing vapor-treated whetlerite. Standing three days in a sealed container at room temperature resulted in practically complete redistribution of the pyridine.

4. The upper permissible pyridine concentration on PCI ASC whetlerite is 2%. Above this concentration the odor of pyridine becomes detectable. The upper limit for picoline is 3 g per 100 ml of solution. Both pyridine and picoline are selectively adsorbed from the impregnating solution.

5. Equilibration to 80% RH results in the evolution of considerable ammonia from some batches of ASCP whetlerite, but the amount of pyridine desorbed is not detectable by present analytical methods.

6. The introduction of a uniform, small concentration of pyridine or picoline into whetlerite in loaded canisters does not appear feasible by the aeration method since a tremendous volume of air would be required to distribute the pyridine.

7. A somewhat lower temperature than that used for ASC should be used to dry ASCP and ASCPi absorbents in which the pyridine or picoline is incorporated in the impregnating solution. At the normal temperature used for the laboratory preparation of ASC (180 C), frequent ignition of the pyridine or picoline-treated materials occurs. Because the presence of the organic base accelerates the release of volatile ammonia, a temperature of 150 to 160 C for 2 hr will produce a material which meets the ammonia specification.

Actual plant production of ASCP whetlerite has been carried out in the CWS impregnating plant at Zanesville, Ohio. The material (officially designated as Type E 11 impregnated charcoal) was produced with existing equipment without difficulty. The only

condition changed was the maximum drying temperature, which was lowered slightly. Type E 11 impregnated charcoal showed a slightly greater tendency to ignite than ASC whetlerite at the temperature ordinarily used for ASC plant production (400 F). At 370 to 390 F, no ignition occurred. The following observations were made at the time this particular plant production was carried out.[88]

1. Type E 11 impregnated charcoal gives slightly less protection in canisters against all gases than does ASC impregnated charcoal made from the same base charcoal. The extent of the loss in protection is approximately proportional to the amount of pyridine present.

2. The CK protection of Type E 11 impregnated charcoal decreases more slowly during moist closed storage at elevated temperatures in canisters than does Type ASC impregnated charcoal made from the same base charcoal. The use of pyridine, therefore, considerably lengthens the period during which a canister gives adequate protection against CK.

3. Type E 11 impregnated charcoal can be made in existing charcoal impregnating plants without difficulty.

4. Type E 11 impregnated charcoal can be dried at a lower temperature than Type ASC impregnated charcoal because pyridine appears to accelerate the release of volatile ammonia.

5. Seattle and PCI Type E 11 impregnated charcoals containing as much as 2% of pyridine showed no significant desorption of pyridine and possessed no odor of pyridine.

The inclusion of pyridine, picoline, or other organic bases in ASC whetlerite appears to be a useful method of improving the aging properties of this type of absorbent. If such an improvement proves to be necessary, practically no changes in existing plants, or plant procedures are required to convert to the new process.

It has been observed that aging toward CK of Type ASC whetlerite in canisters in the field is not as serious as first supposed. Hence the advantages of the use of pyridine or picoline are not as significant as laboratory tests indicated.

4.7 ABSORBENT RESINS AS SUBSTITUTES FOR ACTIVATED CHARCOAL

4.7.1 Introduction

Simultaneously with the developments in charcoal impregnation was the investigation of possible non-charcoal materials which might be used as gas mask absorbents. Two distinct types were investigated: (1) reactive materials such as granular magnesia, Hopcalite, and aminated Xerogels; (2) inert catalyst carriers such as silica gel, activated alumina, and kieselguhr which have no chemical reaction with adsorbates and act chiefly as catalyst carriers.

The first class of materials have a definite capacity for specific agents depending upon the amount of chemical reaction which occurs with the agent. The second group are able to adsorb vapors to some extent quite similarly to charcoal, and rarely have any chemical reactivity with the material adsorbed. They must be impregnated, just as charcoal, in order to gain a satisfactory capacity for specific materials. Class I materials have a definite disadvantage in that they have a negligible capacity for materials with which they do not react chemically.

Among inert absorbents, charcoal is far better than any other similar material in having a much larger surface area, a more diversified pore structure, and a greater absorptive capacity for capillary condensible gases. Silica gel, activated alumina, etc., are not suitable for impregnation with ASC solution. No results were obtained in the impregnation of materials of this type which compared favorably with the results of the charcoal impregnation.

In the search for a good CK absorbent many Class I (chemically reactive) materials mentioned above were tried. Granular magnesia and Hopcalite showed some ability to destroy CK at elevated temperatures, but none at room temperature. Attempts at impregnation of granular magnesia were uniformly unsuccessful.

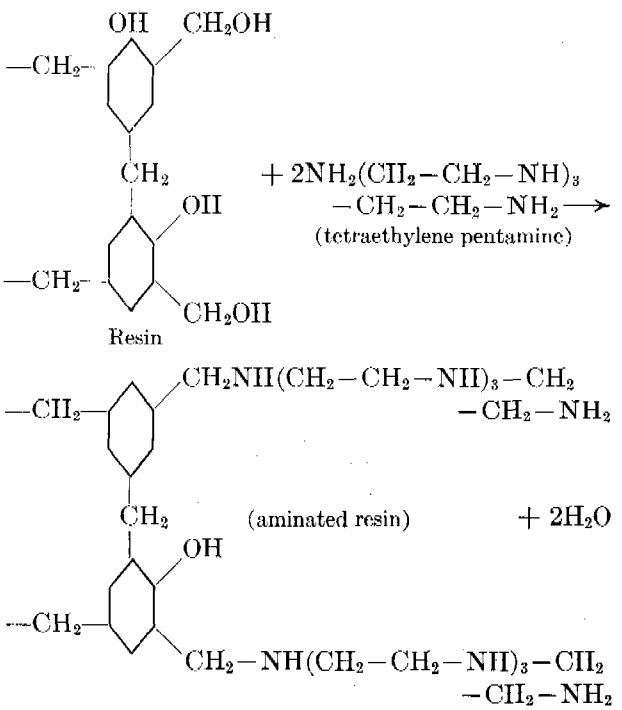
4.7.2 Aminated Phenol-Formaldehyde Xerogels[70]

Resins of this type were originally developed to purify water by removal of acidic ions. In conjunction with a hydrogen-ion exchange resin, they are capable of completely removing ions from aqueous solutions. In the preparation of such ion-exchange materials the phenol-formaldehyde resins were impregnated with a polyamine such as tetraethylene pentamine. The amine reacts to form a part of the resin structure, and yet retains part of its ability to act as an amine. For this reason the aminated resins react readily with CK and certain acid bases. By the addition of metallic constituents the resin can be

modified to absorb SA and AC. AC is apparently too weakly acidic to be removed by a neutralization reaction with the aminated resins.

4.7.3 Preparation

Aminated resins are prepared from porous phenol-formaldehyde resins. The porous resin is granulated, dried, and made to react with a polyamine, as follows:



The polyamine may react with one or more reactive $-CH_2-OH$ groups, but experiments indicate that a considerable portion of the polyamine molecules is attached to the resin by one bond only. The aminated resin may be pictured as a large porous granule, the exposed surfaces of which are covered with molecular flagellae. The length of the flagellae is determined by the kind of polyamine used in the amination process.

During amination the resins swell to an extent depending upon the amount of condensation which has taken place in the original resin. If over-condensed (few –OH groups remaining), the resin will not react with enough amine to produce a good product. Under-condensation results in too much amine entering the molecule. The result is that the resin swells uncontrollably and the mechanical strength of the product is poor. The resin finally chosen for amination was intermediate, and when aminated at 120 to 150 C it swelled about 100%. Upon removal of the excess amine and drying, a shrinkage of approximately 25% occurred. The resulting product had good mechanical strength and good absorptive capacity for CK.

The gas absorbing capacity of aminated resins is dependent almost entirely upon a chemical reaction of the gas in question with the aliphatic amine groups in the resin or with metallic impregnants introduced during preparation. Resin absorbents have very small surface areas compared to a good physical adsorbent like charcoal (see Chapter 6). Comparative values are shown in Table 35.[71]

TABLE 35. Surface areas of resins.

Adsorbent	Surface area from nitrogen adsorption sq m/g	Surface area from water adsorption sq m/g
Aminated resin TR–2	63.0	139
Aminated resin TR–4	62.5	188
Aminated resin TR–4A	59.5	148
Non-aminated resin HCR 5/25	164	···
Non-aminated resin HCR 3/9	108	···
Type A whetlerite	1400–1800	···

Because the surface area of aminated resins are approximately one-twentieth of those of whetlerites, it is apparent that their absorptive capacities must be dependent on chemical reaction rather than physical adsorption. In order to be useful for gas masks, such absorbent should be capable of a specific reaction with every possible type of toxic agent. Absorbents of the aminated resin type are at a distinct disadvantage, compared to charcoal, because their absorptive capacity for toxic agents which did not react probably would be small or nonexistent. The property of physical adsorption possessed by charcoal is a tremendous advantage.

Aminated resins exhibit an objectionable volume change with variation in the relative humidity of the air with which they are in contact. Swelling of from 15% to 25% occurs as the relative humidity varies from 0% to 100%. Between 21% and 71% relative humidity the corresponding resin volume changes are 8% to 12%. This is decidedly undesirable in an absorbent to be used in a gas mask canister. Impregnation with metals which form amine-complexes reduces somewhat the tendency of the resin to shrink as the relative humidity decreases. The effect of such impregnants is apparently to reduce the hydrophylic nature of the amine groups on the resin surface. This

results in an increased contact angle between the meniscus of the liquid in the pore and the wall of the pore. This, in turn, results in a less effective exertion of the constricting effect of the surface tension of the liquid. Therefore, the mechanical strength of the resin is better able to resist constriction. The overall effect is the lowered shrinkage of the resin. On this hypothesis resins with high mechanical strength should show negligible shrinkage, and indeed some resins do show these properties.

When amine resins, metal-impregnated or non-impregnated, are tested against CK at 0% RH, after having been dried at 50 C and 0% RH, they show a greatly reduced capacity. This loss of activity does not extend to such gases as AC, SA, and HCl. When the resins, dried as above, are tested against a gas stream of CK at 80% RH, a normal life is obtained, indicating that enough moisture is taken up from the gas stream to restore its activity. A possible explanation is that the molecular flagellae, with which the CK reacts, may be coiled up against the surface when dry, and hence are not available for reaction. The presence of moisture makes the flagellae again available for reaction. If this is true, then the use of a material such as glycerine to keep moisture on the surface, or the complete replacement of the moisture by a high molecular weight hydrocarbon (the replacement of the water film by an oil film to keep the flagellae in an extended position) should result in resistance to deterioration upon drying. Accordingly, glycerine and clear mineral oil were applied to aminated resin to test this hypothesis. Both failed to alter the properties as desired. The treated materials had fair CK protection at 0-80 conditions, but had very slight protection at 0-0 conditions.

Shrinkage can be reduced to about 9.6% for the aminated resin, and to 6.6% for the Ag_2O impregnated resin in a change of RH from 0% to 100%, by careful control of preparative conditions and the addition of a small amount of an aliphatic long chain amine in isopropyl alcohol to the amination solution.[72]

4.7.4 Impregnation of Aminated Resins

Aminated resins are impregnated with metallic constituents capable of forming stable complexes with amines. Impregnation is accomplished by adsorption from aqueous solution. Copper, silver, nickel, chromium, and zinc have been used. Silver must be present to effect the removal of SA, but presence of other metals with silver seems to improve the action. SA removal is presumably catalytic oxidation as in the case of whetlerites. AC appears to be removed by complex formation with the metal impregnants. Apparently the metals combine with the resin by formation of the normal ammonia-type complex. Aminated resin capable of absorbing two moles of hydrochloric acid can absorb one-half mole of copper, indicating that each mole of copper combines with four moles of amine, probably in the usual amine-complex form $[Cu(RNH_2)_4^{++}]$. It is possible, of course, that part of the copper or other complex-forming metal may be absorbed as the mixed aquo-ammino complex.

4.7.5 Effect of Impregnants

The general effect of the impregnants on each gas considered may be summarized as follows:

CK

With the exception of Ag_2O, all metallic impregnants tend to reduce CK protection. The effect is greater when the impregnant is in the form of a salt than when in the form of an oxide.

SA

Silver must be present to effect removal of this gas, which is removed by catalytic oxidation. Silver may be present as metal, compound, or oxide. Other metallic constituents present as oxides promote the catalytic effect of silver, although they have no effect in the absence of silver.

AC

AC is too weakly acidic to be removed by amine-cyanide salt formation. Oxides of metals capable of forming stable cyanides remove AC in proportion to the amount of metal present. Metals capable of forming cyanide complexes are particularly efficient. Cupric copper is avoided because of the possible formation of cyanogen. Impregnation has little effect on the capacity of aminated resins for HCl. Metal oxides may improve the HCl capacity slightly. The effect is similar to that for other active acid gases.

CO

Sodium nitroprusside reacts with both carbon monoxide and amines. Hence, by reaction with aminated resin, sodium nitroprusside is incorporated into the resin, thereby conferring an absorptive ca-

pacity for CO on the resin. The reactions proposed are:

$$\underset{\text{Resin}}{RNH_2} + Na_3[Fe(CN)_5NO] \longrightarrow$$

$$R[-NH_2Fe(CN)_5]Na_3 + NO$$
nitroprusside impregnated resin

and

$$R[-NH_2Fe(CN)_5]Na_3 + CO \longrightarrow Na_3[Fe(CN)_5CO] + RNH_2$$

The reaction with carbon monoxide is not very rapid. Resins prepared in this way showed a 90% penetration by a 0.1% CO test mixture after 5 min. The resin is not effective enough to be useful in a canister, but may be developed into a satisfactory material for other purposes.

Silver nitrate-nickel nitrate impregnated aminated resins and ruthenium chloride impregnated aminated resins also show some carbon monoxide capacity.

4.7.6 Evolution of Ammonia from Aminated Resins

A distinct disadvantage of aminated resins as gas mask absorbents is the evolution of ammonia when used. Intolerable concentrations are found in the effluent stream from certain resins at normal breathing rates. Oxygen, moisture, and free alkali are active in promoting ammonia evolution. The ammonia is attributed to (a) action of water and oxygen upon the resin amine groups, with the formation of alcoholic groups and ammonia, and (b) the action of ammonia present in the commercial tetraethylene pentamine on the resin, producing an aminated resin which is split hydrolytically by moisture to form an alcohol and ammonia.

Use of an anti-oxidant to reduce reaction (a) resulted in decreased SA protection without appreciable decrease in ammonia evolution. The best resins from the point of view of low ammonia evolution were produced by washing the aminated resin with water prior to impregnation with silver oxide. The resulting impregnated aminated resin had only a slight odor of ammonia.

4.7.7 Other Types of Absorptive Resins

The very reactive $-CH_2-OH$ groups in phenol-formaldehyde resins are capable of reacting with substances such as Na_2HSO_3, H_2S, PH_3, etc. The resulting resin contains the groups $-CH_2$, $-SO_3H$, $-CH_2-SH_3$, $-CH_2-PH_2$, et cetera. These reactive groups in turn are capable of a variety of reactions and therefore offer the possibility of the development of a specific absorbent for any particular material of known chemical properties.

Chapter 5

SURVEILLANCE OF IMPREGNATED CHARCOAL

By *W. Conway Pierce* and *Thurston Skei*

5.1 INTRODUCTION

NEXT TO INITIAL PROTECTION the most important requirements for a gas mask canister are that the adsorbent shall not deteriorate with age and that the canister shall have mechanical strength to remain effective after rough usage. While it would be possible to provide for frequent and periodic replacement of gas mask canisters, this would entail a tremendous additional burden on supply organizations. It is highly desirable to provide canisters whose lives under normal conditions of use are in excess of 6 to 12 months. Throughout the gas mask development program much emphasis has been placed upon surveillance and rough-handling characteristics.

Prior to the development of ASC whetlerite, the only surveillance problem concerning the gas adsorbent was the effect of moisture on performance. It is now well established that canisters issued to field troops pick up moisture to an amount depending upon the prevailing relative humidity. This happens whether the canisters are used or not, but the rate of water pickup is much faster if the canisters are being worn. A canister worn for 10 to 15 hours in rainy weather may be completely equilibrated with water vapor. In the tropics, the equilibrium amount of water adsorbed by charcoal is about that which corresponds to equilibration at 80% RH.

The Type A whetlerite used in U. S. canisters prior to 1943 was fairly stable indefinitely as long as it remained dry. In the period before the war, gas masks were packaged in tin cans to insure dryness of the charcoal until the mask was issued. After a mask was issued, the protection against some gases fell off rapidly as water was picked up by the charcoal. The protection against CG was not affected, but the PS and AC protection was lowered somewhat, the latter because of the C_2N_2 penetration which occurred when a humidified canister was exposed to AC:

$$2HCN + CuO \xrightarrow{\text{moist}} Cu(CN)_2 + H_2O$$
$$2Cu(CN)_2 \longrightarrow 2CuCN + C_2N_2.$$

The CK and SA protections fell to nearly zero as the moisture content approached the saturation value.

Because of the effect of moisture on protection and the knowledge that moisture is absorbed when canisters are used, the British have (and still do) "wet up" the charcoal in manufacturing. They use a coppered charcoal which is sprayed with dilute silver nitrate [a] solution to a water content about two-thirds the moisture saturation value [MSV]. By addition of water, CG protection is gained without use of the heavy CuO impregnation which is necessary to impart dry CG protection. After humidification, the gas protection of the British canister is about the same as that of corresponding U. S. canisters with Type A whetlerite; both are weak in CK and AC protection.

The recognized weakness in 80-80 CK protection led to attempts at improvement.[17, 21] The most promising of these, prior to the ASC development, was the thiocyanate treatment (see Chapter 4). This was never put into production because Type E 6 whetlerite was not stable in storage.

The problem of CK protection at high humidity, as well as improved AC protection, was solved by the development of the ASC process which went into production in 1943. Shortly after this process was developed it was discovered that it, too, had surveillance problems. When an ASC whetlerite has become humidified and is then stored in absence of air, particularly at elevated temperatures, its effectiveness toward CK and AC decreases and, in the limiting case, the protection becomes equivalent to that of humidified Type A whetlerite. In normal times, adoption of the ASC process would doubtless have been postponed for perhaps a year or two, pending a thorough surveillance study. However, because of the emergency and the knowledge that ASC at its worst

[a] Silver nitrate is added to impart SA protection. This is perhaps unnecessary, since no good method has yet been found to disperse SA; but since it adds little to the cost, the use of silver is continued as a precaution. The same is true of silver in U. S. ASC whetlerite.

would never be inferior to Type A whetlerite, it was decided to initiate production and, if necessary, provide for frequent canister replacements. Concurrently, very extensive surveillance tests were made.[1] Current opinion is that the aging of ASC whetlerite under field conditions is not a serious problem, but it is recognized that some loss in protection does occur with use and that a canister cannot be continued in service indefinitely. The experimental programs and the data on which these conclusions are based are reviewed in the following sections.

5.2 SURVEILLANCE METHODS

5.2.1 Early ASC Surveillance

The first studies of the stability of ASC whetlerites were made under conditions which were known to give accelerated aging. Equilibrated samples were stored in sealed bottles [2, 3] at elevated temperatures, up to 85 C. Control was by CK life tests, since it had been found that the first and most important effect in aging was a loss in CK protection. At this stage tube tests were used, since the available sample was usually small. From these early tests the following facts became apparent: [1]

1. Tube tests are not reliable indices of the protection given by a sample in the thin-bed canister such as the M10, which was in use at the time of the tests. A sample which appeared to have undergone a slight decrease in effectiveness, as judged by the tube test life, might give zero life in an M10 canister. Later, it was recognized that the first step in aging is an increase in the critical depth while the capacity remains about constant. Because of this, the tube life did not drop greatly until the sample was badly aged. This is shown in the tube and canister data of Table 3 in Chapter 2.

2. The accelerated aging was too severe. All samples soon lost CK protection and became equivalent to Type A whetlerite. This extreme aging did not permit any conclusions regarding the stability which an ASC-filled canister might have in field usage where conditions are not so drastic.

3. The rates of aging were found, even by tube tests, to vary from one type of charcoal to another. This is discussed later.

4. The presence or absence of air and the moisture content of the charcoal played important roles in the rates of aging.

5.2.2 Canister Aging Programs

When it was recognized that absence of air and elevated temperatures drastically accelerate aging, and that canister tests are necessary for control of aging programs, the attempts to conduct accelerated aging programs with tube tests were discontinued. Instead, efforts were made to set up conditions similar to those found in the field. With these changes, it was realized that accelerated aging procedures may produce misleading results because of effects which may not be present in normal use of a canister.

A variety of conditions has been employed in the aging studies of the Chemical Warfare Service [CWS] and National Defense Research Committee [NDRC] laboratories.

Edgewood Arsenal Chambers [15]

To simulate various climatic conditions the following canister storage chambers are used at Edgewood Arsenal:

1. Arctic: operated at −40 F and saturated RH.
2. Desert: operated at 150 F and 10% RH.
3. Tropical: operated at 113 F and 87% RH.

Canisters are either placed open in these chambers and allowed to take up moisture or, in some tests, particularly in the tropical chamber, pre-equilibrated canisters may be used.

NDRC Cyclic Chamber [1, 7]

This chamber was designed to operate with cyclic-temperature changes to simulate day and night variations, on the assumption that the "breathing" of canisters might have a different effect on aging than constant temperature conditions. Daily operation was for eight hours at 130 F and 60% RH, and sixteen hours at 90 F and 90% RH. There was some lag in the transition period from one condition to the other. A continuous automatic record was kept of both temperature and humidity.

Storage Methods. A variety of storage methods was tried in the NDRC cyclic chamber as questions arose about the correlation of laboratory and field results. The following were used for bulk charcoal:

1. Closed-dry: samples were sealed in pint fruit jars, with *as received* moisture contents. This represented unused canisters in storage.

2. Open-dry: samples were originally dry but were stored in open containers which permitted access to humid air. These represented canisters after issue, originally dry, but exposed to atmospheric humidity.

3. Open-wet: equilibrated samples (80% RH) were stored in open containers.

4. Closed-wet: equilibrated samples were stored in tightly sealed jars. This condition represented canisters which had been used, then tightly stoppered by plugging the inlet and outlet.

Since storage of bulk charcoal was always open to the objection that reloading into test canisters would mix the outer and inner portions (which might have different moisture contents) the more important surveillance programs were carried out with four types of preloaded canisters stored in a variety of conditions.

The Types of Canisters. The four types of canisters used included the following:

1. M10, old style, 5/8-in. baffle.[b]
2. M10, new style, 1/4-in. baffle.
3. M10A1.
4. M11.

Storage Conditions. The more important storage conditions were:

1. Sealed-dry: canisters were sealed, as in normal depot storage. This simulated depot storage in a tropical climate.

2. Open-dry: canisters were stored with the inlet valve in place but with the nozzle open so that there was free access to moist air. This represented the condition of canisters issued to troops, that were not used but stored in carriers permitting free access to air.

3. Sealed-partially equilibrated: this represented canisters which had picked up some moisture in the assembly plant and had then been sealed and put in depot storage.

4. Open-wet: canisters were equilibrated at 80% RH, then stored open. This condition partially simulated canisters which had been worn a few hours in a humid climate and were then stored where they might have access to fresh air.

5. Open-wet carrier: limited numbers of canisters were stored wet, completely assembled in the carrier with which the canister is normally used. This condition was the most realistic approach to actual field use since the assembled mask in its carrier does not have completely free air interchange with the surrounding atmosphere. Of particular interest were the tests with M11 canisters in M7 carriers, which are practically airtight.

[b] The baffle in radial-flow canisters covers the end sections of the central tube. Its function is to prevent a gas channel at the top or bottom of the adsorbent bed if the packing should become loosened by rough handling. The first M10 canisters had a baffle 5/8 in. in length, but later this was changed to 1/4 in. to gain the added protection of an additional length of charcoal at each end.

Field Tests

From the beginning, it was realized that laboratory aging tests were useful to indicate the relative stability of samples, but that there was not a direct correlation between the useful lives in laboratory surveillance and in the field. It was very difficult, however, to obtain canisters of known history which had been in field use in tropical climates, and it was not until February 1945, that reliable data were obtained for canisters of known history. The available field test data are the following:

1. Wearing tests (I) at Camp Sibert, Alabama.[4,5] In the summer of 1943, canisters with various types of absorbents were issued to troops at Camp Sibert. These were used in normal training activities for three months, then withdrawn for gas testing.

2. Wearing tests (II) at Camp Sibert. Following a wearing period from September 1943 to May 1944,[6] canisters were tested against gas.

3. Canisters from Finschafen.[20] In September 1944, wearing trials were conducted at Finschafen, New Guinea, for the purpose of obtaining data on the magnitude of ammonia evolution under tropical conditions. At the conclusion of these tests, selected M1, M10, and M10A1 canisters were sent to the United States for gas tests. The canisters did not arrive until early in 1945, almost a year after some of them had been issued.

4. Miscellaneous canisters returned to Edgewood Arsenal for testing. Numbers of canisters have now been gas-tested at Edgewood Arsenal, after return from the field. Unfortunately, in most cases, there were not any data regarding the date of issue, the amount of wear, the amount of water picked up in the field, and the amount of time spent in the tropics.

5. San José canisters.[1] Selected canisters were equilibrated at 80% RH, assembled with the mask, and stored for three months in the open at San José Island near Panama. They were then returned to the laboratory for gas tests. Both M10A1 and M11 canisters were used, each stored in the carrier normally used.

5.2.3 Results of Aging Studies of ASC Whetlerites

This section presents a résumé of the present knowledge regarding the aging of ASC whetlerites

and the factors which contribute to, or accelerate, the rate of deterioration. From the thousands of tests which have been made, quite definite conclusions can now be drawn. These are based chiefly upon data from NDRC reports, but are confirmed by extensive data from the CWS laboratories.[11–14]

Moist Storage

When an ASC whetlerite is stored moist, the following changes occur:

1. The 80-80 CK protection drops to that of the base charcoal; that is, the effect of the impregnant disappears.
2. Hexavalent chromium is reduced to the trivalent state. There appears to be, for a given sample, a correlation between the rate of loss in CK protection and the rate of reduction of chromium.
3. The AC protection at high humidity decreases, but at a slower rate than the CK protection. Eventually, the AC protection becomes that of Type A whetlerites.
4. There is some decrease in CG protection.[7, 8] This appears to be due to a decrease in activity of the adsorbent and not to a change in capacity. It is not of practical importance.
5. The protection for SA and PS is not affected by aging but is dependent upon the water content of the charcoal.

Rate of Aging

The rate of aging is affected by the following factors:

1. Presence or absence of air.[2, 3] Moist samples in a sealed container age far more rapidly than if free access to air is permitted. Oxygen is consumed and carbon dioxide formed in the aging process. In a sealed container, all the oxygen may be used.
2. Amount of moisture adsorbed. Partially equilibrated samples age more slowly than those which contain saturation amounts of water. The end result on prolonged storage is the same regardless of the water content.
3. Temperature of storage. There is a large temperature coefficient for the reactions which occur on aging. Numerical values for this temperature coefficient have not been determined, but all data indicate that as the temperature is elevated, aging is accelerated.

Dry Storage

Samples which are stored dry and kept in a dry condition are quite stable. Canisters in depot storage probably remain usable for years if they are originally dry and are kept dry. At present replacement canisters are sealed in tin cans at the time of manufacture. It is extremely important to take every possible precaution to insure that no moisture is picked up by the charcoal prior to sealing, since even slight amounts of moisture eventually cause aging, particularly in the absence of air. In humid weather, any delay in the assembly line may easily permit adsorption of enough water to cause aging. An M10A1 canister should not contain more than 5 to 10 g of water when put into storage and preferably the amount should be less than 5 g.

Rate of Aging

The rate of aging varies with the base charcoal used. This is illustrated in the accelerated aging data from Edgewood Arsenal shown in Table 1 for a variety of base charcoals. Available data indicate that the rate of field aging is relatively in the same order for these samples as in the accelerated aging.

Several points of interest may be noted in Table 1.

1. The M10 canisters subjected to sealed-wet aging at 113 F had aged badly in three days. From other data, it is now known that this is due to a rapid increase in the critical bed depth for CK and that at slower flow-rate tests these canisters might still give good protection.
2. From the open-wet data for M10A1 canisters it is seen that PCC, Seattle, and Atlas apricot charcoals give the best initial lives and stability and that most of the nut-shell charcoals deteriorate rapidly. It is because of this that most of the present production is of PCC and Seattle charcoal (see Chapter 3).
3. When the canister is stored open-dry in a humid atmosphere, the rate of aging is far less than if the charcoal is equilibrated before storage.

In view of the varying stability exhibited by different base charcoals, present whetlerite specifications (No. 197-52-123 C, December 20, 1944) contain a stability clause:

> *Accelerated Aging.* The Grade I impregnated charcoal aged for 7 days (168 hours) as described in C.W.S. Pamphlet No. 2, Part II, Section N, and tested as prescribed in Paragraph F-8b shall have a minimum life of 20 minutes against CNCl and the life after aging shall be at least 40.0 per cent of the initial life.

CK Protection Effect

The first effect noted for CK protection on aging is an increase in the critical bed depth. (See Table 7.) Later, as aging proceeds, there is a drop in capacity

TABLE 1. Summary of tropical storage surveillance data, ASC impregnated charcoal.

Charcoal base	Lot No.	Approximate date of mfg.	Type canister	Concn. CK mg/l	CK gas lives 80–80, 50 lpm				Type* stored	References
					Original min	After simulated tropical storage				
						3 days min	7 days min	14 days min		
Atlas W	ID–239	1943	M10(⅝″)	4	14, 16	3.3	2	2, 1.5	A	TCIR 35
Atlas OW	ID–244	1943	M10(⅝″)	4	12, 14	2.5, 2.5	1, 2	2, 1	A	TCIR 35
Atlas OA	ID–251	1943	M10(⅝″)	4	12, 14	2, 3	1, 1.5	1.5, 1.5	A	TCIR 35
Seattle	HD–140	1943	M10(⅝″)	4	14, 16	4, 3.5	2.75, 2	3	A	TCIR 35
PCC	AD–255	Sept. 1943	M10(⅝″)	4	21, 23	6, 7	6, 5	4, 4.5	A	TCIR 35
PCC	BD–1063	Jan. 1944	M10A1	4	57	48	40	41	C	TCIR 153
PCC	AD–255	1943	M10A1	4	43	31	27	15	C	TCIR 210
Seattle	HH–529	....	M10A1	4	50	..	30, 31	..	C	TCIR 210
Seattle	HH–531	....	M10A1	4	43	..	22, 27	..	C	TCIR 210
BC pecan	CC–1105	1944	M10A1	4	44	14, 25	16, 12	18, 19	C	TCIR 189
BC pecan	..	1944	M10A1	4	26	12	5	..	C	TCIR 210
BC flash bake coal	..	1944	M10A1	4	35	30, 30	11, 21	19, 20	C	TCIR 179
BC std extruded coal	..	1944	M10A1	4	46	31	16, 28	21	C	TCIR 179
BC mixed nutshell	..	1944	M10A1	4	53	36, 33	15, 20	26, 20	C	TCIR 179
BC peach pit	..	1944	M10A1	4	29	21, 25	9, 11	12, 16	C	TCIR 210
Atlas apricot	..	1944	M10A1	4	82	..	52, 56	..	C	TCIR 210
Atlas walnut	..	1944	M10A1	4	56	..	3, 3	..	C	TCIR 210
						2 months min	4 months min	6 months min		
BC	A–116	1943	M10(⅝″)	2.5	21	7	3	2	B	TCIR 110
Seattle	HD–140	1943	M10(⅝″)	2.5	55	26	6	5	B	TCIR 115
Atlas	ID–244	1943	M10	4	10	4	2	1	B	TCIR 172
Atlas	ID–239	1943	M10	4	21	5	3	1.5	B	TCIR 175
PCC	AD–255	1943	M10	4	26	13	5	4	B	TCIR 158
Atlas W	ID–251	1943	M10	4	18	5	4	1.5	B	TCIR 185
National Carbon	196B1X	1943	M10	4	35	23	6	2	B	TCIR 188
Seattle	Composite of July 1944 production		M11	4	32, 29	18, 21, 15 (D)	..	..	B	..
PCC	same		M11	4	25, 27.5	27, 27, 22 (D)	..	..	B	TCIR 188
BC pecan	same		M11	4	26, 21	8, 8, 6.5, (D)	..	..	B	TCIR 188

* A Canisters equilibrated to 80 per cent relative humidity and sealed airtight before storage.
B Canisters stored with open nozzles, *not* equilibrated before storage.
C Canisters equilibrated to 80 per cent relative humidity, then stored, with nozzles open.

and a further increase in critical bed depth. Because of the bed-depth effect, aging occurs far more rapidly for a thin-bed canister, such as the M10, than for one of thicker bed depth, such as the M10A1 or M9A2. Another consequence is that a canister which is apparently badly aged, as tested at high flow rate, may still give excellent protection at a lower flow rate. This is shown in the data of Table 2.

TABLE 2. CK lives at different flow rates M10A1 canister. Life in minutes.

Condition	50 lpm	16 lpm
Original	40	280
Aged	5	120

Since a flow rate of 16 lpm is far more typical of breathing rates under normal exercise conditions than 50 lpm, which corresponds to very vigorous exercise, a badly aged canister may still give very good protection against CK. Further data in substantiation of this are shown in the following section.

CANISTERS USED IN FIELD

The overall picture for canisters which have been used in the field for various lengths of time is quite reassuring.

New Guinea. Canisters from wearing trials in New Guinea were shipped to the United States in September 1944. These canisters had been worn for 14 hr. Some were freshly issued from depot stock and others had been issued at the POE in May 1944. Data for the water contents and gas lives are shown in Table 3. Since the tests were made in February 1945, the period of use may be taken as the total

SECRET

TABLE 3. Data for used canisters from New Guinea.

Date issued	Can. No.	Type can.	Type char.	Lot number	Grams H_2O at start of wearing test	Grams H_2O end of wearing test	Grams H_2O as received at laboratory	Grams H_2O at 80% RH	ΔP mm H_2O 85 lpm	Life in min 50 lpm	Life in min 25 lpm
CK AR–80 performance 4 mg/l, SIP indicator											
5/44	621	M10	AD	JJ–3–4–6	23	31	44	..	60	24	173
5/44	622	M10	AD	JJ–3–4–5	23	32	44	..	57	18	155
8/31/44	718	M10A1	HH	SC–12–4–2	4	19	36	..	55	84	299
8/31/44	719	M10A1	CC	EV–10–4–5	7	23	40	..	55	52	229
1943	894	M1A1	AD	EV–C941–6A	..	..	..	..	58	3	42
CK 80–80 performance 4 mg/l, SIP indicator											
5/44	623	M10	BD	JJ–4–4–3	33	33	45	49	58	13	135
5/44	626	M10	AD	JJ–3–4–5	24	31	44	50	58	14	151
8/31/44	726	M10A1	HH	SC–10–4–12	5	14	32	53	50	48	214
8/31/44	736	M10A1	CC	EV–10–4–5	6	17	34	57	59	23	210
1943	896	M1A1	AD	EV–C941–6A	..	..	..	2.4*	61	2	36
AC AR–80 performance 4 mg/l, AgI indicator											
5/44	629	M10	AD	JJ–3–4–5	20	28	42	..	59	49	...
8/31/44	832	M10A1	CC	EV–10–4–5	6	34	45	..	57	53	...
AC 80–80 performance 4 mg/l, AgI indicator											
5/44	627	M10	AD	JJ–4–4–2	23	29	44	52	53	43	...
8/31/44	722	M10A1	HH	SC–15–4–2	6	22	35	57	55	58	...
8/31/44	7110	M10A1	CC	EV–10–4–5	5	14	38	61	54	50	...
CG AR–50 performance 10 mg/l, KI–acetone indicator											
8/31/44	7111	M10A1	CC	EV–10–4–5	7	19	38	..	55	49	...
CG 80–50 performance 10 mg/l, KI–acetone indicator											
5/44	631	M10	AD	JJ–3–4–5	23	30	44	51	60	19	...
8/31/44	721	M10A1	HH	SC–15–4–2	5	17	30	56	50	56	...
SA 80–80 performance 4 mg/l, $KMnO_4$–HgI_2 indicator											
5/44	632	M10	AD	JJ–3–4–5	23	26	41	52	55	57	...
8/31/44	7210	M10A1	HH	SC–10–4–12	4	12	32	58	52	>75	...

* M1A1 canister No. 896 was almost equilibrated when received. It adsorbed only 2.4 g more of water at 80% RH.

elapsed time from the date of issue to February 1945. In shipment, the canisters were intentionally left unstoppered, to permit at least a limited access to air. Weights were recorded before and after the wearing period, and after arrival in the U. S. some canisters were tested as received and some at 80-80.

The data of Table 3 show that the CK protection was still good, particularly at a 25 lpm flow rate, and protection for other gases was apparently unimpaired, as judged by comparisons with data for fresh canisters. The water content of the used canisters was almost up to the 80% RH equilibrium value, but the M10A1 canisters which were issued from depot stocks at the start of the test had gained only about two-thirds the saturation value.

These tests provide the most reliable information available at present for field aging, and they indicate that average M10 and M10A1 canisters in the field give good protection.

CBI Theater. Tests at Edgewood Arsenal on M10

SECRET

TABLE 4. Data for used canisters from CBI theater.

No.	Type	Humidity Can	Humidity Air	Flow lpm	Gas	Concentration life mg/l	Concentration life min
4145B	MIXA1	AR	80	50	CK	4	3
4148B	MIXA1	AR	80	50	CK	4	7.5
4152B	MIXA1	AR	80	50	CK	4	4.5
4155B	MIXA1	AR	80	50	CK	4	3.5
4174D	M10	15	80	50	CK	4	27
4176D	M10	AR	80	50	CK	4	19
4177D	M10	AR	80	50	CK	4	16
4180D	M10	80	80	50	CK	4	5
4180D	M10	80	80	25	CK	4	55
4192D	M10	80	80	50	CK	4	6
4192D	M10	80	80	25	CK	4	74
4194D	M10	80	80	50	CK	4	23
4195D	M10	80	80	50	CK	4	14
4195D	M10	80	80	25	CK	4	84
4146B	MIXA1	AR	80	50	SA	4	17
4150B	MIXA1	AR	80	50	SA	4	27
4154B	MIXA1	AR	80	50	SA	4	3
4156B	MIXA1	AR	80	50	SA	4	13
4178D	M10	80	80	50	SA	4	40
4179D	M10	80	80	50	SA	4	52
4181D	M10	80	80	50	SA	10	7
4182D	M10	80	80	50	SA	10	6
4158B	MIXA1	AR	50	32	CG	20	70
4183D	M10	AR	50	50	CG	10	18
4184D	M10	AR	50	50	CG	10	20
4189D	M10	AR	50	32	CG	20	34
4187D	M10	AR	50	32	AC	10	23
4188D	M10	AR	50	32	AC	10	25
4144B	MIXA1	AR	50	32	PS	50	26
4151B	MIXA1	AR	50	32	PS	50	17
4185D	M10	AR	50	32	PS	50	10
4196D	M10	15g H_2O	50	32	PS	50	19

and MIXA1 canisters used by troops in the CBI theater gave the data of Table 4. The MIXA1 canisters contained only about 9 to 17% moisture when received, indicating that they had been used very little and had been kept in a rather dry place. M10 canisters contained about 30 g of water or three-fourths the MSV at 80% RH. MIXA1 canisters were tested as received; part of the M10 canisters were equilibrated before testing, some were dried, and some were tested as received. Breather tests were made at 50 and 25 lpm and constant flow tests at 32 lpm, the choice depending upon the conditions in use for the various gases.

The data of Table 4 show that the CBI theater canisters have aged in CK protection but that the life is still good at low flow rates. There is no obvious deterioration in the protection for other gases. Since the M10 canisters were from a lot manufactured in 1943 and the tests were made in 1945, it would appear that, in general, the canisters used in the field give adequate protection. The data for MIXA1 canisters were included merely for a comparison as they are not currently used by combat troops. Obviously these canisters are weak in CK and SA protection.

San José Island. Few data are yet available for field surveillance of the M11 canister. In view of the known fact that free access to air is beneficial in preserving CK protection of moist ASC whetlerite, it has been feared that the M11 canister stored in its airtight carrier will not stand up as well as M10 and M10A1 canisters. Laboratory findings confirm this view. Only one carefully controlled field experiment has been reported. Fresh canisters were equilibrated at 80% RH and stored, assembled with the mask, in the regular carriers from April to September 1944 at San José Island, a typical tropical location with prevailing high humidity and a mean temperature of 80 to 90 F. CK test data for these canisters are shown in Table 5. It is seen from these data that the M11 canisters deteriorate much more rapidly than M10A1 canisters but that after 5 to 6 months (elapsed time from equilibration to testing) there is still ample protection at 25-lpm flow rate. These data do not indicate that M11 canisters in the field at present have

TABLE 5. Comparison of CK protection for M10A1 and M11 canisters aged in carriers for 5 to 6 months.

No.	Type	Filling	H_2O canister grams	CK life (breather pump)* 50 lpm	25 lpm
Control	M10A1	PCI	25	43	..
Control	M10A1	PCI	25	46	..
1	M10A1	PCI	26	36	..
2	M10A1	PCI	27	24	..
3	M10A1	PCI	26	36	..
Control	M11	Seattle	33	21	..
Control	M11	Seattle	33	22	..
Control	M11	Seattle	33	25	..
Control	M11	Seattle	33	22	..
4	M11	Seattle	33	2	70
5	M11	Seattle	34	3	81
6	M11	Seattle	32	11	102

* The 25-lpm tests were made following 50-lpm tests to a break and lives are computed as additional 25-lpm life plus 2 × 50 lpm life.

deteriorated to this extent, for in a non-gas condition these canisters have not been worn much and, stored in the airtight M7 carrier, the majority of canisters have probably picked up very little water. If an emergency should develop it would be possible to screen out doubtful canisters very rapidly by weighing, since all M11 canisters show the original weight at the time of manufacture. Those whose weight-gain was slight could be considered safe, and probably even those with weight-gains of 20 to 30 g might give adequate protection.

Camp Sibert. The field tests on M1XA1, M10, and M10A1 canisters at Camp Sibert agree with the previously cited data for canisters from tropical theaters. As might be expected with a temperate climate, the rate of aging at Camp Sibert is less than in the tropics and the rate of water pickup is less. There is a decrease in CK protection, but no marked effect for other gases other than the effect of humidification. It seems safe to conclude that ASC-filled canisters used in this country have a useful life of well over a year, and perhaps much more.

5.2.4 Surveillance of ASM and ASV Whetlerites [1,9]

Early in 1943 the surveillance results with ASC whetlerite that had aged sealed-wet (under accelerated conditions) caused considerable alarm and the search for other impregnants which would be more stable was intensified. The most promising of the other impregnants were made by replacing chromium with molybdenum [ASM] or vanadium [ASV]. The first results, based upon sealed-wet aging, looked as if these impregnants were much more stable than ASC (see Chapter 4); but later, when aging conditions were made less drastic, the ASM and ASV whetlerites were found to be less satisfactory than ASC. When aged in presence of air, ASM is actually less stable than when aged in absence of air. In the final recapitulation, these processes were discarded for the following reasons:

TABLE 6. Typical CK aging for ASC and ASM whetlerites.

Conditions of storage	Days aging	80–80 CK life M10A1 — PCI ASC	ASM
None	None	63, 59	40, 41
Open initially dry	14	56	...
	28	61	32, 30
	42	52	...
	56	39	...
	66	...	19, 21
	84	44	...
	99	...	6, 8
	112	39	...
	131	...	8, 3
	340	...	4, 3
	400	17, 19	...
Sealed-wet	None	...	40, 41
	10	...	36
	18	...	26
	28	4	27
Sealed-dry	14	57	...
	28	61	...
	56	42	...
	112	34	...

1. It was found difficult to prepare them with present plant equipment.
2. ASM was less stable than ASC when aged in presence of air.
3. ASC stability was found to be more satisfactory than the early sealed-wet aging results had indicated.

4. The properties of pyridine and picoline in inhibiting ASC aging had been discovered and it was felt that if a more stable adsorbent were needed it could best be obtained by use of one of these in conjunction with the ASC process.

The data of Table 6 are presented to show typical ASC and ASM performances for comparison. Aging was in the NDRC cyclic chamber.

5.2.5 Pyridine and Picoline Impregnations [10, 16, 19, 22]

The use of pyridine and similar organic bases as charcoal impregnants to increase CK protection was first discovered by the British. Preliminary studies made at Edgewood Arsenal in 1943 looked very promising so that further investigations were undertaken along these lines. Descriptions of the conditions used for addition of pyridine, picoline, and related compounds and the performance given by these impregnants are found in Chapter 4. Early surveillance studies were made by layer depth-life studies with tube tests.[18] Data for samples aged sealed-wet at 40 C are shown in Table 7 to illustrate the effect of pyridine. Picoline and other organic bases behave similarly.

TABLE 7. Critical layer depth and capacity for CK of aged charcoals (OSRD 4013); Charcoal PCI — Sample A.

Impregnant	Hours aging sealed-wet 40 C	Critical depth cm	Capacity mg CK/ml char
None	None	2.9	9.7
P (3%)	None	2.2	23
ASC	None	1.9	84
	281	2.9	63
	480	3.7	54
	954	4.5	34
ASC + 1% P	0	1.7	68
	281	1.7	48
	480	2.2	55
ASC + 3% P	0	1.6	39
	290	2.0	37
	479	2.0	23
	1440	2.2	33
	1922	2.4	31
	2401	2.4	29

TABLE 8. Effect of pyridine on CK protection of M11 canisters aged in M7 carriers; Charcoal PCI.

Whetlerite	CK life at 50 lpm and 25 lpm (in parentheses)			
	Initial	14 days	28 days	56 days
ASC	32, 35	13, 12	4, 5	2 (50)
+ 0.84% P	31, 33	20, 20	14, 17	9, 10 (59)
+ 1.6% P	34, 36	25, 26	16, 17	13, 16
+ 2.4% P	31, 33	16, 23	15, 18	17, 17

From the data of Table 7, and from numerous other series for various charcoals, it is concluded that pyridine has the effect of enhancing the CK protection of aged ASC whetlerite. The first effect of aging is to increase the critical depth. When pyridine is added, its effect is to hold the critical depth constant, regardless of the aging of the other components. That is, the effect of pyridine is superimposed upon the effects of other components. Since the CK capacity due to pyridine is small in comparison with that of unaged ASC, addition of pyridine has little effect on an unaged sample; in fact, the protection is lowered slightly because adsorption of pyridine covers some of the available active centers and decreases the adsorptive capacity. But as the aging destroys the ASC effectiveness toward CK, the influence of the pyridine becomes apparent and aging lowers protection only to that which pyridine alone gives.

With the accumulation of aging data for canisters used in the field, it became more and more apparent that aging is not a serious problem for the M10A1 canister and, consequently, interest in the addition of a pyridine impregnation decreased. At the time of writing, however, there is still some interest in the possibility of using pyridine in the M11 canister which is, as mentioned above, perhaps subject to more drastic aging conditions than the M10A1 because of the airtight M7 carrier. In view of this possibility, an extensive program has been carried out in the NDRC cyclic chamber to study the effect of pyridine on the aging of M11 canisters stored wet in M7 carriers. Typical data are reproduced in Table 8. The beneficial effect of the pyridine is obvious. Whether such a treatment will ever be put into production depends upon what is learned from further field data, the applicability of present plant processes to addition of another constituent in impregnation, and further studies of any deleterious effects which might follow the use of pyridine.

Chapter 6

ADSORPTION AND PORE SIZE MEASUREMENTS ON CHARCOALS AND WHETLERITES

By *Paul H. Emmett*

6.1 INTRODUCTION

As part of a fundamental program designed to throw light on the surface area, pore size and structural characteristics of an "ideal" charcoal, a great many measurements have been made during the last five years, both in NDRC and in British and Canadian research laboratories. The present report is an attempt critically to discuss and summarize such work, taking due cognizance of the current concepts of area and pore size measurements of porous solids. Tables and figures incorporated have been selected to illustrate the nature of the work that has been carried out and the conclusions that have been reached. For more detailed accounts of the work, the reader is referred to the original articles listed in the extensive bibliography.

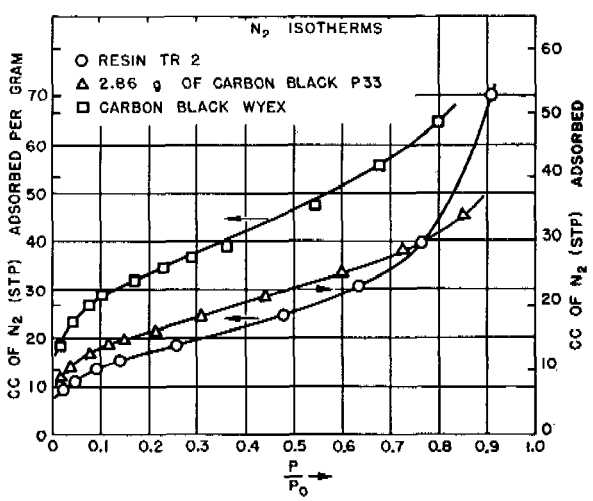


FIGURE 1. Method for measuring surface areas of various solids by means of low temperature adsorption isotherms.

It must be realized at the start that it is not always possible to give a final, categorical interpretation to the experimental results. The writer will endeavor to summarize accurately the experimental work and to give his own opinions as to its meaning. It is hoped that the present writeup will serve to bring up to date our thinking relative to the surface characteristics, the pore size and the pore size distribution that we should aim to incorporate into a charcoal which is to be used for gas mask work.

6.2 MEASUREMENT OF SURFACE AREAS

6.2.1 Theory of the Adsorption Method and General Application

During the last few years [1, 2] a method has been developed for measuring the surface area of various porous and finely divided solids by means of low-temperature adsorption isotherms (Figure 1). It has been shown [3] that the adsorption data can be plotted according to the equation:

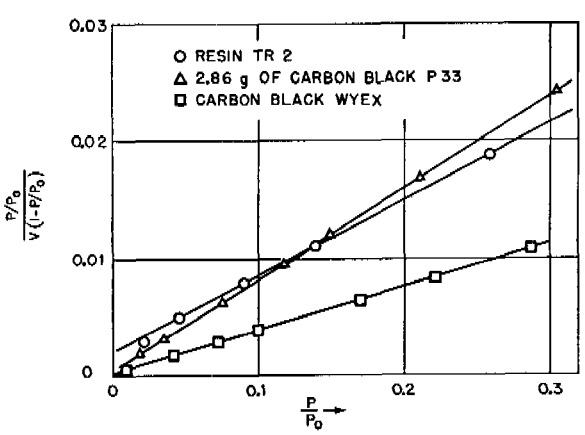


FIGURE 2. Linear Brunauer, Emmett, and Teller plots from Figure 1.

$$\frac{P/P_0}{V(1 - P/P_0)} = \frac{1}{V_m C} + \frac{(C - 1)}{V_m C}\frac{P}{P_0} \qquad (1)$$

and yields straight lines over the relative pressure range of 0.05 to 0.35 (Figure 2). From this V_m, the

volume of gas required to form a monolayer on the adsorbent can be evaluated. A simple multiplication of the number of adsorbate molecules in a monolayer by the average cross-sectional area of each adsorbate molecule will then yield a value for the surface area of the solid. In equation (1), V represents the volume of gas adsorbed (expressed at standard temperature and pressure) at the pressure P. P_0 is the liquefaction pressure of the adsorbate. C is a constant related to the heat of adsorption, E_1, by the equation

$$C = \frac{a_1 b_2}{a_2 b_1} e^{(E_1 - E_L)/RT} \qquad (2)$$

where a_1, b_2, a_2, and b_1 are constants and E_L is the heat of liquefaction of the adsorbate.

The validity of surface area calculations by equation (1) has been greatly strengthened recently by an independent approach to the problem by Harkins and Jura.[4] By pre-saturating a non-porous solid TiO_2 with several layers of adsorbed water vapor and then measuring the heat of immersion in water of the TiO_2 covered with adsorbed water, they are able to calculate directly the surface area of the solid. The heat of immersion, expressed in ergs, divided by the surface energy equal to 118.5 ergs per sq cm of surface, yields an absolute value for the area of the finely divided TiO_2. By this direct method, Harkins and Jura obtained a surface area value of 13.8 sq m per g for the adsorbent compared to 13.9 sq m per g by use of equation (1). This latter value involved the assumption that the cross-sectional area of the nitrogen molecule is 16.2 A^2, as calculated from the density of liquid nitrogen. Harkins and Jura [5] also developed a new equation for plotting the adsorption data to yield directly a value for the surface area of finely divided and porous materials. Their equation involves a constant, the numerical value of which is fixed by calibration with TiO_2, using the surface area value obtained by the heat of immersion. These alternative methods of plotting the low temperature adsorption data need not be discussed in detail here.[6] It will suffice to point out that, for a large number of porous and non-porous solids, there is good agreement between the plots of Harkins and Jura and those making use of equation (1).

Equation (1) has been applied to hundreds of different samples of adsorbents with apparent success.[7-9] S-shaped isotherms of the type [12] shown in Figure 1 are invariably obtained if nitrogen is used as adsorbate and the measurements are made at −195 C, provided the adsorbent does not have a large surface area located in small pores. Thus it has been applied in measuring surface areas of carbon black,[7] paint pigments,[7] zinc oxide particles,[7] metallic catalysts,[8] metallic oxides,[7] gel catalysts,[8] and many other materials.[8, 9] Thermodynamic [10, 11] as well as kinetic derivations lead to results expressed in equation (1) if one postulates that curves of the shape illustrated by Figure 1 represent the building up of multilayers of adsorbed molecules on the surface. The higher the relative pressure, P/P_0, the greater the average statistical thickness of the adsorbed layer. In view of all of the experimental evidence thus far obtained, it may be concluded that by plotting low temperature nitrogen adsorption isotherms according to equation (1), one can obtain reliable relative surface areas that are accurate to at least 5%, and absolute values that are entirely reproducible on a given solid but might be in error by as much as 20% due to uncertainties of molecular diameters and molecular packing.

In the original paper by Brunauer, Emmett, and Teller,[3] it was pointed out that if, for any reason, the maximum thickness to which adsorbed layers could build up on a surface is n molecular diameters, then the equation that one obtains to represent adsorption as a function of relative pressure (here designated for convenience as x rather than as P/P_0) is

$$V = \frac{V_m C x[1 - (n+1)x^n + nx^{n+1}]}{(1-x)[1 + (C-1)x - Cx^{n+1}]}. \qquad (3)$$

Here the symbols have the same meaning as in equation (1). Attention was also called to the fact that if $n = 1$, equation (3) reduces to the form

$$\frac{P}{V} = \frac{P_0}{CV_m} + \frac{P}{V_m} \qquad (4)$$

which is identical with the Langmuir equation.

For materials such as charcoal having a large number of very fine pores, n is conveniently interpreted as one-half the diameter (expressed as number of molecular diameters) of the pores, cracks, or crevices in which the adsorption occurs. It has been shown by Deitz and Gleysteen,[13] and by Joyner, Weinberger, and Montgomery [14] that equation (3) can be applied successfully to the adsorption isotherms for a number of materials having too many fine pores to fall in the class represented by equation (1). Figure 3 contains a number of isotherms that follow equation (3) over the pressure range 0.1 to 0.4; the values of n, C, and V_m that fit well into the equation are also indicated.

Pickett [15] has recently questioned equation (3) on

the grounds that at relative pressures of 1.0 it does not postulate the complete filling of a crevice with adsorbate but only a fractional filling equal to $(n+1)/2(1+1/Cn)$. He carried out the summation up to n layers in a different manner than that employed by Brunauer, Emmett, and Teller [3] and arrived at an equation of the form

$$V = \frac{V_m Cx(1 - x^n)}{(1 - x)(1 - x + Cx)} \cdot \qquad (5)$$

This equation has the advantage of representing the complete filling of the capillaries at a relative pressure of 1; however, the value of V_m obtained by equation (5) is substantially the same as that obtained by equation (3). Hence, Pickett's suggestion

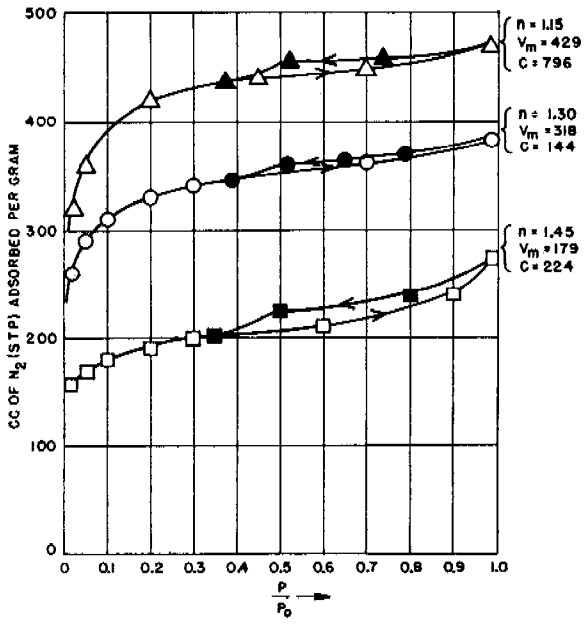


FIGURE 3. N_2 isotherms for three carbons.

is much more pertinent to the question of pore volume than to that of surface area. Furthermore, equation (3) and not equation (5) is obtained by a statistical mechanical [16] or thermodynamic derivation. It seems probable, therefore, that equation (3) may be relied upon for surface area measurements of materials having small pores even though there may be some question as to the course followed by the adsorption isotherm near saturation.

It should be made clear in passing, however, that the measurement of the surface area is much less exact for materials such as charcoal, chabazite and some gels, having pores which in size approach molecular dimensions, than for non-porous substances or those having large pores. For example, equations (3) and (5) have both been derived on the assumption that the adsorption is taking place on cracks having plane parallel walls. Without doubt, the actual pores and capillaries have no such simple structure. Indeed, it may be that the small pores might better be described as cylinders or cones rather than cracks or crevices. A further cause of uncertainty arises from the lack of any good independent means of checking the area of substances having pores of molecular dimensions. There is no way of solving these uncertainties at the present time; their existence, however, should always be kept in mind.

6.2.2 Measurement of Surface Area of Charcoals and Whetlerites

The detailed calculation of surface areas by equation (3) has not been used in most of the work that has been done on charcoal during World War II because the calculations involved are too time-consuming. For most samples, equation (4) has been employed; in a few instances [17] even equation (1) has

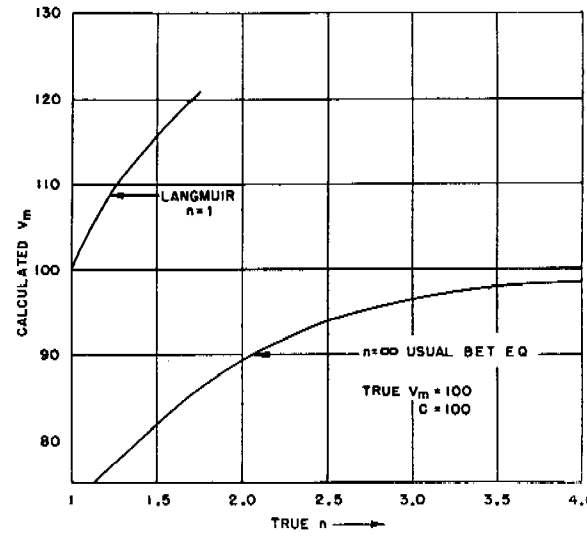


FIGURE 4. Ratios between areas obtained by equations (4) and (3) as a function of the value of n.

been used. However, as pointed out by Joyner and co-workers,[14] the use of equation (4) for adsorption isotherms for which $n = 1.5$, yields an area value about 15% higher than that obtained by using equation (3), whereas employing equation (1) for plotting the adsorption data will yield a value 18% lower than obtained by equation (3). The exact ratios between the area obtained by equations (4) and (3) as

a function of the value of n are shown in Figure 4, the figure having been taken from their paper. Accordingly, even though equations (1) and (4) have been used extensively as approximations for measuring the surface areas of charcoal, nevertheless, in the writer's opinion, the most reliable surface area values on nitrogen adsorption are obtained by fitting the adsorption isotherms to equation (3) and evaluating V_m after determining the values of n and C that are needed to fit the data to the equation over the range 0.1 to 0.4 relative pressures. The area values obtained for charcoals by equation (4) probably represent upper limits, and those obtained by equation (1) represent lower limits to the correct areas.

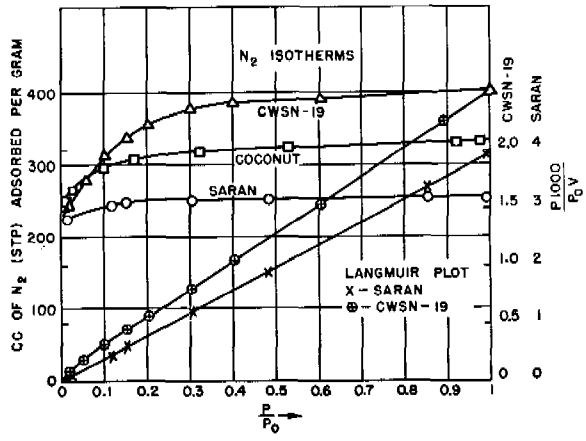


FIGURE 5. N_2 isotherms at −195 C for three small pore charcoals.

The numerical value of the surface area that one will obtain by the use of equations (1), (3), or (4) will, of course, depend markedly on the gas used as adsorbate. Even on non-porous or coarsely porous solids, there is some indication that surface areas obtained by the use of large molecules are a little smaller than those obtained by the use of smaller molecules, providing the molecular cross sections are calculated from the density of liquids in the usual way.[18] For materials with fine pores this effect of molecular size is much magnified. For example, it has been known for many years that chabazite when properly dehydrated will exhibit a screening action on molecules larger than ethane.[19] It has been shown that it is possible to make the pores so small in dehydrated chabazite as to permit the adsorption of hydrogen molecules but not nitrogen;[20] nitrogen but not C_4H_{10};[20] and straight-chain hydrocarbons but not branched chain.[21, 22] On charcoal, similar screening effects are very much in evidence. On a charcoal such as Saran [23] shown in Figure 5, the adsorption of isooctane is only one-twelfth as large as it should be if nitrogen and isooctane were being adsorbed on the same pore walls.[23] On charcoals with larger pores (Figures 5 and 6), such as are produced

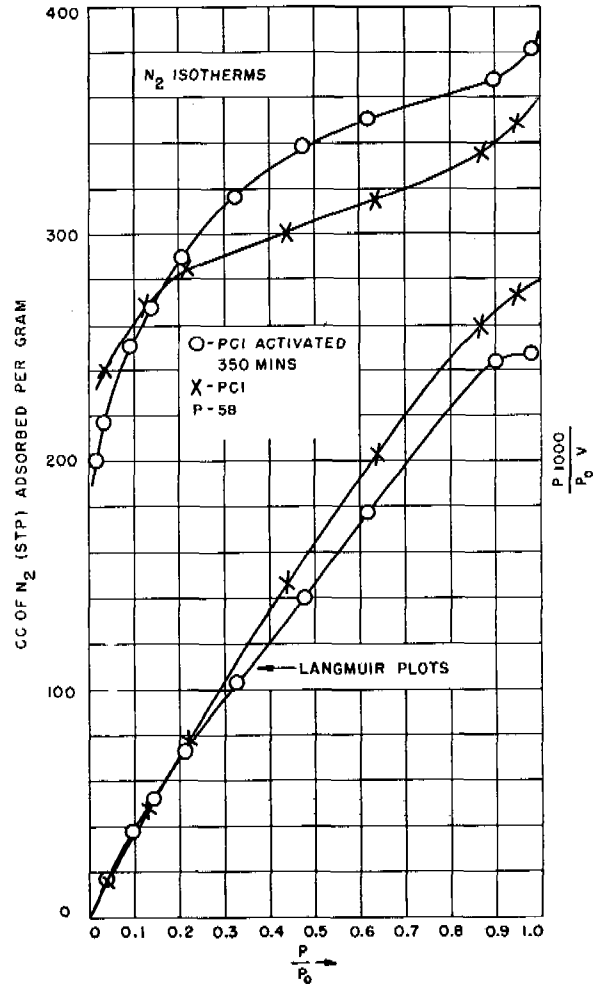


FIGURE 6. N_2 isotherms at −195 C on two charcoals with large pores.

by more extensive activation, the screening is still in evidence but much less pronounced. A plot of surface area [calculated by equation (4)] as a function of molecular size is shown in Figure 7. As indicated, a surface area value for charcoal will, in general, so decrease in size as the molecule employed for the adsorption measurements increases in size.

For obvious reasons it seems likely that the surface area measured by gases will be more important in judging the properties of charcoal than the areas

TABLE 1. Maximum millimols of acids adsorbed, and surface areas in sq m, per g charcoal. Taken from C. E. 151, Report 1, III-1-1232, Sept. 20, 1943 by Lemieux and Morrison.

Measuring acid	Measurement	Charcoal number 1	2	3	4	5	6	7	8
Acetic acid	Millimols†	2.15	2.55	2.85	3.22	3.25	3.70	4.00	*
	Sq m‡	338	402	449	507	512	583	630	
Propionic acid	Millimols	1.63	2.04	2.47	2.91	2.93	3.46	3.75	3.96
	Sq m	257	321	389	458	462	545	590	624
Butyric acid	Millimols	1.24	1.66	2.06	2.63	2.74	3.43	3.84	4.25
	Sq m	195	262	324	415	432	540	605	670
Valeric acid	Millimols	0.88	1.31	1.75	2.40	2.41	3.18	3.66	4.01
	Sq m	139	203	276	378	380	501	577	632
Benzoic acid	Millimols	0.89–	1.26	1.71	2.25	2.31	2.91	3.38	3.70
	Sq m	140	198	269	354	364	458	533	583

* Insufficient charcoal.
† Areas measured in millimols per gram.
‡ Area range in square meters per gram.

measured by adsorbing molecules from a suitable liquid solvent. This is primarily due to the difficulty involved in causing a solute to diffuse through a solvent and cover the surface of capillaries when the latter are the order of a few molecular diameters in size. Nevertheless, some measurements of the surface area of charcoal by the adsorption of molecules from the solution have been made. In Figure 7 a comparison is made between the area values obtained by phenol and methylene blue from solution and those obtained by adsorbing gas molecules of comparable size. The agreement on the crushed sample is fairly good; the areas on the uncrushed sample seem to be about 40% lower by adsorption from liquid than by adsorption from gas. It is interesting to note that the areas obtained by Lemieux and Morrison [25] using acetic, propionic, butyric, valeric, and benzoic acids, all lie in the range 583 to 670 sq m per g on a given sample of well activated charcoals (Table 1). As would be expected, the area measured by acetic acid was much larger for small degrees of activation than that measured by valeric acid, just as the area measured by PS or other large molecules is much smaller [17, 23] than that measured by nitrogen in the early stages of activation when, presumably, the smaller pores are predominant. No areas by nitrogen adsorption methods are available for their charcoals though the combined effect of molecular screening and incompleteness of equilibration probably cause all these solution results to be low by a least 50%.

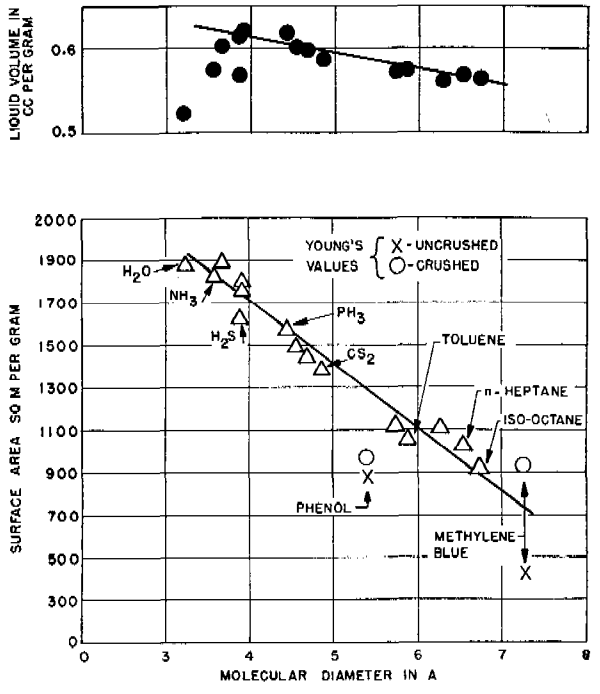


FIGURE 7. Charcoal CWSN-19. Liquid volume and surface area vs molecular size.

6.2.3 Application of Area Measurement in Predicting the Performance of Charcoals

The application of surface area measurements in charcoal research is much less extensive and significant than the application of pore size measurements. This arises from the fact that *rate of adsorption* as well as the sorption capacity enters into the actual process by which a poisonous gas is removed from a stream of air on passage through a sample of charcoal. Nevertheless, many hundreds of such measurements have been made.[25a, 25b] There have been a few uses for the area measurements, however, that are worth mentioning.

1. Some limited conclusions as to the whetlerizability of a charcoal can be deduced from the nitrogen adsorption isotherm. For example, a charcoal giving

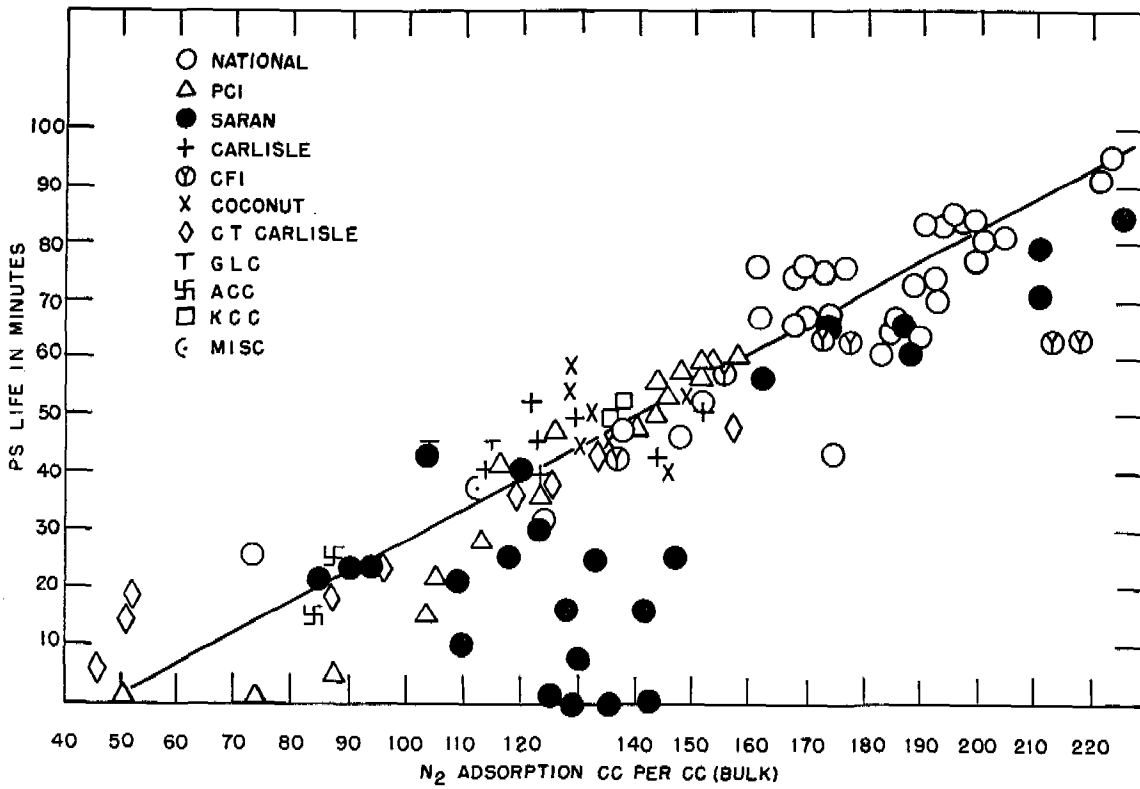


FIGURE 8. PS life vs N_2 adsorption at $P/P_0 = 0.4$.

an isotherm as flat as that of Saran (Figure 5) cannot be expected to be suitable as a support for the catalyst material that is added in whetlerization because apparently, as judged by a plot of the data by equation (3), the pores are all very small. At one time it was suggested that a gently rising nitrogen adsorption isotherm of the type shown in Figure 6 was a necessary prerequisite to a good charcoal.[26] It may still be said that such a rise usually exists for a charcoal capable of being effectively whetlerized for the removal of CK under 80-80 conditions. Actually, one must take into consideration the shape of adsorption isotherms not only up to relative pressures of 0.99 but also to much higher ones.[27] This application, however, involves the question of pore size measurements and will be considered in a later section.

2. For charcoals that are sufficiently well activated to have a large supply of pores wide enough to accommodate PS molecules, it seemed likely that some correlation should exist between the nitrogen adsorption capacity and the PS life. Actually a plot [23] of the PS life (Figure 8) as determined by standard tests against $V_{0.4}$ (volume of nitrogen gas adsorbed per cc of charcoal at a relative pressure of 0.4) seems to give an approximately straight line that fits the equation

$$\text{PS life (in minutes)} = 0.53\ (V_{0.4} - 48), \quad (6)$$

over the life range of 20 to 60 min with an accuracy of about 10 min.

3. Surface area measurements on charcoals that have been partially saturated with water vapor are an essential part of the methods [17, 28, 29] used by Juhola in measuring pore size. They will be discussed in the following section.

In this section only adsorption data for nitrogen have been discussed. Adsorption of water vapor, PS, and a variety of other gases will be considered in other sections of this chapter.

6.3 ADSORPTION OF WATER VAPOR

6.3.1 Adsorption Isotherms for Various Charcoals and Whetlerites

For a number of reasons [17, 23, 24, 27, 30] hundreds of water adsorption isotherms have been determined in the course of the present work on a variety of char-

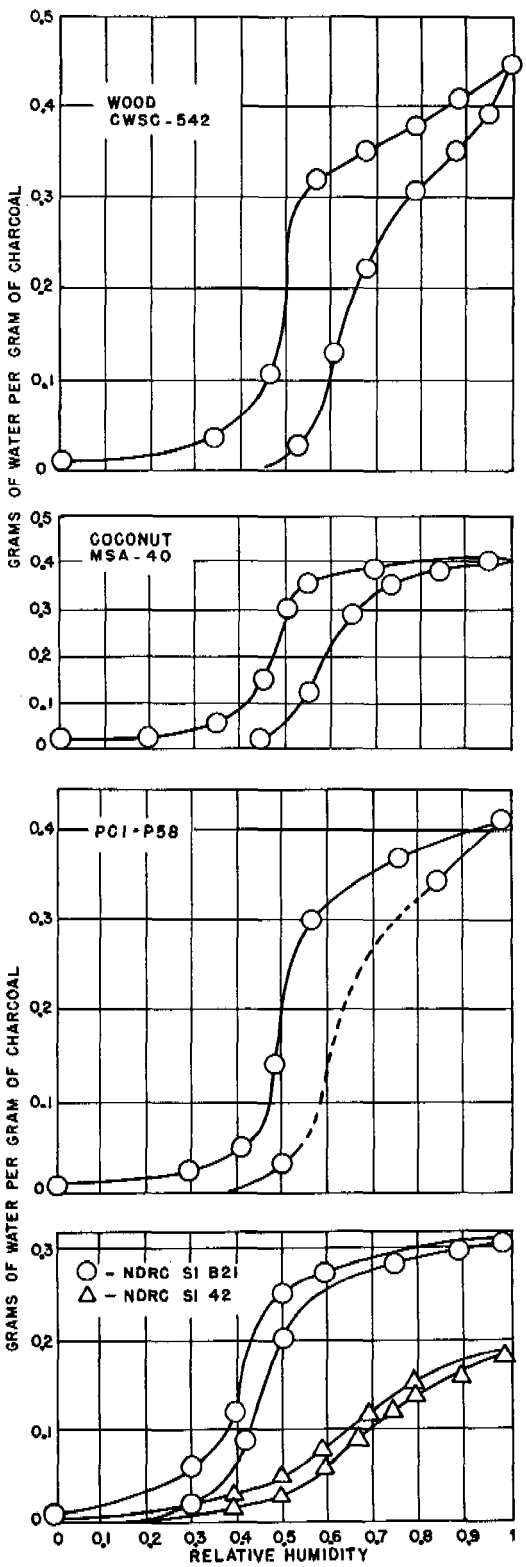


FIGURE 9. Water adsorption on charcoals at room temperature.

coals and whetlerites. To begin with, the 80-80 activity of many whetlerites toward CK may be vanishingly small even though the 0-80 activity might be high. This raises the question as to the amount of the catalyst surface that is left uncovered when the whetlerite is equilibrated with water at 80% RH. Secondly, water is known [23] to be capable of inhibiting the adsorption of PS by charcoals and hence will influence the PS life of a canister. Finally, water adsorption isotherms have proved to be of great value in estimating the pore size and pore size distribution according to a method developed by Juhola.[17, 28, 29]

Figure 9 illustrates a number of various types of water isotherms [32] that have been found on charcoals by adsorbing and desorbing water vapor from a stream of air passing through the sample. Most of the adsorptions are characterized by hysteresis that extends clear back to zero pressure when the isotherms are determined by a flow technique using air as a carrying gas. When the adsorption is measured by a static system after thorough evacuation of the sample, the shape of the hysteresis loop is somewhat altered and the desorption curve on some charcoals rejoins the adsorption curve at about 0.4 relative pressure [17, 23] as illustrated in Figure 10. However, Juhola has found [17] a number of examples of partially activated charcoals for which even in a static system hysteresis persists down to approximately zero relative pressure. Any such hysteresis in physical adsorption extending to relative pressures below those corresponding to condensation on pores at least four molecular diameters in diameter, is to be questioned seriously. Slow chemical adsorption and gradual evolution of CO or CO_2 from surface complexes [27] in the presence of water vapor may both be factors in apparent low-pressure hysteresis in water adsorption.

It has long been known that the shape of the adsorption isotherms for water vapor on a charcoal is radically influenced by the amount of oxygen present as a surface complex. For example, it was pointed out by Lawson [33] that the presence of an oxygen complex on the charcoal surface shifts the adsorption isotherm to lower pressures than in the absence of such a complex. The influence of oxygen-coating a sample is graphically illustrated by Figure 11 in which the water adsorption isotherm is shown for charcoal CWSN 19 both before and after exposing it to oxygen at 400 C.[24, 30] During this exposure the nitrogen isotherms remained practically unchanged.

The amount of water adsorbed has proved to be substantially independent [39] of the temperature at a

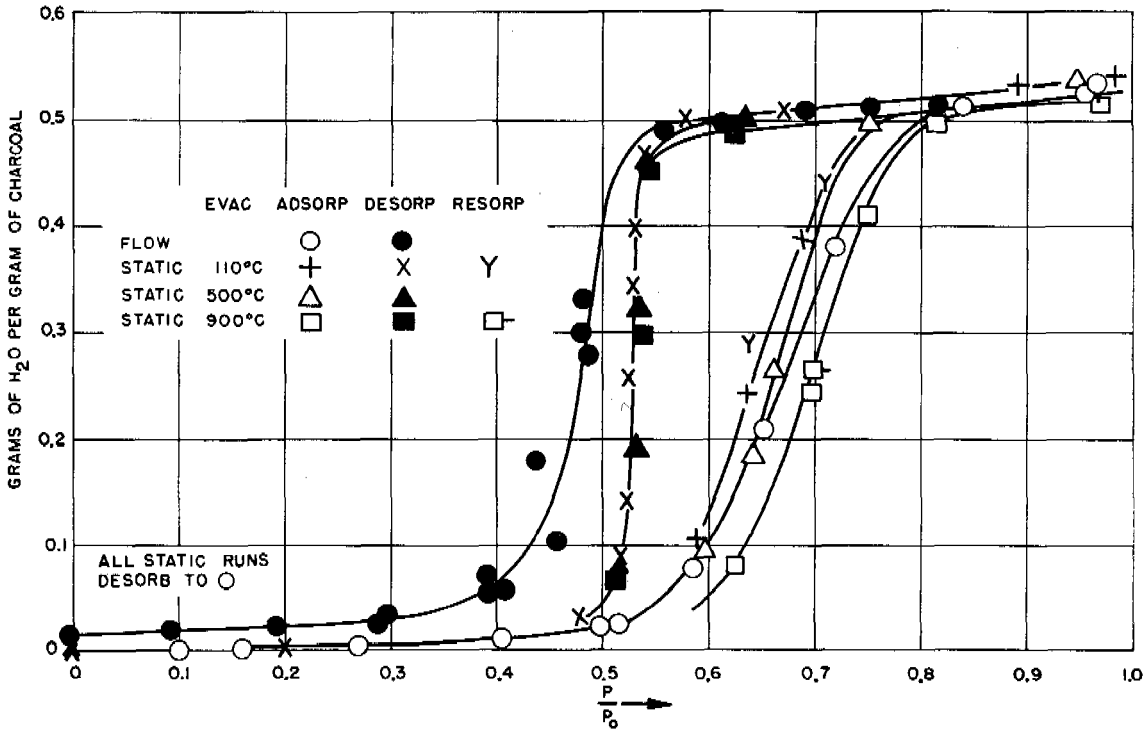


FIGURE 10. Water on CWSN–19 in flow and static systems. All static runs desorb to zero.

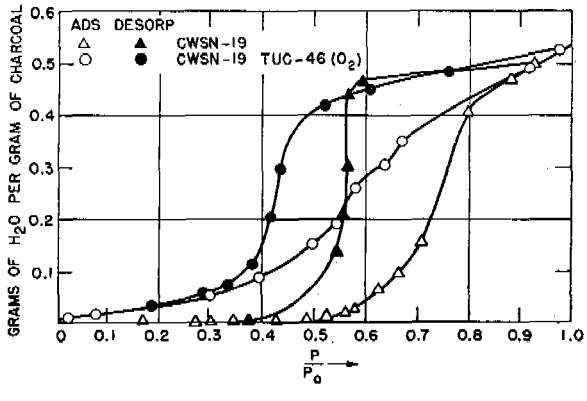


FIGURE 11. Water isotherms as a function of the amount of surface oxygen complex.

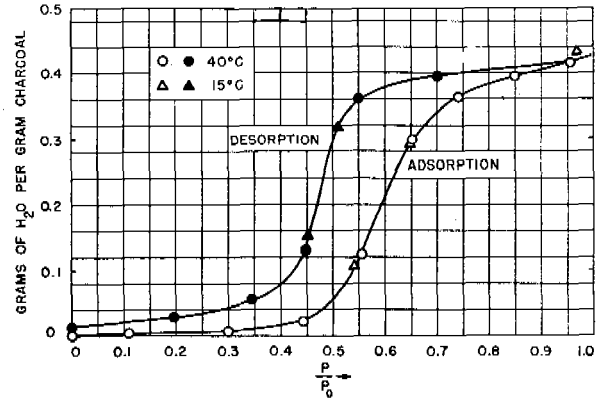


FIGURE 12. Adsorption of water on Navy charcoal MSA Grade 40.

given relative pressure for a number of [24, 30] charcoals. One of these is illustrated [30] in Figure 12 for water isotherms determined by a flow system for two different temperatures. This is not surprising because it is known that $E_1 - E_L$ in equation (2) is small for water. Consequently, the influence of temperature on the value of C, and hence the amount of adsorption according to equation (3), is negligible over short temperature ranges.

RATE OF ADSORPTION OF H_2O

The rate of adsorption of water vapor has received considerable attention because of the importance of knowing the rate at which canisters might be contaminated by picking up water vapor and the rate at which they could be dried out when necessary by sucking dry air through them. The following conclusions have been reached although no complete mathe-

matical analysis of the rates of adsorption and desorption have been reported.

1. The rate of adsorption of water vapor by whetlerites is a little faster and the rate of desorption somewhat slower than for the corresponding base chars.[30] This is probably due to the fact that the equilibrium water vapor curve is shifted toward lower relative pressures by whetlerization. Hence, for a gas stream of a given RH (relative humidity) the driving force for adsorption is greater than for the base char; similarly, the driving force for desorption into a dry gas stream is less for the whetlerites than for the base chars and hence the rate is slower.

2. The rate of equilibration increases with the rate of gas passage [35–37] at a given RH in the entering gas stream. This is probably due to the increase in the average partial pressure of water vapor throughout the charcoal column, as a result of the higher gas velocity.

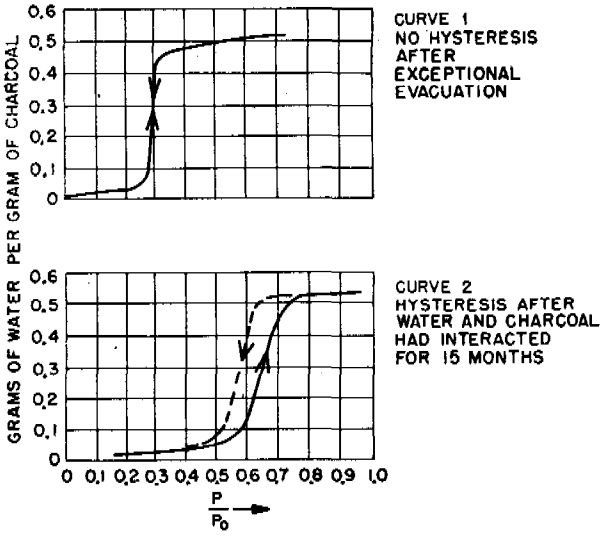


FIGURE 13. Water adsorption on charcoal. McBain Porter & Sessions (J.A.C.S. **55**, 2294, 1933). Temperature of runs, 120 C.

3. Apparently [35] the slow step in the equilibration of charcoal with water vapor is not the mass transfer of the water vapor from the stream of gas to the charcoal particles, but the resistance encountered by the passage of the water vapor from outside the particle into the tiny capillaries. This has been pointed out by Colburn [35] who showed that the HTU (height of a transfer unit) for charcoal samples ranged from 3 to 25 in. under his experimental conditions compared to values of 0.2 to 1 in. for silica gel particles of similar size. This observation is consistent with the idea that some of the penetration of gases into the smallest capillaries is due to surface migration on the adsorbent. If the adsorption of water vapor is low, it would naturally follow that the transport of water vapor into the pores of the capillaries by surface migration, and hence the rate of equilibration, would be slow.

4. At 30 C and a gas flow of 600 ml of air per min per g of charcoal (a space velocity that is close to that of normal breathing rates through canisters) the time [30] for half-equilibration of several typical base chars ranged from 48 to 90 min; the time for half-desorption into a stream of dry air at this same flow rate was about 30 to 40% of the time of adsorption. The time required for equilibration (by adsorption) on the whetlerites was from 30 to 60% of the time required for equilibration of the base charcoals.

6.3.2 Nature of Water Adsorption on Charcoal and Whetlerlites

Much has been written [38–40] relative to the nature of water adsorbed on charcoal. This is understandable since the interpretation of the water isotherms may be a key to the calculation of the pore size and pore size distribution of the adsorbent. If water is adsorbed in or desorbed from a state that may be called capillary condensation, then the adsorption or desorption curves may be used together with the Kelvin equation to estimate the pore size distribution. In the next section we shall see how this method has actually been applied by Juhola and others. For the present we shall limit our discussion to a presentation of the evidence that has accumulated as to the nature of water adsorption. In particular, the evidence will be presented on the question whether water pickup by charcoal is adsorption, capillary condensation, or a mixture of both.

McBain [40, 41] and his co-workers have contended that the sorption of water vapor by charcoal is an adsorption phenomenon rather than a capillary condensation. In favor of this point of view are the following experimental facts:

1. When water vapor is taken up by charcoal the latter expands [40] rather than contracts. It seems agreed that pure capillary condensation would lead to a tension in the pores of the charcoal and hence to a slight contraction.

2. McBain [40] succeeded in drying and evacuating a sugar charcoal sufficiently to eliminate all hysteresis in an isotherm at 120 C. The results of his measure-

ments are shown in Figure 13. The water sorption rises abruptly at a relative pressure of about 0.3 until about 80% of the sorption capacity of the charcoal is satisfied. It then levels off gradually to a constant saturation value. Desorption follows the same curve. On the other hand, after the charcoal stood in contact with the water vapor for a year with the development of detectable amounts of hydrogen, a repeat adsorption run showed the conventional type of adsorption curve (Figure 13) with hysteresis in desorption.

3. The shape of the lower part of water isotherms such as shown in Figures 9 and 10 are not very different from the shape of the water isotherms obtained by Emmett and Anderson [42] on samples of degassed carbon black (Figure 14). It will be noted that the nitrogen isotherm on the carbon black before and after evacuation at 1000 C are practically identical. On the other hand, the water adsorption isotherms are greatly changed. The sample, after the high temperature evacuation, adsorbs no water at low relative pressures but increasing amounts as the relative pressure is increased. The isotherms apparently indicate a heat of adsorption that is smaller than the heat of liquefaction. The water isotherm before evacuation rises almost linearly with relative pressure in much the way one would expect if the heat of adsorption is substantially equal to the heat of liquefaction. It seems clear that on the degassed carbon black the water adsorption cannot be due to capillary condensation since there is no evidence of any capillaries being present. Certainly, the high temperature evacuation did not produce capillaries or the nitrogen adsorption isotherms would have been quite different before and after the evacuation. The similarity between the shapes of the two carbon black water adsorption isotherms and the shapes of the isotherms of water vapor on charcoals is striking; accordingly, one must certainly be cautious about interpreting the water adsorption isotherms on charcoal as due to capillary condensation. Both the capillary size measurements of Lowry,[38] and those of Fineman, Guest, and McIntosh,[43] based upon the assumption that the adsorption isotherms for water are due entirely to capillary condensation, are to be questioned.

The evidence for interpreting the desorption part of the isotherms as capillary condensation may be also reviewed here.

1. No satisfactory explanation of hysteresis in desorption has been advanced so far for any process other than capillary condensation. On the other hand, in the water isotherms on the degassed carbon black [42] in Figure 14, hysteresis appears to exist. If these observations are confirmed by further work they will tend to undermine the capillary condensation interpretation of hysteresis since the particle size in the carbon black work is such that even capillary condensation between the particles seems to be ruled out.

2. By assuming that the shape of the desorption isotherms of water vapor on charcoal is due to capillary condensation and that $\cos\theta$ in the Kelvin equation

$$\ln\frac{P}{P_0} = -\frac{2\sigma V\cos\theta}{RT} \tag{7}$$

has a value of 0.5 to 0.6, Juhola has been able to calculate pore size distribution for charcoals that yield good values for the surface areas measured by nitrogen adsorption. This is considered in detail in the next section.

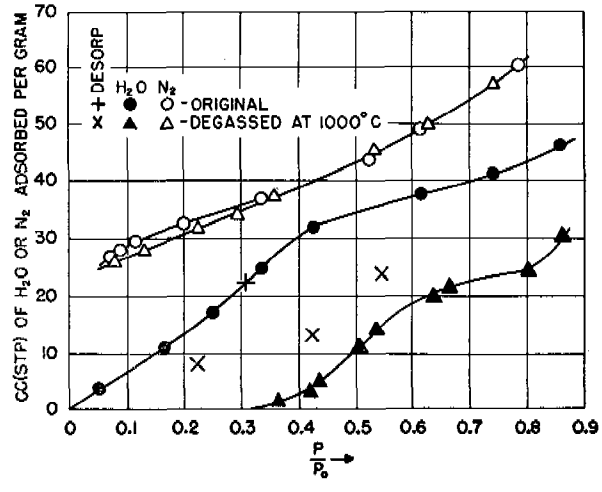


FIGURE 14. Adsorption on carbon black Grade 6.

3. The most convincing evidence that even the adsorption curve is partly capillary condensation has been obtained by Juhola in his scanning runs.[17] A typical set of these is shown in Figure 15. Unless some explanation for hysteresis based purely on adsorption is forthcoming, these scanning runs must be considered definite evidence that part of the adsorption isotherms are due to capillary condensation.

Perhaps the soundest interpretation of water isotherms at the present time is that they may be almost any combination of adsorption and capillary condensation. In water isotherms such as shown in Figure 15, it seems reasonable to assume that on the

SECRET

adsorption part of the curve, the adsorption increases with relative pressure, passes through a maximum, and then decreases as more and more of the surface is eliminated as a result of the capillaries filling with water vapor. At high relative pressure near saturation most of the water pickup is due to capillary condensation. It should be noted, however, that if this picture is adopted and if the same angle of wetting, density, and surface tension characterizes the

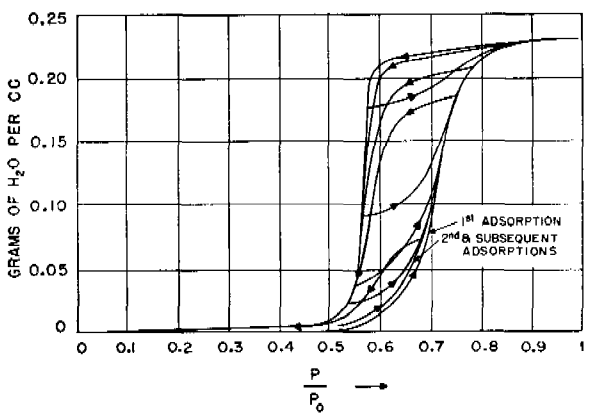


FIGURE 15. Water adsorption isotherms for CWSN 291 AY1.

condensed liquid during both adsorption and desorption, then one must conclude that the capillary condensation on the adsorption part of the curve does not occur at the relative pressures indicated by the Kelvin equation. For some reason that is not yet certain, it would appear that capillaries of a particular size fill with condensation only at relative pressures that are considerably higher on the adsorption side of the curve than on the desorption isotherm. Perhaps the bottleneck theory of Kraemer [44] or the *open pore* theory of Cohan [45] can supply the explanation for the hysteresis.

Some idea as to the nature of water in capillaries might be expected to be obtainable from measurements of freezing points and measurement of the density of the water sorbed by the charcoal. Two sets of measurements of the density of the water in the charcoal have been made. They disagree sharply with each other. Morrison and McIntosh [46] obtained values ranging from 1.02 to 1.166 when the charcoal was exposed to relative humidities below 100%. On the other hand, two runs with pure water at 100% RH resulted in the water picked up by the charcoal having an apparent density of about 0.957. In contrast to this, Juhola [17a] has found consistently that the apparent density of water is less than unity, values of approximately 0.93 and 0.90 characterizing adsorption and desorption parts of a run. It is difficult to be sure of the cause of this discrepancy. The procedure used by the Canadian workers for getting relative humidity values smaller than 100% is subject to suspicion. The use of sulfuric acid to decrease partial pressure of water vapor in their experiments might have contaminated the charcoals with small amounts of acid spray or SO_3. Either of these would have a much higher density than water and would cause the apparent density values to be erroneously large. In agreement with this, it should be noted that the values obtained by Morrison and McIntosh [46] using pure water for saturating the sample are in satisfactory agreement with Juhola's results. Because of the fact that the blocking of submicropores by capillary condensation of water or the placing of water under tension in capillary condensation would both tend to make the density less than one, it seems likely that the values obtained by Juhola for the apparent density of water are more nearly correct than the high density values obtained by McIntosh and Morrison.

Freezing methods have also failed [23a] to help much in revealing the nature of adsorbed water. Johnstone and Clark [47] found that charcoals such as CWSN 19, when equilibrated with water sufficient to cause a 45% weight increase on dry basis (probably equilibrated at about 75% RH), failed to yield an ice pattern (X-ray diffraction) at −30 C. On the other hand, a sample soaked in water initially and then air-dried to a damp powder showed ice crystals that were much smaller than those obtained by allowing moisture from the air to condense on the cold cassette. It seems likely that the water picked up during adsorption at 75% RH is either held by adsorption as a monolayer or else is in the form of capillary condensation in capillaries as small as 20 A in diameter. It is therefore understandable why the sample equilibrated at 75% RH failed to show an X-ray pattern. The pattern shown by the sample, initially exposed to liquid water vapor and retaining about 75% water by weight, could easily be due to a thin film of water located in the larger capillaries of the charcoal or adhering to the outer periphery of the particles. A 75% weight increase is considerably higher than one would expect from adsorbed water on CWSN 19 even at saturation. Accordingly, this observation does not reveal the nature of the water that is contained in the capillaries in normal water adsorption up to say 99% RH.

Another approach toward throwing some light on

SECRET

the question of the nature of adsorbed water was made by comparing the nitrogen adsorption on dry charcoal with that on samples that had been partially equilibrated with water vapor. Such measurements [23] showed that on both PCI and CWSN 19 charcoals there is no sudden expansion of water as the temperature is dropped until some point between −78 and −195 C is reached. This seems to point to the conclusion [23a] that the water held by the two above-mentioned charcoals at 83.5 and 96% RH, respectively, is not water having a normal freezing point. However, much further work would be required before one could be sure of the influence of the size of a capillary on the freezing point of liquid contained in it. Hence, even this observation is a bit indefinite as an indication of the nature of the water held in capillaries.

6.4 PORE SIZE AND PORE SIZE DISTRIBUTION

No entirely satisfactory method has been discovered for measuring pore size and pore size distribution in charcoal and other similar small pore materials. The difficulties encountered are many. Perhaps one of the principal complications has to do with the shape of the capillaries. Not only is it impossible to ascertain whether the capillaries are cylinders, cracks with parallel walls, crevices, cones, or other regular geometric shapes, but it is impossible to tell what combination of all of these and other irregular forms may be involved. Furthermore, it must be realized that in dealing with capillaries that are from one to ten molecular diameters in size, one has little information as to the way in which density, surface tension, and other properties of the adsorbed molecules may differ from those of the adsorbate in bulk form. It would probably, therefore, be difficult to specify *pore size* even if we knew the exact shape of all capillaries present of the adsorbate in bulk form. Accordingly, progress in estimating pore diameters of charcoal is possible only by virtue of making assumptions as to the shapes of the capillaries and the properties of the adsorbed molecule. It is gratifying that, in spite of the numerous assumptions and approximations that had to be made, methods were worked out during the recent war that are certainly more satisfactory than any previously available and that give results that are useful in trying to approach the ideal type of adsorbent for gas mask work.

Methods that have been employed for measuring pore size may be listed in the following five classifications:

1. Study of adsorption as a function of the size of the adsorbate molecules.[23]
2. Application of the Kelvin equation to the adsorption and desorption of any gaseous adsorbate other than water vapor.[23]
3. Application of the Kelvin equation to the adsorption [38, 43] and desorption [17] isotherms of water vapor.
4. Measurement of the change of surface area resulting from the pickup of water by the charcoal.[17, 28, 29]
5. Measurement of the pressure required to force mercury [17, 27, 50, 65] into the charcoal capillaries.

These five methods will now be considered in turn.

6.4.1 Molecular Size as a Criterion of Pore Size

In a general way it would seem to be possible to tell a great deal about the size of pores in charcoal by comparing the relative amounts of adsorption with the size of the adsorbate molecule. For example, experimental work on chabazite has shown rather clearly that it is possible to prepare the adsorbent [19–22, 51] so as to make the pores capable of adsorbing molecules of a given adsorbate and yet screen out molecules of only a slightly larger size almost completely. Thus, as a function of the temperature and time of dehydration, as pointed out in an earlier section, chabazite can be made to adsorb hydrogen, but not nitrogen; oxygen, but not nitrogen; nitrogen but not butane; and normal hydrocarbons but not branched-chain hydrocarbons. However, this apparently simple method becomes very complicated if the adsorbent is one in which only a partial screening out of the larger molecules occurs. One is then faced with the task of differentiating between screening effects and the influence of the tightness of packing of odd-shaped molecules in capillaries of unknown shape. For example, it is known that if one compares the surface area obtained by the adsorption of nitrogen by CWSN 19 with that obtained by use of successively larger molecules, the result (Figure 7) is a decrease of about 50% in going to isooctane.[23] It is not at all certain, however, that this means that one-half the area is located in pores intermediate in size between that of the nitrogen molecule (about 3.9 A) and that of the isooctane molecule (about 6.7 A). Much of the decrease may be attributed to the less

efficient packing of large molecules onto a given area than the corresponding packing of smaller, more symmetrical molecules. Indeed, it is not even yet well established that, for non-porous adsorbents, the same areas can be obtained by using large molecules as measuring sticks, as by using smaller ones.[6, 18] In spite of this, the use of adsorbates whose molecules are of different sizes has been used effectively for at least qualitative appraisal of the relative pore sizes of two different charcoals. For example, it is well known [38, 41] that large dye molecules are almost completely excluded from the pores of many charcoals. In fact, decolorizing carbons used commercially to remove color from sugar solutions are known to have much larger pores than the charcoals or activated carbons intended to adsorb large quantities of gas. Furthermore, some unmistakable screening effects can be noticed for molecules differing as little in size as those of nitrogen and isooctane. For example, charcoals made from carbonization of certain plastics are known to have uniformly small pores. These Saran charcoals (Chapter 3) will adsorb as much as twelve times [23] as many molecules of nitrogen as of isooctane and will equilibrate very much faster with nitrogen than with isooctane. It seems likely that most of the pores of this material are in the size range 5 A to 10 A. Again, it is well known that charcoals made by the activation of coal develop pores capable of adsorbing nitrogen much earlier than they develop pores capable of adsorbing molecules as large as PS or isooctane. Accordingly, in a qualitative sense, the relative amounts of adsorbate picked up as a function of the size of the adsorbate molecule can be used to obtain some idea as to the distribution of pore sizes in charcoal.

Attention should, perhaps, be called to one other precaution in judging the size of capillaries by the size of the adsorbate molecules. If one compares the amount of adsorption in terms of the volume of adsorbate (calculated as normal liquid) picked up, some odd results are obtained. For example, on two samples of charcoals on which the pores had been partially plugged by the product from the oxidation of arsine, the volume of liquid isooctane adsorbed near saturation was greater [52] than the volume of nitrogen (as liquid) adsorbed near saturation. Specifically, the ratios of the volumes of isooctane to nitrogen were 1:3 and 1:6 respectively, for the two samples. This can be understood if one remembers that if two plain, parallel walls were completely covered with adsorbate molecules and were exactly 12 A units apart, then the volume of liquid calculated for an adsorbate that had molecules 6 A units in size would be nearly 50% greater than that of an adsorbate that had molecules 4.2 A in size. Such extreme cases are rarely encountered, though it is observed that the liquid volume of adsorbates of successively larger size picked up by a charcoal do not fall off (Figure 7) as rapidly as do the apparent surface areas as calculated from the molecular cross section. This may result from the effect of the thickness of the adsorbed molecule entering into a calculation of the volume of liquid picked up when much of the adsorption is necessarily only a single layer in thickness.

6.4.2 Pore Size from Isotherms of Adsorbates other than Water

A general method for measuring the diameter D of pores that has often been suggested makes use of the Kelvin equation,

$$D = -\frac{4\sigma V \cos\theta}{RT\ 2.303\ \log P/P_0} \tag{8}$$

where V is the molal volume, σ is the surface tension, T the temperature at which the adsorption is measured, P/P_0 the relative pressure of the adsorption, and θ is the angle of wetting of the walls of the capillaries by the adsorbate. The equation in this form assumes that the capillaries are circular in cross section.

Two serious complications arise from trying to use this method in practice. For substances having large enough pores to give smooth S-shaped curves of the type shown in Figure 1, it becomes very difficult to differentiate between an increase in adsorption due to capillary condensation and one due to multimolecular adsorption. Indeed, some [53] interpret the upper part of the adsorption isotherms of curves such as those shown in Figure 1 and also those shown in Figure 16 for porous glass, some silica gels, and similar substances as due entirely to multilayer adsorption rather than to capillary condensation. Wheeler [54] is having some success in separating the multilayer adsorption effect from the capillary condensation effect and thereby is able to obtain fairly satisfactory pore distributions from nitrogen adsorption isotherms on gels at −195 C. For the most part, however, this confusion between multilayer adsorption and capillary condensation effects has not been satisfactorily resolved.

A second difficulty encountered in attempting to calculate pore diameters by use of the Kelvin equation has been pointed out in the literature [20, 55, 56] on a number of occasions and is especially applicable to fine-pore solids such as charcoal. It is concerned with the question of whether the diameter mentioned in the Kelvin equation [equation (8)] is the diameter of the capillary *after* a monolayer has been adsorbed or before it has been adsorbed. If the capillaries are

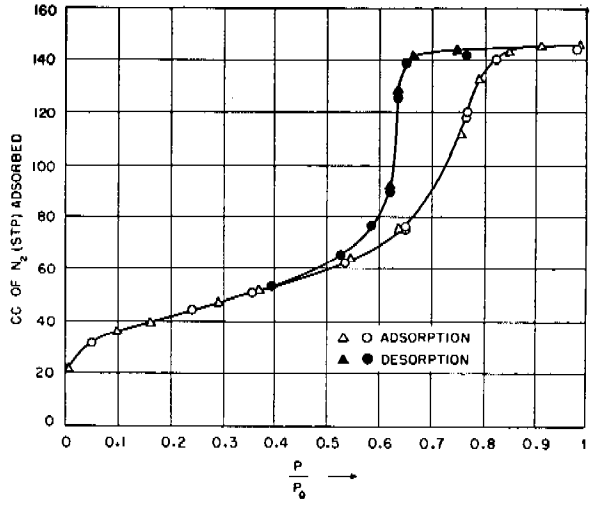


FIGURE 16. Adsorption isotherms of porous glass.

large enough to permit multilayer adsorption, the thickness of the layer left on the surface after a capillary empties at some given desorption pressure also comes into consideration, since, according to the multilayer theory [3] one may have several statistical layers left on the surface at sufficiently high relative pressures. This second difficulty can perhaps best be discussed in connection with Figure 17 showing the adsorption and desorption isotherms for nitrogen on several typical charcoals. It will be noted that the desorption isotherms show some hysteresis compared to the adsorption isotherms. The desorption curve, however, rejoins the adsorption curve at about 0.35 to 0.4 relative pressure.

It has been pointed out by Cohan [45] that for a large number of adsorbates, the desorption isotherms rejoin the adsorption isotherms at a relative pressure which, according to the Kelvin equation, figures out to correspond to 4 molecular diameters. On such a basis the adsorption of nitrogen on the charcoals shown in Figure 5 would indicate only a comparatively small pore volume in excess of about 20 A diameter and less than about 2000 A diameter (the

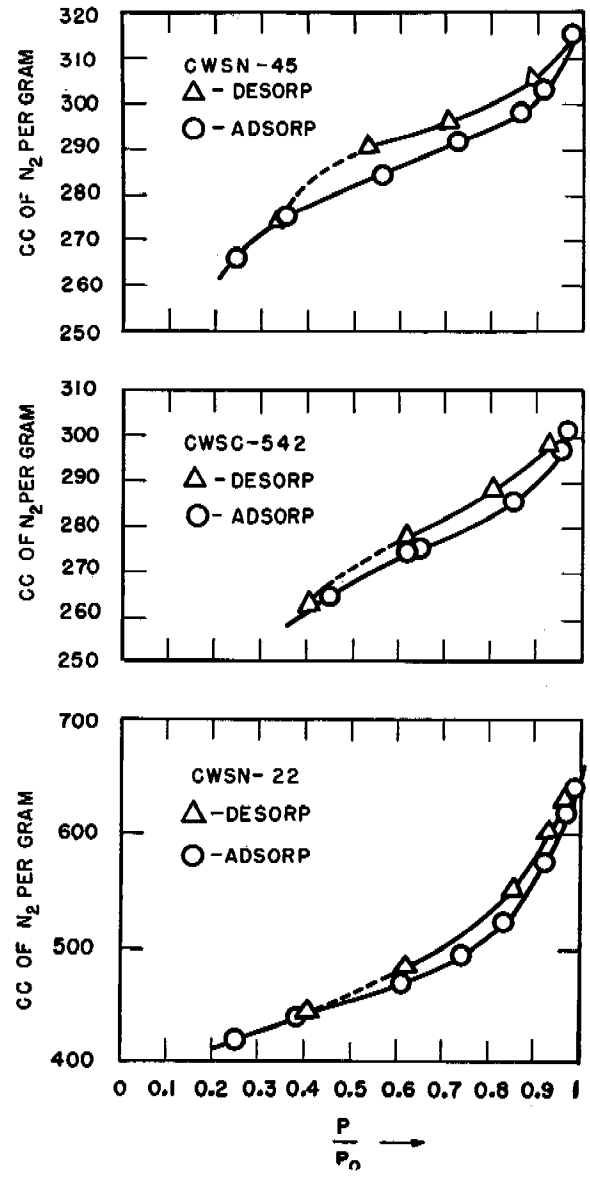


FIGURE 17. Adsorption and desorption isotherms for nitrogen on several typical charcoals.

upper limit fixed by the highest relative pressure 0.99 to which the runs were carried). These curves also make it clear that for nitrogen, at least, emptying of a capillary by evaporation of the portion of the adsorbate held by capillary condensation, leaves at least a monolayer of adsorbate on the surface. For charcoals such as those shown in Figure 17, on the other hand, definite qualitative evidence is given by the nitrogen isotherms as to the presence of capillaries in the range 20 A to 2000 A in diameter.

The two complications discussed thus far are in-

volved even when the desorption curve shows marked hysteresis in comparison to the volume of gas picked up at a given relative pressure during adsorption. Matters are made even more complicated by the fact that, according to some interpretations of capillary condensation, one may not obtain any hysteresis [45] even though capillary condensation is occurring. It is claimed for example that if capillaries are wedge shaped no hysteresis is to be expected. Also, if they are cylindrical but have some narrow portion less than four molecular diameters in diameter they will not, according to certain hypotheses,[45] give hysteresis. For all these various reasons it may be concluded that deductions as to capillary size and distribution based on the adsorption of molecules other than water vapor are susceptible to only qualitative interpretations at best. Even if hysteresis (the usually accepted criterion for capillary condensation) occurs, the interpretation of the results on a quantitative basis is made very difficult if not impossible by the uncertainty as to the thickness of the adsorbed layer left after evaporation of the portion of the sorption that is due to capillary condensation.

There is one adsorption region in which the Kelvin equation may be applied to nitrogen isotherms with a somewhat greater assurance than indicated above. It is the range near saturation extending up to the highest relative pressures that can be conveniently measured. By the use of the Pearson gauge [27] for measuring pressures very close to saturation, nitrogen adsorption measurements have been made on several charcoals. Typical adsorption data [27] are plotted in Figures 18 and 19. The adsorption in the range 0.99 to 0.999 covers diameters between 1800 and 18,000 A, if one assumes that the Kelvin equation is valid for the calculation. The question may be asked whether the abrupt rise in some of the isotherms in this relative pressure range may not be partially caused by the formation of multilayers on the surface of the large pores. It is difficult to give an exact answer in the absence of any certain knowledge as to the thickness of films that will be built up without capillary condensation. The BET equation,[3] if followed, would predict layers 1,000 molecular diameters in thickness at a relative pressure of 0.999 and a C value of 100. However, this is certainly much on the high side since the BET equation predicts adsorption that is too high at all pressures above 0.35. It seems more likely from the few measurements reported in the literature [4, 5] that no more than 50 layers would be built up. This would mean that the

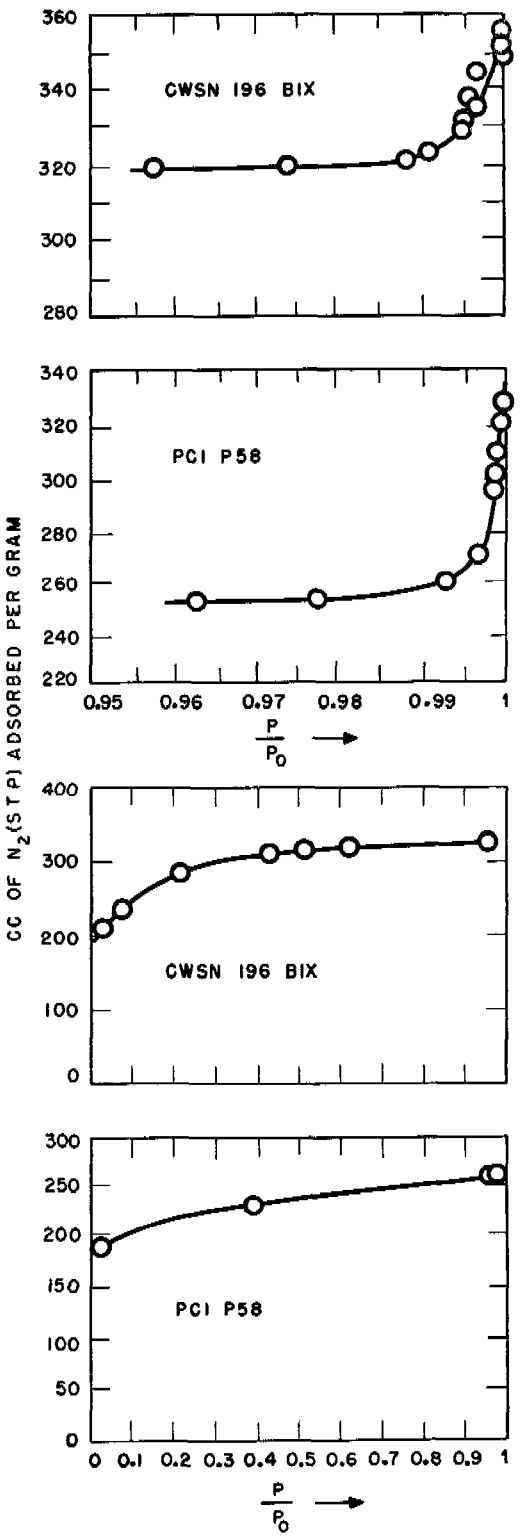


FIGURE 18. Typical adsorption data of various charcoals carried to high relative pressures.

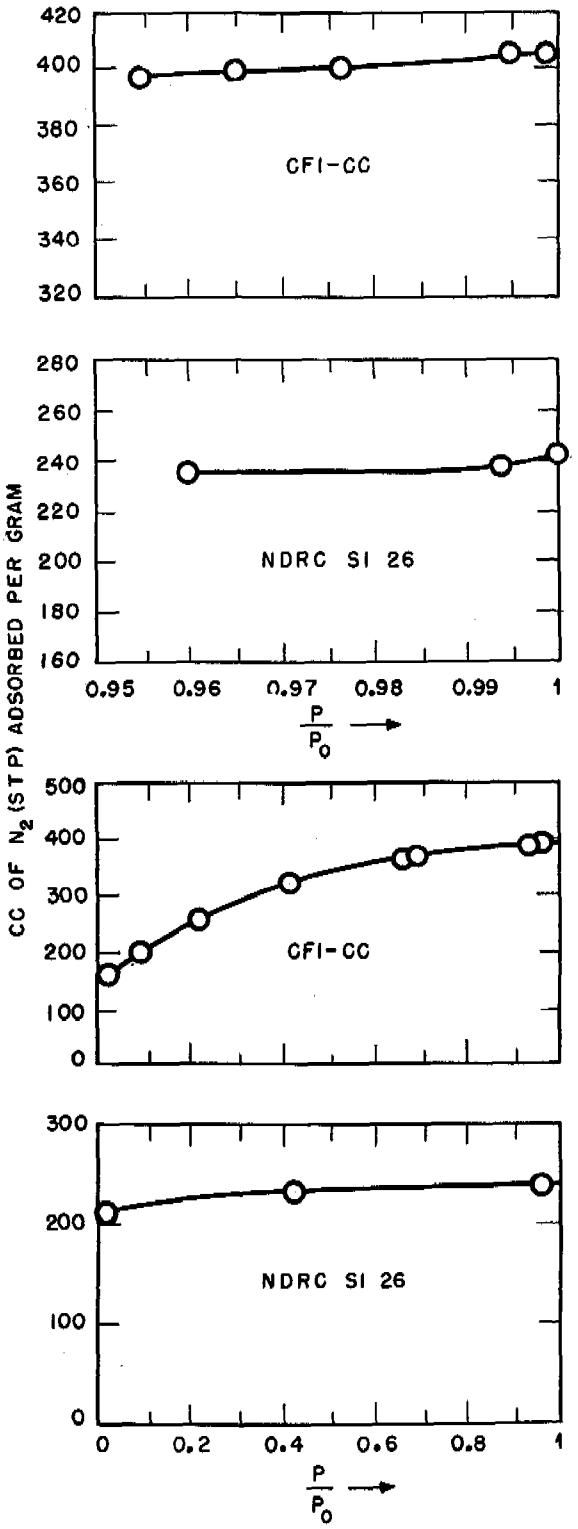


FIGURE 19. Typical adsorption data of various charcoals carried to high relative pressures.

multilayer built up would be no more than about 10% of the total volume of liquid required to fill pores of this size and, hence, could be neglected. The exact utility of these measurements will be discussed in a later section though it may well be pointed out here that, as shown in Figure 19, both Saran and CFI "CC" charcoals show no adsorption increase between 0.99 and 0.999 and are very poor bases for whetlerization; on the other hand, the charcoals shown in Figure 18 can both be converted into whetlerites and have a considerable increase in adsorption in this range of relative pressure.

It has been pointed out that by selecting proper adsorbates having large products of $V\sigma/T$ [see equation (7)] it is possible to extend the pore measurements to larger diameters without working at higher relative pressures. CCl_4,[57] pyridine,[58] and tributyrin [59] have been employed in this way to extend the measurements to 4000, 5000, and 13500 A, respectively.

6.4.3 Pore Size from Water Adsorption and Desorption Isotherms

It was suggested many years ago [38] that adsorption isotherms for water vapor on charcoals could be used for calculating pore size distributions. However, as pointed out in an earlier section, there seems good reason to doubt that all of the water picked up by charcoal during adsorption is held by capillary condensation. The similarity between the adsorption isotherms for water vapor on well degassed, nonporous carbon black [42] and those for charcoals such as shown in Figures 11, 12, and 15 suggests caution in making any pore size calculations from the adsorption curves. On the other hand, the desorption isotherms for some of the charcoals give every indication of representing the emptying of capillaries with little or no residual adsorption. Calculations such as those made by Juhola, therefore, seem entirely warranted provided the charcoals used are those having negligible adsorption below about 0.4 relative pressure.

If one applies the Kelvin equation to a desorption isotherm such as shown in Figure 15, and uses a value of unity for $\cos\theta$, one obtains pore diameters in the range 30 to 40 A for most of the sample. These are clearly too large for they would not afford a sufficiently large area to account for the surface area measured by nitrogen adsorption or by the adsorption of other gases. There seem to be two alternatives in interpreting the desorption curves. The possibility

exists that the angle of wetting is not zero degrees but an angle of such size as to yield a $\cos\theta$ between 0.5 and 0.6. As will be seen in the next section, such a choice of $\cos\theta$ yields pore distribution curves that appear to be very reasonable. On the other hand, one might be inclined to interpret the result to mean that $\cos\theta$ is equal to 1, but that attached to each of the pores of the 30 to 40 A pores are a sufficient number of smaller pores in the range 10 to 20 A which adsorb water only when the larger pores are filled. An obvious weakness with this latter interpretation is that it does not account for the absence of an appreciable number of pores in the range 20 to 30 A in which it is generally believed capillary condensation can occur.

It must be kept in mind that it is entirely within the realm of probabilities that the value of $\cos\theta$ changes as a function of the relative pressure. As a matter of fact, the heat of adsorption would be expected to increase to a value corresponding to the heat of liquefaction of water vapor as soon as the surface is covered with a monolayer of adsorbed water vapor. From experiments on carbon black [42] that has been stripped of its surface complex by high temperature evacuation, it appears that a monolayer of a sorbed water formed at about 0.85 relative pressure. It might not be surprising, therefore, by analogy to expect the $\cos\theta$ term to become substantially unity above 0.8 to 0.9 relative pressure. Furthermore, the shift [24] of the steep part of the desorption part of a water isotherm to lower relative pressures as one coats the surface with chemisorbed oxygen is an indication that $\cos\theta$ for a complex covered surface is greater than for one without a surface coating.

6.4.4 Pore Size from Surface Area Changes Resulting from Water Take-up by Charcoals

For cylinders, the diameter D, the volume V, and the area A, are related by the equation

$$D = \frac{4V}{A}. \tag{9}$$

Similarly, if one pictures charcoal as a collection of cylindrical capillaries and imagines that a group of capillaries of a particular size are filled by capillary condensation, then the small change in available volume in the charcoal will be related to the diameter of the capillary and the change in available area by the equation

$$D = \frac{4\Delta V}{\Delta A}. \tag{10}$$

Juhola was the first to point out that by measuring the surface area of a charcoal with nitrogen (at liquid nitrogen temperature) as a function of the amount of water present, one could obtain a curve from which the pore diameter distribution of the charcoal could be calculated. The H_2O desorption isotherms for the charcoals used are shown in Figure 20. The change in

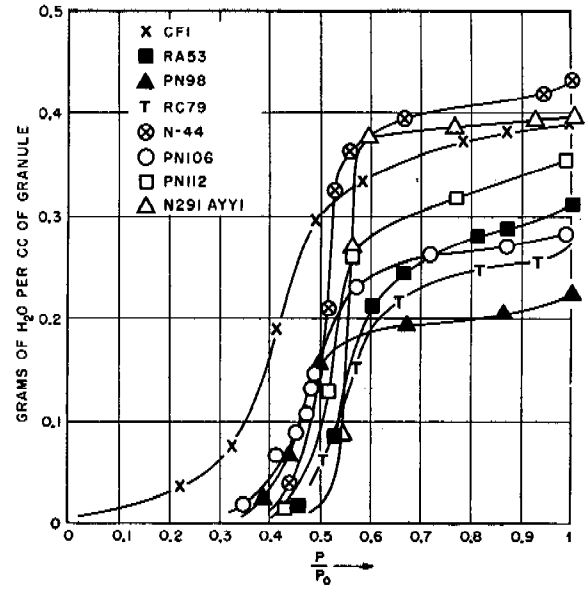


FIGURE 20. Water desorption isotherms.

area vs volume curves are shown in Figure 21, and the resulting plots of pore diameters against relative pressure of condensation of water are shown in Figure 22. It soon became apparent, however, that the technique of measuring pore diameters by this procedure would be quite laborious. Juhola, therefore, suggested using the method merely as a means of evaluating the $\cos\theta$ term of equation (7) and thereafter using this latter equation for pore size measurements in conjunction with water adsorption data. He has used this method extensively [17] for obtaining pore size distributions over the range up to about 100 A.

Juhola states [17] that the Kelvin equation, with $\cos\theta$ equal to about 0.53, agrees satisfactorily with the values obtained when equation (9) is applied to the surface area vs volume experiments at relative pressures up to about 0.9. Above this, he reports, the

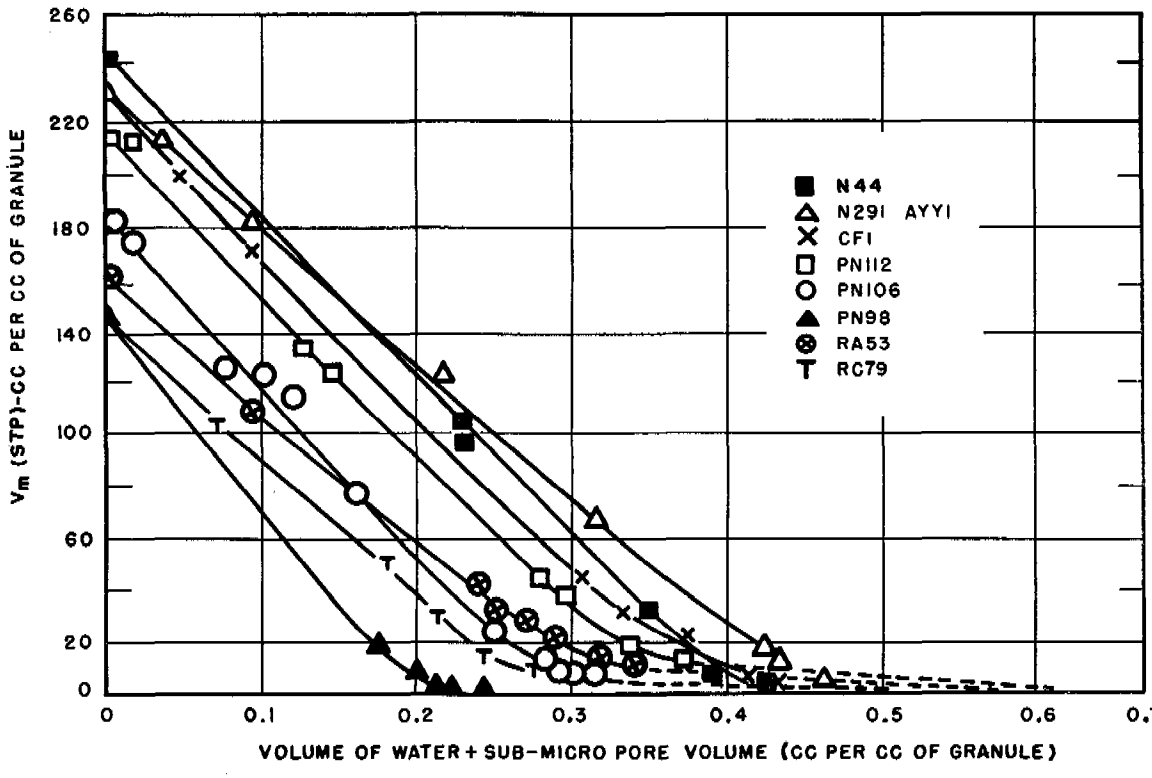


FIGURE 21. Area vs volume curves.

Kelvin equation does not hold. Actually, there is less reason to expect the Kelvin equation to fail at relative pressures above 0.9 than at lower relative pressures. From comparison with the water adsorption experiments on degassed carbon black, it seems probable that at a relative pressure of 0.9 the portion of the charcoal not covered by capillary condensation has at least a monolayer of adsorbed water vapor on it. Hence the angle of wetting is likely to be much more nearly zero than for lower relative pressures where no such film exists. Hence, one would expect that cos θ above relative pressures of 0.9 might equal unity. Presumably, the objection to interpreting the water isotherms in this way has to do with the lack of smoothness with which the pore diameter vs pore volume curves (such as shown in Figures 23 to 25) extrapolate from the lower pore diameter range into the curves for the higher range determined by the mercury method discussed below. At any rate, Juhola has elected to leave the region between about 100 A and 2000 A diameters as undetermined in most of the materials he has studied.

In the application of the Kelvin equation to water desorption isotherms for pore diameter measurements, the cos θ term has been considered as taking into account only the angle of wetting. Actually, it may be, perhaps, a constant that takes into consideration any variation in (1) the surface tensions, σ; (2) the molal volume, V; and (3) the angle of wetting in the small pore regions where we have no direct information as to the validity of the values for these terms as determined from bulk water.

The choice of the value of 0.53 for cos θ is, as pointed out by Juhola,[17] attended with considerable uncertainty. Depending upon the density selected for water and for the adsorbed nitrogen in the experimental work, this cos θ term might vary from 0.44 to 0.58. Nevertheless, for those charcoals in which there is negligible water adsorption at relative pressures below about 0.4, the method appears to give very reasonable values for pore diameters. Distribution curves for about 110 charcoals or charcoal-producing materials are given by Juhola in his final report.[17]

6.4.5 Measurement of Pore Size by High Pressure Mercury Method

Washburn [50] was the first to suggest that one could measure the diameter of pores by measuring the pressure necessary to force mercury into them. It can

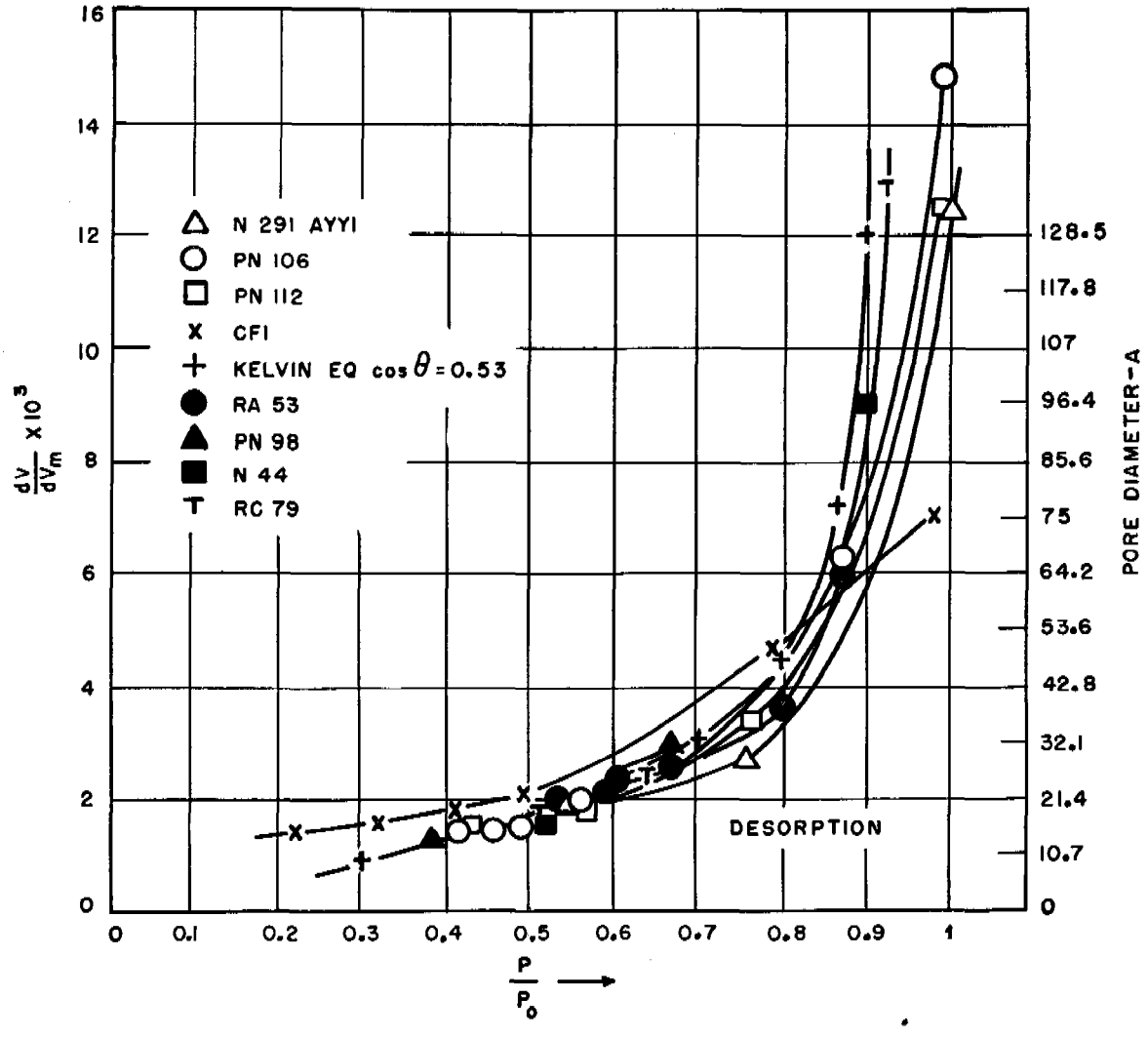


FIGURE 22. Variation of pore diameter with P/P_0 of water.

be shown that the diameter of a cylindrical capillary is related to the density ρ, and surface tension σ of mercury by the equation

$$D = \frac{4\sigma \cos\theta}{\rho h g} \qquad (11)$$

where θ is the angle of wetting (taken as -180 degrees), h is the pressure applied and g is the gravitational constant. This method was selected and applied [32] to a number of charcoals using pressures up to 100 atmospheres in some of the early war work at Johns Hopkins University; it has been much more extensively studied and applied by Juhola [17] on more than a hundred charcoals. Juhola [17] tested the method on a block of briquetted, carbonized coconut shell charcoal by boring a hole 0.015 in. (3.81×10^6 A) in diameter and measuring the pressure required to force mercury through it. Four runs gave results of 3.39, 3.96, 3.43, and 3.75×10^6 A, which agree well with the actual value, 3.81×10^6 A.

Recently, Ritter and Drake [61, 62] have published details of the method as applied to cracking catalysts and also to a number of commercially available charcoals. Their runs have extended up to 10,000 psi pressure and, therefore, include measurements to pore diameters as small as 200 A diameter. A number of their resulting curves are shown in Figures 26 and 27.

Several inherent characteristics of the mercury method should be noted. If bottleneck capillaries exist, it must be realized that the pore diameter measured will be that of the narrow neck rather than the

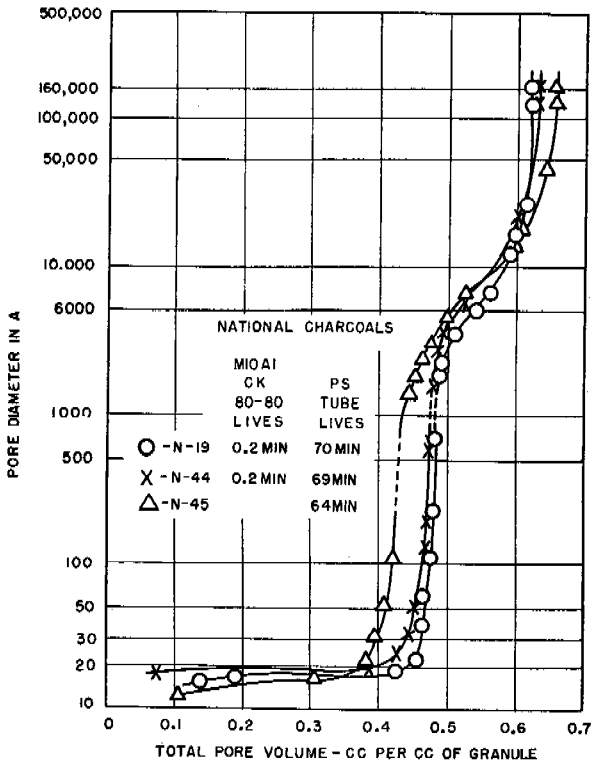


FIGURE 23. Pore diameter vs pore volume curves.

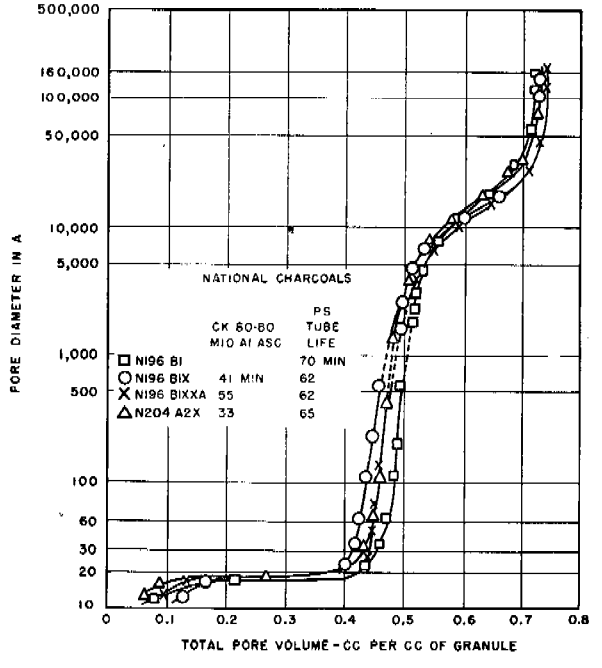


FIGURE 24. Pore diameter vs pore volume curves.

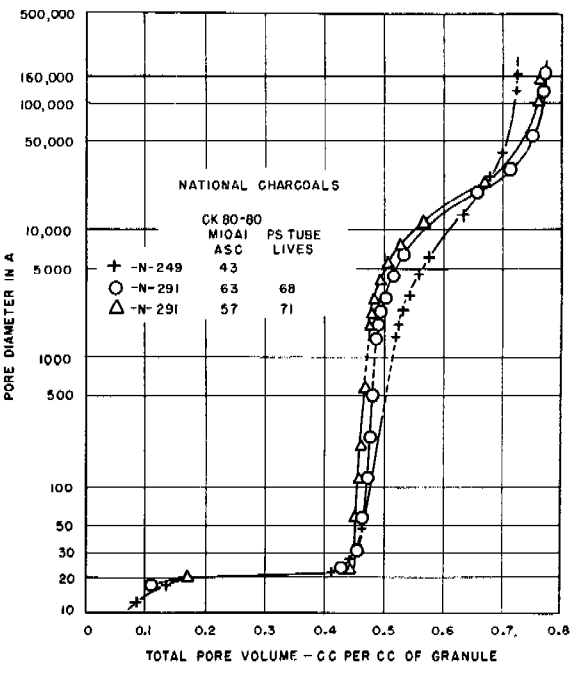


FIGURE 25. Pore diameter vs pore volume curves.

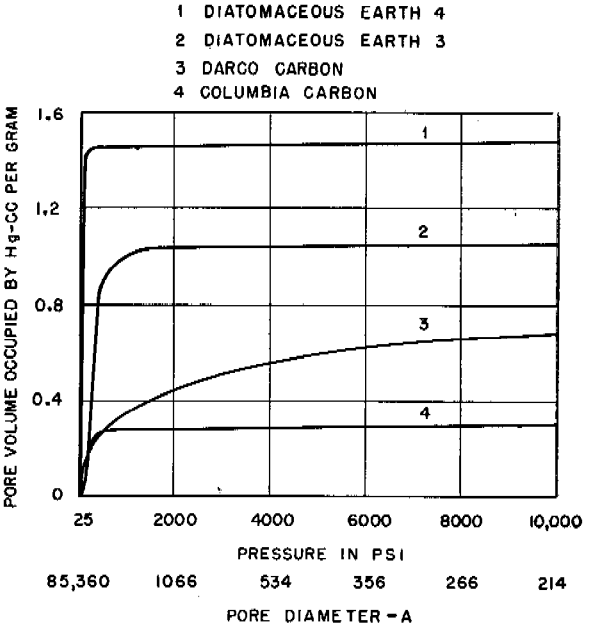


FIGURE 26. Pore diameter measurement curve by high-pressure mercury method.

larger bulk of the capillary. Accordingly, on an average, one would expect that the pore diameters obtained by the mercury method will be somewhat too small. This would mean that all the curves in Figures 23 to 25 should be shifted to somewhat larger pore sizes if some method were available for estimating the difference on an average between the narrow necks and the larger main portion of the bottleneck-shaped capillaries. No method for making this cor-

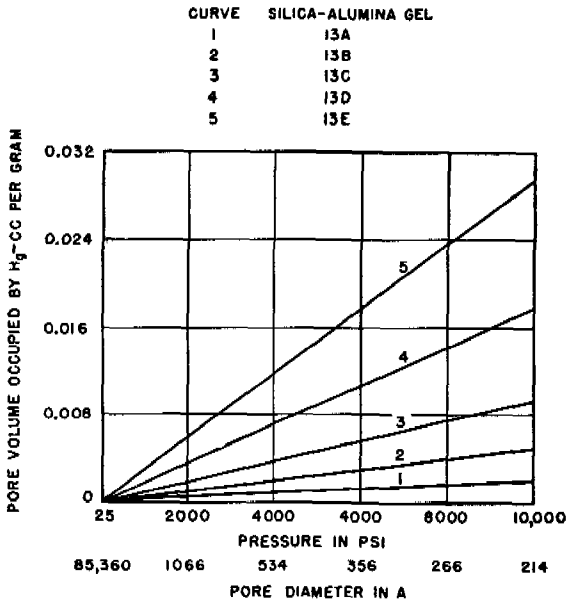


FIGURE 27. Pore diameter measurement curve by high pressure mercury method.

rection is now apparent. It is not surprising in this connection to note that the few measurements [27] on nitrogen adsorption in the pressure range 0.99 to 0.999, corresponding to pore sizes from 1800 to 18,000 A, show much smaller volumes for a given pore size than are shown by the mercury runs. A comparison of seven charcoals is shown in Table 2.

TABLE 2. Macropore volume in the 1800 to 18,000 A diameter range.

Charcoal	Pore volume By N_2 ads	By Hg method
CWSN 19	0.04	0.148
CWSN 196 B1X	0.042	0.308
CWSN 196 B1X TH 427	0.039	0.327
CWSN 196 B1X TH 410	0.050	0.301
NDRC SI 26	0.006	0.0044
CFI "CC"	0.0016	0.019
PCI P58	0.062	0.106

The mercury pore measuring experiments are accompanied [17] by a hysteresis which, for devolatilized or activated charcoals or charcoal materials, is usually equal to 90 to 95% of the mercury in the pores. On the other hand, some of the baked charcoal stocks show prior to activation as little as 35% of the total mercury retained in the sample when the pressure is released. It is a curious fact that the samples showing the smaller mercury hysteresis are also those that show little or no water hysteresis. Juhola [17] has suggested that this may be interpreted as evidence for the formation of *bottleneck* pores during activation, the narrow constrictions in the small pores being responsible for the water hysteresis and the narrow constrictions in the larger pores, for the mercury hysteresis.

6.5 INFLUENCE OF PORE SIZE AND DISTRIBUTION ON CHARCOAL PERFORMANCE

The object of all the pore distribution and size measurements described in the preceding sections has been the elucidation of the factors responsible for the activity of charcoals for gas mask work. Such activity is of two kinds. The charcoal, by virtue of its adsorptive properties, is able to remove some of the poison gases that are likely to be encountered. Other gases can be removed only by adding chemicals to the charcoal capable of catalyzing the oxidation of the poison gas or of chemically reacting with it. For this latter type of action, the charcoal acts as a catalyst support or a support for chemically active reagents. Accordingly, all correlations between pore distributions and activity are concerned with these two general methods, adsorptive and chemical, by which the charcoal in the mask accomplishes its purpose. In this section, we shall summarize such conclusions as have been reached between the structure of the charcoal and its activity.

6.5.1 Definition of Terms

At the outset it will be convenient to define a few arbitrary terms that will be useful in the discussion of activity. The terms to be defined are *free volume*, *submicropore* volume, *micropore* volume, and *macropore* volume.

Free volume is the term used [63] to designate the pore volume of a charcoal that is not filled with nitrogen at a relative pressure of 0.99. It is obtained by subtracting from the total pore volume, as measured by immersing charcoal in mercury at one atmosphere pressure, the volume equivalent to the amount of nitrogen taken up by the charcoal at a relative pressure of 0.99. A value of 0.808 was assumed for the density of nitrogen in this calculation. To a first approximation, the value of the free volume should agree with the pore volume measured by mercury up to pressures of 100 atmospheres since the latter, as well as the 0.99 relative pressure measurement for nitrogen, corresponds (as calculated by the Kelvin

equation) to pore diameters of about 1800 A. In Table 3 are shown the values obtained [27] by the mercury method and by the free volume calculation on typical charcoals and whetlerites. The agreement between the two methods is probably within the combined experimental errors. For example, the change in the calculation of the free volume for the charcoals and whetlerites listed that would result from assuming that the density of the liquid nitrogen in the capillaries is 1.0, rather than 0.808, would more than equal the largest differences between the mercury penetration and the free volume results in Table 3.

TABLE 3. Free volume of charcoals compared to macropore volume to 100 atm by Hg method.

Charcoal	Free Volume*	Volume by Hg method to 100 atm
CWSN 19	0.162	0.199
CWSN 196 B1X	0.402	0.475
CWSN 196 B1X TH 427	0.482	0.491
CWSN 196 B1X TH 410	0.467	0.461
NDRC SI 26	0.007	0.026
CFI "CC"	0.009	0.050
PCI P58	0.265	0.304

* Free volume is the difference between the total pore volume and the nitrogen adsorption at 0.99 relative pressure (calculated as liquid).

Zabor and Juhola [64] arbitrarily defined *macropores* as those that are too large to fill with water vapor by capillary condensation at 80% RH. The macropore volume is the difference between the pore volume as measured by mercury at one atmosphere pressure and the apparent volume occupied by the water picked up at 80% RH during adsorption as judged by helium displacement. *Micropores* are then defined as the pore volume filled with water at 80% RH. *Submicropores* were defined originally [64] as those too small to permit water to condense in them but large enough to admit helium atoms. The volume of the submicropores was determined by measuring by helium displacement the apparent volume occupied by the water picked up at 80% RH and subtracting from this volume the calculated volume for the water based on the assumption that the water condensed in the capillaries has a density of 1.

6.5.2 Free Volume and Activity of Whetlerites Toward CK (80–80)

Early in the work it was discovered that CK removal under 80-80 conditions by whetlerites made from some base charcoals was much less effective than by whetlerites made from other charcoals. As a first suggestion as to the possible cause of the differences in base charcoals, it was pointed out [66] that the better base charcoals had nitrogen isotherms in which the adsorption between 0.4 and 0.99 relative pressure range increases 5% or more. This was construed as a qualitative indication that some pore volume in the range 20 to 1800 A diameter was essential to a base charcoal for a good whetlerite. It soon became evident, however, that although this seemed to be necessary, it was not a sufficient property of a base charcoal to assure it being useful for making whetlerites. For example, CFI charcoals yielded isotherms that increased 18% over this relative pressure range, yet would not make good whetlerites.

It was next suggested [63] that the free volume of the charcoal would be a more useful criterion by which to judge the effectiveness in making whetlerites. This suggestion was based on the belief that possibly pores larger than 1800 A were also important in determining the quality of whetlerite. A comparison [23] of a number of charcoals showed that unless 10% or more of the pore volume was free volume the charcoal would not make a good whetlerite. Thus, Saran and CFI "CC" charcoals, with practically no free volume formed almost inactive whetlerites. However, there were clearly other factors entering into the picture, for a number of charcoals giving free volumes equal to 15% or more of their total pore volumes yielded poor whetlerites, whereas others gave good whetlerites.

All attempted correlations between the 80-80 CK activities of whetlerites and the free volume as judged by nitrogen adsorption were based on the belief that the nitrogen isotherms and free volumes might indicate the amount of pore space that would not be filled with water by capillary condensation at 80% RH. Obviously, this correlation would be rather approximate since a Kelvin equation calculation for water vapor would indicate that a capillary retaining water at 80% RH would be 95 A or less in diameter if $\cos\theta$ is taken equal to 1, whereas nitrogen at 0.99 relative pressure should be held in capillaries 1800 A or less in diameter. Use was, therefore, made of a corrected free volume [27] based on the volume not occupied by nitrogen at a relative pressure of 0.745. This should agree with the volume not occupied by water at 80% RH if $\cos\theta$ for the water desorption is about 0.7. In Table 4, the activities of a series of whetlerites are shown together with values for free volume and corrected free volume. Also, values for

TABLE 4. Comparison of different pore measurements and 80–80 CK activities.

Charcoal	Methods of preparing base charcoals	Free vol cc per g	Corrected* free vol cc per g	Macropore vol per Zabor and Juhola	80–80 CK Lives (min)
CWSN 19	. . . . .	0.13	0.14	0.22	0†
NDRC SI 26 (Saran)	. . . . .	0.007	~0.007	. . .	0†
CFI "CC"	. . . . .	0.007	~0.007	0.02	0†
CWSN 196 B1X TH 423	Impregnated 2% Cr_2O_3. Steamed to 22% weight loss at 950 C; heated in N_2 10 hr 1100 C.	0.25	. . .	0.47	13, 15
CWSN 196 B1X TH 426	Impregnated 5% Fe_2O_3; steamed 9% weight loss, heated 10 hr in N_2 1100 C.	0.26	0.36	0.46	19
CWSN 196 B1X TH 427	Impregnated 5% Cr_2O_3, steamed 16% weight loss at 950 C; heated 10 hr, N_2 1100 C.	0.28	0.38	0.48	14, 18
CWSN 196 B1X TH 432	Impregnated 1% Fe_2O_3, heated in N_2 10 hr at 1100 C to 60% weight loss.	0.30	0.34	0.34	24
CWSN 196 B1X TH 433	Impregnated 2% Cr_2O_3, heated in N_2 10 hr at 1100 C to 8.5% weight loss.	0.26	0.37	0.46	12, 12
CWSN 196 B1X TH 434	Impregnated 5% Cr_2O_3, steamed 20% weight loss at 750 C; heated 10 hr at 1100 C.	0.30	0.42	0.46	16, 20
CWSN 196 B1X TH 437	Impregnated 0.2% Cr_2O_3, heated in N_2 10 hr at 1100 C to 5% weight loss.	0.27	0.30	0.34	22, 26

* Calculated from N_2 adsorption for 0.745 relative pressure.

† *M10 canister test; others are 2.5-cm tube test.*

TABLE 5. Pore volume differences between base chars and whetlerites for samples prepared from CWSN 196 B1X.

Sample	Weight of whetlerite components g per cc granule	Volume of whetlerite components cc per cc granule	Vol difference between base and whetlerite (Hg penetration at 100 atm) cc per cc granule	Vol difference between base and whetlerite (N_2 adsorption at $P/P_0 = 0.99$) cc liquid per cc granule
CWSN 196 B1X TH 432	0.182	0.036	0.005	0.0527
CWSN 196 B1X TH 436	0.127	0.025	0.001	0.0681
CWSN 196 B1X TH 429	0.132	0.026	0.009	0.0620
CWSN 196 B1X TH 427	0.157	0.031	0.003	0.101

the volume of macropores are shown as defined by Zabor and Juhola.[64] It will be noted, in general, that all the active whetlerites have macropore volumes and corrected free volumes that agree with each other and are large compared to those of the base charcoals that do not produce active whetlerites. These limited data afford no direct correlation between the activity and the macropore or corrected free volumes, but they do seem to indicate the necessity of a macropore or corrected free volume larger than some minimum the exact value of which is not clearly defined.

One other conclusion seems evident from measurement of the volume of pores greater than 1800 A by the mercury displacement method.[27] Of the whetlerites made from the four charcoals listed in Table 5, the impregnated chemicals do not appear to be located in pores larger than 1800 A to any great extent. Specifically, from 5 to 30% only of the whetlerizing materials are so located. This observation is checked by the fact that the decrease in volume of pores below 1800 A in size, as judged by the nitrogen adsorption isotherms of impregnated and unimpregnated charcoal, is more than enough to account for the entire volume of whetlerizing components. Presumably, the whetlerizing materials are not only located in pores smaller than 1800 A for the most part, but are in pores sufficiently small to cause some pore blocking. The data in this table point to the conclusion that the necessity of a considerable macropore or corrected free volume in good charcoals may be to furnish a sufficient number of channels through which the gases can reach the whetlerite responsible for their removal. Nothing in these results throws any light on the question of the size pore in which most of the actual removal of the CK occurs.

6.5.3 Macropore Volume and CK 80–80 Activity

Zabor and Juhola [64] and later Juhola [17] have made extended comparisons between the macropore vol-

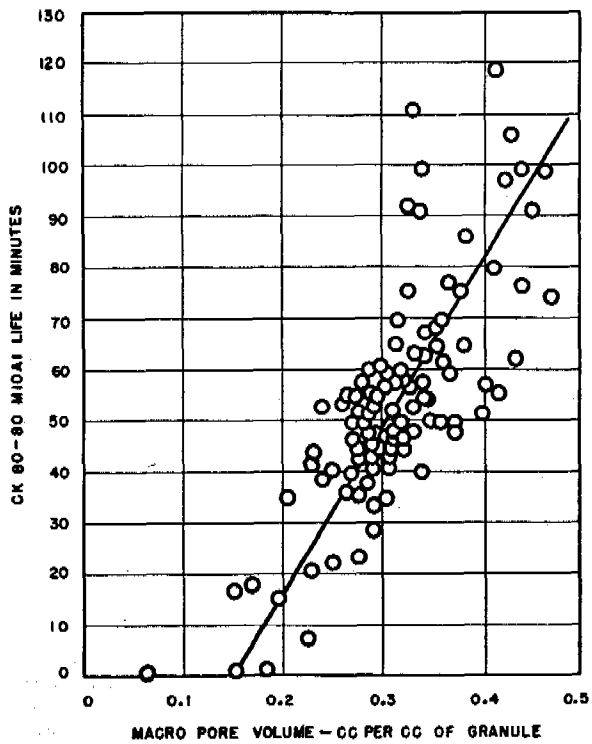


FIGURE 28. Break time for CK 80-80 M10A1 canister tests as a function of macropore volume.

umes of charcoals and the CK 80-80 activities of their whetlerites. A plot of the break time in minutes for the CK 80-80 M10A1 canister tests [17] is shown in Figure 28 as a function of macropore volume. The results for this large number of samples are less definite than indicated by the first paper of Zabor and Juhola,[64] in the fixing of a minimum macropore value below which a whetlerite will have practically zero activity. They indicate clearly, however, that the larger the macropore volume, the better the chance of the whetlerite having a high CK 80-80 life. Apparently macropore volumes below about 0.15 cc per cc granules are too small to yield active whetlerites.

Juhola [17] has discussed in detail the various factors that could conceivably cause the scatter of the results in Figure 28. They are (1) location of impregnant, (2) macropore surface area, (3) pore size distribution in the macropores, (4) carbon surface properties, (5) state of the impregnant, and (6) pore size distribution in the larger micropores. Apparently all the blame for the scattering cannot be placed on any one of these factors. On the other hand, there is considerable evidence that slight variations in whetlerizing technique, in the length of time elapsing between the preparation of the whetlerites and their testing, and in the nature of the surface of the charcoals in themselves, account for a considerable scatter in the CK 80-80 activity tests. Juhola [17] calls attention to two examples in which leaching the initial whetlerite and rewhetlerizing increased the CK 80-80 life from 0 to 27 min in one case, and from 57 to 90 min in another. Obviously, this change is not connected with pore alteration in the charcoal. Accordingly, the agreement indicated by the data in Figure 28 is probably as good as could be expected. It is certainly sufficiently good to indicate the extreme importance of macropore volume as a criterion for selecting base charcoals for making ASC whetlerites.

6.5.4 Pore Size in Relation to the PS, AC, SA, and CG Life of a Charcoal or Whetlerite

In a previous section (Figure 8) attention has already been called [23] to the apparent relation between the PS life of a charcoal and the amount of nitrogen adsorbed at a relative pressure of 0.4. Since this is a pressure that probably will form from one to one and a half monolayers of adsorbed nitrogen on the charcoal, it may be considered as a rough estimate of the surface area. It would be even better to plot the PS life against the surface area values for the various charcoals but, unfortunately, this is made difficult by the lack of precision in obtaining surface area values for adsorbents with pores as small as those of charcoal. An even better correlation was pointed out between the PS life and the adsorption of PS or other molecules of similar size.

Juhola [17] has plotted the micropore volume of a number of charcoals against the PS life with the result shown in Figure 29. As he points out, there is considerable doubt as to whether a plot of this kind is significant in view of the fact that almost certainly PS will be adsorbed as at least a monolayer on the entire charcoal surface at the relative pressure of 0.25 (47 mg of PS per liter) at which most PS life tests are made.

Insufficient work has been done to draw very definite conclusions relative to the relation existing between pore volume, pore distribution, and the activity of a charcoal toward the removal of AC and SA. From the study of activity vs time of activation of PCI charcoals, Blacet and Skei [68] obtained data which indicate that SA activity is very low for the

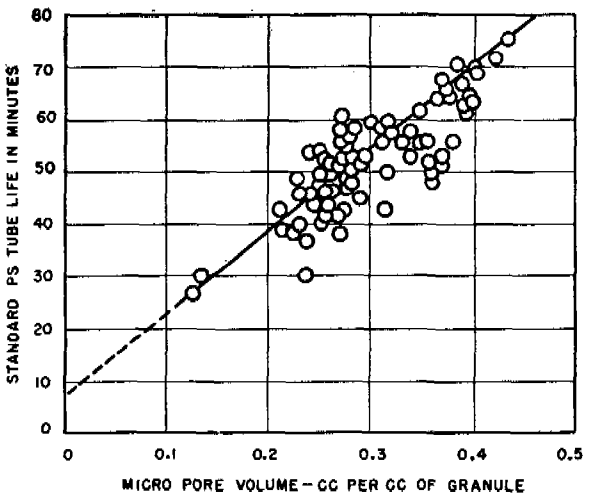


FIGURE 29. Micropore volume of various charcoals vs PS life.

first 100 min of activation and then rises sharply, almost linearly, with time of activation. Unfortunately, pore size measurements were not made on the samples in this series of runs. However, according to a similar series reported by Juhola [17] (Figure 19 of his June 1945 report) the pore size that increases abruptly at about 100 min of activation is the range 18 to 2000 A diameter. Presumably, therefore, pores in this range are essential to SA removal. In contrast to this, AC activity, according to Blacet's and Skei's results, increases from the start and for the 80-80 tests has reached about 60% of its maximum by the end of 100 min of activation. This suggests that perhaps the smaller pores and capillaries (those under 18 A in size) are especially necessary for AC removal. Doubt is thrown on both of these conclusions, however, by the fact that the 80-80 CK activity behaves quite differently as a function of the time of activation in Blacet's and Skei's [18] tests and in those reported by Juhola.[17] In the former, the CK activity begins rising abruptly after about 30-min activation and reaches a life that is, at least, 80% of the smoothed maximum by 100-min activation. In contrast to this, according to Juhola's report,[17] the CK 80-80 activity is very low during the first 90-min activation and then rises linearly with time to an activation of 300 min, the longest activation period employed. This makes one believe that conditions during the activation of the two series were not the same and that, accordingly, the pore size measurements, as a function of time, on the series reported by Juhola may not be the same as on the series reported by Skei. It should be emphasized, however, that with the completion of the methods for measuring pore distributions in charcoals and whetlerites it is now possible to carry out experiments that should throw more light on the mechanisms of removal of the various gases by charcoal than has been possible in the past.

The CG test data reported by Zabor and Juhola [64] indicate that macropore volume is as important to the removal of CG (80-80 test conditions) as it appears to be to the removal of CK under 80-80 test conditions. In both cases, according to these authors, there is a minimum macropore volume below which the CK and the CG lives are substantially zero. No further information is available relative to the CG activity as a function of macropore volume. The preponderance of evidence certainly indicates the importance of macropore volume for CG as well as for CK removal.

6.6 PORE SIZE ALTERATION

When it appeared that pore size distribution might be largely responsible for the failure of certain charcoals to make good whetlerites, work was undertaken [69] with a view to altering the pore size of the base charcoals that would not make good whetlerites. In particular, it appeared that the charcoals made at that time by the $ZnCl_2$ process were good adsorbents but very poor supports for making whetlerites. A typical nitrogen isotherm of such a charcoal is illustrated in Figure 5. On the other hand, charcoals made from coal by certain procedures were excellent both as an adsorbent and as a base charcoal for making whetlerites. The intensive work on pore alteration, accordingly, originated with the idea of trying to alter the product of the $ZnCl_2$ process so as to permit the large plant capacity producing charcoal by this process to be usable.

The alteration in pore size has been judged mostly by the change in the appearance of the nitrogen adsorption isotherms up to relative pressures of 0.99. Furthermore, most of the discussion will be centered upon the actual pore alteration rather than on the improvement in the whetlerized product-result from such alteration. The procedure in making these whetlerite tests was not up to the usual standard of whetlerization and testing because all samples of the base charcoal had to be shipped, and because whetlerizing technique and whetlerite testing were in the process of change during the period of this work, making it impossible to compare adequately one group of samples with another.

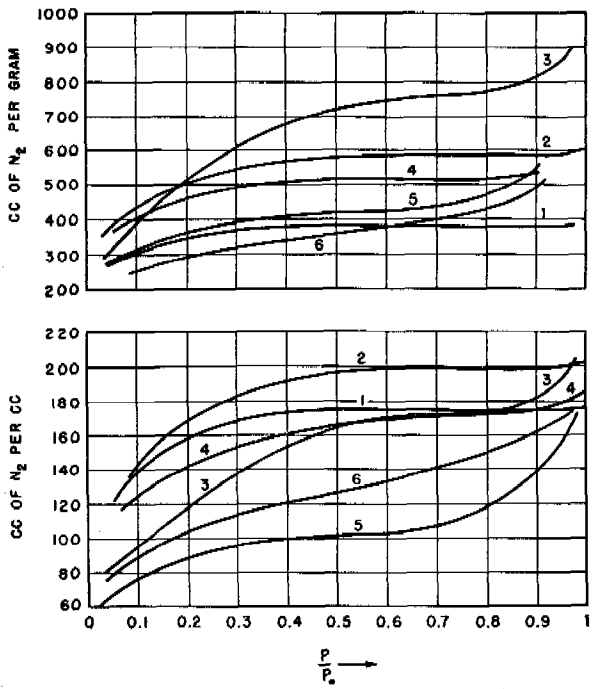


FIGURE 30. Effects of treating CWSN 19: (1) Normal CWSN 19; (2) Steamed at 750 C, 43% loss; (3) H_2 at 1000 C, 74% loss; (4) 5% Fe_2O_3, steam at 750 C, 37% loss; (5) 5% Fe_2O_3, H_2 at 600 C, 50% loss; (6) 5% Fe_2O_3, air at 350 C, 48% loss.

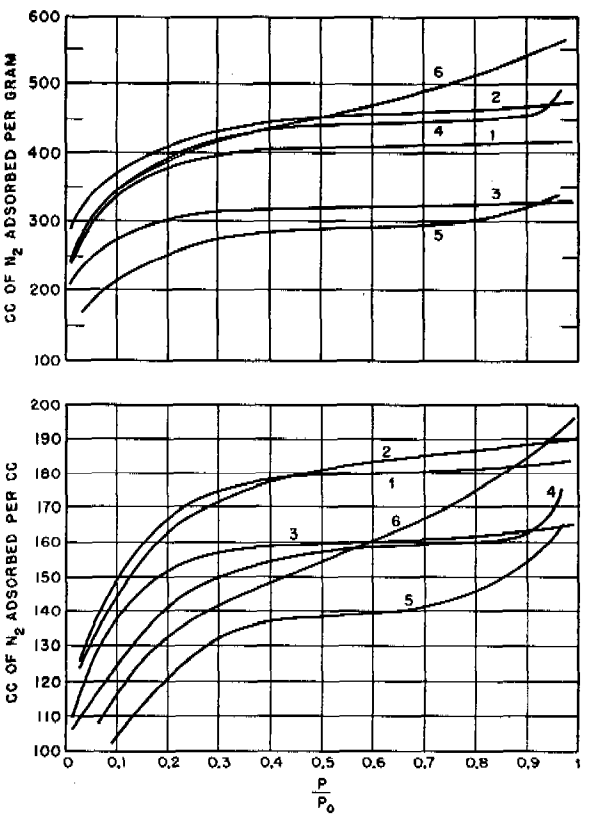


FIGURE 31. Effects of treating CWSN S5: (1) Normal CWSN S5; (2) Heated in pure N_2 to 1200 C then steamed at 750 C to 69% loss; (3) Heated for 2 hours in pure N_2 at 1200 C; (4) H_2 treated at 1000 C to 37% loss; (5) 5% Fe_2O_3, tank N_2 at 1000 C to 25% loss; (6) 5% Fe_2O_3, H_2 treated at 500 C to 30% loss.

In discussing the influence of various factors on the shapes of the isotherms, it will be convenient to differentiate between the total adsorption in the region up to 0.4 (called AB), the slope of the isotherm between 0.4 and 0.7 (called BC; this is roughly the pore size that would be filled with water vapor by capillary condensation at 80% RH if cos θ for water is about 0.6), and the slope of the isotherm between 0.7 and 0.99 (called CD; this region is the portion of the macropore region lying between about 60 and 2000 A).

It is also important to differentiate between changes in isotherms per gram of charcoal and changes per cubic centimeter of granules (this means per cubic centimeter of actual charcoal volume as measured by mercury pycnometers at 1 atmosphere pressure).

In a general way it can be said that it is possible [69] to tailor-make the pore distributions in charcoals by a combination of steaming and hydrogenating (with and without impregnants), that is, to change charcoals having flat sotherms of the type shown in Figure 5 for CWSN 19 to isotherms having steeper slopes. The region AB can be increased or decreased on either a per gram or a per cubic centimeter basis; both BC and CD can be left unchanged in slope or can be increased in slope. An increase in slope of either of these last two regions is interpreted as an increase in pore volume in these respective ranges. On the other hand, an increase in AB might mean an increase in the number of small pores, or it might mean an increase in the total surface area caused possibly by increases in the number of pores n the BC region.

A few typical examples [69] of the effect of steaming, air oxidizing, hydrogenating and, to a limited extent, treatment with impregnants are shown in Figures 30 - 34. For more examples, the reader is referred to the original report [69] where a total of 17 figures show all the results that were obtained on pore alteration. Below are discussed the influence of a few of the operations on the shape of the isotherms in so far as any general conclusions can be drawn.

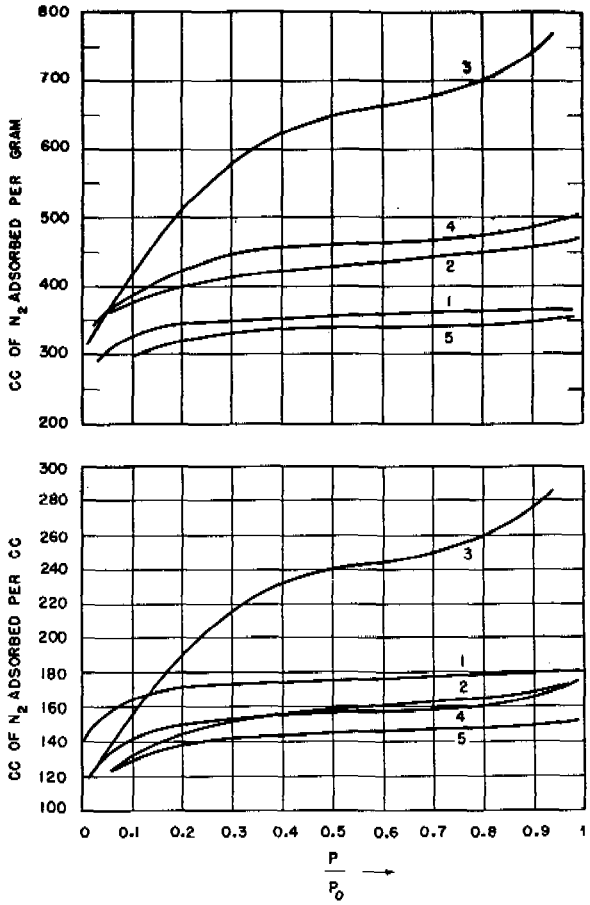


FIGURE 32. Effects of treating coconut charcoal. (1) Normal coconut charcoal; (2) Steamed at 750 C to 40% loss; (3) 0.2% Cr_2O_3, steamed 750 C, 33% loss; (4) H_2 treated at 1000 C to 31% loss; (5) 5% Cr_2O_3, H_2 at 1000 C to 38% loss.

6.6.1 Steaming without Impregnating

Moderate steaming at 750 C on standard charcoal samples increased the adsorption in region *AB*. This presumably means that added steaming beyond the point usually used for steam-activated charcoals continues to open up small pores. This was always true on a weight basis for the four charcoals studied, CWSN 19, CWSN 55, coconut charcoal, and PCI P58. The adsorption per cc was increased in the *AB* region for the first of these four but decreases slightly for the other three. Examples are given by curves in Figures 30 to 34. There is nothing unusual in these steaming results since new small pores can certainly be opened up by the treatment with a resulting increase in adsorption per gram. If the steaming is carried too far, of course, the adsorption per cubic centimeter of granules must start to decrease because of overlapping of the small pores.

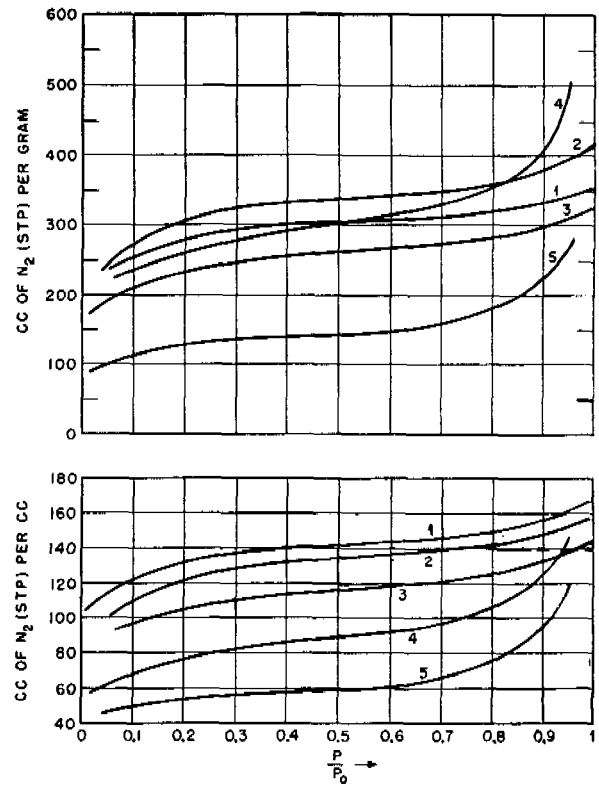


FIGURE 33. Effects of treating PCI P58. (1) PCI P58; (2) Steamed 750 C to 31% loss; (3) 5% Cr_2O_3, steam 750 C, 36% loss; (4) H_2 at 1000 C to 48% loss; (5) 5% Cr_2O_3, H_2 at 1000 C, 43% loss.

6.6.2 Hydrogenation without Impregnation

It does not seem to be generally recognized in the literature that hydrogenation can alter pore sizes and distribution just as effectively as can steaming. Usually, however, a somewhat higher temperature is needed for hydrogenation than for steaming. Figures 30 to 34 show curves illustrating the effect of hydrogenation of the four charcoals studied. For all of them, the adsorption in the *AB* region per gram either increases or remains constant; the slope of the adsorption in the intermediate *BC* region remains unchanged, and the slope of the adsorption in the *CD* region increases sharply with an especially rapid increase close to a relative pressure of 0.99. In fact, the rapid rise in the adsorption between 0.9 and 0.99 relative pressure is rather characteristic of hydrogenation in the absence of impregnants.

Only for charcoal CWSN 19 is there an increase in the total adsorption per cubic centimeter of granules during mild hydrogenation. Presumably, the major attack is on pores in the *CD* region.

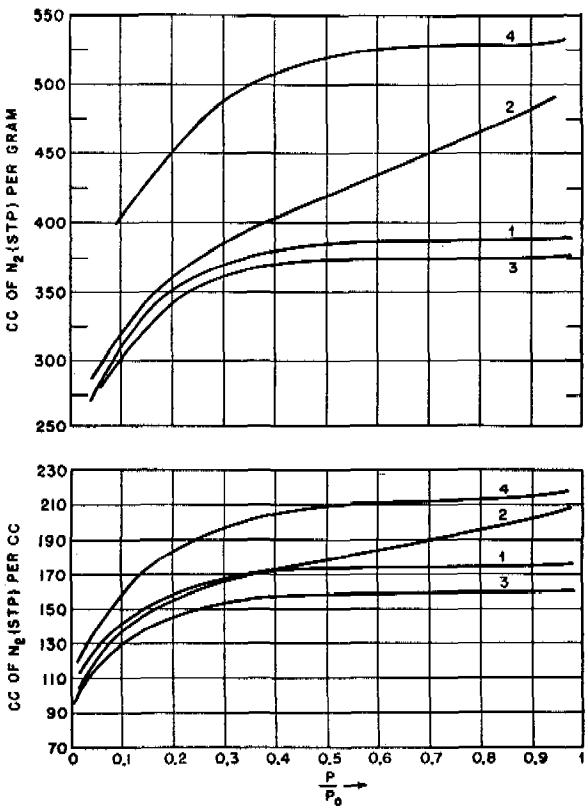


FIGURE 34. Effects of hydrogenation of CWSN 19. (1) CWSN 19; (2) 5% NiO. H_2 at 1000 C to 27% loss $Ni(NO_3)_2$; (3) 5% NiO, H_2 at 1000 C to 25% loss ($NiCl_2$); (4) H_2 treated at 1000 C to 26% loss.

6.6.3 Partial Combustion in Nitrogen Containing Limited Amounts of Oxygen and No Impregnants

Mild oxidation of CWSN 19 increased the adsorption in the *AB* region (Figure 30) by a small amount both on a per gram and a per cubic centimeter basis. On the other hand, it had little influence on the slope of the isotherm above 0.4 relative pressure. Presumably such oxidation primarily effects the formation of new small pores.

6.6.4 Influence of Impregnants on Steaming, Hydrogenation, and Partial Oxidation

In the course of the work, the action of Cr_2O_3, Fe_2O_3, Mo_2O_3, Na_2CO_3, and NiO on the various processes for altering pore size were studied. These compounds were formed in amounts ranging from 0.2 to 5.0% by various procedures.[69] It is sometimes difficult to generalize because the impregnant produced results at times that differed as a function of the particular compounds used in getting the given oxide on the sample. However, in a general way the results were as follows.

1. Fe_2O_3 gave definite evidence of catalyzing the attack on the charcoal. For example, at 600 C in the presence of 5% Fe_2O_3 impregnant a 50% weight loss of CWSN 19 was brought about by hydrogenation, whereas in the absence of the impregnant practically no loss occurred. Another evidence is the fact that even on a weight basis, the adsorption up to 0.4 relative pressure decreased in a majority of treatments with Fe_2O_3 as impregnant. This is definite evidence of an attack on the smaller pores greater in extent than any formation of small pores that is taking place. The iron oxide invariably causes a considerable rise in the isotherms between 0.7 and 0.99 regardless of the gas being employed for activation.

One result with iron oxide is especially puzzling. In a run using 5% iron oxide and carried out with tank nitrogen at 1000 C to a 13% weight loss, the total pore volume on both the per gram and per cubic centimeter basis dropped about 20%. Unless some error in calculation was involved (the original notebooks are not available at this writing) this means that the closing up of enough small pores by the 1000 C treatment more than compensates for the increase in the number of pores indicated by the 0.7 to 0.99 relative pressure region. This is the only instance in which positive evidence was obtained of a pore closing effect on CWSN 19.

2. Cr_2O_3 impregnation combined with steaming on CWSN 19 seems to have little added effect over steaming by itself. On hydrogenation, however, the effect is similar to that of the iron in that a considerable decrease in the *AB* region occurs on a volume basis with a marked increase in the *CD* region.

The results on CWSN S5 are confused by the fact that heating this charcoal to 1200 C even in pure nitrogen causes a shrinkage as a result of which the adsorption per unit weight decreases *more* than the adsorption per unit volume (Figure 31). In other words, the apparent particle density increases. At 750 C, steaming after impregnation with chromium oxide produces a very different effect than steaming alone. The low-pressure adsorption decreases per cubic centimeter of charcoal, whereas the slopes of both the *BC* and *CD* regions are increased by about 15%. The hydrogenation at 1000 C with Cr_2O_3 present seems to produce the same sintering effect caused by heating this charcoal to 1200 C but in addition

causes a 20% increase in the slope of the *CD* portion of the isotherm.

On coconut charcoal, impregnation with 0.2% Cr_2O_3 caused nearly a 100% increase in the adsorption up to 0.4 relative pressure on a weight basis, a 30% increase on a volume basis and a 15% slope increase in the *CD* region (Figure 32). Strangely enough, 5% Cr_2O_3 and steaming produced very little more effect than straight steaming to a similar weight loss, though the slope of the *BC* and *CD* regions were 10 to 20% greater than those resulting from steaming alone. Hydrogenation of coconut charcoal impregnated with 0.2 or 5% Cr_2O_3 caused none of the slope change characterizing similar runs on CWSN 19 or CWSN S5, the slope of the isotherms being identical to that of the original charcoal; in fact, the marked turn-up of the isotherm between 0.9 and 0.99 produced by straight hydrogenation is absent when Cr_2O_3 is present (Figure 32).

PCI P58, impregnated with Cr_2O_3, behaved little differently on steaming from samples not impregnated as regard the slope of the isotherms; however, the larger (5%) Cr_2O_3 content caused a drop in the absolute adsorption of 15 or 20% on both the weight and volume basis (Figure 33). Hydrogenation after impregnation with Cr_2O_3 produced the same slope increase in the *CD* region that was obtained without any impregnation; the total pore volume, however, of this charcoal was decreased by the impregnation both on the weight and volume basis (Figure 33), much as though a sintering effect had taken place that shifted the adsorption to smaller values on both a weight and volume basis.

It is apparent that Cr_2O_3 as an impregnant can effect marked changes in charcoals when combined with steaming and hydrogenation, and that the effects are apparently quite specific and dependent on the kind of charcoal used.

3. On steaming, NiO on CWSN 19 produces no change in slope of the isotherms, just as was true of straight steaming; however, it appears to drop the total pore volume on both a weight and volume basis by about 35% compared to the volume after steaming in the absence of NiO. For hydrogenation, the nickel results are especially noteworthy in that they show a decided specificity upon the particular nickel salt used in impregnation. For example, if the nitrate is used together with precipitation by NH_4OH, hydrogenation to a weight loss of 29% results in a nitrogen isotherm that is a straight line from 0.4 to 1.0 relative pressure with an increase in volume of 20% over this range. In contrast to this, the same percentage of NiO produced from $NiCl_2$ plus NH_4OH caused no change in slope and only a few per cent decrease in total adsorption compared to the initial CWSN 19 (Figure 34). In fact, the NiO from the chloride appeared to have little effect on the hydrogenation.

The single experiment tried on CWSN 5 indicated that impregnation with 5% NiO combined with hydrogenation at 1000 C resulted in no change in slope of the isotherm compared to the original, and a decrease of about 15% total adsorption on both a weight and volume basis.

4. Impregnation (5%) with Mo_2O_3 produced no specific effects in either steaming or hydrogenating CWSN 19 other than those observed without the impregnation. Likewise, 5% Na_2O from sodium carbonate produced no noticeable modification to the hydrogenation of CWSN 19 at 1000 C.

The two experiments on steaming Type A whetlerites (Cu impregnation) behaved quite differently. On CWSN 19, steaming a whetlerite to a 26% loss at 750 C resulted in an isotherm unchanged in slope from that of the original charcoal but about 35% smaller in volume than would have resulted from a steaming to a 40% weight loss in the absence of the impregnant. On the other hand, steaming a Type A whetlerite made from CWSN S5 caused the slope of the *BC* and *CD* section of the isotherm to increase greatly, the adsorption at 0.99 relative pressure being about 20% greater than at 0.4 relative pressure.

6.7 OXYGEN SURFACE COMPLEXES ON CHARCOALS

6.7.1 Introduction

It has long been known [33, 38, 70–72] that charcoals and activated carbons are covered with carbon-oxygen complexes, the composition of which varies as a function of the method of treatment of the sample. Research on surface complexes of charcoal during the war has been carried out primarily because of the help it might furnish in (1) showing the proper surface treatment to give maximum adsorption of certain gases such as ammonia that are apparently very sensitive to the nature of the charcoal surface; (2) interpreting the aging of base charcoal that from time to time was thought to be taking place on storage under humid conditions; (3) interpreting the aging of ASC whetlerites that is known to occur under high

humidity; and (4) indicating the type of surface complex that might be most effective in minimizing the adsorption of water vapor by the whetlerites.

The actual results obtained that are applicable to the four main objects of the work are, for the most part, restricted to item (1) above. The surface complex studies failed to throw much light on items (2) and (3).[27] This may be due in part to the fact that the surface complex work was carried out in a different laboratory from that in which the whetlerization and aging work was done. Consequently, the delay in getting samples whetlerized, the uncertainties surrounding the treated base charcoals during shipment for whetlerization, and the changing of whetlerizing procedures in the course of this work, all tended to complicate the drawing of any rigorous conclusions as to the influence of surface complexes on the aging of either the base charcoals or the whetlerites. As for (4), the behavior of whetlerites toward water vapor appears to be much more dependent on the pore size distribution in the region between that corresponding to capillary condensation at 0.8 relative pressure and that at 1.0 relative pressure than it does on the nature of the surface complex. The latter is more likely to influence the amount of water adsorption occurring at low relative pressures but is less influential on the adsorption at high relative pressures.

The work that has been done on the surface complexes divides itself rather naturally into two parts: (1) the study of oxygen adsorption by the charcoal in relation to the adsorptive properties toward ammonia, acids, and bases; and (2) the measurement of the gas evolution as a function of the temperature to which the various charcoals have been heated. The first of these two groups of experiments were carried out chiefly by Young[24, 73] and his co-workers; the second, by Anderson.[27] These two research studies contribute a great many useful data and correlations that will now be briefly summarized even though they fail to give a definite answer to the question of the relation between the surface composition and the aging of charcoals and whetlerites.

6.7.2 Oxygen Adsorption by Charcoals and its Influence on their Properties

As pointed out by Young,[73] it has long been known [74, 75, 75a, 79a, 80a] that several different carbon-oxygen surface complexes may exist on charcoal and carbon black. Two [76–78] of these appear to be formed by the picking up of oxygen at room temperature; another is claimed to be formed by exposure of charcoal to oxygen at about 400 C; and a fourth [79] is supposed to form above 850 C in the presence of oxidizing gases. Oxygen complexes have been reported for graphite and diamond [80] as well as for charcoal and carbon black. The experiments reviewed and summarized in the present section were directed not so much toward the verification of these various complexes as toward the study of the influence of the complexes formed at 400 C in free oxygen upon the properties of the various charcoals as adsorbents for acids, bases, ammonia, HCl, and water vapor. A few experiments were also made upon the rate of oxygen pickup by various charcoals at room temperature. These various results and observations made during this work may be summarized as follows.

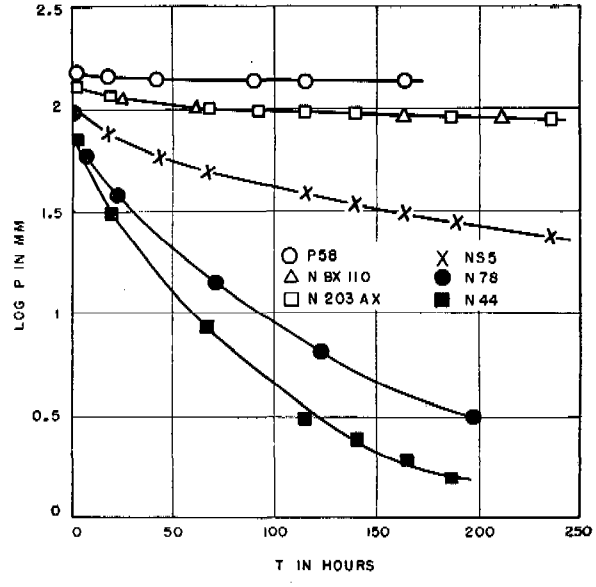


FIGURE 35. Oxygen sorption at 25 C on charcoals.

1. Oxygen pickup by charcoals: Lowry [38] pointed out that oxygen is slowly picked up by charcoals at room temperature in the form of a chemical adsorption. In addition, there is a rapid physical adsorption which is easily reversible and which amounts to about 10% of a monolayer at one atmosphere pressure. The slow chemical adsorption varies in amount and rate with different charcoals. Figure 35 shows the results obtained by Young [24] on a typical group of charcoals. The total oxygen picked up irreversibly by even CWSN 44 is apparently only a small fraction of a monolayer.

By exposing charcoals to oxygen at 400 C, Young has succeeded in building up an oxygen content of as

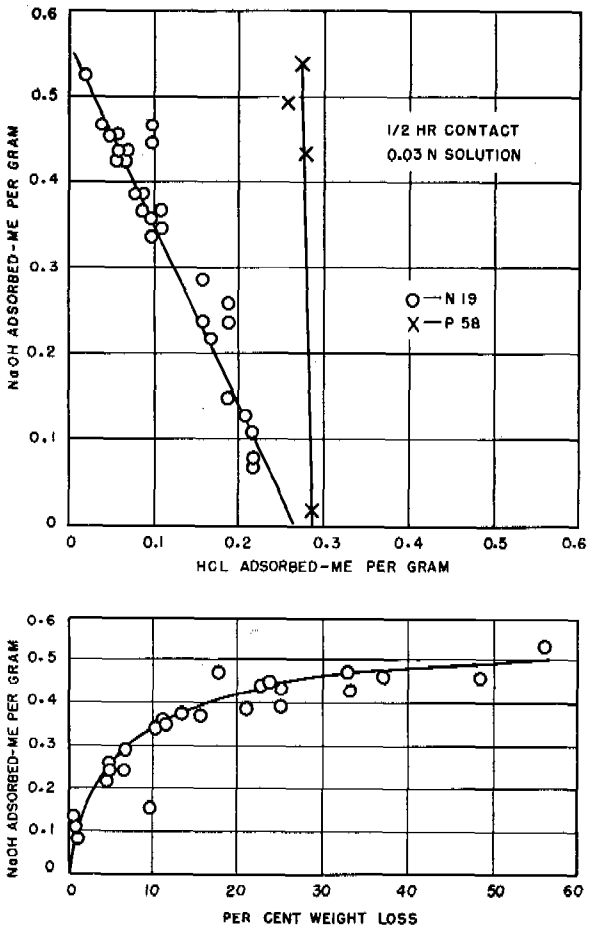


FIGURE 36. Influence of oxygen treatment on the base and acid adsorptive properties.

much as 18% on the charcoals. This oxygen coating was accompanied by a 56% weight loss. It should be noted that even 18% oxygen corresponds to only a monolayer of oxygen on the surface of the carbon.

2. Influence of oxygen treatment on the base and acid adsorptive properties: CWSN 19, upon which most of the early oxygen complex work was done, adsorbed [73] 0.27 milli-equivalents of HCl per gram and no NaOH. The time allowed for equilibration in adsorption in these experiments was 30 min and the original concentration of the adsorbate solution was 0.03*N*. Oxygen-treating the charcoal increased the base adsorption and decreased the acid adsorption. The results are shown in Figure 36 taken from the paper of Young.[73] In the same figure is shown the NaOH adsorption as a function of the weight loss in the oxidation process.

In Figure 37 is shown the variation of the rate of NaOH pickup with time, temperature, and the

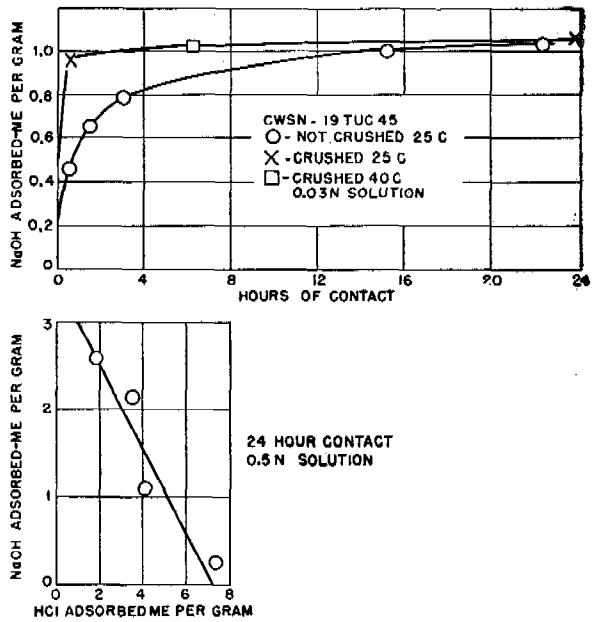


FIGURE 37. Variations of the rate of NaOH pickup with particle size.

amount of crushing to which the sample has been subjected. Evidently, crushing the sample and increasing the temperature increases the rate of adsorption greatly. Neither temperature increase nor crushing has any effect on the final equilibrium value of the adsorption. Figure 37 also shows the adsorption curve obtained by allowing 24-hour equilibration and by using adsorption solutions that were 0.5*N*. As pointed out by Young, the slope of this curve indicates that for every equivalent of acid-forming power lost by the charcoal, four to five equivalents of base-forming power are gained.

Experiments by King [79] and also by Young [73] lead to the conclusion that both the H^+ and the Cl^- are adsorbed from solutions by the charcoals. Also, both Na^+ and OH^- are adsorbed. It is still unknown whether the alkali *adsorption* is a process by which the Na^+, by base exchange, displaces a H^+ from the surface which then reacts with the OH^- or whether the Na^+ and OH^- are actually adsorbed.

Washing experiments showed that most of the HCl adsorbed by the untreated CWSN 19 and most of the NaOH adsorbed by the oxygen-treated samples were irreversibly adsorbed. In other words, they were not removed by thorough washing. However, these quantities of *irreversibly held* adsorbates could be titrated with base and acid respectively, washed, and caused to re-adsorb the original amount of adsorbate. For example, the original CWSN 19 held 0.24 milli-equiv-

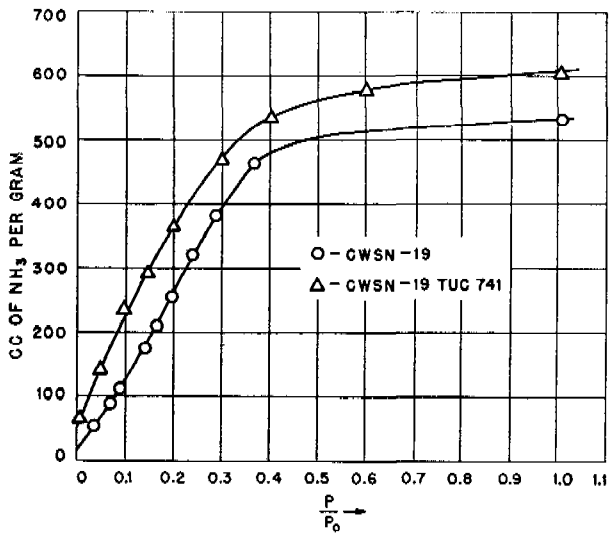


FIGURE 38. Typical curves of effects of oxygen coating on NH_3 adsorption.

alent of HCl irreversibly. This, on titration, picked up 0.24 milli-equivalent of NaOH with the evolution of this amount of NaCl into the solution. The sample, after washing, could then again pick up 0.24 milli-equivalent of HCl and the process could be repeated.

3. Influence of surface complex on the adsorption of water vapor: It has already been pointed out in the section on water adsorption that adding oxygen complex to a charcoal increases the low pressure adsorption of water vapor and displaces the desorption hysteresis loop to lower relative pressures. Conversely, treating charcoals with hydrogen or with steam at high temperature tends to shift the adsorption curves to higher relative pressure and decreases markedly the adsorption below 0.5 relative pressure. It should also be noted that similar effects have been observed for carbon black samples as shown in Figure 14.

4. Influence of surface complex on the adsorption of ammonia and of HCl gas: Oxygen-treating a charcoal at 400 C increases its tube life for ammonia ten to forty fold and increases the ammonia adsorption over the entire relative pressure range.[23, 73] In Figure 38, two typical curves that illustrate the effect of oxygen coating are shown. The extra ammonia pickup would appear to be due to a kind of chemical adsorption of ammonia since the increase in adsorption is between 75 and 100 cc throughout the entire pressure range. However, the heat of binding of such chemisorption is not great, as is evidenced by the fact that the extra ammonia will pump off slowly at 25 C, and completely in a short time at 100 C.[23] It should also be recorded that nitrogen isotherms prove that this enhanced ammonia adsorption is definitely not the result of an increase in surface of the charcoal resulting from the oxygen treatment. It is due to the specific nature of the surface containing the oxygen complex.

The adsorption of HCl gas by CWSN 19 is not altered [81] in any marked way by oxygen coating. The changes in the adsorption are small and apparently no greater than the corresponding changes in the nitrogen adsorption.

5. Heat of binding of oxygen to carbon in the surface complex: By a series of careful measurements of the heat of combustion of charcoal as a function of the amount of oxygen complex on the surface, Young [73] has been able to show that the oxygen is held to the surface of a carbon by a heat of about 60,000 to 65,000 calories per mole of oxygen. The heat of adsorption at 400 C thus estimated appears to be independent of the fraction of the surface covered by complex. These heat of adsorption values are in good agreement with the value 70,000 calories found by Keyes and Marshall [82] for charcoal at 0 C, 60,000 calories reported by Blench and Garner [83] for adsorption at room temperature, and 70,000 to 129,000 calories reported by Marshall and MacInnes.[84] There can be no doubt that the oxygen is held to the carbon surface by very strong chemical bonds.[85, 86]

6.7.3 Gas Evolution from Charcoals as a Function of the Temperature to Which They are Heated

Lowry [38] has described the apparatus used and the results obtained in degassing a series of charcoals which at the end of World War I could be considered as typical of those used by the United States, Great Britain, and Germany. In general, he showed that all charcoals evolved considerable quantities of CO, CO_2, and water vapor up to about 900 C. Between 900 and 1200 C, increasingly large quantities of hydrogen were given off. Part of this hydrogen appeared to come from the surface of the charcoal though it is also possible that part of it resulted from decomposition of hydrogen-carbon complexes that were not located at the actual surface of the charcoal.

Using a very similar apparatus, Anderson [27] has made an extended series of experiments on various charcoals of interest in the recent research work in

TABLE 6. Degassing experiments on charcoals — total gas evolved ml (STP) per g.

Sample	25–300 C			300–600 C				600–900 C				900–1200 C				
	CO	CO_2	H_2O	H_2	CO	CO_2	H_2O	H_2	CO	CO_2	H_2O	H_2	CO	CH_4	CO_2	H_2O
CWSN 19	0.2	0.3	0.4	0.3	3.8	1.5	1.3	10.4	11.7	0.5	0.4	46.4	1.0	2.1	1.0	0.0
CWSN S5	0.5	2.0	2.3	1.0	4.6	2.3	5.3	92.0	21.7	1.4	6.0	36.9	0.6	0.6	0.0	0.0
CWSN S5 Extracted with HF	0.9	3.0	5.8	2.5	87.2	39.9	1.9	66.9	27.7	1.2	2.0	21.8	0.4	0.6	0.7	0.1
CWSN 44	0.7	3.3	3.5	1.4	6.6	3.2	4.6	97.5	22.8	1.1	4.0	51.8	2.6	3.3	0.1	0.0
CWSN 196 B1	0.5	2.7	3.3	1.4	5.5	3.0	4.6	93.0	29.5	0.5	1.8	36.5	0.5	0.8	0.2	0.0
CWSN 196 B1X	0.2	1.5	1.6	1.0	3.3	6.8	1.6	53.1	11.8	0.2	0.1	33.8	0.4	0.8	0.2	0.1
PCI P58	0.1	0.2	0.9	0.1	1.2	0.7	0.7	16.2	11.4	0.5	0.2	38.3	97.8	4.7	0.0	0.0
CWSC 1242	0.3	0.6	0.9	0.0	0.7	1.2	1.1	5.8	4.0	0.3	0.2	19.3	0.9	0.1	0.2	0.1
CFI "CC"	0.1	0.2	1.2	0.0	0.7	0.3	1.1	7.8	5.5	0.2	0.2	38.5	63.4	0.8	0.2	0.0
CWSB–X2	0.2	3.1	2.3					13.4*	7.8*	2.2*	1.9*	36.3	5.4	0.6	0.3	0.1
	25–120 C			120–600 C												
PCI P25	0.0	0.0	0.5	0.5	2.0	1.0	3.0	10.5	9.9	0.4	0.5	35.3	88.5	2.7	0.3	0.0
PCI 1042	0.0	0.2	0.6	0.3	2.6	1.2	1.3	7.5	9.6	0.3	0.3	43.2	93.1	2.3	0.4	0.0
PCI 1042 Extracted with HF	0.0	0.0	0.7	0.6	51.2	9.4	4.3	20.8	20.9	3.0	0.3	22.3	0.8	0.8	0.4	0.0

* 300-900 C.

TABLE 7. Degassing experiments on charcoals — total gas evolved ml (STP) per g.

Sample	25–900 C				25–1200 C					H_2 evolved	O_2 evolved	O_2 in ash
	H_2	CO	CO_2	H_2O	H_2	CO	CH_4	CO_2	H_2O			
CWSN 19	10.7	15.7	2.3	2.1	57.1	16.7	2.7	3.3	2.1	0.58	1.81	0.04*
CWSN S5	93.0	26.8	5.7	13.5	129.9	27.4	1.4	5.7	13.6	1.31	3.74	2.0†
CWSN S5 Extracted with HF	69.4	115.8	44.1	9.7	91.2	116.2	1.8	44.8	9.8	0.93	16.10	
CWSN 44	98.9	30.1	7.6	12.1	147.5	32.7	8.3	7.7	12.1	1.58	4.30	0.8*
CWSN 196 B1	94.4	35.5	6.2	9.7	130.9	36.0	1.8	6.4	9.8	1.29	4.18	0.6*
CWSN 196 B1X	54.1	15.3	8.5	3.3	87.9	15.7	1.5	8.7	3.4	0.84	2.59	1.0*
PCI P58	16.3	12.7	1.4	1.8	54.6	110.5	5.0	1.4	1.8	0.59	8.22	
CWSC 1242	5.8	5.0	2.1	2.1	25.1	5.9	0.2	2.3	2.3	0.25	0.91	
CFI "CC"	7.8	6.3	0.7	2.5	49.7	13.4	0.8	5.6	4.3	0.50	2.06	
CWSB X2	13.4	8.0	5.3	4.2	46.3	69.7	0.8	0.9	2.5	0.45	5.28	
PCI P25	11.0	11.9	1.4	4.0	46.3	100.5	2.8	1.7	4.0	0.40	7.70	
PCI 1042	7.8	12.2	1.7	2.2	51.0	102.3	2.5	2.1	2.2	0.58	7.76	
PCI 1042 Extracted with HF	21.4	72.1	12.4	5.3	43.7	72.9	1.2	12.8	5.3	0.46	7.42	

* Ash was assumed to be zinc oxide in computation of these values.
† Reported by Wiig and Flagg (Informal Report 10.1-26 June 11, 1943).

World War II. The evolved gas was collected during periods of about seven hours for each temperature interval studied. The experiments were grouped to cover the range 25 to 300 C; 300 to 600 C; 600 to 900 C; and 900 to 1200 C. The variables studied included the nature of the charcoal, the ash content [87] of the charcoal, and the type of treatment to which the charcoal had been subjected. The principal results [27] obtained may be briefly summarized as follows.

1. In Table 6 are shown the volumes of CO, H_2, CO_2, CH_4, and H_2O evolved from a number of typical charcoals as a function of the temperature to which they were heated. In Table 7 the results are summarized to cover the region up to 900 and up to 1200 C; also in this latter table are shown the results of gas evolution to 1200 C calculated in terms of equivalent per cent of hydrogen and oxygen in the original charcoal. For comparison, Table 7 also shows the per cent oxygen present in the ash wherever ash analysis was available or could be guessed from the method of preparation of the charcoal.

Several general conclusions can be drawn from the results in these two tables. In the first place it should be noted that the CO and CO_2 evolution is smaller from the PCI, CWSC, CFI, and CWSB–X (nutshell) than from the National samples prepared by the $ZnCl_2$ process. However, a detailed study of

the gas evolution from one of the National samples, CWSN 5, at 60-degree intervals showed that most of the CO and H_2O were evolved in the temperature range 600 C to 800 C. Concomitantly with the gas release, a deposit of zinc was formed on the cooler part of the reaction vessel. In all probability, therefore, the excessive evolution of CO and H_2O from the National samples in the temperature range up to 900 C may be attributed to a large extent to the reduction of ZnO ash by C and by H_2. Consistent with this interpretation is the fact that CWSN 19, which had only 0.04% ash, yielded volumes of CO and H_2O in the temperature range up to 900 C approximately the same as obtained from charcoals not made by the $ZnCl_2$ process.

At temperatures above 900 C, a burst of CO was obtained from all the charcoals that had appreciable percentages of ash other than ZnO. There seems to be little doubt that this higher temperature CO evolution is caused by the reduction of the ash components by C. Ash for the most part on analyzed samples was found to consist of SiO_2 and Al_2O_3.[87] Data in the literature [88] indicate that for the reduction of SiO_2 by C to form silicon carbides and CO, the partial pressure of evolved gas at 900 C at equilibrium is about 0.1 mm, and at 1200 C is about 10.7 mm. Accordingly, since the maximum pressure in the present experiments was about 0.02 mm, it is entirely possible that the higher temperature (at temperatures in excess of 900 C) CO evolution could have come from the reduction of silica components in the ash. In line with this conclusion is the fact that the gas evolved from a sample of PCI that had been rendered substantially ash free by extraction with HF contained practically no CO.

One other peculiarity of these results should be noted. Two different samples that had been extracted by HF evolved excessive amounts of CO and CO_2 in the region between 300 and 900 C. Thus, CWSN S5 after extraction evolved 115.8 ml of CO and 44.1 ml of CO_2 compared to 26.8 ml of CO and 5.7 ml of CO_2 from the sample that had not been extracted. Corresponding results for PCI 1042 showed 72.1 ml of CO and 12.4 ml of CO_2 after extraction, compared to 12.2 ml of CO and 1.5 ml of CO_2 before extraction. The cause of this excessive gas evolution from the extracted samples is not clear. Possibly, the reagents used have a catalytic effect on the oxidation of the surface by air during extraction or drying.

Strong hydrogen evolution from certain charcoals was noted a number of years ago.[38] The runs in Tables 6 and 7 show that some of the charcoals evolve as much as 147 ml of H_2 per gram on being heated to 1200 C. In general, it appears that the $ZnCl_2$ charcoals evolved much more hydrogen than the others. Furthermore, with the exception of CWSN 19, all of the $ZnCl_2$ charcoals tested appeared to evolve most of their hydrogen in the 600 to 900 C region rather than the 900 to 1200 C region. CWSN 19, for some unknown reason, evolved the normal amount of hydrogen in the higher temperature region but very little hydrogen up to 900 C. The amount of hydrogen present in the charcoals is probably related to their pretreatment since it is known that the higher the temperature of calcining of the various charcoals in the course of preparation and activation, the smaller the percentage of hydrogen that they contain. There is some evidence that steaming at 900 C will put hydrogen onto a charcoal. Thus, a sample of CWSN B1X that had been heat-treated in nitrogen at 1000 C until it would evolve only 15.6 ml of hydrogen to 1200 C, was found to evolve 47 ml of hydrogen after being steamed at 900 C to a 56% weight loss. In contrast to this, short steaming to a few per cent weight loss at 300, 400, and 750 C caused no appreciable increase in the hydrogen evolution above the 15.6 ml of the original sample. There is a chance, of course, that the excessive steaming made possible the escape of some hydrogen that originally was buried so deep in the charcoal as not to be able to escape at temperatures up to 1200 C. Hence, the interpretation of this result must remain uncertain until more work is done.

2. Heat treating samples of charcoal to 1000 C in a stream of nitrogen was found [27] to remove practically all the CO, CO_2, and H_2O from the surface and about two-thirds of the hydrogen. This would be expected on the basis of the degassing experiments shown in Tables 6 and 7 and hence needs no special comment.

3. It is interesting to note [27] that exposure to air at room temperature for a week of a sample of CWSN B1X that had been treated with nitrogen at 1000 C and cooled in a stream of nitrogen, restored the original complex to such an extent that the CO_2 evolution on heating to 1200 C was as large as the original untreated sample, and the CO was two-thirds as large. Exposure of a heat-treated sample of this charcoal to oxygen at 300 C for 30 min put on more complex than was characteristic of the original charcoal as shown in Table 8; the CO and CO_2 content was still, however, much smaller than that of

TABLE 8. Effect of heat treatment on National charcoals — gas evolved ml (STP) per g of sample.

Sample	25–300 C			300–600 C				600–900 C				900–1200 C					Total gas evolved 25–900 C				25–1200 C					[H_2, O_x] evolved	% O_2 in ash
	CO	CO_2	H_2O	H_2	CO	CO_2	H_2O	H_2	CO	CO_2	H_2O	H_2	CO	CO_2	CH_4	H_2O	H_2	CO	CO_2	H_2O	H_2	CO	CH_4	CO_2	H_2O		
7. CWSN 196 B1X heated in N_2 to 1000 C, cooled in N_2 and transferred in N_2	0.0	0.0	0.1	2.1	0.3	0.2	0.8	2.7	0.7	0.1	0.1	33.2	1.3	0.6	0.1	0.0	4.8	1.0	0.3	1.0	38.0	2.3	0.6	0.4	1.0	0.36	0.29	1.0*
8. Same as No. 7 exposed to air for one week	0.3	3.5	3.9	1.2	1.5	5.6	2.6	4.5	6.0	0.3	0.1	33.2	1.2	0.7	0.3	0.1	5.7	7.8	9.6	6.6	38.9	9.0	0.8	9.9	6.7	0.41	2.54	1.0*
11. CWSN 196 B1X exposed to O_2 at 300 C	0.1	0.4	0.7	0.2	4.1	9.5	1.8	42.9	22.9	1.0	0.4	35.0	0.4	0.4	0.1	0.0	43.1	27.1	10.9	2.9	78.3	27.5	0.6	11.0	2.9	0.73	3.74	1.0*

* Ash assumed to be zinc oxide in computations of these values.

some of the National samples treated with oxygen at 400 C by Young.

4. In view of the fact[89] that aging base charcoals by exposing them to a high relative humidity for a long period of time was believed to render the charcoal less useful for making whetlerites, a few experiments were carried out to compare the surface complex of aged and un-aged samples. Also, because heating an aged sample to 110 C for an hour was reported[89] to restore it to a condition in which it would then make a good whetlerite, a sample of aged charcoal was examined after it had been evacuated at 115 C. The oxygen content of the charcoals increased during aging in all cases by 2% in absolute value (33 to 100% relative increase in oxygen). The increase in oxygen[27] found by our degassing experiments on charcoals CWSN S5, CWSN 44, and PCI P58 was 2.12, 1.85, and 1.43 compared to values of 2.6, 2.3, and 1.2 found by ultimate analyses by Young. It should be noted that the 3-hour heating at 115 C of the aged CWSN S5 sample produced no detectable change in composition or amounts of evolved gas. If the improvement in whetlerizability resulting from heating an aged charcoal to 110 C as claimed by Blacet[89] was real, then either his heating conditions were critically different from ours or else the surface complex is not related in an important way to the whetlerizability of a charcoal.

5. English workers[90–95] have reported results which indicate that in the process of adsorbing such vapors as CCl_4 on charcoals, part of the surface complex is driven off into the gas phase. The displaced gases were reported to be equal in some cases to the equilibrium partial pressure of the adsorbate and to cause marked changes in the adsorptive characteristics of the charcoal. The actual volumes of displaced gas were not mentioned. To check this important factor, several experiments shown in Table 9 were carried out[27] on a charcoal made by the $ZnCl_2$ process and on a PCI sample made from coal. The samples were evacuated at 120 C before the run in each instance, at temperature that should cause practically none of the CO or CO_2 in the complex to be removed. The results clearly indicate that the amount of complex evolved by the adsorption of either CCl_4 or C_6H_5Cl is very small, being equivalent in all cases to less than 0.01% of the complex known to be present. Only water vapor displaced an appreciable amount of gas from the charcoals; the gas evolved by water was entirely CO_2 and was limited almost entirely to the sample made by the $ZnCl_2$ process. It seems likely that most of this evolved CO_2 may have resulted from the attack on the $ZnCO_3$ ash content by water condensed in capillaries. The total CO_2 evolution in one case amounted to about 8% of that which would have been evolved by heating the sample to 1200 C. The results as a whole fail to check the English work and certainly give no indication that physical adsorption of vapors is capable of seriously altering the composition of the surface complex on typical charcoals.

TABLE 9. Displacement of complex by adsorption of vapors at 25 C.

Charcoal	Vapor	Vol of liquid ml per g charcoal	Time of ads in hr	Gases evolved ml (STP) per g	
				CO	CO_2
CWSN 196 B1	CCl_4	0.5	18	0.0028	0.0036
CWSN 196 B1	C_6H_5Cl	0.4	5	0.00036	0.00039
CWSN 196 B1	H_2O	0.4	$4\frac{1}{2}$	0.0014	0.495
CWSN 196 B1	H_2O	0.2	$2\frac{1}{2}$	0.0024	0.205
CWSN 196 B1	H_2O	0.1	16	0.0016	0.235
PCI P58	C_6H_5Cl	0.15	3	0.0016	0.00003
PCI P58	H_2O	0.08	1	0.0025	0.0094

6. In view of the fact that most charcoals are activated by steam, it seemed worth while to ascertain the effect of steam activation on the surface complex. In Table 10 the results are shown for such a series of experiments on charcoal CWSN 191 B1X

TABLE 10. Complex formed during steam activation.

A. CWSN 196 B1X sample extracted with HF and heated in N_2 at 1000 C for 3 hr.

Temp range C	Gases evolved during degassing ml (STP) per g charcoal H_2	CO	CH_4	CO_2	H_2O vapor
25–300	0.0	0.0	0.0	0.0	0.6
300–600	0.3	0.0	0.0	0.1	0.2
600–900	1.2	0.1	0.1	0.1	0.1
900–1200	14.2	0.2	0.3	0.4	0.0
Total	15.7	0.3	0.4	0.6	0.9

B. Treated as in *A*, then exposed to water vapor at 300 C for 3½ hr (weight loss = 0.4%).

25–300	0.0	0.0	0.0	0.1	0.8
300–600	0.2	0.1	0.0	0.9	0.8
600–900	1.1	0.6	0.1	0.2	0.1
900–1200	11.4	0.4	0.2	0.2	0.0
Total	12.7	1.1	0.3	1.4	1.7

C. Treated as in *A*, then exposed to water vapor at 600 C for 3½ hr (weight loss = 1.0%).

25–300	0.0	0.1	0.0	0.0	1.3
300–600	0.1	0.0	0.0	0.3	0.6
600–900	1.5	1.8	0.0	0.1	0.2
900–1200	12.3	2.3	0.2	0.3	0.1
Total	13.9	4.2	0.2	0.7	2.2

D. Treated as in *A*, then exposed to water vapor at 750 C for 1 hr (weight loss = 1.6%).

25–600	0.2	0.0	0.0	0.3	1.7
600–900	2.7	2.3	0.1	0.3	0.4
900–1200	16.9	1.9	0.2	0.1	0.0
Total	19.8	4.2	0.3	0.7	2.1

E. Treated as in *A*, then exposed to water vapor at 900 C for 3½ hr (weight loss = 56%).

25–300	0.0	0.0	0.0	0.4	0.6
300–600	0.6	0.1	0.0	1.1	1.1
600–900	5.8	1.3	0.2	0.2	0.2
900–1200	40.5	2.2	0.5	0.1	0.1
Total	46.9	3.6	0.7	1.8	2.0

after it had been extracted with HF and heated 3 hr in nitrogen at 1000 C. In general, the results obtained agree with those of Muller and Cobb [96] who studied the chemisorption of water vapor on an acid-extracted wood charcoal at temperatures ranging from 300 to 1100 C. Steaming at temperatures up to and including 750 C produced only a slight increase in the amount of adsorbed water and a total fixation of only 4.1 ml of water vapor in a form evolved as CO and CO_2 on heating. Over this temperature range, the hydrogen fixed was no greater than that calculated from the amount of oxygen fixed. The sample that was steamed at 900 C to a 56% weight loss clearly fixed more hydrogen than oxygen. This is in agreement with the experiments of Muller and Cobb [97] who noted more hydrogen than oxygen being fixed by steaming in the range 700 to 900 C. The total oxygen fixed at 900 C was no greater than on steaming at 750 C. In view of these results, it is easy to understand why the CO and CO_2 complex is so low on samples of charcoal made by steaming at high temperature and not exposed excessively to air before cooling.

6.8 SPECIAL SURFACE COATINGS ON CHARCOAL

There are statements in the literature [93] to indicate that the relative amounts of different gases adsorbed may well depend upon the exact nature of the surface coating of the charcoal. Because of the obvious importance of knowing the nature of any such changes that might be produced, a few experiments were carried out in an effort to coat charcoals with complexes other than carbon-oxygen complexes. Specifically, the influence of covering the surface with nitrogen, with chlorine, and with sulfur were investigated. The principal results obtained on samples with these coatings will now be considered.

6.8.1 Treatment of Charcoals with Nitrogen

References in the literature [98, 99] indicate that high-temperature treatment of charcoals with ammonia is capable of forming carbon-nitrogen complexes that are more stable than carbon-oxygen complexes. Accordingly, two sets of experiments were carried out [27] in which an acid-extracted, degassed sample of CWSN B1X charcoal was heated in ammonia at 750 C and at 900 C. The samples were then analyzed by being heated by Anderson to various temperatures up to 1200 C and the evolved gases analyzed. The results as shown in Table 11 confirm the previously published work. A nitrogen complex is formed that is evolved only on heating in the 900 to 1200 C region. Most of the nitrogen comes off as free nitrogen, though some is evolved as HCN, C_2N_2, and NH_3. It will also be noted that the hydrogen content of the charcoal is increased by the ammonia treatment from a value of 15.6 for the original sample to values of 30.5 and 39.3 ml for the ammonia treat-

TABLE 11. Complex formed during ammonia activation.

A. Sample exposed to NH_3 at 750 C for three hr. Weight loss = 0.4%.

Temperature of degassing	Gases evolved during degassing ml (STP) per g char					
	H_2	CO	N_2	C_2N_2 HCN	NH_3	H_2O
25–600	0.6	0.0	0.1	0.2	0.1	0.5
600–900	3.3	0.1	0.2	0.1	0.1	0.5
900–1200	26.6	0.4	5.2	2.3	0.3	0.1
Total	30.5	0.5	5.5	2.6	0.5	1.1

B. Sample exposed to NH_3 at 900 C for three hr. Weight loss = 17.1%.

25–300	0.0	0.0	0.0	0.0	0.0	0.6
300–600	2.3	0.0	0.1	0.2	0.2	0.6
600–900	5.2	0.1	0.1	0.2	0.2	0.3
900–1200	31.8	0.7	6.3	2.5	0.8	0.2
Total	39.3	0.8	6.5	2.9	1.2	1.7

ments at 750 C and 900 C respectively. Unfortunately, time did not permit further work with these ammonia-treated samples.

6.8.2 Treatment of Charcoals with Chlorine

Chlorine complexes which are so stable that the chlorine cannot be removed by evacuation at temperatures as high as 600 C, nor by the action of boiling 10% NaOH over the period of an hour, have been reported [100] in the literature. For the present work [27] charcoal has been made to retain as much as 17% of its weight of chlorine after evacuation for an extended period at 400 C. The results are shown in Table 12 and in Figure 39. Apparently the amount of stable chlorine held by the charcoal increases with the temperature of treatment because the amount

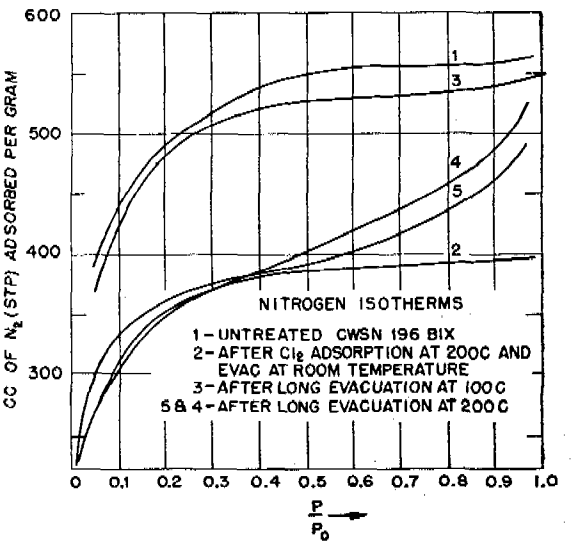


FIGURE 39. Treatment of charcoals with chlorine.

retained at room temperature after evacuation is greater when the temperature of the original treatment is high. This is also true of the fraction of the total chemisorption that is retained on evacuation to 400 C.

Insufficient nitrogen adsorption runs were carried out on the chlorinated sample to answer the question as to the location of the chemisorbed chlorine. In general, it may be said that the chemisorbed chlorine did not decrease the volume of nitrogen held by the charcoal at 0.99 as much as one would expect though conclusions are uncertain until more runs are made. Figure 39 indicates that on treating a sample at 200 C with chlorine and then evacuating it at 200 C a drastic pore size change occurs. If these few experiments are to be believed, the change occurs during the long evacuation at 200 C rather than during the original treatment since evacuation at 100 C left an

TABLE 12. Adsorption of chlorine by CWSN B1X.

Temperature of experiment used in adsorption. Flow system employed.	Weight of chlorine* adsorbed per gram of charcoal at various temperatures				
	Physical adsorption† at room temperature and 1 atm	Chemisorption retained after evacuation at room temperature	100 C	200 C	400 C
Room temp flow expt No. 1	0.6262	0.2523	....	....	....
Room temp flow expt No. 2	0.719	0.202	0.081	....	....
100 C flow expt No. 3	0.6338	0.2502	0.2152	0.142	0.0976
200 C flow expt No. 4	0.665	0.352	0.2734	0.239	0.178
400 C flow expt No. 5	0.722	0.342	0.317	....	....

* Weights of Cl_2 adsorption in columns 3–6 are the weights of Cl_2 retained by sample after extended evacuation at successively higher temperatures from 25 to 400 C.

† Column 2 represents physical adsorption at room temperature when sample was cooled in stream of Cl_2 at 1 atm from T of experiment indicated in column 1.

isotherm similar to, but 11% smaller, than the one of the untreated sample. The attack on the charcoal is not especially surprising in view of the fact that one proposed method of producing active charcoal [104] involves burning hydrocarbons in chlorine under such conditions as to deposit a considerable portion of the hydrocarbon as free carbon.

6.8.3 Treatment of Charcoals with Sulfur

Young and his co-workers [24] prepared a number of samples of charcoal coated with sulfur by heating charcoal and sulfur together at 400 C in a rotating furnace. Comparatively little work was done on the properties of the coated charcoals though the following facts were established:

1. As much as 41% sulfur by weight could be incorporated into the charcoal. The amount of sulfur picked up was proportional to the amount included in the original mix.
2. The 41% sulfur content of one of the charcoals was reduced to 29% by extraction with either of two different solvents. Apparently some of the sulfur is present in an extractable form and part of it in a more tightly bound form.
3. The hydrogen content of the charcoal decreases to about one-third of its original value as the sulfur content increases to 40%.
4. Water adsorption isotherms show that if the sulfurized sample was protected from oxidation it picked up very little water below 0.5 relative pressure. The samples are definitely still hydrophobic. The sulfur, however, apparently decreases the pore volume of the charcoal considerably as evidenced by the fact that the sample containing 41% sulfur had only about 0.12 ml water sorptive capacity at saturation.
5. There seems to be no relation between the acid and base adsorptive properties and the sulfur content.

6.9 RELATION BETWEEN ADSORPTION AND MOLECULAR STRUCTURE

Before considering the work that has been done on the measurement of the adsorption of gases such as chloropicrin, pyridine, CCl_4, and other vapors, it seems well to summarize the results that have been obtained by Kummer [105] and are being reported here for the first time on the relation existing between the adsorption of a gas and the structure and properties of the adsorbate. In view of the fact that the efficiency of removal of war gases by gas mask charcoal is known to depend upon a rate factor and upon a capacity factor N_0, it seemed worth while to carry out a study with a view to predicting the sorption capacity of a given charcoal for a gas at various relative pressures as a function of the properties of that gas. It would be especially helpful to be able to predict approximately the shape of the adsorption isotherm of a gas on charcoal if only a few of the fundamental properties of the adsorbate gas are known. The analysis of the problem and the experimental results presented here give us a much better insight into the factors upon which the adsorbability of a gas depends than we have ever had before and enables us to predict with a fair approximation whether a gas will be adsorbed strongly, medium strongly, or weakly by a sample of charcoal.

Experimental measurements relative to this study were made on a single charcoal CWSN 19, one of the early samples made by $ZnCl^2$. (See Chapter 3.) It had an apparent density of 0.482, a particle density of 0.792, a carbon density (as determined by helium at 25 C) of 2.09; an ash content of about 0.3% made up mostly of ZnO and $ZnCl_2$; a heat of wetting in benzene of 22.69 cal per g, and a PS service life of about 66 min. As indicated in one of the earlier sections, the charcoal is characterized by a comparatively low amount of surface complex; [27] on being heated to 1200 C it evolved 57 ml H_2, 7 ml CO, 2.7 ml CH_4, 3.3 ml of CO_2 and 2.1 ml of water vapor.

6.9.1 Experimental Data for the Adsorption of Gases on CWSN 19

Figure 40 shows the adsorption isotherms for a large number of gases. The data are plotted in the manner suggested by Polanyi [34] as the fraction of the total sorption capacity taking place as a function of RT times the logarithm of the relative pressure. A few regular isotherms plotted with relative pressure as the abscissa are given in Figure 41. The adsorption data are summarized in Table 13. It will be noted that the total liquid volume of gas adsorbed at saturation pressure is substantially constant and independent of the nature of the adsorbate. We shall now turn to the theoretical part of his work and summarize his derivation of relationships that will enable one to predict the general nature of the adsorption

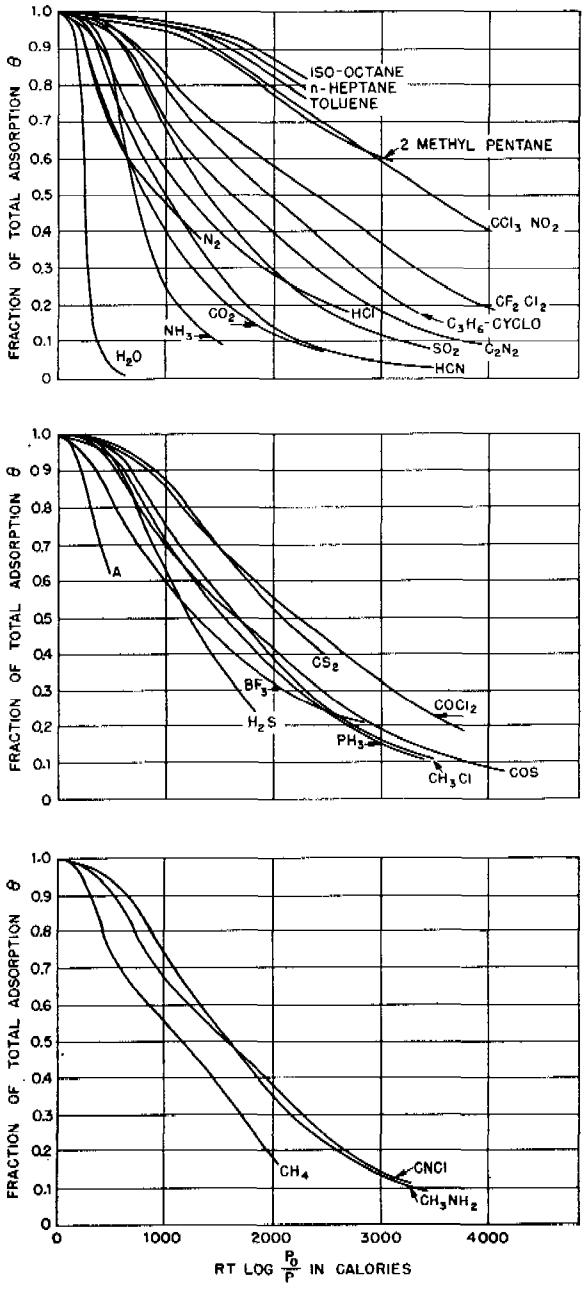


FIGURE 40. Adsorption isotherms for various gases on CWSN 19.

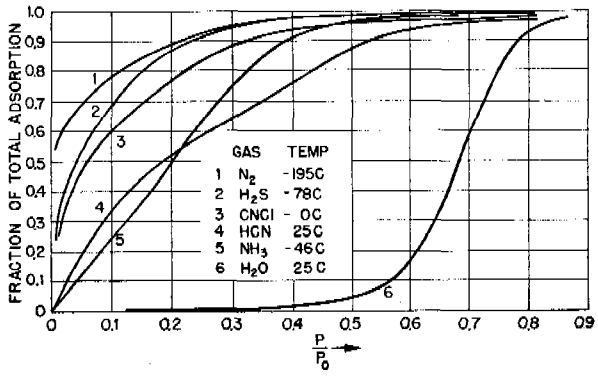


FIGURE 41. Some regular isotherms vs relative pressure for gases on CWSN 19.

TABLE 13. Adsorption data for various gases on CWSN 19.

Gas	Temp of run C	Adsorption at a relative pressure of 0.99. ml of gas STP per gram of charcoal	Adsorption at a relative pressure of 0.99. ml of liquid adsorbate per g of charcoal
N_2	−194	397	0.616
A	−194	490	0.600
CH_4	−160	360	0.610
BF_3	− 78	291	0.600
PH_3	− 78	298	0.615
HCl	− 78	442	0.613
CO_2	− 78	355	0.554 (liquid density)
H_2S	− 78	371	0.566
CF_2Cl_2	− 20	166	0.609
NH_3	− 46	526	0.572
COS	− 46	262	0.608
CH_3Cl	− 20	264	0.600
C_2N_2	− 21	245	0.595
Cyclopropane	− 39	216	0.590
CH_3NH_2	0	296	0.596
SO_2	0	298	0.595
$COCl_2$	0	193	0.596
CNCl	0	267	0.598
HCN	25	350	0.607
CS_2	25	216	0.585
H_2O	40	644	0.520
n-Heptane	25	87	0.567
Toluene	25	120	0.574
CCl_3NO_2	25	128	0.570
2-methylpentane	25	95	0.560
Isooctane (2,2,4-trimethylpentane)	25	76.5	0.563

of any adsorbate from its physical properties and the behavior of some other one adsorbate on the same charcoal.

6.9.2 Theory

In deriving the desired relationship, a number of equations will be used. To begin with, we have the Polanyi [34] relationship to account for the dependence on temperature of adsorption of a given adsorbate

$$T_1 \log \frac{P_1}{P_{0_1}} = T_2 \log \frac{P_2}{P_{0_2}} \qquad (12)$$

where T_1 and T_2 are the two different temperatures of the adsorbent, P_1 and P_2 are the isotherm pres-

sures, and P_{0_1} and P_{0_2} are the vapor pressures of the adsorbate at the two temperatures. This equation is derived to hold for a constant fraction of the total adsorption. In other words, the pressure required to produce the same fractional saturation of a given adsorbate would vary with the temperature in the way indicated.

It will be convenient also to use an empirical equation for the relation between the amount of adsorption and the pressure of the adsorbate. If θ represents the fraction of the saturation value of the adsorption that is occurring at pressure P, the relation

$$RT \log_e \frac{P}{P_0} = K(1-\theta)^{\frac{1}{3}} - B \log_e \theta \qquad (13)$$

is found to hold fairly well for all adsorbates on CWSN 19. It gives an isotherm in which the slope dV/dP decreases monotonously as the pressure increases and equals zero when $P = P_0$. For those charcoals which give an S-shaped isotherm it would not hold above $P/P_0 = 0.5$ but it is to be noted that a mask is rarely called upon to afford protection from gases which have attained a partial pressure in the air equal to one-half the vapor pressure of the liquid adsorbate.

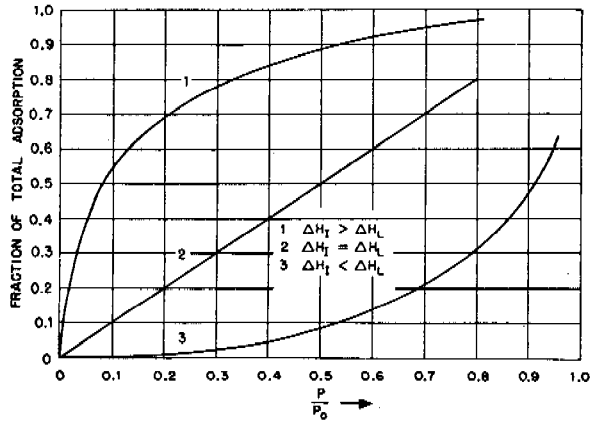


FIGURE 42. Isotherm shape as a function of $\Delta H_I - \Delta H_L$.

If constants K and B could be evaluated from molecular data for the adsorbate, the given problem would be completely solved. It is extremely difficult to do this with exactness. Accordingly, in this section a way will be pointed out to make a somewhat simpler but useful approach to the problem. Specifically, a way will be outlined for calculating the difference between the integral heat of adsorption $-\Delta H_I$, and the heat of liquefaction $-\Delta H_L$, for the adsorbate on the basis of the fundamental properties of the adsorbate molecule. Since it is well established that adsorption isotherms follow curves of types 1, 2, or 3 in Figure 42, depending upon whether the heat of adsorption is greater than, equal to, or less than the heat of liquefaction, then it will be obviously possible to indicate the general nature of adsorption.

A thermodynamic equation for the adsorption of a gas on a solid is

$$RT \log_e \frac{P_0}{P} = -\left(\frac{\partial(\Delta H_a)}{\partial n}\right)_T + \Delta H_L + T\left(\frac{\partial \Delta S}{\partial n}\right)_T \qquad (14)$$

which relates the relative pressure P/P_0 of the adsorption to the differential enthalpy of adsorption for the gas going to the adsorbed phase, $\partial(\Delta H_a)/\partial n$, and the differential entropy change $\partial(\Delta S)/\partial n$ when the bulk liquid is transferred to the surface layer.

Now, if equation (12) holds, it can be shown that the entropy term disappears and that

$$RT \log \frac{P_0}{P} = \frac{\partial(\Delta H_a)}{\partial n} - \Delta H_L. \qquad (14a)$$

Coolidge's data [39] show that the organic gases follow equation (12) very closely, whereas water does not.

In order to estimate the entropy term, some assumptions are necessary. For one thing, it is necessary to assume some shape factor for the capillaries in order to be able to know the fraction of liquid adsorbate which is in contact with the surface of the charcoal. The exact form of the assumption is not too important because with a variety of choices the final answer as to the calculated difference between the integral heat of adsorption and heat of liquefaction does not change much. For simplicity, it will be assumed that the charcoal pores have plain parallel walls and are four molecular diameters apart. Furthermore, usually the entropy term is written in the form $RT \ln \phi/1 - \phi$ where ϕ represents the fraction of the surface covered by adsorption. However, it appears simpler for physical adsorption to assume that the rate of condensation on the surface is proportional to the total surface rather than to $1 - \phi$ and, hence, for $\phi < 1$, the entropy term can be written

$$\frac{\partial(\Delta S)}{\partial n} = -R \ln \phi. \qquad (14b)$$

For $\phi > 1$, the entropy term is 0 since there is the same surface for evaporation as for condensation. If, as is likely, most of the first layer will form before the second begins, then $\phi = 2\theta$.

Combining equations (13), (14), and (14b), we have

$$-\left(\frac{\partial \Delta H_a}{\partial n}\right)_T + \Delta H_L = K(1-\theta)^3 - B\ln\theta - RT\ln 2\theta. \quad (15)$$

The integral heat of adsorption can be found by integrating the entire expression including the last term from $\theta = 0$ to $\theta = 0.5$; and, without the last term, from 0.5 to 1. The integral heat of adsorption $-\Delta H_I$ obtained in this way is

$$\begin{aligned} -\Delta H_I &= -\Delta H_L + \tfrac{3}{4}K + B - \tfrac{1}{2}RT \\ &= -\Delta H_L + \Delta H_x. \end{aligned} \quad (16)$$

We deal with the integral heat of adsorption up to complete filling of the pores because complete filling represents a definite physical state which is the same for all gases and which lends itself to theoretical calculations.

In order to calculate the integral heat at saturation, we can consider the following simple process:

1. Condense one mole of gas into a bulk liquid; the enthalpy change will be ΔH_L.

2. Next, spread this bulk liquid out into a sheet four molecules thick; the enthalpy change will be one-half the energy required to bring a mole of water from the interior or bulk liquid to the surface of the liquid, or $\Delta H_s/2$.

3. Allow both sides of this sheet to come in contact with a charcoal surface, giving an enthalpy change of $\Delta H_c/2$, where ΔH_c is the heat that would be evolved if all the molecules in the mole of adsorbate were brought as a sheet of liquid into contact with the carbon surface. Then

$$\Delta H_I = \Delta H_L + \frac{\Delta H_c}{2} + \frac{\Delta H_s}{2}. \quad (17)$$

Next, we shall proceed to find a means of evaluating ΔH_c and ΔH_s that depends upon the physical properties of the adsorbate molecule. The enthalpy change when a molecule is brought from the interior of a liquid to the surface is largely independent of the temperature and can be calculated by

$$\Delta H_s = +2.22k_e(T_c - 6) \quad (18)$$

where k_e is Eötvos' constant and T_c is the critical temperature. One, therefore, has a ready means of calculating $\Delta H_s/2$, the heat required to form a mole of liquid into a sheet four molecules thick.

The heat quantity ΔH_c can be evaluated by means of the theory of London [105] to be

$$-\Delta H_c = \frac{3N\alpha_c\alpha_g(2)V_{0_c}V_{0_g}}{4h^3(V_{0_c} + V_{0_g})} \quad (19)$$

where α_c is the polarizability of the carbon surface, α_g is the polarizability of the gas molecules, V_{0c} is the fundamental frequency of the carbon surface, V_{0_g} is the fundamental frequency of the gas molecules, N is Avogadro's number, and h is the distance between the carbon surface and the molecules of adsorbate when the sheet is at its equilibrium position. Since we intend to evaluate all the right-hand side of the equation by some given adsorbate, we can write

$$-\Delta H_c = C\alpha_g V_{0_g}. \quad (20)$$

We evaluate C from some one adsorbate and then neglect any change in C produced by possible changes in h involved in using other adsorbates. By substituting (17), (18), and (20), in (16) we now have

$$\begin{aligned} \tfrac{1}{2}[C\alpha_g V_{0_g} - 2.22(T_c - k_e)] &= \tfrac{3}{4}K + B - \tfrac{1}{2}RT \\ &= +\Delta H_x. \end{aligned} \quad (21)$$

This equation can be rearranged in the form

$$\begin{aligned} C\frac{\alpha_g}{2}V_{0_g} &= -\Delta H_x + 1.11(T_c - 6)k_e \\ &= +\Delta H_x + \tfrac{1}{2}\Delta H_s. \end{aligned} \quad (22)$$

Tables 14A and 14B show values of K, B, and ΔH_x calculated from the isotherms together with ΔH_s and physical data for the various adsorbate molecules. Figure 43 is a plot of $\alpha_g V_{0_g}$ against $\Delta H_x + \frac{1}{2}\Delta H_s$. The value of C turns out to be 3.75 and is equal to twice the slope of the plot.

As pointed out above, complete solution of the problem requires a method for evaluating the absolute values of K and B. Several procedures for doing this are now being worked on but have not yet been completed. However, at the present stage of development, it is possible to evaluate $\Delta H_I - \Delta H_L$ for any adsorbate from the experimental adsorption values for some standard adsorbate on a charcoal, together with fundamental data for the adsorbate for which $\Delta H_I - \Delta H_L$ is sought. For the standard adsorbate one can calculate K and B for the given charcoal from an isotherm. Knowing ΔH_L for this standard adsorbate one can then calculate ΔH_x as per equation (21). But ΔH_x is really $\Delta H_c/2 + \Delta H_s/2$ and $\Delta H_s/2$ is known from the Eötvos equation.[108] Consequently, from the experimental data and the Eötvos equation, a value for ΔH_c can be calculated and used to evaluate the constant C. The value of α_g can be readily calculated by the method of Denbigh [110] from the structure of the molecule, and the value of V_{0_g} for organic molecules [109] lies within $\pm 20\%$ of the value 286 kcal per mole. For other adsorbates, then, on the same charcoal, one has merely to insert values

TABLE 14A. Fundamental data on the adsorbate gases.

Gas	Mol wt	Density g per ml	Temp C	$-\Delta H_L$ cal per mole	Molal vol ml	Average liquid radius, Å	Dipole moment $\mu \times 10^{18}$ Debyes	Polarizability $\alpha_g$ml $\times 10^{24}$
N_2	28.02	0.805	−194	1335	34.9	2.16	0.0	1.74
A	39.94	1.454	−194	1590	27.4	2.00	0.0	1.63
CH_4	16.04	0.422	−160	2040	38.0	2.23	0.0	2.54
BF_3	67.82	1.47	− 78	4620	43.0	2.32	0.0	2.40
PH_3	34.04	0.736	− 78	3489	46.3	2.37	0.55	3.50
HCl	36.46	1.174	− 78	3860	31.1	2.08	1.03	2.63
CO_2	44.01	1.26 liq.	− 78	4130	34.9	2.16	0.0	2.57
H_2S	34.08	0.993	− 78	4463	34.3	2.15	1.10	3.64
COS	60.07	1.154	− 46	4423	52.0	2.47	0.65	5.05
C_3H_6	42.05	0.688	− 39		61.1	2.61	0.0	4.55
NH_3	17.03	0.697	− 46	5720	24.4	1.92	1.49	2.14
CH_3Cl	50.5	0.99	− 20	5170	51.0	2.45	1.86	4.41
C_2N_2	52.02	0.953	− 21	5576	54.6	2.51	0.0	4.65
SO_2	64.06	1.432	0	5960	44.7	2.35	1.67	3.76
$COCl_2$	98.92	1.428	0	5990	69.3	2.72		6.51
CNCl	61.48	1.226	0	6300	50.1	2.44		4.58
HCN	27.02	0.695	25	6027	38.9	2.24	2.6	2.46
CS_2	76.13	1.256	25	6490	60.6	2.60	0.0	8.03
n-Heptane	100.2	0.684	25	7650	146.1	3.49	0.0	13.7
H_2O	18.02	0.995	40	10400	18.1	1.74	1.85	1.48
Toluene	92.13	0.862	25	7980	107.0	3.14	0.4	12.3
CH_3NH_2	31.06	0.687	0		45.2	2.36	0.99	3.88
2-methylpentane	86.1	0.654	25	7000	132.0	3.37		11.8
Isooctane	114.1	0.692	25	8200	165.0	3.63		15.5
CCl_3NO_2	164.4	1.641	25		100.0	3.08		10.82
CF_2Cl_2	120.9	1.47	− 20	4760	82.1	2.88		6.55

TABLE 14B. Fundamental data on adsorbate gases.

Gas	Fundamental frequency V_0 kcal	Isotherm constant K	Isotherm constant B	Total surface energy ΔH_s cal per mole	ΔH_x cal per mole	$\alpha_g V_{0g}$	$\Delta H_x + \frac{1}{2}\Delta H_s$
N_2	402			561		700	
A	396			643		645	
CH_4	324	240	1210	817	1268	822	1677
BF_3	435	295	1555	1460	1581	1043	2311
PH_3	(300)	650	1485	1410	1778	1050	2483
HCl	311	394	1300		1401	818	
CO_2	357	292	816	1320	840	916	1500
H_2S	257	1060	608		1208	935	
COS	313	765	1417	1740	1741	1580	2620
C_3H_6	307	1170	1451		2061	1675	
NH_3	271			1290		580	
CH_3Cl	312	1117	1081	1910	1667	1380	2622
C_2N_2	285	870	1290	1840	1689	1322	2609
SO_2	272	1020	915	2050	1407	1022	2432
$COCl_2$	274	1465	1429	2100	2256	1785	3306
CNCl	(300)	938	1150		1581	1372	
HCN	321	552	765	1100	881	790	1431
CS_2	188	1610	1192	2520	2102	1510	3362
n-Heptane				2490			
H_2O	311	360	10	1520	0	460	760
Toluene				2870			
CH_3NH_2	294	1110	990	1145	1549	1140	2121
2-methylpentane							
Isooctane							
CCl_3NO_2	(280)	2620	2000	3640	3667	3030	5487
CF_2Cl_2	(300)	1160	1910	1850	2530	1970	3455

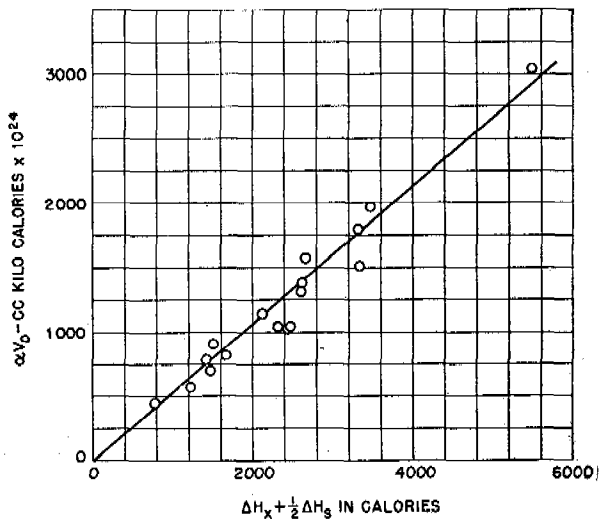


FIGURE 43. Plot of equation (22) for determining the constant C.

for α_0 and V_{0_0} in equation (20) and obtain a value for ΔH_x. Knowing ΔH_s from the Eötvos equation, one can then calculate ΔH_x and hence by equation (17) obtain a value for $\Delta H_I - \Delta H_L$. In other words, by knowing a single adsorption of any one adsorbate on a given charcoal and by knowing the polarizability and fundamental frequency of the molecules of the adsorbate whose adsorption one wishes to evaluate, one is able to tell whether the difference between the integral heat of adsorption and the heat of liquefaction is a large positive quantity, zero, or a negative quantity. From this knowledge, one can by equation (3) or equation (4) tell whether the adsorbate will be strongly adsorbed as in curve 1, weakly adsorbed as in curve 2, or very weakly adsorbed as in curve 3, Figure 42.

To show the usefulness of this method of procedure, there are listed in Table 15 values for $-(\Delta H_I - \Delta H_L)$ for the various adsorbates as determined experimentally and as calculated using the isotherm for CH_3Cl for evaluating the constant C. It is readily apparent that one would not be misled as to the nature of the adsorption isotherm of any of the gases listed by the calculated value for the difference between the integral heat of adsorption and the heat of liquefaction of the adsorbate.

The question naturally arises as to the extent to which the results in Table 15 are dependent upon the nature of the assumption made as to the shape of the pores in the capillary. If one assumes that the adsorption is taking place in pores that are cylindrical and four molecules in diameter, one obtains an equation similar to (16), except that the constant 2 is changed to about 1.5. Evaluation of the difference between the heat of adsorption and the heat of liquefaction calculated for a cylindrical capillary from the absolute physical constants for the adsorbate and the difference between these two heat quantities as calculated by the proper modification of equations (17, 20, 21, and 22) is shown in Table 16; it is evident that to a close approximation, one can estimate the magnitude of the difference between the heat of adsorption

TABLE 15. Calculation of $-(\Delta H_I - \Delta H_L)$ for various adsorbates on CWSN 19, assuming adsorbate is in capillaries with parallel walls four molecular diameters in size.

Gas	Temp of isotherms C	$-(\Delta H_I - \Delta H_L)$ from actual isotherms by equation (16)	$-(\Delta H_I - \Delta H_L)$ calculated from constant C and values for $\alpha_g V_{0g}$ and ΔH_s
CH_4	−160	1269	1131
BF_3	−78	1589	1230
PH_3	−78	1778	1255
CO_2	−78	840	1050
COS	−46	1750	2080
CH_3Cl	−20	1667	1625
C_2N_2	−21	1689	1560
SO_2	0	1407	895
$COCl_2$	0	2256	2290
HCN	25	881	925
CS_2	25	2102	1570
CH_3NH_2	0	1549	1568
CCl_3NO_2	25	3667	3860
CF_2Cl_2	−20	2530	2755
H_2O	40	0	−23

TABLE 16. Calculation of $-(\Delta H_I - \Delta H_L)$ for various adsorbates on CWSN 19, assuming adsorbate is in cylinders four molecules in diameter.

Gas	Temp of isotherms C	$-(\Delta H_I - \Delta H_L)$ from actual isotherm data	$-(\Delta H_I - \Delta H_L)$ calculated from constant C for CH_3Cl and values for $\alpha_g V_{0g}$ and ΔH_s
CH_4	−160	1232	1155
BF_3	− 78	1524	1185
PH_3	− 78	1713	1230
CO_2	− 78	775	1020
COS	− 46	1684	2110
CH_3Cl	− 20	1584	1584
C_2N_2	− 21	1606	1514
SO_2	0	1316	760
$COCl_2$	0	2165	2290
HCN	25	781	965
CS_2	25	2002	1440
CH_3NH_2	0	1459	1582
CCl_3NO_2	25	3567	3854
CF_2Cl_2	− 20	2457	2438
H_2O	40	−113	−64

and the heat of liquefaction without too much error being entailed by the nature of the assumption that has to be made relative to the shape of the pores of the charcoal. The procedure here presented should, therefore, be very useful in quickly evaluating the probable adsorption characteristics of any adsorbate if only the polarizability, the fundamental frequency, and surface energy of the adsorbate molecule are known. If one wished to estimate the adsorption at room temperature, one should divide $\Delta H_I - \Delta H_L$ by 298 and then solve for V at the particular partial pressure being used by inserting $e^{-(\Delta H_I - \Delta H_L)/RT}$ for C in equation (3) or (5), and using an estimated V_m based on a comparison of the size of the molecules being studied with the V_m and size of the molecules used in the standard isotherm. Since actual adsorption usually deviates at low relative pressure in the direction of being greater than that estimated from equation (3) or (5), the above method of estimating the adsorbability of an adsorbate is conservative and would give adsorption values that, if anything, would be too low.

6.10 ADSORPTION OF PS, PYRIDINE, PICOLINE, CCl_4 AND OTHER VAPORS ON CHARCOAL

Most of the adsorption work has been done upon typical war gases such as PS [111] as a function of the kind of charcoal and the amount of moisture present during adsorption, upon gases such as pyridine and picoline [27] that appear to be useful for improving the quality of whetlerites, or upon gases such as CCl_4 [112–114] which have been used in studying pore size and rates of adsorption. Other examples of adsorption have already been included in the discussion of the adsorption of nitrogen and water vapor as they are related to surface area and pore size measurements. Additional data on adsorption, which will be included in the section on retentivity, have been taken primarily with a view to judging the danger of desorption of gases into a stream of vapor-free gas.

6.10.1 Adsorption of PS on Charcoal

The adsorption of chloropicrin on CWSN 19 was determined [111] at 15, 25, and 35 C by passing a gas stream charged with a known amount of PS through a tube of charcoal and determining the increase in weight at steady state. The results are shown as a Polanyi plot in Figure 44. The detailed data are

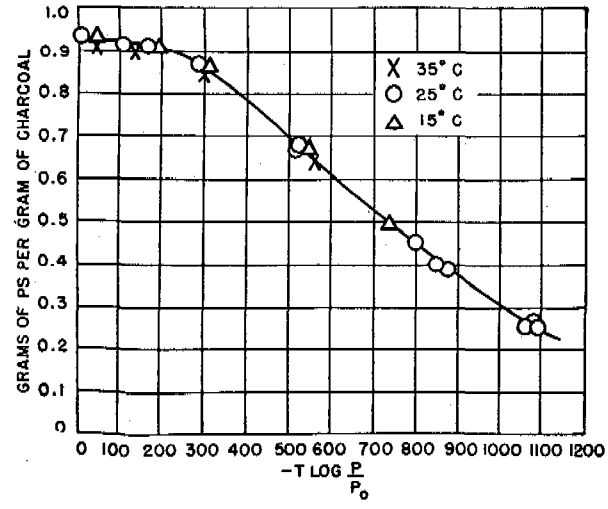


FIGURE 44. Polanyi plot of CCl_3NO_2 on CWSN 19.

given in the original report. It is evident that the data all fall, as would be expected, on the same curve. Hence, at a given relative pressure the fraction of the total adsorption occurring changes only slightly. The isotherm is of the strong adsorption type, large adsorption occurring at low relative pressures. A typical isotherm is shown in Figure 45.

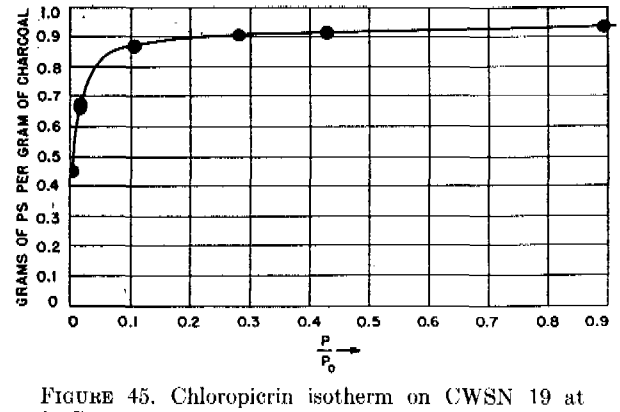


FIGURE 45. Chloropicrin isotherm on CWSN 19 at 25 C.

The influence of water vapor on PS adsorption was also determined.[111] In Table 17 are shown data taken on CWSN 19 in the presence and absence of water vapor equivalent to adsorption equilibration at 0.75 RH. Similar data for the Type A whetlerite CWSN Type 1 are also included in the table.

It will be noted that for high relative pressures of PS the water vapor has little effect on the adsorption. Presumably the water is quickly expelled by the more strongly adsorbed PS. This is true regardless of whether the experiment was started with dry char-

coal or with charcoal that had already been equilibrated with water vapor at 75% RH. However, for small partial pressures of PS, the presence of water vapor equivalent to 75% RH had a marked inhibiting effect on the PS adsorption. This is consistent with the well known fact that under the test conditions usually employed for PS, the presence of water vapor causes a marked decrease in the break time of the mask or charcoal tube.

TABLE 17. Weight of PS adsorbed in the presence of water vapor on charcoal CWSN 19 and whetlerite CWSN 19 Type 1.

Initial condition of charcoal or whetlerite	P/P_0 for PS	P/P_0 for H_2O	Adsorption of PS grams per g	Adsorption of H_2O grams per g
Dry	0.75	0.00	0.925	...
Wet	0.75	0.75	0.92	0.0
Dry	0.75	0.75	0.90	0.0
Dry	0.045	0.00	0.77	...
Wet	0.045	0.75	0.465	0.24
Dry	0.031	0.00	0.72	...
Wet	0.031	0.75	0.41	0.28
Dry	0.034	0.75	0.58	0.11
Dry	0.00	0.75	...	0.50
Dry whetlerite	0.017	0.00	0.57	...
Dry whetlerite	0.017	0.75	0.32	0.24
Dry whetlerite	0.022	0.00	0.59	...
Wet whetlerite	0.022	0.75	0.19	0.33
Dry whetlerite	0.00	0.75	...	0.409

6.10.2 Adsorption of Pyridine and 4-Picoline

In view of the widespread interest shown in the possible use of pyridine and related materials for improving the aging characteristics toward CK under 80-80 tests, some measurements have been made [27] of the adsorption of both pyridine and 4-picoline. The results are illustrated by the isotherms in Figure 46.

The isotherms are of a standard strong adsorption type and indicate that both of these gases would be strongly held by the charcoals. The rates of adsorption observed were extraordinarily low. As much as 20 hr was required in the equilibration of each adsorption point. The extreme slowness is probably connected with the slowness of surface migration of molecules of this molecular weight and strongly polar character into the tiny capillaries of the charcoal. The cause of the slowness cannot be stated with certainty until further studies on similar molecules are made, but there can be no doubt of the reality of the slow nature of the gas pickup. One sample of a Type A whetlerite prepared from a BC charcoal showed

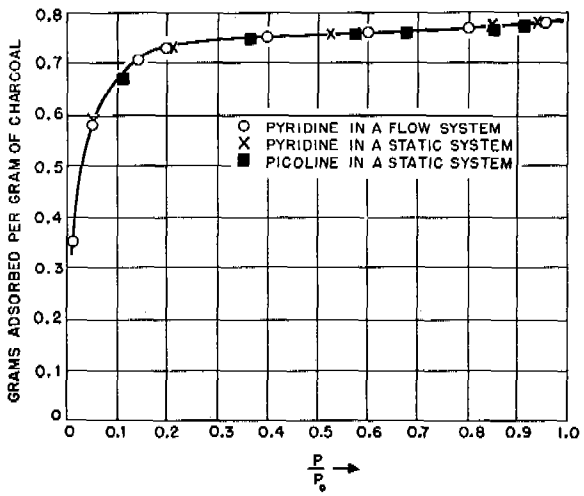


FIGURE 46. Adsorption of pyridine and picoline by CWSN 196 B1X at 23 C.

strong adsorption of pyridine contrary to the observation made at Edgewood Arsenal to the effect that this whetlerite would not adsorb this vapor. The cause of the disagreement is not known.

6.10.3 Adsorption of CCl_4 and Other Vapors by Charcoals

Most of the adsorption work dealing with the pickup of CCl_4 by charcoals has been done with a view to studying the pore size, sorption capacity, and rate of equilibration of various charcoals. The Canadian workers have employed an isopiestic technique [112–114] in their work that seems to simplify greatly the making of comparisons of the sorptive capacities of the various charcoals. By their procedure, a series of charcoals together with some standard charcoal is exposed to CCl_4 or other vapors at various but unknown partial pressures in a desiccator. The samples are left until equilibrium is attained. By knowing the adsorption isotherm for the standard charcoal, they are able to establish the dependence of adsorption of the other charcoals on the partial pressure of adsorbate. Their procedure affords a rapid and easy means of establishing the relative sorptive characteristics of a large number of charcoals. They find a certain correlation between the isopiestic isotherms and the *volume activity* (weight of adsorbate picked up by the charcoal in a standard tube test up to the break point).

In a report by Heise and Slyh,[115] it was stated that an unusually large variation in the capacity and the rate of CCl_4 adsorption was observed for a number of

base charcoals. The saturation values in the temperature range 20 to 23 C were reported to be only about one-third to one-half as large as those of 25 C, and the charcoal was four times as slow in equilibrating. Since there seemed to be no reasonable explanation of this behavior, the results were repeated by Holmes. Measurements on four National samples, CWSN S5, CWSN 19, CWSN 196 B1X, and CWSN B1X TH 410, gave results that contradicted the experience of Heise and Slyh and gave normal adsorption values both as regards the rate of equilibration and the total adsorption. A later recheck by the National workers indicated that the early report was in error. In view of this fact, the results are not being included in the present report, but are merely being called to the attention of the reader.

Canadian workers have studied the adsorption of a number of vapors other than CCl_4 by various charcoals.[112] Most of their work had been done by their isopiestic method and a great deal of it is concerned with determining the saturation adsorption values of charcoals toward miscellaneous vapors. The amount of various vapors taken up by a series of five charcoals at saturation are given in Table 18, the results

TABLE 18. Isopiestic volume activities* at saturation. Weight of adsorbate per 100 cc char.

Vapor	Carbon numbers				
	1	7	8	9	0
Carbon tetrachloride	24.4	26.2	30.2	38.2	39.4
Phosgene	20.6	24.3	28.2	33.5	34.0
Mustard gas	19.8	21.8	25.7	31.9	32.9
Water	14.1	15.9	18.9	23.0	...
Amyl chloride	...	...	18.0	22.6	...
Benzene	13.6	15.5	17.3	22.0	...
Methyl alcohol	12.0	13.5	15.7	19.5	...
n-hexane	...	...	13.3	16.8	...

* From Report No. 2 Project CE 107 by Ferguson Sheffer, and Waldock, April 10, 1942.

being expressed as weight of adsorbate taken up by 100 cc of the charcoal. The same group of experiments showed that the volume activities of any charcoal toward eight different adsorbate vapors bears a constant ratio for all adsorbate vapors against the volume activities of a standard charcoal. For example, the volume activity of charcoal No. 1 in Table 18 was approximately 0.62 that of the volume activity of charcoal No. 9 for all of the vapors shown in Table 18. Such measurements are accordingly very useful for comparing different charcoals and for predicting their behaviors toward adsorbates upon which they have not been tried.

6.11 HEATS OF ADSORPTION AND IMMERSION

Comparatively few measurements have been made as part of the NDRC program on the heats of immersion of charcoals, aside from the standard routine testing of charcoal by measuring the heat evolved when a sample is immersed in benzene. Young has,[24] however, employed an accurate calorimeter and compared his results with those obtained by the standard CWS test method. The heat evolved will increase as the sample being used is made more nearly gas free. Thus, a sample measured in air evolved 28.2 cal per g, one measured in helium evolved 30.2 cal per g; and one measured in vacuum produced 30.85 cal per g. These values are to be compared with 26.5 cal obtained by the usual CWS heat of immersion technique and 29.1 cal when the CWS calorimeter is calibrated by electrical heating technique. He concludes that the usual crude measurements are quite satisfactory and within 3 to 6% of more accurately determined values, depending upon the method used in calibrating the calorimeter.

Young [24] also obtained a few values for the heat of immersion of charcoal in water. For CWSN 19, the evolved heat was 59 cal per g. It was given off over a period of 48 hr and required a special technique and method of calculation for its determination. On the other hand, CWSN 19 TUC 87, which was prepared by oxidizing CWSN 19 in air until it had 15% oxygen, yielded a value of 24.6 cal per g but liberated this heat rapidly. It is easy to understand why the heat should be liberated more rapidly from the oxygen-coated sample. The adsorption at low relative pressures is much greater and, therefore, the rate of saturation in all probability is also greater for the oxygen-treated than for the original CWSN 19. However, the average or integral heat of adsorption would, if anything, be greater on the treated than on the untreated sample. It is, therefore, difficult to account for the smaller heat evolved on immersing the oxygen-treated sample than on immersing the original CWSN 19.

Trost and Morrison [116] measured the heat of adsorption of butyric acid from aqueous solution onto the surface of charcoal. On a series of charcoals that had been activated to different degrees, they found

that the heat of adsorption of the butyric acid was constant at 2.2 kcal per mol of butyric acid adsorbed. It was concluded that within the accuracy of the measurements, the activity of the surface-per-unit area did not change during activation. In other words, the quality of the surface was constant even though the absolute surface area was increasing.

In connection with measurements being made on retentivity, Wiig [117] has determined the heat of wetting in ethyl chloride for various charcoals. The results are shown in Table 19 in comparison

TABLE 19. Heats of wetting in ethyl chloride at 0 C for various chars.

Char	Av heat of wetting cal per g	Density of char	Heat of wetting cal per cc	Heat of wetting in benzene cal per cc
PCI-1143	11.5	0.533	6.13	9.37
DX-134	11.3	0.539	6.09	
DX-166	11.6	0.515	5.97	
DX-184A	12.4	0.482	5.97	
DX-86	12.7	0.472	5.99	
PC-518	10.9	0.545	5.94	
EASC on PCI-1143	10.7	0.617	6.61	
N-204A-2X	17.4	0.324	5.63	8.45
N-291AY-1	17.8	0.283	5.04	
NY-165	14.3	0.380	5.43	
EASC on N-204A-2X	14.2	0.412	5.85	
Seattle	13.9	0.351	4.88	7.95
H-1366	10.4	0.438	4.56	
H-960	14.7	0.356	5.23	
EASC on Seattle	12.0	0.456	5.47	

with a few scattered values for the heats of adsorption in benzene. The measurements were made with the same type of calorimeter employed by Young in the work described in preceding text. Wiig concluded that no consistent correlations between the data on heats of wetting and the amount of ethyl choride adsorbed at the break point or retained during desorption could be made.

6.12 RETENTIVITY OF CHARCOALS

It has long been recognized that a complete appraisal of the performance of a mask in removing a poison gas must concern itself with the relative ease with which the adsorbed gas is given up to a stream of poison-free air as well as with the length of time the mask will give protection when used against a stream of gas containing a definite concentration of the poisonous component. The ability of an adsorbent to retain the gas which it has picked up is generally called the *retentivity* of the adsorbent.

The exact method of determining the retentivity and, hence, of defining its true meaning has varied a great deal. The history of work done is given by Volman, Doyle, and Blacet [118] and by Stevens [119, 120] and need not be reviewed here. It will suffice for present considerations to point out that there are really two extreme cases with which one has to deal in approaching the problem. If a mask is used against a poison gas for only a fraction of its break time and is then permitted to stand unused for a sufficient length of time, it is known that the adsorbed gas will eventually redistribute itself uniformly throughout the mass of adsorbent. When the redistribution is complete and the mask is again put into service, the first bit of air passing through will remove the adsorbed gas at a gaseous concentration corresponding to the adsorption isotherm of the particular adsorbate being used. The seriousness of such redistribution and desorption will then depend primarily upon the shape of the adsorption isotherm. The other extreme case is the one in which the mask is used continuously, but the poison content of the entering air drops to zero before the break time is reached. The question then arises as to how long the mask can be kept in continuous service on poison-free air before the slug of adsorbed gas works itself along the canister bed and into the exit gas stream.

A complete solution of the problem would involve measuring adsorption isotherms for all the known and potential poison gases that are removed by adsorption on all Service charcoals, both under dry and moist conditions, and also measuring the retentive time for all gases as a function of moisture content,[114a] and fraction of the service time during which the sample was being gassed before the beginning of the passage of poison free air through the sample. Many such data have been accumulated and are available for numerous gases and charcoals but the specific results on actual poison gases are not available at the present writing. In this section we shall restrict our attention to two papers by Stevens [119, 120] and one by Volman, Doyle, and Blacet [118] dealing with the adsorption and retentivity of a number of nontoxic organic vapors as a function of moisture content of the charcoal and gas stream, and the relative miscibility of the gas being used and water vapor. Wiig [117] has also been carrying on an extensive study of the retentivity of ethyl chloride but the final report of his work has not yet been received.

By saturating a sample of charcoal with given partial pressures of vapors and then noting the

change in concentration of the effluent gas when vapor free air is passed into the sample, it is possible to construct an approximate adsorption isotherm giving the amount of adsorbate left on the sample as a function of the exit partial pressure of the adsorbate. Ordinarily, the approximate isotherms so obtained will be somewhat lower than a true isotherm because the charge left on the charcoal at any stage in the desorption is not uniformly distributed but is concentrated more at the exit than the entrance to the bed of adsorbent. Nevertheless, such approximate isotherms serve as a useful means of predicting the initial exit concentration of vapor that one could expect in a mask as a function of the amount of adsorbate that had been taken up and permitted to redistribute itself. This technique also permits one to determine the influence of moisture on the retentivity.

By employing such technique, the approximate isotherms were constructed for CCl_4, $CHCl_3$, CS_2, ethylene dichloride, methyl ethyl ether,[118] neopentane, [118] acetone, and methanol.[118] It was concluded that water vapor decreased the amount of adsorbate that could be held at equilibrium and decreased the retentivity very markedly for all vapors that were insoluble in water. For those that were slightly soluble, the effect was less pronounced and for those that are miscible in all proportions with water, no appreciable decrease in the total sorption capacity or retentivity of the charcoal was found to occur. As a matter of fact, it was shown that the isotherm for methanol could be derived in the presence of water from the dry isotherm and the water isotherm.

Time required for the effluent gas to build up to the *break* value depends upon the length of the gassing time and the relative humidity. This is illustrated in Table 20 taken from the reports of Stevens.[119] The *gas time* in column 3 refers to the number of minutes during which the vapor $CHCl_3$ was passed through the adsorption tube. The retentive time in column 6 is measured from the beginning of the gassing period. Columns 4 and 7 represent the percentage of the service time during which the sample was gassed, and the percentage of the service time to which the retentive time is equivalent, respectively. It is evident that the ratio of the retentive time to the service time depends both upon the gassing time and upon the relative humidity during the runs.

The suggestion has been made [118] that retentivity experiments carried out with an organic vapor of medium molecular weight might enable one to anticipate the behavior of unknown poison gases that would have to be removed by adsorption. It may be well to point out that this would be true only in the event that the unknown poison gas had the same adsorptive characteristics as the organic vapor. If one could predict the isotherm of the poison gas from the structure and physical properties of its molecule, one could also anticipate fairly well the retentivity of the gas. Progress has been made in this direction as outlined in Section 6.12 though it cannot be said that the exact shape of the isotherm can yet be predicted with sufficient detail to be very helpful in calculating the retentivity.

TABLE 20. Retentive time* of charcoal SBT 350 in relation to gassing time and relative humidity. $CHCl_3$, 9 mg per min.

Relative humidity	Service time T_s in min	Gas time min	% of T_s	Retentive Charge mg	Retentive time min	% of T_s
0	143	100	70	900	158	110
		71	50	639	235	164
		50	35	450	550	385
60	50	35	70	315	58	116
		30	60	270	60	120
		25	50	225	78	156
		20	40	180	108	216
		17	35	153	230	460
70	32	20	62	180	36	113
		15	47	135	42	130
		10	31	90	60	187
		6.5	19	59	96	300
		5.0	15.5	45	150	470
80	22	11	50	99	25	114
		7.2	25	65	30	136
		4.0	18	36	40	182
		2.2	10	20	55	250

* From C. E. 161 III–1–1806 by W. H. Stevens, September 9, 1944.

6.13 CHEMISORPTION ON THE CuO IN TYPE A WHETLERITES

In order to obtain some idea as to the extent of surface of the inorganic material added to base charcoals in the course of making Type A whetlerites, a search was made for a gas that would not be strongly adsorbed on charcoal and that would form only a layer of chemically bound adsorbate on the CuO attached to the charcoal. At the same time, measurements were made on two different samples of CuO of known surface areas.

The detailed results of the work need not be given

here.[121] It will suffice to point out that H_2S, PH_3, CNCl, BF_3, HCl, C_2H_2 and NO all appear to react at room temperature with the CuO in Type A whetlerites to a depth in excess of a monolayer and hence will not serve for measuring the surface area of the whetlerizing ingredients. H_2S, CNCl, BF_3, and HCl seem especially reactive and probably combine almost stoichiometrically with the copper oxides present. NO reacts extensively even with the base charcoal. CO, SO_2, H_2O, C_2N_2, and NH_3 are all chemisorbed in amounts that do not exceed a monolayer. They combine to indicate that on the three Type A whetlerites investigated, CWSN 19 TP 1, CWSN 19 TU 8, and CWSC 10 T1 15, about 3 ml of gas is required to form a monolayer on the copper oxides of the whetlerite. This corresponds to a particle size of about 100 A for the CuO crystals.

6.14 STRUCTURE OF CHARCOAL

There are very few things about which we can be sure as regards the structure of charcoal. Perhaps one of the few things we can say with certainty is that an active charcoal must contain a network of capillaries, some large and some small. This seems essential in order to provide avenues by which the molecules that are to be adsorbed can gain entrance to the interior of the charcoal particles and to the large surface area that must necessarily be located in small pores. When, however, we come to a discussion of the pore shape and ask whether we should consider charcoal as a honeycomb structure of approximately cylindrical pores, or as a collection of platelets more or less parallel to each other and forming boxlike capillaries of rectangular cross section, or some combination of these, or some arrangement involving pores of still different shapes, we find ourselves in the realm of speculation and unable to speak with certainty. Perhaps the best procedure to follow in summarizing the evidence is to consider the results obtained from each of the principal tools and types of measurement through which we can hope to obtain information as to the pore shape and the general structure of charcoal. These various approaches will include (1) X-ray diffraction studies, (2) microscopic studies, (3) electron microscope studies, (4) area and pore volume measurements and calculations, (5) chemical behavior of charcoal, (6) expansion of charcoal during adsorption, and (7) measurements of the true density of the carbon in charcoal. These will now be discussed in turn.

6.14.1 X-ray Structure Work on Charcoal

In an extended series of papers, Johnstone and Clark [122, 123] have reported the results of their study of the structural characteristics of some 1,200 samples of carbons, cokes, activated charcoals, resins and gas mask adsorbents of all kinds. A number of their observations relating to the charcoals are as follows.

1. Charcoals sinter and turn into graphite much less readily than does petroleum coke.

2. The value of c (twice the spacing between planes in the c direction) is about 7.72 A for a coconut charcoal and 7.47 A for a National charcoal made by the $ZnCl_2$ process, provided the samples have not been heated over 1100 C. This compares with 6.70 A for graphite.

3. The value of a is about 2.45 A for both these charcoals and for graphite.

4. These charcoals appear to contain a number of platelets which in the c direction are about 10 A in thickness; for a few other charcoals this thickness is as high as 12 A.

The disks or platelets of carbon revealed by the X-ray studies are broader than they are thick. For coconut charcoal they range from about 20 A for samples that have been heated to no more than 500 C, to 39 A for samples that have been heated to 1000 C. Values for this L_a dimension for National charcoals start at 20 A for the coconut charcoal but extend up to 45 A on samples heated to 900 C and to 63 A for samples heated to 1100 C.

The X-ray results, taken as a whole, constitute strong evidence that much of the carbon in charcoal is arranged in platelets. The preferential growth of these in one direction seems to be especially convincing evidence of their reality. Johnstone and Clark conclude [123] that "the data obtained from the X-ray study evidently gives credence to the idea that activation is essentially a process of cleaning out capillaries in changing their size, and perhaps their shape without greatly effecting the matrix structure of carbon."

6.14.2 Microscopic Studies

During World War II no extensive microscopic studies of charcoals were reported. However, it is well known from published reports [124, 124a] that it is possible to show the presence of large capillaries in the surface of charcoal particles by photomicrographs. Necessarily, the limit to such studies is

about 05 micron so that capillaries smaller than about 5000 A will not be observable. These microscopic studies, accordingly, will merely confirm the presence of the large connecting channels by which the gases that are to be adsorbed gain access to the interior of the particles. They show nothing about the shape or distribution of the fine pores.

6.14.3 Electron Microscope Studies

Electron microscope pictures push the microscopic observations out to capillaries smaller by perhaps a factor of 50 than those observable in the ordinary light microscope. The results have been well expressed in a summary of the paper by Johnstone, Clark and Le Tourneau: [125]

Thirty-six electronmicrographs of various charcoals are presented. While they do not reveal the ultimate pore structure of the charcoal, they do show a larger pore structure between several hundred and 1000 A in diameter, in the nut shell charcoals as ordinarily prepared, in Carlisle charcoal, in low density National Carbon Company charcoals, and in highly activated (steamed) Saran charcoals. The importance of these large pores is not fully established, but they may effect the rates of adsorption of gases by the charcoal.

6.14.4 Area and Pore Size Measurements

In earlier work, Young [126] calculated the diameter and length of a cylindrical capillary that would be required to be equivalent to the area and pore volumes of typical charcoals. For CWSN 19 using a value of 1,338 sq m per g for the area, he concluded that 2.05×10^{13} cm of pores 20.8 A in diameter would be needed. To illustrate the enormous length of capillary thus involved, he pointed out that the length in a 1-g sample would be equivalent to 40,000 times the circumference of the earth. If one assumes that these cylindrical capillaries are arranged as a honeycomb in a particle of charcoal, it turns out that the minimum wall thickness between the cylinders would be only about 4 A. It is a little difficult to reconcile such a picture with the X-ray observations of platelets 10 A thick and 20 to 60 A wide as making up most of the charcoal. Even though cylindrical capillaries have been used for convenience in calculating pore diameters from water desorption isotherms, the X-ray results, if they can be relied upon, certainly would dictate the use of caution in formulating any such picture of the charcoal structure.

Young also calculated that if all of the capillary space consists of rectangular parallelepiped capillaries with parallel walls, the distance between the walls would, on an average, have to be 10.4 A for CWSN 19, in order to account for the observed area and pore volume. Such a picture would be entirely consistent with the X-ray data. As a matter of fact, it was found that on one particular sample of National charcoal, the apparent area dropped from 2,040 sq m per g to 1,670 sq m per g as the sample was heat treated up to 1100 C. During this heat-treating the L_a dimension of the disks or platelets increased from 20 to 63 A in size. It is entirely reasonable on a platelet structure to explain such particle growth with comparatively little change in surface area. It would be much more difficult to explain if the charcoal consisted of a honeycomb structure of cylindrical capillaries.

6.14.5 Chemical Behavior of Charcoal

It is well known that standard charcoals can all be converted by proper chemical treatment into compounds that appear to have a central nucleus of carbon atoms arranged much as though they were in a plane of graphite. Thus mellitic acid has been reported [127] to be formed in good yield by controlled oxidation with nitric acid. This certainly indicates that much of the carbon is arranged in two dimensional graphite-like sheets or platelets and again is consistent with the X-ray picture of the structure of charcoals.

6.14.6 Expansion of Charcoals During Adsorption

At least two different observers [40, 128] have noted that when charcoal picks up water vapor it expands. This has been construed as evidence against capillary condensation and in favor of an adsorption interpretation of the water vapor picked up by charcoal. It should be noted, as pointed out by Kummer, that it is much easier to imagine the expansion of charcoals if they are made up of platelets capable of being pried apart to some extent by entering water molecules in much the same way that various molecules can pry apart the planes of monotmorillonite and certain other clays. If the pore structure consists of a honeycomb of cylinders the possibility of expansion seems much more limited.

6.14.7 True Density of Carbon in Charcoal

The true density of carbon in graphite is about 2.25 g per cu cm as determined both from X-ray

work and from actual density measurements. If the c dimension in charcoal is as large as 7.5 A as indicated by the X-ray work, and the a dimension is substantially the same as for graphite, it would seem to follow that the apparent density of the carbon in charcoal cannot be as high as 2.25 g per cu cm since the c distance for graphite is only 6.7 A. On the basis of the X-ray measurements the density should be somewhere between 2.0 and 2.1 g per cu cm. Carbon densities determined by helium have been reported over the entire range from 1.77 to 2.36 g per cu cm for various charcoals; a large number of the apparent densities are in the range 1.95 to 2.15 g per cu cm. Accordingly, it may be said that the density values of the carbon in charcoals are also consistent with the X-ray data. It should be noted in this connection that an interplanar distance of 7.5/2 that one would deduce from the c dimension is probably too small to permit the entrance of helium atoms between planes during density measurements. Hence, the helium density determinations would really yield values for the density of the platelets.

6.14.8 General Conclusion as to Structure

As stated in the introduction to this section, it is not possible to speak with certainty as regards the structure of charcoal. When all of the evidence listed above is taken as a whole, however, it seems to speak in favor of capillaries of rectangular cross section for the most part, rather than cylindrical capillaries. Immediately, one is confronted with the question as to what happens to the pore diameter calculations made by Juhola in the event that the pores are really boxlike structures rather than cylinders. The answer is that the distance between parallel walls that one calculates from the Kelvin equation is just one-half as great as the diameter calculated from cylindrical capillaries. Accordingly, capillaries which with a cos θ of 1.0 appeared to be about 36 A in diameter, if present as cylinders, would calculate to be 18 A between parallel platelets. However, the calculation of the distance between parallel planes from the relation of the increment of surface area A covered up by each increment of volume V is given by the equation

$$d = \frac{2\Delta V}{\Delta A} \cdot \qquad (23)$$

Hence if cos θ were taken as 0.53, the measurement of the slope of the surface area vs volume of water curve would lead to a value of about 9 A for the distance d. This is too small a size to permit the occurrence of what we might call capillary condensation. On the other hand, if one assumes that the charcoal is made up of platelets and accepts the distance d as 18 to 20 A the surface area per g of charcoal is computed as about 800 sq m per g; this is to be compared to values ranging from 1,300 to 1,700 sq m per g obtained by different methods of estimating the area. Possibly the answer to the dilemma is to be found by assuming that the capillaries are for the most part rectangular in cross section and for CWSN 19 about 18 to 20 A between platelets, and that even smaller crevices leading off the 20 A openings become covered with adsorbed water only when the larger 20 A openings are full. In desorption, this would mean that the water in the very small cracks and crevices would disappear at the same time that the water was desorbed by capillary condensation from the hemicylindrical surface at the edge of the rectangular capillary opening. Furthermore, this explanation is not inconsistent with the value of d obtained from equation (23) because such a calculation is necessarily an average for the main capillaries and any smaller side capillaries that fill and empty at the same time that the main 20-A capillaries fill and empty. It does, however, entail assuming cos $\theta = 1$, an assumption that does not seem very reasonable at relative pressures at which water vapor is only slightly adsorbed.

Possibly the capillaries are neither cylinders nor rectangular parallelepipeds, but some irregular collection of openings of odd shapes that will not permit any simple presentation. The final answer still seems obscured. As stated above, however, if the choice were between cylindrical capillaries and rectangular capillaries, the bulk of the evidence would, in the writer's opinion, favor the latter.

6.15 SUMMARY

Measurement of Surface Area

By measuring the adsorption of nitrogen at −195 C it is now possible to determine the relative surface area of non-porous, finely divided solids or of porous solids having large pores, to an accuracy of about 5% and the absolute area to an accuracy of about 25%. The method is also applicable to fine pore adsorbents such as charcoal, but for such materials it is attended with considerably more uncertainty than for the non-porous or large pore adsorbents.

Application of Area Measurements in Predicting the Performance of Charcoals

The nitrogen adsorption isotherms used in surface area measurements can be employed to obtain an approximate estimate of the PS life of a charcoal and to give some indication as to the utility of the base charcoal for making ASC whetlerite.

Adsorption of Water Vapor

Water vapor is adsorbed only slightly by most charcoals at relative humidities below 50%; at higher relative pressures, the adsorption rises rapidly and reaches a final saturation value which is about the same as that of other vapors when calculated as volume of liquid. Desorption of water vapor from activated charcoals is almost always accompanied by marked hysteresis, the equilibrium pressure for a given volume of gas adsorbed being much less on desorption than on adsorption. Desorption appears to take place as though the water were held in the capillaries by capillary condensation; adsorption of water vapor seems best explained as a combination of adsorption and capillary condensation.

Pore Size and Pore Size Distribution

Methods for measuring pore size include (1) use of molecules of increasing size in adsorption studies; (2) application of the Kelvin equation to adsorption isotherms of gases other than water vapor; (3) application of the Kelvin equation to water vapor adsorption and especially desorption isotherms; (4) measurement of the relation between the residual surface area and the amount of water held in the capillaries of a charcoal; and (5) measurement of the pressure required to force Hg into capillaries. By a combination of (3), (4), and (5), pore size distribution curves have been obtained on more than a hundred charcoals.

Influence of Pore Size and Distribution on Charcoal Performance

A necessary prerequisite to a good base charcoal for making ASC whetlerites to remove CK under 80-80 test conditions appears to be the possession of a macropore volume in excess of about 0.2 cc per cc of charcoal granule. Micropores suffice for removal of PS provided enough large capillaries are present to permit gas to enter the particle readily. The same pore size criteria appear to apply to the removal of CG that apply to CK. The pore size requirements for the removal of SA and AC are less exactly determined as yet, but are susceptible to determination by methods now available.

Pore Size Alteration

By a suitable combination of steaming, hydrogenation, or partial oxidation in the presence or absence of impregnation with inorganic materials, it is possible to tailor-make charcoals to give any desired distribution of pore sizes. Cr_2O_3, Fe_2O_3, NiO, Mo_2O_3, Na_2CO_3 and CuO have all been studied as impregnating agents to assist in pore size alteration.

Carbon-Oxygen Complexes

The pickup of oxygen at temperatures up to 400 C has been studied in relation to its influence on the properties of charcoal. The adsorption of base from solution, of ammonia from the gas phase, and of water vapor at low relative pressure are all increased by oxygen treating. The surface complexes formed during the treating can all be removed from charcoal as CO and CO_2 by evacuation to 1200 C together with large quantities of hydrogen and smaller amounts of water vapor and methane. No correlation between the nature of the surface complex and the whetlerizability of a base charcoal has been established.

Special Surface Coatings on Charcoal

Samples have been prepared that are coated with partial layers of chemically bound nitrogen, chlorine, and sulfur. The influence of these coatings on the whetlerizability or sorptive capacity toward poison gases has not been measured.

Molecular Structure and Adsorption

Adsorption isotherms of about twenty different gases on CWSN 19 have been used as a basis for working out a theory for predicting the adsorption isotherm of a gas from its structure and physical constants. It has been found possible to predict whether a given adsorbate will be strongly, weakly, or very weakly adsorbed by a charcoal if the surface energy of the liquefied adsorbate, and the polarizability, and fundamental frequency of its molecules are known together with the adsorption isotherm for any known gas on the sample of charcoal to be used.

Adsorption of Vapors by Charcoal

Data are presented for the adsorption of PS in the presence and absence of water vapor and for the

adsorption of pyridine, picoline, and carbon tetrachloride. Adsorption volumes at saturation are shown, in addition, for phosgene, mustard gas, amyl chloride, methyl alcohol, benzene, and *n*-hexane.

Heats of Adsorption and Immersion

Heat of immersion values have been measured for benzene on one charcoal under various conditions; for water on a charcoal before and after treating it with oxygen at 400 C, and for ethyl chloride on a series of charcoals.

Retentivity

The importance of the retentivity of a charcoal for a poison gas has been emphasized as a prerequisite for gas mask use. Detailed studies have been made on the retentivity of a number of vapors that are not miscible with water, of some that are partially miscible, and of several that are completely soluble. Water vapor on the charcoal or in the gas stream used in desorption was found to greatly decrease the retentivity of the first class of vapors, to influence to a smaller extent the desorption of the second class, and to have little influence on the desorption of those vapors that are miscible with water vapor.

Chemisorption of Gases by Whetlerite Components

On Type A whetlerites H_2S, PH_3, CNCl, BF_3, HCl, C_2H_2, and NO appear to react with the CuO at room temperature to a depth in excess of a monolayer and hence were not useful for measuring the particle size of the CuO particles deposited by whetlerization. CO, SO_2, H_2O, C_2N_2, and NH_3 all give promise of being useful for such measurements. On several typical whetlerites the average size of the CuO crystals appeared to be about 100 A.

Structure of Charcoal

It has not been possible to decide definitely as to the structure of the charcoal. Many pore size measurements have been made on the assumption that the pores are cylindrical capillaries. This is almost certainly an over-simplification. Many of the properties of charcoals seem best explained by assuming that the charcoal is made up of sheets of carbon atoms only a few atoms thick, the pores having plain walls and being so crisscrossed as to provide sufficient strength for the particles. In any case, it is certain that a good gas mask charcoal must include a network of large and small pores; the large pores permit ready access to the molecules being adsorbed; the small pores provide the large surface area that is essential for removing gases by adsorption.

Chapter 7

MECHANISM OF CHEMICAL REMOVAL OF GASES

By *J. William Zabor*

7.1 PURPOSE AND SCOPE OF THE INVESTIGATIONS

DURING the past four years a considerable amount of time and effort has been expended in studies of the mechanism of chemical retention or destruction of the various types of chemical warfare agents on base or impregnated charcoals. The research was undertaken in the hope that a better understanding of the mechanisms might lead to such advances as the following.

1. Ideas for new impregnants, which by virtue of stoichiometric or catalytic action, would increase the protection afforded by gas mask absorbents for each type of gas.
2. Clues to the mechanism of deterioration of impregnated charcoals now in use and to possible methods of reduction or elimination of such deleterious aging.
3. Information to guide the search for new war gases toward types which would most readily penetrate enemy gas masks.
4. Suggestions for gaseous agents which might be employed tactically as catalyst poisons — that is, agents designed to reduce the protection afforded by enemy gas masks against standard war gases to such a point that the enemy would be rendered vulnerable to subsequent gas attack; and, conversely, to discover and eliminate such vulnerability in the gas masks of our Armed Forces.

Among the references used in the compilation of this chapter are many reports of studies which were originally directed toward objectives other than the discovery of the mechanism of retention of the gases. Even from these, however, some information pertinent to this subject may be gleaned.

Considerable knowledge of the mechanisms for removal of the more common gases had been accumulated prior to 1940 by the Chemical Warfare Service and by independent workers. Much of the work, or similar investigations, leading to this knowledge was purposefully repeated in order to ascertain whether the more recently developed charcoals and whetlerites behave similarly. Because this chapter does not represent a chronological treatment of the subject, only the more recent evidences are given in cases of duplication.

It is obvious from consideration of the purpose of these investigations that a complete knowledge of the mechanisms, including all minor side reactions, is unnecessary; and understanding of only the principal reactions should suffice in most instances. For this reason, as well as for lack of time and because of the comparative importance of other methods of approach to the general problems at hand, the conclusions to be drawn are fragmentary and in some cases only tentative, pending the results of further investigation.

7.2 CLASSIFICATION OF AGENTS

There are many criteria upon which to base the classification of agents. For the purposes of this discussion it is most convenient to classify them primarily according to their chemical properties. In general, such a classification system naturally separates the mechanisms into general types as well.

On this basis the agents are considered in the following order:

1. Gases retained primarily by physical adsorption.
2. Acidic or acid-forming gases.
3. Basic or base-forming gases.
4. Readily oxidizable gases.
5. Readily reducible gases.

As in any classification system, there is some overlapping of types; some agents exhibit properties characteristic of two or three of the classes.

7.2.1 Gases Retained Primarily by Physical Adsorption

Chloropicrin

It has always been assumed that chloropicrin (trichloronitromethane; CCl_3NO_2; PS) is physically adsorbed. A large volume of work has been done on the nature of this adsorption, its dependence on numerous variables, and its reversibility. Only a few of the experiments and conclusions supporting the assumption of physical adsorption need be quoted in this section; the bulk of the research is beyond the scope of this discussion.

Nature of the Product Desorbed.[1] Base charcoals and whetlerites were brought half way to the break point in standard tube tests with chloropicrin, and desorption was effected by passing dry air through the absorbent bed at 25, 35, 50, and 95 to 100 C. The boiling point, freezing point, and index of refraction of the desorbed gas were determined, alcohol solutions of the desorbed gas were analyzed polarographically, and chloride analyses were made of the pyrolytic products of the gas. All analyses indicated that chloropicrin was at least the chief, if not the only, substance desorbed from either type of adsorbent.

Effect of Humidity of the Gas Mixture.[2, 3] Studies of effluent concentration versus time curves and of the weight-gains of dry charcoal tested with chloropicrin-air mixtures at 0% and 50% RH showed that, within experimental error, the results of either type of test were independent of humidity. Though no attempt was made to ascertain the fraction of the gain in weight due to water adsorption, it is safe to assume on the basis of other experimental data that little or no water was adsorbed. Thus, at least during the course of dynamic tests, it is probable that hydrolysis plays a negligible role in the retention of chloropicrin. Water originally adsorbed by the charcoal does effect adsorption of PS or other gases by rendering part of the charcoal surface inaccessible.

Table 1. Comparison of standard PS tube lives of 12–16 mesh base charcoals and Type ASC whetlerites.

Service time (min)	
Base charcoals	Whetlerites
39	34
50	45
56	51
64	57

Comparison of Base Charcoal and Whetlerite. The reference [2, 3] quoted is only one of many in which chloropicrin lives of base charcoals and whetlerites are compared. Typical performance data extracted from this reference and summarized in Table 1 show that the normal effect of whetlerization is to reduce slightly the amount of PS adsorbed.

Occasionally a sample is found in which the life of the whetlerite is slightly longer than that of the base charcoal. Such infrequent phenomena are best explained either on the basis of additional activation during the drying of the whetlerite, or change of mesh size due to attrition during the whetlerization process. In general, however, the reduction of PS service times by impregnation indicates that the impregnant occupies space on the adsorbent, or in some other way makes this adsorption space inaccessible to chloropicrin. It further indicates that during the course of dynamic tests no beneficial reaction takes place between chloropicrin and the impregnant.

Mustard Gas

By virtue of their low volatilities and high molecular weights persistent agents are adsorbed tenaciously by dry charcoals and whetlerites. As a consequence the protection of the respiratory tract against such agents does not present a problem and little work has been done to determine whether chemical reaction plays any appreciable role in the retention.

One series of experiments [5] on the performance of the M10 canister against H—mustard gas, 2,2′-dichlorodiethyl sulfide; $(ClCH_2CH_2)_2S$—under humid tropical conditions is of interest. Canisters filled with humidified Type A and Type AS whetlerites were tested at 50 lpm against H at 40 to 50 C. Even under these extreme conditions the protection afforded is more than ample. Examination of the weight changes during the tests offers the most interesting and conclusive evidence that the adsorption is primarily physical in nature. In all tests, the weight of H adsorbed exceeded the weight gain; indeed, in some of the experiments the canisters lost weight while adsorbing as much as 34 g of H. Because it is improbable that any volatile decomposition products other than HCl would be formed and since HCl would be retained by the adsorbed water and the impregnants, these observations are best explained on the premise that H, being much more strongly adsorbed than water, displaces the latter from the adsorbent.

Some hydrolysis of H undoubtedly takes place on

the adsorbent, but the evidence for the displacement of water by mustard gas suggests that physical adsorption is of prime importance in dynamic tests.

Similar results and conclusions [6] have been obtained with HN-3—tris β-chloroethyl amine, $(ClCH_2CH_2)_3N$.

Many other gases which are held by physical adsorption have been studied during the past two decades. In general, however, except for carbon monoxide, these gases have little or no promise as toxic agents; those which are toxic are nonvolatile and are well adsorbed by charcoal.

7.2.2 Acidic or Acid Forming Gases

The majority of the nonpersistent gases fall in this classification. The three standard agents, phosgene, hydrogen cyanide, and cyanogen chloride, are examples of this type as well as the many fluorides upon which considerable time and energy were expended in search for new agents during the early part of World War II. Other gases which have been investigated to a moderate extent and which are members of this group are nitrogen dioxide, hydrogen sulfide, sulfur dioxide, and the halogen acids.

Needless to say, the largest bulk of research in the field of reaction mechanism has been directed at the problems arising from consideration of the more important agents of this group. An effort is made, therefore, to summarize the experimental evidence and conclusions with reference to summary reports whenever feasible.

Phosgene

The main features of the mechanism of CG (carbonyl chloride; $COCl_2$) removal by charcoals have long been known.[7] The conclusions from early tube tests with unimpregnated charcoal are briefly summarized as follows.

1. In contact with charcoal, phosgene is hydrolyzed by moisture in the air or in the charcoal; hydrochloric acid and carbon dioxide result.

2. Whichever substance (phosgene or water) is present in deficient amounts is completely used up.

3. For dry charcoal and dry gas mixtures the phosgene is held by physical adsorption.

4. If water is present in deficient amount, hydrochloric acid will penetrate the charcoal before phosgene since hydrochloric acid is less tenaciously adsorbed than is phosgene.

5. If water is present in excess, phosgene will penetrate the charcoal before the hydrochloric acid because hydrochloric acid is very soluble in the excess adsorbed water while phosgene, being relatively insoluble, must be retained principally by adsorption on the surface of the charcoal.

6. The service times of deep layers of charcoal are considerably longer in the presence of excess moisture (either in the gas mixture or in the charcoal) than in absence of excess moisture, by virtue of the increased capacity of the charcoal for HCl at high humidities.

7. The carbon dioxide formed by the hydrolysis of phosgene appears in the effluent stream shortly after the start of the test under any set of conditions. Large excess of water may delay the appearance slightly, but in any case most of the carbon dioxide appears eventually in the emergent gas.

These conclusions have been verified by more recent tests.[8] The results indicate that the phosgene, under dry conditions, is held principally by physical adsorption.

$$C^*OCl_2 = C^*OCl_2(\text{Adsorbed}), \quad (1)$$

$$C^*OCl_2(\text{Adsorbed}) + O(\text{Surface}) = C^*O_2 + 2Cl(\text{Adsorbed}), \quad (2)$$

$$2Cl(\text{Adsorbed}) + C + O(\text{Surface}) = COCl_2. \quad (3)$$

Studies [9] with radioactive carbon [a] as a tracer suggested the possibility that reactions (2), and (3) might take place to a minor extent following reaction (1) on dry charcoal. This series of reactions seemed necessary to explain the presence of CO_2 in the emergent stream in excess of the amount expected from reaction with the small amount of water available. Verification with thoroughly dried charcoal and gas streams is necessary. In any case, however, these reactions are of little interest in the overall mechanism inasmuch as they play a negligible role in the usual circumstances when some water is present; the principal reaction must then be hydrolysis:

$$COCl_2 + H_2O = CO_2 + 2HCl. \quad (4)$$

On whetlerites this reaction is followed by neutralization of the HCl

$$CuO + 2HCl = H_2O + CuCl_2, \quad (5)$$

and regeneration of the water. Thus in the presence of deficient amounts of water the life to the penetration of HCl is considerably lengthened by whetlerization.

[a] Radioactive carbon atoms are indicated by an asterisk.

The observation [9] of considerable C^*O_2 in the effluent gas in tests with relatively dry whetlerite and gas may be explained on the basis of reactions (2) and (3) or by the chain set up in (4) and (5) or possibly by direct reaction with the copper oxide:

$$CuO + C^*OCl_2 = C^*O_2 + CuCl_2. \qquad (6)$$

This reaction is also probably of little significance in the usual circumstances.

Thus the catalytic hydrolysis [equation (4)] followed by neutralization [equation (5)], or by solution of the HCl in adsorbed water, probably represent the overall mechanism adequately. Other basic constituents of the impregnant may enter into reactions similar to equation (5) as well.

The rate [9, 10] of removal of phosgene from the gas stream decreases with increasing moisture content of the whetlerite while the capacity of the adsorbent for the products increases. This is illustrated in the life vs thickness plots in Figure 1 for a Type AS whetlerite prepared from an extruded, zinc chloride-

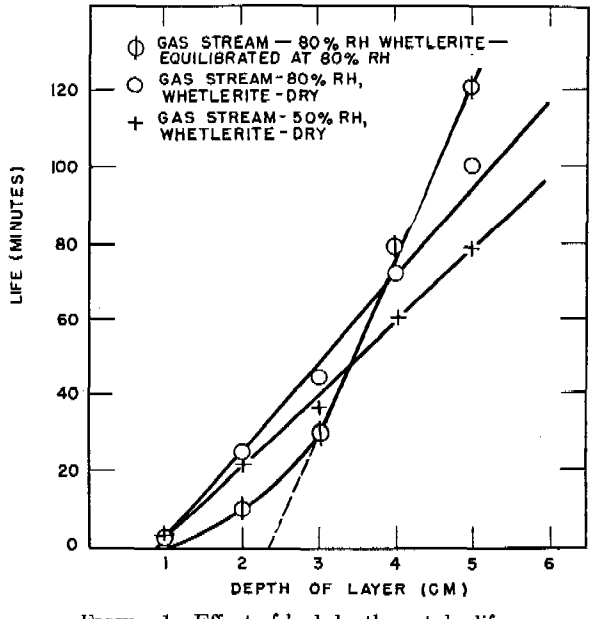


FIGURE 1. Effect of bed depth on tube life.

activated wood charcoal. This effect on the rate of removal of phosgene, together with other evidence, suggests that the reaction mechanism discussed above must be preceded by physical adsorption. This suggestion is deduced from the fact that the rate of physical adsorption must be a function of the accessible adsorptive surface area and consequently should decrease as the moisture content of the adsorbent increases; on the other hand, the rate of hydrolysis should be a function of the amount of accessible water and should increase with increasing moisture content. The extent of this effect depends to a large degree on the pore size distribution of the adsorbent as discussed in Chapter 6.

The CG capacity of dry whetlerites increases with decreasing temperature; [9] at the same time the critical bed depth first increases, probably because of changes in the diffusive properties of the gas, and then decreases as the rate of rise of capacity increases. This is typical of systems in which reversible adsorption is the predominating process. The capacity of whetlerites having a high moisture content remains essentially unchanged with decreasing temperature [9, 12] until approximately −20 C is reached; at this point the capacity of most samples studied drops sharply. This may indicate a change in physical state of the adsorbed water and consequent transition to a mechanism of primarily physical adsorption. The critical bed depth increases at first partially because of the decrease in temperature and because of a reduction in the rate of hydrolysis. Below −20 C there is indication of a rise in rate of adsorption as in the case of dry adsorbents.

The experiments to determine the effects of temperature are only cursory in nature and are quoted only to complete the picture and to show that by reasonable speculation they may be qualitatively interpreted on the basis of the proposed mechanism.

The copper content of a whetlerite is in the range of 5 to 8% on a weight basis and the apparent density is approximately 0.5 g per ml; thus the copper content may be expressed as 0.025 to 0.040 g per ml. In tests of whetlerites as received with 50% RH CG-air mixtures, the capacities of the adsorbents expressed in millimoles of CG lie in the range of 0.6 to 0.9 millimole per ml. Similar tests with base charcoals indicate that excess of the observed range of capacities of whetlerites over the range calculated from the copper content and the proposed mechanism, represents a reasonable capacity for the charcoal base. The critical layers for the whetlerites under these conditions lie in the range of 0.5 to 1.5 cm at a linear flow rate of 500 cm per min and are nearly independent of flow rate over the range of 250 to 1,000 cm per min.

For whetlerites or base charcoals equilibrated at 80% RH, the capacities are in the range of 1.5 to 2.5 millimoles per ml and the critical layers in the range of 1.0 to 2.3 cm at a flow rate of 500 cm per min.

Preliminary tests [13] with monofluorophosgene (COClF) are compatible with the mechanism discussed above. The protection afforded by dry whetlerites against dry gas mixtures is less for COClF than for $COCl_2$. This would be predicted on the basis of the effect of reduced molecular weight and increased vapor pressure on physical adsorption. The protection afforded in moist systems, on the other hand, is greater against COClF than against $COCl_2$ presumably because of the greater ease of hydrolysis of COClF.

Acids

None of the acids HF, HCl or H_2S are of interest as war gases, but studies of protection afforded against these gases and of the mechanism of the retention lend insight to the expected behavior of new agents of this general classification.

Life vs thickness studies [14] with dry Type A whetlerite and dry HF-air mixtures demonstrated that at 25 C and an influent concentration of 1.5 mg per l, the capacity of the whetlerite was 1.75 millimoles per ml of adsorbent while the critical bed depth was 1.2 cm; at 40 C and an influent concentration of 1.65 mg per l, the capacity was reduced to 1.45 millimoles per ml while the critical bed depth remained unchanged. The fact that part of the HF is held by physical adsorption is shown by the reduction in capacity with increase in temperature and by desorption trials. Nevertheless, the amounts of HF retained by 3-cm layers of dry whetlerite taken to the break point were found to be independent of the influent concentration over the range from 0.4 to 2.2 mg per l at 25 C; base charcoal on the other hand not only shows a smaller retention under these conditions, but also a retention which increases with increasing influent concentration. These observations may be considered as good evidence for the predominance of a chemical reaction, presumably

$$CuO + 2HF = CuF_2 + H_2O. \qquad (7)$$

The equality of critical layers for the whetlerite at these two temperatures is an indication that reaction (7) is probably preceded by adsorption and that adsorption may be the rate-governing step. On the basis of equation (7) and approximate calculations such as were made in the section dealing with phosgene, the capacity due to chemical reaction should lie in the range of 0.8. to 1.3 millimoles per ml as compared with the observed capacity of 1.45 millimoles per ml.

The presence of moisture increases the tube lives of either whetlerite or base charcoal several fold, indicating additional retention by solution of HF in the adsorbed water.

If dry or moist adsorbents are exposed to or beyond the HF break point in a tube test and an air stream is subsequently passed through the tube, some of the HF will desorb.[15] The desorption from base charcoal is much greater than from Type A whetlerite. If the desorption curves [15] are extrapolated to the point where the concentration becomes essentially zero, a rough estimate may be made of the amounts of HF retained chemically. Estimates made in two trials with dry Type A whetlerite were 0.7 and 1.1 millimoles per ml; the first estimate may be low since the test was carried only to the break and insufficient time was given to permit redistribution of the slight excess of adsorbed gas in the influent layers to the effluent layers so that reaction (7) could proceed to complete utilization of the CuO or of the HF. Though these estimates are only approximate, the fact that they fall in the range of capacities predicted for this mechanism constitutes additional substantiation. A similar desorption experiment with base charcoal was not conducted over a sufficiently long period to permit an extrapolatory estimate of the retentivity, but it is certain from the data that the retentivity would be less than that of the whetlerite by a large factor.

When 1 g (approximately 2 ml) of thoroughly dried whetlerite was exposed to 21.6 ml (STP), or approximately 1 millimole of HCl gas, the gas was completely and irreversibly adsorbed.[16] Water equivalent to 70% of the HCl was removable. This result is compatible with the proposition of equation (5) as the principal mechanism for removal of HCl by whetlerites in the absence of water. The predicted irreversible capacity is 0.8 to 1.3 millimoles of HCl per ml of whetlerite.

Canister tests with HCl [17] are likewise compatible with this mechanism. M7XA1 canisters tested to the break point failed to evolve any HCl during 6 hr of subsequent passage of air. At the break point the gas input was less than the capacity computed on the basis of chemical reaction.

Hydrogen sulfide behaves in a manner similar to hydrochloric acid when brought in contact with thoroughly dried whetlerite.[16] Even at −78 C the H_2S reacts within a few minutes with all the CuO present in the whetlerite to form H_2O and CuS. Tube tests of whetlerite in comparison with base charcoal [18] substantiate this chemical removal.

Nitrogen Dioxide (NO_2)

By virtue of its oxidizing properties, NO_2 might be classified as a readily reducible gas. However, a study of its behavior in contact with charcoal or whetlerite leads rather to classification as one of the more or less unique members of the acidic group.

No data have been obtained in systems entirely free of water. Since such circumstances are never met in actual practice this lack of information is of little concern except for the light which might be shed on the mechanism of removal of NO_2 by studies of its behavior under these conditions.

In tube and canister tests [19, 20] in the presence of some moisture charcoals and whetlerites exposed to NO_2 are penetrated first by NO. In general, the greater the amount of moisture present, the more rapidly NO forms and penetrates the adsorbent. Charcoals and whetlerites equilibrated at 50 to 80% RH transmit NO immediately when exposed to NO_2.

NO_2 is reduced to NO on the surface of other solids such as silica gel and soda lime, which are not reducing agents. Water is the only substance present capable of accounting for the reduction. It was, therefore, concluded that the reaction

$$3NO_2 + H_2O = 2HNO_3 + NO \qquad (8)$$

is catalyzed by these surfaces at room temperatures; when uncatalyzed this reaction is unimportant compared with the reaction

$$2NO_2 + H_2O = HNO_3 + HNO_2. \qquad (9)$$

That water is involved in the removal of NO_2 is also shown by the observation that the time before penetration of NO_2 increases with increasing moisture content while the time to penetration of dangerous dosages of NO decreases. NO must result mainly from direct reaction with water and not from decomposition of HNO_2 inasmuch as the production of NO takes place on soda lime and whetlerite where no appreciable quantities of HNO_2 may exist in the early stages of the test because of reaction with the bases present.

That reaction (8) is preceded by activated adsorption is suggested by the necessary catalytic nature of the reaction as well as by the observation that NO is produced less rapidly on soda lime than on charcoal.

Reactions (8) and (9) followed by solution or neutralization of the HNO_3 and HNO_2 suffice to explain the material balance of influent and effluent gases observed over fairly long periods of time. After extended periods of time, however, three times the NO concentration in effluent gas plus the penetrating concentration of NO_2 becomes greater than the influent NO_2 concentration. This may be due to reaction between the HNO_3 and the charcoal, resulting in the formation of either NO or NO_2, or both;

$$4HNO_3 + 3C = 4NO + 3CO_2 + 2H_2O. \qquad (10)$$

$$4HNO_3 + C = 4NO_2 + CO_2 + 2H_2O. \qquad (11)$$

When moist whetlerite is tested with NO immediate penetration of a relatively high concentration of NO is observed, but after continued exposure NO_2 is likewise found in the emergent gas; the service time to the penetration of NO_2 increases with increasing moisture content of the adsorbent. Numerous reactions could be postulated to account for these observations, but it seems most likely that the mechanism consists primarily of the adsorption and catalytic oxidation of the NO:

$$NO + O(\text{Surface}) = NO_2, \qquad (12)$$

and that the effect of moisture is to retain the NO_2 by reactions (8) and (9) as well as to reduce the rate of (12) by reducing the accessible adsorptive surface area.

While many side reactions are conceivable and may play minor roles, the overall mechanism of adsorption followed by reactions (8), (9), (10), (11), and (12) is adequate to explain the observations on the removal of NO_2 by charcoals and whetlerites in dynamic systems.

Sulfur Dioxide (SO_2)

Only a few experiments have been performed with SO_2 and these are too few to permit speculation as to the exact nature of the chemical removal. In the absence of sufficient data on the mechanism of reaction, SO_2 is merely mentioned because of the additional evidence it affords for the conclusion that, in general, the first step in the mechanism of removal of gases is that of physical adsorption.

At 25 C the SO_2 tube test lives of Type A whetlerite, considered as a function of humidity, display a maximum at intermediate humidities. The initial increase in life with increasing humidity is in the range where the adsorbed moisture has little or no effect on the rate of physical adsorption. Such behavior indicates that the mechanism definitely involves solution of the SO_2 in water adsorbed during the exposure or

chemical reactions in which water plays an important role. The subsequent fall in life with increase in humidity is in the range in which water renders a considerable fraction of the surface inaccessible to the SO_2 and, therefore, suggests that adsorption is the initial step and a limiting process in the mechanism.

At intermediate humidities the amount of SO_2 removed at the break point decreases with increasing concentration. Because the capacity, regardless of the mechanism, must either remain constant or increase as the influent concentration is increased, this is considered as evidence that even under these conditions the rate of removal is a limiting factor in determining the service time. At higher humidities, the rate of removal should become more dominant as the limiting process.

While the few tests with SO_2 do not permit an unambiguous conclusion as to the mechanism, they are most readily interpretable on the basis of the assumption that the first step in the removal is physical adsorption, followed by chemical reaction and solution of SO_2 in the water condensed in the pores.

Reaction of SO_2 with the CuO, et cetera, of the impregnant in the absence of moisture may or may not occur. Preliminary investigation [16] showed that such reaction may be sensitive to small amounts of alkali.

Fluorides

A considerable research program has been conducted in search for new toxic agents among the compounds containing fluorine. One of these, COClF, has already been mentioned in this chapter. Because of their lower boiling points and molecular weights such compounds are less readily adsorbed physically than the corresponding chlorine derivatives. Nevertheless, most of the toxic fluorides are readily hydrolyzed or decomposed in contact with charcoal and hence under normal conditions the protection afforded by gas mask canisters containing moist charcoals or whetlerites is adequate.

Phosphorus Trifluoride (PF_3). In tube tests [22] in the absence of moisture, the total input of PF_3 to the break points of Type A whetlerites was found to be independent of the influent concentration over the range of 0.5 to 13.4 mg per l. The tube lives at −30 C were longer than those at 25 C under these conditions. These results indicate that physical adsorption is the principal means of retention; reaction with the CuO of the whetlerite can play only a minor role.

With addition of moisture to the adsorbent the service time increases at first and then decreases when more than an optimum amount of water is added. The lives of whetlerites tested with a 50% RH gas stream are longer than those with dry gas when the moisture content of the whetlerite is less than about 10% on a dry basis. The tube life for tests with dry gas decreases with decreasing temperature if the moisture content of the whetlerite is greater than about 10%.

On the basis of these and previous observations it is concluded that the hydrolysis of PF_3 plays a major role in the mechanism of removal of this agent. As in the case of other gases considered, it is probable that this reaction takes place on the surface of the adsorbent and must be preceded by physical adsorption.

Selenium Hexafluoride (SeF_6). The experiments performed with selenium hexafluoride [23, 24] are not as complete as those with phosphorus trifluoride. Nevertheless, the data are consistent with the conclusions drawn above. The mechanism probably consists principally of physical adsorption followed by hydrolysis and subsequent retention of the products by neutralization by the impregnants, solution in the adsorbed water, and physical adsorption. The fact that the service time continues to rise at least to the highest moisture content (75% RH; 30% moisture on the whetlerite) employed, suggests that the initial step is not dominant as the rate controlling step. This conclusion is confirmed by the observation that the dry life does not go through a minimum, but shows a continuous increase as the temperature is decreased.

Sulfuryl Chloro-fluoride (SO_2ClF). A limited number of tube tests with sulfuryl chloro-fluoride [25] yielded interesting results. In tests with dry Type A whetlerite and dry air, SO_2 was the first substance to penetrate the adsorbent; this product probably results from the catalytic decomposition of SO_2ClF following adsorption:

$$SO_2ClF = SO_2 + ClF. \qquad (13)$$

ClF is presumably more strongly adsorbed than SO_2. SO_2ClF was the second gas to penetrate under these conditions

In the presence of moisture, SO_2ClF was found in the emergent stream before SO_2. In all cases the chloride and fluoride in the effluent gas were small

in amount compared with the SO_2ClF. The chloride and fluoride probably appear as HCl and HF formed by hydrolysis:

$$SO_2ClF + 2H_2O = H_2SO_4 + HCl + HF, \quad (14)$$

or

$$2ClF + 2H_2O = 2HCl + 2HF + O_2. \quad (15)$$

Competition of (14) with (13) probably accounts partially for the precedence of SO_2ClF before SO_2 in tests in the presence of moisture. H_2SO_4, HCl, and HF are retained by reaction with CuO and by solution in the adsorbed water; O_2 may either be chemisorbed by the charcoal or appear unnoticed in the emergent gas.

SO_2ClF preceded SO_2 and the halogen acids by longer time intervals when tests were performed with moist whetlerite at −29 C, indicating a probable reduction in rate of reactions (13) and (14).

Sulfur Pentafluoride; (S_2F_{10}); 1120 or Z. When charcoal or whetlerites are exposed to sulfur pentafluoride-air mixtures,[26] a mixture consisting chiefly of SF_6 and SO_2F_2 generally penetrates the adsorbent first; in some cases, however, SO_2 is the first pentrating gas. This initial penetration is followed considerably later by penetration of HF and finally by S_2F_{10}.

Insufficient experimental data are at hand to ascertain the importance of the role played by moisture, but the presence of sulfuryl fluoride and hydrofluoric acid in the effluent stream and some evidence for an increase in the tube life in the presence of moisture suggest that hydrolysis plays a major role in the mechanism of removal.

Because SF_6, SO_2F_2, and SO_2 are relatively innocuous, penetration of these gases is of little concern. While not very toxic, HF is irritant, and penetration of this gas would probably mark the conclusion of the period of usefulness of the canister. Under all conditions of test, protection to the HF break appears to be adequate. Whetlerite and Type D mixtures are more effective than base charcoal in removing the HF. There is some evidence for transmission of small concentrations of toxic substance prior to the S_2F_{10} break; this may be due to slow leakage of this agent at concentrations which appear too small to be effective.

These many observations demonstrate a very complicated mechanism. Nevertheless, with the aid of the results obtained with other fluorides, it is possible to speculate as to the more important reactions in the overall mechanism.

The first step is probably adsorption followed by decomposition:

$$S_2F_{10} = SF_6 + SF_4. \quad (16)$$

Adsorption of SF_6 and SF_4 may then be followed by catalytic hydrolysis:

$$SF_6 + 2H_2O = SO_2F_2 + 4HF. \quad (17)$$

$$SF_4 + 2H_2O = SO_2 + 4HF. \quad (18)$$

Another source of SO_2 in the effluent gas may be a decomposition similar to reaction (13):

$$SO_2F_2 = SO_2 + F_2. \quad (19)$$

F_2 and SO_2F_2 probably undergo hydrolysis similar to (14) and (15):

$$2F_2 + 2H_2O = 4HF + O_2. \quad (20)$$

$$SO_2F_2 + 2H_2O = H_2SO_4 + 2HF. \quad (21)$$

Boron Trifluoride Acetonitrile ($CH_3CN \cdot BF_3$). Tests [25] with $CH_3CN \cdot BF_3$ were insufficient in number to permit much speculation in regard to the mechanism of removal. No tests were made for acetonitrile in the emergent stream because it is relatively innocuous. Moist whetlerite afforded longer service time to the penetration of fluorides than dry whetlerite. Thus the mechanism probably consists of the catalytic decomposition yielding acetonitrile and boron trifluoride, followed by hydrolysis of the BF_3 (and possibly CH_3CN as well). Protection appears to be adequate in any case.

Arsenic Trifluoride (AsF_3). The results of tests [25] with arsenic trifluoride, though inconclusive, indicate strong adsorption followed by rapid hydrolysis. Protection against this gas appears to be excellent under all conditions.

1,2-Dinitro-tetrafluoro-ethane. Investigations of 1,2-dinitro-tetrafluoro-ethane ($C_2F_4[NO_2]_2$) show no evidence for reaction or decomposition of the gas either on dry or moist Type A whetlerite.[25] Indeed, the results of all experiments with this agent indicate reversible adsorption, and adequate protection except at high moisture content of the adsorbent. Being relatively innocuous, dinitro-tetrafluoro-ethane supports the generalization that fluorides sufficiently toxic to be of interest as war gases must be reactive and hence subject to hydrolysis and/or other decomposition on moist whetlerites as exemplified by the other fluorides considered in this section.

Phosphoryl Trifluoride (POF_3). The few experiments performed with phosphoryl trifluoride [25] indicate direct reaction with the CuO of Type A whet-

lerite as well as with adsorbed water in line with the general mechanisms discussed above.

Hydrogen Cyanide (HCN; AC) and Cyanogen (C_2N_2)

Hydrogen cyanide was used on a minor scale during World War I and today is one of the three standardized nonpersistent agents produced by the Chemical Warfare Service. Among the advantages of this agent are its low molecular weight and high volatility which result in inadequate protection by physical adsorption on activated charcoal. As a consequence, considerable effort has been expended in search for suitable impregnants which enhance the protection by chemical retention or destruction, in study of the mechanism of removal, and in consideration of tactics for use of AC against protected enemy troops.

Because of the volume of work and reports dealing with the removal of AC, it is impossible to discuss all of the experimental results in this brief treatment of the subject. Only some of the more important aspects of the research are mentioned. For detail, the reader is referred to summary reports [28, 29] and to the original reports of the research.

Cyanogen is considered concurrently with hydrogen cyanide because of the similarities in many of the reactions in the mechanisms of removal of these two gases. No implication of equal importance is intended.

The AC tube lives of dry base charcoals are short at room temperature, but increase rapidly with decreasing temperature, indicating that physical adsorption is the principal mechanism of retention. The presence of moisture either in the gas stream or on the charcoal effects a small increase in life, probably due to retention by reaction of HCN with the adsorbed water, with possible hydrolysis to ammonium formate. Only HCN is found in the effluent gas.

The C_2N_2 tube test lives of base charcoals are generally somewhat longer than the AC lives under similar conditions. This observation and the effect of temperature on C_2N_2 service times in dry systems indicate that the gas is held primarily by physical adsorption at room temperature. At high humidities, equilibrated charcoals tested at various temperatures exhibit minimum service times at about 25 C, indicating that a chemical reaction occurs in the presence of water. The presence of HCN in the effluent gas under these conditions suggests that hydrolysis is a probable reaction. In the absence of evidence pro or con, however, other reactions such as polymerization must be admitted as additional possibilities.

At high humidities the C_2N_2 lives decrease with increasing humidity of equilibration and test. Such a decrease is probably due, at least partially, to the slowness of the chemical reactions in the destruction of the cyanogen and consequent regeneration of adsorptive surface of the charcoal. The possibility of desorbing cyanogen and observations of recovery of life on standing after initial test lend further support to the thesis that physical adsorption is the primary step and that this is followed by slow reaction of the cyanogen.

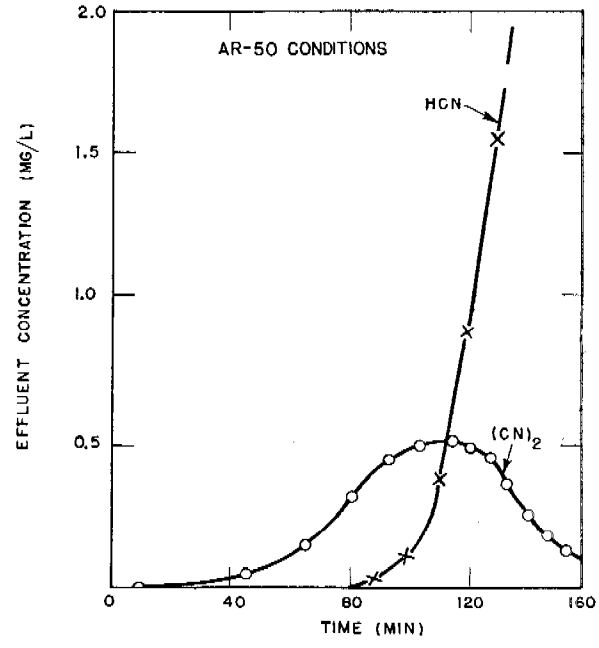


Figure 2. Typical effluent concentration-time curve for tube tests of Type A whetlerite against HCN.

It has long been recognized [30] that cyanogen appears in the emergent gases from whetlerites exposed to hydrogen cyanide. Typical effluent concentration-time curves [31] for tube tests of Type A whetlerite at AR-50 and 80-80 humidity conditions appear in Figures 2 and 3, respectively. By passage of gas-free air through a whetlerite following an HCN exposure, varying amounts of C_2N_2 can be desorbed depending on the extent of the original exposure and the humidity conditions. The greatest amount of C_2N_2 is desorbed under relatively dry conditions, but even in such cases the amount desorbed is not proportional to the amount of HCN adsorbed.

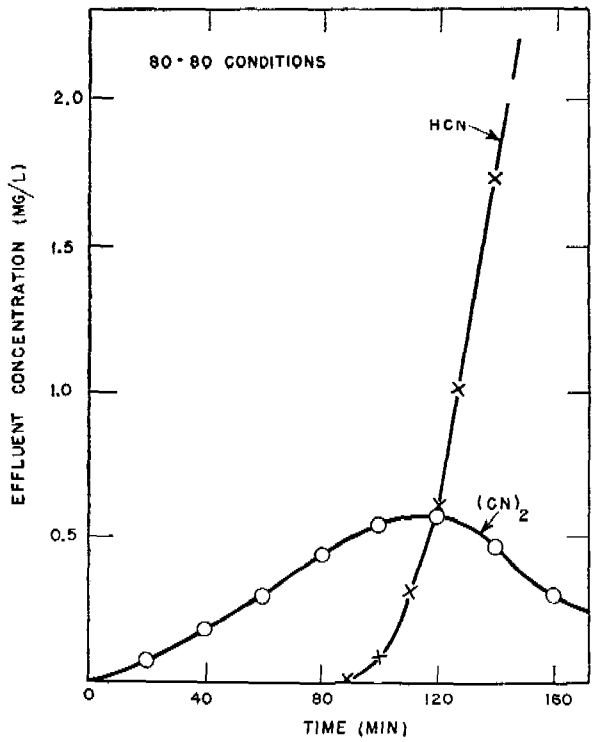


FIGURE 3. Typical effluent concentration-time curve for tube tests of Type A whetlerite against HCN.

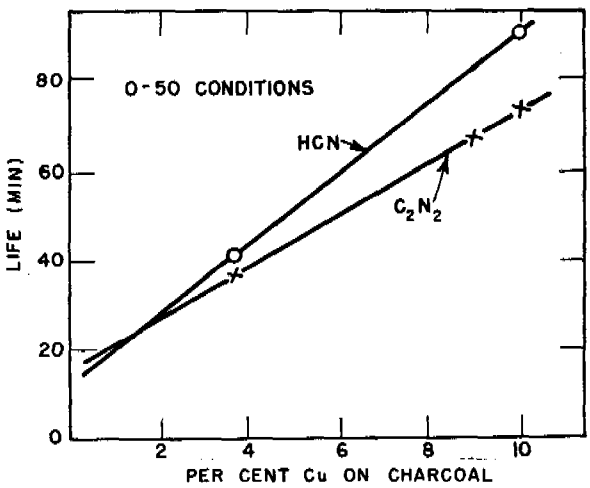


FIGURE 4. Effect of copper content on HCN and C_2N_2 lives of whetlerite.

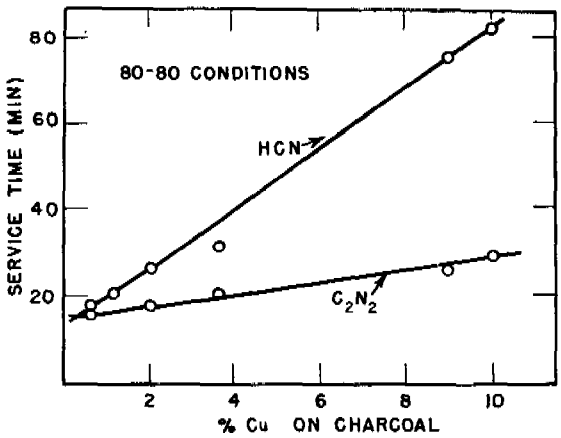


FIGURE 5. Effect of copper content of whetlerite on HCN and C_2N_2 lives.

Since the removal of HCN or C_2N_2 by whetlerite involves the absorption of both, the mechanisms for the removal of these gases cannot be discussed separately. The reactions postulated apply to the absorption of either.

As in all previous instances, it is believed that physical adsorption of the toxic gas is the first step in the mechanism. The AC protection afforded by impregnated resins and soda lime indicate that this step is probably not the major rate-governing process in the case of whetlerites. On the other hand, the ineffectiveness of catalytic cuprous or cupric oxide in granular form, or whetlerized sodium silicate, or exploded mica, are evidence supporting the conclusion that adsorption is a prerequisite to satisfactory removal. Temperature and adsorption studies with C_2N_2 show that it can be appreciably adsorbed without chemical reaction. The short life of whetlerite at 80-80 is evidence that adsorption of cyanogen is the primary step in its retention by whetlerite.

The presence of C_2N_2 in the emergent gases from whetlerites exposed to HCN necessitates the presence of an oxidizing agent on the charcoal surface; oxygen has been found to be unnecessary for the removal of HCN and production of C_2N_2. Furthermore, a stoichiometric reaction with the copper is indicated by the facts that (1) saturation data show that 1.5 to 2.0 moles of HCN are adsorbed per mole of copper and (2) the HCN life is proportional to the copper content of the whetlerite (see Figures 4 and 5). The nitrogen in the HCN is not oxidized, but remains in a form which can be hydrolyzed to ammonia (as nitrile, amide, or ammonia salt). At 100 C about 50% of the absorbed HCN remains on the whetlerite as cyanide, tentatively identified as cuprous cyanide. This abundance of evidence supports the theory that the main reaction for HCN removal is

$$4HCN + 2CuO = 2CuCN + 2H_2O + C_2N_2. \quad (22)$$

This is not the only form of chemical removal. In addition to CuO, cuprous oxide and basic copper carbonate have been identified on whetlerites by

X-ray diffraction studies. Tube tests indicate that cupric oxide is more reactive than basic copper carbonate. Nevertheless, the evolution of considerable CO_2 in the reaction of HCN is best explained on the basis of reaction with the carbonate:

$$4HCN + 2CuCO_3 = 2CuCN + 2H_2O + C_2N_2 + 2CO_2. \quad (23)$$

It is possible that some CO_2 comes from other sources, but the observations supporting equation (23) as the principal reaction involved are that (1) sufficient carbonate was present to account for all the CO_2, (2) CO_2 was found in the absence of water and to a greater extent from HCN than from C_2N_2 and thus does not arise to an appreciable extent from hydrolysis of these gases, and (3) all of the HCN absorbed was found as cyanide or cyanate.

Cu_2O and HCN most likely undergo a straight metathetical reaction:

$$2HCN + Cu_2O = 2CuCN + H_2O. \quad (24)$$

Whetlerites containing copper in the form of Cu_2O instead of CuO exhibit lives slightly more than half those of standard whetlerite.

Polymerization of HCN is possible, but there is no evidence available to substantiate the occurrence of such a reaction; moreover saturation experiments indicate that it does not occur to any great extent.

British investigators claim ammonium formate as the main end-product on their adsorbents. This product has not been found on whetlerite and the general stoichiometric nature of the HCN adsorption with the formation of C_2N_2 precludes the possibility that hydrolysis to the formate plays a very important role on whetlerite.

Cyanogen is held irreversibly on whetlerite [16] in the same amounts as SO_2, CO, and H_2O. This chemisorption or chemical reaction may be represented by:

$$C_2N_2 + CuO \longrightarrow CuO \cdot C_2N_2 \left(\text{Perhaps } Cu\langle \begin{matrix} OCN \\ CN \end{matrix} \right). \quad (25)$$

Such a reaction would explain the greater C_2N_2 life of whetlerite in comparison with base charcoal tested at 0-0 RH. It also would afford at least a partial explanation for the reduction of HCN life of a whetlerite by previous exposure to C_2N_2. Such reduction of HCN life is greater under dry conditions than in the presence of moisture. This may be due to the decomposition of the product of reaction (25) by hydrolysis or to the fact that a greater proportion of the cyanogen may be destroyed by direct hydrolysis:

$$C_2N_2 + H_2O = HCN + HOCN, \quad (26)$$

or

$$C_2N_2 + 2H_2O = (CONH_2)_2. \quad (27)$$

The appearance of HCN in the emergent stream in C_2N_2 tests on whetlerite as well as base charcoal is evidence for reaction (26). The HOCN may undergo polymerization to cyanuric acid, a probable reaction in the absence of strong acids. Since some ammonia has been identified on whetlerite exposed to HCN, it is also possible that HOCN is hydrolyzed to NH_3 and CO_2. However, insufficient NH_3 is found to account for more than one-tenth of the HOCN being destroyed by this hydrolysis, if all the C_2N_2 is removed by reaction (26). Some of the ammonia, however, could be removed by side reactions leading to formation of ammonium cyanate, urea, ammonium carbonate and copper ammonium complexes.

That the oxamide formed by reaction (27) may also undergo hydrolysis is indicated by the identification of both ammonium oxalate and oxamide among the products.

There is no direct evidence for or against the polymerization of cyanogen on whetlerite, but it must be considered as a possibility until such evidence is obtained:

$$xC_2N_2 \xrightarrow{H_2O} (CN)_{2x}. \quad (28)$$

Impregnation of charcoal with chromium or molybdenum oxides alone improves only slightly its ability to remove HCN or C_2N_2. However, in conjunction with copper oxide, they are effective in removing these gases (particularly cyanogen). That reaction (22) occurs with Cu-Cr-Ag and Cu-Mo-Ag adsorbents is indicated by the saturation data, the effect of copper content on the life, and the presence of small quantities of C_2N_2 in the effluent gas. Catalytic hydrolysis of the C_2N_2 with destruction of the CuO may be responsible for the longer lives of these adsorbents. A mole ratio greater than two for HCN to Cu indicates that Cr must give the adsorbent some additional ability to remove HCN. The mole ratio of adsorbed cyanogen to copper and chromium on the char is too great for the reaction to be stoichiometric. Lack of a direct relationship between the life and the copper or chromium contents supports this conclusion.

Reaction (26) cannot be the major reaction, for the amount of HCN generated would be too great to be completely adsorbed. Even after being run to

the C_2N_2 break point, Type ASC whetlerites display long service times against HCN.

Inasmuch as water is necessary to make Type ASC whetlerite effective in removing C_2N_2, but oxygen of the air is not, a catalytic reaction is indicated. The most likely reactions are hydrolysis [reaction (27)] to oxamide and then to ammonium oxalate, or polymerization [reaction (28)]. Qualitative identification of oxalate favor the hydrolysis as the major reaction.

Adsorbents impregnated with zinc, cadmium, and nickel have appreciable HCN lives and probably react to form stable metal cyanides or cyanide complexes. No cyanogen is generated.

Lives of charcoals impregnated only with silver are short in comparison with lives of whetlerites. Hydrolysis to ammonium formate is said to be the major reaction in the removal of HCN. The silver, however, is rapidly attacked; small amounts of HCN poison the catalyst, destroying its action in arsine removal.

Cyanogen Chloride

Cyanogen chloride (CNCl; CK) was standardized and produced by the Chemical Warfare Service as the third nonpersistent gas largely because of the vulnerability of enemy canisters to this agent (see Chapter 11). Prior to 1945 it was known as CC. A considerable amount of time and effort has been expended by Division 10 of NDRC and by the Technical Division of the Chemical Warfare Service in search for new impregnants for charcoal or new adsorbents which would afford ample protection against CK under all conditions. This research culminated in the standardization of Type ASC whetlerite (see Chapter 4). Considerable thought and experimentation was devoted simultaneously to the mechanism of removal of CK for clues such study might uncover toward possible improvements in the impregnation of charcoal, elimination of the deterioration of the proposed impregnants, and optimum tactical employment of the gas as an offensive weapon.

Though the research was prodigious and quite fruitful, the mechanism of retention of CK has proved to be complex and an unambiguous or unique solution has not been found. This was true in the cases of the other gases considered in this chapter, but to a lesser degree. Nevertheless, a brief summary of pertinent observations and tentative conclusions is warranted at this point.[28, 32]

The CK tube test lives of dry or moist base charcoals decrease with increasing temperature over the range of 0 to 100 C. Studies of the kinetics of the adsorption in dry systems [33] show that, at least in the absence of water, this observation is due to a reduction in the capacity of the charcoal which more than compensates for a simultaneous increase in the first-order rate constant for the adsorption. The presence of moisture reduces both the service times at any temperature studied and the capacities of base charcoals (at least at 25 C). Such observations are indicative of physical adsorption as the principal process of retention.

Additional validation of this hypothesis is obtained in the observation that all of the adsorbed chloride can be desorbed from dry charcoal by the passage of air. About 12% of the chloride in one test failed to desorb in 20 min from charcoal tested at 80-80. It is possible that this fraction of the absorbed gas is held by solution in the water condensed in the pores and is thus less readily desorbed; however, part of the remaining absorbate might be destroyed by a slow reaction which can play only a minor role in the overall mechanism. Thin layers of charcoal which appear to be saturated in 5 or 6 min at 80-80 and high flow rates, continue to pick up CK slowly, giving rise to an increase in apparent capacity. For one sample, an increase from 10 to 14.3 mg of CK per ml of charcoal was noted after 180 min. This may indicate a slow displacement of water, a slow rate of reaction, or both. At any rate, the slowness of this removal eliminates it as an important step in the mechanism and hence does not invalidate the conclusion that physical adsorption is the major process involved in dynamic tests. An increase in the CK input to the tube-test break point with increase in influent concentration in the presence or absence of moisture lends further support of this thesis.

Type A and AS whetlerites yielded similar results in regard to the effects of humidity and influent concentration on the tube lives, indicating that the mechanism of rapid removal in dynamic tests at room temperature is essentially the same (physical adsorption) as in the case of base charcoal. The CK tube test lives at AR-50 were found to be practically independent of the amount of copper in the impregnant. Hence it seems that copper oxide does not react to an appreciable extent with CNCl or at least in a rapid stoichiometric reaction. However, whetlerites broken to CK in air streams at various humidities and temperatures recover considerable fractions of their original lives upon standing; furthermore, this regeneration process may be repeated several

times. It is thus apparent that a slow chemical reaction occurs which removes some of the CNCl, permitting additional physical adsorption in subsequent tests. Since this phenomenon was not observed on base charcoal, it must be concluded that the copper oxide plays a role (either catalytic or stoichiometric) in the reaction during recovery. Such a slow reaction is further evidenced by the fact that the amount of desorbable chloride decreases if the exposed whetlerite is permitted to stand before desorption is attempted. Furthermore, preliminary studies seem to indicate that the dry tube lives may pass through a minimum as the temperature is increased and then rise with further increase in temperature, substantiating the conclusion that a slow reaction may be taking place at room temperature.

Cupric chloride has been identified by means of X-ray diffraction on a whetlerite exposed to CNCl. Such a compound could be formed by reaction with HCl produced by CNCl hydrolysis or with Cl_2 from CNCl oxidation. Similarly the presence of CO_2 in the effluent gas long before the CK break point may be explained either by hydrolysis or by oxidation of the CK. However, as pointed out in the section dealing with HCN, much of the CO_2 may result from reaction of HCl with copper carbonate which is likely to be present in the whetlerite. Only faint qualitative tests for cyanate have been found; this may be due to predominance of destruction of CK by oxidation over that by hydrolysis, or it may be explained by further hydrolysis of HOCN.

To increase the protection against CK, particularly in the presence of moisture, the Chemical Warfare Service developed E 6 whetlerite, a standard whetlerite treated with sodium thiocyanate and sodium hydroxide (see Chapter 4). This additional impregnation increases the lives of all whetlerites at low humidities, and at high humidities it increases the lives of whetlerites having the proper distribution of pore sizes and characteristics (see Chapter 6). No desorption is observed from E 6 whetlerites which have been exposed to CK. Upon aging, the E 6 whetlerites lose a considerable fraction of their original lives. Such deterioration in protection appears to be due to the oxidation of part of the thiocyanate to sulfate. From these observations it has been concluded that the CNCl reacts directly with the nitrogen of SCN^-.

An increase in C_0t with increasing C_0 is generally taken as an indication of physical adsorption as the major step in the removal of a gas. Such behavior should also be manifested in cases in which reactions subsequent to adsorption are slow and fail to remove the gas from the adsorptive surface rapidly enough to make appreciable additional adsorption possible; any change in conditions which tends to accelerate the chemical reaction in such cases should decrease this trend of C_0t. The presence of moisture on thiocyanate whetlerites appears to decrease this tendency of C_0t to increase with increasing C_0, probably by accelerating the reactions of adsorbed CK, and hence offers some additional validation to the conclusion that adsorption, the primary step, is followed by a relatively slow chemical reaction.

Search for impregnants affording greater original protection and stability led to the investigation of many metal oxides. Of these chromium, vanadium, and molybdenum were most promising. Study has been concentrated mainly on chromium impregnated charcoal inasmuch as this impregnant offered the best overall characteristics. Many of the speculations and conclusions for chromium impregnated charcoals and whetlerties, however, apply equally to those containing vanadium and molybdenum as well.

Impregnation by copper or chromium alone yields poor adsorbents for cyanogen chloride. Both Cu^{+2} and Cr^{+6} are necessary for optimum protection. The decrease in protection during aging is apparently due to loss of Cr^{+6} by reduction to Cr^{+3}, presumably by oxidation of the charcoal to CO_2. A similar reduction of Cr^{+6} occurs during exposure to CK. In samples of ASC whetlerite exposed to less than the break time, 4.7 equivalents of CK were absorbed per equivalent of chromium reduced; in long exposures, far beyond the normal service time, this ratio was found to be 11.4, although 27% of the Cr^{+6} still remained after the longest exposures attempted. Thus it would seem that there is no direct relationship between the amount of Cr^{+6} reduced and the total amount of CK absorbed; this may be partially due to reaction of CK with CuO, though it is unlikely that such a reaction could afford a complete explanation. It is therefore doubtful that CNCl reacts stoichiometrically with the impregnant. Thus while Cr^{+6} is necessary for rapid reaction, reduction of the chromium may not be a part of the primary process, but of a secondary or side reaction. It is possible that at least part of the reduction is due to oxidation of carbon; this reaction is known to be accelerated in the presence of acid.

The initial rates of sorption of CK are approxi-

mately the same for base charcoal and ASC whetlerite; however, the rate falls off more rapidly with time in the case of the base charcoal. This observation would suggest that the first step in the removal of CK by ASC whetlerite is physical adsorption because only with such a mechanism could the initial rates be equal on base charcoal or ASC whetlerite. This conclusion is validated by indirect evidence that the rate of destruction of CK on ASC whetlerite increases at first during the period when the concentration of adsorbed CK is probably increasing and then decreases during the extended period when the impregnant is being destroyed and part of the adsorptive surface is being utilized or made inaccessible by reaction products.

In tube tests taken to the break point, CK saturation values are never reached in any part of beds of moderate thickness. Under standard test conditions life vs thickness plots are curved and estimates of capacities from such studies yield low values. This is apparently due to the slowness of chemical reaction of the adsorbed CK. The apparent capacities of present ASC whetlerites are within the range of 40 to 100 mg of CK per ml of whetlerite (as compared with 0 to 15 mg of CK per ml of charcoal at 80-80) and are essentially independent of moisture conditions. Longer test lives at low humidities are due to the greater rates of sorption. Calculations based on comparison of results of tests with ASC whetlerites and base charcoals indicate that the specific chemical reaction rate for CK on ASC whetlerite is greater at high than at low humidities. Thus water plays an important part in the mechanism. This naturally suggests hydrolysis as a major step, but catalytic action of water may be important as well. CO_2, NH_3, Cl^-, and small amounts of HOCN are known to be among the products of the reaction; other products may also be present. Practically no CNCl can be desorbed from ASC whetlerite within short periods of time after exposure to the break point. Thus all of the CK must be either destroyed or chemisorbed.

All the chloride ion in CK taken up by charcoal or whetlerite can be recovered by acid distillation; about 90% can be recovered by extraction with water. On the average, less than 40% of the nitrogen can be recovered as NH_3 by basic distillation; somewhat larger percentages can be recovered if the whetlerite was made acid for a period prior to the basic distillation. Approximately 70 to 75% can be recovered as NH_3 by extraction with water and subsequent basic distillation of the extract. From a comparison of NH_3 blanks for these two methods, it is apparent that part of the ammonia originally on the whetlerite is not removable by extraction; it is possible that part of the CK which was not extractable as NH_3 was lost by similar retention. It is also possible that loss is partially due to failure of intermediate products to hydrolyze. HOCN hydrolyzes slowly in basic media whereas urea hydrolyzes less readily in acid media. A third possibility is that CK is destroyed by some other reaction which does not yield NH_3.

The amounts of CO_2 recovered in the effluent gas and from the adsorbent are large but irreproducible. This may be caused in part by variability of original CO_2 on the whetlerite due to different degrees of aging or to varying amounts of CO_2 picked up during equilibration. As mentioned above, part of the CO_2 may arise during the test from oxidation of carbon by the Cr^{+6}. This oxidation may be accelerated by the temperature rise due to the heats of adsorption and reaction of CK and by increased acidity.

In view of these observations, it is possible only to speculate as to the mechanism of reaction of CK on various whetlerites. All reactions are open to some question and need additional verification. Undoubtedly the primary process is physical adsorption. This may be followed by hydrolysis, oxidation, or polymerization catalyzed by CuO and Cr_2O_3 or a complex salt of these metals.

$$CNCl + H_2O = HOCN + HCl, \quad (29)$$

$$2CNCl + 2O_2 = 2CO_2 + N_2 + Cl_2, \quad (30)$$

$$3CNCl \longrightarrow (CNCl)_3(\text{Cyanuric chloride}). \quad (31)$$

Hydrolysis to yield HCl and HOCN is favored by change of free energy over the alternative reaction yielding HOCl and HCN. Furthermore, reaction (29) is necessary to explain the observation of OCN^-.

Oxidation according to reaction (30) has been observed to take place fairly rapidly in experiments with CK and metal oxides on asbestos at 75 C. The fact that the capacity of ASC whetlerite is approximately the same at 0-0, 0-50, and 80-80 RH would seem to indicate that the reaction can go to the same extent in the presence or absence of water and hence that water is merely a catalyst and hydrolysis is excluded as the major reaction. However, there was, undoubtedly, some water present in the 0-0 RH tests because drying procedures employed do not remove all the water either from the

adsorbent or the gas stream and small amounts of additional water may possibly be picked up by the gas in passage through the flowmeters; furthermore, some water may be formed by neutralization reactions such as in equation (5). Thus neither reaction (29) nor (30) can be excluded.

No direct evidence for or against polymerization (31) on the adsorbent has been found. It must, therefore, be included as a possible reaction of minor importance in the mechanism.

The HOCN can undergo further hydrolysis or reaction with NH_3:

$$HOCN + H_2O = NH_3 + CO_2, \quad (32)$$

$$HOCN + NH_3 = CO(NH_2)_2, \quad (33)$$

and the urea could be hydrolyzed:

$$CO(NH_2)_2 + H_2O = CO_2 + 2NH_3. \quad (34)$$

Urea has not been identified as a final or intermediate product, but reaction (34) is known to be possible.

The ammonia would be retained by reaction with HCl or with the metal impregnants, forming complexes. Cl_2 and HCl should be retained by mechanisms similar to those postulated in previous sections.

It has long been known that cyanogen chloride undergoes an addition reaction with amines:[34]

$$R{-}NH_2 + CNCl \longrightarrow \left[R{-}\overset{\displaystyle H}{\underset{\displaystyle H}{N}}{-}CN \right]^{+} + Cl^{-}. \quad (35)$$

That such reactions take place on charcoal adsorbents is evidenced by an increase in rate of removal and of capacity of the adsorbent,[34, 35] upon addition of amines to the impregnant. The nitrogen bases evidently react directly with the CK and do not merely activate the other catalysts, since an efficient adsorbent is formed when pyridine is put on base charcoal; in such cases the life is proportional to the amount of pyridine added.

Pyridine and other bases do not appear to affect the aging of the inorganic catalyst, but merely raise the final life of aged whetlerite.

Use of this additional impregnant has not been standardized since (1) the hazards of deterioration of ASC whetlerite have been found to be much less serious than was originally feared, (2) the addition of organic bases does not appreciably affect the initial overall performance of ASC whetlerite, and (3) many of the organic bases give off objectionable vapors on aging. Hence no detailed mention is necessary at this point.

Because ASV and ASM whetlerites have not been standardized they need not be considered separately nor in detail in this discussion. It is sufficient to say that vanadium and molybdenum, like chromium, probably act as catalysts in conjunction with copper.

For comparison purposes, the ranges of 80-80 CK capacities achieved with variously impregnated charcoals are summarized in Table 2. These values were obtained from the slopes of life vs thickness curves and hence are probably below the true saturation values. Nevertheless, they offer a good comparison of the capacities effective during the useful lives of these adsorbents.

TABLE 2. Ranges of 80–80 CK capacities of variously impregnated charcoals. (Influent concentration = 4 mg per l; flow rate = 500 cm per min).

Impregnation	N_0 range (mg per ml)
None	0–15
P* or Pi*	15–35
ASP or ASPi	25–55
ASM	30–50
ASMP or ASMPi	40–100
ASC	40–100
ASCP or ASCPi	40–100

* P = pyridene; Pi = picoline ($\beta-\gamma$ mixture).

General Conclusions for Acidic or Acid-Forming Gases

It has been concluded that the first step in the removal of acidic or acid-forming gases by gas mask adsorbents is physical adsorption. This conclusion probably applies generally, as shown in the succeeding sections of this chapter.

Acid gases, such as the halogen acids, undergo a rapid metathetical reaction with the metal oxides of the impregnant or, since most of them are very soluble in water, are retained by solution in the water condensed in the pores of the charcoal.

The majority of the probable nonpersistent war gases are halides of one sort or another. The toxicity usually bears some relation to the reactivity of the molecule; the more reactive, the more toxic. Such gases are readily hydrolyzable and acid producing. The second step in the mechanism of removal is, therefore, hydrolysis, followed by reaction of the acid products with the impregnant or by solution of these products in the adsorbed water. Both the charcoal and the metal oxides are effective catalysts for hydrolysis. Frequently, agents of this type react directly with the metal oxides in the absence of water, but this is not an important feature because the

adsorbent in use in the field always contains some moisture, as does the air.

HCN and CNCl are exceptional members of this group. The mechanism of HCN reaction is complicated by the fact that $Cu(CN)_2$, formed by metathetical reaction with the copper, is unstable, decomposing to CuCN and C_2N_2. The resulting cyanogen is less readily destroyed than HCN; nevertheless, chromium in conjunction with copper acts as an effective catalyst for the destruction; probably by hydrolysis. In the case of CNCl it is the original hydrolytic reaction which is the limiting process.

The metal oxides are present in sufficient quantities in the U. S. gas mask adsorbents to afford ample protection against gases of this group by metathetical reaction. Thus a catalyst "poison" designed to destroy the possibility of chemical reaction and render the mask vulnerable to subsequent attack must be employed in sufficiently large dosages to react with most of the impregnant; dosages are comparable to those necessary for penetration of the mask by a lethal agent. Partial destruction of the impregnant produces only a partial loss of protection against the lethal agent, whether it be removed by catalysis or by direct reaction with the impregnant. Thus the tactical use of a nonpersistent catalyst poison prior to attack by a lethal agent, in general, has little advantage except perhaps one of ease of procurement of such poison. A disadvantage in use of a gas as a poison is the resultant complications of logistics and the uncertainty of the result.

However, in cases where the rate of removal of a gas is the limiting factor and the presence of large amounts of adsorbed water reduces the rate to a dangerous level, the use of a persistent agent to enforce prolonged masking during a period of high humidity prior to attack with the nonpersistent agent would be effective.

It is improbable that continued research will produce any new acidic or acid-forming gas which simultaneously is very toxic and readily able to penetrate U. S. gas masks.

7.2.3 Basic or Base-Forming Gases

Little attention has been paid to the nonpersistent basic gases. At one time ammonia was considered by some as a possible harassing agent because of the low dosage required for canister penetration. However, the only basic gases which have been standardized by the armed forces of any country are the nitrogen mustard gases; these amines are persistent agents and, by virtue of their relatively high molecular weights and low volatilities, are strongly adsorbed.

A limited number of experiments have been performed to determine the protection afforded by charcoal adsorbents against NH_3 and a few amines. Though the results of these experiments are inadequate to permit a complete evaluation of the mechanisms of removal, a brief discussion at this point has some value as a guide to future work.

Ammonia (NH_3)

In tests with an influent concentration of 6.8 mg of NH_3 per l, saturation values [36] obtained from the slopes of life vs thickness for five Type A whetlerites ranged from 2.0 to 15 mg of NH_3 per ml of whetlerite under 0-0 conditions; at 80-0 the capacities were increased to 22 to 70 mg per ml. A larger, critical bed depth was found for the equilibrated whetlerites than for the same whetlerites when dry.

Large percentages of the ammonia are desorbable from all types of whetlerites both in the presence and absence of water.[36, 37] In tests with Type AS whetlerite in M10and MIXA1 canisters taken to the break points immediately previous to the desorption, 63 to 75% of the ammonia was desorbed from the dry whetlerite in 22 min and 51% was desorbed from equilibrated whetlerite in 41 min. The effluent desorption concentration had not fallen to zero by the conclusion of the experiment in any of the trials; hence these percentages are minimum values and it is possible that all the adsorbed NH_3 could have been desorbed. Type ASC whetlerite affords considerably greater protection than Types A or AS whether dry or moist, and the desorption from ASC whetlerites proceeds much more slowly; only 33% of the NH_3 is desorbed in 43 min from a previously broken dry Type ASC whetlerite, and the rate of desorption from the moist whetlerite is even slower. Again, these are minimum values, and it is possible that all or nearly all the NH_3 can be desorbed by the prolonged passage of air. Lowering the temperature increases the amount of ammonia adsorbed by canisters filled with Type A or AS whetlerites.

These observations clearly indicate that the major process involved in the retention of NH_3 by dry charcoal or whetlerites of Types A or AS is physical adsorption. On equilibrated adsorbents of these types this process is followed by solution of the ammonia in the adsorbed water. The enhanced protection afforded by ASC whetlerite would seem to indicate

that chemisorption on or reaction with the chromium, probably to form complexes, may play an appreciable role in the mechanism as well as adsorption and solution.

Other Amines

Though a considerable amount of work has been done with ethylenimine [EN], this gas may be dismissed very briefly by a comparison with ammonia.

In the case of a whetlerite which had a 0-0 capacity of 2 mg of NH_3 per ml at an influent concentration of 6.8 mg per l, the capacity for EN at 0-0 and an influent concentration of 3 mg per l was found to be 50 mg per ml. EN, having a higher molecular weight and lower volatility than NH_3, is much more strongly held. Indeed EN is more strongly held by the charcoal than by solution in water and consequently the capacity decreases as the moisture content of the adsorbent is increased.

Like ammonia, EN can be desorbed from whetlerite, but the desorption is slow. The effect of temperature on the performance of a whetlerite against EN is similar to its effect in the case of NH_3. No volatile products are evolved during the adsorption of ethylenimine and there is no regeneration of the adsorbent upon standing. Thus it is reasonable to postulate that physical adsorption is the principal process in the removal of this gas. It is possible that polymerization takes place to a minor extent on the adsorbent, but at best this could only play an insignificant role in the retention.

Other amines whose tube lives have been determined for comparison are trimethylenimine, piperidine, N-methyl ethylenimine, methyl ethylenimine, pyridine, diethyl amine, and allyl amine. The protection against all these amines is greater than that against ethylenimine.

General Conclusions for Basic or Base-Forming Gases

Because of the nature of the impregnation now employed on gas mask adsorbents, basic gases are retained primarily by physical adsorption. However, of all of the basic gases studied to date, only ammonia is inadequately removed from the gas stream. The limitations of molecular weight and volatility for gases of this type to penetrate the gas mask are quite stringent. Even if these limitations were to be circumvented, the resultant gas would probably have to be hydrolyzable in order to be toxic. In such an event the agent would most likely behave more nearly like the acidic gases than like the basic gases even though the intact molecule were basic. Thus it seems unlikely that a gas of this class will be found which at the same time will be very effective against protected troops.

Nevertheless, ammonia is deserving of some consideration. Aside from its potentialities as a harassing agent, it is conceivable that it might be used to good advantage preceding attack with an odorless lethal gas. Poorly disciplined troops might be expected to remove their masks during subsequent attack rather than endure the irritation of the desorbing ammonia. It must be remembered, however, that the presence of NH_3 on the adsorbent increases, rather than decreases, the protection against acid gases.

7.2.4 Readily Oxidizable Gases

Oxidation has been postulated as a possible reaction in the mechanisms of removal of phosgene [reaction (2)], nitric oxide [reaction (12)], and cyanogen chloride [reaction (30)]. The oxidation of phosgene plays an insignificant part in the presence of water. It seems also probable that oxidation of cyanogen chloride is of secondary importance in comparison with hydrolysis under usual conditions. The primary process in the mechanism of chemical removal of nitric oxide, no doubt, is oxidation to NO_2. The lack of adequate protection against NO is probably due, first, to the weakness of the physical adsorption which must precede oxidation, and second, to the regeneration of NO by reactions (8) and (10). At any rate the nature of the reaction products from CG, CK, and NO and the nature of the reactions other than oxidation which these gases undergo, leads to their classification as acid-forming gases.

Arsine is the best known of the gases which are removed solely by oxidation. Since World War I it has been one of the standard test gases used by the Chemical Warfare Service to evaluate gas mask adsorbents. In addition to the innumerable specification tests which have been run, a considerable amount of research has been devoted to the study of the mechanism of its removal. It is possible that other arsenicals undergo similar oxidation on whetlerites. The arsenicals that have been considered as possible war gases, however, have high molecular weights and low volatilities and are consequently strongly adsorbed. Furthermore, they are generally readily hydrolyzed, yielding nonvolatile products. Thus, such gases do

not constitute a hazard to the respiratory tracts of masked men regardless of the nature of the gas mask adsorbent, and hence they have not been studied and are not considered in this discussion.

Carbon monoxide should also be considered a member of this class. A slow oxidation of CO to CO_2 is known to occur on whetlerites.[16] Nevertheless, because of the weakness of adsorption of CO on charcoal and of the slowness of the oxidation, the protection afforded by the gas mask is entirely inadequate. It has been necessary to design special canisters and adsorbents to care for this gas; the research along these lines is discussed in Chapter 12.

Arsine (AsH_3; SA)

When whetlerites are exposed to SA–air mixtures, large rises in temperature are observed.[40] If the whetlerite is exposed to SA in the absence of oxygen, no great thermal effect is observed until air is admitted.[41]

The arsine tube life of Type A whetlerite,[39] both dry and moist, decreases with decrease in temperature until a minimum is reached at about −10 C after which the life increases markedly. Base charcoal exhibits a continued increase in life with decrease in temperature until the life becomes identical with that of the whetlerite at and below −30 C. An important difference between the two, however, is that even at −45 C the passage of pure air through the bed soon after the break point and at the same temperature failed to remove any appreciable amount of arsine from the whetlerite while considerable quantities could be desorbed from the base charcoal.

These observations clearly indicate the occurrence of a rapid oxidation reaction on the whetlerite. At temperatures below −30 C the physical adsorption, which must precede the chemical reaction, becomes the characterizing step because the removal of adsorbed SA by reaction is too slow to appreciably alter rate or effective capacity of adsorption; the whetlerite therefore behaves like the parent base charcoal.

Calorimetric studies of the removal of arsine indicate that the energy production is not the result of a single unique reaction.[42] One of the simplest ways to interpret the observed facts is to postulate that two or more reactions are occurring and that the relative amounts depend on the experimental conditions. Such postulation had been offered previously in explanation of the fact that C_0t to the break point increases with increasing C_0. There are a number of possible reactions which might occur in this system. The three most probable ones are:

$$2AsH_3 + 4O_2 = As_2O_5 + 3H_2O; \quad (36)$$

$$2AsH_3 + 3O_2 = As_2O_3 + 3H_2O; \quad (37)$$

$$4AsH_3 + 3O_2 = 4As + 6H_2O. \quad (38)$$

H_2O, As_2O_3 [41, 42] and As_2O_5 [42] have been identified as the major products of reaction of arsine on charcoals and whetlerites. Though As has not been specifically identified it is possible that reaction (38) plays a minor role in the removal.

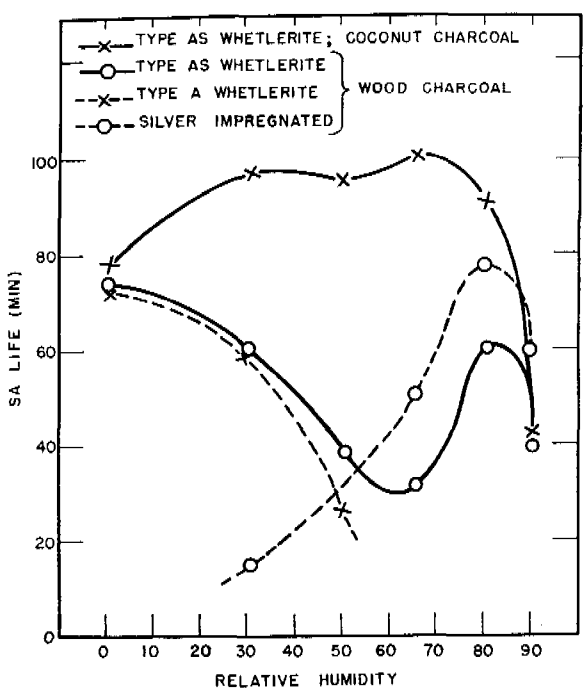


Figure 6. Effect of humidity on SA lines of silver-impregnated charcoal and whetlerites of Type A and AS.

For Type A whetlerites prepared from most types of base charcoals, the SA tube lives [39] increase at first with increasing humidity of gas mixture and charcoal, pass through a maximum between 30 and 50% RH and then decrease rapidly. These observations are consistent with the postulates that physical adsorption is the first step and that water catalyzes the oxidation; at high humidities the adsorbed water causes a reduction in the rate of adsorption to the point that this becomes the limiting process. Type A whetlerites made from some charcoals show a consistent decrease in life with increase in humidity at all humidities; in such cases the rate of adsorption is

probably the limiting factor throughout the whole range of humidities because of the structure of the charcoal.

Silver-impregnated charcoals are quite ineffective against SA at low humidities, but display high maximum lives in the vicinity of 80% RH. Metallic silver, in conjunction with water, is an excellent catalyst for one or more of the oxidation reactions.

Type AS whetlerites exhibit the additive properties of the two separate impregnants (see Figure 6). Type ASC whetlerite behaves like Type AS.

Because the whetlerite in the influent end of a bed does not become saturated [38] during a tube test the life vs thickness plots are definitely curved. Indeed it is difficult to define a saturation value for SA. After a period of relatively rapid removal of SA, whetlerite continues to absorb the gas very slowly over long periods of time. This phenomenon seems to be due to two factors;[41] (1) some of the product oxides are apparently chemisorbed on the catalyst, thus reducing its effectiveness, and (2) the initial rapid reaction takes place near the entrance of each pore and the products partially block the channels, making diffusion into the active inner surfaces and catalyst very slow. At any rate, the amounts of SA absorbed per milliliter of whetlerite are so excessive over the amount required for reaction with the CuO present in Type A whetlerite that it is obvious that the impregnant acts primarily as a catalyst and does not participate solely in a metathetical reaction. This conclusion is in accord with the observation that oxygen is necessary for the reaction to proceed.

General Conclusions for Readily Oxidizable Gases

Because of the insurmountable difficulties involved in the storage and dispersion of arsine, due mainly to its instability, it is not considered as a likely war gas. Therefore, observations made in the preceding section merely serve to indicate the possibility of attaining adequate protection against readily oxidizable gases by suitable impregnation of charcoal, provided that the gas is so strongly adsorbed physically by the charcoal that this necessary initial step does not become the limiting process in the removal.

It seems unlikely that any other nonpersistent gas, which could be removed by such oxidation processes, would be sufficiently stable to undergo dispersion from explosive munitions without chemical change. Such circumstance would present a serious limitation to its use.

7.2.5 Readily Reducible Gases

The only reducible gases which have been studied to date are NO_2 and Cl_2. NO_2 was considered in detail in a previous discussion because it behaves as an acid-forming gas. Chlorine was not used or considered as a war gas in World War II and therefore its behavior was not studied in any of the laboratories dealing with absorbents.

Chapter 8

THE ADSORPTION WAVE

By *Irving M. Klotz*

8.1 INTRODUCTION

THE GENERAL OBJECT in the study of the adsorption wave has been to obtain an understanding of the various factors which determine the variation in concentration of a toxic gas effluent from a bed of charcoal. The study of the adsorption wave includes the consideration, from an experimental and theoretical point of view, of the distribution of toxic gas throughout a bed both on the adsorbent and in the air above the adsorbent.

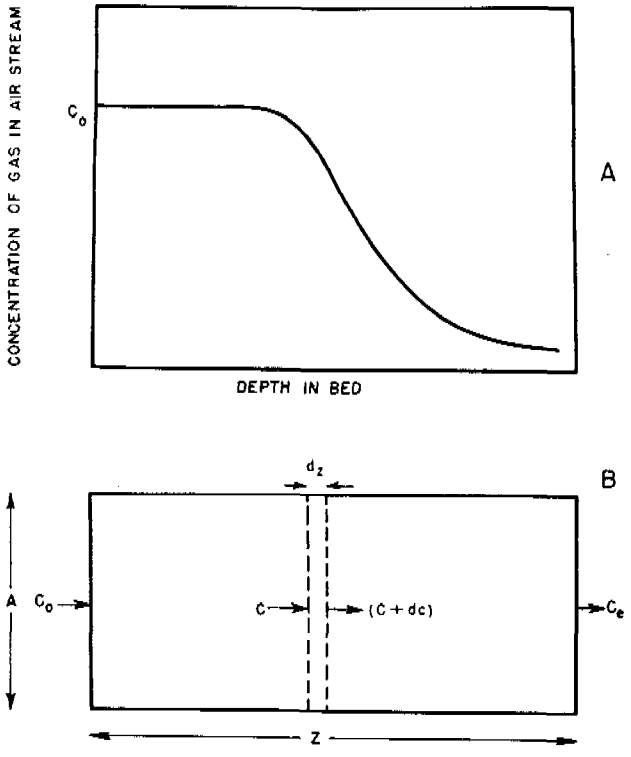


FIGURE 1. A. Distribution curve for the concentration of air above various points in the bed of adsorbent. B. Flow of gas through an adsorbent.

A typical distribution curve showing the concentration of gas in the air above various points in the bed of adsorbent is shown in Figure 1A. The curve for the concentrations which would be in equilibrium with the adsorbed gas at various points in the bed would be similar in shape but displaced slightly to the left. The term *adsorption wave* is generally applied to the movement of these distribution curves (to the right in Figure 1A) during the continuous passage of gas-laden air through the bed of adsorbents.

A complete mathematical description of the wave would effect a number of important consequences. It would be possible to predict the performance of a particular canister from a minimum of experimental data and without exhaustive tests on the canister itself. It would also be possible to devise the best test procedures from which to obtain the information necessary for the prediction and evaluation of canister behavior. A complete understanding of the adsorption wave would lead also to the design of the most efficient type of canister. Equally important would be the elucidation of the mechanism of the adsorption process for various gases on different types of charcoal. Such an understanding would suggest additional treatments for the improvement of the adsorbent and would also indicate when the natural limit to such improvement had been attained.

The problem of the adsorption wave has not been solved in its most general form, primarily because of the prodigious mathematical difficulties entailed. In connection with a similar problem of correlating the performance of small-scale and large-scale reactors in chemical engineering processes, the opinion has been expressed [6] that the correlation is impossible to attain in a truly rigorous manner. Nevertheless, a number of simplified special cases of the adsorption wave have been considered and, with these results as guides, it has been possible to develop several semi-empirical approaches to the problems of performance and mechanism of reaction.

It is recognized generally that the removal of a toxic gas from air by a porous adsorbent may involve one or more of the following steps:

1. Diffusion (mass transfer) of the gas from the air to the gross surface of the granule.
2. Diffusion of the molecules of gas into (or along the surface of) the large pores of the adsorbing particle.
3. Adsorption of the molecules on the interior surface of the granule.
4. Chemical reaction between the adsorbed gas and the charcoal or adsorbed oxygen, water, or impregnant.

The relative importance of each of these four steps may vary widely with the particular conditions under which the removal is taking place. The rate of mass transfer is influenced strongly by the flow rate of the gas stream, by the diffusion coefficient of the gas, and by the particle size of the adsorbent, but is relatively unaffected by temperature. The importance of diffusion in the pores is determined by such factors as the particle size, the structural characteristics of the pores, certain diffusional properties of the system, and the rate of reaction at the internal surface. The speed of adsorption at the interface depends on the nature and extent of the surface as well as on the activation energy for the adsorption of the particular gas under consideration. Chemical reaction is also determined by the properties of the surface, but much more specific effects will be obtained than in adsorption. Since large activation energies may be expected in steps (3) and (4), these processes will be highly sensitive to temperature.

Usually, all four steps in the removal process may proceed with rates of approximately the same magnitude, and hence a problem of extreme mathematical difficulty is presented. On the other hand, in many situations one particular step may be much slower than the others, and hence it may be considered the rate-controlling process. For a single rate-controlling process, a number of mathematical approaches have been developed. A few attempts have also been made to treat situations with more than one rate-controlling step, and for certain special circumstances, partial success has been attained.

8.2 THEORIES PREDICTING EFFLUENT CONCENTRATION AS A FUNCTION OF TIME

The ultimate aim of the mathematical analysis is an expression for the dependence of the effluent concentration on time. Even without such an expression, however, some qualitative description of the shape of an effluent-time curve can be given. Figure 2 illustrates a number of interesting cases. If the reaction on the charcoal were instantaneous and if the adsorbent were infinitely fine-grained, none of the adsorbable gas would penetrate until some time t, when the charcoal would be saturated, and then the gas would penetrate at full influent concentration.

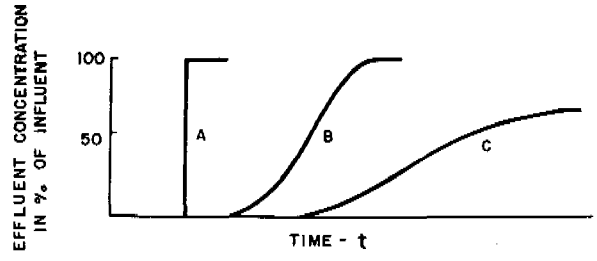


FIGURE 2. Transmission of a gas by an adsorbent.

Such an adsorbent would exhibit a transmission curve such as A in Figure 2. On the other hand, if the reaction is not instantaneous, a curve such as B would be exhibited. This curve would be symmetrical only for certain simple rates of adsorption. In addition to these two examples, cases may be encountered (for example, in the removal of carbon monoxide) where the charcoal, or its impregnant, acts as catalyst for a reaction involving the toxic gas. As a result, the effluent-concentration curve C may rise very slowly; and if the catalyst remains at least partially unpoisoned, the transmission of gas may never reach the full influent value. It is also conceivable, although no such case has been yet encountered, that the rate of catalysis may be very high compared to the rate of supply of gas. In such circumstances the transmission curve would be the time axis, that is, none of the gas would penetrate.

8.2.1 Theories in Which One Step is Rate-Controlling

THE GENERAL DIFFERENTIAL EQUATION

Consider a stream of gas and air flowing through a bed of adsorbent as indicated in Figure 1B. Each layer of the adsorbent removes a portion of the gas from the air, and hence the concentration of gas drops from an influent value of c_0 to an effluent value of c_e. A cross section of infinitesimal thickness dz will reduce the concentration from c to $c + dc$

(dc is negative). From the principle of conservation of mass it follows that:

Quantity of gas entering = quantity of gas picked up by charcoal + quantity of gas leaving. (1)

The quantity of gas entering the infinitesimal section of bed will be equal to the concentration c times the volume rate of flow L times the interval of flow dt:

$$\text{Quantity of gas entering} = cLdt. \tag{2}$$

The amount of gas picked up by the charcoal will be given by the rate of pickup per unit volume $\partial n/\partial t$ times the volume of the infinitesimal section of the bed (area $A \times$ depth), multiplied by the interval of exposure:

$$\text{Quantity picked up by the charcoal} = \frac{\partial n}{\partial t}(A dz)dt. \tag{3}$$

The quantity of gas leaving the section dz will be given by:

$$\text{Quantity leaving} = (c + dc)Ldt. \tag{4}$$

Setting up the equality demanded by the conservation principle, one obtains:

$$cLdt = \frac{\partial n}{\partial t}(A dz)dt + (c + dc)Ldt, \tag{5}$$

which can be rearranged to give:

$$-dc = \frac{A}{L}\frac{\partial n}{\partial t}dz. \tag{6}$$

Since c is a function of the variables z and t, the total differential is:

$$dc = \left(\frac{\partial c}{\partial z}\right)_t dz + \left(\frac{\partial c}{\partial t}\right)_z dt, \tag{7}$$

and since

$$\partial z/\partial t = V \tag{8}$$

and

$$L = VA\alpha \tag{9}$$

where V is the linear velocity through the interstices between the particles of the adsorbent, and α is the porosity (that is, the fraction of voids per unit gross volume of bed) one obtains:

$$-\left(\frac{\partial c}{\partial z}dz + \frac{\partial c}{\partial t}dt\right) = \frac{1}{\alpha V}\frac{\partial n}{\partial t}dz \tag{10}$$

which can be rearranged to give

$$-\frac{1}{\alpha}\frac{\partial n}{\partial t} = \frac{\partial c}{\partial t} + V\frac{\partial c}{\partial z}. \tag{11}$$

It is implicitly assumed in the derivation of this equation that the concentration of gas is small and that diffusion in the direction of flow is negligible.

The solution to equation (11) depends on the mathematical relation one assumes for $\partial n/\partial t$, the local rate of removal of the toxic gas by the granules. The particular mathematical form to be chosen depends on the mechanism of the removal process. No matter which mechanism is visualized, the local rate of removal would be dependent in general on the following variables:

1. The nature of the adsorbent.
2. The nature of the gas to be removed.
3. The geometrical state of the adsorbent.
4. The temperature.
5. The local concentration of the toxic gas, as well as of other gases in the air.
6. The relative amount of the toxic and other gases already adsorbed by the granules.
7. The velocity of the gas-air stream.

In all cases which have been considered, it has been assumed that the first four variables are maintained constant, but that $\partial n/\partial t$ may depend on one or more of the remaining three.

Diffusion as the Rate-Controlling Step

Case A. In some cases, one may encounter a gas which has no back pressure on charcoal, but which ceases to be removed by the granules when the moles of gas on the granules n approaches N_0, the saturation capacity of a unit gross volume of adsorbent for the toxic gas. Under these conditions the local rate of removal would be given by the relation:

$$\frac{1}{\alpha}\frac{\partial n}{\partial t} = \frac{Fac}{\alpha\rho}, \tag{12}$$

where F is the mass transfer coefficient, a the superficial surface per unit volume of granules, and ρ the density of the air-gas mixture.

The solution of the differential equation may be resolved into two cases. For all times up to t_0 when $n = N_0$ at the entrance face, the concentration at a given point in the bed is given by the equation:

$$\frac{c}{c_0} = \exp\left[-\frac{Fa}{\alpha\rho}\frac{z}{V}\right]. \tag{13}$$

For times greater than t_0, the following relation holds:

$$\frac{c}{c_0} = \exp\left[-\frac{Fa}{\alpha\rho}\left(\frac{z}{V} - \frac{c_0 t}{N_0}\right) - 1\right]. \tag{14}$$

Case B. If a gas is adsorbed reversibly on charcoal, the equation obtained for c/c_0 depends on the character of the adsorption isotherm. One of the simplest

SECRET

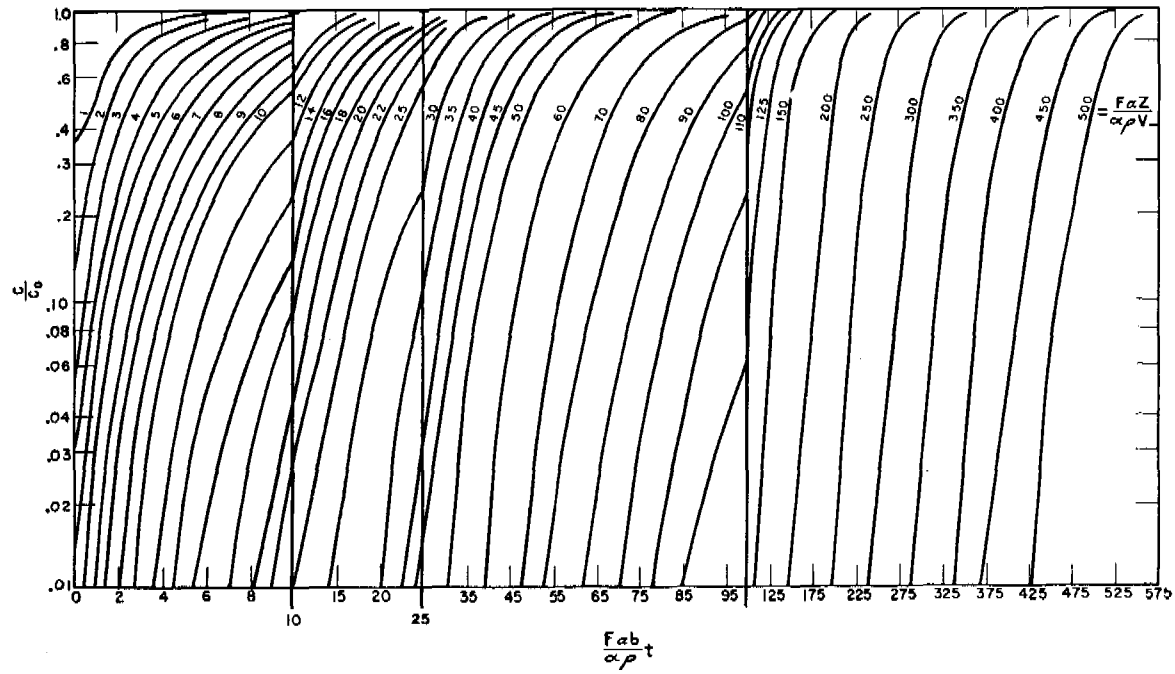


FIGURE 3. Relation of gas unremoved to time and position.

cases that has been considered is that of the linear isotherm, for which

$$c^* = bn \tag{15}$$

where c^* is the concentration of the gas in air stream at a given point in the bed in equilibrium with the charcoal at that point, and b is a constant. With a linear isotherm governing the back pressure of the gas, the equation for the local rate of removal becomes:

$$\frac{1}{\alpha}\frac{\partial n}{\partial t} = \frac{Fa}{\alpha\rho}(c - c^*)\,. \tag{16}$$

The solutions of the differential equations, for the boundary conditions encountered in charcoal, are well known because completely analogous equations have been encountered in the problem of heat exchange in granular beds. Analytical expressions, in terms of Bessel functions, for the solutions are cumbersome to handle, and hence the results are given best in the form of reference curves of c/c_0 as a function of the important variables. The curves worked out by Furnas [14] are very incomplete in regions of low concentrations, the regions of great interest in work on gas transmission. Consequently a semi-logarithmic plot taken from a report by Hougen and Dodge [17] is given in Figure 3. For values of c/c_0 below 0.01 see reference 10.

Case C. Most gases do not exhibit a linear isotherm on charcoal. A better approximation is the Langmuir isotherm which may be expanded in a power series of the form

$$c^* = \frac{K}{N_0}n + \frac{K}{N_0^2}n^2 + \cdots \tag{17}$$

where K is a constant. Using the first two terms in equation (17) as a parabolic approximation to the isotherm, one may substitute for c^* in equation (16). The solutions of the resultant equations in terms of standard graphical procedures have been worked out.[10]

Adsorption or Reaction on the Surface as the Rate-Controlling Step

Case A. The earliest analysis of the adsorption wave was made by Bohart and Adams [4] on the assumption that the toxic gas is adsorbed irreversibly and at a local rate of removal governed by the equation:

$$\frac{1}{\alpha}\frac{\partial n}{\partial t} = k_1 c(N_0 - n), \tag{18}$$

where k_1 is a constant.

A similar treatment has been carried out more recently.[7] Both groups of investigators have derived the following expression for the variation of the concentration of gas in the air stream:

$$\frac{c_0}{c} = 1 + [\exp(-k_1 c_0 t)]\left[\exp\left(\frac{k_1 N_0 z}{V}\right) - 1\right]. \tag{19}$$

This equation in its various forms has been used very widely to interpret and to interpolate data on the performance of various charcoals. Unfortunately, present indications are that there are few cases where the rate of removal of a gas by charcoal is governed primarily by adsorption or reaction at the surface. Diffusion, or mass transfer, seems to make some contribution to the slowness of removal of almost all gases by charcoal, and hence equation (19) is not strictly applicable.

Case B. An attempt has been made by Lister [25] to consider the relations obtained when adsorption on the surface is the rate-controlling step but for the special case where the adsorption is reversible and the adsorbed gas exerts a back pressure. For such conditions, the equation for the local rate of adsorption becomes

$$\frac{1}{\alpha}\frac{\partial n}{\partial t} = k_1 c(N_0 - n) - k_2 n, \qquad (20)$$

where k_1 and k_2 are constants.

No complete solution of the resultant differential equations has been given. Approximations have been given for the conditions obtained with fresh charcoal, but the general validity of these has been questioned.[10]

8.2.2 Theories in Which More Than One Step Contributes to Rate of Removal

Diffusion in Air and Deposition on Surface Contributing

It has been possible to construct [10] a differential equation for the local rate of removal on the assumption that the diffusion of the toxic molecule from the air to the charcoal and the subsequent deposition process, whether chemical or adsorptive in nature, both contribute to the slowness of removal. The general equation for this process has not been solved. Nevertheless, certain special cases have been considered, but each of them reduces to one of the single-step processes discussed in the preceding text and hence does not warrant further elaboration.

Diffusion in Air and Processes Within the Granule Contributing

A very detailed consideration of the nature of the processes involved in the removal of gases by adsorbents has been made.[37] Emphasis has been given particularly to diffusion within the pores and to the various factors which influence the cross-sectional and longitudinal mixing in the intergranular spaces. Where the equilibrium adsorption of a gas follows a linear isotherm, the differential equations have been solved and have been shown to be applicable to the experimental data on the removal of CO_2 at 100 C. For gases with curved isotherms, however, the general solution to the differential equation has not been obtained though certain special cases have been considered.

8.2.3 Comparison of Theories with Experiment

None of the theoretical approaches gives a satisfactory correlation of the experimental data on the removal of a toxic gas by charcoal. Even with gases such as chloropicrin, where (as is shown later) mass transfer seems to be the rate-controlling step, the observed dependence of effluent concentration on time does not agree over any appreciable range with the curves given in Figure 3. The primary cause of the deviation, for other gases as well as for chloropicrin, is the curvature of the adsorption isotherm, a condition which so far has not been incorporated into the wave equations, except in an approximate, empirical manner.[29] In addition to the curvature of the isotherm, a further difficulty that arises with most other toxic gases of interest is the combination of mass transfer with one or more of the succeeding steps in controlling the rate of removal of the gas by the adsorbent. Minor discrepancies may also arise from thermal factors. Temperature changes in the removal process, which in some cases are many degrees, may raise the back pressure of the adsorbed gas or may affect the rate of mass transfer in the carrier stream.

Sufficiently fundamental differences exist in the differential equations for the local rate of removal in the mass-transfer and surface adsorption mechanism so that one can determine the presence or absence of a slow, diffusion step. In equation (18), based on surface adsorption as the rate-controlling step, the velocity V does not appear, and hence, in the integrated equation for c/c_0, V will enter only as z/V as can be verified by glancing at equation (19). Similarly, on expanding and rearranging (19) to obtain an equation for the instantaneous break time, t_b, an expression is obtained in which V enters only as z/V. In contrast, when mass-transfer (diffusion) is the controlling step, the velocity of flow enters the equation for the local rate of removal, inasmuch as F, the mass-transfer coefficient, depends on the rate of flow. In consequence, the instantaneous break

time depends on V as well as on z/V, and a plot of t_b vs z/V gives different curves for different rates of flow. (It should be emphasized that the cumulative break time, that is, the time in which a total quantity of gas sufficient to produce a change in some indicator has escaped from the bed, depends on V and z/V whether or not V enters the expression for the local rate of removal. Therefore, the cumulative break time cannot be used to distinguish between mechanisms of removal.) Thus, a criterion has been established for detecting the presence of a slow diffusional step. In Figure 4, this criterion is applied

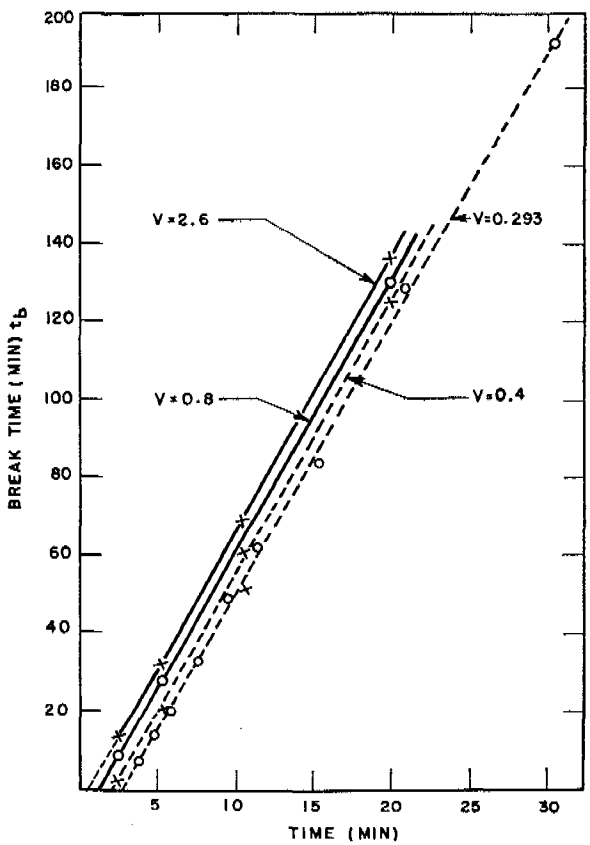


FIGURE 4. Effect of rate of flow on rate of removal of chloropicrin. Time (of contact) = $z/V \times 10^3$ min.

to some data on chloropicrin.[38] It is obvious from the graph that t_b depends on V as well as on z/V, and in consequence, that diffusion contributes to the slowness of removal of chloropicrin by charcoal. Consequently, it is unlikely that the theories based on surface adsorption or surface reaction as the rate-controlling process will be applicable to any charcoal which has sufficient activity to make it useful in protection against toxic gases.

Unfortunately, these relationships were not realized in much of the early work and many extrapolations were made on the basis of the Bohart-Adams-Hinshelwood equation,[4,7] which is based on a surface-deposition, rate-controlling mechanism. The particularly misleading fact is the observation that in many circumstances a plot of log $(c_0/c - 1)$ is linear with time, a necessary condition derivable from equation (19). Unfortunately, such linearity is not a reliable test of the applicability of equation (19), for all the other mechanisms will also lead to such linear equations over wide ranges if suitable values are chosen for the constants. When constants for equation (19) are determined from plots of log $(c_0/c - 1)$ vs time, one finds that both k_1 and N_0 vary with the rate of flow of the air stream. Such behavior is completely at variance with the postulates of the mechanism and illustrates the inapplicability of the equation to the removal of gases by the usual charcoal adsorbents.

8.3 SEMI-EMPIRICAL TREATMENTS

In the absence of a satisfactory comprehensive theory of the adsorption wave, investigators have been forced to develop semi-empirical methods of treating data. Primary emphasis has been given to equations which relate break time to the common variables such as bed depth, rate of flow, particle size, and concentration of influent gas. With the accumulation of results from different modes of approach, it has also been possible to correlate certain relations with particular mechanisms of removal.

8.3.1 Factors Affecting Break Time

NATURE OF FLOW IN CHARCOAL

The flow of fluids through beds of granular solids is very complicated in nature because the channels are very tortuous and nonuniform. It is impossible to fix the dimensions or number of channels, as two streams may frequently merge or a single stream may redistribute itself into several new paths of flow. Since sudden contractions or enlargements in the intergranular spaces may occur, it is quite possible to have both streamlined and turbulent flow occurring simultaneously in different portions of a granular bed. In consequence, there is a much slower transition from conditions of laminar flow to those of turbulent flow in the passage of gas through an adsorbent bed than there is in the flow of fluid through pipes.

Usually the nature of the flow of fluids is studied by measuring the pressure drop in the bed or pipe. Correlations are then made with the dimensionless parameter known as the Reynolds number, $D_p V\rho/\mu$. When a graph of a function of the pressure drop known as the friction factor[15, 16] is plotted against the Reynolds number, two linear portions are observed which intersect at the *critical* Reynolds number, a value corresponding to conditions under which laminar flow is transformed into turbulent flow.

In studies made of the flow of fluids through porous carbon,[16] a critical Reynolds number of about 4 has been found. Extensive work has also been carried out on the flow of gases through beds of charcoal.[24] Two representative curves are shown in Figure 5.

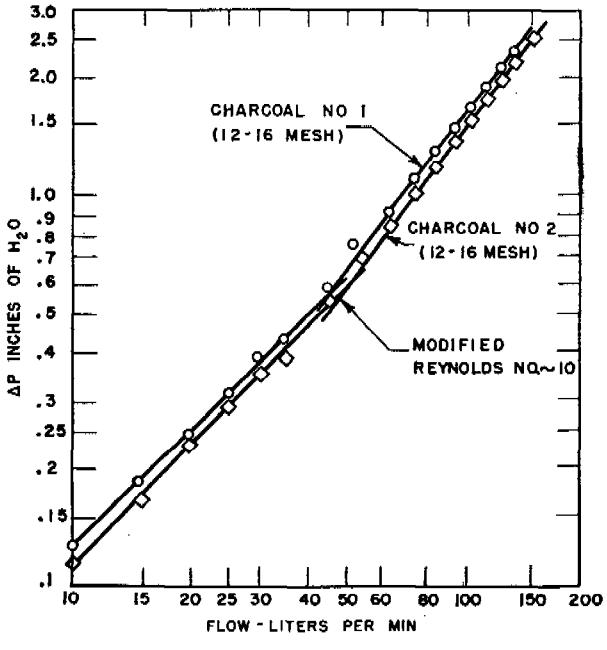


FIGURE 5. Relation of flow rate to pressure drop in charcoal beds.

From these curves and other data, it has been concluded that the critical Reynolds number is about 10 in the charcoals investigated. The Service laboratories[33] and two English workers[20] have found a transition in the same region. But it cannot be certain that the same critical value will be observed with all charcoals of any possible shape since it is quite conceivable that curious shape factors may occasionally be encountered in view of the rather arbitrary use of particle diameter D_p in place of pore size in the Reynolds number. In all the work described here, however, it has been assumed that the critical region is in the neighborhood of a Reynolds number of 10.

The Effect of Bed Depth

The dependence of canister or tube life on the depth of charcoal has been investigated more widely than has the dependence on any other variable. The reason for such emphasis is perhaps obvious, for the amount of adsorbent necessary determines very largely the bulk of the canister. Life-thickness curves have become, therefore, the most common method of representing the performance of a charcoal. In consequence, the interpretation of performance in terms of the mechanisms of removal has revolved around the elucidation of life-thickness curves.

General Character of Life-Thickness Curves. A survey of performance data shows that two types of life-thickness curves are encountered. The simplest case is a linear relation such as is shown in curve A of Figure 6. Most organic gases when tested in a dry

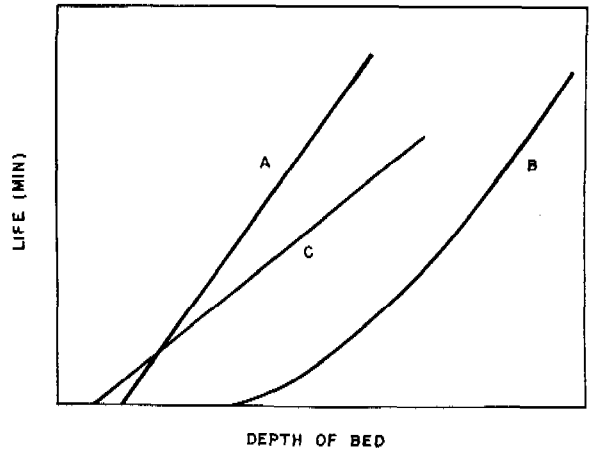


FIGURE 6. Life-thickness curves.

condition against dry charcoal exhibit linear life-thickness curves. In principle, a break-time test using a cumulative indicator should not show a linear relation with bed depth, at least not at small depths, but this lack of linearity is frequently overlooked because few tests are carried out at very small depths. Curve B exhibits a very common observation of curvature at low lives with a tendency to linearity at high break times. Such behavior should always be encountered in cumulative tests of the break time. It is also usually observed when tests are carried out with humidified gases and charcoal, and in some cases occurs in tests under dry conditions.

Whether or not curvature occurs, the life-thickness curve intersects the bed-depth axis at a finite value. It follows then that there exists a critical bed depth below which the life is zero. This critical length varies with the conditions of flow, concentration, mesh size, sensitivity of the detector, and the nature of the charcoal. It is this manifold dependence which has engaged much attention. Numerous attempts have been made to correlate these variables in some convenient analytic expression, for in small beds as in canisters, it is the critical bed depth which primarily determines the degree of protection.

The Mecklenburg Equation. A very convenient expression for the linear life-thickness curve has been derived by Mecklenburg[28] from elementary considerations of conservation of mass. At the break time a negligible portion of the toxic gas has penetrated the bed, and hence one can assume that:

Weight of gas supplied = Weight of gas picked up by adsorbent. (21)

The weight of gas supplied by the air stream is equal to the time of flow (the break time in minutes) times the rate of flow L (in liters per minute) times the concentration (in grams per liter). In turn, the pickup by the charcoal may be *arbitrarily* considered as occurring in a certain portion of the bed instantaneously and up to the saturation value, while the remainder of the bed, defined by Mecklenburg as the *dead layer*, remains completely free of gas. As was emphasized by Mecklenburg, the dead layer is a purely fictional concept devised merely to facilitate the derivation of the following equation and to obviate the necessity of considering in detail the distribution of gas in the bed of adsorbent. With this arbitrary division it follows that the amount picked up by the charcoal is equal to the saturation value per unit volume times the area, times the difference between the bed depth and the depth of the dead layer h. In algebraic terms the equality in (21) may be expressed as follows:

$$t_b L c_0 = N_0 A (z - h). \tag{22}$$

This equation may be rearranged readily to give an expression for the break time,

$$t_b = \frac{N_0 A}{L c_0} (z - h). \tag{23}$$

As has been pointed out previously (Chapter 2), the slope of the life-thickness curve for a fixed rate of flow, input concentration, and bed cross-section is a measure of the capacity (N_0) of the charcoal. For a system which obeys this equation throughout the complete life-thickness curve, the dead layer h and critical bed depth I must be equal, so that

$$t_b = \frac{N_0 A}{L c_0} (z - I). \tag{24}$$

The great deficiency of equation (24) is that it cannot be used to extrapolate information from one set of flow or concentration conditions without further information on the dependence of the critical bed depth on these variables. The wave theories discussed in preceding paragraphs set certain requirements for the variation of critical bed depth, and where these theories are applicable they may be used to extend equation (24). Further details are considered in a subsequent section.

Curvature Due to Cumulative Method of Test. If the break time is defined in terms of the period necessary for a total cumulative amount of gas to penetrate the bed, it can be shown that the life-thickness curve, even in the simplest mechanism of removal, would obey an expression of the form

$$t_c = \frac{N_0 A}{L c_0} k_3 V^{k_4} \ln \left[\frac{k_5 \exp (z/k_3 V^{k_4})}{N_0 A k_3 V^{k_4}} + 1 \right]. \tag{25}$$

In general, equation (25) would not be linear; however, for large bed depths, the first term inside the brackets becomes large in comparison to the second term and the equation as a whole approaches the linear relation:

$$t_c = \frac{N_0 A z}{L c_0} + k_6. \tag{26}$$

These predictions are in agreement with the behavior observed in cumulative tests.

Curvature in Systems Using Instantaneous Tests. In the testing of Type ASC charcoals with cyanogen chloride, it has always been observed that the life-thickness curves for humidified gas streams and humidified charcoal show pronounced curvature at small bed depths but approach linearity with deep beds. Curve B of Figure 6 is a typical example. The increasing slope of this curve with increase in bed depth implies an increasing capacity, per unit volume, of adsorbent for the toxic gas. This expectation has been verified by an examination of the distribution of gas adsorbed on the bed at various time intervals. For a substance such as chloropicrin, which exhibits a linear life-thickness curve on dry charcoal, the amount of gas taken up by a unit volume of charcoal reaches a maximum which is not surpassed by increasing the time of exposure of the

bed to the toxic gas. As a result, the distribution curves behave as shown in Figure 7A. In contrast, a humidified ASC charcoal shows a continuously increasing capacity, per unit volume, for cyanogen chloride and in consequence exhibits a set of distribution curves such as is shown in Figure 7B (Wiig). The capacity of the influent end of the bed approaches, but never quite reaches, a true saturation value, probably because a second slow reaction follows an initial rapid one. Consequently, the distribution curve is displaced upward as well as to the right toward the inside of the bed.

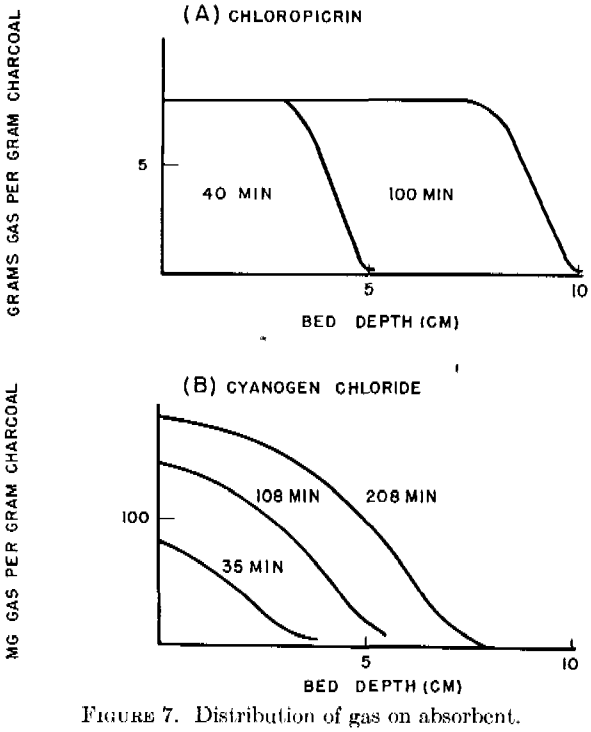


FIGURE 7. Distribution of gas on absorbent.

In a number of cases, tests carried out with dry gases on dry base charcoal have also shown curvature in their life-thickness curves. A typical example would be methyl alcohol or ethyl chloride. The curvature in all such cases, however, is less than that observed with cyanogen chloride. Although no distribution curves were obtained for these dry examples, it seems likely that in these cases also some slow secondary reaction occurs in addition to the initial rapid one. For methyl alcohol it is possible that an oxidation process is being catalyzed by the charcoal. With other inert gases, and perhaps also with methyl alcohol, it seems likely that the slow reaction is a diffusion process within the pores of the granule.

THE EFFECTS OF VELOCITY OF FLOW, CONCENTRATION, AND PARTICLE SIZE

It can be shown [23] from considerations similar to those discussed by Hurt [19] for the design of catalytic reactors, that if more than one step contributes to the rate of removal of a gas from the carrier stream, the critical bed depth I will be the sum of two terms I_t and I_r. I_t represents the portion of the critical bed depth due to the slowness of diffusion of gas from the air stream to the surface of the charcoal, whereas I_r represents the fraction due to processes occurring within a charcoal granule. Since the critical bed depth can be thought of as the distance which the gas may penetrate the bed before its concentration is reduced to the break value, it seems reasonable to expect a certain minimum value of I for a fixed set of conditions, which would represent the smallest penetrable depth possible, even if every process in the granule were instantaneous and the rate were determined entirely by the speed with which the gas diffuses to the particle. This limiting value of I for a fixed set of conditions would be I_t. Any critical bed depth above I_t must be the contribution of the processes within the granule. That this contribution should be an additive term, rather than a multiplicative factor, has been shown in principle by Hurt.[19]

The critical bed depth due to diffusion, I_t, can be expressed [23] in terms of a number of familiar parameters, independent of the nature of the charcoal, but dependent on the properties of the air-gas mixture and on the granular characteristics of the bed. Considerations of dimensional analysis lead to the conclusion that at a fixed ratio of influent to effluent concentration, I_t should be a function of the particle size of the granules, and of two dimensionless parameters D_pG/μ and $\mu/\rho D_v$, the Reynolds number and Schmidt number, respectively. The specific function which has been adopted is essentially that of Gamson, Thodos, and Hougen:

$$I_t = \frac{2.303}{a}\left(\frac{D_pG}{\mu}\right)^{0.41}\left(\frac{\mu}{\rho D_v}\right)^{0.67}\log\frac{c_0}{c_b}. \qquad (27)$$

In the derivation of this equation, it is assumed that c_0/c_b is very large. Strictly speaking, this equation should be applicable only in cases of turbulent flow, but it has been found that in the region of laminar flow in charcoal, I_t is approximated satisfactorily by equation (27). For a fixed ratio of influent to effluent concentration, the equation expresses the variation of the critical bed depth with particle size D_p, rate of

flow G, and diffusion coefficient of the gas D_v. The factor a, the superficial surface of the granule (ignoring pore structure), depends on the particle size and on the percentage of voids in the bed. Values of a have been calculated and are tabulated.[15] Where the absolute value of I_t is not desired but only the form of the equation is necessary, one can substitute the following approximate equation:

$$a = \text{Constant} \times D_p^s. \tag{28}$$

The power s takes into account the variation of percentage voids with particle size and generally has a value slightly less than 1.

For convenience in comparing data on critical bed depths with analogous performance data in chemical engineering processes, the following transformation is useful:

$$H_t = \frac{I_t}{2.303 \log c_0/c_b} = \frac{1}{a}\left(\frac{D_p G}{\mu}\right)^{0.41}\left(\frac{\mu}{\rho D_v}\right)^{0.67}. \tag{29}$$

H_t is called the *height of a transfer unit.*

In contrast to I_t, I_r would be a complex function of the structure and nature of the charcoal and would be specific for the particular gas being removed. While it would be independent of the Reynolds number, it should [judging from consequences of equation (19)] vary directly with the rate of flow of of the gas-air stream, and it may be quite sensitive to temperature. Since many of these variables cannot be estimated in any general way, it is only possible to suggest the following relation for I_r (on the assumption that c_0/c_b is large and that the reaction is first order):

$$I_r = k_8 V \ln \frac{c_0}{c_b}. \tag{30}$$

The total critical bed depth, therefore, should be given by the expression

$$I = I_t + I_r = \frac{1}{a}\left(\frac{D_p V \rho}{\mu}\right)^{0.41}\left(\frac{\mu}{\rho D_v}\right)^{0.67} \ln \frac{c_0}{c_b} + k_8 V \ln \frac{c_0}{c_b}. \tag{31}$$

To determine the relative contributions of I_t and I_r, one may proceed in at least two ways. One approach would be to calculate I_t from equation (27) and obtain I_r by difference from the total critical bed depth. To facilitate these calculations a series of graphs has been prepared in which I_t is plotted as a function of the common variables.[22] A second approach is to obtain data on I as a function of the linear velocity V, and then to plot the data against $V^{-0.59}$. It is obvious from equation (31) that for all conditions, except flow rate, fixed, I/V may be expressed as

$$\frac{I}{V} = k_9 V^{-0.59} + k_{10}, \tag{32}$$

where k_9 and k_{10} are constants. The intercept of the line obtained is a relative measure of I_r and the value of the first term in equation (32) at any particular linear velocity is a relative measure of I_t.

The variation of the critical bed depth with particle size depends on the relative importance of the two terms in equation (31), that is, on the mechanism of the removal process. If the slow step in the granule is some surface reaction, I_r will be independent of particle size, whereas I_t will vary as some power of D_p, usually near 1.4. If diffusion in air and surface reaction contribute about equally, a plot of I against D_p will approach a finite limiting value as D_p approaches zero. This is illustrated by curve A in Figure 8. If mass transfer alone is rate-controlling, one obtains a similar curve (B in Figure 8) but with an intercept at the origin. In contrast, if the surface reaction were rate-controlling, I would be independent of granule size, as is illustrated in curve C of Figure 8.

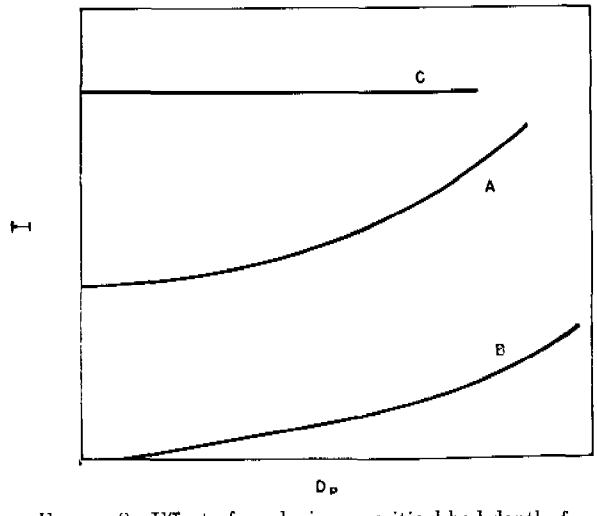


FIGURE 8. Effect of mesh size on critical bed depth, for various mechanisms of gas removal.

Where both terms contribute appreciably to the critical bed depth, one obtains an interesting graph in a plot of break time versus particle size. For large sizes, the life is less than that for small particles, but as the granule size decreases the life rises and approaches a limiting value, corresponding to condi-

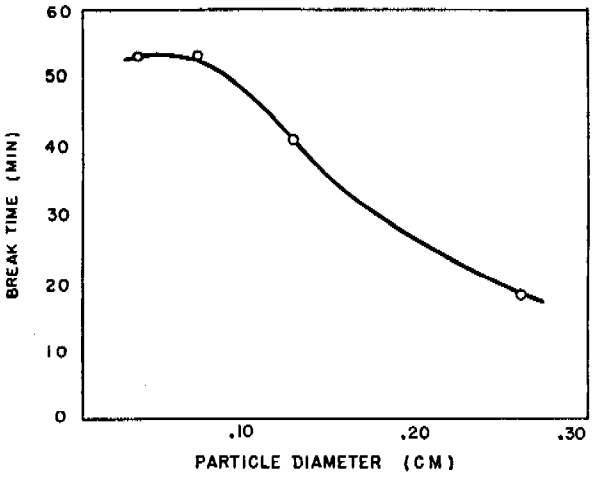


FIGURE 9. Dependence of break time on particle size (for phosgene).

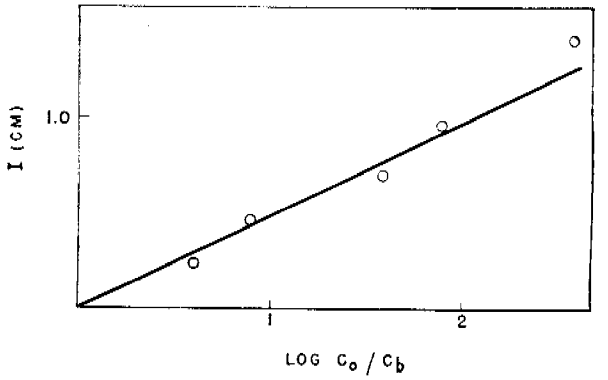


FIGURE 10. Dependence of critical bed depth on ratio of influent to effluent concentration.

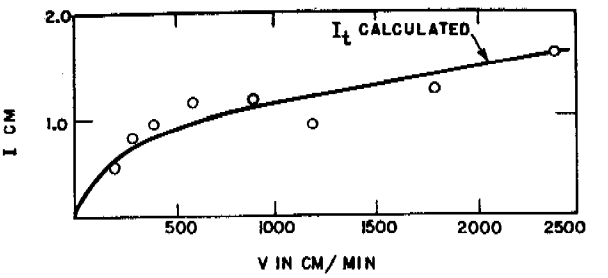


FIGURE 11. Critical bed depths for chloropicrin.

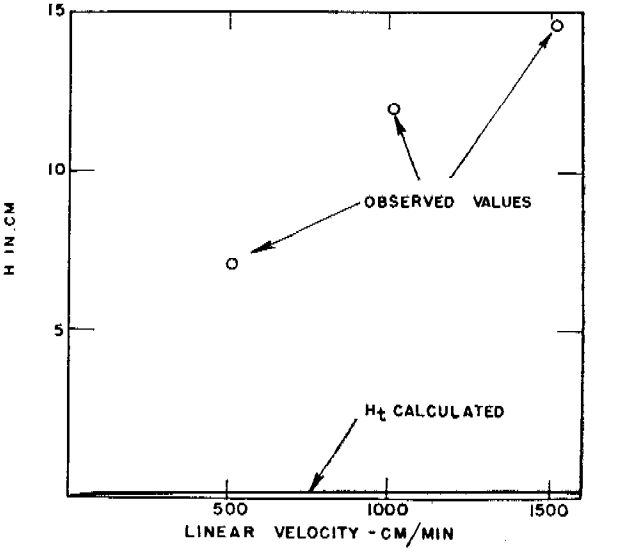


FIGURE 12. Water removal by charcoal. Deviation of observed from computed values of H.

tions where the surface reaction becomes the important factor and mass transfer has been effectively eliminated. A typical curve is shown in Figure 9.

The variation of the critical bed depth with velocity of flow also depends on the relative importance of the two terms in equation (31). If the slow step is a reaction in the granule, I will vary directly with the velocity. In contrast, if mass transfer is rate-controlling I will vary with the 0.4 power of the velocity. Where the two processes contribute, I can usually be expressed in terms of some power of the velocity between 0.4 and 1.0, although it must be realized that such a function would be merely an approximation to the fundamental one of equation (31).

The available evidence indicates that the critical bed depth is a logarithmic function of c_0/c_b. According to equation (31), the logarithmic relation should hold for any mechanism of removal. Sufficient data on effluent concentration as a function of time are available only for a few gases, so that the predicted relation has not been tested adequately. That it does hold for chloropicrin is shown in Figure 10.

Mechanism of Removal of Some Gases. The criteria described for estimating the relative contributions of diffusion in air and physical or chemical reactions in the charcoal to the critical bed depth have been applied to a number of gases with the aim of elucidating the mechanism of their removal.[23]

Chloropicrin is an example of a gas whose rate of removal is governed primarily by the rate of diffusion to the particle surface. In Figure 11 the observed values of the critical bed depth are plotted as a function of the linear velocity, and for comparison the curve calculated for I_t is also shown. The observed values do not deviate significantly from the calculated curve. Such behavior indicates no appreciable contribution of any factors other than mass transfer (diffusion in air) to the removal of chloropicrin, at least not in the initial stages of the process.

In direct contrast to chloropicrin is water, whose rate of removal seems to be governed primarily by some slow surface process. Experimental data on the rate of removal of H_2O[5] have been expressed in terms of a quantity H which may be defined by the equation

$$H = \frac{I}{\ln c_0/c_b} . \tag{33}$$

Values of H on a sample charcoal are shown in Figure 12. In comparison to the values to be expected if diffusion in air were the controlling process, the observed values are very high and indicate the large contribution that is made by factors which appear within or on the granule.

Other gases, such as cyanogen chloride, are intermediate in behavior between water and chloropicrin, in that diffusion in air and surface factors contribute almost equally to the rate of removal of the gas.

Dependence of Critical Bed Depth on Nature of Adsorbent. It must be realized that the relative contributions of various steps to the rate of removal will be very sensitive to the nature of the adsorbent. This dependence is well illustrated in the case of water where different base charcoals, having different pore structures and surface complexes, can react with water with different speeds and hence strikingly influence the critical bed depth or the value of H. Similarly, charcoals treated with impregnants usually react more rapidly with water, apparently because of their ability to form hydrates, and hence the magnitude of H is reduced considerably. In adsorbents such as silica gel, where the combination with water vapor at low pressures is probably due to hydrogen-bonding rather than primarily to van der Waals' forces, the removal reaction is extremely rapid and H approaches the limiting value due to diffusion in air alone. These factors are illustrated by the values of H listed in Table 1.

TABLE 1. Dependence of H on adsorbent.[5]

Adsorbent	H (in cm)
Charcoal, base, CWSN–19	38–64
Charcoal, base, CWSC–11	20–30
Charcoal, impregnated, CWSE1–TE1	7–15
Silica gel	0.5–2.5

The measurement of critical bed depths for charcoals which have been subjected to various treatments is a useful method of analyzing the results obtained. For gases such as chloropicrin, at least some of the available charcoals can react so rapidly that the limiting factor in the removal of gas (the rate of diffusion to the granule) has been reached, and it is futile to attempt to improve the adsorbent any further toward these particular toxic materials. On the other hand, toward most possible toxic agents there is still sufficient room for additional treatments or impregnations which may speed up processes which occur within the granule.

The Effect of the Capacity of the Charcoal

A clear statement of what is meant by *capacity* of a charcoal is not as readily available in a flow type of experiment as it is in the static case. In the latter situation, capacity refers to the amount of gas picked up by a unit weight of charcoal after sufficient time has elapsed for equilibrium to have been attained. The inapplicability of such a definition is particularly evident for a gas such as cyanogen chloride where, as is illustrated in Figure 7B, the influent end of a bed still has not reached a static state even after 200 min.

The primary value of a measure of capacity is in the prediction of the dependence of life on bed depth. Consequently, it is customary to define N_0 in terms of the slope of a life-thickness curve [see equation (23)]. In this manner, two samples which show linear life-thickness curves can be compared reliably in their performance under a set of conditions requiring a slight extrapolation from the measured ones. It is realized of course that such a capacity may be far different from the final equilibrium value, even for gases removed by adsorption alone. Nevertheless, it is more useful than a definition based on a static experiment.

For small bed depths, the break time is determined primarily by the critical bed depth of the adsorbent, inasmuch as the critical bed depth is a large fraction of the total bed. On the other hand, as the bed is made deeper, the critical bed depth becomes less important, whereas the capacity becomes increasingly significant and in large depths is the determining factor. These relations became evident in a comparison of the lines A and C in Figure 6.

The capacity is also a useful function for estimating the maximum possible life one can obtain from a sample. By assuming a critical bed depth of zero, one can calculate the total amount of gas that could be picked up by the bed and, from the flow conditions, the maximum limit for the break time (see "Efficiency of Canister," Chapter 2).

8.3.2 Equations for Canister Life

To predict the performance of canisters under any set of conditions other than those used in routine tests, it is necessary to have convenient analytic relations for life as a function of the common variables. This problem has not been solved satisfactorily except in a few special cases. Where the life-thickness relations show distinct curvature, no suitable analytical method has been evolved for extrapolating data. Since many tests are carried out under humid conditions, in which curvature is generally observed, this large field of testing still remains to be considered. However, in testing under dry conditions, where linear life-thickness curves are obtained, useful equations for the break time have been developed.

Cases in which Diffusion in Air is the Rate-Controlling Step

Under these conditions it is a simple matter to combine the Mecklenburg relation for t_b and equation (27) for I_t. The result is the expression:

$$t_b = \frac{N_0 A}{L c_0}\left[z - \frac{1}{a}\left(\frac{D_p G}{\mu}\right)^{0.41}\left(\frac{\mu}{\rho D_v}\right)^{0.67} \ln\frac{c_0}{c_b}\right]. \qquad (34)$$

It allows the prediction of the complete break-time history for any gas whose removal is controlled by mass transfer after the determination of one constant N_0, the capacity of the charcoal for the particular toxic material. The diffusion coefficient D_v of the gas can be estimated readily from relations available in the literature, or in most cases can be estimated sufficiently from the molecular weight curve illustrated in Figure 13. Tables of a, the superficial area, for various particle sizes and percentage of void spaces are listed.[15] All other constants may be evaluated from the conditions of flow and from the dimensions of the adsorbent bed.

Cases in which More Than One Step Contributes to Rate

It has been shown that under these conditions the critical bed depth may be expressed as a sum of two terms, each of which contains the linear velocity V to a different power. Equation (31) for I could be inserted into the Mecklenburg relation but the resultant expression is not as convenient for manipulation as an alternative developed.[23]

It has been observed in most experiments that a plot of the critical bed depth versus the logarithm of the rate of flow can be approximated sufficiently well by a straight line. Because of the large errors

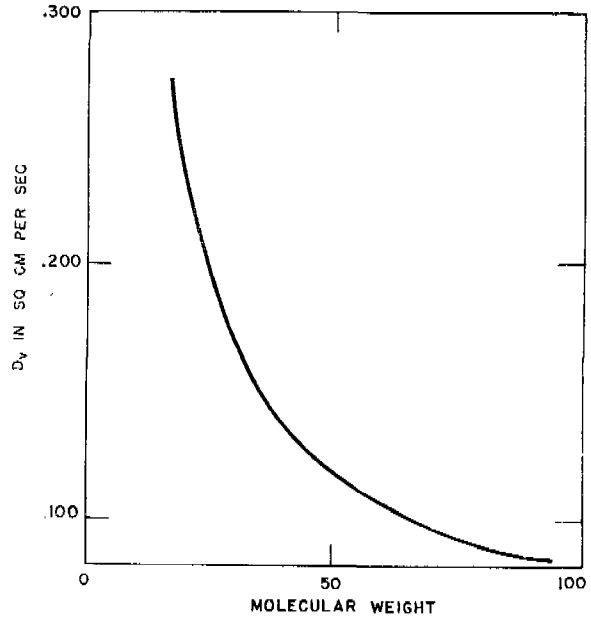


FIGURE 13. Relation between diffusion coefficient and molecular weight.

inherent in the determination of the critical bed depth, the relation

$$I = \text{Constant} \times V^d, \qquad (35)$$

where d is a constant, can be used in place of the two-term expression of equation (31). The insertion of this simple relation into the Mecklenburg equation gives:

$$t_b = \frac{N_0 A}{L c_0}\left[z - g\left(\frac{L_e}{A_b}\right)^d \log\frac{c_0}{c_b}\right], \qquad (36)$$

in which g is a constant which depends on the mesh size of the charcoal and the particular gas being removed, d is a constant determined by the test gas, A_b is the open area of the baffle at the effluent end of the canister and L_e is the steady flow rate equivalent to the pulsating rate of flow actually used. As has been described in a previous chapter, canister tests are made with a *breather* apparatus, designed to simulate respiratory conditions, in which the flow may vary from a high peak rate down to zero. The equivalent steady flow may be determined by measuring critical bed depths for a series of different constant flow rates and plotting I vs V. Then in a subsequent experiment with pulsating flow, the value of I is determined and from the reference graph a corresponding equivalent steady flow is read off. The reference curve may vary with the test gas as well as with large changes in the shape factor of the charcoal.

The use of equation (36) requires the evaluation of three constants, N_0, g, and d. The other parameters would be fixed by the conditions of flow and the geometric properties of the bed.

The equation has been applied [33] to five test gases (arsine, chloropicrin, cyanogen chloride, hydrogen cyanide, and phosgene) and to a number of different charcoals and found to be reliable within the precision of the experimental data. Thus, it affords a very convenient interpolation formula for the prediction of the performance of axial-flow canisters.

The principles used in the derivation of equation (36) have been applied to the radial-flow canister also. The result depends on the geometrical configuration of the canister.[33]

8.4 CONCLUSIONS

In examining the whole of the theoretical and experimental results of the work on the adsorption wave, it is seen that progress has been attained in the following respects. The nature of the steps involved in the removal of a toxic gas from air by a granular adsorbent has been clearly stated. Where the rate-controlling process is a single one of these steps, it has been possible within recognized restrictions to develop a complete analytical expression for the adsorption wave. Where two steps contribute to the rate of removal, a complete theory is still lacking, but it has been possible to develop criteria for the evaluation of the relative importance of diffusion in air and reactions in the granule in the removal process. These criteria have been applied to a number of different gases and the mechanism of their removal has been elucidated. From the general nature of the various equations for the adsorption wave it has been possible to develop semi-empirical relations for the prediction of canister lives under dry conditions and to predict qualitatively the effects of mesh size, flow rate, and concentration under dry or wet conditions.

The great gap in the present work is a suitable analytical treatment of results obtained under humid conditions or in other cases where non-linear life-thickness relations are obtained. Related to this is the absence of a complete treatment of the adsorption wave where many steps contribute to the rate of removal. These failures, however, are bound very closely to the general obscurity of the structural characteristics of granular adsorbents and of the nature of catalytic reactions. As fundamental relations in these latter fields are gradually evolved, one may anticipate further progress in the treatment of the adsorption wave and in canister design.

SYMBOLS

a superficial surface of the granule (ignoring pore structure) per unit volume of bed
A cross section of adsorbent bed
A_b open area of the baffle at the effluent end of the canister
b constant in equation for linear adsorption isotherm
c concentration of toxic gas in air stream at any point in bed of adsorbent
c^* concentration of toxic gas in air stream at any point in the bed in equilibrium with the charcoal at that point
c_b concentration of toxic gas in air stream chosen as the *break* value
c_e concentration of toxic gas in air stream at exit face of bed
c_0 concentration of toxic gas in air stream at entrance face of bed
d constant in equation for critical bed depth
D_p diameter of granule
D_v diffusion coefficient of the toxic gas (units of area per unit time)
exp notation for the exponential e
F mass transfer coefficient
g constant in equation for canister life
G mass velocity, that is, weight per unit time per unit cross section of bed
h depth of the "dead layer"
H height of a removal unit; $I/\ln c_0/c_b$
H_t height of a transfer unit; $I_t/\ln c_0/c_b$
I critical bed depth, that is, the actual intercept of a life-thickness curve on the thickness axis
I_r fraction of critical bed depth due to slowness of processes occurring within a charcoal granule
I_t fraction of critical bed depth due to slowness of diffusion of gas from air stream to the surface of the charcoal
k_1 constant in rate equation
k_2 constant in rate equation
k_3 constant in equation for t_c
k_4 constant in equation for t_c
k_5 constant in equation for t_c
k_6 constant in equation for t_c
k_7 constant in equation for critical bed depth
k_8 constant in equation for critical bed depth
K constant in the expanded form of the Langmuir isotherm
L rate of flow in liters per minute
L_e rate of steady flow equivalent to rate of pulsating flow
n moles of toxic gas on or in the granules contained in a unit volume of bed
N_0 saturation capacity of a unit gross volume of adsorbent for the toxic gas
s constant in equation for superficial area
t time
t_b *instantaneous* break time, that is, the time at which the effluent concentration reaches a value specified as the break concentration
t_c *cumulative* break time, that is, the time necessary for a given total amount of gas to penetrate the adsorbent
V linear velocity through the interstices between the particles of the adsorbent; $G/\alpha\rho$
z distance from the entrance face of the bed
α porosity, that is, the volume of intergranular voids per unit gross volume of bed
μ viscosity of gas-air stream
ρ density of gas-air stream

Chapter 9

CANISTER DESIGN

By *W. Conway Pierce*

9.1 INTRODUCTION

THE FACTORS that govern the amount of gas protection which can be obtained from a given volume of adsorbent (of given capacity, N_0) have been discussed in Chapter 8. In this section, the factors of practical importance which must be considered in the development of a gas mask canister are discussed. These are:

1. Amount of gas and smoke protection sought.
2. Weight and size permitted for the canister.
3. Resistance of canister.
4. Effect of mesh size on resistance and protection.

The factors listed above are so interrelated that, in practice, it is usually necessary to effect a compromise to obtain the desired protection; an understanding of the way in which they are related one to another is necessary in the development.

9.2 AMOUNT OF PROTECTION

There is, to date, no general agreement as to the amount of gas and smoke protection which the gas mask canister should provide. Moreover, it is improbable that a general agreement will ever be reached on this question even if gas is actually used, since it is not possible to increase protection without increasing weight, bulk, and pressure drop. Two somewhat opposing views are held. One group thinks chiefly in terms of protection and strives for the maximum safety, while the other group would sacrifice protection to achieve lightness and compactness and would take a considered risk of some casualties to obtain the lightest possible mask.

Several years ago a standard was empirically set up at Edgewood Arsenal of 6-g protection for all gases. This was based upon the 32-lpm flow rate used for testing at that time and for a gas concentration of 10 mg per l. It corresponded to a minimum life of 19 min. It was an easy matter to achieve this degree of protection for H, CG, and dry SA and AC but prior to the introduction of Type ASC whetlerite the 80-80 protection for SA, AC and CK was much less than 6 g for all canisters.

In 1943, a joint committee representing the British, Canadians, CWS and NDRC was set up to consider the question of how much protection is needed. This committee set up as the desired standard a protection against a gas dosage (Ct) of 100 mg min per l (100,000 mg min per cu m). No reference was made to the breathing rate except for the statement that this protection should be afforded under all conditions likely to be encountered. While this approach is more realistic than the previous value of 6-g protection it is necessarily empirical.

The ASC filled canisters of today will easily meet the desired protection, even when badly aged, except at high breathing rates which correspond to vigorous sustained exercise. When new, and tested at 25 lpm, an M11 canister will protect against a Ct of several hundred mg min per l (see data of Chapter 11).

On the basis of field experiments with gas arguments may be found in favor of almost any desired degree of gas protection. In the open, a high Ct rarely can be obtained except under certain restricted conditions. On the other hand, in the jungle, one can obtain a Ct of several thousand with reasonable munition expenditures. It is characteristic of these high dosages, however, that the gas cloud hugs the ground and tends to flow down slopes or ravines like a liquid. Under most conditions of terrain, and with most gases, simple evasive action could materially reduce the dosage to which a man is exposed.

Protection against a dosage of 50 to 100 is probably almost as good as one against a dosage tenfold greater. That is, Army canisters that protect against a dosage of 50 to 100 mg min per l will probably not have much greater percentage of gas casualties than canisters that protect against a Ct of 500. The arguments favoring this hypothesis are as follows:

1. Exposures to very high dosages will probably be very rare since a high dosage can be obtained only under such specialized conditions:
   a. In woods or heavy vegetation, where wind velocities are very low.
   b. Under inversion conditions.
   c. On level ground or in ravines and depressions.
   d. In enclosed places such as caves.
2. Unless a gas attack can be accompanied by sustained heavy fire to force troops to remain under cover, it is usually possible to escape from a region

of high concentration by moving to an elevated position. Since large gas concentrations over large areas can be laid down only by aerial bombs, it is not very feasible to provide covering-fire during the period of gas attacks. Friendly troops must be kept at a safe distance from the area under attack. Therefore, it is probable that in a heavy gas attack the majority of individuals can seek the comparative safety of higher ground.

3. In view of the difficulties attendant upon setting up high dosages over large areas the use of nonpersistent gas, except against enclosures is likely to be for the purpose of surprise rather than for canister penetration. If so, a small degree of protection will be sufficient since alertness rather than the degree of protection is important.

4. Whenever it is possible to exceed dosages of 50 to 100 by large margins, canister penetration is a possibility. With properly chosen weapons, the use of gas against caves, pill boxes and other enclosures can lead to casualties by canister penetration.

5. When high dosages are achieved, there will be casualties from leaky valves, poorly fitting facepieces and causes other than canister penetration, but the number is difficult to predict and would decline as troops became accustomed to gas warfare. Heavy canisters with large protection may even increase the danger of casualties from facepiece leakage for those gas masks with canisters attached directly to facepieces.

If the above premise is accepted (that protection against a dosage of 50 to 100 is adequate) it does not follow that better protection is undesirable. Every effort should be made to get the maximum protection consistent with other features such as weight and resistance. Low protection should be accepted only when it is not feasible to aim for higher values.

Filter protection should be made as high as possible, consistent with breathing resistance and canister design. Present filters will permit penetrations of the order of 0.01 to 0.1% of the incident aerosol.

The relation of pressure drop to protection in filters is such that it is not feasible to lower protection from the present level in order to obtain decreased resistance. As the thickness of filter is reduced, the resistance is decreased linearly but the protection decreases logarithmically.

9.3 WEIGHT AND SIZE OF CANISTER

The weight and size permissible for a gas mask canister depend upon how the canister is mounted and used. The trend today is toward developing facepiece-attached canisters but there are still large numbers of hosetube masks with the canister mounted in a knapsack carrier. In the facepiece canister models both the weight and size are of importance but in the hosetube type, weight is of secondary importance.

Choice of Type

It should be pointed out that, despite the present trend of facepiece canister masks, data on the relative merits of the two types are very meager. Neither the British nor the U. S. gas defense organizations have adequate facilities for testing the field behavior of gas masks. Present opinions as to the relative merits of hosetube and facepiece canister models are based upon limited wearing trials under non-gas warfare conditions and there is no real knowledge regarding the relative merits of the two types. If gas warfare were initiated, the choice would depend upon the conditions found to prevail in the field. It is believed that if it is found necessary to wear masks for long periods the hosetube type may be superior because of greater comfort but if gas attacks are infrequent and of short duration the facepiece attached type may be superior because of lightness and decreased interference with other activities. Much more protection can be built into a hosetube-type canister since weight is not important and this type can be of far more rugged construction than the facepiece type. On the other hand it is easier to waterproof the facepiece type and easier to wear it in active combat.

It is fortunate that in the absence of real knowledge of the relative merits of the two types, the British and U. S. Armies had large supplies of both. In the event that gas warfare had been started, all combat troops could have been readily equipped with the type of mask which proved to be most desirable as new conditions were encountered.

Hosetube Canisters

It is much easier to design a canister which is attached by a hosetube and carried in a knapsack than one which is directly carried on the facepiece. The only important limitation of the knapsack canister is that of bulk, or more specifically, of diameter. It is undesirable to have a canister of diameter greater than about 3 in. since the amount of interference depends upon the distance the canister projects from the body. Weight is not important, within limits, since a change of a few ounces is not noticeable and

as much as 2 lb (the weight of the M9A2 canister) can be tolerated.

For many years the U. S. canisters of the hosetube type have been of a radial-flow design. There are several advantages in this construction, which is possible only when weight is not a limiting factor.

1. Charcoal bed resistance is low. For large canisters the filter resistance may be kept quite low.

2. Radial-flow canisters are more rugged than flat-bed, axial-flow types because the chemical container is a separate can mounted within an outer jacket which furnishes protection.

3. In a radial-flow design as compared to a flat-bed type, it is easier to pack the absorbent tightly so that it does not loosen or channel. Baffles at the top and bottom of the inner tube of the chemical container effectively prevent any channeling if the granules become loosely packed.

4. The large surface area on the outside of the chemical container provides for large filter area.

The weights of these radial-flow canisters vary from about 1 lb for the M10 to 2 lb for the M9A2. Nearly half this weight is in the metal parts. If desired, the weight might be materially lightened by use of aluminum or light alloys in place of steel parts. This, however, has not been thought necessary.

The ultimate in low resistance and high protection has not been attempted in the hosetube canisters since there has been no apparent need for further improvement. An obvious change that could be made without making the canister more bulky or increasing the weight too much is to increase the length of the M10A1 canister which is the most efficient of the radial-flow models. An increase in length of 1 in. would lower the resistance at least 20% and increase the protection by much more than 20%, perhaps by as much as 50%, because of decreased critical depth at the lower flow rate. This is mentioned to illustrate the possibility but is not recommended since the protection of the M10A1 canister already seems adequate for all needs.

Facepiece Canisters

There are two general methods of attaching canisters to the gas mask facepiece, at the chin and on the left cheek. The former method is used in German masks and the latter in British and U. S. masks. Each has advantages and disadvantages.

Both weight and size of the canister are important considerations. More weight can be tolerated in a chin-mounted canister than in a cheek-mounted because the unbalanced weight on the cheek tends to break the face seal. Tests conducted by the CWS development laboratory indicate that the weight of a cheek-mounted canister should not be much greater than 250 g and that above this weight there is far greater tendency to break the face seal when the head is moved quickly. A weight of nearly a pound can be tolerated in a chin-type canister, since the pull is exerted on the head harness and does not break the face seal.

Because of the necessity to conserve weight it is not feasible to use a radial-flow canister for mounting on the facepiece. The U. S. training mask is the only case of such a usage and this mask is not satisfactory for field use. All other facepiece-attached canisters of this and other nations are of the flat-bed, axial-flow type. To conserve resistance the diameter is made as large as can be tolerated, usually about 4 in. The volume of charcoal ranges from about 225 ml in the British canister and 250 ml in the U. S. M11 to over 410 ml in the latest model German canisters (FE42).

Relation of Weight and Protection

Since weight and protection vary somewhat inversely with one another, it is necessary in designing a canister to know the relation of the two for a given type. This relation may be discussed for the M11 canister to illustrate the general principles involved.

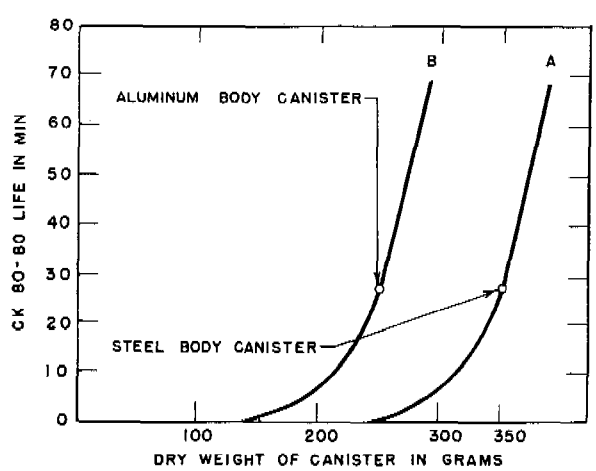


Figure 1. The relation of weight and protection against CK in M11 canisters.

The M11 canister with steel parts (now discontinued, but with several million in stock) weighs about 350 to 400 g. Of this, only about 175 g is taken up by the adsorbent when the canister is dry and 200 g when humidified. An increase or decrease of

SECRET

10% of the charcoal volume (which does not affect the weight appreciably) may cause a large change in protection. This is illustrated in curve A of Figure 1 which shows protection against CK as a function of weight. Similar curves can be drawn for other gases but with the inflection points located somewhat differently, depending upon the critical bed depths for the gases in question. The protection of the present canister, with a volume of 250 ml is indicated by an arrow. It is noted in Figure 1 that if the weight is reduced by 30 g (1 ounce) the gas life drops from 27 to 11 min. Conversely an increase in weight of 30 g more than doubles the gas life. The reason that this is not done is that the corresponding increase in the amount of charcoal makes the bulk too great for a canister worn on the cheek (one argument for a snout canister is that greater bulk can be tolerated).

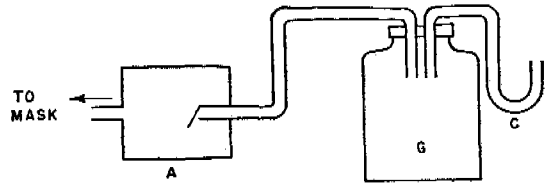


FIGURE 2. Scheme of apparatus used to measure peak resistance.

Since it is not feasible to reduce the weight by using less absorbent, the only other possibility is in the use of lighter metal parts. The CWS development laboratory has designed a satisfactory M11 canister which uses aluminum components, thereby affecting a material weight reduction. A life-weight curve for such an aluminum canister is shown in Figure 1, curve *B*. There is a weight saving of about 100 g for the same protection. This is the canister now in production.

Similar relations hold for weight and protection in the radial-flow canisters. The M10A1 canister with 340 ml absorbent gives a much higher gas protection than the M10 with 275 ml absorbent, although weighing only 40 to 50 g more; as mentioned in a preceding section, a still further increase in protection could be obtained by an increase in the length.

The present aluminum body M11 canister is still not the ultimate that can be expected in reduction of weight but is near the ultimate in bulk. Using present grade charcoal and the present mesh size it is impractical to reduce the charcoal volume materially since protection falls off much more rapidly than weight. It might be possible to effect a small saving in volume by using finer mesh charcoal, but it would not be safe to go far below the present volume of 250 ml. Use of a charcoal of lower apparent density is feasible and has been done experimentally. The present PCC charcoal when impregnated has an apparent density of about 0.65. It is possible to obtain good whetlerites with an apparent density of 0.40 to 0.45. The weight saving in 250 ml is therefore near 50 g.

9.4 CANISTER RESISTANCE

The first impression received on wearing a gas mask is that it is difficult to breathe, particularly if vigorous exercise is attempted. From the start of gas warfare one of the most important considerations in gas mask design has been to keep the breathing resistance low. This section reviews the factors which cause resistance and their effect on canister design.

MEASUREMENT OF RESISTANCE

For many years it has been customary to express the resistance of a gas mask canister as the pressure drop in millimeters (or inches) of water when air is passed through the canister at a flow rate of 85 lpm. The choice of flow rate is purely empirical since this rate is higher than average flow but lower than the peak flow for men at vigorous exercise.

During World War II devices have been developed to measure peak resistance for canisters and complete masks worn by men at heavy exercise. One of these is shown schematically in Figure 2. It consists essentially of a bottle *G* to which a water manometer *C* is attached, connected by rubber hose to the gas mask facepiece. Valve *A* permits air to be drawn from the bottle until an equilibrium pressure is attained; the pressure is then read from the manometer. The valve *A* must open at low resistance and have low leakage characteristics. The same apparatus may be used for expiratory resistance by arranging the valve so that pressure is built up in the reservoir to equal the static pressure of the gas mask valve.

Typical results for several subjects at heavy exercise and for a standard mechanical breather pump are given in Table 1.

These data show that the peak resistances vary over wide ranges for different subjects, because of different breathing rates. The mask for which the data are given was of poor design and had an unusually high expiratory resistance. In the better masks peak expiratory resistances were much less than the inspiratory resistances; this is achieved by

proper design of the outlet valve. Incidentally, it may be pointed out, as shown in Table 1, that the subjects at heavy exercise showed peak flow rates of the order of twice that for the mechanical pump, which had a flow rate of 50 lpm and a peak of near 155 lpm. The exercise conditions were chosen as the most severe that the subjects could endure for a few minutes.

TABLE 1. Maximum inspiratory and expiratory resistance for a gas mask.

Subject	Max. resistance in in. of water	
	Inspiratory	Expiratory
1	2.7, 2.7, 2.9	2.7, 2.8, 2.7
2	3.1, 3.2, 3.4, 3.2	5.0, 4.5, 4.9, 5.1
3	5.7, 5.8, 6.3, 6.2	.....
4	3.3, 3.4, 3.4, 3.3	3.1, 3.3, 3.3, 3.2
5	5.5, 4.7, 4.9, 5.3	5.1, 5.0, 5.5
Mechanical pump (50 lmp)	2.6, 2.9, 2.8, 2.9	2.8, 3.2, 3.3

PHYSIOLOGICAL EFFECTS OF CANISTER RESISTANCE

It is not easy to arrive at definite conclusions regarding the amount of resistance that can be permitted in a gas mask. Tests conducted at the Department of Physiology, Harvard School of Public Health, indicate that for subjects at exercise no marked difference is found in physical stamina up to resistances of nearly 75 to 100 mm of water (measured at 85 lpm flow). These tests were made on the basis of measurements of pulse, temperature, et cetera, for subjects who did not know how much resistance was interposed. Tests by Medical Division CWS indicate also that there is no marked impairment of efficiency so long as the breathing resistance does not exceed 75 to 100 mm water. (Reports from Division 11 NDRC and Medical Division CWS should be consulted for details.) On the other hand, experience with troops wearing gas masks in field trials tends to indicate that the efficiency of the average man is markedly lowered by wearing a gas mask of resistance near 75 mm water and that the endurance at heavy work is greatly decreased. Some claim that in field tests with mustard gas the comfort of the mask is increased by removing the particulate filter, thereby halving the resistance. How much of the handicap of the mask is due to its discomfort in binding the face, how much to the breathing resistance, and how much to psychological factors, is not known. The writer feels that the subject warrants a more thorough study than has yet been made and that in particular more data should be obtained on the ability of men to become acclimated to wearing the mask. Possibly a rigorous training program might enable men to be as efficient when breathing through a 75- to 100-mm resistance as when no resistance is present.

Lacking good data on the effect of resistance, current practice is to permit masks to have a resistance as high as of 75 mm water. Efforts are made to keep the resistance as low as is compatible with the amount of protection desired, but in general, the 85 lpm resistance of M3-10A1-6 masks is near 60 mm and that of the M5-11-7 mask near 70 mm. The fact that no serious objections have been raised to these resistances is not proof that they are satisfactory since, to date, masks are worn by the average soldier only for a few hours in training.

SOURCES OF RESISTANCE

In a complete gas mask assembly the inspiratory resistance is the summation of the following:

1. Particulate filter of canister.
2. Chemical container.
3. Fittings, connections and facepiece.

In a properly designed mask most of the resistance is in the canister, divided between the filter and chemical container. The proportion due to each depends upon the type of construction. In the radial-flow models the filter resistance is about three-fourths the total, while in axial-flow canisters of the M11 type the resistance of the filter is usually less than that of the chemical container.

The chemical container resistance is due to the intergranular resistance within the charcoal bed and to the retaining screens and dust filter. In early stages of the M11 development, the interfacial resistance between charcoal and screen was high but suitable pad and screen combinations were later found to give a low canister blank. The effect of screens and pads cannot be determined from the resistance of an empty container but must be measured with charcoal present by plotting pressure drops vs volume of charcoal and extrapolating to zero volume.

Since the chemical container resistance of radial-flow canisters, like the M10A1, is inherently small no difficulty is met in holding within tolerances in the assembly plant. Such is not true of the flat-bed M11 canister. Unless the operation of filling machines is carefully controlled and care is taken to avoid excessive amounts of fine-mesh charcoal the resistance may go very high. Normally the resistance of the assembled M11 chemical container is about 35 to

SECRET

40 mm. It varies somewhat with the different charcoals now on procurement.

The resistance of complete canisters shows some variations as filter materials and charcoal from different sources are used, but in general it is:

Source	Resistance
M1XA1 or M9A2	50 mm
M1 or M1A1	60-65 mm
M10 or M10A1	60–70 mm
M11	60–70 mm

Relation of Resistance to Size of Canister

In the development of the M11 canister certain simple principles were noted, relating resistance to cross section of the canister. These are:

1. The resistance of the filter is inversely proportional to the area or to the square of the diameter.

2. The resistance of the chemical container is, for a given charcoal volume, roughly inversely proportional to the square of the cross-section area or the fourth power of the diameter. This relation is based upon the fact that both the flow rate and the bed depth depend upon the cross section. Protection, however, is almost constant, within certain limits, for a given charcoal volume. Data to show this point are given in Table 2. The calculated resistances are based on the relation

$$\frac{R_1}{R_2} = \frac{(D_2)^4}{(D_1)^4}.$$

These are net values, corrected for the container blank.

Although it is not likely that an increase in the diameter of the M11 canister will ever be used, these data show why it was not possible to use a smaller canister than the present 4-in. size. In a 3-in. can the chemical container resistance would be for the same charcoal volume about three times that for the 4-in. can.

Table 2. Effect of variation in diameter on resistance and gas protection for 250 ml adsorbent.

Diameter	Resistance		Gas lives		
	Observed	Calculated	CK	CG	AC
10.6 cm ($4\frac{5}{32}$ in.)	25	..	32	42	53
11.2 cm ($4\frac{13}{32}$ in.)	21	20	33	40	47
11.8 cm ($4\frac{21}{32}$ in.)	17	16	26	39	51

Effect of Mesh Size on Resistance and Protection

It is present U. S. practice to use 12-30 mesh (U. S. standard) for gas mask adsorbents. Considerable tolerance is given the manufacturer in the distribution of sizes but in general this distribution is approximately 20–50–30 (20% 12–16; 50% 16–20; 30% 20–30). The British, Canadians and Australians employ a more uniform mesh distribution.

There is no theoretical basis for the mesh size now used; rather the requirements are based upon practical considerations of what the manufacturers can supply without undue wastage and how much pressure drop can be tolerated in the chemical container. A more efficient ratio of protection to resistance could be obtained by use of a narrower mesh spectrum but at present the wastage in producing such a charcoal renders a change inadvisable.

Considerable work has been done on the relation of resistance in the charcoal bed to the size and distribution of granules, and tests of gas lives have been performed with various mesh distributions. The results of such tests can be qualitatively summarized in a curve of the form shown in Figure 3, which represents gas life as a function of resistance for a given volume of charcoal.

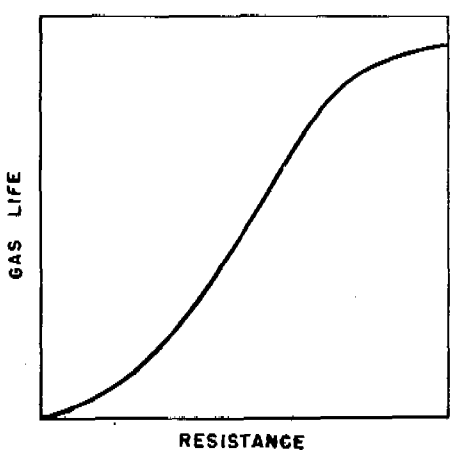


Figure 3. Relation of gas life and resistance for given volume of charcoal.

A curve of this type is readily explained from the considerations given in the preceding chapter. At a low resistance, or with large particles, the protection is low because the critical depth is large. As the particle size is decreased, protection increases more rapidly than resistance, due to the fact that when the critical depth is near the total bed depth a slight decrease in the critical depth may cause a disproportionate increase in the thickness of the saturated layer. At still higher resistances, which correspond to smaller intergranular distances, the critical depth becomes a small fraction of the total bed depth. When

this occurs, any further increase in resistance causes little increase in protection since the bulk of the absorbent is in the saturated zone already. At this point the curve flattens out.

From such considerations it is obvious that for a given canister design it is desirable to obtain the resistance-protection curve for typical gases, in order to select the optimum mesh size of absorbent. These tests should be made both with gases whose I_r values are small and large to cover the extremes which may be encountered. The curves for small I_r values may be quite unlike those for large I_r values.

9.5 CONCLUSIONS

In light of present knowledge as to the requirements for the gas mask canister it is felt that the two most modern U. S. canisters, the M10A1 and M11 models, represent about the best overall performance that can be obtained with present charcoals and filters. Both canisters have high efficiencies of the order of 50 to 75% when new.

$$\text{Efficiency} = \frac{\text{Weight of gas retained at break}}{\text{Weight of gas at saturation}}.$$

It is felt that an increase in efficiency at the expense of weight or bulk is not now justified. Conversely, it is felt that a reduction in weight or bulk at the expense of protection is not justified unless it can be shown by large scale field trials that such a reduction is urgently needed. Should such needs develop, the principles of design are now well understood and if new requirements are set up it is a simple matter to redesign the canister to meet them. At the present time canister design is ahead of facepiece design and extensive canister development is not needed until the designers of facepieces demand something different.

Attention should be called to one weakness in present canister design; that is, in the lack of ruggedness. The M10A1 and other radial-flow canisters were so rugged in construction that they could be carried in a cloth knapsack without damage. The Germans have used a fragile canister for years but keep it in a sturdy metal carrying case. It is not at all certain that a fragile canister like the M11 aluminum model can be safely carried in a cloth knapsack. It is quite probable that many canisters will be dented and the bottoms mashed in so that the rubber plug cannot be used for waterproofing, thereby sacrificing one of the advantages of this type of canister.

Chapter 10

THE AEROSOL FILTER

By *W. Conway Pierce*

10.1 INTRODUCTION

At the end of World War I the development of aerosol filters for gas masks was well under way. The Germans had first realized that a gas mask canister could be penetrated by airborne particles, which are not absorbed by charcoal. They had developed the use of diphenylchloroarsine smoke for this purpose and, in the latter days of the war, this agent was used on a rather large scale. Dispersion was effected by placing solid diphenylchloroarsine in high explosive shells. The smoke so obtained was poorly dispersed, according to modern standards, and although it was effective against masks which had no filter the smoke could be stopped by a very crude filter pad. By the end of the war all masks were equipped with some type of filter to stop smoke particles.

In the period between World War I and II the smoke protection of gas masks was greatly improved and at the start of the present war the gas masks of all nations provided at least moderately good protection against all known toxic and harassing aerosols. A variety of types was used.

10.1.1 United States

The filter of the MIXA1 and M1 canisters was composed of several sheets of porous paper impregnated by aspiration of carbon black (from a smoky flame) through the paper. The filtering action was due to deposition of carbon filaments of small diameter across the large pores of the cellulose fiber network of the paper. This filter was very effective against solid particle smokes, particularly at low humidity. It would, however, break down on exposure to liquid smokes.

10.1.2 German

The filter was a single sheet of asbestos-bearing paper, folded so as to present a large area with low resistance. It was the best of the prewar filters when both resistance to flow and protection were considered. Later U. S. filters were based upon developments resulting from studies of German and British filters. However, the theory underlying filter action was carefully studied as a basis for later developments.

10.1.3 British

Two types were used. The large box canister contained pads of wool into which asbestos fibers had been carded. Later, when the assault mask was developed, the asbestos was replaced by a resin which was carded into the wool. This filter functioned because of electrostatic charges. Under optimum conditions it was very effective but it had the weakness that the charge might be dissipated with age, by acid gases, or even high humidities. When this happened the filter permitted high penetration of aerosols.

10.1.4 Japanese

The filter was made of cloth that was pleated so as to present a large surface to the air stream. The filters on some types of canisters were excellent.

10.2 DEVELOPMENTS OF THE WAR PERIOD

The first chemical warfare problem to reach the NDRC was CWS-1. The Service directive requested that fundamental scientific information be obtained on the dissemination and filtration of aerosols. Intensive work on this subject began in 1940–41, by both NDRC and CWS, and led to a more fundamental understanding of the problem. The following generalizations appear in early reports.[1–6]

1. An aerosol filter is a network of fine fibers. It does not function as a sieve; all but the largest particles may pass through the holes.

2. A particle is caught by the filter only when it comes into contact with one of the fibers, where it is held by van der Waals' forces and is not removed by air currents which flow at moderate speeds.

3. A mathematical theory was developed [5,6] that took account of the mechanism whereby the particle reaches the fiber surface, and that predicted the effect of particle size, flow rate, and other factors on filtration. It was shown that the fiber diameter should be

of the same order of magnitude as the particle diameter. The predictions of this theory were confirmed by experiments.

4. Presence of an electrostatic charge on the filter fibers increases their interception radius and improves the efficiency of filtration. All filters display, under certain conditions, some electrostatic action but, in general, it is not safe to rely chiefly upon this effect which may be lost on exposure to humidity or to certain types of liquid aerosols. The safest filters are those which act by interception even when electrostatic charges are not present. Testing of filters should be carried out at high humidity to avoid spurious effects due to transient electrostatic charges. Liquid smoke (that is, the dispersed phase is liquid droplets) should be used for testing filters, since such smokes are more penetrating than smokes which contain solid particles.

5. It was stated [1] that "Apparently the ideal filter would consist of a series of grids made up of proper sized filaments placed in series and staggered so that the stream lines will not pass straight through the filter." This ideal filter must be of finite depth since a shallow grid is more readily clogged than a deeper one of the same resistance.

6. The filter should contain fibers of 1 to 2 microns diameter but a support of heavier fibers may be necessary to prevent matting of the fine fibers. The cellulose fibers of alpha web paper used in the prewar mask are some 20 microns in diameter. Carbon impregnation of this paper presumably gives finer filaments which span the large pores in the cellulose network.

Recognition of the above generalizations was followed by an intensive study of means for producing filters of optimum efficiency and low pressure drop. Several sources of fine fibers were investigated, including asbestos, glass wool, organic fibers, and rock wool. Excellent filters were made from all of these, but asbestos combined with paper was found to be best suited to rapid, large scale production. All U. S. gas mask filters of the M9A2, M1A1, M10, M10A1 and M11 canisters were equipped with asbestos-paper filters. A brief account of the various fine fiber studies follows.

10.2.1 Glass Wool [5]

This material is readily available and has small fibers, usually less than 10 microns in diameter. The first tests, with laboratory material of fiber diameter 6 to 8 microns, appeared very promising but it was soon realized that fibers of this size were not adequate at high humidity. At low humidity, where electrostatic effects may aid the filtration, these fibers are excellent. In view of these findings, the Owens-Corning Fiberglas Company undertook to make an ultrafine glass wool with fibers 2 to 3 microns in diameter. Experimental lots appeared to be very good and in 1942 Rodebush reported [5] "It may be considered therefore that the glass wool research has been completed and that the problem is now in a development state.... Glass wool is superior to paper as a filter material for two reasons: (1) the small diameter of the fibers and (2) the better distribution in space. Paper is ill adapted to use as a filter because it is made of large fibers which are matted together with a minimum of open space between them.... In glass wool the fibers are uniformly dispersed throughout the volume with a relatively large amount of free space and the glass wool, therefore, gives a very low pressure drop for a given degree of penetration."

Following the research studies on glass wool, a CWS contract was given to Owens-Corning Fiberglas Company for development of a filter suitable for wrapping on the M10 canister. Sheets were prepared which gave excellent filtrations with low pressure drop, but by the time development work had proceeded far enough to warrant production, an excellent asbestos-bearing paper was in production and it was not deemed desirable to make a change which would involve retooling and bring about new problems in manufacture.

It appears in retrospect that had the glass wool development been made earlier it might have won out in competition with asbestos. One of the peacetime studies needed is a thorough comparison of glass wool and absestos filters, particularly for the axial-flow type of canister. Theoretically, glass wool appears to be superior in structural make-up but it is not certain that it can replace asbestos paper in practical application (which involves questions such as mounting, handling, and uniformity of production material).

10.2.2 Rock Wool [5]

The use of rock wool as an aerosol filter was suggested to the CWS in 1941. This suggestion was referred to NDRC and extensive investigations were made. Rock wool is manufactured in large tonnage for use as a heat insulator. The fibers are very similar

to those of glass wool, with diameters ranging from 1 to 2 up to about 7 microns, the average being about twice that of the ultrafine glass wool made experimentally. In commercial manufacture, a binder is added and the rock wool is felted into pads. The commercial product has several disadvantages for gas mask filter use: (1) the pads are often uneven, having thin and irregular spots; (2) it is difficult to control the fiber size; (3) the wool contains a considerable amount of shot or beads of fused glass which occupy space but contribute nothing to filter action; and (4) adequate protection could not be obtained without excessive bulk or pressure drop.

Because of these disadvantages, no serious consideration was given to the use of rock wool for military canisters. However, its availability in large amounts and its quite excellent filtering power led to consideration of rock wool for use in canisters for civilian or noncombatant masks. In 1942 the Johns-Manville Company undertook, without charge, an experimental development of a civilian canister. Later, this was continued at Edgewood Arsenal. Some excellent and cheap canisters were made by placing a layer of charcoal between two rock wool pads. Before this development was completed all need of a civilian canister had ended and the study was discontinued. Should it ever become necessary to produce large numbers of noncombatant canisters quickly, rock wool might well be considered for use in the filter pad; it does not appear, however, to hold any promise for use in military canisters.

10.2.3 Organic Fibers

In the search for fine fibers for use in filters, it was a natural development to investigate organic materials which could be prepared by the methods used in the rayon and nylon industry. Research contracts were set up with American Viscose Corporation, E. I. duPont de Nemours Company, and Tennessee Eastman Corporation. It was found that superfine fibers could be produced, with diameters ranging down to 0.01 micron and that these fine fibers could be prepared in uniform sizes. By the time these results were achieved, the asbestos filter program was proceeding so satisfactorily that no attempt was made to set up production facilities, to solve the many problems attendant upon changing over from a laboratory to a commercial scale, or to devise methods for the fabrication of these fibers into gas mask filters. Thus, beyond the production of fibers by a relatively expensive process, the field of organic fibers is practically untouched.

Unfortunately only one report of the work on fibers has been distributed.[7] Contractors' final reports in the Division 10 files should be consulted for details.

10.2.4 Asbestos

The first material to be investigated in the search for fine fibers was, of course, asbestos since this was known to contain fibers of the proper size. It was in use in British and German gas masks, and it was readily available. Early tests with laboratory asbestos of Gooch crucible grade showed that it made an excellent filter. Work was begun immediately by CWS and NDRC on methods for incorporating asbestos into filters by combining it with paper. Two general lines of attack were made on the problem: (1) by impregnating an open structure paper with asbestos, much as the older type paper was impregnated with carbon black; (2) incorporating asbestos into the paper so that it was interspersed throughout the cellulose network. Papers made by the former process are designated *asbestos impregnated* and those in which the asbestos is incorporated in the paper as *asbestos bearing* papers.

Methods for impregnating thin-sheet paper for use in wrap-on, multilayer filters were developed by the Services. In dry impregnation, shredded asbestos was aspirated through the paper by a method similar to that formerly used for carbon black impregnation. Apparently the fine asbestos fibers were pulled into the large holes of the cellulose network at the paper surface so as to form a network of fine fibers superimposed upon the coarser cellulose fiber network. The filters made by wrapping on several layers of this paper gave excellent protection. Similar results were obtained by a wet impregnation in which the paper was treated with a thin coating of asbestos slurry which was allowed to dry, leaving a deposit of asbestos fibers.

While asbestos-impregnated paper gave filters which were distinctly superior to carbon-impregnated paper, they were not wholly satisfactory and were never used on a large scale. Asbestos-bearing paper, when good manufacturing processes had been developed, was used exclusively during the latter part of the war.

Numerous problems had to be solved before a satisfactory asbestos-bearing paper could be produced. Among these were methods for preparing the asbestos

fibers of proper size, of removing dirt and foreign matter from the asbestos, of dispersing the asbestos uniformly throughout the paper pulp, and of retaining a satisfactory tensile strength in the finished product. Through close cooperation between the Services, the paper manufacturers, and the research group, all these problems were solved and several types of asbestos-bearing papers were developed.[8] For multilayer, wrap-on filters, where tensile strength was of paramount importance, a reinforced paper backed by scrim was used. All later Model M10 and all M10A1 canisters were wrapped with this paper. In fact, the availability of this paper made possible the development of the M10A1 canister with the same outer dimensions as the M10 canister. The scrim-back paper was so efficient that the number of layers of paper was reduced and the space saved thereby was utilized for increasing the charcoal bed depth by $^{3}/_{32}$ in.

The development of effective procedures for incorporating asbestos into the paper made possible the design of an axial-flow canister of the M11 type. Before such a canister could be designed, a single-sheet paper was necessary that could be fluted to present a large filter area since in the axial-flow canister it is not feasible to use a wrap-on multilayer paper. The single-sheet paper produced eventually was comparable to, and probably better than, the German filter in protection and resistance.

During the filter paper development, extensive study was made [8] of the effect of cellulose fiber on the resistance and efficiency of the paper. The incorporation of special fibers, such as esparto grass, and the development of methods for treating wood to obtain the best size and distribution of cellulose fibers, all contributed to the success of the asbestos-paper filter, particularly by giving the necessary mechanical properties.

Chapter 11

PERFORMANCE OF U. S. AND FOREIGN GAS CANISTERS

By *J. William Zabor*

11.1 INTRODUCTION

THE PURPOSE of this chapter [a] is to summarize the data on the protection afforded by allied and enemy canisters against nonpersistent agents under a variety of conditions simulating circumstances likely to be met on the battlefield. As indicated in Chapter 7, the protection afforded by all canisters against persistent agents is more than adequate and, consequently, need not be considered in this résumé.

It is obvious that only those enemy canisters which have been captured and returned to allied nations are considered. These canisters do not necessarily represent the enemy canisters which would appear under gas combat conditions because the enemy may possess, or be able to produce in a short time, canisters that afford better protection than those considered herein. Furthermore, in comparing the protection afforded by enemy canisters with that afforded by allied canisters, it must be emphasized that many of the enemy canisters suffer the disadvantage of having been carried by troops, or having been subjected to climatic conditions causing corrosion, whereas most of the allied canisters were new and in their best condition.

The general test methods employed have been described in Chapter 2. Concentrations, humidities, and flow rates were varied and are specified in each case. Only results with breather-type pumps are given. Whenever possible, the results of the following three types of tests are given: (1) absorption to initial penetration of physiologically significant concentrations, (2) absorption to the penetration of a dosage which is considered to be lethal, and (3) initial absorption followed by desorption. It must be remembered in this connection, however, that penetration of a lethal dosage during a given exposure in the laboratory does not insure that a casualty is produced in combat by a similar exposure; there is usually sufficient warning in the early stages of penetration to permit a change of canisters or of gas masks if such replacements are available.

The agents to be considered are the three U. S. standard agents (CG, CK, and AC), plus PS, and NO_2. As was pointed out in Chapter 7, these gases represent the typical as well as the exceptional nonpersistent gases which are apt to be met on the battlefield. Sulfur pentafluoride, and any other fluoride which might conceivably be employed, behaves much like CG, and protection may be expected to be comparable. The results obtained with PS offer an estimate of the protection which would be afforded against a semi-persistent agent whose destruction on charcoal by hydrolysis or other reaction is likely to be too slow to affect the dynamic retention. Though few tests have been made with NO_2, it is considered because it has often been proposed as a potential war gas. SA is not discussed in this chapter; it is not under consideration by the U. S. Army as a possible war gas, and therefore performance data of enemy canisters toward SA would be of little interest. Allied canisters afford more than adequate protection against this agent and thus it is of little concern from a defensive point of view. Furthermore, any deficiencies in protection of enemy canisters against SA could very easily be remedied. Performance data are considered separately for each agent in order that a direct comparison of the several canisters may be drawn.

The majority of the work done on foreign canisters has been done by the Chemical Warfare Service [CWS] laboratories and more complete data may be obtained by direct reference to the original technical reports of that Service. The summary given in this chapter gives a sketchy overall picture of gas mask performance and is intended only to render the first part of this book more complete. Reference is made only to summary reports whenever possible.

11.2 GAS MASK CANISTERS

All U. S. gas mask canisters, except the U. S. Army M11 canister, are radial-flow design. These canisters are adequately described in Chapter 1. All foreign canisters discussed herein are of the axial-flow design. It is unnecessary to describe these canisters in detail in this summary, but a few of the physical characteristics of the more important canisters should be

[a] This chapter was written before V-E Day but the conclusions regarding enemy equipment have not been materially altered by developments of the immediate postwar period. —Ed.

Table 1. Physical characteristics of foreign canisters.

Canister	Overall weight (g AR)	Resistance at 85 lpm (mm H_2O)	Volume of adsorbent (ml)	Wearing position	Moisture content as issued	Principal impregnants
British Mk II/L	313	63	233	Cheek	ca 20%	Cu, Ag (Pyridine)
Canadian Mk II/L	...	..	...	Cheek	ca 20% (or dry)	Cu, Ag, Cr
German FE41	340	59	260	Snout	Dry	K, Na, Zn, Cu, Ag
German FE41P	320	68	270	Snout	Dry	Same as FE41; also Pyridine or Picoline
German FE42	455	75	410	Snout	Dry	Same as FE41
German FE42P	455	75	420	Snout	Dry	Same as FE41P
Japanese Army 99	508	47	315	Hose	Dry	Cu, Mn
Japanese Army 95	691	55	425	Hose	Dry	Cu, Mn
Japanese Navy 93	918	53	610	Hose	Dry	

mentioned before consideration is given to the gas protection the canisters afford. A brief physical description is given in Table 1.

It will be noted in Table 1 that British and some Canadian canisters are moistened before issue. This practice was started originally to provide added CG protection without impregnation. Inasmuch as the canisters soon become humidified in the field, the practice has been continued. All "AR" test-results summarized in succeeding sections were performed on the moist canisters as received. All other canisters are issued dry and "AR" represents a nearly dry canister.

The German canisters have the adsorbent separated into two layers in the FE37, FE41, and FE41P, and three layers in the FE42 and FE42P models.

Table 2. Comparison of CG protection afforded by allied and enemy canisters to the break points.

	Influent dosages required to the initial penetration of physiologically effective concentrations under various conditions					
	Flow rate (lpm)					
	50	50	50	50	25	25
	Influent concentration (mg per l)					
	10	10	20	50	10	10
	Relative humidity					
Canister	AR–50	80–50	80–50	80–50	AR–50	80–50
U.S. Army M1	200[1]	160[1]				
U.S. Army M1A1	200[1]	150[1]				
U.S. Army M10	350[1]	320[1]	300[1]	200[1]		
U.S. Army M11	430[1]	380[4]	360[4]	325[4]		
U.S. Army M10A1	450[1]	450[1]	140[1]	325[4]		
U.S. Army M9A2	1000[1]	1000[1]				
U.S. Navy (Old Type)		200[1]				
U.S. Navy Mark B	330[1]	250[1]				
U.S. Navy Mark B1	570[1]	620[1]				
British Mk II/L	280[1, 7]					
Canadian Mk II/L	300[1]	330[1]				
German FE37						
German FE41	100[1]	350[1, 3]				
German FE41P		390[3]				
German FE42		790[3]				
German FE42P		950[3]				
German Civilian					80–210[5, 6]	
Japanese Army 99	20–170[1, 2]				235[1, 2]	160[1, 2]
Japanese Army 95	80–400[1, 2]					530[2]
Japanese Navy 93		1160[2]			1310[1]	1130[1]
Japanese Civilian	350[1]					960[1]

Note. Superscript numbers refer to bibliographical references.

This permits the use of two or three different adsorbents without blending. It also facilitates the insertion of a specific absorbent in the advent of the use of a new gas.

The Japanese Army 99 canister contains about 28% by volume of a modified Hopcalite. The Japanese Army 95 and Navy 93 canisters, respectively, contain 26% and 17% by volume of soda lime. The Navy canister is the latest type captured from Naval and Marine units; it is equipped with a carbon monoxide auxiliary canister containing a poor grade Hopcalite.

TABLE 3. Comparison of CG protection to initial penetration and to lethal penetration. (Influent concentration = 10 mg per l; flow rate = 50 lpm; humidity = 50–50.)

Canister	Influent dosage (mg min per l)	
	Initial penetration	Lethal penetration
U.S. Army M1A1	195	380
U.S. Army M10	290	540
U.S. Army M10A1	500	750
U.S. Army M9A2	820	1000
German FE41	180	220
Japanese Army 95	440	730
Japanese Civilian	350	475

11.2.1 Protection against Phosgene

The comparative CG protection afforded by allied and enemy canisters to the break points is summarized in Table 2. The superscripts refer to the bibliography of this chapter and represent the sources of these data. Average values are given except in cases where the range of values is large. Such large discrepancies are due to the testing of a limited number of canisters which were probably subject to considerably varied treatment prior to receipt and test in this country. In such cases, the higher figures probably more nearly represent the average protection to be expected in combat.

A few tests have been conducted to determine the influent *Ct*'s required to produce a lethal effluent *Ct* (considered to be 7 mg min per l). These tests [1] were all performed at 50 lpm, an influent concentration of

TABLE 4. Comparison of CK protection afforded by allied and enemy canisters to the break points.

	Influent dosages (mg min per l) required to the initial penetration of physiologically effective concentrations under various conditions										
	Flow rate (lpm)										
	50	50	50	50	50	32	32	25	25	12.5	12.5
	Influent concentration (mg per l)										
	4	4	4	10	20	4	4	4	4	4	4
	Relative humidity										
Canister	AR–80	80–80	AR–50	AR 50	AR–50	AR–80	80–80	AR–80	80–80	AR–80	80–80
U.S. Army M1	16[1]	4[1]				36[1]			8[1]		
U.S. Army M1A1		24[1]	90[1]								
U.S. Army M10	140[1]	80[1]	125[1]	120[1]	110[1]	300[1]	120[1]				
U.S. Army M11		140[1]	190[1]								
U.S. Army M10A1	300[1]	160[1]	200[1]	190[1]	190[1]	500[1]	340[1]		1000[2, 3]		
U.S. Army MIXA1	30[1]	4[1]					16[1]				
U.S. Army M9A2	400[1]	280[1]									
U.S. Navy Mark B	140[1]	70[1]					190[1]				
U.S. Navy Mark B1	290[1]	190[1]									
British Mk II/L	28[7]							85[7]			
Canadian Mk II/L		20[1]	140[1]								
German FE41	24[3]	4[1, 3]	16[1]					55[3]	8[1, 3]	130[3]	12[3]
German FE41P	24[3]	4[3]						105[3]	32[3]		195[3]
German FE42	40[3]	4[3]						125[3]	12[3]	315[3]	70[3]
German FE42P	65[3]	8[3]						245[3]	70[3]		
German Civilian											
Japanese Army 99	12[2]	4[2]						24[2]	4[2]	55[2]	8[2]
Japanese Army 95	60[2]	4[2]						80[2]	8[2]	240[2]	28[2]
Japanese Navy 93	88[2]	8[2]			160[2]			225[2]	24[2]	535[2]	110[2]
Japanese Civilian								85[1]	17[1]		

Note. Superscript numbers refer to bibliographical references.

SECRET

TABLE 5. Comparison of CK protection to initial penetration and to lethal penetration.

Canister	% RH	Flow rate (lpm)	Influent concentration (mg per l)	Influent dosage (mg min per l) Initial penetration	Lethal penetration
U.S. Army M1A1	50–50	50	10	40	147[1]
U.S. Army M10	50–50	50	10	140	340[1]
U.S. Army M10A1	50–50	50	10	180	415[1]
U.S. Army M10A1	80–80	50	4	175	550[2]
U.S. Army M10A1	80–80	25	4	1000	1760[2]
U.S. Army MIXA1	50–50	50	10	40	180[1]
U.S. Army M9A2	50–50	50	10	320	547[1]
German FE41	50–50	50	10	20	95[1]
German FE41	0–80	50	4	24	85[3]
German FE41	80–80	50	4	4	30[3]
German FE41	0–80	25	4	55	150[3]
German FE41	80–80	25	4	4	60[3]
German FE41	0–80	12.5	4	170	290[3]
German FE41	80–80	12.5	4	12	160[3]
German FE41P	0–80	50	4	24	110[3]
German FE41P	80–80	50	4	4	80[3]
German FE41P	0–80	25	4	105	245[3]
German FE41P	80–80	25	4	32	170[3]
German FE42	0–80	50	4	40	145[3]
German FE42	80–80	50	4	4	50[3]
German FE42	0–80	25	4	125	255[3]
German FE42	80–80	25	4	12	110[3]
German FE42	0–80	12.5	4	315	490[3]
German FE42	80–80	12.5	4	70	380[3]
German FE42P	0–80	50	4	65	165[3]
German FE42P	80–80	50	4	8	100[3]
German FE42P	0–80	25	4	245	390[3]
German FE42P	80–80	25	4	70	284[3]
Japanese Army 99	0–80	50	4	12	90[2]
Japanese Army 99	80–80	50	4	4	30[1, 2]
Japanese Army 99	0–80	25	4	24	170[2]
Japanese Army 99	80–80	25	4	4	40[1, 2]
Japanese Army 99	0–80	12.5	4	55	310[2]
Japanese Army 99	80–80	12.5	4	8	85[1, 2]
Japanese Army 95	0–80	50	4	60	150[2]
Japanese Army 95	80–80	50	4	4	40[2]
Japanese Army 95	0–80	25	4	80	250[2]
Japanese Army 95	80–80	25	4	8	100[2]
Japanese Army 95	0–80	12.5	4	240	520[2]
Japanese Army 95	80–80	12.5	4	28	170[2]
Japanese Navy 93	0–80	50	4	90	205[2]
Japanese Navy 93	80–80	50	4	8	70[2]
Japanese Navy 93	0–80	25	4	225	395[2]
Japanese Navy 93	80–80	25	4	24	130[2]
Japanese Navy 93	0–80	12.5	4	535	785[2]
Japanese Navy 93	80–80	12.5	4	110	345[2]
Japanese Navy 93	0–80	50	1	48	120[2]
Japanese Navy 93	80–80	50	1	5	57[2]
Japanese Navy 93	0–80	50	20	160	320[2]
Japanese Navy 93	80–80	50	20	20	120[2]

Note. Superscript numbers refer to bibliographical references.

10 mg min per l, and 50-50 humidity conditions. The results are tabulated in Table 3. It is noted that, on the average, the protection to lethal penetration is 25 to 50% greater than the protection to the initial penetration. The data in Table 3 are for single tests; this explains the differences between the *Ct*'s to initial penetration given in Tables 2 and 3.

No results on desorption are available. It is well to point out, however, that under normal conditions of high moisture content, it is unlikely that appreci-

TABLE 6. Time for penetration of a lethal dosage of CK including desorption after various exposures. (Flow rate = 50 lpm.)

Canister	% RH	Influent concentration (mg per l)	Influent dosage (mg min per l)	Time to penetration of lethal dosage (min)
German FE42	0–80	4	88	55[3]
German FE42	0–80	4	100	44[3]
German FE42	0–80	4	128	34[3]
German FE42	80–80	4	32	15[3]
German FE42	80–80	4	38	12[3]
German FE42	80–80	4	44	10[3]
Japanese Army 99	0–80	4	45	45[2]
Japanese Army 99	80–80	4	19	12[2]
Japanese Army 95	0–80	4	46	54[2]
Japanese Army 95	80–80	4	21	16[2]
Japanese Navy 93	0–80	4	73	84[2]
Japanese Navy 93	0–80	1	80	140[2]
Japanese Navy 93	0–80	20	80	130[2]
Japanese Navy 93	80–80	4	31	26[2]
Japanese Navy 93	80–80	1	42	60[2]
Japanese Navy 93	80–80	20	29	30[2]

Note. Superscript numbers refer to bibliographical references.

able amounts of CG could be desorbed. Continued passage of air would probably remove only the hydrolysis products, HCl and CO_2.

It is obvious from these data that all canisters provide adequate protection against phosgene under normal conditions. The element of surprise must therefore be relied upon to a large degree in the offensive use of this agent.

11.2.2 Protection Against Cyanogen Chloride

The comparative CK protection afforded by allied and enemy canisters to the break points is summarized in Table 4. Average values are given in all cases. The superscripts refer to the bibliography of this chapter and represent the sources of these data. It should be noted that, when humidified, German and Japanese canisters are penetrated by harassing concentrations of CK after short exposures even at breathing rates corresponding to moderate exercise.

Comparisons of influent dosages required under a variety of conditions to produce initial penetration of harassing concentrations and those required for penetration of a lethal dosage (considered to be 10 mg min per l at concentrations exceeding 0.2 mg per l) are summarized in Table 5. In all cases the data under a given set of conditions are for single tests. In general, the protection to lethal penetration is several fold greater than the protection to initial penetration; this is particularly true at high humidities where protection to initial penetration is at a minimum.

Little or no desorption of CK is possible from exposed British Mk II/L, Canadian Mk II/L, German FE41P, or German FE42P canisters, or from exposed U. S. canisters which are filled with Type ASC whetlerite; the impregnants in these canisters destroy the CK. Desorption is possible, however, from exposed German FE41 and German FE42 canisters and from all Japanese canisters tested to date. Tests have therefore been conducted to determine the rate and extent of the effective desorption (concentration exceeding 0.2 mg per l). In Table 6 the results are summarized of a few tests to determine the time for the penetration of a lethal dosage including desorption after various exposures under a variety of conditions. Such a situation could be met in combat only if a CK attack is accompanied or followed by an attack with an agent which is at least semi-persistent, in order to insure continued wearing of the mask. All the tests given in Table 6 were performed at 50 lpm; considerably longer periods would be required at breathing rates corresponding to rest or moderate exercise.

It should be noted that the Germans were aware of the possibility of eliminating desorption of CK and increasing the protection against this agent by impregnation with pyridine or picoline. The canisters issued at the end of World War II contained pyridine. Some Japanese canisters are amenable to this method of improvement but it was not used by the Japanese. Both German and Japanese canister protections can

TABLE 7. Comparison of AC protection afforded by allied and enemy canisters to the break points.

	Influent dosages (mg min per l) required to the initial penetration of physiologically effective concentrations under various conditions							
	Flow rate, lpm							
	50	50	50	50	25	25	12.5	12.5
	Influent concentration, mg per l							
	4	4	20	40	4	4	4	4
	Relative humidity							
Canister	AR–80	80–80	80–80	80–80	AR–80	80–80	AR–80	80–80
U.S. Army M1	60[1]	25[1]						
U.S. Army M1A1	90[1]	90[1]						
U.S. Army M10	130[1]	130[1]	80					
U.S. Army M11	155[1]	155[1]						
U.S. Army M10A1	180[1]	180[1]	160[1]	160[1]				
U.S. Army MIXA1	140[1]	80[1]						
U.S. Army M9A1	300[1]	300[1]						
U.S. Navy Mark B	130[1]	140[1]						
U.S. Navy Mark B1	210[1]	210[1]						
British Mk II/L	28[7]							
Canadian Mk II/L	100[1]	90[1]						
German FE41	16[3]	10[13]			44[3]	24[3]	120[3]	36[3]
German FE41P		8[3]				28[3]		
German FE42	44[3]	56[3]			235[3]	275[3]	425[3]	530[3]
German FE42P		52[3]				235[3]		
Japanese Army 99	8[2]	4[2]			110[2]	12[2]	160[2]	75[2]
Japanese Army 95	12[2]	8[2]			36[2]	30[1, 2]	75[2]	70[2]
Japanese Navy 93	32[2]	12[2]			55[2]	35[1, 2]	160[2]	125[2]
Japanese Civilian					24[1]	25[1]		

Note. Superscript numbers refer to bibliographical references.

likewise be improved and desorption eliminated by impregnation with copper and chromium. Thus, it is obvious that for this reason, as well as those listed in the introduction of this chapter, the figures quoted in Tables 4, 5, 6, represent minimum CK protection afforded the enemy soldier at the advent of gas. Nevertheless, it is apparent that it would be very difficult to obtain CK casualties by canister penetration even at the present level of minimum protection, unless the enemy were attacked during periods of strenuous activity when his canisters were well humidified and replacement canisters were unavailable.

11.2.3 Protection Against Hydrogen Cyanide

A comparison of AC protection afforded by allied and enemy canisters to the break points for various conditions is given in Table 7. The superscripts again refer to the sources of the data. In general, the protection afforded by dry canisters to initial penetration is less against AC than against CK, and vice versa for humidified canisters; thus, the protection against AC is slightly better balanced. The Japanese Army 99 canister, containing Hopcalite, is an exception to this general rule; the protection afforded by this canister when dry is considerably greater than that afforded against CK.

Table 8 shows AC protection to initial penetration and to lethal penetration. In general, the factor of difference between influent dosage to these two types of penetration is less in the case of AC than in the case of CK. In other words, the rate of increase of effluent concentration with time is generally more rapid for AC than for CK. In many instances, the protection to lethal penetration is lower for AC than for CK at moderate breathing rates.

The results of a few penetration experiments, including desorption, are summarized in Table 9. Desorption from the German FE42 and Japanese Army 99 canisters is slow and limited. Desorption from German FE41 and Japanese 95 and 93 canisters is much more extensive and rapid. Little or no AC can be desorbed from Type ASC whetlerite or from charcoals impregnated with many other metal oxides, such as ZnO. Furthermore, as noted in the case of the Japanese Army 99 canister, Hopcalite eliminates or reduces this possibility and increases the protection.

TABLE 8. Comparison of AC protection to initial penetration and to lethal penetration.

Canister	% RH	Flow rate (lpm)	Influent concentration (mg per l)	Influent dosage (mg min per l) Initial penetration	Lethal penetration
U.S. Army M1A1	50–50	50	10	90	165[1]
U.S. Army M10	50–50	50	10	140	215[1]
U.S. Army M10A1	50–50	50	10	200	270[1]
U.S. Army M9A2	50–50	50	10	300	415[1]
German FE41	50–50	50	10	30	65[4]
German FE41	0–80	50	4	16	40[3]
German FE41	80–80	50	4	8	44[3]
German FE41	0–80	25	4	44	75[3]
German FE41	80–80	25	4	24	100[3]
German FE41	0–80	12.5	4	120	176[3]
German FE41	80–80	12.5	4	36	128[3]
German FE41P	80–80	50	4	8	44[3]
German FE41P	80–80	25	4	28	105[3]
German FE42	0–80	50	4	44	76[3]
German FE42	80–80	50	4	56	160[3]
German FE42	0–80	25	4	235	300[3]
German FE42	80–80	25	4	275	380[3]
German FE42	0–80	12.5	4	570	665[3]
German FE42	80–80	12.5	4	705	855[3]
German FE42P	80–80	50	4	52	120[3]
German FE42P	80–80	25	4	235	385[3]
Japanese Army 99	0–80	50	4	8	56[2]
Japanese Army 99	80–80	50	4	4	44[2]
Japanese Army 99	0–80	25	4	110	240[2]
Japanese Army 99	80–80	25	4	12	96[2]
Japanese Army 99	80–80	25	1	38	258[2]
Japanese Army 99	80–80	25	18	18	126[2]
Japanese Army 99	0–80	12.5	4	160	340[2]
Japanese Army 99	80–80	12.5	4	75	335[2]
Japanese Army 95	0–80	50	4	12	40[2]
Japanese Army 95	80–80	50	4	8	32[2]
Japanese Army 95	0–80	25	4	36	80[2]
Japanese Army 95	80–80	25	4	24	64[2]
Japanese Army 95	0–80	12.5	4	75	135[2]
Japanese Army 95	80–80	12.5	4	70	130[2]
Japanese Navy 93	0–80	50	4	32	60[2]
Japanese Navy 93	80–80	50	4	12	44[2]
Japanese Navy 93	0–80	25	4	75	125[2]
Japanese Navy 93	80–80	25	4	40	85[2]
Japanese Navy 93	0–80	12.5	4	160	220[2]
Japanese Navy 93	80–80	12.5	4	135	225[2]

Note. Superscript numbers refer to bibliographical references.

The Japanese auxiliary CO canisters would provide ample protection against this agent. In view of these remarks, it must be concluded that the Japanese would soon be able to increase protection against AC amply if the present protection were found to be inadequate at the advent of gas warfare.

11.2.4 Protection Against Chloropicrin

As stated in the introduction to this chapter, PS is considered only because test results with this agent offer an estimate of the protection which would be afforded against a semi-persistent agent whose destruction on charcoal by hydrolysis or other reaction is likely to be too slow to affect the dynamic retention.

Only a comparatively few breather tests have been performed with PS. The results of some of these tests are tabulated in Table 10 [1] for a cursory comparison of canisters. Because the protection is substantial for all canisters in spite of the strenuous conditions of the tests, it is obvious that all Allied or enemy canisters would provide more than adequate protection against agents like PS under normal combat conditions.



TABLE 9. Total AC penetration and time to the penetration of a lethal dosage including desorption after various exposures. (Influent concentration = 4 mg per l.)

Canister	% RH	Flow rate (lpm)	Influent dosage (mg min per l)	Time to penetration of lethal dosage (min)	Total penetration at concentration >0.1 mg per l (mg min per l)
German FE41	80–80	25	40		8.1
German FE42	0–80	50	60		1.9
German FE42	80–80	50	80		0
Japanese Army 99	80–80	25	80		3.0
Japanese Army 99	80–80	25	87	55	5.0
Japanese Army 99	80–80	25	100		8.3
Japanese Army 99	80–80	25	120		13.0
Japanese Army 99	80–80	25	140		19.0
Japanese Army 95	80–80	25	20		3.6
Japanese Army 95	80–80	25	24	65	5.0
Japanese Army 95	80–80	25	40		15.0
Japanese Army 95	80–80	25	80		41.3
Japanese Navy 93	80–80	25	20		2.2
Japanese Navy 93	80–80	25	25	38	5.0
Japanese Navy 93	80–80	25	40		15.0
Japanese Navy 93	80–80	25	60		27.5

TABLE 10. Comparison of PS protection afforded by enemy and allied canisters to the break points.

	Influent dosages (mg min per l) to initial penetration			
	Flow rate (lpm)			
	50	50	50	50
	Influent concentration (mg per l)			
	10	10	50	50
	Humidity			
Canister	AR–50	80–80	80–80	AR–50
U.S. Army M1A1	580	100		
U.S. Army M10	670	140		
U.S. Army M11	720	160		
U.S. Army M10A1	...	200		
U.S. Army MIXA1	800	200		
U.S. Army M9A2	1200	350		
British Mk II/L	330	...		
Canadian Mk II/L	...	160		
German FE41	...	...	600	
Japanese Army 99	...	450	...	1200

TABLE 11. Comparison of NO_2 protection afforded by allied and enemy canisters to the penetration of lethal dosages of NO.

	Influent NO_2 dosage (mg min per l) to penetration of a lethal dosage of NO					
	Flow rate (lpm)					
	32	32	16	32	32	16
	Influent concentration (mg per l)					
	4.3	4.3	4.3	21.4	21.4	21.4
	Humidity					
Canister	AR–50	80–50	80–50	AR–40	80–40	AR–40
U.S. Army M11	800	500	750	...	...	...
U.S. Army M10A1	1000	550	1250	550	310	1200
U.S. Army M9A1	1450	950	1500			
German FE42	750	400				
Japanese Army 99	375	270				

11.2.5 Protection Against Nitrogen Dioxide

NO_2 has frequently been proposed as a war gas because of its reduction to NO on charcoal and the early penetration of this product. A few tests have been run on U. S. and enemy canisters to determine the protection to penetration of lethal dosages (considered as 15 mg min per l at concentrations exceeding 0.24 mg per l), inasmuch as the effluent concentration of NO builds up slowly after initial penetration. The average results of these tests are summarized in Table 11.

The protection afforded by all canisters at moderate breathing rates and influent concentrations less than 1.5 mg per l is practically unlimited if the threshold concentration considered is correct. At these low influent concentrations, the effluent concentration of NO will not exceed 0.24 mg per l for very long periods of exposure.

Naturally, the presence of NO even at low concentrations will have a harassing effect, but the protection against serious injury to the respiratory tract is more than adequate for all canisters under normal conditions.

[redacted]

11.3 CONCLUSIONS

All U. S. canisters that are filled with Type ASC whetlerite and that are issued at present for combat use provide adequate protection against all known nonpersistent war gases. Indeed, the U. S. canisters provide better all-around protection than any canisters now issued by ally or enemy.

All Allied and enemy canisters afford ample protection against CG, NO_2, PS, or similar gases under normal conditions while German and Japanese canisters are most vulnerable against AC and CK.

Chapter 12

PROTECTION AGAINST CARBON MONOXIDE

By *Ralph N. Pease*

12.1 INTRODUCTION

IT HARDLY NEEDS to be emphasized that carbon monoxide is a potential hazard wherever air is contaminated with the products of incomplete combustion. Fires that are in enclosed spaces (a ship's hold, for example), gunfire (with high explosives generally), products from flame-throwers, and engine exhaust (particularly when rich mixtures are employed) may give rise to dangerous concentrations.

The situation is the more serious since the gas, being colorless and odorless, gives no real warning of its presence. The first physiological effects (headache, drowsiness, dizziness, nausea) may easily go unrecognized. Even if a simple, reliable chemical or physical test were available, there would still remain the problem of specifying a critical concentration under each set of conditions since variables such as exposure-time, activity of the subject, oxygen partial pressure, and similar factors must be taken into consideration. For practical purposes [4] the following table gives critical concentrations.

Concentration CO vol. %	Effect
0.01	No symptoms for 2 hours
0.04	No symptoms for 1 hour
0.06–0.07	Headache and unpleasant symptoms in 1 hour
0.10–0.12	Dangerous for 1 hour
0.35	Fatal in less than 1 hour

Values as low at 0.0025 to 0.0050% (25-50 ppm) have been specified as permissible upper limits under extreme conditions (high-altitude flight). In these circumstances, the only safe procedure would be to supply complete protection for personnel wherever there is a chance of exposure.

Such protection may be achieved in some cases either by efficient ventilation, provided this does not introduce new sources of the gas, or by the use of the relatively bulky oxygen helmet, especially when CO concentration may be high and oxygen concentration low, or where high oxygen content itself is essential. However, when mobility is a consideration and CO concentrations are not too great (less than 2%), the best solution is a suitable gas mask.

Such a mask must depend for its effectiveness on an efficient canister filling material. The subject was widely investigated during World War I.[5] Direct adsorption is apparently out of the question with known adsorbents, though there seems to be no reason why a synthetic analogue of haemoglobin may not ultimately be prepared. (Dried blood is of no use.) Several oxidants have been evolved, such as "hoolamite" (I_2O_5 + fuming H_2SO_4), silver permanganate, and some oxide mixtures. Most successful solution of the problem was the development of Hopcalite catalyst, which utilizes oxygen of the air for oxidation of CO. Hopcalite is a mixture of MnO_2 with other oxides, particularly CuO. It has become a universal standard material in CO canisters.

12.1.1 Hopcalite

Hopcalite is an extraordinarily active catalyst. Properly prepared and used, it can give almost complete protection at a space-velocity (hours) as high as 50,000 at room temperature. This is roughly equivalent to passage of contaminated air (dry) at 2 lpm through a layer of 2.5 cc of catalyst. Unfortunately, Hopcalite has several undesirable characteristics. Since it is prepared from finely divided, precipitated hydrous oxides, the catalyst granules are often soft and friable. More serious is its high sensitivity to poisoning by water vapor, which necessitates the use of a pre-drier. Further, Hopcalite does not completely remove CO at temperatures below 0 degree C, though it still shows some activity as low as −79 C. Finally, as an inevitable consequence of the high heat of oxidation of CO (67,600 cal per mole) exceptionally high-temperature rises result from its use (98 C for only 1% CO). Efforts have been directed at reducing some of these limitations.

12.1.2 Charcalite Drier [1]

The advantage in long life which might be expected to accrue from use of Hopcalite catalyst is largely lost in practice because of poisoning by water vapor. Effective life then depends on the efficiency of the pre-drier. For this purpose, $CaCl_2$ granules and silica gel have usually been employed. However, the former

is unsatisfactory because drying is never complete, and liquefaction of the granules at high humidities leads to the danger of channeling. Silica gel, though more efficient initially, has relatively short life and tends to swell and crack on wetting.

In searching for an improved pre-drier, advantage has been taken of the tremendous surface, per unit volume, of activated charcoal. Charcoal itself is not a good drying agent, though its ultimate capacity is large. A surface coating of high moisture retentivity is obviously needed. After several trials $CaCl_2$ was chosen for the purpose, with HPO_3, $MgCl_2$, or $ZnCl_2$ as alternatives. Distributed thinly over the charcoal surface, (perhaps in a unimolecular layer) its residual aqueous tension is reduced far below that of the salt in bulk. The best charcoals for the purpose proved to be a series of $ZnCl_2$-activated products manufactured by National Carbon Company; for example, CWSN 177 B3. These charcoals combine exceptionally large surfaces and pore volumes (average density about 0.25 to 0.30 g per cc). They take up not only a maximum quantity of impregnating solution, but also retain saturated solution satisfactorily during use in drying. That the salt is well dispersed through the charcoal is indicated by the fact that a product containing 40% by weight $CaCl_2$ is still coal-black except for occasional white flecks of effloresced salt.

Charcalite has about twice the effective life of $CaCl_2$ granules, and 4 to 5 times the life of silica or alumina gel. In a layer 2.5 cm deep by a 4-sq cm section at 25 C, with air at 2 lpm, and 50% RH (11.5 mg H_2O per l) there is no detectable escape (condensation at −79 C) for perhaps 30 min, a cumulative total of 50 mg H_2O in 70 min, and of 400 mg (the effective life) in 130 min. Overall, a total of nearly 3 g of water would have been retained by 10 cc apparent volume of Charcalite. Protection is proportionately as good over a range of conditions, except that at higher temperatures (toward 50 C) there is a considerable loss in retentivity, though not relative to either $CaCl_2$ granules or silica gel. At these higher temperatures, HPO_3-impregnated charcoals have a marked advantage.

Incidentally, it is of interest to find that Hopcalite catalyst itself is superior to silica gel as a drier. This is in harmony with the known poisoning action of water vapor.

The general method of preparing Charcalite includes soaking active charcoal in 40% by weight $CaCl_2$ solution and then draining, and drying. In the last operation the material is first oven-dried at 110 C with frequent mixing to prevent efflorescence. Subsequently, it is heated to about 250 C in a large flask until the water content is 2% or less. (The charge catches fire in air at 180 C or above.) An essentially similar process was employed successfully for large-scale production.

12.1.3 Gel-Type Hopcalite [2]

The many shortcomings of Hopcalite have already been noted. The method of preparation developed during World War I involves the addition at 50 to 70 C of solid $KMnO_4$ to a strong solution of H_2SO_4 containing $MnSO_4$. This is said to form manganese disulfate. On pouring the solution into water, a finely divided precipitate of hydrated MnO_2 (containing some excess oxygen) is formed. This is washed by decantation until free of sulfate. Copper (or other metal) basic carbonate or hydroxide is precipitated in the suspension, or separately. After mixing and further washing, the precipitate is filtered off, dried, compressed, and meshed.

It has been found that under certain conditions it is possible to obtain the product in the form of a gel. First experiments utilized solutions of $NaMnO_4$, which is far more soluble than the potassium salt. When it became apparent that this salt was not available in quantity, the method was altered so that solid $KMnO_4$ could be employed. It was found that a similar hard product was obtained by the following procedure.

To a solution of 4 moles H_2SO_4 and 16 moles H_2O one-quarter mole of $MnSO_4$ is added. This is heated to 50 to 70 C; then three-quarter mole of $KMnO_4$ (solid) is added slowly (temperature tends to rise) with vigorous stirring. This mixture is poured into 40 liters of cool, distilled water. A very bulky flocculent precipitate separates after a minute or two. The precipitate is washed free of sulfate and filtered. After drying, this yields hard granules of high activity without compressing. If copper is to be added, the basic carbonate is separately precipitated from Na_2CO_3 and $CuSO_4$ solutions, and the suspended precipitates mixed after washing. Again a hard active product results. This catalyst shows less sensitivity to water vapor than commercial grades under certain conditions.

One variant containing silver and palladium in the atomic ratio 3Mn:2Ag:1Pd is exceptionally active, and was considered for use in detector equipment. Attempts were made to obtain large-scale prepara-

tion but these failed to give active products. It was found that heat effects due to adsorption-desorption of carbon dioxide were especially troublesome with this catalyst (perhaps because of its silver content) in connection with detector operation, and the development was dropped.

The question of thermal activation subsequent to actual precipitation and washing is an important one. It might be assumed that the sole requirement is reduction in water content, but this proves to be only partially true. Samples dried at 110 C and containing as much as 20% of H_2O have appreciable activity, whereas samples heated to 400 C, and containing less than 1% of H_2O are relatively inactive. Furthermore, a sample deliberately dried in a stream of humid air (50% RH at 25 C) at 350 C, is found to be inactive even though water content is low. Other samples dried in open flasks at 300 to 400 C are also of low activity. Optimum activity is obtained only when a lively stream of dry air is applied, or when the sample is thoroughly evacuated (Langmuir pump); this only when temperature is below 350 C.

It seems fairly clear that the residual moisture content of the atmosphere surrounding the particles is a factor, though the reason is not obvious. Possibly it is a question of crystal growth. The available oxygen content (as MnO_2) does not prove a satisfactory index of activity. Many active samples, especially after vacuum treatment, run as low as 75% available oxygen. On the other hand, totally inactive commercial MnO_2 powder registers 100%. Surface determinations (N_2 adsorption by the Emmett-Brunauer method) show some correlation with activity (especially after higher temperature treatment) but not in any simple proportion. The precise sort of surface alteration involved remains a mystery.

It seems quite definite that pronounced improvement in both the hardness and the activity of commercial Hopcalite can be attained. Formation of gel-type products is merely a question of altering concentrations in the preparation of MnO_2. As to effectiveness of thermal activation and drying, commercial lots of Hopcalite sometimes contain as high as 5% of H_2O. The customary oven-drying at 200 to 250 C reduces this only moderately, depending on atmospheric humidity. For optimum activity a figure below 1% must be attained. This requires higher temperatures and closer control of drying conditions as well as subsequent protection from moist air in the canister filling operation. Just how much improvement in practice may be made remains to be seen, but experience with break-down tests indicates there is a large margin.

12.2 CARBON MONOXIDE REAGENTS

Over against the MnO_2-base Hopcalite catalysts are substances which oxidize carbon monoxide at the expense of their own oxygen. Two such catalysts, silver peroxide and silver permanganate, have received some attention in England and Canada and merit consideration.

Silver Peroxide

This catalyst is prepared by adding silver nitrate to an alkaline solution of potassium persulfate containing a little manganous sulfate, which is said to act as a stabilizer. The precipitate may be combined with shredded asbestos for preparation of granules. These granules remove CO from air, for a time, at a rate comparable to that of Hopcalite. A marked advantage is their insensitivity to water vapor. Disadvantages are their thermal instability, and the extremely large weights of silver required.

Silver Permanganate

This catalyst is easily prepared by precipitation from solutions of $AgNO_3$ and $KMnO_4$. It has been combined with $CaCl_2$ and CaO, or with kieselguhr, before compressing into granules. Such granules also remove CO from air at a rate comparable to Hopcalite, and have the advantage of water insensitivity, although thermal instability is again a handicap.

It may be noted that the preparation in which $CaCl_2$ and CaO are incorporated dry with $AgMnO_4$ yields a markedly more active product, but one which is less stable at higher temperatures than that in which $AgMnO_4$ is mixed with kieselguhr. It remains to be seen whether a suitable compromise between activity and stability can be achieved.

12.3 CANISTER DEVELOPMENT

There was at one time a demand for an assault-type canister for use of LST personnel. Development was undertaken by the CWS Development Laboratory, Massachusetts Institute of Technology. Ultimately it was determined that about 160 cc Hopcalite and 90 cc Charcalite in an M11 assault canister would give the protection required for a 30-min period.

Another matter, at one time believed to be a pressing one, concerned the protection of aircraft personnel. It was suggested by the Bureau of Navigation, U. S.

Navy, that a unit might be developed as an adjunct to diluter-demand oxygen regulator equipment. Exact requirements were not specified but a long life (up to 5 hr) was indicated. Pressure drop had to be low, breathing rates and CO concentrations were not to be high, and allowance was to be made for a wide range of temperature. After some experimentation,[3] it was concluded that a unit of 80 sq cm cross section (or larger) containing about 150 cc Hopcalite and 300 cc Charcalite, would be suitable. It was also shown that a mixed filling might be employed, though with some loss in life. Such a canister would protect for 5 hr from −30 to 0 C up to 0.01% of CO or less against an influent concentration of 0.05% of CO at 15 lpm.

In both these cases it is understood that the problem was ultimately solved by improved ventilation.

Chapter 13

CRITICISMS AND RECOMMENDATIONS

By *W. Conway Pierce*

13.1 INTRODUCTION

THE PRECEDING CHAPTERS of this report were largely written in the period February to June 1945, and they reflect, therefore, the viewpoints held while World War II was still in progress. The present chapter is written in 1946, as the report goes to press. At this time it seems proper to review briefly the accomplishments in gas mask development made during the war period and to point out some of the things that were left undone. Such a résumé may be of use at some future date, even though the problems of the future promise to be very different than those of the present because of the development of the atomic bomb.

In this section the writer will, as in preceding sections, treat the Service and NDRC work as a unit, since in many instances the problems were attacked jointly.

In discussing the deficiencies of the program, the remarks will necessarily represent the writer's personal opinion, which in some instances at least will be conjectural, since gas warfare was not used. Exception may be taken to some statements, since frequently the all-too-meager data are subject to various interpretations. These comments are offered, therefore, as the basis for discussion and with the hope that such discussion may lead to further improvement in the U. S. gas mask.

13.2 ACCOMPLISHMENTS

A brief review may be made of the accomplishments in gas protection during the war period.

1. Two types of domestic charcoal, from wood and coal, were developed and put into large-scale production, replacing coconut charcoal. These domestic charcoals were not only more available and cheaper than nut charcoal; they were, after impregnation, decidedly superior in gas protection.

2. New impregnants were developed which, when used with the domestic charcoals, gave an adsorbent that furnished complete protection against all known war gases, both dry and humidified.

3. A lightweight mask was developed with the canister attached directly to the facepiece, thereby eliminating need for a hosetube.

4. Lighter and more efficient canisters were developed.

5. Protection against aerosols was improved by development of asbestos-incorporated and asbestos-impregnated filters. All the later model canisters, M9A2, M10, M10A1 and M11, had asbestos filters.

6. A single sheet, folded, asbestos-incorporated filter of high efficiency and low resistance was developed. This made possible the development of the axial-flow M11 canister which was directly mounted on the facepiece. It is reported that the Germans considered the M11 to be the best canister they had examined.

7. Many components of the gas mask, such as the eye lenses and the outlet valve, were improved.

8. Methods for testing the performance of adsorbents, filters and completed canisters were made more realistic and rigorous. As a result, the overall standards for procurement were raised.

9. Advances were made in theoretical knowledge of the factors which govern the removal of gases and aerosols by gas mask canisters.

10. Useful studies were made of the relation of the surface structure of charcoal to adsorption, retentivity, and effectiveness as a carrier for chemical agents. Knowledge was gained concerning the activation process and the variables which affect the nature of the charcoal surface.

11. Extensive studies were made of the aging of impregnated charcoal under a variety of storage and use conditions. These studies led to the development of adsorbents whose field life was increased, and to better methods for packaging masks and canisters. Improved laboratory methods for surveillance were developed.

12. A better understanding was gained of the extent to which water is adsorbed by impregnated charcoal and of the effect which this adsorbed water has on gas protection.

13. Studies were made of the mechanism of removal of the important war gases by impregnated charcoal and of the possibility of "poisoning" the adsorbent by one gas so that the canister may be

penetrated readily by a second gas. It was concluded that present ASC charcoal is not poisoned by any known gas and that the U. S. canisters are not vulnerable to such a sequence of gas attacks.

14. Extensive comparisons were made of the gas protection of U. S. and foreign gas mask canisters. It was found that, in overall protection under a variety of conditions, U. S. canisters are superior to corresponding types of foreign canisters.

15. A superior drying agent, Charcalite, was developed for use in carbon monoxide canisters to protect the Hopcalite catalyst against the poisoning action of water vapor.

13.3 CRITICISMS

The accomplishments of the war period, listed in part in the preceding section, are a source of satisfaction to all who participated in the gas defense program. But despite these developments and improvements, criticisms may be made of the overall program and of the status of gas protection at the close of the war.

Perhaps the major criticism is that it has never been possible, because of manpower shortages and organizational difficulties, to provide truly adequate field tests of gas masks under conditions that might prevail if gas warfare were employed. The only field tests made during the war were limited in scope and usually designed to test some particular item. In combat operations, the gas masks were usually discarded as soon as it was found that the enemy was not using gas.

It is felt that much useful information might have been gained by the establishment of a test unit whose sole duty was to use anti-gas equipment in field operations under simulated gas warfare conditions. Such a unit was formed in 1918. Despite the fact that actual gas warfare was used then, the reports made at that time indicate that information gained from the field test unit was a great help in solving problems of design and use of masks.

Because of the lack of adequate field testing, there are many questions concerning gas masks which are not yet completely answered. Some of these may be listed:

1. Which is the better mask for all-round use, a hosetube or facepiece canister type? Certainly the latter is preferable on the basis of lightness and freedom from interference. But if it becomes necessary to wear masks continuously for 12 to 36 hours, which mask is preferred?

2. For all-round use is it better to mount the canister on the cheek, as in the combat mask, or on the snout, as in the German mask? Each position may be superior for certain requirements.

3. What degree of waterproofing of the canister is needed by combat troops operating under various conditions, such as living in the jungle and landing from boats? Will the waterproofing devices now provided prove adequate under various field conditions? The writer suspects that they are not adequate, particularly for the M3–10A1–6 mask.

4. Does the M7 carrier for the combat mask provide adequate protection for the canister? Will this carrier stand up under severe usage? Will it maintain its waterproofing? Should a fragile canister, such as the M11, be provided with a metal carrier to protect it against damage?

5. What is the tolerance of well-trained troops to prolonged wear of a mask under jungle warfare conditions? To what extent does the wearing of masks reduce the efficiency of trained men operating as in jungle warfare? Tests by the Medical Division indicate that under tropical conditions the tolerance for a mask is very limited.

6. How much of a handicap to vision is imposed by present masks, for men at various types of activity?

7. Of how much importance is the canister breathing resistance? Will a reduction of resistance by 30 to 40 mm decrease the amount of fatigue caused by wearing the mask? (It has been reported by participants in the jungle trials at Innisfall that if the aerosol filter is removed from a British canister the mask is much more comfortable to wear.) What limits should be set for the breathing resistance of the mask, both for inhalation and for exhalation?

8. How important are the weight and bulk of the mask?

9. If troops are forced to don masks after several days under combat conditions, what is the incidence of serious facepiece leakage because of dirt and beards?

10. How important is it to have better speech transmission? Should all masks be of a diaphragm type?

11. Will freezing of valves cause trouble if masks are used intermittently by troops operating at subzero temperatures?

12. Are nose cups desirable?

13. Is it possible to fight effectively in a tropical

climate while wearing a mask and full protective clothing? If not, the plans for distribution and use of clothing should be modified.

When conclusive answers are obtained for these questions it will then be possible to delineate more definitely than at present the objectives which should be sought in the design of the gas mask and accessory equipment.

13.4 RECOMMENDATIONS

The whole question of gas and aerosol protection is, at this time, very much confused. The lack of gas warfare in World War II, the possibility of deadly aerosols such as bacteria or radioactive dusts, and the certainty that future wars will be fought with different weapons than in the past, all combine to make it impossible to make a clear statement of future objectives. Some would advocate making the mask as impenetrable as possible, perhaps going so far as to recommend self-contained units with oxygen supply. Others feel that it is not possible to protect against all possible hazards and that a considered risk should be taken in order to make the mask as light and comfortable as possible.

In view of present uncertainty, it is believed that immediate development should be focused on improving the comfort of the mask, keeping the standards of protection about as in the M4–11–7 unit. When a thoroughly satisfactory mask has been developed along these lines, it will be possible to make a better evaluation of the overall policy regarding protection against hypothetical agents of future wars. If such a development is undertaken, the following points should be considered.

1. Placement of canister, on cheek or snout.
2. Improvement of vision.
3. Improvement of speech transmission.
4. Use of mustard resistant facepiece materials.
5. Waterproofing.
6. Light weight of complete assembly.
7. Facepiece leakage.
8. Ease of carrying the mask.

PART II

MICROMETEOROLOGY AND THE BEHAVIOR OF CHEMICAL WARFARE GAS CLOUDS

Chapter 14

GENERAL METEOROLOGICAL PRINCIPLES

By *Wendell M. Latimer*

14.1 ATMOSPHERIC STABILITY

14.1.1 General Principles

AIR IS in a stable state of equilibrium when a volume of the air, which is displaced a small distance up or down, tends to return to its original position. Unstable air, when displaced upward, is acted upon by forces which tend to accelerate it in the direction of the impulse, while stable air is decelerated. The acceleration, which acts upon a volume of unstable air, depends upon the difference in density between it and its surrounding air; but since air is a compressible medium, changes in pressure and temperature occur, so that the difference in density of both the displaced volume and its surrounding air vary from the initial conditions. When resulting temperature changes cause condensation of aqueous vapor, the heat of vaporization is liberated and the density changes are further complicated by this heat.

Atmospheric pressure decreases with increasing elevation and from the first law of thermodynamics

$$dT = \frac{dQ}{C_p} + \frac{RT}{C_p}\frac{dp}{p}, \qquad (1)$$

where T is absolute temperature, Q the heat added to the system, R the gas constant, C_p the specific heat of the air at constant pressure, and p is the air pressure. If no heat flows in or out of the system, $dQ = 0$ and the process is called *adiabatic*. Then

$$T = T_0\left(\frac{p}{p_0}\right)^{(C_p - C_v)/C_p}, \qquad (2)$$

where C_v is the specific heat at constant volume. From the average decrease of pressure with altitude, the rate of change of temperature for the adiabatic transfer of air from low levels to higher levels is about 1 degree C per 100 m or 5.4 degrees F per 1,000 ft. This is known as the *adiabatic lapse rate.*

The condition for the stability of dry air is not that the density must decrease and the temperature increase with altitude, but that the temperature shall not decrease more rapidly than the dry adiabatic lapse rate.

The normal lapse rate, that is, the normal decrease of temperature with altitude, is about 3.3 degrees F per 1,000 ft. An air mass with this lapse is stable, as is indicated in Figure 1.

To interpret Figure 1, let a volume of air be taken from the level k to the level l. If it is dry air (or air which will not become saturated in the process) its temperature decreases by the adiabatic rate, that is, line lk is parallel to line CD. Its temperature at l is less than that of the surrounding air which has a temperature corresponding to m. Therefore its density is greater than that of the surrounding air, and

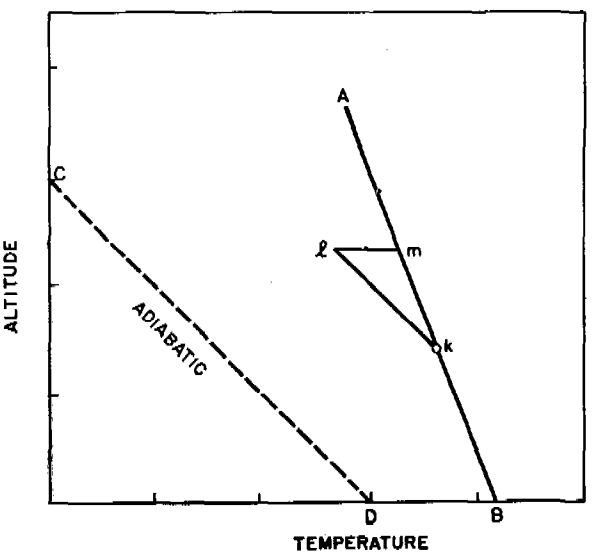


FIGURE 1. Relation of stability to lapse rate.

the displaced mass tends to return to its original level. If the rate of decrease of temperature with increase in altitude for AB had been greater than for CD, the temperature at l would have been warmer than that of its environment and the air mass would have been unstable.

The dependence of the lapse rate upon the rate of fall of pressure has been indicated in the last paragraph. However, there is an interdependence of the two factors as indicated by the following argument.

The rate of fall of pressure with height is proportional to the density d.

$$\frac{dp}{dz} = -gd, \qquad (3)$$

where g is the acceleration due to gravity. But for a

gas $d = p/RT$, and if the temperature were constant at all heights, by integration

$$\log \frac{p}{p_0} = \frac{gz}{RT} . \tag{4}$$

Actually, however, temperature falls off and may be represented usually by a straight line function

$$T = T_0 - az, \tag{5}$$

where T_0 is the ground temperature (absolute). Hence

$$\log \frac{p}{p_0} = \frac{g}{aR} \log \frac{T - az}{T_0} = \frac{g}{aR} \log \frac{T}{T_0} . \tag{6}$$

In dealing with air masses which are subject to changes in both temperature and pressure, it is convenient to have some standard reference condition for the sake of comparisons. Such a factor is the *potential temperature* Θ, which is defined as the temperature the air would have if brought adiabatically to a standard pressure (1,000 millibars). From equation (2)

$$\Theta = T \left(\frac{1000}{p} \right)^{(C_p - C_v)/C_p} . \tag{7}$$

At 25 C the specific heats of dry air are $C_p = 0.2396$ and $C_v = 0.1707$ cal per g. Hence

$$\frac{C_p - C_v}{C_p} = 0.288. \tag{8}$$

Atmospheric stability may be defined in terms of potential temperature.

For stability, the potential temperature must decrease with height. For instability, the potential temperature must increase with height.

14.1.2 Moist Air Stability

The criteria for the stability of dry air apply with sufficient accuracy to moist air, even though there is a slight difference in the specific heat values, as long as the movement of the air fails to produce saturation. The value for the saturated adiabatic lapse rate depends upon the temperature and pressure of the air but is not simply related to the altitude. A number of graphical thermodynamical methods are in use for solving problems involving ascending saturated air. An example of such is the aerogram. In this method $\log T$ as abscissa is plotted against $T \log p$ as ordinate. Isotherms are shown as vertical lines and isobars as nearly horizontal lines. The graph has three sets of lines: (1) constant, maximum, specific humidity (dew point lines), (2) dry adiabatic, and (3) moist adiabatic. At low temperatures and low pressures, lines (2) and (3) are nearly parallel but they diverge greatly at high temperatures and pressures.

By means of such a diagram measurements of temperature and relative humidity permit the calculation of the level at which ascending moist air will form a cloud and also the thickness of the cloud. Since the purpose of this discussion is to give a foundation for consideration of problems on the earth's surface, it is not necessary to amplify the problem of saturated air and cloud formation. Reference should be made to a standard text.[12]

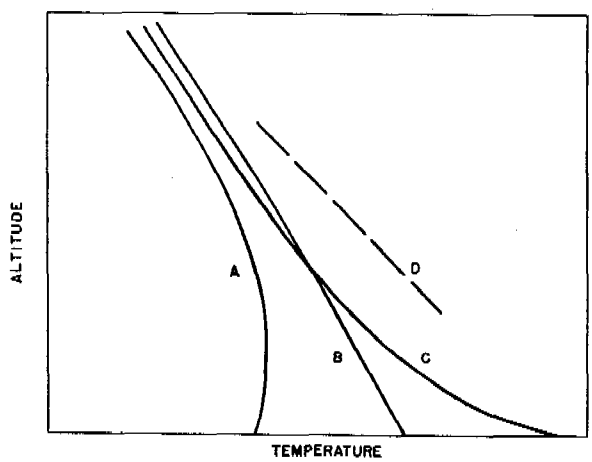


FIGURE 2. Diurnal variation in air temperature near the ground; (A) night; (B) evening; (C) midday; (D) day-adiabatic.

The arguments in the previous paragraphs have assumed that a volume of air could be displaced vertically without disturbing its environment. Actually an ascending current is normally balanced by a descending current. The coexistence of such adjacent currents modify somewhat the conditions for stability. They give rise to *solenoid-producing* terms. These do not greatly affect dry air problems but do lead to slight changes in the criteria for the stability of saturated air.

14.2 METEOROLOGY OF THE GROUND LAYER

The layer of air near the ground tends to assume the ground temperature. The large diurnal heating and cooling of the earth's surface is thus accompanied by corresponding changes in the air next to the surface. These effects are illustrated in Figure 2 and Figure 3.

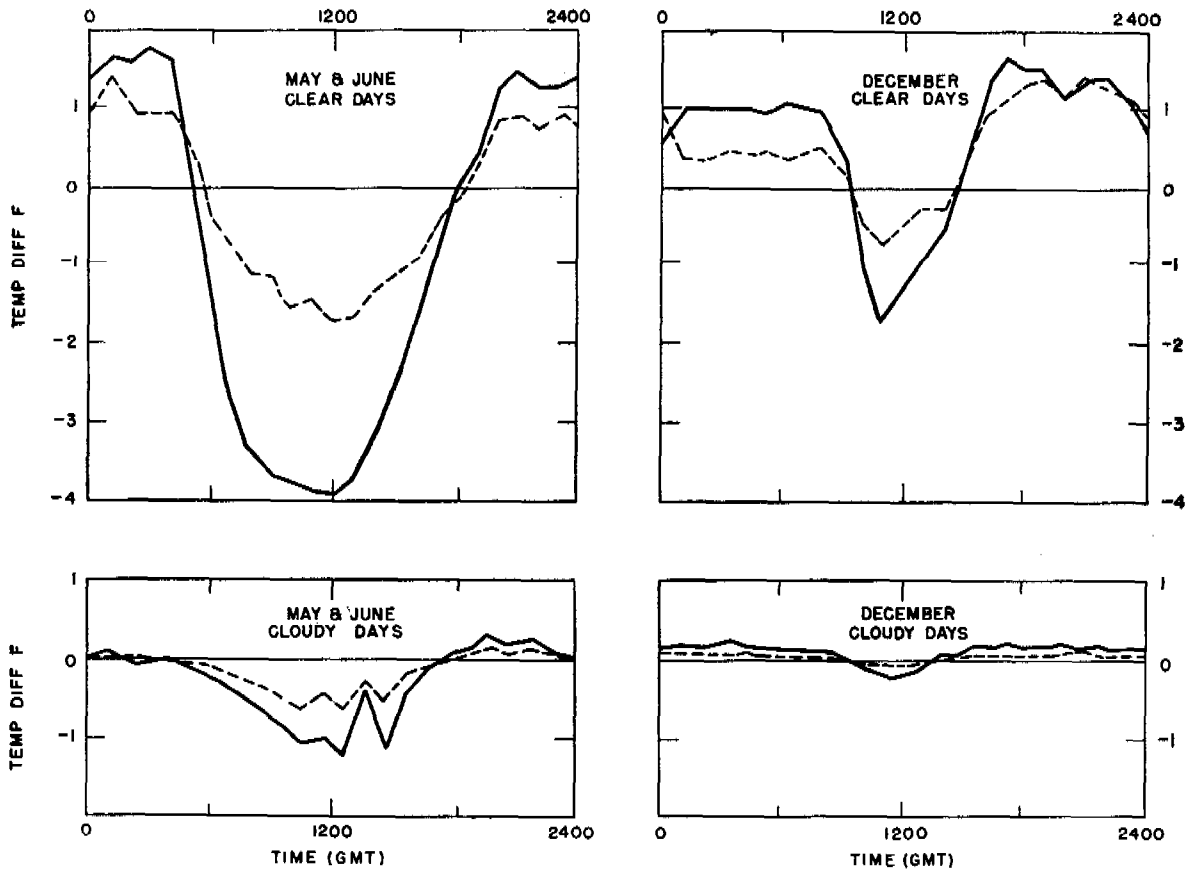


FIGURE 3. Mean diurnal curves showing temperature differences over the height intervals 2.5 to 30 cm (full line) and 30 cm to 1.2 m (dashed line) on clear and cloudy days in summer and winter (after Best).

The very high ground temperatures in midday and early afternoon give rise to temperature gradients in the air which are in excess of the dry-adiabatic lapse rate. These conditions are referred to as *superadiabatic lapse* or often as high lapse or strong lapse. As the ground cools at night the temperature gradient of the air near the ground inverts from the normal decrease with height to an increase with height. This condition is referred to as *inversion*. A cross-over occurs in the morning and evening where there are zero or normal lapse gradients; these are known as *neutral conditions*.

14.3 FACTORS INFLUENCING TEMPERATURE GRADIENTS NEAR THE GROUND

14.3.1 Radiation Effects

The mean energy of solar radiation just outside the earth's atmosphere is given as 1.93 cal per min per sq cm. On the average, 38% of the incoming radiation is scattered or reflected back into space. This reflection is due to such surfaces as dust clouds or earth's surface and for any region is subject to considerable variation. Thus, clouds and snow-covered ground may reflect 80% of the radiation, and the reflection from water surfaces is much greater than from the ground.

Most of the sun's radiation lies within the limits of wavelengths 0.2 to 3 μ, about half within the visible range 0.4 to 0.7 μ and half on the infrared side of the visible. The absorption by oxygen and nitrogen molecules is negligible except in the ultraviolet below 0.3 μ. Most of this appears to be due to atomic oxygen at 100-km levels and to ozone around the 40-km level. Carbon dioxide absorbs in a narrow band around 15 μ. The absorption of water vapor lies in the region 5 to 8 μ and 15 μ to longer wavelengths.

Since both the CO_2 and H_2O vapor absorption regions are so far out in the infrared, these absorptions do not remove an appreciable amount of energy from

the direct solar radiation, but they do play an important part in both the emission and absorption of atmospheric-temperature radiation.

Because the average yearly temperature of the earth is fairly constant and the amount of solar energy absorbed by vegetation is a small fraction, it follows that the energy of the temperature (black body) radiation of the earth's surface and atmosphere must be approximately equal to the amount of solar radiant energy.

From the Stefan-Boltzmann equation,

$$E = 8.22 \times 10^{-11} T^4, \tag{9}$$

the effective black-body temperature of the earth as a radiator to space may be calculated. Using 38% as the loss of solar energy by reflection and dividing by 4, the ratio of the area of the surface of a sphere to the area of a circle, we have

$$\frac{0.62 \times 1.93}{4} = 8.22 \times 10^{-11} T^4$$

or

$$T = 246 \text{ K}.$$

This value is too low by about 40 degrees C. The assumption that the earth radiates as a black body is far from exact, and the actual value of the temperature should be higher than that calculated. Moreover,

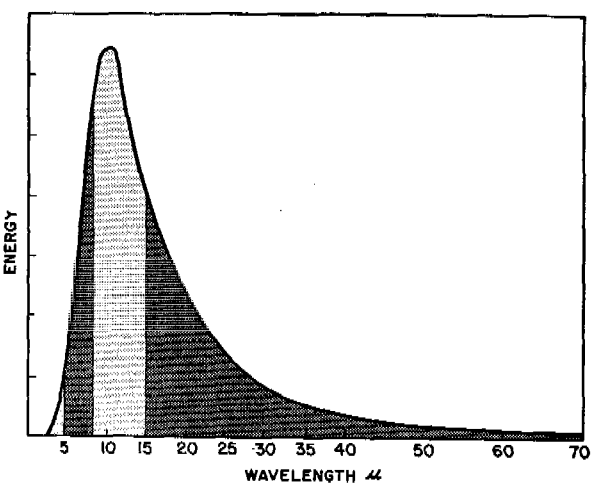


FIGURE 4. Energy distribution in black-body radiation at 300 K. Shaded portions are regions of water-vapor absorption.

the earth's temperature is dependent upon evaporation, condensation, and turbulent wind convection; these factors are also involved in the departure from black-body conditions.

Since the wavelength of maximum energy in black-body radiation is inversely proportional to the absolute temperature, and since the ratio of the temperatures of the sun and earth is about 20 (that is, 6,000/300), the maximum energy of the earth's black-body radiation lies around 10 μ. This is in the region of the water vapor bands and much of the outward radiation from the earth's surface is therefore absorbed by the atmospheric water vapor (see Figure 4). However, it is noted that there is a transparent region in water vapor between 8 and 15 μ, and it follows that an appreciable fraction of the radiation is transmitted.

The water vapor and carbon dioxide of the atmosphere emit radiation in the same regions in which they absorb. This gives rise to an atmospheric radiation back to the earth's surface which is highly important. If the temperature of the atmosphere is much colder than the earth's surface, the atmospheric radiation is small in comparison to that of the surface because of the T^4 dependence of the energy, but if the temperatures are nearly the same, as they normally are, they differ only by the amount of radiation transmitted by the water vapor in the 8 to 15 μ region.

With clear skies the incoming atmospheric radiation (sky radiation) is between 50 and 85% of the black-body value corresponding to the temperature of the air near the ground. The variations are largely due to changes in the relative humidity or weight of water in the air, but the total pressure and temperature differences in the upper atmosphere are also factors.

Various formulas have been proposed to calculate the sky radiation. Angstrom gave

$$\frac{R}{F_b} = 0.806 - 0.236 \times 10^{-0.052e}, \tag{10}$$

where R is the incoming radiation, F_b the black-body radiation at the temperature of the air near the ground, and e is water vapor pressure in millibars. Brunt found that the experimental data are quite accurately expressed by the equation

$$\frac{R}{F_b} = 0.526 + 0.065\sqrt{e}.$$

Rabitzsch wrote

$$\frac{R}{F_b} = \frac{0.135p + 6.0e}{T}, \tag{11}$$

where p is air pressure in millibars and T is absolute temperature.

Taking as an example the set of conditions, $p = 1{,}000$, $e = 15$, and $T = 300$, one may calculate from equation (11) $R/F_b = 0.75$. F_b at 300 K is 0.60

cal per cm per min. Hence R, the sky radiation, is 0.45 cal per min per sq cm and the effective outward radiation of a black body on the earth's surface would be 0.60 − 0.45 = 0.15 cal per min per sq cm.

For the same set of data, Brunt's equation would give:

$$\frac{R}{F_b} = 0.526 + 0.065\sqrt{15} = 0.78 .$$

Angstrom and Asklof have shown that there is a simple linear relation between the effective outward radiation when the sky is clear, R_0, and when the fraction $w/10$ of the sky is overcast, R_w;

$$R_w = R_0\left(1 - \frac{kw}{10}\right). \qquad (12)$$

The value of k depends upon the type of cloud: for low clouds 1 to 2 km above the ground (stratus, nimbus, stratocumulus) $k = 0.9$; middle clouds (altostratus at 3 km) $k = 0.7$; very high clouds (cirrostratus and cirrus, at about 7 km) $k = 0.2$.

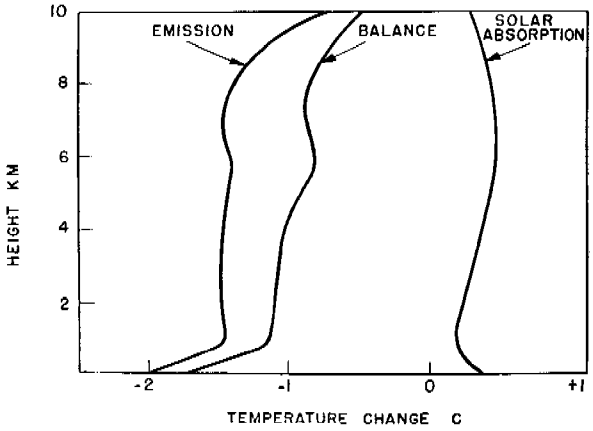


FIGURE 5. Heat balance of the free air over Ludenberg in June, clear sky (after Möller).

The atmospheric counterradiation must depend upon the mass of the atmosphere and therefore decrease with elevation. Angstrom gave the following data, but it should be kept in mind that they represent average conditions and are subject to variation with changes in temperature and humidity.

Elevation, meters	0	1,000	2,000	3,000	4,000	5,000
Counterradiation, cal per min per sq cm	0.44	0.37	0.31	0.25	0.21	0.18

The net outward radiation also depends upon elevation. Absorption diminishes as the amount of water vapor in the atmosphere (above) decreases, but at the same time the outward radiation decreases as the water vapor decreases, and also as the temperature

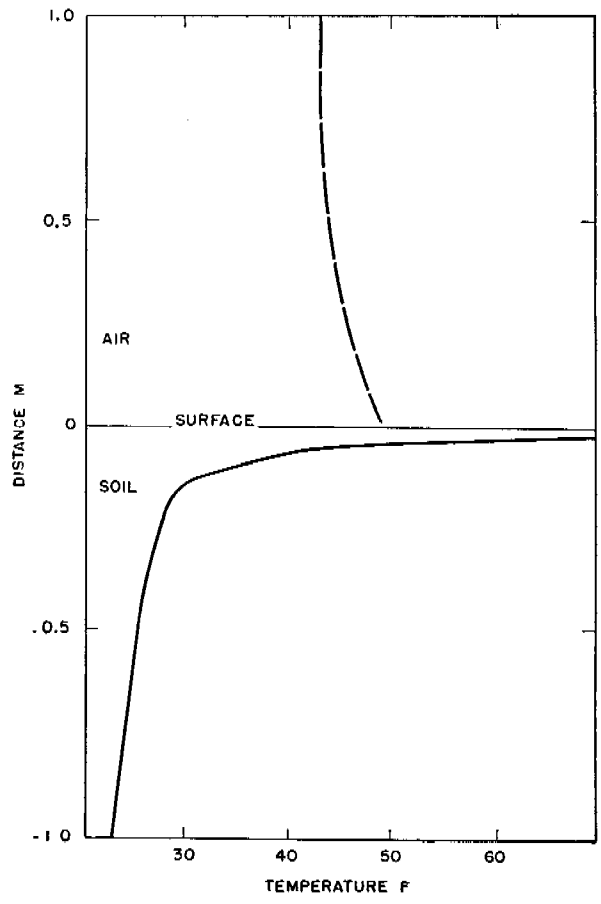


FIGURE 6. Vertical distribution of temperature in air and soil (midday).

falls with elevation. As a result of these opposing factors, there is a maximum in the effective outward radiation at elevations around 2,000 to 3,000 meters above sea level. The ground surface gains energy from the solar radiation, but the net effect of radiation on the atmosphere is always cooling.

Figure 5 (from Möller) indicates the radiation balance on a clear day. With clouds present, the situation is markedly altered as water particles check the outward flow of radiation and increases the counterradiation of the atmosphere.

14.4 GROUND TEMPERATURES

The black-body temperature corresponding to maximum energy density of the solar rays on the earth's surface, 0.62 × 1.93 cal per min per sq cm (that is, sun directly overhead and corrections made for scattering), is 347 K or 74 C. The theoretic maximum may exceed this value as a clear dustless sky may transmit more than the assumed 62%. Maxi-

mum ground surface temperatures have been reported of 71.5 C at the Desert Laboratory, Tucson, Arizona, and 69 C in Agra, India.

Results of Sinclair at the Desert Laboratory in Tucson, Arizona, are given in Figure 6 to illustrate air and earth gradients with respect to the ground surface.

It is observed that the temperature falls rapidly in the soil below the surface. In fact this rapid falling off makes it very difficult to measure surface temperature accurately. At the surface there is a discontinuity between the air temperature and the surface temperature. At least there is a region in which no accurate measurements of the air gradient have been made, and from the very nature of the problems the convection air currents must be such as to render the temperature indefinite.

The surface temperature is obviously a function of the rate of transfer of heat to the air and the conductivity of heat down into the soil. The first of these depends upon the velocity of the air and its turbulence. The conductivity of the soil and other surface materials varies greatly. Values for various substances are given in Table 1.

TABLE 1. Heat conductivity (cal per cm sec C).

Air 0 C	5.6×10^{-5}
Basalt	5.2×10^{-3}
Clay	2×10^{-3}
Concrete	2.2×10^{-3}
Diatomaceous earth	0.13×10^{-3}
Brick	1.1×10^{-3}
Granite	8.2×10^{-3}
Gypsum	3.1×10^{-3}
Paper	0.3×10^{-3}
Peat	0.4×10^{-3}
Snow	0.1×10^{-3}
Soil (heavy)	1.5×10^{-3}
Soil (light)	0.7×10^{-3}
Water	1.3×10^{-3}
Wood	$0.4 - 0.8 \times 10^{-3}$

Because of the low conductivity of air, types of ground which contain high proportions of air show low heat conductivity. The conductivity of grass and other vegetation is also low and it is noted from the table that the value for snow is the lowest listed.

If two substances have the same albedo but differ in thermal conductivity, the substance with poor conductivity will be heated to a higher temperature by the solar radiation in the day time and will be cooled to a greater degree by the thermal radiation at night. Thus the diurnal variation in temperature will increase in the following order: granite, concrete, clay, heavy soil, light soil.

The variation will be greater over grass than over bare soil. Snow forms a highly insulating blanket, but at night the surface temperature of the snow will fall more rapidly than ordinary ground. In the daytime, snow reflects such a high fraction of the sun's radiation that it does not show an abnormal heating. The effect of the low conductivity of wood is noticeable on frosty mornings when the coating of frost will be much heavier on a board walk than on a concrete walk.

The presence of moisture on the surface greatly reduces the diurnal temperature variations. If the soil is moist, part of the energy which would otherwise heat the soil will be expended in vaporizing the water. This effect increases with the porosity or water content of the surface material. Thus, for granite the effect is slight, for moist sand, half of the radiant energy may be so expended, and for peat as high as 80% of the energy may be used up in this way. The process of vaporization essentially transfers the energy to the atmosphere as the subsequent condensation of the water vapor will again release the equivalent energy.

The effect upon night radiation cooling is not so direct, since a moist surface may be an effective black-body radiator. However, if the atmosphere is near saturation, the cooling of the surface results in the formation of dew or frost and the heat liberated on condensation will increase the surface temperature.

Diurnal temperature variations of the ocean's surface are small, about 1 degree C being the maximum change between day and night. The solar radiation is not absorbed on the surface as in the soil, but penetrates to a considerable depth before the absorption is complete. Thus the heat is distributed over a large volume of water with a correspondingly small rise in temperature. However, in very shallow pools, the sand on the bottom will absorb the radiation and transmit it to the water so that in this case appreciable temperature rise may result.

At night, the surface radiates its corresponding temperature radiation but as the temperature of the surface decreases, the increase in density causes the surface water to sink, and thus again, the total heat change is distributed over a large column.

14.4.1 Albedo Effect

An average value for the solar radiation reflected and scattered by the earth's surface has been given

as 38%. The specific effect for various types of substances is obviously an important factor in determining the surface temperatures and accounting for thermal differences which exist along the horizontal. The albedo (ratio of reflected to incident radiation) for a number of substances is given in Table 2.

TABLE 2. Albedo values for various materials.

Material	Dry	Wet
Black soil	0.14	0.08
Granite	0.14	...
Sand	0.18	0.09
Short grass	0.25	...
Tall grass	0.32	0.22
Old snow	0.70	...
New snow	0.81	...

14.5 CONVECTION, TURBULENCE, AND GUSTINESS

Turbulence and convection are more important in the transfer of heat in the atmosphere than is radiation. Petterssen estimates that, under normal conditions, eddy transfer of heat is about 100 times as large as the radiative transfer. Most of this eddy transfer occurs in the daytime under high lapse conditions.

The vertical movement of unstable air is called convection. Whenever the temperature gradient exceeds the dry adiabatic lapse rate, the air is unstable and should rise, but actually no overturning occurs unless a considerable impulse is applied. Thus, very near the ground, the lapse rate may be 800 to 900 times the adiabatic.

Geiger gives the following calculation of the acceleration of a parcel of air which has a temperature gradient of 0.84 degree between the heights 5 and 10 cm. Expressing g, the acceleration of gravity in meters per square second and t, the time in seconds, the acceleration in meters per square second is:

$$\frac{d^2z}{dt^2} = g\frac{T - T'}{T} . \qquad (13)$$

If the particle is lifted from the 5-cm level to the 10-cm level and T is 300 K,

$$\frac{d^2z}{dt^2} = 980\frac{0.84}{300} = 2.8 \text{ cm per sec}^2 . \qquad (14)$$

The particle, displaced only 5 cm from its original position, would move 1.4 cm in the first second and after 4 seconds would be 0.25 m above its original position. The acceleration would increase so that these values are too small. At these velocities an adjustment to the temperature of the surroundings is not probable with parcels of any considerable volume. However, the very existence of superadiabatic lapse rates argues that an initial impulse must be given to start the upward movement.

The initial impulses may be regarded as due to (1) unequal heating, and (2) wind. Natural surfaces are neither smooth nor homogeneous in material. Differences in reflectivity, radiation, blackness, and heat conductivity, as well as sunny and shady sides of surfaces, will give rise to temperature differences, and gravity differences in the horizontal will be converted into up and down movement. These differences in density may be observed visually over heated ground in the middle of the day as the familiar shimmering of the air.

Air is seldom at rest and the friction and roughness of the earth's surface tend to convert any horizontal motion along the surface into turbulent motion. Under lapse conditions, these impulses provide the initial displacements necessary to set up convection currents, and thus break down the high superadiabatic lapse rates. At high wind speeds on a clear afternoon the lapse rate will tend to approach the adiabatic rate. Under inversion conditions the stability of the air tends to damp out vertical displacements, but if the wind is high much irregular movement will be present. This is frequently referred to as *turbulent motion*. The effect of turbulence is to carry the slower moving air upward and to replace it by faster moving air from above. In this way the ground speed is maintained. As indicated, turbulence is at a minimum with low wind velocity under inversion conditions.

Taylor sought to express the power of eddies for the diffusion of heat as a constant K, the eddy diffusivity which is roughly proportional to $0.5wd$, where w is the vertical component of velocity in the eddy and d the mean diameter of the eddy. K varies from 10^3 to 10^5 cgs units, depending upon the nature of the surface and the atmospheric stability.

Schmidt introduced the idea of the Austausch coefficient, A, to represent the behavior of groups of turbulence bodies. From a consideration of the turbulent convection of heat, the coefficient is seen to be analogous to k/σ, the ratio of the heat conductivity to the specific heat. Its magnitude may be evaluated from the change of temperature with height.

$$A = \frac{\pi\rho}{T}\frac{\ln(x_2 - x_1)^2}{\ln \delta_1 - \ln \delta_2} , \qquad (15)$$

where x is height, δ temperature, and ρ density. Geiger gave the following values for A from observations at Schleissheim in the middle of the day.

Height (cm)	A
140	0.015
100	0.010
50	0.0028
20	0.0005
10	0.0002
0	0.000

For pure heat conductivity

$$\frac{k}{\sigma} = \frac{0.000048}{0.238} = 0.0002 \cdot \tag{16}$$

Thus, at the ground, A is zero because there is no vertical turbulence. Just above the surface it is the same magnitude as k/σ and it increases with height.

Components of gustiness are defined in a Cartesian coordinate system as

$$G_x = \frac{|\overline{u'}|}{\bar{u}}, \quad G_y = \frac{|\overline{v'}|}{\bar{v}}, \quad G_z = \frac{|\overline{w'}|}{\bar{w}}, \tag{17}$$

where $\bar{u}$ is the average x component of the wind velocity, the direction of x being the mean wind direction, and u', v', and w' are the differences between the instantaneous and average values of the x, y, and z components of the velocity, respectively.

The vertical component of gustiness is obviously significant in the transfer of momentum, or heat, or dust and smoke particles from the lower to the higher altitudes; experimental observations confirm this correlation. However, the measurement of these components involves peculiar difficulties. A bilateral vane described by Best gives a fair approximation to the relative values of the horizontal and vertical components.

Best has discussed the effect of stability and wind speed upon gustiness. For low wind speeds (0.5 to 1.0 m per sec) gustiness is much less during inversions than during heavy lapses, and the same is true for speeds between 1.0 and 1.5 m per sec. For speeds between 1.5 and 4 m per sec the effect is much smaller, and for higher speeds there appears to be no variation with changing temperature gradient. For lapses less than 0.9 degree F and for inversion, the gustiness in both lateral and vertical directions increases with wind speed. The small gustiness is maintained for higher speeds in the greater inversions. The ratio G_y/G_z appears to be independent of temperature gradient but decreases slightly with increasing speeds. Best gave a value of 1.81 as an average for this ratio. Additional data on the correlation of gustiness with wind and temperature gradients are given in Table 3.

14.6 WIND FLUCTUATIONS

A fluctuation or eddy velocity may be defined by the equation

$$u' = u - \bar{u}, \tag{18}$$

where u is the instantaneous velocity and $\bar{u}$ the average velocity. Best has studied the mean value of the fluctuation ratio

$$\bar{g} = 100\,\frac{|\overline{u'}|}{\bar{u}}, \tag{19}$$

which is the ratio of mean eddy velocity to mean velocity, expressed on a percentage basis. His data indicate that $\bar{g}$ decreases as the temperature gradient changes from lapse to inversion and the effect is more marked at low velocities than at high velocities.

14.6.1 Wind

Gradient wind is defined as the speed of the air at which the deflective force, due to the rotation of the earth, and the centrifugal force jointly balance the horizontal pressure gradient. The direction of the gradient wind is along the isobars and, at heights sufficiently great to be unaffected by surface friction (2,000 ft), its value may be calculated with considerable accuracy from the pressure gradient and the latitude of the station. For a general equation, see any standard text on meteorology.

Closer to the ground, frictional forces cause the *surface wind* to blow between 20 and 30 degrees across the isobars toward the low pressure center. The speed at 30 ft will be about half the gradient wind, depending upon the stability of the air, roughness of the surface, and local topography.

At heights between 10 and 400 m, the variation of wind speed with height is given fairly accurately by the equation of Chapman

$$u = a \log h + b, \tag{20}$$

where a and b are constants dependent upon a given time and place.

For speeds near the ground, Sutton derived the expression

$$\frac{u}{u_1} = \left(\frac{h}{h_1}\right)^{n/(2-n)}, \tag{21}$$

in which n is a constant varying from 0 to 1 with an average value about 0.25. The value of n depends upon the stability of the atmosphere and the roughness of the surface. Best states that a power law can be used provided only a shallow layer is considered,

TABLE 3. Correlation of temperature gradient, velocity gradient, and gustiness components over long grass in Sacramento Valley.

u_{2m} mph	$\frac{u_{2m}}{u_{1m}}$	$\frac{u_{4m}}{u_{1m}}$	ΔT,F 2m–1m	ΔT,F 6m–3.5m	G_y	G_z	Time
4.5	1.12	1.29	−0.4	−0.2	0.67	0.43	7:18 p.m.
5.5	1.13	1.43	−0.4	...	0.57	0.38	7:44 a.m.
5.6	1.16	1.44	−0.3	−0.2	0.70	0.46	7:19 a.m.
6.7	1.17	1.37	−0.4	−0.2	0.90	0.45	3:00 p.m.
5.2	1.17	1.42	−0.8	−0.6	0.52	0.42	3:40 p.m.
5.9	1.19	1.33	−0.4	−0.4	0.66	0.43	7:49 a.m.
5.6	1.23	1.23	0.0	0.0	0.58	0.43	6:53 a.m.
6.2	1.24	1.55	0.5	0.3	0.70	0.52	8:45 p.m.
9.3	1.25	1.54	0.3	0.2	0.63	0.48	8:45 p.m.
4.3	1.25	1.53	0.6	0.3	0.58	0.36	10:23 p.m.
5.3	1.25	1.59	0.4	0.3	0.60	0.44	8:18 p.m.
5.9	1.29	1.63	0.6	0.5	0.58	0.40	8:48 p.m.
4.3	1.31	1.74	0.5	0.6	0.50	0.40	9:43 p.m.
3.5	1.35	1.91	0.5	0.8	0.41	0.27	5:48 a.m.
3.5	1.39	1.73	1.0	0.6	0.59	0.24	11:04 p.m.
3.4	1.43	1.98	1.0	1.1	0.32	0.23	10:00 p.m.
4.0	1.45	...	0.9	2.6	0.28	0.16	10:45 p.m.
3.2	1.50	2.08	0.9	0.7	0.32	0.23	9:46 p.m.
3.0	1.53	2.32	1.6	2.3	0.32	0.22	9:20 p.m.
3.2	1.66	2.78	1.8	2.7	0.21	0.15	9:56 p.m.
3.0	1.68	2.54	1.8	2.0	0.18	0.08	10:24 p.m.
3.5	>1.8	...	>5.0	1.5	0.08	0.0	9:58 p.m.
1.9	1.95	3.61	1.0	1.5	0.25	0.17	11:14 p.m.
4.0	2.2	4.6	..	..	0.07	0.06	9:26 p.m.

and that the index for zero temperature gradient may vary from about 0.43 in the lowest layers to 0.13 at greater heights. This index can increase considerably during light winds and big inversions.

If the wind at two levels is different, a frictional stress, τ, which is a function of the velocity gradient, is set up.

$$\tau = \nu \frac{du}{dz}, \tag{22}$$

where ν is the eddy viscosity of the air. For neutral conditions Rossby defines ν by the equation

$$\nu = 0.02\,(z + z_0), \tag{23}$$

where z_0 is the roughness coefficient, approximately one-thirtieth of the height of the roughness elements of the ground. The value of ν also varies with atmospheric stability and becomes smaller with inversion conditions.

Extensive investigations have been made of the dependence of the velocity gradient upon atmospheric stability. In many of these measurements the wind speeds have been determined at heights of *two* and *one* meters and the ratio determines the so-called *R value*,

$$R = \frac{u_2}{u_1}. \tag{24}$$

The effects of temperature gradient upon the R value over short grass at Leifield were summarized by Best.

1. For light winds (less than 1.5 m per sec), R is about 1.06 for lapses of 1 degree C per m or greater; R is about 1.35 for inversions of 1 degree C per m, and R varies linearly for lapse rates between −1 degree C per m and +1 degree C per m.

2. For moderate winds (1.5 m per sec to 4.0 m per sec) R varies from about 1.08 to 1.16 from lapse to inversion conditions.

3. For strong winds (4.0 to 8.0 m per sec) R is approximately constant at about 1.11.

It should be emphasized that this summary applies to short grass and level surfaces. The R values increase with the roughness of the surface and will increase by some 0.05 unit as the grass length changes from 2.0 to 4.5 cm.

An extensive study of R values, temperature coefficients, and gustiness was made [11] in the Sacramento Valley. The surface was flat and covered with high dry grass which was bent over. The data are summarized in Table 3. The following points will be noted. High values for R occur with high inversion. High inversion existed only at wind speeds of 4 mph or under. Both G_y and G_z decrease with inversion conditions. The correlation of R values and temperature gradients is shown graphically in Figure 7.

TABLE 4. Wind speed at various heights over flat open country of different surface roughness. (In all cases wind speed is 1.00 in arbitrary units at 30 ft.)

Surface roughness	High lapse low or moderate wind				Neutral or very high wind				High inversion low wind			
Height in ft	20	10	6	3	20	10	6	3	20	10	6	3
Smooth snow field					0.99	0.94	0.89	0.81	0.97	0.87	0.81	0.69
Close cropped grass	0.97	0.90	0.86	0.80	0.95	0.84	0.77	0.68	0.88	0.68	0.53	0.44
Grass 12 to 24 in. high	0.93	0.79	0.68	0.50	0.92	0.75	0.65	0.48	0.86	0.63	0.50	0.32
Desert brush 2½ ft high and 4 ft diameter covers 10 — 20% of ground					0.90	0.71	0.60	0.43				

Best found that, for low lapse and inversion, R increased with decreasing wind speeds, but for lapses greater than 0.9 degree F per m the velocity gradient increased with increasing velocity. He concluded, "The chief factor which tends to minimize velocity gradients is mixing due to turbulence and it appears that mixing accompanying high lapse rate is greatest when there is little or no wind."

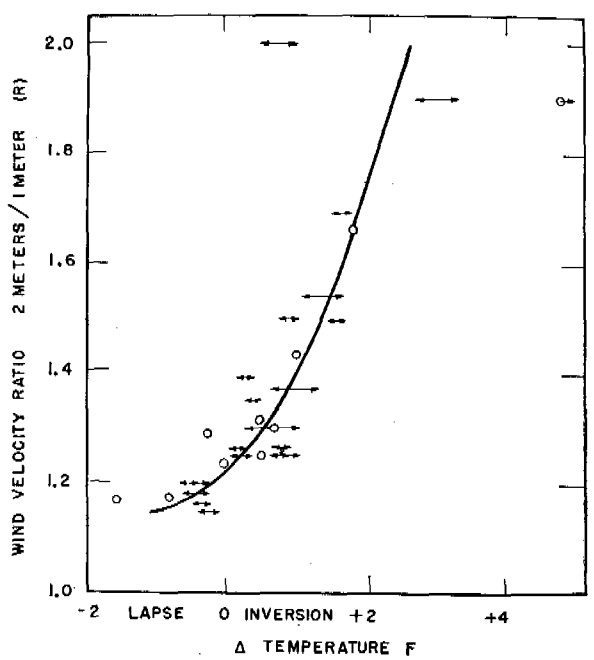


FIGURE 7. Wind velocity ratio versus temperature gradient.

Dickinson, Gilman, and Johnston have given a table[6] of factors by which the wind speed at heights of 20, 10, 6, and 3 ft over various surfaces and under lapse, neutral, and inversion conditions may be predicted from the value at 30 ft. This table is useful since the speed at 30 ft is normally given by the Air Corps forecast. The influence of the various factors are in agreement with principles already discussed.

14.6.2 Gravity Winds

Under inversion conditions, the surface layer of air on a slope is colder and heavier than the air on the same level away from the surface. The surface air then tends to flow down the slope under a force,

$$f = gw \sin \theta, \tag{25}$$

where g is the acceleration of gravity, θ the angle of slope, and w a factor that depends upon the difference in density between the air in the surface layer and that of the free atmosphere at the same level. A steady state is usually reached in which

$$gw \sin \theta = kv^n, \tag{26}$$

in which k is the coefficient of friction as the surface air moves with the velocity v, and n is a numerical exponent. This gravity flow is also known as mountain wind, canyon wind, or *katabatic wind*. These winds show their greatest development over high snow-covered mountains or gently sloping plateaus such as exist in Greenland or the Antarctic Continent. In these regions katabatic wind speeds of 100 to 200 mph occur. However, on most slopes these flows are normally only a few miles per hour and the air currents quite shallow. Latimer, Ruben, Gwinn, and Norris studied the katabatic currents which exist on clear nights on the slope of Mt. Shasta at a distance about ten miles from the summit. The slope at the site was approximately 2%. The data in Table 5 illustrate the type of velocity and temperature gradients which normally existed.

TABLE 5. Temperature gradient and wind speed at base of Mt. Shasta 11:27 p.m., August 27, 1943.

Temperature gradient	Wind speed at various heights	
	Height, m.	Miles per hour
$T_{2m} - T_{1m} = 1.5$ (inversion)	1	1.69
$T_{3.5m} - T_{2m} = 1.3$	2	1.55
$T_{6m} - T_{3.5m} = 1.9$	4	1.32
$T_{9.4m} - T_{6m} = 0.7$	8	1.08
		$R_{2m/1m} = 0.92$

It will be observed that the air next to the ground is moving more rapidly than at higher levels and that the R value is less than unity. This occurred in spite of the inversion present, so it is obvious that R cannot be used as a measure of stability under these conditions.

Light gravity winds may occur on the shaded side of a mountain in the afternoon. In general, it may be stated that gravity flow of air under inversion conditions tends to follow the natural water flow from the area. Both the depth and speed of the stream will be greater down ravines, canyons, and river beds. An example of aerial drainage down a narrow canyon is the fierce wind which sometimes develops in Santa Ana Canyon in Southern California during a high-pressure area over the mountains. At night, level valleys surrounded by high mountains tend to fill with cold air, often up to well-defined levels which are known as *thermal belts*.

In the daytime, high lapse conditions on mountain slopes give rise to upward surface convection currents or *anabatic winds*. The following effects were described by Jelinek from experiments with theodolite balloons on the slope winds of a mountain 1,100 m high near Innsbruck, Germany.

1. Upslope winds developed from 15 to 45 min after sunrise.

2. Speeds were greatest (max 3.7 m per sec) and depth of upslope wind layer highest (max 280 m) on the south slope. The north slope also showed the least development both in speed (max 1.6 m per sec) and depth of layer (max 170 m).

3. The speed and depth of layer of the upslope winds increased steadily during the morning to a maximum before noon, decreased toward noon with the development of cumulus clouds on the top of the mountain, increased in the afternoon when the clouds drifted away and decreased to zero near sunset.

4. Both uphill and downhill winds are best defined when the pressure gradient over the area is small.

Wexler has given the following examples of valley winds in the region around Dugway Proving Ground.

1. Dugway Proving Ground has a general drainage from the mountains to the east and southeast. During the early morning the winds are prevailingly from the southeast. During the afternoon the winds are from the northwest direction up the area toward the mountains. A tendency has been observed for the direction of the wind to follow the sun in the morning. This can be explained by the fact that the slopes facing the sun receive more heat than other slopes, causing a rising air from the slopes and a thrust of air from the valley toward these slopes. The southeast winds in the morning are light, averaging less than 5 mph.

2. During the afternoon, the northwest winds are slightly stronger, averaging about 8 mph during the summer months. With cloudiness during the morning, the shift from southeast to northwest may be delayed. Strong pressure gradient or storms in the vicinity will overcome the diurnal cycle of winds. The depth of these local winds are in the vicinity of 2,000 ft.

14.6.3 Land and Sea Breezes

As a result of the comparative constancy of the ocean temperature, it can happen that during the day the air over the land heats above the temperature of the air over the ocean, and during the night cools below it. In daytime the hot air over the land may rise and be replaced by air flowing in from the sea. Such a wind blowing *from* the *sea* is called a *sea breeze*; the wind that blows similarly *from* the *land* at night is called a *land breeze*.

Both land and sea breezes are shallow and do not extend many miles from the shore. The sea breeze is likely to be rather stronger than the land breeze. The former generally reaches 10 to 25 miles inland but the latter seldom extends more than 5 to 6 miles to sea. If hills come near the shore line, the land and sea breeze effect can combine with the mountain and valley effect. Land and sea breezes are most prominent when strong radiation effects occur along with weak general winds; they are often important in the tropics.

The thermal stability of the air near a coast line needs special consideration. The ocean surface is much more constant in temperature than the land surface. When air flows landward or seaward it may flow from a region where one stability condition prevails to a region where there is a different stability condition. For example, if approximately neutral air from the ocean moves inland over a sunny beach, a short travel (for instance, 50 ft) may suffice for the development of a distinct lapse in the lowest foot or two of the air. If a very small flat island is being considered, air may move entirely across the island, retaining its neutral structure in all but the lowest levels. Even if the air is moving in over a large land surface, an examination of the temperature gradient

in the lowest levels alone will give misleading information concerning the thermal stability unless the air has moved a sufficient distance over land to modify all the levels of interest. Similar remarks apply to air moving out from land over water.

A small island can modify the turbulence and the thermal stability of the lowest layers of air; but the land and sea breeze effect may be unimportant even on larger islands. On a wooded tropical island 5x7 miles, the land and sea breeze effect was difficult to detect; and this was in the region of the doldrums. The size that an island must have in order to show land and sea breeze effects evidently depends on the magnitude of the general wind and on radiation conditions as well as on the mountainous or flat character of the topography.

14.7 THE EFFECT OF AIR MASS CHARACTERISTICS

An air mass which has moved from a cold area to a warmer area will be heated from below and thus become unstable. This instability will be a maximum in the afternoon and a minimum at night, when a radiation inversion may be set up if the area is land. Over ocean the diurnal effects will be slight.

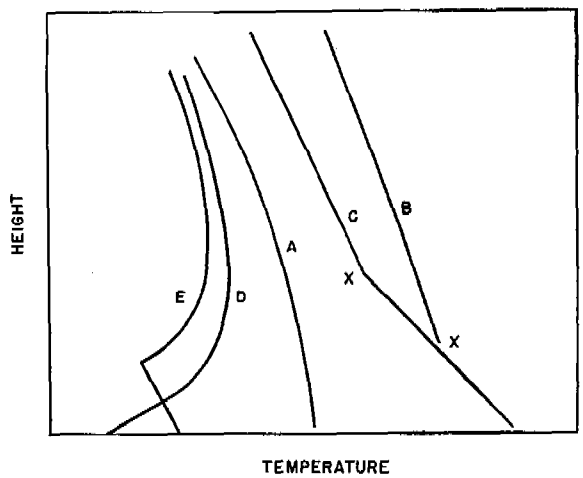


FIGURE 8. Types of temperature-height curves in traveling air masses. A, initial curve; B, after travel over warmer ocean; C, after travel over warmer continent; X, condensation level; D, after travel over a colder surface, slight wind velocity (slight turbulence); E, after travel over a colder surface, high wind velocity (strong turbulence).

Conversely, an air mass which travels toward a colder area will be cooled from below and develop stability in the surface layers. Since turbulence will be a minimum, convection will be small and the effects of cooling will be confined to the lower levels.

Petterssen,[12] in discussing Figure 8, notes that "the development from A to B results in numerous convective clouds and a low condensation level, whereas the development from A to C results in a smaller number of convective clouds at a considerably higher level. The development from A to D usually results in formation of fog, whereas the development A to E results in formation of stratus or strato-cumulus below the base of the inversion." It should also be noted that case E is important in smoke screening as the smoke will tend to rise and level off at the base of the inversion.

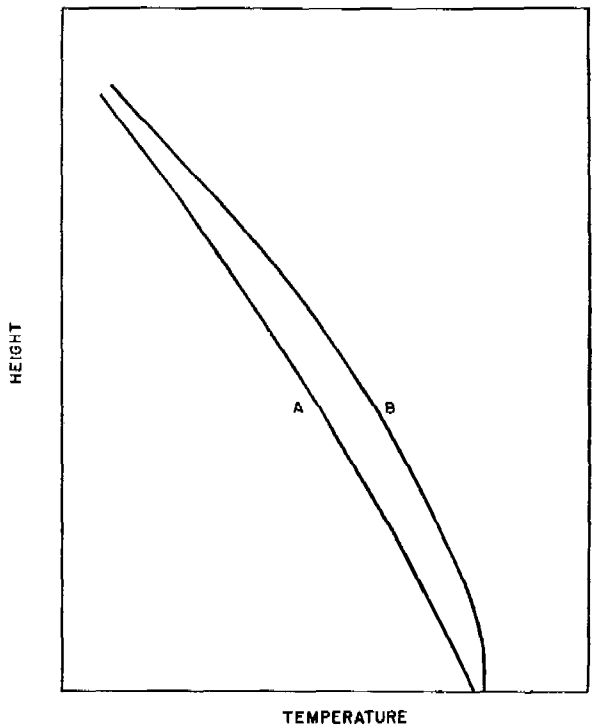


FIGURE 9. The diurnal variation in stability over oceans: A, night; B, day.

Subsidence in high pressure areas may produce inversions and intensify existing inversions. These effects are often difficult to recognize from temperature measurements alone but are disclosed by the vertical distribution of humidity. Petterssen has given the data in Figure 10.

The relative humidity in the inversion layer near the ground is always high. If the inversion is produced by surface radiation alone, there is no rapid decrease in the humidity above the inversion layer.

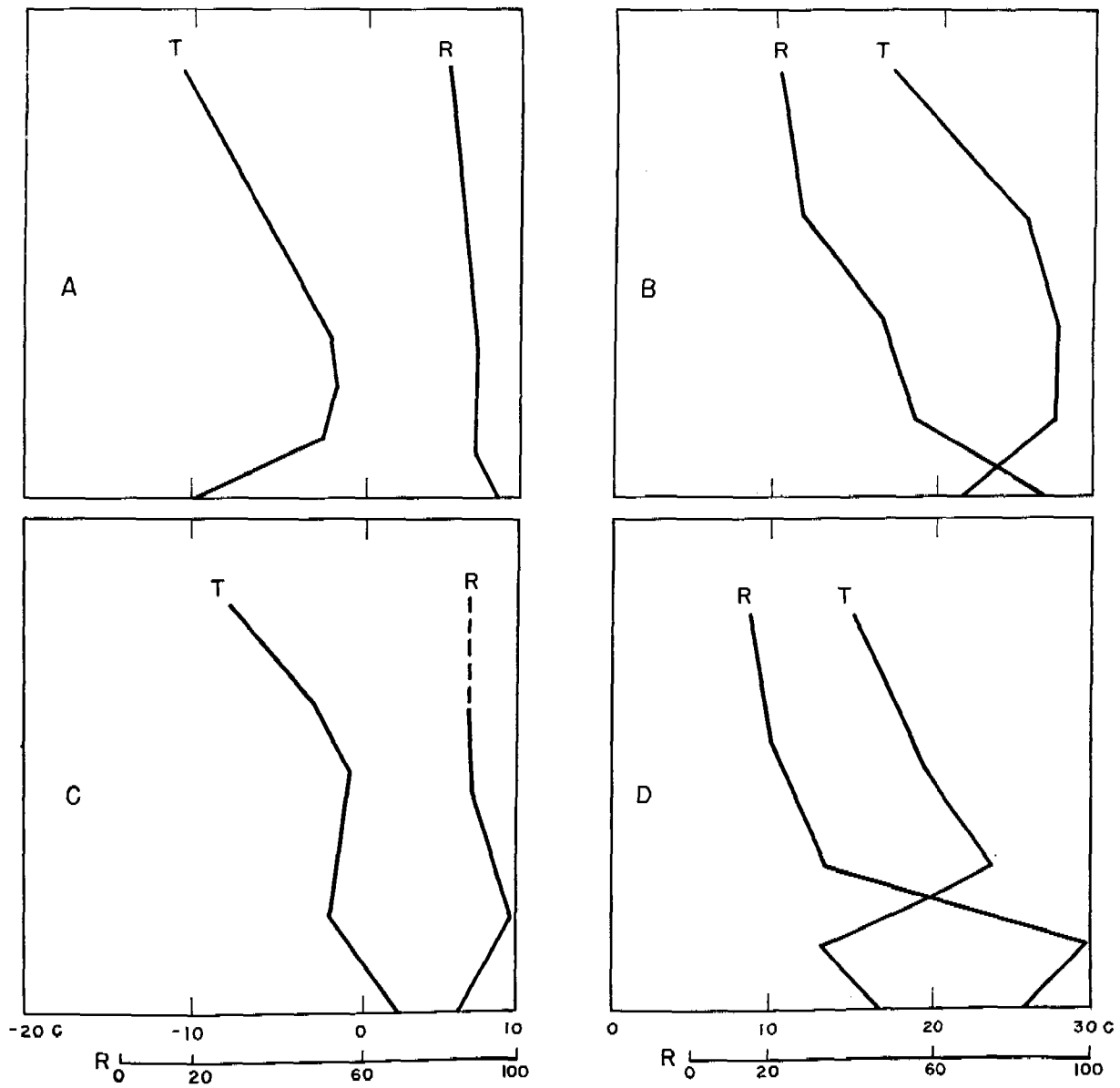


FIGURE 10. Types of inversions. A, Kjeller, 21 Feb. 1938, inversion produced by cooling from below; B, Fargo, 27 July 1938, inversion produced by subsidence aloft and cooling from below; C, Mildenhall, 17 Dec. 1938, inversion produced mainly by cooling and turbulent mixing; D, San Diego, 6 Oct. 1938, inversion produced by subsidence aloft and heating and turbulent mixing below.

In the case where subsidence is a factor the descending cold air is dry and the humidity will fall rapidly with increasing altitude.

Since the wind normally increases with elevation, advection of air aloft may alter the stability of the atmosphere over an area. However, conditions are rarely favorable for potentially colder air to overrun potentially warmer air, but, if the air temperature decreases in the direction opposite to that of the wind, this type of instability may be produced. In cold fronts, cold air may overrun warmer air largely owing to the friction of the ground layer. Such conditions result in great instability and high turbulent winds.

14.8 CORRELATION OF CONTINUOUS MICROMETEOROLOGICAL OBSERVATIONS

Probably the most complete micrometeorological measurements in America have been made by Dr. M. D. Thomas of Salt Lake City, Utah, in connection

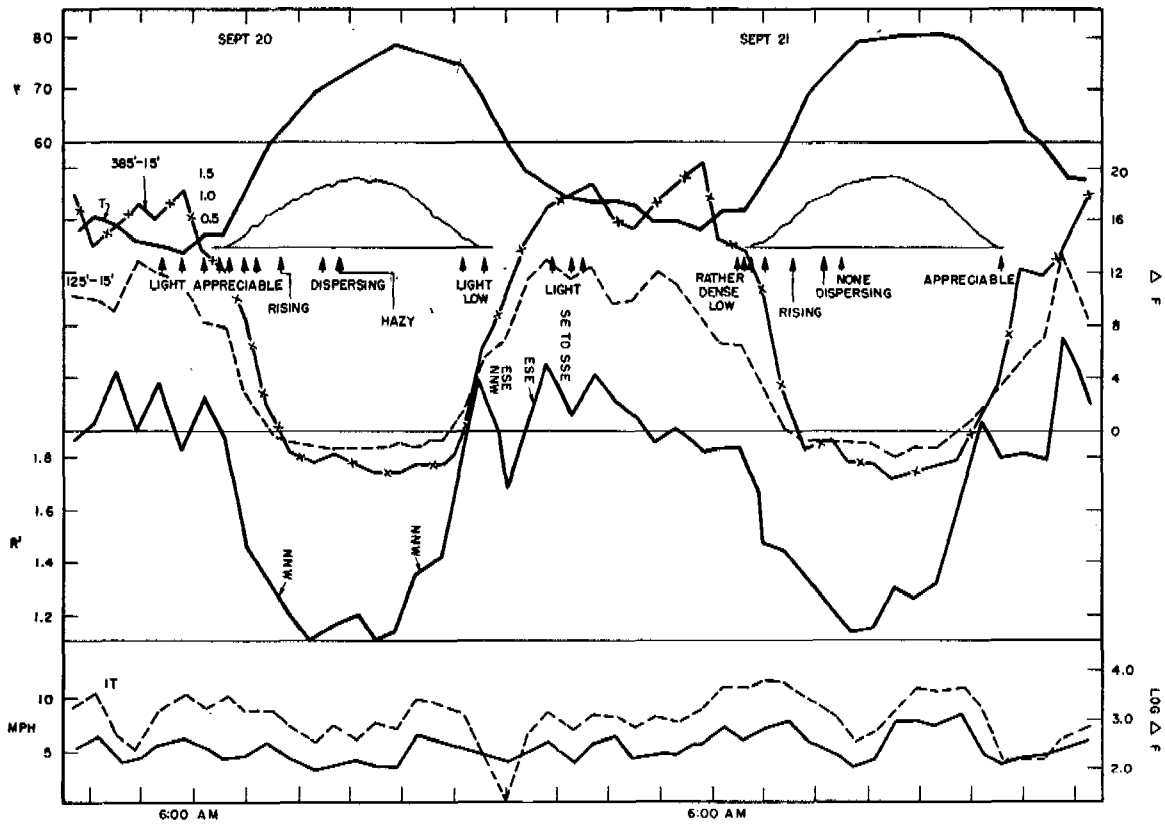


FIGURE 11. Typical daily recordings of meteorological data.

with smoke problems in that region.[19] The work was undertaken by the American Smelting and Refining Company and was supported in part by Division 10, NDRC. A discussion of these measurements will be given as an illustration of the principles presented in this chapter. Some of the conclusions are based upon a study of the Thomas data.[20]

The data consist of the following elements.

1. Continuous temperature records (10 ft above ground).
2. Temperature differences for the intervals: 110 to 10 ft, 220 to 10 ft, 330 to 10 ft, 440 to 10 ft. (After August 1943 the intervals were for the heights: 15, 125, 255, and 385 ft.)
3. Wind direction.
4. Wind speeds at 7 m, 2 m, and 1 m.
5. Pyroheliometer traces.
6. Degree of turbulence.

The above measurements are automatically recorded throughout the 24 hr of the day. Observations are also made on the density of smoke in the valley. From the data, continuous plots have been made of the various elements. Figure 11 is given as an example of this record. The items included on this chart are:

1. Temperature at 10 ft (top curve).
2. Intake of solar radiation in cal per min per sq cm (inserted curves).
3. Temperature differences for the height intervals 385 to 15 ft and 125 to 15 ft (second and third curves).
4. R' values. The ratio of the wind speed at 7 m to that at 1 m. R (2 m to 1 m) given in some instances (fourth curve).
5. Index of turbulence of the wind. Defined as the logarithm of the number of degrees per hour through which the wind vane rotates in one direction (fifth curve).
6. Wind speed (mph) at 7 m (sixth curve).
7. Smoke observations (noted on line below solar radiation).

A study of Figure 11 discloses the diurnal variations in temperature, temperature gradient, and wind gradient previously discussed in this chapter. In general ΔT and R' are high at night, due to the stability set up by radiation cooling, and are low in the

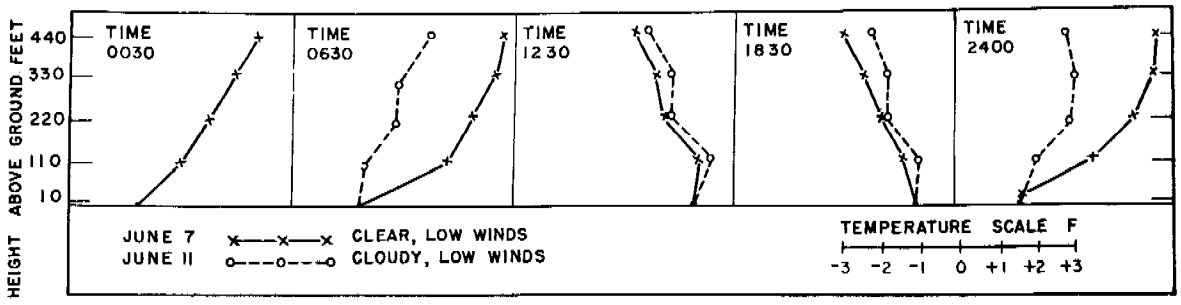


FIGURE 12. Temperature profiles for days in June.

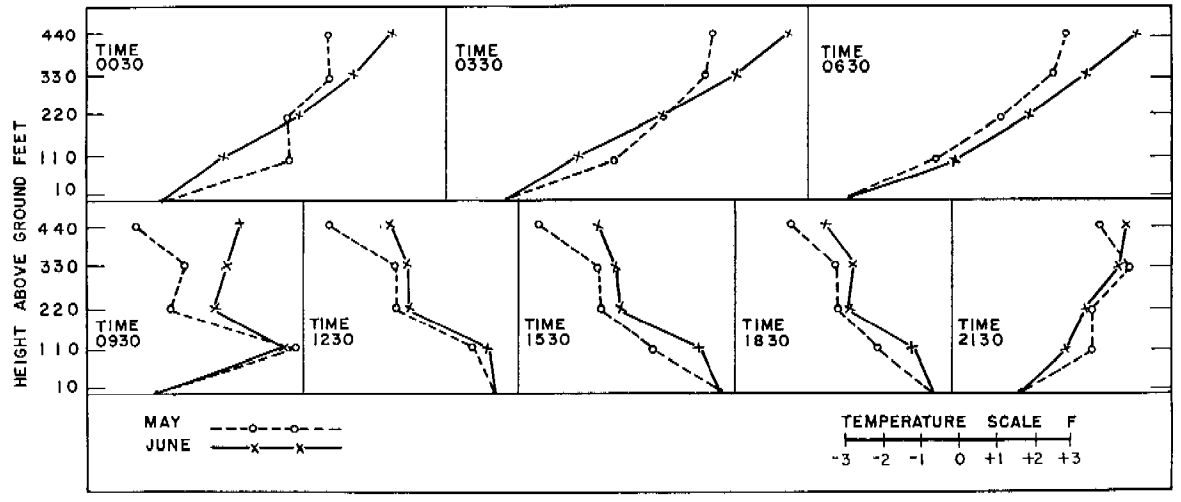


FIGURE 13. Temperature profiles for May and June, all weather.

daytime under the convection currents of high lapse conditions. The curves at ΔT and R' are roughly similar but there are certain interesting divergencies. Thus about 8 p.m. there is a sudden drop in R' without a corresponding large drop in ΔT. This appears to be due to a very shallow katabatic wind flowing down from the mountains and occurs with a change of the wind direction from northwest to southeast. In general, there is a close correlation between the wind speed and the index of turbulence; high turbulence is associated with high wind speed. A remarkable drop in the values of the index of turbulence is also associated with the shallow katabat, but as the katabat deepens and develops into a valley wind, the values of both the index of turbulence and R' again rise. An inverse relationship exists between R' and the index of turbulence but it is often masked by the effect of the wind speed upon both of these quantities.

The effect of clouds upon the temperature profile is illustrated in Figure 12. It will be observed that both the night inversion and the day lapse were greater on a clear day (June 7) than on a cloudy day (June 11). On foggy days ΔT is mainly lapse.

Figure 13 summarizes the average temperature profiles for the months of May and June 1943. May inversions terminated rather sharply at the 330-ft level, and the June inversions were stronger in general than those of May. On the other hand, the intensity of the lapse was greater in May than in June, which is not to be expected, but these data include all weather and the normal trends will be influenced by the wind velocity and number of cloudy days.

In Figure 14, the difference in the maximum temperature on the preceding afternoon and the minimum temperature before sunrise is plotted against the maximum inversion. It will be observed that the two quantities are roughly proportional; this is to be interpreted as the effect of temperature on the net nocturnal radiation loss. Thus, when the ground surface is hot, the radiation loss will be proportionally larger and the resulting inversion greater. The rate of cooling is probably the most important factor in

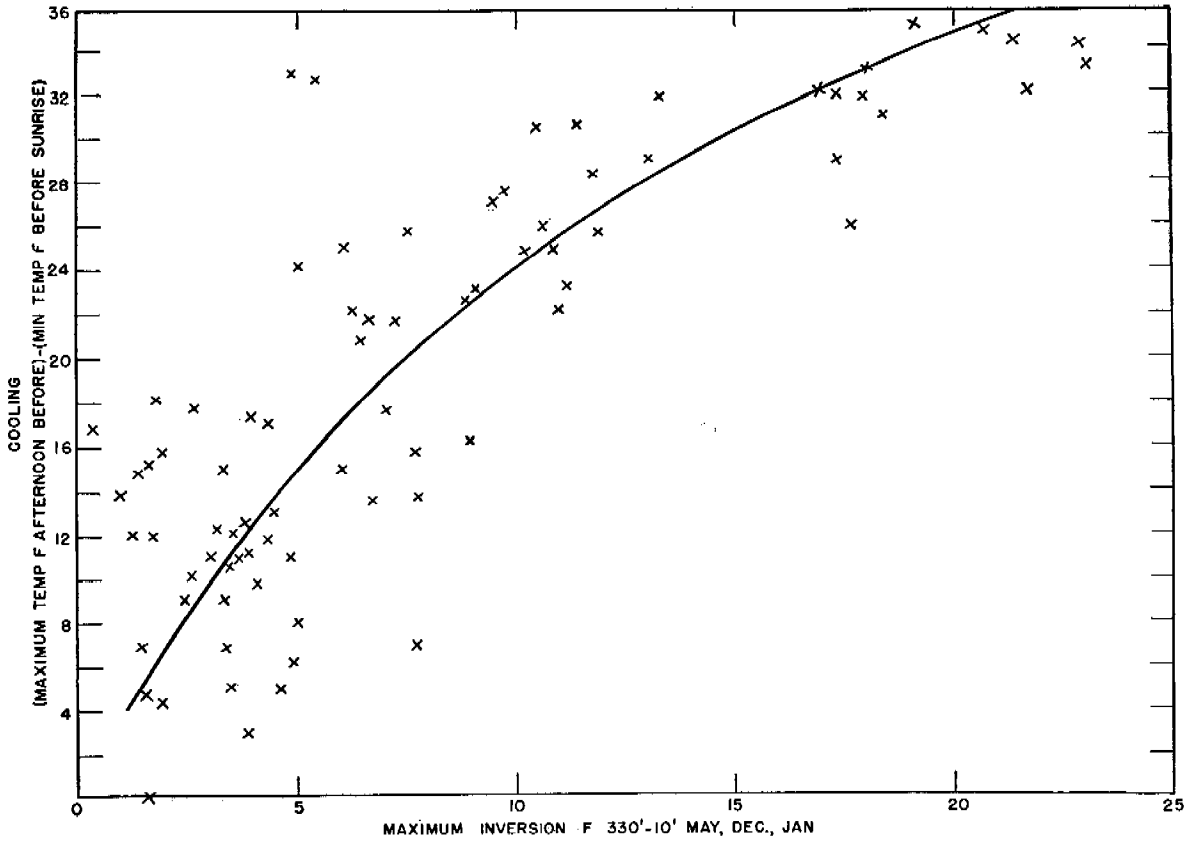


FIGURE 14. Plot of difference in maximum and minimum temperature against maximum inversion.

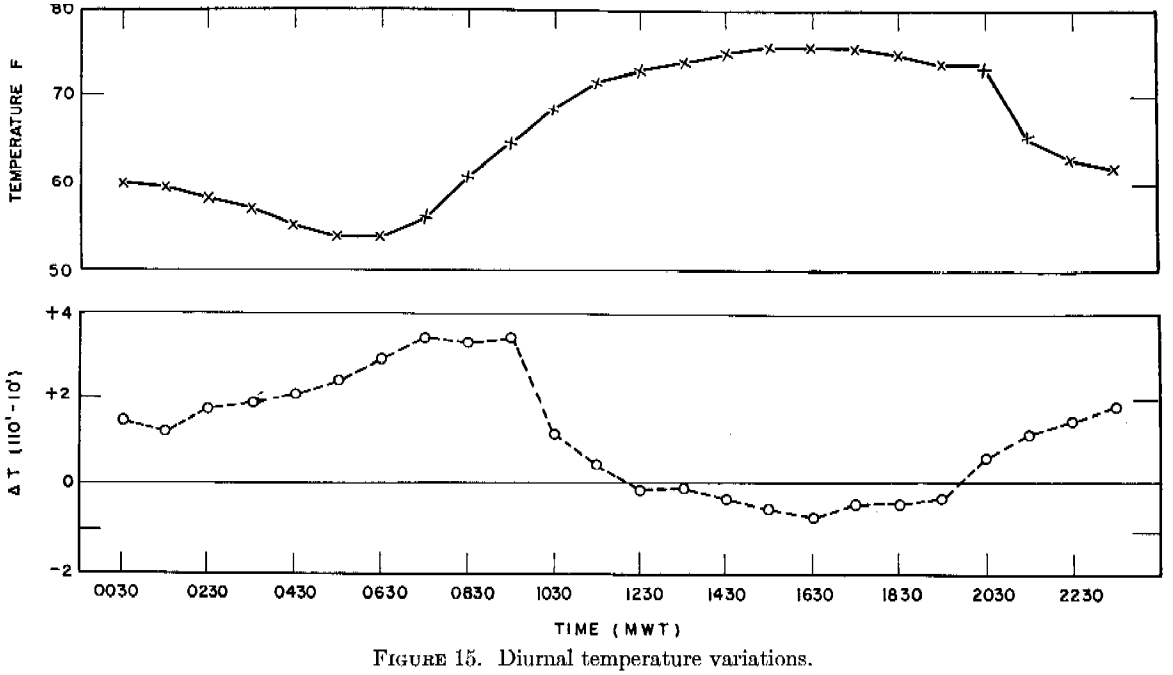


FIGURE 15. Diurnal temperature variations.

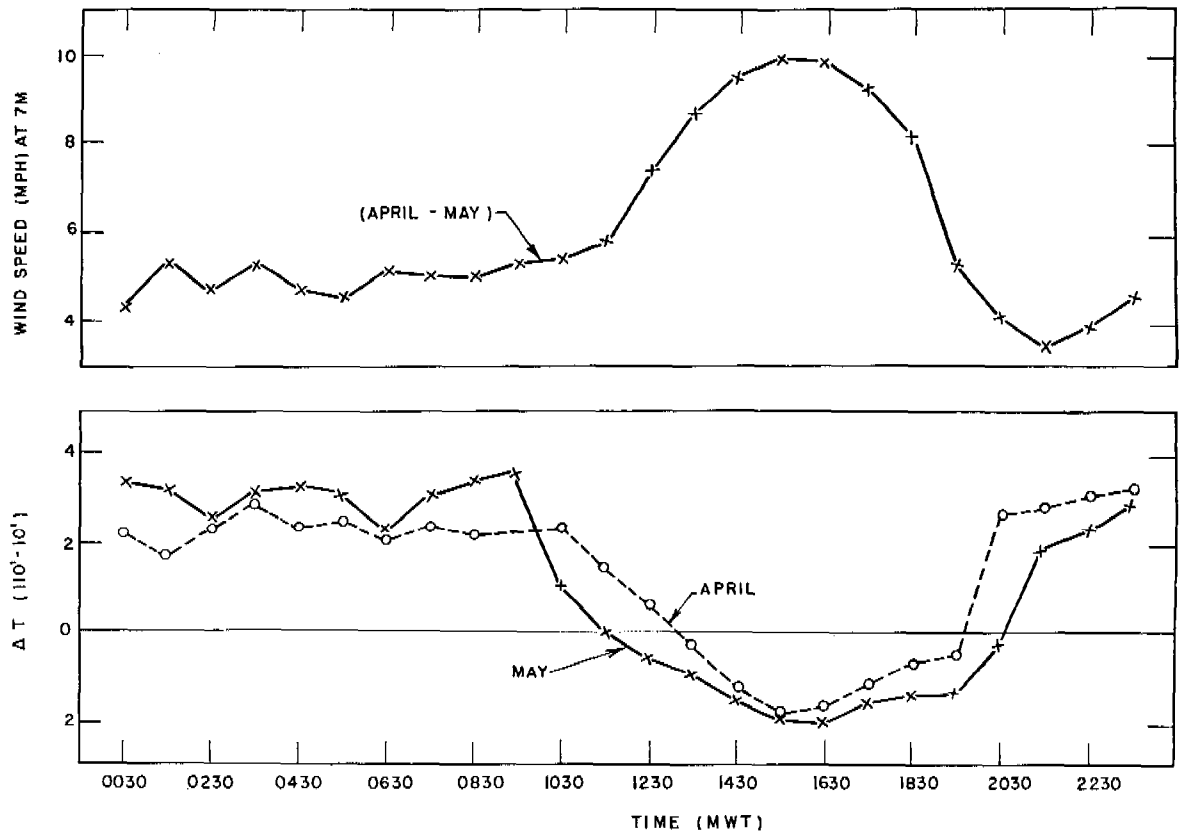


FIGURE 16. Wind velocity at $\Delta T'$ on clear days.

determining the extent of inversion. The time of maximum inversion for small heights is generally after the period of most rapid cooling but for gradients over several hundred feet inversion may occur after the time of minimum temperature. The time of maximum lapse generally follows the time of maximum temperature closely. Figure 15 gives a comparison for T and ΔT curves for June.

Figure 16 is a plot of monthly average values of ΔT for hourly recording throughout the day and, for comparison, a plot of the corresponding hourly averages of the wind velocity. Figure 17 gives similar plots of R' and velocity. The conclusion might be drawn that inversion produces low winds and lapse high winds. While of course there are effects in these directions, it must be kept in mind that high winds tend to break down both inversion and lapse conditions to neutral. If the higher wind velocities had not existed during the day, the lapse values would have been considerably larger. The effect of wind speed upon stability is so great that it is frequently difficult to differentiate between the wind factor and radiation factor. This is illustrated in Figure 18, which gives R' values for a clear day with low winds in each of the months of April, May, and June. The inversions at night intensify as the days get hotter and the humidity of the desert region decreases. However, for the days chosen, the R' values under lapse conditions do not show the expected order.

The region around Salt Lake is so mountainous that orographic factors are usually more important than frontal activity or cyclonic convergencies. However, the air mass characteristics play an important role in determining the ground conditions. In the wintertime, high-pressure areas of stable marine polar air, or even continental polar air, prevail over Utah; subsidence occurs, wind velocities are low and smoke tends to accumulate in the valley in spite of the fact that nocturnal inversions are not so great as in the summer months.

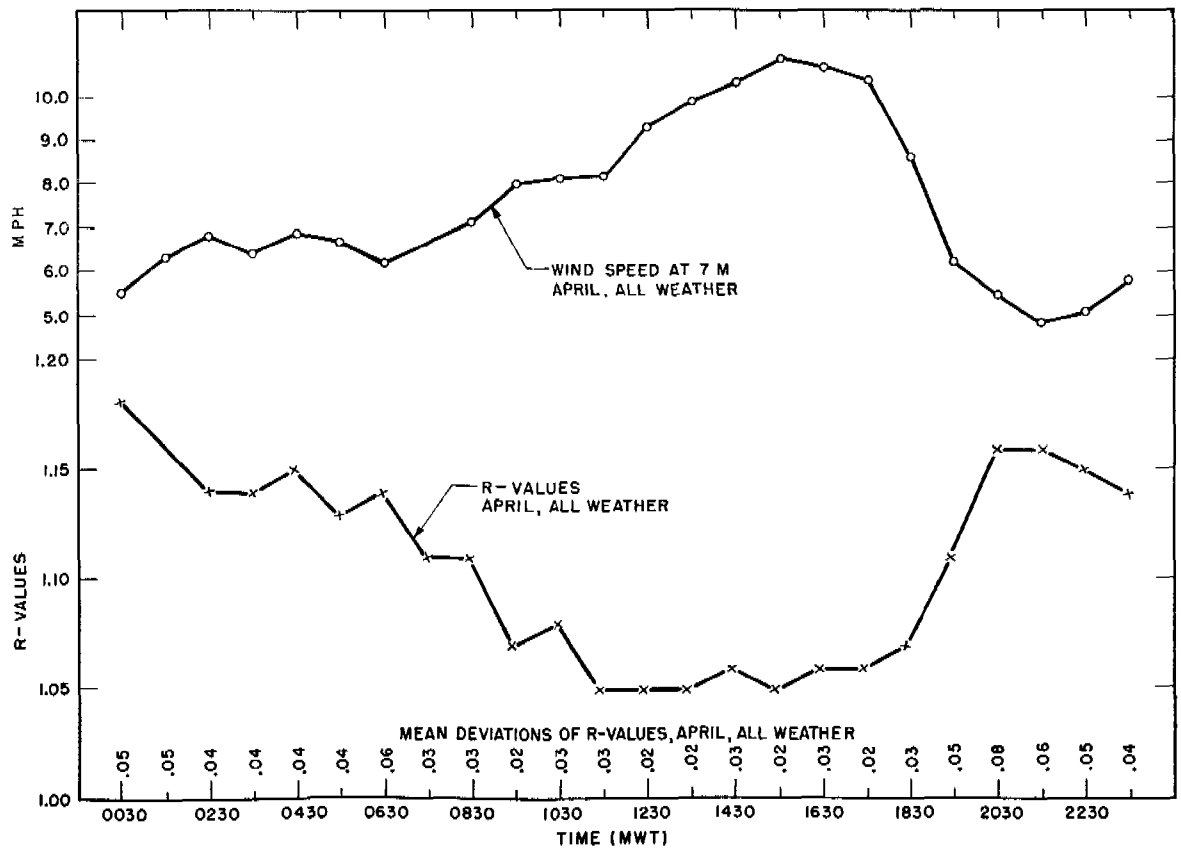


FIGURE 17. Diurnal variation in R values and wind velocities.

14.9 MICROMETEOROLOGY IN WOODED AREAS

14.9.1 General Considerations

For the sake of simplicity, wooded areas are treated here as distinct from open country. Actually there is no sharp demarcation between open and wooded terrain. There is, in reality, a continuous gradation in vegetation from close-cut grass to dense jungle. And there is also a continuous gradation in the complexity of meteorological factors. The same general principles apply to the air over and in a forest as do in the open. In the forest, however, emphasis has to be placed on the character of the vegetation and the effects it imparts.

The types and characteristics of wooded areas and their relation to climatic conditions will not be discussed in this report. In this section, the role played by meteorology is treated in relation to wooded areas in general. It must be left to the individual to apply the principles stated in the following text to the particular type of forest where operations are planned. Furthermore, the following sections dealing with wind, turbulence, and temperature are intended to apply to forests on level terrain. Important effects of topography have been treated elsewhere.

A great variety of vegetative covers can occur. For definiteness, remarks will be made with a particular type in mind; the effect of departures from this type can then be discussed. Consider a fairly dense jungle with a canopy of irregular height; the tops of the trees may be mostly at, for example, 30 to 50 ft. Suppose that there is a moderate amount of undergrowth and that little direct sun reaches the forest floor even at midday.

14.9.2 Wind Speed

WIND ABOVE AND IN CANOPY

The wind in the free air above a forest canopy has a somewhat reduced velocity because of the drag

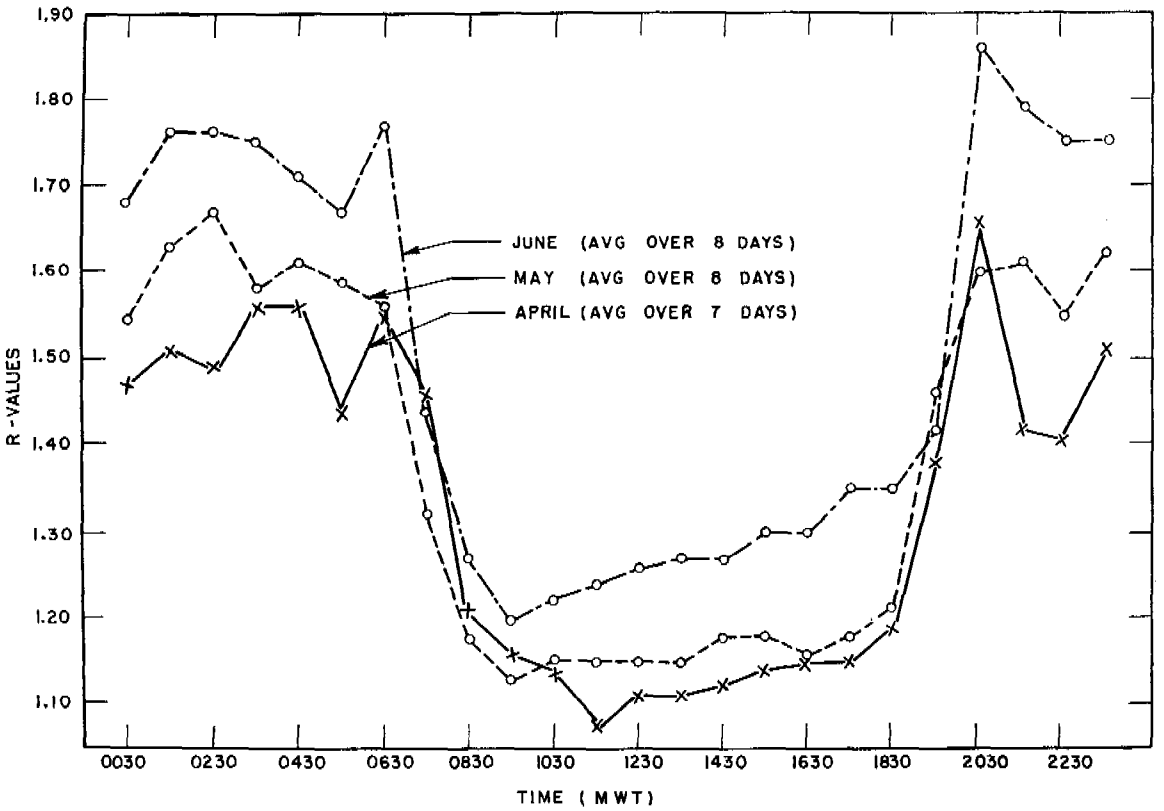


FIGURE 18. Diurnal variations in R' values.

effect of the comparatively rough surface offered by the canopy. On passing from the free air down into the tops of the tree-crowns, there is a large and sudden decrease in wind velocity. The heavier the forest growth, the greater is the magnitude of this decrease. Some typical wind profiles in a forest are shown in Figure 19.

WIND UNDER THE CANOPY

The winds below the tree-crowns are usually induced by the overhead wind. Under given thermal conditions the relation between the forest wind speed and that of the overhead wind is controlled by the thickness of the canopy and the development of the undergrowth. Speeds of greater than 2 mph below a moderate to heavy forest-cover are relatively infrequent. In fact, it is not uncommon to encounter speeds below ½ mph, particularly at night time.

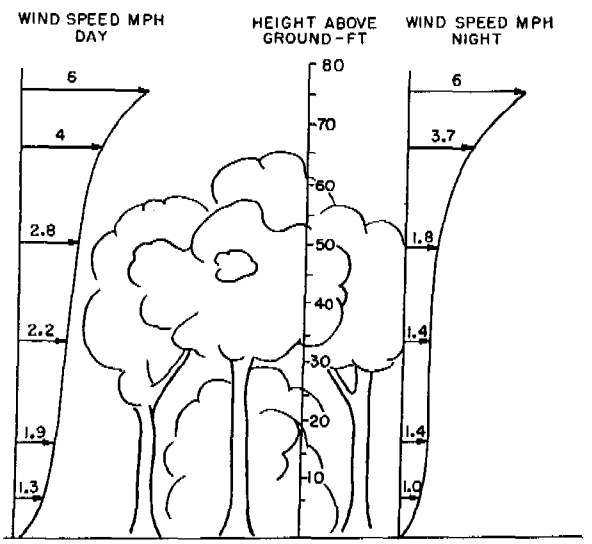


FIGURE 19. Wind speed at various heights in forest.

RELATION BETWEEN WINDS ABOVE AND BELOW A FOREST CANOPY

The wind near the floor of a forest (say at 2 m above the ground) is generally caused by the motion of the air above the trees. As the horizontal motion is transported downward through turbulence, most of the energy of the wind is dissipated by the stationary obstacles in its path so that the speed near the ground is much less than that above. The thicker the foliage, the greater will be the difference in speeds.

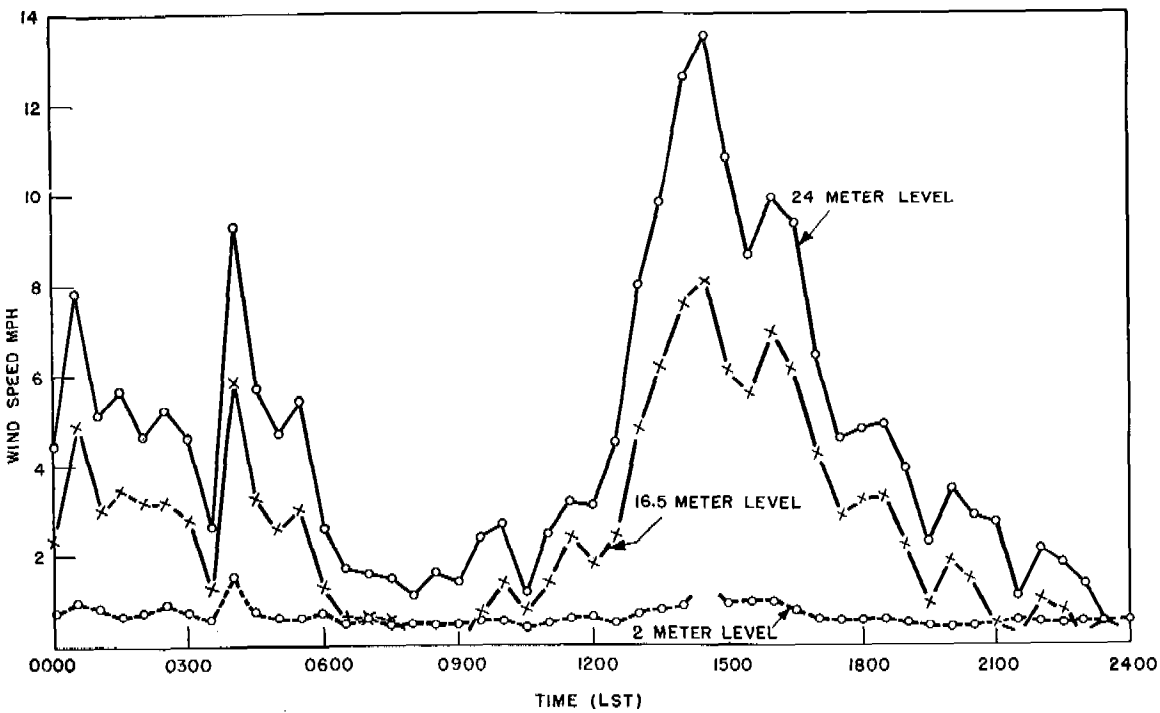


FIGURE 20. Wind profile record.

In addition, this downward transfer of motion from above is affected by the thermal structure of the air in and over the trees. The question of air stability in a forest will be taken up later. It is sufficient to say that when the air is stable, the transfer of motion is curtailed. For a given overhead wind, the wind speed at 2 m will be less under stable conditions than under unstable conditions. When the air is unstable, vertical mixing is enhanced; hence, there is less tendency for the existence of a large vertical velocity gradient. Thus, if the wind overhead is constant day and night, it is to be expected that the winds in the woods will be generally lower at night than during the daytime.

Under given stability conditions the wind speed in a moderately heavy jungle is nearly independent of the wind speed over the canopy if the latter is not over 5 mph. With higher wind speeds overhead, those in the woods increase and become more nearly proportional to those overhead. The jungle speeds are then roughly one-eighth of those overhead.

The wind profile of a typical day in the San José Forest is illustrated in Figure 20. The heights are 2 m in the jungle, 16.5 m at the top of the canopy, and 24 m above the canopy. Throughout the day the speed at 16.5 m closely follows the speed at 24 m. The speed at 2 m hardly follows even the peaks and troughs. Worth noting is the fact that while the wind speed above the jungle is greater than 10 mph, the speed in the jungle is only about 1 mph. In contrast, while the speed above the jungle is about 0.5 mph near midnight, the speed in the jungle is also 0.5 mph.

Figure 21 is a plot of the ratio: wind speed at 24 m divided by wind speed at 2 m vs the wind speed at 24 m. It is apparent that the ratios measured with inversion conditions are well enough separated from those measured under lapse so that separate curves for average values may be drawn. The implication here is that the speed in the jungle is more dependent on the speed above the jungle under lapse conditions than under inversion conditions. Since there is more downward transfer of momentum under lapse, greater turbulence will also result under these conditions.

14.9.3 Wind Direction

The wind direction above a wooded area is generally the same as in open terrain.

Insofar as the wind below the canopy is caused by the overhead wind, the average wind direction inside a forest coincides with that above. The air movement, however, as a rule is much more irregular than that above. Hence, at any given instant the direction

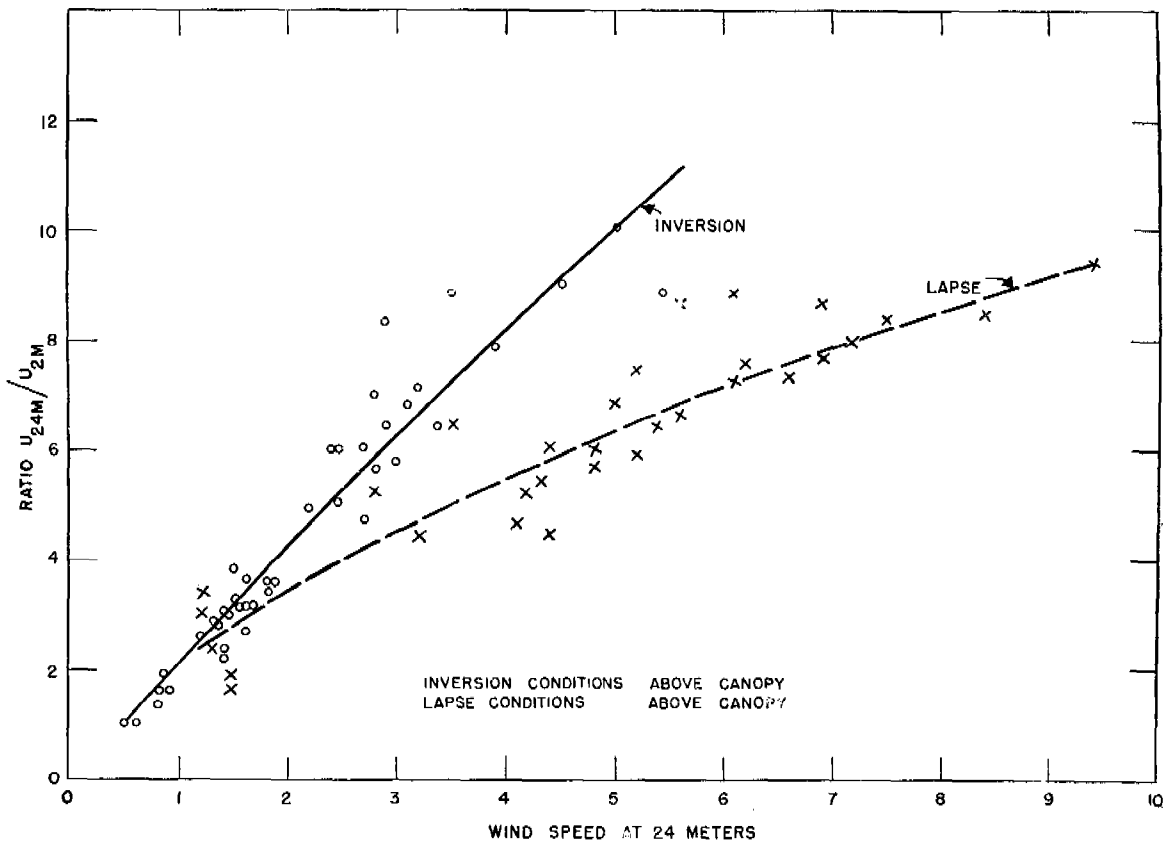


FIGURE 21. Effect of wind speed on R' for lapse and inversion.

near the ground may be considerably different from the average. It is not uncommon for the slowly moving air in a wooded area to execute two complete 360-degree changes in direction in the space of one minute. Moreover, at any moment the direction of winds at two points at the same level in a forest usually differ considerably.

On clear days or on cloudy days with moderate to high overhead wind speeds, the wind directions in a forest fluctuate rapidly over a wide range because of the turbulent condition of the air. When there is a heavy overcast and low winds during the daytime, the fluctuations are more subdued. At night, especially with clear skies and a low overhead wind, turbulence is at a minimum, and the direction observed at one point in the woods usually exhibits slow and random changes.

This last mentioned situation seems to result from the wind in the woods being relatively independent of the wind above. It is presumed that the stability of the air under these conditions makes this possible. Apparently the air movement below the canopy is caused not so much by the transfer of motion from above as by effects such as the settling of cold air and uneven radiational cooling whose origins are purely local. There results, therefore, a low local wind which does not fluctuate rapidly and which is not necessarily in the same direction as the wind above the trees, but which gradually shifts as one local effect becomes more predominant than another.

These effects are further indicated by Figure 22, which compares the frequency of the wind direction at 24 m (above the canopy) to that observed in the jungle. The fact that the daytime data show larger deviations in the directions than do the night data is consistent with the greater turbulence under lapse conditions.

A comparison of the low- and high-wind speed traces from a hot wire anemometer is given in Figure 23. Again, greater turbulence is to be noted for lapse conditions.

An important exception to the above remarks about wind directions in woods at night is found in the remarkably steady winds on slopes. These katabatic winds have been discussed in preceding text in some detail.

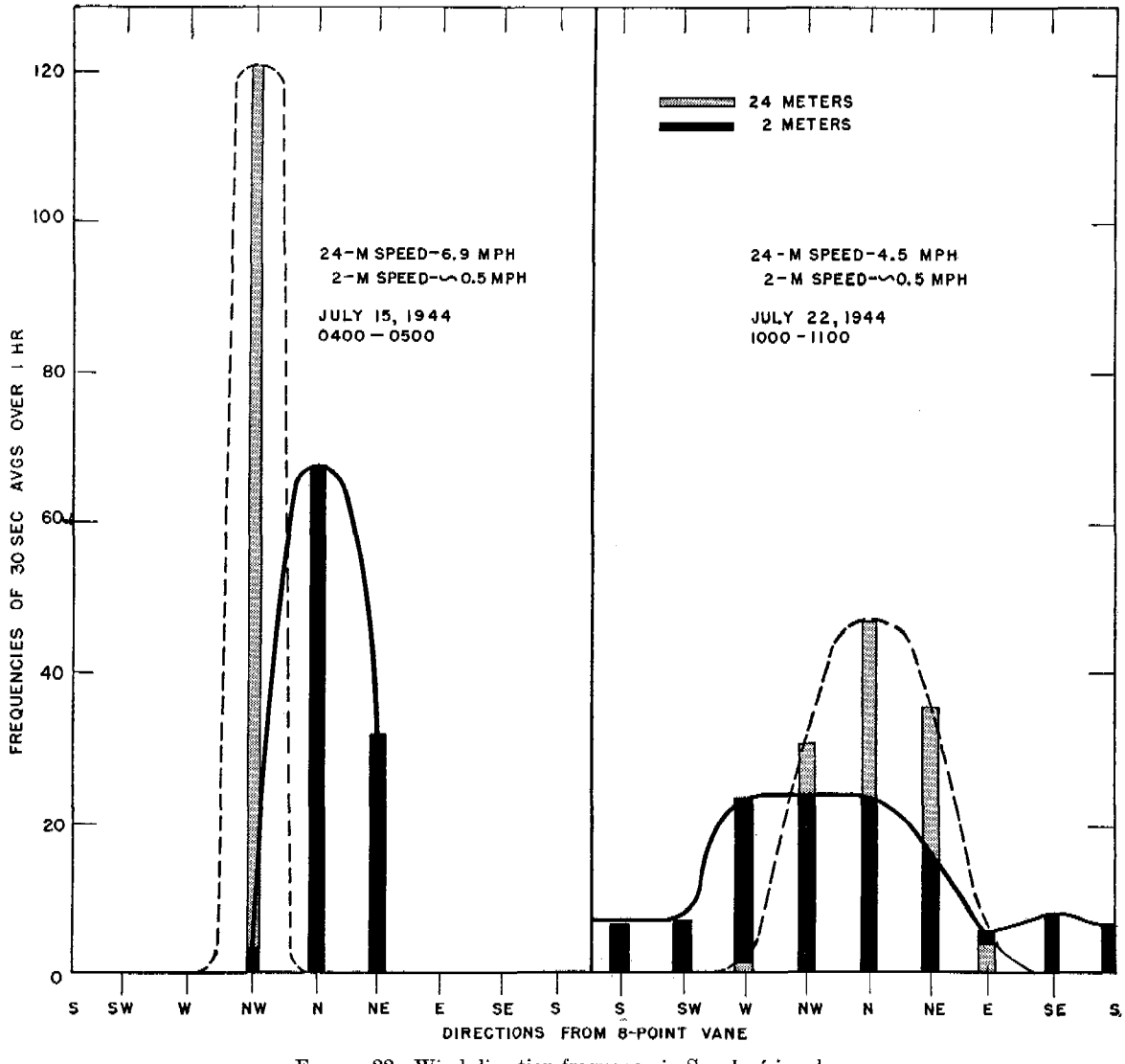


FIGURE 22. Wind direction frequency in San José jungle.

14.9.4 Forest Temperatures

TEMPERATURES IN AND ABOVE THE CANOPY

In the free air above the tree tops, conditions are much the same as over open ground with the tree tops taking the place of the ground surface for radiation purposes. The surface temperatures of living leaves in the sun are often 10 degrees F, or hotter than the surrounding air; and dried leaves can give larger differences. Accordingly, the canopy and the air above it undergo a diurnal variation with a maximum in the afternoon and a minimum before sunrise. Furthermore, above the canopy, lapse conditions develop in the sunshine, and inversion conditions develop on clear nights just as they do over open ground. Some difference arises from the fact that the canopy does not show nearly so well defined a surface as the open ground; the temperature gradients are consequently not so large in the air over the tree tops as over an open field. Again, the ground of an open field presents a solid obstruction while the canopy of a forest does not; air, cooled by open ground during an inversion, pools on the ground but when cooled by the cold leaves of a canopy it sinks down through the canopy.

TEMPERATURES BELOW THE CANOPY

If the surface of the ground or of some low vegetation lies under a heavy forest canopy and has little or no direct exposure to the sun or sky, then the surface temperature undergoes a smaller diurnal varia-

DATE	TIME	AVERAGE WIND SPEED (2 METERS)	GUSTINESS CHARACTERISTIC	TEMPERATURE DIFFERENCE, °C	
				$T_{24M} - T_{12M}$ (ABOVE CANOPY)	$T_{12M} - T_{1.0M}$ (BELOW CANOPY)
8-24-44	1000	0.5 M P H	HIGH	-0.9° (LAPSE)	1.2° (INVERSION)
8-25-44	0100	0.5 M P H	LOW	2.1° (INVERSION)	-0.4° (LAPSE)

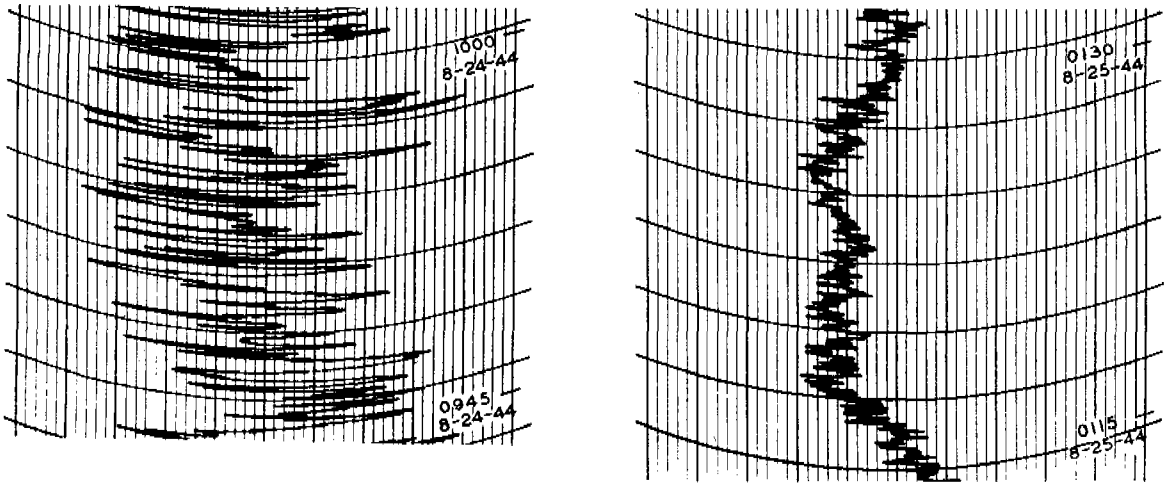


FIGURE 23. Low and high gustiness wind-speed traces.

tion than it would if the surface were exposed. In woods in Florida during May and June, the average daily range in ground surface temperature on clear days was only 16 degrees F while that of the grass in a nearly open area was 40 degrees F. A range of only 5 degrees F has been found in the jungle on a tropical island.

Also, the temperature of a well-shaded surface does not depart greatly from that of the nearby air. For the Florida woods, the air was usually cooler than the ground surface at night and warmer in the middle of the day; but the difference was usually less than 2 degrees F.

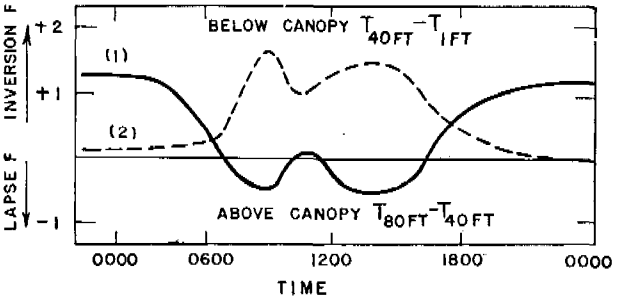


FIGURE 24. Temperature differences in jungle between air above and in canopy; and between air in canopy and near ground.

LAPSES AND INVERSIONS UNDER THE CANOPY

In the open, inversions usually develop at night and lapses occur in the day. Under a fairly heavy canopy the reverse occurs; lapses develop at night and inversions occur in the day. This is illustrated by Figure 24 drawn from observations in a jungle on a small tropical island. For various times of the day and night there are shown two temperature differences: one, $T_{80\text{ ft}} - T_{40\text{ ft}}$, is the temperature of the free air well above the crown minus that of the air in the crown; the other, $T_{40\text{ ft}} - T_{1\text{ ft}}$, is that in the crown minus that of the air near the ground. Positive differences indicate inversions.

Rapid changes in the temperature profile occur rather frequently under the jungle canopy. These are illustrated [23] in Figures 25 and 26. Thus, in Figure 25, a change from inversion to lapse occurs between 10 and 13 m in a few minutes. These rapid changes are indicative of the vertical and horizontal motions of the air due to heating and cooling of the vegetation and it may be concluded that any single measurement of the temperature profile during the day may not be representative of the average condition.

SECR[redacted]

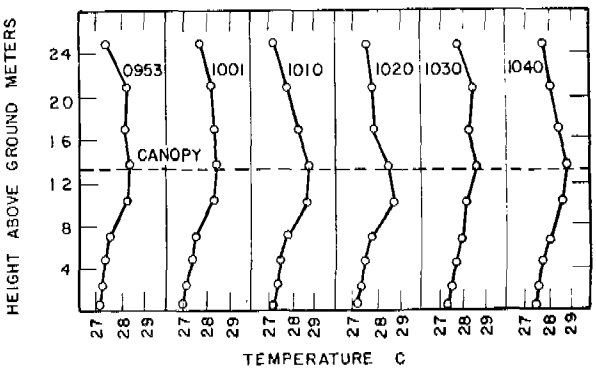


FIGURE 25. *Variation of jungle temperature profiles under uniform cloud cover.*

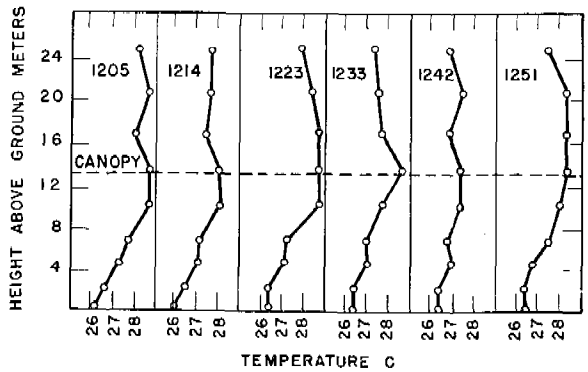


FIGURE 26. Modification of jungle temperature profile by passing small clouds.

THERMAL INSTABILITY IN THE FOREST

Although the inversions under a heavy canopy occur in the daytime, it is not to be concluded from this that day is the time of air stability in the woods; for at any one height in the crown, horizontal temperature differences with consequent circulation doubtlessly exist.

To understand this daytime inversion, consider that when the sun strikes a forest canopy many leaves at the tree tops receive direct sunshine and are heated to temperatures distinctly greater than of the surrounding air. The leaves then warm this air. Below the tree tops, fewer leaves are exposed to the sun; if the canopy is fairly heavy, very few spots receive direct sunlight at the lowest levels. From the ground on upward into the canopy there is, then, an increasing number of hot spots with the result that the average air temperature increases from the ground well into the canopy. Although this is an average temperature distribution corresponding to an inversion, its manner of production by hot spots results in convective turbulence.

Similarly, on clear nights many leaves at the top are exposed to the sky; they radiate freely and become cooler than the surrounding air which is then cooled by the leaves. At lower levels, fewer leaves are exposed so that, on the whole, the air is cooler in the canopy than somewhat below it, that is, the temperature distribution here is that of a lapse.

This simple picture requires modification in a less dense forest. If considerable sun is able to reach the forest floor at midday but not in the morning or afternoon, it can happen that there is a lapse near the ground at midday but an inversion morning and afternoon. If the forest is very thin, lapses by day and inversions by night may be expected somewhat as in the open. Evidently, within the woods, the knowledge that a lapse or inversion exists is of no value alone.

14.9.5 Turbulence in the Forest

From what has been said it is clear that thermal stability and turbulence in the woods cannot be estimated simply from average temperature gradients. However, a good idea of the turbulence in the woods can be formed from a knowledge of the wind speed and temperature gradient *above* the canopy.

If lapse conditions exist above the canopy, a turbulence of convective origin is present in addition to that due to canopy roughness. But, if an inversion exists above the canopy, even the turbulence of mechanical origin tends to be damped out. Accordingly, with a lapse over the canopy, much turbulence is present which can, to a greater or lesser extent, be communicated through the canopy to the air below. With an inversion over the canopy there is relatively little turbulence present for communication to lower levels.

The turbulence in the forest also depends on the speed of the wind. With a given size of lapse or inversion over the canopy, the turbulence below is least when the magnitude of the wind speed over the canopy is least.

These relations are illustrated by Figure 27, which shows qualitatively the amount of turbulence (low, medium, or high) in the jungle of a tropical island under various conditions over the canopy. The turbulence was estimated from the fluctuations of a hot wire anemometer 6 ft from the ground.

The figure shows that low turbulence in the woods is favored by low winds aloft (5 mph or less) and an inversion above the canopy. These conditions are

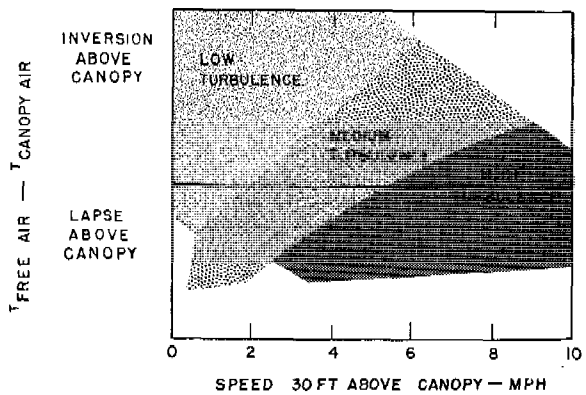


FIGURE 27. Turbulence under canopy.

most apt to be found in the very late afternoon, night, or early morning.

In addition to suppressing turbulence in the woods, an inversion over the canopy tends to seal gas or smoke in the woods, since by the inversion, an agent reaching the canopy is prevented from going further. However, with a lapse, any agent reaching the canopy is carried away in the upper air and lost to the operation.

If it is not possible to estimate the temperature gradient and wind velocity over the canopy, the same quantities estimated for a near-by open field may be used with some success.

14.9.6 Low Canopy Jungle or Heavy Brush

The San José project investigated the condition inside a heavy, low-canopy jungle. Measurements were made of wind speed at heights of 5 m (above the canopy) and 2 m (inside the canopy). The following text is quoted from their results.

The relationship between the winds at the 5- and 2-m levels and the temperature profiles showed that the same general effects occur in a low- as in a high-canopy jungle, except that the effects are concentrated over a much smaller height interval. In fact, the effects are intensified by the extremely heavy cover which at times produces effectively a second ground surface at the top of the jungle in typical areas. For example, between the free air and the jungle floor (a height interval of roughly 20 m in high-canopy terrain) a ratio of 8/1 is common for the wind speeds when the overhead wind is 6 mph. In a heavy, low-canopy jungle this ratio would be 12/1 or 15/1 and the height interval would be only 3 to 5 m. Whereas a lapse or inversion of 1 degree C might be found in a layer 10 m deep over a high canopy, the

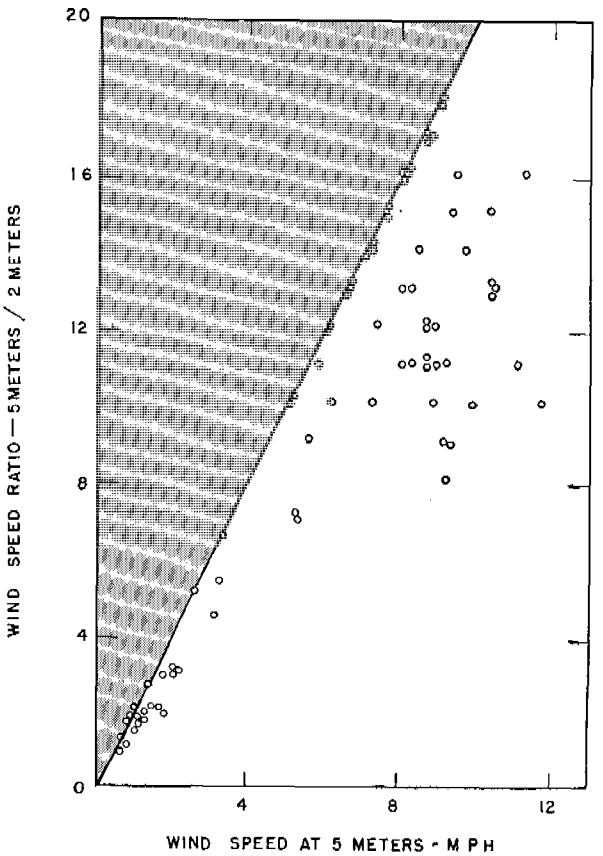


FIGURE 28. Low canopy jungle.

same temperature difference is possible in only 1 m over a low canopy because of the compactness which makes the top akin to a ground surface.

As in the high-canopy jungle, it was found that the ratio of the wind speeds above and down in the low-canopy jungle depended on the overhead wind. Figure 28 illustrates this dependence. The ratios obtained with the higher overhead winds were independent of the time of day. All the low-wind ratios were obtained at night or in the early morning. In the daytime the ratios were generally so large that, unless the overhead wind were greater than 5 mph, the wind below the canopy was too light to be measured with a cup anemometer (a wind with speed less than 0.5 mph). The shaded portion of Figure 28 represents the region in which no definite speed could be assigned to the lower wind and hence no ratio determined.

A further similarity between the high- and low-canopy jungles was found in the comparable situations which exist in each at night with low overhead wind. This is the condition most favorable for the

formation of inversions (provided it is not too cloudy). On a calm night, it is found that the air underneath the canopy is relatively independent of the air above. Its movement is not caused so much by the downward transfer of momentum from the air above the jungle as by the existence of drainage or gravity wind currents inside the jungle. Under such conditions, the ratio of the wind speeds can fall below unity. This effect was undoubtedly enhanced by the location of the low jungle station on a slope, where drainage winds are most likely to occur. On a flat region, it would be expected that, with a strong inversion above the canopy, the air underneath a low canopy would be stagnant.

Chapter 15

MICROMETEOROLOGICAL INSTRUMENTS

By *Wendell M. Latimer*

15.1 INTRODUCTION

The various micrometeorological instruments employed on Division 10 and CWS field projects are described in this chapter. While, in general, they proved adequate for the acquisition of the desired data, it is realized that many of them were developed rapidly under the stress of an emergency and can be further improved. In some cases it would have been desirable to make the instruments self-recording. This may be accomplished readily for permanent locations but is difficult for portable field equipment. The following instruments are described in this chapter.

1. Anemometers.
   a. Magnetic cup anemometer.
   b. Mercury cup anemometer.
   c. British anemometer.
   d. Hot wire anemometer.
2. Wind direction recorder.
   a. CIT-type vane.
   b. Commercial eight-point vane.
3. Temperature apparatus.
   a. Aspirated thermocouple system.
   b. Aspirated resistance thermometer system.
   c. Surface thermometer system.
4. Vanes for gustiness.
5. Miscellaneous.
   a. Smoke puffer.
   b. Photocell illumination recorder.
   c. Humidity measurement.
6. Dugway portable recording system.

15.2 ANEMOMETERS

15.2.1 Magnetic Cup Anemometer [a]

The anemometer is of the cup type with three cups rotating about a vertical axis (see Figure 1). The rate of rotation of the cups depends on the wind speed but is independent of direction for horizontal winds. For each rotation of the cup system, a set of small electric contacts close and open a circuit once (see Figure 2). Through a relay, one count is registered on a counter for each rotation of the cup assembly.



FIGURE 1. Anemometer and box ready for use. The cable from the anemometer is attached to the box through a weatherproof fitting.

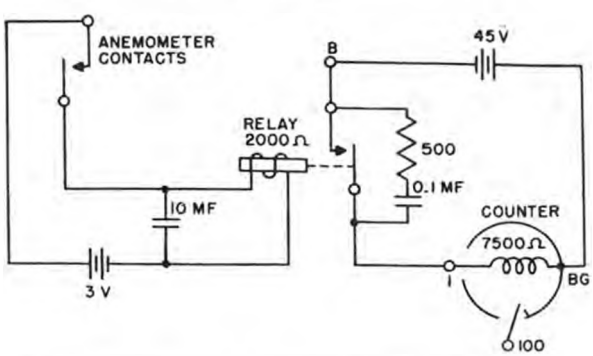


FIGURE 2. Diagram of wiring of anemometer, relay, and counter.

[a] This anemometer was developed by the Lane-Wells Company of Los Angeles in accordance with requirements set forth by Contract OEMsr-861. Since it was the anemometer most widely used in the field experiments, it will be described in some detail.

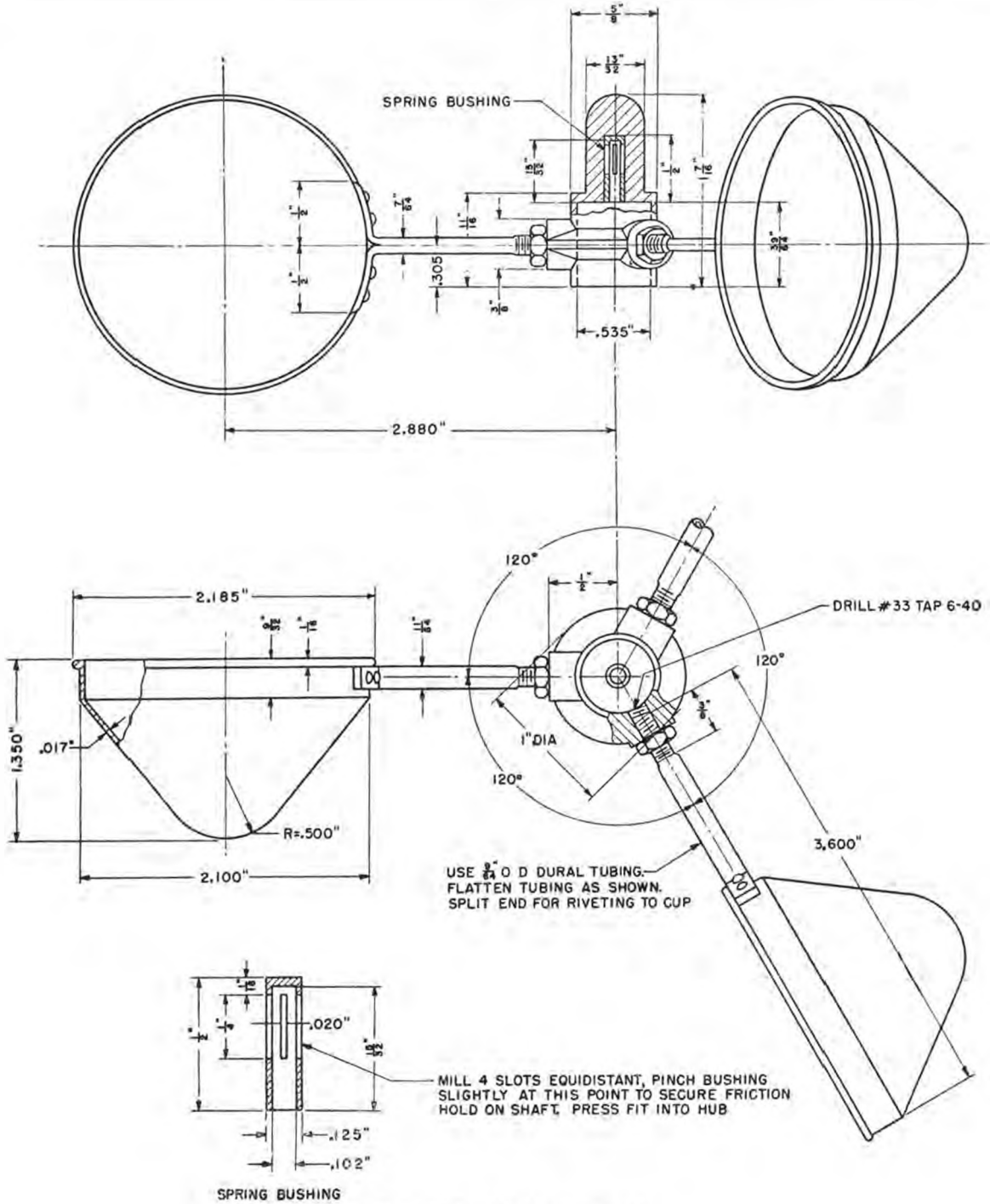


FIGURE 3. Cup and hub sub-assembly.

By observing the number of counts recorded in a calibrated instrument in a measured lapse of time, the average wind speed over a given time interval is obtained. The instrument will operate at wind speeds varying from a little less than 0.5 mph to perhaps 30 mph. The instrument has been left in the rain for days without having water reach the internal working parts.

The cup assembly rides on a jeweled bearing at the bottom and is guided by a circular Phosphor-bronze bearing near the top. The coupling between the rotor and the electric contacts is magnetic. The rotor shaft carries a horizontal semicircular segment of iron which moves under one pole of a permanent U-shaped magnet once for each rotation. In the field of the magnet is an armature supported in jeweled bearings. The armature carries one of the electric contacts and is moved a small amount on each approach of the iron semicircular segment. The armature is restored by a hairspring.

If it is desired to record the indications of the anemometer, an appropriate chronograph pen may be connected in place of the counter.

Since the cup assembly gives about 20 rotations per min per mph of wind (fewer at low speeds), direct counting by a chronograph pen may often be inconvenient. An auxiliary contact built into the counter makes it possible to record every hundred rotations instead of single rotations.

Details of the Anemometer

Cup System. The cup system is held on the rotor shaft by a spring bushing and is simply lifted off when the instrument is to be packed away. The cups are matched by weighing before assembling so that the rotor is carefully balanced. From one instrument to another the rotor dimensions are held closely similar; except at the lowest wind speeds, the calibration curves should be substantially the same for all instruments.

The cups (Figure 3) are somewhat deeper than those of the British anemometer Meteor No. 4 but are otherwise the same and will interchange with the cup system of the British instrument.

Rotor. Figure 4 shows the semicircular iron piece which is carried by the vertical rotor shaft. This drawing also shows the pivot point of the bearing on which the rotor stands.

Upper Bearing. The shaft housing carries a circular Phosphor-bronze bearing near the top. If this bearing is made too tight, the low-speed sensitivity of the anemometer is seriously impaired. The design of the instrument is such that dirt should not collect in this bearing too readily; but experience on this point is not extensive. The bearing is readily removable for cleaning; the bearing retainer at the top may be unscrewed and the bearing shaken out.

Inner Case. This is a small housing which carries the shaft housing. The inner case is cut away on one side to permit interaction of the soft iron segment with the armature, and on the other side to permit the introduction of a compensating magnet. A rubber packing ring is placed on the beveled top of this housing for waterproofing purposes.

Compensating Magnet. There is, naturally, a force between the U-shaped magnet and the semicircular iron piece which is carried by the rotor. This force might be expected to have some influence on the starting wind speed. With the idea of compensating it, a bar magnet has been mounted on a post on the opposite side of the rotor from the U-shaped magnet. Care must be exercised in selecting and placing this bar magnet; if the field from it is too strong, it can easily do more harm than good.

Electric Contacts Subassembly. This assembly is shown in Figure 5. The base (1) carries the subassembly and is fastened by two screws to the outer case bottom. The upright piece (3) is screwed to the base (1) and carries the moving parts of the subassembly. The permanent U-shaped magnet is (4). The armature (11) is mounted on an axis (7) and rocks slightly when the soft iron swings under it. This axis moves in jeweled bearings; one of these bearings is rigid in the upright (3) and the other bearing (12) is adjustable. A restoring force is exerted on the armature by a hairspring (13); tension on this spring may easily be altered somewhat by rotating (8) about the axis. The purpose of all this is to move an electric contact; this is carried by the right-angled piece (10) which is rigidly attached to the armature axis. The stationary contact is carried on the upright (5) which is electrically insulated from the base by the bakelite piece (2). The upright (5) carries two screws which limit the motion of the contact carried by (10). One of these two screws is tipped with a platinum contact; the other screw is insulated from the upright and is simply a stop. (In later instruments these two screws have been interchanged from the positions shown in the working drawing. In these instruments the hairspring closes the circuit and the magnetic effect opens it.)

External Electrical Connection. Within the instrument the electric circuit, when made, passes through the base, the hairspring, the contact, the upright (5), and a wire from (5). The circuit is brought to the outside of the outer case through an Amphenol part No. CL-PCLM. This can be connected to the cable by an Amphenol part No. MC1F on the end of the cable. The other end of the cable attaches to a receptacle in the carrying case.

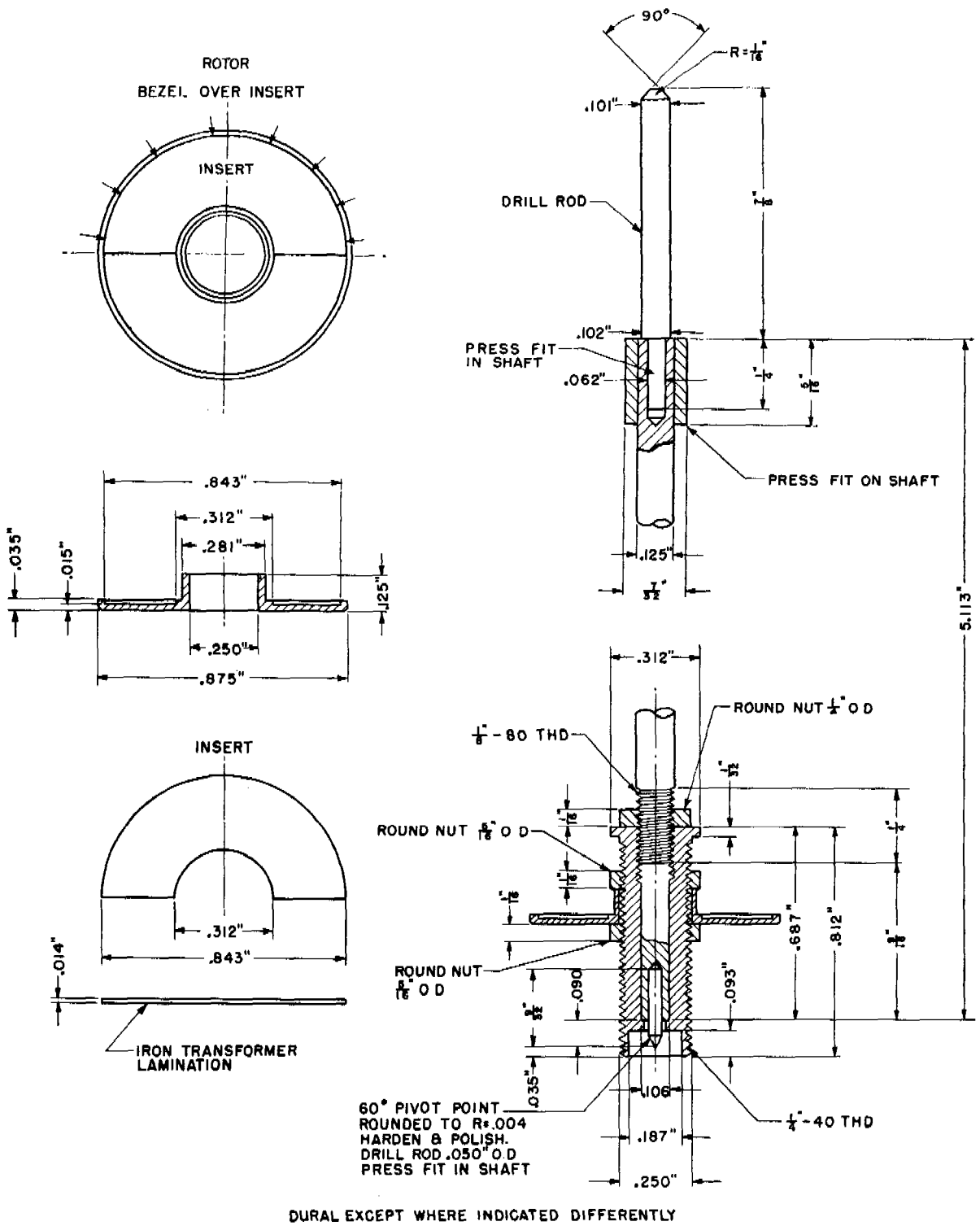
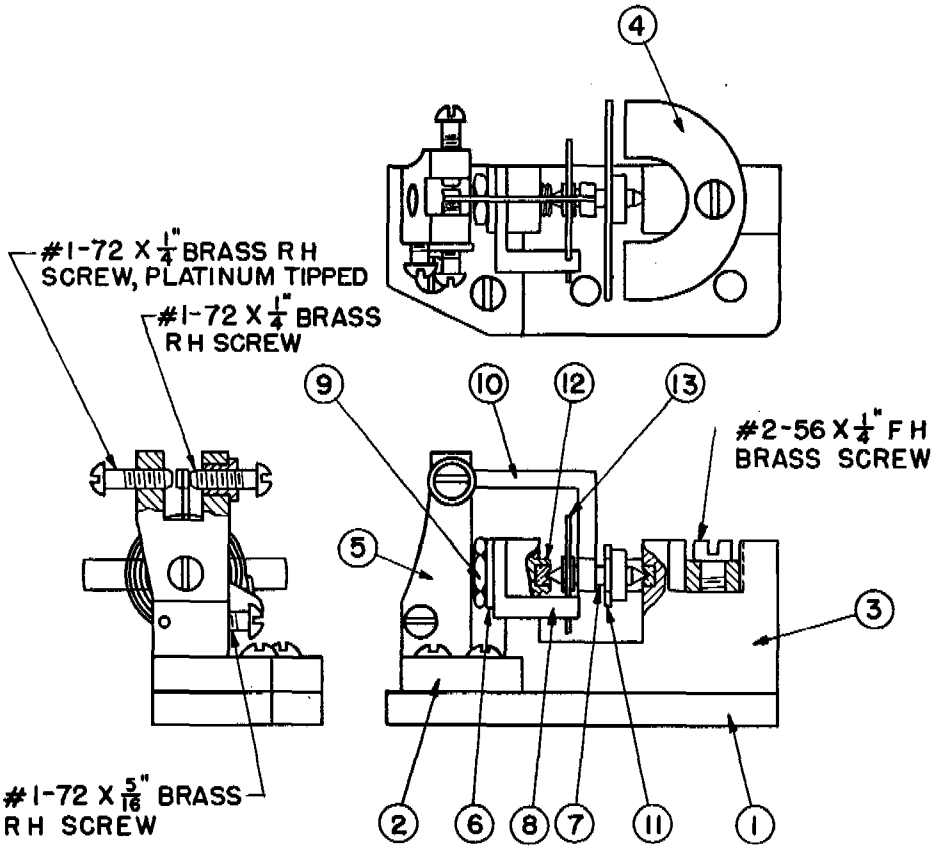


FIGURE 4. Shaft and rotor sub-assembl.



NOTE: TO FASTEN 5 ON TO 2 USE 1 #1-72 X 3/16" F H BRASS SCREW
TO FASTEN 2 ON TO 1 USE 2 #1-72 X 3/16" R H BRASS SCREWS
TO FASTEN 3 ON TO 1 USE 2 #2-56 X 3/16" F H BRASS SCREWS

FIGURE 5. Contact sub-assembly.

ACCESSORIES

A wiring diagram showing the connections of the anemometer to relay, batteries, and counter is shown in Figure 2.

The anemometer is connected through a small 3-v dry battery to the coil of a 2,000-ohm relay. Under these operating conditions the relay is extremely critical in its behavior toward adjustment; a small fraction of a turn of the screw controlling the relay hairspring makes the difference between operating satisfactorily and not operating at all.

Across the coil of the relay is placed a 10-μf electrolytic condenser. Without a large condenser, the contacts of the anemometer are very apt to stick and thus cause the instrument to cease indicating.

The counter is one made by the Cyclotron Specialties Co. It has a resistance of about 7,500 ohms and is actuated by a 45-v B battery. Although not imperative, a small condenser (0.1 μf) has been connected across the relay contacts through a 500-ohm resistance to reduce sparking. The carrying box is built to receive a standard-size B battery but not a heavy-duty battery. One end of the counter coil has been connected to the counter case and to the binding post marked *BG*.

An auxiliary contact has been built into the counter which allows a second independent circuit to be closed every 100 counts. The terminals for this circuit are the posts marked 100 and *BG*. Any apparatus employing this feature is additional to that shown in the photographs.

The box, which has been designed as a carrying case, in addition to holding the anemometer, relay, and counter, has compartments for the batteries, a

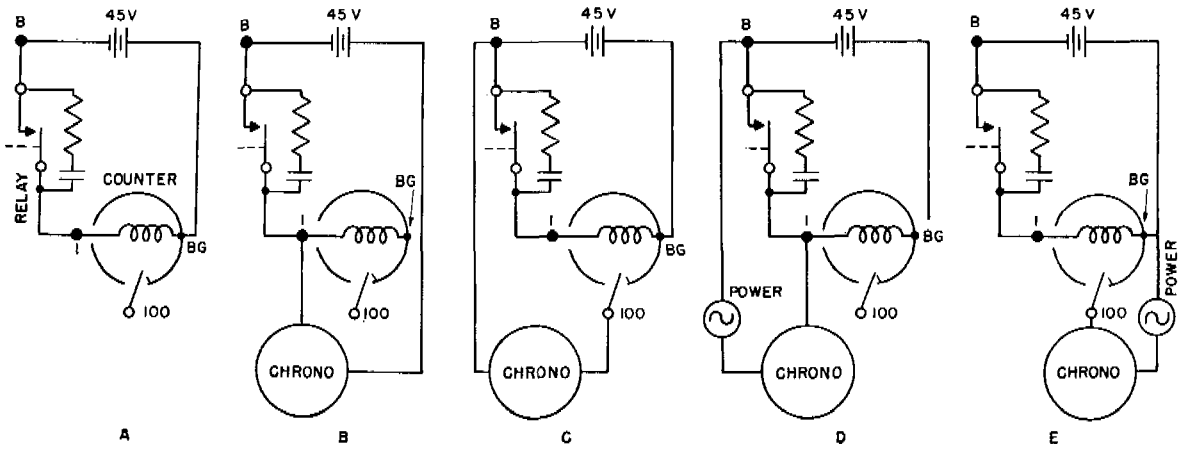


FIGURE 6. Diagram of alternative wiring arrangements.

cable, and calibrations. The outer dimensions of the box exclusive of handle and clasps are 12½ x 10¾ x 8¼ in. The weight of the complete outfit including batteries is about 25 lb.

WIRING ARRANGEMENTS FOR RECORDING

In the wiring diagram of Figure 2, the apparatus is arranged to give one count on the counter for each rotation of the cup system (case *A* of Figure 6). If it is desired to record by using a chronograph pen on a moving paper the connections may be made in any of the several ways shown in Figure 6. In these diagrams the anemometer circuit is like that of Figure 2 and has been omitted. The points labeled *B*, 1, 100, and *BG* are the similarly labeled binding posts. The necessary connections may all be made at the binding posts or at the wires connected to them without removing the panel on which the counter is mounted.

In case *B* the chronograph pen is arranged to be actuated by the B battery of the anemometer and receives one impulse per rotation of the rotor. The counter is shown disconnected. The chronograph pen of some Esterline-Angus milliammeters can be actuated by 45 v; but this power supply may not be appropriate in all cases.

In case *C* the B battery is again used for the chronograph but the chronograph receives only one impulse for each 100 rotations of the rotor. The counter is actuated once per rotation. If a chronograph is used with any except very low winds this arrangement or case *E* is desirable.

Case *D* is similar to *B* except that an external power supply is used for the chronograph.

Case *E* is similar to *C* but has an external power supply.

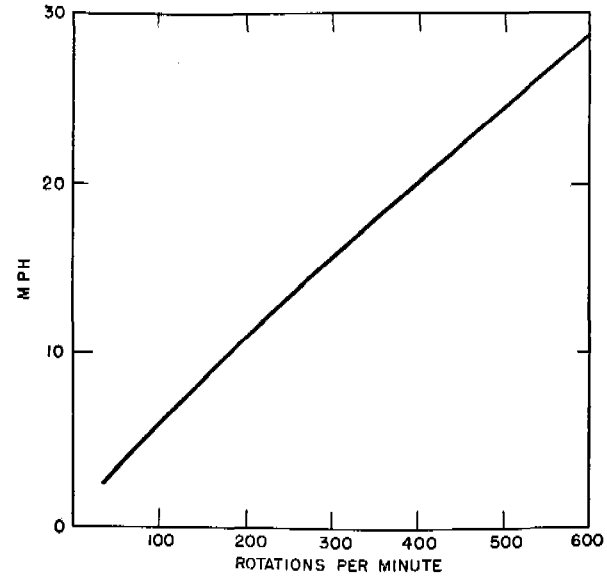


FIGURE 7. Anemometer calibration for higher speeds.

CALIBRATION CURVES

Calibration curves which are typical of all instruments are shown in Figures 7 and 8.

15.2.2 Mercury Cup Anemometer

Another anemometer which is capable of measuring wind speed as low as 0.5 mph is the mercury cup instrument.[b] This principle is quite simple. With each revolution, two small curved stainless steel knife edges attached to the cup arms make contact with two mercury surfaces contained in small iron

[b] This anemometer was designed and constructed on NDRC Contract 126, University of California.

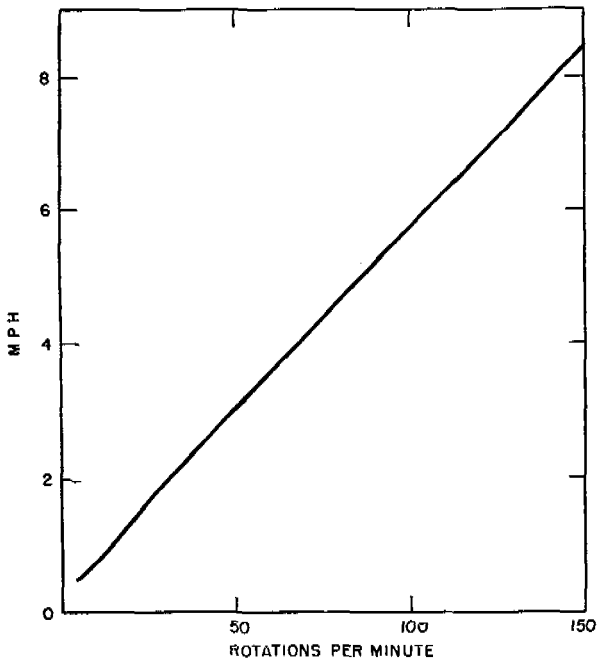


FIGURE 8. Anemometer calibration for low speeds.

cups attached to, but insulated from, the shaft. The current from a 45-v dry battery actuates the mechanical register. A schematic diagram is shown in Figure 9. The mercury contacts offer no detectable resistance to the rotation of the cups. This method was employed to replace a photoelectric counter and had the advantages of (1) simplicity, (2) no required vacuum tubes or amplifiers, (3) low voltage and current consumption, thereby making it independent of 110-v power supply.

15.2.3 British Anemometer

This instrument is the 3-cup type, the cups being 5.4 cm in diameter and the centers of the cups being at a distance of 7.0 cm from the axis of rotation. In early models the counting mechanism consists of a high-grade stop watch, the lever escapement of which is operated indirectly by the rotation of the anemometer spindle. The train of wheels is driven by the spring of the watch and thus imposes no frictional load upon the anemometer. As a result, this anemometer will function accurately to wind velocities as low as 1 mph. The provision of a beaded edge to the cups ensures a nearly constant factor for the instrument.[c] In later models the stop watch mechanism has been replaced by the more orthodox

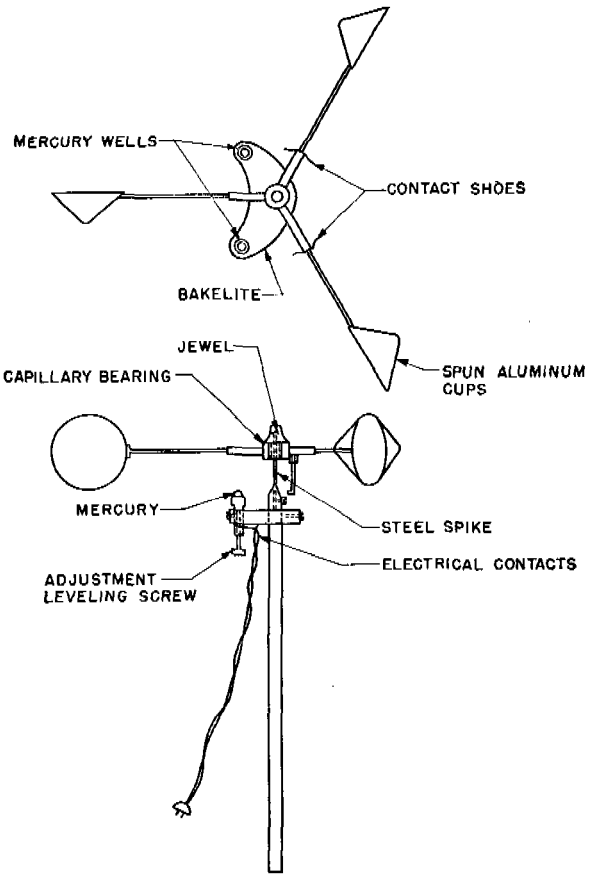


FIGURE 9. Schematic diagram of mercury cup anemometer.

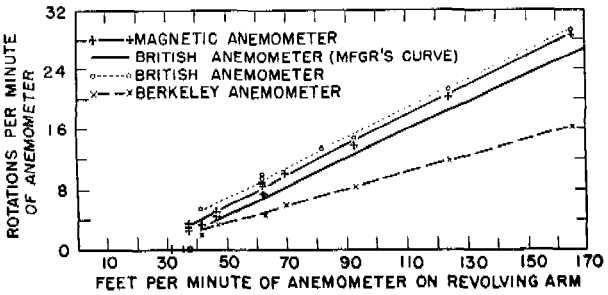


FIGURE 10. Comparison of magnetic, mercury (Berkeley), and British anemometer.

direct drive to a train of gears, but careful design of the bearings has resulted in this instrument being practically as sensitive at low wind speeds as the earlier model.

A comparison of the three anemometers was made [d] and is shown in Figure 10. The starting velocities of all three ranges between 30 and 40 fpm and the run-over or coasting rates are also comparable.

[c] The design of this anemometer is due to P. A. Sheppard.

[d] Contract NDCrc–137.

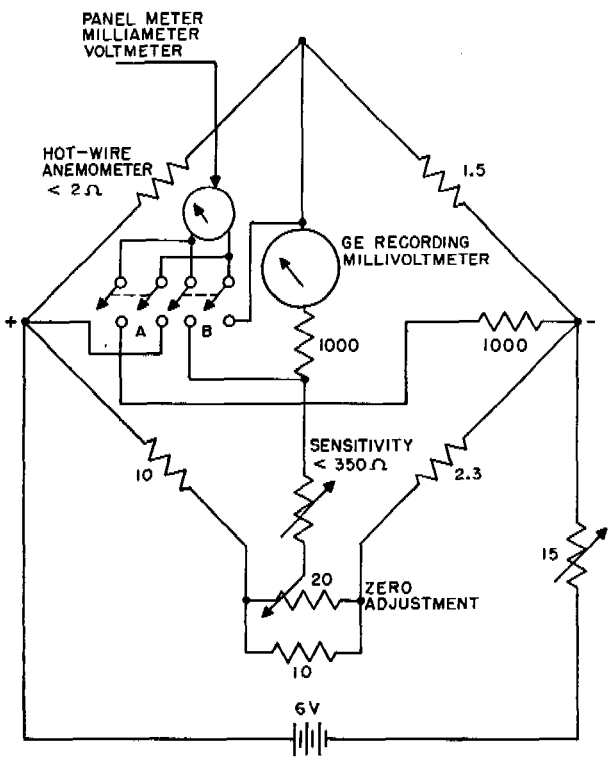


FIGURE 11. Diagram of recording-type hot wire anemometer.

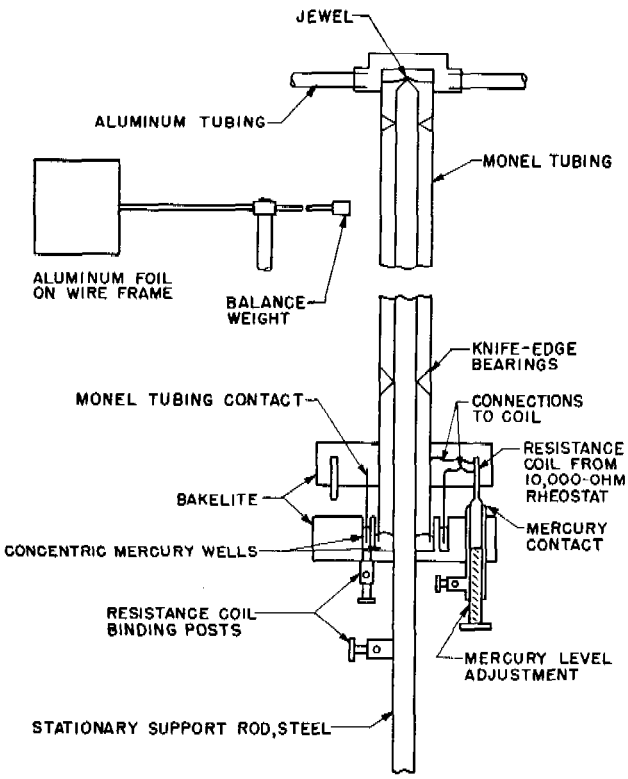


FIGURE 12. Diagram of CIT-type vane for wind recording.

15.2.4 The Hot Wire Anemometer

The hot wire anemometer, because its sensitivity is greatest at very low wind speeds, was found to be the most useful instrument in the jungle where winds of less than 0.5 mph (the starting velocity for the cup anemometers) are common.

The electrical circuit of the anemometer consists of a Wheatstone bridge, one arm of which is a short, fine wire (usually 50 in. of 0.003-in. Pt wire in the form of a bird cage) which is exposed to the wind. Through this wire is passed a given current, supplied by a storage battery, which causes the wire to heat. The wire will assume a certain temperature (and hence a certain resistance) when wind of a given speed blows by. The bridge is balanced with the anemometer covered; when the cover is removed, the resistance of the platinum wire will change by an amount corresponding to the wind speed. This causes the bridge circuit to be out of balance. The amount of this unbalance is measured by observing the reading of a milliammeter or by a suitable recording meter. A General Electric recording millivoltmeter was used for this purpose. A diagram of the circuit used in the San José work is given in Figure 11.

15.3 WIND DIRECTION RECORDERS

15.3.1 The CIT-Type Vane

This vane was designed and built at the California Institute of Technology [CIT] for the specific purpose of enabling the recording of wind directions at speeds of a few tenths of a mile per hour. This high sensitivity was made possible by the use of (1) lightweight materials, (2) circular knife edge and jeweled bearings, and (3) mercury contacts for the electric circuit. A diagram of the working parts of the vane is given in Figure 12. Omitted from the figure are the brass cover and collar which slip over the electrical part and protect it from the weather. A schematic circuit diagram is given in Figure 13.

The electrical circuit of the vane is essentially that of a potentiometer. By means of a B battery, a potential difference is applied across the 10,000-ohm coil in the vane. A certain fraction of this difference, which depends on the orientation of the vane, is tapped off by a small drop of mercury which touches the coil, and which in turn is connected with the recording meter. The current passing through the meter, then, is a function of the direction in which the

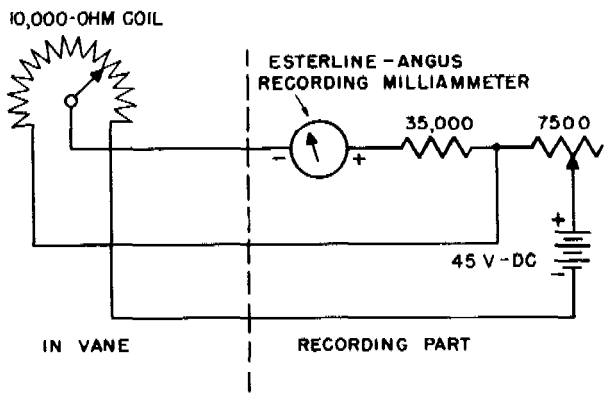


FIGURE 13. Diagram of electrical circuit of continuous recording vane.

vane is pointing. By having a high resistance in series with the meter, the current is made practically linear with the direction. Thus, if south is selected as zero, then east will read 0.2, north 0.4, and west 0.6 ma. The variable 7,500-ohm resistor in the circuit is used to adjust the proper maximum current which can flow through the meter. Since there is of necessity a gap of 15 to 20° in the vicinity of the switch-over direction (that direction corresponding to zero or the maximum current) the vane is set up so that the switch-over occurs at the direction, if any, which is least likely to be recorded. This keeps the record obtained from being confused and readings are kept away from that part of the scale which is least linear.

This type of recording vane was used in the winds normally encountered in the open, with just as satisfactory results as in the light jungle winds. A smaller tail was generally installed when higher wind speeds were encountered.

15.3.2 The Eight-Point Commercial Vane

At more or less permanent installations, the wind directions at the 2-m height were recorded by means of two eight-point vanes. As originally constructed, the vanes were designed merely to indicate direction by causing lights to go on inside a panel. They were not at all sensitive to low winds because of the heaviness and poor balance of the vane assembly. However, by devising a lighter assembly quite similar in its dimensions and construction to the CIT-type vane (the CIT tails were used), it was found that these vanes could be made adequately sensitive to winds as low as ½ mph. Instead of indicating directions on a lighted panel, the nine leads from each vane (see diagram) were wired to eight coils of a

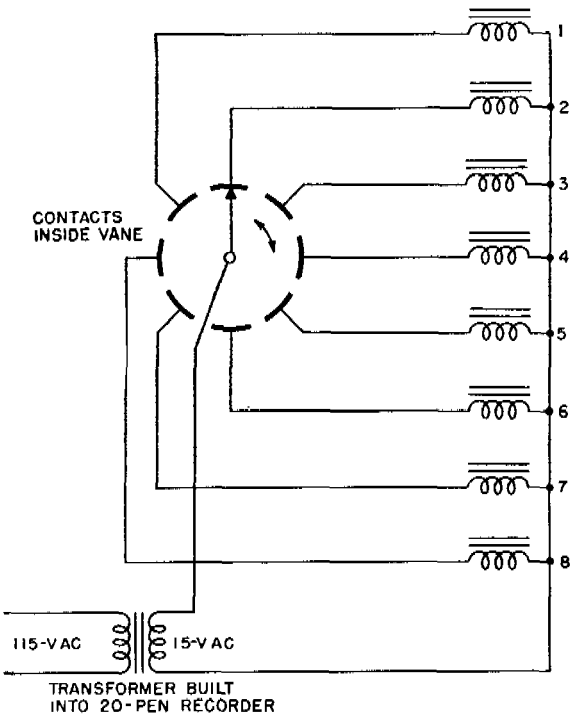


FIGURE 14. Diagram of eight-point vane.

twenty-pen recorder. A diagram of the electrical circuit is presented in Figure 14. These vanes were in operation for over two months without requiring any attention; the performance has been most satisfactory.

15.4 TEMPERATURE APPARATUS

15.4.1 Aspirated Thermocouple Systems

The apparatus consists essentially of a hollow mast carrying the radiation shields, aspiration occurring through the mast itself. With it, temperature differences between various thermoelements are read on a sensitive portable galvanometer. The apparatus is not recording but could be so modified. It was not designed for quantity production (only four have been made) nor for rough handling, although it is reasonably sturdy. It is, however, believed to give reliable results when properly used.

RADIATION SHIELDS

The radiation shields are the right-angled pieces attached to the mast as shown in Figure 15. They consist simply of the elbow (see Figure 16) of thin-walled tubing of 1-in. OD with an $1\frac{1}{16}$-in. inner tube of the same material held in the vertical part of the

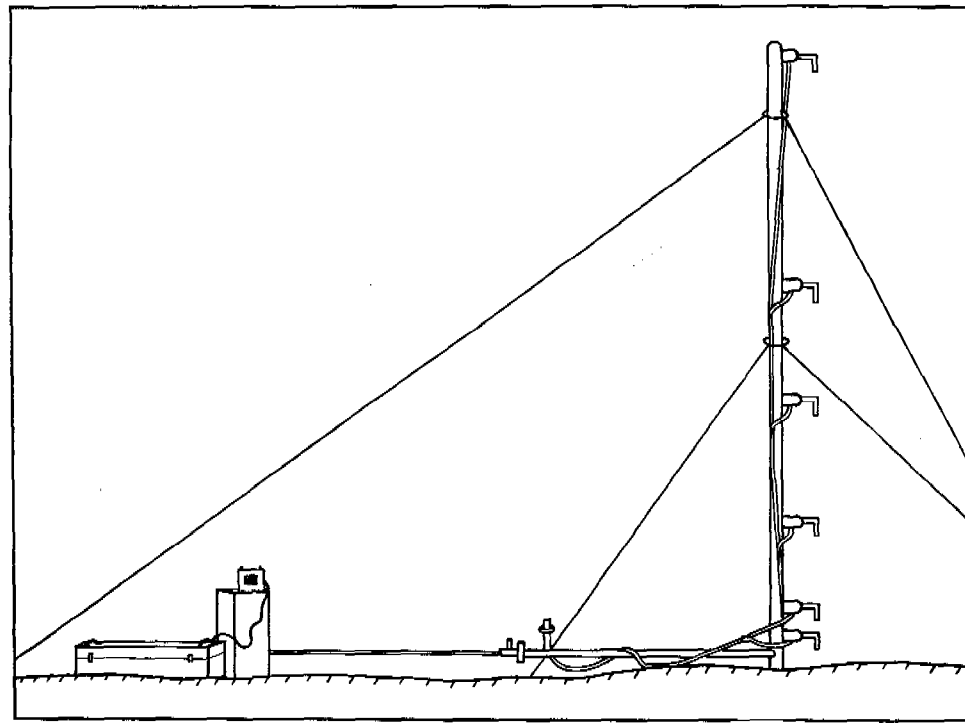


FIGURE 15. Diagram of mast with thermocouple system.

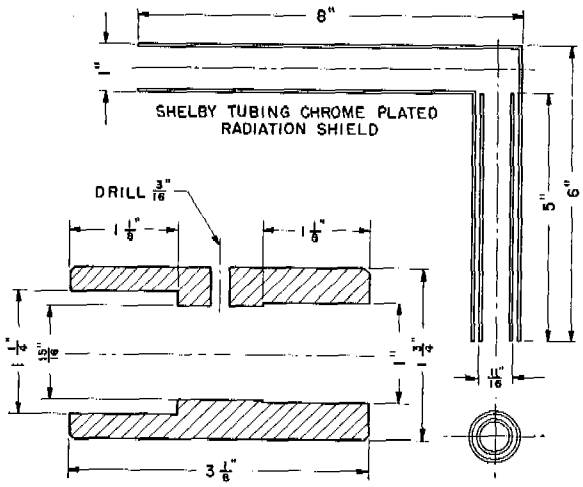


FIGURE 16. Diagram of radiation shield.

elbow by small pieces of rubber. The exposed thermoelement is placed just inside the outer opening of this inner tube and is held in the center by light pieces of wood. These various pieces of rubber and wood must not be so large as to impede aspiration.

The shields fit tightly into hardwood adapters which, in turn, slip over short open tubes protruding from the mast at appropriate levels. These adapters would be better if made of plastic.

The wires from the thermoelement continue through the length of the shield into the adapter and emerge from a hole in its side.

The type of shield shown here is a simplification of that used by A. C. Best.[1] The principal disadvantage compared with that of Best is the slight uncertainty as to the exact level at which air is being taken in; experiments with smoke suggest that the uncertainty is not more than 2 or 3 cm. In addition to simplicity, the present shield has the advantage that the air examined strikes the thermoelement before striking any part of the shield.

THE MAST

The free opening of the highest radiation shield is 5 m from the ground. (Higher masts with the same construction could doubtlessly be used.) The mast is made of 3-in. No. 18 Shelby steel tubing (cadmium plated). To give portability, it is made in five sections (see Figure 17); these fit together with the aid of end sleeves of 3-in. ID. The top section is closed at the top. The top section and the middle section are each provided with a loose ring carrying three eyes

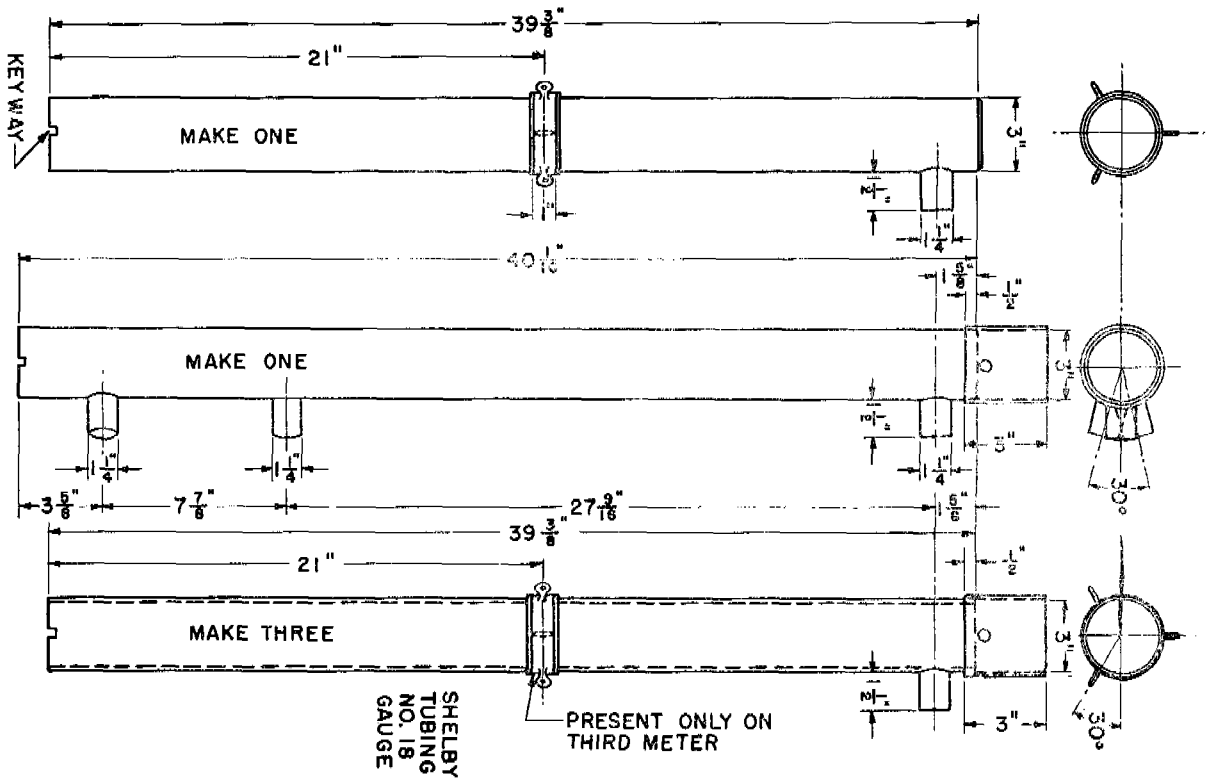


FIGURE 17. Diagram of 5-meter mast sections.

for light guy ropes. The various sections are provided with short side tubes to receive the radiation shield adapters. The heights provided by the mast are 5, 4, 3, 2, 1, 0.3, and 0.1 m; however, the side tube for a 4-m shield has never been used and might well be omitted. The bottom section of the mast fits into an L joint mounted on a base plate (Figure 18). The base plate is designed to assist in erecting the mast. The L joint receives a horizontal stretch of Shelby tubing leading to the aspirator. This horizontal member consists of two plain 1-m sections (not shown in the drawings); it is necessary that the aspirator be somewhat removed from any of the shields so as not to disturb the air around them.

The base plate carries a hinged flap with two $\frac{3}{8}$-in. holes, shown at the top of Figure 18. Before the mast is erected, this flap is pinned to the ground through these two holes. After the entire mast with shields is assembled on the ground, it is erected by rotation about the horizontal axis of the hinge; a third pin is then placed in the ground through the base plate and the mast is guyed.

Without moving the guys or base plate, the mast and the horizontal section leading to the aspirator may be rotated about the vertical axis of the mast. This is necessary so that the radiation shields may be kept up-wind of the mast, auxiliary apparatus, and observer in case the wind shifts.

THE ASPIRATOR

An ordinary aluminum household vacuum-cleaner blower has been found satisfactory for aspiration. To drive it, a 6-volt model locomotive motor No. 117-4 was used, made by Kendrick and Davis Co. of Lebanon, New Hampshire. A blower with its motor is indicated in Figure 15 at the left end of the horizontal 3-in. tube. The motor was operated from a storage battery, but alternating current may be used if available.

With the arrangement described, the radiation shields are found to be adequately and substantially equally aspirated. The air flow past the thermoelement is 1,200 fpm or more. The shields and their aspiration have been considered adequate if no significant temperature difference developed when two shields were placed side by side in the sun and a shadow was thrown on one shield.

A squirrel-cage blower, No. 3, made by the L-R Manufacturing Co. of Torrington, Connecticut, can

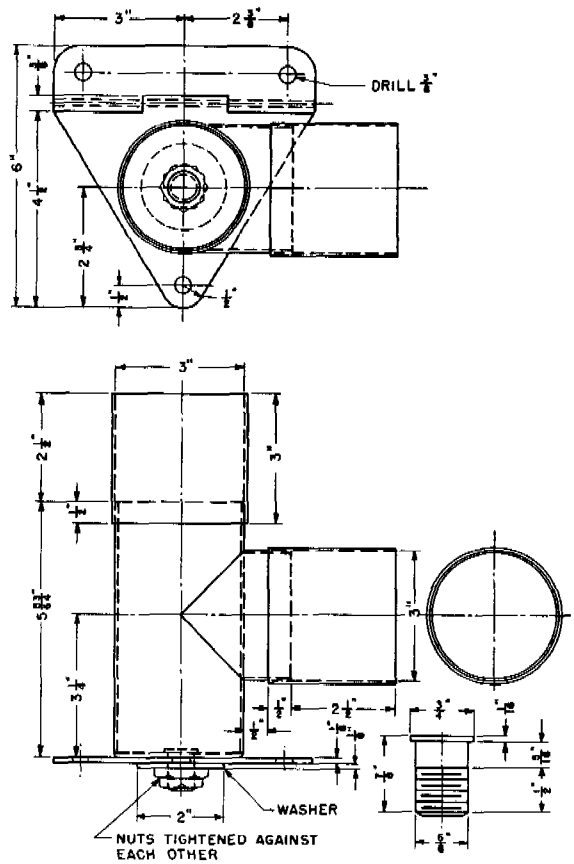


FIGURE 18. Diagram of base plate and L joint.

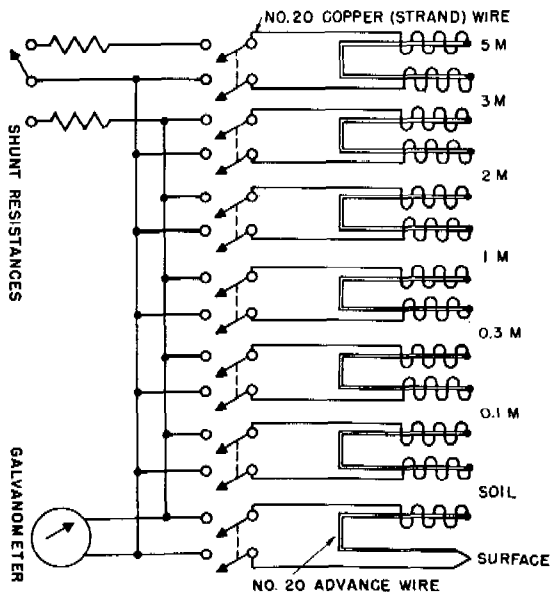


FIGURE 19. Diagram of thermocouple system.

easily be mounted so as to be used instead of the vacuum-cleaner blower. Although the squirrel cage blower would appear to be satisfactory, field trials have not been made with one.

If it is desired to measure profiles through heights of more than 5 to 10 m, such as is the case if a profile is desired from the ground up through the tree crowns in a forest, it may be more convenient to dispense with aspiration through a mast and provide each junction with an aspirator at its own level.

THE ELECTRICAL SYSTEM

Single-junction copper Advance thermoelements were used. Number 20 wire was employed; and, at the junction, several turns of one wire were wound closely around the other and the whole soldered. This gave a junction of moderate heat capacity, which was desired since it was not the intention to follow momentary temperature fluctuations. The arrangement of the various junctions is shown in Figure 19. Thus, there was one junction in the top radiation shield and two junctions in each of the other shields, so that temperature differences between adjacent levels were measurable.

In order to obtain temperatures as well as differences, one thermocouple had one junction in an aspirated shield (that at 0.1 m) and the other in a pointed copper piece inserted about 2 in. into the ground. In the copper piece was also placed a mercury thermometer graduated to 0.1 C and with its bulb in good thermal contact with the thermoelement. The *soil temperature* as given by this mercury thermometer was relatively steady. Aside from its own interest it afforded the basis of determination of the air temperatures.

In the soil thermometer there was also one junction of a couple, the other junction of which was in a device to measure surface temperatures. This was a piece of heavy felt with a fine wire junction in its surface. The felt was mounted in a convenient handle. In use, the junction is pressed against the ground for a second or two and then moved to a new spot presumed to be similar to the first. This is repeated as many times as may be necessary to obtain a constant reading. This procedure appears to give intelligible results in case the ground presents a reasonably well-defined surface on which to make measurements.

Although not imperative, it is highly convenient to

have all thermocouples built with the same resistance so that deflections on a galvanometer may be converted to temperature differences, using the same calibration for each couple. It was found convenient to build all thermocouples into a single waterproof rubber-covered cable with appropriate taps leading to each shield. (Thus, the top section of cable between 3 and 5 m contains only two wires, one copper and one Advance, with increasing numbers of wires at lower levels. The wires in the part of the cable leading to the galvanometer are all copper.)

The electromotive force given by a copper Advance thermocouple is only 40×10^{-6} v per centigrade degree of temperature difference. Consequently, care must be exercised with the insulation to avoid the introduction of extraneous electromotive forces; and precautions must be taken to eliminate thermoelectromotive forces other than those due to the couples.

The thermocouple cable leads to a set of switches; these are contained in the upright box at the left of Figure 15. (This box serves as a carrying case for all parts except the mast, which packs in the horizontal box.) Ordinary copper knife switches are used; attempts to replace these by a compact multiselector switch have been unsuccessful because of the introduction of spurious electromotive forces presumably originating at the silvered switch contacts. With the aid of double-pole single-throw switches any desired couple may be connected to the galvanometer.

The galvanometer should be a low-resistance instrument with as high sensitivity as is compatible with ready portability. A Leeds and Northrup galvanometer No. 2420B with enclosed lamp and scale has been found convenient. A galvanometer chosen to have adequate sensitivity for small temperature differences may give too large deflections with large temperature differences. Therefore, it is convenient to provide one or two shunts which may be quickly thrown in if desired; these may be chosen so that the factor for converting deflections into temperature differences is made a small integer and thus the apparatus is made substantially direct reading.

Observational Procedure

With the apparatus set up in the desired location, and with the radiation shields up-wind from the mast and the rest of the apparatus, the blower is started 2 or 3 minutes before observations are to start. The zero position of the galvanometer is read with the instrument shorted through a resistor; this observation is repeated frequently. A series of deflections is then read, starting with the 5- and 3-m junctions and proceeding down the mast, ending with the 0.1-m soil thermocouple. Because of fluctuations in the individual temperatures, the series is immediately repeated. About 5 min are required to make four series of readings; thus any one temperature difference is measured four times at intervals of a little over one minute and the results averaged. Along with this group of observations, the mercury soil thermometer is read and, if desired, the soil-surface difference.

15.4.2 Recording Resistance Thermometers

A convenient method of measuring and recording a series of temperatures in order to establish the gradient in the atmosphere is by means of resistance thermometers. The temperature difference between two thermometers at different levels may be measured by placing the resistance coils in the arms of a Wheatstone bridge. The unbalanced bridge circuit may be employed to operate a Leeds and Northrup Micromax, or the unbalanced potential may be registered directly on a recording General Electric millivoltmeter. The following is a description of the system employed on the San José program. Figure 20 is a diagram of the circuit. There are ten pairs of arms, any two pairs of which can be connected by means of automatic rotor and base selector switches to form a bridge. T_1 through T_9 are the arms whose resistance indicates the desired temperatures. They are coils of fine copper wire inserted in the aspirated shields at various levels from 0.3 to 24 m on the tower. When two of these arms form part of a bridge, a temperature difference between them will cause the bridge to be out of balance, and a potential difference proportional to the unbalance will be set up across the meter and recorded. T_{10} is a coil of Manganin wire. Because of the low temperature coefficient of resistance of Manganin, a bridge formed with this arm and the one selected for the reference temperature will be out of balance by an amount indicative of the actual temperature of the base thermometer. Either of the bottom two thermometers is used for the reference because the short period temperature fluctuations are smallest at these points.

When in operation, the rotor switch is actuated by a synchronous motor in such a way that the bridge

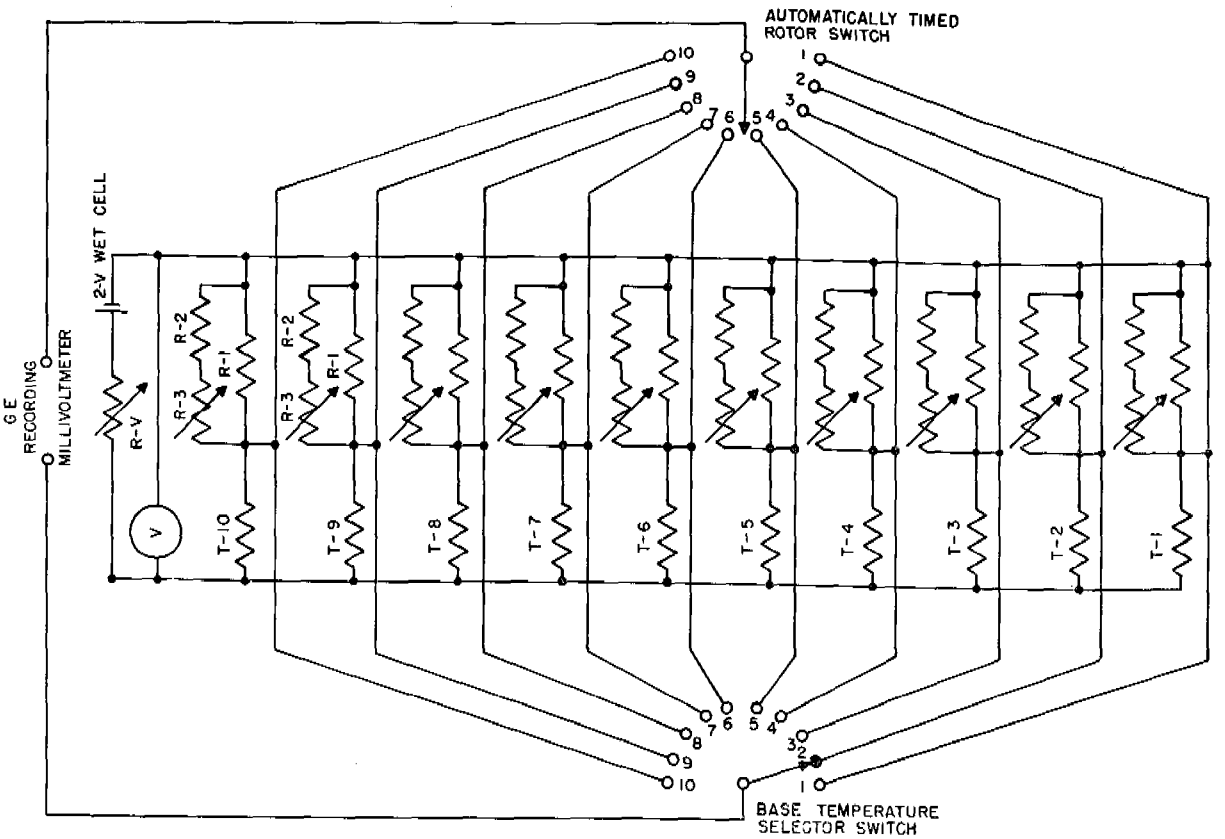


FIGURE 20. Diagram of resistance thermometer system.

circuit is changed every minute. A complete cycle, then, is made every 10 min. Each time a new circuit is made, the synchronous motor also causes the meter to make a mark on the record roll, thus permitting the separate temperature differences to be distinguished readily. A sample record is given in Figure 21. A typical cycle with T_1 as the reference thermometer will have the following sequences. First, when T_1 is in the circuit, the meter records the zero reading, because there is no potential difference across the meter. Then, with T_2 through T_9 succeeding one another, the temperature differences between each thermometer and T_1 are recorded. Readings to the right of the zero indicate that that thermometer is warmer than T_1; to the left, cooler. Finally, when T_{10} is in the circuit, the actual temperature of T_1 is recorded. After an open circuit, the cycle repeats itself.

Certain of the important details of the electrical circuit will be mentioned below. Reference is made to Figure 20. The thermometers T_1 through T_9 are wound with No. 38 copper wire and have a resistance of exactly 5 ohms. Since the nine arms containing these thermometers must all have the same resistance, the leads to them are all of the same length. (At the tower station 40-m lengths were used.)

The T_{10} is a 3-ohm Manganin coil. The ten resistors R_1 are Manganin coils each with a resistance equal to the total resistance of its opposite arm. R_2 and R_3 are fixed and variable 500-ohm resistors, respectively. The resistances of the 10 arms on the left-hand side of Figure 20 are adjusted by means of the variable resistors to be exactly equal to one another and as close to 5 ohms as possible. The variable resistor R_v is used to adjust the voltage applied across the bridge and the sensitivity of the scale.

15.4.3 Surface Thermometers

In general, the moving felt pad method of measuring surface temperatures was employed with either a thermometer or a thermocouple junction in the pad.

A description of the San José project thermocouple system follows.

An Advance copper couple of No. 32 wire was used. One junction was fixed on the bottom of a rubber

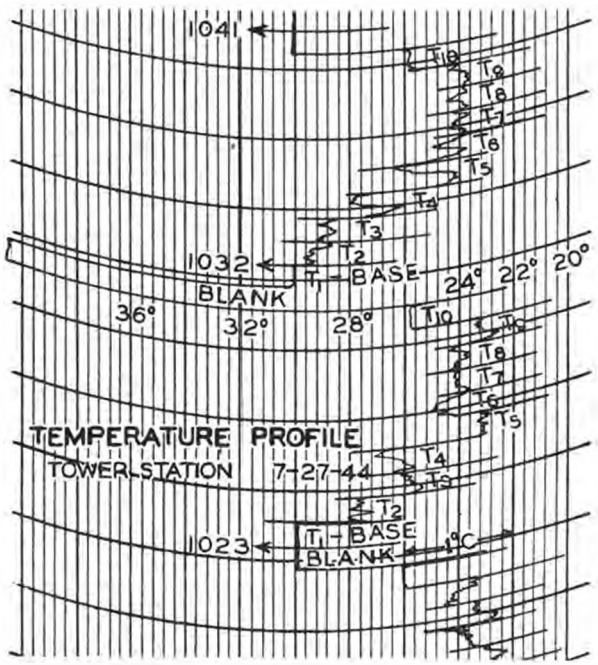


FIGURE 21. Diagram of a thermometer profile recording.

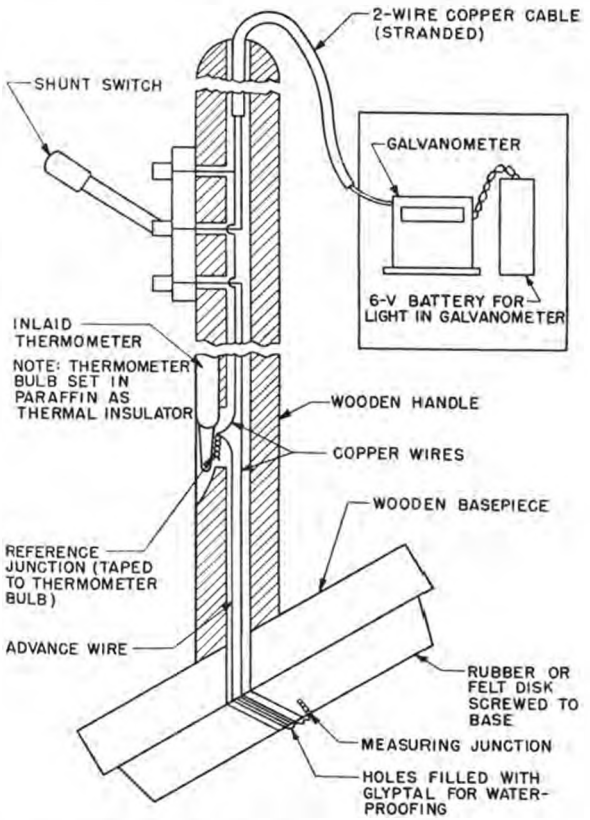


FIGURE 22. Diagram of a surface temperature measuring device.

disk which was attached to a wooden handle 4 ft long. The other junction was set in the handle of a thermometer which gave its temperature. A Leeds and Northrup low-resistance (25-ohm), high-sensitivity galvanometer was mounted on a portable stand and connected to the circuit at the end of 20-ft leads. Thus, while one operator recorded the galvanometer reading, another would apply the junction to various surfaces, reading the reference temperature occasionally. A schematic diagram of the assembly is given in Figure 22.

15.5 VANES FOR GUSTINESS

The British bidirectional vane is probably the most satisfactory instrument used to obtain gustiness factors. However, two other instruments were developed and employed to a limited extent. One, designed at Berkeley, was a vane which consisted of a single lightweight weathervane with a single turn of No. 40 Chromel wire mounted on the rim of a bakelite disk attached to the stationary shaft. A brush is attached to and rotates with the vane. A suitable potential difference (depending on the desired sensitivity) is applied along the full length of the Chromel wire and as the brush rotates with the vane, the difference in voltage between the brush and one end of the Chromel wire is recorded on the moving chart of an Esterline-Angus recording milliammeter.

The other, developed at CIT, is a bidirectional vane whose movements are registered by Cenco electric impulse counters. The shaft of the vane is mounted in brass gimbals, and on each of the two axes of the gimbals, brass wheels are mounted which turn with the axes. These contact wheels are slotted around the periphery, and the slots are filled with an insulating material. As the wheel turns, a sliding contact alternately makes and breaks an electric circuit and records on the counters the magnitude of movement of the wheel, and, hence, of the vane itself. One wheel registers lateral movements of the vane and the other vertical movements. Each is slotted over one-half its circumference to make contacts so spaced that the attached counter registers once for each 3° movement of the wheel. A single slot is cut in the center of the unslotted portion of each wheel, and the orientation of the wheel and sliding contact is made in such a way that this slot breaks the contact whenever the vane is in a mean position.



FIGURE 23. Photograph of British bidirectional vane.

Two sliding contacts are mounted 180° apart on each wheel, and each registers on a separate counter. One measures the total amount of deflection which the vane experiences and the other records the number of times that the mean position is crossed. The four counters required are mounted in a conveniently transportable box. The gimbals are mounted on a brass tube which can be supported by a surveyor's tripod, and from the tube a cable connects the contact points in the gimbals with the counter box.

The British bidirectional vane was constructed after the design by Best. In his original paper Best gives the following discussion.

The bidirectional vanes were constructed for this particular investigation and in their construction, special attention was paid to the following points:

1. The vanes should be as sensitive as possible to light winds.

2. The sensitivities in horizontal and vertical directions should be as nearly equal as possible.

3. The supports and chart holders should be arranged to cause the least possible interference with the vane.

4. The two vanes should possess similar characteristics.

5. The vanes should be fairly robust in order to prevent accidental damage.

The first two points were satisfied by making the vanes light, reducing the friction at the bearings to a minimum, making the moment of the pressure due to the wind about the axis as large as possible, and making the vanes symmetrical about their axes. Allowance was made for the third point by ensuring that the center of the vane should be at least five times the height of the chart holder above the base of the chart holder.

A photograph of one of the vanes is shown in Figure 23. As may be seen, the actual vane was constructed of stiff wire and balsa with a brass balance weight at the nose. The bearings were all point bearings, and stops were provided to prevent the vanes from being deflected too far in either direction. Suspended from the framework of the vane was a wire pen arm to the end of which was attached a small glass pen. Every movement of the point of suspension of the pen on the vane arm was reproduced, to a close approximation on the same scale, on a chart which formed part of a cylinder having the same vertical axis as the vane. The glass pen was made by drawing out a piece of glass tubing and bending the fine end suitably.

15.6 MISCELLANEOUS

15.6.1 Smoke Puffer

A simple and practical means for estimating wind speed and direction in the jungle without the use of elaborate recording instruments is by observing the travel of a small smoke cloud. The smoke from an H–C mixture is fairly satisfactory, but because of its heat, this smoke tends to tower in low winds. On mixing with moist air, titanium tetrachloride ($TiCl_4$) forms a cool white smoke. Figure 24 gives the essential features of a simple device which employs this material to produce puffs of smoke which can be followed with ease for distances of 10 to 20 ft through the jungle. A rubber tube of suitable length permits the operator to generate the smoke by "remote control."

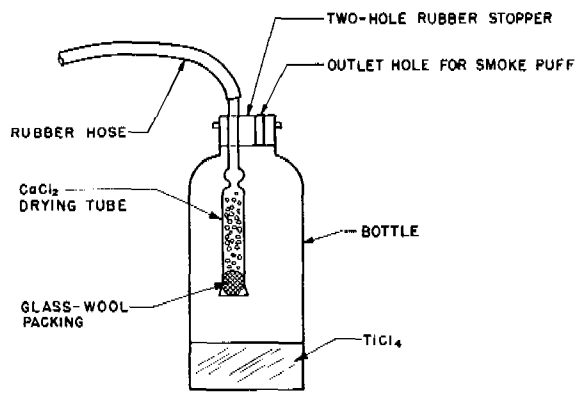


FIGURE 24. Diagram of a smoke puffer bottle.

15.6.2 Photocell Illumination Recorder

The primary factors influencing the magnitude of the daytime lapse in a given area are: (1) the altitude of the sun, (2) the wind speed, and (3) the amount of cloud cover. The first two factors can be ascertained readily by direct measurement and from knowledge of the time of day, time of year, and the approximate latitude of the area under consideration. The amount of cloud cover, however, is a different quantity to handle, especially in a jungle, and when more or less continuous observations are necessary. An instrument which records a quantity related to the intensity of the solar radiation should yield data varying with cloud cover. Such an instrument was designed and constructed at San José and installed at the tower station. It was essentially an electronic circuit which amplified the current of a photocell.

The cell with vacuum tube and batteries was mounted in a waterproof box at the top of the tower, one side of the box being made of Plexiglas, a transparent plastic. A sheet of white celluloid, fixed in the horizontal plane, reflected the light from the sun, sky, and clouds through the window to the photocell. The current induced in the cell was amplified by the vacuum tube and then passed through long leads to a recording milliammeter at the instrument shack.

15.6.3 Humidity Measurements

Sling psychrometers were generally used to measure relative humidity. A hygrograph may frequently be employed to follow general diurnal trends in the forest, although it is not accurate in detail because of shifting of the zero point. The dry bulb of the sling psychrometer was used regularly in some projects as a check against the temperature profile apparatus.

15.7 DUGWAY RECORDING INSTRUMENTS

15.7.1 The Selection and Plan of Operation of Field Micrometeorological Instruments

The most usual practice in the testing of chemical warfare munitions from which a gas cloud is produced is to function the munition in a selected area over which samplers are distributed in a known pattern. These samplers produce a record at each sampling point of the total Ct, the Ct produced within a given time interval, or of the time-concentration curve.

These chemical sampling results are dependent on the characteristics of the munition, the influence of the agent on the natural air-flow pattern (for example, the gravity effect), and the air-flow pattern itself. The effect of the latter may be stated most simply in terms of a wind speed representative of the area, a wind direction representative of the area, and a temperature gradient representative of the area. The time interval involved is the same as that used in the chemical sampling.

For preparing munition requirement tables as well as for the intercomparison of different munitions, it is evident that the accuracy requirements of the micrometeorological assessment are fixed by the accuracy requirements laid down for the chemical sampling; if it is desired that the chemical results be known to $\pm 20\%$, then, for example, the tolerance of the wind velocity measurement should be selected so that it is found from a consideration of gas cloud behavior that this amount of change in the wind velocity will affect the Ct by not more than $\pm 20\%$.

The instrumental accuracy of the anemometers will ordinarily be much better than this, but because of the natural variations in wind speed over the target area, several anemometer locations may be required in order to fix the representative wind velocity within these limits, particularly if the sampling time is short. For the sake of increased accuracy, the instruments will frequently be located within the area considered dangerous to personnel; hence the instruments should be self-recording or remote-indicating.

Similar considerations apply to measurements of temperature gradient, except that ordinarily this quantity is steadier and more nearly uniform over the target area than is wind velocity. For a desired accuracy of $\pm 20\%$ as reflected in the chemical sampling, the required accuracy in the measurement

of temperature gradient between 2 and 0.3 m turns out to be on the order of ± 0.05 degree C, for open terrain.

Another variable micrometeorological factor, usually observed if present, but not measured, is the presence of updrafts and downdrafts over the target area. Ordinarily the value of the micrometeorological data will be much enhanced by photographic and visual notes; an overall estimate of the weight, which should be given to the results of a particular field trial, can be given only after a review of all the observations taken, preferably as soon as possible after the operation.

Another closely allied objective of chemical warfare meteorology is to enable the prediction of gas-cloud behavior at a given time and location, both for offensive and defensive purposes as well as for selecting the optimum time at which to run field experiments. In this case the accuracy requirements are less strict than for most proving ground work, but it is desirable to collect long-period records from unattended instruments, and to have them in such form that they may be quickly scanned without further treatment.

15.7.2 A Representative Selection of Recording Instruments for Field Use

The most satisfactory instruments covering the optimum ranges and fulfilling the above requirements, as indicated by NDRC experience at Dugway, consist of the following:

1. For wind speeds from 1 to 15 or 20 mph: A light, contacting, 3-cup anemometer such as the Lane-Wells or Friez 339-L used with a relay-type frequency meter and an Esterline-Angus recording milliammeter.

2. For wind direction (down to about 0.3 mph): A wind vane with a potentiometer-type head, in conjunction with another Esterline-Angus recorder.

3. For temperature gradient: Thermocouples mounted between the two selected levels (now usually 0.3 and 2 m), aspirated (or if unaspirated, then proven by experiment to fulfill the desired accuracy requirements) and connected to a photocell galvanometer-amplifier the output of which is recorded on a third Esterline-Angus recorder.

4. For wind speed from 0 to 2.5 mph: A hot wire anemometer, the output of which is recorded by a less sensitive photocell galvanometer-amplifier with Esterline-Angus meter.

The above instruments (with the exception of the hot-wire anemometer, for which a satisfactory design has already been described) have all been made battery-operated and self-contained in weatherproof cases capable of being transported by vehicle over rough roads, of being handled and set up in the field by one operator, and of operating for several hundred hours without attention or significant change in calibration.

Although the above instruments have been thoroughly tested by actual use over a period of a year, and although they can be operated and maintained by selected enlisted men, and have in their operation entailed a tremendous saving in manpower where extensive records were to be taken, in many cases the simpler hand-read devices will suffice, particularly for measurements of temperature gradient, surface temperature, and long-time averages of wind velocity.

The wind speed recorder, 1 to 15 or 20 mph, has in particular shown itself to be a far more useful instrument than was first anticipated by properly evaluating in the simplest manner the representative wind speed over an area.

15.7.3 The Relay-Type Frequency Meter

The most satisfactory means found for recording wind velocity from a rotating anemometer consists of an Esterline-Angus milliammeter used with a relay-type frequency meter. This system presents the advantages that (1) the record is immediately available without further treatment, (2) the record is not far from linear in calibration, (3) there is a choice of paper speeds ranging from $\frac{3}{4}$ in. per hr to 3 in. per min depending on the purpose for which the record is required, and (4) that the records may be preserved in compact form in such a way that although any portion may be intensively studied, there is no further measuring or computation to be done.

This type of circuit, shown in Figure 25, is referred to [14] as a condenser discharge anemometer. It operates as follows:

When the anemometer contacts are closed, the relay (see Figure 25) is energized and C_1 is charged through the lower relay contact to essentially the full voltage of battery B. When the anemometer contacts are opened, condenser C_1 discharges almost completely into the smoothing condenser C_2 (much larger than C_1) and eventually the charge passes through the milliammeter. This process is repeated for every make and break of the anemometer con-

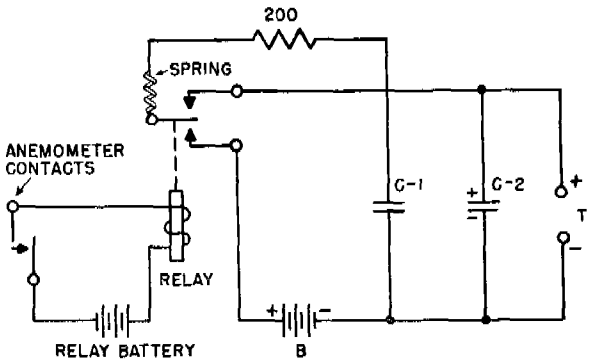


FIGURE 25. Circuit diagram of a relay-type frequency meter.

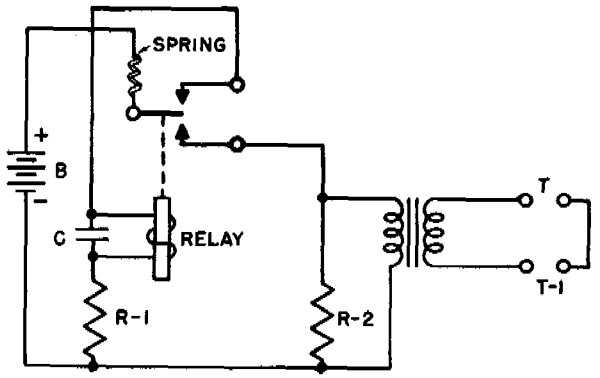


FIGURE 26. Circuit diagram of a keep-alive relay oscillator.

tacts, the quantity of electricity transferred each time being equal to the $V_b \times C_1$, where V_b is the battery voltage and C_1 is in farads. The current through the milliammeter is then equal to $F \times V_b \times C_1$, where F is the number of anemometer contacts per second.

Since the resistance of the milliammeter is fairly high, the voltage drop across the terminals T is an appreciable fraction of V_b, and C_1 will not be completely discharged when the milliammeter shows a deflection. The exact formula relating I_m, the current in milliamperes passing through the recording meter, to F is given below:

$$I_m = \frac{1{,}000\, C_1\, F\, V_b}{1 + C_1\, F\, R_m}$$

where R_m is the meter resistance.

The number of contacts per second corresponding to each successive mile per hour of wind speed can be obtained from the anemometer calibration curve; V_b and C_1 can then be so chosen that the resultant calibration curve (milliamperes against wind speed) is nearly linear and corresponds in some way to the lines on the chart paper. Since the anemometer will not turn at all below a threshold of ½ to 1 mph, the zero of the milliammeter may be intentionally set a little to the right of the first chart line and then the uniformly spaced chart divisions will correspond quite well over the whole range to uniform steps of miles per hour.

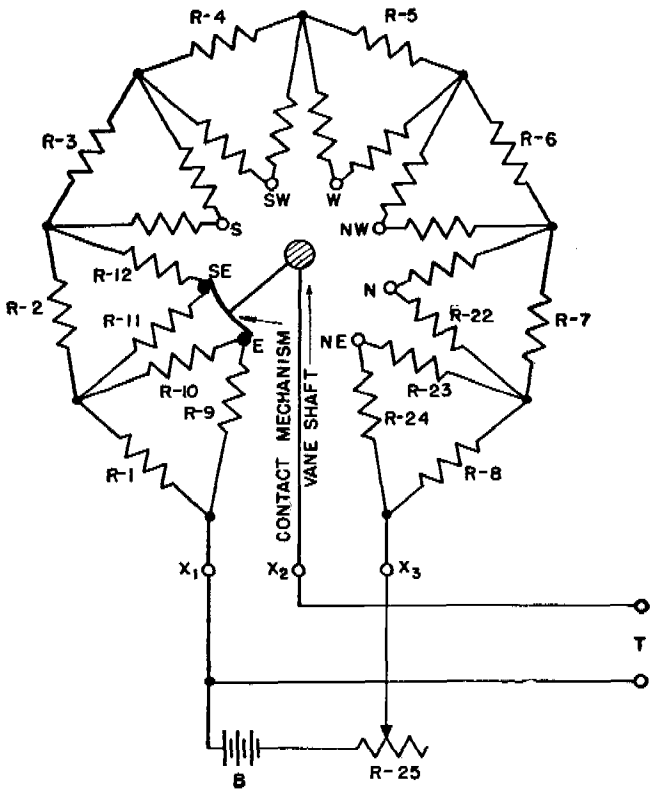
The smoothing condenser C_2 is chosen to be large enough so that each individual pulse from C_1 will cause, even at the lowest wind speeds, only a tolerable wavering of the recording pen. A larger value of C_2 will unnecessarily reduce the speed of response of the system, tending to give a weighted time average of the wind velocity over the past period of time. The overall speed of response of the system then depends on the response time of the milliammeter, the introduced time delay, and hence the number of contacts per revolution of the anemometer, and the relation between the moment of inertia of the anemometer cups and their effective area which is exposed to the force of the wind.

Both the CIT model of the Lane-Wells anemometer and the Friez 339-L anemometer (preferably modified so that it gives two contacts per revolution) have proven satisfactory; the use of photocells with a faster-acting similar type of vacuum-tube frequency meter has also been used with the Biram anemometer with good field results and a somewhat faster speed of response. In practice, the Lane-Wells anemometer with its recording circuit will in a few seconds (depending on the wind speed) give a 50% response to an abrupt change in wind speed.

15.7.4 The Keep-Alive Circuit

Experience with the Esterline-Angus meters in the field has indicated that far more satisfactory records are obtained with them if, in addition to the measuring current, a small low-frequency alternating current is passed through the moving coil. This "keep-alive" current, just enough to cause the pen to tremble visibly, serves to make the pen continually assume its true equilibrium position; if it is not present the pen will not follow rapid fluctuations in the measuring current with a high degree of accuracy, and particularly at low paper speeds the pen will tend to move in jumps.

The most economical way of obtaining this small alternating current, of a frequency of about 10 c, is by the use of a relay oscillator together with a small transformer, condenser system, or pair of batteries



Parts List for Recording Wind Vane Circuit

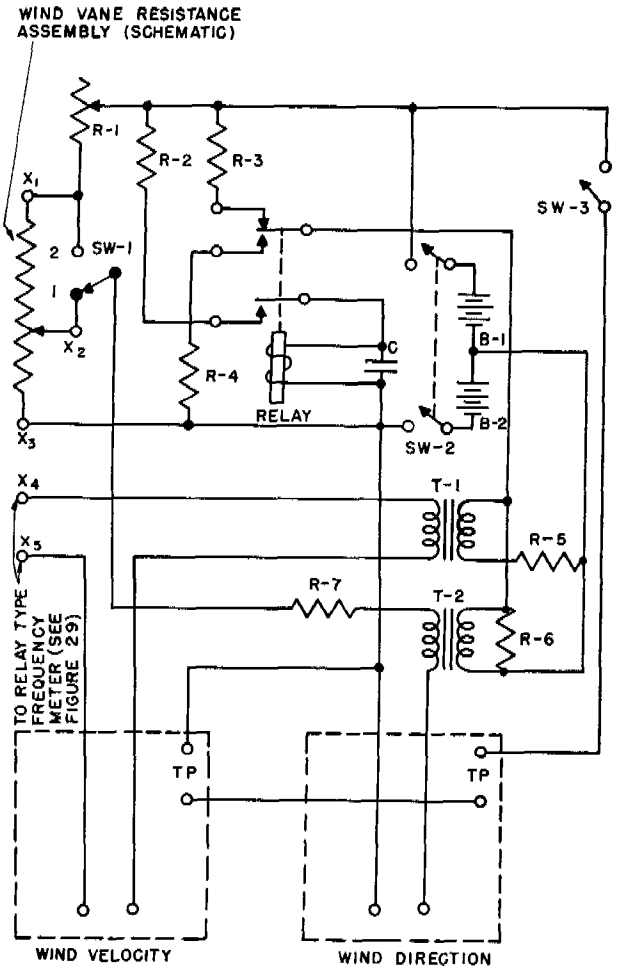
12 Volt Model:

R_1 to R_8	75 ohm 1 watt carbon resistors (selected for uniform resistance).
R_9 to R_{24}	1000 ohm ½ watt carbon resistors (selected for uniform resistance).
R_{25}	200 ohm 4 watt rheostat.
B	Two 6 volt dry batteries in series (Burgess Uniplex No. 4F4H).
T	Terminals to Esterline-Angus recording milliammeter connected in series with 12,000 ohms or more.

2 Volt Model:

R_1 to R_8	5 ohms each (see above).
R_9 to R_{24}	200 ohms each.
R_{25}	15 ohm rheostat.
B	2 volt charge-retaining storage battery.
T	Terminals to E–A meter connected in series with 800 ohm wire wound resistor.

FIGURE 27. Diagram of a resistor assembly with Friez 363–C wind vane.



Parts List for 12-Volt Wind Direction and Velocity Recorder.

B_1,B_2	Burgess Uniplex No. 4F4H dry batteries.
C	150 mfd 50 volt electrolytic condenser.
Relay	Advance No. 500 DPDT 6 volt, 1000 ohm coil.
R_1	200 ohm rheostat.
R_2	450 ohm 1 watt carbon resistor.
R_3,R_4	10 ohm 1 watt carbon resistor.
R_5	5000 ohm 1 watt carbon resistor.
R_6	1500 ohm 1 watt carbon resistor.
R_7	13,500 ohms total, wire wound.
SW_1	SPDT toggle switch (ordinarily in position 1; for adjusting R_1 to give standard deflection of wind direction meter, switch to position 2).
SW_2	DPST toggle switch.
SW_3	Push-button type microswitch [for simultaneous actuation of chronograph pens (TP)].
T_1,T_2	Doorbell transformers, 110 volt to 10 volt, 60 c.

FIGURE 28. Diagram of a circuit for 12-volt wind direction and velocity recorder.

controlled by the relay contacts. A simplified diagram of the shunt-type relay oscillator with transformer is given in Figure 26, and the explanation is as follows.

When the battery B is first connected, condenser C is charged through resistance R_1 and as soon as the voltage across C becomes high enough, the relay armature is pulled down and a pulse of current is sent through the transformer. When the connection at the upper contact is broken, however, the relay armature is not released immediately because the current stored in C continues to flow through the relay coil. Since the air gap in the magnetic circuit is reduced when the armature is held down, the armature can be held down by a current considerably smaller than that required to pull it down initially. Finally the condenser current through the relay coil

decreases sufficiently to allow the spring tension to release the armature, and the cycle can then be repeated.

In practice it has been found that considerable experimentation is required to get a given type of relay to function dependably over long periods of time; the exact analysis of the action is complicated and there are numerous possible variations of the circuit. The time the relay remains in the open and closed positions depends on the capacity of C, the battery voltage, the relay resistance, and the adjustment of the spring and relay contacts. The inertia of the armature and the resonant frequency of the condenser-resistance-inductance combination appear to have quite an effect on the stability of operation. When properly designed, however, the circuit appears capable of giving year-long uninterrupted service from a dry cell.

15.7.5 The Recording of Wind Direction

Figure 27 shows a means of obtaining an indication of wind direction by a resistor assembly attached to a standard Friez 363–C wind vane. The eight contacts of the vane are made to indicate 16 steps of direction, 15 of them as successive steps in the milliammeter, and one as a single position about midway in the deflection. It has been found in practice that the latter indication, although nearly the same as one of the other steps, causes no confusion in interpretation because the vane will not ordinarily turn abruptly through an angle of 180° without leaving an indication of the intervening directions, and this anomalous position can in any case be oriented away from the prevailing directions.

Since the circuit is a modified potentiometric circuit, the resistance of the contacts is unimportant, and a completely open contact will show zero voltage on the milliammeter; this indication is different from that of any wind direction. The use of a specially designed wind vane would reduce the bulk and weight of the apparatus, and light-friction units are now commercially available for changing a circular indication into linear meter indication, with a negligible transition interval from low-scale to high-scale readings.

15.7.6 Examples of Complete Circuits as Used in the Field

Figures 28 and 29 show the complete diagrams with circuit constants of two field sets for recording wind direction and velocity. The 12-v model, containing two recording meters in one case, is too heavy for convenient transportation away from a vehicle, but has the advantage of being self-contained. It will record for a week without attention to the meters, and the self-contained batteries will give about 1,500 hr of service before it is necessary to replace them.

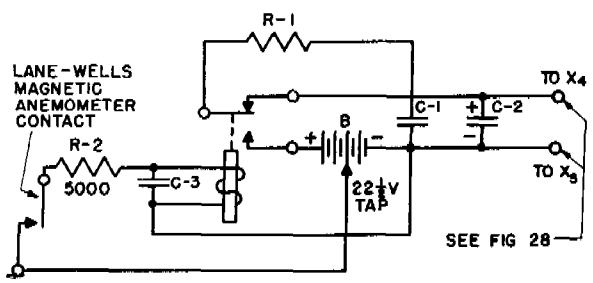


FIGURE 29. Diagram of a frequency meter circuit for 12-volt recorder.

The 2-v model, using a charge-retaining lead-acid storage battery, will withstand temperatures far below 20 F, where dry cells would freeze and become unreliable, and contains only the recording meter for wind velocity; the wind-direction recording milliammeter can be easily carried separately and attached. In all cases the milliammeters must be properly shock-mounted to withstand transportation.

Chapter 16

BEHAVIOR OF GAS CLOUDS

By *Wendell M. Latimer*

61.1 INTRODUCTION

THE NORMAL OBJECTIVE in the use of clouds of nonpersistent toxic agents is to produce casualties among personnel on or near the ground level. For that reason the greatest efficiency is obtained when the cloud remains close to the earth's surface and the importance of the factors influencing atmospheric stability, discussed in Chapter 14, are obvious. In general, under inversion conditions, the cloud will travel along the ground with a minimum of vertical displacement, and casualty-producing dosages may be expected at great distances from the source; while under lapse conditions the large convection currents arising from the instability of the air near the ground will tend to lift the cloud and the efficiency will fall off rapidly with the distance from the source.

The Chemical Warfare Service [CWS] is interested in munition requirements for certain specific tactical objectives. In determining such requirements, it is generally necessary to know the dosages of toxic material which are set up by a given munition. The quantity of toxic gas which a man may breathe is proportional to the average concentration C of the gas and the length of breathing time t, or more exactly,

$$\text{Dosage} = \int_{t_1}^{t_2} C dt . \qquad (1)$$

The value of this integral is generally referred to as the Ct value. The actual quantity of toxic material breathed also depends upon the rate of breathing which may vary from 15 to 50 lpm. This fact is taken into account in assigning lethal dosages, but the overall Ct value is the significant quantity used in assessing the munition efficiency. One unit often employed for nonpersistent gases is *milligram minutes per liter*. This unit is 1,000 times as large as milligram minutes per cubic meter, the unit generally used.

For a definite set of field conditions the efficiency of the munition is also governed by the area covered by a stated minimum Ct. Thus, for example, a bomb may give Ct values of at least 20 mg min per l over 1,600 sq yd, and Ct values at least 3 mg min per l over 10,000 sq yd. This is generally stated as $Ct = 20$ area of 1,600 sq yd (0.16 artillery square) and $Ct = 3$ area of 10,000 sq yd (1 artillery square).

In some reports the integral of Ct over all areas is given and referred to as CtA. This quantity is of value in the comparison of relative bomb efficiencies, and also in calculating the overlapping of clouds in multiple bomb shoots. However, it has no particular military or tactical significance in itself.

As indicated above, the atmospheric stability is a highly important factor in the efficiency of a gas cloud. However, the most important single factor affecting the dosage or Ct value is the wind speed. With a source of finite time which produces a cloud of a given diameter, the time of passage of the cloud over a point, and, therefore, the dosage at the point, is inversely proportional to the wind speed. With a source of infinite output time and definite rate of output, the dosage in a given time for a given weight of material is also inversely proportional to the wind speed, since the volume of air into which the material is injected is proportional to the wind speed, and hence the concentration of the material is inversely proportional to the speed. For clouds of finite size the effect of wind velocity upon the area of a given Ct value is more complicated, but for high winds the area is inversely proportional to the square or cube of the velocity.

Other factors that affect the efficiency of gas clouds, in addition to atmospheric stability and wind, are gravity flow, turbulence and large eddies, and the nature of the ground surface, including roughness and vegetation. In this chapter the behavior of gas clouds with respect to these various effects is considered.

16.2 LINE SOURCES

16.2.1 Open Terrain

In the early use of gas in World War I the *line source* was frequently employed. The gas was released from cylinders on a line from 1 to 5 miles in length and the time of emission was from 2 to 5 min. A steady, moderately high wind blowing toward the enemy positions was required. The moderately high wind reduced efficiency by the dilution effect, increased the turbulence, and was unfavorable for the existence of high inversion conditions. Thus the loss of gas in traversing the territory between the lines

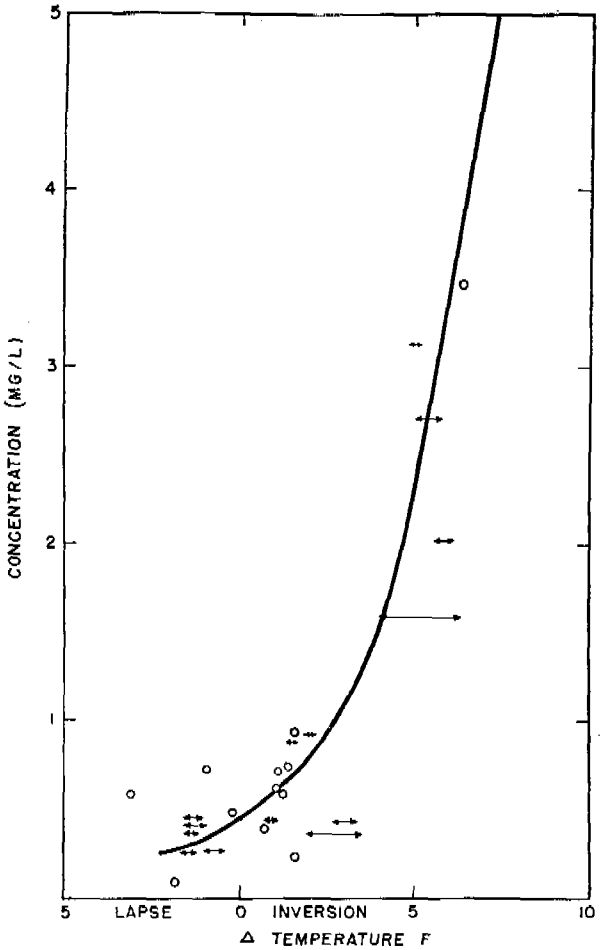


FIGURE 1. Concentration at 1-foot height 150 yards from source versus temperature gradient between 1 and 6 meters.

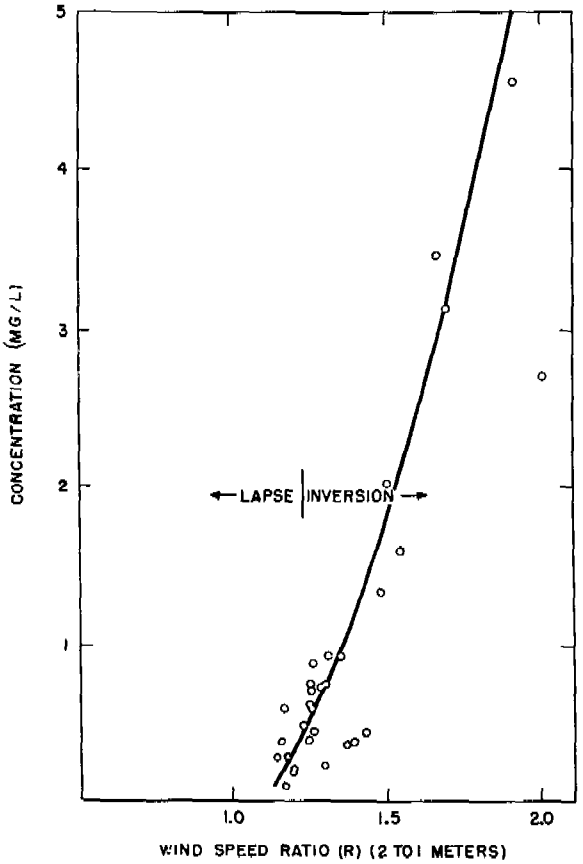


FIGURE 2. Concentrations at 1-foot height 150 yards from source versus wind velocity ratio between 1 and 2 meters.

was very great and the method was replaced by munitions such as the Livens projector and chemical mortar which placed the gas directly on the enemy positions. However, considerable theoretical and experimental work has been done on the travel of gas clouds from line sources. The well-defined character of the source has many advantages in controlling experimental conditions, and in most cases, area sources may be treated as line sources; therefore knowledge of the travel of gas clouds generated at a line may be applied to many problems. For this reason the line source is considered in some detail.

An extensive investigation was carried out in the Sacramento Valley of California on the concentration of butane from a line source. Because of the very high inversion prevalent in this region, this study included the effect of atmospheric stability over a wide range of conditions.

The correlation of the concentration at the 1-ft level, 150 yd from the source (0.5 lb per min per yd) with the temperature gradient is given in Figure 1, and a similar correlation with the R values is given in Figure 2. The general dependence upon atmospheric stability is apparent and the conclusion may be drawn that both the temperature gradient and the wind gradient are satisfactory measures of the stability. However, the correlation is slightly better with the R values. Although the wind velocities were mostly in the general range of 3 to 5 mph, a better correlation might be expected if the product of the concentration and the wind velocity were plotted. Such a plot against R is given in Figure 3. The points fall fairly well on the curve and the deviations may be ascribed to experimental errors arising from fluctuations in the wind. These fluctuations include both speed and direction, the latter being the more annoying in line source experiments as the conclusion assumes that the wind direction remains constantly at right angles to the source.

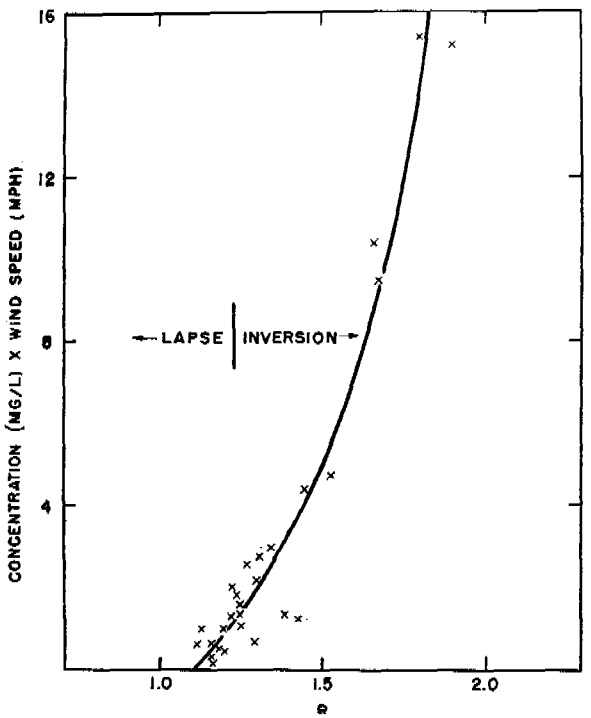


FIGURE 3. Concentration times wind velocity against R.

The surface of the ground was covered with grass 2 ft high and partly bent over. As a result of this roughness the R values are higher by about 0.10 unit than the corresponding values over smooth ground. The value for neutral conditions (zero temperature gradient) is 1.23. Values of R above 1.45 are not generally experienced in regions of moderately high relative humidities. However, at this value of R the efficiency is some 4 or 5 times as great as that obtained for moderate lapse. At an R value of 1.8 the efficiency is 40 to 50 times the lapse value.

In the preceding paragraph the word "efficiency" is used to indicate the tendency of the gas to remain close to the ground and not to diffuse upward. It is to be noted, however, that if the gas settles to the ground in a thin layer, a person may be able to take steps to avoid the high dosages of the gas; for example, he may be able to stand or to hold his canister above the gas cloud. In this case, the efficiency (as used above) is not an indication of the true effectiveness against personnel.

The temperature gradient for the gas clouds was determined over various heights, but the interval of 1 to 6 m appears to give the most satisfactory correlation. Measurement of temperature at 0.1 m is subject to larger experimental errors because of the

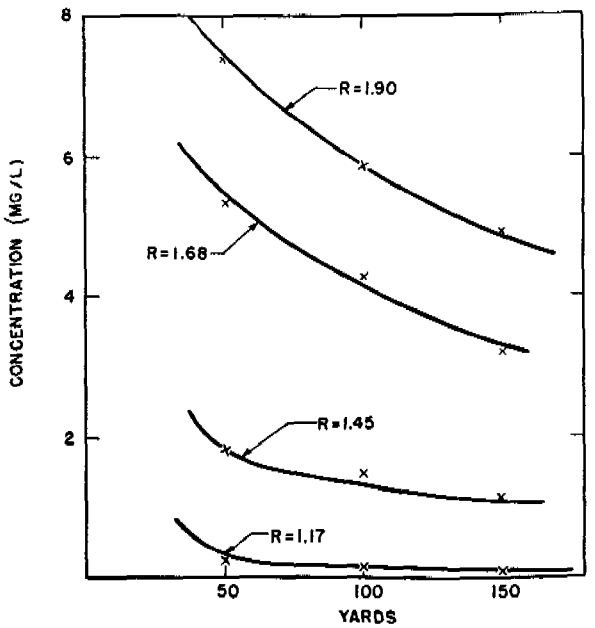


FIGURE 4. Concentration against distance at 1-foot level.

steeper gradient near the surface. In the same way, velocity ratios were obtained between various heights and there was some evidence that the ratio for 6 to 1 m was more satisfactory than the generally employed ratio of 2 to 1 m.

Values for the horizontal and vertical gustiness were obtained. In general, under inversion conditions both components were small; there was no simple correlation with the gas concentration.

The variations of concentration with distance are shown in Figure 4 for several R values at the 1-ft level. At a given wind velocity and source strength

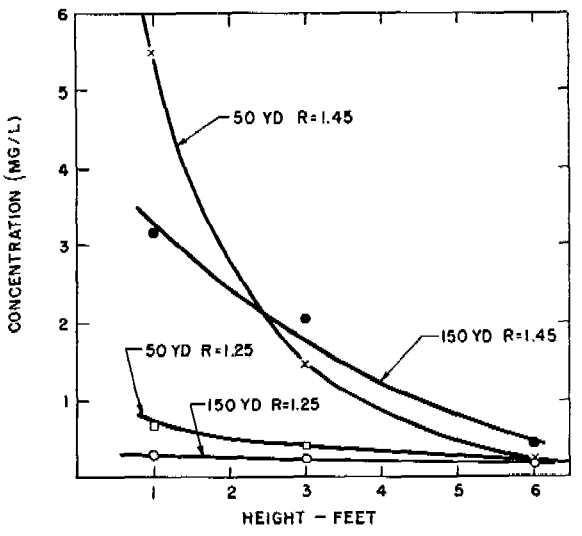


FIGURE 5. Variation of concentration with height.

the concentration depends upon some inverse power of the distance, and this power is a function of R.

$$C = \frac{k}{X^{f(R)}} \tag{2}$$

The theoretical treatment of the problem is discussed later.

Figure 5 shows the variation in concentration with height. Under high inversion most of the gas lies close to the ground. In fact, in the highest inversions studied in the Sacramento Valley, the stability was such that streamline flow was approached with almost no diffusion into higher levels. Under lapse, even at 50 yd from the source, the diffusion and turbulence are so great that the concentration gradient is small within the first 6 ft.

The suggestion has been made that the travel of gas clouds should be related to the Richardson number

$$R_i = \frac{g\left(\frac{dT}{dz} + \gamma\right)}{T\left(\frac{du}{dz}\right)^2} \tag{3}$$

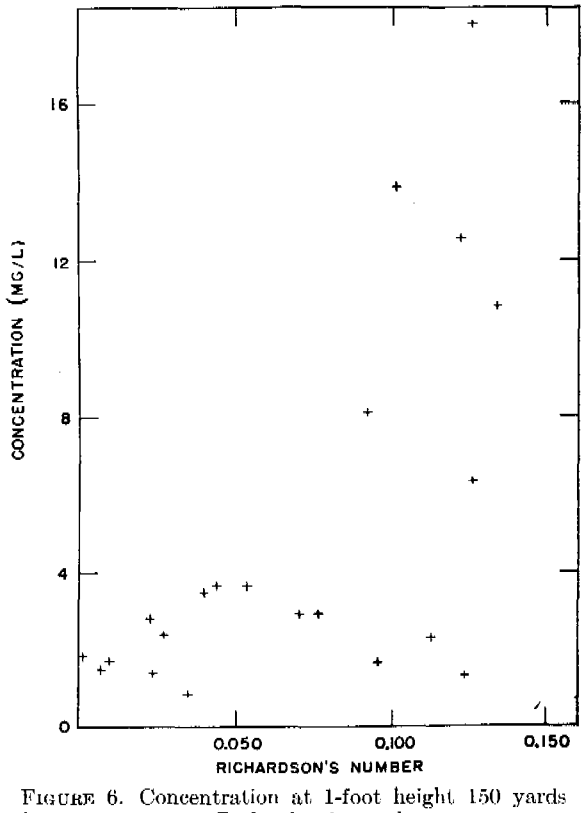


FIGURE 6. Concentration at 1-foot height 150 yards from source versus Richardson's number.

where g is the gravity constant; γ the adiabatic lapse rate; T the absolute temperature; and u the mean wind velocity. A plot of concentration against the Richardson number, shown in Figure 6, gives no indication of any simple correlation.

16.2.2 Forested Areas

Each forested area is a problem in itself, depending upon the height of the vegetation and its density at various levels. A pine forest with a heavy canopy of interlacing branches and open (brush free) space below is quite different from a tropical jungle with tall trees intertwined with vines and thick ferns covering the ground.

There are practically no data for line sources in the tropical jungle. Data for a typical pine forest were obtained but the problem was complicated by the existence of strong katabatic winds at night. The following experiments illustrate the cloud travel observed.

EXPERIMENT 1

Type, source, and strength	Line 0.25 lb/min yd	
Wind velocity 1.70 mph	1	2
R	0.99	
Temperature difference	$T_{1m} - T_{0.1m}$ -1.8 to -2.4 (lapse)	$T_{2m} - T_{1m}$ -0.4 to -0.7 (lapse)
Gas concentration, mg/l		
Distance	Height	
	1 ft	6 ft	10 ft
100 yd	0.02	0.02	0.03

EXPERIMENT 2

Type, source, and strength	Line 0.25 lb/min yd	
Wind velocity, 1.10 mph	1	2
R	0.76	
Temperature difference	$T_{1m} - T_{0.1m}$ 0.15 (inversion)	$T_{2m} - T_{1m}$ 0.75 (inversion)
Gas concentration, mg/l		
Distance	Height	
	1 ft	6 ft	10 ft
70 yd	2.2	1.5	0.35
100 yd	1.7	0.82	0.16
125 yd	1.5	0.52	...
150 yd	1.3	0.65	0.26

The large difference between lapse and inversion conditions is due in part to "chimney effects" set up under lapse around openings in the canopy. In the heavy brush type of forest in Florida and in typical tropical jungle the night and day values probably do not differ by more than a factor of 3 or 4. The inversion values given in experimental data are comparable to the behavior with $R = 1.35$ in the open.

16.2.3 Beach Areas

The behavior of gas on a beach area with a land breeze corresponds to that of a gas on any other land area with a similar wind. With a sea breeze, the behavior for several hundred yards inland is modified by the character of the wind. In general, since no marked lapse or inversion conditions exist over the ocean, the behavior tends toward neutral conditions; however, considerable variation may be expected, depending upon the air-mass stability. On the California coast the sea breeze consists of warm air from the Japanese current which has traveled over the cold coast current. It has been thus cooled near the surface and has great stability and low turbulence. Rather fragmentary data obtained in this region indicate that under afternoon lapse conditions, gas cloud travel in the sea breeze is somewhat more efficient than under neutral conditions with a land breeze.

16.3 BRITISH THEORY OF CLOUD TRAVEL FROM LINE AND POINT SOURCES

The theory of cloud travel developed at Porton describes the travel of gas clouds from point and line sources with considerable accuracy. It is based upon sound theoretical reasoning and was supported by a fair amount of experimental data, especially under neutral atmospheric conditions.

The basis of the theory is the assumption that the vertical eddy velocity w_t', associated with a mass of fluid at time t, is correlated with the subsequent velocity $w_l'_{+\xi}$ of the same mass at time $t + \xi$, by a correlation coefficient R_ξ. This coefficient is defined as

$$R_\xi = \left(\frac{\lambda}{\lambda + \overline{w'^2}\xi}\right)^n, \tag{4}$$

where λ is a quantity independent of time and identified with the kinematic viscosity of the medium and n is a dimensionless parameter given by the velocity gradient expression

$$\bar{u} = \bar{u}_1\left(\frac{z}{z_1}\right)^{n/(2-n)}, \tag{5}$$

where $\bar{u}$ is the mean velocity at height z. The parameter n varies between 0 and 1. It has been shown that the scatter of a group of particles in a diffusing medium is given by

$$\overline{X^2} = 2\,\overline{u'^2}\int_0^T\int_0^t R_\xi d\xi dt, \tag{6}$$

where X is the distance traveled by a particle in time T, and R_ξ is the same as defined in equation (4).

Define the component velocities u, v, w, and mean velocities $\bar{u}$, $\bar{v}$, $\bar{w}$, and $u = \bar{u} + u'$, $v = \bar{v} + v'$, $w = \bar{w} + w'$, and consider the instantaneous generation of matter at a point in space by taking axes moving with the mean wind velocity $\bar{u}$. The scattering due to disturbances of mean energy $\overline{u'^2}$, $\overline{v'^2}$, and $\overline{w'^2}$ along the three axes after time T is

$$\overline{X^2} = \sigma_x^2 = 2\,\overline{u'^2}\int_0^T\int_0^t R_{\xi(x)}\,d\xi dt, \tag{7}$$

and similar equations for $\overline{Y^2}$ and $\overline{Z^2}$. Then,

$$R_{\xi(x)} = \left(\frac{\lambda}{\lambda + \overline{u'^2}\xi}\right)^n \tag{8}$$

and similar equations for $R_{\xi(y)}$ and $\overline{v'^2}$, and $R_{\xi(z)}$ and $\overline{w'^2}$. One then obtains

$$\begin{aligned}\sigma_x^2 &= \tfrac{1}{2}\,C_x^2\,(\bar{u}\,T)^{2-n}\\ \sigma_y^2 &= \tfrac{1}{2}\,C_y^2\,(\bar{v}\,T)^{2-n}\\ \sigma_z^2 &= \tfrac{1}{2}\,C_z^2\,(\bar{w}\,T)^{2-n}\end{aligned} \tag{9}$$

with

$$C_x^2 = \frac{4\lambda^n}{(1-n)\,(2-n)\bar{u}^n}\left(\frac{\overline{u'^2}}{\overline{u^2}}\right)^{1-n} \tag{10}$$

and similar equations for C_y^2 and C_z^2.

These are the basic formulas in the simplest form. To apply, assume C_z independent of height. This is equivalent to regarding the lower atmosphere as one in which the mean wind velocity and gustiness components may be regarded as independent of height as far as such variations affect actual diffusion, but the variation of wind with height is actually used to determine the value of n. In other words, the slow variation of wind with height on this approximate theory is looked upon merely as an indicator of the degree of turbulence present. The method adopted is then to seek expressions for the density distribution which satisfy equation (9) and the equation of continuity.

The general solutions obtained are:

For continuous point source, Q g per sec; X at (x,y,z); x, downwind; y, across wind; z, vertical.

$$X = \frac{Q}{\pi C_y C_z \bar{u} x^m}\exp\left[\frac{-1}{x^m}\left(\frac{y^2}{C_y^2} + \frac{z^2}{C_z^2}\right)\right]. \tag{11}$$

For continuous infinite line source, Q g per sec m.

$$X = \frac{Q}{\pi^{\frac{1}{2}} C_z \bar{u} x^{m/2}}\exp\left[\left(\frac{-1}{x^m}\right)\left(\frac{z^2}{C_x^2}\right)\right]. \tag{12}$$

In all cases $m = 2 - n$. If the source is at ground level, all concentrations must be doubled to allow for ground reflection.

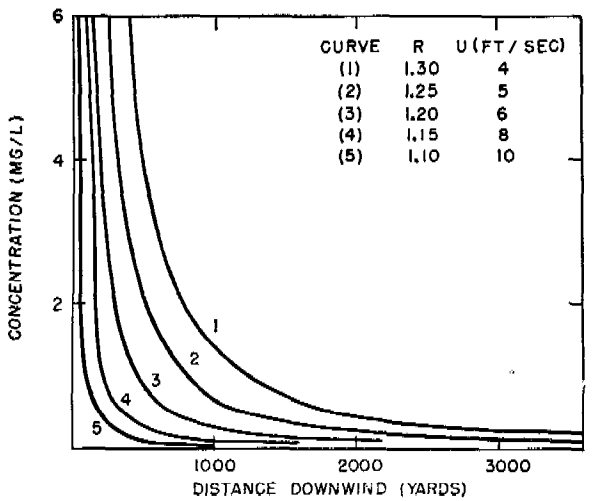


FIGURE 7. Concentration from a continuous point source. British theory.

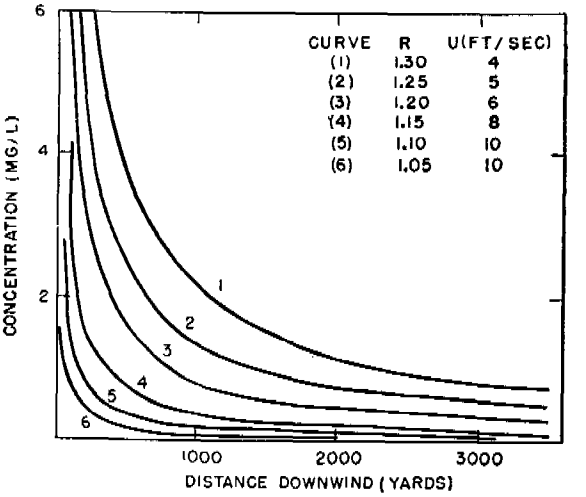


FIGURE 8. Concentration from a continuous line source. British theory.

It has been the practice of the British to measure $\bar{u}$ at 2 m, and to evaluate m from R values; that is, the ratio of $\bar{u}_{2\text{ meters}}/\bar{u}_{1\text{ meter}}$.[a] Also since the components of gustiness vary roughly with R and $\bar{u}$, average values for these quantities are employed. The following tables give these values.[8]

TABLE 1. Continuous point source 1 lb per min approximate concentration in mg per cu m on axis of cloud at ground level.

Conditions for use of gas	Unfavorable	Moderate	Favorable
Value of R	1.05	1.13	1.25
Index of X	1.85	1.74	1.60
Wind velocity, mph	10	10	5
Distance downwind, yd	Gas concentration		
100	2.2	14.0	150.0
200	0.6	4.0	48.0
500	0.12	0.85	11.0
1,000	0.03	0.26	3.5

TABLE 2. Continuous line source 1 lb per min yd concentration in mg per cu m at ground level.

Conditions for use of gas	Unfavorable	Moderate	Favorable
Value of R	1.05	1.13	1.25
Index of X	0.93	0.87	0.80
Wind velocity, mph	10	10	5
Distance downwind, yd	Gas concentration		
100	130	320	1400
200	65	170	800
500	28	76	380
1,000	14	41	210

For other values of Q, u, and x, the concentration is:

1. Directly proportional to Q.
2. Inversely proportional to $\bar{u}$.
3. Inversely proportional to x raised to the index of X. Graphical presentation of data for various values of R and u are given in Figures 7 and 8.

Since R is also dependent upon roughness, observed values must be corrected to a standard condition. This is taken as a close-cut grass surface, having grass about 1 in. long. To find the correction factor for any given site (allow 50 yd of representative terrain upwind), reading should be on a completely overcast day or night in a steady wind, preferably of about 10 fps (about 6 mph). The value over the standard surface should then be 1.15. If the observed value due to roughness is greater, for example 1.24, the correction factor may be found from Table 3.

TABLE 3. Correction factors in R for roughness.

R (observed)	Correction
1.15	0
1.16	0.01
1.17	0.03
1.18	0.04
1.19	0.06
1.20	0.07
1.21	0.08
1.22	0.10
1.24	0.13
1.26	0.15

From this table the correction here is 0.13 and the value to be used is 1.11. The correction is composed of two parts: (1), a correction for additional drag, in

[a] The recent trend has been to evaluate the parameter R from other meteorological factors without reference to wind speed ratios.

TABLE 4. Finite line source. Axial concentrations at distance x from a continuous source of width L expressed as percentage of concentration from infinite line source.

	R = 1.07				R = 1.14		
L yd	50	100	500	1,000	50	100	500
x yd							
50	93	100	100	100	100	100	100
100	74	94	100	100	98	100	100
500	25	44	96	100	55	82	100
1,000	14	26	81	97	33	59	100
5,000	3	6	29	51	9	18	68

	R = 1.20			R = 1.25		R = 1.35	
L yd	50	100	200	50	100	50	100
x yd							
50	100	100	100	100	100	100	100
100	100	100	100	100	100	100	100
500	77	97	100	95	100	100	100
1,000	53	87	98	76	97	95	100
5,000	16	30	55	27	49	44	75

this example 0.09; and (2) a correction for increased turbulence, in this case 0.04.

The equations give concentrations for infinite time of emission and for infinite width of line sources. To correct for finite time and length of line sources, the following procedure is employed.

1. To find the concentration from a line source continuous in time, but finite in length, multiply the value from the equation by the factor in Table 4 for the appropriate value of R, x, and L. Divide by 100.

2. To find the concentration from a source which emits at a uniform rate for a finite time: (a) find the initial length (yards) z, by multiplying the wind velocity by the time of emission; (b) multiply the value from the equation by the factor in Table 5 for the appropriate values of R, x, and z. Multiply by 100. This rule applies only if x is greater than z.

3. For both finite length and time apply both corrections.

TABLE 5. Finite time source. Mean (axial) concentration over central portion of the cloud at a distance x from a source emitting for a finite time t, expressed as a percentage of the axial concentration from a corresponding continuous source.

	R = 1.07				R = 1.14			R = 1.20			R = 1.25		
z* yd	20	50	100	200	20	100	200	20	50	100	20	50	100
x yd													
50	69	88	100	100	88	100	100	94	97	100	96	99	100
100	48	71	88	100	79	96	100	89	96	97	93	97	99
500	13	30	53	75	34	84	92	62	85	93	77	91	95
1,000	3	17	33	56	22	71	85	43	73	87	62	85	92
5,000	1	4	8	15	2	28	49	13	32	55	24	50	74

* z = distance traveled by gas during time of emission = wind velocity yd per sec multiplied by time of emission (sec).

16.3.1 The Gas Concentration Slide Rule

In order to permit the rapid calculation of concentration from given source strengths under various conditions and at various distances from equations (11) and (12), the British developed a special slide rule.

The gas slide rule resembles an ordinary slide rule in that it consists of three parts, the stock, a slide, and a cursor. The graduations or scales are its special feature.

The stock carries two scales, marked Scale A and Scale D. Scale A at the top gives concentrations in milligrams per cubic meter. Scale D at the bottom shows rates of emission of gas, either in pounds per minute (point source) or pounds per minute per yard (line source). The mixed metric and British units are adopted in order to agree with the units in general use for chemical warfare purposes.

The center slide, which is rather wide, also carries two scales on its face. Scale B is toward the right and indicates distance downwind from the point of emission (beam discharge). Scale C is towards the left and is the wind velocity at a height of 2 m. These two scales extend across the whole width of the center slide, being in the form of curved lines for Scale B and almost straight lines for Scale C. The reverse side of the slide carries a further two scales, B_1 and C_1, which are the corresponding scales for a line source (that is, trench discharge).

A seventh scale is engraved vertically on the cursor and refers to R, the ratio of the wind velocity at a height of 2 m to that at a height of 1 m. This scale reads from 1.05 at the bottom to 1.35 at the top.

For detailed description of the operation of the slide rule and its application to various types of problems, reference should be made to the British manuals.

16.3.2 Application of British Theory to Bombs

Table 6 gives values of the concentrations which were calculated from the British theory for a single 250-lb tail-ejection bomb for neutral (15-mph wind) and inversion (5-mph wind). The general method of treating the problem is indicated in the discussion following the table.

Concentrations are at ground level. For a burster-type bomb, concentrations would vary from 1/20 to

TABLE 6. Gas concentration from a single tail-ejection 250-lb LC bomb charged CG.

Distance from burst yd	Peak conc mg/cu m	Mean ground axial conc during passage mg/cu m	Mean ground conc over entire cloud mg/cu m	Width of cloud yd	Time of passage sec
For R = 1.15; 15 mph wind					
75	...*	...*	20,000†	25	29
50	...*	...*	10,000†	30	30
100	5,800	4,800	3,800	37	31
200	2,200	1,700	1,200	50	34
500	500	330	230	90	42
1,000	150	95	60	145	53
2,000	30	20	12	250	74
For R = 1.25; 5.5 mph wind					
75	...*	...*	62,000†	22	36
50	...*	...*	35,000†	24	37
100	26,000	20,000	18,000	27	38
200	13,000	10,000	8,900	33	40
500	8,500	6,300	3,300	46	45
1,000	1,500	950	670	66	52
2,000	450	270	180	100	65

* Not estimated at short ranges.
† Very approximate.

1/4 of those given, depending on range. Figures given are for open-type country. The time of emission is taken as 20 sec. It is assumed that 130 lb of CG is rained down onto an area 40 yd downwind by 20 yd crosswind, from which it evaporates in 20 sec. The area source is treated as a line source across the center, emitting at the rate of 20 lb per min yd. Calculations are made by use of the concentration slide rule.

To determine mean axial concentration at given distance from source, such as a bomb or shell which has a short time of emission:

1. If Q is source strength per unit time, that is, gas content divided by the time of emission t, and T the time of passage of the cloud,

$$\textit{mean axial concentration} = \frac{\textit{Concentration from continuous point source of strength } Q}{T}$$

The time T of passage of a cloud may be calculated by finding the width of the point source cloud at the given distance, dividing by the wind velocity, and adding t the time of emission.

The assumed time of emission t for a Livens drum and for a 250-lb LC bomb is 30 sec, for a volatile nonpersistent gas.

2. If the dimensions of the puff of gas from a single weapon are known, the concentration can be determined by assuming that the cloud is identical with that part of the cloud from a continuous point source at a distance from its origin where the width is equal to the width of the puff. The concentration then decreases with the distance in accordance with the usual curves for a continuous point source.

3. Approximately, the width of a puff is one-half that of a cloud from a continuous point source, and its length equal to its width. The length of a cloud from a finite point source is obtained by taking the width (or length) of a puff and adding the initial dimension, that is, the product of wind velocity and duration of emission. From this value the time of passage of the cloud can also be found.

Dugway Proving Ground gave the following comparison of observed bomb data with the British theory.

Dugway: 1,000-lb CG; lapse; $R < 1.1$; Wind < 1 ft per sec

Distance, yd	Ct observed	Ct calculated
40	2,380	2,200
80	1,180	1,300
120	304	810

Targhee Forest; 1,000-lb CG; inversion; wind, 2.25 ft sec

Distance, yd	Ct observed	Ct calculated
50	9,800	1,200
100	3,710	700
150	499	500
200	297	400

While the agreement is very good in the open under lapse conditions, quite the reverse is true for inversion conditions in a forest.

16.3.3 Discussion of British Theory

The agreement between calculated and observed concentrations is excellent for moderate source strengths, especially under neutral and small inversion conditions. Because of the assumption that the velocity gradient is negligible in the diffusion process itself, there is considerable divergence between calculated and observed values when R is above 1.45, but this is not serious since these conditions are seldom encountered. However, the application of the theory to clouds produced by large aerial bombs introduced serious difficulties. These arose because the theory neglected gravity effects and in the case of large aerial bombs the heavy clouds tended to flatten or "pancake" to a very pronounced extent. The weight of the clouds was due in part to the fact that the molecular weight of most of the agents was greater than the average molecular weight of air, and in part to the greater density arising from the cooling pro-

duced by the rapid evaporation of a large quantity of liquid. This effect also greatly enhanced the stability of the ground layer. It could be said that the large gas bomb tended to create its own meteorological conditions, and these predominated over the first hundred yards or more of the cloud travel.

In addition to the unsatisfactory handling of the large bomb problem, the original British approach had certain practical difficulties. For example, the exact measurement of the wind velocity gradient is difficult, especially at velocities below 1 mph, since in this range none of the common cup-type anemometers are accurate. In addition, with katabatic or gravity winds, which generally occur at night on hillsides, the ground air velocity may be even larger than the velocity at higher levels, thereby giving R values less than unity, which are difficult to correlate. Also the corrections for the roughness of the surface, that is vegetation, are large and are often impossible to make accurately. Inside a forest or jungle both the temperature gradient and the velocity gradient are generally small, and show little variation with lapse and inversion, although there may be considerable variation in cloud travel under the two conditions. Finally, the efficient use of the relatively complicated British manual requires an extensive training program. In the rapid development of an army from civilian personnel, which occurred in the American Army in World War II, such a training program would have been very difficult.

16.4 CLOUDS FROM CW BOMBS

16.4.1 Gravity Effects

Upon impact, the explosive force of the burster causes the liquid filling of a nonpersistent agent to be dispersed as small droplets. Most of these vaporize in the air, but a small amount of the liquid reaches the ground and under temperate conditions vaporizes immediately. The normal crater loss is very small with CG or CK but, in the case of AC, an appreciable amount of liquid remains in and around the crater.

The concentration of gas in the initial cloud varies from 15 to 50 mg per l or higher, depending upon the size of the bomb, the weight of burster, and the thickness of the bomb case. If the weight of agent, CG for example, is 20 mg per l, the increase in density of the air is about 14 mg per l, taking into account the relative molecular weights of phosgene, 98, and air, 28.8. The heat of vaporization of CG is 60 cal per g, or 1.2 cal for 20 mg. The specific heat of air is 0.3 cal per l. Hence the vaporization of 20 mg per l would produce a cooling of about 4 C. If the initial temperature were 20 C where air has a density of 1.2046 g per l, the final temperature would be 16 C, with a density of the air of 1.2213 g per l. This represents a gain of about 17 mg per l in weight, neglecting the heat liberated by the explosion of the bomb.

Thus, the air in the gas cloud is heavier by 14 mg per l because of the greater molecular weight of the phosgene and by 17 mg per l because of the cooling effect. In other words, the two effects are approximately the same for CG. For CK the two effects are also of the same order of magnitude, but for AC the molecular weight is about equal to that of air and the increased weight of the cloud is due to the cooling effect alone.

The heavier gas cloud tends to fall or pancake under the force of gravity and the rate of fall is proportional to the square root of the difference in density and to the square root of the initial height of the cloud.

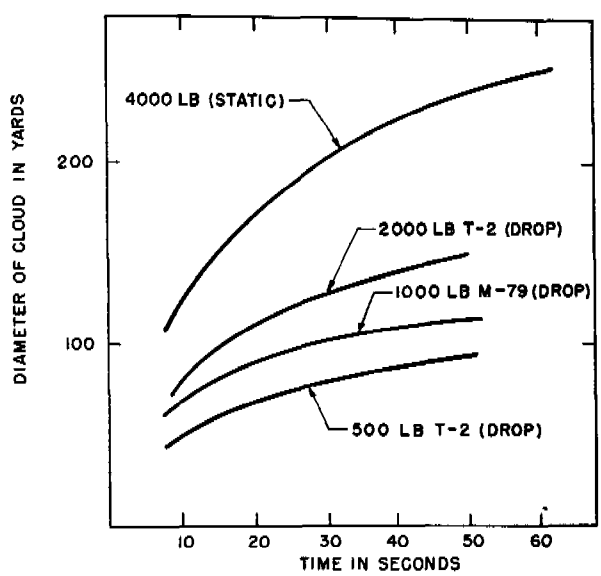


FIGURE 9. Cloud diameters against time after burst.

Figure 9[7] illustrates the increase in diameter of the cloud in the first 60 sec after the burst due to the pancake effect. Figure 10, from the same report, gives a comparison of the concentration of gas and temperature of the cloud.

The initial height of the cloud depends to some extent upon the hardness of the ground; with very soft ground the bomb tends to bury itself and the

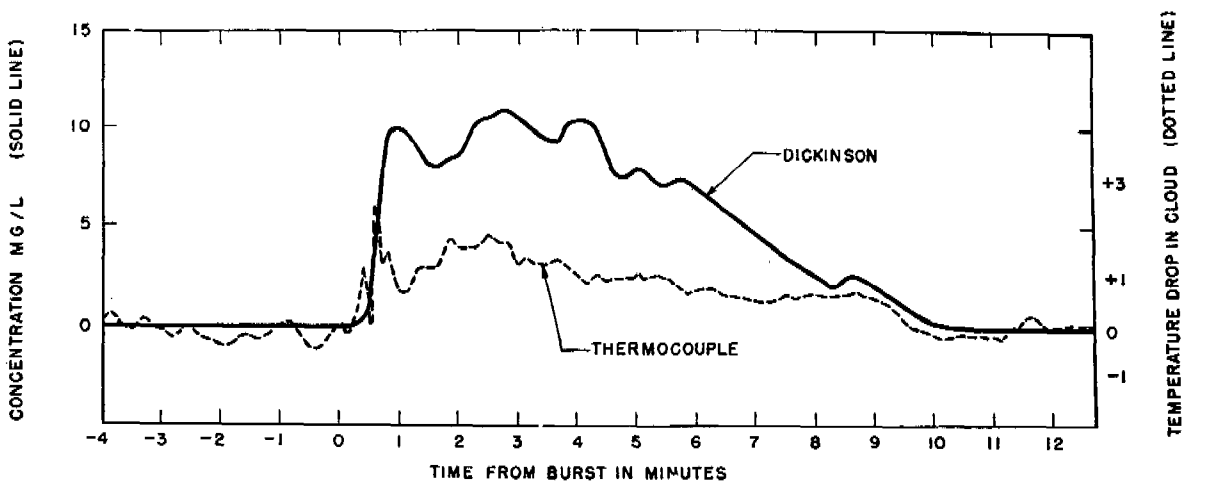


FIGURE 10. Comparison of temperature and CG concentration in the gas cloud.

gas cloud is shot upward to a greater height. In the open, the final height of the cloud is usually around 10 ft, but with low wind velocity and high inversion it may drop to as low as 2 ft.

The gravity effect in heavy jungle was studied by the San José Project on the 1,000-lb M79 bomb.[14] The following conclusions can be drawn.

1. The burst cloud radius, with either CG or CK and static burst, is between 35 and 55 ft (average about 50 ft).

2. The pancake cloud radius of the bomb is between 80 and 100 ft. The time required for the gas to reach this distance is approximately 30 sec.

3. Sixty seconds after the burst at a radius of 90 ft, most (80%) of the cloud was below the 18-in. level.

On the basis of mathematical theory [24] the gravity spread of heavy gas clouds has been discussed.

The equation of motion of the cloud along the ground in the initial stages where friction may be neglected is

$$\frac{d\beta}{dt} = bB\sqrt{\frac{x^6 - x^4}{1 + \frac{b}{a}x^4 + \frac{b^2}{2a^2}x^6}} \qquad (13)$$

where b is the initial radius; β the radius at time t; $x = \beta/b$; a the initial height; and B is given by an expression involving the density of the cloud and the surrounding air ρ_1 and ρ_2, respectively, and of the acceleration of gravity g,

$$B = \sqrt{\frac{15g\,(\rho_1 - \rho_2)}{16\,\rho_1\,a}}. \qquad (14)$$

Neglecting friction, the terminal velocity would be

$$\frac{d\beta}{dt} = a^{\frac{1}{2}}\left[\frac{15}{8}g\left(\frac{\rho_1 - \rho_2}{\rho_1}\right)\right]^{\frac{1}{2}}. \qquad (15)$$

For the slowing-down process, it is assumed that the frictional conversion of kinetic energy into heat is approximated by the case of flow between two parallel plates,

$$\frac{d\beta}{dt} = \sqrt{2}\,aBe^{-(f/2)(b/a)x^3} \qquad (16)$$

where f is the dimensionless friction factor. From these equations calculations have been made giving the gravity spread which are in reasonable agreement with experimental observations.

Under inversion conditions and at low wind velocities the effect of gravity flow is very pronounced in large clouds even after the initial pancake effect. This is especially true in heavy forests. This point is discussed [17] and on the basis of data obtained on the San José Project, the conclusion was drawn that "a slope of 6 degrees is sufficiently steep to cause the gravitational force of the relatively dense cloud released from a single 1,000-lb M79 bomb of CK or CG to predominate over a 0.5- to 0.7-mph wind in determining the movement of the cloud during its early stages in this jungle." As a consequence clouds under these conditions tend to follow the natural course of the watershed and dosages are extremely high along stream beds.

16.5 DATA ON CLOUDS FROM SINGLE BOMBS

16.5.1 Open Terrain

Dugway has studied the behavior of the 1,000-lb M79 T2 bomb in a large number of single shoots. Unfortunately the experiments were not planned to cover all ranges of wind speed and stability and in

some cases the sampling data were erratic. However, approximate values can be given for the behavior of clouds from these bombs and these data are summarized in Table 7. At a wind speed of 1 mph the

TABLE 7. Data on 1,000-lb bombs charged approximately 410 lb CG.*

Area, Ct = 1, in artillery squares per bomb				
Wind speed, mph	1	2	4	8
Strong inversion	21	10	4.5	..
Moderate inversion	16	7	3	1.4
Neutral	11	5	2	0.9
Lapse	3	1.8	1.5	0.9
Area, Ct = 3, in artillery squares per bomb				
Wind speed, mph	1	2	4	8
Strong inversion	14	6	2.9	..
Moderate inversion	10	4.5	2.0	1
Neutral	6	3	1.5	0.7
Lapse	2	1.5	1.0	0.6
Area, Ct = 30, in artillery squares per bomb				
Wind speed, mph	1	2	4	
Strong inversion	1.5	0.8	0.3	
Moderate inversion	1.0	0.4	...	
Neutral	0.5	0.2	...	
Lapse	0.3	0.1	...	
Maximum Ct on axis of cloud				
Wind speed, mph	1	2	4	8
Strong inversion	120	60	30	..
Moderate inversion	100	50	25	8
Neutral	70	32	12	5
Lapse	60	30	10	3

* Values for 18-in. height.

area covered by (Ct = 3) varies from about 16 artillery squares (16×10^4 sq yd) for high inversion to 2 artillery squares for lapse. At low wind speeds the area under inversion conditions decreases inversely proportionally to the speed to the first power but at higher velocities the decrease corresponds to a power between 1 and 2. The length of the (Ct = 3) area under inversion conditions may be 500 to 600 yd. At a distance 100 yd from the source, the width is about 100 yd at low wind speeds, and increases to about 200 to 300 yd downwind to give an egg-shaped area. With high winds the width is somewhat less. Under lapse with low wind the cloud tends to rise with very little spread. Higher wind speeds break down the lapse conditions and this operates to hold the cloud down to the ground and increase the dosage area, and thus counteracts the effect of the shorter time of passage. For this reason the area covered by (Ct = 3) does not change so much with wind speed under lapse as it does under inversion. These effects are illustrated in Figure 11.

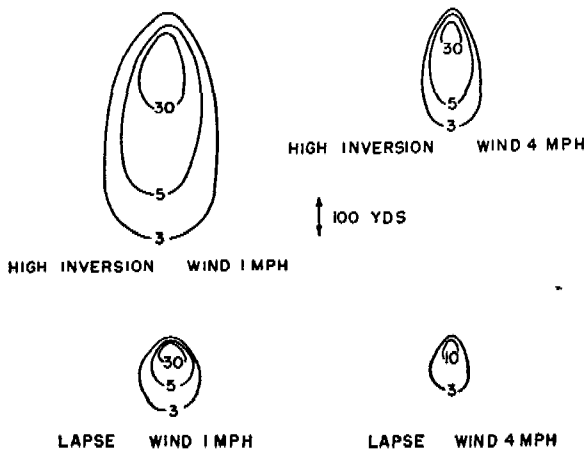


FIGURE 11. Areas for single 1,000-lb bombs charged CG.

For low wind speeds the areas covered by various Ct values are roughly proportional to the square root of the Ct values. This relationship obviously breaks down for greater wind speeds, as the time factor becomes so small that the product Ct never attains the higher values.

The concentration of gas in the initial cloud is independent of meteorological conditions, so that at winds of 1 mph it might be expected that the Ct of the impact area would be constant for lapse and inversion. However, under inversion the cloud sinks to a lower level and the actual concentration is probably about twice that obtained under lapse condition.

Experiments on other fillings besides CG include CK and AC. In general the Ct values are proportional to the weight of agents per bomb. For CK the results are about equivalent to CG. For most of the shoots the weight of CK was 360 lb per bomb as compared to 406 to 430 lb for the CG; this difference in weight was not reflected in the Ct areas obtained. For AC the filling was 215 to 240 lb per bomb, and the area for (Ct = 3) was about half that obtained with the same bomb charged CG under similar conditions.

16.5.2 Results on 500-Lb Bombs

The data on 500-lb bombs are not very complete since the rather brief field experiments have been carried out on various bomb types with widely varying weights of charge. The results seem to indicate that, per hundred pounds of agent, the areas for low values of Ct are slightly greater for the smaller bombs, but that the areas for large values of Ct are less.

16.5.3 Results on 2,000- and 4,000-Lb Bombs

The experiment on one 2,000-lb T2 bomb charged 822 lb of CG gave an area covered by (Ct = 3) of 15 artillery squares under high inversion and wind speed of 2 mph. The corresponding value for a 1,000-lb bomb charged 410 lb of CG from Table 7 is 7 artillery squares. Thus the areas appear to be proportional to the weight of charge. The same is true for areas of (Ct = 3) for the 4,000-lb bomb M56 charged 2,341 lb of CG. Thus under neutral conditions and 4.6 mph the observed area was 9.4 artillery squares, which may be compared with the value of 1.5 from Table 7. However, the maximum Ct values observed were considerably higher than the values for 1,000-lb bombs. For a 2,000-lb bomb with wind speed 1.9 mph and neutral conditions the maximum Ct recorded was 48. The corresponding value for the 1,000-lb bomb is about 35. A 4,000-lb bomb, lapse conditions and wind 11.4 mph, gave a maximum of 43. Under the same conditions a 1,000-lb bomb would probably give a maximum Ct of about 2.

16.5.4 Multiple Shoots — Bombs in Line

The Dugway reports give data on two field experiments with six 1,000-lb bombs charged CG. The bombs were placed at 100-yd intervals crosswind and fired statically. The following comparison gives the observed areas for various Ct-values and six times the value for a single bomb under similar conditions. The meteorological conditions were high inversion with wind speed 2.6 mph. Areas are in artillery squares.

Ct mg min per l	6 bombs in line	6 × single bomb
1	119	58
3	96	34
5	85	..
10	57	27
30	2*	4
Maximum	59	50

* Value low, probably sampling error.

It is observed that the reinforcement given by the merging of the clouds tends to increase the areas of low Ct values by a factor of 2 or 3. Little reinforcement occurs over the target area and the maximum Ct remains approximately the value for a single bomb. Under lapse conditions the distance of cloud travel decreases and the diminished effect of the reinforcement tends to make the total Ct areas more nearly the value for six single bombs.

16.5.5 Multiple Bombs Over Area

Dugway carried out 6 shoots using in each 11 to 41 of the 1,000-lb bombs on area targets. Unfortunately, none of the experiments was under high inversion conditions. Table 8 summarizes the results on three of these trials.

These results indicate that for (Ct = 1) and (Ct = 3) the multiple shoots under lapse or neutral conditions gave about the same area per 100 lb of agent as observed for single bombs. For low inversion the efficiency was about 2 or 3 times that of a single bomb due to the reinforcement of the cloud from one bomb by adjacent clouds. In the 41-bomb shoot a large area was covered by (Ct = 50) which is a greater dosage than could have been obtained from a single bomb under these conditions. Figure 12 gives the Ct contour map obtained for this shoot.

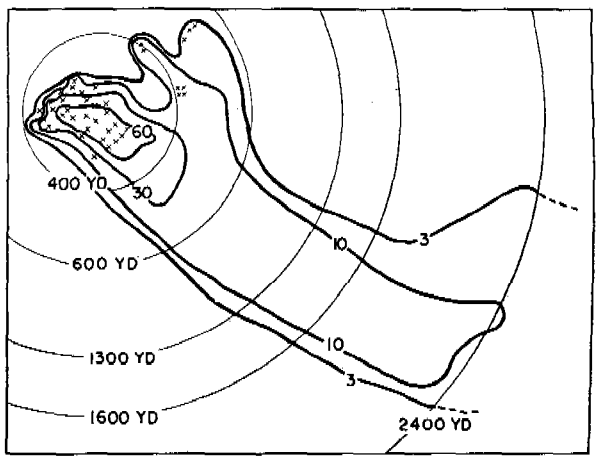


FIGURE 12. Ct areas for 41-bomb shoot of M79 bombs, charged CG + 5 per cent NO_2.

16.5.6 Variation of Dosage with Height

From the previous discussion of gravity effects in clouds from large bombs, it follows that the pancaking of a cloud under inversion conditions and low wind results in large concentration gradients. For good inversion, Dugway states "the dosage at 5 feet is only about 30–40 per cent of the dosage at 18 inches as determined as the average of a large number of measurements. Under neutral conditions this percentage is between 50 and 75 while under lapse it is still higher." Downwind dosages at 18 in. and 5 ft become nearly identical under all conditions.

TABLE 8. Summary of Dugway results on area targets with 1,000-lb bombs.

No. of bombs	Wt of agent, lb	Wind speed, mph	R	$T_{2m}-T_{0.1m}$	Area covered by various dosages Ct at 18 in., in artillery squares						Area of impact	Average Ct over impact area
					1	3	5	10	30	50		
12	5,136	2	1.45	+1.4°(I)	64	53	43	29	11	4	12	37
12	5,148	4.8	1.2	−1.0(L)	40	26	20	15	2.3	<1	12	18
41	17,163	3.3	1.4 − 1.7	N to I	>332	>266*	>216	155	28	14	16 for † 32 bombs	40

* Cloud off target area, value estimated 350 artillery squares.
† 9 bombs short distance away.

16.5.7 Surprise Areas

In view of the importance which has been attached to the use of nonpersistent gases as surprise agents, Dugway has discussed this subject with respect to two concepts: (1) a dosage of 5 mg min per l established in 30 sec, and (2) a dosage of 3 mg min per l in 2 min. Their results are summarized in Table 9.

TABLE 9. Surprise areas for large bombs.

1. Thirty-second surprise area at low winds (Ct = 5 mg min/l in 30 sec)

Bomb, lb	Area, artillery square
500	0.2
1,000	0.3
2,000	0.5
4,000	1.0

2. Two-minute surprise area (Ct = 3 mg min/l in 2 min)

Bomb, lb	Wind, mph	Area, artillery square	Downwind distance, yd	Crosswind distance, yd
500	<1	0.6	90	90
1,000	<1	1.0	110	110
1,000	3	0.7	125	60
2,000	<1	1.8	150	150
2,000	11.0	1.8	240	100
4,000	<1	4.9	250	250
4,000	11.0	4.5	380	120

Suffield reported 30-sec surprise areas (Ct = 3.2) for a 4,000-lb bomb (charged 2,160 lb CG) of 1.0 and 1.35 artillery squares for wind speeds of 5 and 10 mph, respectively.

16.5.8 Munition Requirements — Bombs, Open Terrain

In order to state bomb requirements it is necessary to specify the objectives to be attained. In addition to the objectives of surprise given above, the following tactical uses have received general consideration.

1. Masking [M_a]; troops forced to mask to escape injury (Ct = 1 mg min per l for CG and CK and 0.5 for AC). In general, troops would mask at a lower dosage, but this dosage requires enemy personnel to mask to avoid disablement.

2. Casualty producing among unprotected personnel [C_u]; this depends on the lethal dosage [b] which for CG was chosen as a Ct = 3; for CK, Ct = 6; and for AC, Ct = 2. The area covered by this dosage is called the lethal area. (These dosage values were chosen during the early stages of the war from the best experimental data available at that time. It is to be noted that they do not agree with the values adopted in 1944 by the U. S.–U. K.–Canadian committee: for CG, Ct = 3.2; for CK, Ct = 11; for AC, Ct = 5.)

3. Casualty producing among imperfectly protected troops [C_i] (considered as 10 times the lethal dosage); this dosage will cause casualties among troops with a 10% mask leakage. In combat this leakage may occur even with well disciplined troops because of the difficulty in obtaining tight-fitting facepieces and because of valve leakage or defects due to manufacture or subsequent damage.

4. Casualty producing among protected troops [C_p] (Ct = 200 for CK). Canister penetration; this dosage will penetrate the present enemy canisters with CK, provided the time of required wearing of mask is 1 hr or more. Canister penetration is probably not feasible for CG. A dosage of Ct = 200 will also cause casualties, if not fatalities, with all gases on troops with a 1 to 3% mask leakage.

The munitions required to attain these objectives, that is, Ct values of 1, 3, 30, and 200 for CG and CK, may be deduced from the experimental data presented above (at least to a fair approximation) al-

[b] Although the dosage necessary to produce a casualty varies with time, the variation of the value of the lethal Ct in a time greater than 1 min and less than the time of passage of a gas cloud in the open is not great enough to affect appreciably the ammunition requirements. In the woods, even though the time of passage of the cloud is considerably longer, the requirements will not be appreciably altered, since they do not change rapidly as the time increases.

though more experiments with multiple shoots under inversion conditions would have been desirable.

16.5.9 Uniform Distribution

Dugway gave the values listed in Table 10 for the 1,000-lb bomb requirement.

TABLE 10. *Ammunition expenditures uniform coverage* for open terrain (bombs per 100 artillery squares); 1,000-lb M79 bombs filled CG or CK.*

Wind	$Ct = 3$			$Ct = 30$ †		
mph	Inversion	Neutral	Lapse	Inversion	Neutral	Lapse
2	30	50	130	110	180	600
4	50	70	150	190	280	700
8	160	200	220	550	700	1,100

* For AC, multiply by 1.5.
† For $Ct = 200$, multiply ($Ct = 30$) values by 6.

The requirements given in Table 10 are very high and it is obvious that a uniform coverage of a target area is quite inefficient. Thus the 41-bomb shoot at Dugway gave a ($Ct = 3$) area of at least 350 artillery squares compared with the 30-bomb for 100 squares given in the table. Thus to attain the required dosage over the target area, large additional areas downwind will be covered by dosages almost as large as those over the target. The values in Table 10 could be cut in about half if two-thirds of the bombs were distributed over the upwind half of the target. A uniform distribution is also open to the objection that in actual application any nonuniformity in the distribution, especially along the upwind edge, results in dosages in that area which are below the desired value. These statements apply in particular to nonpersistent gas clouds and not to the persistent agents.

For other bomb sizes the figures in Table 10 may be multiplied by the appropriate factor to give an equivalent weight of agent.

16.5.10 Expenditures for Line and Upwind Distribution in the Open [c]

The following is quoted from the Dugway Report No. 18.[7]

For the purpose of obtaining the actual values to be used, the results of the field experiments have been analyzed in the following manner.

To estimate the number of 1,000-lb M79 bombs needed under various conditions, the areas covered by a given dosage at 18 inches in the field experiments were plotted on a per bomb basis against the wind speed in several different ways (chiefly as log-log plots). From the curves for inversion, neutral, and lapse conditions the variation of area with wind speed could be determined, and the areas covered per bomb under inversion, neutral, and lapse conditions for wind speeds at 2, 4, and 8 mph could be obtained. In calculating the number of bombs required for an area of 100 artillery squares, the most weight was given to the areas observed in the larger scale tests.

The dimensions of the experimentally measured Ct areas were used to determine the maximum allowable spacings for the bombs. The overlapping of areas of low dosage (from nearby bombs) to form an area of higher dosage has been taken into consideration.

CtA was also employed to determine the requirements for the highest dosages, and wherever possible the values were checked by extrapolation from lower dosages. Plots of the variation of CtA per 100 pounds of agent with wind speed were made for inversion, neutral, and lapse so that the values of CtA corresponding to the conditions given in the table could be obtained. However, it is to be noted that the CtA values per 100 pounds of agent (or area for a given dosage) cannot be used directly for the present calculations, since additional bombs will be needed to compensate for the portion of the total CtA (or area) which will be lost outside the 100 artillery square area. For the woods, an additional number of bombs above that calculated by CtA will be necessary to take care of the fraction of CtA lost in building up dosages above $Ct = 200$. For areas larger than 100 artillery squares and dosages higher than 200, these corrections will become less important.

The ammunition expenditures obtained in the manner described above are shown in Table 11.

COMMENTS ON THE USE OF TABLE 11

1. The requirements in Table 11 are based on the use of an attack area obtained by circumscribing the designated target with a straight-edged figure approximately 50 yd larger in every direction than the target area. If the upwind edge of the target area is bounded by water or other natural obstacles which prevent dropping of bombs on this part of the attack area, it is assumed that the bombs for this area will be dropped along the upwind edge of the target area.

[c] The reported results of bombing missions in World War II demonstrated the impossibility of putting bombs down in an orderly pattern on the target. For mutual protection the planes flew in definite patterns; generally the bombs were released upon signal from the lead plane; bombings were usually made from high altitudes. For all of these reasons, the pattern of the impacts was essentially random. This is why the Project Coordination Staff adopted for their own use the random distribution method developed by two members of Division 10, NDRC. In World War II acceptance of such randomness of impact was a much more realistic approach than the use of any planned pattern on the target. However, this early work from Dugway is recorded here, since it may be that developments and changes in attack will some day permit placing bombs at predetermined points. In such event, these considerations should be of value in planning attacks.

TABLE 11. Ammunition requirements for M79 bombs filled CG and CK. Open terrain. Bombs per 100 artillery squares.

		Inversion			Neutral			Lapse		
	Wind, mph	2	4	8	2	4	8	2	4	8
$Ct = 1$	No. of bombs	11	20	54	20	36	90	55	60	95
	Max crosswind spacing, yd	150	125	75	150	125	75	125	90	60
$Ct = 3$	No. of bombs	16	30	96	27	50	140	110	120	180
	Max crosswind spacing, yd	125	90	60	125	90	60	100	75	50
$Ct = 30$	No. of bombs	54	130	440	110	220	640	600	700	1,100
	Max crosswind spacing, yd	50	40	30	50	40	30	45	35	25
$Ct = 200$	No. of bombs	350	800	2,700	550	1,100	3,200	Prohibitive		

2. The size of the attack area is measured in artillery squares and the requirement for a given area is computed from the table by comparison with that for 100 artillery squares. In the open, for objectives M_a and C_u, the tabular requirements (per artillery square) are satisfactory for areas larger than 10 artillery squares. For smaller targets, the requirements per artillery square will be approximately double the values given in the tables, with a minimum of 1 bomb per artillery square for area in the neighborhood of 2 artillery squares. For objectives C_i and C_p the requirements for areas less than 50 artillery squares can be obtained by multiplying the tabular values (per artillery square) by a factor of 2 for areas near 10 artillery squares, and by 1.5 for areas near 30 artillery squares. An alternative method for the calculation of requirements for small targets is by the use of the values for uniform coverage given in Table 10.

3. For open terrain at wind speeds greater than 8 mph the requirements become large, but they may be estimated by extrapolation from the tabular values. Above 10 mph the atmosphere tends toward neutral conditions at all times.

4. The type of distribution is determined from the nature of the target and the meteorological conditions. For open terrain, if the wind direction is known, the expenditures for the following types of bomb distribution may be obtained from Table 11.

a. Line distribution. For line coverage all the bombs are dropped in a line along the upwind edge of the target. As already stated, the number of bombs needed to cover a given area can be calculated from the values in the table for a 100 artillery square area, but if the calculated requirement is not as large as the number of bombs obtained by dividing the crosswind dimension of the area by the maximum crosswind spacing, the latter value should be used. Under conditions similar to those used in the field experiments, the gas from a single line source cannot be depended upon to cover a target under inversion conditions more than 1,000 yd downwind for $Ct = 1$ to 5, and 500 yd downwind for $Ct = 30$. Under neutral conditions, the distances are 600 and 300 yd, respectively. If an area with a considerably greater distance downwind is to be covered, it is possible to divide the area into smaller areas with shorter downwind distances and to cover each of the smaller areas in an identical manner by a line of bombs on the upwind edge of each small area. If conditions are very favorable, the downwind effect of gas in the upwind areas will add to the effect of the lines of bombs in the areas farther downwind.

b. Upwind distribution. Bombs are distributed over the attack area. The downwind effect is employed to some extent by displacing the bombs toward the upwind edge of the area.[d] This can be accomplished by placing the first row of bombs on the upwind edge of the attack area and spacing the remaining bombs in rows at equal distances downwind on the target area, with no bombs on the downwind edge.

For example, in Figure 13 it is assumed that the requirements and distribution of bombs for a dosage of 3 for CG (task C_u) for the accompanying area consisting of open, flat terrain under inversion conditions and a wind speed of 4 mph are to be calculated. The size of attack area is (1,050/100) x (1,110/100) equals 117 artillery squares. The requirement for 100 artillery squares equals 30 bombs with maximum crosswind spacing of 90 yd. The requirement for 117 artillery squares equals 35; bombs in first row 1,050/90 equals 12. Number of rows 35/12 equals 3. Downwind spacing between rows 1,110/3 equals 370.

[d] For objective $Ct = 200$, approximately 60% of the bombs should be dropped in the upwind half of the target area.

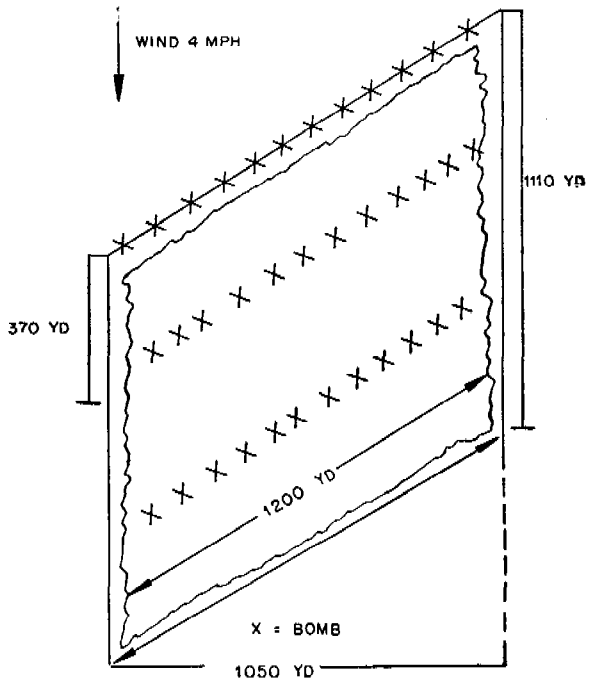


FIGURE 13. Upwind distribution.

Bombs in second row equal 12. Bombs in third row equal 11 (or 12 as shown).

5. The economy of munitions usually obtained when the effect of wind is utilized makes desirable the use of upwind or line distribution wherever possible. For these types of coverage the wind direction must be reasonably well known; with upwind coverage it is estimated that for most targets of approximately 100 artillery squares, 90% of the area or more will still be covered with a wind shift of $\pm 30°$. It is apparent that a shift in wind direction will be more serious for line distribution than for upwind.

6. The distribution and spacings suggested in this report are made chiefly on the basis of efficient use of the gas clouds produced, but it is expected that modifications will have to be made in any actual operational use. No increases have been made in tabular value to allow for operational difficulties in bombing. However, in the case of nonpersistent gas bombs, small errors in placement of bombs are not serious (except on upwind edge of target) since the gas clouds from different bombs will probably expand and merge together to cover the target.

7. The tabular requirements are not intended to apply to gas-proofed fortifications, since many additional bombs will be needed for such an attack.

The Project Coordination Staff [PCS] of the Chemical Warfare Service have made a careful study of all available data on nonpersistent gases. From the integral $\int A\, d(Ct)$ they have obtained the values for CtA given in Table 12 for a 1,000-lb bomb with approximately 400 lb of agent.

TABLE 12. CtA values for 400-lb agent at 18-in. height.

Wind speed mph	Clear day	Neutral	Clear night
2	12	20	50
4	7	11	20
8	4	5	6
10	2	2.5	3

Table 12 has been used to calculate the overlapping in multiple bomb shoots and hence munition requirements. These are summarized in Table 13.

TABLE 13. PCS munition requirements. Area targets Ct values for 18-in. height. Bombs per artillery square, assuming statistical distribution.

Speed (mph)	Clear day	Neutral	Clear night
	1. M79 for $Ct = 30$ *(from Table 10)*		
2	2.3	2.3	0.9
4	6.4	4.1	2.3
8	11	9	7.5
16	22	18	15
	Comparison with Dugway report		
2	6	1.8	1.1
4	7	2.8	1.9
8	11	7	5.5
	2. M79 for $Ct = 200$ with agent CK*		
2	21	12	5
4	35	23	12
8	62	50	41
16	124	100	83
	3. M79 for $Ct = 11$ with CK or $Ct = 5$ for AC†		
2	2.5	1.5	0.7
4	3	2.5	1.5
8	5	4	3.5
16	8	6.5	5.5
	4. M79 for $Ct = 3.2$ with CG‡		
2	0.9	0.6	0.3
4	1.5	0.8	0.6
9	2	1.5	1.5
16	3	2.5	2

* For M78 multiply by 2.2.
† For M78 multiply by 1.8.
‡ For M78 multiply by 1.7.

The comparison mentioned in (1) Table 13 refers to the values given in Table 10 for uniform distribution, and it will be observed that except for lapse and

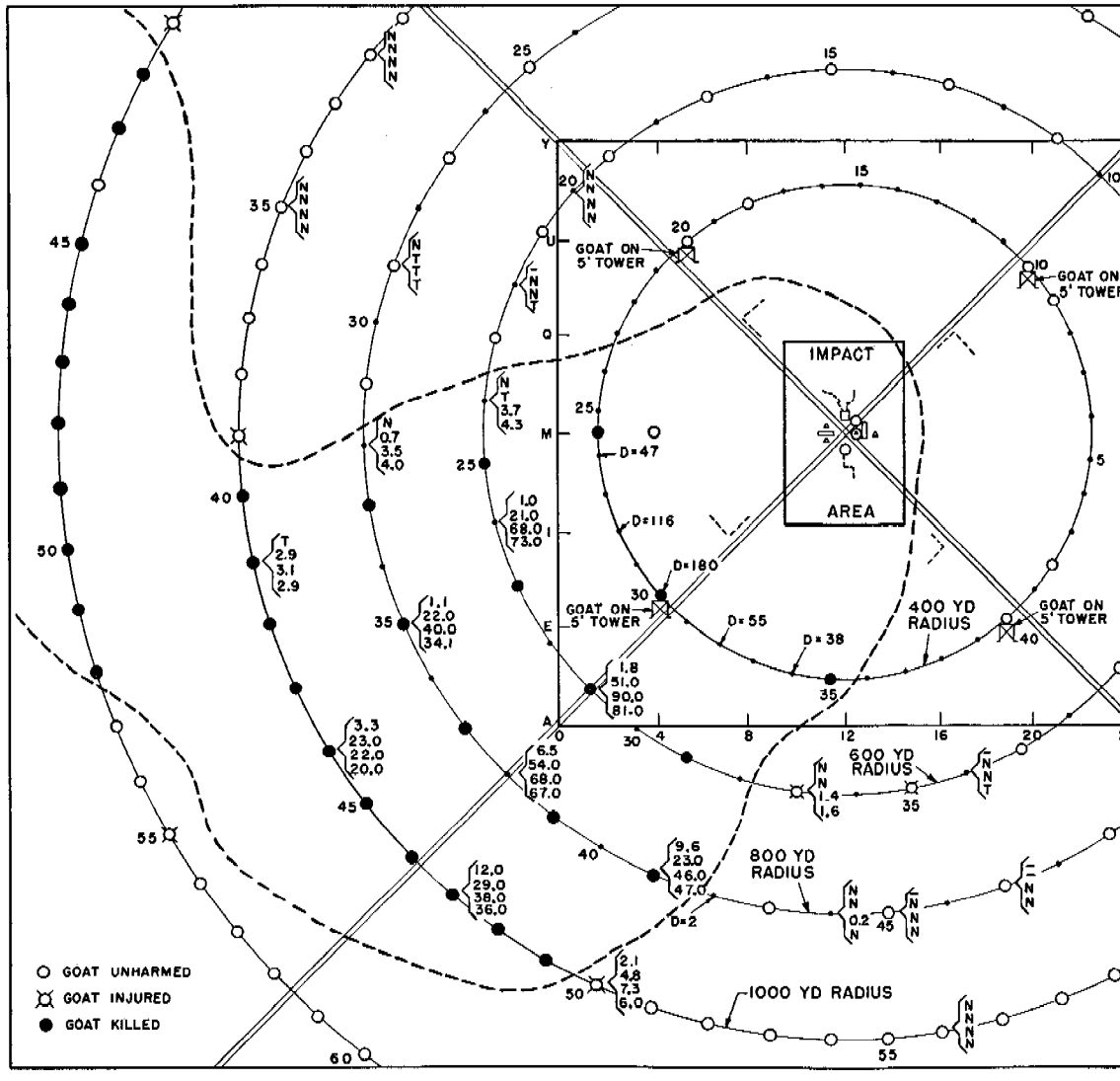


FIGURE 14. Sampling data on Dugway 4.2-in. mortar shoot.

low winds, the values are essentially the same. As noted in the discussion of that table, these requirements give large areas downwind which have very high Ct values. If this region is occupied by enemy troops this may be looked upon as an extra premium obtained in the operation. However, it seems to the reviewer that the placement of 80% of the bombs on the upwind half of the target would cut the number of bombs required by 30% to 50%, depending upon the size of the target, and if such a procedure should ever be possible from the operational standpoint, it should be recommended in place of statistical distribution over the whole target. The same comments apply to all sections of Table 13.

16.5.11 Munition Requirements for Surprise

The following discussion [2] was given of the requirements for surprise effects with the M79 bomb.

To set up a lethal dosage of CG (5 mg min per l) over 90 per cent of an open area within 30 seconds requires a density of at least three M79 bombs per artillery square (dropped within 5 seconds): for a lethal dosage over 80 to 90 per cent of the area within 2 minutes (3 mg min per l) requires at least one M79 bomb per artillery square.

There is little advantage in using gas bombs under high wind speeds for surprise since the 30 second and 2 minute surprise areas are not appreciably increased by higher wind speeds. On the other hand, if gas bombs are used for surprise under conditions where gas is not dissipated rapidly, other objectives will be usually achieved in addition to surprise.

The Project Coordination Staff give the values tabulated in Table 14. The 30-sec requirements apply to well-trained personnel and the 2-min values to men poorly trained, or sleeping.

TABLE 14. Munition requirements for surprise casualties.

Type of bomb	Agent	Ct	Number of bombs per artillery square 30 sec	2 min
British 250 LC	CG	3.2	12	6
British 500 LC	CG	3.2	8	4
M78 500-lb	CG	3.2	8	4
M78 500-lb	CK	3.2	12	6
M78 500-lb	AC	5.	12	6
M79 1,000-lb	CG	3.2	4	2
M79 1,000-lb	CK	11.	6	3
M79 1,000-lb	AC	5.	6	3

16.5.12 Clouds from Area Sources Set Up by 4.2-In. Mortar Shells

At the Dugway Proving Ground 18 shoots were carried out with the 4.2-in. mortars charged CG and at San José 2 shoots with the shells charged CK. Data on the larger Dugway trials and the two at San José are summarized in Table 15, and a typical Dugway concentration plot is given in Figure 14.

Open Terrain

On the basis of the Dugway trials it was concluded that the behavior of the gas cloud over flat open terrain is comparable with the behavior of a cloud set up by large aerial bombs, and comparisons for equal weights of agent indicate that the mortar and the bomb are about equally efficient for covering areas with dosages up to 30 mg min per l. An analysis of the factors affecting the efficiency was made by Walters and Zabor and their conclusions follow.

Effect of Wind Velocity

The area covered at 18 in. above the ground varies inversely as a power of the wind velocity — a power which increases with increasing wind speed, with increasing degree of inversion, and with increasing dosage. For example, for a dosage of 1 mg min per l under neutral conditions, the area varies inversely as the 1.1 power of the wind velocity between 2 and 4 mph and inversely as the 1.5 power between 8 and 10 mph; for $Ct = 3$ mg min per l these exponents are increased to 1.4 and 2.0, respectively, and for $Ct = 30$ mg min per l the area is inversely proportional to the 1.6 power in the range of 2 to 4 mph. For high inversion in the range of 2 to 4 mph the area varies as the reciprocal of the wind velocity to the 1.1 power for $Ct = 1$ mg min per l, the 1.5 power for $Ct = 3$ mg min per l, and the 1.9 power for $Ct = 30$ mg min per l. The rate of increase of this exponent with the wind velocity increases with increasing degree of inversion and decreases with increasing degree of lapse.

Effect of Atmospheric Stability

The temperature profile offers the best measure of atmospheric stability; in restricted cases only can the wind profile be used as a quantitative measure of the effective stability. An unsuccessful attempt was made to use the temperature difference from the surface to 2 m above the surface. The failure of this difference is probably due to two factors: (1) the difficulty of trying to obtain a representative macro surface temperature and (2) the fact that the surface temperature is only effective inasmuch as it governs the temperature profile of the air above the surface. Consequently, it was found to be convenient to employ the temperature difference from 1 to 3 m as a measure of the atmospheric stability; this is defined as $\Delta T'$ and is expressed in degrees centigrade.

TABLE 15. Data on 4.2-in. mortar shoots.

Wind speed, mph	ΔT	R	Target area for 80% of shell yd × yd	Weight of agent lb	Max Ct†	Area* Ct† = 3	Area* Ct† = 10	Area* Ct† = 100
				Dugway				
3.5	3.5I	1.7	267 × 195	920	430	72	...	...
2.8	1.6I	1.7	223 × 154	2,100	140	150	120	...
2.9	1.3I	1.8	243 × 187	2,110	180	128	...	...
5.6	1.0I	1.2	275 × 216	1,660	27	50	...	...
calm	2.7L	...	240 × 193	1,550	42	24	...	...
				San José				
0.5	I	...	100 × 400	6,615	780	...	>46	10
0.5	I	...	100 × 400	6,589	325	...	>30	15

* Areas in artillery squares.
† Ct values for 18 in.

TABLE 16. Ammunition requirements for the 4.2-in. chemical mortar shell charged CG over open terrain.

Time of day	Objective Mg min/l for Ct	Requirement (round per artillery square) at indicated wind velocities 2 mph	4 mph	6 mph	8 mph	10 mph
Inversion	1	45	45	45	45	50
	3*	45	45	60	105	165
	5 (in 2 min)	180†	180†	180†	185†	285†
	30*	50	170	375	660	995
	..‡					
Neutral	1	45	45	45	65	90
	3*	45	55	110	185	290
	5 (in 2 min)	180†	180†	180†	300†	465†
	30*	100	295	580	925	1,300
	..‡					
Lapse	1	60	130	210	305	410
	3*	110	265	480	745	1,055
	5 (in 2 min)	180†	340†	650†	1,100†	1,760†
	30*	1,015	1,600	2,120	2,615	...
	..‡					

* When using shell charged CK multiply these requirements by a factor of 1.5.
† Must be fired in 30 to 45 sec or less.
‡ For Ct = 200 fire 7 successive attacks using requirements for Ct = 30, at 10-min intervals.

The area covered by a given dosage at any height above the ground and at a specified wind velocity varies approximately as $(\Delta T + 0.37)^{\frac{1}{2}}$. This variation is essentially independent of the dosage and the wind velocity. From this it is noted that the munition requirement for a given mission increases very rapidly as the lapse rate increases; for $\Delta T = -0.36$ C, the requirement is ten times the requirement under inversion when $\Delta T = +0.63$ C. However, this relationship should be used with caution, especially under lapse conditions. When $\Delta T = -0.37$ C, the area indicated is zero, while actually the area is not zero even when $\Delta T = -1$ C, as it has been observed to be at times at Dugway. Under neutral and inversion conditions, the relationship is perhaps rather more valid. Inversions as great as +3.5 degrees have been observed at Dugway.

EFFECT OF DOSAGE

At low dosages (Ct = 1 to 5 mg min per l) the area varies inversely as the 0.45 power of the Ct at a wind velocity of 2 mph. This exponent increases to 0.8 at 6 mph and to 1.1 at 10 mph. It also increases with increasing dosages; for Ct = 10 to 30 mg min per l it is about 0.8 at a wind velocity of 2 mph. Variations of the power of the Ct with atmospheric stability and height above the ground are of second order.

The area enclosed by a specified dosage contour is inversely proportional to the height above the ground raised to a power which increases with increasing wind velocity, Ct, and degree of inversion.

On the basis of this analysis of the experimental data Walters and Zabor recommended the munition requirements given in Table 16.

From a study of the Dugway data the PCS gave the following munition requirements for the 4.2-in. mortar.

TABLE 17. Munition requirements for 4.2-in. mortar. Open terrain.

1. CG for Ct = 3.2 on 80% of target

Wind mph	Shell* per artillery square Neutral to moderate inversion
2	30
4	55
8	100

2. CK for Ct = 200 on 80% of target

Wind mph	Shell* per artillery square Neutral	Inversion
2	600	300
4	1,800	1,000

* 6.25 lb of CG per shell.

Because of the slow firing rate and low weight of agent per shell, the 4.2-in. mortar is impractical for attainment of surprise lethal dosages in 30 sec. However, Table 16 includes a requirement to give a Ct of 5 in 2 min. It has been argued that the fragmentation of the shells will cause troops to seek shelter and thus delay the adjustment of their masks for a period of about 2 minutes.

Wooded Areas

The two San José mortar shoots do not provide sufficient data to permit an experimental evaluation of munition requirements for wooded areas. In the second of these shoots 300 shells per artillery square on four squares gave Ct of 100 on 85% of the target, but the total area for $Ct = 100$ was some 15 artillery squares, mostly beyond the target. The area for $Ct = 200$ was about 4 artillery squares, but again much of this was beyond the target. When the cloud moved off the region of the target, the dosages were still very high, so the total area for lower dosages was unknown. The slow motion of clouds in forests or jungles would appear to make it possible to use the mortar to maintain low concentrations over large areas for long periods of time. Whether this would result in very high dosages per pound of agent expended is at present unknown. However, the requirements stated in Table 17 for 2 mph may be employed with the assurance that they are ample for average conditions inside the forest.

Bombs in Wooded Areas

The salient features of the micrometeorology inside a forest and jungle canopy, as discussed in Chapter 14, included: (1) low wind velocities, (2) zero or small temperature gradients both night and day, and (3) fairly large vertical air mass movement even with good inversion over the canopy. These factors result in considerable deviation in the travel of gas clouds in wooded areas from that observed in open terrain. The following comparison of Ct values for the 1,000-lb bomb is typical.

Table 18. Comparison of Ct areas in artillery squares for 1,000-lb bomb charged CK in open terrain and in forest. Wind speed 1 mph, clear night, 18-in. level.

	Areas			
	$Ct = 3$	$Ct = 30$	$Ct = 100$	Max Ct
Open	10	1	0.05	100
Woods	3	1	0.3	130

It is observed that (1) the area covered by ($Ct = 3$) is much greater in the open but (2) the maximum Ct, and (3) the areas covered by ($Ct = 100$) are much larger in the forest. Effect (1) is understandable because of the larger vertical air movement in the forest, and the vertical component which is constantly being introduced by a parcel of air in horizontal motion striking a branch or leaf. Effects (2) and (3) are harder to understand and doubtless are not true at all levels since they appear to be related to the smaller gravity spread and lower concentration gradients in the forest. In the open, many drops of the liquid from a bomb burst will fall nearly to the ground before they vaporize, thus setting up an initial concentration gradient, while in the forest considerable vaporization will occur from the surface of the foliage high above the ground. The observed temperature decrease in the cloud is much less in the forest than in the open, which indicates that heat has been absorbed from the vegetation. This decreases the density of the gravity effect. The friction of the vegetation tends to slow down the gravity spread of the cloud and it comes to rest with the top of the cloud considerably above the height observed in the open. As a result of these effects the concentration gradient is considerably smaller in the forest, and Ct values at higher levels will be greater. Under inversion, with low winds in the open at 100 yd from the burst, most of the gas from the charge will lie below the 18-in. level.

The difference between open terrain and woods indicated in Table 18 for the area of high Ct values is further accentuated by the fact that the average wind speed at night in a forest is around 0.5 mph and the average in the open certainly above 2 mph. It is this general occurrence of low wind speeds at night in forests and jungles which enhances the efficiency of nonpersistent agents in these areas.

Experiments with single 1,000-lb bombs were carried out in the Shasta, Targhee, and Florida forests, and the jungle of San José Island. The data obtained are adequate to give a fairly complete picture of the cloud travel under wide ranges of meteorological conditions. Figure 15 gives typical Ct contour for a bomb charged CK at Bushnell. While it is difficult to summarize in a single table the behavior of the 1,000-lb bomb for forests of varying density of foliage and height of canopy, it is believed that Table 19 gives representative values for the agent CK.

It should be emphasized that these values are for level ground. At the low wind speeds generally prevalent in the forest, gravity flow may be more important than the wind in determining the course of the cloud, if the terrain is sloping. In this case extremely high Ct values may be observed in stream beds and in general along the natural water course. This effect has been discussed in detail.[17]

For the agent phosgene [CG] considerable reaction occurs with the foliage, and the fall-off of concentration with distance is greater than that observed with the agent cyanogen chloride [CK]. CG is also

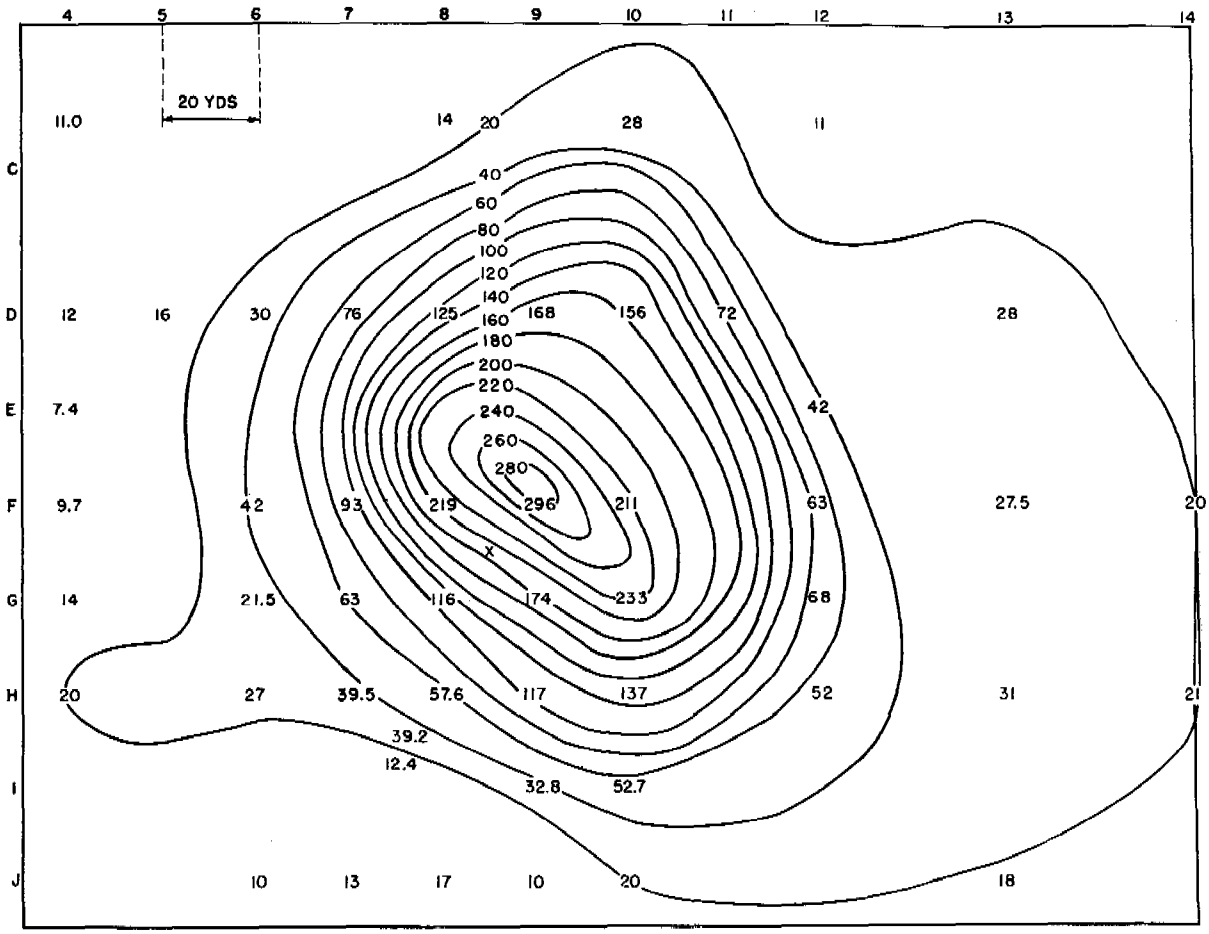


FIGURE 15. *Ct* contour map for 1,000-lb bomb charged CK.

TABLE 19. Summary for 1,000-lb bomb charged CK in heavy forest.

	Wind speed in forest, mph	Area in artillery squares covered by given *Ct* value*				Maximum *Ct*, mg min/l
		Ct = 3	*Ct* = 30	*Ct* = 100	*Ct* = 200	
Clear night	1	3	1	0.3	0	130
	0.5	8	2	0.5	0.1	225
	0.3	14	3	0.8	0.2	300
Clear day	1	1.5	0.5	0.02	0	120
	0.5	2.5	1	0.25	0	190
	0.3	3.5	1.6	0.4	0.05	250

* 18-in. height.

hydrolyzed by water, and following a rain or in a wet jungle much of the agent may be lost by this process. Rate constants for the absorption by a definite density of foliage were determined.[16]

The experimental field data for multiple bomb shoots in forest areas are not complete either with respect to the variation of meteorological conditions or the number of bombs per artillery square. Two multiple bomb CK shoots were carried out at Bushnell and two at San José. In all cases inversion over the canopy and low wind velocities beneath the canopy prevailed. Unfortunately the bombs were highly concentrated in a few artillery squares so that it is difficult to draw conclusions as to probable dosages

TABLE 20. *Ct* area and maximum *Ct* values from multiple bomb CK shoots (values for 18-in. height).

No. of bombs	Bombs per artillery square	Wind mph	Area covered by stated *Ct* in artillery square					Maximum *Ct*
			Ct = 5	*Ct* = 30	*Ct* = 100	*Ct* = 200	*Ct* = 1000	
				Bushnell				
10	8	0.4	20	14	11	7.5	1.4	2,000
8	9	0.7	14	9	7.5	6	0.6	1,900
				San José				
18*	4	0.4	..	..	> 5	2	..	470
96	5–9	0.5	..	..	>55	38	10	7,500
8	4	0.3	18	..	8	4	1	1,185
8	2–6	0.3	20	..	8	4.5	0.7	1,600

* 500-lb bombs. All others shoots 1,000-lb bombs.

with more normal bomb distributions. The observed *Ct* areas and the maximum *Ct* values are summarized in Table 20.

A comparison of the multiple shoots with the single bomb shoots indicates that the maximum *Ct* obtained is roughly the maximum for the single bomb multiplied by the number of bombs per artillery square. On the other hand, the overlapping of the single bomb effects results in a correspondingly smaller area per bomb for (*Ct* = 5) for the multiple shoots.

In general, the concentration gradient in the forest was less than that observed in the open. Over the target area, the concentration at 72 in. was from one-sixth to one-half the value at 18 in. with an average of about one-third. At a distance of 200 yd there was little difference in the values at the two heights except in stream beds where gravity flow was occurring.

The gas CK remained in covered fox holes and dugouts for fairly long periods. Although the maximum concentrations were generally lower than the outside, the *Ct* values were 30 to 50% greater.

TABLE 21. Munition requirements in wooded areas for 1,000-lb bombs charged CK; number of bombs per 100 artillery squares after Walters and Zabor; wind speed over woods.

	Inversion wind, mph		Neutral wind, mph		Lapse wind, mph	
	4	8	4	8	4	8
Ct = 3	36	45	42	54	50	64
Ct = 30	72	90	85	100	110	144
Ct = 200	140	230	150	270	170	320

16.5.13 Munition Requirements in Wooded Areas

By referring to the rather meager Bushnell data and by superimposing *CtA* data for single bombs, Walters and Zabor derived the munition requirements given in Table 21 for the 1,000-lb bomb. It is estimated that the requirements for CG would be about double that for CK.

The Project Coordination Staff reviewed all the data from Bushnell and San José and calculated $\int A\, d(Ct)$ for single and multiple bomb shoots. From their study they recommended the requirements given in Table 22.

TABLE 22. Requirements for 1,000-lb M79 bomb.

Wind over canopy in mph	Bombs per artillery square		
	Clear day	Neutral	Clear night
Charged CK in wooded terrain for Ct = 200*			
0–10	4.5	1.5	1.0
Charged CG for Ct = 200			
0–10	4.5	2.5	2.0

* Jungle terrain, multiply by 1.4. For other bomb sizes, multiply by 344/(lb of agent per bomb).

16.6 GAS CLOUDS IN URBAN AREAS

The following discussion is taken from Porton Memorandum No. 6.[1]

16.6.1 Air Circulation in Streets and Courtyards

As a preliminary, qualitative studies have been made of circulation of air in London streets. The results are best explained by diagrams.

Under calm conditions the circulation is controlled by temperature, and is as shown in Figure 16. A wind of about ½ m per sec is sufficient to mask this thermal circulation. When the wind blows along a

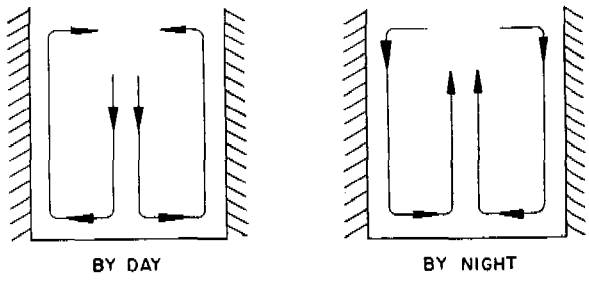


FIGURE 16. Temperature effect on circulation.

street, the air in the street flows in the same direction, continuing down the street until it is forced to rise over the houses at the end. At junctions with side streets, stationary eddies are formed which extend up these streets for a distance about equal to the width of the street; the flow in these horizontal eddies is away from the main street at the downwind side of the junction and toward it at the upwind side. If houses form a barrier across the top of the main street, the wind must flow over these houses before reaching the main street so that an eddy is formed. This extends down the street for a distance approximately equal to the height of the barrier. This triangular eddy maintains an upward current at the lee wall of the barrier, so that for a short distance downwind of the barrier the flow of the air near the ground is opposite to the undisturbed wind.

When the free wind blows across a street, the air descends at the downwind side of the street and rises at the upwind side. At street level the flow is therefore opposite to the wind direction as shown in Figure 17.

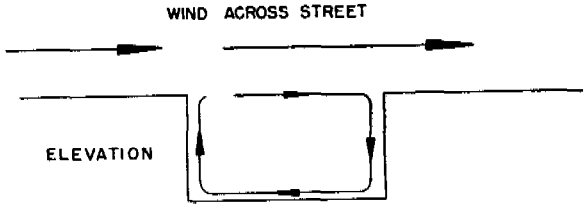


FIGURE 17. Flow of wind at street level.

For winds blowing diagonally across a street the circulation is a combination of the simple cases discussed, and the main flow can be roughly represented by a helix.

The circulation in a courtyard is the same as that in a street when the wind is blowing across the street. When the walls of the street or the courtyard are very high, however, the *dynamical* circulations extend only to a depth below the roofs approximately equal to the breadth of the street or yard. In these cases there is thermal circulation below the critical depth.

To illustrate how the circulations can be superposed for the case of the diagonal wind, observations taken at Porton provide an example. A site was made to simulate a blind alley 50 m long with no obstructions at the open end so that the wind could approach undisturbed. A typical observed circulation is shown in Figure 18.

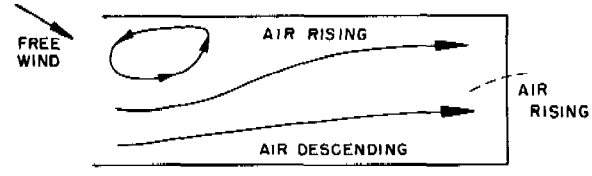


FIGURE 18. Observed circulation of air in a blind alley.

The circulation of air in drains and sewers is found to be independent of the direction of flow of the water, but is determined by the direction of the wind. When the wind blows along a street the direction of the flow of air in the sewers is opposite to that of the wind.

CONCENTRATIONS IN A SIMULATED BUILT-UP AREA

The potential dangers due to a large aircraft bomb charged with phosgene have been examined in a simulated built-up area at Porton. The site chosen was a space between 2 one-story buildings whose height was increased to 12 m by false roofs, the "street" being really a cul-de-sac some 50 m in length. Two types of bombs were examined under conditions of lapse, zero gradient, and inversion. The tail ejection bomb, which was sunk into the ground to a depth equal to its own length, was an aircraft bomb, 250-lb LC Mk I charged 41.3 l phosgene, and the burster-type of bomb was simulated by five Livens drums each charged 30 lb (13.6 kg) phosgene.

It was found that high concentrations were produced in the area, particularly in inversion conditions. The initial cloud, which filled about half the area, gave concentrations as high as 1 part in 50, and up to a height of 10 m concentrations of approximately 1 part in 10,000 persisted for some minutes, while appreciable amounts of gas were found to persist for about 40 min. As a general result, it was found that rooms with sound windows afforded a reason-

able degree of protection, which was considerably enhanced by simple measures of gas protection.

It is a matter of considerable difficulty to extend these results to the densely populated areas of a large city, but it is already clear that cul-de-sacs and courtyards may be very dangerous in the event of an attack with gas bombs. In the Porton cul-de-sac, it was found that the decay of concentration with time could be represented fairly well by the law

$$C_t = C_0 \exp(-kt)$$

where C_0 is the maximum concentration at the point in question and C_t the concentration after a lapse of t seconds. The decay coefficient k was found to vary with the site, meteorological conditions, and with the wind velocity, the ariation with the last factor being linear. Trials with smoke in London courtyards showed that the same law applies, and brought out the interesting fact that the cul-de-sac at Porton was much less dangerous than certain London areas, where the value of k may be as low as 5×10^{-3} sec^{-1}.

Chapter 17

FIELD SAMPLING METHODS FOR NONPERSISTENT GASES

By *Francis E. Blacet*

NONPERSISTENT AGENTS are those which normally enter the gas phase quickly after being dispersed. Phosgene, hydrocyanic acid, and cyanogen chloride are examples of such gases. In contrast to these agents are persistent gases, those with low vapor pressures at normal temperatures, of which mustard gas is the outstanding example. In general, the gas concentration ranges encountered in the study of the two classes of agents are of a different order of magnitude, and hence sampling devices which are satisfactory for one class usually do not prove good for the other. Accordingly, in studying the behavior and effects of toxic agents, a logical division of endeavor has taken place and Division 10 of NDRC was given problems pertaining to the nonpersistent gases. The sampling methods and equipment described on the following pages were developed for this type of agent. The merits of each instrument are discussed, including the possibility of its use with persistent gases.

17.1 HYDROSTATIC HEAD PUMP SAMPLER [9]

This device, which was developed for field use by Division 10 at Dugway Proving Ground, makes use of the simple and well known fact that a liquid flowing by gravity from a bottle tends to produce a reduced pressure and, therefore, can be used to draw air or gas through an absorption tube.

Figure 1 is a schematic diagram of the apparatus as used extensively in the field. It contains two independent pumping units which can be used to collect two samples at the same level, or with the aid of rubber tubing can collect single samples at any two positions at reasonable heights or distances from the pumps. The 2½-l acid bottles used in the pumps are graduated in 100-ml divisions. Approximately 1-mm capillary tubing forms the connection between the upper and lower bottles. The diameter of the capillary is selected to give approximately the flow rates desired. Flow rates of ½ to 1 l per hr prove to be satisfactory and hence sampling can be carried on over periods of from 2 to 4 hr without attention from an operator. The U-tubes in the bottles insure constant hydrostatic head during operation of the apparatus. The glass parts are mounted and securely held inside substantial wooden frames so that the pumps can be transported over rough terrain with little loss from breakage. The apparatus is completely symmetrical and can be used with either end up. Thus the same water is used over and over again for pumping purposes. All-glass bubbler absorption tubes are used for the absorbing solutions. Each bubbler has a 30-ml graduation mark.

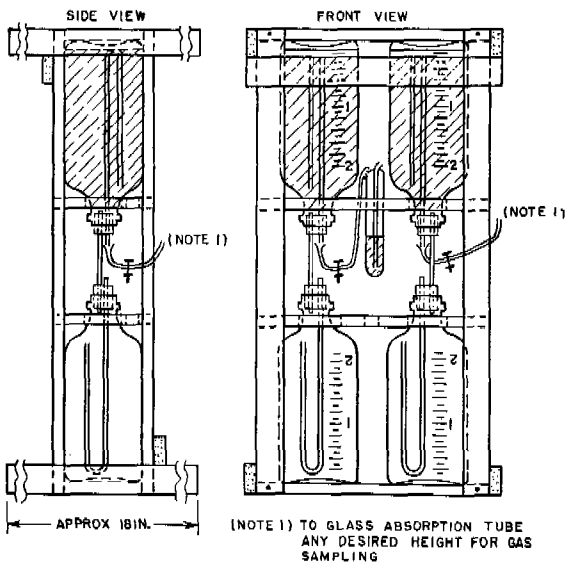


FIGURE 1. Diagram of hydrostatic head pump sampler.

17.1.1 Operation of Sampler

When the sampler is not in use, the water is in the lower upright bottles. In preparation for sampling, the entire apparatus is inverted and the absorption tubes attached by means of appropriate lengths of rubber tubing. The heights of the tubes and the water levels in the two inverted bottles are recorded. The time of reading the water levels is also recorded. Regardless of the nature of the experiment, the samplers are allowed to operate until at least 1 liter of water drains from each of the upper bottles. Upon completion of sampling, the final time and the water levels in the upper bottles are recorded, and the absorption tubes are detached and taken to the laboratory for analysis.

17.1.2 Preparation and Analysis of Solutions

The sampler has been used extensively in the study of CG, CK, and AC. For all three agents conductimetric analyses are employed.

Phosgene

The absorbing solution for this gas is made by mixing equal volumes of 95% ethyl alcohol and a good grade distilled water, and then adding sufficient HCl to bring the blank within the range of the conductance meter.

Twenty-five ml of this solution are placed in each absorption tube. After the gas is absorbed the tubes are brought back to the laboratory and more solution added to bring the total volume in each to exactly 30 ml. The solutions are allowed to stand for at least 8 hr to insure complete hydrolysis of the phosgene. Thereafter, they are passed in rapid succession through the cell, and the conductance readings and temperature are recorded.

From the conductance values and previously prepared concentration (mg per 30 ml) vs specific conductance curves the concentration of each solution is obtained. These data combined with the gas volumes and times recorded in the field make possible the calculation of the total gas dosage Ct attained at each sampling point.

$$Ct = \frac{\text{mg of agent}}{\text{flow rate, l per min}} = \frac{\text{mg min}}{\text{l}}$$

Cyanogen Chloride

The absorbing solution for this gas is made by mixing the following substances in the proportions given: ethyl alcohol, 250 ml; distilled water, 775 ml; formaldehyde (37%), 10 ml; and hexamethylenetetramine, 10 g. The sampling and analytical methods used for this gas are essentially the same as those used for phosgene.

Hydrogen Cyanide

This gas is absorbed in a 0.5% solution of mercuric chloride in distilled water. The sampling and analysis are the same as for phosgene, except that it is not necessary to allow a minimum time to elapse between gas absorption and the conductance measurements.

17.1.3 Notes

1. With this apparatus Ct values from 0 to at least 10,000 mg min per l can be obtained without difficulty. Over the majority of this range results may be expected to average an accuracy within about 10%.

2. This sampler is simple and cheap to construct, and proved to be very reliable in the field. The only replacement problem was due to breakage from bomb fragments and the loss from this cause was light.

3. Because of the simplicity of this sampler, personnel with little education and no background in science could be trained to do the field work. That proved to be a very important factor in trials in which a large area of rugged terrain had to be covered in a short time.

4. In the laboratory two men with one conductance meter could handle about 100 samples an hour. The biggest laboratory problem was the rinsing and filling of the absorption tubes. This work could be done by unskilled labor.

5. This method will work with other gases. For example, ammonia and sulfur dioxide can be absorbed in distilled water and analyzed by conductivity. Other analytical methods can be used if necessary.

6. Because of the small total volume of sample which it can take, no way has been devised so far to use this sampler for persistent agents.

7. The apparatus, constructed and used as described above, gives only the total dosage Ct attained at the sampling point. However, in certain limited experiments in which the operator can stay at the location of the sampler, it is possible to get a series of samples from which can be obtained points for a concentration vs time curve. This was done in early field and indoor experiments with ammonia, sulfur dioxide, and phosgene. The apparatus was modified by replacing the capillary connecting the two bottles by a rubber tube and pinch clamp, the quantity of water was adjusted so that just 1 l would flow from one bottle to the other. By means of the clamp the flow rate was made approximately 1 lpm. The operator had a rack full of bubbler tubes and during an experiment used them at recorded times. Because of the rapid flow rates involved it was necessary to use absorbents which could not be analyzed by conductivity means. Ammonia was absorbed in 1.5% boric acid and titrated with HCl. Sulfur dioxide was absorbed in 10% NaOH to which had been added a trace of stannous chloride. The excess of NaOH was neutralized by 6 N acetic acid and the sulfurous acid titrated with iodine. Phosgene was absorbed in 1 N NaOH in 50% methyl alcohol and the chloride determined potentiometrically.

17.2 DIAPHRAGM PUMP SAMPLER

This sampler was developed by Division 10 at Dugway Proving Ground and Northwestern University. It makes use of the fact that an electrically operated vibrating diaphragm, operated in conjunction with two simple check valves, may be caused to circulate a gas against a small hydrostatic head.

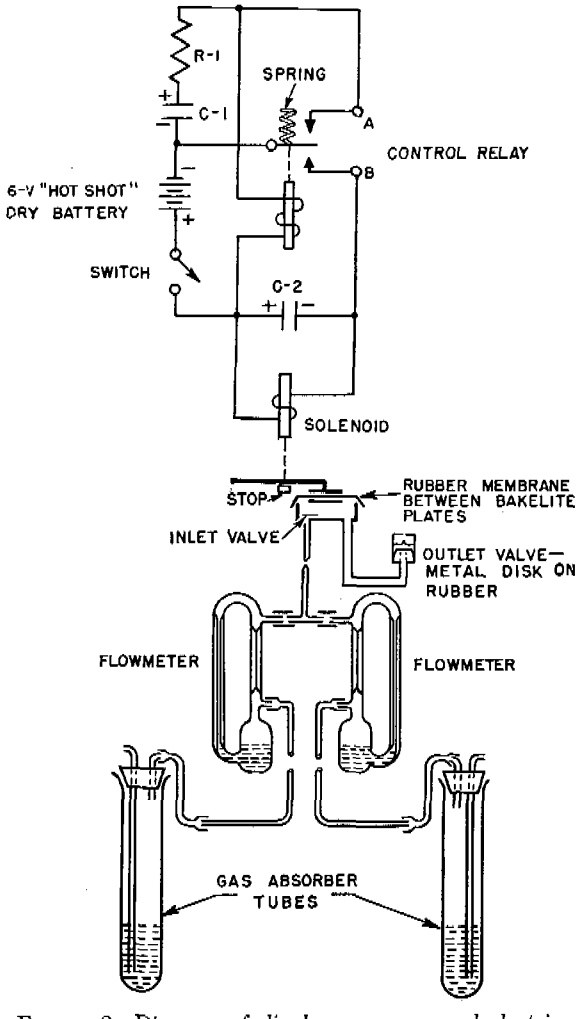


FIGURE 2. Diagram of diaphragm pump and electric circuits.

Figure 2 contains a diagram of the pump and electrical circuits. The entire pump, including battery and flowmeters, is enclosed in a rainproof box of dimensions 9x9x10 in. equipped with handle for carrying. The capacity of the pump is between 600 and 800 ml per min when operated against a 2-in. water head. Since half of this flow rate is sufficient for sampling purposes the apparatus is designed to operate two gas absorption tubes at the same time. A separate flowmeter is provided for each bubbler. The bubblers are 8-in. test tubes fitted with rubber stoppers and an inlet tube leading to the bottom. With the aid of rubber tubing, the bubblers can be placed at any desired reasonable height or distance from the pump.

17.2.1 Operation

Because of minor changes in pumping rate during the time the electrical circuit is reaching thermal equilibrium, it is found desirable to start operation of the sampler at least 15 min before taking the initial flowmeter reading. Flow rates are taken before and after the cloud is sampled and the average is taken in calculating results.

17.2.2 Preparation and Analysis of Solutions

PHOSGENE

The solution for this agent is made by mixing equal volumes of 95% ethyl alcohol and aqueous 2 *N* sodium hydroxide. Twenty-five ml are used in each absorption tube. After the gas is absorbed the tubes are returned to the laboratory and titrated for chloride by a standard procedure. From the data thus obtained and the recorded flow rates, total dosages are calculated in the same manner as discussed in Section 17.1.

CYANOGEN CHLORIDE

The same solution and analytical method are used for this agent as previously described for phosgene.

HYDROGEN CYANIDE

This gas is absorbed in aqueous 2 *N* sodium hydroxide and titrated for cyanide by a standard method. The calculation of dosage is the same as given for phosgene.

17.2.3 Notes

1. This type of pump will operate for a total of from 30 to 50 hr on a single 6-v dry battery (Burgess 4F4H). For this reason it is especially suitable for distant and inaccessible places where it can be started well before a gas trial is scheduled, thus giving the operator ample time to leave the area.

2. Because of the comparatively high capacity of the pumps, they will measure low dosages with considerable accuracy. Thus they are especially useful in defining the outer fringes of a gas cloud.

3. For the same reason, this apparatus has some promise for the sampling of persistent agents with low vapor pressures.

4. The major fault which developed in this sampler was the gradual pitting and finally, the sticking of the electrodes of the vibrating relay. The contact points are silver. Laboratory studies indicate that points of platinum or tungsten would be very much better.

5. In brief trials with mustard vapor in a moist tropical atmosphere there was considerable corrosion of the electrical parts. This served to emphasize that the sampler could be improved by enclosing all the electrical parts in a gasproof box.

17.3 HOT WIRE ANALYZER [7]

This instrument, which was developed under a Division 10 contract at the University of California, made use of the fact that many gases are induced to react by oxidation or decomposition when they come in contact with a hot wire. The reaction in turn affects the temperature, and therefore the electric resistance, of the wire. The wire filament in the apparatus is incorporated in a Wheatstone bridge and used with a continuously recording, photoelectric microvoltmeter.

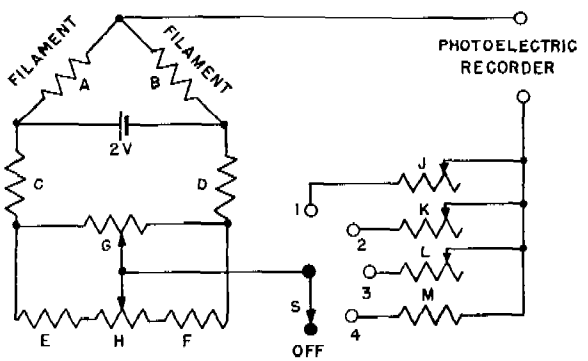


FIGURE 3. Diagram of hot wire analyzer electric circuit.

Figure 3 is an electrical circuit diagram of the analyzer in its simplest form. The photoelectric recorder, a General Electric Model 8CE1CM57Y1, covers the range 0 to 1 mv. The filaments are embedded in a brass block as indicated in Figure 4. By means of a suitable pump, the gas-air mixture to be analyzed is drawn over one filament, and air, which had been purified by first passing through a canister filled with type ASC charcoal, is drawn over the other. Capillary tubes are placed between the filaments and the pump to provide a critical orifice and hence a flow of approximately 1 lpm past each filament.

In order to conserve electric cable, triple unit samplers as diagrammed in Figure 5 usually were used in field experiments but the operation of these was essentially the same as given here for the single unit. If conservation of wire is no important object it is better to use single units, because in the triple units there is some coupling between the bridge circuits which materially reduces the sensitivity in the low gas concentration range.

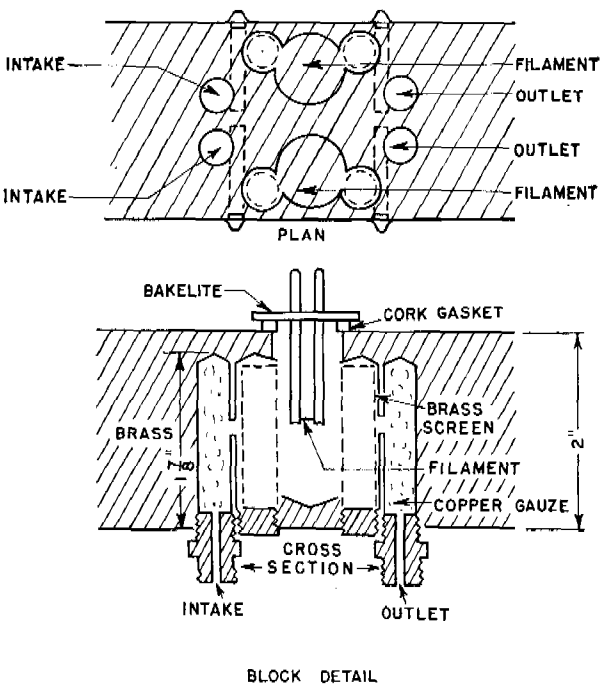


FIGURE 4. Diagram of reaction cell of hot wire analyzer.

17.3.1 Operation

In the field, the filament block, battery, and pump (No. 4F5, Gast Mfg. Co., Benton Harbor, Michigan) are located near the desired sampling point. Tygon (plastic) tubing, which does not in any way affect the gases studied, is used to convey the gas-air mixture from the sampling point to the filament block. The remainder of the apparatus is located at a control center, which at times may be as much as 1,200 ft from the sampling point.

At least 20 min before sampling is to begin, the pump is turned on (after that the filaments are connected to the 2-v battery). Care is taken never to heat the filaments before starting the pump, never to have more than 2-v battery potential, and always

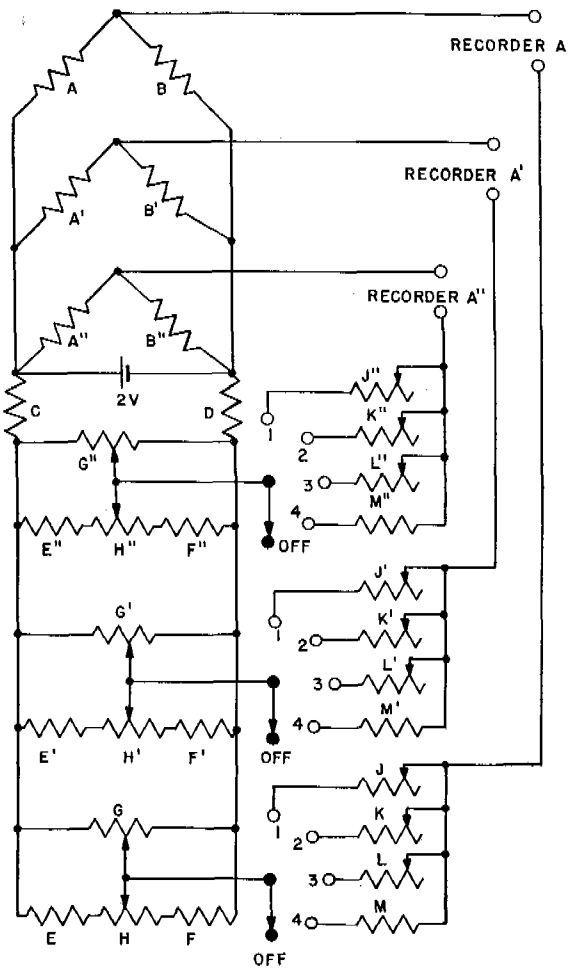


FIGURE 5. Diagram of triple unit sampler.

to have the recorder disconnected during the time the block is coming to equilibrium temperature.

Just before measurements are expected to start, the bridge circuit is balanced so that on high sensitivity (Circuit 1, Figure 3) the zero position is at about 0.2 of the full recorder scale. This is done by making a preliminary bridge adjustment on circuit 4, switching to 3 and adjusting with potentiometer G, switching to 2 and adjusting with both G and H, then finally switching to circuit 1 and adjusting by means of H.

Whenever possible the recorder is kept under constant observation, and when the gas concentration increases to the point where there is danger of the needle going off scale, the switch is changed to the medium scale (position 2) and a notation made on the tape to indicate that change. By shifting to different ranges of sensitivity in this way, a continuous record may be obtained for the duration of the experiment. Time and rate of tape movement are recorded. If drifts occur which make it necessary for the zero position to be ajdusted during an experiment, the magnitude of this adjustment is noted so that suitable corrections can be made in the final calculation of concentrations.

17.3.2 Calibration

Each analyzer is calibrated in its field position by getting meter readings in each sensitivity range for five or six known gas-air mixtures. The known mixtures are prepared by allowing pure gas, contained in gas pipets of known volume, to flow into partially evacuated 20-l carboys. After equilibrium pressure has been established with the atmosphere the pipets are removed, and the bottles are allowed to stand sealed until uniform concentrations are established. In use, each bottle is opened and gas is drawn immediately from near its bottom through the Tygon sampling tube and over the hot filament. In response to this the recorder needle quickly levels off and remains for a short time at a maximum value representing the specific concentration involved. From such measurements, calibration curves of meter readings versus concentration are obtained.

17.3.3 Calculation of Results

The time of arrival and the duration of a gas cloud at the sampling point is read directly from the record. The concentration at any time is obtained with the aid of the calibration curves. The total dosage is obtained by integrating the area under the total recorder curve.

17.3.4 Notes

1. This type of apparatus has been used successfully in the field with AC, CG, CK, NH_3, NO_2, and butane. Doubtless it could handle practically all other nonpersistent gases as well.

2. The lower range of sensitivity of the apparatus varies with the gas. With butane, a concentration of 0.05 mg per l can be measured with fair accuracy. For AC, the lowest concentration which can be detected is approximately 0.1 mg per l; for CK, 0.3 mg per l; and for CG, 0.3 mg per l. The magnitude of these limiting values will vary with the quality of the instrument and with climatic conditions at the time of the test. Scale readings are not necessarily linear

functions of concentrations. The character of the calibration curve varies with the gas and also from filament to filament. However, the average instrument may be expected to give reliable results up to concentrations of 50 mg per l and good approximations can be obtained up to 100 mg per l.

3. A minimum of chemical laboratory equipment is required. Except for the possible necessity for a chemical analysis of the calibration gas, all measurements are physical in nature and, accordingly, all data are available for the calculation of results as soon as the gas cloud experiment is finished.

4. No other field instrument will handle inert gases such as butane. Likewise, no other instrument will give arrival times of gas cloud fronts or instantaneous concentrations so exactly. Because of these latter features the hot wire analyzer is an ideal instrument for studying the characteristics of clouds formed from single bombs.

5. Along with the attractive features of the apparatus must, of course, be listed its drawbacks. The more important of these are as follows:

a. For even a moderate sampling layout a large amount of well insulated electric wire is required. For example, one triple unit located 400 yd from the control center requires the equivalent of 1¼ miles of single strand wire. To install the necessary wire to cover adequately, an experimental plot is no small task. Because of this, in forested areas where most liberated gases will destroy the foliage and hence the worth of the area for testing in a very short time, it is doubtful whether this apparatus should be adopted for general use to the exclusion of all others.

b. The large amount of exposed wire is vulnerable to bomb fragments, and it has been common experience to have crucial sampling points missing from the records, because of wires being cut.

c. The filaments used in the apparatus have neither been so rugged nor so long lived as one would like. When a new one is installed a new calibration is required.

d. Variations in the absolute humidity may seriously affect the accuracy of results in the low concentration range.

e. The relatively large lower limit of sensitivity for most gases means that a dangerous or lethal dosage could be built up at a sampling point without being detected by this instrument. It is for this reason that the hot wire analyzer in its present design cannot be used for persistent gases such as mustard, which have low vapor pressures.

f. In order to obtain the best results the recording instruments must be under observation at all times. In large scale aerial trials it was not practical to do this because of the hazard to personnel.

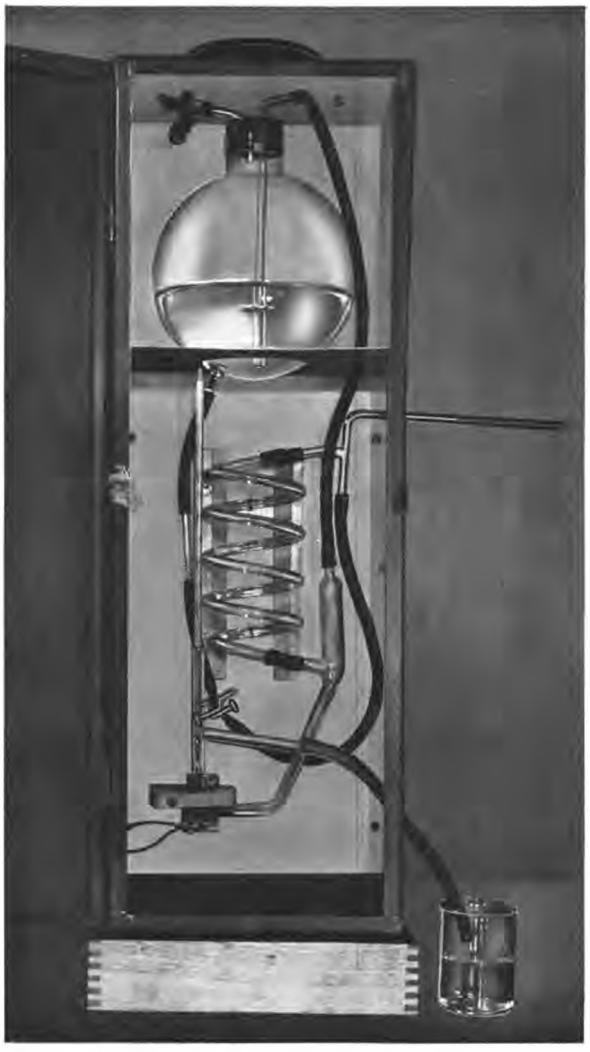


FIGURE 6. Photograph of absorption unit and conductance cell.

17.4 FIELD CONDUCTIVITY ANALYZER [4, 5, 6, 8]

This instrument, which is referred to frequently as the Dickinson meter, was developed at the California Institute of Technology. It made use of the fact that

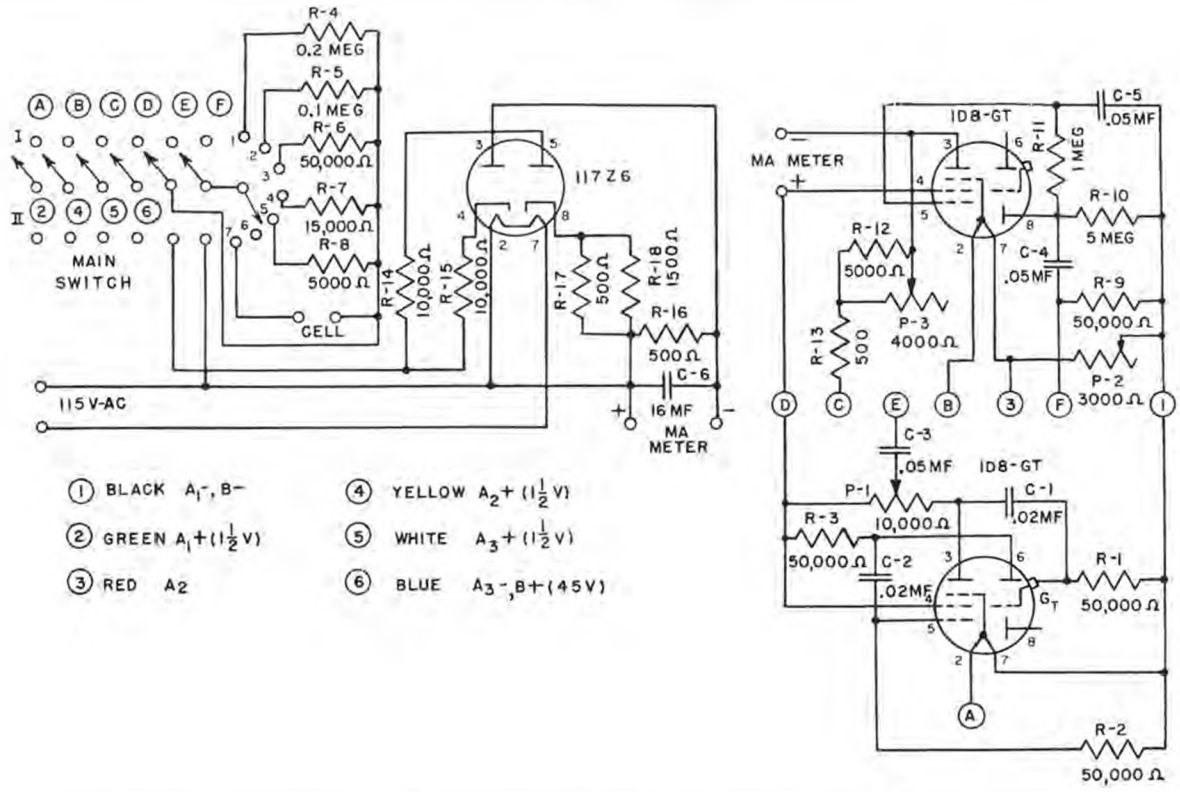


FIGURE 7. Diagram of electronic circuit for alternating-current model (left) and battery model (right).

the nonpersistent gases, when absorbed by an appropriate solvent, cause large changes in conductivity. The agent is absorbed continuously with fresh solvent and the solution so formed is then passed through a conductivity cell. The amplitude of an alternating current passing through the cell is a function of the concentration of dissolved gas, and with the aid of a rectifier, it can be recorded continuously on a recording milliammeter.

Figure 6 is a photograph which shows the manner in which the agent is absorbed and passed through the conductance cell. The solvent flows by gravity, at a controlled rate of approximately 10 ml per min, through a capillary T-tube which serves to aspirate the gas-air mixture into the spiral where absorption occurs. Then it passes through the cell, and finally around a thermometer bulb and out of the system as waste. The purified air after passing through the spiral escapes by way of a constant-head tube to the space above the remaining solvent in the reservoir.

The analyzer can be operated either with batteries or with 115-v alternating current. Wiring diagrams for both circuits are given in Figure 7.

In the last model developed, the complete electronic circuits and batteries are enclosed in a weatherproof and gastight can. The recorder, an Esterline-Angus Model A.W., is protected in a gastight metal container fashioned after the conventional bell jar. The recorder can be placed either near the sampler in the field or in a distant central shelter.

17.4.1 Operation of Sampler

Preliminary to an experiment the reservoir is filled with the appropriate solvent, the capillary intake is inspected to make sure that it is dry, the flow rate is tested and, if the battery system is used, this is turned on well ahead of time. A calibration curve is obtained on the record both before and after the experiment by means of the fixed resistors R4-R8, (Figure 7). The lag time of the instrument is obtained by noting the period elapsing between the time an open bottle of ammonia is held to the intake tube and the response of the recorder needle.

Other necessary data taken during an experiment are reference times on the record, time of gas release, speed of meter tape, and solution temperature.

17.4.2 Solutions

A good grade of distilled water must be used in making up all solutions.

PHOSGENE

This gas can be absorbed in water, but best results are obtained by using 20% ethyl alcohol. Sufficient HCl is added if necessary to bring the cell resistance down to 200,000 ohms.

CYANOGEN CHLORIDE

Cyanogen chloride is absorbed in 20% ethyl alcohol to which 14 g of hexamethylenetetramine per l have been added.

HYDROGEN CYANIDE

Hydrogen cyanide is absorbed in 20% ethyl alcohol to which 400 mg of mercuric chloride per l are added. Sufficient HCl is added, if necessary, to bring the cell resistance down to 200,000 ohms.

17.4.3 Calibration of Results

If battery-operated circuits are used, the records are corrected for scale drift at as many points as necessary with the aid of the calibration points recorded at the beginning and at the end of the experiment. If constant voltage alternating current is used, the meter readings are changed to cell conductances and these converted to gas concentrations with the aid of the known cell constant and the temperature. Actually, from data obtained in laboratory experiments, charts and scales are constructed for each gas, from which the gas concentrations can be obtained directly from corrected meter readings.

17.4.4 Notes

1. This instrument was designed originally to operate as an independent battery-powered unit. As such, it has no peer among present field sampling devices for overall performance. It gives arrival times, duration, total dosage, maximum concentration, and other characteristics of gas clouds with sufficient accuracy for practically all purposes. It will perform all functions especially ascribed to the various samplers previously described, but may not perform some functions as well as will some of the other instruments. For example, the response is slower than that of the hot wire analyzer, and consequently, if the interval of time between a bomb burst and the arrival of the gas is extremely short this time interval can be measured more accurately and more easily by the hot wire instrument.

2. The instrument is much easier to service when operated on a 115-v a-c circuit and since there is no drift in the calibration points the records are simpler to evaluate. However, the use of alternating current restricts the location of the instrument and introduces all the disadvantages of a wired experimenting area mentioned previously in discussing the hot wire analyzer.

3. The lower limit of sensitivity varies somewhat for the different gases but, in general, concentration measurements below 0.3 mg per l will not be reliable. Accordingly, total dosages from low concentrations over a long period of time cannot be obtained satisfactorily with this sampler.

4. In addition to the toxic gases mentioned above, this analyzer has been used successfully with ammonia and sulfur dioxide. Distilled water was the solvent in each case.

17.5 ROTARY DISTRIBUTOR SAMPLER [9]

The first model of this apparatus was designed and built by a member of Division 10 at Dugway Proving Ground. Subsequent changes in design were made in cooperation with the Chemistry Section there.

17.5.1 Operation of Sampler

This sampler was designed to pull air at a known rate through a bubbler tube for a controlled interval of time, and then shift to another tube and so on up to as many as 20 samples with some models. This was done by use of a continuously acting pump which could be connected successively to different absorption tubes by the intermittent movement of a rotary mechanism. The latest model was designed to operate by electrical impulses from a central control point. The current activated a solenoid which permitted a ratchet mechanism to move forward one space. A clock spring mounted in the instrument and attached to the rotary arm produced power for rotation. The motion was quite rapid so that there was little time lost between the termination of sampling through one bubbler and the beginning of sampling on the next.

The absorbing solutions and methods of analysis were essentially the same as those described in Section 17.2.

17.5.2 Notes

1. When the instrument was used for the duration of the cloud, it was possible to calculate the total Ct at the sampling point. However, it was more than a

total dosage meter, for it could be used to give the dosage, and, hence, the average concentration over short periods of time up to the limit of sample tubes. Thus, it proved especially useful for obtaining "surprise" dosages from single munitions. The dosages for the first 30 seconds first minute, etc., could be obtained very well.

2. The sampler was used with power and control wires emanating from central points, and, hence, was subject to hazards caused by wire being cut by bomb fragments and to other disadvantages associated with the wiring of an area for tests.

3. An early model made use of an automatic starter and was designed to be self-contained with no necessary external wiring. A pair of conductivity cells was arranged in a bridge circuit and connected to a pump so that air was pulled through the cells in series. The presence of CG or any agent producing a conductivity change upset the bridge balance and tripped a relay in the plate circuit of a single tube amplifier. The relay in turn started an alarm clock equipped with contact on one gear which activated the rotary distribution solenoid. Further, by noting the time of gas release and the reading of the alarm clock after the test, the time for the gas to reach the sampler could be found within limits.

17.6 THE FIELD CANISTER TESTER

This apparatus, which is sometimes referred to as the *mechanical goat*, was developed in the Division 10 Central Laboratory, Northwestern University. It was able to draw air through canisters in a manner designed to simulate the human breathing cycle and was used to evaluate the performance of canisters in actual gas clouds.

Figure 8 is a schematic diagram of the field tester. The bellows pump C is operated by a small 120-v a-c motor D which is geared down internally to 25 rpm. The connecting rod which works the bellows can be connected to either one of two positions on the crank disk which correspond to pump capacities of 16 and 32 lpm, respectively. Air is drawn into the bellows through the canister and valve A and then forced out through valve B.

By means of the small pump H, which maintains reduced pressure in chamber I, continuous sampling of the canister effluent stream is done at point E and the gas is drawn through an appropriate absorbing reagent in G. The capillary J keeps the flow constant at a known rate. By sampling with a conductivity meter at point F a continuous effluent concentration curve can be obtained. The pumps and motor are enclosed in a weatherproof case and are protected from the corrosive gases by a breather canister K.

17.6.1 Operation of the Tester

The tester is always placed in the field beside one of the sampling devices previously described so that the total dosage of exposure is obtained. The solutions used in G are the same as used with the diaphragm pump samplers. The operation of the conductivity meter, which is attached at point F, is described in the previous section.

17.6.2 Notes

1. This apparatus was designed and used on the assumption that since the lethal dosages of the several gases were known, it would give more data, and more reliable data, concerning the penetration of canisters in the field than could be obtained by the use of animals. For a known exposure, it will give the total effluent dosage at a known breathing rate, the shape of the effluent curve, and a measure of the amount of desorption from the charcoal. In animal field experiments so far devised, if the animal survives the gas cloud it is certain that he did not draw a lethal quantity of agent through the canister, but if he dies, it is not known (a) whether the agent came through the charcoal or from facepiece leakage, (b) whether he died exclusively as a result of the agent or a combination of agent and strangulation,

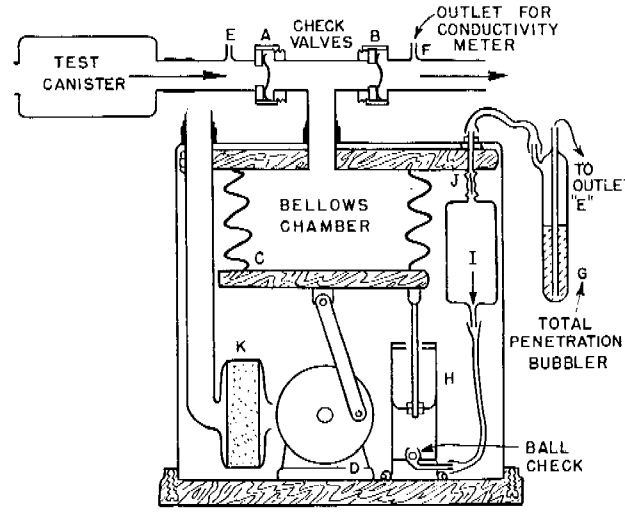


FIGURE 8. Schematic diagram of field canister testing apparatus.

(c) whether the dosage which came through the canister was large or small, or (d) whether the animal died as the result of direct canister penetration or desorption from the charcoal after the gas cloud had passed.

2. With canisters that broke slowly, the conductivity meter gave only moderately valuable results when used in conjunction with this apparatus, because it did not measure low effluent concentration with sufficient accuracy. Accordingly, it was found desirable, whenever practical to do so, to go into the field and change bubblers G, at known times. In this way, effluent Ct values could be obtained accurately and the shape of the effluent Ct curve could be obtained approximately.

17.7 OTHER SAMPLING DEVICES

Mention is made in this section of several sampling methods which were developed and used by other United States and Allied agencies but which were not used in field experiments by Division 10. Reference is made also to some methods which offered promise but which never got beyond the developmental stages.

17.7.1 The Snap Sampler

In this device an evacuated vessel is opened at a selected time in a gas cloud, the air enters and subsequently the amount of agent is determined. An almost instantaneous sample is obtained, but since gas clouds are not homogeneous especially in the first few minutes of their existence, the results from snap samplers may be misleading. If a number of consecutive samples are taken the discrepancies tend to be eliminated, and a fairly accurate total dosage can be obtained by plotting concentrations vs time, and drawing a smooth curve through the points.

An instrument which operated on this principle was made under a Division 10 contract at Stanford University, and was used extensively at Dugway Proving Ground by the Chemical Warfare Service. It contained ten evacuated tubes which were opened at known time intervals by means of a clock mechanism. Various modifications of the device were made at Dugway. A sampler operating on the same principle and known as the *Berthelle* is used at Suffield, Canada.

17.7.2 The Ultraviolet Photometer [1]

This instrument, which was developed at Northwestern University for gas sampling, will give concentrations of gases (such as phosgene) which absorb strongly at a wavelength of 2537 A. It is used with a continuous recorder. It is probably an ultimate standard in sampling for those gases for which it is applicable. The response is rapid and the calibration can be very exact. However, as originally built, the instrument was not sufficiently rugged for field use and, since it could analyze only gases which absorbed the above-mentioned wavelength, it was not used extensively.

17.7.3 The Air Injector

At Suffield, Canada, compressed air injectors were used to obtain total dosage during the passage of gas clouds of small duration. Over short periods of time the injectors could aspirate the gas through an absorbing tube at a very nearly constant rate. The absorbing solutions were analyzed by standard methods.

17.7.4 The Tape Recorder

This sampler was developed under a Division 9, NDRC, contract at the University of Chicago. It draws a known volume of gas through a *frame* on a strip of specially impregnated filter paper. An automatic mechanism then moves the strip forward one frame and repeats the process. The gas cloud is sampled at 2- or 6-sec intervals. The tape, which is cut and perforated like a 16-mm movie film, is analyzed by a photoelectric measurement of the intensity of the color produced on the paper by the gas. The instrument can be set to cover a fortyfold range of concentration, within the anticipated range. The instrument is portable and completely self-contained in a single small box. Considerable difficulty was encountered in developing satisfactory tapes for the various gases, and, as a consequence, the samplers were not used to an appreciable extent in the large-scale field experiments discussed elsewhere in this volume.

17.7.5 Radio Control for Samplers

The rotary distributor sampler and other samplers described in this chapter could be adapted to radio control. This would eliminate the problems associated with wiring a testing area, and possibly would simplify many of the other problems connected with large-scale experiments. At Northwestern University experimental models of a radio transmitter and a receiver were made which appeared to operate a rotary

sampler very well. However, at the time this was done, the need for performing field tests without delay was so great that the models were set aside, and the experiments were carried out with the equipment available. With the new developments which are being made in electronics, there is no doubt that, in the future, excellent remote radio controlled samplers can be made.

17.8 SUMMARY AND SUGGESTIONS

In the course of the many field experiments with nonpersistent gases performed or cooperated in by contracts of Division 10, most of the samplers described in this section have proved very useful. The nature of the experiment to be performed determines the types of sampler that should be used. Accordingly, an installation designed to do a large variety of tests should have several kinds of samplers available.

If the characteristics of clouds liberated from single munitions are to be determined, recording instruments with a rapid response are necessary. In multiple bomb tests made over a comparatively large area the relative importance of recording instruments diminishes, although some should be used; a large number of total dosage samplers, such as the hydrostatic head pump and the diaphragm pump, should be employed.

If a test area is in the open country, without vegetation, where many experiments (usually of short duration) may be run, it is doubtlessly advantageous to wire the area for alternating electric current in order to operate samplers. However, in wooded and jungle areas where wiring is difficult to accomplish and where only a few experiments can be performed before the trees are defoliated as a result of the action of the gas, it is desirable to use independent, self-contained samplers as much as possible, and thus reduce the stringing of wires to a minimum.

In large-scale experiments of from ½ to 4 hr duration it was found satisfactory to use a limited number of recording instruments at strategic locations to get arrival times, maximum concentrations, and cloud durations, and to depend on total dosage, bubbler-type samplers to furnish the remaining necessary sampling information. Hydrostatic head samplers were used in parts of the area where the dosages were expected to be high, and diaphragm pumps were placed at distant points where only traces of gases were expected. The hydrostatic head pumps operate only for a limited time and hence must be serviced shortly before the gas is liberated. Accordingly, it is best to have them at accessible points. Also, they are easy to make from nonstrategic material, and thus, being expendable, can be placed right up in the target area without danger of an irreplaceable loss. Because the diaphragm pumps will operate for hours, they are good to put in distant and inaccessible places since they can be serviced long before an experiment is scheduled to start, giving the operator ample time to leave the area before the cloud is released.

PART III

AEROSOLS

Chapter 18

GENERAL PROPERTIES OF AEROSOLS

By *W. H. Rodebush*

18.1 INTRODUCTION

The term *aerosol* is used to designate particles dispersed in a gaseous medium. The term *particulate* is preferred in Great Britain and more specific and familiar terms such as *smoke, fog,* and *dust* should be used whenever applicable. For example, an aerosol of particles of diameter less than about one micron will exhibit the characteristic behavior of a smoke and may be properly so designated. The particles of which the aerosol is composed may be either solid or liquid. If liquid the particles will be spherical, but solid particles will usually behave approximately as spheres.

18.2 STABILITY

Aerosols, like most colloidal forms of matter, are essentially unstable, and will usually disappear with the passage of time either by evaporation or precipitation. Evaporation will occur if the substance of which the aerosol is composed has an appreciable vapor pressure at room temperature. The vapor pressure of a small drop is larger than that from a large mass of substance, but this effect is not important for a drop diameter greater than 0.01 micron.[1]

Precipitation may occur as a result of diffusion or settling. The diffusion constant varies inversely as the particle diameter, and the rate of diffusion to a wall depends upon the concentration of aerosol in the surface layer. Unless the surface layer is constantly renewed the concentration quickly falls to zero, and only by very violent stirring can the surface layer be kept moving with sufficient velocity to maintain the diffusion process.

These statements concern ordinary or kinetic diffusion. Thermal diffusion is the process by which an aerosol is deposited on cold surfaces. It is a much more effective process in the precipitation of aerosols but the theory of thermal diffusion is not in very good agreement with the observed facts.

Settling, ordinarily, accounts for the precipitation of aerosols of diameter 1 micron or greater. According to Stokes' law a particle falls with a steady velocity which is proportional to the square of the diameter. The instantaneous rate of precipitation is independent of the amount of stirring (within limits) because the layer of air in contact with the surface remains stationary and the particles fall through this layer at constant velocity.

It follows, therefore, that aerosols of large particle diameter disappear by settling, and those of very small particle diameter by diffusion. For particles in the range of 0.1 to 1.0 micron diameter, the diffusion constant is small and the Stokes' law rate-of-fall is small. Smokes, which are usually composed of particles in this size range, therefore, are remarkably stable, and remain dispersed for long periods of time. The foregoing statements apply to aerosols which do not carry electrical charges. The behavior of charged aerosols will be discussed later.

18.3 COAGULATION

When a particle of small diameter collides with a surface it adheres because of surface forces. Large dust particles may be dislodged by a strong blast of air so that air cleaners are often coated with a film of oil or sticky liquid, but small particles will adhere regardless of the surface. Similarly, the collision is inelastic and a single particle is the result when two particles collide. If the particles are liquid they coalesce to a single drop whereas solid particles form aggregates which often take the form of chains and resemble fibers on casual inspection. This coagulation resembles a bimolecular mechanism, and is described by the equation for a second order reaction. Table 1 gives the approximate times necessary to reduce the number of particles to one-tenth of the original number [computed on the basis of equation (19), Chapter 19].

TABLE 1. Rates of coagulation (t_0) equals time required to reduce the number of particles to one-tenth of the initial number. W equals mg per l, assuming diameter equals 1μ, and density equals 1.

No. per cm^3	W mg per l	t_0 sec
10^{10}	5,236	3
10^{9}	523.6	30
10^{8}	52.36	300
10^{7}	5.236	3,000

As a result of this coagulation a smoke of uniform small particle size will become heterogeneous, and the larger particles will settle out. It follows, therefore, that a smoke with a concentration of particles greater than 10^7 per cubic centimeter will not be stable. There is no method known for preventing the coagulation of aerosols. The stabilizers which are effective for preventing the coagulation of solids or liquids dispersed in a liquid medium are completely ineffective with aerosols.

18.4 FORMATION OF AEROSOLS

Natural-occurring fogs are of relatively large particle size, 10 to 50 microns diameter, and of relatively low concentrations, a few droplets per cubic centimeter. Each droplet is formed by the condensation of water on a nucleus, which in the neighborhood of cities may be a particle of dust or soot. Near the ocean, minute salt crystals, which are thrown into the air by spray, serve as nuclei, and the water collected always contains dissolved salt. Therefore, fogs are more common near the ocean, or in the neighborhood of large cities, or industrial areas.

Because of the large particle size, fogs tend to fall out as a fine mist or rain, and this process is accelerated by the tendency of the small drops to evaporate; the vapor condensing on the larger drops. Thus, fogs will only persist if meteorological conditions are such that new drops are constantly forming to replace those that fall.

The droplets of natural fogs often carry considerable electrical charges and the accumulation of these charges accounts for the electrical effects that occur in thunderstorms when the small drops coalesce rapidly to form larger drops. It may be remarked that the conditions which produce rapid coalescence and the heavy downfall of rain are not compatible with the conditions that produce fog, and vice versa.

The methods of producing aerosols artificially fall into two categories: mechanical dispersion, and vapor condensation. Mechanical dispersion appears at first thought to offer the most promise. The work required to break up a liquid into drops of 1 micron diameter is negligible when compared to the heat of vaporization. There are two difficulties. The first is that the only method for bringing about this breakup is that of turbulent flow through a nozzle which is, of course, a very inefficient process mechanically. An even more fundamental difficulty, however, is that the concentration of drops leaving the nozzle is so high that most of the small drops coagulate before leaving the immediate vicinity of the nozzle. This difficulty can be avoided only by using an aspirator nozzle, and maintaining a very high air velocity to scatter the drops before they can coalesce. One hundred and fifty cubic feet of air at 50 lb pressure per gallon of liquid will give only a fair dispersion. The dispersion of solids is even more difficult. The solids must be ground to the required particle size, which is a very inefficient process mechanically, and then dispersed in an air jet. It has been pointed out earlier that the surface forces which cause particles to adhere are relatively very strong so that it is difficult to bring a sufficient shearing force to overcome them by a blast of air. The operation of grinding and dispersal may be combined in one operation by the use of a *micronizer* but the process remains an inefficient one.

The most satisfactory way to produce an aerosol is to imitate the process by which natural fogs are produced. Any substance which can be vaporized without decomposition can be converted to an aerosol by blowing a jet of the vapor into cool air. When the degree of supersaturation is small, drops will not form by condensation except on nuclei which may be present in the form of ions, dust particles, etc. When the degree of supersaturation is great, as when the vapor of a high boiling oil escapes into the atmosphere at high velocity, an enormous number of very small droplets will be formed. It is difficult to see what sort of nuclei can be present in such enormous numbers but it cannot be stated categorically that nuclei are not present. It may be in the case of the oil that the larger molecules behave as nuclei. Coagulation takes place very rapidly as described in Chapter 22 but the size range remains narrow as the process

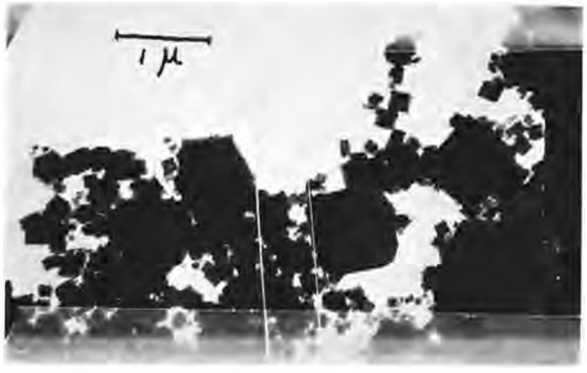


FIGURE 1. Electron microscope picture of magnesium oxide smoke particles.



FIGURE 2. Electron microscope picture of titanium oxide smoke particles.

goes on, so that it is possible to control the size of droplets quite precisely by regulating the rate of vapor flow.

A modification of the vapor condensation process is used when smokes are produced by combustion. When magnesium ribbon is burned, the ultimate particles produced are nearly perfect crystals of magnesium oxide which are too small to be seen by the ordinary microscope, but are revealed by the electron microscope [2] as shown in Figure 1. These submicroscopic crystals agglomerate into chains and clusters of fantastic shape and structure, which appear under the microscope as though they were solid particles. Figure 2 is an electron microscope photograph of titanium particles produced by thermal dispersion. When carbon smoke is produced by incomplete combustion the small crystals of graphite tend to form filaments that resemble a string of beads (see Figure 3). This tendency of soot and dust particles to form filaments often deceives the housewife who supposes these "cobwebs" to be produced by spiders.

18.5 ELECTRICAL PROPERTIES OF AEROSOLS

Except for special cases, which will be discussed later, electrical charges are of minor importance. Most of the particles produced are uncharged, particularly if the concentration of the aerosol is high, since normally there are only a few ions present per cubic centimeter. Even in the case where ions are produced by special means to serve as nuclei, the resulting aerosol will contain many uncharged particles, since the positively and negatively charged particles have a tendency to neutralize each other by agglomeration. If it is desired to precipitate aerosols in a uniform field, it is necessary to charge the aerosol before the process will be effective.

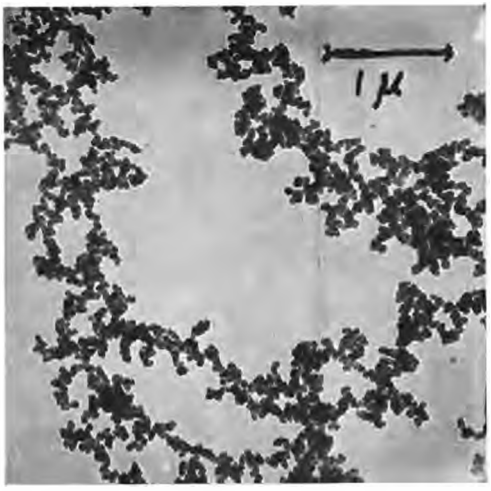


FIGURE 3. Electron microscope pictures of carbon particles from camphor smoke.

18.6 FILTRATION

Neither electrical nor thermal precipitation have proved in the past to be practical for the rapid removal of aerosols. Filtration appears to be, by long odds, the most satisfactory method of precipitation. Aerosol filters consist of loosely aggregated fibers, and, in order to avoid excessive resistance to the flow of air, the mesh of the filter must be large compared to the size of the particle to be removed. There is therefore no screening action; the removal of a particle depends entirely upon a chance collision of the particle with a fiber of the filter. Once having collided, the particle adheres by the natural forces which are always operative.

Very large particles can be precipitated by centrifugal action as in a cyclone separator. For smaller particles whose diameter is in the neighborhood of 1 micron the centrifugal action is no longer effective since the inertia of the particle is not sufficient to overcome the resistance of the air. Thus the air flows

around the fibers of a filter in stream lines and the particles are carried around with the stream lines. There is a range of particle sizes for which a higher velocity will improve the operation of the filter since the inertial effects will carry the particles across the stream lines into collision with the fibers of the filter. For particles smaller than 1 micron diameter no inertial effects exist, but the kinetic diffusion becomes of greater importance in the smaller particle. Very small particles($\approx$ 0.01 micron) are precipitated very rapidly by diffusion. The process is analogous to the condensation of a vapor on a cold surface. The particles most difficult to remove by filtration are those in the range 0.1 to 1.0 micron, i.e., smokes. In order to obtain efficient filtration without excessive resistance the filter must contain fibers of small diameter approaching that of the particles themselves.

18.7 BULK DENSITY OF AEROSOLS

It will be apparent from reference to Table 1 that the increase in density of the air due to the presence of an aerosol cannot be very great unless (1) the number of particles per cubic centimeter is very large, or (2) the particle size is very large. If the number of particles per cubic centimeter is large, however, the particle size will increase rapidly so that the second condition is actually the only one under which a considerable mass of aerosol can be present. If the particle size is very large, the particles will fall so rapidly under the force of gravity that the aerosol concentration cannot persist. If a high concentration of aerosol particles of 10 microns diameter could be produced, a very great increase in the bulk density of the air would result, but there is no simple method of doing this. In general, therefore, the density of an aerosol cloud does not differ greatly from that of the air itself.

18.8 OPTICAL PROPERTIES

Lord Rayleigh called attention to the very important optical properties of finely dispersed particles in his theory of the blue color of the sky. The theory of optical behavior is still obscure for opaque or reflecting particles but for transparent spheres such as oil drops the behavior is now well understood (see Chapter 21). The maximum scattering effects are obtained when the particle size approximates the wavelength of the light being scattered. The greatest scattering is in the forward direction and the maximum polarization is at right angles to the incident light. It is entirely a coincidence that the particle size which gives the greatest stability against precipitation and filtration lies in the range which gives the maximum scattering for visible light.

18.9 SMOKE SCREENS

Smoke screens composed of small drops of transparent liquids actually have greater obscuring power than those of opaque particles. The reason for this is that the transparent drop transmits a background of light which makes it difficult for the observer to distinguish inconspicuous objects. This effect is particularly important when the observer is facing the sun so that the forward scattering causes a glare.

Chapter 19

STABILITY OF AEROSOLS AND BEHAVIOR OF AEROSOL PARTICLES

By *David Sinclair*

19.1 DEFINITIONS

An aerosol is an assemblage of small particles, solid or liquid, suspended in air. By small particle is meant a particle with a radius less than about 50 microns. The usual range of particle radii in aerosols is from 0.1 to 10 microns, although particles as small as 0.01 micron may be encountered.

Aerosol is the generic term for dust, smoke, fog, and haze. Dust is commonly thought of as solid particles of any material blown up by the wind, smoke as solid particles of ash or carbon resulting from fires, and fog as water droplets. These definitions are satisfactory for natural aerosols. For artificial aerosols, a smoke is defined as an aerosol of solid particles, and fog is defined to include droplets of any liquid such as water, oil or acid.

The different types of aerosol frequently overlap. Carbon may produce a smoke or a dust. Tobacco smoke is very hygroscopic and consists chiefly of water droplets. When fresh, stearic acid aerosol is a fog of supercooled droplets, which slowly change to a smoke of crystal particles. Haze may be composed of fine particles from any source.

19.2 RANGE OF PARTICLE SIZE

The range of particle sizes in the various types of aerosol is considerable. Dust may range from fine particles of 0.1 micron radius or less, which produce haze, to sandstorms having large particles beyond the range considered to be aerosols. Smoke is often composed of extremely fine primary particles which have coagulated to form groups (see Figures 1 and 2 in Chapter 18, 1 and 2 in Chapter 22). Carbon smoke is composed of small primaries about 0.01 micron radius which coagulate into long irregular filaments that may reach several microns in length (see Figure 3, Chapter 18). Screening oil for droplets should be about 0.3 micron radius for maximum screening. Water fog droplets are much larger, ranging from 4 to 40 microns in radius.

19.3 STABILITY

The stability of an aerosol is determined by a number of factors. The individual particles may move about under the influence of several different forces: (1) Brownian movement, which consists of random oscillations and rotations causing coagulation, accompanied by drift which results in diffusion to any solid object such as the walls of a containing vessel or the ground; (2) settling under gravity; (3) thermal forces, causing movement of the particles toward any object colder than its surroundings; (4) electrical forces; (5) acoustical forces; and (6) centrifugal forces.

In addition, convection currents are usually present which consist of motion of large or small regions of the aerosol relative to other regions.

Finally, there may be evaporation, causing the particles to decrease in size and even disappear, and condensation which may cause the particles to increase in size until they fall out very rapidly.

Under ordinary conditions the stability of an aerosol is chiefly affected by the Brownian oscillations and by gravity settling. Owing to the Brownian oscillations the particles collide and either adhere or coalesce. If the particles are solid they adhere to form more or less loose aggregates which may be roughly spherical in shape as those for ZnO or albumin, or filamentary like carbon. If the particles are spherical droplets such as oil or water fog, they coalesce to form larger spherical droplets. As a result of this coagulation process, the number of particles per unit volume of aerosol and the number concentration decreases, and the average size of the particles increases.

Filtration of fine particles is largely a diffusion process (see Chapter 23). Otherwise, except for an aerosol of very fine and highly concentrated particles in a small containing vessel,[1] diffusion is unimportant.

The question often arises as to the efficiency of collision, i.e., what proportion of the colliding particles will adhere rather than rebound. It would be difficult to observe the process directly under the microscope, but indirect experiments indicate that the collision process is 100% efficient. In most experiments, the observed coagulation of solid particles is greater than that calculated from the simple theory, and not less, as it would be if the efficiency of collision were appreciably less than 100%. In the case of

liquid droplets it can be safely assumed that all droplets will coalesce on collision. Whytlaw-Gray [2] finds that his experiments on coagulation justify the assumption of 100% efficiency. We know of no experiments to contradict it.

Numerous attempts have been made to surface-treat solid particles,[3] or charge them electrically so that they would be less likely to adhere on collision, but no significant effect has as yet been observed. The only observed effect has been either to cause aerosol particles to disappear more rapidly, or to cause the particles in powder form to adhere less tightly, thus making them more easily dispersed in an air jet or by explosion. In the aerosol state, the forces of adhesion are always greater than any ordinary forces of separation.

Under the force of gravity, aerosol particles settle onto any surface having a horizontal component. The large particles settle out faster than the small particles, the rate of settling being proportional to the cross-sectional area of the particle. As a result, both the number concentration and the average particle size decrease.

Because of their comparatively small size, the particles adhere to whatever type of surface they settle upon, and the efficiency is again 100% as in the case of coagulation. The forces of adhesion are greater than the ordinary forces tending to pull the particle away from the surface.

Whenever aerosol particles are found adhering to vertical or inverted surfaces, forces other than gravity must be present.

Thermal and electrical forces are more common than generally realized. Dust near steam pipes or other hot bodies is precipitated onto the neighboring walls or ceiling. Ink fog in printing plants or dust in textile mills is precipitated onto the walls or ceiling by static electrification from the rollers or other machinery. Filtration is in some cases due largely to static electrification.

Acoustical forces are also fairly common. Sound vibrations above a certain minimum frequency, depending on the particle size, increase the rate of coagulation. Intense vibrations in factory buildings may cause precipitation, particularly in pipes. Thunder claps and explosions are known to precipitate rain and dust. Air raid sirens and similar sound sources will precipitate natural and artificial water fog.

Centrifugal forces large enough to cause coagulation or precipitation are less common. Small particle aerosols will travel around bends in pipes or through constrictions (provided they are free of sharp edges) without serious precipitation. For example, a particle of 0.1 micron radius requires a centrifugal acceleration of one million times gravity to precipitate it in a centrifugal separator.[4] Much of the coagulation of small particle aerosols in pipes and ducts is attributable to thermal, electrical, or acoustical forces rather than to centrifugal forces. This is not true, however, for aerosols of large particles, i.e., radii above a few microns.

One or the other of these factors may dominate in determining the stability of an aerosol. In a natural water fog, settling is the predominant factor, as it usually is in large particle aerosols. In flue gases, which contain very large numbers of very fine particles, coagulation is very rapid at first. Later, settling becomes more important, usually after emission into the atmosphere. In the case of screening oil fogs, evaporation and wind are the important factors.

Dilute aerosols of fine solid particles that neither coagulate nor evaporate may be so stable as to persist almost indefinitely. For example, volcanic dust, which may be expelled into the air several miles above sea level and which has a particle radius of 0.3 micron, falls at the velocity of about one mile per year. This is the size of the droplets of a screening oil fog. It is the slow rate of fall of fine particles that makes it possible to maintain a smoke screen for long periods.

19.4 SETTLING OF AIRBORNE PARTICLES UNDER GRAVITY

19.4.1 Uniform Particle Size or Homogeneous Aerosols

In aerosols of uniform particle size, which may be produced in the laboratory by a method described in Chapter 20, two cases may be distinguished: (1) settling when the aerosol is completely free from convection currents, called tranquil settling, and (2) settling when the aerosol is kept stirred so that the concentration throughout the containing vessel is uniform at all times.

Tranquil Settling

In tranquil settling all the particles fall with the same velocity. The cloud will have a well-defined flat top which will be observed to fall with a constant velocity equal to that of a single particle. This is the basis of a method of measurement of the particle radius of a uniform aerosol, described in Chapter 22.

The velocity of fall in centimeters per second is given by Stokes' law [5] of fall of small spheres in a continuous viscous medium. In air

$$v = \frac{2}{9}\frac{r^2\rho g}{\eta} = 1.2 \times 10^6 \rho r^2 , \qquad (1)$$

where r is the particle radius in centimeters, ρ the particle density, η the coefficient of viscosity of the air, and g the acceleration of gravity.

This law is correct to 5% or better for spherical particles between 1 and 50 microns radius. The particles fall with a velocity less than that given by Stokes' law when they are so large [6] that $vr = \eta/\rho_1$, where ρ_1 is the density of the air. For air $\eta/\rho_1 = 0.15$ and when $r = 50\mu$, $vr = 0.15$ for particles of unit density. For such particles the velocity becomes so large that turbulence occurs, decreasing the velocity more than does the viscous drag alone.

For smaller particles whose size is comparable with the mean free path of the air molecules, a correction must be applied to compensate for the tendency of the particles to "slip" between the air molecules, and thus move faster than predicted by Stokes' law. This correction has been calculated from Cunningham's equation [5] and it was found that the true radius is given quite accurately by subtracting 0.04 micron from the Stokes radius (in microns), for all radii between 2 and 0.1 microns.

For still smaller particles the correction is much larger. However, the velocity of fall of particles below 0.1 micron is so small that it is extremely difficult if not impossible to make observations of their settling velocity.

Stokes' law applies strictly only to spherical particles. Millikan [7] has shown, however, that the law holds quite well for particles whose shape is somewhat different from spherical.

Stirred Settling

In stirred settling the motion of the particles is complicated by random convection currents. Except for very large particles or violent stirring there is little or no impingement on the walls or ceiling. Nearly all the particles eventually settle on the floor.

The horizontal components of convection current have no effect on the velocity of fall. Since the upward convection currents will, on the average, exactly compensate for the downward convection currents they also have no effect on the velocity of fall. The convection currents merely serve to keep the concentration uniform throughout the containing vessel. The result is that the concentration continuously decreases as the settling continues so that the amount of aerosol settling out per unit of time continuously decreases.

The number of particles dn that settle out during a small interval of time dt is proportional to the number concentration n at the time t. The fraction of particles having velocity of fall v that settle out of a rectangular box of height h in time dt is

$$\frac{v}{h}dt = -\frac{dn}{n} .$$

By integrating this equation we find that

$$n = n_0 e^{-vt/h} , \qquad (2)$$

where n_0 is the initial concentration in the box. Thus the rate of settling (in terms of the number of particles per second), as well as the number concentration, decreases exponentially with time.

19.4.2 Heterogeneous Aerosols

In ordinary aerosols, composed of particles of many sizes, the settling process is more difficult to analyze. Again the two cases of tranquil and stirred settling will be considered separately.

Tranquil Settling

In tranquil settling, a differential separation according to size will occur, which may be analyzed as follows. Suppose at time $t = 0$ the concentration is uniform throughout the containing vessel and no convection currents are present. The particles of radius r will begin falling with the constant velocity v_r corresponding to that radius, and will continue to fall with that velocity independent of larger or smaller particles.

Consider a layer in the aerosol at a height x below the top of a containing vessel. At a time $t_1 = x/v_1$ there will be no particles in or above this layer, of radius greater than r_1. At a greater time $t_2 = x/v_2$, there will be no particles in or above this layer of radius greater than r_2, where r_2 is less than r_1. Consequently, observation of the decrease in number concentration at a height x, during the time interval $t_2 - t_1$ will give the number of particles having velocities of fall between v_2 and v_1, or radii between r_2 and r_1, given by Stokes' law.

This is the principle of the differential settler, described in Chapter 22, in which the decrease in number concentration is measured by the decrease in scattered light.

STIRRED SETTLING

The analysis of stirred settling of heterogeneous aerosols is more complicated. Each group of particles of radius r will settle exponentially, at a rate given by equation (2). The following discussion is based on the assumption that the particles have a logarithmic probability distribution.

Most natural distribution curves are found to be skewed from the symmetrical probability distribution. The number at larger sizes decreases more slowly than at smaller sizes in such a way that the distribution curve is made symmetrical when the number at a given size is plotted against the logarithm of the size.[8,9] This type of distribution has been found approximately in the thermally generated smokes produced in the laboratory (see Chapter 20).

One can characterize a given physical property of a heterogeneous aerosol, such as particulate volume or cross-sectional area, by an average diameter. For example, the total cross-sectional area of N spherical particles is $\frac{1}{4}\pi N d_2^2$, where

$$d_2 = \sqrt{\sum(nd^2)/\sum n}$$

is the diameter of the sphere having the average area; and the total volume of these N particles is $\frac{1}{6}\pi N d_3^3$, where

$$d_3 = \sqrt[3]{\sum(nd^3)/\sum n}$$

is the diameter of the sphere having the average volume.

If the aerosol has a logarithmic probability distribution of sizes, the number of particles per cubic centimeter having diameter d is:

$$n_d = \frac{N}{\log \sigma_g \sqrt{2\pi}} \exp\left[-\frac{(\log d - \log d_g)^2}{2 \log^2 \sigma_g}\right]. \quad (3)$$

Here N is the total number per cubic centimeter of particles of all sizes, d_g is the geometric mean diameter, i.e.,

$$\log d_g = \frac{\sum(n \log d)}{N},$$

which is equal to the number median diameter in this type of distribution and σ_g is the geometric standard deviation, i.e.,

$$\log \sigma_g = \sqrt{\frac{\sum(n \log d - n \log d_g)^2}{N}}.$$

It follows that

$$d_2^2 = \frac{\sum(n_d d^2)}{N} = \frac{1}{\log \sigma_g \sqrt{2\pi}} \int_0^\infty d^2 \exp\left[-\frac{(\log d - \log d_g)^2}{2 \log^2 \sigma_g}\right] \delta \log d, \quad (4)$$

with similar expressions for d_3, d_4, d_m. These equations have been integrated [9] and it is found that, in general,

$$\log d_m^n = n \log d_g + 2.303 \frac{nm}{2} \log^2 \sigma_g. \quad (5)$$

At time $t = 0$, when the aerosol is formed, the number of particles per cubic centimeter having diameters between $\log d$ and $\log d + \delta \log d$ is $n_d \delta \log d$. Therefore the initial total cross-sectional area per cubic centimeter of particles is:

$$C_0 = \frac{\pi}{4} \int_0^\infty d^2 n_d \delta \log d = \frac{\pi}{4} N_0 d_2^2. \quad (6)$$

Similarly the initial mass concentration in grams per cubic centimeter is:

$$M_0 = \frac{\pi}{6} \rho \int_0^\infty d^3 n_d \delta \log d = \frac{\pi}{6} N_0 \rho d_3^3. \quad (7)$$

Due to stirred settling, the mass concentration and cross section per cubic centimeter decrease exponentially with time according to equation (2). Therefore, at time t:

$$C_t = \frac{\pi}{4} \int_0^\infty d^2 n_d \exp\left(-\frac{v_d t}{h}\right) \delta \log d, \quad (8)$$

and

$$M_t = \frac{\pi}{6} \rho \int_0^\infty d^3 n_d \exp\left(-\frac{v_d t}{h}\right) \delta \log d. \quad (9)$$

In Stokes, settling [equation (1)] the velocity v_d in centimeters per second is

$$v_d = 3.0 \times 10^5 \rho d^2. \quad (10)$$

Taking the logarithm (to the base 10) of C and differentiating with respect to t, we obtain on substituting the value of v_d given by equation (10):

$$-\frac{d}{dt} \log C_t = 1.3 \times 10^5 \frac{\rho}{h} \cdot \frac{\int_0^\infty d^4 n_d \exp\left(-\frac{v_d t}{h}\right) \delta \log d}{\int_0^\infty d^2 n_d \exp\left(-\frac{v_d t}{h}\right) \delta \log d}. \quad (11)$$

For time t, small compared to h/v, equation (11) becomes:

$$-\frac{d}{dt} \log C_t = 1.3 \times 10^5 \frac{\rho}{h} \frac{\int_0^\infty d^4 n_d \delta \log d}{\int_0^\infty d^2 n_d \delta \log d}, \quad (12)$$

or

$$-\frac{d}{dt} \log C_t = 1.3 \times 10^5 \frac{\rho}{h} \frac{d_4^4}{d_2^2}. \quad (13)$$

Similarly:

$$-\frac{d}{dt}\log M_t = 1.3 \times 10^5 \frac{\rho}{h}\frac{d_5^5}{d_3^3}. \qquad (14)$$

Making use of equation (5), we find that equations (13) and (14) become:

$$-\frac{d}{dt}\log C_t = 1.3 \times 10^5 \frac{\rho}{h} d_6^2, \qquad (15)$$

and

$$-\frac{d}{dt}\log M_t = 1.3 \times 10^5 \frac{\rho}{h} d_8^2. \qquad (16)$$

It can be readily shown [10] that d_6 is the median weight diameter, which is equal to the geometric mean weight diameter in a logarithmic probability distribution. Consequently, when the particle density is known, the median weight diameter can be obtained by measurement of the decrease in cross section per cubic centimeter. Measurement of the decrease of mass concentration will yield d_8.

By substituting the values of d_6 and d_8 into equation (5), the number median diameter d_g, and the geometric standard deviation σ_g, may be calculated. By substituting the values of d_g and σ_g into equation (3), the particle size number distribution curve may be calculated.

This is the basis of a method of particle size distribution measurement described in Chapter 22, in which the geometric cross section is obtained by measuring the scattering cross section.

19.5 BROWNIAN MOTION. COAGULATION

19.5.1 Brownian Motion

In the preceding discussion it was assumed that coagulation and the other effects of Brownian motion were negligible. Due to the random Brownian motion, the top of a tranquil settling cloud of uniform particles will become blurred. Similarly, the upper boundary of the region of occurrence of particles of radius r in differential settling of nonuniform smoke will be spread vertically. This effect is unimportant except for very small particle sizes.

According to Einstein's [11] and Smoluchowski's equation of Brownian movement, the average displacement $\bar{x}$, in a given direction of a spherical particle of radius r in air in the time t, is

$$x = \sqrt{\frac{RT}{N}\frac{t}{3\pi\eta r}} = 4.8 \times 10^{-6}\sqrt{\frac{t}{r}}\ \text{cm} \qquad (17)$$

at $T = 293$ K. For a particle of radius 0.2 micron, in 1 hr $\bar{x} = 6.4 \times 10^{-2}$ cm, or slightly over ½ mm.

If this displacement is taken to be upward, then during the same time other particles will move an equal distance downward, so that after 1 hr the top of a cloud of uniform particles falling in still air will be spread vertically over a distance of about 1¼ mm. During this same time the whole cloud would have fallen through a distance, given by the Stokes-Cunningham equation of fall, of 2.5 cm.

The spread of 1¼ mm in 2.5 cm corresponds to a particle size spread of 2½%. This is considerably less than the spread of particle size in the most uniform aerosols.

19.5.2 Law of Atmosphere

Since the particles of an aerosol are in constant random motion, they exert a pressure just as do the molecules of a gas. Due to gravity, the pressure and particle concentration, i.e., the density of the aerosol, will ultimately vary with height according to the law of atmosphere: [12]

$$n_h = ne^{-mgh/KT} = ne^{-mh \times 2.46 \times 10^{16}}, \qquad (18)$$

when $T = 293$ K. Here n_h is the number concentration at a height h above the region where the concentration is n, and m is the mass of a particle.

As the aerosol particles fall under the action of gravity, and diffuse due to Brownian motion, the cloud approaches a concentration gradient given by equation (18). The time required to reach this concentration gradient decreases with the size of the particle, according to equation (17). Due to the settling and adhering of the particles onto the floor, the magnitude of the concentration at any point will finally decrease to zero, although the rate of disappearance is retarded by the Brownian movement.

It is seen that the concentration gradient increases rapidly with particle size. For example, particles of unit density of 0.01 micron radius will approach a concentration gradient of 10% per centimeter. For such particles the rate of diffusion is approximately equal to the rate of fall. For particles of 0.03 micron the final gradient is 90% per centimeter.

Above this size the final gradient is so large as to be practically equivalent to complete settling. Such sizes are well below the limit of usefulness of settling methods. Thus the law of atmosphere has no practical significance in aerosols of particle size greater than 0.05 micron in radius.

Perrin [12] found considerable effect in hydrosols for

particles of about 0.5 micron radius. Due to the buoyancy of the water, the concentration gradient is much less than in air.

19.5.3 Coagulation in a Homogeneous Aerosol

It has been found experimentally that due to coagulation alone the particle concentration in a uniform aerosol varies inversely with the time [13] that is:

$$\frac{1}{n} - \frac{1}{n_0} = \mathcal{K}t, \tag{19}$$

where n_0 is the initial particle concentration, and $\mathcal{K}$ is the coagulation constant. The differential equation of this process is evidently:

$$-\frac{dn}{dt} = \mathcal{K}n^2 \tag{20}$$

showing that the rate of coagulation is proportional to the square of the concentration.

According to the theory of Smoluchowski [13] $\mathcal{K}$ is equal to $4kT/3\eta = 3.0 \times 10^{-10}$ cc per sec in air at $T = 293$ K. Thus the rate of coagulation is independent of particle size. The equation is, of course, true only during the initial stages of coagulation before the process has introduced appreciable nonuniformity of particle size.

The coagulation equation has been tested experimentally by Whytlaw-Gray [13] who obtained good agreement with the theory when using approximately uniform particle size aerosols.

This equation holds only for particles that are large compared to the mean free path l. For smaller particles, the Cunningham correction must be applied. Equation (20) then becomes [13]

$$-\frac{dn}{dt} = \mathcal{K}\left(1 + \frac{0.9l}{r}\right)n^2 . \tag{21}$$

In air at room temperature, the mean free path $l = 10^{-5}$ cm. Consequently, due to the Cunningham correction 1 micron radius particles coagulate 8% faster, and 0.1 micron radius particles 88% faster than 10 micron radius particles.

The rate of coagulation at ordinary concentrations is quite low. For example, rewriting equation (20) in terms of the per cent coagulation per hour, gives:

$$-100\frac{dn}{n} = 1.08 \times 10^{-4}n . \tag{22}$$

Taking $n = 10^5$ (the concentration of a screening oil fog of 133-ft visibility) it is seen that approximately 11% of the particles coagulate per hour. A concentration of 10^5 particles per cubic centimeter is also frequently encountered in the laboratory. Due to the Cunningham correction, the rate for 1 and 0.1 micron particles would be increased to 12 and 21% respectively.

19.5.4 Coagulation and Stirred Settling Combined

Elementary Theory

The calculation of the rate of disappearance of particles due to both coagulation and settling is more complicated.

In the early stages of the life of a stirred uniform particle size aerosol the decrease of particle concentration is given approximately by adding equation (20) to the differential equation of equation (2). That is:

$$-\frac{dn}{dt} = \mathcal{K}n^2 + \frac{v}{h}n . \tag{23}$$

The solution of this equation is

$$\frac{1}{n} = -\frac{\mathcal{K}h}{v} + \left(\frac{\mathcal{K}h}{v} + \frac{1}{n_0}\right)e^{-vt/h} . \tag{24}$$

For times short compared to h/v, $e^{-vt/h} = 1 + vt/h$ so that equation (24) becomes

$$\frac{1}{n} = \frac{1}{n_0} + \left(\mathcal{K} + \frac{v}{h}\right)t . \tag{25}$$

For particles of 1 μ radius when $h = 100$ cm, $h/v = 10^4$ sec. Therefore equation (25) is reasonably correct for a period of about 15 min provided the concentration is not much over 10^5 per cubic centimeter.

If $1/n$ is plotted against time a straight line will be obtained having the slope $\mathcal{K} + v/h$ and the intercept $1/n_0$. Thus if $\mathcal{K}$ is known r may be calculated, and conversely.

This is the basis of a method of particle size measurement, described in Chapter 22, in which n is measured by measuring the intensity of light transmitted by the aerosol.

General Equation

The general equation of coagulation of a heterogeneous aerosol in stirred settling was derived by Goldman.[14] It was assumed that the aerosol is composed of spherical fog droplets which coalesce on collision to form larger spherical fog droplets.

Let the distribution of particle size be given by $dn(r) = n(r)dr$ = number of particles between r and $r + dr$. Then $\int_0^\infty n(r)dr = N$ = total concentration.

Since the distribution changes with time, $n(r) = n(r,t)$. The total concentration N does not depend upon r, so that $N = N(t)$.

The Smoluchowski expression for the number of collisions per second between particles of radius r_1 and r_2 in a heterogeneous smoke is:

$$\nu(r_1,r_2) = 4\pi kT[w(r_1) + w(r_2)](r_1+r_2)\cdot n(r_1)dr_1n(r_2)dr_2 \quad (26)$$

$w(r)$ is the mobility of the particle, given by the Stokes-Cunningham law, as:

$$w(r) = \frac{r+\alpha}{6\pi\eta r^2}, \quad (27)$$

where: $\alpha = Al$; A = constant; l = mean free path of air molecule; η = viscosity of air.

Let $\mathcal{K}_0 = (4/3)(kT/\eta)$, the coagulation constant for large particles, and let

$$\phi(r_1,r_2) = \left(\frac{r_1+\alpha}{r_1^2} + \frac{r_2+\alpha}{r_2^2}\right)(r_1+r_2). \quad (28)$$

Then

$$\nu(r_1,r_2) = \frac{\mathcal{K}_0}{2}\phi(r_1,r_2)n(r_1)dr_1n(r_2)dr_2. \quad (29)$$

This is the general equation of coagulation[15] of which equation (21) is a special case.

The number of particles of radius r settling out onto the floor per second [see equation (2)] is

$$\nu(r) = \frac{v}{h}n(r)dr. \quad (30)$$

h is the height of a rectangular box, or the ratio of the volume to the floor area, v is the Stokes-Cunningham velocity of fall:

$$v = mgw(r), \quad (31)$$

where

$$m = \frac{4}{3}\pi r^3\rho.$$

Let

$$u = \frac{2\rho gr}{9\eta h}(r+\alpha). \quad (32)$$

Then

$$\nu(r) = u(r)n(r)dr. \quad (33)$$

At each collision with one another the particles are destroyed as such, but a new particle is formed by coalescence having a radius corresponding to the sum of the masses of the two original particles. Hence the total rate of change of particles of radius r is:

$$\frac{\partial}{\partial t}n(r)dr = -\int_{x=0}^{\infty}\nu(r,x) + \frac{1}{2}\int_{x^3+y^3=r^3}^{\infty}\nu(x,y) - u(r)n(r)dr, \quad (34)$$

or

$$\frac{\partial n(r,t)}{\partial t} = -\frac{\mathcal{K}_0}{2}\int_0^\infty \phi(r,x)n(r,t)n(x,t)dx + \frac{\mathcal{K}_0}{4}\int_{x^3+y^3=r^3}^{\infty}\phi(x,y)n(x,t)n(y,t)\frac{dy}{dr}dx - u(r)n(r,t). \quad (35)$$

In the second integral the range of x is from 0 to r, and y is determined by the equation $y^3 = r^3 - x^3$. This equation expresses the fact that, in coalescence, the volumes add.

The above is the fundamental equation whose solution gives the number of particles of any size at any time when a given initial distribution is placed in the box.

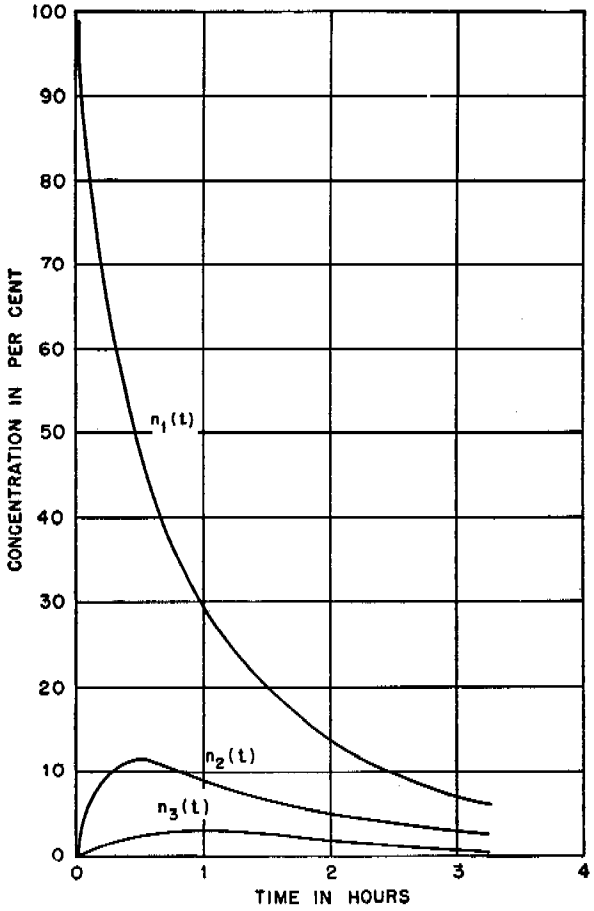


FIGURE 1. Coagulation and settling in stirred homogeneous aerosol.

This is a nonlinear integro-differential equation whose solution has been obtained in certain special cases,[16] namely: in an initially homogeneous aerosol when either the coagulation or the settling is predominant. Since the equations are rather complicated they will not be given here.

Figure 1 shows a numerical solution for a particular case of the differential equations derived from equation (35). The smoke was initially homogeneous, of radius $r_1 = 0.83$ micron, and concentration $n_1 = 5.8 \times 10^5$ per cubic centimeter. Terms $n_1(t)$, $n_2(t)$, and $n_3(t)$ are the relative number of particles of radii r_1, $\sqrt[3]{2}r_1$, and $\sqrt[3]{3}r_1$ present after time t.

19.6 DEPOSITION IN CENTRIFUGAL FIELDS

A particle in a field of force of acceleration a, will move with a terminal velocity v given by Stokes' law [equation (1)] as follows:

$$v = \frac{2}{9}\frac{r^2\rho a}{\eta}. \tag{36}$$

As stated in Section 19.4.1, this equation will hold as long as $vr < \eta/\rho_1 = 0.15$ for air.

When $vr \gg 0.15$ the motion becomes turbulent and the terminal velocity of the particle (relative to the air) is given by Newton's law for bodies in turbulent motion:

$$v = \sqrt{\frac{8r\rho a}{3\rho_1}}. \tag{37}$$

Here ρ is the density of the particle and ρ_1 is the density of the air. It is seen that the velocity is no longer dependent upon the viscosity of air. Allen [17] found that this equation holds when vr is about 100 times greater than η/ρ_1.

If aerosol particles are given a sufficiently high centrifugal acceleration by causing a sudden change in the direction of flow, they can be precipitated out of the aerosol. Various forms of such precipitators have been constructed, such as centrifugal separators, impingers or impactors. They may be very effective for large particles but are frequently ineffective for small particles.

The particles may be precipitated by directing a jet of aerosol against a collecting surface. In this type of precipitator the jet must have a high velocity and the change of direction must take place in a small distance in order that the acceleration may be high. Consequently the length of time during which the particle is in the high centrifugal field must of necessity be very small.

The centrifugal acceleration $a = V^2/R$, where R is the radius of curvature of the path of the particle, and V is the jet velocity.

Substituting the value of the acceleration a, into equation (37) yields the following value for r, the minimum radius of the particle which will be precipitated:

$$r = \frac{3}{8}\frac{\rho_1}{\rho}\frac{v^2}{V^2}R = 4.5 \times 10^{-4}\left(\frac{v}{V}\right)^2 R \tag{38}$$

for a particle of unit density in air.

If we replace v by d_p/t, where d_p is the distance the particle must travel *relative to the jet of aerosol* in order to reach the collector during the time t, and if we replace V by d_a/t, where d_a is the distance traveled by the jet of aerosol during the same time, we obtain:

$$r = 4.5 \times 10^{-4}\left(\frac{d_p}{d_a}\right)^2 R. \tag{39}$$

Consequently, if R or the ratio d_p/d_a or both are small, small particles will be precipitated.

In the impinger or impactor, R is made small by placing the end of the jet tube near the collecting plate.

The ratio d_p/d_a may be made small by passing the aerosol through a long spiral tube of moderately small radius. This results in a considerable separation of the particles according to size, the larger particles being, of course, deposited first. The use of this type of separator is described by Abramson.[18]

19.7 ELECTRICAL EFFECTS. PRECIPITATION

19.7.1 Charge on Homogeneous Smoke Particles

The electrical charge on the particles of homogeneous smoke was investigated. The homogeneous oleic acid fog produced in the usual way with electric spark (Chapter 20) is electrically almost neutral.[19] Only 5% of the particles are charged, mainly positive, and with small numbers of electronic charges (1 to 4) per particle. These observations were made in a Millikan oil drop apparatus using an electrical intensity of 500 v per cm.

19.7.2 Unipolar Smoke

Unipolar charged smokes are produced by a direct current corona discharge from a needle point at a potential of 10,000 v. This potential is obtainable from a 2V3G RCA rectifier tube. The needle point was placed in the center of a 2-l, three-neck flask through which the electrically neutral homogeneous smoke was passed. The other electrode consisted of an aluminum strip placed inside on the bottom of the flask. The characteristics of the negative unipolar charged smoke, obtained when the needle point was negative, are as follows:

1. About 99% of the droplets are charged.
2. Droplet charges are high, 25 to 50 electrons per droplet. These charges were observed in a Millikan oil drop apparatus using an electrical intensity of 90 v per cm.
3. Dilution with air from 1,000 to 32 μg per l has no significant effect on the droplet charge.
4. High humidities have no effect on the droplet charge.
5. The mass concentration of the neutral smoke may be decreased by as much as 65% due to passage through the corona discharge.
6. The number of spectra (Chapter 21) in the Tyndall beam as counted by the naked eye may be decreased by ½ to 1 spectrum on passage between the electrodes.
7. This smoke disappears with great rapidity when introduced into a flask or other chamber.

19.8 MOVEMENT OF PARTICLES IN A THERMAL GRADIENT

Aerosol particles in a temperature gradient are acted on by a force directly proportional to the temperature gradient,[20] and inversely proportional to the absolute temperature. When introduced into a region between two bodies at different temperatures, particles will move toward the colder body and deposit on it.

The method of calculation of the force acting upon a spherical particle in a thermal force field depends upon the relative values of the particle radius r, and the mean free path l of the gas molecules.[21] When $r \gg l$ the force is proportional to $(l^2rp/T)(dT/dx)$, and when $r \leq l$ the force is proportional to $(lr^2p/T) \cdot (dT/dx)$, where p is the pressure and T the absolute temperature.

It was found[21] that when $r > 0.5$ micron the velocity is independent of particle size. In the region between 0.05 micron and 0.5 micron, there is a twofold decrease in velocity with increasing particle radius (Figure 2). Hence there exists a definite possibility in this range of using a thermal gradient for the separation of smoke particles according to size, and thence obtaining the size distribution.

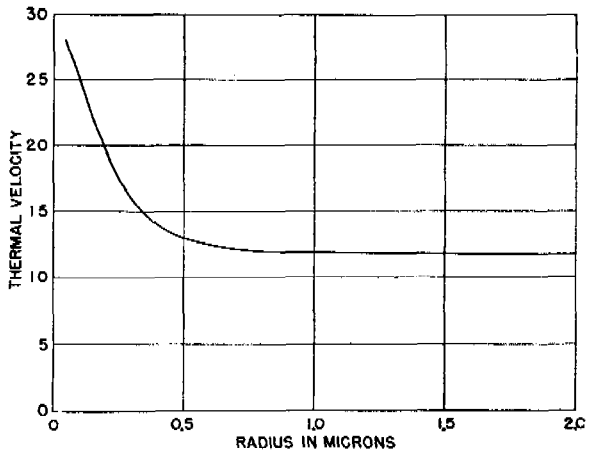


FIGURE 2. Thermal velocity vs particle radius.

Various types of thermal separators have been discussed elsewhere.[21,22] Because of the limited size range of applicability, this method of size distribution measurement has not as yet been developed experimentally.

A method of sampling smoke particles without separation according to size is described in Chapter 22.

19.9 COAGULATION BY SONIC AND SUPERSONIC VIBRATIONS

It is well known that sound of supersonic frequency and high intensity will cause the rapid coagulation of smoke. For example, Andrade[23] and Parker[24] observed the coagulation of magnesium oxide smoke using frequencies of 22,000 c, and Brandt and Hiedemann[25] coagulated tobacco and ammonium chloride smoke using frequencies of 10,000 to 20,000 c. St. Clair[26] found that a frequency as low as 4,000 c at an intensity of 0.2 w per sq cm (153 db) caused rapid coagulation of ammonium chloride smoke of 1 micron radius.

Large particle aerosols, including natural and artificial water fogs of droplet radii from 4 to 16 microns, can be coagulated by sound of 250 to 1,000 c provided sufficient energy is generated. The available

theory of the phenomenon indicates that sound of 350 c should cause nearly as rapid coagulation of natural water fog as any higher frequency.

At such frequencies, the absorption of sound in air is negligible. At a frequency of 10,000 c, however, the sound intensity is reduced 10 db (a factor of 10) every 150 ft. At higher frequencies, the adsorption is much greater.

19.9.1 Theory

The coagulation of an aerosol by sound vibrations is due to at least three effects: (1) the motion of different sized particles relative to each other, (2) attractive forces set up between particles by the air vibrating between them, and (3) vortex motion which occurs around large particles.

These effects vary in different ways with the size and density of the particle and the frequency and intensity of the sound.

1. For supersonic frequencies in small particle aerosols and for audible frequencies in large particle aerosols, the different size particles will vibrate with different amplitudes, the smaller particles having the larger amplitude. The largest particles will have practically zero amplitude. Consequently, the velocities of the particles relative to one another will be increased and the probability of collision thereby increased.

In order to determine the dependence of the particle velocity upon frequency and particle size it is necessary to assume some law for the force on the particle moving through the gas. In an intense sound field the velocities vary from about 7 cm per sec at 120 db (10^{-4} w per sq cm) to about 2,000 cm per sec at 170 db (10 w per sq cm).

As stated above, Stokes' law holds only when $vr < \eta/\rho_1$. In a sound field, v is the velocity of vibration of the air relative to the particle. For air, $\eta = 1.81 \times 10^{-4}$ poise and $\rho_1 = 1.2 \times 10^{-3}$ g per cu m, so that $\eta/\rho_1 = 0.15$. When $r = 10$ microns and $v = 100$ cm per sec, $vr = 0.1$ so that Stokes' law is valid only for the smaller particle sizes and air velocities. When $r = 1$ micron or less, Stokes' law is valid for much higher intensities.

Koenig [27] has shown that, in general, the force depends upon the acceleration as well as the velocity. However, the approximate frequency necessary to obtain the maximum velocity of the particle relative to the air can be obtained by assuming Stokes' law to hold. According to this law, the force of resistance acting on a spherical particle of radius r, moving through a viscous medium with velocity v is $F = 6\pi\eta rv$.

On this assumption St. Clair [26] has derived the following expression for v, the amplitude of the velocity of a particle *relative to the air* in a sound field.

$$v = v_0 \frac{\omega}{\sqrt{k^2 + \omega^2}} \cdot \tag{40}$$

Here v_0 is the velocity amplitude of the sinusoidal air vibration, $\omega = 2\pi$ times the frequency and $k = (9/2)(\eta/r^2\rho)$ where ρ is the density of the particle.

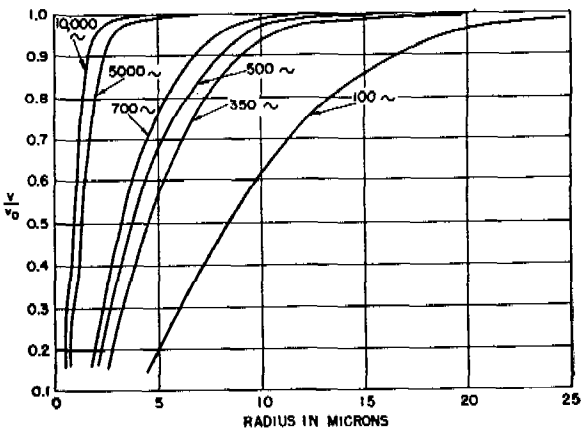


FIGURE 3. Relative velocity v/v_0, as a function of frequency and particle radius, r.

Figure 3 shows v/v_0 plotted against r for several values of the frequency. It is seen that in the neighborhood of 440 c, the relative velocity has nearly reached its maximum at a radius of 10 microns.

Various estimates [28] of the radii of natural fog droplets give the limits to be 4 to 40 microns, the large sizes predominating in radiation fogs. Although the above calculation may give only the order of magnitude of the relative velocity, it is evident that different sized particles will have different amplitudes and phases of vibration, which will increase the rate of coagulation.

It should be pointed out that this particular effect is greatest for comparatively low frequencies. Figure 3 shows that 100 c might be more effective than 440 c in a large droplet radiation fog. Droplets of 5 micron radius would have very low relative velocities and droplets of about 20 microns radius, very large relative velocities. On the other hand, at 5,000 c, all droplets above about 5 microns radius would remain motionless in the vibrating air. Smokes of particle

radii less than 1 micron would require frequencies above 5,000 c to impart different relative velocities to the particles.

2. The increased motion of the particles relative to each other appears to be of secondary importance in causing coagulation when compared to the hydrodynamic forces of attraction between two particles resulting from the motion of the air between them. These forces are greatest when the relative velocity of air and particles is greatest, which does not necessarily mean when the particle is motionless.

Due to the inertia of the particle, its vibrations are more or less out of phase with the vibration of the air. Consequently, when the relative velocity first reaches a maximum, the particle will not be standing still but will be vibrating with considerable amplitude, 180° out of phase with the air. For example, since the actual velocity amplitude u of the particle [26] is:

$$u = v_0 \frac{k}{\sqrt{k^2 + \omega^2}}, \tag{41}$$

a 10-micron particle whose relative velocity amplitude is 0.95 v_0 at 440 c has an actual velocity amplitude of 0.28 v_0.

Koenig [27] derived the following equations for the components of force between two spheres in a sound field. Suppose the particles are stationary and lie in the X–Y plane, their line of centers making an angle θ with the Y axis, and the sound vibration is in the Y direction. The force components are then:

$$X = \frac{-3\pi\rho_1 r_1^3 r_2^3 v_0^2}{2d^4} \sin\theta\,(1 - 5\cos^2\theta) \tag{42}$$

$$Y = \frac{-3\pi\rho_1 r_1^3 r_2^3 v_0^2}{2d^4} \cos\theta\,(3 - 5\cos^2\theta)\,. \tag{43}$$

Here r_1 and r_2 are the radii of the particles, d is the distance between them, ρ_1 is the density of the air, and v_0 is the velocity amplitude of the sinusoidal air vibration.

The derivation of the above equations is also given by St. Clair.[26] It is interesting to note that the same distribution of forces exists around two magnets when their axes are parallel, at distances large compared to the lengths of the magnets.[29]

For two particles of the same size whose line of centers is perpendicular to the air velocity ($\theta = \pi/2$), the resultant force is an attraction along the line of centers of magnitude:

$$X = \frac{3\pi\rho_1 r^6 v_0^2}{2d^4}\,. \tag{44}$$

When the line of centers is parallel to the air velocity ($\theta = 0$), the resultant force is a repulsion along the line of centers of magnitude:

$$Y = \frac{3\pi\rho_1 r^6 v_0^2}{d^4}\,. \tag{45}$$

These forces have been checked experimentally by Georg Thomas.[30]

Some idea of the rate of coagulation caused by the hydrodynamic forces can be obtained by integrating the equation of motion of two particles attracted by the force X. Assuming that the motion of the particles toward each other obeys Stokes' law, St. Clair [26] obtains the following expression for the time of approach of two particles, separated by a distance d, whose line of centers is perpendicular to v_0:

$$t = \frac{2}{5}\frac{\eta}{\rho_1 v_0^2}\left(\frac{d}{r}\right)^5. \tag{46}$$

If d is the average distance of separation of the droplets in a uniform fog, t is the average time for each pair of droplets to collide once, thus halving the number of droplets. At constant mass concentration, the scattering per unit mass is inversely proportional to the radius for large particles (see Chapter 21). Therefore, halving the number of particles will increase the visibility by 26% since the radius will be increased by the factor $\sqrt[3]{2} = 1.26$.

Expressing d/r in terms of c, the mass concentration in grams per cubic centimeter, we have for an aerosol of spherical particles of unit density:

$$t = \frac{0.66}{v_0^2 c^{5/3}}\,. \tag{47}$$

Thus for a given mass concentration, the time required to halve the number of particles in a uniform aerosol is independent of the particle size, or the distance between them.

This equation is based on the assumption that the concentration remains constant after coagulation, which, of course, it will not do because of precipitation of large coagulated particles. However, as discussed below, the coagulation is quite rapid, particularly for dense aerosols, so that the equation is valid for short times.

Since the average acoustic energy per cubic centimeter of air is $\frac{1}{2}\rho_1 v_0^2$, the intensity of the sound is $\frac{1}{2}\rho_1 v_0^2 V$ where V is the velocity of sound in air and is 3.44×10^4 cm per sec. Thus the time to halve the number of particles is inversely proportional to the sound intensity and to the five-thirds power of the mass concentration.

A dense water fog of 10 microns radius droplets, having a visibility of about 20 ft (99% of light scattered in 20 ft), has a concentration of about 10 g per cu m. For a fog of this concentration, t would be of the order of 300 sec at 160 db and 3×10^4 sec at 140 db.

In experiments on water fog, the observed time required to double the visibility was of the order of one hundredth the time calculated from the above theory. For example, a 4½ micron radius fog of 50 ft visibility ($c = 2$ g per cu m) gave double the visibility in about 1 min at 135 db.

This discrepancy is due in part to the assumption that d is the average distance of separation of the particles in a uniform aerosol. If the aerosol is not uniform the different sized particles will have different amplitudes and phases relative to each other, as already described. Consequently, different sized particles will frequently approach much closer than the distance d (about equal to the amplitude of the sound vibrations). Since the force of attraction varies inversely as the fourth power of the distance, the small values of d will predominate in their effect on coagulation. For instance, if a value of ½d were used in the above calculation, the time would be reduced by a factor of 32.

St. Clair [26] found the same discrepancy between the calculated and observed time in his experiments. He observed the coagulation of 1 micron radius ammonium chloride smoke by sound of 4,000 c to be 30 times faster than calculated according to the above theory.

3. The third cause of coagulation, which has not been taken into account, is the vortex motion of the air around the larger particles which are not vibrating with the air. At the higher intensities, eddy currents are set up in the air around such particles.

Andrade [31] has observed that vortex motion causes neighboring particles to be attracted or repelled depending upon their orientation relative to the sound field and their initial distance apart. He showed that vortex motion occurs around a large spherical particle in air when $vr > 0.35$. Thus 10 microns radius particles would cause vortex motion when the velocity exceeded 350 cm per sec or at about 155 db.

Andrade showed also that vortex motion is the cause of the striations in the large dust particles in a Kundt tube. The distance between the striations is, consequently, not equal to twice the amplitude of the sound vibration as might be expected from the experiments of Koenig [27] and Robinson.[32] Therefore, the sound intensity cannot be obtained from the spacing of the striations. Andrade measured the sound intensity by observing the amplitude of vibration of the 0.25-micron radius particles in tobacco smoke which vibrate with the sound amplitude of the air.

Vortex motion inhibits the hydrodynamic forces so that the Koenig equations for these forces do not apply when $vr > 0.35$. The anomalous experimental results obtained by Gorbatchev and Severnyi [33] are probably due to vortex motion. They observed the forces between two water drops, supported on separate glass threads in a wind tunnel, as well as in a "sound" field of frequency 10^{-3} c. They found the directions of the forces to be just the reverse of those given by the Koenig theory. In the wind tunnel experiments the wind velocity was 15 cm per sec and the droplet radius of the order of 0.5 mm, so that vr was of the order of 0.75. The anomalous results obtained by several other investigators have been shown by Andrade [31] to be due to vortex motion.

The results of the theory may be summarized as follows.

1. No accurate value of the absolute rate of coagulation of an aerosol by sound can be calculated from the present theory.

2. The relative rate of coagulation of uniform aerosols varies directly with the sound intensity, and inversely with the five-thirds power of the mass concentration of the aerosol.

3. Insofar as the coagulation is due to the relative motion of different sized particles, there may be an optimum frequency for which the coagulation rate of a nonuniform aerosol is a maximum.

19.9.2 Experiments

Laboratory experiments at Columbia University and field tests at Lunken Airport, Cincinnati, Ohio, have shown that sound of audible frequency (300 to 700 c) and high but practicable intensities (130 to 160 db) will dissipate natural water fog and artificial sprays having the mass concentration and particle radius found in nature.

In field tests at Lunken Airport, a radiation fog was partially cleared by four Chrysler-Bell victory sirens. The visibility was increased by the sound from 200 ft to 300 or 400 ft.

The clearing occurred in about one minute over a region 300 ft long and 75 ft wide, where the average sound intensity was 140 to 150 db at a frequency of 440 c. The height of the clearing was not measured

but, from the known intensity distribution of the sirens, probably extended about 50 ft upward. The droplet radius of this fog, measured microscopically (see Chapter 22), ranged from 4 to 16 microns and the mass concentration was about 1.0 g per cu m.

In the experiments in a Columbia University tunnel, the visibility of a continuously produced spray of 4½ microns radius droplets was increased from 35 ft to 70 ft by a 2-hp Federal Electric Company siren. The average sound intensity was 135 db at a frequency of 600 c.

In a small-scale laboratory experiment, a spray of the same droplet radius but of much higher concentration was completely dissipated in 15 sec by sound of 150 db intensity and a frequency of 500 c emitted by a loudspeaker.

The details of these and other tests are described elsewhere.[34]

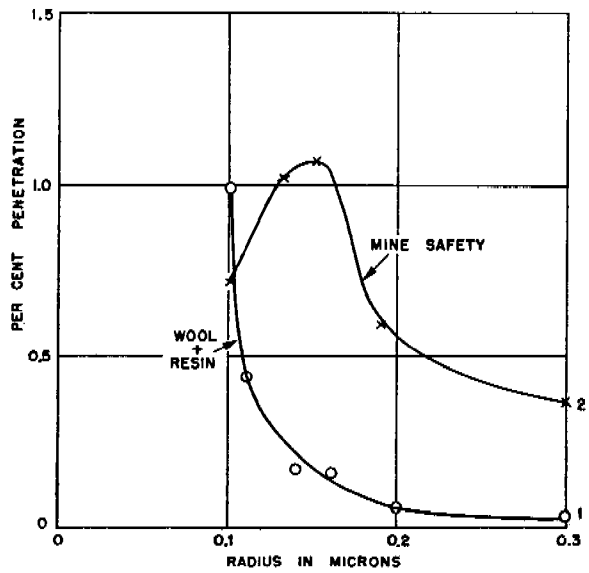


FIGURE 4. Penetration of wool-resin and Mine Safety Company canisters.

19.10 FILTRATION — GENERAL

19.10.1 Effect of Particle Size

Numerous experimental measurements[35] have shown that particles of radius about 0.17 micron penetrate most readily an ordinary type of smoke filter such as rock wool, glass wool, asbestos paper or cellulose paper (α-web). The Canadian wool-resin filter does not show this effect.

The results of some measurements are shown in Figure 4. Curve 1 shows that as the particle radius is decreased from 0.3 micron to 0.1 micron, the penetration of a wool-resin filter rises from 0.016% to 1%. Curve 2 shows a comparison series of measurements on an ordinary Mine Safety Company type of canister, for which the maximum penetration occurs at 0.15 micron radius.

19.10.2 Electrical Effects

In general, the negative unipolar smoke described in the preceding section has a negligible effect on the penetrability of filters. The optical mass-concentration meter (Chapter 22) was used to measure the penetration of a variety of filters, including a German filter paper and a Canadian wool-resin, and the penetration found to be practically the same for the unipolar as for the uncharged homogeneous smoke. However, the smoke penetration through a glass wool filter was decreased 90% or by a factor of 10. With rock wool filters, the penetration decreased 15% in one case and 36% in another.

The per cent penetration of the charged smoke as a function of time for Canadian wool-resin filters remained constant over a period of 30 min. A low smoke concentration, about 2.5 μg per l, was used in this latter test since the Canadian wool-resin is readily broken down by oleic acid.

These filter materials have only a slight effect on the electrical properties of the smoke. With filters of low penetrability, the dilute issuing smoke is mostly uncharged, with a few particles carrying comparatively small charges, whether charged or uncharged test smokes are used. When a filter of high penetrability is used (10% or larger), the electrical characteristics of the issuing smoke are practically the same as those of the entering smoke.

A detailed discussion of filtration is given in Chapter 23.

Chapter 20

FORMATION OF AEROSOLS

By *David Sinclair*

20.1 CONDENSATION METHODS

20.1.1 Condensation in Vapor Jets

AEROSOLS OF VERY UNIFORM particle size may be produced in the laboratory by slow and uniform condensation of vapor, well mixed with air, containing condensation nuclei. The size of the particles is determined by the ratio of the mass of condensable vapor to the number of nuclei. When the cooling and other pertinent factors are *carefully controlled*, it is possible to produce aerosols having a particle size which does not vary by more than 10% from the average, as shown by direct microscope measurement of the droplets.

The substance from which the smoke or fog is to be formed is contained in the *boiler*, a 2-l Pyrex flask (see Figure 1). The flask and contents are heated electrically in an asbestos board box to between 100 and 200 degrees C depending upon the substance and the particle size desired.

The condensation nuclei are formed in the *ionizer*, a 1-l Pyrex flask fitted with two electrodes sealed into standard tapered joints. The ionizer is mounted above the heater box and connected to the boiler by a standard tapered joint. The condensation nuclei are formed by a high-voltage electric spark or an electrically heated coil of wire which has been dipped in sodium chloride.

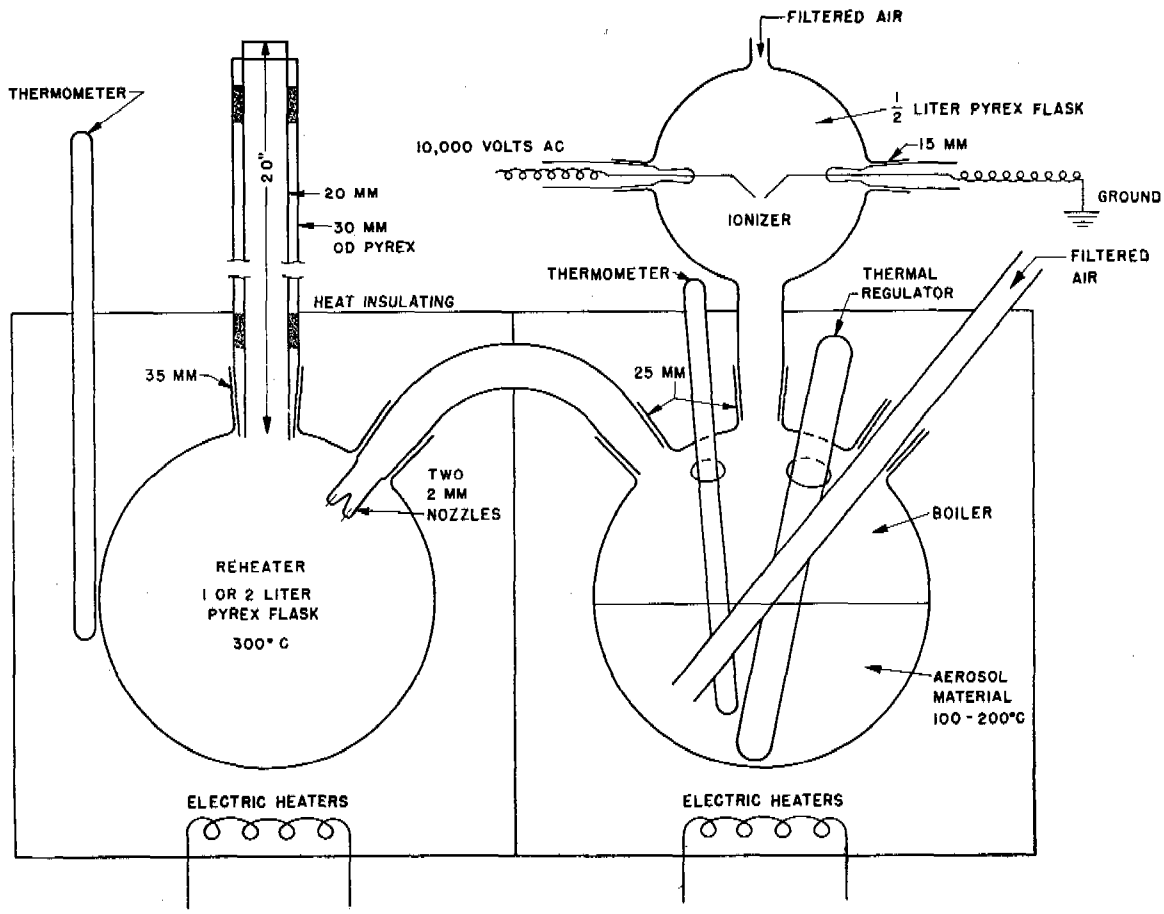


FIGURE 1. Homogeneous aerosol generator.

The *reheater* is a 2-l Pyrex flask in an adjacent asbestos box heated electrically to about 300 C. A double walled Pyrex glass chimney 20 in. long is connected to the reheater by a large standard tapered joint. The boiler and reheater are connected by a Pyrex tube having a standard tapered joint at each end. The outlet of this tube into the reheater consists of a jet having two holes of 2-mm diameter.

Smoke is produced by bubbling air through the hot liquid in the boiler, through the glass tube shown in the diagram. At the same time, air is blown in through the ionizer. The total rate of flow is usually from 1 to 4 lpm. The mixture of nuclei, spray, and vapor-laden air then passes through the two jet holes into the reheater. Here the spray is vaporized and the nuclei well mixed with the vapor.

The mixture then rises through the chimney, the vapor condensing uniformly upon the condensation nuclei. The smoke which issues from the chimney is found to be of quite uniform particle size. When the column of smoke is examined in front of a white light it is seen to be brilliantly colored, the colors varying markedly with the angle of observation.

The smoke has a high mass concentration, about 1 to 10 mg per l, depending upon the particle size. In order to avoid destroying the uniformity of particle size by coagulation, the smoke should be immediately diluted 10 or 100 times with dry, filtered air. Small tubes or jets should not be used for this purpose since turbulent flow destroys the uniformity of size.

The particle size is increased by increasing the temperature of the boiler, or by increasing the flow of air through the liquid relative to that through the ionizer, or by decreasing the rate of production of ions. A little practice with any given piece of apparatus will show the conditions that will yield the most uniform smoke of a given particle size.

The temperature can be automatically maintained constant by a thermal regulator inserted directly into the liquid or into the heater box. *The air must be dried and well filtered.* If it is not, the moisture, dust and oil fog droplets in the air from a compressor, or even a tank, will provide so many condensation nuclei that the control of particle size by the ionizer will be lost.

To produce the larger particle sizes above 1 or 2 microns radius, it is necessary to increase the proportion of vapor by bubbling the air through a porous disk beneath the liquid surface. Care must be taken to avoid decomposition of the material by excessive heating.

A substance having a range of boiling points or an impurity, particularly of higher vapor pressure, is not suitable for producing uniform smoke by this method. The different components condense at different rates in the chimney, causing nonuniformity in the particle size. A volatile impurity sometimes condenses so readily that it forms sufficient nuclei to destroy the control of size by the ionizer.

Uniform aerosols have been produced from oleic and stearic acid, triphenyl and trichresyl phosphate, rosin, menthol, ammonium chloride, lubricating oil and Aroclor. The range of particle radii is from 0.1 to 5.0 microns. Smaller sizes may be produced, but it is difficult to measure the size or uniformity. In general, the large particle aerosols are more uniform in size.

The condensation nuclei may be ionized air molecules or molecules of such compounds as NO_2, H_2, O_2, or NH_3. When a too intense, flaming spark is used, NO_2 is readily detectable by its odor and color.

The construction and operation of this generator is described more fully elsewhere.[1]

20.2 THE DISPERSAL OF PRE-GROUND SOLIDS

20.2.1 Air-Jet Dispersion

Pneumatic dispersion is capable of producing aerosols of solid particles whose size is as small as the primary size of the ground material. This method does not usually break up single particles but does tear apart aggregated particles. The method is very inefficient in that a very large volume of air is required, producing a dilute aerosol.

One form of apparatus,[2] called the *geyser* (see Figure 2) has been used to produce aerosols of lithopone, Kadox (zinc oxide), and egg albumin, of mass concentration up to 30 μg per l. Using Kadox of primary particle size 0.1 to 0.3 micron, the particles dispersed by the geyser are 0.3 to 0.5 micron on the average. Egg albumin was dispersed down to its primary particle size of 0.5 to 10 or 15 microns radius.

It is quite necessary to use well dried and filtered air for the dispersal. The water vapor and oil fog in raw air from an air compressor cause materials such as lithopone to pack into an intractable mass.

The filter and powder chamber are both made of standard 3 in. galvanized iron pipe although they have been drawn to different scales in the diagram. The connections are all made with standard ¼-in. pipe fittings, as shown.

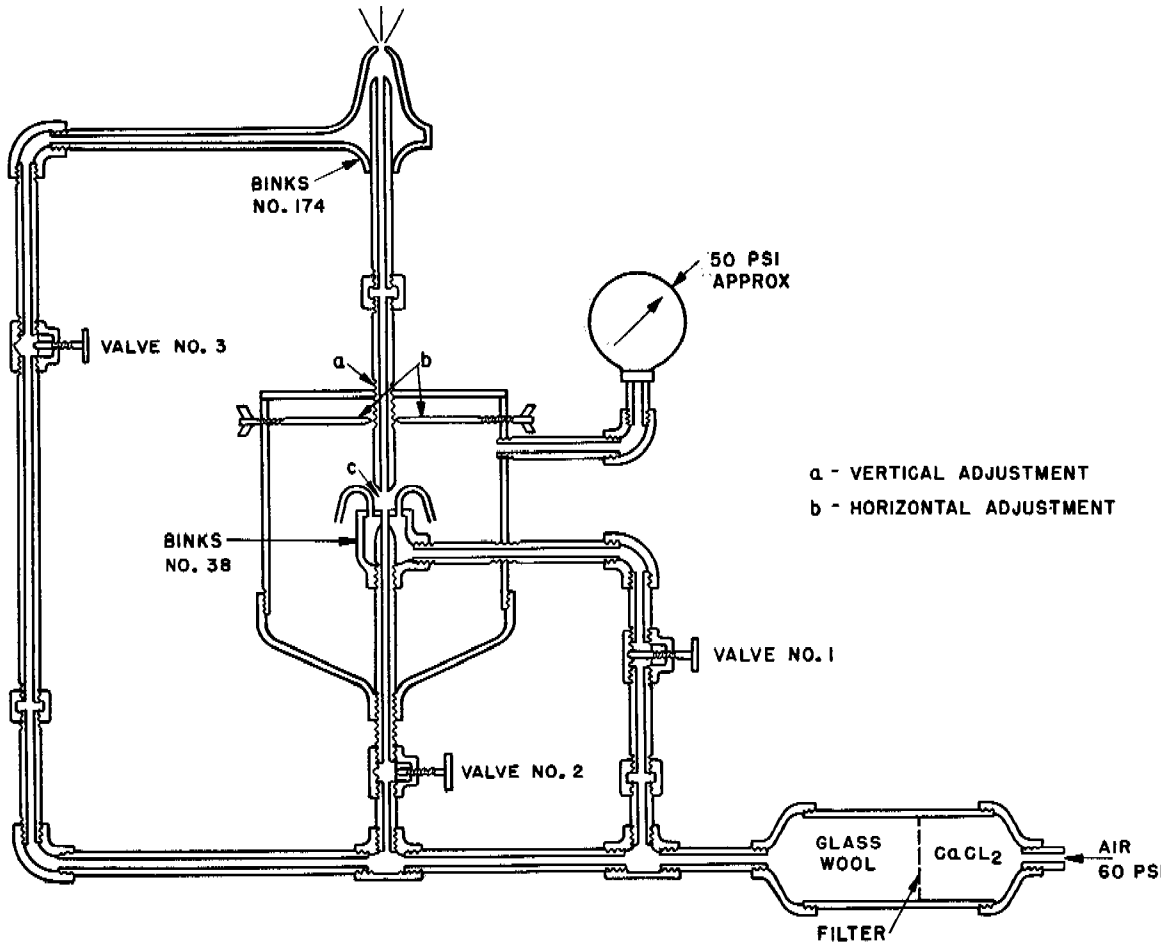


FIGURE 2. The geyser (pneumatic disperser).

Two spray nozzles of different types, made by the Binks Manufacturing Company of Chicago were adapted to this apparatus. The No. 174 nozzle, which gives the final dispersal, was altered by removing the air cap and the needle, and drilling out the central hole to $\frac{1}{16}$ in. diameter.

In order to eliminate a constriction and a right-angle bend, the hole that carried the needle adjustment was enlarged and the pipe from the powder chamber connected to this opening. The regular inlet (stamped WAT on nozzle) is closed off. With this arrangement the powder comes straight from *c* out through the No. 174 nozzle without any turns. This eliminates a tendency of the powder to collect at the turns and then break loose later in large pieces.

The Binks No. 38 nozzle was altered by removing the screw cap and soldering in its place a flat disk having a 1-mm central hole concentric with the central air outlet. All the air from this outlet flows out through the 1-mm hole. In addition, the plate has three symmetrically placed holes to which bent tubes $\frac{1}{16}$ in. ID are attached as shown in the diagram.

The air from these tubes serves to stir up the powder. Air from the central hole of the Binks No. 38 nozzle blows up through the nozzle above at *c*, which should be tapered. This air stream carries more or less of the powder-laden air with it, depending upon the adjustments *a* and *b*. The upper nozzle at *c* is a convex cone having a $\frac{1}{16}$-in. diameter hole.

The top plate of the powder chamber is sealed with a gasket and fastened with screws which are loosened slightly while the adjustments are being made. Three horizontal adjusting screws *b* are used for lateral adjustment, and adjustment at *a* is made by loosening the union directly above it and screwing the pipe up or down a small amount.

The rate of flow out of the No. 174 nozzle is about

140 lpm. Most of this air flows through valve No. 3 and is used to disperse the aggregates blown up from the chamber.

A more convenient, portable form of geyser was made by attaching a Binks 174 nozzle to a DeVilbiss-type GB flock gun. The powder is stirred in the flock gun by a thin stream of air and the concentrated aerosol dispersed by the Binks nozzle as in the above described model.

20.2.2 Gas Ejection Bomb

A bomb of 22 cc capacity was used to disperse Kadox, egg albumin and lycopodium spores in a 22-cu m room. The particle size in the Kadox aerosol was greater than obtained with the geyser. With egg albumin and lycopodium, a primary dispersion was obtained, when using a bursting pressure of 1,800 psi.[3] (See also Chapters 22 and 35.)

Chapter 21

OPTICAL PROPERTIES OF AEROSOLS

By *David Sinclair*

21.1 SCATTERING OF LIGHT BY A SINGLE SPHERICAL PARTICLE

THE SCATTERING OF LIGHT by spheres has been extensively studied, both theoretically and experimentally. In the case of transparent dielectrics, that is, nonabsorbing substances, the scattering properties have been found to provide convenient measures of particle size and size distribution.

The theory of scattering by a spherical particle was originally developed from Maxwell's equations by Gustave Mie [1] in 1908. Since that time, numerous calculations [2] have been made of the total energy, and the angular distribution of the intensity of light scattered by both transparent and absorbing particles. The derivation of the equations is given in a compact form by Stratton.[3]

Since the calculations available in the literature were incomplete, additional calculations on both absorbing and transparent particles were made by the Bureau of Standards. Most of the calculations on transparent particles have already been published.[4] The calculations on absorbing particles and additional calculations on transparent particles are described in following text.

Numerous experimental measurements have amply confirmed the Mie theory, with one exception, described in the discussion that follows.

For transparent, spherical particles that are small compared to the wavelength of light, the Mie theory is in complete agreement with the more elementary theory of Rayleigh,[5] derived to account for the blue of the sky. According to this theory the total amount of light of wavelength λ scattered by a small sphere of radius r per unit intensity of illumination (unit energy per unit area) is

$$S = 24\pi^3 \left(\frac{m^2 - 1}{m^2 + 2}\right) \frac{V^2}{\lambda^4} . \qquad (1)$$

Here V is the volume of a small particle, and m is its refractive index relative to that of air ($= 1$). S is thus the effective scattering area of one particle.

This equation holds for extremely small particles such as air molecules. For such sizes the particles need not be spherical. The equation holds for spherical particles when $r < 0.1\lambda$. It is seen that the total scattered energy varies directly as the sixth power of the radius, and inversely as the fourth power of the wavelength, so that blue light is scattered much more than red.

Consequently, the diffuse light of the sky is blue when free of haze. However, when the sun is near the horizon the sky may exhibit other colors even when free of haze as explained in the following text.

When the particle is illuminated with unpolarized light, the intensity scattered at an angle γ to the incident light is

$$I_\gamma = \frac{9\pi^2}{2R^2} \left(\frac{m^2 - 1}{m^2 + 2}\right)^2 \frac{V^2}{\lambda^4} (1 + \cos^2 \gamma) . \qquad (2)$$

R is the distance from the particle to the point of observation. This equation holds only when R is very large compared to the radius of the particle. The angle γ is the angle between the direction of propagation of the scattered light and the *reversed* direction of propagation of the incident light.

When observing at right angles to the incident light, i.e., when $\gamma = 90°$, the scattered light is plane-polarized with the light vibrations perpendicular to the plane of observation. The plane of observation is the plane containing the direction of observation and the incident beam.

If a very small particle is illuminated by polarized light the intensity of light scattered at an angle ψ is [4]

$$I_\psi = \frac{9\pi^2}{R^2} \left(\frac{m^2 - 1}{m^2 + 2}\right)^2 \frac{V^2}{\lambda^4} \sin^2 \psi . \qquad (3)$$

Here ψ is the angle between the direction of observation and the direction of the electric vibrations in the incident polarized light. The scattered light is plane-polarized, no matter what the direction of observation.[4]

As the particle radius increases to about the same size as the wavelength of the light, the scattering becomes a very complicated function of the radius, wavelength, and refractive index. The Mie theory shows that the total scattering by one spherical particle per unit intensity, is:

$$S = \frac{\lambda^2}{2\pi} \sum_{\nu=1}^{\infty} \left(\frac{a_\nu^2 + p_\nu^2}{2\nu + 1}\right). \qquad (4)$$

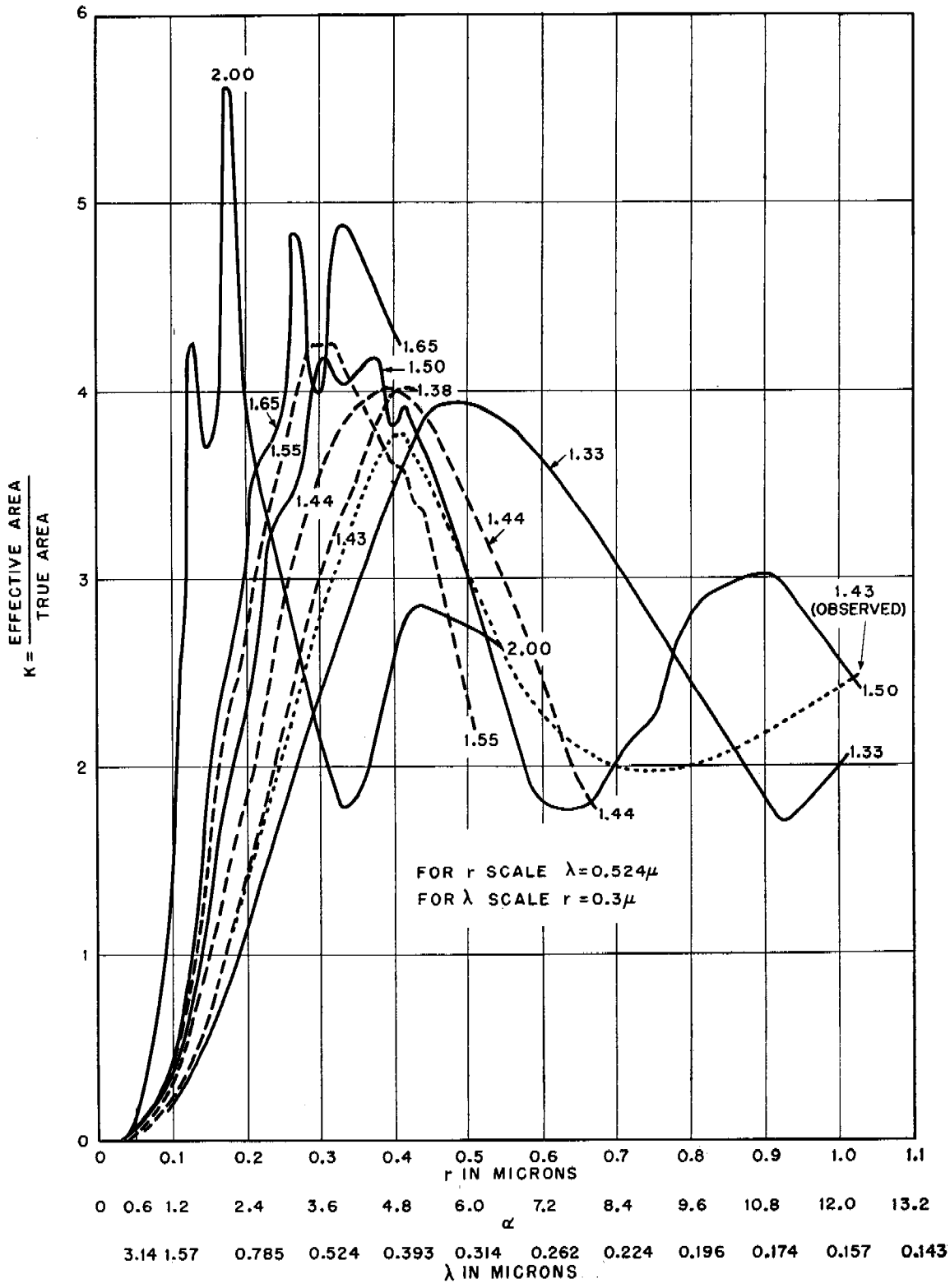


FIGURE 1. Scattering coefficient for spherical particles. K vs α, r and λ.

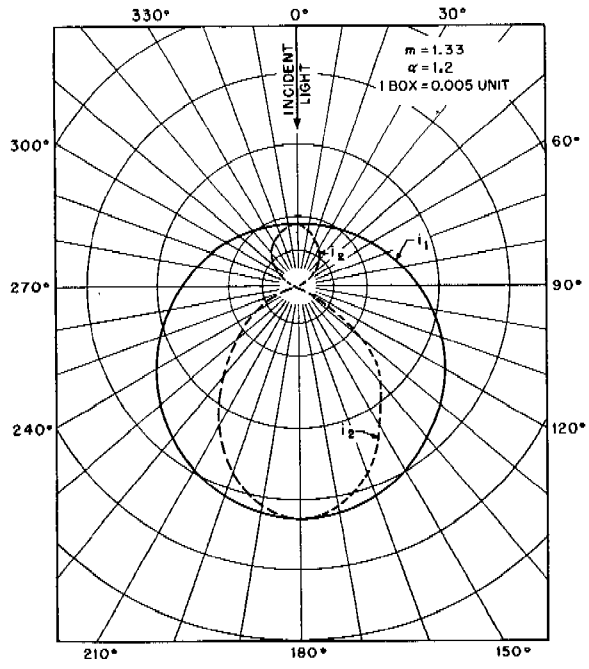


FIGURE 2. Angular distribution of intensity of light scattered by a spherical particle. i_1 and i_2 vs γ.

The a_ν's and p_ν's are functions of $\alpha = 2\pi r/\lambda$ and $\beta = 2\pi rm/\lambda$.

The scattering coefficient K, the scattering per unit cross-sectional area of particle, is obtained by dividing equation (4) by πr^2. Thus:

$$K = \frac{2}{\alpha^2}\sum_{\nu=1}^{\infty}\left(\frac{a_\nu^2 + p_\nu^2}{2\nu + 1}\right). \qquad (5)$$

K is therefore a function of r/λ. This means that once the scattering coefficient is known for a particular value of r and a particular value of λ, it will be known for all values of r and λ which bear the same ratio.

Since the functions are extremely complicated and have already been published,[3, 4] they will not be given here.

The scattering coefficient for particles of different radius and refractive index is shown in Figure 1. The ordinates are the scattering coefficient K, and the abscissas are $\alpha = 2\pi r/\lambda$. The radii corresponding to a wavelength of $\lambda = 0.524$ micron and the wavelengths corresponding to a radius of 0.3 micron have also been given as abscissas, so that these curves show the variation of total scattering with radius at a constant wavelength, and with wavelength at a constant radius.

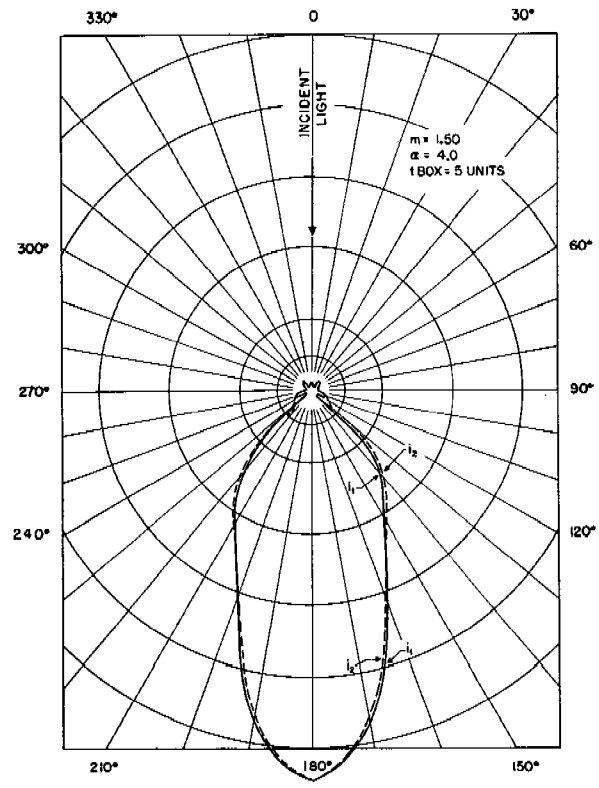


FIGURE 3. Angular distribution of intensity of light scattered by a spherical particle. i_1 and i_2 vs γ.

It is seen that the peak of the curve, and therefore the radius for maximum scattering, moves toward smaller radii as the refractive index increases. There is also a secondary peak in the neighborhood of 1 micron or less.

The angular distribution of intensity varies according to the same function of r/λ. For Rayleigh scattering by small particles, the angular distribution as shown by equation (2) is symmetrical about a plane normal to the incident illuminating beam. That is, as much light is scattered backward as forward. As the particle radius increases, the forward scattering becomes much greater than the backward. For a particle whose radius is equal to or greater than the wavelength of light, the ratio of forward to backward scattering may be 1,000 or more.

The angular distribution of intensity is an extremely complicated function of the scattering angle γ, and the complexity increases markedly with increase in particle size. Numerous equations and angular distribution curves are given in references.[2,3]

The Mie theory predicts, and observations confirm, that the scattered light is partially polarized. That is,

the scattered light is composed of two incoherent plane-polarized components, whose planes of polarization are mutually perpendicular. One of these components, of intensity i_1, has its light vibrations perpendicular to the plane of observation; the other, of intensity i_2, has its light vibrations parallel to the plane of observation.

Figures 2 and 3 show the angular distribution of intensity scattered by spheres of different sizes and materials when illuminated by unpolarized light of $\lambda = 0.524$ micron. Figure 2 is for a 0.1 micron radius water droplet (index 1.33). Figure 3 is for a 0.33 micron radius oil droplet (index 1.50, taken from a paper by Blumer[2]).

The angular distribution of intensity varies with wavelength. For example, a 0.2 micron radius water droplet would have, for a wavelength of 1.048 micron, an intensity distribution like that of Figure 2. This results from the reciprocal relationship between radius and wavelength which states that the intensity distribution is constant when r/λ is constant.

The plane-polarized component, i_1, is the component observed in Rayleigh scattering at an angle $\gamma = 90°$. At this angle, i_2 is zero, as shown by equation (2), since the $\cos^2 \gamma$ term in the brackets is proportional to i_2. The unity term is proportional to i_1, so that i_1 alone is constant for all angles of observation in Rayleigh scattering.

21.2 SCATTERING BY UNIFORM PARTICLE SIZE SPHERICAL AEROSOLS

In aerosols, the particles scatter light independently of one another when the distance between the particles is 10 or preferably 100 times the radius of the particle. In small particle aerosols, of radius 1 micron and number concentration 10^6 per cc, the ratio of distance of separation to radius is $10^{-2}/10^{-4} = 100$. However, for a 10-micron particle aerosol of the same concentration the ratio is reduced to 10. In such an aerosol some interference between the scattering by neighboring particles would be expected, but such high concentrations are not found in practice.

In a water fog of 10 microns radius droplets having a number concentration of 10^3 per cc, the mass concentration would be 4.2 mg per l. This is a concentration found in dense natural fogs. However, the usual concentration found in screening oil fogs and in the laboratory is a few hundred micrograms per liter or less. Consequently, the optical properties of a single spherical particle can be observed by a study of the optical properties of a uniform particle size aerosol.

21.2.1 Angular Distribution of Color

Observations of the scattering were made on a spherical flask of uniform droplet-size fog traversed by a bright and nearly parallel beam of light (called a Tyndall beam), about 1 in. in diameter. The fog was produced in the homogeneous aerosol generator described in Chapter 20.

The angular distribution of color in the scattered light was found [6] to agree closely with the theory. Oleic and stearic acid fogs were illuminated with unpolarized, white light, and the plane-polarized component i_1 was observed as the angle of observation θ (measured from the forward direction, i.e., $\theta = 180° - \gamma$) was varied from near 0 to near 180°. The component i_2 exhibits a different and less distinct series of colors.

As the angle of observation is varied from the forward toward the backward direction, a series of colors is seen which resembles the spectrum of white light. The order of the colors is violet, blue, green, yellow, orange, and red. This series may then be repeated several times, depending on the particle size. Near 90° the order of colors reverses, becoming red, orange, yellow, green, blue, and violet. This reverse series may then be repeated until the backward direction is reached.

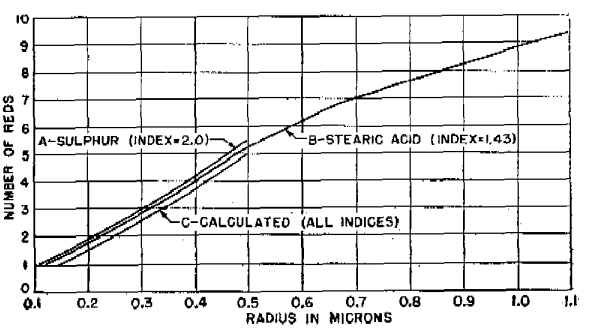


FIGURE 4. Number of reds vs particle radius.

The purity and brightness of the colors increases with the uniformity of particle size. The number of times the color sequence is repeated increases with particle size. This is the basis of a method of particle size measurement, according to which the particle size is given by the number of times red, the most distinctive color, is repeated (see Chapter 22).

In Figure 4, curves A and B are the experimental

curves obtained with oleic acid fogs and sulfur smokes, showing the number of times red is observed as a function of particle size.

Calculations for radii up to 0.5 micron and for indices of refraction 1.33, 1.44, 1.55, and 2.0 show that the number of *reds* corresponding to a given radius is independent of refractive index. Curve *C*, Figure 4, shows the calculated curve which differs throughout from the experimental curves by about 0.025 micron. Since the curves for all indices of refraction approximately coincide up to 0.5 micron, it seems likely that they will continue to coincide up to 1.0 micron.

The calculated curves were obtained from the Mie theory as follows. A curve was plotted for each particle radius showing the ratio of the intensity i_1 in the red ($\lambda = 0.629$ micron) to the intensity i_1 in the green ($\lambda = 0.524$ micron) for scattering angles from 0 to 180°. The number of maxima of magnitude, greater than 0.45, is taken equal to the number of reds observed visually, for the following reason.

The calculated values of i_1 refer to unit intensity of illumination at all wavelengths in the incident beam. Since, in sunlight (i.e., white light) the intensity ratio of red to green at the above wavelengths is 0.9, it was assumed that the observed scattered light would have a reddish hue when the ratio i_1 (red) to i_1 (green) was greater than 0.9. In the tungsten light used for observation, the intensity

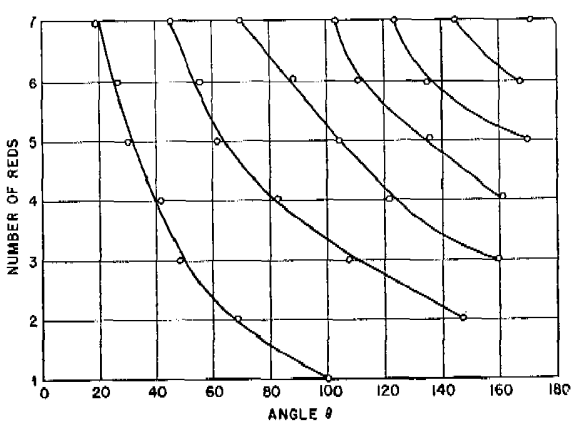


FIGURE 5. Angular position vs number of reds.

ratio of red to green was 2.0. Consequently a calculated ratio i_1 (red) to i_1 (green), greater than 0.45, would correspond to an observed red since the ratio i_1 (red) to i_1 (green) in the observed scattered light would be greater than $2 \times 0.45 = 0.9$.

Figure 5 shows the angular position of the reds seen in i_1 in stearic acid smokes of 1 to 7 spectra. The ordinates show the number of reds and the abscissas their angular position, θ. With the exception of sulfur, most of the calculated points for other indices of refraction lie on the stearic acid curves to within $\pm 5°$.

21.2.2 Polarization

The polarization for various angles θ was found, both experimentally and theoretically, to vary in a regular manner from the Rayleigh region up to about 0.2-micron radius. The relative intensity of i_2 to i_1 was found to vary from a low value up to greater than one. The polarization can thus be used as a measure of particle radii up to 0.2 micron (see Chapter 22). Above 0.2-micron radius, the polarization varies more rapidly with particle radius and is multiply valued.

The polarization may be conveniently measured with a polarization photometer. A Tyndall beam of approximately monochromatic light is observed through a bipartite disk with its dividing line parallel (or perpendicular) to the plane of observation. The bipartite disk is a plane-polarizer having one half of its plane of polarization perpendicular to the dividing line and the other half parallel to the dividing line. One half of the bipartite disk, therefore, transmits i_1 and the other half transmits i_2. Between the observer and the bipartite disk is a plane polarizer, called the analyzer, which can be turned so that its plane of polarization makes a given angle with the plane of observation.

The analyzer is turned so that the intensities of the two halves of the bipartite disk are equal. If the angle between the direction of the light vibrations transmitted by the analyzer and the plane of observation is ϕ, then:

$$\frac{i_2}{i_1} = \tan^2 \phi \cdot \qquad (6)$$

Figure 6 shows the calculated values of ϕ as a function of radius for five different refractive indices when the angle of observation $\theta = 90°$ and $\lambda = 0.524$ micron. Figure 7 shows ϕ as a function of radius for four different values of θ when the index of refraction $m = 1.44$ and $\lambda = 0.524$ micron.

The blue tobacco smoke that rises from the end of a cigarette exhibits Rayleigh scattering approximately when illuminated with white light ($\lambda = 0.4$ to 0.7 micron). If a Tyndall beam is examined in a direction at right angles to the beam through a plane

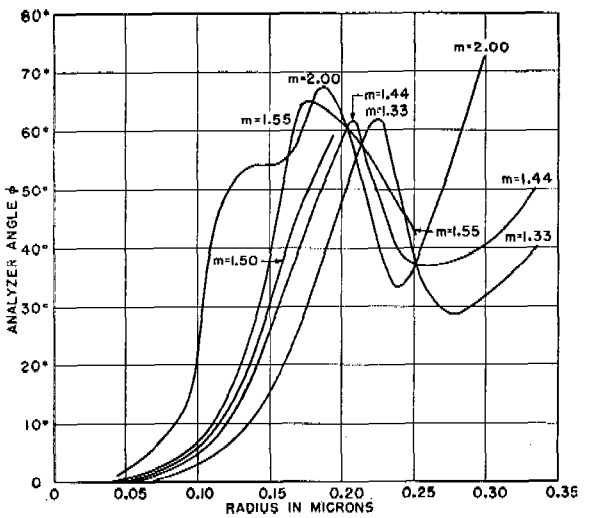


FIGURE 6. Calibration curves for Owl. Analyzer angle ϕ at $\theta = 90°$, vs refractive index.

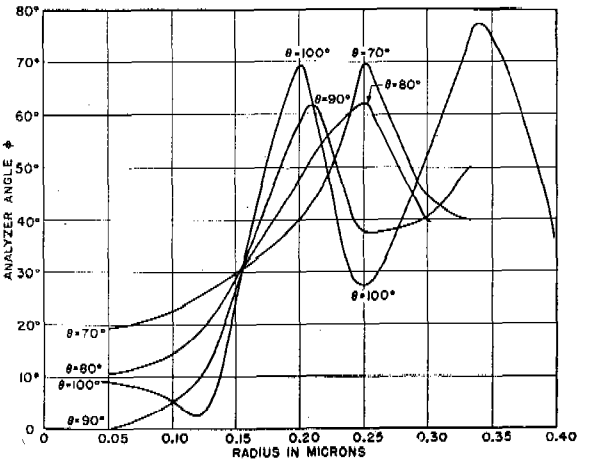


FIGURE 7. Calibration curves for Owl. Analyzer angle ϕ at refractive index 1.44 vs θ.

polarizer, it will be seen to be virtually extinguished when $\phi = 0°$.

When fresh, the particles of tobacco smoke are 0.15-micron radius or less. If this smoke is allowed to age in a flask, or if exhaled smoke is examined, much less polarization will be observed. Aged tobacco smoke particles are 0.2 or 0.25-micron radius, due to the accumulation of moisture. Such smoke may be sufficiently uniform in size to exhibit some color when examined through a polarizer.

21.2.3 Total Scattering

Measurements were made of the angular distribution of intensity of the light scattered by uniform stearic acid and oleic acid fogs. The details of the method of measurement have been given elsewhere.[7]

A fog of known concentration (measured by weighing a known volume of fog collected in a glass wool filter) was observed while streaming out of the generator. A suitable volume was uniformly illuminated and the intensity scattered into a given small solid angle was measured with a photometer. Measurements were made at angles from 3 to 175° at frequent intervals. The intensities were then integrated over all possible directions. In order to obtain the total scattering coefficient, the integrated scattering was compared with that of a diffuse reflector of known reflectivity.

The results are given in Figure 1. The dotted curve shows the experimental measurements made on uniform particle size stearic acid fog, refractive index = 1.43. The agreement with the theoretical curve for index 1.44 is considered to be satisfactory. The discrepancy is due to the difficulties inherent in this type of measurement.

It was found that the theoretical values of both total scattering and angular distribution of intensity are too high by a factor of 2 when the particle is illuminated by unpolarized light. This was due to a mistake made in the original derivation of the theory when transferring from polarized to unpolarized light.[4] The error was made originally by Rayleigh [5] and was first pointed out by Stiles [8] in a paper, which was brought to the author's attention after reference 4 had been distributed. Rayleigh's original error has been propagated unchanged in a number of texts. In the *Handbuch der Physik*, the error is compensated by making an improper integration over the sphere.[9]

The values of the scattering coefficient given in Figure 1 are the correct values. They are equal to the values obtained directly from the Mie theory when derived for polarized light, and to half the values given by the Mie theory for unpolarized light.

The total amount of light scattered by 1 cc of aerosol is equal to the product of the amount of light scattered per particle and the number concentration n. Figure 8 shows S the scattering cross section per particle ($\times 10^8$) as a function of particle size and wavelength for water (index = 1.33), screening oil (Diol, index = 1.50) and sulfur (index = 2.0). These curves may be obtained from equation (4), or they may be obtained from the curves of Figure 1 by multiplying the values of the scattering coefficient K by the cross-sectional area of the particle πr^2. The scattering per cc is then $K\pi r^2 n = Sn$.

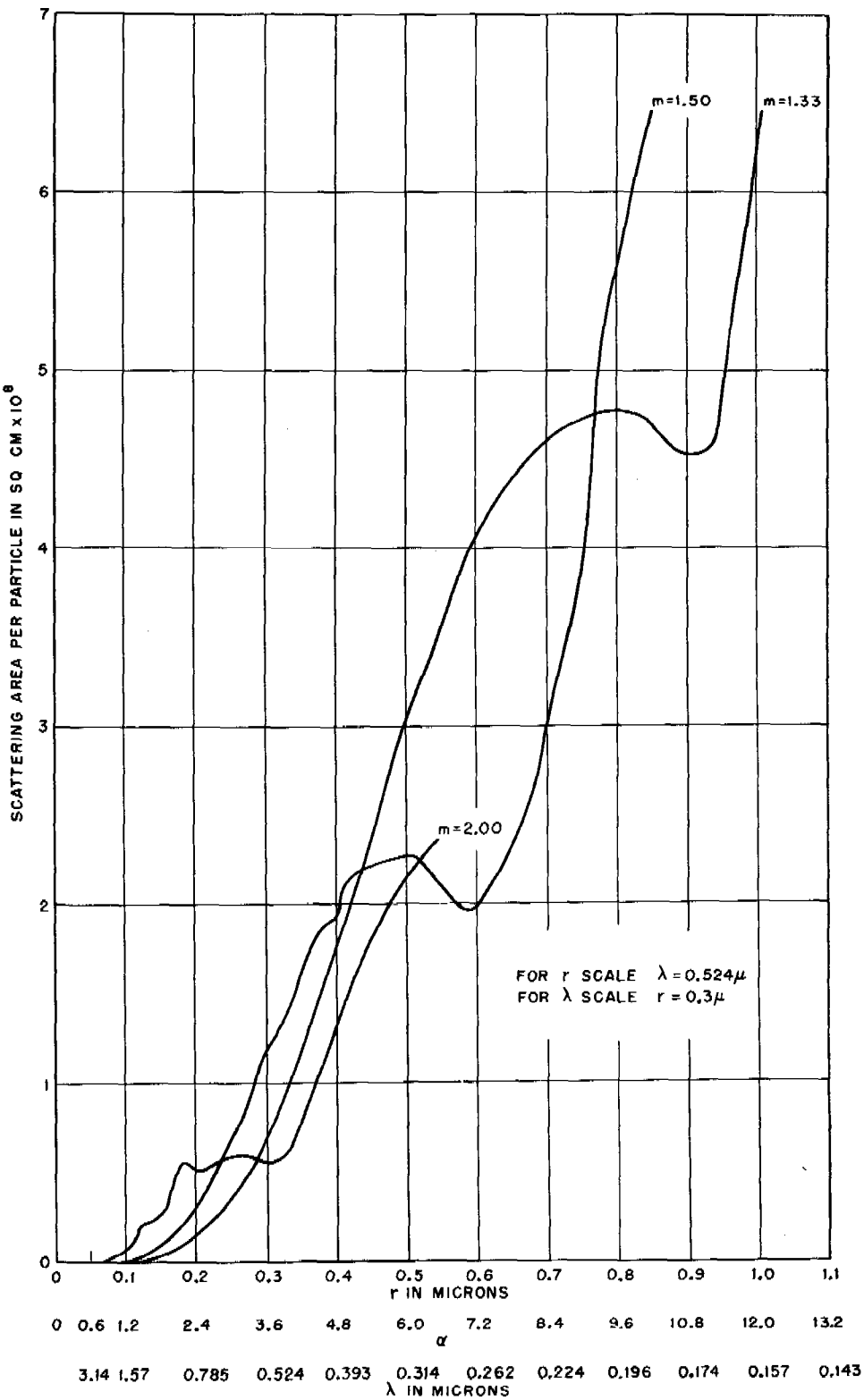


FIGURE 8. Total light scattered per particle. S per particle vs α, r and λ.

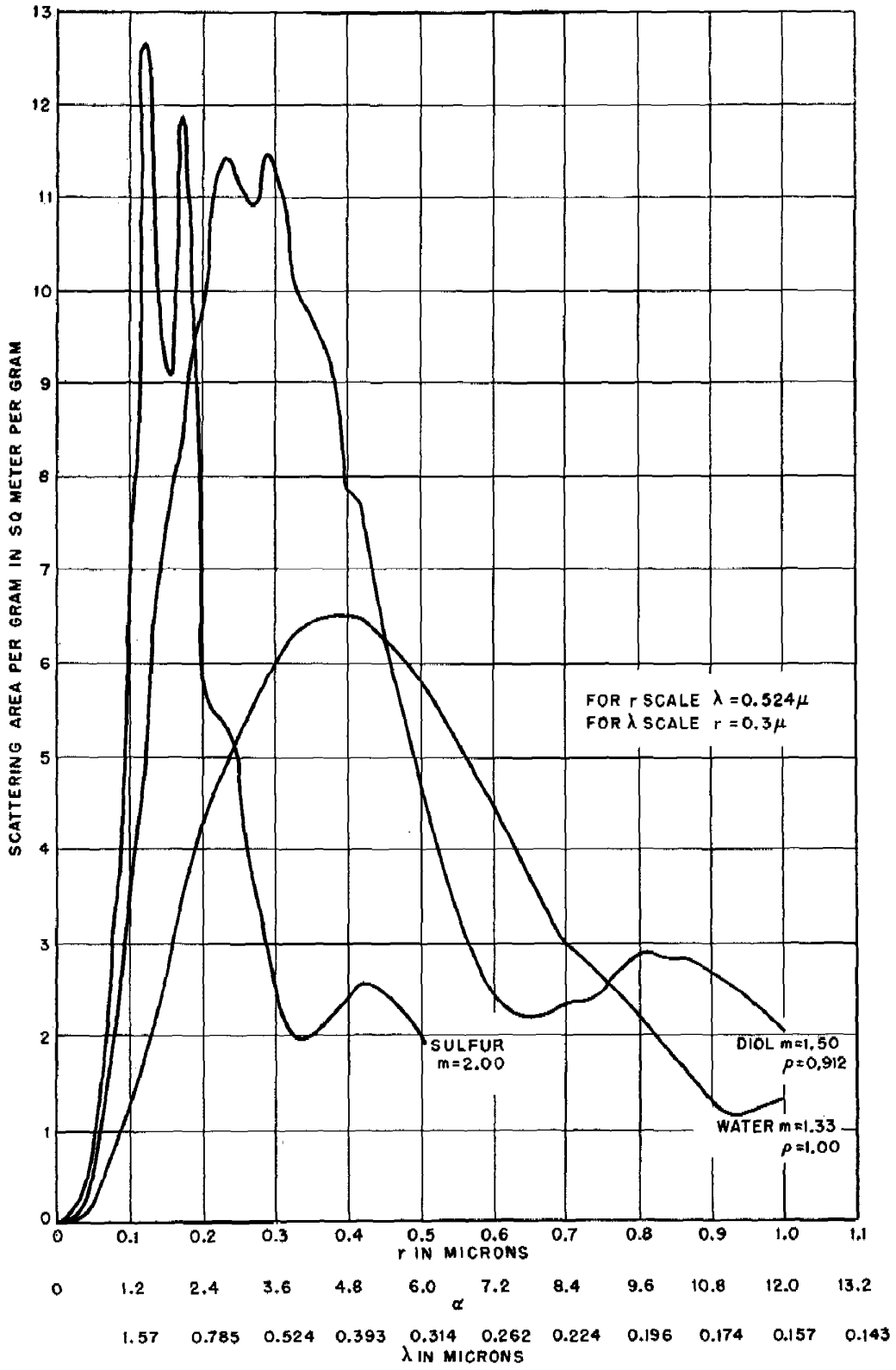


FIGURE 9. Total light scattered per gram of particles. S per gram ($=J$) vs α, r and λ.

The total scattering may also be expressed in terms of the scattering per gram of material. This is the quantity most important in determining the performance of a screening smoke. Figure 9 shows the scattering cross section in square meters per gram for some of the materials of Figure 8. These curves were obtained from Figure 8 by dividing the scattering per particle by the mass of one particle. Thus, the scattering per gram is $J = 3K/4r\rho$, where ρ is the density of the material.

21.2.4 Transmission

The total scattering may be more conveniently obtained by measuring the decrease of intensity of the transmitted beam. For small particles, the intensity of the transmitted beam of wavelength λ decreases exponentially with the distance traversed through the aerosol, that is:

$$I = I_0 e^{-Snl} = I_0 e^{-Jcl}. \tag{7}$$

Here l is the distance, and c is the mass concentration of the aerosol in grams per milliliter. The term Snl ($Snl = Jcl$) is defined as the optical density D.

The intensity I transmitted through a given distance l in a stirred homogeneous aerosol will decrease exponentially with the time, due to the decrease in n, according to equation (2), Chapter 19. Combining equation (2) with equation (7),

$$\log \frac{I_0}{I} = Snl = Snl_0 e^{-(vt/h)}. \tag{8}$$

Thus the optical density $D = Snl$ will decrease exponentially with the time. However, for times short compared to h/v the change will be small. If the concentration n is maintained constant by replenishing the aerosol from a homogeneous generator, the transmitted intensity will be constant.

A beam of monochromatic light was passed into a photocell through a homogeneous aerosol of constant concentration, and the transmission measured as a function of particle size and wavelength. The concentration and distance were also measured and the scattering coefficient then calculated from equation (7). Good agreement was found between experiment and theory for oleic acid [4] (index = 1.46), sulfur [4] (index = 2.0), and Diol [10] (index = 1.5).

In the case of oleic acid and sulfur, it was convenient to plot curves showing the variation of $J\lambda$ [$\propto K(\lambda/r)$] with r/λ. These curves are similar in form to the K vs α curves of Figure 1.

For Diol a series of curves showing the variation of $\log J$ with $\log \lambda$ at constant radius was plotted. It was found that the slope of these curves varied markedly with particle size. For the wavelength 0.65 micron, the slope was -1.9 at $r = 0.3$ micron ($\alpha = 2.9$), reached a maximum of $+2.1$ at $r = 0.7$ micron ($\alpha = 6.8$) and fell to $+1.7$ at $r = 0.76$ micron ($\alpha = 7.3$).

At $r = 0.1$ micron or less the slope should reach the value -4, according to the Rayleigh equation [equation (1)]. The curve of scattering per gram for Diol (Figure 9) shows a variety of slopes of positive and negative values.

A negative slope means that the scattering per gram decreases with increasing wavelength. In other words the transparency of the aerosol increases with increasing wavelength. This is the general situation for aerosols whose particle radii are smaller than the radius (or radii) corresponding to the principal maximum of the scattering curve. Conversely, aerosols whose particles are somewhat larger than this optimum size will be more transparent to shorter wavelengths.

It has been observed that the color of the sun's disk, viewed through a cloud of Diol fog produced in the field, is red when the droplet radii are less than 0.23 micron, and blue or green when the radii are greater than 0.3 micron. Inspection of Figure 9 shows that the optimum radii for Diol are between the above values (for green light, $\lambda = 0.524$ micron).

The observations should be made when the sun's light is nearly extinguished, since the residual rays will exhibit the most distinctive color. The purity of the color will vary with the uniformity of particle size. It is evident that a considerable range of sizes, great enough to span the peak of the curve, would exhibit little or no color. This is a simple criterion for estimating the particle size and size distribution of a fog (see Chapter 22).

If the particles are all considerably smaller than the optimum size, they may have a large range of size and still produce a red color in the transmitted light. The setting sun appears red, usually because of the small particles of haze which exhibit approximately Rayleigh scattering. And the color of the sun deepens as it sets, due to increased selective scattering, until the residual color becomes a deep red just before the sun is extinguished.

Even when free of haze the color of the sky at sunset will differ from the usual blue. The sky color will vary with the color of the transmitted sunlight, which varies with the path length as follows:

Combining equations (1) and (2) into an equation of the form of equation (7),

$$I_\gamma = \frac{9\pi^2}{2R^2}\left(\frac{m^2-1}{m^2+2}\right)\frac{V^2}{\lambda^4}\cdot (1+\cos^2\gamma)\exp\left[-24\pi^3\left(\frac{m^2-1}{m^2+2}\right)^2\frac{V^2}{\lambda^4}nl\right]. \quad (9)$$

This equation is a maximum when

$$\lambda = \sqrt[4]{n\alpha V^2 l}$$

where

$$\alpha = 24\pi^3\left(\frac{m^2-1}{m^2+2}\right)^2. \quad (10)$$

Thus the wavelength of maximum Rayleigh scattering increases with the particle radius, the length of path and the number concentration.

This phenomenon is very striking when observed in a dense homogeneous aerosol exhibiting Mie scattering. The color of the Tyndall beam varies from blue through green and orange to red, before it is extinguished.

The particle radii may be obtained quite accurately by measuring quantitatively the transmission as a function of wavelength. This is the principle of an instrument called the *Slope-o-meter* described in Chapter 22.

21.2.5 Scattering by Large Particles

The Mie equations hold, theoretically, for any value of the radius. However, when α is greater than 10 or 12, the practical difficulties of calculation become excessive. Consequently Figure 1 shows no points beyond $\alpha = 12$.

However, when r is extremely large, approximation methods show [3] that K approaches the value 2. At first sight this appears false since it says that a very large sphere scatters twice as much light as falls on it. Brillouin [11] has recently shown theoretically that the light scattered by a relatively large metallic sphere ($r > 12$ microns) could be divided into two *equal* parts, that scattered into a small solid angle around the forward direction (i.e., into the geometrical shadow), and that scattered in all other directions. This means that although the correct value of the scattering coefficient is 2, the actual value, measured experimentally, will be 1 for very large spheres, since for such spheres the angular divergence of the shadow is extremely small.

This result was confirmed by the following experiment. A cloud of lycopodium spores was allowed to settle on to a glass plate. The radii of these spores were found to be very uniform, 15.0 ± 1 micron. The plate was then placed in a parallel beam of light in front of a photocell, and the transmitted intensity measured at different distances between plate and photocell. The reading of the photocell increased by the factor 2.1 when the distance from the plate to the photocell was decreased from 18 ft to 6 in. Calculation checked this result and showed that at 18 ft the observed scattering cross section was $2\pi r^2$ and at 6 in. it was πr^2. At 6 in., half of the scattered light (i.e., that part scattered into the geometrical shadow) was picked up by the photocell.

This conclusion is further confirmed by a consideration of diffraction by large obstacles. According to the theory of diffraction, the total amount of light diffracted by an opening is equal to the area of the opening (in the case of unit intensity of illumination). For a circular hole of radius r, the amount of light diffracted would be πr^2.

According to Babinet's principle, a circular obstacle of radius r will diffract the same amount of light as a circular hole of radius r. But the obstacle will also intercept an amount of light equal to its area πr^2. Consequently the total amount of light, both intercepted and diffracted, is $2\pi r^2$, and the transmission experiment described above will yield a scattering cross section of $2\pi r^2$, provided the distance from the obstacle to the measuring device is made large enough.

However, for very large obstacles, this condition is not realizable in practice. The diffraction pattern is so small that all the light contained in it is received by the collector. The collector then measures only the amount of light intercepted by the geometric cross section πr^2.

Therefore, it is evident that the total amount of light absorbed and scattered (i.e., diffracted at any angle from its original direction) is $2\pi r^2$, as the Mie-Stratton theory shows. However, any experimental measurement of a very large particle will yield the value πr^2, the amount of light absorbed by an opaque disk, or in the case of a reflecting sphere, light scattered outside of the geometrical shadow.

21.3 SCATTERING BY NONUNIFORM PARTICLE SIZE SPHERICAL AEROSOLS

Ordinary aerosols, having a large range of particle size, exhibit the scattering which would be observed from a mixture of a large number of uniform particle

size aerosols, mixed in varying proportions. The different colors in the scattered light overlap so that the aerosol appears more or less white depending on how much one particle size predominates. The polarization is also a mixture of that from many sizes, the effect of the large particles predominating because of the great increase of intensity with size.

If a nonuniform aerosol, such as tobacco smoke, is allowed to settle in a convection-free chamber, considerable separation of sizes will occur. If the upper layers of the cloud are examined with a beam of white light, various colors will be seen depending upon the height and direction of observation. An approximate idea of the size and size distribution of the smoke particles can be obtained by examining the colors and polarization at different heights and angles.

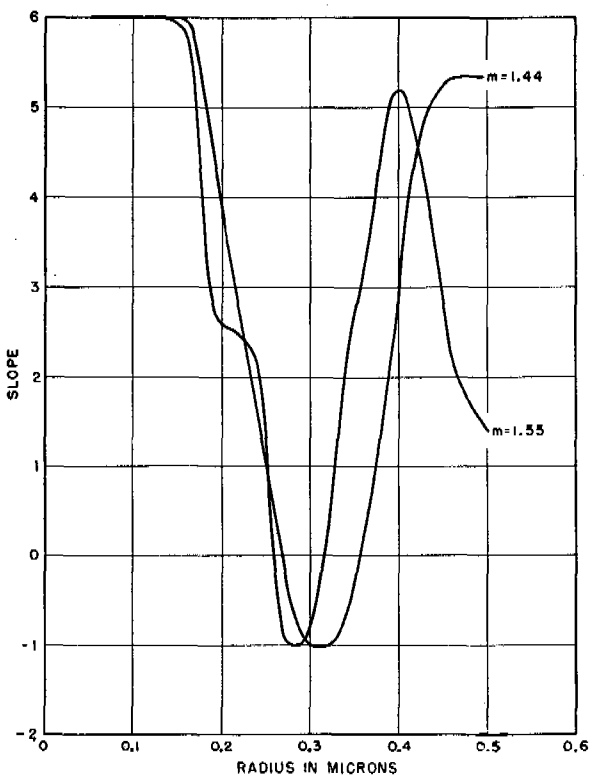


FIGURE 10. Angle scattering as function of particle size. p vs r in eq. $\Delta I = kr^p \Delta n$ at $\theta = 45°$.

21.3.1 Scattered Intensity vs Particle Radius

The intensity scattered at any wavelength by a given volume of smoke at a fixed height will decrease with time since the number of particles in that volume will decrease due to differential settling as explained in Chapter 19. If coagulation is negligible, the rate of decrease of intensity at any time depends upon the particle size and size distribution, and the scattering as a function of size.

The change in the scattered light intensity, ΔI, observed at a given angle and wavelength is proportional to the change in the particle concentration Δn, and the radius raised to some power p, that is

$$\Delta I = kr^p \Delta n. \tag{11}$$

The value of p at a given value of r and angle of observation, θ, is obtained from the calculations of the angular distribution of intensity referred to above.[4] The values of log $(i_1 + i_2)$ vs log r were plotted and the value of the slope p as a function of r was obtained for several angles.

Figure 10 shows the variation of p with r at θ = average of 40°, 45°, 50°, for refractive index 1.44, and 1.55 at the wavelength 0.524 micron. It is seen that p has the value 6 for radii below 0.1 micron as is to be expected in the region of Rayleigh scattering. The region of negative values of p corresponds roughly to the region of the curves of Figure 8 where the slope is negative. Sufficient calculations are not available to carry these curves beyond $r = 0.5$ micron.

Similar curves were drawn showing p as a function of r for total scattering. For Rayleigh scattering, p should again have the value 6, and for very large particles, the value 2. These curves were found to be quite different from those of Figure 10 in the useful range from 0.1 to 1 micron so that they cannot be used to supplement the curves of Figure 10.

The use of these curves in conjunction with the differential settler for the determination of particle size and distribution is described in Chapter 22.

21.3.2 Transmission in Tranquil Settling

The intensity transmitted by an aerosol in tranquil settling will vary in a similar manner. However, the practical difficulties of this measurement were found to be insurmountable. In order to obtain sufficient optical density and avoid coagulation, the smoke chamber must be large in order that the path length may be large since n must be not over 10^5 per cc. It has been found impossible to eliminate convection currents in anything but a chamber so small that the transmission is very nearly 100% when n has a suitable value.

21.3.3 Transmission in Stirred Settling

The optical density $D = Snl$, of a homogeneous aerosol in stirred settling and undergoing coagula-

tion, will vary according to equation (24), Chapter 19, as follows.

$$\frac{1}{n} = \frac{Sl}{D} = -\frac{\mathcal{K}h}{v} + \left(\frac{\mathcal{K}h}{v} + \frac{S_0 l}{D_0}\right) e^{-vt/h}. \quad (12)$$

For times short compared to h/v, this becomes

$$\frac{1}{D} = \frac{1}{D_0} + \left(\frac{\mathcal{K}}{Sl} + \frac{v}{hD_0}\right) t. \quad (13)$$

If $1/D$ is plotted against time a straight line will be obtained, having the slope $\mathcal{K}/Sl + v/hD_0$. The quantities l, h, D, and D_0 are readily measurable. If the particle radius is known, v, S, and $\mathcal{K}$ may be calculated, or if $\mathcal{K}$ is known, then v, S, and r may be calculated. (See Chapter 22.)

This equation neglects the change in particle size (but not the change in number) due to coagulation. As a result of coagulation, v and S would not be quite constant.

21.3.4 Heterogeneous Aerosol without Coagulation

The total scattering cross section of N spherical particles of different sizes can be obtained by measuring the optical density $D = SlN$. In a heterogeneous aerosol, S is the scattering cross section of an average particle. In the range of particle sizes where K is nearly constant and equal to 2 ($r > 1$ micron, see Figure 1), S will be the scattering cross section of the sphere having the average geometrical cross section. Therefore, according to equation (6), Chapter 19, the scattering cross section per cc at zero time is

$$S_0 = \frac{\pi}{4} N_0 K_2 d_2^2, \quad (14)$$

and according to equation (8), Chapter 19, the scattering cross section at time t is:

$$S_t = \frac{\pi}{4} K_2 \int_0^\infty d^2 n_d \exp\left(-\frac{v_d t}{h}\right) \delta \log d. \quad (15)$$

Here K_2 is the scattering coefficient of the sphere of diameter d_2.

Equation (15), Chapter 19, may then be transformed to:

$$-\frac{d}{dt} \log S_t = 1.3 \times 10^5 \frac{\rho}{h} \frac{K_4}{K_2} \frac{d_4^4}{d_2^2}, \quad (16)$$

or

$$-\frac{d}{dt} \log S_t = 1.3 \times 10^5 \frac{\rho}{h} \frac{K_4}{K_2} d_6^2. \quad (17)$$

Thus d_6 can be obtained by measuring the average scattering cross section provided K_4 and K_2 can be determined.

The scattering per gram at zero time A_0 is obtained by dividing equation (14) by equation (7), Chapter 19.

$$A_0 = \frac{S_0}{M_0} = \frac{\frac{\pi}{4} N_0 K_2 d_2^2}{\frac{\pi}{6} N_0 \rho d_3^3} = \frac{3}{2} \frac{K_2}{\rho d_5}, \quad (18)$$

making use of equation (5), Chapter 19.

A further useful relationship is obtained by dividing equation (16) by equation (14), Chapter 19. Writing $d/dt \log M_t = u_m$ and $d/dt \log S_t = u_s$ we have

$$\frac{u_s}{u_m} = \frac{K_4}{K_2} \frac{d_3^3}{d_5^5} \frac{d_4^4}{d_2^2}. \quad (19)$$

Multiplying equation (19) by A_0 [equation (18)] gives

$$A_0 \frac{u_s}{u_m} = \frac{3}{2} \frac{K_4}{\rho} \frac{d_4^4}{d_5^5} = \frac{3}{2} \frac{K_4}{\rho d_9}, \quad (20)$$

making use of equation (5), Chapter 19.

The use of these equations for particle size measurement is described in Chapter 22.

21.3.5 Complete Analysis of Scattering

The complete analysis of the light scattered or transmitted by a heterogeneous aerosol is extremely difficult. The absence of distinctive color in the scattered light is an indication of heterogeneity, but the distribution curve cannot be obtained by this means. Similarly, the polarization in the range of radii below 0.2 micron, may be used to detect the presence of a distribution of sizes, although it is extremely difficult, if not impossible, to obtain any quantitative results by this means.

The general theory has been discussed elsewhere.[12] The conclusions reached may be summarized as follows.

The determination from scratch of the nonhomogeneity of a smoke is possible only in principle. But if we already know enough about the size and distribution of a heterogeneous smoke, the knowledge of the scattering functions of homogeneous smokes will enable us to find out more. For example, the determination of the proportions of a mixture of two homogeneous smokes of known particle size is relatively easy.

The relative proportions of a mixture of two homo-

geneous smokes of known radii less than about 0.2 micron can be obtained by measuring the polarization at the scattering angle θ. Let x and $1 - x$ be the proportion of particles of radius r_1 and r_2 respectively. Let $i_1(r_1,\theta)$ and $i_2(r_1,\theta)$ be the intensities of the polarized components scattered per particle of radius r_1 at the angle θ, with similar expressions for r_2; and let the wavelength be λ.

Then the ratio of the intensities observed at the angle θ will be according to equation (6)

$$R = \frac{xi_2(r_1,\theta) + (1-x)i_2(r_2,\theta)}{xi_1(r_1,\theta) + (1-x)i_1(r_2,\theta)} = \tan^2\phi. \quad (21)$$

Since the i_2's and the i_1's are known from the Mie theory, this equation may be solved for x.

If the radii were unknown they could be obtained by observing the polarization at three different angles θ.

For radii greater than about 0.2 micron this method would not yield a unique solution since the absolute values as well as the ratio of the intensities are multiple valued.

Usually, however, no such simple distribution of sizes is encountered. Calculations have been made showing the effect of various size distributions on the polarization.[13] The conclusion is that this method cannot be used to obtain the size or size distribution of heterogeneous smokes.

One can merely determine whether or not the smoke is homogeneous by observing the polarization at several angles. If, for example, the polarization of a stearic acid smoke were observed at 90°, 80°, and 70°, and the same size were obtained from each of the corresponding curves of Figure 7, then the smoke would evidently be homogeneous.[14] However, this method would fail for radii near 0.15 micron where the curves cross.

Similarly, the color of the transmitted light serves as an approximate measure of the particle size, and an unsaturated color indicates a distribution of sizes (see preceding text and Chapter 22); but the distribution curve cannot be obtained from the wavelength intensity distribution of the transmitted light.

21.4 THE SCATTERING OF LIGHT BY SOLID PARTICLES

21.4.1 Polarization

The angular distribution of intensity of the light scattered by irregularly shaped particles has not been analyzed in detail. The Rayleigh theory is applicable to extremely small particles no matter what their shape. However, for larger particles near the limit of the Rayleigh region, shape and internal structure have an effect on the scattering. The ratio i_2/i_1, called the *depolarization factor*, is greater than for spherical particles. Lotmar [15] has shown that the internal crystal structure of solid particles has a much greater effect on the polarization than does the external shape of the particle.

When very small particles are illuminated by polarized light the Rayleigh theory shows [equation (3)] that i_2 is zero everywhere. For larger spheres exhibiting Mie scattering, or for irregular particles exhibiting depolarization, i_2 is not zero. Krishnan [16] has shown theoretically and experimentally that the component i_2 (scattered when the incident light is polarized with its electric vibrations perpendicular to the plane of observation) is equal to the component i_1 (scattered when the incident light is polarized with its electric vibrations parallel to the plane of observation). These two components will be referred to as the *rotated* components. This relationship holds for a mass of particles of all shapes and sizes, and for all angles of scattering, provided the orientation of the particles is random.

The Mie theory for spherical particles shows that the rotated components are both equal to zero.[4] Consequently when the incident light is unpolarized, the component i_2, which is observed, is produced by the incident electric vibrations which are parallel to the plane of observation, and the component i_1 is produced by the incident electric vibrations which are perpendicular to the plane of observation.

However, when irregularly shaped particles are illuminated by unpolarized light, the rotated components are no longer equal to zero. Consequently, comparison of the polarization of the light scattered by particles when illuminated with unpolarized and polarized light would provide a measure of the shape or anisotropy of the particles.

It would be expected that the polarization by particles of a given form could be used as a measure of their size, provided a calibration could be obtained. This would require a series of smokes of uniform size. Attempts were made to produce or obtain solid particle smokes sufficiently uniform for this purpose, but they were not successful.

21.4.2 Scintillating Particles

Some useful qualitative information can be obtained by observing the effect of Brownian rotation.

When a bright Tyndall beam is observed in a solid particle smoke, the particles will be observed to scintillate due to random reflections from the crystal faces. Large particles, which are observed to fall rapidly, produce intermittent flashes at a much lower frequency than those from the more slowly falling particles. Stearic acid smokes that have been aged for an hour or more exhibit these scintillations, while fresh smokes do not. This indicates that in the course of time the supercooled stearic acid droplets crystallize.

21.4.3 Transmission in Stirred Settling

The optical density of solid particle smokes in stirred settling may be analyzed according to the methods described in preceding text.

The aerosol, composed of irregularly shaped aggregates of a wide range of sizes, is compared with a hypothetical aerosol of equivalent spherical particles having a logarithmic-probability distribution of sizes. Microscope examination of Kadox (see Figure 1, Chapter 22) and albumin particles has shown them to be fairly compact aggregates that show no tendency to form filamentary particles; particle size exhibits a distribution curve that follows approximately the logarithmic-probability law.

In ground materials it is probable that the number of particles at very small sizes is greater than appears from the measurements, due to the difficulty of observing them. However, since the scattered light decreases with the sixth power of the radius for particles below about 0.1-micron radius, and the contribution to the mass decreases as the third power of the radius, such particles are relatively unimportant so that the approximation appears to be good enough for practical purposes. Bailey has found a logarithmic probability distribution in ground pigments.[17]

Consequently one can calculate various average diameters in a manner similar to that described in Chapter 19. The average scattering cross section and scattering per gram may be expressed as described in preceding text, provided the scattering coefficient is known.

In the case of Kadox and other small particles less than about 2-micron diameter, the Mie theory shows (see Figure 1) that the scattering coefficient usually has a value between 2 and 4 except for extremely small particles exhibiting Rayleigh scattering. It was found empirically by Bailey [17] that if the values of the diameter are multiplied by $(m^2-1)/(m^2+2)$, where m is the refractive index, then all the scattering curves approximately coincide.

It has been found that this relationship is also approximately true for the scattering curves calculated from the Mie theory. Figure 11 shows the average of the curves obtained by plotting the values of K in Figure 1 against the corresponding value of $d(m^2-1)/(m^2+2)$. It is seen that maximum values of the scattering coefficient occur when $d(m^2-1)/(m^2+2) = 0.2$ and 0.5 micron (dashed line in Figure 11). Figure 11 is a universal scattering curve for all transparent materials of any refractive index. The heavy line was drawn to average out the trough and minor peak since they are within the precision of measurement. (See Chapter 22.)

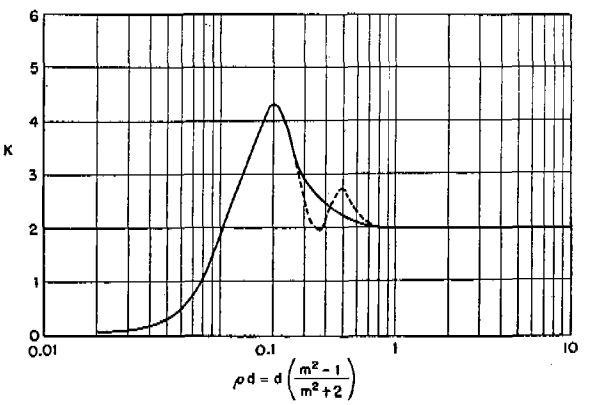


FIGURE 11. Universal scattering curve for all transparent materials of any refractive index.

Since solid aerosol particles are aggregates of small primary particles, they will have an effective density and an effective refractive index less than the true density and refractive index of the material. The effective density has been found experimentally to be about equal to the density of the powder before dispersal, i.e., the average of the density of the solid particles plus the air in the spaces between the particles. The effective refractive index has been found to be given approximately by the same average.

The author has found that the effective density ρ and effective refractive index m are related according to the Lorenz-Lorentz relation, ρ = Constant $\times$ $(m^2-1)/(m^2+2)$. The value of the constant for a given aerosol material is found by substituting the true density ρ_0 and the true refractive index m_0 into the equation. The constant is equal to 11 for Kadox and 4 for albumin. It is seen that the factor $(m^2-1)/(m^2+2)$ is the factor which brings the scattering curves for all materials into approximate coincidence.

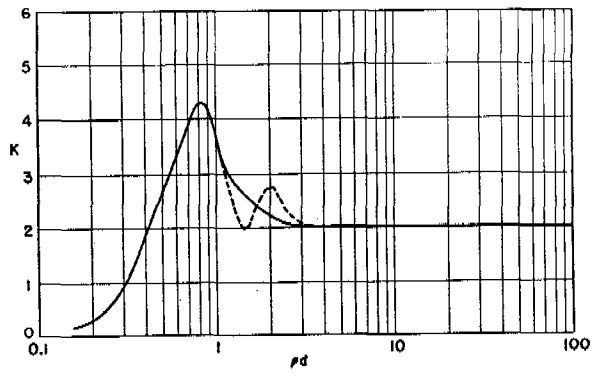


FIGURE 12. Scattering curve for Kadox. K vs ρd.

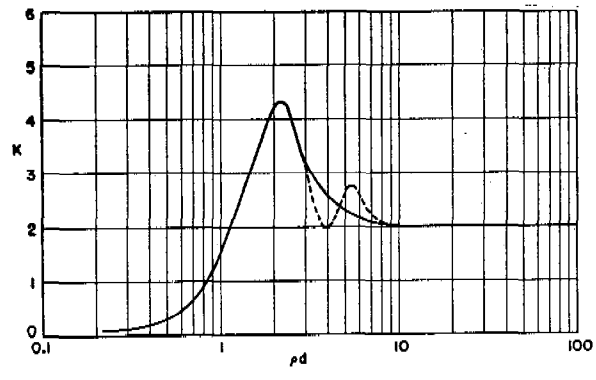


FIGURE 13. Scattering curve for albumin. K vs ρd.

Two curves (Figures 12 and 13), one for Kadox and one for albumin, were plotted, showing the variation of the scattering coefficient K with

$$\rho d = \text{Constant} \times d\left(\frac{m^2 - 1}{m^2 + 2}\right). \qquad (22)$$

Such a curve will yield the scattering coefficient of a loosely aggregated particle of a given material when the product ρd of the diameter and effective density is known.

It has been assumed that the effective density is a constant for all sizes of aggregated particles formed. This means that the packing of the primary particles is the same for all aggregates, which seems probable since most of the aggregates contain large numbers of primary particles, 20 or more.

The assumption that the refractive index of the aggregated particle is a smeared out index appears to be justified since the primary Kadox particles are about one-fifth to one-tenth the wavelength of light. Since the primary particles are packed in contact with each other, they will not individually give rise to Rayleigh scattering but will behave collectively as a single large particle showing Mie scattering. In the case of albumin the particles are all so large that the refractive index has little effect on the scattering, K having the constant value 2 as explained in preceding text.

Figures 12 and 13 may be used to obtain the particle size and size distribution as described in Chapter 22.

21.5 SCATTERING BY LIQUID OR SOLID PARTICLES WHICH ALSO ABSORB

21.5.1 General Characteristics

The scattering of light by colored particles is a combination of the selective scattering by transparent particles having a real refractive index, plus the selective absorption by absorbing particles having a complex refractive index. In selective scattering all the light not scattered is transmitted, but with selective absorption, some of the light not scattered is also not transmitted.

In colored materials the absorption and the refractive index vary markedly with wavelength. For example, solutions of the orange dye (Calco Oil Orange Y-293) used in orange smoke signals have a low value of absorption in the yellow and red, a high value in the green and blue and an intermediate value in the violet. This means that, for the green and blue wavelengths, dye particles and oil droplets containing dye will have complex scattering and absorbing properties, while for the red and yellow wavelengths such particles will exhibit approximately the selective scattering by transparent particles.

At wavelengths of low absorption the optimum particle size of a colored particle will be approximately the same as that of a transparent particle of the same real refractive index. In the case of dye dissolved in oil of real refractive index 1.50, the optimum particle size would be about 0.3 micron for red and yellow. Since the absorption of green and blue is higher, the refractive index at these wavelengths will be higher, and therefore, the optimum particle size will be smaller since it decreases with increasing refractive index. (See Figure 9.)

The exact form of the dispersion curve for pure Y-293 dye is not known. The refractive index of the pure dye for red and yellow is 1.8. For green and blue it is probably higher; for violet, probably lower. In any case, the optimum particle size is lower than for Diol or for dye dissolved in Diol. It is probably near

that of sulfur, index = 2.0, for which the mean optimum particle radius is 0.15 micron. (See Figure 9.)

The observed optical density of pure dye smoke (of unknown particle size), measured with blue light ($\lambda = 0.44$ micron) outdoors,[18] was about one-half the observed and calculated optical density of both sulfur and Diol for green light ($\lambda = 0.524$ micron) at the optimum particle size. Diol has a scattering cross section of 11 to 12 sq m per g (see Figure 9) for radii between 0.22 and 0.34 micron, and sulfur has about the same scattering cross section for the radii 0.12 to 0.18 micron. The dye smokes should have at least the same scattering cross section at their optimum radius (probably about 0.2 micron). The fact that the observations on the dye smoke were made for blue light and the measurements on sulfur were made with green light does not invalidate this statement since the optical density of sulfur smoke near the optimum particle size ($r = 0.12$ to 0.18 micron) is practically the same for all visible wavelengths. This can be seen in Figure 9 by dividing the λ scale by 2 to correspond to $r = 0.15$ micron.

The indications are that the dye smoke particles produced by the orange smoke signals are smaller than the optimum size when produced outdoors and larger when produced indoors. The dye smoke particles produced indoors were examined with a high power microscope of high resolution. They were too small to be measured accurately but appeared to be not greater than 0.3 or 0.4 micron in radius. The particles produced outdoors appeared smaller for the following reasons.

In a dye smoke, the color of the transmitted light is an indication of the size just as it is in the case of transparent particles. For example, the dye smoke produced by burning the orange signals in a 22-cu m room appeared pale green by transmitted light. This occurred because the particles had grown large due to rapid coagulation of the dense smoke. They became somewhat greater than the optimum size so that the transmitted light appeared green as it does through a screening oil fog whose droplets are somewhat greater than the optimum size (green sun's disk). On the other hand, deep red or orange is frequently transmitted by the dye smoke produced outdoors showing that the particles are smaller than the optimum size.

It has been observed frequently that the color of a cloud of dye or other colored smoke becomes paler with dilution. This is a necessary consequence of the absorbing properties of such smokes. A dense cloud of small orange dye particles appears orange by scattered light and deep red or orange by transmitted light. The cloud transmits red and yellow as does an oil solution of the dye, and the color of a cloud becomes paler with dilution, as the color of a solution becomes paler with dilution.

A dense cloud of small orange dye particles appears orange because of *multiple scattering* and *absorption*, and not because of primary scattering, which is practically colorless. At each rescattering, slightly more green than red is abstracted from the light by selective absorption in a particle, so that the light which is finally scattered from the interior of a dense cloud has had much of the blue and green abstracted from it and consequently appears red or orange. In a dilute cloud, however, the multiple scattering is greatly decreased. A great deal of primary scattering is seen, which is practically colorless.

However, in a cloud of large particles, the color decreases less rapidly with dilution. Due to greater selective absorption, larger particles abstract a greater proportion of blue at each scattering process so that less multiple scattering is required to produce a strong orange color. Again, as with the dye smoke produced indoors, if the size is somewhat greater than the optimum, then selective scattering may cause the transmitted light to appear green.

21.5.2 Tables of Calculations

Tables of calculations, based on the Mie theory for absorbing particles, have recently been completed. They can be used to obtain the total scattering by a droplet of transparent oil of real refractive index $m_0 = 1.50$ containing dye in solution. When the absorption index k of the dye solution is known as a function of wavelength, the total scattering can be calculated for a complex refractive index m, ranging in value from $m = 1.44(1 - ik)$ to $m = 1.55(1 - ik)$ for values of α up to 6.0. The index k can have values up to 0.03, which corresponds to high absorption. These calculations cannot be used for pure dye smokes whose real refractive index is 1.8.

It should be pointed out that these calculations will also yield the total scattering by a transparent particle of refractive index from 1.44 to 1.55 when k is made equal to zero. Approximately correct values will be obtained for refractive indices as small as 1.33 and as large as 1.65.

These tables have been published by the Mathematical Tables Project.[19]

Chapter 22

MEASUREMENT OF PARTICLE SIZE AND SIZE DISTRIBUTION

By *David Sinclair*

22.1 MICROSCOPIC EXAMINATION

22.1.1 Light Microscope

THE LIGHT MICROSCOPE has long been the standard method of observation of the particle size and distribution of smokes. It possesses the advantage that the true shape and size of the particles can be obtained, provided the radii of the primary particles are not less than 0.3 micron. It has the disadvantage that a long and tedious series of measurements is required to obtain a distribution curve.

Solid particles are usually composed of more or less loosely bound aggregates of primary particles too small to be resolved by the light microscope. To reveal the true structure of such particles, the electron microscope is required.

When liquid droplets are observed on slides, the true diameter is not observed since the drop is flattened, more or less, by its weight. The amount of flattening depends to a marked extent on the properties of the surface of the slide as well as the nature of the droplet. If a carefully cleaned slide is used, a definite relationship exists for a given drop material, between the observed diameter of the flattened drop and its focal length.

May [1] has given equations and curves from which the true diameter can be read when the lens diameter and focal length have been measured. The amount of flattening of the drop can be reduced by coating the slide with an oleophobic film.[2]

This method has sometimes been found unreliable. Observation of 4 microns radii droplets (determined by the gravity fall method and also by weighing a known number of droplets) gave results 25% too small when the radius was calculated from microscope measurements of the lens diameter.

Volatile droplets on slides may evaporate so rapidly that the true diameter cannot be obtained. This may be avoided by allowing the drop to settle into a viscous liquid film in which it is insoluble.[1]

This method has been successfully applied to the measurement of the radii of water fog droplets.[3] A small drop of castor oil is placed in a depression slide and spread into a film. The water drops are allowed to settle onto the oil and then immediately covered with a cover glass coated with oil. The water drops are thus imprisoned and may be observed at leisure. The true diameter of the drops is observed, since they assume a spherical form while floating in the oil.

Because the density of castor oil is 4% less than that of water, the droplets will finally sink to contact with the slide. They will usually spread and change their shape. This may occur for large drops before they can be measured. The spreading may be prevented by coating the depression with a thin, transparent film of paraffin.



FIGURE 1. Electron microscope photo of ZnO particles.

The light microscope may be used to measure smoke particles in situ. This method has been investigated in great detail by Whytlaw-Gray.[4] The difficulties of this method have been analyzed and some of the defects corrected by Stumpf.[5]

In general, the light microscope is most useful as an auxiliary to other methods. These methods, described below, make possible rapid measurements on a mass of particles in their actual state of dispersion, either in the laboratory or in the field.

22.1.2 Electron Microscope

The electron microscope reveals details of the shape, structure, and size of particles completely unobservable by any other method. For example, some magnesium oxide particles of 1 or 2 microns diameter, as seen in the light microscope, are found to be irregular aggregates of a large number of cubical crystals as small as 0.01 micron on a side (see Figure 1, Chapter 18). Carbon particles are found to be long filaments of extremely small spherical particles (see Figure 3, Chapter 18). Similarly, the structure of particles of zinc oxide and lithopone are revealed by such photographs as Figures 1 and 2. Extensive observations of the structure of aerosol particles have recently been made with the electron microscope by Eyring,[6] McGrew,[7] and others.

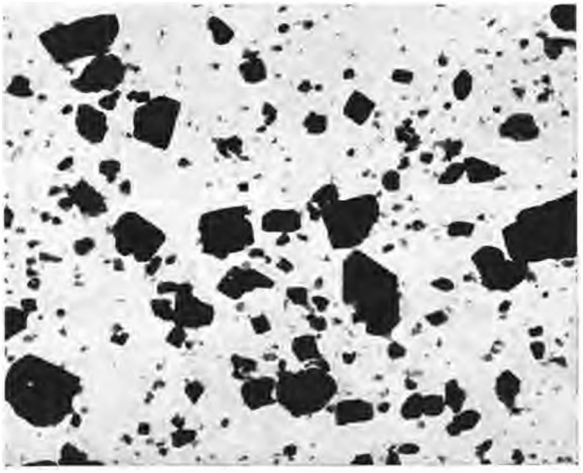


FIGURE 2. Electron microscope photo of lithopone.

The electron microscope has some of the disadvantages suffered by the light microscope. The particles are not observed in the dispersed state and may be altered during or after sampling. This is especially true of fog droplets which are evaporated and distorted by the energy in the electron beam. For this reason, particles must have a vapor pressure at room temperature of not over 10^{-5} cm of Hg, if they are to be observed in the electron microscope. The problems presented by various sampling methods are described in the next section.

The difficulties of obtaining a true particle size distribution curve are even greater with the electron microscope than with the light microscope. Because the magnification is high, the field of view of the electron microscope is so small that a large number of photographs must be taken in order to obtain a representative picture. This greatly increases the time and labor involved in making a count.

Furthermore the details of individual particles observable with the electron microscope are often unimportant, or are averaged out in the mass of particles in an aerosol. For example, the obscuring power of a smoke of solid particles is determined by the average cross section of the particles, their shape and structure being unimportant. For such problems a method of size measurement is desired which will yield the particle area distribution as rapidly as possible.

Similarly, the rate of fall of particles is determined by their geometric cross section and particle density (generally less than the true density of the solid material), so that these quantities can be obtained by suitable measurements of the rate of fall. It would be extremely tedious if not impossible to obtain the particle cross section and density from electron microscope photographs.

In general, the method of measurement should be adapted to obtaining the properties of the aerosol of particular interest.

The electron microscope, even more than the light microscope, is not suitable for measurements in the field. For these reasons the electron microscope, like the light microscope, is most useful as an auxiliary to the methods of measurement of particle size and distribution in the aerosol state, described in following text.

22.2 SAMPLING METHODS

22.2.1 Centrifugal Separation

The cascade impactor is a form of centrifugal separator developed at Porton Experimental Station.[1] It is suitable for particles above 1-micron radius. The aerosol is forced in succession through a series of jets directed at microscope slides perpendicular to their surface. For each succeeding jet the velocity of flow V is increased by decreasing the area of the jet opening; and the radius of curvature R of the path of flow is decreased by placing the jet nearer the surface of the slide.

Particles having a radius equal to or greater than r_1 [given by equation (39), Chapter 19] will be thrown out onto the first slide. Particles having a radius equal to or greater than r_2 will be thrown out onto the second slide, and so on, where $r_1 > r_2 > r_3 \cdots$, $V_1 < V_2 < V_3 \cdots$, $R_1 > R_2 > R_3 \cdots$.

As stated in Chapter 19, the values of $r_1, r_2, r_3, \cdots$

may be determined by the construction of the apparatus, which determines the length of time the particles are in the given centrifugal field, as well as by the values of V and R. The apparatus is usually constructed so that all the particles down to 1 micron radius are collected in four stages. Smaller particles may contribute a large amount to the total number of particles but they contribute a negligible amount to the total mass of large particle aerosols.

In order to obtain a constant range of sizes on each slide the velocity of flow must be kept constant. This can be done by drawing the air through a critical pressure orifice. For example, this may be an opening in a glass tube, adjusted so that the pressure drop across it is appreciably greater than one-half an atmosphere when the flow has the desired value.[8] Under these conditions, moderate changes in the pumping rate have no effect on the flow through the orifice.

The cascade impactor, like the *impinger*,[9] has the disadvantage that the particles are likely to be distorted by the violent impact with the slide. Solid particles are frequently broken, resulting in too high a count of small particles, and droplets are spread out and greatly distorted from their spherical shape. Consequently, only an approximate idea of the true size can be obtained by direct microscope measurement of the impinged particles. An independent measure of size should be made so that the instrument can be calibrated for a given rate of flow and particle density. The cascade impactor has the advantage of compactness, and rapidity and ease of operation in the field.[1]

22.2.2 Thermal Precipitator

The thermal precipitator is particularly suitable for sampling heterogeneous smokes of particle radii less than 1 micron. As described in Chapter 19, aerosol particles will move in a temperature gradient from a hot body toward a colder body with a velocity directly proportional to the temperature gradient. With a high temperature gradient, the force acting on a particle is many times the force of gravity and the particle is deposited quickly. By placing the hot and cold bodies close together, the temperature gradient can be made high when the temperature difference is low (50 to 100 C).

All the particles can be removed quickly from a small volume of smoke in a few minutes so that a true sample can be obtained. Thus, this method is superior to deposition by gravity, which discriminates against small particles because of their lower rate of fall.

This method is superior to centrifugal separation of solid particles since it does not shatter or distort the particles by high velocity impact. It is not suitable for collecting volatile droplets because the hot body causes evaporation.

A type of precipitator that gives 100% precipitation is described by Watson.[10] A similar piece of apparatus was constructed at Columbia University and used to sample both solid and liquid smokes, which were also analyzed with the differential settler.

The apparatus consisted of a heated wire 0.007 in. in diameter, placed midway between two cold microscope cover glasses which were 0.015 in. apart and mounted with their planes vertical and parallel. Each cover glass was supported on one end of two brass plungers which fitted into a brass cylinder. The wire was stretched across the center of the cylinder, perpendicular to the axis. The wire was insulated from the cylinder and was heated to about 100 C by an electric current. The plungers carrying the cover glasses were inserted at opposite ends of the cylinder and held against stops so that each cover glass was at a distance of about 0.004 in. (about 100 microns) from the surface of the wire.

The method of sampling was as follows. The flask of smoke from which a sample was taken for the differential settler was immediately connected by a rubber tube to the thermal precipitator. Smoke was then drawn in between the cover glasses through an inlet tube in the top of the cylinder. The direction of flow was at right angles to the length of the wire. The smoke particles were all deposited on each of the two cover glasses in a strip parallel to the wire and a little ahead of a line opposite the wire.

The rate of flow was kept constant at about 3 cc per min by allowing water to flow slowly out of a reservoir connected to an outlet tube in the bottom of the cylinder. One to three minutes were required to obtain a sample, depending on the particle concentration and size of the smoke.

The efficiency of collection was tested by drawing the air from the precipitator through a spherical flask illuminated by an intense Tyndall beam. Any particles, even extremely small ones, can be readily detected by this method. When the flow was less than about 5 ml per min, no particles could be found in the flask.

The deposits were measured and counted, using a

microscope having an objective of numerical aperture about 0.85 and magnification of 120 diameters. This was used with a micrometer eyepiece, magnification 20 diameters, which was calibrated with a Zeiss stage micrometer. One division on the ocular micrometer = 0.86 micron. The diameter of particles of 0.3 micron radius and larger could be read to ± 0.1 division or about ± 0.1 micron in diameter, i.e., ± 0.05 micron in radius. Particles below 0.3 micron radius could only be estimated.

Distribution curves were obtained by counting about 200 particles. A count of a larger number of particles would be necessary for an accurate distribution curve, but the number counted seemed sufficient for the purpose of testing the performance of the differential settler.

There was some indication of separation of sizes along the direction perpendicular to the hot wire. The smaller particles seemed to be deposited sooner than the larger, in conformity with the theory (Chapter 19). Consequently, in order to obtain as true a count as possible, the counts were made along several lines which completely traversed the deposit.

The particles were deposited in two strips about 1 mm wide and 1 cm long, i.e., over an area of 0.2 sq cm. In 2-min flow at a rate of 3 cc per min, a smoke of 10^5 particles per cc would yield a deposit of 6×10^5 particles. These 6×10^5 particles of 1 micron radius have a total cross-sectional area of 0.002 sq cm, or 1% of the area on which they are deposited. Thus 1% of these particles should be expected to touch and form some sort of double particle. An equal number of smaller particles are less likely to touch, and the time of sampling can be shortened for larger particles.

The normal appearance under the microscope of a deposited smoke prepared from undecomposed stearic acid is that of solid spheres, which are probably supercooled liquids of high viscosity. (The melting point of pure stearic acid is 69 C.) Frequently, however, the particles were not spherical. There were a few doublets which could have been formed either by coagulation in the aerosol or by collision at the time of deposition. Sometimes the slides showed many crystals, either leaves or tetrahedra. These were most numerous when using an old batch of stearic acid which had turned dark brown from the decomposition products.

Crystallization may have occurred in the aerosol, but more probably at the time of deposition on the slide. (It was frequently found that particles, originally deposited as spheres, had changed their shape by the following day.) Scintillating crystal particles are always observed in an aged smoke and only rarely in a freshly made heterogeneous smoke. No scintillating particles were observed in many fresh smokes which, after deposition on the microscope slide, showed leaf or tetrahedral crystals. It seems probable, therefore, that the condition of the surface of the cover glass caused the observed variety of shapes of the particles.

As has already been mentioned, drops will spread when deposited on a hard surface so that the diameter observed in the microscope will be too large.

The thermal precipitator was also used to obtain deposits of lithopone and zinc oxide on electron microscope slides. A brass disk, having a depression cut to fit an electron microscope screen, was used in place of one of the light microscope cover glasses. This method was found to be very unreliable since most of the particles were deposited onto the plastic film on top of the wires where they could not be observed. Furthermore, the heat from the wire tended to break the film on the screen.

A microscopic examination of the plastic film on a new screen revealed the fact that the film sagged between the wires. The center of the film was as much as 20 microns lower than the part touching the wires. This is one-fifth of the distance between the screen and the hot wire of the thermal precipitator. The result is that the thermal gradient is 25% greater over the wires than over the center of the film, so that the particles tend to deposit on top of the wires.

Figure 1 shows one of the few good thermal deposits of ZnO obtained. The sample for Figure 2 was prepared from a liquid dispersion of lithopone. The latter appears to be the only reliable method of preparing electron microscope screens.

22.2.3 Gravity Settling

Gravity settling yields a slide on which the particle number distribution usually differs from that in the aerosol. Unless the slide is left in so long that all the particles settle out, the number of particles of smaller radii which settle out will be less than the true distribution in proportion to the square of the radius. [See equation (1), Chapter 19.] In general, it is impractical to wait for all the smallest particles to settle out.

Consequently, the slide is usually placed in the aerosol for a few minutes and the number distribution corrected by multiplying the observed number of

particles of radius r by r_0^2/r^2. This correction is valid only in tranquil settling, and is applied only to particles of radius $r < r_0$ where r_0 is the radius of the particle for which the distance of fall during the time of exposure of the slide is equal to the distance from the slide to the top of the settling chamber.

According to equation (2), Chapter 19, in stirred settling the fraction f_s of particles having a given velocity v, which settle out during the time t of exposure of the slide is

$$f_s = 1 - e^{-vt/h}. \quad (1)$$

Consequently, the correct number distribution can be obtained by dividing the number of particles of a given size by the corresponding value of f_s.

In general, the type of settling of an aerosol in a closed chamber is somewhere between tranquil and stirred settling, so that an exact correction cannot be applied unless care is taken to maintain either tranquil or stirred settling. For small particles, gravity settling is not suited to obtaining a representative sample because of the length of time required.

22.2.4 Mass Concentration

The mass concentration of an aerosol can usually be readily measured by collecting a known volume in a glass wool filter and weighing. A small drying tube is half-filled with fine fiber glass wool, which should be packed in fairly tightly. The aerosol is drawn through the tube for a given length of time at a rate of about 10 lpm, measured with a flow meter, or a critical pressure orifice.

The efficiency of collection is observed by drawing the filtered air through a spherical flask illuminated with a Tyndall beam. If an appreciable number of particles are observed, more glass wool should be inserted, or the rate of flow decreased. Small particles pass through more readily than large particles.

This method is suitable for aerosol concentrations down to about 10 μg per l. At this concentration and a flow rate of 10 lpm for 30 min, an efficient filter would collect 3 mg, which can be measured with fair accuracy. For lower concentrations a microfilter, developed at Porton,[11] may be used.

22.2.5 Optical Mass-Concentration Meter

The optical mass-concentration meter may be used, when calibrated, to measure concentrations from 200 μg per l down to 10^{-3} μg per l. The instrument is a form of Tyndall meter, modified so that dark field illumination is used. The light scattered forward at angles from about 5 to 30° is observed, instead of that scattered at 90°. As the Mie theory shows, the observed intensity may thus be 100 or even 1,000 times greater. The instrument was developed for measurement of filter penetration.[12]

A schematic diagram of the apparatus is shown in Figure 3. The source S is a 6-v, 32-cp automobile

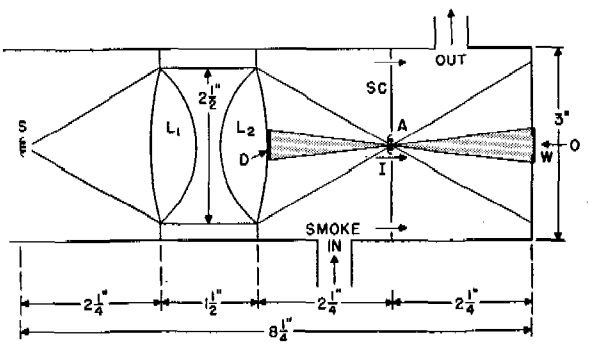


FIGURE 3. Schematic diagram of optical mass-concentration meter.

headlight bulb. L_1 and L_2 are aspheric condenser lenses of about 2¼-in. focal length and 2½-in. diameter. The source is placed at the focal point of L_1. A high intensity image of the source is formed by L_2 at its focal point. At this point the conical beam passes through a 3/16-in. diameter aperture A in the screen S_c. The smoke enters through a glass tube below A, passes through A and several peripheral holes in the screen and leaves the chamber through the tube above A.

A black, opaque disk D of about ½-in. diameter is painted or glued onto the lens L_2. This disk D blocks out a cone of central rays. Observation along the axis of the cone through the window W (about ¼-in. diameter) shows the smoke brilliantly illuminated, but no direct rays reach the eye. The observer sees only the rays which are scattered along or near the axis of the cone, the direct rays from the source being absorbed by the blackened end of the chamber. Stray light is reduced to a minimum by blackening the whole of the interior of the chamber, preferably with soot.

When no smoke or dust particles are present, the observer sees only the black background of the disk D, provided the aperture A is small enough. The aperture A must be so small that no scattered light from the edge of D or from dust particles on the lenses reaches the window. The aperture A must be larger than the image of the source. When the lenses

are not achromatic, violet rays strike the edge of A but are so faint that the resultant stray light is quite weak.

The sensitivity of the apparatus is such that the dust in ordinary room air appears brilliantly illuminated. Consequently, the chamber must be airtight. The zero reading for no smoke in the chamber is made while well filtered air is passing through.

The instrument is calibrated for a given smoke by observing the intensity at several concentrations high enough to be measured by collection in a glass wool filter. The concentration of more dilute smokes is then directly proportional to the intensity.

Because of turbulence the smoke fills the chamber completely. For this reason, a smoke of concentration higher than about 200 μg per l should not be used. At higher concentrations the loss in intensity of the direct beam due to scattering becomes appreciable, so that the linear relationship between observed intensity of scattered light and concentration no longer holds.

The calibration is correct over a wide range of mass concentrations provided the particle size remains unchanged. For this reason the smoke must not be so dense that appreciable coagulation occurs. This sets an upper limit to the mass concentration which decreases with particle size. Because of the short time of flow the maximum allowable number concentration is 10^6 per ml (see Chapter 19). Therefore, a 0.5 micron radius homogeneous smoke will not show appreciable coagulation up to 500 μg per l while a 0.15 micron radius smoke must not be over 14 μg per l (see preceding text).

The measurement or other purpose for which the aerosol is used must not change the particle size appreciably. For example, when using heterogeneous smoke to measure filter penetration, the dilute smoke which issues from the filter usually has a smaller average particle size than the more concentrated smoke entering the filter (see Chapters 19, 23, and 24). Consequently a fairly homogeneous smoke is particularly necessary when measuring filter penetration with the optical mass-concentration meter.

22.3 METHODS BASED UPON GRAVITY SETTLING

22.3.1 Measurement of Individual Particles

The velocity of fall of particles under gravity may be used in a variety of ways to measure their size. The simplest method is to observe with a low power microscope the individual particles when brightly illuminated in a small closed chamber. The radius may be calculated from the observed velocity of fall by means of the Stokes-Cunningham law of fall. (See Chapter 19.)

This method is suitable only for qualitative measurements. In order to obtain quantitative results a large number of particles must be observed and it is difficult to make the measurements representative. The tendency is to select the larger, brighter particles. Furthermore, the smaller particles are difficult to follow because of Brownian movement and the larger particles are likely to fall out before they are observed.

22.3.2 The Homogeneous Smoke Settler

The particle size of a homogeneous smoke may be conveniently measured by observing the rate of fall of the top of the cloud in a settling chamber free from convection currents. (See Chapter 19.) The observation is made with a Tyndall beam from a source which may be held in the hand or mounted so that it can be moved up and down conveniently. If care is taken to shield the chamber from radiation, the top of the smoke cloud will remain quite flat and sharp for an hour or more.

A form of settling chamber, previously described,[13] consisted of a 3-in. diameter Pyrex tube 18 in. long, closed at the bottom with a rubber stopper and at the top with a brass plate cemented to the glass. This chamber is submerged in distilled (dust free) water contained in another glass cylinder and kept at a uniform temperature by stirring.

Smoke is introduced through two brass tubes soldered to holes in the brass top of the settling chamber and extending above the water level. These tubes contain needle valves which are operated from above the water level by wires or strings. This apparatus avoids mechanical and temperature disturbances.

Tranquil settling may best be obtained by placing the chamber in a darkened room free from draughts or other causes of rapid temperature change. A water cell should be used to remove the heat from the Tyndall beam, which is turned on only when a reading is being taken.

The height of the cloud is recorded at suitable time intervals by sighting along the top of the cloud and marking the position on the wall of the water

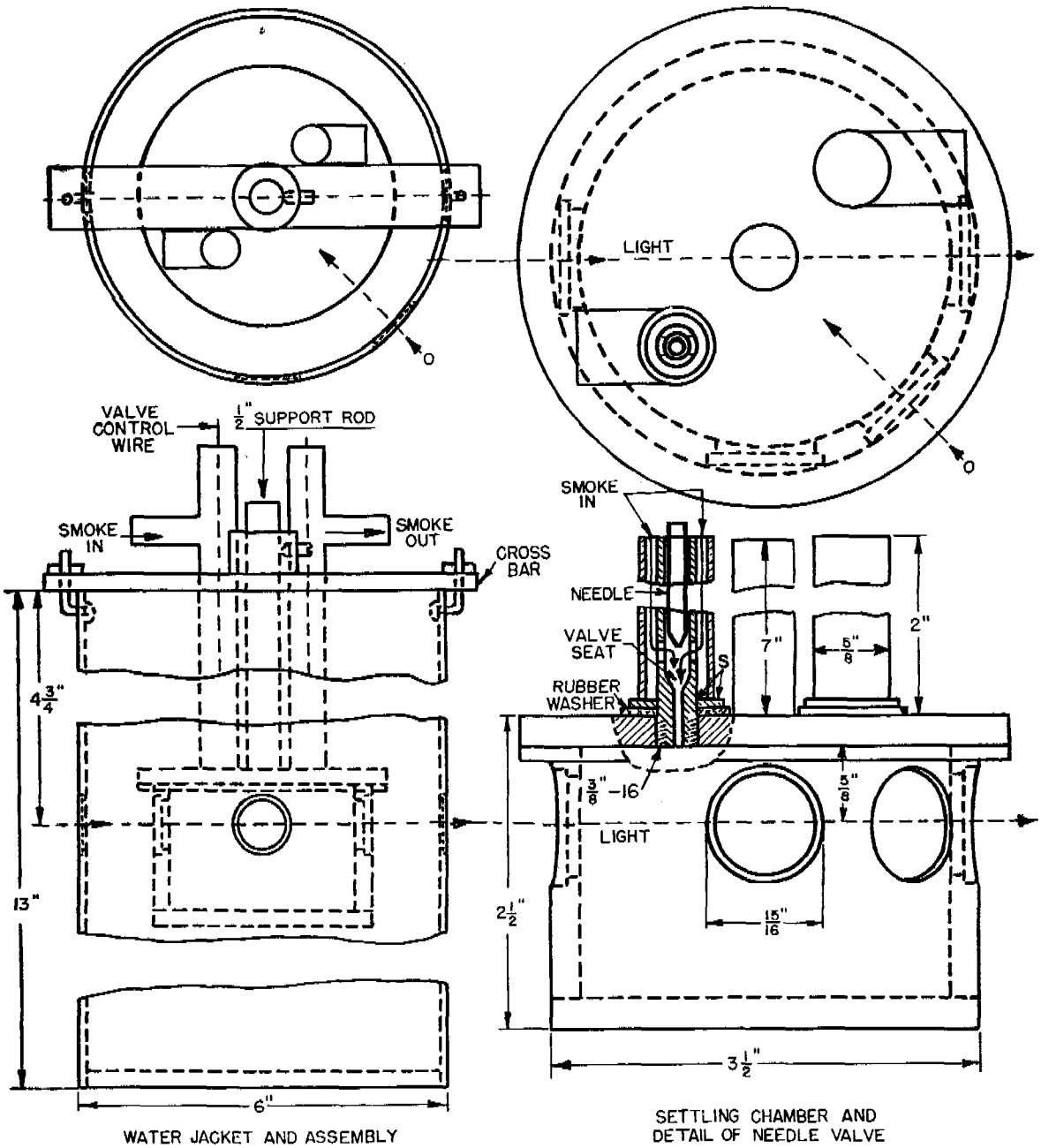


FIGURE 4. Differential settler.

jacket with a wax pencil. A precision of 5% or better can be obtained readily from four successive readings.

This method can be used for rates of fall from about 4 cm per hr up to 160 cm per hr, corresponding to radii from 0.3 to 2 microns for a material of unit density, and radii from 0.2 to 1½ microns for material of density 2 g per cc, such as sulfur.

Radii down to 0.1 micron may be measured by observation (with a low-power microscope) of the individual droplets in a small chamber. Frequently, the microscope observation can be made on the top of the cloud. Although the top becomes considerably spread due to Brownian movement (see Chapter 19), an average position can be measured with fair accuracy. This method yields sufficiently accurate re-

sults with a few measurements in the case of a homogeneous smoke.

For radii below 0.1 micron the Brownian movement becomes so large that the results are unreliable.

22.3.3 Differential Settler

The differential settler is an instrument designed to measure the size and size distribution of a heterogeneous smoke. As described in Chapters 19 and 21, the rate of change of the number of particles, $\Delta n/\Delta t$, at a fixed height in an aerosol in tranquil settling is proportioned to the rate of change of the scattered light intensity $\Delta I/\Delta t$.

Figure 4 is a diagram of the apparatus constructed and used to measure the size distribution of a variety of smokes having spherical particles.[14]

The settling chamber consists of a hollow brass cylinder closed with brass end plates, 3 in. in diameter and 2 in. high, inside dimensions. The walls of the chamber are ¼ in. thick.

The smoke is illuminated and observed through plane glass windows cemented over circular holes bored in the side of the chamber. The chamber is submerged in distilled (dust free) water contained in a brass water jacket and kept at a uniform temperature by a stirrer (not shown in diagram). The water jacket also carries windows, located opposite the windows in the settling chamber.

Smoke is introduced through two brass tubes soldered to holes in the top of the settling chamber and extending above the water level. These tubes contain needle valves which are operated from above the water level by wires. This apparatus avoids mechanical and temperature disturbances.

In order to make reliable intensity measurements and also to prevent convection currents, it is necessary to reduce stray light to a minimum. For this purpose, clear plane windows consisting of polarimeter tube cover glass 23.7 mm in diameter are used. By means of a slit 2 mm high and 8 mm long, the illuminating beam is made small enough so that it enters one window and leaves by a diametrically opposite window without touching the chamber walls. The light is made roughly monochromatic with a green filter and is completely screened off between readings.

The illuminated smoke is observed at an angle O of $45° \pm 5°$ to the incident beam, as shown in the diagram. The intensity is measured with a Luckiesh-Taylor brightness meter. The 8-mm depth (in the direction of observation) of the illuminated volume of smoke provides sufficient intensity of scattered light for accurate measurement. The smoke should be as dilute as possible in order to prevent coagulation during the time of a run. With fine particle smokes, this time may be as much as an hour or more.

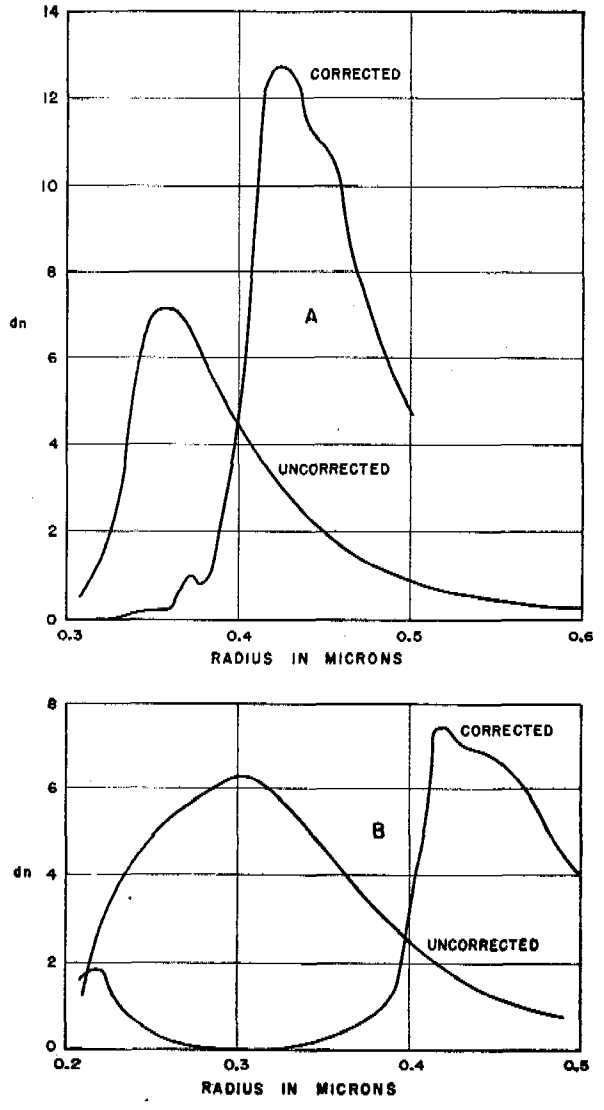


FIGURE 5. Corrected and uncorrected differential settler curves.

The 2-mm thickness (in the vertical direction) of the illuminated volume is the least that will provide a large enough field of view for good matching with the Luckiesh photometer. The thickness of the illuminated region should be kept as small as possible relative to the height of the top of the chamber above the illuminated region. A convenient height is 1.5 cm. A greater height makes the length of some runs exces-

sive, and a smaller height introduces too large an error in the determination of the starting time of a short run. With the above dimensions the intensity observed at any one time is that due to all particles within the region 1.5 ± 0.1 cm from the top. This introduces an error such that a smoke of uniform particle size appears to have a spread in size of about 7%. This is not considered excessive.

When the particle density is known, the particle size can be calculated from the relative intensity at any time provided the law of scattering of light with particle size is known. In the previous measurements described elsewhere,[14] it was assumed that the law of scattering for spherical particles was given with sufficient accuracy by making p [see equation (11), Chapter 21] equal to 3 for all values of the radius. This yielded a distribution curve which was not even approximately correct in some cases.

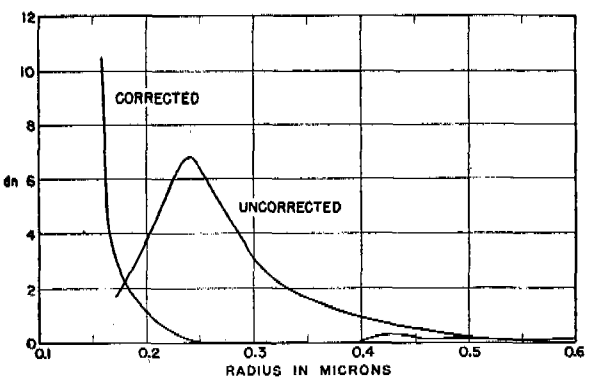


FIGURE 6. Corrected and uncorrected differential settler curves.

The true law of scattering is given in Figure 10, Chapter 21. Some of the distribution curves, previously given, were corrected by means of Figure 10, Chapter 21. The results are shown in Figures 5 to 8 which show the relative number of particles dn of radius r microns.

It will be seen that some of these curves, notably those in Figures 6 and 8, are completely altered. It is not certain that the curves of Figure 10, Chapter 21, are the proper correction curves. In correcting the distribution curves, the observed 7% spread in particle size as well as the 10° spread in angle was taken into account as far as possible.

A more reliable method would be to obtain an experimental calibration curve using very homogeneous smokes. In addition, a type of illumination similar to that used in the optical mass-concentration meter might be used. This would provide a greater angular spread in illumination which would tend to smooth out the calibration curve.

Furthermore, more intense illumination would make it possible to use smokes of low concentration, thus avoiding coagulation which may have been a

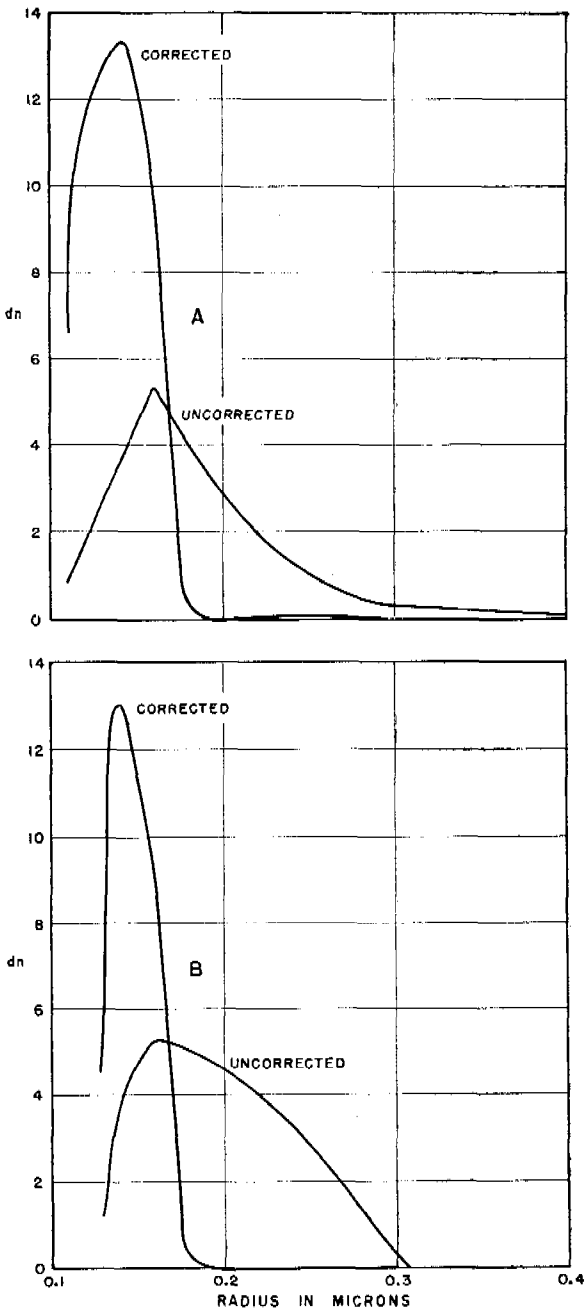


FIGURE 7. Corrected and uncorrected differential settler curves.

disturbing factor in the measurements made with the differential settler thus far.

22.3.4 Stirred Acrosols

The equations to be used in the measurement of particle size and size distribution of uniformly stirred acrosols have been given in Chapter 21.

Homogeneous Aerosol with Slow Coagulation

If the aerosol is initially homogeneous and undergoes slow coagulation, equation (13), Chapter 21, describes the early stages in the life of the aerosol. Some experimental results obtained by this transmission method have been described elsewhere.[15]

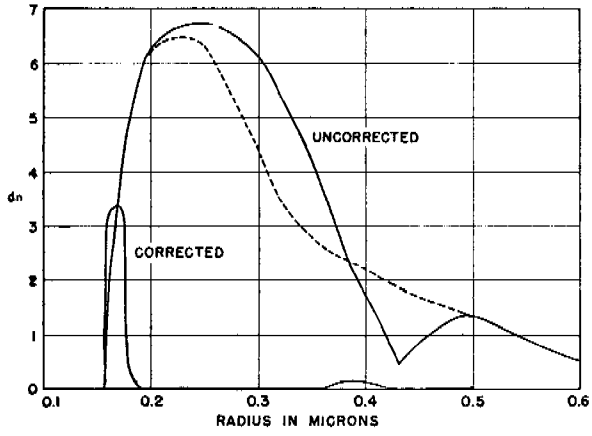


Figure 8. Corrected and uncorrected differential settler curves.

Heterogeneous Aerosol without Coagulation

When a heterogeneous aerosol is sufficiently dilute so that coagulation is negligible, equations (14) to (20), Chapter 21, may be employed. This transmission method has been used [16] to obtain the initial size distribution of aerosols of zinc oxide and egg albumin dispersed with the *geyser* and with the gas ejection bomb described in Chapter 20.

The average diameters of the equivalent spheres (see Chapter 21), that is, spheres having the density, rate of settling, refractive index and scattering cross section of the actual particles, were obtained from measurements of the initial scattering per cc of aerosol, S_t [equation (15), Chapter 21], and the mass concentration, M_t [equation (9), Chapter 19]. The values of S_t and M_t were plotted on semi-log paper.

Extrapolation of these curves to zero time gives the initial scattering per cubic centimeter, S_0, and the initial mass concentration, M_0, from which the initial scattering per gram, $A_0 = S_0/M_0$ [equation (18), Chapter 21], is obtained. The slopes of these two curves at zero time give the initial values of $u_s = d/dt \log S_t$ [equation (17), Chapter 21], and $u_m = d/dt \log M_t$ [equation (16), Chapter 19].

In order to facilitate the analysis of the experimental measurements, figures were drawn from which the values of ρ, d_g and σ_g can be picked off when the experimental quantities u_s, u_m and A_0 are known. These figures were calculated by means of equations (5) and (16), Chapter 19, and (18) and (20), Chapter 21, as described in following text. They are particularly useful when the particles are so small that the scattering coefficient is greater than 2. This is the case for all Kadox particles and for the smaller statistical diameters of egg albumin, although in the latter case K_2 is only a little greater than 2.

Figure 9 shows the values of σ_g and ρd_g corresponding to a set of values of A_0 and R for egg albumin, where $R = u_m/u_s$. To obtain this figure, appropriate values of σ_g and ρd_g were chosen and from these, ρd_2, ρd_4, ρd_5, and ρd_9 were calculated by means of equation (5), Chapter 19. Using Figure 13, Chapter 21, K_2 and K_4 corresponding to ρd_2 and ρd_4 are read off, and these values, together with ρd_5 and ρd_9, are substituted in equations (18) and (20), Chapter 21, to calculate A_0 and $A_0(u_s/u_m)$.

Figure 10 shows the values of ρ corresponding to a set of values of ρd_8 and hu_m calculated by means of equations (5) and (16), Chapter 19.

The figures are used by finding on Figure 9 the value of σ_g and ρd_g corresponding to the experimental values of A_0 and $R = u_m/u_s$. Using the value of σ_g and ρd_g thus obtained, ρd_8 is calculated by means of equation (5), Chapter 19. Using this value of ρd_8 and the experimental value of hu_m, the value of ρ is obtained from Figure 10. The weight median diameter d_6, or other statistical diameter may then be calculated from equation (5), Chapter 19, using the values of σ_g and d_g just found. This calculation of d_6 may be checked by means of equation (17), Chapter 21.

22.4 OPTICAL METHODS

22.4.1 The Owl

As described in Chapter 21, the colors and polarization of the scattered light may be used to determine the particle size of a homogeneous smoke of spherical particles. An instrument, called the *Owl*, has been constructed and used for this purpose.[17] It

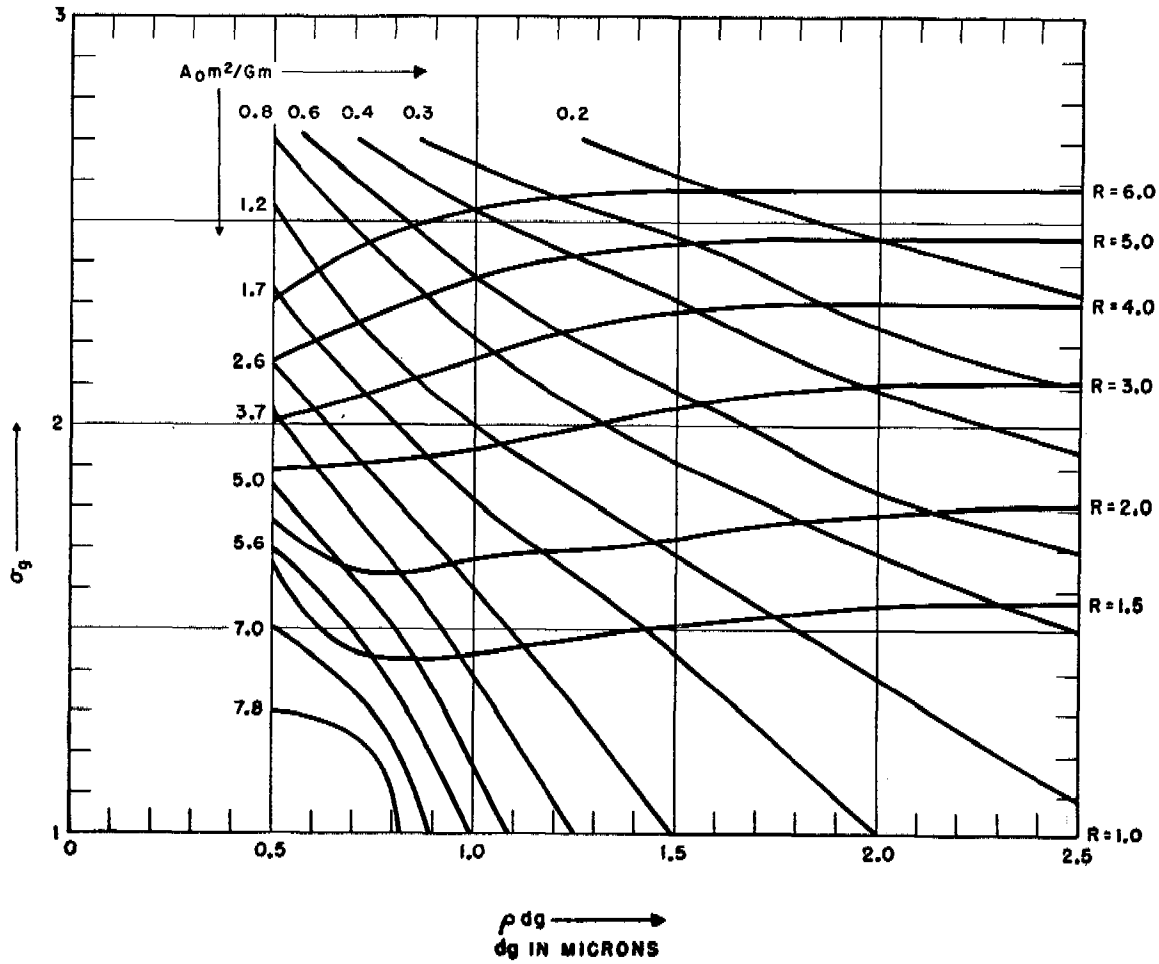


FIGURE 9. Values of σ_g and ρd_g for values of A_0 and R for albumin.

consists of an observation chamber and light source which may be held in the hand and rotated while observing the smoke through a low power microscope.

The observation chamber is a hollow metal cylinder 3 in. in diameter and 1 in. high (ID) having flat end plates, Figures 11 and 12. A window ½ in. high is cut in the side for an angular distance of a little more than 150°. Over this is cemented a section of a cylinder of uniform glass whose inside diameter is equal to the outside diameter of the chamber. This window enables observations to be made at all angles between 15 and 165° by rotating the chamber (and attached illuminator) about an axis through its center. The axis of rotation is perpendicular to the plane of observation.

The illuminator is constructed from microscope eyepieces and an automobile headlight bulb as shown in Figure 11. The arrangement shown provides a sufficiently intense light beam, parallel to ±3°. When the illuminator is properly adjusted, the light beam just clears the open end of the light trap.

On the opposite side of the chamber from the illuminator is a light trap consisting of a ⅝-in. diameter tube 2½ in. long with the far end closed with a metal plate. Except for the window, the inside of the chamber should be blackened with high quality, *dull* black optical lacquer and, preferably, also covered with soot. This can be conveniently done by means of the flame from burning camphor.

A semicircular scale, graduated in degrees, is mounted on the bottom of the chamber as shown in Figure 11. The illuminator should be located at 180° and the light trap at 0° to within 1°. A fiduciary mark should be placed on the supporting bar, extended, for reading the angle of observation, θ. The chamber is rotated by using the light trap as a handle.

By means of an atomizer bulb, smoke is blown in at

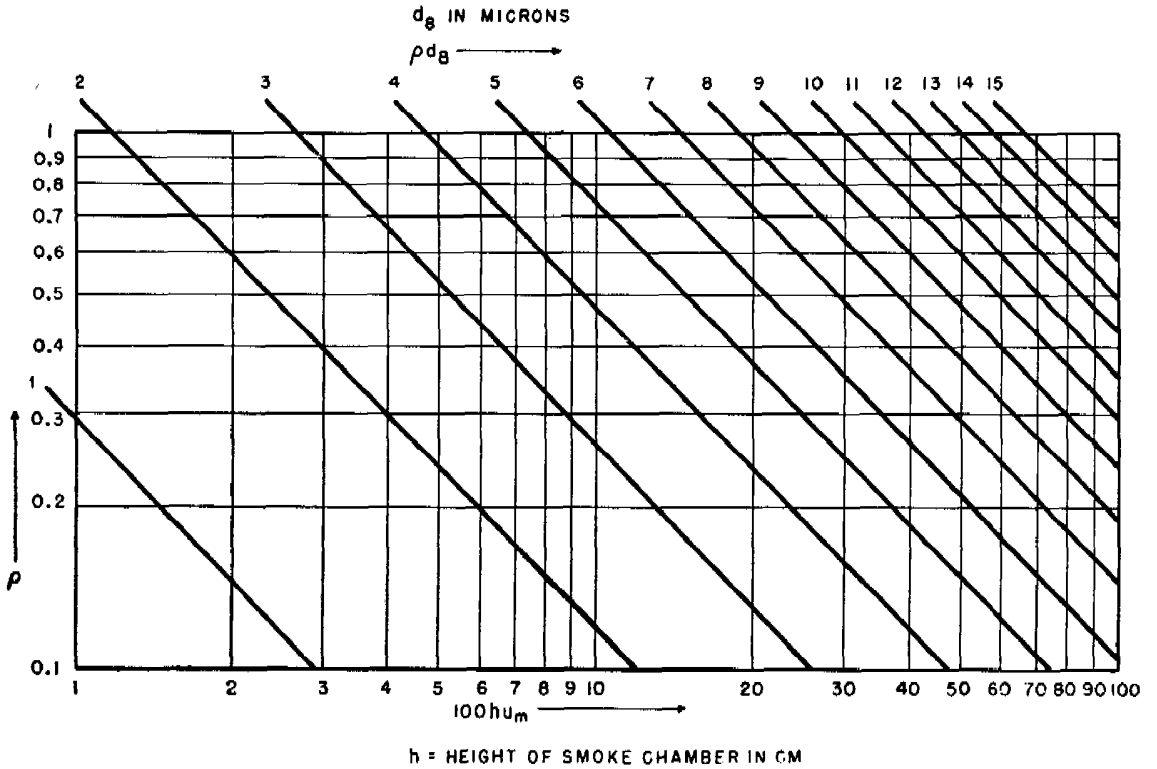


FIGURE 10. ρ vs hu_m for values of ρd_s.

the bottom and out through the top of the chamber. A ball valve is located at the bottom of the bulb, and another at the top of the chamber. A type of valve which does not stick easily is required.

The observations are made through a long focus microscope, of magnification 6×, constructed from ordinary microscope eyepieces as shown in Figure 11. The microscope is focused on the smoke particles in the center of the chamber.

The polarization photometer (see Chapter 21) is made by mounting a bipartite Polaroid disk in the eyepiece of the microscope, in good focus, with the dividing line parallel to the plane of observation to ±1°. This setting may be made as follows. Remove the chamber and illuminator from their supports and mount the illuminator so that the direct beam can be seen through the photometer and microscope. Mount a Polaroid (hereafter referred to as the *polarizer*) between the illuminator and telescope. The polarizing axis of the polarizer is set parallel (or perpendicular) to the plane of observation and the analyzer (see following paragraph) is set perpendicular (or parallel) thereto. When the polarizer and analyzer are thus *crossed* and the bipartite disk is oriented correctly, no light (except for the residual violet always transmitted by Polaroids) will be transmitted. If any white light is transmitted, rotate the bipartite disk until extinction is obtained, and fix it in this position.

The bipartite disk was made by the Polaroid Corporation (Cambridge, Massachusetts) using their new Polaroid-H laboratory-type film which, they report, gives about 99.99% polarization throughout most of the visible region. The polarizing axes of the bipartite disk are respectively perpendicular and parallel to the dividing line to ±1°. The dividing line between the two halves should be as inconspicuous as possible.

The analyzer is placed in front of or in the eyepiece *between the bipartite disk and the observer*. It consists of a piece of Polaroid-H laboratory glass mounted so as to be readily rotated about a horizontal axis. The angular setting, ϕ, is read off a quarter circular scale graduated in degrees. The scale is mounted so that the setting of the analyzer is accurate to ±1°. When $\phi = 0°$ the vibration or polarizing axis of the analyzer lies in the plane of observation.

A piece of Wratten 58B green gelatin filter is also mounted in front of, or in, the eyepiece. This filter should be fastened to the front face of the analyzer. Both the analyzer and filter should be readily removable out of the line of sight.

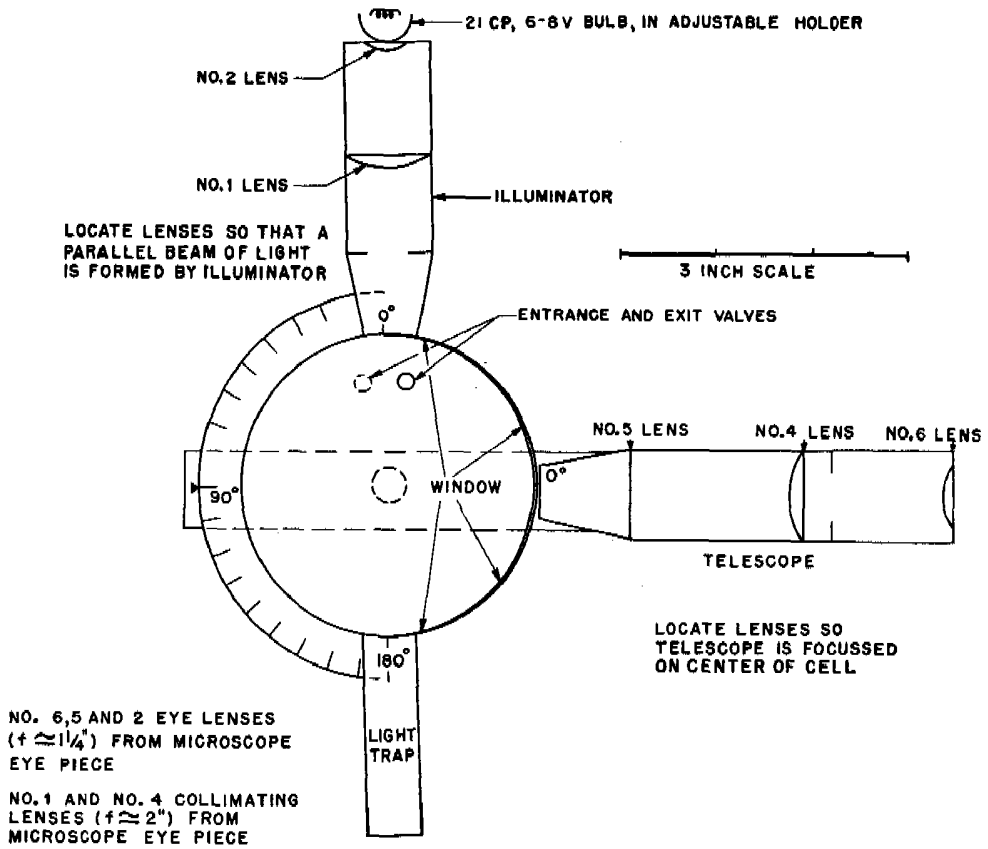


FIGURE 11. Plan of Owl.

In order that observation may be made in daylight, the microscope objective and window should be completely covered. One satisfactory method is to use a conical bag of opaque black cloth open at both ends. The small end fits over the microscope so that it does not interfere with the rotation of the chamber.

A tapered metal sleeve extending to just in front of the window is fitted over the microscope. This prevents the black cloth from obstructing observation. In addition, a black cloth hood is fastened around the eyepiece end of the microscope and thrown over the observer's head.

The foregoing description refers particularly to models made at Columbia University. Another model has been made commercially which is of improved design. Among other features, this model has a fine adjustment for setting the analyzer, and a facepiece which eliminates the need for the black cloth hood.

The particle radius corresponding to the observed angular setting of the analyzer is given in the calculated calibration curves, Figures 6 and 7, Chapter 21. The polarization at a radius of 0.11 micron for sulfur and at 0.17 micron for oleic acid has been checked experimentally by observing the rate of fall of homogeneous smokes under gravity in the small settling chamber described in preceding text.

The calibration curves extend down to 0.05 micron but readings below 0.10 are not reliable. It must be emphasized that these curves can be used *only* for small particle smokes of radii below 0.2 micron (for sulfur and tryphenyl phosphate only below $r = 0.15$ micron). In other words, they should not be used when the number of spectra (reds) observed is two or more.

For measurement of particles of radii from 0.20 up to 1.0 micron, remove the analyzer and green filter and count the number of times red is seen in i_1 as the observation chamber is turned from near 0 to near 180°. The description of the colors observed is given in Chapter 21, and the calibration curve is shown in Figure 4, Chapter 21.

The observations of the number of reds must be made on the scattered component i_1 alone, since the component i_2 exhibits a different series of spectra. The component i_1 is seen when the vibration axis of the analyzer is vertical. In a Polaroid-H disk, this

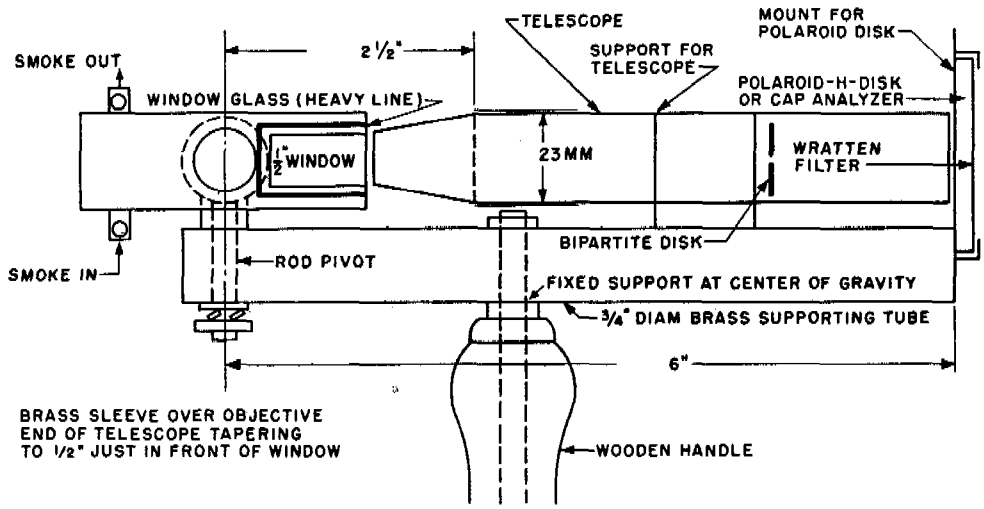


FIGURE 12. Assembly of Owl (vertical projection).

axis is parallel to the diameter through the diamond etched on the disk.

When observing without the analyzer, the two spectral series in i_1 and i_2 are seen simultaneously and adjacent to each other and the contrast between them frequently aids in the analysis of rather heterogeneous smokes.

When observing the spectra, attention should be paid to the angular position of the reds (Figure 5, Chapter 21) as well as their number. It is seen clearly how the position of the first red shifts from 100 to 20° as the number of spectra increases from one to seven, i.e., as the particle radius increases from about 0.1 to 0.7 micron.

22.4.2 Coronae

The radii of transparent fog droplets of 5 or 10 microns and over can be obtained by observing the diffraction rings or *coronae* formed around either a point source of light located in the fog, or, preferably, a beam of light shining through the fog. These diffraction rings are similar in appearance to the colors observed in Mie scattering by smaller droplets, except that the angles at which the colors appear are much smaller.

According to the theory of diffraction for opaque disks, the angular radius θ_1 of the first bright ring is given by $\sin\theta_1 = 0.819\lambda/r$ where λ is the wavelength of the light and r the radius of the droplet.[18] The second bright ring is given by $\sin\theta_2 = 1.346\lambda/r$, the third by $\sin\theta_3 = 1.858\lambda/r$, and the fourth by $\sin\theta_4 = 2.362\lambda/r$. The relative intensity of the first four rings is approximately 1, ¼, 1/10, 1/20.

The angular radii of the *dark* rings are given simply by $\sin\theta = (n + 0.22)\lambda/2r$ where n is the order of the ring.

The rings are observed most clearly in a fog of uniform droplet size. Experience has shown, however, that the uniformity need not be so great as in the case of Mie scattering. Kohler [19] has used this method for the measurement of the droplet size in water fogs of about 8 microns radius. He found that the rings are usually produced by the predominant size, with the larger sizes being favored since they produce the smallest and brightest rings. The writer has observed several colored rings in water fogs which contained droplets varying in radii from 4 to 16 microns or greater.

It is seen that the size of the rings is independent of the index of refraction of the droplets. This is so because the equations are derived for diffraction by opaque disks. For this reason, Wilson [20] states that the equations are not accurate for radii less than 10 microns and scattering angles θ greater than 10°.

For accurate measurement of radii below 5 or 10 microns, down to 1 micron (below which the Mie scattering can be used) the coronae radii could be calibrated against droplets of known size. However, an approximate value of the radius can be obtained for radii between 2 and 10 microns by the use of the above equations.

For this purpose Humphreys [18] gives a calculated curve showing the angular radii of the first and

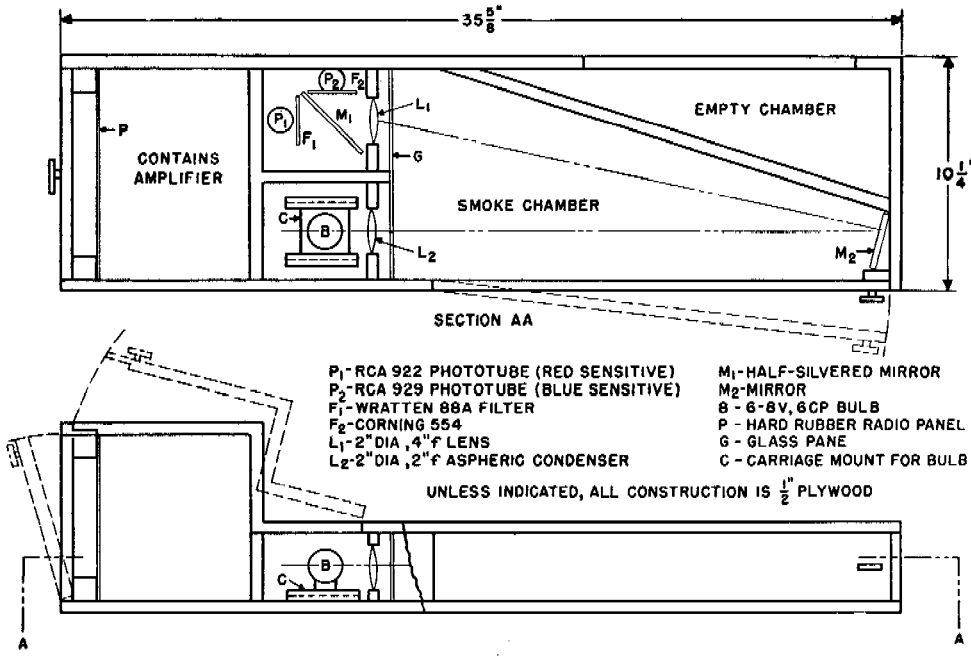


FIGURE 13. Slope-o-meter (layout of parts).

second red rings as a function of the radii of water droplets between 1 and 10 microns. It will be seen that these two curves are roughly extensions of the first two curves of Figure 5, Chapter 21.

The coronae were used to measure the size of lycopodium spores of fairly uniform size. The radius of these spores, as measured in a light microscope, was found to vary from 13.6 to 16.0 microns.

The spores were allowed to settle on a glass plate which was then placed in a beam of light of parallel rays and also in a slightly divergent beam from a point source. Measurements were made of the angular diameter of two orders of both the light and dark diffraction rings in both red and green light. From these measurements the spore radius was calculated to be 15.5 $\pm$ 0.2 microns, in good agreement with the microscope measurements.

Similar measurements were made on a uniform droplet size oil fog in a flask. The radius, as measured by two independent methods was 4.0 $\pm$ 0.1 microns. The agreement here is less good, as is to be expected for such small, transparent spheres.

22.4.3 The Slope-o-Meter

The particle size of a homogeneous smoke, or an average size of heterogeneous smoke, may be obtained by measuring light transmission as a function of wavelength (Chapter 21). An instrument, called the *Slope-o-meter*, has been constructed and used for this purpose.[21]

The instrument is essentially a photoelectric spectrophotometer which compares the intensity of light transmitted at two wavelengths through a sample of smoke. Extensions of the same mechanical and electrical system may be used to compare the transmission at three or more wavelengths. Two types of Slope-o-meter designated as Type I and Type II have been constructed. The following is a description of Type II. Type I is described elsewhere.[21]

METHOD

Photo-emissive photoelectric cells of the vacuum type are used to measure (1) the intensity of blue light (wavelength, 4400 A) transmitted through the aerosol sample, and (2) the difference between the intensities of infrared light (wavelength, 8000 to 9000 A) and blue light transmitted.

CONSTRUCTION

The optical and electrical systems have been assembled in a single box, one compartment of which serves as a smoke chamber (Figure 13). A second box contains three 45-v portable B batteries and an 8-v portable storage battery. Power is transmitted to the optical and electrical systems via a six-wire cable

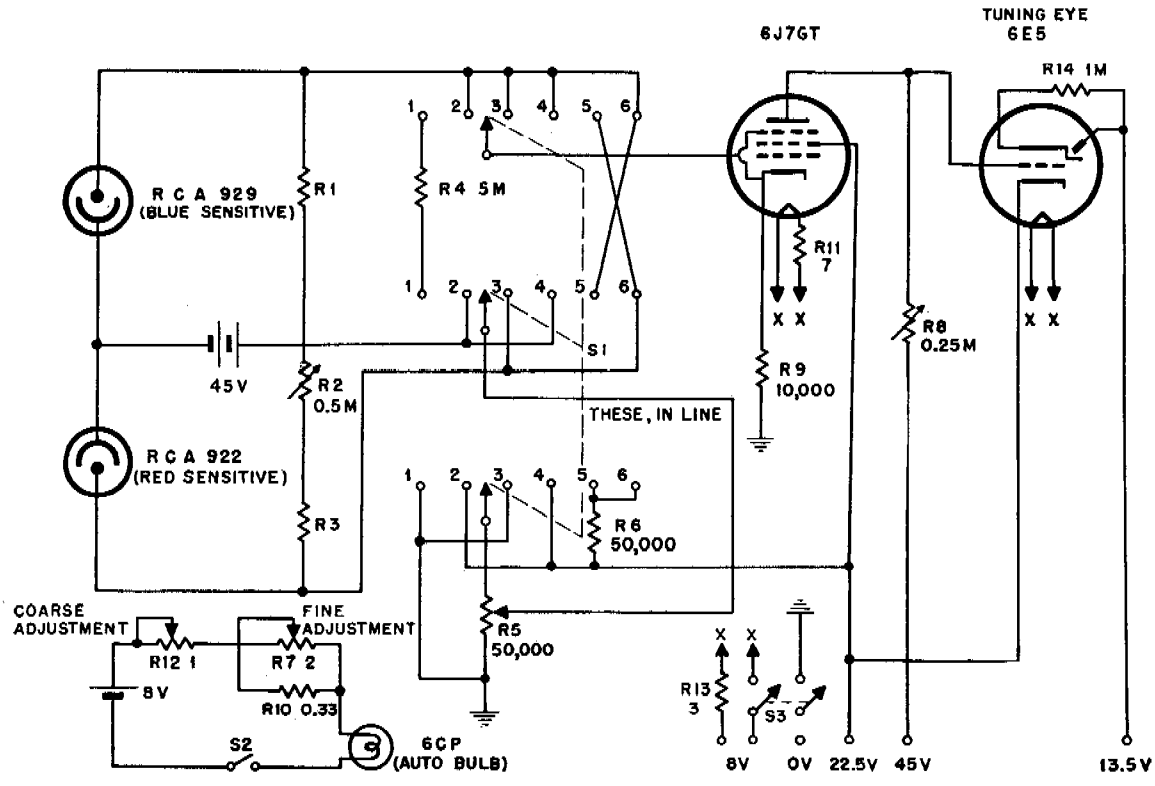


FIGURE 14. Slope-o-meter (wiring diagram).

and suitable plugs and jacks. The optical system consists of a 6-cp automobile bulb (Mazda No. 81), a condensing lens which sends a beam of light through the smoke and a semitransparent mirror directing it finally onto the phototubes. The purpose of the semitransparent mirror is to enable a single beam of light through the smoke to suffice for both phototubes. Color filters are interposed between the semitransparent mirror and the phototubes.

Rigid mounting of all parts of the optical system is necessary for reliable operation. The possibility of warping should be reduced to a minimum, although slight warping is corrected by the normal adjustment of the Slope-o-meter.

The electrical system (Figure 14) consists of suitable resistance loads (R_1, R_2, and R_3) for the phototubes, selector switch S_1 and a slide-back vacuum tube voltmeter. Three 45-v B batteries provide plate and slide-back voltage and an 8-v portable storage battery provides current for the 6-cp lamp and for the heaters of the vacuum tubes.

The resistors, R_1, R_2, and R_3, vary from one machine to the other but are selected so that with no smoke in the chamber, and with the 6-cp bulb operating at its proper current, the emf developed by each photocell is just below 22.5 v, the maximum slide-back voltage. The proper current is selected so that it can be maintained constant for all working voltages of the storage battery through adjustment of R_7.

When the selector switch S_1 is at position 1, the grid of the 6J7 GT is connected through R_4 to ground and the slide-back potential is zero. R_8 may then be adjusted so that the shadow of the tuning eye (6E5) is open to some selected angle near the middle of its range. This angle is marked and used for all subsequent balancing operations and indicates that zero emf is impressed on the grid of the 6J7 GT.

When the selector switch is at position 2 or 4, the emf developed by the blue sensitive phototube (RCA 929) is impressed on the grid of the 6J7 GT and this may be balanced manually by the slide-back emf developed in R_5. The dial reading of R_5 is a measure of the total amount of blue light striking the phototube.

When the selector switch is at position 3 the difference between the emf's developed by the blue and and by the infrared light is impressed on the grid 6J7 GT and the slide-back potential is again zero. The

load resistance ($R_2 + R_3$) of the infrared sensitive phototube may then be adjusted to bring the tuning eye to the balance position. The effect of this operation is to make the response of the instrument to blue light the same as the response to infrared light. This compensates for changes in the color of the light emitted by the lamp as it ages and for other changes in the apparatus such as drift in the value of the phototube load resistors or small amounts of warping.

When the selector switch is at position 5 or 6, the difference between the emf's developed by the infrared and by the blue light may now be balanced by the slide-back potential developed in R_5. With the selector switch in these positions, however, the magnitude of the slide-back voltage corresponding to full scale of R_5 has been reduced by the insertion of R_6. The increase in sensitivity is desirable here because a difference between two quantities is measured which may often be small.

OPERATION

1. Adjustment: No smoke in smoke chamber.
   a. Switches S_2 and S_3 are thrown to "on" position.
   b. Selector switch on 1. Adjust R_3 to balance.
   c. Selector switch on 2. Set R_5 on preselected value near maximum. Adjust R_7 and R_{12} to balance.
   d. Selector switch on 3. Adjust R_2 to balance.
2. Measurement: Put smoke in smoke chamber. For field use, open the door of the smoke chamber while in the smoke and close it.
   a. Selector switch on 4. Adjust R_5 and note dial reading.
   b. Selector switch on 5. Adjust R_5 and note dial reading. If no balance is possible, turn selector to position 6, balance with R_5 and note dial reading.

The dial readings of R_5 for selector switch positions 4 and 5 (or 4 and 6) fix the particle concentration and the radius (respectively) of the smoke in the chamber. See typical calibration curve in Figure 15.

The concentration lines on the calibration curves were obtained by means of calculations based on the Mie theory. As described in Chapter 21, the Mie theory yields the droplet radius from observations of the color and polarization of the scattered light. The theory also gives the scattering coefficient for a known droplet size and wavelength, so that the concentration can be obtained by observing the decrease of intensity at a known wavelength and known length of light path through the smoke.

MEASUREMENT OF PARTICLES BELOW 0.18 MICRON RADIUS

For very fine particles the sensitivity of the Slope-o-meter decreases markedly. For instance, all smokes fine enough to exhibit Rayleigh scattering fall on the same particle size calibration line. Accordingly, for fine particles the Owl described previously should be used to determine the particle size, and the Slope-o-meter used to measure concentration. For this purpose, it is necessary to measure only the transmission of blue light (dial reading of R_5 for selector position 4).

LIMITATIONS AND PRECAUTIONS

For particles above 0.5-micron radius, index of refraction 1.50 to 1.55, the particle size calibration curves are duplicates of the curves obtained for smaller particles.

It is apparent that a reading of particle size and concentration will be obtained no matter how inhomogeneous the smoke may be. For a homogeneous smoke, which shows orders in the Owl, the results will be as accurate as the initial calibration. For heterogeneous smokes, a complex weighted average is obtained, where the effect of particles larger than the average tends to cancel the effect of particles smaller than the average, provided there are few particles of 0.5-micron radius or larger. The smoke from large-scale generators of the coil or combustion gas type is apparently homogeneous enough and the particle sizes are within the proper range for use of the Slope-o-meter.

22.4.4 Color of the Transmitted Light

Visual observations of the color of white light transmitted through an aerosol provide a measure of the particle size (Chapter 21). It must be emphasized that this method does not provide an absolute, but only a relative measure of size relative to the optimum size for material of a given refractive index.

If the residual rays transmitted by a Diol fog are blue or green, it indicates that the average radius is greater than 0.33 micron, the optimum radius for Diol. However, a similar observation through sulfur smoke indicates an average particle radius greater than 0.17 micron, the optimum radius for sulfur. If the residual rays are red, it indicates an average radius less than 0.33 micron for Diol fog and less

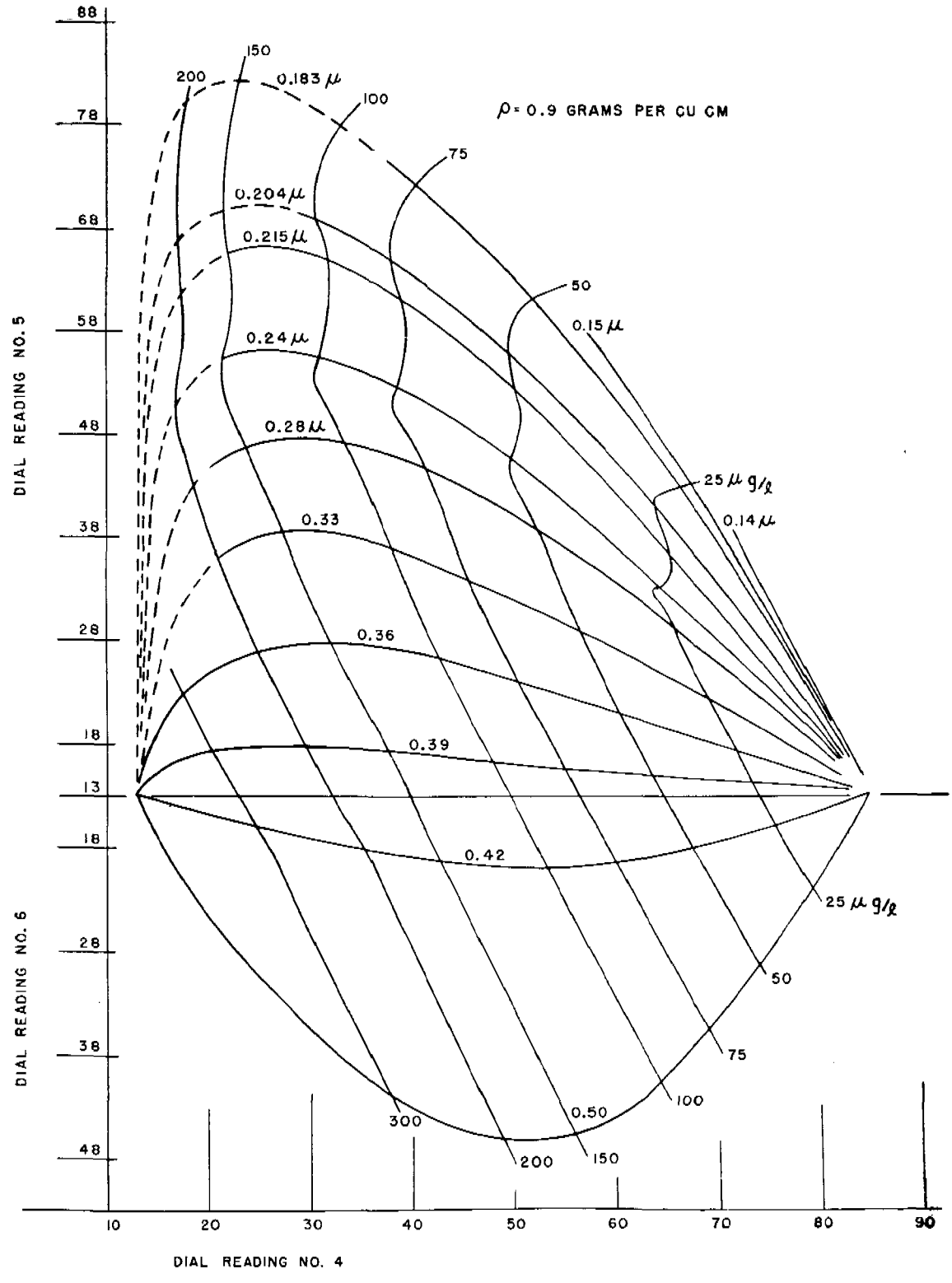


FIGURE 15. Slope-o-meter (calibration curves). Note: Diol $m = 1.50$.

TABLE 1

Date	Generator	Owl radius, microns	Slope-o-meter radius, microns	Sun's disk color	Comments
Nov 10, 1942 am	Esso	0.18	0.15		Fairly homogeneous
		0.16	0.16		
Nov 10, 1942 am	Servel	0.29			Moderately homogeneous
		0.33			
Nov 10, 1942 pm	Servel	0.29	0.28, 0.33, 0.22, 0.33. After turning off and on again: 0.20		
Nov 10, 1942 pm	Haslar	0.5 estimate		Blue	Brownish color, heterogeneous
Nov 23, 1942 pm	Servel 50 gal	0.32		Purple	15 ft from generator
		0.40		Blue	115 ft from generator
Feb 23, 1943 pm	Servel 25 gal	0.22		Red	30 ft from generator, some carbon
Feb 23, 1943	Chrysler			Lavender	Sample unobtainable. Blower
				White	sends smoke 35 ft up
Feb 23, 1943	DeVilbiss	estimate medium size		Lavender	Heterogeneous
				White	
Feb 24, 1943 am	Esso	0.3		Lavender	Owl colors indistinct
				White	
Feb 25, 1943 am	Hickman	0.4 approx	0.5 approx	Blue	Heterogeneous
		0.3 approx			Standard nozzle
Feb 25, 1943 pm	Hickman	0.27	0.30	Lavender-white to red	Multiple-hole nozzle
		0.22	0.26		
Feb 25, 1943 pm	Williams	0.20	0.18	Red	Multiple-hole nozzle
		0.25	0.25	Red	
Feb 25, 1943 pm	Williams	0.32	0.35	Red	Multiple-hole nozzle
		0.35		Blue	
Feb 25, 1943 pm	Hickman	0.29	0.31	Too cloudy	Multiple-hole nozzle
Feb 25, 1943 pm	Hickman	0.35	0.38–0.42	Too cloudy	Standard nozzle
Feb 25, 1943 pm	Esso	0.29	0.25	Reddish white	50 ft from generator
Feb 24, 1943	Esso	0.27	0.24	Red	18 mph wind from propeller
		0.22	0.19	Red	

then 0.17 micron for sulfur smoke. A magenta color indicates the optimum particle size.

Langmuir has developed a set of color filters which enable this measurement to be made more precisely. Several transparent filters, whose colors match the residual colors of the sun when the droplet radius of Diol fog is at or near the optimum, are mounted in a frame and viewed against a white background. The particle size can then be obtained by matching the observed color of the sun with the color of one of the filters.

22.4.5 Field Measurements

During November 1942, and again in February and March 1943, optical methods were used to measure the droplet size of oil fogs from screening smoke generators operated at Edgewood Arsenal, Maryland. The droplet radii in the fog produced by the Esso, Servel, Haslar, Chrysler, DeVilbiss, Hickman, and Williams generators, using Diol 55 as the fog oil, were measured with the Owl and the Slope-o-meter. Observations of the color of the sun's disk were made whenever possible.

TABLE 2. Esso generator.

Owl radius, microns	Sun's disk	Nozzle diameter inches	Diol temperature degrees F	Remarks
0.2	Red	3/16	1,000	Homogeneous
0.2	Red	3/16	950	Homogeneous
0.25	Red	3/16	900	
0.3	Lavender	3/16	850	Indistinct
0.3	Lavender	3/16	800	Indistinct
0.3	Red	1/4	900	
0.3	Lavender		900	
0.3	Lavender-white	5/16	1,020	Homogeneous
0.35	Blue	5/16	1,000	
0.3	Lavender	5/16	900	Homogeneous
0.3	Blue	5/16	800	Homogeneous
0.3	Red	3/8	1,000	Homogeneous
0.35	Lavender-white	3/8	900	Indistinct
0.4	Purple	3/8	800	
0.4	Blue	3/8	825	Indistinct

The results are summarized in Table 1. They represent only the results obtained for the particular

settings of the generators and are not to be taken as the only particle radius that may be obtained from these generators. At the bottom of the table it is shown that an 18 mph wind decreased the droplet radius 0.05 micron.

Special tests were performed on the Esso generator to test the effect of high wind, of nozzle diameter and of oil temperature as shown in Table 2. The standard nozzle diameter in the Esso generator is $\frac{3}{16}$ in. When the diameter was doubled to $\frac{3}{8}$ in. the average droplet radius was increased by 0.1 micron, provided the temperature of the oil was constant. For a given size nozzle, when the Diol temperature was raised from 800 to 1000 F, the average droplet radius was decreased by 0.1 micron. The pressure was not observed. It is seen that the droplet radius could be increased from 0.2 to 0.4 micron by doubling the nozzle size and lowering the temperature simultaneously.

Additional field and laboratory measurements made on various types of smokes are described in an unpublished report.

Chapter 23

FILTRATION OF AEROSOLS

By *W. H. Rodebush*

23.1 INTRODUCTION

As has been pointed out in Chapter 18, aerosol filters do not behave as sieves or screens which stop particles larger than the mesh and let through smaller particles. It is theoretically possible to construct such a filter, but it would offer so much resistance to the flow of air that it would be useless from a practical point of view. Thus, the filter papers used in analytical chemistry for the separation of precipitates are very inefficient as aerosol filters. All mechanical aerosol filters must, in practice, be of open construction, with the openings large compared to the size of the particles to be removed, in order to reduce the resistance offered to the flow of air. The removal of the particles is therefore by chance collision rather than positive action, and the percentage removed is a statistical function of the thickness of the filter; a filter of infinite thickness would be required to remove 100% of the particles from the air stream.

In practice all mechanical filters are made up of fibers, some of which must be of small diameter (i.e., comparable to the diameter of the aerosol particles) if the filter is to be efficient. An efficient filter may be defined as one which offers a low resistance and at the same time a low penetration. These two quantities are mutually interdependent variables, and for a given filter material one can be decreased only at the expense of the other.

It will be obvious from the theory of filtration why an efficient filter must be made up of fibers. The ideal filter would consist of a series of grids of fibers parallel to each other and at right angles to the direction of air flow. In practice it is impossible to obtain any such perfect orientation of the fibers although, in general, they will lie at right angles to the direction of flow.

In theory, the smaller the fiber diameter the better the performance, but it is clear that if the fiber diameter is too small the fiber will not have sufficient mechanical strength to resist the air currents. Furthermore, the forces which cause a particle to adhere to a fiber must depend to some extent upon the area of contact, and a very small fiber would not retain a large particle against the forces exerted by gravity, air currents, etc., which would tend to remove it. In practice, there is a limit to fiber diameter, but fibers of 0.01 micron or less prove to be very effective.

23.2 THE MECHANISM OF THE FILTERING ACTION

It has been pointed out in Chapter 18 that small particles adhere to any surface with which they come in contact, because of van der Waals forces. If electrical charges are present the adhesion forces may be increased; but electrical behavior will be discussed in a separate section. Mechanical filtration depends upon the actual impingement of the particles on the fibers of the filter. In order to consider the mechanism of the filtering action, consider a single fiber placed at right angles to the air stream. Assume in this discussion that the velocity is low enough so that the flow is nonturbulent, since it can be shown that this condition must hold in any filter that operates with a reasonably low pressure drop. There are several different mechanisms which may bring about the impingement of the particle on the fiber.

23.2.1 Direct Interception

Imagine the center of the particle of radius r to lie on a stream line which passes within a distance r of the fiber, in which case the particle will be caught. In the limit of the fiber diameter d, approaching zero, the particle will be removed from a cross-sectional area $= 2r$ per unit length of fiber. For larger fiber diameters the number of particles removed will not be greatly increased and will be independent of velocity, since the stream lines do not change with changes in flow rates. Direct interception is restricted, however, to particles whose centers remain in coincidence with a given stream line. This will occur only if the particles are too large to show appreciable Brownian motion and too small to have an appreciable Stokes' law rate of fall. There is no particle size for which the Brownian motion and the Stokes' law rate of fall are both zero, and simple calculations show that the efficiency of filters is far greater than

could be accounted for by direct interception.[1] These two effects, which prevent particles from following the stream lines around a fiber, evidently play an important role in the mechanism of filtration, and each will be considered in turn.

23.2.2 Stokes' Law Deposition

If a particle is large enough so that it has an appreciable Stokes' law rate-of-fall, its path will no longer coincide with any particular streamline in the air flow. It might be assumed, at first thought, that Stokes' law deposition would not in itself be important, since a particle is likely to fall away from, as well as toward, a fiber of the filter. The following consideration, however, shows that the Stokes' law fall is important in deposition. Suppose that the air flow through a filter be suddenly stopped. Within a short period, all of the larger particles which are present will be deposited on the upper surfaces of the fibers of the filter; and this period will be short because the distances through which the particles must fall are short. Although the same process goes on without interruption when the air is moving through the filter, it appears that it will make no difference whether the direction of flow is horizontal or vertical. The rate of deposition will vary with the particle size and concentration, and the total area that the upper surfaces of the fiber project into a horizontal plane. The flow will maintain the concentration uniform locally, but the concentration will decrease with increasing depth of-penetration of the filter. If the particle is below 0.3-micron radius, the Stokes' law rate of fall is so low that this mechanism of removal is likely to prove unimportant. The rate of deposition is not affected by variation in the rate of flow, but important inertial effects appear at higher velocities (particularly with larger particles), which give rise to another mechanism of filtration.

23.2.3 The Inertial Effect

If a streamline bends sharply around a fiber, a heavy particle at high velocity will not follow the sudden bending but will tend to continue in a direct course and collide with the fiber.

The extent to which a particle may be carried by its own inertia across the stream lines may be measured by the so-called stopping distance. The stopping distance, S, is the distance a particle with a velocity V and a mass m will penetrate a gas which is assumed to be at rest before being brought to rest by the viscous forces. The force resisting the motion of the particle through the gas is $f = 6\pi\eta r V$. Since

$$-\frac{d(mV)}{dt} = f,$$

integration gives

$$V = V_0 e^{-6\pi\eta r t/m},$$

where V is the velocity of the particle at the time t, and V_0 the initial velocity. Integration of

$$S = \int_0^\infty V dt,$$

gives the value

$$S = \frac{mV_0}{6\pi\eta r} = \frac{2r^2\rho V_0}{9\eta},$$

where ρ is the particle density. Substituting the values $\eta = 1.8 \times 10^{-4}$ for the viscosity of air, particle density unity, and a velocity of 3.5 cm per sec (a reasonably high rate of flow), the following table of values in centimeters is obtained:

r, cm	S, cm
0.5×10^{-4}	10^{-5}
5×10^{-4}	10^{-3}

S is the maximum distance that the particle could travel across stream lines if the stream lines bent at right angles. One sees that this distance could have no consequence for impingement if the particles were of 0.5-micron radius, but that with particles of 5-micron radius a considerable increase in the number impinging on a given fiber could be expected. Furthermore, an increase in velocity will increase the number caught.

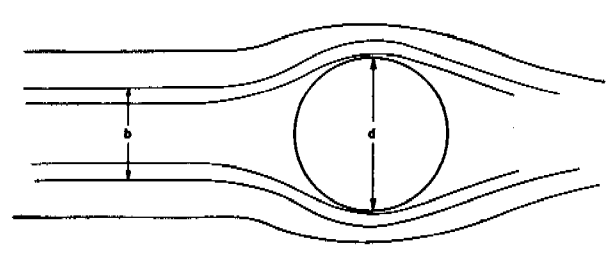


FIGURE 1. Stream lines around fiber and effective diameter b as compared with actual diameter d.

The *effective* diameter of a fiber may be defined as the width b between the bordering stream lines such that particles initially located in them will just clear the fiber (see Figure 1). Particles lying within this boundary will impinge upon the fiber. The ratio b/d is

always less than unity and may approach zero for low velocity of flow, large fiber diameter, or small particle diameter. If the dimensionless ratio, $Vr^2\rho/d\eta$, where V is the velocity of flow, r the particle radius, ρ the particle density, d the fiber diameter, and η the coefficient of viscosity, is plotted against the ratio of the effective diameter b to the actual fiber diameter a curve of the form given in Figure 2 is obtained.

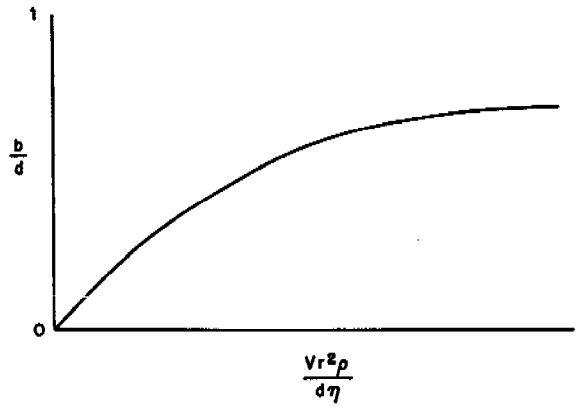


FIGURE 2. Inertial effect for large particles. Ratio of effective diameter to actual diameter, b/d, plotted against dimensionless ratio $(Vr^2\rho)/(d\eta)$.

For particles of large diameter, the effects of direct interception become appreciable and must be superposed on the curve of Figure 2 to give an increased filter efficiency. The effective diameter b is in this case increased by the amount $2r$. When the particle diameter is of the same order of magnitude as the fiber diameter, this correction becomes very important.

23.2.4 Diffusion

THE IMPINGEMENT OF SMALL PARTICLES

For particles of 1 micron diameter or less, inertial effects should not be important, and this is confirmed by the fact that penetration increases rather than decreases with increasing velocity. Similarly, the direct interception effect ($2r$) becomes very small for small particles. Yet, provided the fibers are of small diameter, the filtration efficiency is high and increases with decreasing particle size. The diffusion coefficient D varies inversely as the radius, and this quantity may be combined with the fiber diameter and velocity of flow in a dimensionless ratio D/dV to plot the ratio of effective diameter to actual diameter, as before (Figure 3). The value of b/d now becomes greater than one; but b no longer represents a sharp boundary between particles which impinge and those which escape, since on account of the Brownian motion, the probability of impingement is a matter of chance which decreases with increasing distance measured at right angles to the axis of the fiber and the direction of flow.

Actually, b is a mean distance; the total number of particles impinging on the fiber is equal to the number lying within the limits of b, but many of the particles within these limits do not impinge and many of the particles impinging come from outside these limits. The ratio b/d is of course greater, the greater

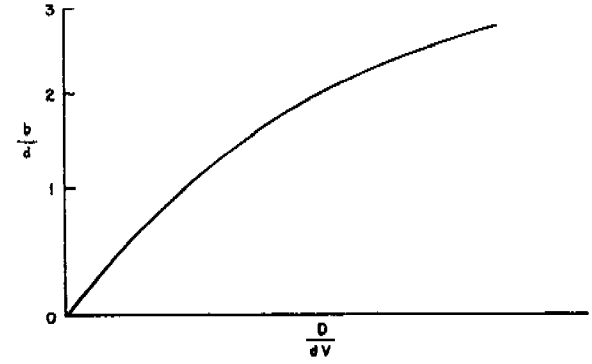


FIGURE 3. Diffusion effect for small particles. Ratio of effective diameter to actual diameter, b/d, plotted against dimensionless ratio D/dV.

the diffusion constant. The number impinging is greater the slower the velocity of flow, since the particles remain in the neighborhood of the fiber for a longer time. The ratio also increases as d approaches zero because b does not approach zero but a finite value which depends upon the mean distance of diffusion.

23.3 THE THEORY OF FILTRATION

It is practically impossible to give an exact mathematical theory of filtration. In the first place the differential equations can be solved only in an approximate manner, either for the inertial or the diffusion mechanism.[2, 3]

Even if satisfactory solutions are obtained for the behavior of a single fiber, a filter is made up of fibers with a random deposition and orientation, which cannot be taken into account in any exact manner. However, certain general considerations can be deduced, and these conclusions have been verified in a general way.

For example, very small particles will be removed

effectively by the diffusion mechanism [4] and very large particles by the inertial effects. It would be expected, therefore, that particles of intermediate size would be most difficult to remove. This prediction has been confirmed by experiment, but the size with a radius of about 0.2 micron [5] turns out to be the most difficult to remove. This maximum of penetration appears to be independent of fiber size. The decrease in penetration for particles above 0.2 micron radius can scarcely be due to the inertial effect, which was shown previously to be unimportant even for particles of 0.5 micron radius. It has been suggested that the effect of direct interception must account for the decreasing penetration of particles of greater than 0.2 to 0.3 micron radius, and it can readily be seen that the direct interception will contribute to the filtering action as the particle size increases. It would not appear however that a sharp maximum of penetration should be found which is apparently quite independent of rate of flow and fiber diameter.

The answer to the question seems to be given by experiments with glass plates, where the filtering action at lower particle size must be entirely due to diffusion and the filtering action for large particles can only take place through Stokes' law deposition. The same sharp maximum of penetration in the neighborhood of 0.2 to 0.3 micron is observed. Hence it must be concluded that the decrease in penetration above 0.2 micron is due to the increasing rate of Stokes' law deposition.

The effect of velocity on filtering efficiency depends upon the particle size. Small particles are removed more effectively at low velocities by diffusion, while large particles are removed more effectively at higher velocities by inertial effects. At some point in the intermediate range, perhaps in the neighborhood of 1 micron radius, the filtering efficiency will not be affected by changes in velocity.

Small fibers are more effective than large fibers in collecting particles from an air stream, because the smaller the diameter of the fiber the closer the stream lines lie to the fiber surface. A fiber may be considered to be surrounded by an envelope of nearly stationary air which is thicker the larger the periphery of the fiber. Also, the stream lines bend more sharply when the fiber diameter is smaller which will make the inertial mechanism of filtration more effective. The correctness of the foregoing statement has been demonstrated experimentally with fibers of 1 micron diameter and particles in the range 0.2 to 0.5 micron radius. It is possible that the statement is not true for very small particles whose diffusion range is very large, but these particles are so readily removed by a filter that they do not constitute a problem.

From the foregoing, one sees that a filter made up of a given number of fibers disposed in a certain way will be more effective when the fiber diameter is smaller, and at the same time the resistance will be less. Actually, a filter made up of smaller fibers will be more closely packed and have a higher resistance. Hence, if very small fibers are used, in order to avoid too high a resistance it is necessary to support the fine fibers on a loose network of coarser fibers.

23.4 FILTER MATERIALS

Most naturally occurring fibers, such as cotton, wool, and silk, are 10 to 20 microns or more in diameter. These fibers are much too large to be effective, and filters made of these materials will have to be very thick and have a high resistance, if the penetration is to be reduced to a low figure.[6]

Paper is a particularly unsuitable material for a filter, since the fibers are flat and ribbon-like and are matted together in such a way as to offer a minimum porosity. Certain fibers obtainable in tropical countries, such as esparto grass, are narrower than the fibers of ordinary paper stock, and papers made of these fibers are more open and have less resistance to the passage of air. In general, however, these fibers can be used only as a supporting grid for finer fibers such as asbestos.[7] There is no apparent limit to the fineness of dispersion which may be obtained with asbestos fibers, and mixtures of asbestos fibers with wool or paper are in use, and make excellent filters.[8] If paper is used, it must be very porous and, hence, of little mechanical strength, but this defect is easily remedied by a backing of gauze.

23.4.1 Glass Wool

Glass fibers of diameter down to 1 micron can be produced by special methods. By coating the glass fibers with a suitable binding, they can be matted into a paper-like web which is very strong and shows excellent filtering characteristics. Such a material is relatively expensive, but is unexcelled in many respects as a filter material.[9]

23.4.2 Rock Wool

Rock wool is composed of glass fibers which are produced from blast furnace slag or special limestone

silica mixtures. The material is fused in a cupola furnace, and the fibers are produced by blowing the molten fluid. The material is produced in carload lots for use as thermal insulation at a cost of a few dollars a ton. By control of the process, it is possible to produce fibers of a few microns diameter, and the material has great possibilities for use as a filter,[10] particularly where bulk is not limited.

23.4.3 Synthetic Fibers

Various types of synthetic textile materials such as cellulose acetate, polyvinyl acetate, or polyvinyl chloride, can be produced in the form of fibers of very small diameter.[11] The methods for producing these fibers are either a modification of the ordinary process of spinning and drawing, or electrostatic spinning. These materials have not been produced on a commercial scale, but experimental samples show the excellent performance that is to be expected. In order to use these very fine synthetic fibers, it is necessary to support them on a gauze backing.

23.4.4 Methods of Testing Bulk Filter Materials

The testing of a material in bulk in order to determine its suitability for use as a filter material is a different process from the testing of a fabricated filter. It is desirable to test the material at varying rates and over long periods of time. In order to detect clogging or breakdown, the penetration and resistance must be recorded as a function of the time.

A filter material may be conveniently tested in the form of layers or pads of uniform thickness arranged in series. The pads are compressed together to a suitable degree by means of metal gauze placed at the front and back of the series of pads. A radioactive smoke such as triphenyl-phosphate is passed through the material for a length of time, after which the pads are separated and each one counted separately with a Geiger counter. During the run, the pressure drop through the series of pads is recorded at intervals.

If the pads are of uniform thickness and homogeneous, and the smoke itself is homogeneous, each layer will remove from the smoke a constant fraction of the number of particles entering the layer. Thus if the number entering the nth layer is N_n, and the number entering the n plus first layer is $N_{(n+1)}$, then their ratio is given by:

$$\frac{N_{(n+1)}}{N_n} = e^{-k\Delta X}, \qquad (1)$$

where k is the stopping coefficient per unit thickness, and ΔX is the thickness of the pad. If the logarithm of the numbers of counts per pad is plotted against the ordinal number of the pad, a straight line results with a slope $S = k\Delta X$. If the pressure drop per pad is p, then the ratio s/p becomes an index for the filtering efficiency of the material; the higher the value of s/p, the better the performance of the material. Since, in general, both s and p will vary with the velocity of flow, it is necessary to test the material at various flow rates.

23.4.5 Clogging and Breakdown

An increase in pressure drop during a run is an indication of clogging. The filtering efficiency may or may not be affected, but the resistance will continue to go up until the filter becomes inoperable.

Breakdown of a filter material is often observed with liquid smokes. It is characterized by the fact that the plot of the logarithm of the counts is no longer a straight line but is a convex upward as shown in Figure 4. This is because the penetration

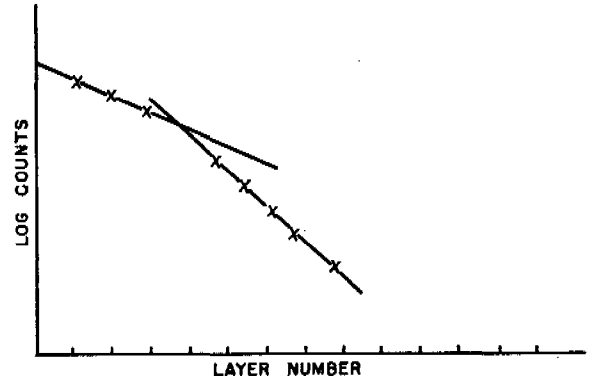


FIGURE 4. Plot of quantities of smoke caught by successive layers of a filter showing evidence of breakdown.

has gone up in the first layers which have become "saturated" with the smoke. This saturation effect is presumably due to the fact that the liquid wets the fine fibers of the filter and draws them together by surface tension forces, thus leaving open passages through the filter.

23.4.6 Electrostatic Filters

It is a matter of common observation that filters show a higher penetration when the relative humidity is high. The explanation of this must be that at low humidities static charges are accumulated on the filter

fibers and these charges are effective in collecting particles from the air even though the particles may be uncharged. Certain types of materials will retain static charges even at high humidities, and the Canadian wool-resin filter furnishes us with a striking example of this behavior. The wool-resin filter is made by carding various types of naturally occurring or synthetic resins into wool. The resulting material has excellent filtering power with, of course, a very low resistance. It retains this power for long periods of time at high humidities and, if the filtering power is lost, it may be restored by recarding the wool of the filter. There seems to be no question that the action of this filter is electrostatic. Wool and resin are classical materials for the production of static charges by friction, and the carding process undoubtedly produces high static charges on the filaments. In the neighborhood of the filaments the field intensities would rise to thousands of volts per centimeter.

Most of the particles in a smoke are uncharged, but they will be polarized in these strong fields and attracted to the filament. The polarization varies as the cube of the radius of the particle, whereas the resistance to motion through a viscous fluid is inversely proportional to the radius. The situation is the same, therefore, as with the fall due to gravity according to Stokes' law. The velocity with which a particle is drawn toward a filament will be proportional to the square of the radius. Large particles will be removed much more effectively than small particles. The filters are very effective, however, for particles in the ordinary smoke range of 0.2 to 0.5 micron radius (see Figure 4, Chapter 19).

Oil smokes appear to break the filter by dissolving, or perhaps merely wetting the resin. Some resins are more resistant to oil smokes than others.

Methods of testing fabricated filters are described in Chapter 24.

Chapter 24

METHODS OF TESTING SMOKE FILTERS

By *Frank T. Gucker, Jr., Hugh B. Pickard, and Chester T. O'Konski*

24.1 GENERAL PRINCIPLES OF SMOKE FILTER TESTING

THE PRINCIPLES DISCUSSED in the preceding chapters clearly indicate that, for use against troops equipped with the U.S. masks or any Service smoke filter except the wool-resin type employed by the British and Canadians, the most penetrating toxic smoke which could be set up in the field would consist of nearly uniform liquid particles about 0.3 micron in diameter. The production of such a smoke is a problem for the maker of CW munitions.

The most effective mechanical filter for this smoke should consist of fine fibers, e.g., of asbestos, supported on a web of larger fibers which give the filter mechanical strength and allow passage of the air with minimum resistance. The production and comparison of such filter materials and the manufacture and testing of completed filters is a problem for the CW defense.

The critical evaluation of a smoke filter should include many different considerations. The smoke penetration and pressure drop should be determined over a considerable range of flow rate, including any to which the filter would be subjected in use in the field. The smoke penetration should also be studied over a range of particle size, and correlated with toxicity studies which should indicate both the total number of particles and the total mass of smoke which could be tolerated. Other important characteristics of a filter are its capacity to remove smoke before clogging and its resistance to breakdown due to severe climatic conditions, CW agents, or other factors met in the field.

Once the general characteristics of a filter material are known, routine tests of pressure drop and filtration can be made under a single set of conditions if these are suitably chosen.[1]

Since filter penetration depends on the flow rate, the standard flow rate should be chosen after consideration of actual field conditions. A rate of 32 lpm was used in many of the tests at the beginning of the war. However, studies of breathing rates showed that a man exercising vigorously breathed at an average rate of 50 or 60 lpm, and that the instantaneous rate at the peak of the cycle may be as high as 200.[2] The rate of 85 lpm was taken as a standard for measurement of pressure drop and filter efficiency of canisters, and 320 cm per sec of linear flow for testing filter material, at a pressure drop of 30 mm of water.

The measurement of pressure drop is simple enough, and discussion will be confined to the measurement of smoke penetration. Here the test smoke should be of the most penetrating size. The test apparatus must include a reliable smoke generator and a rapid and sensitive method of measuring inlet and outlet smoke concentration. For poor filters, chemical or other methods of analysis of samples filtered from the smoke are adequate, although the process is extremely slow. Such methods are totally inadequate for the best types of modern filter, which require much more sensitive analytical methods, usually based on the measurement of the light scattered from the smoke. Such methods are more rapid as well as more sensitive. Instead of giving the average penetration integrated over a long period of time, they give instantaneous values of effluent concentration. Unless the instrument is differential and compares inlet and effluent concentration simultaneously, it must be used with a smoke generator which is adjusted to produce a smoke of constant size and constant mass concentration. With any type of instrument the test smoke must be homogeneous or nearly so, otherwise the filtration will cause a change in the particle-size distribution. The particles of the more penetrating sizes will comprise a larger proportion of the effluent than of the original smoke, and the light scattered in the two cases may not be strictly proportional to the respective quantities of smoke.

The actual development of methods of testing smoke filters paralleled the increased understanding of the process of filtration and the improvements in filter material which took place during World War II. The production of test smokes will be taken up first, then the methods of smoke-filter testing designed for laboratory use, and finally those which were adapted to production-line testing.

24.2 CHEMICAL TEST-SMOKE GENERATORS

Most of the generators used for the production of uniform test smokes employed condensation of supersaturated vapors, as described in Chapter 20.

24.2.1 The NDRC Homogeneous Aerosol Generator [3]

This apparatus already has been described in Chapter 20. In the hands of a skilled operator it produces smokes which are beautifully homogeneous as judged by their spectra. However, this generator is temperamental, is not easily adjusted to give fine smokes, and cannot be run for long tests without continuous care and adjustment.

24.2.2 The MIT–E1R7 Smoke Generator

The CWS Development Laboratory perfected a standard test-smoke generator which was widely used in smoke filter testing. The MIT–E1R7 generator [4] employs a stream of humidified air at 88 lpm. This is divided so that a flow of 17 lpm passes through a heated chamber where it picks up dioctylphthalate vapor from an open cup. The vapor-laden air is mixed with the larger stream of air at a Venturi orifice, under highly turbulent conditions (Reynolds number of 45,000 to 50,000) so that the rapid cooling yields a fine smoke. The mass concentration is adjusted to about 100 μg per l by regulation of the boiler temperature. The particle size is adjusted if necessary by means of a small filament heater in the large air stream, so that the MIT–E1R2 particle-size meter (see The Owl, Chapter 22) gives a reading of 29° ($\pm 1°$). This corresponds to the standard smoke of 0.3 micron diameter. The generator is connected to convenient clamp holders for canisters and sheets of filter paper. The generator furnishes a sample of 3 lpm of raw smoke for the penetrometer and 85 lpm for the filter test.

24.2.3 The NRL Smoke Generator [5]

Work at the Naval Research Laboratory paralleled that at the CWS Development Laboratory. The MIT smoke generators were tested and several basic modifications were made, which added to the stability of operation. The MIT generators were designed to furnish a test smoke under pressure, which was forced through the filter. The insertion of the filter increased the resistance in the line and this changed the concentration and characteristics of the smoke. The NRL generator was designed to furnish smoke to a 5-gal reservoir at a rate somewhat greater than that required for test. Excess smoke escaped to the atmosphere through a vent, while that required for test was *sucked* through the filter by a vacuum connection. Although this arrangement required a tight test system to avoid diluting the test smoke or introducing dust from the room air into the filtered smoke line, the NRL group considered that it stabilized the test smoke by keeping the pressure in the generator constant, and by allowing the smoke to cool to room temperature before it was used.

A propeller stirrer in the reservoir of dioctylphthalate helped improve the control of temperature and rate of evaporation of the liquid. Later, a water jacket was put around the quenching air stream to keep its temperature constant, and this also helped to stabilize the particle size of the smoke.

24.2.4 Smoke Materials

The material for a test smoke should be a liquid with a low vapor pressure at room temperature. It should be stable for long periods of time at the boiler temperature. Triphenyl phosphate [TPP] was used in much of the earlier work. It has the disadvantage of being a solid melting at 50 C. Although it forms a supercooled liquid smoke, this solidifies when it deposits in any cool parts of the generator, and eventually clogs the apparatus. Oleic acid also was used in the early work. It has a lower melting point than TPP and also supercools to form a liquid smoke. It has the disadvantage of decomposing at the temperature of the boiler. Tricresyl phosphate [TCP] has the advantage of being a liquid at room temperature, and was used to some extent, but later was given up because of its tendency to decompose and the fact that it is somewhat toxic. Dioctylphthalate [DOP] was the most useful smoke material, and became a standard test material by the end of the war. It is liquid at room temperature and is fairly stable, although it decomposes somewhat after a considerable time in the boiler.

24.3 LABORATORY TEST METHODS

When the United States entered the war, the CWS at Edgewood Arsenal used two standard laboratory methods of testing smoke filters. The first employed toxic test smokes [DM or DA], the second utilized nontoxic methylene blue [MB] introduced by the British.

24.3.1 DM and DA Smoke Tests [6]

Smokes of DM [7] are produced by dripping a 1% solution of DM in acetone upon a hot plate held at a temperature of about 245 C. The smoke is generated in a closed box, which is kept at a temperature of 45 to 50 C. The resulting smoke particles are solid crystals. Microscopic examination on a thermal-precipitator slide showed a particle-size distribution curve with a peak at 0.2 micron diameter, which is only slightly smaller than the most penetrating size (0.3 micron diameter) and no particles larger than 0.6 micron diameter. The smoke, at a concentration of about 50 μg per l, is passed through the test filter at 32 lpm. The effluent smoke is analyzed for arsenic by a modified Gutzeit method sensitive to 0.01 μg per l, or 0.02% penetration.[8] A charcoal bed is placed between the filter and the analyzer to absorb any DM vapors which may come from the generator. This arrangement improves the consistency of the results, but removes 20 to 25% of the DM smoke. The test therefore does not yield absolute per cent penetration, although it can be used to grade a series of canisters or samples of paper. Additional disadvantages of this test are the toxicity of the agent, the excessive time required to carry out the chemical analyses, and the fact that solid smokes with irregularly shaped particles are less penetrating than liquid smokes with the same number of spherical particles.

The DA test [9] obviates this difficulty, since this material forms a liquid smoke. The method of production is similar to that for DM smoke. An acetone solution of about 2.6 g per l is dropped at the rate of 80 drops per minute on a hot plate to form the smoke. Experimental tests also were run with DC smoke produced in the same way.

24.3.2 The Methylene Blue Test [10]

In the methylene blue test carried out at Edgewood Arsenal in the EA–E1 meter,[11] the smoke is generated by atomizing a 1% aqueous solution of methylene blue and evaporating the water by mixing the spray with a larger quantity of dried air. Microscopic examination showed that most of the particles were nearly spherical with a diameter of 0.2 micron, and only a few were larger than 0.4. The smoke is drawn through the filter or canister at a rate of 32 lpm and then passes through a strip of filter paper for a definite length of time. The test strip is "developed" by exposing it to steam and the color is compared with a set of standard stains. One disadvantage of this method of comparison is that the rate of drawing off standards is different from the rate used in making a test strip. This may lead to error, since velocity has a considerable effect upon the penetration of smoke through paper, especially the alpha-web paper which is used as the standard strip. The lower limit of the methylene blue test is about 0.005% penetration.

The CWS Development Laboratory at MIT designed the MIT–E2 methylene blue penetration tester [12] to overcome some of these difficulties in the testing of filter paper. The MB smoke, generated as before, is passed through a pad of a number of sheets of the filter paper under test and the stains produced on the single sheets are compared. The penetration per sheet can be calculated from the filtration law. A series of tests at Edgewood Arsenal [13] indicated that the MIT E2 tester gave less reproducible results than the EA–E1 tester, was not sufficiently sensitive to discriminate closely between filter papers of different filtering qualities, and required 25 min for a test, compared with an average of 4 min per test on the EA–E1. It can be used only for filters in sheet form. An indirect method, which is still less sensitive, must be used when the filter sheet is colored.

24.3.3 The Radioactive Smoke Test [14-16]

Early in the NDRC smoke program (November 1940) a method of testing the filtering power of sheets of paper or bulk material was devised, using radioactive test smokes. The sheets, or bulk material made into pads of uniform thickness, are arranged in series, and the test smoke (e.g., triphenyl phosphate containing radiophosphorus) is passed through these. After a sufficient length of time the sections are tested separately with a Geiger counter which registers counts proportional to the amount of smoke removed by each section. This test served to compare the filtering power of many materials and played an important role in the early NDRC smoke program. It suffers from the disadvantage of requiring radioactive materials and techniques, and later was given up in favor of more rapid, simple, and sensitive optical methods.

24.3.4 Optical Smoke Penetration Meters [17]

The NDRC Optical Mass-Concentration Meter [25]

Before the introduction of photoelectric meters, the NDRC optical mass-concentration meter was devel-

oped and used for many of the decisive tests on various filter materials. An appreciation of the advantage of small-angle forward scattering, and thorough familiarity with optical systems led to the design of the instrument already described in Chapter 22. It was operated in a small dark room and, in the hands of a skilled operator, was sensitive to 0.001 μg per l of a 5 order (1 micron diameter) oleic acid test smoke or the standard DOP smoke of 0.3 micron diameter and 100 μg per l. Thus, the instrument was sensitive to 0.001% penetration. The optical comparisons were very tiresome for the operator, and required considerable skill and experience as well as time.

THE MIT–E1R1 OPTICAL MASS-CONCENTRATION METER [18,19]

An optical system nearly identical with that of the NDRC optical meter was developed independently at about the same time at the CWS Development Laboratory and used in the MIT-E1R1 optical meter. This was designed as a rapid, portable, and simple instrument for testing filter papers or canisters with liquid smoke furnished by the MIT-E1R7 generator [4] described in a previous section. It utilized two smoke cells, with identical lamps and identical optical systems, employing small-angle forward scattering. Unfiltered smoke passes through one cell and filtered smoke through the other. The light scattered from the filtered smoke passes directly through a small rectangular hole in the center of the silvered face of a prism forming one half of a photometer cube, while that scattered from the raw smoke is reflected from a single prism and then from the opposite side of the silvered face. Thus the field, viewed by a low-power microscope, consists of the central rectangle of light coming from the filtered smoke, surrounded by the light from the raw smoke. Before measuring smoke penetration, raw smoke first is passed through both smoke cells, and a neutral screen filter in the optical system is adjusted to give uniform illumination of the photometer cube. Then filtered smoke is put into one cell and the intensity of the light scattered from the raw smoke is reduced by means of a calibrated optical gradient until the field is again uniform. The penetration is read directly from a 3-cycle logarithmic scale on the same shaft as the optical gradient. If the filtered smoke concentration is very low, the intensity of the light from the raw smoke can be further reduced by means of optical filters to 0.1, 0.01, or 0.001 of the reading on the gradient.

This instrument is compact, portable, and simple to operate. A small light shield over the eyepiece allows it to be read in the ordinary daylight. It gives absolute penetrations, and has the advantage of any comparative method in that a single reading gives relative light scattering, and gradual changes in the concentration of the test smoke are compensated. Its chief disadvantage is that it requires visual comparison of two fields, which is tedious. It was the experience of the Division with the instrument furnished that under optimum conditions individual readings vary by as much as 10%, and a series of readings are required for 5% accuracy. The limit of sensitivity of this instrument was found to be about 0.05% of a 100 μg DOP smoke, being determined chiefly by stray light in the effluent smoke cell which could not be reduced below this value.

24.3.5 The Australian Ionization Penetrometer [20]

An ionization penetrometer was developed at the Munitions Supply Laboratories, Maribyrnong, Australia. A 1% solution of sucrose is sprayed under a pressure of 30 psi to give a cloud of charged particles. Mobility measurements indicate a mean diameter of 0.03 micron. The spray is diluted to a flow of 1 cu ft per min, yielding a positive ion concentration of about 400,000 per ml. The electrical conductivity of the smoke is measured before and after filtration. The sensitivity of the penetrometer is 0.0002% per mm deflection on the scale, on the highest sensitivity range. Four to five minutes are required per test. The ions are found to be only about one-fifth as penetrating as a carbon smoke at a carbon penetration of 0.1% and only one-hundredth as penetrating as methylene blue. Comparative tests of this method apparently have not been made in this country, but it should be investigated, since it might be useful either for the study of the penetration of very fine smokes, or if larger ions could be produced, as a penetrometer for use with the standard smoke of 0.3 micron diameter.

24.3.6 Photoelectric Smoke Penetrometers

HILL'S PHOTOELECTRIC SMOKE PENETROMETER [21]

At the start of the war, the most sensitive laboratory instrument available was the photoelectric smoke penetrometer developed by A. S. G. Hill for the testing of commercial dust respirators, which is described in the British Journal of Scientific Instruments. Hill's test smoke consisted of carbon particles,

which he stated had an average diameter of 0.16 micron. The smoke was made by the carefully controlled incomplete combustion of butane in a bunsen burner. The smoke contained 6.8×10^9 particles per liter, at a mass concentration of about 25 μg per l. The absorption of light by a 50-cm column of this smoke was measured by means of a photocell connected to a triode amplifier, the plate current of which was balanced with a suitable resistor and a highly sensitive galvanometer. Although the total absorption of the raw smoke was only about 9%, penetrations could be read to 0.02% (1 mm galvanometer deflection). This arrangement required careful adjustment of the flame to give a uniform smoke, and careful regulation of the light current and the batteries, in order to measure the minute changes in the intensity of the transmitted light.

English and Canadian Carbon-Smoke Penetrometers [22, 23]

In the early days of the war, a carbon-smoke penetrometer was developed and used in England for testing gas mask filters, and was employed in Canada as an acceptance test. The English apparatus was sensitive only to 0.5% and was superseded by the MB test. A penetrometer, using carbon smoke also, was developed at the Pulp and Paper Research Institute of Canada. Butane is burned in a bunsen jet with a variable amount of air bled into the gas stream before combustion. The penetrometer consists of two smoke cells separated by a filter holder. The light, scattered by the smoke in either cell, is measured by means of an RCA 929 vacuum phototube and a balanced d-c amplifier of the *cathode follower* type.

It was found that the penetration of rayon-asbestos filters increased markedly as the amount of air bled into the gas stream was increased. Electron microscope photographs showed only a slight increase in the relative number of particles of optimum size as the gas is diluted. This change was not considered great enough to account for the large increase in penetration. It was concluded that the phenomenon was a mass-concentration effect, the carbon smoke forming a *pre-filter* upon the rayon asbestos fibers. The more concentrated the smoke, the greater was the pre-filtering action.

Since the mass concentration must be controlled with care to insure significant penetration data, and since liquid smokes are 50 to 100 times more penetrating than carbon smoke, the carbon penetrometer seems to be of little practical use.

The Kimberley-Clark Nephelometer [24]

This instrument was developed for testing samples of filter paper. A single 50-cp automobile headlight supplied light to two smoke cells set at right angles to each other. In each cell the light was focused by means of a lens system upon a small area where the light, scattered from the smoke at right angles, was viewed by a Type 931 photomultiplier tube. The stray-light current in each cell was balanced out electrically. Raw smoke flowed through one cell and filtered smoke through the other. The current due to the scattered light in each case was read and the ratio of the two gave the smoke penetration. The sensitivity of the instrument was about 0.1% penetration when using the standard 100-μg test smoke.

By 1943, smoke filters were improved to the point where they transmitted only a few hundredths of a per cent of a standard DOP smoke, of 0.3 micron particle diameter (as judged by a 29 degree Owl reading). At a standard concentration of 100 μg per l for the test smoke, the effluent from such a filter could not be measured by means of the MIT–E1R1 optical mass-concentration meter. The NDRC optical mass-concentration meter has the necessary sensitivity only in the hands of a skilled operator. However, a penetrometer for routine testing, sensitive to 0.001%, was evidently needed, and tests in this range are extremely difficult by any visual method. Neither the Kimberley-Clark nephelometer nor any of the photoelectric photometers then in use by the Armed Forces in this country, Great Britain, or Canada, had the desired sensitivity. The only photoelectric penetrometer of sufficient sensitivity was that of Hill to which reference has been made.[21] This instrument, however, measured the *absorption* of light and required extreme control of light intensity as well as an extremely sensitive galvanometer. Since only about 10% of the light was absorbed by the raw smoke, the intensity of the light had to be kept constant to 0.002% in order to obtain Hill's sensitivity of 0.02% in the penetration. If the *scattered* light is measured, however, the variation in light intensity can be of the order of the desired accuracy of measurement, e.g., 1%, provided the background light intensity is kept low. Hill's instrument also required a galvanometer with a sensitivity of 1,500 mm per μa, which cannot be used conveniently except in a research laboratory.

As a result of the need for a sensitive and simple penetrometer for routine tests, several instruments were developed for photoelectric measurement of the intensity of the light *scattered* from the standard

test smokes, using electronic amplification and small rugged galvanometers which could be operated anywhere.

The NDRC Balanced Photoelectric Smoke Filter Penetrometer [25]

This apparatus was developed from the NDRC optical mass-concentration meter already described. A single 50-cp bulb supplies light to two of the forward-angle scattering cells placed at 130° to each other. The scattered light falls on two Type 931 photomultiplier tubes. With raw smoke in one cell and filtered smoke in the other, the currents from the scattered light in the two cells pass through resistors, one of which can be varied so that the IR drops are balanced in a bridge circuit. If the currents are proportional to the smoke concentrations in each case, the ratio is the smoke penetration. Careful tests showed, however, that the Type 931 tubes were far less reliable than had been expected, when appreciable currents were drawn. Individual tubes also varied widely in their characteristics and suffered fatigue so that a current of 0.5 ma would fall off by 25% to 50% in an hour of steady illumination. This meter was studied in some detail at the Central Laboratory of Division 10, but reliable results below 0.05% penetration never could be obtained. Therefore the use of the Type 931 tube in such an arrangement was given up in favor of the more stable vacuum-type phototube in conjunction with suitable amplifying circuits.

The NDRC E1R2 Smoke Penetrometer [26]

This compact, direct-reading photoelectric penetrometer, designed especially for rapid and accurate readings to 0.001% of the standard DOP smoke, is shown schematically in Figure 1. It was developed between March 1943 and June 1944. The photoelectric current passing through the resistance R produces across it a potential drop E_R which can be balanced by means of the potentiometer so as to bring the galvanometer in the plate circuit of the amplifier tube to zero.

The smoke-cell arrangement is shown in Figure 2. The smoke from any suitable generator can be used. The CWS Development Laboratory MIT E1R7 generator [4] was widely used for test purposes. The smoke enters at A and leaves the cell at B. The converging beam of light from the aspheric lens system C illuminates the smoke intensely at the focus D where the image of the filament falls. Stray light is reduced to a minimum by use of the light trap E to absorb the diverging beam, the baffles F, G, and the slits H, H, which limit the field of view of the photocell. This reduction of background compensates for the reduction of intensity in using right-angle instead of small-angle forward scattering.

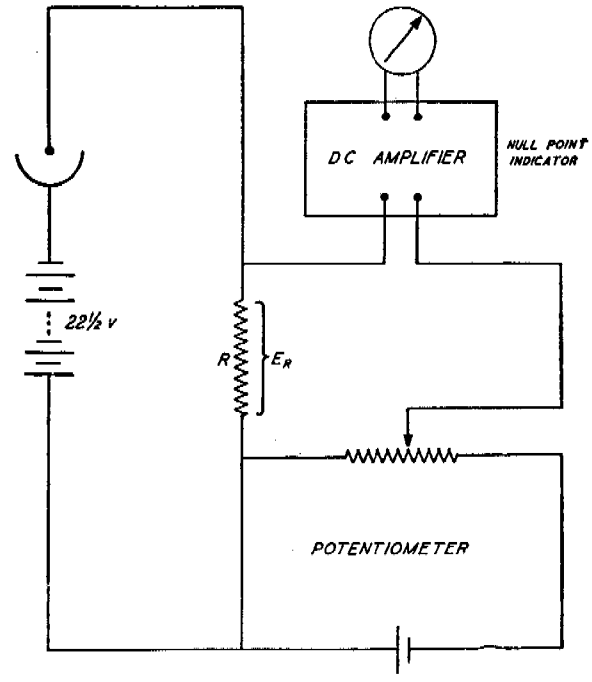


Figure 1. Schematic diagram of penetrometer circuit.

The Type 929 vacuum phototube was removed from its base to reduce leakage currents and connected through a very high resistance to the grid of a Type 38 tube which serves as a single stage of d-c amplification. As the photocurrent is reduced (to 5×10^{-13} a for a smoke concentration of 0.001 μg per l), the potential drop is kept within the range of measurement by increasing the high resistance by decimal steps from 10^7 to 10^{10} ohms. A special circuit was introduced, which compensates for any deviation of the high resistors from their nominal values.

A photograph of the instrument is shown in Figure 3. To make a measurement, the switches are turned on, the grid bias is adjusted and the stray light knob is turned to balance the stray light electrically. Then raw smoke is passed through the cell, the scale switch is set on 1 (connecting the 10^7-ohm resistor in the circuit), the per cent penetration dials are turned to 100, and the sensitivity is adjusted to give a zero reading on the galvanometer. Next the filtered smoke

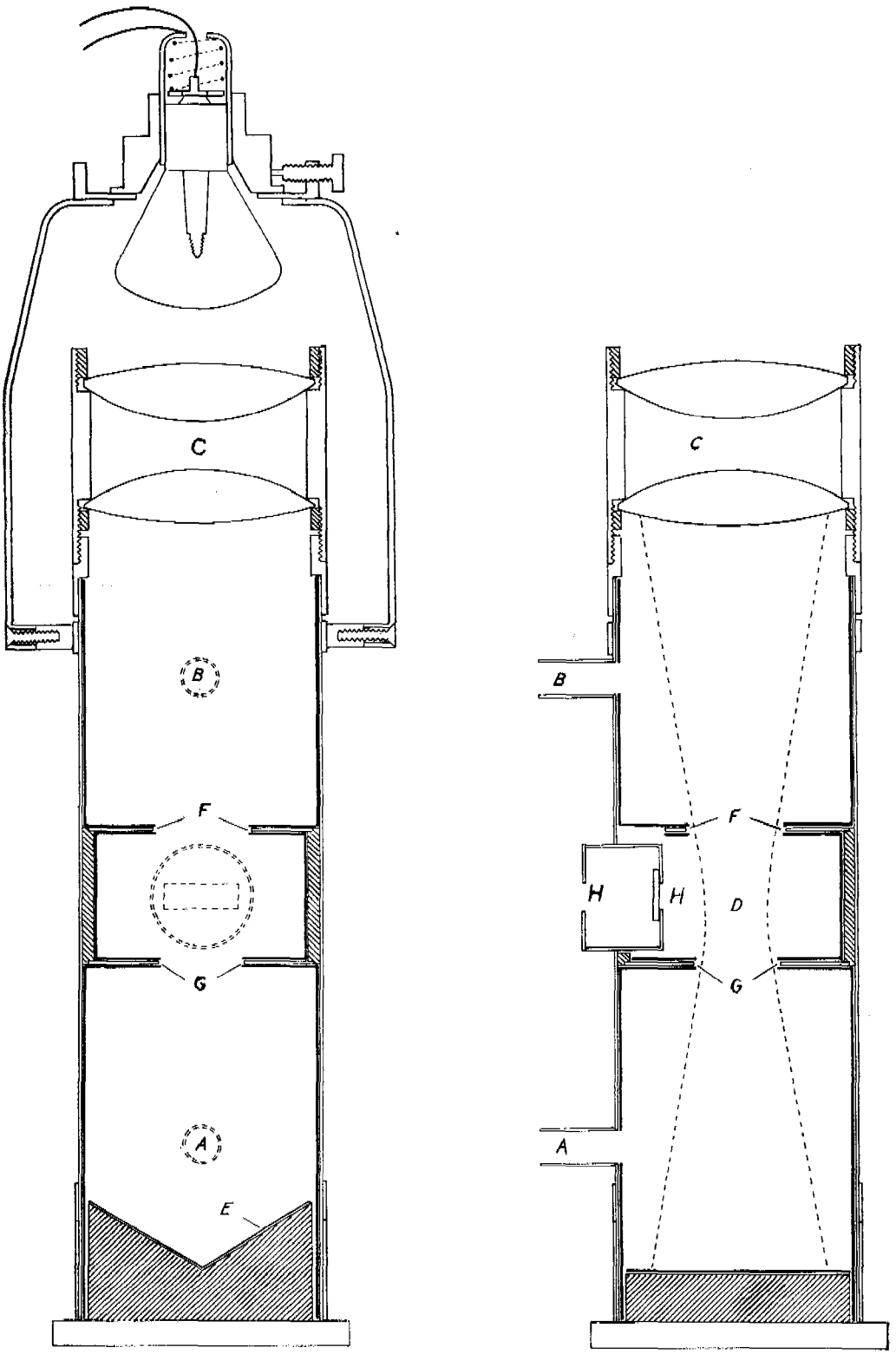


FIGURE 2. Smoke cell arrangement.

is passed through the cell, the scale switch turned to the appropriate value, and the per cent penetration dials adjusted to balance the galvanometer. The resulting readings give the penetration directly. Thus 85% on scale 0.001 (10^{10}-ohm resistor) corresponds to 0.085% penetration. On this scale a change of 0.001% gives a galvanometer deflection of 1 mm, which is significant.



FIGURE 3. NDRC–E1R2 smoke penetrometer.

Auxiliary circuits are supplied to check the adjustment of the scale switch to decimal steps, to check the emf of all cells, and to read the stray light, grid, and leakage currents. Arrangements are also made for reading plate currents, so that the characteristics of the Type 38 amplifier tubes can be determined. The unit is self contained, and all these readings are made without auxiliary equipment.

In addition to the NDRC–E1R2 smoke penetrometer built and used in the Central Laboratory of Division 10, at Northwestern University, three instruments were furnished to the Services. The first was sent to the CWS Development Laboratory at MIT, the second to the Naval Research Laboratory, and the third to Edgewood Arsenal.

THE CWS PHOTOELECTRIC SMOKE PENETROMETER, MIT–E2 [27]

This apparatus was developed between June 1942 and August 1945 by adapting the optical system of the MIT–E1R1 optical smoke penetration meter to the measurement of light intensity with an electrical system using a Type 931 photomultiplier tube. It was designed not as a penetrometer but as a versatile instrument for studying the optical properties of smokes at low light intensity. It is sensitive to 0.001% of the standard 100-μg DOP smoke, but is more complicated than the instruments designed as penetration test meters.

The apparatus included two separate smoke cells for measuring forward scattering, with a separate Type 931 tube and associated circuits for each. Great care was taken to supply a regulated constant voltage to the dynodes of each tube, the output of which was kept to 50 μa or less, and amplified by a cathode-follower circuit. Compensation of the stray light and leakage current was accomplished by means of an adjustable compensating lamp and Type 926 phototube. Arrangements were also made to calibrate the intensity of the light falling on the Type 931 tube by means of an incandescent lamp which could be compared with a standard lamp.

In practice, one optical system was used to measure the intensity of the light from the raw smoke. This light was cut to 1% by means of an optical attenuator. The other optical system was used for measuring the intensity of the light from the filtered smoke, and the ratio of the two intensities gave the penetration.

THE NRL SMOKE PENETRATION METER E2 [6]

This meter, developed at the Naval Research Laboratory for laboratory use and factory tests of filter paper, comprised the NRL smoke generator previously described, an Owl particle-size meter, a smoke cell, and an indicator unit. The smoke cell, based on the NDRC optical mass concentration meter, employed small-angle, forward scattering. Careful arrangement of light baffles reduced the stray light to 0.008% of that from the standard 100 μg DOP test smoke. The light was focused upon a Type 931 photomultiplier tube. At first, the output current was measured with a galvanometer sensitive to 0.03 μa per division. Later a vacuum-tube current amplifier was used with a microammeter in a bridge arrangement in the plate circuit, so that the indicator would be immune to the vibrations of factory operation.

In order to insure stable operation of the Type 931 tube by limiting its output photocurrent to 30 μa, the light from the raw smoke was reduced by means of a calibrated optical filter, made from a perforated disk of metal inserted between the condensing lenses so that it was perpendicular to the light beam.

The stray light was compensated electrically. Adjustment of a sensitivity control made the galvanometer read directly in per cent penetration. A scale switch allowed the range to be reduced by factors of 0.01 or 0.001, so that readings could be

made to 0.001% penetration of a standard DOP smoke. The whole operation was rapid and convenient.

24.3.7 Comparative Tests of Various Penetrometers

The photoelectric penetrometers are so sensitive that independent tests by other means are difficult. However, careful comparisons were made at the CWS Development Laboratory [27] and at the NRL.[5] Penetrations were measured by collecting standard DOP smoke for a sufficient length of time on a weighed glass-fiber filter, and comparing the penetrations so measured with the readings of the photoelectric meter on the same sheets. In each case, the results agreed within a standard deviation [a] of ±3%, which is less than the experimental uncertainty. These comparisons could not be made with any accuracy for penetrations less than a few per cent.

Each of the penetrometers was tested individually for self-consistency by measuring the penetrations of a series of filter papers singly and in series. Plots of the logarithm of the penetration against the number of sheets showed a straight line as required by the filter law.

In November 1943, two series of measurements were made with the NDRC–E1 penetrometer. This was the original model from which the direct-reading E1R2 was developed. Measurements of 2, 4, 6, 8, and 10 sheets of Brown and Company paper gave penetrations of 33 to 0.4%, with a standard deviation of ±6.6% from the average penetration for 2 sheets. Omitting one result, the standard deviation was ±3.4% for the other 9 sheets. A similar series of experiments on 1 to 12 sheets of paper at MIT gave penetrations of 50 to 0.01%, with a standard deviation of ±5.5% from the mean penetration per sheet. Two series of measurements at the NRL on 1 to 5 sheets gave penetrations of 50 to 2%, with a standard deviation of ±3.7% from the mean penetration per sheet. These results tested simultaneously the smoke generator and the uniformity of the filter paper as well as the penetrometer. The observed deviations include errors due to variations and inhomogeneity in the smoke and paper, as well as experimental errors in the penetrometers.

The self-consistency of the MIT–E2 meter was checked in a series of twenty consecutive tests on a group of canisters over a period of four months. The standard deviation of the results on any one canister averaged ±8% at penetrations of 0.04 to 0.14%. The results for a series of canisters all appeared to vary in the same direction from one day to another, suggesting that a change in the smoke may have caused the differences.

Tests with two different NRL meters showed a standard deviation of ±3% for the penetration of the same canister measured with the same meter over a period of about a month, and ±2% standard deviation for the penetration of a single canister measured with the two meters over a period of seven months. The excellent agreement of this series of results shows the advantage of the close control of the smoke generator which was developed at the NRL.

A series of 27 comparisons of filters and papers, using the same smoke and two different indicator units, gave an average ratio of 1.01 with a standard deviation of ±0.03% over the range from 0.01 to 73% penetration. A comparable series of experiments with two completely separate meters, each including its own smoke generator, cell, and indicator unit, gave an average ratio of 1.02 with a standard deviation of ±0.06%. This indicates that about half of the observed differences were due to difference in the smoke. However, the agreement is very satisfactory, and speaks well for the operation of both NRL smoke generators and indicator units.

A number of comparative tests of the different penetrometers were made. The CWS Development Laboratory [27] made a series of comparisons between their E2 photoelectric meter and their E1R1 optical meter, and NDRC–E1R2 photoelectric penetrometer and an NRL–E2 meter. The results were given in terms of the average value of the ratio of the reading of any meter, referred to the corresponding reading of the MIT–E2 meter. These values are given in Table 1 together with the corresponding standard deviations [SD] of the individual pairs of readings. A series of comparisons was also made at the NRL between their E2 meter and an NDRC–E1R2 meter. The average of these results, most of which are given in the NRL Report,[5] is also given in the table. Since the NRL–E2 meter gives results which are about the average of the others, all of the values have been calculated on the basis of 1.00 for this meter. These results are given in the last column of Table 1.

The Particle-Counting Smoke Penetrometer

By the spring of 1944, work at Camp Detrick had shown that the best canister smoke filters gave almost

[a] Defined as the square root of the average values of the individual deviations.

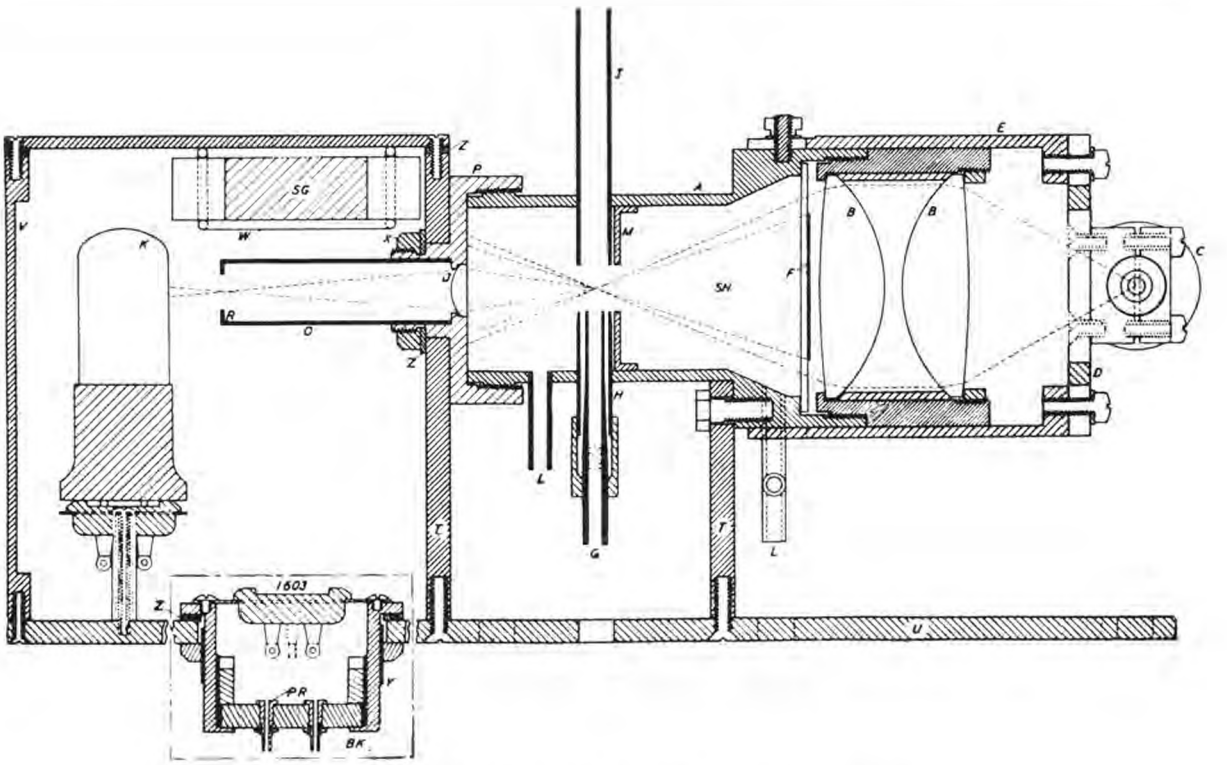


FIGURE 4. General arrangement of particle-counting penetrometer.

TABLE 1. Summary of comparative tests of penetrometers.

Meter	Experiments	Range (%)	Average ratio	SD	Average/NRL
NDRC–E1R2	29	0.07–55	NDRC/NRL 1.05	0.09	1.05
NDRC–E1R2	140	0.002–50	NDRC/MIT 1.05	0.19	1.01
NRL–E2	36	0.01–30	NRL/MIT 1.04	0.07	1.00
MIT–E2	...	.....	... ...	...	0.96
MIT–E1R1 optical	17	0.15–50	MIT–E1R1/MIT–E2 0.97	0.04	0.93

perfect protection against the BG spores which were being used as simulated BW agents. Many canisters, however, which showed low penetration for the standard DOP smoke, leaked an appreciable number of the BG spores. These spores, which are elliptical in shape with major axis of about 1.2 microns and minor axis of about 0.8 micron, evidently were stopped almost completely by the filter paper but penetrated any cracks due to faulty crimping of the edges of the filter paper, or pinholes in the paper or the metal can.

The method of determining penetration at Camp Detrick was to collect the spores from the effluent air on a cotton-wad impinger, wash them off onto an agar plate, and count the number of colonies which developed in 24 hours' time. There was urgent need for a rapid method of detecting defective canisters and of comparing the best canisters, which only allow the passage of a few particles per minute. Some indication of defective canisters was obtained by increasing the size of the DOP test smoke and decreasing the flow rate used in production-line tests with the MIT–E1 canister tester. This is because smoke penetration through the filter paper decreases with decreased flow rate much more rapidly than leakage through pinholes. However, a more direct method was needed, comparable both in sensitivity to the biological test and in rapidity to the ordinary photoelectric penetrometer. The problem was solved by developing the photoelectric particle-counting penetrometer described below.

Preliminary tests were made with a uniform DOP

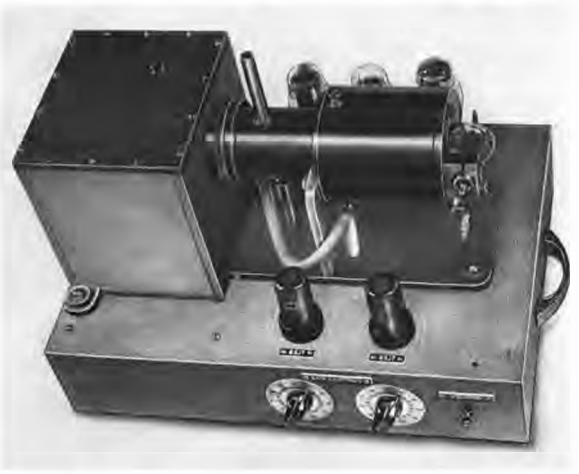


FIGURE 5. Cell unit of particle-counting penetrometer.



FIGURE 6. Time recorder and power supply unit.

smoke of 0.4-micron radius from a generator [3] like that described in Chapter 20. When this smoke was used in the NDRC–E1R2 photoelectric penetrometer described in a previous section, the lower limit of measurement was found to correspond to the light from only about 10 smoke particles. The sensitivity for counting individual particles therefore did not seem unattainable, particularly if the added intensity of small-angle forward scattering were utilized instead of the right-angle scattering of the photoelectric penetrometer. The d-c electronic amplifier of the earlier penetrometer could not be used, but an a-c pulse amplifier and counter had the advantage of eliminating the effect of any nonfluctuating stray-light background.

The smoke cell contained a dark-field system of illumination similar to that in the NDRC optical smoke penetration meter described in Chapter 22. The general arrangement is shown in Figure 4. The smoke enters the cell A through G, the smaller of the two concentric tubes, while a sheath of filtered air flows through the outer tube H at the same linear rate and prevents the smoke stream from spreading out before it passes into the tube I. The well-defined smoke stream is narrower than the light beam at the focus. Hence every smoke particle is illuminated and scatters light into the conical shadow beyond the focus. Most of this light, indicated in Figure 4 by the inner dashed lines, enters the lens J and is focused on the photosensitive cell K to produce an electrical impulse of about 0.003-sec duration for each particle. The vents L, L, are used to flush the cell with filtered air before use. The cell K, coupling condenser and resistors, and first amplifier tube (Type 1603) are mounted in an airtight brass box, desiccated with silica gel to reduce electrical leakage.

The 50-cp automobile headlamp C was held in a massive clamp. The cell was of heavy construction, mounted on a solid brass plate U which rested on a felt pad. These precautions eliminated mechanical vibrations of the lamp filament which would lead to *optical microphonics* and spurious counts. The appearance of the cell unit is shown in Figure 5.

In preliminary tests neither vacuum nor gas-filled phototubes were found to give a high enough signal-to-noise ratio to allow successful counting. Even the best available RCA Type 931 electron-multiplier phototube gave a ratio so small that counting was unsatisfactory because of the background. Fortunately a thalofide cell, [28] developed in Division 16 of the NDRC, was made available for this work. This cell gave a high enough signal-to-noise ratio so that background counts could be reduced to one every few minutes and the operation of the counter became practical.

The original pulse was fed into the Type 1603 amplifier, chosen for its low microphonics, followed by two Type 6SJ7 tubes, giving a maximum amplification of about 500,000. The output of the amplifier was fed into a thyratron *trigger* circuit which activated the mechanical recorder. A control of the grid bias of the thyratron regulated the size of the pulse needed to fire the tube. The amplifier and thyratron voltages were taken from a rectifier with a filter and a number of VR (voltage regulator) tubes which gave a closely-regulated, stable power supply. Filters were



FIGURE 7. Rear view of time recorder and power supply unit.

used to eliminate the feedback between the stages of the amplifier.

The success of the particle counter depended upon three things: (1) the use of the thalofide cell with its high signal-to-noise ratio, (2) the construction of a compact and rigid optical system which eliminated optical microphonics due to vibrations, and (3) the development of a remarkably stable amplifier which eliminated electrical background counts.

Two mechanical recorders were used, in order to provide a check of their functioning. These and an electric timer were so arranged that in a normal test a single button started the recorder and timer which were then stopped after 100 counts by a contact on the counter. The time for 100 counts thus recorded was determined with a statistical uncertainty of not over 10% in each experiment. Figures 6 and 7 show the timer, recorder, and power supply units.

Although the electrical stray counts were reduced to a negligible quantity, the background due to dust blown from the filter was troublesome unless the filter was blown off for 5 min or more before a test. Then the counts could be reduced to a value of about 1 to 5 per min which is negligible for most tests.

The particle counter was tested by measuring the penetration of the same filter paper, first with smoke of standard concentration and the photoelectric penetrometer, and then with greatly diluted smoke of known dilution and the particle-counting penetrometer. The results agreed up to about 1,000 counts per min, above which an increasing number of the counts were lost.

The range of the instrument is from about 3 to 1,200 counts per min. If the inlet smoke concentration is 10^8 particles per l, which is attainable with BG, one count per min corresponds to 10^{-6} per cent penetration. Hence the sensitivity range of the instrument is 3 micro-per cent to 1.2 milli-per cent.

A particle-counting smoke penetrometer, E1R2, was made for use at Camp Detrick, where it was compared with the BG tester. The work at Northwestern University is being continued under a contract with the War Department and should yield results of considerable interest.

21.4 PRODUCTION-LINE TESTERS

21.4.1 The Edgewood Arsenal E3 Canister Tester [30–33]

The EA–E3 meter, employing an oil smoke, was used extensively at the beginning of the war for production-line filter testing. The oil smoke is produced by spraying amyl stearate into an electrically heated furnace mounted on one side of a large smoke chamber. The furnace is heated to about 450 C, and the smoke is formed by condensation of the oil vapor in the large chamber. The smoke is sucked through the canister at 40 lpm and then through a cell where the light, scattered at right angles from a Tyndall beam, is measured, using a Westinghouse Type SK-60 phototube and a Wheatstone bridge circuit amplifier. The meter is standardized by the use of master standard filters and used as a pass-reject instrument. The mechanical arrangements of the canister holder are well designed for rapid and convenient production-line tests by unskilled operators.

The concentration of the oil smoke originally used in the E3 meter was maintained as uniform as possible, but was not determined accurately. According to the estimate of H. Scherr, it was about 40 mg per l. With this inlet smoke concentration, the sensitivity of the E3 meter was better than 0.02%.[34]

NDRC tests [25] about April 1941 showed that oil smoke caused considerable deterioration of the carbon-impregnated paper then used in the smoke filter. Apparently this is because the liquid smoke wets the fine carbon filaments bridging the openings in the filter paper, causing these fine filaments to coalesce with the coarser cellulose fibers. Later, considerable attention was paid to the harmful effect of oil screening smokes on filters.[35–38]

When the highly concentrated test smokes were

shown to be harmful to the filters on the production line, the concentration of the test smoke was reduced to about 2 to 5 mg per l.[39] However, this reduced the sensitivity of the meter to somewhat better than 0.2% penetration.

24.4.2 The CWS Development Laboratory MIT-E1 Canister Tester [40, 41]

The great improvement in Service canisters rendered the EA–E3 meter obsolete, and the much more sensitive MIT–E1 canister tester was developed to take its place on the production line. This tester is provided with the MIT–E1R1 generator [4] which produces a liquid smoke of DOP. A stream of air is bubbled through the liquid DOP in a boiler maintained at a constant temperature within ± 0.5 C by a thermostat. The vapor-laden air is cooled rapidly as it is mixed with a large volume of diluting air in a Venturi tube. By proper adjustment of the temperatures of the boiler and diluting air, the smoke-particle size is maintained at about 0.3-micron diameter, as measured by an Owl reading of 30° (± 1°). Originally, the smoke concentration was between 200 and 250 μg per l, at a flow of 85 lpm in the MIT–E1 canister tester. Later, the flow was cut to 32 lpm and the concentration was increased to 750 μg per l in the MIT–E1R1 canister tester. This change was made in order to make the tester more sensitive to pinhole leaks and canister imperfections, as explained in discussing the particle-counting smoke penetrometer.

All the smoke stream put through the canister also traverses the smoke cell. Hence it is flushed out almost instantly. The cell is designed to minimize fouling of the lenses by smoke or by lint blown off from the filters, so as to allow long periods of operation before the background light becomes too high. Since the test-smoke concentration is reduced to avoid damage to the filter, and the scattered light from the smoke cell is viewed at right angles to reduce background scattering as much as possible, the amount of light scattered from the filtered smoke is so minute as to require a very sensitive photoelectric circuit. A Type 929 photocell is employed. A light chopper between the lamp and the smoke cell gives 90-c pulses from the Type 929 tube, which are fed to a 4-stage 90-c amplifier operated at a gain of about 2×10^6. Thus the small current due to the light pulses scattered by the filtered smoke is separated from the much larger d-c leakage current in the Type 929 tube. The background light, scattered by the cell, is compensated by a zero adjustment.

When the instrument has been calibrated against a standard filter, the percentage penetration may be read directly. However, in a production line, it is used as a pass-reject instrument. The rejection limit may be set as low as 0.01% penetration.

Another advantage of the tester is its speed. Since only about 5 sec are required per canister, it is well adapted for use on a production line. The disadvantages are the complicated electronic circuits, which make the initial cost high and require maintenance men who are specialists in electronics to service the meter.

24.4.3 The NRL-E3 Smoke Penetration Meter [5]

This meter employed the smoke generator, small-angle forward scattering cell, and indicator units of the NRL–E2 meter described in an earlier section, adapted to rapid production-line testing. The volume of the smoke cell was reduced by a wooden sleeve, which filled most of the space around the cone of light, so as to reduce the time for equilibration of the cell. With a test smoke of 125 to 150 μg per l, this instrument had a sensitivity of 0.001% and measured absolute penetrations. This was an advantage over the MIT–E1 canister tester, which was calibrated against a standard filter.

The validity of standard filters is always open to some question, due to change of penetration with use. The CWS Development Laboratory supplied standard canisters with filters of glass fiber, which is less affected by DOP smoke than paper filters. The MIT–E1 canister tester, calibrated with such a standard, was found to give results with other glass fiber filters which agreed well with the NRL-E1 meter (the original laboratory model from which the production-line tester NRL–E3 was developed). However, the penetrations of paper filters measured with the MIT–E1 meter were nearly twice as large as those obtained with the NRL–E1 meter. All the measurements were in the range 0.05 to 0.10% penetration. The discrepancy was greatly reduced when the MIT test smoke was used with both indicators. This fact suggested that the test smokes were not equally uniform, and that selective filtration was different with the two filter materials. Even with the same test smoke, unless it were homogeneous, the selective filtration could cause a different reduction of

the intensity of the light viewed at right angles in the MIT–E1 meter, and at small forward angles in the NRL–E1 meter.

The complete explanation of all these facts awaits the development of a method of measuring particle size distribution in these fine smokes before and after filtration. If such a method were comparable in ease with the owl reading for average particle size, it would give a tremendous amount of useful information. However, a practical solution in this case was obtained by using paper filters as primary standards for the MIT–E1 meter, and the glass wool filters as secondary standards which were checked against the primary ones and then used for routine tests the rest of the day. The primary standards were replaced frequently.

24.4.4 The Carbon-Smoke Penetrometer [42]

This instrument, which has been described in a previous paragraph, was used by the British and the Canadians as a production-line tester. The sensitivity of the British apparatus was only 0.5%. The Canadians employed a photoelectric detector sensitive to 0.01% penetration. However, the penetrometer had the disadvantage of using a solid smoke consisting of many chain-like particles made up of small primary carbon nuclei. These particles are less penetrating than spherical liquid particles of the same mass. Also, they tend to clog the filter, decreasing its penetration for the moment by impregnating it with fine carbon filaments. However, this improvement disappears in the presence of oil smokes, which wet the carbon filaments and cause them to coalesce with the larger fibers of the filter, as explained in the discussion of the Edgewood Arsenal E–3 canister tester.

24.4.5 The Sodium-Flame Penetrometer [43]

The sodium-flame apparatus was developed by the British [44, 45] as a 100% filter tester for use in the production of canisters. The smoke is generated by atomizing a 2% solution of salt and diluting the spray with air, allowing the drops to dry to a smoke of solid sodium chloride. As originally designed, the apparatus employed visual comparison of the intensities of sodium light from two hydrogen flames, one burning in the unfiltered smoke, the other in the effluent leaving the test filter. A comparison spectroscope is used so that the D lines of the two flames appear to be separated by a dividing line. The intensity of the flame burning in the unfiltered smoke is cut down by means of an optical wedge to match that of the test flame. At balance, the percentage transmission of the wedge is a measure of the concentration of the filtered smoke. Since the intensity of the flame may not be proportional to the concentration of salt in the air about the flame, and since the intensity may change with the alignment of the spectroscope with respect to the flames, the value at balance is not absolute but only relative. Thus, one of the disadvantages of this type of tester is that it yields percentage penetrations only after it is calibrated with filters standardized by some other method such as the methylene blue tester. A second disadvantage is that it requires visual comparisons of intensities, which is rather fatiguing, although the British reported no complaints of eye strain from the observers in their factories.

The advantages of this tester are its high sensitivity, the rapidity with which canisters can be tested (over 400 an hour by one observer), and its simplicity, which reduced the initial cost and required a smaller amount of strategic materials than did more complicated testing apparatus.

The sodium-flame apparatus was later modified by the Canadian Chemical Warfare Laboratories [46] so that visual comparisons are replaced by the use of the RCA Type 931 electron-multiplier type phototube, the output of which is passed through a microammeter. The meter can be made to give absolute penetrations by comparison with a standard filter, the penetration of which has been measured by means of a methylene blue tester. The hydrogen flame is adjusted so that 1 μa corresponds to a penetration of 0.005%. After a careful study of the penetration of wool-resin filters, it was concluded that the sodium-flame penetrometer gave results as consistent as did the methylene blue and DOP penetrometers. The sodium-flame penetrometer might well be adopted as a production-line tester if all canisters were tested against a solid smoke.

24.4.6 Possible Use of a Particle-Counting Canister Tester

The particle-counting smoke penetrometer has definite possibilities as a production-line tester, if the need should arise for such an apparatus. The control of test smoke concentration by a photoelectric device is now under investigation at Northwestern University under a contract with the Army Service Forces at Camp Detrick. The smoke cell and electrical circuits

would require little change to arrange for a count of 5 or 10 sec duration. The chief problem would seem to be removal of all dust from the filter, which might be accomplished by blowing filtered air through the canisters on the assembly line before they reached the testing station. The maintenance and servicing of the electronic apparatus probably would be simpler than for the MIT–E1 canister tester.

Chapter 25

SMOKE SCREENS

By *W. H. Rodebush*

25.1 INTRODUCTION

A SMOKE SCREEN is an artificially generated cloud of smoke particles, or more usually fog droplets, produced for the purpose of obscuring vision. Because of the scattering of light by the individual droplets, the visibility of an object in or beyond the cloud may be reduced to a low value or to zero. A small or dilute cloud produces a diffuse glare of light between the object and the observer which decreases the contrast between the object and its surroundings (see Chapter 27). A large or dense cloud may provide a completely opaque screen.

25.2 TYPES OF SMOKE SCREENS — BLANKET SCREENS AND CURTAIN SCREENS

A smoke screen laid over an area to conceal it from aerial observation may be termed a blanket screen. A smoke screen laid along the ground to conceal objects at ground level from observers on the ground may be termed a curtain screen. If a curtain screen rises to a sufficient height it may interfere with aerial observation, and a blanket screen becomes a curtain screen if it settles to the ground. The distinction is important only for defensive screening. In the offensive use of smoke, where the object is to blind the enemy by enveloping him in a dense cloud at ground level, the distinction between blanket and curtain screens no longer exists.

25.2.1 Meteorological Conditions Favoring Different Types of Screens

It is often stated that stable air conditions are favorable to the use of smoke, but this is by no means necessarily the case. If smoke is being produced by a number of generators under strong inversion conditions with a wind blowing over a smooth terrain, the smoke plumes will not spread enough to merge and will not rise to great enough height to form a satisfactory curtain screen. A blanket screen is entirely out of the question under such conditions.

On the other hand, by the proper choice of munition, one may produce a curtain under any conditions. Under high inversion a cluster type munition of white *phosphorus* will give a continuous screen and a sufficient rise, because of the large quantity of heat liberated. If the wind direction happens to be parallel to the screen, a long screen can be generated by a few munitions. It is, of course, equally possible to produce a curtain screen under unstable conditions using a cluster type munition, but one giving less heat than white phosphorus is to be preferred. Under neutral conditions a long curtain screen downwind may be produced by a single generator.

25.2.2 Blanket Screens

The first use of blanket screens in World War II was by the British who used the orchard heater to produce a black or brown carbon smoke by burning fuel oil. These screens were used to protect industrial areas from night bombing raids. They were satisfactory for the following reasons.

While the orchard heaters are very inefficient smoke producers, only a small quantity of smoke is required to produce obscuration at night. The smoke is dark colored, so that the canopy was not conspicuous by moonlight. It is necessary that the smoke blanket lift off the ground to permit visibility and movement, and that the cloud rise to a sufficient height to cover tall objects. Under the inversion conditions usually prevailing at night, the large amount of heat produced by the generators served to cause the smoke blanket to rise to a considerable height and then level off, as is characteristic of smokes which consist of carbon in an atmosphere of carbon dioxide.

The oil vapor smoke generator, which has largely replaced the orchard heater because of its increased efficiency, behaves in a very different manner. Because of the large volume of brilliant white smoke produced, it is better adapted for daytime screening. Furthermore, since there is little heat liberated in the smoke production process there is little tendency for the smoke to rise. Unstable air conditions will be required to form a defensive blanket screen. If these generators are used at night under inversion conditions, the smoke will cling to the ground and paralyze

traffic. Conditions of extreme instability are not desirable, of course, because a blanket screen which has risen to a height of five or six thousand feet is of little use.

25.3 SMOKE COVERAGE

The smoke coverage may be defined as quantity of smoke per unit area of a blanket screen necessary to give obscuration. It may be stated in terms of grams per square meter, or pounds or gallons per square mile. (1 g per sq m = 5,700 lb per sq mile.) As pointed out in Chapter 27, the smoke coverage will vary enormously with the varying conditions of illumination, contrast of target, etc. An amount of 0.25 g of oil smoke per square meter, when dispersed in optimum particle size, will give obscuration under severe conditions. This is equivalent to 200 gal of oil per square mile.

25.3.1 The Number of Generators Required to Give a Stated Smoke Coverage

If Q is the output of a generator (gallons per hour), C the smoke coverage (gallons per square mile) required, and V the wind velocity in miles per hour, then the number n of generators per mile of front required to maintain this smoke coverage is

$$n = \frac{CV}{Q} \cdot \qquad (1)$$

The foregoing statement requires qualification. The smoke plumes will not merge until the smoke has traveled a long way downwind, particularly under stable air conditions over smooth terrain. The smoke will never be distributed uniformly over the area, because of local variations of wind direction, so that the minimum smoke coverage for obscuration will not give obscuration. Finally, the smoke blanket usually spreads out over an increasing width of terrain as it travels downwind, so that the actual coverage is less than the calculated.

25.3.2 Rule of Double Output

Hence, if complete obscuration at all points is desired, double the output given by equation (1) will give a moderate factor of safety.

25.3.3 Degree of Obscuration Required for Protection

It is by no means necessary in all cases to obtain complete obscuration for adequate protection. Complete obscuration may be a disadvantage. Thus, in the Italian campaign near Salerno, it was found possible to protect a rear area several miles in extent by maintaining a haze over this area. This reduced visibility to a few hundred yards, but still permitted free mobility of vehicles and troops in the congested area on the ground. There was good visibility between an airplane directly overhead and the ground, but this was of advantage to the ground forces since it enabled them to direct antiaircraft fire, whereas it was a disadvantage to the attacking plane because its pilot must have visibility at an angle in order to begin a bombing run. A plane can do little damage to an objective that is only visible from directly above.

25.4 SMOKE MATERIALS

The primary requirement is that the material be cheap and available. Since the only methods of producing a satisfactory smoke are by vaporization and condensation, the material for this must volatilize without decomposition and at the same time have a low enough vapor pressure so that a few hundred pounds will saturate a cubic mile of atmosphere. These last requirements are almost contradictory, and the only materials that can be used practically are the stable petroleum oils with a boiling range in the neighborhood of 400 C.

Sulfur is an interesting material in that it is cheap and available and has almost ideal volatility. It has a high refractive index and the optimum particle size is about 0.15 micron radius (see Figure 9, Chapter 21). The difficulty with the use of sulfur is that this particle size is very critical and lies in a range which is difficult to obtain.

Since heavy lubrication stock oils are about the only materials available for the production of smoke, it follows that the only feasible method for setting up large-scale smoke screens is the vapor condensation method.

25.4.1 Practical Considerations Concerning Particle Size of Oil Smokes

Oil vapor smoke generators obtain particle size control by the rapid dilution of the oil vapor with cool air. As the mixing and cooling occurs, the vapor condenses with a high degree of supersaturation. We must assume that sufficient nuclei are present, so that many more particles are formed than are finally

present in the smoke. A very rapid rate of coagulation occurs for a very short time, and the particle size grows to the proper size without developing any appreciable heterogeneity of particle size. The dilution occurs so rapidly that the process of coagulation is checked after a few thousandths of a second.

It is, of course, a matter of coincidence that the condensation process produces particles within the proper size range when the oil vapor is allowed to escape through a jet with a few pounds excess pressure at temperatures slightly above the boiling point. This conclusion is confirmed by the fact that it has not been possible to increase the particle size, e.g., to 1 micron. The vapor issues at high velocity, at or near the boiling temperature, and is rapidly diluted with cold air. It must be assumed that the high degree of supersaturation produces a very high concentration of very small particles, and that these particles grow by coagulation to their final size in the first few feet of travel. Since the time of coagulation is very short, a remarkably narrow range of particle size results.

The particle size is variable within limits, possibly over a tenfold range, but it is very difficult to produce a particle size greater than 1 micron diameter. This is understandable if we grant the initial high concentration of very small particles. Whatever may be the nature of the nuclei which produce the condensation, they appear to be present in large numbers, and there is no obvious method of controlling them. The oil is a mixture of many different hydrocarbons and it is possible that very large molecules may act as condensation nuclei. Some control of particle size is obtainable by varying the rate of mixing with the air, which varies the length of the period of coagulation (see Table 3, Chapter 22). In view of the fact that each tenfold reduction in particle number (corresponding to a little more than a twofold increase in particle diameter) requires ten times as long as the previous tenfold reduction (Table 1, Chapter 18), it is seen that a given design of nozzle cannot be operated to give any great range of particle size. A thousandfold change in coagulation time would be required to produce a tenfold change in particle size. Furthermore, a long coagulation period must result in a nonuniform particle size.

25.4.2 Inflammability

When the vapor of a high-boiling oil is rapidly diluted with cold air, the zone of inflammability (where the vapor concentration is within the limits to support combustion) is very narrow and fluctuating. Consequently, even if the jet is ignited with a hand torch, it will blow out almost instantly. This freedom from inflammability depends on the proper operation of the equipment. There are several conditions which will almost certainly result in spontaneous flaming of the vapor jet. One of these is the cracking of the oil to produce light hydrocarbon vapors plus carbon particles. The danger of this is obvious.

A second cause of flaming is the occurrence of large drops. If a slug of unvaporized liquid is thrown out into the air, it retains its heat until it is completely surrounded by pure air. While the flash point of the oil is high because of the low vapor pressure, the combustion temperature is probably lower than for the lighter hydrocarbons. The large drop will therefore inflame spontaneously.

A final cause of flaming occurs in the combustion type of oil vapor smoke generator when the excess oxygen present exceeds 100% or more. Under these conditions ignition occurs directly from the combustion chamber, and by the time the oxygen present is consumed, the jet has become mixed with additional air which continues to support combustion. In other words, a combustible mixture exists through the vapor cloud instead of merely in a narrow zone bordering the issuing jet.

25.5 OIL VAPOR SMOKE GENERATORS

Two general types of oil vapor smoke or fog generators have been built. These may be referred to as the coil type and the combustion type. The coil type was perfected first, and examples of this type are the Esso Jr., the Beslar, and the DeVilbiss. In the coil-type generator the oil is vaporized in a coil which resembles that of a tubular steam boiler. In order to avoid coking and to reduce the amount of decomposition of oil in the coil, the standard refinery practice of introducing a small amount of water along with the oil is followed. The oil vapor and steam mixture escapes through jets into the atmosphere with an excess pressure of ½ atm or more to insure a high velocity. The combustion type of smoke generator is illustrated by the Williams (never perfected), the York-Hession, and the Todd. In the combustion type, the fog oil is sprayed directly into the combustion gases from an oil fire. The resulting mixture of gases issues from relatively large apertures at a fairly high velocity but only slightly in excess of atmospheric pressure.

25.5.1 Advantages and Disadvantages of the Two Types

From the operational standpoint the coil has a great advantage, since the oil is separated from the fire and the control of combustion and oil flow can be carried out independently. From the standpoint of mechanical durability, however, the coil is a liability. Because of the high boiling point of the oil, the heat transfer per unit area is very low compared with that for a tubular water boiler. Since the coil is in direct contact with the fire, local superheating is likely to occur, with the deposition of coke and the formation of a "hot spot" which will quickly burn through. Unless a large, heavy coil is used, it must be replaced at frequent intervals.

Since light weight is usually an important consideration in the design of a smoke generator, the combustion-type generator possesses obvious advantages. Still further reduction in weight can be achieved by the use of air cooling in this type, but the design involves difficulties. Since the combustion must be carried out with a small excess of oxygen, the temperature of the combustion chamber is very high, and heat resistant metal must be used for the chamber. Cooling fins must be placed on the outside of the chamber, and a rapid circulation of air maintained over these fins.

25.6 SMOKE MUNITIONS

The standard smoke munitions used by the Chemical Warfare Service (such as FS, HC, and WP) are, in general, hygroscopic or deliquescent substances, or produce substances of this character by a chemical reaction. The resultant smoke is a fog composed of droplets of a concentrated water solution with a refractive index 1.40 or thereabouts. Such droplets constitute an effective obscuring screen, and, since the water is condensed from the air, a small quantity of the original material will produce a great deal of smoke. From the standpoint of logistics therefore, these munitions would be very satisfactory were it not for one difficulty. There is no satisfactory control of the particle size produced by these munitions, and it is generally much too large to give an efficient area of obscuration per unit weight of material.

25.7 METHODS OF LAYING SMOKE SCREENS

There are three general methods of laying smoke screens.

25.7.1 Smoke Screens Drifted into Position

This is the method commonly used in defensive area screening. A line of stationary oil generators or smoke pots is placed upwind of the area to be screened. A high steady wind is more favorable than a low variable wind, since it takes less time to develop the screen and there is less danger of sudden shifts in the wind. In the use of this method it is necessary to anticipate sudden shifts in the wind direction, which may prove disastrous. With no wind this method becomes practically useless.

25.7.2 Smoke Laid from Moving Craft

Smoke may be laid from generators mounted on moving planes or boats. When planes are used, one attains the practical results of the third method in that the smoke is laid right where it is wanted within a matter of a minute or two. The lead plane in a smoke mission is exposed to fire, but once a screen is established, it may be maintained with a minimum of exposure. Boats are so much slower that their use in laying smoke screens involves the character of the first method to a considerable extent. The smoke may be produced either from generators mounted on the boat or from floats which are thrown overboard at intervals. The latter method anchors the screen to a fixed point or line of generation. If the generator is mounted on the boat, a straight plume of smoke trails from the boat in a straight line in the direction of the relative wind, i.e., the direction recorded by an anemometer mounted on the boat. Such a screen maintains its direction, i.e., travels with the boat, so that to the stationary observer it becomes a curtain screen with a lateral drift. Because of the relatively low speed of a boat, the laying of screens from boats calls for a degree of anticipation, and, hence, some uncertainty occurs in the results.

25.7.3 Projected Munitions

The third method of laying screens is by projected munitions, such as bombs, shells, or rockets. This method has the advantage of the placement of the screen exactly where it is needed (within the limits of accuracy of aim) at the instant that it is needed, and without undue exposure to enemy fire. In order to get a proper distribution of smoke, a bursting munition is desirable, but if the screen is to have any

duration, a slow-burning munition is necessary. The ideal munition is a combination of the two, and for use in landing operations it should also be amphibious, i.e., function either on land or water.

25.8 OPERATIONAL TACTICS

The primary use of a smoke screen is obscuration of vision, and to the extent that viewing devices render the obscuration futile, a smoke screen is useless. Military tactics have always depended heavily upon the protection afforded by darkness or natural fog. The smoke screen affords the same protection as darkness or natural fog plus the advantage that it can be placed where it is wanted and be initiated and discontinued at will, so that the user need not have his own movements handicapped by poor visibility. For many operations, it would be desirable to duplicate natural conditions of poor visibility rather than to produce a dense screen, but the processes of atmospheric diffusion are too slow and uncertain to achieve the former.

With respect to the disposition of the screen and the occasion of its use, smoke screens may be classified as defensive or offensive.

25.8.1 Defensive Screens

A blanket screen placed over an area as a protection against aerial bombing is a common example of a defensive screen. Such screens vary greatly in their effectiveness depending upon the area to be defended and the equipment of the attackers. For example, when fixed installations are subjected to pattern bombing, the attackers are able to use navigational and viewing instruments to do about as good a job as if the screen were not there, and, once fires are started, they will be able to judge the results by photographs. On the other hand, with mobile targets such as troops on the ground or ships in a transparent area, blanket screens may prove to be of very great actual protection, since the enemy can form no adequate picture of the disposition of the targets, which are being constantly relocated.

It should also be mentioned that an area screen (provided it is maintained at such an elevation that it does not reduce the visibility at the surface to a point where it hampers movement) is likely to be a great aid to the morale of the men working in the area.

25.8.2 Offensive Screens

Offensive smoke screens find their greatest use in assault or landing operations where personnel are exposed to directly aimed enemy fire. In the offensive use of smoke, the purpose is to blind the enemy, and to achieve this purpose the smoke should be placed immediately upon him. The second or third method of laying smoke screens must be used here as a rule, and special attention must be given to the probable wind directions. With the wind blowing in the face of the assault troops, the smoke will be blown back and blind the assault troops instead of the enemy.

Blinding the enemy serves two purposes: (1) it prevents directly aimed fire against the assault troops, and (2) it handicaps the enemy's movements, cuts down his efficiency, and affects his morale. The importance of the second effect above should not be minimized. Anyone who has attempted to work in dense smoke will realize how difficult it is to work effectively.

The argument commonly urged against the use of smoke in assault operations, namely, that it interferes with the effective fire of the attacking troops, is fallacious. While they are advancing, their fire will be badly aimed and ineffective; when they have reached a hold point where they have some protection, the smoke screen can be lifted. A smoke screen placed upon an enemy does not reduce the accuracy or effectiveness of general fire at him by more than a small percentage.

Chapter 26

TRAVEL AND PERSISTENCE OF AEROSOL CLOUDS

By *W. H. Rodebush*

26.1 FORMATION AND TRAVEL OF SMOKE CLOUDS

THE BEHAVIOR OF SMOKE (when used, for example, for the purpose of obscuring vision) is subject to the same laws of micrometeorology which apply to gases liberated for military purposes. As in the case of the gases, the smoke is usually emitted from the generator in a jet of considerable velocity, so that mechanical turbulence produces a rapid mixing with the air. This effect quickly damps out and is no longer effective at a distance of a few feet from the generator. More persistent effects are due to differences in density. The ordinary toxic gases are usually vapors of molecular weight much greater than air. In addition, because of the absorption of the heat of vaporization, the gas is much cooler than the air with a resultant tendency for the gas cloud to settle.

With a smoke, the situation is quite the opposite. The density of a smoke cloud is but little greater than that of air (smoke density of 1 mg per l is a very dense cloud), and the formation of smoke is usually accompanied by the liberation of sufficient heat which more than offsets any increase in density. In the case where smoke is formed by burning oil or white phosphorus, for example, the heat liberation is so great that the smoke exhibits a very strong tendency to rise because of the reduced density. Even in the case of an oil vapor smoke or chlorosulfonic acid, the condensation of the oil vapor or of moisture from the air causes a rise in temperature sufficient to more than compensate for the increase in density due to the smoke particles present.

Table 1 is self-explanatory. A temperature rise of 0.25 C will offset an increase in density of 1 mg per l.

26.1.1 Thermal Behavior of Smokes

It will be seen from Table 1 that there will be a tendency for smoke to rise in every case, this tendency being especially pronounced for white phosphorus.

When a smoke appears to be "heavy," there is usually a gas of high molecular weight present. For example, even on hot sunshiny days, the black smoke from a factory chimney usually rises at first, but may occasionally fall to the ground after some travel. This happens because the carbon dioxide present loses its heat by radiation and then sinks because it is heavier than air. The carbon dioxide receives no heat directly from the sun because there is sufficient carbon dioxide in the air above to remove all the radiation of the wavelength that is absorbed by carbon dioxide. Particles of soot will, of course, absorb heat and tend to prevent the cooling effect which causes the smoke to fall.

26.1.2 Atmospheric Diffusion

The initial condition of turbulence, which accompanies the generation of smoke, disappears by the time the smoke has traveled a short distance from the generator. The buoyancy effect resulting from the higher temperature of the smoke will continue to be effective, causing the smoke cloud as a whole to rise. As the smoke becomes more and more diluted with the cooler air, this effect will be less and less observable, unless (as in the case of white phosphorus) there is a very great initial rise in temperature when the smoke is formed.

TABLE 1. Effect of temperature rise on density; relative humidity, 70%; smoke density, 1 mg per l.

Material	Per cent by wt of condensed water in smoke	Temperature rise
Oil vapor	0	1.0
FS	66	1.6
HC	60	2.2
WP	83	7.0

The process by which the smoke is diluted and mixed with air is called *atmospheric diffusion*. This process is often termed *eddy diffusion* to distinguish it from *molecular diffusion*, since eddy-like motions of one to many feet in diameter are commonly observed. Eddy diffusion takes place at the same rate for a gas as for a smoke while molecular diffusion depends upon the size of the molecule or particle. The rate of atmospheric diffusion is measured by the angle of rise and angle of spread of the smoke plume as it travels downwind from the source.

Photographs taken at right angles to the smoke

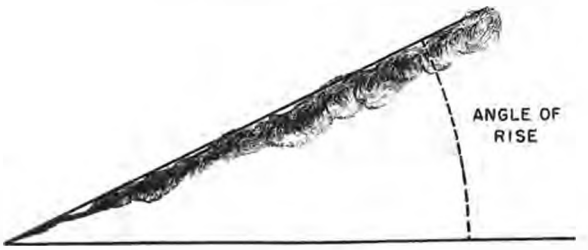


FIGURE 1. Angle of rise of smoke plume (from photograph).

plume, both horizontally and vertically, furnish a convenient method of measuring the angle of rise and angle of spread (see Figures 1 and 2). Such photographs show that the smoke plume usually has initial angles of rise and spread which differ from the angles farther away from the point of generation. It has already been indicated that the initial behavior is a transient effect of the heat and turbulence resulting from the process by which the smoke is generated. Its behavior as the smoke travels farther away from the generator depends upon the meteorological conditions prevailing, and these require detailed discussion.

26.1.2 Meteorological Factors

The principal meteorological factors affecting the travel of a smoke cloud are wind speed, direction, and turbulence, in the lower atmosphere. These are, of course, the same micrometeorological factors that affect the behavior of war gases, but the effects are not the same, and the conditions favorable to the use of one may not be favorable for the other in a given set of circumstances.

If it is desired to cover an area with smoke from a limited number of stationary sources, a wind velocity of fixed speed and direction is desirable. Too high a wind speed will require an excessive rate of production of smoke to maintain any sort of coverage. On the other hand, too low a wind speed means that too long a time will be required to develop the screen in the first place.

If there is no wind, the smoke screen can only be obtained by laying the smoke from a moving vehicle such as a plane or boat, or by projecting smoke munitions into the area. The latter method is usually only feasible in offensive operations.

Conditions of very low wind speed are likely to be accompanied by sudden variations in the wind, which may carry the smoke into areas in which it is not desired.

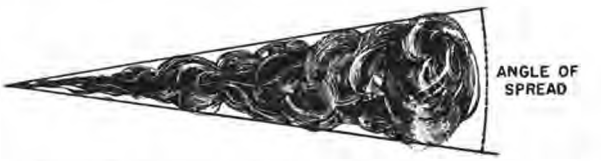


FIGURE 2. Angle of spread of smoke plume (from photograph).

When smoke is emitted by a stationary generator in a steady wind, the smoke plume travels downwind with the speed of the wind, and the axis of the plume is parallel to the wind direction. The density of the smoke at any point downwind will be, in general, inversely proportional to the wind speed, but this statement is only approximately true because of other factors which must be taken into account.

When smoke is laid from a moving source, the above statements will still be true if one substitutes the relative wind speed and velocity for the true wind speed and velocity. By the relative wind speed and velocity, one means the wind speed and velocity as recorded by an anemometer that is mounted on the vehicle carrying the smoke generator. Thus, if a boat carrying a smoke generator moves due south with a speed of ten knots when the wind is blowing from due east at ten knots, the smoke plume will appear to an observer on the boat to lie exactly downwind, i.e., northwest, and to have a density corresponding to a speed of 14.14 knots. The above statement, however, is not so simple as it sounds, and it only holds for an observer on the boat. To a stationary observer, the smoke plume no longer lies with its axis parallel to the wind (see Figure 3).

If the wind speed and direction are recorded by sensitive instruments, very rapid and violent fluctuations of both quantities will often be observed. Thus, the exact direction of the wind can be established only as an average measurement over a considerable time, and the wind may momentarily veer by as much as 180°. Zero wind may be recorded momentarily. The wind vane records variations only in the horizontal component of wind velocity, but, if a vane is mounted to turn in a vertical plane, vertical components of velocity will be observed. These latter must, of course, approach zero as the measuring instrument approaches the ground surface.

The unsteadiness in wind velocity and direction can be considered, therefore, as being due to pulsations taking place in three directions, namely, in the general direction of the wind, and in horizontal and vertical directions at right angles thereto. The mean

values of these pulsations in the different directions, measured over a period of time, would be expected to be equal if the motions of the lower air were isotropic, but the vertical direction is unique in this respect. If thermal instability exists, strong vertical gusts may be expected at considerable altitudes. At the ground level, however, the vertical component must fall to zero.

The sum total of the pulsations in the different directions measures the gustiness or turbulence of the atmosphere.

26.1.3 Causes of Turbulence

One obvious cause of turbulence is mechanical. The higher the wind velocity, the greater the turbulence, particularly over a rough terrain. Over a smooth surface of water there will be no turbulence produced by mechanical causes at low wind speeds. Wind speeds greater than 10 to 11 knots, however, will produce waves which in turn will produce mechanical turbulence in the lower air layers.

26.1.4 Thermal Stability

The most important factor in producing turbulence is thermal instability in the lower atmosphere. During the day, in bright sunshine, the ground surface receives a great deal of heat from the sun, and since the earth is a poor conductor, the temperature of the surface will rise many degrees. The layer of air in contact with the ground is heated in turn, and becoming lighter by expansion, it rises. Since the warm lower layer of air cannot rise everywhere uniformly, it must break through the upper cooler layers somewhat as bubbles burst upward through a liquid. The actual driving force is, of course, the weight of the cooler air, which settles toward the ground to be heated in turn. These upward convective currents cause the bumpiness of the air which is noticeable in an airplane, and, if there is sufficient humidity, cumulus cloud formation is likely to take place at moderate altitudes.

On clear nights the ground loses heat by radiation and cools the lower layer of air so that the density is greater near the ground, and a condition of extreme stability prevails. When the sky is overcast, heat is neither received nor lost by the earth, and a neutral condition prevails in which there is no tendency for upward convection.

The foregoing statements do not hold for changing weather conditions. The passage of a warm or cold front may completely alter the temperature relation between ground surface and air and produce stability or instability regardless of time of day or sky conditions.

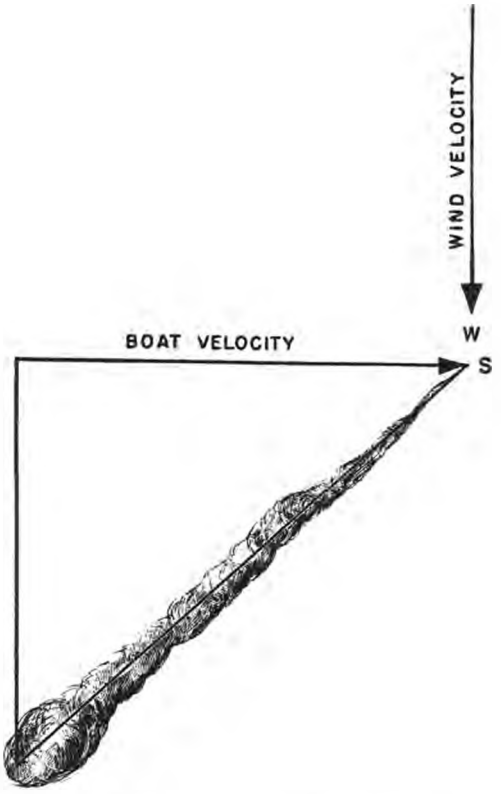


FIGURE 3. Curtain screen laid from a boat.

The situation over large bodies of water is also different. Water is a heat reservoir of great capacity, so that there is no significant variation in temperature between day and night. On the other hand, the air is usually not at the same temperature as the water, so that we may expect to find conditions of stability or instability prevailing continuously (throughout the twenty-four hours) for long periods. Changes in stability will usually take place only with changes in wind direction or in seasons. Thus, a wind blowing offshore from the New England coast will probably produce stable air conditions in summer and unstable air conditions in winter, over the ocean. Near the equator the ocean receives so much heat from the sun that a considerable degree of instability is likely to prevail.

26.1.5 Thermal Gradient

Although stability relations have their cause in differences in temperature between the earth's surface and the lower layers of the air, the actual stability conditions are determined by the temperature gradient in the air itself. If the temperature decrease with height is more than 1 C per 100 m, the air will be unstable, that is to say, the lower layer of air will tend to rise and to keep on rising as long as this condition prevails. This is caused by the rising mass of air which, even though it expands and cools as it rises, will be warmer and lighter than the surrounding air at any altitude. On the other hand, if the gradient is less than −1 C per 100 m, i.e., zero or positive, there will be no tendency for the air to rise, because a mass of air carried upward would be colder and heavier than the surrounding air.

It is, of course, not an easy matter to measure the temperature gradient, but it is usually much exaggerated near the ground, so that unless the gradient is near zero a temperature difference of a degree or more will be observed between two thermometers placed a few inches and a few feet, respectively, above the ground.

This critical gradient of −1 C per 100 m is termed by the meteorologist the *adiabatic lapse rate* for dry air, and the degree of stability or instability will depend upon the extent to which the temperature gradient departs in one direction or the other from the critical value. The extreme condition, when the temperature gradient is actually positive, is known as *inversion* and is characterized by extreme stability of the lower atmosphere. (See Figure 4.)

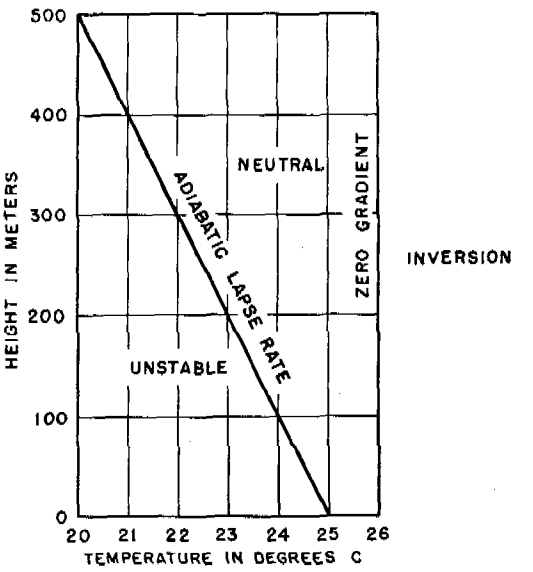


FIGURE 4. Thermal stability and instability. This gradient is 1¼ degrees centigrade per 100 meters.

26.1.6 Stability Relations at Land-Water Boundaries

Since a diurnal cycle of stability exists on land and no such variation occurs over water, it might be anticipated that a sharp discontinuity in meteorological conditions might occur at land-water boundaries, which would greatly complicate the use of smoke in landing operations, for example. It turns out, however, that this is not the case, except for discontinuities due to such terrain as high cliffs or other sharp differences in elevation. There is a tendency for the air to be stable over beaches which are bordered by low-lying terrain. This comes about in the following way. The diurnal variation in stability relations often results in the so-called land and sea breezes. During the day, the air over the land becomes heated and the cooler, stable air from the sea flows in over the beach. This air mass must in turn become heated and unstable by contact with the ground surface, but the instability will not be set up until the air mass has penetrated some distance inland.

On the other hand, at night the land is cooled by radiation, and a cool air mass flows from inland out over the beach. This air mass may be cooler than the water and may, therefore, become unstable as it travels to sea, but the air in the vicinity of the beach will remain stable.

The foregoing generalizations are only statements of tendencies. There will be many departures from this regularity, and the whole situation may be illustrated by a discussion of the stability conditions prevailing over the east coast of Florida in summer. Very few fronts pass through the subtropical regions of the world in summer. This is particularly true in the neighborhood of large water areas where the disturbances due to land areas are at a minimum. Under these conditions the highs and lows are static, and the gradient wind which blows along the isobars maintains a steady velocity day after day. At sea, this wind prevails practically down to the sea surface, where it is known as a trade wind. Off the east coast of Florida a northeasterly wind blows throughout the summer. The warm Gulf Stream lies some distance off the coast, and the air mass becomes unstable over the Stream. This instability is evidenced by the

cumulus clouds which can nearly always be seen from the shore.

The water mass between the Gulf Stream and the shore is cooler, so that the air mass may be cooled enough to become stable over this intervening water. When it passes across the beach over the land in the daytime, it will become unstable before it has traveled very far inland. On the other hand, the air at night becomes cooled over the land and flows out to sea as a land breeze. This land breeze is usually strong enough to oppose the gradient wind, but its effect does not extend very far out to sea, nor to a very high altitude. The gradient wind still blows a few hundred or a few thousand feet aloft. At some time during the forenoon, the gradient wind will overcome the land breeze and blow across the beach once more as a sea breeze. The exact time at which this happens depends upon the relative strengths of the two winds, and it cannot be forecast with exactness. Similarly, when the air temperature is near that of the water, the change from stability to instability over the water may take place with slight changes in wind velocity or other variables. The temperature of the water itself is likely to undergo sudden changes such as an offshore wind which may bring up cooler water from below near the beach.

26.1.7 Theory of Atmospheric Diffusion

In order to describe the travel of smoke clouds, it would be desirable to develop a mathematical theory in terms of such certain measurable quantities that when the meteorological structure of the lower air is known, it is possible to calculate the smoke concentration at any point downwind. The British meteorologists have developed such an equation (on a frankly empirical basis) for gas clouds, and it has been proposed to apply this equation to the travel of smoke. Certain very serious limitations exist, however, to the use of such an equation.

In the British equation the degree of turbulence existing in the air is taken account of by the so-called R ratio which is the ratio of the wind velocity at 2 m to the wind velocity at 1 m. Actual values of the R ratio vary from about 1.05 for very unstable air to 1.30 for stable air over a very smooth terrain.

Such an equation, however, has a very limited applicability. If the air is thermally unstable, a smoke cloud will lift clear of the ground before it travels very far. This will happen as soon as it encounters an upward convection current, but the point at which it will occur cannot be predicted by a statistical equation. On the other hand, under stable conditions over a smooth terrain, there is no natural tendency for a smoke cloud to rise or spread. This conclusion is supported by the evidence of many photographs which have been made of smoke streamers under stable air conditions. The only use that remains for the British equation which applies to smoke is to take account of the mechanical turbulence produced by rough terrain. This is done by means of on-the-spot measurements of R made at ground level. Such measurements will not apply to the smoke cloud after it has reached an elevation of 100 ft. The British equation is, of course, not calculated to take care of the initial transient rise and spread of a smoke cloud which is due to the heat and turbulence produced by the smoke generator.

26.2 BEHAVIOR OF SMOKE CLOUDS UNDER VARIOUS METEOROLOGICAL CONDITIONS

26.2.1 Stable Conditions

Under inversion conditions over a smooth terrain such as calm water, the only tendency shown by the smoke cloud to rise and spread is the initial transient effect due to the heat and turbulence produced by the smoke generator. The turbulence is quickly damped out but the heat produced may be sufficient to cause a very pronounced rise as is the case with white phosphorus smoke munitions. In the case of oil smoke where the heat produced is small, the temperature of the smoke at any dilution is only slightly greater than the temperature required to produce a buoyancy sufficient to offset the increase in density caused by the presence of the smoke material. As the smoke rises, the temperature falls because of two effects, namely, further dilution with cool air, and the adiabatic expansion due to the decrease in barometric pressure. Since, in an inversion, the temperature of the surrounding air increases with increasing altitude, an elevation is soon reached at which the smoke is stable; having the same density as the surrounding air, it has no tendency either to rise or sink.

Oil vapor smoke is often observed to level off (Figure 5) at an elevation of approximately 100 ft under stable air conditions. Certain types of smoke will show an erratic behavior because of abnormal density. Examples of these are (1) the smoke produced by burning oil in an orchard heater, in which

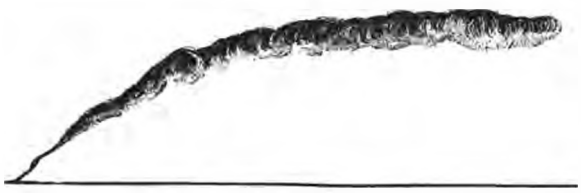


FIGURE 5. Smoke leveling off under inversion conditions.

particles of carbon and carbon dioxide are present, and (2) HC smoke, in which large particles of zinc chloride and other heavy materials are formed. While a good deal of heat is produced in the formation of these smokes, a good deal of it is quickly lost by radiation, particularly at night.

Since the heat produced in the generation of the smoke will usually cause the smoke cloud to rise, even under the most stable conditions, it may be anticipated that the cloud will lift entirely off the ground after a short distance of travel. If, however, a wind of considerable velocity is blowing, this lifting from the ground will not occur for reasons which will be explained later.

Although the heat produced in the smoke generator produces a rise, it has little effect upon the spread of the smoke cloud. Such spread as takes place is due to the initial turbulence, and this soon damps out. Consequently, if it is desired to produce continuous clouds of smoke from a series of individual generators, it is necessary to place the generators very close together, otherwise the individual plumes may not merge for a long way downwind. This situation holds for smooth terrain. If, however, the terrain is covered with shrubbery, for example, the lateral spread of the cloud is greatly increased as a result of the mechanical turbulence produced by the wind flowing through the shrubbery.

26.2.2 Behavior of Smoke Under Unstable Conditions

When the air current is turbulent because of thermal instability, atmospheric diffusion takes place to such an extent that the initial transient behavior of the cloud due to the heat and turbulence of the generator is of little significance. The smoke cloud continues to rise and spread as it travels downwind until the cloud becomes so thin that its boundaries are no longer distinguishable to the eye. If a time exposure were to be taken of the cloud it would appear as a cone with its apex at the generator and its axis rising at an angle from the horizontal, the angle of rise depending upon the degree of instability and the wind velocity. An instantaneous view of the cloud will show that it is furrowed and broken by variations in wind direction and sudden upward convective currents.

26.2.3 Convective Pattern

As has been stated previously, when the air is thermally unstable, upward convective currents occur. Over a rough terrain these currents are apt to be located at certain points. An upward current may be anchored at the windward brow of a hill, for example. Over a smooth terrain the convective currents are constantly shifting, and the distance between two upward currents depends upon various factors such as wind velocity and degree of instability. (Some idea of the convective pattern may be obtained by observing cumulus clouds.) Between these convective upbursts, the atmosphere is slowly settling over the whole area. Hence, the smoke cloud will appear to hug the ground until it encounters an upward current, when it will appear to change direction suddenly and rise at a considerable angle. The dimension of the convective patterns (distance between up currents) may be as much as ½ mile over a very smooth terrain. Since the convective pattern involves a complete circulation of the air, it might be supposed that, eventually, smoke which has been carried upward would be widely diffused and brought back down with the descending air. This must happen eventually, but whether or not it happens within a short distance from the point of generation depends upon the height of the convective ceiling.

26.2.4 Convective Ceiling

The lower air is thermally unstable when a negative temperature gradient greater than 1 c per 100 m of elevation exists at the ground level. This negative gradient may continue indefinitely upward. Thus, in thunderstorms, cumulus clouds often rise to a height of several miles, and a smoke cloud would be carried to the same height.

Under other circumstances, a current of warmer air may be blowing at an elevation of a few hundred feet, so that the temperature gradient may become zero or even positive, giving an inversion at this elevation. There is no tendency for the lower air to rise

through this warmer lighter layer, and a definite ceiling will be established for the convective turbulence. Within this layer the atmosphere turns over and over, and the smoke may become diffused throughout the layer before it has traveled very far. It must be remembered, of course, that eddy diffusion always takes place at the boundaries of the upward convection currents, so that some smoke will become diffused throughout the settling layer of cooler air even with a high convective ceiling.

26.2.5 Angle of Rise

The rate of rise of the convective current increases with the thermal instability. The angle of rise of the smoke cloud (as a statistical average) is inversely proportional to the wind velocity. With zero wind, the convective currents rise directly upward. As the wind increases, the direction of the convective current must incline more and more away from the vertical.

26.3 EVAPORATION AND DEPOSITION OF AEROSOLS

Travel of smoke clouds has been discussed in the first part of this chapter, from the standpoint of meteorological conditions. Since the particles of which screening smokes are composed are too small to fall out appreciably by Stokes' law, and have too low a vapor pressure to evaporate, screening smokes will persist almost indefinitely, i.e., until the cloud is so diluted by atmospheric diffusion that it is no longer apparent to the observer. Naturally occurring fogs, however, disappear both by evaporation and by Stokes' law deposition, and clouds of aerosols may be set up which are subject to attenuation by one or both processes.

The fundamental factor in estimating the rate of either process is the concentration of aerosol at the ground level or at some stated height above the ground. The difficulties that arise in estimating this quantity have been emphasized and need not be reiterated here. Rather, the discussion will be limited to conditions where some sort of satisfactory estimate of concentration over a considerable area can be made. The discussion will be limited to the following conditions.

1. The thermal gradient at ground level is positive, or in the limit, neutral, so that the lower atmosphere is stable.
2. Wind velocity is moderate.
3. Terrain is level with uniform vegetative cover.
4. The aerosol drops are not larger than 5 microns radius.

If the foregoing conditions are satisfied, the only turbulence in the air will be the mechanical turbulence produced by the vegetative cover of the terrain. The drop size is large enough so that Stokes' law deposition occurs, but not large enough so that a major portion will fall out before the transient effects of the generator have disappeared and the clouds have become stabilized. The concentration will decrease from the ground upward and, under the conditions postulated, will probably become negligible at a point two to three times the height of the vegetative cover. It is not possible to judge the height of the cloud by the eye, since considerable concentrations of the larger drops will be inconspicuous while a small amount of smoke of smaller drops (about 1 micron) will be very noticeable. If the cloud is generated from a plane, the initial height of the cloud will be very much greater than if the generators are located on the ground.

26.3.1 Approximate Rule for Concentration in Cloud

Under the stable air conditions assumed above, and with a line of generators at right angles to the wind, one may use the following approximate rule. Assume that the height of the cloud is the same as the height of the vegetative cover and that the concentration does not vary with height. This will be approximately true for fog of uniform particle size. The concentration near the ground will then be the concentration expected, if the foregoing conditions are satisfied.

To illustrate, suppose that with a wind velocity of 5 m per sec, 100 g of aerosol are generated per sec per m of front, and that the height of the vegetative cover is 25 m. The mass concentration to be expected when the cloud is initially diffused is 0.8 mg per l.

The foregoing rule may lead to errors of 100% or more, and it becomes meaningless when applied to nearly bare ground. When measurements of R can be made, the British diffusion equation may be used to give a more exact result. But, unless the measurements are made on the spot, the use of the equation is not likely to decrease the error very much.

26.3.2 The Evaporation of Aerosols

A satisfactory formula for the evaporation of drops whose vapor pressures range from that of water to nitrobenzene appears to be the equation of Fuchs,

[redacted]

$$\frac{dn}{dt} = \frac{2\pi kd}{RT}(p_0 - p). \tag{1}$$

Here dn/dt equals the rate of formation of vapor in moles per second per drop, k the diffusivity of the vapor in air, d the drop diameter, R the gas constant, T the absolute temperature, p_0 the vapor pressure of the liquid, and p the actual partial pressure of the vapor present in the air; CGS units are required for the formula.

The mass rate of evaporation is proportional to the drop diameter. The rate of change of drop diameter at a constant mass rate varies inversely as the square of the diameter. Thus, if both sides of equation (1) are multiplied by M/ρ where M is the molecular weight and ρ the liquid density,

$$\frac{M}{\rho}\frac{dn}{dt} = -\frac{dv}{dt} = \frac{2\pi kMd}{\rho RT}(p_0 - p). \tag{2}$$

Here v is the volume of the liquid drop. Substituting $2r$ for d,

$$\frac{dv}{dt} = \frac{4\pi r^2 dr}{dt} = -\frac{4\pi kMr}{\rho RT}(p_0 - p). \tag{3}$$

Hence,

$$\frac{dr}{dt} = -\frac{kM}{\rho RT}\left(\frac{p_0 - p}{r}\right). \tag{4}$$

This may be integrated to

$$r^2 = r_0^2 - \frac{2kM}{\rho RT}(p_0 - p)t, \tag{5}$$

or

$$d^2 = d_0^2 - \frac{8kM}{\rho RT}(p_0 - p)t. \tag{6}$$

Hence, as the drop evaporates, the rate of decrease of drop diameter varies inversely as the drop diameter. A curve showing the decrease of drop diameter with time is shown in Figure 6, plotted from the data shown in Table 2. As the drop size becomes smaller the drop decreases in diameter more and more rapidly.

TABLE 2. Diameter of evaporating drop as a function of the time for a typical liquid.

Mol wt = 100; density = 1; k = 0.1 cm² per sec; p_0 = 0.01 mm; p = 0; T = 298 K.

Drop diameter (microns)	Time (seconds)
10.0	0
7.5	10
3.7	20
3.09	21
2.24	22
0.95	23
0	23.2

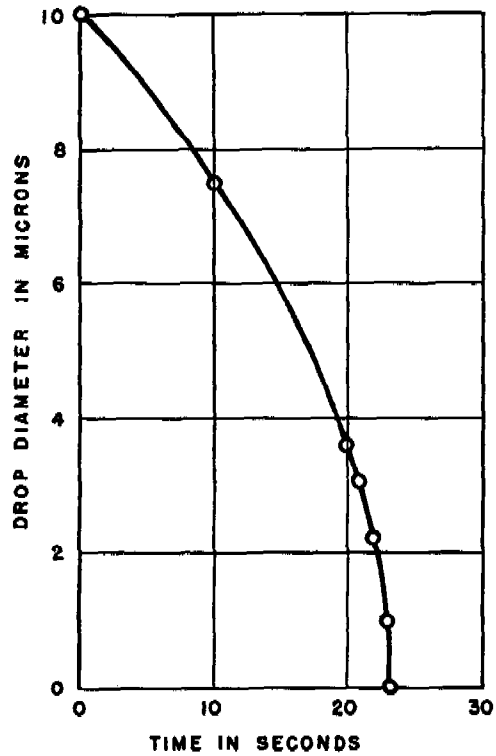


FIGURE 6. Evaporation of 10-micron drop.

If it is desired to estimate the vapor concentration in equilibrium with an aerosol, an estimate must be made of the original concentration, and a step-by-step integration must be made to estimate the change in concentration with time and distance of travel downwind.

26.3.3 Deposition of Aerosols

If the concentration is known at any point in an aerosol cloud, the rate of deposition per unit area through Stokes' law fall can be estimated. Let V_0 = the Stokes' law rate of fall for the particular aerosol particles forming the cloud. Then the rate of deposition per unit area is

$$V_0 C,$$

where C is the concentration per unit volume. If the cloud is assumed to be of uniform concentration at all times, and of height h, then the rate of change of concentration with time is

$$-\frac{dC}{dt} = \frac{V_0 C}{h}. \tag{7}$$

Integrating

$$\ln\left(\frac{C_0}{C}\right) = \frac{V_0 t}{h}. \tag{8}$$

The concentration at any point downwind could be calculated if the wind velocity were known.

The above calculation assumes a single surface for deposition and would hold for a cloud traveling over bare ground. When the area is covered with vegetation, the area of deposition may be doubled.

26.3.4 Inertial Effects

With wind velocities of several miles per hour, inertial effects become very important in deposition, especially because the leaves of many plants are covered with hairs of small dimensions, which prove to be very effective in filtration. The deposition due to inertial effects in dense vegetation may prove to be several times that due to Stokes' law deposition. When one considers that an aerosol will usually not be of uniform particle size and that the concentration at any point in the cloud is a highly variable quantity, one sees that the estimate of rate of deposition from an aerosol cloud in a jungle area may be in error by several hundred per cent.

Chapter 27

THEORY OF OBSCURATION

By *W. H. Rodebush*

27.1 THE CONTRAST LIMEN

IN ADDITION TO physiological and psychological factors affecting visibility of a target through fog or smoke clouds, there are at least two physical factors of fundamental importance. These are the contrast offered by the target and the amount of light scattered by the cloud. The contrast of the target is measured roughly by the reflectivity of the target, although color affects the contrast to a degree. The ordinary smoke box experiments are usually made with a target consisting of a white square on a black background. The white square has a reflectivity near unity and the black background is near zero, so that the contrast is nearly equal to the intensity of illumination of the target. With actual targets, however, which are usually camouflaged to a certain extent, the differences in reflectivity may not be more than 10%. An exception is the case of the wake of a vessel viewed from the air, where the contrast becomes very great.

If the reflectivity of target and surroundings is r_1 and r_2 respectively, then the contrast C may be defined as the difference in intensity of the reflected light, that is,

$$C = (r_1 - r_2)\, I_t = \Delta r I_t \qquad (1)$$

where I_t is the intensity of illumination on the target and its surroundings.

The contrast limen is defined as the critical ratio C/I_1 necessary for visibility. C is now the observed difference in intensity and I_1 is the total intensity of light received by the eyes from the general direction of the target. The contrast limen depends upon the total intensity of illumination, the angle subtended by the target, and various other physical and physiological factors. It is not the same for different observers, nor for the same observer at different times. However, under ordinary daylight conditions, it may be stated that for complete visibility C/I_1 must not be less than 1% and for complete obscuration not greater than 0.3%.

27.1.1 Visibility in a Natural Fog

When both target and observer are enshrouded in a natural fog, the intensity of illumination reaching the target and entering the eye of the observer is the same. The contrast ratio C/I_1 becomes, therefore,

$$\frac{(1-\alpha)\Delta r I_1}{I_1} = (1-\alpha)\Delta r, \qquad (2)$$

where $1 - \alpha$ is the fraction of the light reflected by the target that reaches the eye of the observer without being scattered. If it were not for the fog, the eye would receive only the light reflected from the target, but because of the scattering and diffusion of light by the fog, the intensity of illumination is uniform everywhere.

27.1.2 The Extinction of Light by a Fog

The transmission factor, $1 - \alpha$, for light traveling a distance l centimeters through a fog is given by an expression of the general form, $1 - \alpha = e^{-\kappa l}$ where κ is the scattering coefficient per unit distance in a fog. Since [from the theory of scattering (Chapter 21)] the effective scattering area for small drops is known, it is possible to calculate by statistical methods with a fair degree of approximation the scattering coefficient for a fog.

Assume that the fog consists of drops of uniform size, each drop having an effective scattering cross section of $1/N$ sq cm and that there are n drops per cc. Imagine a cross section of 1 sq cm at right angles to the line of vision to be divided into N equal squares with area equal to the effective scattering area of a drop. If only one drop is present, the chance that the center of this drop will lie in any of these small squares is $1/N$, and the probability that the center of the drop will not lie in any specified small square is $1 - 1/N$. If there are n drops per cc, the probability that no drop will have its center in a specified square is $(1-1/N)^{nl}$. The total area of squares per sq cm in which the center of a drop does not lie will be just $(1 - 1/N)^{nl}$. Since nl and N are large, this expression becomes $e^{-nl/N}$.

This result does not mean that a fraction of the total area equal to $e^{-nl/N}$ will be unobstructed for vision, for there will be overlapping of drops whose centers lie in areas adjacent to a vacant square. In order to appraise the extent of this overlapping, the

assumption will have to be made that the squares adjacent to an empty square contain the average number of drops randomly distributed. This cannot, of course, always be the case, but the errors introduced will perhaps be as often positive as negative, and the estimate will be a good first order approximation. By a process of counting, the fractional obscuration due to overlap is estimated to be $0.3nl/N$ where nl/N is the average number of drops per square. The fraction of light transmitted unscattered becomes

$$1 - \alpha = \left(1 - 0.3\frac{nl}{N}\right)e^{-nl/N} . \qquad (3)$$

This formula agrees with reported results. For example, it is reported that visibility is 200 m in a natural fog of 0.18 g water per cu m. This would correspond to $n = 8$ drops of 35 microns diameter per cc. Taking the effective scattering area for the drop as $2\pi r^2$ (Chapter 21), $nl/N = 3.1$, which approaches the limiting value, and $1 - \alpha = 0.32\%$. One notices that when nl/N becomes 3.33, the result indicates that even a square in which no centers of drops lie will be completely obscured. One, therefore, concludes that when the effective obscuring area of the drops present in a region is 3.33 times the actual area measured at right angles to the line of vision, the visibility will be zero.

27.1.3 The Extinction of Light by a Screening Smoke

Since $1/N = a$, the *effective scattering area* for a drop, equation (3) may be written

$$1 - \alpha = (1 - 0.3nla)e^{-nla} \qquad (4)$$

The expression nla represents the total effective scattering area of all the drops that lie in the line of sight, per unit of cross-sectional area. This expression is equivalent to, and may be replaced by, the expression Aw, where A is the total effective scattering area per unit weight of the material as dispersed, and w is the weight of material dispersed per unit of cross-sectional area. Since the expression is dimensionless, any units may be used as long as the same units are used for A and w; w is often expressed in grams per square meter.

Thus, for Diol 55 dispersed in particles of optimum size for screening smoke (about 0.3-micron radius), A is about 10 sq m per g. The expression for extinction [equation (4)] then becomes

$$1 - \alpha = (1 - 0.3w)e^{-10w}. \qquad (5)$$

27.1.4 Conditions Approaching Extinction

The remarkable property of a fog or smoke of considerable density is that an object either appears visible or disappears completely, there being no appreciable zone of partial visibility as long as the illumination is adequate. This is partially due to the sharpness of the contrast limen, but it is also due in part to the effect of the overlapping drops. The formula above shows that, as the exponent approaches a value which is estimated to be in the neighborhood of 3.33, the light transmission, instead of continuing to fall off exponentially with the increasing depth of fog penetrated, suddenly becomes zero. This result agrees with experience. It will not be possible to check this expression by observations of visibility in natural fogs because of the difficulty of estimating the exact number and size of drops present per cubic centimeter of air, but it may be taken as a reasonably reliable formula.

27.1.5 Variation of Visibility with Concentration

It has been assumed in the foregoing considerations that the interference of a fog with vision depends only upon the total number of fog particles per unit area of cross section that lie in the line of vision and in no way upon the distribution in space of these particles. That is to say, a high concentration along a short path would produce the same obscuration as a low concentration over a long path. This assumption is at least approximately correct, and it follows that the limiting distance for visibility for a given drop size will be given by the relation

$$l_0 \sim \frac{1}{n} ,$$

where n is the number of drops per cubic centimeter. In very dense fogs the visibility is likely to be reduced, because the contrast limen depends upon the total intensity of illumination.

27.1.6 Visibility in Artificial Fogs; Smoke Screens

The artificially produced fog cloud differs from the naturally occurring fog in that it may occupy only a relatively narrow region between the target and the observer, with both the target and observer entirely out of the cloud. Under these circumstances, the intensity of illumination may be very different at the target and at the eyes of the observer. Because of this fact, the quantity of fog or smoke required for

complete obscuration is a highly variable quantity, and no reasonable figure can be given that will be adequate under all conditions.

The general formula for visibility may be written

$$\frac{\Delta I_1}{I_1} = \frac{(1 - \alpha)\Delta r I_t}{I_1}. \tag{6}$$

Here I_t is the intensity of light on the target and I_1 the total intensity of light reaching the eye of the observer. The contrast at the target is $\Delta r I_t$, and $\Delta I_1 = (1 - \alpha)\Delta r I_t$ is the contrast perceived by the observer as diminished by the screen. $\Delta I_1/I_1$ must be less than 0.003 for complete obscuration. For a screening smoke of Diol 55, $1 - \alpha$ is given by equation (5).

The greatest difficulty lies in estimating the values of I_t and I_1. Before we can estimate values for these quantities, we must consider the penetration of light in fog. The fraction of the total intensity that penetrates a fog without being scattered is a far different quantity from the total intensity of light that penetrates a fog after repeated scattering. Because of the complicated way in which it is scattered as a function of angle, and because multiple scattering occurs, it is not possible to calculate the penetration factor exactly, but an approximation is given by the following considerations. Imagine the cloud to be made up of a large number of single layers of particles. Light which is scattered by one of these layers is scattered in all directions, but a major fraction of it is scattered in the forward direction. On the other hand, a certain fraction $1/k$ is scattered in the backward direction. A complete analysis of the problem shows that the total fraction of incident light returned by m layers is

$$f_m = \frac{m}{m + k - 1}. \tag{7}$$

Hence, the fraction that penetrates m layers is

$$1 - f_m = \frac{k - 1}{m + k - 1}. \tag{8}$$

It has been shown that the equivalent of more than three *continuous* layers of drops is required for complete obscuration. Estimating a value of $1/k = 1/4$, one sees readily that the equivalent of three layers would not reduce the penetration to less than one-half. If the cloud is of sufficient depth and concentration to correspond to many layers, practically all the light entering a cloud must be returned to the same side of the cloud which it entered and from which it is now scattered in a backward direction. Thus, a thick cloud must behave as a perfectly *white body*, one which returns by diffuse reflection (scattering) 100% of the light which falls upon it. The upper surface of a cumulus cloud appears a brilliant snowy white in the sunshine while the under side of the cloud may appear black because of the failure of light to penetrate.

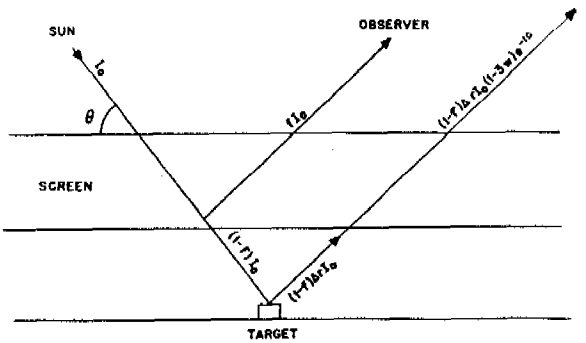


FIGURE 1. Obscuration by a blanket screen. I_0 = incident light. fI_0 = light scattered back by cloud. $(1 - f)I_0$ = light reaching target.

It is possible now to set up the expression showing the exact dependence of the degree of obscuration by a blanket screen upon the various factors. Referring to Figure 1, the contrast ratio will be

$$\frac{\Delta I_1}{I_1} = \frac{(1 - f)\Delta r I_0(1 - 3w)e^{-10w}}{fI_0}. \tag{9}$$

The greatest amount of smoke will be required when both sun and observer are directly overhead. Assume $w = 0.25$ g per sq m. Assuming $\Delta r = 0.1$, then $\Delta I_1/I_1 = 0.0025$, which is below the limen for obscuration. On the other hand, a greater contrast (larger Δr) would not give obscuration. A Δr of 0.1 might be expected in an area which has been camouflaged to give low visibility. A dark object on snow or the wake of a ship against quiet water would, on the other hand, give values of Δr approaching unity.

When the sun and the observer are at angles less than 90° with the horizon, the quantity of smoke required will be less. The effective value of w will be increased in the ratio $1/\sin\theta$, where θ is the angle with the horizon. The penetration will be less for smaller values of θ, and in particular, if the sun and observer are at 180° azimuth, the value of f in the denominator will no longer be the same as the value for f in the numerator, but will be much greater.

At low angles for sun and observer, when the observer is facing the sun, the cloud behaves as if it were a mirror giving specular reflection, because of

the tendency toward forward scattering. The top of the cloud will then have a brightness several times that of a perfectly white body.

Thus it happens that the amount of smoke required for obscuration by a blanket screen is greatly reduced: (1) by the reduction in illumination of the target, and (2) by the glare thrown back from the top of the cloud into the eye of the observer. If the cloud is of small extent and high, the illumination of the target will not be reduced, and any artificial illumination of the target at night, for example, will require a larger quantity of smoke for obscuration.

With curtain screens, the illumination of the target will not be reduced, and the second effect mentioned above will be present only when the observer and sun are on opposite sides of the screen.

27.2 COLORED SMOKE

The theory of the scattering of light by absorbing or reflecting particles has not been perfected to the same degree as the theory for transparent particles. Hence, it is not possible to make positive statements as to the variation of the *effective scattering area* as a function of particle size and wavelength. Certain thermally stable dyes can be vaporized to give colored smokes. Such smokes may show some of the characteristics of solutions, such as fluorescence and selective reflection. If the particle size is too small, the color may not be that of the original dye. For colored smoke signals it is satisfactory to produce a particle size somewhere between 1 and 5 microns diameter.

27.2.1 Colored Smoke Screens

White smoke screens (transparent particles) may be very conspicuous, particularly on moonlight nights or over water, so that they serve to point out the target rather than to conceal it. It would be desirable to produce screens of neutral or pastel tints ranging from blue-green to dark brown or black for tactical operations. Dyes are obviously too expensive to be used in a pure state on such a scale.

It is evident that the high screening efficiency per pound of material that is obtained with Diol 55, for example, is due to the very careful control of particle size, a particle being produced which has an effective screening area several times its geometrical area. About the only materials that can be used for making smoke are transparent or nearly colorless materials such as hydrocarbon oils. Carbon is, of course, a cheap and available material, but carbon smoke cannot be produced in the particle size desired, and even carbon black is a relatively expensive material.

A few per cent of oil soluble dye dissolved in a fog oil will give a smoke which in high concentrations shows a good deal of color. When the smoke thins out to a screening concentration, however, the color fades and the smoke appears to be white or nearly so. The explanation for this behavior is not difficult. Very little absorption takes place when light is scattered by a particle of the optimum particle size for scattering, but after repeated scattering, enough absorption will have occurred to give a pronounced color. If the smoke cloud is of great density and depth, all of the light will be thrown back by repeated scattering, and a strong color will be observed. As the cloud thins out, much of the light penetrates clear through the cloud, and the light that is scattered backward has undergone only two or three scatterings. The cloud now behaves as a white body of poor reflecting power, but it is scarcely less conspicuous than if the dye were not present.

PART IV

NEW MUNITIONS FOR SMOKE AND TOXIC GASES

Chapter 28

INTRODUCTION

By *H. F. Johnstone*

28.1 ORGANIZATION

EARLY IN THE PREPARATION for World War II, work was started on the development of new methods for dispersing smoke and toxic aerosols. Some of the first contracts supported by Section B5 of NDRC were on the development of new smoke generators and improved munitions for dispersing DM and CN. Later, following the inauguration of an extensive field testing program in which concentrations of toxic gases from standard munitions were measured, and estimates made on the munition requirements for various tactical situations and meteorological conditions, Section B6 was requested to undertake work on the improvement of gas munitions. When the two sections were reorganized as Division 10, the munitions work was concentrated in one contract at the University of Illinois which operated under Service Projects: CWS-1, "Aerosols: Their Generation, Stabilization and Precipitation," and CWS–27, "Simple and Unusual Munitions for Setting up Field Concentrations of Chemical Warfare Agents." In this section the technical aspects of several new munitions and devices, which were developed for dispersing smoke, toxic and insecticidal aerosols, and toxic gases, will be discussed.

28.2 NEW SMOKE MUNITIONS

Fundamental studies on the evaporation of liquids, carried on in connection with the development of new designs of the DM candle and CN generators, led to suggestions of new methods for the dispersal of aerosols. These formed the basis of several new munitions which were developed later. It was shown that extremely rapid rates of heat transfer could be obtained by finely atomizing a liquid as it was injected into a hot gas stream. The atomization was accomplished by injecting the liquid at the throat of a Venturi through which hot gases were passed at high velocities. In this way, complete evaporation of relatively high boiling liquids could be accomplished within a few milliseconds, so that decomposition of heat-sensitive agents was reduced to a minimum. Several new oil smoke generators were developed on this principle. These included smoke pots and floats and a smoke generator to be attached to the exhaust of airplane engines. The possibility of setting up oil smoke clouds in this way was especially attractive because, as a substitute for HC, it eliminated the toxicity and the glow of the burning pyrotechnic mixture, both of which were serious handicaps to the standard pot. During the later stages of World War II, when it was necessary to set up smoke screens of long duration, the need for the oil smoke pot became particularly pressing and the work on the new developments proceeded under high priority.

The lightweight exhaust generator for airplanes had an output of 40 to 50 gal of fog oil per min, when installed on the single engine 1,900-hp TBM-3 plane. It produced satisfactory smoke screens of 2 to 10 min duration under all meteorological conditions when the plane was flying at a speed of 200 knots. The possibility of using a formation of planes with this equipment, for providing rapid protection of harbors and task forces at sea, was recognized as a possible defense against *kamikase* attacks, and equipment for 72 planes was procured during the summer of 1945. These planes were not used, however, before the war ended.

The extensive use of phosphorus smoke munitions in the Sicilian and Italian campaigns resulted in an urgent request in the fall of 1943 for work on the improvement of this type of smoke filling, especially with the view of eliminating the pillaring characteristic. The possibility of mechanically reinforcing the filling with steel wool, gauze and tubes had been tried with only partial success. The idea of incorporating the phosphorus granules in a matrix of rubber was then suggested and this resulted in the development of plasticized white phosphorus [PWP]. Field tests on the new smoke agent in bombs, rockets, and mortar shells were carried on during the summer and fall of 1944. Its superior quality finally led to its adoption as a standard smoke-filling in place of WP for all nonrotating projectiles and rockets used by the Army Ground Forces, as well as for the 4.2-in. chemical mortar and for the 3.5-in. and 4.5-in. Navy rockets, and for the M–47 bomb.

The thermal generator method described above was also adapted for evaporating heat-sensitive

organic dyes for new and efficient target identification markers and floating distress signals. This was the basis of a new target identification bomb (Bomb, Target Identification, Smoke, Mark 72, Mod 2), which was demonstrated in June 1945. A number of these bombs were manufactured for Service test.

Because of the possibility of a short supply of chemicals for the hexachloroethane smoke mixture, in 1942 an intensive study was made of possible substitutes. New mixtures were developed containing the anhydrous chlorides and complexes of more readily available salts. A sulfur nitrate smoke mixture was also developed and demonstrated to the Chemical Warfare Service. Attention was also given to a sulfur smoke generator built on the thermal generator principle. A successful model of this device was completed in May 1943. The unit, although quite light, had only a small capacity, and the limitations imposed, coupled with considerable improvement in the oil smoke generators at the same time, made it undesirable to continue with the project. The information obtained, however, was valuable in the development of the direct combustion-type oil smoke generator, such as the Hesson-York unit, which utilized the Venturi design.

28.3 TOXIC VAPORS AND AEROSOLS

While toxic gas was not used during World War II, considerable effort was spent in developing new weapons for dispersing it in the most effective manner. With the improvement of the gas mask and other protective measures, it was realized that either agents of much greater toxicity must be found, or else much greater concentrations of the known agents must be established to be of value in tactical situations. The value of dispersing the liquid agents as aerosols to establish high concentrations was recognized by both sides. The Germans had made elaborate field studies in which they demonstrated the potency of mustard gas and Tabun (MCE) when dispersed from shells and bombs with extremely heavy bursters which shattered the chargings into fine droplets, most of which remained airborne until evaporated. The important tactical use of these weapons was mainly to set up high initial concentrations to achieve casualties before protection could be gained. The Germans claimed that a single 250-kg bomb charged with H-arsenöl mixture, with a 34-lb TNT burster, could produce a lethal area of 4,000 to 4,500 sq m for a 1-min exposure.

The great potency of mustard vapor was recognized even in World War I. A method for taking full advantage of this effect was developed in the form of a thermal generator bomb which operated on the Venturi principle already described. Field tests indicated that it was easily possible to set up mustard vapor concentrations which exceeded the lethal dosage even of masked men within less than a minute, using clusters of bombs identical in size with the oil incendiary bombs and having the same dispersion pattern. Tests on cave fortifications with similar devices showed that dosages could be established with a small expenditure of munitions which exceeded the best protection of impregnated clothing. While the limitation of the small thermal generator bomb (designated E29R1) was recognized in that it must impact and remain in a vertical position in order to function properly, a larger bomb was developed near the end of World War II which did not have this restriction.

Work similar to that of the Germans on dispersing aerosols by means of an HE burster was also carried on by the Munitions Development Laboratory [MDL]. In this case, however, the size of the bomb was intentionally made small so that it could be carried in standard clusters and take the maximum effect of the burster. It was contemplated that this bomb might also be used for dispersing solutions of insecticides from airplanes over enemy-held territory.

Because of the considerable interest in the development of new highly toxic powders, work on a new munition for dispersing these agents was also carried on. Several of the materials considered were quite sensitive to even moderate temperatures and to explosive shocks. It was desirable, therefore, to find other means of dispersing the powders than by high explosives. Preliminary tests showed that good dispersal could be obtained by the sudden release of a gas under high pressure through the agent compartment. This principle was incorporated in a bomb which used either a small cylinder of air at 4,000 lb pressure or a cylinder of liquid carbon dioxide. The gas was released by the action of a mechanical fuze, or an explosive train.

Work on several miscellaneous devices and munitions was also carried on at the MDL. Some of these proved to be unsuccessful and were abandoned, while others were developed with the utmost dispatch but failed to be used during the war, either because they were developed too late or because need for them did

not arise in the later campaigns. One of the interesting problems on which the staff of the MDL cooperated, because of its experience in the dispersal of solid particles, was the development of means for dispersing herbicides. It was decided that the most feasible method of dispersal was by means of an aimable air burst bomb. This necessitated a study of the fall of granules of the material through air and the measurement of dosage patterns to determine the most desirable size of the particles and the containers. Here again, the sudden ending of World War II in the Pacific made use of this weapon unnecessary.

Chapter 29

ATOMIZATION OF LIQUIDS

By *H. F. Johnstone*

29.1 INTRODUCTION

THE EFFECTIVENESS of many liquid agents used in warfare depends upon atomization to produce small droplets. This is true not only of chemical agents, but also of smokes and insecticides and even applies to liquids used in other ways, since atomization is necessary for carburetion and combustion of fuels. The degree of atomization desired depends upon the nature of the agent and the use to which it is being put. In the generation of oil smokes, for instance, it was found that the optimum drop size for maximum obscuration is considerably below the range attainable by mechanical atomization. Consequently, it was necessary to evaporate the oil completely and to produce the droplets by condensation following discharge of the vapor into the air. The evaporation of oil by heat transfer from hot gases takes place most rapidly when the liquid is atomized as completely as possible. On the other hand, in the application of insecticides it was found that the drop size useful for screening smokes is entirely too small to give efficient results. The optimum size occurs when the particles are just small enough to be dispersed by the wind and still produce the maximum contact effect on insects as well as give an efficient coverage when they are deposited on foliage and water surfaces. The optimum drop size for this purpose appears to lie between 10 and 50 microns diameter.

In the dispersal of the vesicant chemical warfare gases the so-called *persistent* effects for the denial of terrain and contamination of personnel are best obtained when the drops are fairly large, i.e., within the range of 1 to 5 mm diameter. During the war, the perfection of the gas mask and development of protective clothing shifted the emphasis to other tactical uses of these agents which depended upon surprise and the setting up of high concentrations of vapor and aerosols which would produce lethal dosages before the protection of the mask could be gained. Much attention was given to mechanical and thermal methods of dispersing mustard gas and other vesicant agents as aerosols. The atomization of liquid agents by high explosives was the principal method adopted for the dispersal of these agents by the Germans.

In this chapter a review will be made of the principles of atomization on the basis of present knowledge. These have led to the development of several new chemical and smoke munitions.

29.2 ATOMIZATION BY NOZZLES

29.2.1 Mechanism of Droplet Formation

The basic mechanism of the formation of finely divided drops consists of drawing out the liquid into slender streams or filaments. Such filaments are unstable and any slight displacement causes them to contract in some places and expand in others so that eventually they collapse into droplets. High-speed photographic studies show clearly the formation and disruption of the filaments in a manner which depends on the air velocity. At low velocities, the relative motion between the air and the liquid stream produces a bead-like swelling and contraction with continuously increasing amplitude until the liquid jet finally breaks up into separate drops. As the velocity of the air is increased somewhat, a fluttering action of the jet begins, forming a twisted ribbon of liquid. A portion of the ribbon is caught up by the air stream and, being anchored at the other end by surface tension, is drawn out into a fine ligament. This ligament is quickly cut off by the rapid growth of a dent in its surface and the separated mass is swiftly drawn up into spherical drops. At still higher air velocities, there is a flattening action of the twisted ribbon to form a cobweb-like film which is so thin that it is readily torn apart into microdroplets.

There is some evidence that there is a minimum average drop size attainable in the atomization of a liquid by air.[1] Sauter[2] measured by photometric means the size of the drops formed when water is atomized in an air stream, and found that, at high air speeds, the mean diameter approaches asymptotically a value of about 12 microns at air velocities of 330 to 400 fps. The idea of a limiting degree of atomization of liquids in air, however, is opposed by Littaye.[3] In any case, it is evident that, from a practical point of

view, it is very difficult to secure complete atomization to the sub-micron range. It is true that a large percentage of the drops from an atomizing nozzle may exist in this range but the actual percentage of the mass of the liquid below 1 micron is very small. This conclusion, which is based on the amount of energy required to provide a high-velocity air stream with large ratio to the liquid rate, indicates that no air atomizing nozzle can be perfected which will efficiently produce a screening smoke from a non-volatile liquid.

29.2.2 Types of Nozzles

Spraying devices may be classified as pneumatic, hydraulic and mechanical, according to the principle employed in effecting the dispersion of the liquid. These types differ characteristically in the degree and uniformity of the dispersion produced and in their industrial applications.

1. Pneumatic nozzles in which compressed air or steam is used to effect atomization are capable of producing the finest dispersion. They are commonly used for paint spraying, humidification of gases and atomization of oil for burning. Industrial pneumatic nozzles are classified as internal mixing and external mixing, according to the relative positions of the liquid and gas jets. A nozzle is described as external mixing if the contact between the fluid and the gas takes place entirely outside the nozzle, and internal mixing if the contact occurs within a chamber from which the spray exits through an orifice.

2. Hydraulic nozzles are available in a variety of forms and sizes. The most common is the so-called hollow-cone nozzle in which the liquid is led into a whirl chamber through tangential passages or through a fixed spiral so that it acquires a rapid rotation. In either case, the liquid emerges through a relatively large orifice which is placed at the axis of the whirl chamber. The basic principle is that of imparting angular motion to the liquid which causes it to be thrown out as a thin hollow cone moving at a high velocity. The relative volume of air which is engaged for atomization depends upon the angle of the cone and the design of the orifice. These nozzles are characterized by low power consumption and large capacity, but the atomization obtained is relatively poor, compared with air-atomizing nozzles, unless extremely high pressures are used. In one form of hydraulic nozzle the liquid, under high pressure, is forced through a very small orifice or slit. This type of nozzle has found some application in diesel engine fuel injection. Another type of hydraulic nozzle which is used for special purposes and apparently gives good atomization, but still somewhat less than the pneumatic nozzle, is the impact nozzle. Here, a solid stream of liquid under pressure is caused to strike a solid surface or another similar stream to give the necessary dispersion.

3. Mechanical nozzles are used when the liquid to be atomized has a high viscosity or carries suspended particles which may clog a small orifice. Atomization is obtained by discharging the liquid onto a disk rotating at high speed. The centrifugal force hurls the liquid into the air, thus providing the velocity necessary to produce atomization. These devices have found extensive use in spray drying.

29.2.3 Performance of Pneumatic Nozzles

In spite of the importance of the degree of atomization obtained from commercial nozzles, there have been actually very few measurements made of the drop size distribution in a spray pattern. Few nozzle manufacturers are in position to report the actual degree of fineness produced by their products. Possibly the reason for this is the difficulty in collecting representative samples of the droplets from the spray, and in measuring the actual diameters after the droplets are collected. Some of the studies reported have used obviously imperfect methods which have led to erroneous conclusions regarding nozzle performance. The most complete study in this interesting field was made by two Japanese engineers, S. Nukiyama and Y. Tanasawa [4] at Tokyo Imperial University. This work led to two empirical correlations on the drop size distribution and performance of pneumatic nozzles. These have served as a basis for a more extended study made at the Munitions Development Laboratory in which it was found that the same methods of correlation could be used for large exhaust atomizers, airplane sprays, and, in a limited way, to explosive bursts.[5]

Nukiyama and Tanasawa studied the atomization of several liquids of varying physical properties with small gas atomizing nozzles of various types operated with compressed air. They collected samples of the spray droplets from several points in the spray by means of a cylindrical shutter device which gave an exposure time of 0.002 to 0.01 sec. The drops were received on a cover glass coated with a film of oil which was then photographed under a microscope

so that the size distribution could be measured. The following factors influenced the degree of atomization.

1. The effect of the relative velocity of the air past the droplets.

2. The effect of the physical properties of the liquid, including surface tension, viscosity and density.

3. The effect of the relative quantity of air expressed by the ratio of the volume of air to the volume of liquid.

Within a limited range of these variables, that is, for densities between 0.8 and 1.2, surface tensions between 30 and 73 dynes per cm, viscosities between 0.01 and 0.3 poises, and for air velocities below the acoustic velocity, the following empirical equation represents the degree of atomization:

$$D_0 = \frac{585\sqrt{\sigma}}{v\sqrt{\rho}} + 597\left(\frac{\mu}{\sqrt{\sigma\rho}}\right)^{0.45}\left(\frac{1{,}000Q_L}{Q_a}\right)^{1.5}, \qquad (1)$$

where D_0 = diameter, in microns, of a single drop with the same ratio of surface to volume as a representative sample of the drops in the spray;

v = difference in velocity between air and liquid at the *vena contracta*, in meters per second;

Q_a/Q_L = volume flow rate of air/volume flow rate of liquid;

ρ = liquid density, grams per cubic centimeter;

μ = liquid viscosity, poises;

σ = liquid surface tension, dynes per centimeter.

The distribution of the drop sizes in a spray can be represented by a relatively simple empirical formula of the type:

$$\frac{dn}{dx} = ax^p e^{-bxq}, \qquad (2)$$

where x = drop diameter, in microns;

n = total number of drops in the sample with diameters between zero and x microns;

a, b, p, and q are constants.

Nukiyama and Tanasawa found that when the velocity and the quantity of the air were both high and sufficient, i.e., velocities above 450 fps and for air/liquid ratios greater than 5,000, the values of the constants were $p = 2$ and $q = 1$. For poor atomization, which is obtained at low air velocities and low air/liquid ratios, the value of q decreases to ½ to ⅙, but p appears to remain constant.

The significance of the constants a and b in equation (2) is of interest. These relationships follow from the fact that by definition,

$$D_0 = \frac{\int_0^\infty x^3 dn}{\int_0^\infty x^2 dn}. \qquad (3)$$

If p, q, D_0, and the total volume of sample under consideration (or the total number of drops) are known, the integration can be carried out and the constants a and b determined. The relationships among a, b, q, D_0, and the total volume of sample are shown in Table 1 for the case when $p = 2$. If $1/q$ is an integer, the calculations may be performed by the usual methods of calculus and an ordinary integral table; but the labor is considerably less if a table of gamma functions is utilized. If $1/q$ is not an integer, the use of table of gamma functions is advisable.

TABLE 1. Relationship between q, a, b, V, and D_0, when $p = 2$.

q	D_0 as a function of b	a as a function of b and V*
2	$1.50/\sqrt{b}$	$1.91b^3V$
1	$5/b$	$1.59 \times 10^{-2}b^6V$
½	$110/b^2$	$2.39 \times 10^{-8}b^{12}V$
⅓	$4{,}080/b^3$	$1.79 \times 10^{-15}b^{18}V$
¼	$213{,}000/b^4$	$1.84 \times 10^{-23}b^{24}V$
⅕	$14{,}300{,}000/b^5$	$5.32 \times 10^{-32}b^{30}V$
⅙	$1{,}170{,}000{,}000/b^6$	$3.08 \times 10^{-41}b^{36}V$
General case when $1/q$ is an integer	$\frac{(6/q)!}{(5/q)!} \times \frac{5}{6} b^{-1/q}$	$\frac{36b^{6/q}V}{(6/q)!\pi}$

* V = total volume of sample in cubic microns.

The value of q is a measure of the flatness of the drop distribution curve. If $q = 2$, the curve has a relatively high and narrow apex. As q decreases, the peak of the curve becomes lower and flatter. Accordingly, a high value of q means that most of the mass of the liquid lies within a narrow range of sizes, whereas a low value of q corresponds to a scattering of the drops over a considerable range of sizes. The volume frequency curves for three values of q are shown on a comparable basis in Figure 1. The corresponding cumulative volume curves are shown in Figure 2. For any given nozzle, it appears that q is constant over a wide range of operating conditions. However, q is affected markedly by the

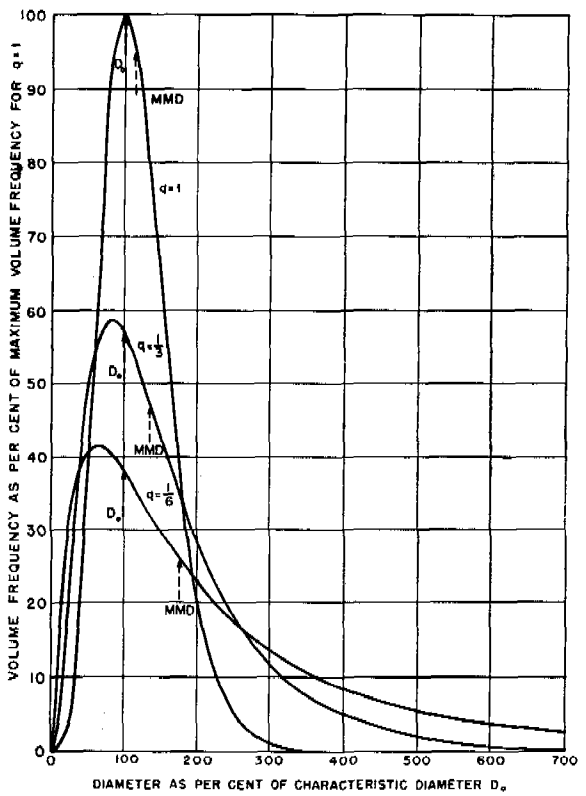


FIGURE 1. Volume frequency curves for typical nozzle coefficients.

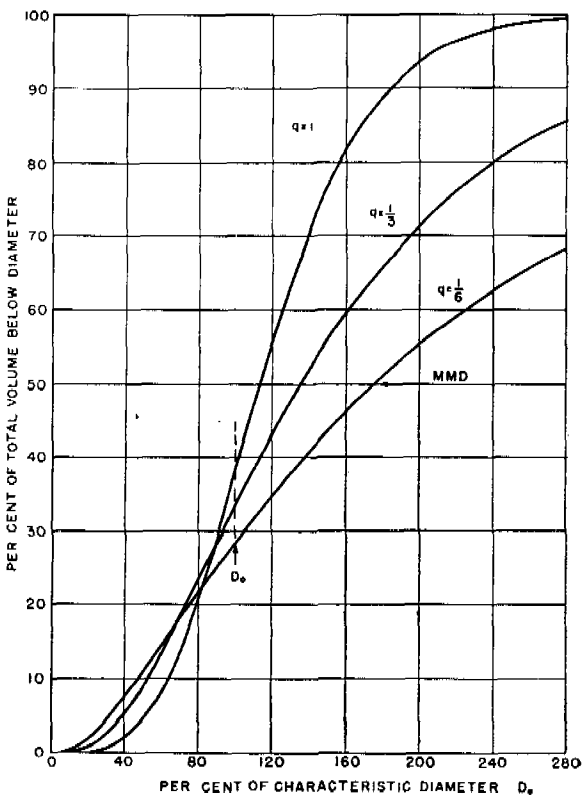


FIGURE 2. Integrated volume distribution curves for typical nozzle coefficients.

type and size of the atomizing device used. Hence its value must be determined experimentally for each type and size. Values thus far encountered range from $\frac{1}{3}$ to 1 for gas-atomizing nozzles and from $\frac{1}{8}$ to 2 for spray nozzles.

For some purposes, it is of more interest to know the *mass median diameter* [MMD] of the droplets in a spray than it is to know D_0. If the drop size distribution in a spray fits the empirical equation for dn/dx, and if $p = 2$, and $1/q$ is an integer, it can be shown mathematically that the ratio of the MMD to D_0 depends only on the value of q.

$$\frac{\text{MMD}}{D_0} = \frac{(5/q)!}{(6/q)!} \times \frac{6}{5} Y^{1/q}, \tag{4}$$

where Y is found by trial-and-error solution of the equation following.

$$\frac{1}{2} = e^{-Y} \sum_{z=0}^{z=\frac{6-q}{q}} \frac{Yz}{z!}. \tag{5}$$

These equations have been solved for the case when $q = 1$, for which it is found that $\text{MMD}/D_0 = 1.14$.

If $p = 2$, then the equation for drop size distribution can be written as follows:

$$\log\left(\frac{1}{x^2}\frac{dn}{dx}\right) = \log a - \frac{bx^q}{2.3}. \tag{6}$$

If sufficiently small intervals are used in the drop count, a plot of $\log (1/x^2)(\Delta n/\Delta x)$ against x^q should give a straight line with slope equal to $-b/2.3$. This relationship makes it easy to test experimental data to see if they fit the empirical equation, since the distribution data are normally available in terms of Δn, the number of drops in a small size range, Δx, at various values of x. Various values of q are assumed, and for each value, a plot is made of $\log (1/x^2)(\Delta n/\Delta x)$ vs x^q. The correct value of q is the one that gives a straight line plot. The value of b is obtained from the slope of the straight line. From the values of q and b, one can then calculate D_0 through use of the second column in Table 1. Examples of the use of this method for various types of nozzles are shown in Figures 3, 4, and 5.

It will be noted that, in some cases, deviations of some of the observed points from the straight lines

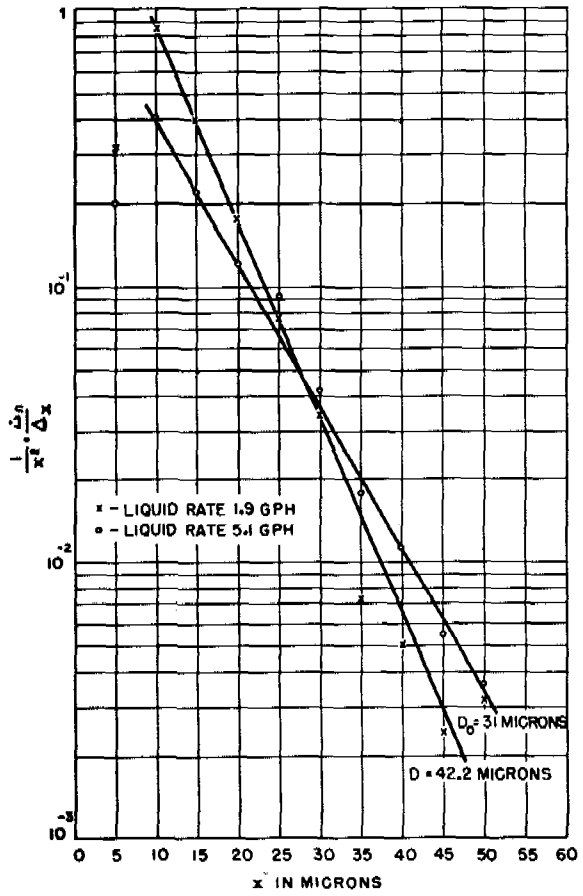


FIGURE 3. Performance of exhaust Venturi atomizer on Dodge truck dispersing Diol 55 oil.

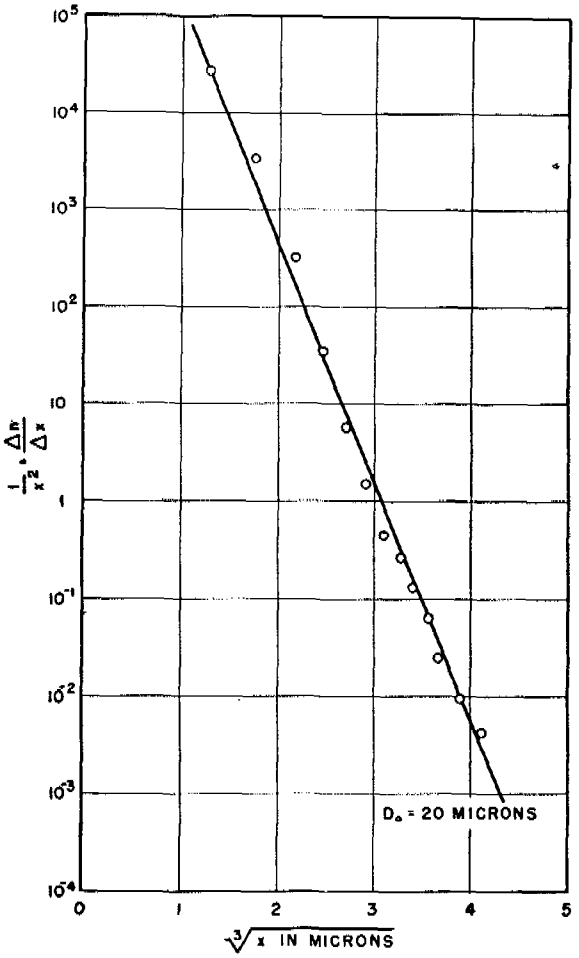


FIGURE 4. Drop size distribution from a small air-atomizing nozzle.

occur in both the low and high ranges of drop sizes. These are to be expected since, with the usual methods of sampling, it is difficult to collect the very small drops and, unless an extremely large number of droplets is counted, a statistically significant number of large drops is not included in the area of the slide surveyed. In fact, this is one of the advantages of this method of analyzing drop count data since it is usually possible to determine the value of q and the slope of the line from a relatively few points determined by counting the number of drops in small increments of diameter. For representative samples of sprays which are relatively homogeneous, the values of D_0 and MMD determined from the above formulas will agree quite closely with those obtained by summing up the actual drop counts. For less homogeneous sprays, however, when q is small, the value of D_0 may actually exceed the diameter of the largest drop measured if only a small number of drops is counted. In this case the graphical method permits extrapolation of the data, and gives a more exact picture of the drop spectrum. The value of q cannot be determined precisely by the trial-and-error method but this is of no great importance. Small errors in the determination of the slope of the line, however, may cause large deviations in the calculated value of D_0 and the method of least squares should be used to determine the best line.

29.2.4 Venturi Atomizer

The air for most industrial pneumatic nozzles is supplied at pressures ranging from 20 to 150 psi and the liquid is supplied under only a small head. In spite of the large volume of air required and the low energy efficiency of these nozzles, the power requirement generally is not excessive for industrial purposes. In munitions, which are usually limited to a

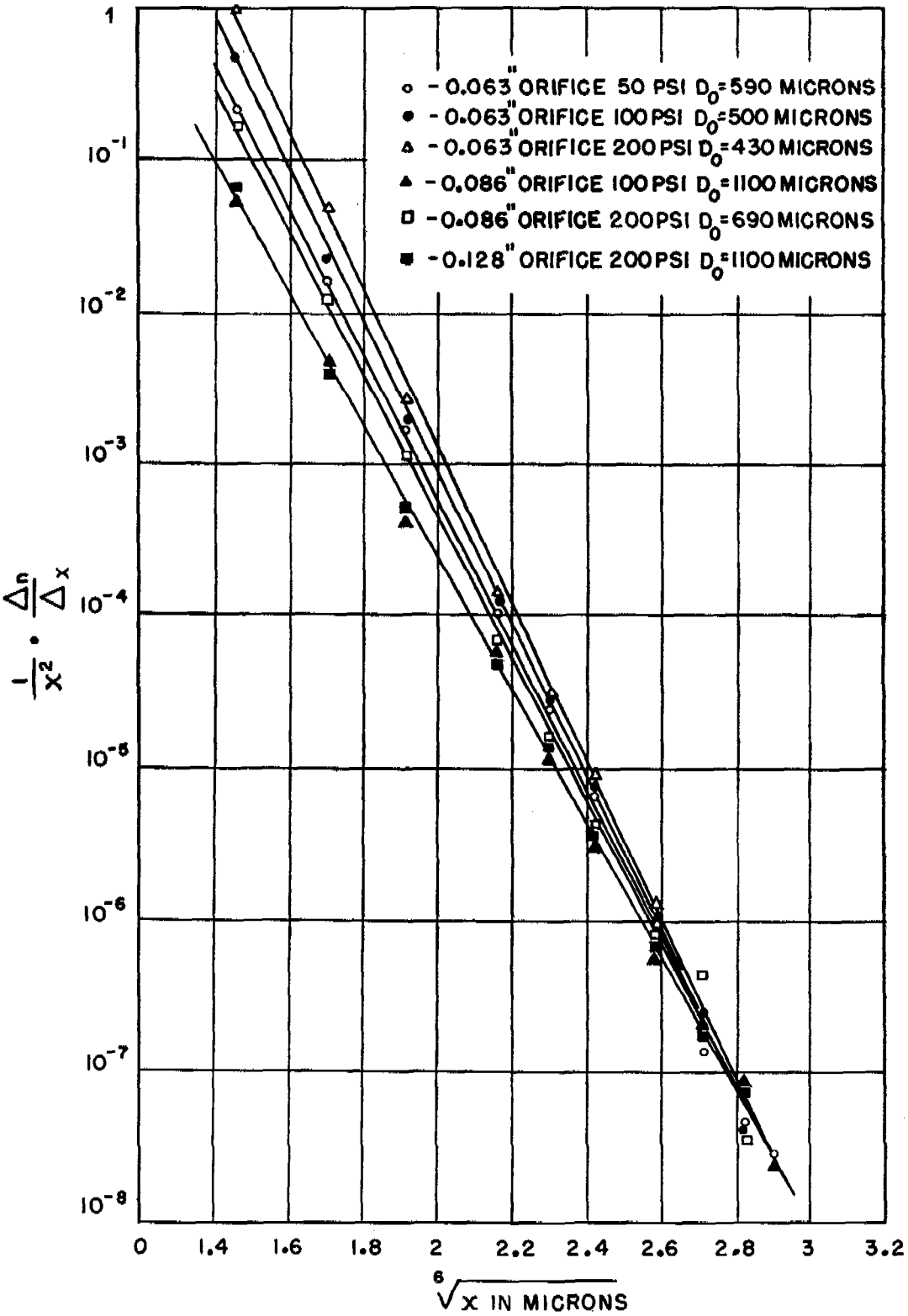


FIGURE 5. Drop size distribution from Spraco Type T nozzles.

small supply of gas from a pyrotechnic fuel block at low pressures, or when the exhaust gases from an airplane engine or the slipstream around a plane are employed for atomization, it is essential that the gas pressure be low.

A practical device for providing high gas velocity and still maintaining low overall pressure drop is the familiar Venturi tube, consisting of a converging section, a high velocity throat and a tapered divergent section. The important element is the diverging section which should not have a total angle of more than 7°, while the converging section is the frustum of a cone with a vertex angle of 25 to 30°. The use of the Venturi tube to secure a zone of high velocity largely avoids the substantial loss of kinetic energy occasioned when the jet from a simple nozzle or orifice discharges downstream into a slowly moving fluid. The pressure difference between the upstream and the throat of the Venturi may be calculated from the usual adiabatic orifice formula.[6] The overall pressure loss for a single-phase fluid, gas, or liquid, is from 10 to 20% of this difference. Design calculations for a Venturi used for the atomization of oil by means of the exhaust gases from an airplane engine are shown in Chapter 33. It will be seen that it is possible to approach the acoustic velocity in the Venturi throat and still have an overall pressure loss of only a few pounds per square inch. This loss is perhaps increased by a factor of 1.5 to 3 when liquid is fed to the Venturi throat during atomization depending on the ratio of liquid to gas and on the gas velocity.

The Venturi atomizer is especially adaptable to the production of small droplets for high rates of evaporation in hot gases. Even with viscous oils it is possible to produce a spray in which essentially all of the droplets are less than 100 microns diameter and the value of D_0 is approximately 40. This will correspond to about 6,000 sq ft per gal of liquid fed to the atomizer. This type of pneumatic atomizer is especially suitable for the dispersal of insecticides, since the exhaust gases from an internal combustion engine are readily available either for airplane spray or ground spray. The greatest use of the Venturi atomizer for war purposes, however, was contemplated in the development of a new floating oil smoke generator and in munitions for the dispersal of vesicant gases, both of which depended upon the vaporization of a liquid by means of hot gases from a pyrotechnic fuel block.

A brief study was made of the performance of Venturi atomizers in various sizes ranging in throat diameter from 0.11 in. to 3.3 in., and using gases of various densities and viscosities and several types of liquids.[7] For the small Venturis the atomization of oil in a stream of nitrogen was somewhat better than that indicated by equation (1). Since neither the viscosity nor the density of the gas is included in this equation, it was desirable to determine what effect these properties would have on the resulting atomization. From experiments using ethylene and helium, it was found that a decrease of gas viscosity at constant gas density improved the atomization of the liquid. A viscosity decrease of approximately 60% resulted in a decrease in D_0 of about 60%. On the other hand, a decrease in gas density at constant gas viscosity had an unfavorable effect on the atomization of the liquid. When the density was reduced to ¼ by substituting helium for nitrogen the value of D_0 was increased by a factor of 2 to 3.

In the case of the small Venturi atomizer, it was found that incomplete atomization of the liquid sometimes took place and resulted in dribbling of the liquid from the exit of the atomizer. This appeared to be a wall effect occasioned by the impingement of the droplets on the downstream section. It could be eliminated entirely by cutting off the Venturi so that the exit diameter was not greater than twice the throat diameter.

For the large Venturis the agreement between the observed drop sizes and those predicted by the empirical equation of Nukiyama and Tanasawa was surprisingly good. In all cases for the Venturi atomizers operating at high gas velocities, the value of q was 1. This indicated that the atomization was good and that a relatively uniform drop spectrum was obtained. Figure 3 shows the correlation of the data for the atomization of Diol 55 oil in a Venturi attached to a Dodge truck engine. Although sampling of the aerosol from airplane dispersal using the Venturi atomizer was somewhat more difficult than for ground dispersal, surprisingly good agreement with the predicted drop sizes was also obtained when the drop count data from stationary and waved slides were analyzed by means of equation (2).

In this work several types of nozzles were used to introduce the liquid into the Venturi throat. These included low-velocity jets which allowed the liquid to run along the wall of the Venturi throat, coarse spray nozzles which gave an initial break-up to the liquid, and a concentric axial spray jet. No particular difference was found in the performance of the Ven-

turi atomizers using these types of injectors, although in practice it is better to use large-diameter liquid jets so as to avoid clogging and the disadvantage of high liquid pressure. As long as the liquid jet discharges into the throat the angle of flow does not seem to make much difference.

29.2.5 Performance of Hydraulic Nozzles

The few complete measurements on drop sizes from commercial hydraulic nozzles which have been reported by Houghton [8] have been analyzed by means of equation (2). The results are shown in Figure 5. The data follow straight lines which converge at a point when the exponent q is $\frac{1}{6}$. From the slope of the lines the characteristic drop diameter is found to vary from 430 to 1,100 microns. It is apparent therefore that this type of atomizing nozzle gives a relatively inhomogeneous coarse spray. The only data on fine sprays which have been analyzed by this method are those by Lee [9] who measured the atomization of fuel oil through nozzles with very small orifices at pressures up to 5,700 psi. The variables studied were the effects of oil pressure, air density, nozzle design, orifice diameter, and the ratio of orifice diameter to orifice length. It was found that the degree and uniformity of atomization were favored by increasing the oil pressure and decreasing the orifice diameter, and were insensitive to air density and ratio of orifice length to diameter. With a given oil pressure and orifice diameter, modifications of the details of the nozzle construction appeared to have no effect on the average diameter of the spray, but did affect the uniformity of drop distribution. Analysis of the data from a typical series of runs shows the surprisingly high value of 2 for the exponent q in equation (2). Values of D_0 varied from 122 microns at 450 psi to 70 microns at 5,700 psi.

An attempt was made to correlate these results with equation (1) so that the performance of hydraulic nozzles could be predicted. In order to do this, it was necessary to estimate the interfacial velocity of the liquid leaving the nozzle and the relative volume of air effective in the atomization. Because of the limited amount of data, the correlations are only roughly quantitative. They are based on two assumptions: (1) the velocity at which the conical sheet of liquid formed by the nozzle leaves the orifice is given by Bernoulli's equation, i.e., $v = 3.72\sqrt{P/\rho_l}$, where v is the velocity of the sheet in meters per second, P is the pressure on the nozzle in pounds per square inch gauge, and ρ_l is the density of the liquid in grams per cubic centimeter. The value of v estimated in this manner may be used for the velocity term in equation (1); (2) the *effective value* of Q_a, when applied to interaction between stagnant air and a high-speed sheet of liquid issuing from a spray nozzle, is proportional to the surface of the sheet and the rate at which it is traveling. This is equivalent to saying that $Q_a = cd\sqrt{P/\rho_l}$, where d is the orifice diameter in inches and c is a constant. If Q_L and Q_a are expressed in gallons per minute, the value of c for Houghton's data appears to be about 85 and for Lee's data approximately 6,600. The wide discrepancy in these two values indicates the greatly different atomizing efficiencies of different types of hydraulic nozzles, but correlation with the design of the nozzle has not been attempted.

29.2.6 Attempt to Produce Screening Smokes by Mechanical Atomization

Early in the war it was suggested that artificial fogs could be produced by atomizing solutions or suspensions of nonvolatile materials in water. Favorable results were obtained in laboratory experiments using solutions of sodium chloride and other salts and suspensions of bentonite clay in water.[10] It was also proposed that the refuse from the beet sugar industry, known as *Steffen's waste*, could be dispersed through pneumatic nozzles to set up artificial fogs for the protection of large industrial areas.[11, 12] Various types of spray nozzles were evaluated, first according to the persistence of the suspension formed by spraying solutions of various concentrations into a large room, and second, on the basis of the power consumed in spraying.[13, 14] It was possible to produce artificial fogs roughly equivalent to natural fogs, with visibility noticeably impaired at a distance of 20 ft in the laboratory when the concentration of one gram of sodium chloride per cubic meter existed. With the best hydraulic nozzles, however, not more than 2% of the total solvent sprayed at nozzle pressures up to 5,000 psi remained suspended in the air longer than five min.[15] While no measurements of the drop sizes were reported, this observation alone indicates a half-life of about one min, for which it can be shown that the MMD of the initial cloud was between 20 and 30 microns.[a]

[a] The half-life of a coarse aerosol cloud dispersed in a closed room is a convenient method of measuring the MMD. See Figure 2 in Chapter 35.[16]

The most promising nozzles from the standpoint of fog production were the pneumatic types furnished by the Spraying Systems Company and the Binks Manufacturing Company, and the oil burner Nozzle SA–O of the National Airoil Burner Company. Fogs produced by these humidifying nozzles in the laboratory had a half-life of from 6 to 15 min, corresponding to MMD's of 5 to 10 microns. The best operation was obtained with the nozzles operating on compressed air at 50 to 60 psi at which the consumption of air was 165 cu ft per gal of liquid sprayed.

The futility of trying to produce screening smokes by mechanical atomization should be apparent on the basis of the preceding discussion. It is evident that, even if aerosols with MMD's of 5 microns could be produced by the use of large quantities of air for atomization, less than 10% of the mass of the liquid would be below 2 microns, according to the curves in Figure 2. Even if dilute solutions were used, only the droplets of this size would evaporate to leave residues sufficiently small to produce light scattering. The whole process, therefore, is extremely inefficient and there is no possibility that mechanical atomization of this type could be used for the formation of screening smokes.

29.3 ATOMIZATION IN AIRPLANE SPRAYS

Aircraft may be used for the dispersal of smoke, insecticides, and vesicant agents by the discharge of the liquid into the slipstream. The degree of atomization depends upon the speed of the plane and the properties of the liquid. For FS smoke, it is desirable to atomize the liquid as completely as possible so that vaporization of the sulfur trioxide will take place readily as the drop falls through the air. The desirable limits of atomization for insecticides have already been mentioned. The problem in the dispersal of vesicant agents, however, is to prevent fine atomization from taking place so that the drops will remain of sufficient size to produce casualties. This problem has been thoroughly studied, and numerous measurements have been made on the drop-dispersal spectrum from thickened and unthickened liquids. It is beyond the scope of this chapter to discuss the details of this work since it is treated elsewhere in this series. This report will be concerned only with the mechanism of break-up and methods of increasing the efficiency of atomization when desired.[17]

The problem of break-up of liquids in an aircraft spray has been studied mathematically by the British.[18, 19] The study of ripples on a liquid surface over which a steady stream of air is flowing shows that ripples of certain wavelengths are hydrodynamically unstable and grow rapidly in amplitude. An approximate theory of break-up was developed by correlating the wavelengths of the most unstable ripple with the diameter of the most frequent drop in the drop spectrum. This led to the conclusion that the *main* drop will have dimensions proportional to $\mu^{2/3}v^{-4/3}\sigma^{1/3}$ where μ is the viscosity of the liquid, σ is the surface tension, and v is the velocity of the air in the slipstream. Elaboration of this theory predicted drop-size distributions which were in fair agreement with those found experimentally. The theory was tested for a range of values of μ and v. A change in v gave a variation in drop sizes which was in satisfactory agreement with the theory, but there was less satisfactory agreement with the results in which μ was varied. These deviations may have been due to the existence of a tough surface film with the rubber gels used for increasing the viscosity. This would in a sense give a very large increase in σ, and may account for the results with the thickened agents.

29.3.1 Design of a Venturi Air Scoop for Atomization

Several attempts have been made, by using a Venturi scoop, to increase the velocity of the air at the point at which the liquid is discharged, above that of the speed of the aircraft. The designs of suitable devices have been empirical for the most part, but they have been successful when used on a small scale. The problem of designing a large Venturi air scoop arose in connection with dispersing insecticide solutions at a high flow rate from the B-25 medium bomber, which has only a moderate speed. Because of the quantity of liquid to be atomized and the belief that it was necessary to secure as small droplets as possible, the size of the air scoop became quite large. Approximate design calculations were based on mechanical energy balances making allowances for the acceleration of the injected liquid[b] and the friction of the scoop. Calculations were made for a speed of the aircraft of 300 fps (205 mph) and throat velocities of 600 and 900 fps. The effect of friction loss in the Venturi itself

[b] In these calculations it was assumed, on the basis of experiments made on small Venturis, that the liquid injected into the throat of the Venturi was accelerated to 61% of the velocity of the air in the throat.

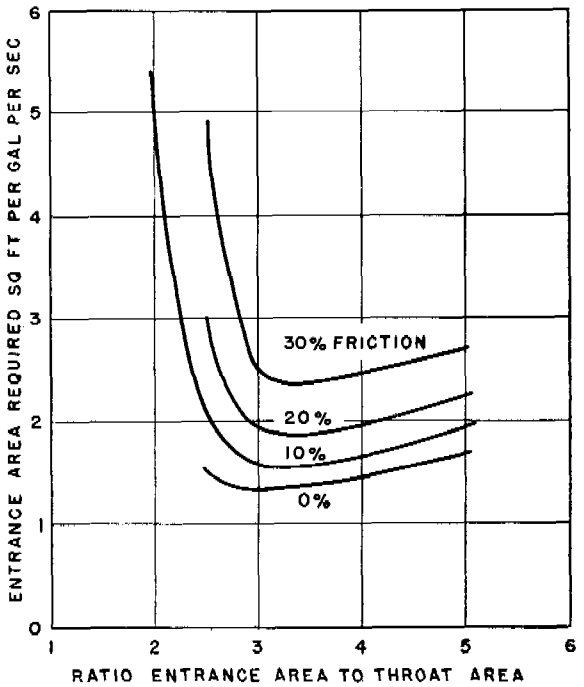


FIGURE 6. Dimensions of Venturi air scoop for spraying DDT solutions. Throat velocity = 600 fps; plane velocity = 300 fps.

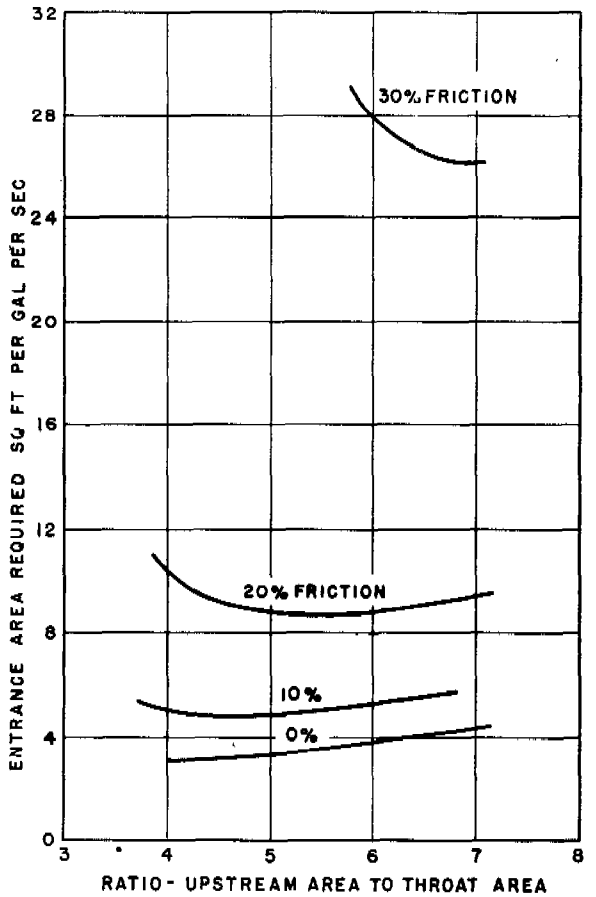


FIGURE 7. Dimensions of Venturi air scoop for spraying DDT solutions. Throat velocity = 900 fps; plane velocity = 300 fps.

was taken at 0, 10, 20, and 30% of the difference in head between the upstream and throat section to show the degree of care needed in the fabrication of the unit.

The results are shown in Figures 6 and 7 which give the entrance areas of the Venturi, as square feet per gallon of liquid sprayed per second, for different ratios of upstream to throat areas, to produce the indicated throat velocities. Several conclusions may be drawn from these curves.

1. If it is desired to have an air velocity of 600 fps at the throat, or twice the IAS, the friction in the Venturi scoop is not serious; that is, the upstream area is not increased excessively if the overall pressure loss *due to friction* is 30% rather than 10% of the energy loss between the entrance and the throat. However, if it is desired to have a velocity of 900 fps at the throat in order to produce better atomization, it is necessary to keep the pressure loss due to friction to an absolute minimum, otherwise the area of the entrance becomes excessively large.

2. For an air velocity of 600 fps at the throat, an entrance area of 1½ to 2½ sq ft per gal of liquid sprayed per sec is sufficient, provided the throat area is one-third to one-fourth as large.

3. It appears that it is better to have the throat area too small than too large, as the entrance area required to produce a given air velocity at the throat decreases rapidly as the ratio increases and then reaches a broad minimum before increasing.

Table 2 shows the dimensions of the Venturis required for dispersing DDT solutions from a plane, assuming that 0.5 lb of agent is required per acre and that the plane can lay a swath of 100 ft when traveling at a speed of 300 fps and a velocity of 600 fps at the throat is necessary for the atomization.

The Venturi scoop, shown in Figure 8, was constructed of Duralumin sheet riveted to 2½ x 2½ x ¼ in. Duralumin angles. The solution to be sprayed was fed into the Venturi throat through two streamline distributing tubes with orifices in the downstream edges.[20] The Venturi was installed beneath the fuselage of a B-25 plane at Wright Field. Flight tests were made to observe the degree of atomization when a solution of DDT in fuel oil was

TABLE 2. Dimensions of Venturi air scoop required for atomizing DDT solutions to give 0.5 lb per acre. Throat velocity, 600 fps; speed of plane, 300 fps; swath width, 100 ft.

Tons of solution per sq mile	Solution strength % DDT by weight	No. of Venturis on plane	10% Friction Entrance diameter in.	10% Friction Throat diameter in.	20% Friction Entrance diameter in.	20% Friction Throat diameter in.	30% Friction Entrance diameter in.	30% Friction Throat diameter in.
3.2	5	1	15.9	9.20	17.5	10.1	19.8	11.5
3.2	5	4	7.95	4.60	8.75	5.05	9.9	5.73
0.8	20	1	7.95	4.60	8.75	5.05	9.9	5.73
0.8	20	4	3.98	2.30	4.38	2.53	4.97	2.87

fed by gravity to the distributor.[21] Unfortunately, no opportunity was provided in these tests for determining the air velocity at the throat. The atomization was so fine, however, that, in turbulent air, recovery of the solution on the ground was poor. Because of the complexity of the unit, it was decided that a simple discharge tube cut at the exit at an angle of 45° on the trailing side was suitable for dispersing DDT solution. While the atomization with this was admittedly much poorer than with the Venturi air scoop, the results over open terrain where there was no screening of the large drop sizes by the foliage appeared to be reasonably good.[22]

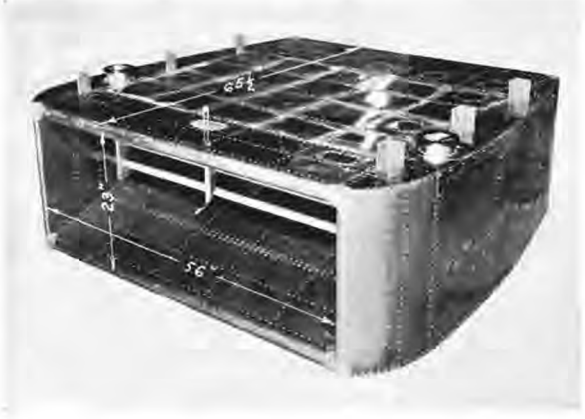


FIGURE 8. Rectangular Venturi spray device for attachment under fuselage of B-25 bomber.

Later, a small Venturi scoop for dispersing DDT solutions was developed empirically for the Navy Bureau of Aeronautics by the Curtiss-Wright Research Laboratory.[23] The final unit had a throat area of 3.2 sq in. and an entrance area of 50 sq in. Its capacity was 0.5 gal fuel oil per sec for a plane speed of 300 fps. This device produced droplets from 115 to 185 microns diameter.

A considerable study was also made at Edgewood Arsenal on the atomization of DDT solutions of low viscosity when discharged from modified M-10 spray tanks. Chemical and physical methods were developed for assessing the spray. It is interesting to note that the characteristic diameter of the spray spectrum could be determined by the graphical method outlined above.[21]

29.4 ATOMIZATION IN EXPLOSIVE BURSTS

There is no difficulty in obtaining a satisfactory degree of dispersion with liquid chargings of low viscosity in shells and bombs. With gunpowder bursters, a mean drop size of 50 microns may be obtained, and with high explosives the mean size is 10 to 20 microns.[19] The Germans had several shells of the 10.5-cm and 15-cm size equipped with heavy bursters ranging from 0.5 lb to 4.5 lb RDX/wax and 1.7 lb TNT for dispersing mustard gas and other vesicant agents as aerosols. They also had bombs and rockets for the same purpose. Some of these contained bursters with as much as 15.5 kg of TNT for a 250-kg bomb.

29.4.1 Mechanism of Atomization by Explosion

A study of the mechanism of atomization by explosion was made by Whytlaw-Gray by means of a spark photographic apparatus.[25, 26] From these experiments, it appeared that the fragmentation occurs before or at the moment of opening of the container, while subsequent shattering by projection of the liquid through the air is of little importance. In short, fragmentation is caused by cavitation of the liquid. It is not clear whether the passage of the explosive shock wave through the fluid leaves the highly cavitated liquid which is then ejected before the cavities have time to collapse, or whether the liquid under compression in the bomb forms cavities on sud-

den release of the pressure. In either case fragmentation is due to cavitation which, in turn, is due to the expansion of the liquid, giving tensions in excess of the tensile strength of the liquid. It was found that cavitation in the liquid can be inhibited by outgassing or by applying external pressure. Furthermore, water, which has a low compressibility and a high tensile strength, is fragmented much less than organic liquids under comparable conditions.

Davies [27] found no evidence supporting the theory that pre-ejection effects such as cavitation play an important part in the atomization of chargings from a base ejection bomb. His experiments were carried out with liquids of varying viscosity in a small model bomb, one end of which was closed by a copper diaphragm which was burst by compressed air at 45 atm pressure. Flash photographs of the order of 10^{-5} sec exposure were taken at various distances from the explosive release. The break-up of the liquid was brought about primarily by the shattering of the liquid plug which was ejected more or less intact from the bomb. The plug appears to fissure along planes parallel to the axis into rods of liquid held together by sheets. In normal liquids, unless the viscosity is very high, the sheets disappear rapidly and the rods break up into comparatively fine drops. It was found that the mean velocity of ejection of the viscous filling from the experimental bomb when the bursting pressure was 32 atm was 5,000 cm per sec. This velocity is probably much lower than that attained in the burst of a high-explosive bomb, but it is likely that the mechanism of break-up of liquid charging from base ejection shells is essentially the same as that found for the experimental bomb.

If it is assumed that the following factors determine the degree of atomization in an explosive burst, dimensional considerations may be used to define the conditions which account for the results.

p = pressure within the bomb at instant of fracture;
ρ = density of liquid;
ν = kinematic viscosity of liquid;
τ = surface tension of liquid;
d = diameter of bomb;
l = length of bomb;
a = length characterizing the drop spectrum.

Then, assuming the atmosphere to be constant and no secondary disturbances to be present, dimensional reasoning indicates

$$f\left(\frac{\rho\nu^2}{\tau a}, \frac{pd^2}{\rho\nu^2}, \frac{d}{\rho}, \frac{d}{a}\right) = 0 \cdot \qquad (7)$$

Increasing any of these factors favors fine dispersion. In the case of base ejection from shells in flight, other terms involving velocity of spin may be required.

29.4.2 Drop Size Distribution from Explosive Bursts

Data available from field tests at Suffield Experimental Station on the dispersion of liquid chargings from bursting weapons have been analyzed by means of equation (2) to determine whether the distribution of drop sizes from an explosive burst is similar to that from an atomizing nozzle. In this test, which is reported in Suffield Technical Minutes No. 37,[28] two *double-day* bombs, containing 2.82 l of aqueous solution of 5% egg albumin and 1% rhodamine B dye, were functioned simultaneously on separate layouts. The bombs were fitted with bursters of 723 g CE/TNT 30/70, 170 g CE, No. 8 detonator. One of the bombs was charged with CO_2 at 500 lb pressure in order to determine if the dissolved gas would aid in the atomization. The bomb used was an experimental type made from the British 30-lb light case Mk 1 bomb and was characterized by the heavy axial burster which runs the full length of the case.[28]

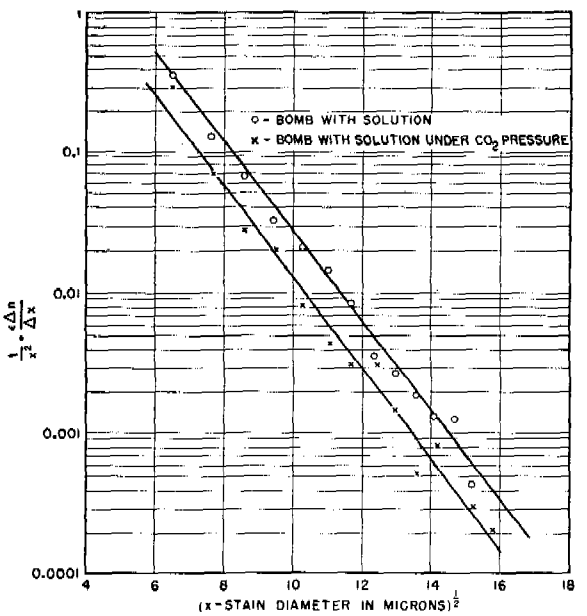


FIGURE 9. Analysis of drop size data from explosive bursts.

The data shown in Figure 9 were taken from swinging impactor samples collected on the 50-yd line, and are corrected for the efficiency (ϵ) of the impactor as

shown in the report. They are presented here simply to show that the method of analysis of drop size data from nozzles is also applicable to atomization by explosive bursts. For the particular charging and conditions of these tests, the value of the coefficient q is ½. The characteristic diameter D_0 of the stains, which is approximately twice that of the drops, is 197 microns for the bomb containing CO_2 and 200 microns for the other bomb. Since, for this drop spectrum, the mass median diameter is 25% larger than D_0, the values of MMD is about 125 microns. The atomization of the charging was no better from the bomb containing CO_2 under pressure than from the bomb without CO_2. It was concluded that less than 1% of the material at 50 yd is present as droplets smaller than 20 microns diameter.

Chapter 30

THERMAL GENERATOR MUNITIONS

By *E. W. Comings*

30.1 INTRODUCTION

THERMAL GENERATORS are devices which use a self-contained fuel as a source of heat to vaporize a substance with a relatively high boiling point. Several munitions of this type were available at the beginning of World War II or shortly thereafter. One example is the colored smoke grenade which uses an intimate mixture of a volatile organic dye and a fuel which carries its own oxygen supply. The 9-lb DM candle was another example. The agent and fuel in this candle were in separate compartments and the hot gases passed over the liquid agent and carried away its vapors.

The thermal generators described in this chapter are an improved type and provide for highly efficient and short-time contact between the hot fuel gases and the agent. The improved design has increased the agent capacity and permitted the use of less volatile and also less thermally stable agents in the thermal generators.

The improved thermal generator has been tested with a number of agents for setting up screening and toxic smokes as well as highly concentrated vapors. The materials which have been vaporized successfully are paraffin wax, oleum, sulfur, CN, DM, DC, tertiary butyl stearate, methyl salicylate, triethylphosphate, Glaurin, Diol and other high-boiling hydrocarbon oils, solutions of DDT in oil, and several varieties of mustard gas, including extracted Levinstein, distilled mustard, and mustard from the thiodiglycol process. In every case an excellent aerosol or concentrated vapor cloud was produced without undue decomposition of the agent. The design has been applied to pots, bombs, and larger generators.

30.2 FUNDAMENTAL PRINCIPLES

Every thermal generator design must meet certain general requirements in addition to the special requirements of each individual application. These general requirements are discussed below.

Thermal Stability of the Agent. The agent to be vaporized will begin to decompose when it is heated above a temperature range which is characteristic of each agent. The amount of decomposition depends on the temperature and the time the agent is held at this temperature. Relatively high temperatures in this range will result in little decomposition if the time of exposure is very short. The capacity of the generator will be greater if the agent is heated to quite high temperatures for the shortest possible time rather than to lower temperatures for a longer time.

Heat Requirements. The heat from the fuel is needed for several purposes.

1. It raises the temperature of the agent to the vaporizing temperature range. This is the range in which the agent has an appreciable vapor pressure. It may be well below the boiling point.
2. It supplies the latent heat of evaporation of the agent.
3. It raises the temperature of the agent vapor to the final temperature of the hot emerging gases.
4. If the agent is initially solid it supplies the latent heat to melt it.
5. It heats the metal components of the generator and supplies heat lost through the walls of the generator.
6. The fuel gases themselves leave the unit at an elevated temperature, and the fuel must supply the heat in these exit gases. When these gases leave the unit, saturated with agent vapor, this heat requirement is at a minimum for a given fuel burning temperature. When the gases carry out less vapor than that needed to saturate them, the exit gas temperature will be higher and this heat requirement greater. A higher fuel burning temperature will also result in a higher exit gas temperature, but if this gas is saturated with vapor the heat requirement will be less when compared on the basis of a unit weight of agent evaporated. This is so because less fuel gas is needed to carry off a unit weight of agent vapor. The higher the fuel burning temperature and the more nearly saturated the exit fuel gases, the lower will be the fuel requirements.
7. In some cases *inert materials* such as carbonates have been added to the fuel *to reduce the fuel burning temperature* in order to avoid decomposition of the agent. The fuel must then heat these materials and in some cases supply additional heat to decompose or vaporize them. These additions increase the fuel requirements by absorbing heat and by increasing the

heat requirements of exit fuel gases due to the lower fuel burning temperatures. These additions to the fuel have been avoided where possible in the improved thermal generator designs. Thermal decomposition of the agent has been avoided by reducing the time that the agent is exposed to the higher temperatures.

Heat Transfer. The design must provide for the transfer of the heat supplied by the fuel to the agent. Merely making the heat available is not enough. The design must insure that it reaches the agent at a fairly uniform rate. Direct radiation from the fuel to the agent compartment may provide for part of this transfer. It is preferable to transfer the heat through the liquid surface in direct contact with the hot gas. The transfer will be more rapid if a large area of liquid surface is exposed and also if the gas velocity over this surface is high. A large amount of experimental and theoretical evidence indicates that these conditions are best provided by a spray of small liquid drops in a high-velocity gas stream.

Vapor Transfer. The agent vapor is transferred from the liquid surface to the gas stream. The conditions which permit this transfer to take place readily are the same as those which promote the transfer of heat from the gas to the liquid, namely, a large liquid surface area and a high gas velocity over this surface. Thus, a spray of small liquid drops in a high-velocity gas stream also provides the best conditions for the transfer of vapor.

Experiments on the vaporization of high boiling organic liquids from flat surfaces into a stream of hot gas [53, 54] indicated that the same principles apply as when evaporating lower boiling liquids. An excessive extent of surface is needed to obtain practical evaporation rates by this means. Evaporation from the surface of packing material, such as used in a commercial absorption tower, also requires more space than can be allotted in a compact munition.

Carrier Gas. The agent vapor is carried out of the thermal generator by the gases from the fuel. The supply of a large volume of carrier gas is an important function of the fuel. The amount of vapor which the gas will carry is limited to the vapor which will saturate the gas at its exit temperature. A large volume of fuel gas will permit operation of the generator at a lower temperature and protect the agent from decomposition. Thus, a fuel that supplies heat but does not give a large volume of gas is not a satisfactory fuel for thermal generators. The fuels selected for the improved thermal generators provide a maximum amount of heat and carrier gas and a minimum of solid residue and slag.

30.3 PERSISTENCE OF THE AEROSOL

The agent vapor mixed with the gases from the fuel issues from the thermal generator in jets. These jets entrain the surrounding air and are chilled rapidly to a temperature approaching that of the atmosphere. The vapor condenses during this cooling and forms an aerosol cloud.

When a liquid aerosol cloud is formed by condensation of vapor or by mechanical disintegration of liquid, the cloud is carried downwind and diluted by the turbulence of the air and by precipitation of the large droplets onto vertical and horizontal surfaces. Evaporation of the droplets commences as soon as the partial pressure of the vapor in the cloud falls below the saturation value. The rate of evaporation depends primarily on the size of the droplets and on the difference between the saturation vapor pressure and the actual partial pressure of the substance in the air. Only when the concentration of droplets is high and their diameter is small will the rate of evaporation be sufficient to maintain the air in the cloud essentially saturated.

With highly nonvolatile agents such as fog oil, very little vapor is needed to saturate the air and the cloud will persist for long distances before it is diluted sufficiently to evaporate all the aerosol. The oil smoke generators depend on this nonvolatile characteristic of fog oil for the persistence of the smoke screen. The factors influencing the persistence of screening smoke have been discussed in connection with the large oil smoke generators.[1, 2] With more volatile agents, the aerosol cloud will be less persistent.

The cloud of mustard gas aerosol from a thermal generator is very similar to a cloud of nonpersistent gas. The degree of saturation of the cloud has been predicted from differential equations [3] written for the rate of evaporation of an aerosol cloud based on the British equations for atmospheric diffusion and the laws of vaporization of spherical droplets. Both continuous point and infinite line sources were considered. Step-wise integration of these equations showed that the degree of saturation of mustard gas aerosol clouds depends very much upon the diameter of the drops, the source strength, and the atmospheric conditions. An approximate solution to determine the maximum initial drop diameter that will maintain essentially saturated conditions throughout the

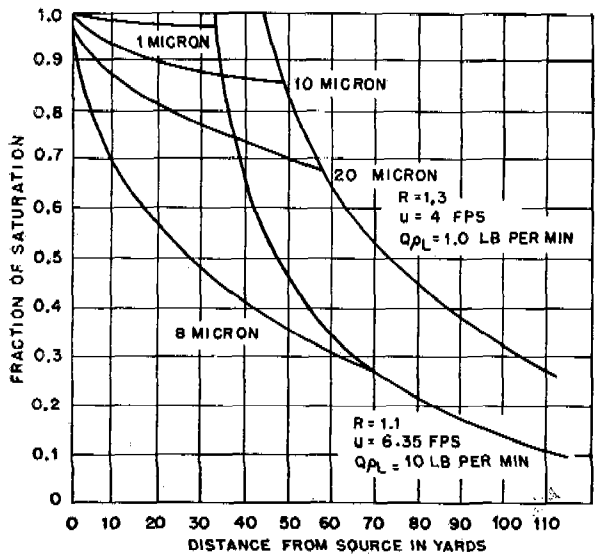


FIGURE 1. The effect of distance from a point source on the degree of saturation of a mustard gas aerosol cloud for particles of various initial sizes.

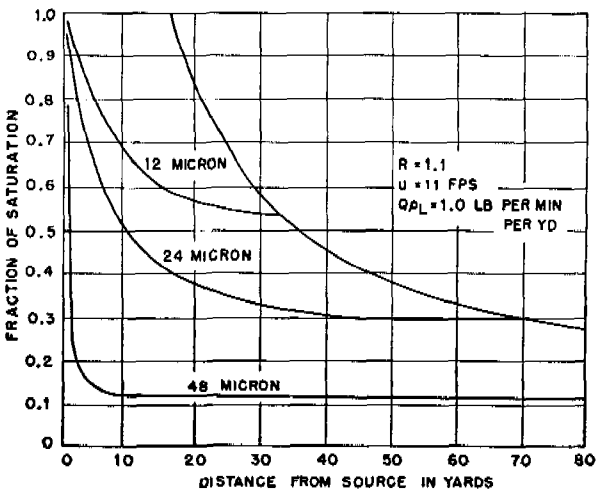


FIGURE 2. The effect of distance from a line source on the degree of saturation of a mustard gas aerosol cloud for particles of various initial sizes.

life of the cloud has shown that the droplets in aerosols generated by mechanical spray nozzles or by explosive bursts are much too large. Only thermally generated mustard gas aerosols may be expected to be saturated. Nonvolatile impurities soluble in the agent reduce the rate of vaporization of the agent and leave a persistent cloud of droplets with a residual drop diameter of the same order of magnitude as the original droplet.

Figures 1 and 2 show some typical integral curves for point and line sources for several different atmospheric conditions, source strengths, and initial droplet sizes. The curves on the right show the distance from the generator at which the droplets in a homogeneous aerosol of pure mustard gas would disappear. They represent also the total concentration of mustard gas as vapor plus aerosol, at any distance from the source. Thus, they do not end at a fraction of saturation of unity, but could be extended to the source position through the region in which the aerosol would exist, regardless of the size of the droplets.

30.3.1 Effect of Temperature on Vapor Concentration in the Cloud

The shape and location of the integral curves representing the degree of saturation in the cloud are affected little by changes in air temperature since the diffusivity of the agent vapor changes only slightly with changes in temperature. This means that a homogeneous aerosol cloud from a given source, and under fixed meteorological conditions, should have the same percentage saturation of vapor at all air temperatures. The actual concentration of vapor will increase with temperature in proportion to the volatility of the agent. The aerosol cloud will persist longer at lower temperatures. After all the droplets evaporate and the aerosol cloud has disappeared, the vapor concentration becomes independent of temperature and depends solely on the strength of the source and on the meteorological conditions.

30.3.2 Maximum Drop Size to Maintain the Aerosol Cloud Essentially Saturated

It is of interest to know the maximum initial size of drops in a homogeneous aerosol cloud that will maintain a saturated condition throughout the life of the cloud. If only the vapor is effective as a casualty agent, it is evident that the larger droplets would be undesirable because the concentration and dosage during the passage of the cloud from a given source would be decreased by the slower rate of evaporation.

Only infinitesimal droplets can keep the cloud completely saturated at all distances up to that at which the cloud disappears. Small droplets maintain high degrees of saturation. Figures 3 and 4 show the largest original diameter of uniform drops that will keep the cloud better than 90% saturated throughout its life for several atmospheric conditions. The values

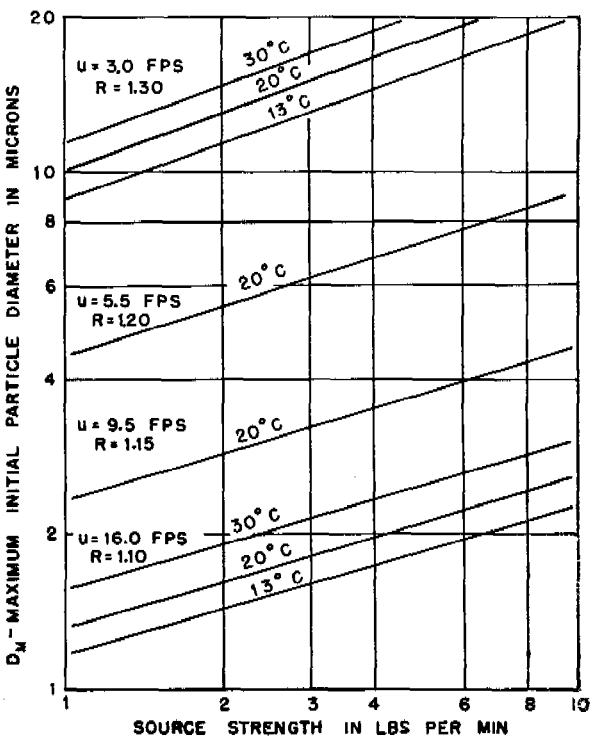


FIGURE 3. The maximum initial drop diameter which will maintain essentially saturated conditions in a mustard gas cloud from a point source.

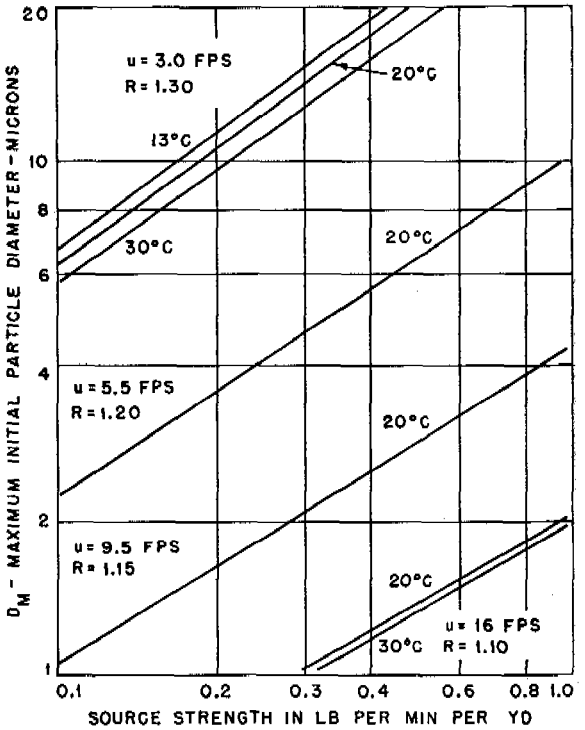


FIGURE 4. The maximum initial drop diameter which will maintain essentially saturated conditions in a mustard gas cloud from a line source.

of wind velocity chosen for the high "R" values in the figures are about the maximum to be expected.[18] Consequently, these charts show the upper limit of drop sizes that may be used for essentially saturated clouds. Aerosols containing large drops could be saturated only under conditions of low atmospheric turbulence. Under such conditions, however, these drops would settle out rapidly. Since the drop sizes in mists from explosive bursts and from all commercial spray nozzles are considerably larger than 10 microns,[19] it is evident that mustard gas aerosols from such sources cannot be saturated. The only method known at present for the field generation of aerosols with droplets less than 1 micron in diameter is the thermal generator.[8] It appears that all mustard gas clouds from such munitions will remain essentially saturated under all atmospheric conditions as long as the aerosol of mustard gas droplets persists.

30.3.3 Effect of Nonvolatile Impurities

If the aerosol droplets contain a nonvolatile residue, the aerosol cloud will not disappear by evaporation. The appearance of such a cloud produced from Levinstein mustard is apt to be misleading. The drop diameter then decreases to such a small extent, when only the nonvesicating impurity is left in the drop, that it may still form a screening smoke. Even materials of high purity, when dispersed as aerosols, may leave visible clouds after the evaporation is essentially complete. Figure 5 shows the residual diameter of drops containing various percentages (by volume) of nonvolatile impurities.

The rate of evaporation of a droplet is decreased by the presence of a soluble impurity due to the lowering of the saturation vapor pressure. If the vapor pressure follows Raoult's law, as in the case of Levinstein mustard,[4] the differential equations can be modified to allow for this impurity. These equations [3] can be integrated in a step-wise manner. Such an integration has been performed for a certain field test at Edgewood Arsenal on a mustard thermal generator. The candle was charged with Levinstein mustard. The calculated axial concentration of mustard gas vapor in the cloud is shown in Figure 6 in comparison with the curve calculated for a pure mustard charging. The initial uniform drop diameter used in the calculations was 0.6 micron, which is the average size

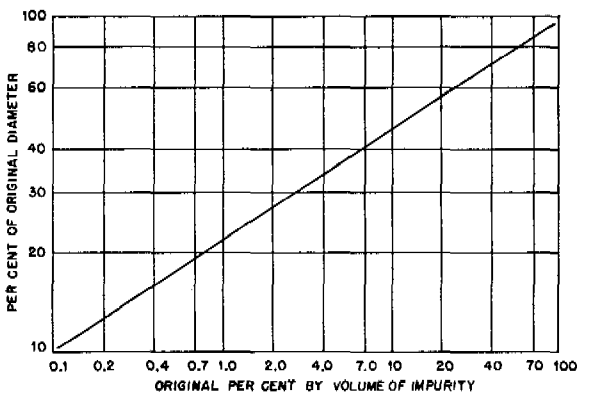


FIGURE 5. The effect of small amounts of nonvolatile impurity on the residual drop diameter.

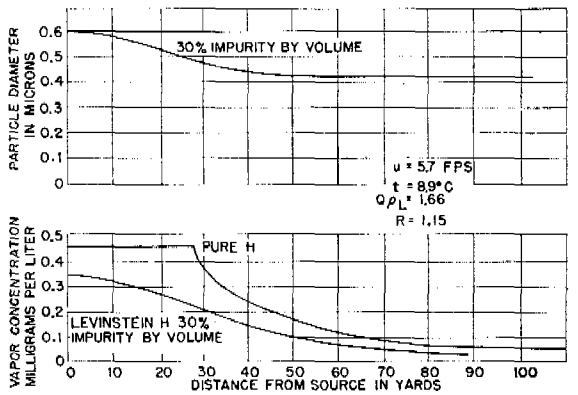


FIGURE 6. Comparison of calculated concentrations of mustard gas vapor in clouds from thermal generator. Test No. 1, Edgewood Arsenal, February 1943.

measured for simulant clouds set up in the same way. It is evident from the curves that the vapor concentration in the Levinstein cloud is considerably less than that of a cloud from pure mustard gas. Furthermore, whereas the cloud of pure mustard gas should have visibly disappeared at about 30 yd, the evaporation of the Levinstein droplets was still continuing at 100 yd. The calculated residual diameter of the droplets is shown in the upper curve in Figure 6.

30.4 CALCULATION OF EVAPORATION OF AEROSOL CLOUD

30.4.1 Derivation of Equations

For aerosols of small particles, the effect of gravity is negligible. The cloud is diluted in the same way as a gas cloud and the same laws of turbulent diffusion are applicable. The theory of atmospheric diffusion derived by the British workers requires a knowledge of the wind velocity, the vertical gradient of wind velocity, and the components of gustiness near the ground.[16] The axial, or peak, concentration of gas near the ground is given by the equations

$$c = \frac{Q}{Aux^m} \quad \text{for a continuous point source;} \tag{1}$$

$$c = \frac{Q}{Bux^{m/2}} \quad \text{for a continuous infinite line source.} \tag{2}$$

For a gas cloud, Q is the source strength in grams per second, or grams per second per centimeter, respectively, u is the wind velocity near the ground, and x is the distance from the source, both in cgs units. The index m is determined from the velocity gradient and is conveniently expressed in terms of the "R" value, which is the ratio of the wind velocity at 2 m to that at 1 m,

$$m = \frac{2}{1 + \dfrac{\log \text{"}R\text{"}}{\log 2}}. \tag{3}$$

The scale factors of diffusion, A and B, are actually complicated functions of the wind gradient, wind velocity and gustiness. Various simplifying approximations have been made in the use of these equations, such as for the concentration range slide rule [47] for field use, where A and B are assumed to be unique functions of the wind gradient and velocity. For the solution of the equations derived in the following text, a step-by-step integration is required, and even the above simplification is not sufficient to avoid laborious computations. Consequently, for this calculation A and B have been considered *constants for all values of* "R" and wind velocities. Actually, proofing of the equation against the Service slide rule has shown that the concentrations calculated will not deviate by more than 30% from the values based on the closer approximation, even for a large range of wind gradient and velocity. Since it is desired here to obtain only the approximate degree of saturation of the cloud and the effect of the droplet size, this simplification is warranted. Accordingly, the values of the constants were calculated from the slide rule for neutral conditions, "R" = 1.15, and for u = 5 mph (223 cm per sec), whence A = 0.34 (for axial concentrations) and B = 0.31.

For an aerosol cloud, N will be considered as the source strength expressed as number of particles per second (or number per second per centimeter for a line source), and c is the number of particles per cubic

centimeter at any point. The volume of air associated with one particle of the aerosol for a point source, therefore, is

$$V = \frac{1}{c} = \frac{Aux^m}{N} \cdot \tag{4}$$

Applying the gas law, the number of moles of vapor already evaporated from the droplet in this volume of air is

$$n = \frac{p}{RT} \cdot \frac{Aux^m}{N} \cdot \tag{5}$$

The rate of vaporization of small droplets in moving air has been investigated by Frossling,[17] who measured the evaporation of aniline, nitrobenzene, naphthalene, and water. All his data were correlated by means of the dimensionless equation

$$Nu' = 2(1 + 0.276 Re^{1/2} Sc^{1/3}) . \tag{6}$$

Here the dimensionless groups are

$$Nu' = \frac{RTk_g d}{k}, \quad Re = \frac{dv\rho_g}{\mu}, \quad Sc = \frac{\mu}{\rho_g k}$$

where d = diameter of the drop;
k = molecular diffusivity of the vapor in air;
ρ_g = density of gas;
v = interfacial velocity of the drop in the air;
μ = viscosity of air;
k_g = molar mass transfer coefficient.

When $Nu' = 2$, the rate of vaporization is

$$\frac{dn}{dt} = k_g S(p_s - p) = \frac{2\pi kd}{RT}(p_s - p) , \tag{7}$$

which is identical with the equation of Fuchs for the evaporation of a spherical drop in still air, where

p_s = saturation vapor pressure of the liquid at the drop surface;

p = actual partial pressure of the vapor in the ambient air.

The value of the Schmidt group, Sc, for mustard gas in air is 2.25. Since the inertial effects of the atmospheric eddies on the droplets of an aerosol are negligible, any interfacial velocity of air past the drop must be essentially that due to gravity fall. From Stokes' law, a 50-micron mustard gas drop falls at the rate of 9.5 cm per sec and $Re = 0.393$. For a 20-micron drop, the fall is 1.5 cm per sec and $Re = 0.025$. Thus, for any mustard gas aerosol cloud containing drops which do not readily settle out, Nu' is essentially equal to 2, and the Fuchs equation for evaporation in still air is satisfactory.

The diameter of the drop at any time is related to the original diameter D at the source by

$$d = \left(D^3 - \frac{6nM}{\pi\rho_l}\right)^{1/3} \cdot \tag{8}$$

Substituting equations (5) and (8) in equation (7), and letting f represent the fraction of saturation, p/p_s, gives the equation for a cloud from a point source,

$$\frac{d(fx^m)}{dt} = \frac{2\pi kN}{Au}\left(D^3 - \frac{6Au}{\pi N} \cdot \frac{p_s M}{RT\rho_l} \cdot fx^m\right)^{1/3}(1 - f) \cdot \tag{9}$$

Equation (9) may be simplified by noting that

$$\frac{p_s M}{RT} = W_s , \tag{10}$$

which is the saturation concentration of the vapor, and

$$\frac{\pi N D^3}{6} = Q , \tag{11}$$

where Q is the liquid volume rate of generation of the aerosol, which is here assumed to be perfectly homogeneous, and also that

$$udt = dx .$$

Then

$$\frac{df}{dx} = \frac{12kQ}{Au^2D^2}\left(1 - \frac{AuW_s}{Q\rho_l} fx^m\right)^{1/3} \frac{(1 - f)}{x^m} - \frac{mf}{x} . \tag{12}$$

This represents the equation for the degree of saturation in an aerosol cloud at any distance from the point source up to the disappearance of the droplets. It is convenient to write the equation in the form

$$\frac{df}{dx} = \frac{K_1}{x^m}(1 - K_2 fx^m)^{1/3}(1 - f) - \frac{mf}{x} , \tag{13}$$

where

$$K_1 = \frac{12kQ}{Au^2D^2} \quad \text{and} \quad K_2 = \frac{AuW_s}{Q\rho_l} \cdot \tag{14}$$

The analogous equation for a line source is

$$\frac{df}{dx} = \frac{K_1'}{x^{m/2}}(1 - K_2' fx^{m/2})^{1/3}(1 - f) - \frac{mf}{2x} , \tag{15}$$

where

$$K_1' = \frac{12kG}{Bu^2D^2} \quad \text{and} \quad K_2' = \frac{BuW_s}{Q\rho_l} \cdot \tag{16}$$

30.4.2 Integration of Equations

No general solutions of equations (13) and (15) have been obtained. Consequently, the integration has been performed by a step-wise method. The particular method used was as follows.

As a starting point, it was assumed that $f = 1$ when $x = 100$ cm. This means essentially that the cloud is saturated very near the source, although a few trials with $f = 0$ at $x = 100$ showed that the conditions at the start are not critical as the curves originating from these extremes converged rapidly. Values of K_1 and K_2 (or K_1' and K_2') were chosen for the conditions of the atmosphere, and source strength, and the particle size. Then df/dx at x_1 was found. The increment Δx_1 corresponding to Δf_1 was then found from

$$\Delta x_1 = \frac{\Delta f_1}{(df/dx)_1} .$$

A new point on the curve was then determined from

$$f_2 = f_1 + \Delta f_1$$

$$x_2 = x_1 + \Delta x_1$$

and $(df/dx)_2$ were found by substitution. The process was repeated indefinitely to give the integrated curve. If the chosen values of Δf were sufficiently small, a smooth curve resulted. Too large values of the increment would reverse the direction of the curve.

The integral curves were tested from the relationship

$$\int_0^{x_B} (1 - f)dx = \frac{3}{2K_1K_2} . \qquad (17)$$

As shown later, this integral is the area above the curve of f vs x up to saturation.

Figures 1 and 2 show some typical integral curves for point and line sources for several different atmospheric conditions, source strengths, and particle sizes. It is evident that, for the conditions chosen, the clouds are saturated only very near the source unless the drop size is below 1 micron. Drops as large as 24 or 48 microns evaporate slowly and cause the cloud to persist for considerable distances even for the small source strengths chosen. For higher "R" values or greater source strengths, the integral curves are shifted upward toward the saturation line and the boundary curve is displaced farther to the right.

30.4.3 The Boundary Curves

The curves on the right in Figures 1 and 2 show the distance from the generator at which the particles from a homogeneous aerosol of pure mustard gas would disappear. They represent also the total concentration of mustard gas, as vapor plus aerosol, at any point in the cloud. As such, they do not end at a fraction of saturation of unity but could be extended to the source position, through the region in which the aerosol cloud would exist regardless of the size of the droplets.

The boundary curves, representing as they do the concentration of matter in a cloud, could be calculated by means of the concentration range slide rule. As derived from equations (13) and (15), they were obtained by equating the terms $(1 - K_2fx^m)^{1/3}$ and $(1 - K_2'fx^{m/2})^{1/3}$ to zero and solving for f as a function of x. Thus they serve as a check on the accuracy of the simplifying assumptions described above. From equations (8) and (9), it may be seen that these terms represent the fraction of the original particle diameter of the droplet existing at any point.

The boundary curves can be represented by straight lines on log-log paper. The position of the lines depends on the value of the meteorological constant m (or "R"), the saturation concentration W_s, and the parameter u/Q. For constant source strength and meteorological conditions (i.e., turbulence and wind velocity) the logarithmic lines for different temperatures are parallel. The actual concentration, equal to fW_s, along the boundary curve, however, is essentially independent of the temperature of the air.

30.4.4 Maximum Drop Size to Maintain Essentially Saturated Clouds

The integral curves for small droplets, lying near the saturation ordinate, are practically linear up to the boundary curve.

Equation (13) may be written in the form

$$-d(1 - K_2fx^m)^{2/3} = \frac{2K_1K_2}{3}(1 - f)dx . \qquad (18)$$

The left side of this equation represents the decrease of the fraction of the original surface of a drop in the distance dx. In the distance from $x = 0$ to $x = x_B$ where the drop disappears, this quantity is equal to unity, or

$$\int_{x=0}^{x=x_B} d(1 - K_2fx^m)^{2/3} = 1 . \qquad (19)$$

Therefore

$$\int_{x=0}^{x=x_B} (1 - f)dx = \frac{3}{2K_1K_2} . \qquad (20)$$

The value of this integral depends upon the path of $(1 - f)$ vs x. Let us assume that the cloud is essentially saturated throughout its life, provided that it is at least 90% saturated when it disappears, that is,

$f = 0.9$ when $x = x_B$. Then, from the area under the curve,

$$\int_{x=0}^{x=x_B} (1 - f)dx \cong \frac{0.1}{2} x_B \cdot \quad (21)$$

But x_B is determined by

$$(1 - K_2 f_B x_B^m)^{1/3} = 0. \quad (22)$$

Substituting from equation (20),

$$K_1 \cong \frac{30(0.9)^{1/m}}{K_2^{(m-1)/m}}. \quad (23)$$

Again substituting the values of K_1 and K_2 from equation (14)

$$D_m^2 \cong \frac{12k}{30(0.9A)^{1/m}} \left(\frac{W_s}{\rho_l}\right)^{(m-1)/m} \frac{Q^{1/m}}{u^{(m+1)/m}}, \quad (24)$$

which gives the maximum original drop diameter that will keep the cloud from a point source better than 90% saturated throughout its life.

A similar treatment for a line source gives

$$D_m^2 \cong \frac{12k}{30(0.9B)^{2/m}} \left(\frac{W_s}{\rho_l}\right)^{(m-2)/m} \frac{Q^{2/m}}{u^{(m+2)/m}}. \quad (25)$$

It may be noted that the value of D_m is not so sensitive to decreasing the value of f_B as it is to increasing it. That is, the maximum drop diameter could be approximately 40% greater if it were assumed that the cloud is only 80% saturated at the point of disappearance. On the other hand, the permissible size would decrease considerably if it were desired to keep the cloud 99% saturated, or better.

30.4.5 Effect of Nonvolatile Impurities

When a nonvolatile impurity is present and if the vapor pressure follows Raoult's law, as it does in the case of Levinstein mustard,[4] equation (13) becomes

$$\frac{df}{dx} = \frac{K_1}{x^m}(1 - K_2 f x^m)^{1/3}(N_A - f) - \frac{mf}{x} \cdot \quad (26)$$

The mole fraction of the solvent N_A may be expressed in terms of z, the original concentration of the impurity, and the quantity $K_2 f x^m$, so that equation (26) for a point source becomes

$$\frac{df}{dx} = \frac{K_1}{x^m}(1 - K_2 f x^m)^{1/3} \cdot \left[\frac{(1 - z) - K_2 f x^m}{\left(1 - z + \frac{\rho_B z}{\rho_A}\right) - K_2 f x^m} - f\right] - \frac{mf}{x} \cdot \quad (27)$$

The corresponding equation for a line source is

$$\frac{df}{dx} = \frac{K_1'}{x^{m/2}}(1 - K_2' f x^{m/2})^{1/3} \cdot \left[\frac{(1 - z) - K_2' f x^{m/2}}{1 - z + \frac{\rho_B z}{\rho_A} - K_2' f x^{m/2}} - f\right] - \frac{mf}{2x} \cdot \quad (28)$$

These equations can be integrated in a step-wise manner similar to that described for equations (13) and (15).

The approximations made in these mathematical derivations leave much to be desired before the actual concentration of vapor in a mustard gas aerosol cloud can be estimated. Such clouds, of course, would not be uniform in particle size, and this would add a complication not considered here. Furthermore, the deposition of droplets greater than 5 microns in diameter on horizontal and vertical surfaces probably proceeds at a finite rate comparable with the rate of vaporization, so that the calculated concentration for aerosols of large droplets is too great. Nevertheless, it appears fairly certain that aerosol clouds made up of droplets of pure mustard gas less than 1 micron in diameter would always be saturated as long as the cloud persists. On the other hand, fine sprays and mists from explosive bursts [20] are by no means saturated, and atomizing nozzles would be of little use in a munition designed to generate high concentrations of vapor.

Nomenclature for Section 30.4

- A Gustiness factor for point source = 0.34.
- B Gustiness factor for line source = 0.31.
- c Axial concentration in gas or aerosol cloud.
- d Drop diameter at distance x.
- D Initial drop diameter in a homogeneous cloud at the source.
- D_m Maximum initial drop diameter to maintain the cloud essentially saturated.
- f Fraction of saturation, p/p_s.
- f_B Fraction of saturation at the point of disappearance of the aerosol cloud.
- k Molecular diffusivity.
- k_g Molar mass transfer coefficient.
- K_1, K_2, K_1', K_2' Parameters.
- m Meteorological constant.
- M Molecular weight.
- μ Viscosity of gas (air).
- n Moles of agent in the air as a vapor.



FIGURE 7. The F7A thermal generator pot.

N Source strength of aerosol cloud expressed as number of droplets/time for a point source; or number/(time)(length) for a line source.
N_A Mole fraction of solvent in a binary liquid agent.
Nu Dimensionless group $= RTk_v d/k$.
p Partial pressure of vapor in air.
p_s Saturation vapor pressure of pure agent.
Q Source strength expressed as volume/time for a point source; or volume/(time)(length) for a line source.
ρ_v Density of gas (air).
ρ_l Density of liquid agent.
ρ_A, ρ_B Molar liquid densities.
"R" Ratio of wind velocity at 2 m to that at 1 m.
R Gas constant.
Re Dimensionless group, Reynolds' number, $dv\rho_0/\mu$.
S Surface area of drop.
Sc Dimensionless group, $\mu/\rho_v k$.
T Absolute temperature, K.

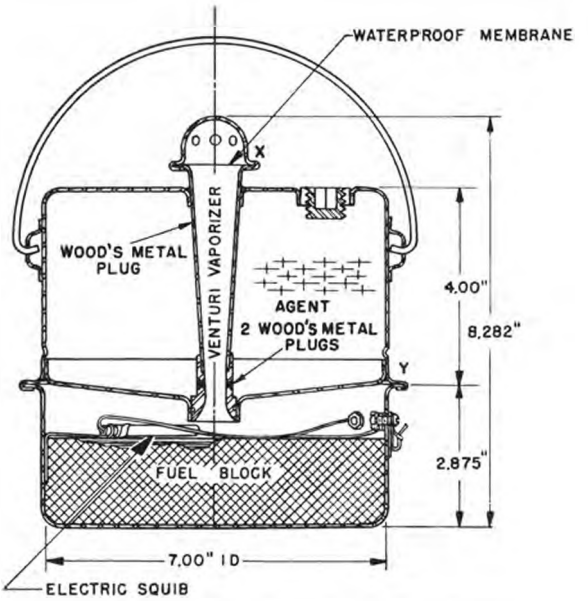


FIGURE 8. The F7A thermal generator.

t Time.
u Wind velocity.
v Interfacial velocity of drop in air.
V Volume of air associated with a drop.
W_s Saturation concentration of vapor.
x Distance downwind.
x_B Distance from source to point of disappearance of cloud.
z Initial volume fraction of impurity in binary liquid mixture.

Note: The units used in the derivation of the British diffusion equation are uniformly in the cgs system. Because of the exponential factors, conversion of the equations to the English system cannot be made conveniently. The integrations were therefore performed in the cgs system and the concentrations and distances, etc., then expressed in the units commonly in use.

30.5 MUSTARD GAS FROM THERMAL GENERATORS

30.5.1 Thermal Generator Pots

The improved thermal generator is well illustrated by the experimental pot [6] known as the F-7A shown in Figures 7 and 8. This pot is a practical munition for hand carrying in field use. It has been produced by production methods in a small quantity of approximately 2,000 units. The pot has not been recom-

mended for adoption as a standard munition because of the general conclusion that gas cloud attacks from hand-placed generators are no longer practical in modern warfare. The small quantity of pots was produced for use in testing the tactical advantages of mustard vapor clouds from thermal generators.[5] The application of this general design to aerial bombs is practical in modern warfare and such a bomb will be described later.

Description of the F-7A Thermal Generator Mustard Pot

This pot consists of a fuel block and agent in separate compartments. The liquid agent is fed into the hot gas stream from the fuel block in a high-velocity Venturi vaporizer. The high-velocity gases atomize the liquid agent, and the atomized liquid evaporates rapidly into the high-velocity hot gases. The feed rate is so adjusted that all but a small fraction of the atomized agent is evaporated in one pass through the vaporizer. This small fraction which is not vaporized is emitted with the vapor-gas mixture as a fine spray.

The pot is 7 in. in diameter and approximately 8¼ in. high. It is made up of two major assemblies which are crimped together. These are (1) the agent compartment assembly, and (2) the fuel container assembly. With the exception of the machined parts, the munition is fabricated throughout from 20 gauge sheet steel of deep drawing quality.

The *fuel mixture* is pressed into the fuel container under a dead load of about 1,000 psi. The composition of this mixture is as follows.

Slow base mixture, 1,000 g	NH_4NO_3	80.7%
	Charcoal	13.1%
	NH_4Cl	3.2%
	Linseed oil	3.0%
Fast base mixture, 400 g	NH_4NO_3	83.5%
	Charcoal	13.5%
	Linseed oil	3.0%
Starter mixture, 20 g	KNO_3	53.0%
	Silicon	39.2%
	Charcoal	5.8%
	Linseed oil	2.0%

The surface of the block is sprayed with a pyroxylin lacquer for protection against moisture. The fuel is ignited by a one-delay electric squib held in place on the surface of the block by a metal clip. The tip of the electric squib is coated with a 34% aluminum/66% potassium perchlorate mixture to insure ignition of the fuel block. The details of making these fuel blocks are described in Chapter 31.

The *agent container assembly* is made up of five parts, as follows: (1) agent container top, (2) agent container bottom, (3) Venturi tube, (4) Venturi throat, and (5) filler cap sleeve. These are joined in one operation by copper-brazing all joints simultaneously in a special furnace. Prior to crimping this assembly to the fuel can, the feed holes (No. 30 tap drill size — 0.1285 in. diameter) and the vent hole located near the top of the Venturi are soldered closed with Wood's metal alloy. A pressure test for leaks is specified with air at 35 psi. The lugs for the carrying handle are then soldered to the outside of the container. The diffuser cap is crimped onto the flanged end of the Venturi tube which projects above the top of the unit. A waterproof membrane of 0.010-in. thick aluminum foil placed over the end of the Venturi tube prevents moisture from reaching the fuel.

The unit, charged with distilled mustard gas, ready for functioning, weighs approximately 13 lb. This weight is distributed as follows: distilled mustard gas, 6.5 lb; fuel, 3.12 lb; metal components, 3.38 lb.

30.5.2 Operation of Unit

The F-7A thermal generator charged with 6.5 lb distilled mustard gas functions from 3½ to 4 min, emitting a dense mustard gas aerosol which evaporates downwind of the generator to form mustard gas vapor. To ignite the unit, an electric current is applied to the squib, and the spit from this ignites the fuel block. The initial pressure surge from the fuel gases fractures the waterproof membrane. The hot gases pass upward through the Venturi, causing the fusible plugs in the two feed holes and the vent hole to melt. The liquid agent then feeds into the Venturi throat, entering the high-velocity hot gas stream at right angles. The agent feed rate is controlled by the size of the two feed orifices and the pressure differential between the agent compartment and the Venturi throat. The agent is broken up by the velocity of the gas stream and partial vaporization of the agent takes place in the throat section. The contact time of the agent with the hot gases is extremely short, being of the order of several thousandths of a second. Further vaporization takes place as the hot gas-vapor-droplet mixture passes through the divergent section of the Venturi. The mixture issues to the atmosphere from the top of the munition through the diffuser cap, which contains eight No. 2

holes, 0.2210 in. diameter, at an angle of 22½° above the horizontal. These holes are designed to avoid flaming of the vapor, by rapid cooling with entrained air. The vapor condenses to form an aerosol upon being cooled by dilution with the air. A small fraction of the agent is deposited in the vicinity of the munition as droplets of unvaporized agent.

30.5.3 Development of the Pots

The development of these pots is of importance because a major part of the work on the improved thermal generators was done with them. Field tests

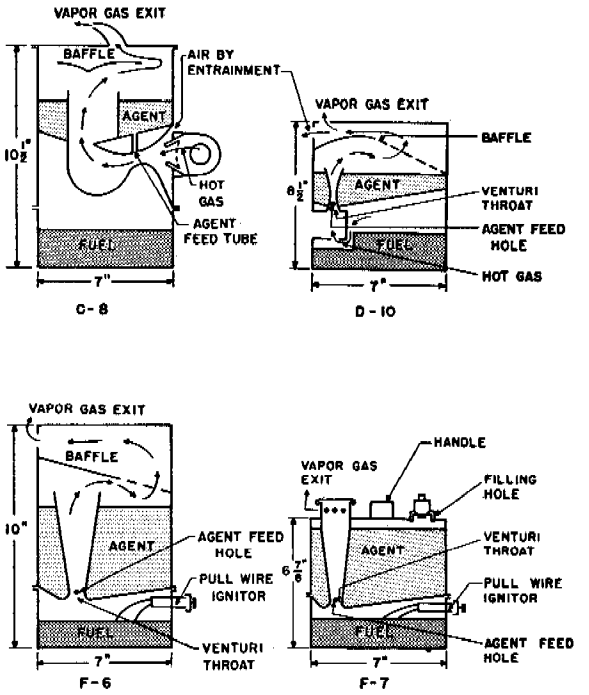


FIGURE 9. Thermal generator experimental pots.

with these pots provided the basis for interest in the use of thermally generated clouds of concentrated mustard gas vapor. This interest lent support to the development of the 10-lb, E29R1 thermal generator bomb described in the following text. In addition to the 13-lb size pot, units weighing 25, 35, and 125 lb were also built.[51] The last held 80 lb of mustard gas which could be dispersed in 10 to 12 min.

The F-7A thermal generator pot was the last of a series of experimental models and the only one which was manufactured by production methods. Some of the earlier models were built in lots of a few hundred by hand-welding methods and were used for field tests. Outline sketches of these various designs are shown in Figure 9, and significant comments on some of the designs will be made.

The early work[10,11] was directed toward an improved generator for solid agents which melt at a temperature above normal atmospheric temperature. These early models (C-8, D-10, and F-6) make no provision for sealing the agent in a closed compartment as would be necessary with a liquid agent. It was also believed at that time that the agent could not withstand direct contact with the hot fuel block gases without serious decomposition. The first pots were, therefore, designed to cool the fuel gases by entraining outside air before the gases came in direct contact with the agent. A series of experiments were carried out to provide a basis for the design of the air entrainment feature.[9] It was realized that using part of the heat from the fuel to heat the entrained air reduced the amount of agent that could be vaporized by a given amount of fuel. The quantitative relation between the amount of agent that can be vaporized and the ratio of entrained air to fuel gases was predicted.[9]

The development of the Venturi vaporizer resulted in such extremely short times of exposure that direct contact of agent and hot gases was possible and the air entrainment feature was eliminated in later models (see F-6 and F-7). The C-8, D-10, and F-6 models were provided with a baffle above the vaporizer. This separated unevaporated liquid drops from the gas stream and returned the liquid to the agent compartment for recycling through the vaporizer. The feed orifice at the throat of the Venturi was then designed to feed the agent at a higher rate than it could be evaporated. This recycling feature could not be readily incorporated in a unit with a sealed agent compartment for liquid agents, and it has not been included in the F-7 design. The agent feed orifice must then be of the proper size to feed the agent at such a rate that it will nearly all be evaporated in one pass through the vaporizer. This was accomplished satisfactorily.

C-8 Design. This was the original Venturi vaporizer design.[7] The fuel gases passed through an external tube and entered the entrance to a Venturi in a jet. This jet entrained air and the mixture passed through the Venturi. The lowest static pressure and the highest gas velocity are attained in the throat of the Venturi and this point was chosen for the introduction of the agent. A contact chamber downstream from the Venturi was provided, but this was later

found to be unnecessary because of the extremely good contact between the liquid and gas in the Venturi itself. This pot evaporated from 600 to 700 g of liquid Glaurin (diethylene glycol monolaurate) or solid paraffin wax in 3 to 4 min with 1,190 g of fuel block. The liquid temperature in the agent compartment ranged up to 240 F and the contact time of the agent with the hot gases was of the order of 0.01 sec. These agents have estimated average boiling points of 700 to 800 F.

D–10 Design. This is a more compact arrangement of the C–8. The model D–10, with air entrainment, has been found to disperse DM, Cyan DA, CN, sulfur, paraffin wax, Glaurin (diethylene glycol monolaurate) and tertiary butyl stearate. It is recommended for toxic smoke agents which are too thermally unstable to be used in the simpler pots without air entrainment. This candle is 8½ in. high by 7 in. in diameter and the experimental model weighs 11 lb when charged with 2 lb of agent and 3 1/16 lb of fuel. The burning time averages 3½ to 4 min and the particle size of the smoke is probably between 0.2 and 0.3 micron radius.

The features of the candle include an air entrainment device, a means of spraying the liquid agent into the hot gas stream, and a special baffle to remove liquid droplets from the gas stream. The candle dispersed 84.4% of the DM charged, as undecomposed smoke in one test, and averaged 67.9% in two other tests. This compared with 56.1% dispersed by two DM irritant smoke M-2 candles. The D–10 candle also dispersed Cyan DA with 91% of this agent appearing in the smoke undecomposed. Earlier tests with tertiary butyl stearate [12] as a simulating compound, indicated that the D-10 model would disperse 89% of this material as smoke undecomposed, compared with 53% dispersed by the M–2 candle. The D–10 model is not adapted to field use with agents which may be liquid at times. Other modifications [8] of this design were tested briefly and ratios of entrained air to fuel gas as high as 6/1 were attained. Attention was then directed to the design of a pot without air entrainment.

F–6 Design. In this design the upper compartment contains the agent. A Venturi-shaped tube connects the fuel compartment with the agent compartment and the hot gases pass through the Venturi at a velocity of about 700 fps. The agent compartment, up to the top of the Venturi, has a total capacity of somewhat over 2,500 cc. The bottom of the agent compartment is slightly conical, allowing the liquid to drain to the throat of the Venturi. Two feed holes (0.024 in. diameter) are provided in the throat. The liquid flows through these holes from the agent compartment into the hot gases passing through the Venturi tube. This flow is caused by the pressure in the agent compartment (about 20 to 30 in. of water) plus the liquid head, and is aided by the vacuum in the throat of the Venturi. The liquid enters at right angles to the high velocity hot gas stream, and is broken up into fine droplets which evaporate rapidly in the turbulent gases in the diverging section of the Venturi. This cools the hot gases quickly. The agent is thus exposed for a very short time to the high temperatures. The mixture of gas, vapor, and liquid particles then impinges on a baffle where the unevaporated particles are thrown out and allowed to drain back into the agent compartment. The vapors then pass around the baffle and are emitted to the air through three ½-in. holes. On mixing with the cooler air they cool rapidly and partially condense to an aerosol. Temperatures in a pot similar to the F–6 are shown in Figure 10.

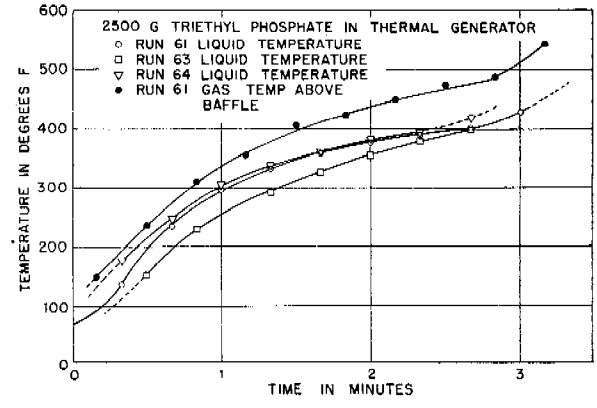


FIGURE 10. Temperature of agent in agent compartment of thermal generator.

30.6 RESULTS OF EXPERIMENTS

30.6.1 Composition of Vapor from the Pot

An attempt was made to determine the extent of decomposition of Levinstein mustard in the pot.[8] The pot was connected directly to a suitable air-cooled condenser followed by a water-cooled condenser. A relatively large amount of aerosol passed through the apparatus uncondensed and it was not possible to account for more than 50% of the agent charged in the condensate. The purity of the condensate was determined by three independent methods.

1. Melting points and mixed melting points were measured.

2. A sample of the condensate was tested on the same men for vesicant action in comparison with Levinstein redistilled mustard.

3. A method of determining the purity of mustard by means of the rate of evaporation of small droplets [4] was used.

All these methods indicated that the condensate had a higher mustard content than the agent charged. A Cottrell-type electrostatic precipitator was then designed and used later to recover as condensate 80% of the agent charged to a thermal generator bomb.

30.6.2 Field Test on the Thermal Generator at Suffield Experimental Station

The F-6 design was used in a field test at the Experimental Station, Suffield, Alberta, in October 1943.[15] In this test 96 pots were tried. They were charged with 5 lb of stripped mustard (90% pure) and placed in a straight line at 1½-yd intervals. The meteorological conditions were as follows.

Air temperature, F	74
Ground temperature, F	84
Relative humidity, %	25
Sky	Clear
Time	12:37 to 12:42 p.m.
Wind velocity	24 fps, 16 mph
"R" value	1.12
Gustiness, G_y	0.61
G_z	0.35

On a line 50 yd downwind, 6 yd long, and opposite the center of the line of generators, four observers were seated on chairs at 2-yd intervals. Immediately upwind from each observer was a chemical sampler 3 ft above the ground. The observers were completely protected by masks and impregnated clothes, except for a spot 2x2 in. on each upper arm.

At 75 yd downwind, chemical samplers were placed on a line 300 yd long at 15-yd intervals, except at the center where they were at 5-yd intervals. An observer dressed in battle dress with impregnated underpants and wearing a gas mask was stationed at each of these center samplers.

On a line 150 yd downwind, four observers dressed in the same way as those on the 75-yd line were stationed at 24-yd intervals, and carried portable sampling apparatus.

Of the 96 pots, 5 did not fire. Five blew the lids loose and twenty more blew the lids completely off. The vapors from one ignited near the end of the run. These lids were applied with a pressed fit, and they could easily have been fastened on more securely if the need for this had been anticipated. As it was, the lids that were blown off remained in position in most cases during a large part of the burning time and apparently did not seriously affect the functioning of the candles.

A summary of the analytical results and the physiological effects reported from Suffield is given in the table below.

These results are in reasonable agreement with the doses predicted from the British diffusion equation, as shown in the table. All men exposed on the 75-yd line showed effects which would correspond to a Ct between 300 and 400 mg-min per cu m. It is possible from these results that the pot dispersed from 75 to 100% of the mustard gas charged as mustard gas vapor. Of six men exposed on the 75-yd line, three became true casualties within ten days after the trial, due to lesions in the armpits. One casualty developed out of the four men on the 150-yd line. The estimate is therefore probably not greatly in error since the temperature was only 74 F. It was estimated that a 20 to 40% increase in concentration would have resulted in a large proportion of casualties, which proportion would have been markedly increased if no impregnated underpants had been provided.

The high wind velocity and low "R" value during the test are unfavorable for obtaining casualties with a small expenditure of agent. They were chosen here because they gave conditions which could be pre-

Position downwind	Analyzed dosages mg-min/cu m Iodoplatinate	Chloramine-T	Pyridine	Predicted dosages (diffusion theory)*	Dosages from physiological results (estimated)
50 yd	450	Not done	Not done	750	Not reported
75 yd	380	350	420	535	3 casualties out of 6 men 300–400
150 yd	350	Not done	Not done	350	1 casualty 2 definite lesions 1 negligible

* These dosages were based on a purity of 90% in the charge.

dicted with considerable certainty at the positions of the human observers used for assaying the physiological effects of the cloud.

F–7 Design. The F–7A thermal generator shown in Figures 7 and 8 is the production model of the F–7 type shown in Figure 9. The latter was developed as an improvement over the F–6 model which was quite efficient in operation, but could not be transported once it was charged with liquid mustard gas. The agent was not confined to a sealed compartment and could slop over through the vaporizer tube, and thence onto the surface of the fuel block, if handled roughly after loading. In the F–7 the agent was completely sealed in the agent compartment resulting in a practical pot for field use. There was no provision for recycling unevaporated agent and it was therefore necessary to obtain a proper balance between the agent feed-hole size, the diameter of the vapor exit orifices, and the weight of fuel and agent charged. The agent vapor issued horizontally over an angle of approximately 120° from five $^{17}/_{64}$-in. diameter holes. Vertical discharge through a ½-in. diameter hole was also tried, and, under neutral conditions at low wind velocity, the aerosol cloud rose to a height of about 20 ft and was considerably diluted before it reached the ground. The horizontal discharge placed the aerosol along the ground.

Field Tests

Six field tests with F–6 and F–7 thermal generator pots were carried out at Bushnell, Florida, in January and February 1944.[13] The first two trials were for the purpose of determining the functioning characteristics of the F–7 generators when charged with either Levinstein or distilled mustard. These tests indicated that Levinstein mustard is unsuitable for use in these thermal generators because of flaming of the agent. It is also anticipated that storage of Levinstein mustard in the generators would frequently result in deposition of solids which would interfere with proper operation by plugging the feed holes. Distilled mustard is relatively free from these two disadvantages and is recommended for use in the generators. In the other four trials, two of which were in the open meadow and two in the forest, vapor sampling data were obtained. Physiological data were obtained in one of the meadow trials with the aid of human observers.

The official report of these trials [13] states:

> On the basis of the rather limited data obtained . . . the thermal generator is capable, under proper conditions, of setting up in a short time at some distance from the source dosages of mustard vapor which will produce a high percentage of casualties in troops protected only by gas masks.

There was a difference in the behavior of the cloud in the meadow and in the forest. Under inversion conditions in the meadow, the cloud remained in a compact mass, close to the ground, moving downwind. Under the same meteorological conditions, in the forest, the cloud tended to rise at first to treetop level and then slowly diffused downward to the ground.

No large-scale tests have been carried out with the F–7 type thermal generator since the Florida trials. However, several small-scale experiments have been reported at Dugway Proving Ground using the F–7A, charged with distilled mustard.[21–23] In one of the tests, an F–7A pot was functioned 10 ft in front of the entrance to a cave. Although most of the visible cloud was seen to flow past the opening, total dosages at all stations within the cave were in excess of 2,000 mg-min per cu m.

An F–7A was functioned at the bottom of an old mine shaft.[23] The mine tunnels extended for a total of 818 ft in different directions and had a volume of approximately 25,000 cu ft. Observed dosages were between 20,000 and 40,000 mg-min per cu m obtained over a 20-hr period.

Two small-scale tests with the F–7A have been carried out at the Suffield Experimental Station [49] at 35 and 26 F, respectively. The generators functioned satisfactorily at these temperatures but only 65% of the distilled mustard gas charging was emitted. The approximate composition of the agent in the cloud produced was 60% as mustard gas vapor, 10% mustard gas droplets with a MMD of 30 to 40 microns, and 30% mustard gas droplets of less than 3 microns diameter. There was no evidence of decomposition products of mustard gas, and the fall out close to the point of emission was small. The effects on physiological observers exposed to the cloud were greater than would have been anticipated for the dosages to which they were subjected. This may have been due to the droplets in the cloud.

30.7 CONCLUSIONS

The following conclusions can be drawn from the tests on the F–7A.

1. The F–7A thermal generator, charged with distilled mustard gas, is a practical hand-carry munition for use in the field.

2. No tactical requirement for a hand-carry pot exists or is anticipated.

3. The pot described disperses distilled mustard gas as an aerosol which evaporates to form mustard gas vapor having a physiological activity at least as great as that of pure mustard gas vapor.

4. This thermal generator is capable of setting up concentrations of mustard gas vapor of physiological importance in a fraction of the time required by bursting-type munitions.

5. The F-7A type thermal generator does not function satisfactorily when charged with Levinstein mustard, due to flaming of the vapor as it issues from the generator. When charged with distilled mustard gas, functioning is satisfactory.

30.8 THERMAL GENERATOR BOMBS

30.8.1 Introduction

Field tests with mustard gas in the thermal generator pots indicated that the chief characteristics of the thermal generator are:

1. It produces high concentrations of vapor that are effective against masked men and these effective concentrations are set up in from 2 to 10 min. This is to be compared with 30 min to 4 hr for bursting munitions which disperse the liquid on the ground.

2. It disperses mustard vapor as a nonpersistent gas. This leaves a minimum of residual contamination on the target area and the target may therefore be occupied by friendly troops shortly after the conclusion of an attack.

3. In open terrain with a moderate breeze the dosages will be comparable to those from an equal amount of nonpersistent agent.

4. In the forest or in open terrain at low wind velocities, the dosages are comparable to those developed in a longer time by an equivalent amount of liquid mustard dispersed on the ground. They are less than the dosages from a typical nonpersistent agent because the thermal generator does not set up self-inversion as do the nonpersistent agents.

Designing a bomb to function as a thermal generator involves several innovations. Unlike high-explosive bombs, this bomb must remain in good mechanical working condition after impact. It must then function as an evaporator for several minutes, and vaporize a liquid without appreciably decomposing it. The liquid is somewhat unstable, and, if boiled at its atmospheric boiling point, an appreciable part decomposes. The vaporization of this liquid by the most modern industrial equipment would require several times the volume of space allotted to this operation in the bomb.

After these requirements had been provided for in the design of the bomb, the center of gravity was found to be farther back from the nose than in any other bomb. To operate properly it must not land flat. This meant that a new and more effective tail had to be developed. A new fuse and ignition system were necessary. Even the standard procedure for applying a protective coating inside the agent space could not be used. The present design is successful in meeting these problems. It has not yet been produced or used in large quantities and, since the design is so new, it is to be expected that additional minor faults will become apparent from time to time.

The bomb must land upright and penetrate into the ground a short distance so that the agent can be completely discharged. It is realized that perfect functioning is not to be expected on hard surfaces.

30.8.2 Description of 10-lb, E29R1 Thermal Generator Bomb

An assembly drawing of the bomb [14] is shown in Figure 11 and a picture of an assembled bomb is shown in Figure 12. The overall dimensions of the cylindrical bomb are $2\frac{3}{4}$ in. in diameter by $19\frac{3}{8}$ in. long. It is composed of two pieces, the main body of the bomb and the streamer tail unit which screws onto the body. Approximately 5,000 of these bomb bodies and 2,000 of the streamer tail units were fabricated and assembled by production methods.

The Bomb Body

The body consists essentially of an impact nose, a fuel compartment, an agent compartment, and a Venturi vaporizer passing through the center of the agent compartment. The agent compartment is separated from the fuel compartment by a steel cup which also houses the Venturi vaporizer. The vaporizer consists of a Venturi and a vapor mixing tube. The Venturi includes a rounded inlet, a short straight section at the Venturi throat, and a diverging section. It is screwed into a Venturi sleeve brazed into the agent compartment bottom. There are two shoulders on the Venturi which seat against the Venturi sleeve. These seats are sealed with copper-clad asbestos gaskets. The Venturi sleeve contains eight liquid

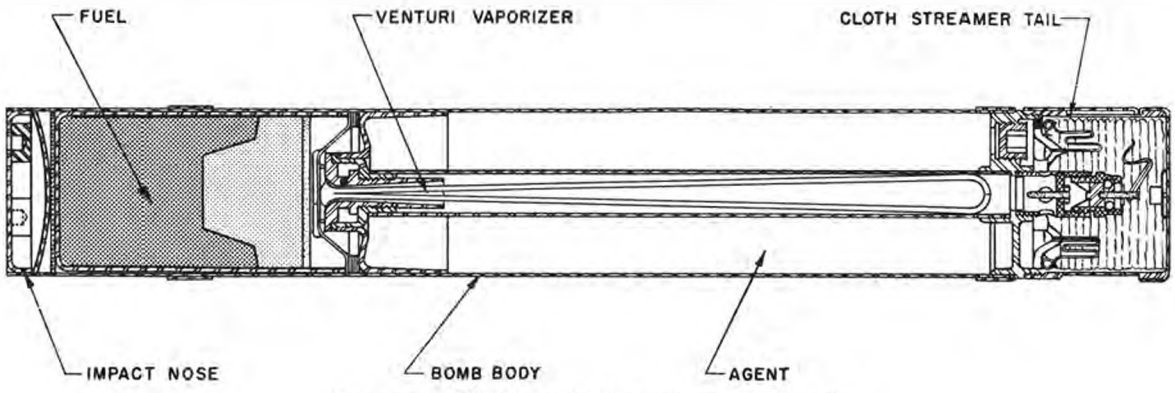


FIGURE 11. E29R1 – 10-lb thermal generator bomb.



FIGURE 12. E29R1 – 10-lb thermal generator bomb.

feed holes which allow the agent to flow into the annular space between the Venturi gaskets. The main feed hole in the Venturi throat is sealed with a low melting solder. In operation, this solder melts out and allows the agent to feed into the Venturi throat.

Below the entrance to the Venturi, is a circular baffle which keeps slag from the burning fuel out of the Venturi throat and liquid feed hole.

The vapor mixing tube connects the Venturi sleeve with the agent compartment top. The agent compartment top is threaded to receive the tail housing cup and also the fuze base. It also contains the filling hole and two index bosses with holes which are used to register the bomb in the filling apparatus. The filling hole is designed to avoid contamination of the threads. A shoulder is provided below the threads. The filling head seats on this shoulder, sealing the threads off from the agent. As an added precaution in filling the bomb, the agent compartment top contains an annular trough for decontaminating solution. After filling, the hole is closed with a $\frac{3}{8}$-in. pipe plug.

The inside of the agent compartment is coated with a bakelite-type resin to reduce the pressure caused by the reaction between steel and mustard.

THE FUEL BLOCK

The fuel block is pressed into a cylindrical steel can lined with heavy paper which is then inserted into the fuel compartment. The fuel consists of two layers and a starting layer with the following compositions:

Bottom layer	243.5 g (84%) NH_4NO_3
	5.9 g (2%) NH_4ClO_4
	31.9 g (11%) Charcoal
	8.7 g (3%) Linseed oil
	290.0 g
Top layer	139.4 g (82%) NH_4NO_3
	6.8 g (4%) KNO_3
	18.7 g (11%) Charcoal
	5.1 g (3%) Linseed oil
	170.0 g
Weight of fuel	460.0 g
Starting layer (or first fire)	5.3 g (53%) KNO_3
	3.9 g (39.1%) Silicon
	0.6 g (5.9%) Charcoal
	0.2 g (2%) Linseed oil
	10.0 g
Total weight of fuel block	470.0 g

In the production of the fuel blocks the percentages of ammonium perchlorate and potassium nitrate were varied slightly to compensate for variations in the burning characteristics of the charcoal. Blocks made with a batch of charcoal which burned too slowly were made to burn at the proper rate by increasing these percentages. Blocks made with a batch of charcoal which burned too fast were slowed down by decreasing these percentages. Several thousand of these fuel blocks were manufactured by the Unexcelled Manufacturing Company. The weight of the fuel block is limited by the space available in the bomb, and in about 15% of the production blocks, it was necessary to reduce the weight of fuel used to within the range 455 to 470 g because of variations in the density.

The fuel block [26] is discussed at length in Chapter 31 and only a few details will be mentioned here. The bottom layer is first pressed into the fuel can with a stepped ram. The top layer is added and smoothed with a flat ram but not pressed. The starting layer is added and these layers are then pressed in with a flat ram. A dead load of 8 tons is used in both these pressing operations.

No. 1 Navy Quickmatch is inserted through the Venturi and vapor mixing tube. A doubled piece is used with the loop near the top of the tube, and two knots tied below the Venturi, one on either side of the baffle. The lower knot is coated with a small amount of primer powder. This powder contains 65.8% potassium perchlorate and 34.2% finely powdered aluminum, and is mixed with a solution of 5% celluloid in acetone to a pasty consistency. When the bomb functions, the top of the Quickmatch is ignited by the flash of the powder in the fuze booster tube. The Quickmatch ignites the primer and the flash from this powder ignites the starting layer of the fuel block.

A chipboard buffer ring separates the fuel container from the agent compartment bottom and acts as a cushion. Below the fuel container is a chipboard disk, a metal impact disk, and the nose cup. The nose cup contains two bosses with index holes to orient the bomb in the filling line. The nose cup is silver-soldered in place by induction heating after the fuel block has been placed in the bomb. In this operation a suitable jig is used, and water is sprayed around the case of the bomb to keep the fuel block below its ignition temperature.

The Fuze

The fuze shown in Figure 13 for use with the cloth streamer tail is an inertia impact fuze provided with

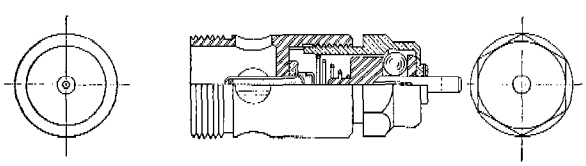


Figure 13. Impact fuze for use with cloth streamer tails on the 10-lb — E29R1, thermal generator bomb.

a safety arming pin which is pulled out by the cloth streamers after the bomb leaves the cluster. The fuze is mounted in the tail of the bomb and screws into the top of the agent compartment. It spits a flame into the vapor mixing tube. The fuze case is aluminum and consists of two parts, the base and the firing pin cylinder, which screw together. The firing pin is a cylindrical steel pellet with the striker at the lower end and the upper end, fitted with two safety balls in a radial hole. When the safety pin is in place, these balls are forced apart and engage a groove in the upper part of the fuze case preventing the firing pin from moving forward. When the safety pin is removed, the balls slip into the firing pin and the latter is free to move forward on impact and strike the primer. A small keeper-spring holds the firing pin away from the primer when the fuze is armed.

The primer is an M -29 percussion cap mounted in the base of the fuze. The primer ignites a booster tube which is also mounted in the fuze base. This is a brass tube $\frac{1}{8}$ in. in diameter by $\frac{3}{4}$ in. long, filled with powder, and with its lower end closed by a small wad of chipboard. The booster powder contains 65.8% potassium perchlorate and 34.2% grained aluminum. The mixture is grained with a 5% solution of celluloid in acetone. It should then pass a 40-mesh screen and be held on a 100-mesh screen.

The Bomb Tail

The cloth streamer tail is assembled as a separate unit which screws onto the bomb after the latter has been filled, and the fuze inserted. The tail consists of three cloth streamers 3 in. wide and 40 in. long. These are fastened to a shroud ring which is attached to the bottom of the tail housing by three nylon shroud lines 10 in. long. The streamers are packed into the tail-housing cup and held by a cover plate. The ends of the streamers are fastened to the cover plate by a spring clip. This plate pulls the streamers out during flight and then drops off. The cover plate is sealed by a fiber gasket and held in place against the tail-housing cup by a spring clip. When in the cluster, this clip is held in place by an adjacent bomb. When the bomb is released from the cluster the spring clip flies off and releases the housing cover. The safety pin in the fuze is attached to the streamer by a wire clip. When the streamers pull out, the fuze arms. In flight the cloth streamers are about 8 in. behind the bomb body and extend back to about 48 in. They are held in this position by the shroud ring which is in turn connected to the bomb body by the 10-in. long shroud lines.

Metal Telescoping Tail for the E29R1 Bomb

A metal telescoping tail has been developed [27] to replace the streamer tail described above. This tail causes the bomb to spin during its fall, reaching 3,500

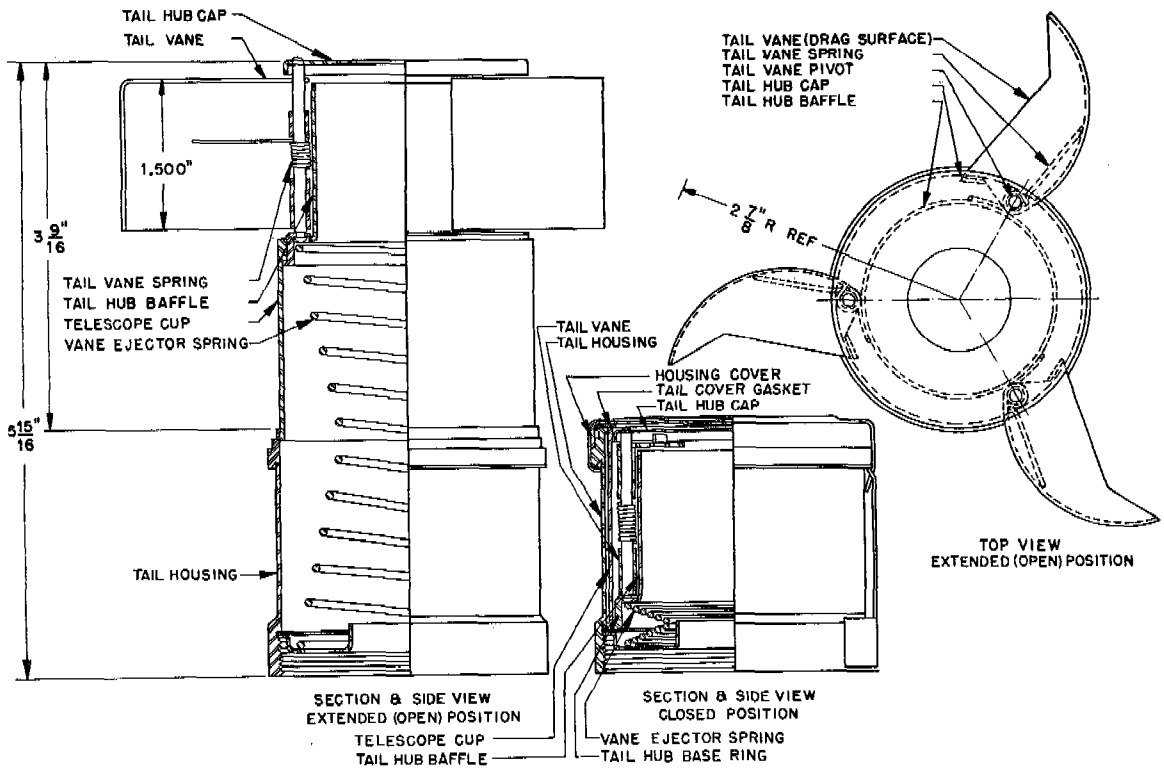


FIGURE 14. Telescoping metal tail.

rpm when dropped from 2,500 ft. This spin stabilizes the flight and also makes it possible to use a centrifugal arming fuze which is easier to seal against moisture.

The metal telescoping tail is shown in Figure 14. It is composed of a housing cup (this is the same housing cup used for the streamer tails, and the two tails appear identical when assembled on the bomb), a telescoping cup, and a telescoping hub with three folding vanes. The hub and telescoping cup are inside the housing cup when the bomb is clustered, and the housing cup cover is held in place in the same way as with the cloth streamer tail. When released from the cluster the telescoping cup and the hub spring out, and the vanes in the hub open out.

A relatively small number of these tails have been built and tested. They gave excellent promise and it is recommended that a sufficient number be made to provide for adequate field testing, with a view to adopting this tail as standard for the E29R1 bomb.

CENTRIFUGAL ARMING FUZE FOR USE WITH THE TELESCOPING METAL TAILS

The centrifugal arming fuze [14] for use with the above telescoping metal tail is shown in Figure 15 and the component parts in Figure 16. The operation of the fuze is quite simple. The firing plunger shown in Figure 16D is held in place by two centrifugal arming pins (Figure 16F), which fit into a continuous groove in the firing plunger. These make the fuze safe until sufficient centrifugal force pulls the pins away from the grooves in the firing plunger. This action can be regulated at any rpm by varying the strength of the arming springs (Figure 16G) behind the arming pins. A keeper spring (Figure 16C) is used to prevent the firing plunger from drifting onto the primer after the fuze is armed. The advantages of this fuze are its increased sensitivity after arming, complete sealing of the fuze mechanism from moisture, elimination of external safety pins, ease of assembly into the bomb, absolute safety during handling, and elimination of air bursts.

Some two hundred fuzes of this type have been dropped. The arming rpm has been varied from 1,750 to 3,200. A final rpm of 2,200 was used as an average operating speed.

30.8.3 Chemical Efficiency of the Bomb

A number of tests were made to determine the extent of the decomposition of mustard gas in the E29

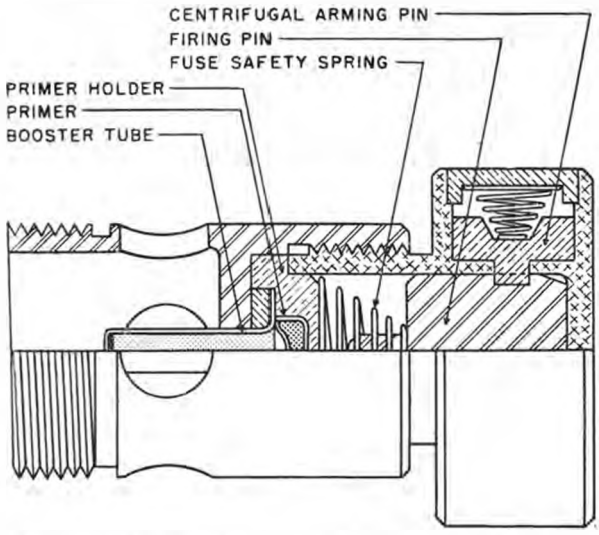


FIGURE 15. Centrifugal arming fuze for use with telescoping metal tails.

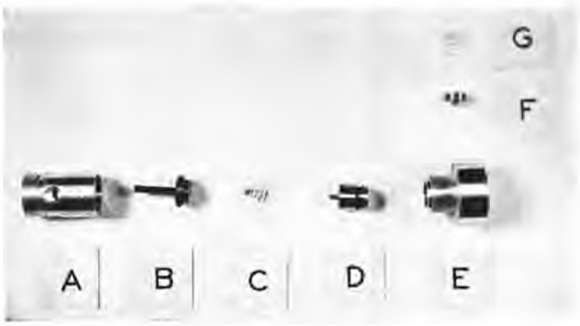


FIGURE 16. Component parts of centrifugal arming fuze. (A) fuse base; (B) primer and booster tube assembly; (C) firing plunger creep spring; (D) firing plunger; (E) fuse head; (F) centrifugal arming pin (only one shown, two are used); (G) centrifugal arming pin spring.

and E29R1 bombs. This was done by collecting the mustard issuing from the bomb and analyzing it.

Two methods of recovering the mustard were used. One method consisted of passing the vapors from the bomb through an absorption column where the mustard gas was absorbed in *butyl Cellosolve*. This method was used on an earlier model E29 bomb. The efficiency of removal of the mustard gas from the hot gases by this method was open to question. The tests indicated however that approximately 80% of the mustard charged left the unit undecomposed.

The method [4] used on the E29R1 bombs consisted of cooling the hot gas-vapor mixture in a water-cooled condenser, where most of the mustard gas was condensed and collected as a liquid. The remainder of the mustard gas which did not deposit in the condenser was present as an aerosol and was removed by a Cottrell electrostatic precipitator. These tests indicated that approximately 78% of the mustard charged was expelled from the bomb undecomposed.

30.8.4 Choice of Size of Bomb

The E29R1 is a small bomb compared to other chemical bombs. This raises the question of whether a larger size would be more generally effective. It may be desirable eventually to develop three or four sizes for a variety of atmospheric and tactical situations. Further development of the bomb and additional field tests will be needed to answer these questions. Some information on this subject is available now and is discussed below.

Single or widely scattered E29R1 mustard bombs impacting in open or wooded terrain are ineffective since personnel may easily move out of the cloud. The effective dosage area from a single bomb is not large. As the number of bombs dropped on an area increases, the effectiveness will begin to increase rapidly when the effective dosage areas from adjacent bombs overlap, and it becomes impossible to escape from the cloud.

The results expected from 64 bombs per artillery square have been calculated as a percentage of the target area covered with a given dosage under several meteorological conditions. These are given in Table 1.

TABLE 1. Expected results from a density of 64 E29R1 bombs per artillery square on a large target area.

	Wind speed	% of target area covered with a given dosage Dosage, mg-min/sq m				
	(mph)	10,000	4,000	2,000	1,000	500
Clear day	2			74	92	100
	4				76	
	8				57	81
Neutral	2		82	95	99+	100
	4			77	92	100
	8				72	89
Clear night	2	79	97	100	100	100
	4			83	95	100

The calculations should be confirmed by field trials. The table indicates that the bombs are large enough to set up effective dosages on the target. Under the best meteorological conditions, such as a clear night with a 2-mph wind, dosages of 10,000 mg-min per cu m are predicted over 79% of the target area. Un-

der unfavorable conditions, as on a clear day with an 8-mph wind, dosages of 500 mg-min per cu m over 81% of the target area may be expected.

Derivation of Results Predicted in Table 1

The following theoretical treatment is based on methods used by the Project Coordination Staff, CWS, which have been applicable to nonpersistent and persistent gas bombs, from data on a large number of field trials.

Only the dosages in open level terrain have been calculated and no consideration has been given to possible pillaring of the cloud.

The basic equation of the British diffusion theory is

$$D = \frac{2kjW}{\pi u x^m} e^{-k^2y^2/x^m} e^{-j^2z^2/x^m}, \qquad (29)$$

where D is the dosage developed at a point x,y,z in space, when a weight W of agent is released at a point with a wind speed of u, and turbulent meteorological conditions represented by k, j, and m.

$$m = \frac{2}{1 + (\log \text{“}R\text{”})/(\log \text{“}R\text{”} + \log 2)}, \qquad (30)$$

where “R” is the ratio of wind velocity at 2 m to that at 1 m above the ground over a standard prepared area.

The center line dosage near ground level can be given as

$$D_C = \frac{K_1}{(x/100)^m}. \qquad (31)$$

The *integrated crosswind dosage* near ground level is given by

$$ICW = \frac{K_2}{(x/100)^{m/2}}, \qquad (32)$$

and the half width of the cloud (defined as the distance from the centerline of the cloud to the point at which the dosage is 0.1 of the centerline dosage) as

$$\text{Half width} = K_3\left(\frac{x}{100}\right)^{m/2}, \qquad (33)$$

where $K_3 = 0.93K_2/K_1$.

The following table of “R” values represents average values for the gross meteorological conditions shown.

Table 2. Summary of “R” values to be used for meteorological combinations.

Wind speed mph	Clear day	Neutral conditions	Clear night
2	1.08	1.14	1.25
4	1.08	1.14	1.18
8	1.08	1.14	...

For “R” = 1.14 and u = 4 mph, the value of m is 1.794. Several values of D_C and ICW are read from the concentration range slide rule and values of K_1, K_2, and K_3 computed. Table 3 contains the values

Table 3. Calculation of the numerical values of K_1,* K_2,† and K_3‡ for neutral conditions, with wind speed of 4 mph for a source strength of 1 lb of agent.

x (yd)	D_C (mg-min/cu m)	$\left(\frac{x}{100}\right)^m$	K_1	ICW (mg-min/sq m)	$\left(\frac{x}{100}\right)^{m/2}$	K_2
100	40	1	40	780	1	780
150	18	2.07	37	550	1.438	790
200	11	3.47	38	420	1.86	780
400	3.5	12	42	230	3.47	800

* Average K_1 = 39.
† Average K_2 = 790.
‡ Average K_3 = 18.7.

thus calculated for a source strength of 1 lb of agent.

By a series of such calculations, the values summarized in Table 4 were obtained. These values are

Table 4. Summary of the numerical values of K_1, K_2, K_3, m, and $m/2$ for various gross meteorological conditions for a point source of 2.34 lb of agent.

Wind speed (mph)	Constant	Clear day	Neutral conditions	Clear night
2	K_1	32.2	177	550
	K_2	1,710	3,400	6,450
	K_3	49	18	11
	m	1.818	1.794	1.610
	$m/2$	0.909	0.897	0.805
4	K_1	18.2	92	164
	K_2	865	1,850	2,100
	K_3	44	18.7	13
	m	1.818	1.794	1.674
	$m/2$	0.909	0.897	0.837
8	K_1	11	54	.....
	K_2	468	1,000	.....
	K_3	40	17.3	.....
	m	1.818	1.794	.....
	$m/2$	0.909	0.897	.....

for 2.34 lb of agent, which is the amount given off by the E29R1 bomb.

The distribution of dosage across the width of the cloud is given by

$$D = D_C e^{-a^2(y/Y)^2}, \qquad (34)$$

where Y is the half width of the cloud. This is presented graphically as curve A in Figure 17. For convenience in the later mathematical treatment, this is replaced by the straight line marked B, whence

$$D = D_C \frac{1.17 \times \text{Half width} - y}{1.17 \times \text{Half width}}, \qquad (35)$$

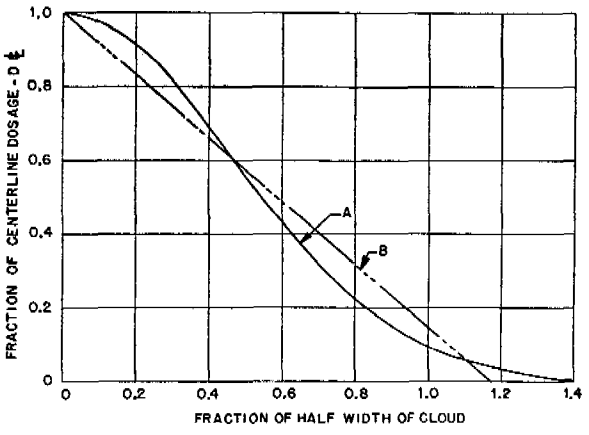


FIGURE 17. Variation of dosage across cloud.

or

$$D = \frac{K_1}{(x/100)^m} \cdot \frac{1.17K_3(x/100)^{m/2} - y}{1.17K_3(x/100)^{m/2}} \cdot \quad (36)$$

The values of y and x for D equal a constant (i.e., an isoline) and are given by

$$y = 1.17K_3\left[\left(\frac{x}{100}\right)^{m/2} - \frac{D}{K_1}\left(\frac{x}{100}\right)^{3m/2}\right], \quad (37)$$

and the area enclosed by the isoline of dosage equal to D is

$$A_D = 2\int y\,dx, \quad (38)$$

or

$$A_D = 2.34\int_0^{(K_1/D)^{1/m}}\left[K_3\left(\frac{x}{100}\right)^{m/2} - \frac{K_3}{K_1}D\left(\frac{x}{100}\right)^{3m/2}\right]d\left(\frac{x}{100}\right), \quad (39)$$

or

$$A_D = 2.34K_3K_1^{(m+2)/2m} \cdot \left[\frac{2}{m+2} - \frac{2}{3m+2}\right]D^{-(m+2)/2m}, \quad (40)$$

where A_D = area in hundreds of square yards. This can be written as

$$A_D = K_4(D)^{-K_5}. \quad (41)$$

For the meteorological combinations given in Table 2, the values of K_4 and K_5 are given in Table 5. This equation predicts the area enclosed by any isoline and the numerical value of the dosage on that isoline. This type of equation has been quite useful in correlating data from field experiments on mustard gas bombs.

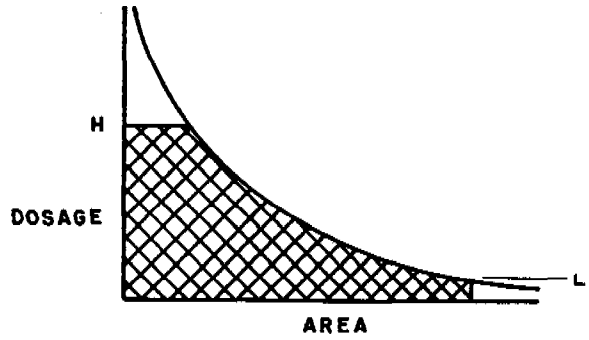


FIGURE 18. Area-dosage relation for a gas munition.

TABLE 5. Summary of coefficients for the area-dosage equation (41) for a point source of 2.34 lb of agent.

Wind speed (mph)	Constant	Clear day	Neutral conditions	Clear night
2	K_4	1,110	2,530	7,940
	K_5	1.0501	1.0574	1.1211
4	K_4	554	1,320	2,130
	K_5	1.0501	1.0574	1.0974
8	K_4	297	690	.....
	K_5	1.0501	1.0574	.....

Let a quantity be defined that measures the effectiveness of a munition in producing a dosage H. This is the quantity used by the Project Coordination Staff in computing munition expenditures. Graphically it is defined as the cross-hatched area in Figure 18. Mathematically it is given as

$$E_H = HK_4H^{-K_5} + \int_{A_D=H}^{A_D=L} D\,dA, \quad (42)$$

or

$$E_H = K_4H^{1-K_5} + \int_L^H DK_4K_5D^{1-K_5}dD, \quad (43)$$

or

$$E_H = K_4H^{1-K_5} - \frac{K_4K_5}{K_5-1}\left[H^{1-K_5} - L^{1-K_5}\right]. \quad (44)$$

In evaluating E_H, L is chosen to be taken either as 50 or as the centerline dosage 100 yd downwind from the source, whichever gives the larger value of E_H. This is, of course, somewhat arbitrary, but it conforms to some extent with the procedure used by the Project Coordination Staff.

If N bombs are dropped in a target area T, the fraction of the area covered with a dosage equal to, or greater than, H is given by

$$f = 1 - \left[1 - \frac{E_H}{H \times T}\right]^N. \quad (45)$$

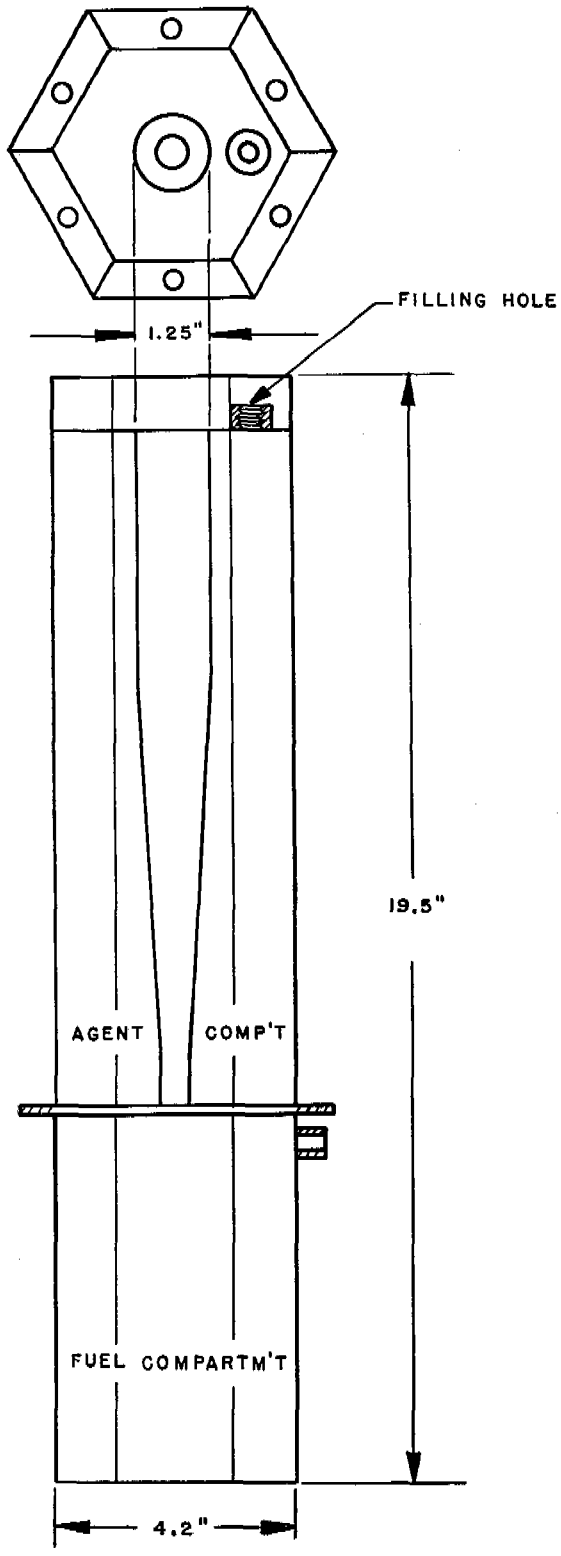


FIGURE 19. Preliminary model K–1 of thermal generator bomb.

For the units used here, and for an impact density of 64 E29R1 bombs per artillery square, which represents approximately the maximum concentration of bombs that may be expected from aimable clusters, this becomes

$$f = 1 - \left[1 - \frac{E_{II}}{100H}\right]^{64}. \qquad (46)$$

Using equations (46) and (44) and the values of Table 5, the expected results from a density of 64 bombs per artillery square were computed. These are given in Table 1.

30.9 A LARGER THERMAL GENERATOR CLUSTER BOMB

Experimental work was also started on a larger thermal generator bomb of the type described above. This was designated the K model. It was 19½ in. long with a hexagonal cross section 3.64 in. across the flat sides. A sketch of the experimental model is shown in Figure 19. It contained 1,500 g of fuel and had an agent capacity of 2,000 ml. Several successful static runs indicated that a thermal generator of this size and shape would function satisfactorily. The work was stopped to concentrate all effort on the smaller E29 size. This latter was a size and shape which would fit into existing cluster adaptors. The K model was not a suitable size to fit existing cluster adaptors, and development of this size cluster bomb would have required a new cluster adaptor. A better choice for a larger bomb would be a cylindrical bomb about 4.6 in. in diameter and 19⅜ in. long. This size could probably be clustered in existing 500-lb cluster adaptors with 14 bombs per cluster.

30.10 A 50-LB NONCLUSTERING THERMAL GENERATOR BOMB

A 50-lb nonclustering thermal generator colored-smoke bomb for use in target identification has been developed for the Navy [28] and designated Mark 72 Model 2. The bomb functions best in a horizontal position but is not critical as to functioning position. It is intended for use from low altitudes and employs a parachute to reduce its impact velocity. Tests have been made with mustard gas in this bomb, and promising results were obtained.[48, 50] This bomb might prove especially useful for setting up high concentrations on local strong points, pill boxes, caves, etc. The bomb is described later in this chapter.

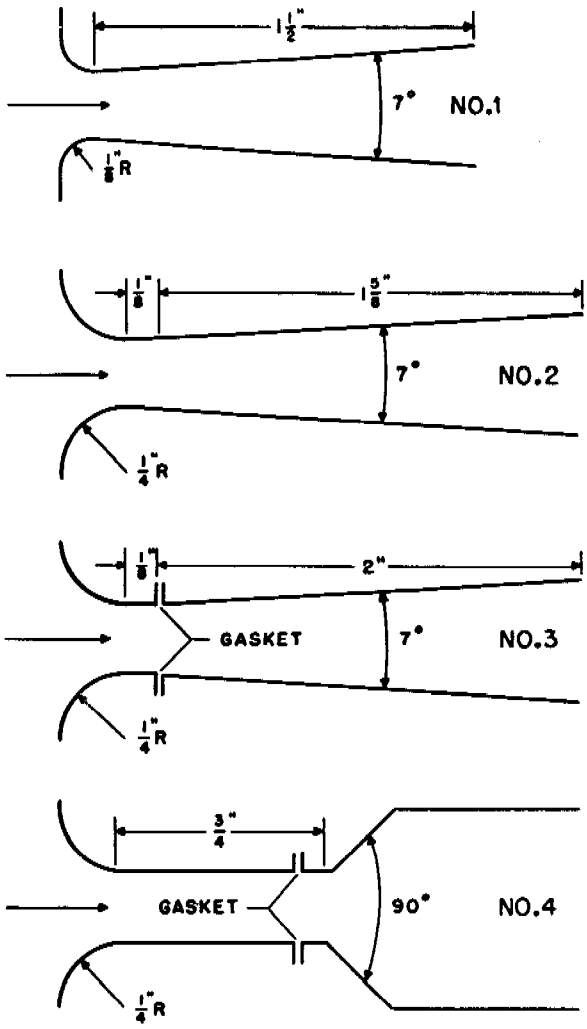


FIGURE 20. Dimensions of Venturi sections. All Venturi throats are ¼ inch in diameter length of parallel section as indicated:
No. 1 — Rolled from sheet metal and welded
No. 2 — Highly finished machined Venturi
No. 3 — Roughly finished machined Venturi
No. 4 — Machined and highly finished.

30.10.1 Development of the E29R1 Bomb

The salient problems encountered in the development of the E29R1 bomb and the solutions to these problems will be discussed briefly. For further details[14] as to the actual tests the original report should be consulted.

Feeding the Agent to the Hot Gas Stream

The development of the bomb was carried out concurrently with that of the pots (F-7 and F-7A) which incorporated a completely closed agent compartment. The problem of feeding the liquid agent into the high-velocity hot gas at the proper rate was therefore encountered. It was proposed to use the pressure from the fuel gases to feed the liquid by drilling a small hole in the agent compartment bottom and sealing this hole with a low-melting alloy. This design was unsatisfactory because variations in the fuel-block pressure, caused by irregularities in the burning rate, allowed the liquid to flow into the fuel compartment and quench the fuel. This difficulty was eliminated by placing the vent hole near the top of the vapor mixing tube. The pressure difference between the Venturi exit and the Venturi throat was then used to feed the liquid into the throat. The use of a tube connecting the fuel compartment with the void space above the agent, or a check valve to keep the agent from leaking into the fuel, were discarded because they would complicate the construction.

The High-Velocity Vaporizer

The results from a few early models made it evident that the design of the vaporizer would have a pronounced effect on the feeding of the agent. Tests were therefore made to study the effects of variation in this design. Two modifications of the Venturi, intended to simplify large-scale manufacture, were tried: (1) The 7° diverging section was replaced by a welded sheet metal 90° diverging section, and (2) the Venturi was machined in a separate piece which screwed into a Venturi sleeve. The first design of the separate Venturi contained a 90° divergent section. The 7° divergent section was omitted because it was thought difficult to manufacture. The Venturi was designed as a separate part because it would be difficult to obtain access to the main feed hole for the soldering operation in production, if the Venturi was an integral part of the bottom of the agent compartment. The designs containing the 90° divergent section were unsatisfactory because the pressure differential between the vapor discharge tube and the throat was not sufficient to feed the liquid agent. Several tests were then made with air (but no liquid) flowing through various nozzles in which the pressure at the throat and the pressure in the vapor-mixing tube were measured. Figure 20 shows sketches of the nozzles which were tested. Figure 21 shows the pressure available for feeding liquid as a function of the air velocity for each nozzle. This pressure was negative at any air rate when a 90° divergent section was used. When a 7° divergent Venturi section was used, the pressure available for feeding liquid increased to

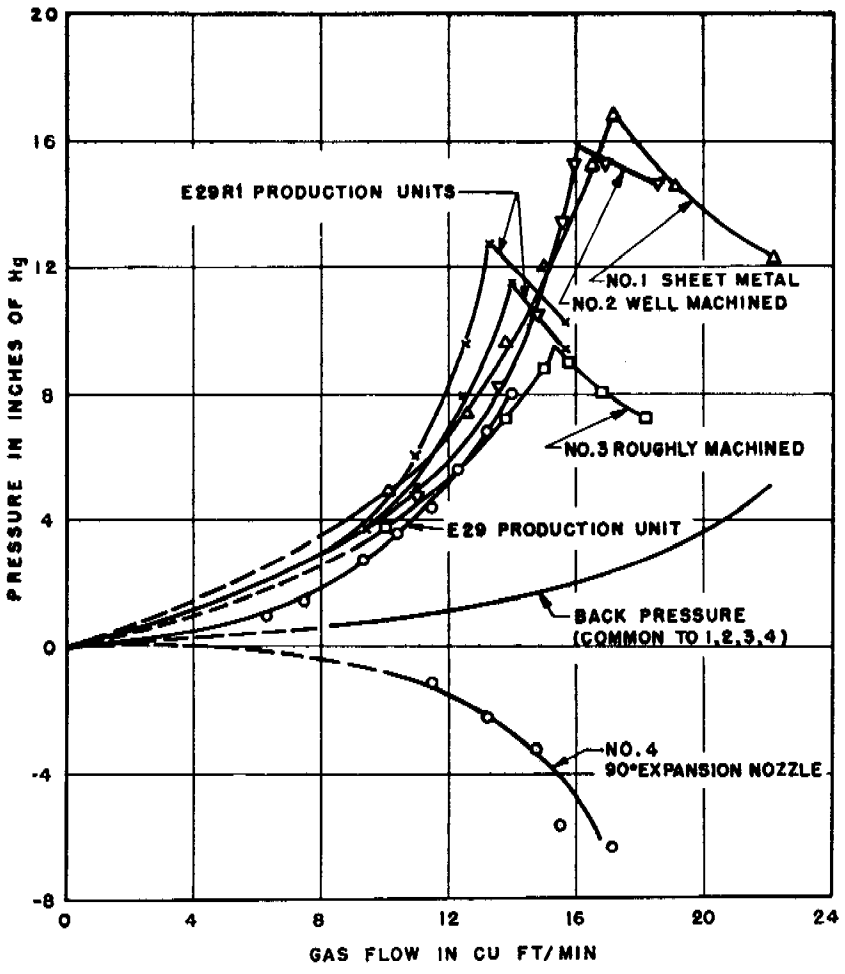


FIGURE 21. The static pressure available to feed liquid. No liquid was fed (vent pressure — throat pressure).

a maximum and then decreased with increasing air rate and became negative at high air rates. The Venturi used in the E29 was the same as No. 2 (Figure 20), and was a separate piece. Additional qualitative tests indicated that the cylindrical section at the throat should be no longer than the throat diameter, and that the cylindrical throat and conical divergent section should be coaxial. A well-rounded inlet was used to minimize the fuel compartment pressure.

Figure 22 shows the effect of gas rate (or fuel burning rate) on the pressure available for feeding liquid as measured with no liquid flowing. Pressure taps were mounted on the bomb before assembling it with a fuel block in the regular way. With a fast-burning fuel block in the bomb, the pressure available for feeding the liquid increases to a maximum, then falls off and becomes negative for an instant as the fuel burns progressively faster. With a slower-burning block this pressure is positive throughout the run. The pressure reversal with fast blocks was responsible for failure of the liquid to feed during part of the run in some cases. The pressure available for feeding liquid is less than shown in the figures when liquid is actually being fed.

Measurements of the feeding pressure in the bomb Venturi were made when water was being fed and comparable measurements were made with oil on a Venturi installed in an airplane smoke generator. Tests were also made with air flowing through the Venturi and water being forced through the feed hole with a pump. The fuel compartment pressure and agent compartment pressure were measured. The throat pressure was calculated for the same air rate by subtracting the pressure difference from the fuel compartment to the throat when no liquid was flow-

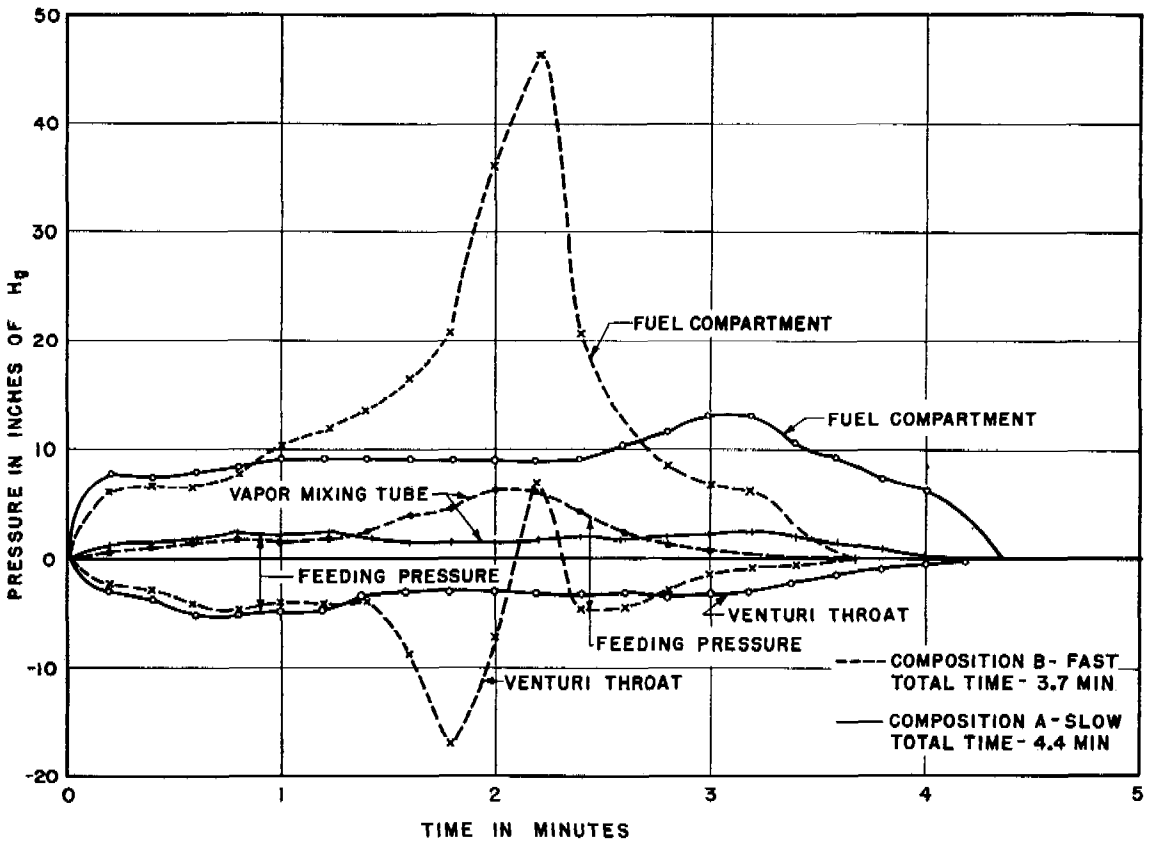


FIGURE 22. Pressures in fuel compartment, Venturi throat, and vapor mixing tube of E29 bomb during burning of fast and slow fuel compositions. No liquids fed.

ing from the measured fuel compartment pressure when liquid was being fed. By direct measurement in another apparatus it was found that within the range of flow rates used, this pressure difference is independent of the liquid feed rate. In Figures 23 and 24 the rate of liquid feed at a given pressure drop across the feed orifice can be compared at several gas flow rates. The pressure required to feed the liquid (measured pressure drop across the feed hole) and the pressure available in the bomb for feeding liquid (gas discharge pressure minus throat pressure) are given as functions of the liquid feed rate for three different air rates. The intersection of each of these pairs of lines gives the expected liquid feed rate in the bomb corresponding to a given air rate. For the narrow range of expected liquid feed rates covered by the data, these rates appear to be relatively constant and independent of the gas flow rate. This conclusion is not definitely established but both Figures 23 and 24 indicate this.

This conclusion must necessarily break down at the pressure reversal and probably at lower gas flow rates.

Figure 25 shows the relation between the liquid feed rate and the pressure upstream from the Venturi.

30.10.2 The E29 Design

The first design produced in any quantity by production methods was given the CWS designation E29. About 500 bomb bodies of this design were manufactured. These were hexagonal with a cylindrical tail cup. Tests in which this bomb was fired from a mortar against concrete indicated that the fuel would withstand such impact without breaking.

Booster Tube Powder

A problem was encountered in carrying the flash from the primer in the fuze down to the Quickmatch in the vapor mixing tube. A small booster tube was used below the primer. Several types of powder were tried in this booster tube. To avoid blowing back

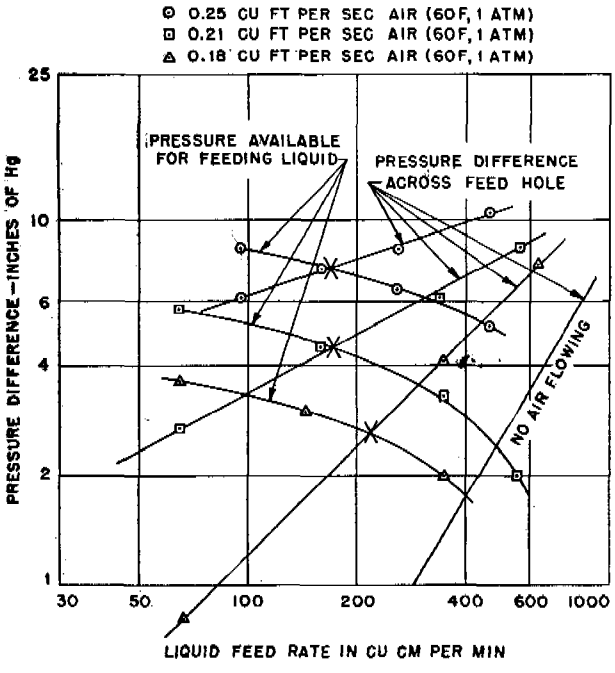


FIGURE 23. Effect of air flow rate on rate of feeding water in an E29 Venturi, with 0.073-inch feed hole.

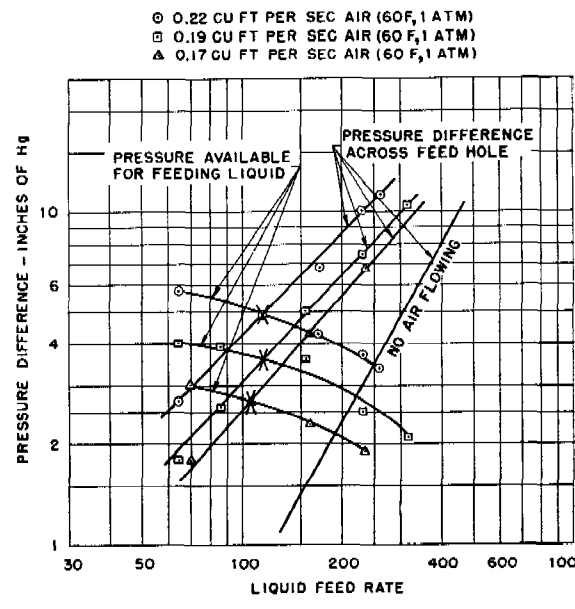


FIGURE 24. Effect of air flow on rate of feeding water in E29 Venturi with 0.046-inch feed hole.

through the primer, it was necessary that this powder should not pack tightly in the tube. A grained powder containing potassium perchlorate and grained aluminum gave the best results.

THE CLOTH STREAMER TAIL

The E29 bomb was fitted with a cloth streamer tail attached to a ring in the tail cup. A number of drop tests were made with this bomb. These indicated that the bomb was not sufficiently stable in flight. Many of the bombs landed flat. The center of gravity of the thermal generator bomb is farther back from the nose than in the M–69 incendiary bomb. Therefore it requires a different tail design.

These first production bombs functioned well enough to give promise that a satisfactory thermal generator bomb could be developed. Several faults were evident and a new design was made to eliminate these.

30.10.3 The E29R1 Bomb

Clustering Bands. When the hexagonal shape of the E29 bomb was changed to the cylindrical E29R1 it was not certain that the latter could be held firmly in the cluster adaptors without shifting. Hexagonal bands were therefore provided at each end of the bomb as an aid in clustering. The outside diameter of the bomb was made slightly smaller to allow room for these bands in the clusters. After several clusters had been assembled it was clear that the round bombs were no more difficult to cluster than hexagonal ones and that the bands were not needed.[29]

Agent Feed System. With the separate Venturi design there is the problem of holding the agent in the agent compartment without leakage during storage and handling and at the same time providing for its easy flow during functioning. Several designs involving gaskets and fusible seals were tested.[25] An excess of fusible metal in the feed channels must be avoided since this is often slow in melting and can solidify and block the channels when the cold agent flows over it. Intermittent feeding in a number of cases was traced to this cause. The latest design used in the bomb is satisfactory but could be simplified.

Slag from the starter layer of the fuel block was frequently blown up into the Venturi and lodged in the feed hole. A baffle was provided to avoid this. This baffle is a disk of sheet iron, $\frac{1}{8}$ in. below the entrance to the Venturi, held in place by three radial arms. Three stops are also provided above the baffle to prevent it from closing the entrance to the Venturi. The baffles first used did not have these stops and a number of bombs burst when the fuel block gases could not escape.

Coating the Agent Compartment. A protective coat-

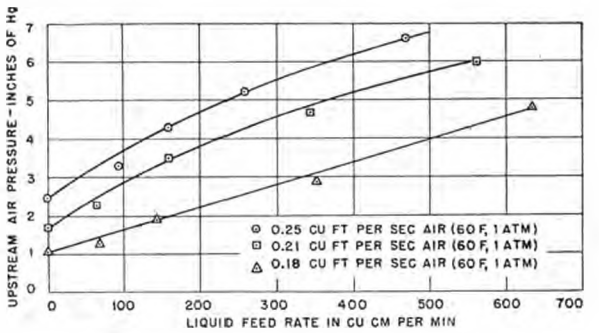


FIGURE 25. Effect of feeding water on upstream air pressure, in E29 Venturi at constant mass rate of flow of air. 0.073-inch liquid feed hole.

ing was applied to the inside of the agent compartment. In using thin-walled containers such as the agent compartment of the E29R1 bomb for storing mustard, it is important to keep the pressure developed by the corrosive action of the mustard on the iron at a minimum. In the E29R1 bomb, it is also important to eliminate any formation of sludge which would clog the feed holes. A protective phenolic coating (specification CWS 196-131-207) has been used in other munitions for this purpose. Preliminary trials in which several E29 bombs were coated, indicated that the vapor-mixing tube which passes through the center of the agent compartment complicated the coating process. A special technique was required to insure complete coverage with the coating. When the bomb was heated in the oven to bake the coating, the bomb case would heat first and the solvent would evaporate and condense on the vapor-mixing tube which was cooler. This condensed solvent would then flow down the tube and wash off the phenolic resin. This problem was solved by controlling the amount of solvent used, the amount of resin solution applied, and the method of heating.

Development of an Improved Tail

Folding Metal Tail. The development of a metal tail for the E29R1 bomb was undertaken. Wind-tunnel tests showed that it was not possible to stabilize the bomb with simple cloth streamers of a practical length when the center of gravity was back farther than about 8.5 in. from the nose. It was recommended that a folding tail similar to the AN-M52 tail be used. Preliminary results indicated that a proper design of such a tail would include six fins, so proportioned that the tail surface contained an area approximately equal to the nose area, set on bars at an angle of 45° with the bomb axis, and extending 5 in. out from the bomb (measured normal to the bomb). With this tail, stability was attained in the wind tunnel when the center of gravity was as far as 9⅞ in. from the nose. It was pointed out that to have a stabilizing effect, the fins should be far enough out from the bomb so as not to be in the turbulent wake from the nose. They should be out in the *virgin air* or region of undisturbed air.

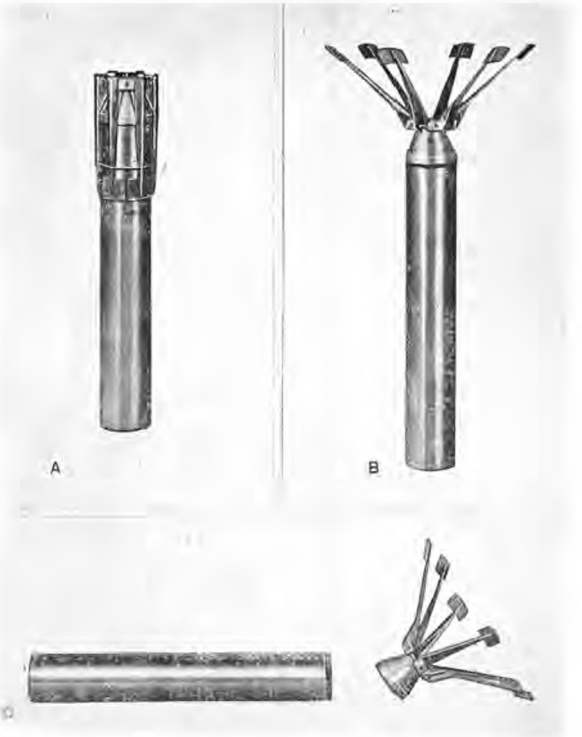


FIGURE 26. Thermal generator bomb with folding vane tail. (A) Vanes folded for clustering. (B) Vanes in flight position. (C) Tail removed for loading bomb.

Several tails were constructed according to these recommendations. Pictures of this tail in the open and closed positions are shown in Figure 26. In the closed position, the tail lies within a hexagon, the size of the M-69 cross section. The length, width, and number of fins, and the angle between the bars and the bomb axis were varied. However, none of the tails tested gave the bomb stability when actually dropped from an airplane. An unexplained difference existed between the conditions in the wind tunnel and those in the atmosphere. The bombs yawed and landed flat when dropped.

Streamer Tail with Shroud Lines. The improvement of the cloth streamer tail was undertaken. The mass center of the E29R1 is only slightly less than



FIGURE 27. Types of metal tails used in drop tests. (A) Four-vane sheet metal tail (vanes fixed). 3½-inch tail extension. (B) Three-vane sheet metal tail (vanes fixed). 7½-inch tail extension. (C) Three-vane sheet metal tail (vanes fixed). 5½-inch tail extension. (D) Complete telescoping metal tail, three-vane. 5½-inch tail extension with no baffle between vanes. (E) Complete telescoping metal tail fixed at acute ejection angle with baffle between vanes. 5½-inch tail extension. (F) Complete telescoping metal tail, three-vane. 5½-inch tail extension with baffle between vanes. (G) Complete telescoping metal tail, three-vane. 3.6-inch tail extension with baffle between vanes.

8.5 in. from the nose, and the wind-tunnel tests indicated that this bomb might possibly be stabilized with cloth streamers. Preliminary tests showed that the stabilizing effect of the streamers could be increased by mounting them on a ring which was attached to the bomb body by several nylon cords or shroud lines. In flight, the ring trailed behind the bomb about 8 in. and allowed the air to pass through inside the streamers. This increased the drag surface of the tail and made possible the use of shorter streamers than would be possible if the streamers were attached directly to the bomb body. Since the available space into which the tails could be folded was limited, this is an important factor.

Metal Telescoping Tail. The first work on this type of tail was done with 24-gauge sheet metal tails as shown in Figures 27A, B, and C. Work on the four-vane unit shown in Figure 27A was soon discontinued because of poor ballistics caused by the relatively small vane diameter. The use of three vanes allows the vane surfaces to extend further radially from the bomb body than the four-vane unit. In the three-vane unit, the vanes extend radially 1.43 in. from the bomb body; the four-vane unit has an 0.98-in. radial extension. This extension is very important in obtaining good ballistics with this type of tail.

The distance that the vanes should be extended longitudinally from the end of the bomb body was also important in the functioning of these tails. The first drop tests were made using the tail shown in Figure 27B. This unit had an extension length of 7½ in. It gave good ballistics, but was objectionable because of its length, and tests were made with the shorter units shown in Figure 27C. The tail shown in Figure 27C has an extension length of 5.6 in. It also gave good ballistics. After impact with one of these tails on medium soft ground, the bomb penetrated 20 in. The impact angle was approximately 86°. These tests established the vane profile and extension length necessary for good ballistics.

A complete telescoping tail, as shown in Figure 27D, was then made. Its total weight was 13 oz. Drop tests with this unit, however, proved that it had very poor ballistics. Further work indicated that baffles between the vanes, as shown in Figure 27F, were necessary. Fifty of these units were made using this baffle and a tapered type of joint between the telescoping sections. Tests using this tail at an acute ejection angle, shown in Figure 27E, were made. At this ejection angle the ballistics were still good.

Forty-three of these metal tails were dropped at Edgewood Arsenal from a B-25 airplane in quick-opening and aimable clusters.[16] The results showed that 37 of the 43 tails failed at the tapered telescoping joint. Those which did not fail at these sections gave very good ballistics.

A new design was then developed which used a square shoulder in place of the tapered joint. This design gave a much stronger joint and provided a positive means of preventing the telescoping parts of the unit from canting when these parts were ejected by the ejector spring.

Further tests were made using a tail unit having one telescoping cup in place of two, as shown in Figure 27G. The vane assembly was modified to provide a ¼-in. longer radial vane extension from the body of the bomb. This unit consistently gave good ballistics when dropped singly from a slow plane. It was not tested in clusters from fast planes. This metal tail ready for assembly onto the bomb is shown in Figure 28.

The production cost of this unit was materially reduced by eliminating the second telescoping cup. The costs of this metal tail and the streamer tails are very nearly the same.

Considerable data on the rotative speed of the one-cup unit was obtained by the use of a centrifugally operated recording instrument.[27] This instrument uses a small, weighted, spring-loaded, recording stylus. The centrifugal force caused by the rotation



FIGURE 28. Complete metal telescoping tail ready for assembly onto bomb body.

of the bomb causes the stylus to move outward from the center of the instrument against the spring tension. The sensitivity of the instrument was changed by using different sizes of retaining springs. During flight the stylus records its path on waxed record paper. On impact, a small hole is punched into the record paper as a record of the impact rotational velocity. The average rpm recorded by this instrument for the one-cup tail was 3,500.

Work was done to record the impact velocity of the bomb with the metal tail. The velocity recording instrument [27] used the ram effect of the air to move a piston and record the air velocity. Measurements with this instrument have recorded an impact velocity of approximately 270 fps. However, these records were obtained from altitudes of 2,000 ft and do not represent the terminal velocity of the bomb. The terminal velocity of the bomb with this tail is 350 to 375 fps.

Sealing the Fuel and Ignition System. The fuel block used in the bomb and some of the powder in the ignition system are adversely affected by high humidity. Therefore, it is necessary to seal the interior of the bomb from the atmosphere. Several methods were tested.

1. The use of waterproof paper over the exit holes was satisfactory for only short periods of time under relatively dry conditions but would not withstand tropical or cyclical temperature conditions.

2. The whole bomb including the tail was hermetically sealed with a thin (0.006 in.) brass diaphragm under the tail cover plate. Two methods of tearing open this diaphragm after the bomb broke away from the cluster were tried. In one, a cutter ring was used, and in the other, a tear wire was attached to the cover plate. Both were promising but not quite satisfactory because of difficulties with the tear features.

3. The fuel and ignition system was sealed by arranging the fuze as a solid plug in the end of the vapor-mixing tube with a Morse taper fit. The fuze was to be blown out by pressure from the fuel block after ignition. The design was objectionable because it was difficult to reproduce the pressure at which the fuze blew out. Some bombs blew up when the fuze failed to be expelled.

TABLE 6. Static tests on E29R1 bombs, Brooksville Army Field, December 5, 1945; an average of 2.23 lb of distilled mustard was charged in each bomb.

No.	Burning time (min)	End of agent emission (min)	Amount of agent left (oz)	Remarks
1	4.0	3.0	nil	
2				Dud
3				Dud
4				Dud
5	4.9	2.5	nil	
6	4.6	4.3	6	Fair cloud
7	4.9	4.9	10	Fair cloud
8				Dud
9	4.8	4.3	nil	Very good cloud
10				Dud
11	4.8	4.8	nil	
12	4.7	3.1	nil	
13	5.5	5.3	13	Erratic feeding, 3.9 to 5.3 min
14	4.75	4.75	nil	Did not feed, 4.0 to 4.3 min
15	5.2	3.3	10	Probably plugged part of the time
16	5.0	5.0	19	Erratic feeding 3.9 to 5.3 min
17	5.0	5.0	18	Poor cloud, 1.7 to 3.0 min
18	5.1	5.0	nil	Poor after 3.3 min
19	5.1	4.9	4	Fair cloud
20				Dud
21	4.75	2.5	nil	
22	4.8	4.9	nil	
23	4.8	4.9	17	Poor at first
24	5.1	3.6	nil	Very good cloud
25	5.1	3.7	nil	
26	4.7	4.7	nil	
27	5.2	3.7	11	Probably plugged
28				Dud
29	4.5	3.3	nil	Very good cloud
30	5.2	5.1	11	Erratic 1.4 to 2.5 min

4. The method finally adopted in the E29R1 bomb consists of a fusible diaphragm between the fuze base and the agent compartment top. This is made of a low melting alloy (50% bismuth, 31% lead, 19% tin) 0.015 in. thick, with a reinforcing ring around the periphery. It is ruptured by the flash from the fuze and does not impair ignition.

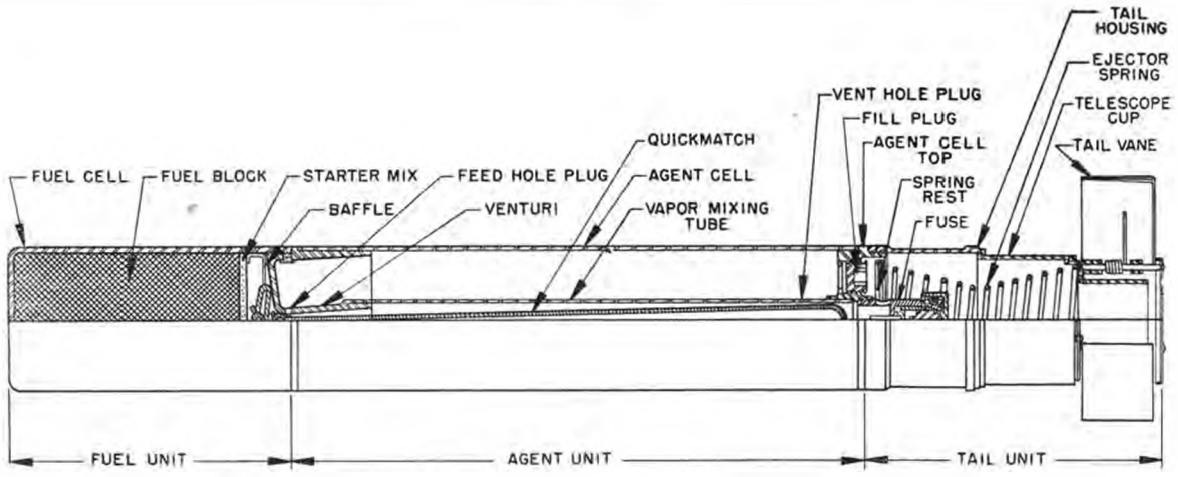


FIGURE 29. Proposed modification of E29R1 bomb.

30.10.4 Field Test of E29R1 Bomb

Tests were made in December 1945 at Brooksville, Florida,[14] on 30 bombs chosen at random from the production lot and charged with distilled mustard. These are listed in Table 6. A number of duds were caused by failure of the Quickmatch in the ignition system to burn completely. Twenty-three bombs functioned and were generally satisfactory. On the average these bombs discharged 85% of the agent charged to them. A few of these bombs apparently plugged either partially or completely during part of their functioning period. As a result of these tests, plans for field-sampling tests on statically fired bombs, and on large-scale drop tests have been made by the CWS.

30.10.5 Recommendations for Improving the E29R1 Bomb

During the manufacture and testing of the E29R1 bomb it became apparent that a number of improvements could be made.

1. The presence of the impact diaphragm in the nose structure is undesirable since on impact it flattens out and tends to push the case away from the nose cup at the silver-soldered joint.

2. The operation of silver-soldering the nose cup after the fuel block is in place has been carried out successfully, but it would be preferable to eliminate it if possible because of the hazard involved.

3. The separate Venturi section is complicated and offers opportunity for leaks at the two gaskets. The Venturi should be made an integral part of the agent compartment bottom and a satisfactory method of sealing the feed hole devised.

4. The outside diameter of the bomb should be increased to $2^{13}/_{16}$ in. This will increase the filling capacity and will make the bomb almost the same diameter as the distance across the flat sides of the M-69 bomb.

5. The cloth streamer tails are undesirable for the following reasons:

   a. They tend to cause flaming of the vapors.
   b. They cause the bomb to have too low an impact velocity to insure good functioning of an impact fuze when the latter conforms with military safety requirements on sensitivity.
   c. The hand work required in the assembly operations is complicated, and this increases the cost of the tail to a figure comparable with the cost of a metal tail.
   d. The tail is subject to tangling when released from the cluster. Twisting of the shroud lines makes the bomb unstable in flight. Improper packing of the streamers may result in failure of the tail to open.

30.10.6 Proposed Improved Design of Thermal Generator Bomb

A new design for a thermal generator bomb of the same size as the E29R1 has been partially prepared. An assembly drawing is shown in Figure 29. A bomb of this design has not yet been built. The entire impact nose structure of the E29R1 has been eliminated. The fuel block container serves as both the outer

case and the nose. It has a wall thickness approximately equal to the combined thickness of the fuel container and bomb case of the E29R1 bomb. The large number of impact tests made on the E29 and E29R1 bombs indicated that the fuel block can withstand impact without the protection of a special nose structure. By eliminating the void space in the nose, the capacity is increased and the mass center is nearer the nose.

The Venturi is to be forged as an integral part of the agent compartment bottom. The fuel compartment is threaded to screw onto the agent compartment. The feed hole is readily accessible for soldering before assembling the fuel block to the bomb. The rest of the agent compartment is essentially the same as in the E29R1. The bomb is equipped with the metal tail described earlier and the centrifugal arming fuze.

The proposed design includes three separate assemblies: the nose containing the fuel, the body containing the agent, and the tail. These assemblies fit together with screw threads and permit inspection and separate storage of the fuel, agent, fuze, and tail.

30.11 OIL SMOKE POTS

30.11.1 Floating Oil Smoke Pot, E-23

A thermal generator floating oil smoke pot utilizing the high velocity vaporizer principle was developed [31] to meet specifications set by the Naval Bureau of Ordnance.[30] These specifications were as follows:

1. It should be the thermal generator type.
2. It should produce a nontoxic smoke.
3. It should have a burning time of 10 to 15 min duration.
4. It should produce a volume of smoke comparable to the M4A2 pot.
5. It should be suitable for mass production from readily available materials.
6. It should not be subject to spontaneous ignition from the effects of moisture, water, or rough handling.
7. When burned at night, it should not be visible from aircraft flying at an altitude of 1,000 ft or higher.
8. It should have a mechanical type of igniter, such as either a bouchon or scratcher igniter, and it should also be equipped for electrical ignition.
9. It should occupy a space no greater than 13½ in. diameter by 13½ in. high.
10. It should be completely waterproof and moisture proof, and should function in a satisfactory manner from 0 F to 120 F after being subjected to the standard Chemical Warfare Service desert, tropical, and arctic surveillance tests for 90 days.
11. It should function satisfactorily after being subjected to a drop of 40 ft into water from a stationary position. It should also function satisfactorily after being subjected to a rough handling test simulating the handling normally encountered in shipping, storing and use.
12. *Satisfactory functioning* is considered to be at least 90% functioning with normal volume of smoke.
13. It is considered desirable to incorporate a feature in the floating smoke pot which will insure that it will sink within 45 min after the completion of burning so that ships dropping floating smoke pots at sea will not mark their course with them. This feature should be incorporated only if it will not interfere with or delay the fulfillment of the above requirements.

The pot was designated, *Pot, Smoke, Oil, Floating, E-23* by the Chemical Warfare Service. Apparently it will meet the specifications set by the Navy, except that no provision has been made for the empty pot to sink within 45 min after functioning. This was a casual requirement and the final model was considered to be satisfactory.

Principle of Operation

The principle of operation involves vaporizing a high-boiling petroleum oil in a high-velocity stream of hot gases. The vaporized oil-gas mixture leaving the unit is cooled by entrained air, and condensation of the oil vapor into small droplets forms a screening smoke.

The unit consists of (1) a fuel block in one compartment to produce hot gases, (2) the oil in a separate compartment, and (3) a high-velocity vaporizer tube in the form of a Venturi. Another tube connects the agent compartment and the fuel compartment, and permits pressure from the fuel compartment to force the oil through an orifice into the Venturi throat. Here the oil mixes with the hot gas stream flowing through the Venturi. The high gas velocity atomizes the incoming oil stream and the droplets are quickly vaporized.

The rate of feeding is governed by the pressure differential between the agent compartment and the throat, the size of the feed orifice, and, to a minor extent, by the resistance to flow through the feed

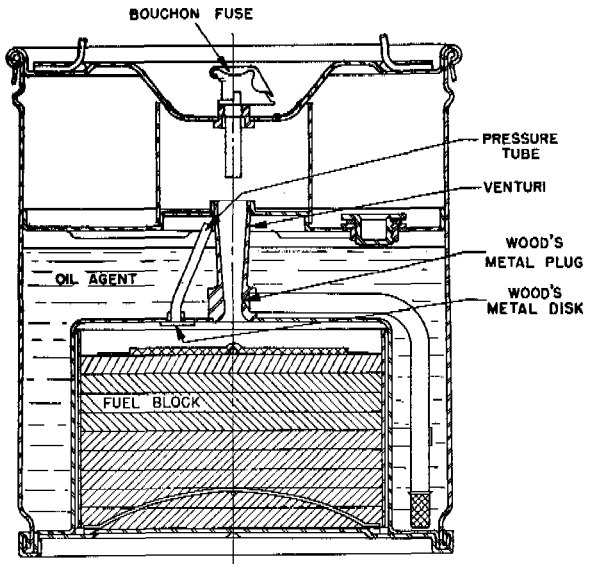


FIGURE 30. Pot, smoke, oil, floating, E–23.

tube. The ratio of agent to fuel is limited by the available heat in the fuel gases and the efficiency of the vaporization process.

DESCRIPTION OF THE FLOATING SMOKE POT

Figure 30 shows the design of the floating smoke pot. The completed unit weighs 36.5 ± 0.2 lb. This includes 14.5 lb of SGF No. 1 oil and 12.16 lb of fuel. A bouchon fuze, modified to give a delay of 12 to 22 sec, serves as the ignition system. The *spit* from the fuze ignites the Quickmatch on top of the fuel block; this in turn ignites the British starter. Hot gases from the fuel block immediately melt the fusible plugs, opening the feed orifice and the *pressure* tube. Oil is fed from the bottom of the annular space through a feed tube into the feed orifice at the throat of the Venturi, and the mixture of hot gases and oil vapor pass through the Venturi into the air chamber and then to the atmosphere through four ½-in. diameter exit ports in the cover. A 4-in. diameter "collar" in the air chamber prevents condensation from taking place at this point.

Fuel Block. The fuel block is composed of three layers. Table 7 shows the compositions and weights of each of these layers. A complete discussion of the fuel is given in Chapter 4.[31]

The ammonium nitrate and ammonium chloride are placed in an edge runner mixer and the oil is slowly added over a 4-min period during mixing. Charcoal is then added and mixed for 16 min. Transition mixtures are made by blending top and base compositions in the desired ratio for 3 to 4 min in the edge runner.

These mixtures are pressed under a dead load of 36 tons, or 1,380 psi in six increments. A wooden ram and a steel form are used during the pressing operation. The pressure is held on each increment for about 5 to 10 sec. Before pressing the final increment, 40 g of British starter is placed in a ring about 1½ in. in from the edge of the can. The British starter has the following composition:

Charcoal	6%
Linseed oil	2%
KNO_3	53%
Silicon	39%

The block is allowed to cure for one day, and then two coats of a special pyroxylin base lacquer are applied to the surface. Waterproof Navy Quickmatch is then fastened to the surface with tacks. The completed block is stored for at least three weeks in a dry room (relative humidity below 50%) at a temperature below 85 F. During the curing period, the linseed oil polymerizes causing the block to harden and its burning rate to increase. The block, after curing, has a burning time of 12 min ± 1.5 min when burned in the E 23 smoke pot.

The fuel block described above was used in the later models of the E–23 and served for the completion of the design. It was realized that it had certain faults such as, (1) a tendency for the burning time to vary somewhat, (2) occasional fast burning periods, (3) information needed for the specification of the charcoal was incomplete, and (4) the pressing procedure and the number of mixtures used could probably be simplified. Paper liners for the fuel block

TABLE 7. Composition of fuel block for E 23 (expressed in weight per cent).

Top				Base					
Wt g	NH_4NO_3	Charcoal	Linseed oil	Wt g	NH_4NO_3	Charcoal	Linseed oil	NH_4Cl	Transition
700	86	11	3	3,000	82	7	3	8	1,800 g of two parts top mix to one part base

cans were used by others. These prevented the fuel from burning down the side and consequently gave a more uniformly burning block.

Agent Compartment. The outside of the agent compartment is formed by the standard outer can of the M4A2 pot. A flanged air partition serves as a top for this compartment and a sheet metal shell, which encloses the fuel block and leaves an annular space for oil, is the agent compartment bottom. The agent specified is SGF No. 1, or fluid (oil), Fog No. 1 (Standard Stock No. 7-F-500). A 5% void space is allowed when filled with oil. The Venturi vaporizer passes vertically through the center of the agent compartment and contains a feed orifice 0.0890 in. in diameter (No. 43 drill) at the throat. The pressure tube is open to the fuel block at one end and extends above the oil level in the agent compartment.

A 16-mesh wire screen is placed over the entrance to the feed tube to prevent foreign matter from reaching the feed orifice. The filler plug is placed directly above the feed tube and the weight of these two parts is off center and causes the unit to tilt to that side. The feed tube is thus able to discharge all but a very small amount of the oil charged.

Buoyancy Chamber. The space between the top of the agent compartment and the can cover acts as a buoyancy chamber for the floating unit. A 4-in. diameter collar, placed around the exit of the Venturi and extending to the top of the chamber, prevents oil from condensing in this space.

Cover. The cover has a lug-type seal. The center of the cover is dished in to house the bouchon fuze. The four exit holes are ½ in. in diameter placed on a radius ⅝ in. from the center. These holes are covered by waterproof adhesive tape. A fuze adapter is welded in the center of the cover. An auxiliary cover with a ring-type seal is used to protect the bouchon fuze from moisture.

Ignition System. The ignition system was developed by the Technical Command, Chemical Warfare Service, and has been designated, *Fuze, Igniting, E-10.* Figure 31 is a drawing of this fuze. It has a delay of 12 to 22 sec and ignites the Quickmatch on the fuel block by "spitting" through the Venturi tube.

Assembly. The outer can and the agent compartment form a complete unit assembly into which the fuel block is placed. The bottom of the unit is then double-seamed to the outer can and the unit is filled with oil. After the cover has been crimped in place, the bouchon fuze is screwed into the fuze adapter. White lead paste in oil is used to lute the threads of

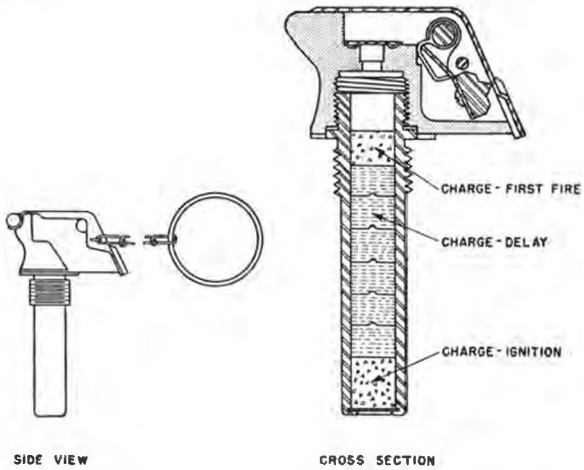


FIGURE 31. E-10 igniting fuze for E-23 floating oil smoke pot.

the fuze adapter. The addition of the secondary fuze cover completes the assembly.

Figure 32 shows a complete pot and one of the pots in operation.

DEVELOPMENT

The E-23 floating smoke pot was developed from the thermal generator nonfloating oil smoke pot known as the E-20 described later. Problems common to all design stages during the development will be discussed in this section. For a description of the various designs, the individual problems encountered and their solution, as well as data on typical runs, the original report should be consulted.[31]

Control of Oil Feed Rate. It was necessary to balance the heat and gas output of the fuel block against the feed rate of oil. A slow-burning fuel block usually produces gases at a low temperature and this reduces the amount of oil that can be vaporized. When this condition exists, the unvaporized oil is thrown out as spray and less oil is converted into smoke. If the feed orifice is too large, the oil feed rate is excessively high and the oil is exhausted early in the burning period. There is then insufficient heat for evaporation during this shorter discharge period and this also results in spraying. On the other hand, if the feed orifice is too small, the oil does not feed rapidly enough and the vapors issue at a high temperature. The resulting smoke is dry and oil may be left in the unit. The pot should use all its oil uniformly with a minimum of spraying.

Flaming. Flaming at the start of functioning was eliminated by applying the British starter in the

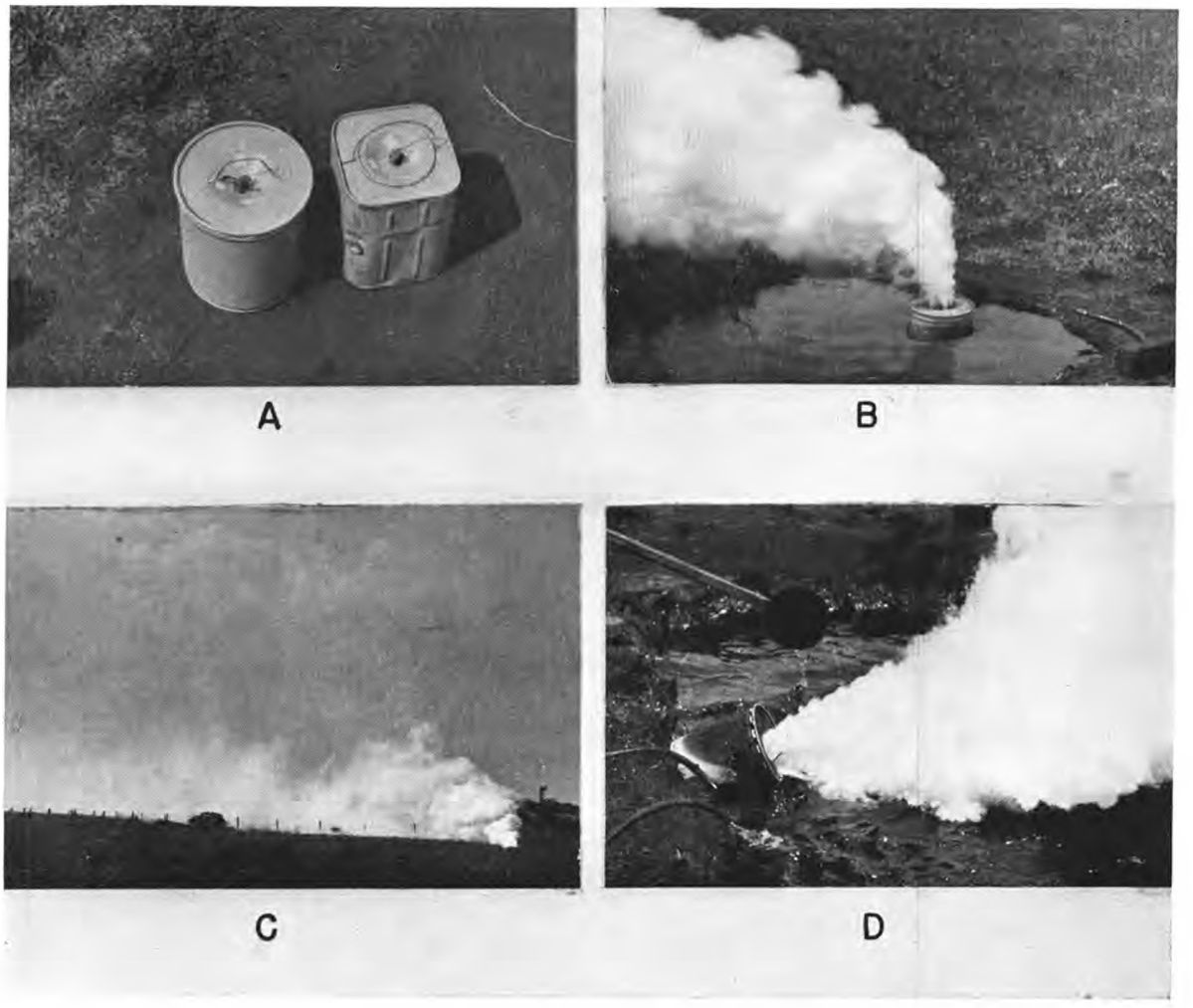


FIGURE 32. E-23 oil smoke pots in operation. (A) The round and square can completely assembled. (B) 15 seconds after emission. (C) Cloud 6.1 minutes after emission. (D) Cloud 10 minutes after emission. The square can shown in upper left-hand picture is an alternative shape of experimental pot.

shape of a ring. This removed the starter from directly below the Venturi throat and prevented the initial flash from igniting the oil.

Terminal Surge. During the last few minutes of the burning period, the unit floats nearly horizontally in the water, and there was a tendency for the fuel block to come loose from the bottom and give a surge of gas at this time. When this happened, pressure sufficient to blow open the bottom seam was sometimes developed. Reinforcing wires were placed across the bottom of the fuel can to hold the block in place and prevent this difficulty.

Functioning the Pot on Land. The floating smoke pot will function satisfactorily out of the water. A slightly shorter smoke emission time results.

Effect of Temperature of Pot on Functioning. Pots were stored overnight at 0, 70, and 150 F and functioned shortly after being removed from storage. The pots at 70 and 150 F functioned satisfactorily except that the pot at the higher initial temperature gave a shorter smoke emission time. The pot at 0 F did not feed oil properly. It is evident that the fuel block does not readily heat the oil in the bottom of the pot near the feed tube inlet. The oil used in these tests had a pour point about 0 F, and consequently would not flow at this temperature. For satisfactory operation at 0 F, an oil with a pour point below this temperature should be used.

Toxicity. Tests on the toxicity of SGF No. 1 oil were made.[32] Monkeys were exposed for 30 min of

SECRET

every hour for 100 consecutive days to a concentration of 63 mg per cu m of SGF No. 1 oil in the air. The conclusion was drawn that similar exposure of men would be without serious pulmonary effects.

Further tests on the toxicity of oil smoke were made in connection with the E–21 training smoke pot.[33]

Two chamber tests were made: in each, two goats, five rabbits, and five rats were exposed for one hour to the smoke and gases, and gas samples were taken from the chamber and analyzed. Two candles were burned.

Three candles were burned to provide increased concentration of smoke and gases.

In both cases, analysis showed no CO_2, CO, saturates, unsaturates, or acidic constituents (percentages to the first decimal place) in the chamber atmosphere; the rats and rabbits showed no ill effect at any time, the goats were only very slightly affected — slight lung rales the next day, clearing up quickly, and a slight tendency toward diarrhea the second day after the test.

Floating Stability. The initial problem with the floating pot was to design the pot to float and function in a satisfactory manner. In the earlier pots for use on land, the oil was carried in a compartment above the fuel compartment. Since the weight of the oil is greater than the weight of the fuel, this made the pot top-heavy and caused it to turn over in the water. Buoyancy may be provided by simply increasing the void volume in the oil compartment, but this allows the oil to run to the top of the pot when the latter is inverted in the water. The pot would then be stable in this inverted position and would not right itself. The pot was thus designed to confine the oil as near the bottom as possible and to provide a separate buoyancy chamber at the top. About half the oil is carried in an annular space around the fuel block and the other half directly above the fuel compartment.

The next step was to provide for feeding the oil from the bottom of the pot up to the high-velocity vaporizer above the fuel. This could be arranged by leading a feed tube from the bottom to the feed orifice. However, the pot tends to float on its side and this tube would not feed oil if it happened to be on the high side with its inlet end out of the oil. This was overcome by weighting the pot eccentrically so the pot would float with the feed tube on the low side.

Pressurized Feeding. With the arrangement just described the suction at the feed orifice was not enough to lift the oil and feed it uniformly. A pressurizing tube was provided connecting the fuel compartment with the upper part of the oil compartment.

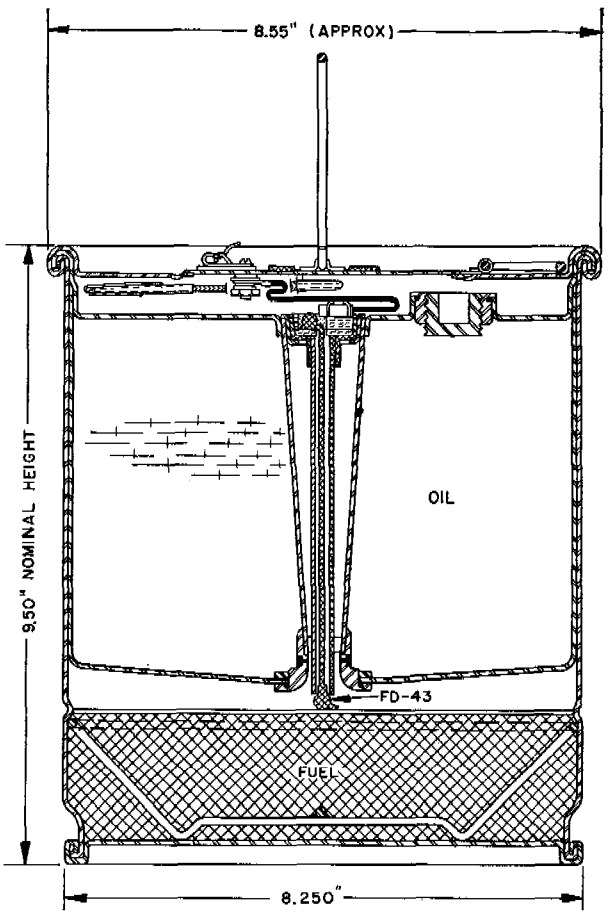


FIGURE 33. E–20 oil smoke pot (nonfloating).

This raised the pressure in the oil compartment and forced the oil up through the feed tube and feed orifice.

30.11.2 Nonfloating Oil Smoke Pot, E-20

The E- 20 thermal generator oil smoke pot for use on land or in boats is shown in Figure 33. The pot functioned on land for 6 min and weighs 21.5 lb. Ten pounds of fog oil in a separate agent compartment is used as the smoke-producing agent, while hot gases are supplied by a *cast fuel block* weighing 6 lb. The unit is ignited either electrically or manually.

Tests were made on the E–20 pot at the Amphibious Training Base, Little Creek, Virginia, in January 1945. The following conclusions[34] were reached.

1. That the volume of smoke produced from the E-20 smoke pot is slightly greater than one-half that produced by the Mk-3 smoke pots.

2. That the effective burning time of the E-20 smoke pot is slightly less than that of the Mk-3 smoke pot.

3. That the short period of glow from the E-20 smoke pots will not pin-point the moving smoke boat at night.

4. That when functioning properly the E-20 smoke pots are capable of producing a lengthy and an effective screen.

The principle of operation of the E–20 pot is similar to that of the E 23 smoke float. Oil is sucked from a vented agent compartment through two feed holes into the Venturi throat. The agent compartment is not pressurized from the fuel compartment and all the agent is contained in a compartment above the fuel.

30.11.3 Training Oil Smoke Pot, E-21

A thermal generator pot, of the size of an M–8 grenade, was developed.[35] This unit contains a small fuel block in a separate compartment and uses oil, such as "Diol 55," or SGF 1, as a smoke agent. The pot operates best in a vertical position. A single pot fills a 13,000-cu ft room with smoke that totally obscures objects 4 to 6 ft away. The present CWS designation is *Pot, Smoke, Oil, Training, E 21*. The specifications [36] for the development were:

1. The burning time should be from two to three minutes.

2. The rate of emission of smoke should be approximately equal to that of the HC training candle M-2.

3. The smoke produced should be non-corrosive to material and equipment, particularly delicate instruments aboard ship.

4. No serious harmful effects should be experienced by unmasked personnel when exposed for sixty minutes to the smoke from two candles in a compartment of 5,000 cu ft.

5. The size should be as small as possible consistent with the requirements of (1), (2), (3), and (4), but should not exceed 2 x 4 x 6 inches.

The E 21 pot meets these specifications with the exception of the burning time. This is less than the 2 to 3 min specified.

Principle of Operation

The principle of operation involves vaporizing a high-boiling petroleum oil by injecting it into a high-velocity stream of hot gases. The oil vapors thus formed are cooled rapidly when they mix with the air outside the unit and condense to small droplets. These condensed oil droplets form the screening smoke.

The unit consists of (1) a fuel block in one compartment to produce the hot gases, (2) the oil in another compartment, and (3) a high-velocity vaporizer tube. This latter is in the form of a Venturi and the low pressure at the throat is utilized to suck the oil into the hot gas stream. The high gas velocity atomizes the incoming oil stream and the small droplets are quickly vaporized.

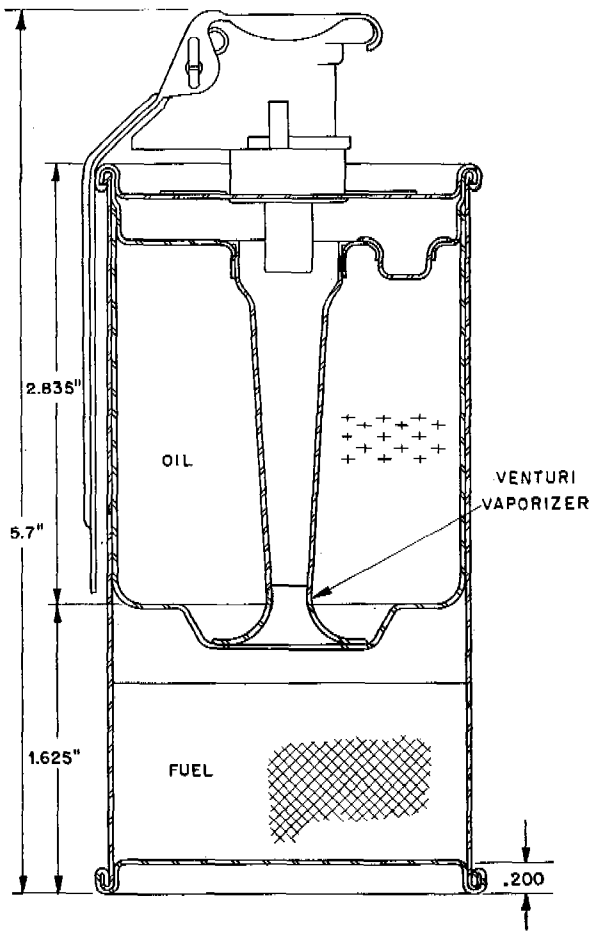


Figure 34. E–21 oil smoke pot (training).

The rate of feeding oil is governed by the pressure differential between the oil compartment and the throat, as well as by the size of the feed orifice. The ratio of oil to fuel is limited by the available heat in the gases and the efficiency of the vaporization process.

Description

Figure 34 shows an assembly drawing of the E 21 smoke pot and Figure 35, a photograph.

Oil and Oil Compartment. The oil compartment contains 107 g of SGF–1 oil or Navy Fog Oil No. 1. The Venturi tube, which serves as the high-velocity vaporizer, passes vertically through the center of the agent compartment and has a feed orifice 0.076 in. in diameter (drill size No. 48) drilled radially at the throat. Both the feed hole and the vent hole at the



FIGURE 35. E-21 oil smoke pot (training).

top of the Venturi tube are closed by fusible metal plugs. These plugs melt out immediately upon ignition of the fuel block and allow the unit to function. A 5% void space is left in the agent compartment.

Fuel Blocks. The fuel block used in the E-21 has the following composition: 82% ammonium nitrate, 11% charcoal, 4% potassium nitrate, and 3% boiled linseed oil. The dry ingredients, with the exception of the carbon, are weighed and placed in an edge runner. The linseed oil which serves as a binder is added slowly, and this is mixed for 4 min. Carbon is then added to the mixer and the mixing operation is continued for 16 min until the mixing time totals 20 min.

Each block consists of 95 g of the above mixture with 6 g of British starter placed on top. This is pressed into an M-8 grenade can held in a pressing form, under a load of 14,000 lb or a pressure of 3,500 psi. The pressed blocks are stored in a room having a relative humidity below 50%, to cure for at least 21 days before use. During the curing period, the linseed oil polymerizes causing the block to harden and also "speed up." The block, after aging, has a burning time of 1.2 ± 0.25 min.

British starter is a powdered mixture of 54% potassium nitrate, 40% silicon, and 6% carbon. Linseed oil is used as a binder for this mixture.

Ignition System. The ignition system consists of a "fuze, igniting grenade, M-201." This fuze "spits" through the Venturi and ignites the British starter on the surface of the fuel block.

Assembly. The agent compartment is a complete unit assembly. After it is filled with oil it is placed into the M-8 grenade can, which already contains the pressed fuel block. A modified M-8 grenade can cover is then rolled on with a double seam. This modified cover contains three $\frac{5}{16}$-in. diameter exit holes instead of the four used in the standard cover. The bouchon fuze is screwed into the fuze sleeve. The threads of the sleeve are luted with white lead paste in oil. Waterproof adhesive tape is used to close the three exit holes in the grenade cover.

Functioning. The pot functions best in an upright position. To ignite it, the arm of the bouchon fuze is held down, the safety ring is pulled out, the pot is set on a smooth surface, and the bouchon fuze arm is released.

Burning Time. The specifications call for a burning time of 2 to 3 min. This has not been met since the fuel block and vaporizer tube in a unit of this small size are better adapted to a shorter burning time. The disadvantages of a longer burning time are:

1. At the lower gas rate it requires a very small vaporizer tube and oil feed orifice. These would have a greater tendency for plugging and malfunctioning.

2. The slower burning fuel block generates less heat, and consequently less smoke, than the composition now used. When used indoors the effective screening time of the smoke is not significantly influenced by the emission time of the smoke pot.

When the pots are burned in a closed room there is an initial flash from the British starter and an instantaneous generation of smoke. The jet of smoke rises to the ceiling and gradually diffuses down. In the course of a few minutes the whole room is obscured. A photograph of a unit functioning indoors is shown in Figure 36.

Toxicity of the Smoke. The almost complete absence of toxic effects from the oil smoke is described in the preceding text in connection with the E-23 floating oil smoke pot.

Inflammability. Tests were made on the inflammability of oil smokes.[37]

These tests were carried out in a chamber 7 x 7 x 10 ft and also in the open. The smoke from the pots at various concentrations was subjected to a continuous 25 watt spark,

SECRET



FIGURE 36. The E-21 training oil smoke pot functioning indoors.

10,000 v, $\frac{3}{8}$ in. spark gap, to a lighted kerosene torch, to the flash from 15 grams of guncotton, to an electric squib, and to the flame of a gasoline blowtorch. A number of these tests were repeated several times under various conditions, and no evidence of ignition or flaming of the oil smoke was encountered.

Conclusions: It is concluded that oil smokes, made from Diol 55, of 0.35–0.45 micron radius, at all concentrations and in a confined space are safe from ignition in the presence of a spark, squib, lighted gasoline torch, and a flash of guncotton.

It is further concluded that the E-21, Pot, Smoke, Oil, Training (Navy) which produces an oil smoke of about 0.40 micron radius, at all concentrations and in a confined space is safe from ignition in the presence of a spark, squib, lighted gasoline torch and a flash of guncotton.

The jet of smoke as it issues from the pot may be ignited with a torch placed within 6 in. of the top of the pot. The jet can be ignited from 6 to 12 in. but usually extinguishes itself. Above 12 in. the jet has cooled sufficiently so that it will not ignite.[38] No case of spontaneous ignition of the smoke jet from the design previously described was found and the smoke cloud itself was never ignited, exploded, nor gave any indication of toxic effect on personnel working in the chamber.

30.11.4 Limited Persistence Smoke

Control of the persistency of oil smoke especially for use with amphibious landings is desirable. Specifications were set up for a bomb to be carried in 100-lb quick-opening clusters, and to function on land or water for a period of 6 to 10 min. The smoke was to dissipate completely at 100 yd at a temperature of 75 F and a wind velocity of 5 to 10 knots. The screen should persist at 50 yd at even higher temperatures. Oils of different volatilities were tested in the F-7A pots.[52] The results indicated that a volatility about that of burning oil should be satisfactory. The design of a bomb based on the thermal generator principle which would float upright and also function on land was not successfully devised. It is suggested that a modification of the Mark 72 Model 2 bomb described in the following text may hold promise.

Preliminary tests on an intimate mixture of a pyrotechnic fuel and diphenyl were promising. This agent has a melting point of 70 C and a volatility in the correct range.

30.12 SULFUR SMOKE GENERATORS

At least three continuous sulfur smoke generators have been built. Two of these were heavy fixed installations while the third was suitable for modification as a mobile field unit.

30.12.1 MIT-Freeport Sulfur Company Generator

This generator [39] was in the form of a stainless steel tubular sulfur boiler fired with natural gas. Undiluted sulfur vapor passed from the boiler through a nozzle directly into the air where it was cooled by entrainment of the air and condensed to a cloud of sulfur particles which formed an obscuring smoke. Particle size determinations were made on this smoke. These indicated that the best covering smoke was produced using a $\frac{3}{32}$-in. diameter nozzle and a boiler pressure of 85 psia. These conditions yielded a particle size distribution curve with a peak at 0.23 micron radius. Sulfur rates as high as 275 lb per hour were achieved.

It was found that above a nozzle pressure in the vicinity of 8 psi gauge, burning of the vapor neither occurred spontaneously nor could be it sustained by the application of a flame to the vapor jet. Below this pressure, however, the vapors always ignited spontaneously, and burned completely. Smokes of excellent covering power of an order of magnitude of 1,000 lb per sq mile were produced.

Prolonged exposure to the densest parts of the smoke cloud, a few feet from the source, caused minor irritation of the throat and lungs. In no case was this effect seriously uncomfortable.

30.12.2 Texas Gulf Sulphur Company Generator

This generator [40] was in the form of a unique direct-fired sulfur boiling pot in a firebrick setting. Steam

was introduced into the pot and used to aid in the vaporization of the sulfur. A mixture of steam and sulfur vapor under pressures up to 12 psi passed from the pot through nozzles to the atmosphere where the sulfur condensed to an obscuring smoke. Sulfur and steam rates of the order of 600 and 250 lb per hour, respectively, were obtained.

30.12.3 University of Illinois — Kimberly Clark Corporation Generator

This generator [11] was an experimental model intended as a step toward a relatively small, compact, mobile field unit. In this respect it was a competitor of the continuous oil smoke generators. The model was of intermediate capacity between the small smoke pots and the larger continuous oil smoke units for rear-area screening. The generator itself was designed for complete hand operation, and incorporated no powered unit such as motors, pumps, or fans. There were no moving parts of any kind except valves. The use of critical materials was kept to a minimum. The unit could be produced with the use of very little stainless steel and possibly without it.

Briefly, it was a unit weighing 197 lb when uncharged, and standing 3½ ft high by 20 in. in diameter. One hundred twenty-five pounds per hour of sulfur was converted to smoke, while at the same time 10 lb of gasoline and 30 lb of water were consumed. The unit incorporated a Venturi high-velocity vaporizer for converting the molten sulfur to vapor. The combustion of gasoline was carried out in a space surrounded by a tangentially wound coil for generating steam. This steam was used to provide draft through the unit by means of a steam injector nozzle.

Certain disadvantages of the design were evident. First, the steam ejector proved to be an inefficient means of forcing the combustion gases through the unit. This resulted in a somewhat larger consumption of fuel and water than should be necessary on the basis of the smoke capacity. A more efficient steam ejector would make the design appear more favorable.

Second, it is a characteristic of sulfur smoke that the size [1] of these smoke particles which give the most effective screen is somewhat smaller than that required for oil smoke particles. These smaller particles were produced by the unit, but the design of the vapor dispenser is much more critical than with oil smokes. This is a disadvantage, since it means that the orifices or slots through which the sulfur vapor is emitted must be quite small, and therefore numerous



FIGURE 37. Experimental continuous sulfur smoke generator.

or of considerable extent, in order to obtain the desired capacity. This is evident from the design of the wing jet smoke dispenser on the unit.

Third, it is an inherent property of a sulfur smoke generator that a melting pot must be provided for the solid sulfur. This melting pot adds weight and bulk to the smoke generator over that required by a comparable oil smoke generator. It seems unlikely that the preliminary melting and starting period can be reduced to less than 5 or 10 min. The melting pot also introduces the problem of disposing of its contents of molten sulfur when the unit is shut down. Probably the most convenient way of handling this would be to provide a drain for emptying this molten sulfur onto the ground. In any case, the sulfur melting pot, with its somewhat longer starting time, its additional bulk and weight, and its content of hot liquid, makes the generator less mobile than an oil smoke generator.

DESCRIPTION OF THE GENERATOR

The experimental generator is shown in Figure 37. It is producing sulfur smoke in Figure 38. The internal construction of two of the principal parts is shown in Figure 39. Figure 40 is an assembly drawing of the generator (the hand-pressured gasoline and water tanks are not shown).

The unit consists of a cylindrical angle iron frame which supports and encloses the four essential parts of the apparatus, namely, the burner, the boiler, the sulfur pot, and the sulfur vapor dispenser. The unit is constructed so that it can be easily disassembled



FIGURE 38. The sulfur smoke generator in operation.



FIGURE 39. The two lower parts of the sulfur smoke generator.

into the four essential parts by the removal of a few bolts.

A standard design of gasoline or kerosene burner, modified for application to an enclosed combustion chamber and to burn the fuel completely in a small volume of combustion space, is attached at the bottom of the unit and is used for supplying heat. White gasoline is fed to the burner from two 4-gal hand-pressured tanks of commercial design. The combustion space is enclosed on the sides by a coil of steel tubing, which makes up the steam generating and super-heating surface of the boiler. The coil section is insulated from the atmosphere with a 2-in. thick Fiberglas blanket, which is, in turn, covered by light-gauge sheet iron for holding the insulation against the outside of the coils, and sealing the combustion chamber against excess air. The No. 16 BWG $\frac{3}{4}$-in. OD tubing from which the coils were made will withstand over 300 psi. A convergent-divergent nozzle is affixed to the end of the tubing and directed through the entrance to the Venturi vaporizer in the bottom of the sulfur melting pot. The steam produced by the boiler passes through this nozzle. Water is fed to the boiler at the lower end of the coil by means of hand-pressure tanks of commercial design.

A hinged covered hopper is provided for charging the raw solid sulfur to the sulfur melting pot. This pot forms the top section of the apparatus so that the bottom of the pot is the roof of the combustion chamber. The combustion gases sweep against this roof and are ejected through the Venturi vaporizer by means of the steam jet described above. Two valves control the flow of molten sulfur from the sulfur melting pot into the throat of the vaporizer.

A sulfur vapor dispenser is provided on top of the unit. This is equipped with a baffle to remove unvaporized liquid sulfur and return it to the melting pot. This dispenser consists of a partial cylinder divided into two sections by the baffle. Sulfur vapor passes to the upper section from the lower section, and liquid sulfur particles are retained in the lower section. The upper section of the dispenser is provided with wing-type slotted jets through which the sulfur vapor is ejected into the atmosphere by the slight pressure inside.

Operation of the Generator

To operate the generator, solid lump sulfur is charged to the hopper on the melting pot and pressure is pumped up in the water and gasoline tanks. The burner is then lighted and the combustion gases are at first allowed to escape through a vent in the combustion chamber. With a bleeder valve in the upper end of the coil open, water is then admitted to the lower end. Dry steam will issue from the bleeder valve in a few minutes and this is then closed to allow pressure in the coil to build up. The vent is likewise closed and the gases pass out through the vaporizer. As soon as the temperature at the top of the steam coil reaches the range 500 to 700 F and operation is steady, the sulfur control valve is opened and liquid sulfur flows from the melting pot to the vaporizer. Sulfur smoke is then produced immediately. Additional sulfur is charged to the hopper from time to time, duplicate gasoline and water tanks are switched on, and the empty tanks recharged to maintain continuous generation of sulfur smoke.

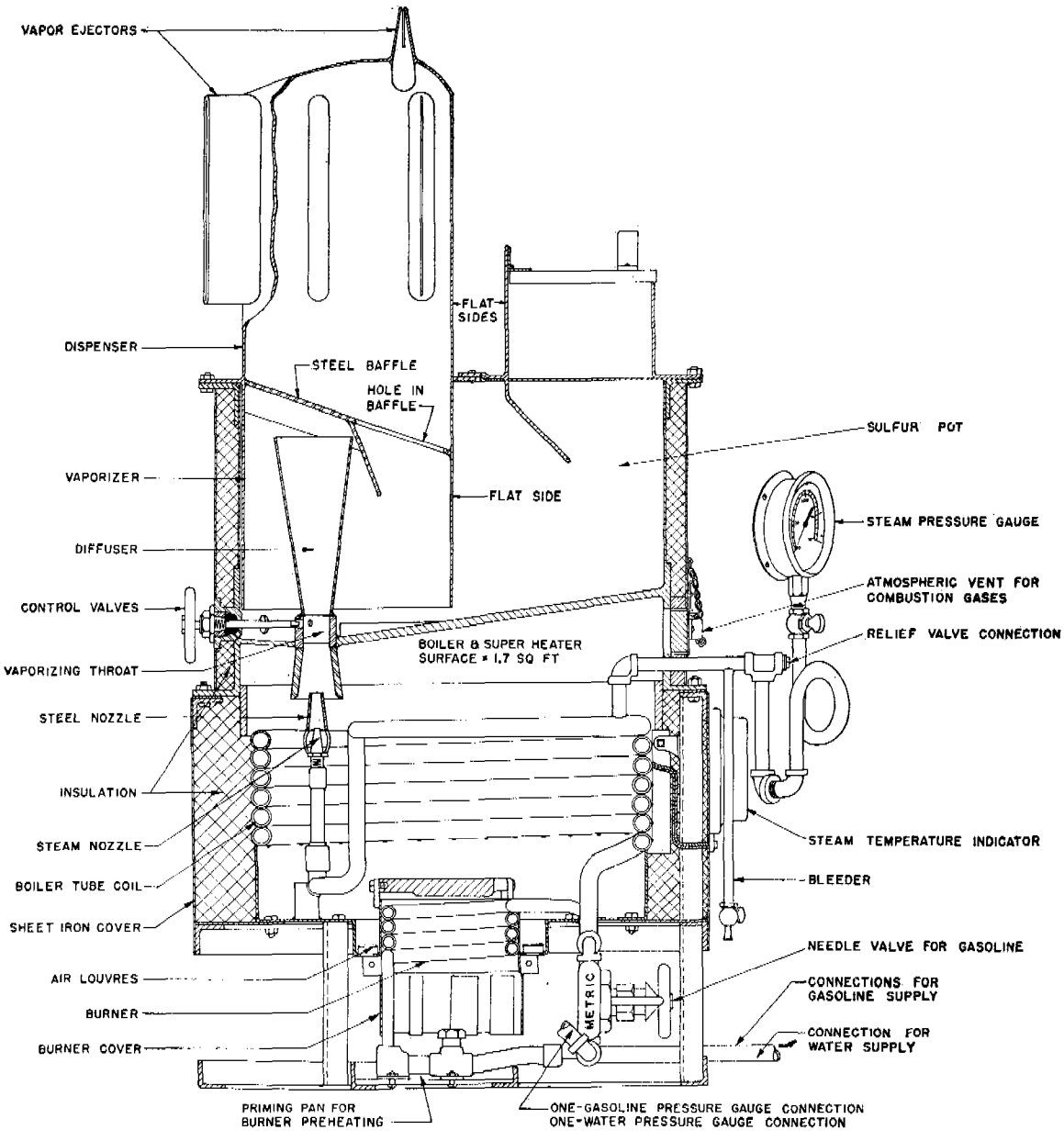


FIGURE 40. Continuous sulfur smoke generator.

30.13 COLORED SMOKE MUNITIONS

30.13.1 Floating Colored Smoke Signal (DS-4)

SPECIFICATIONS

The development of an improved daytime floating distress signal was requested at a conference with representatives of the Air-Sea Rescue Agency in September 1944. It was specified that the signal should conform to Coast Guard specifications which limited the size to 7 in. in diameter and 10 in. high. The signal was to give an orange smoke visible from 5,000 ft altitude and two miles distance for a period of at least 4 min.

HISTORICAL

Colored smoke signals are commonly made of intimate mixtures of pyrotechnic fuels and volatile

organic dyes (for example, mixtures of $KClO_3$, lactose, $NaHCO_3$ and dyes). These mixtures require a fuel with a relatively low heat of combustion. There are also restrictions on the shape of the compressed block and on the burning rate. In general, the colored smoke clouds are small in volume and variable in color.

Several commercial floating distress signals utilizing the intimate mixture principle have been on the market for a number of years. It was felt that a signal utilizing the Venturi thermal generator principle could be developed that would be superior to these. This opinion was verified by tests made on several commercial signals compared with an experimental model of the thermal generator.[43]

A number of tests were made on different models. The results indicated that the Model F–6 thermal generator, in which there is a baffle over the Venturi tube, would disperse the pure dye efficiently and without decomposition. Several units of this type had been made up and demonstrated to representatives of the Coast Guard and the Air-Sea Rescue Agency on Long Island Sound in August 1944. The consensus was that the new signal [44] put out a greater volume and a better quality of smoke than the commercial signals. Some difficulty was experienced with the uniformity of the feeding of the dye, and it was recommended that further work be carried on to improve the signal and that its size be made to conform with the specifications.

Theoretical

The Venturi thermal generator principle has been discussed in the preceding text. This principle was developed to produce a smoke cloud by atomizing a liquid agent in a high-velocity hot gas stream. Essentially, the generator consists of an agent compartment and a fuel compartment. The hot gases from the burning fuel pass through a Venturi vaporizer and the molten dye mixture from the agent compartment feeds into the hot gas stream at the throat section. The dye mixture is atomized and vaporized in the gases and this mixture is discharged to the atmosphere. It issues in a vertical jet which is cooled by entraining air and the dye vapors are condensed to a colored smoke.

The problem of developing a new type of daytime floating distress signal resolved itself into three phases.

1. Investigation of the properties of a number of dyes and dye mixtures and the choice of the most suitable for use in this unit.

2. Design of the unit to obtain the desired heat transfer for melting the dye mixture.

3. Design of the unit to obtain the desired floating characteristics.

In the past, agents such as Diol 55, which remain liquid over most of the temperature range encountered under field conditions, have been used as smoke agents in the thermal generator. The percentages of dye compounds which can be dissolved in these agents, however, is insufficient to produce a smoke having the color intensity necessary for a signal. There are several organic dyes having melting points near 100 C which, when used in the thermal generator, can be melted by the heat of the fuel block and fed into the Venturi as liquid agents.

Proposed dyes were divided into two categories, (1) those that do not melt but decompose with evolution of gas in the neighborhood of the melting point, and (2) those which melt in the vicinity of 100 C and remain stable at temperatures above the melting point for at least 5 min. Dyes in group (1) are obviously unsuitable and were identified by a simple test tube heating test. Dyes in group (2), following the test tube test, were tried in the signal. Upon locating the most suitable dyes, an investigation of compatible organic diluents was carried out. The purpose of the diluents was to give a mixture having a melting point considerably below that of the pure dye. Such a mixture would facilitate melting and insure more uniform operation.

The unit was designed with a maximum of the outer surface of the agent compartment exposed to the hot gases from the burning fuel. The greatest amount of heat to melt the dye is transferred by radiation from the surface of the fuel to the bottom of the agent compartment. An annular region between the agent compartment and the outer case allows a certain amount of convection transfer of heat from the hot gases to the dye mixture. Furthermore, this region serves to insulate the agent compartment from the cold outer wall.

The signal functions in any position from approximately 10° above horizontal to the vertical. The weight of the unit is so distributed that it tilts near the end of the emission and floats with one side lower than the others. The entrance to the feed tube is located at the lowest point in the agent compartment in either the upright or tilted position. This design gives a higher loading efficiency than one in which

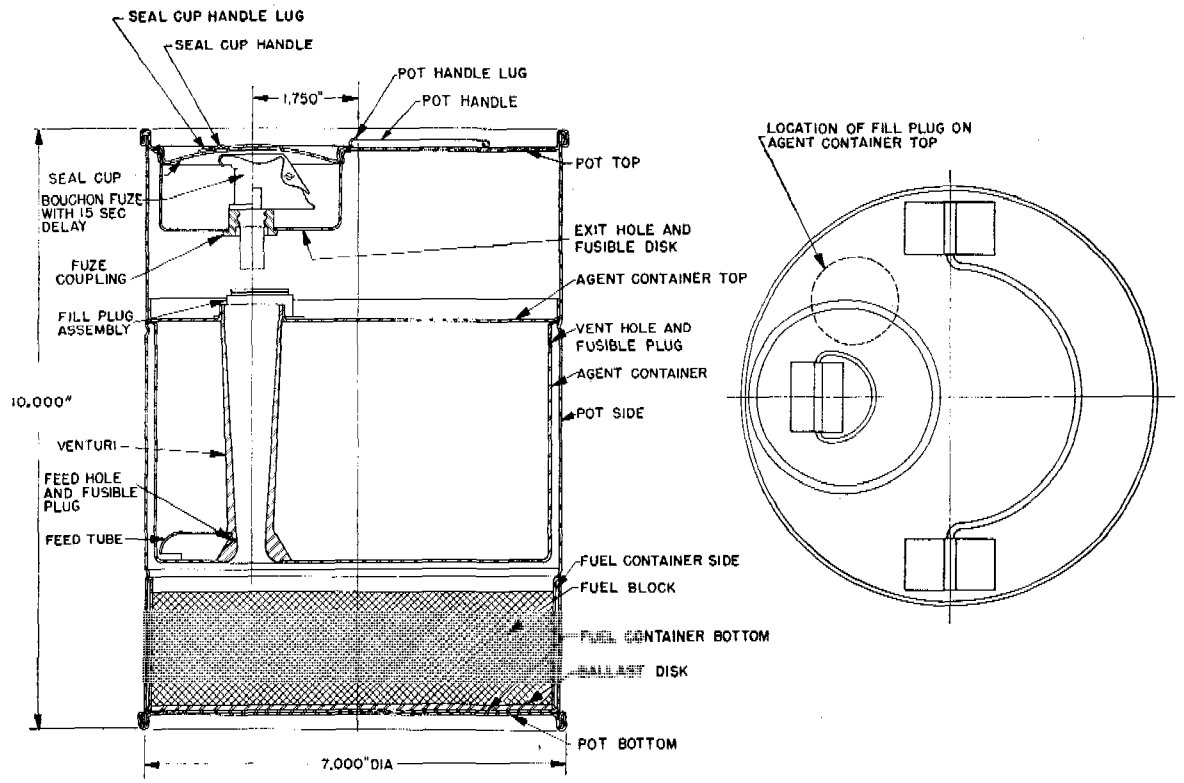


FIGURE 41. Colored smoke floating distress signal, Model DS–4.

vertical functioning only is possible. The latter design requires the use of more ballast to keep the unit floating upright.

DESCRIPTION OF THE FLOATING COLORED SMOKE SIGNAL (DS–4)

The proposed design [42] is shown in Figure 41. This is known as the *floating distress signal*, Model DS–4. Hand-fabricated units embodying the essential features of this model have been made and tested successfully. However, no units have as yet been constructed precisely as shown in the drawing.

The floating distress signal, Model DS–4, is 7 in. in diameter and 10 in. high. The complete unit including dye and fuel weighs about 12 lb. Of this, approximately 5 lb are dye mixture and 3.3 lb are fuel. The assembly is composed of three subassemblies: the fuel container, the agent container, and the outer can or pot.

The fuel mixture is pressed into the fuel container in one charge under a dead load of about 1,000 psi. The composition of this mixture is as follows:

Slow base mix	1,200 g
NH_4NO_3	86 %
Charcoal	9.9%
Naphthalene	1.1%
Boiled linseed oil	3 %
Fast base mix	300 g
NH_4NO_3	86 %
Charcoal	11 %
Boiled linseed oil	3 %
Starter composition	20–24 g
KNO_3	53 %
Silicon	39.2%
Boiled linseed oil	2 %
Charcoal	5.8%

The top surface of the block is coated with a pyroxylin lacquer for moisture protection. A waterproof Quickmatch is then fastened to the block. This picks up the spit from the fuze and insures subsequent ignition of the fuel.

The agent container is assembled from its com-

ponent parts, and all joints are copper brazed. The feed hole and vent hole are soldered closed and the container tested for leaks. The agent container is then seam-welded onto the pot. The molten dye mixture composed of 50% Calco Oil Orange Y–293 and 50% diphenylamine is charged through the filling hole and the plug inserted.

The final assembly consists of registering the fuze assembly directly over the Venturi and crimping the top cover, then slipping the loaded fuel can in from the bottom and crimping the bottom cover.

Operation of the Signal

The first step in functioning the DS–4 signal is to remove the seal cup protecting the bouchon fuze. The cotter pin is then removed from the fuze, thereby initiating a 15-sec delay igniter composition. The spit from the fuze travels down the Venturi and is picked up by the Quickmatch on the surface of the block. The initial pressure surge from the burning fuel ruptures the fusible disks covering the exit holes. The heat from the fuel block melts the fusible plugs and the dye mixture. The liquid dye feeds into the Venturi due to the pressure from the fuel compartment vented into the agent compartment through a hole near the top of the annulus. The dye mixture is atomized and vaporized in the hot gases and this mixture is discharged to the atmosphere, where it condenses to form a colored smoke.

Comments on the Proposed Design

Although the design shown in Figure 41 has not been built, it is based on the experience from considerably more than a hundred tests on numerous experimental signals which were built and functioned. These tests indicated that the high-velocity thermal generator principle is a more efficient method of vaporizing dye for colored smokes than is the intimate mixture of dye and fuel. Since the design shown in Figure 41 has not been built and tested, certain dimensions and weights cannot be specified until this is done.

The DS–4b model is the latest design that has been built and operated a limited number of times. The DS–4a model preceded it. The general arrangement of these designs together with several earlier ones is shown in Figure 42.

The Model DS–4a depended on the suction in the Venturi throat to feed the molten dye and required up to 40 sec for smoke emission to start. It then generated an intensely colored orange smoke cloud having several times the volume of the cloud emitted by the best available commercial signals. After being cooled below 32 F it functioned satisfactorily in water at 32 F.

The DS–4b utilized the pressure in the fuel compartment to aid in feeding the molten dye. Smoke emission then began in a shorter time.

The DS–4 can be expected to give smoke within 10 to 15 sec after the fuel is ignited.

Development

The development proceeded along two parallel lines. On the one hand, it was necessary to find a suitable colored smoke dye or dye mixture for use in the signal, and on the other, to design the unit to function efficiently and to meet the requirements of the Air-Sea Rescue Group.

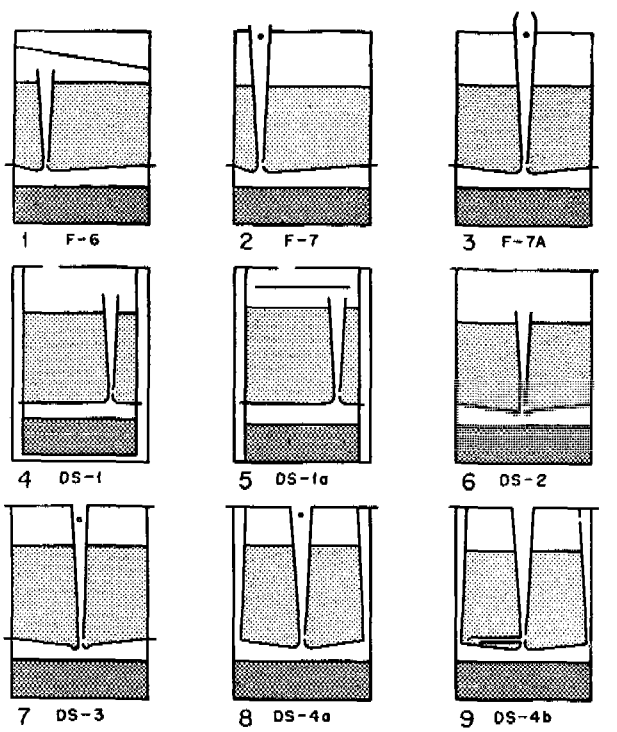


Figure 42. Outlines of several of the models tested in developing the floating distress signal.

Open Dye Chamber. The initial work on the colored smoke signal was done with the F–6 type thermal generator shown in Figure 42. This functioned very well in a number of tests with Calco Y–293 dye but the emission time could not be extended to the required 4 min without frequent plugging of the feed holes and intermittent smoke emission. This design allowed free access to the dye chamber by the hot

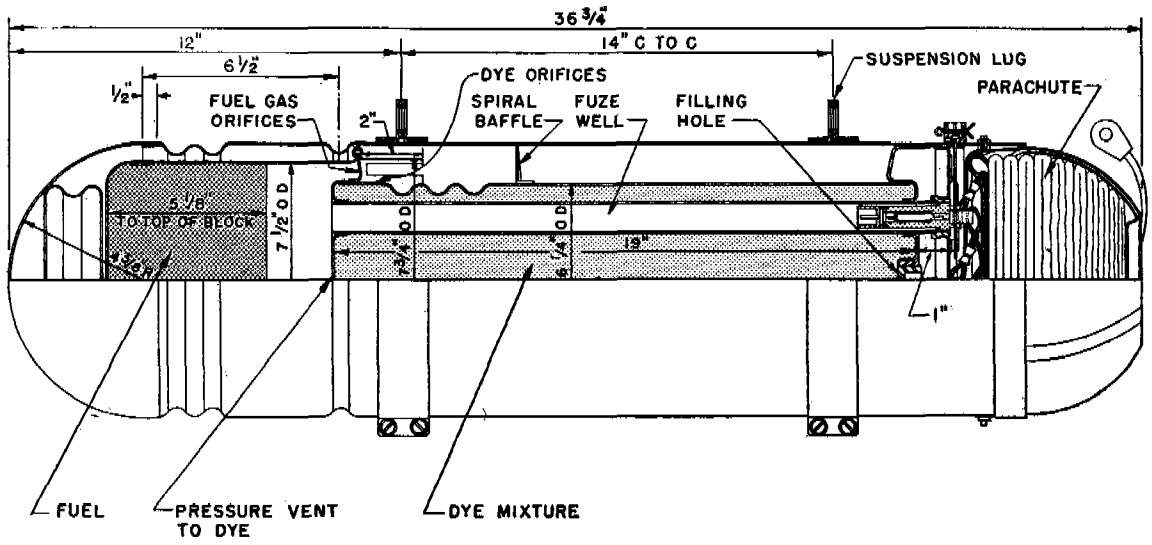


FIGURE 43. Smoke target identification bomb, Mk 72, Mod 2.

gases from the vaporizer. This aided in melting the solid dye. Unevaporated dye from the vaporizer was returned to the dye chamber and recycled.

Dyes. The following dyes were satisfactory in the F–6 pot: Calco Oil Orange Y–293, Calco Oil Green CG, duPont Oil Orange, and duPont Oil Yellow N.

Addition Agents in the Dye. Addition agents, such as diphenyl oxide and diphenylamine, were used with the dye in amounts up to 50%. These were effective in lowering the melting point, diluting both the dye and decomposition products, avoiding the plugging of the feed holes, and giving a longer and more uniform smoke emission time. The low melting point of the dye mixture, however, made the open dye chamber unsuitable.

Closed Dye Chamber. The work was then directed toward adapting the F–7 type thermal generator with its closed agent compartment for use as a signal. The hot gases from the vaporizer do not enter the dye chamber in this design, and no provision is made for recycling unvaporized dye. The rate of feed of dye must, therefore, be controlled more accurately to avoid spraying liquid dye from the signal. This design was carried over into the DS–3. Irregular smoke emission was encountered with the closed dye chamber. This was first attributed to a recurrence of the feed hole plugging difficulties noticed when pure dye was used in the open dye chamber design. It was later found that it was due to the slow rate at which the dye melted in the chamber. A considerable amount of solid dye was left on the cold outer walls of the hamber.

Hot Gas Jacket for Dye Chamber. This led to the DS–4a with the dye chamber completely surrounded with hot gases from the fuel block. This greatly increased the melting rate of the dye and eliminated the difficulty from erratic smoke emission. This design, modified by pressurizing the dye chamber and providing a feed tube for operation in a tilted position, resulted in the design proposed in Figure 41.

30.13.2 Colored Smoke Target Identification Bomb, Mk 72, Mod 2

A colored smoke target identification bomb, equipped with a nylon parachute to be dropped from high-speed combat aircraft at low altitudes was developed [28] at the request of the Navy Bureau of Ordnance. The bomb, designated *Bomb, Target Identification, Smoke, Mk 72, Mod 2* is shown in Figure 43. It weighs about 53 lb, consisting of: metal parts, 22.0 lb; fuel, 9.4 lb; dye, 18.7 lb; and parachute assembly, 3.4 lb. The bomb generates a dense colored smoke for 4.5 to 6.5 min. The colors now available are yellow, yellow orange, a bright orange, and red orange. The bomb functions on a thermal generator principle and contains fuel and dye in separate compartments.

The original specifications indicated that the bomb was to be launched at about 200 ft altitude from a plane diving at 300 knots. It was to be equipped with a parachute which was to act only as a snubber. The fuze was to function when the parachute opened and have a delay of about 5 sec. The bomb was to emit a

colored smoke for 5 min, 10 sec, ± 40 sec. Orange and red smokes were preferred, but there was a definite interest in yellow, green and violet smokes.

Colored smokes have generally been produced by burning intimate mixtures of dye and fuel. A typical mixture of this type contains the following: 22% $KClO_3$, 9% sulfur, 24% $NaHCO_3$, and 45% dye. These materials are thoroughly mixed and then pressed into the munition. The dye is vaporized by the burning fuel, and upon issuing from the generator, condenses to form a colored smoke. There are a number of limitations to this type of smoke munition. In general, the intimate mixtures are suitable for small units, such as colored smoke grenades, but are not so suitable for use in large munitions. The chief difficulties encountered in large colored smoke munitions is in controlling the burning rate of the fuel and the tendency toward decomposition or flaming of the issuing dye vapor when the fuel is too hot. The incorporation of cooling agents such as sodium bicarbonate to prevent undue decomposition of the dye decreases the thermal efficiency of the fuel. The dyes used are often expensive, especially the anthraquinone type, and certain mixtures have a tendency to explode when ignited. The maximum amount of dye that can be incorporated in a mixture is about 50% by weight.

Preliminary tests indicated that a Venturi-type thermal generator described above was capable of generating a colored smoke cloud superior to that generated by the standard intimate mixture compositions.

The 12-lb F-7A experimental thermal generator pot was tried for this use. This was not designed for dropping from aircraft, and provision had to be made to retard its fall by means of a parachute. Tests with this unit were unsatisfactory, due to the tendency of the parachute to tip the munition over on its side. When in this position, the dye would not discharge completely. For this reason, the design of a thermal generator which would function in a horizontal as well as a vertical position was undertaken.

Principle of Operation

The design consisted of two compartments, one of which contained fuel and the other the dye in a solid cake. The dye compartment was surrounded by an annulus through which the hot gases passed. The dye fed into the annulus through several holes located at the base of the compartment. Vaporization took place in the annulus and the vapor issued through a single orifice in the top of the unit. The development of the target identification bomb was based on this principle.

The fuel block consists of ammonium nitrate and carbon, and is pressed into a container in the nose end of the bomb. The dye is cast into a separate compartment above the fuel. Hot gases from the burning fuel block pass through orifices in the top of the fuel chamber into the annulus surrounding the dye compartment. Heat from these gases is transferred through the walls of the dye compartment and melts the dye which then flows, through holes in the bottom of the dye compartment, into the annulus. Here the hot gases come in contact with the molten dye and vaporization takes place. A spiral baffle is used in the annulus to insure better contact between dye and gas. The fuel gas-dye vapor mixture issues from an orifice in the tail of the bomb.

Description of the Target Identification Bomb

The metal components of the bomb consist of three major assemblies: (1) the outer case, (2) the fuel compartment, and (3) the dye compartment. The fuel container and dye compartment are crimped and riveted together and constitute the inner assembly. This is slipped into the outer case and brazed in place. The parachute pack is located on the tail end of the bomb.

The fuel block has the following composition:

Base mixture	3,000 g
NH_4NO_3	86 %
Boiled linseed oil	3 %
Charcoal	8.3%
Naphthalene	2.7%
Top mixture	1,250 g
NH_4NO_3	86 %
Boiled linseed oil	3 %
Charcoal	11 %
Starter	30 g
KNO_3	53.0%
Silicon	39.2%
Charcoal	5.8%
Boiled linseed oil	2.0%

The mixture is pressed in three increments into the fuel can under a dead load of 35 tons, or about 1,600 psi. The surface of the block is sprayed with a pyroxylin lacquer for protection against moisture. A waterproof Navy Quickmatch is attached to the top of the block in a web-like pattern. This picks up the

flash from the fuze and ignites the block uniformly over the surface.

The flange which projects from the bottom of the agent compartment contains eight No. 2 holes for the hot fuel gases to pass through. It also forms the bottom of the annulus. Eight dye feed holes of the same size are provided opposite the holes for the fuel gas. These are closed with 50/50 solder before the dye is cast into the dye compartment.

After the inner assembly is placed in the outer case, the top plate of the agent compartment is brazed to the outer case. A fusible diaphragm 0.10 in. thick is soldered over the vapor exit hole after the bomb is charged with dye. With the fuze assembly in place, complete protection from moisture is assured.

The nylon parachute is a *baseball* type. Four steel cables, $\frac{1}{8}$ in. in diameter, are attached to the shroud lines of the parachute and to load lugs on the tail plate of the bomb. A fifth cable, $\frac{1}{16}$ in. in diameter, is attached to the parachute and fastened to the arming plug of the fuze. The parachute case slips into the recess at the tail of the bomb and is bolted to the outer case. This parachute was manufactured by General Textile Mills, Inc., New York.

The fuze is a modification of the Navy submarine identification flare firing mechanism, Mk 10, and is actuated by the opening of the parachute. When the arming plug is pulled back by the opening of the parachute, it compresses a spring which acts on the firing pin. When the plug has been pulled far enough, it disengages the firing pin, and the latter strikes the primer which sets off the ignition mixture in the spitter tube. The flash travels down the fuze well and ignites the Quickmatch and then the fuel mixture.

The bomb, completely assembled and ready for dropping, is approximately 37 in. long and has a diameter of $8\frac{3}{4}$ in. It weighs $53\frac{1}{2}$ lb.

Development

The early experimental designs tested prior to the design described in the preceding text are omitted from this account. When the work reached a promising stage 15 units were fabricated by hand. These incorporated most of the principles of the later design. These functioned satisfactorily in static tests and one functioned when dropped from 15 ft in free fall onto concrete. Corrugations had been provided in the case and in the walls of the agent compartment to localize deformation on impact. These corrugations were effective in this respect. Twelve of these bombs were fitted with rayon parachutes and delivered to the Naval Proving Grounds at Dahlgren, Virginia. There, 11 were dropped from a Navy F-6-F fighter plane. They were released at an altitude of 75 to 125 ft and at a speed of from 270 to 300 knots. Five of the bombs were duds due to fuze failure. Five functioned satisfactorily for varying lengths of time until the issuing dye vapors flamed. Further tests showed that the rayon parachutes caught fire and ignited the dye vapor. One bomb functioned satisfactorily.

Twenty-five bombs equipped with noninflammable nylon parachutes and improved fuzes were made and taken to Dahlgren for further drop tests. These were loaded with four different orange dye mixtures and a yellow dye. Twelve of these were dropped as before from an F-6-F plane. One fuze failure was encountered, and two bombs flamed after emitting about one-half the dye. The remaining eight bombs functioned satisfactorily, giving a colored smoke emission time of about $5\frac{1}{4}$ min.

To determine whether these bombs would present a hazard when exposed to enemy gunfire, three bombs were set up on a firing range. Single shots were fired into the bombs using a special .50-caliber incendiary bullet. When one of these bullets was fired into the nose of the bomb, the fuel was ignited in such a manner that the nose of the bomb was blown off. When the test was repeated later, after aging the fuel blocks, no ignition of the blocks could be obtained with incendiary bullets.

One hundred twenty-nine additional target identification bombs were delivered to the Navy Bureau of Ordnance for further tests. These were charged as follows:

45 with Calco Oil Orange Y–293
40 with duPont Oil Yellow N
44 with Calco Oil Scarlet II with 15% diphenylamine, or National Oil Scarlet 6G with 15% diphenylamine.

The parachutes on these bombs were of $2\frac{1}{4}$-oz nylon instead of the 4 oz used on the 25 bombs previously delivered to Dahlgren.

Control of Flaming. The chief difficulty has been with flaming of the dye vapor, usually as a result of the hot bomb case igniting either the parachute or dry grass in contact with the case. In 53 trials using bombs without parachutes or with nylon parachutes, five inflamed spontaneously or as a result of grass fires. Four were ignited intentionally to test flaming inhibitors. Out of eight trials with rayon parachutes attached, seven bombs inflamed.

Tests were made using Calco Oil Orange Y–293 mixed with hexachlorobutadiene and with Chlorpropane Wax 130, (the latter supplied by the Hooker Electrochemical Company, 85% octachloropropane, 15% pentachloropropane). The purpose of these diluents was to inhibit flaming of the issuing dye vapor by raising the flash point. These agents had much the same effect as diphenylamine on the intensity of the color of the smoke. Insufficient data are available to draw any conclusions as to the merits of these agents as flame inhibitors.

Ignition of the cloud has been prevented until near the end of the color emission, even in the presence of burning grass, by reducing the diameter of the vapor exit hole from 1⅛ in. to ¾ in. or by adding 25% Chlorpropane Wax to the dye.

Effect of Position. The bomb was found to operate best with the long axis horizontal. However, it has operated successfully in a vertical position nose down; with the long axis at a 30° angle to the horizontal and the nose high; and in intermediate positions. In general, the dye emission time decreases as the bomb is changed from the horizontal to a vertical position.

Dyes. The desirable properties for a dye suitable for use in colored smoke munitions of the thermal generator type munition having separate agent and dye compartments are as follows.

1. The dye should preferably be a crystalline compound and have a melting point under 150 C, or a melting point of 100 C when mixed with a small proportion of a melting point depressant, such as diphenylamine (less than 25% diphenylamine should be necessary). The dye should not undergo decomposition when heated to high temperatures for a short time. It is desirable for the dye to be stable for about 3 to 4 min at temperatures 50 to 100 C above the melting point.

2. A rapid preliminary test may be run on a new dye by heating 5 g in a test tube and observing how it melts. If it melts and flows freely then 100 g should be tested in a small smoke generator. If this gives promising results the final and conclusive test is carried out in the full-scale munition.

Four dye mixtures were found to give excellent smoke clouds: (1) Calco Oil Scarlet II, or National Oil Scarlet 6G with 15% diphenylamine (red orange cloud), (2) Calco Oil Orange Y–293 (bright orange cloud), (3) Calco Oil Orange 7078–V or duPont Oil Orange with 15% diphenylamine (yellow orange cloud), (4) duPont Oil Yellow N (bright yellow cloud).

These dyes are all common azo dyes made by simple coupling reactions and are readily available from several manufacturers. The addition of diphenylamine generally lowers the melting point. If added in too large quantities, however, it dilutes the color of the cloud. The Oil Orange (Color Index No. 24) dye is particularly sensitive to an excess of diphenylamine.

The search for a satisfactory violet dye or a blue dye for mixing with red has so far been unsuccessful. The majority of blue and violet dyes are of the anthraquinone type and are less suitable than azo dyes. This is due to the high melting point characteristic of this class.

Chapter 31

FUEL BLOCKS FOR THERMAL GENERATOR MUNITIONS

By *E. W. Comings*

31.1 INTRODUCTION

A NUMBER OF the munitions described in Chapter 30 function by vaporizing a liquid agent. This vaporization is carried out with a hot gas generated by a fuel block within the munition. The fuel block burns slowly and smoothly during the functioning time of the munition. It burns without using air or oxidizing agents other than those included in the block itself. In this way hot gases are generated under sufficient pressure to cause flow through the channels in the munition without using pumps or blowers.[4–8] The latter would be needed if combustion with atmospheric air were used to supply the hot gases.

Fuel blocks giving satisfactory performance in a number of munitions ranging in size from a 1-lb training candle to a 125-lb generator have been made.[1] Blocks for two munitions were successfully carried through limited production.

Blocks of two types were made, (1) pressed, and (2) cast. The pressed mixture consisted of NH_4NO_3, charcoal, a linseed oil binder, and an additive such as KNO_3, NH_4ClO_4, or NH_4Cl to regulate the burning rate. This mixture was formed into blocks in a hydraulic press. Cast blocks consisted of NH_4NO_3, charcoal, 1.0*M* H_3PO_4, NH_4Cl, and an additive such as $NaNO_3$ or starch to regulate the burning rate. These were melted and poured into the fuel container at a temperature of around 115 C.

The factors involved in the control of burning characteristics have been systematically studied. Of the ingredients used, charcoal is the least uniform and causes the greatest variation in block-burning characteristics. Treatment of charcoal with K_2CO_3 makes the block burn more rapidly; treatment with H_3PO_4 reduces the block-burning rate. The block-burning rate can be changed by (1) varying the charcoal particle size, (2) modifying the charcoal surface properties as by treatment with K_2CO_3 or H_3PO_4, and (3) by formula variation. The latter was the method most commonly used. Substitution of KNO_3, $NaNO_3$, or NH_4ClO_4 for part of the NH_4NO_3 increased the burning rate. Addition of NH_4Cl to the mixture or substitution of naphthalene (or starch in the cast block) for charcoal decreased the burning rate. The method of changing charcoal surface properties has not been thoroughly investigated but offers promising possibilities.

The conditions under which the block burns affect the burning characteristics. Increasing the initial block temperature, and increasing the gas pressure on the block during burning, increases the burning rate. For blocks pressed into metal cans, a cardboard or stencil board inner liner in the can between the block and the metal prevents burning down the side.

A curious type of irregular and objectionable burning known as *surging* has been observed in a few cases when these mixtures were burned under pressure. Data indicate that this is caused by two reducing agents present in the mixture at the same time. These may be two different chemical compounds or the same compound (charcoal in this case) with different activities.

A waterproof lacquer (Special 6C) was effective in waterproofing the exposed surface of a fuel block against tropical storage conditions for 15 days.

Pressed NH_4NO_3–charcoal–linseed oil blocks show an increase in burning rate with age for the first three weeks after pressing. After three weeks no further change is observed.

Gases from a surging and a smooth burning block have been analyzed and a surging mechanism postulated.

All the fuel blocks used in the thermal generator munitions described in Chapter 30 have, up to the present time, included powdered hardwood charcoal as a major ingredient. Hardwood charcoal is not manufactured to specifications which will insure reproducible burning properties of the fuel blocks, but it is likely that it could be manufactured to such specifications. A fuel block which does not contain charcoal has also been carried through preliminary development, and offers much promise.[3] It contains guanidine nitrate.

31.2 DESCRIPTION OF THE FUEL BLOCKS FOR THE THERMAL GENERATOR MUNITIONS

Many different sizes and shapes of thermal generator munitions, ranging from a 1-lb training pot to a

TABLE 1. Summary of physical and burning characteristics of fuel blocks for thermal generator munitions.

Unit	Agent‡ discharged lb	Weight of complete munition lb	Block weight g lb	Block diameter in.	Block surface area sq in. sq cm	Block* height in.	Normal operating gas pressure psi	Block burning time in unit min	Burning rate† in./min	Burning rate† g/(min)(cm)	Block§ density g/cc	Press. increments	Press. psi	Agent/fuel ratio
F7A	6.5 HD	10.0	1,420 3.15	7	38.5 248.5	1.87	2.3	3.5 ± 0.5	0.54	1.62	1.20	1	1,040	2.05
F9	Diol 55 22	44.0	5,000 11.0	10	78.6 508	2.75	Not measured	12.5 ± 1.5	0.22	0.79	1.4+	Cast	Cast	2.0
E20	Diol 55 10	21.5	2,720 6.0	8.25	53.5 345	2.12	Not measured	6.0 ± 0.5	0.35	1.30	1.45±	Cast	Cast	1.67
E23	Diol 55 14.5	36.3	5,540 12.1	8.12	51.7 334	4.75	1.5–2.5	11.5 ± 1.0	0.41	1.43	1.37	5	1,400	1.2
E21	Diol 55 0.24	1.1	101 0.22	2.30	4.15 26.8	1.10	Not measured	1.2 ± .25	0.94	2.96	1.40	1	3,380	1.12
E29R1	HD 2.3	10.0	485 1.06	2.52	5.0 32.3	4.10	2–3	4.75 ± .25	0.86	3.10	1.44	2	3,300	2.15
DS3	Dye + DPA‡ 5	12.0	1,530 3.3	7	38.5 248.5	2.00	2	5.0 ± 0.5	0.41	1.21	1.20	1	1,040	1.5
Mark 72 Mod 2	Dye 18.7	53.0	4,280 9.45	7.5	44.2 285	5.12	3–4	5.5 ± 0.5	0.93	2.72	1.15	3	1,600	1.98
B1	HD 60.0	125.0	13,690 30.0	14.0	154 994	3.75	Not measured	11.0 ± 1.0	0.34	1.24	1.45	Cast	Cast	2.00

* Block height in normal production operations varies ±0.1 inch from values given.
† Weight of starter mix not included.
‡ DPA: diphenylamine. HD: distilled mustard gas.
§ Block density calculated from weight and dimensions given.

TABLE 2. Fuel block formulas for thermal generator munitions.

Unit	Mix	Weight g	Per cent by weight												
			British‡ starter	Cellulose acetate in acetone	Boiled linseed oil	NH_4NO_3	Charcoal	NH_4Cl	NH_4ClO_4	KNO_3	$NaNO_3$	Cornstarch	Naphthalene	1.0 *M* phosphoric acid	
F7A mustard gas generator; 12 lb	Starter	20	98		2										Pressed
	Top	400			3	83.5	13.5								
	Base	1,000			3	80.7	13.1	3.2							
F9 nonfloating smoke pot; 44 lb	Starter	60	70*	30	..										Cast
	Top	300				84.0	9.0	2.7			1.0			3.0	
	Base	4,700				84.0	6.4	3.0				3.6		3.0	
E20 nonfloating smoke pot; 21 lb	Starter	50	70*	30											Cast
	Top					78.0	11.0	2.0			6.0			3.0	
	Base					83.2	7.7	3.0				3.1		3.0	
E23 floating smoke pot; 36 lb	Starter	40	98		2										Pressed
	Top	700			3	86.0	11.0								
	Int.	1,800			3	84.0	9.0	4.0							
	Base	3,000			3	82.0	7.0	8.0							
E21 training candle	Starter	6	98		2										Pressed
	Base	95			3	82.0	11.0			4.0					
E29R1	Starter	10	97.5		2.5										Pressed
	Top	180			3	82.0	11.0			4.0					
	Base	295			3	84.0	11.0		2.0						
DS4 colored smoke signal	Starter	20	98		2										Pressed
	Top	300			3	86.0	11.0								
	Base	1,200			3	86.0	8.8						2.2		
Mk 72 Mod 2 target marker†	Starter	30	98		2										Pressed
	Top	1,250			3	86.0	11.0								
	Base	3,000			3	86.0	8.3						2.2		
B1 nonfloating mustard gas generator; 125 lb	Starter	90	70*	30											Cast
	Top	454				84.3	9.0	2.7			1.0			3.0	
	Base	13,200				84.3	6.2					3.5		3.0	

* Starter is poured on block as a thick slurry.

† Not a Venturi unit.

‡ 40% Si, 54% KNO_3, 6% charcoal.

125-lb generator, have been made during the development work. Differences in size, shape, and required burning times of these munitions necessitated a wide range in the burning rate of the fuel. In Table 1, the physical characteristics of the more important thermal generator munitions are compared. In Table 2, the formulas of fuel mixtures for the munitions are listed. These formulas are varied as necessary to compensate for variations in the ingredients.

Pressed blocks have been used much more extensively than cast, and a major part of the work was done on mixtures that were pressed into E29 [a] and E29R1 [a] type fuel cans.

Cast mixtures have been used for the slower burning compositions of large diameter and low block height. Cast and pressed mixtures will be discussed separately because of the differences in their properties and methods of manufacture.

31.3 PRESSED FUEL MIXTURES CONTAINING CHARCOAL

These mixtures are composed of charcoal, NH_4NO_3, a linseed oil binder, and an additive such as KNO_3 or NH_4Cl to regulate the burning rate.

31.3.1 Block Properties

The volume of gas, reduced to a standard temperature of 60 F and a pressure of 760 mm of mercury, produced by a burning pressed block ranges from approximately 12.0 to 14.6 cu ft per lb of mixture (0.75 to 0.92 l per g). The theoretical volume of gas measured under the same conditions for the reaction

$$NH_4NO_3 + C \longrightarrow CO + 2H_2O + N_2$$

is 16.35 cu ft per lb of mixture (1.02 l per g). For the reaction

$$2NH_4NO_3 + C \longrightarrow CO_2 + 4H_2O + 2N_2$$

the theoretical volume of gas is 15.4 cu ft per lb of mixture (0.96 l per g).

Analysis of the gases from a burning E29 block showed the following gas composition:

H_2O	48.8%	CO_2	13.5%
NH_3	0.6	CO	5.2
NO_2	0.0	N_2	26.1
NO	0.0	H_2	5.8

This corresponds roughly to the reaction

$$6NH_4NO_3 + 4C \longrightarrow 11H_2O + CO + 3CO_2 + 6N_2 + H_2$$

which gives 0.98 l per g of mixture at 16 C and 760 mm Hg. The calculated amount of heat evolved is 0.685 kcal per g of mixture. This compares with 0.72 to 0.75 for black gunpowder. A fuel mixture containing 5% charcoal instead of 11% will yield slightly more gas per gram of mixture but 17% less heat.

By using the sodium "D" line reversal technique,[12] the flame temperature 0.5 in. above the top of the fuel can was measured for an E29 block burning in the open. Values ranged from 2600 to 3000 F. Gas temperatures measured [b] by a shielded thermocouple placed about 8 in. above the enclosed burning mixture ranged from 1100 to 2100 F. In general, lower temperatures were associated with slower burning compositions.

Burning rates for any composition in grams per minute are roughly proportional to the burning surface. This relation can be conveniently expressed as grams of mixture burned per minute per square centimeter of burning surface. Rates from 1.2 to 4.8 g per min per sq cm have been obtained in pressed units burned in surroundings at 25 C and 1 atm pressure. This corresponds roughly to a gas evolution rate of from 1.08 to 4.3 l (at 16 C and 760 mm Hg) per min per sq cm.

The density of the block is 1.30 ± 0.20 and is influenced by pressing technique, particle size, and nature of the ingredients. This density range corresponds to 24 ± 12% void space in the pressed block.

The ignition temperature and nature of the decomposition of the mixture are dependent upon the rate and method of heating. The ignition temperature of the mixture used in the E29 fuel block, as determined by heating the loosely packed powder in a No. 8 brass detonator tube (0.218 in. diameter x 1.88 in. long) was 200 to 240 C. A complete E29 block heated in a Wood's metal bath at a rate of 12 C per min ignited at 220 C.

Heat conductivity of the pressed mixture is poor. A thermocouple, pressed in the center of an E29 block about 1¼ in. from the edge, lagged a thermocouple at the edge by 110 C when a heating rate of 12 C per min was maintained at the edge.

The pressed mixture, in the absence of moisture,

[a] The E29 can is hexagonal, with the dimensions: 2.65 in. across flats, height 5 in., area 36.6 sq cm. The E29R1 can is round, with the dimensions: 2.52-in. diameter, height 5 in., area 32.3 sq cm.

[b] Measurements were made in a standard volume tester described in the following text.

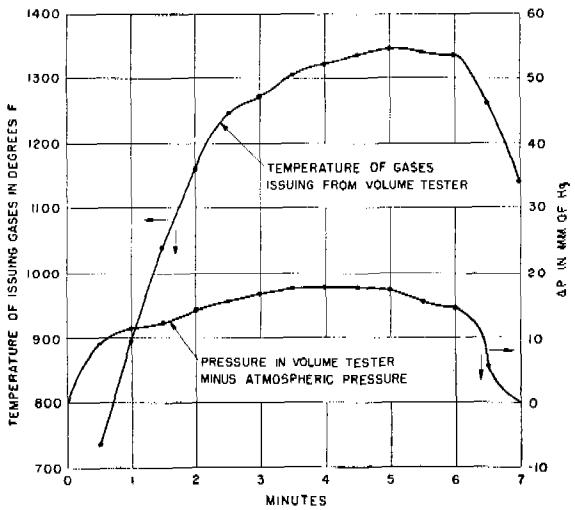


FIGURE 1. Temperature and pressure of gases from burning E29R1-type fuel blocks.

is not particularly corrosive to steel. Corrosion is serious when the mixture is moist.

When properly made, blocks show good mechanical stability. E29 blocks are able to withstand impact on concrete at 300 fps without serious breakup.

31.3.2 Manufacturing Procedure

Salts such as ammonium nitrate, potassium nitrate, and ammonium chloride, were dried at 100 to 110 C for 6 hr and stored at a relative humidity less than 50%. Charcoal was blended into uniform lots by tumbling in a large mixer of about 13 cu ft capacity. Ingredients were mixed in a 2-ft diameter Simpson intensive mixer for 20 min in an air-conditioned room. British starter composition was mixed by hand on a glass plate.

The mixture was pressed into cans in several increments with a hydraulic press and the starter mixture was pressed on with the last increment. Steel retaining forms were used to prevent the cans from deforming. The rams were made of wood and in some cases wooden rams were fitted with a brass face.

After pressing, every effort was made to protect the blocks from moisture. Many were stored in metal cabinets containing $CaCl_2$. Most of the blocks were coated with a special pyroxylin base lacquer designated as Special 6C made by Pyroxylin Products Co., Chicago, Illinois.

31.3.3 Testing Fuel Blocks

The burning properties of the blocks were tested by burning them in four ways: (1) in their appropriate unit, (2) in the open, (3) in a special gas flowmeter known as the volume tester, and (4) in a unit known as the surge tester.

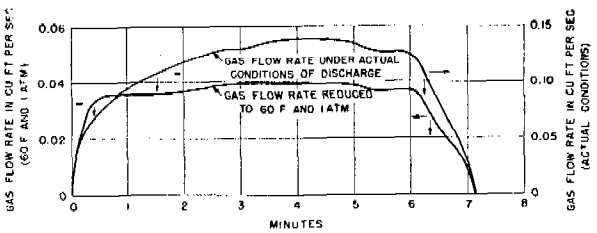


FIGURE 2. Typical gas flow rate — time curves for an E29-type block.

THE VOLUME TESTER

The volume tester is a flowmeter in which the gas is discharged through a sharp-edged orifice. The pressure drop across the orifice, along with the temperature of the effluent gases, is measured and used to compute the instantaneous rate of gas flow at any time during a test. By graphical integration of the instantaneous flow rate over the burning time of the block, the total volume of gas produced is measured.

From this apparatus two types of volume flow rate vs time curves may be obtained. In the first, the gas

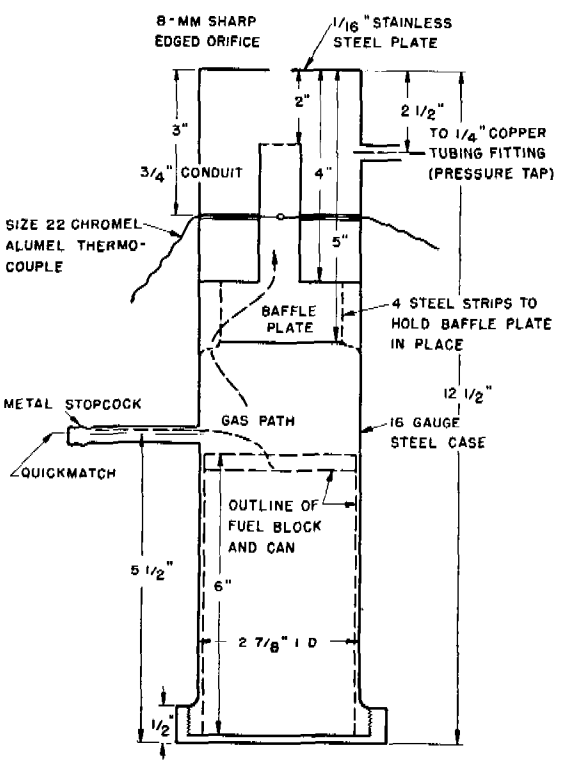


FIGURE 3. Standard volume tester for E29 fuel blocks.

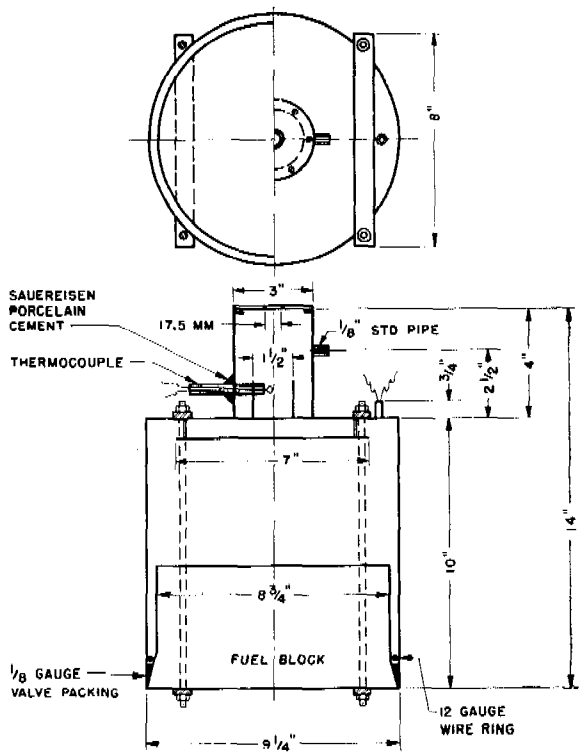


FIGURE 4. Tester to measure volume and temperature of gases from E23 fuel block.

volume under the conditions of temperature and pressure existing at the orifice is used. In the second, the gas volume is reduced to a standard temperature of 60 F (16 C) and 1 atm pressure. The latter volume rate is proportional to the mass flow rate, assuming that the gas has a constant molecular weight. Data for flow rates under actual conditions seem to show slightly better correlation with unit performance. Representative flow rate vs time curves of both types are shown in Figure 2 for an E29-type block. The gas pressure on the block inside the unit above that of the surroundings and the effluent gas temperature are shown in Figure 1. The volume testers used for the E29- and E23-size fuel blocks are shown in Figures 3 and 4.

THE SURGE TESTER (FOR 0–100 PSI)

A surge tester for E29 blocks is shown in Figure 5. The surge tester permits variation of the pressure on a burning fuel block by increasing or decreasing the size of the gas exit orifice in a closed cylindrical vessel containing the block. For the E29 fuel block, the cylindrical vessel was made from 3-in. extra strong steel pipe. One end was welded shut with ¼-in. steel

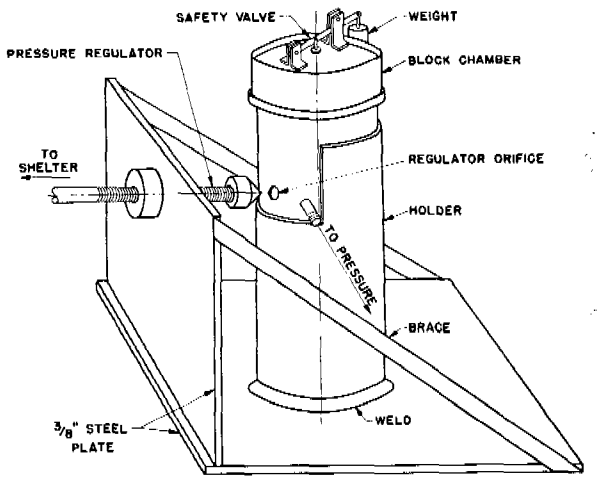


FIGURE 5. E29 surge tester.

plate. The other end was threaded and was closed by a pipe cap which allowed insertion and removal of the fuel block.

The gases of combustion are vented through a ⅜-in. orifice drilled in the side of the pipe. The gas exit area is varied by moving a conical plug into or out of this orifice with the screw adjustment shown.

A safety valve is incorporated in the equipment. The simple weighted orifice plug-type shown in the sketch has proven satisfactory. The area of this safety orifice should be at least $\frac{1}{25}$ the area of the fuel block surface. The operator should be protected by a steel-covered or concrete shelter. The safety valve, set for the highest pressure to be reached, should be checked before each test to be sure it is not jammed. The pressure regulator threads should be oiled and free to turn easily. A test should not be started without this preparation. At the beginning of the run the exit orifice is completely open. The regulator plug is gradually screwed in, slowly increasing the pressure. If surging occurs it can be detected immediately both by the sound and by the characteristic rhythmic motion of the pressure gauge needle or manometer fluid.

31.3.4 The Control of Pressed Block Characteristics

The variables involved in the control of block characteristics may be grouped under four headings: (1) variables due to ingredients used, (2) variables due to manufacturing procedure, (3) variables due to formula change, and (4) variables due to the condi-

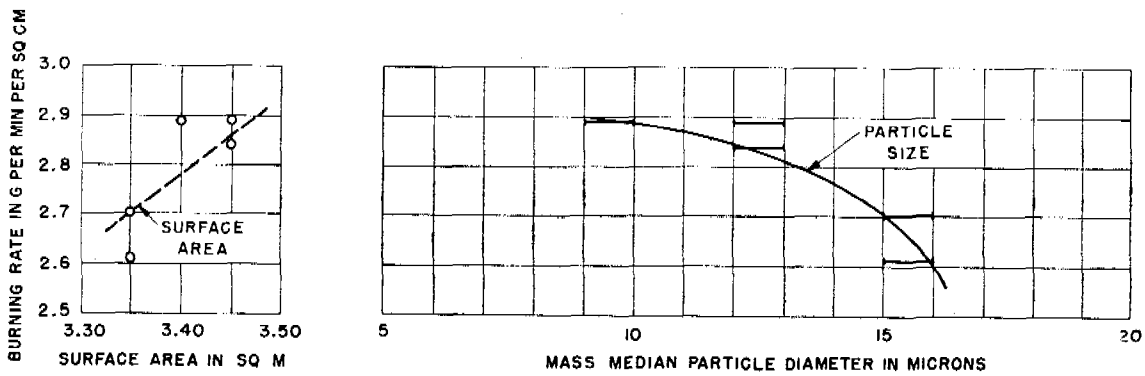


FIGURE 6. Burning rates of E29R1-type blocks made from different bags of Flower City charcoal vs particle size and surface area of charcoal.

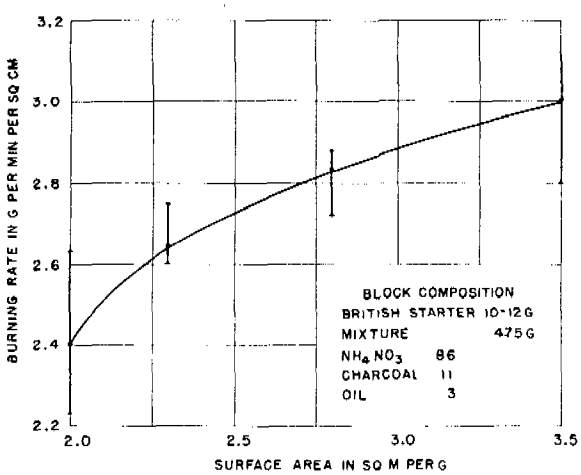


FIGURE 7. Burning rate of E29R1-type blocks as a function of the surface area of the charcoal.

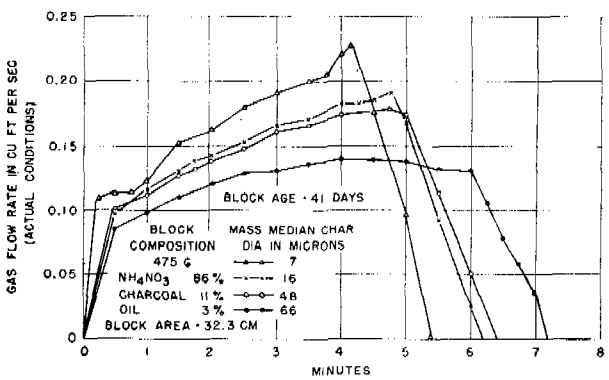


FIGURE 8. Gas flow rate vs time for E29R1-type blocks made with different charcoal size fractions.

tions under which the block burns. Discussion follows.

VARIABLES DUE TO INGREDIENTS

Variables in Charcoal. The charcoal is a source of major variation in burning time. Rather pronounced differences in burning time for different bags of charcoal are obtained.

Samples from each of five bags were examined to determine (1) particle size distribution by microscopic count, (2) per cent ash, (3) per cent volatile matter at 105 C, and (4) surface area by dye adsorption. No definite correlation between burning rate and per cent ash or per cent volatile matter was apparent; however, a fairly good correlation between burning rate and particle size was observed, the burning rate increasing with a decrease in particle size. This is shown in Figure 6.

1. *Effect of charcoal particle size.* In a systematic study of the effect of carbon particle size on burning characteristics, oak charcoal flour of airflow grade, which was supplied by the Tennessee Eastman Corp., was separated into four particle size fractions using an air classifier. E29R1-type fuel blocks were made from each fraction and burned in the volume tester after predetermined periods of aging. Each charcoal fraction was analyzed for particle size distribution, per cent ash, volatile matter, and surface area as determined by methylene blue adsorption. The block burning rate is shown as a function of the charcoal surface area in Figure 7. The instantaneous gas flow rates under actual conditions for blocks from each charcoal size fraction are plotted against time in Figure 8. The block-burning rate is shown as a function of the mass median charcoal particle diameter in Figure 9. The maximum gas temperature, maximum pressure differential, and block density are shown as functions of the mass median charcoal diameter in Figures 10, 11, and 12, respectively. The values given are the average of eight blocks from each charcoal fraction. The block ages range from 6 to 200 days. In

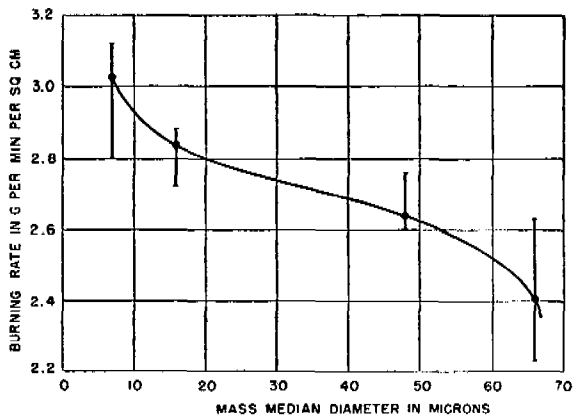


FIGURE 9. Burning rate of E29R1-type blocks as a function of mass median charcoal diameter.

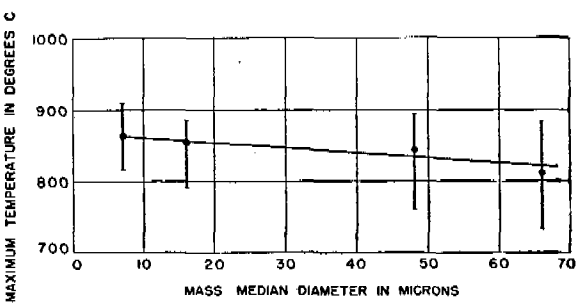


FIGURE 10. Maximum gas temperature vs mass median diameter of charcoal.

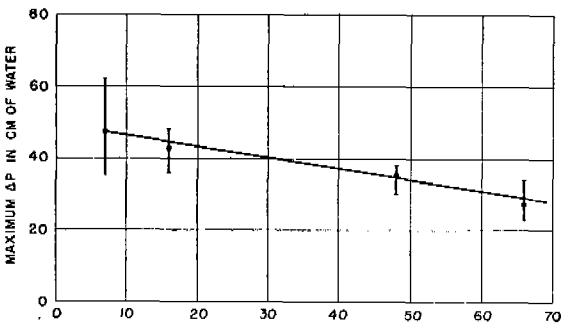


FIGURE 11. Maximum pressure differential above fuel block vs mass median charcoal diameter.

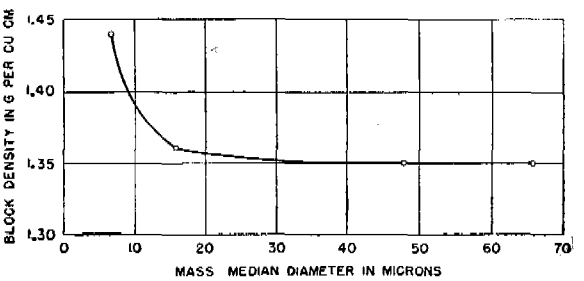


FIGURE 12. Block density vs mass median charcoal diameter.

each figure the average value is represented by a dot; the range is indicated by the line.

2. *Alkali "activation" of charcoal.* A number of investigators have found K_2CO_3 to be a catalyst in the oxidation of charcoal.[14–17] To extend these observations to the burning characteristics of fuel blocks, the following solutions were made up: 1.5*M* H_3PO_4, 5% K_2CO_3, 10% K_2CO_3, 25% K_2CO_3, and water. To 1,000 g of each of these solutions, 750 g of Flower City 5CC charcoal was added. These slurries of charcoal were kept for 24 hr with occasional hand stirring. They were then vacuum dried at 85 C. After cooling, the solid masses were reground to pass a 48-mesh screen. Nine blocks of 500 g each were made with each treated charcoal as well as with an untreated charcoal. The composition used is given below. The weight of charcoal was corrected in each case for the weight of impregnant adsorbed on the surface so that the weight of actual charcoal was the same in each case.

NH_4NO_3	83 parts
Oil	3 parts
Charcoal	11 parts
Block weight:	500 g

Blocks were pressed into E29R1 cans equipped with paper insulating liners, and were burned in the open and in the surge tester after aging three and nine days. These data are summarized in Table 3, and indicate that pretreatment of charcoal has a large effect on the burning rate of the block. A burning rate range of from 1.35 to 3.4 g per min per sq cm has been obtained in blocks of identical composition by controlling the charcoal activity through pretreatment with phosphoric acid or K_2CO_3. These data offer a reasonable explanation for the ability of KNO_3 to increase the burning rate. Since KNO_3 forms K_2CO_3 on burning with carbon, an alkali activator is supplied for the remaining charcoal.

3. *Other factors influencing the reactivity of charcoal.* Charcoal properties such as degree of carbonization, volatile matter content, and other factors as yet undefined, which are influenced by the type of material carbonized and the methods of carbonization, are no doubt also important. A complete study of the oxidation of charcoal should include detailed data on the source and type of wood used, on the methods of carbonization, and on the storage and handling of the charcoal before use. Such data are not available for commercial charcoal. Crude temperature and ventilation controls in the retorts, poor timing control for

TABLE 3. Activation of charcoal with solutions of H_3PO_4 and K_2CO_3.

Solution for treating charcoal	*p*H of* charcoal	Age of block days	Burning time: Taper min	Burning time: Total min	Burning time: Effective min	Burning rate g/min sq cm	Surging
1.5*M* H_3PO_4	1.70	3	11.6	12.0	11.8	1.36	None to 10 lb/sq in. = maximum obtainable
		9	11.5	12.0	11.7	1.37	
		9	11.7	11.8	11.7	1.37	
Water	6.76	3	6.3	6.5	6.4	2.51	None to 50 lb/sq in.
		9	5.6	6.4	6.0	2.68	
		9	5.6	6.4	6.0	2.68	
Untreated		3	6.3	6.5	6.4	2.51	None to 50 lb/sq in.
		9	6.2	6.6	6.4	2.51	
		9	6.2	6.4	6.3	2.55	
5% K_2CO_3	9.20	3	5.4	5.6	5.5	2.92	None to 50 lb/sq in.
		9	5.1	5.4	5.3	3.03	
		9	5.2	5.4	5.3	3.03	
10% K_2CO_3	9.44	3	5.1	5.4	5.3	3.03	None
		9	5.2	5.3	5.2	3.08	
		9	5.0	5.2	5.1	3.15	
25% K_2CO_3	9.36	3	4.81	5.1	4.9	3.28	None
		9	4.5	4.9	4.7	3.41	
		9	4.5	4.8	4.7	3.41	

Block composition — 500 g mix

NH_4NO_3	83 parts
Linseed oil	3 parts
Charcoal	11 parts

Blocks in E29R1 cans with paper liners
Block area: 31.1 sq cm

* *p*H of slurry made with 10 g charcoal plus 10 g boiled distilled water. Addition of an extra 10 ml of water had no appreciable effect on *p*H values.

the carbonization process, and division of management between processes, make control of the product difficult.

Attempts to specify the properties of charcoal by laboratory tests have not as yet been successful. At the present time, the most practical method of charcoal characterization is by making a test fuel block.

4. *Variables in ammonium nitrate.* The ammonium nitrate used in these investigations has been sufficiently uniform so that differences in block performance cannot be attributed to differences in this ingredient. Data taken from pilot plant production of fuel blocks have shown no consistent correlation between changes in burning time and changes in lots of ammonium nitrate.

5. *Particle size of ammonium nitrate.* The ammonium nitrate in particle size ranges larger than 20 mesh, between 20 to 35, and 35 to 60 mesh showed no consistent variation in burning rate. The fractions smaller than 60 mesh burned somewhat faster. That the burning rate is relatively independent of the particle size suggests that the ammonium nitrate either vaporizes or undergoes thermal decomposition before it reacts in the block. This seems much more probable than a solid-solid reaction between charcoal and ammonium nitrate.

6. *Moisture content of ammonium nitrate.* Moisture in excess of 0.75% in the ammonium nitrate affects the burning properties of the block. The tendency of ammonium nitrate to corrode steel also increases with an increase in the moisture content. Detailed surveillance tests were not made at higher moisture contents. Burning tests only, made on blocks 17 days old, indicated that 0.5% moisture is a safe maximum limit for moisture content of ammonium nitrate as far as its effect on burning properties is concerned. Figure 13 shows the effect of moisture. This moisture content of 0.5% should not be considered as a final specification, since the effect of moisture on the storage and surveillance of the final munitions has not been thoroughly tested. In any such tests, the effect of moisture in the block on corrosion of the can should be noted. It has been reported[11] that moisture increases the powder breakup due to phase changes of NH_4NO_3. This may have to be considered also.

It has been the practice of this laboratory to dry the ammonium nitrate until the moisture content, as determined by perchlorethylene extraction, is below

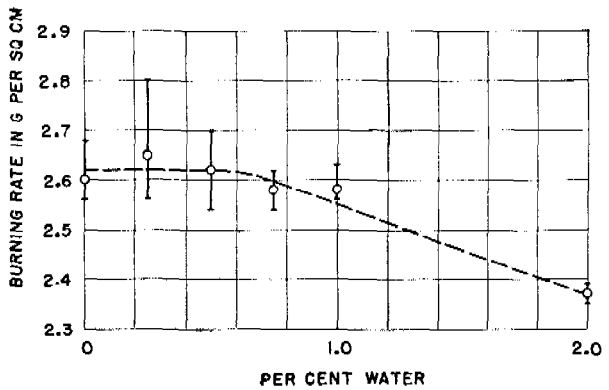


FIGURE 13. Burning rate of E29R1-type fuel blocks as a function of the per cent water in NH_4NO_3.

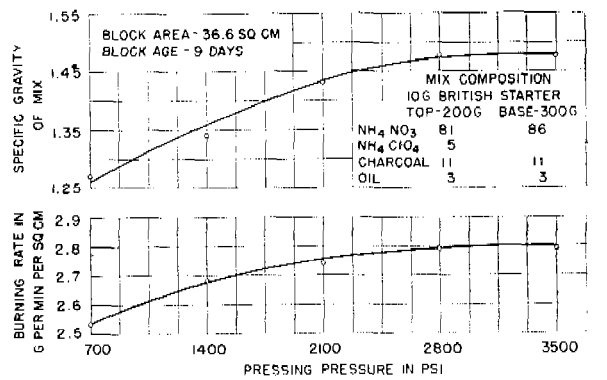


FIGURE 14. Specific gravity and burning rate of an E29-type block as a function of pressing pressure.

0.01%. In the light of the above data, it might be possible to modify this specification to allow up to 0.5% H_2O in the ammonium nitrate.

7. *Physical properties of ammonium nitrate.* Ammonium nitrate is preferred over any other oxidizing agent because of the large volume of gas and heat produced in its decomposition. It has two rather serious limitations: (1) It is hygroscopic. (2) It exists in five different crystalline modifications, and the change in crystal volume which accompanies the change from one form to another has been reported to cause powder breakup. The phase modifications of ammonium nitrate are:

$$\text{Vapor} \rightleftharpoons \text{Liquid} \overset{169.6^\circ}{\rightleftharpoons} \text{Cubic I} \overset{125.2^\circ}{\rightleftharpoons} \text{Tetragonal II}$$

$$\text{Tetragonal II} \overset{84.2^\circ}{\rightleftharpoons} \text{Tetragonal V} \overset{-18^\circ}{\rightleftharpoons} \text{IV Rhombic} \overset{32.1^\circ}{\rightleftharpoons} \text{Monoclinic III}$$

The most troublesome transitions are those occurring at −18 C and 32.1 C. Powder breakup due to the change from III to IV has been one of the main objections to the use of ammonium nitrate in rocket mixtures. Wallerant [18] stabilized form V throughout the entire range −18° to 82° by adding isomorphous $CsNO_3$. Crystallization with small percentages (5 to 20%) of potassium nitrate together with very small amounts of magnesium nitrate hexahydrate have been useful in suppressing the 32° transition.[11] In fuel blocks with a boiled linseed oil binder, as described here, this transition has not appeared to be serious. The other objection to the use of ammonium nitrate, its hygroscopic nature, has been partially overcome by the use of an oil binder and by coating exposed surfaces with a waterproof lacquer.

VARIABLES DUE TO MANUFACTURING PROCEDURE

Mixing. Various mixers have been used successfully for blending the ingredients. The product obtained should be uniformly blended and the oil should be worked into the composition thoroughly. All mixers give some grinding action. In some cases the amount of grinding was of major importance in determining the properties of the block produced. If, however, a mixer gives a uniform product with the proper particle size distribution, it should be satisfactory. Some changes in the preparation of the ingredients might be necessary with other types of mixers. In practice it is desirable to keep both mixing time and the size of the charge for a given mixer constant, since the extent of grinding is increased by an increase in the mixing time and decreased by an increase in the size of the charge.

Pressing. The factors of major significance in the pressing of fuel blocks include the following.[19]

1. Pressing pressure.
2. Distribution of the mixture in the can.
3. Flow characteristics or fluidity of the mixture.
   a. Temperature of the mixture.
   b. Amount and fluidity of the binder.
   c. Particle size.
   d. Efficiency of coating of the mixture with the binder.
   e. Presence of wetting or flow agents.
4. Pressing technique.
   a. Time and means allowed for the escape of air entrapped in the mixture.
   b. Time pressure is maintained in the mixture.
   c. Type of press, as single or double end pressing arrangements.
   d. Rate of pressure release.

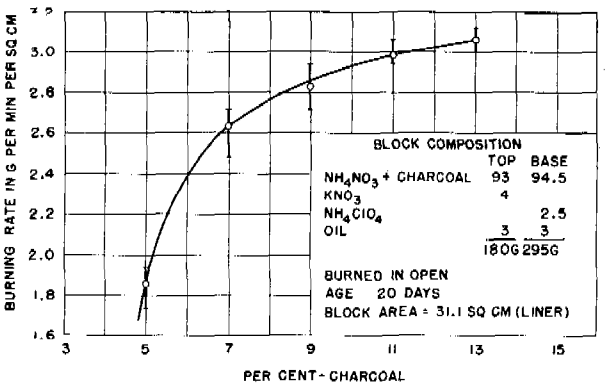


FIGURE 15. Burning rate of E29R1-type block as a function of per cent charcoal in block.

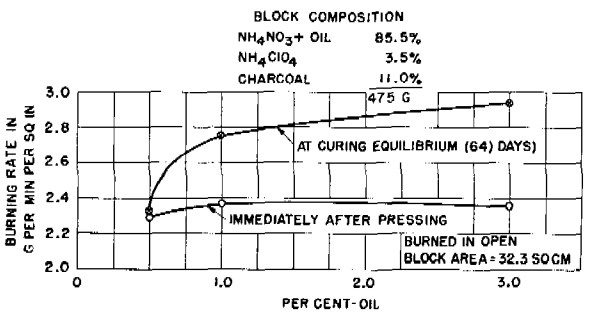


FIGURE 16. Burning rate of E29R1-type block as a function of per cent linseed oil in block.

Of these factors, only the first has been systematically investigated in this laboratory. A series of E29-type blocks was made in which the pressing pressure ranged from 700 psi to 3,500 psi. After aging nine days at room temperature, the block dimensions were measured and they were burned in the open. The block density and burning rate are shown as functions of the pressing pressure in Figure 14.

In connection with the remaining factors, only qualitative data are available. The fluidity of the mixture is increased by an increase in temperature and an increase in the amount of liquid binder. An increase in fluidity results in more uniform pressure distribution throughout the block. In mixtures of low fluidity it is essential that the mixture be evenly distributed in the can before pressure is applied, and it is frequently desirable to press in several increments to insure uniform pressure distribution and block density.

It has been found [19] that rocket fuel pellets could be pressed in large single increments by control of mixture fluidity and application of pressure over periods of time up to 10 to 12 min. Special techniques in the application of pressure were essential to allow

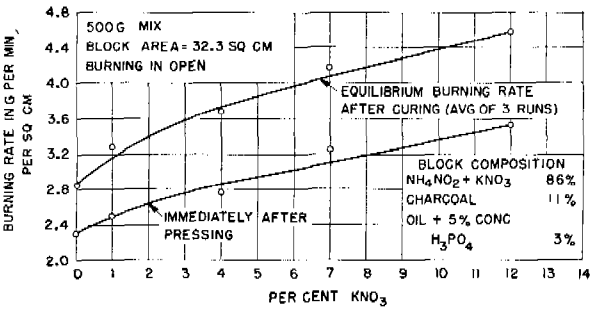


FIGURE 17. Burning rate of E29R1-type blocks as a function of per cent KNO_3 in block.

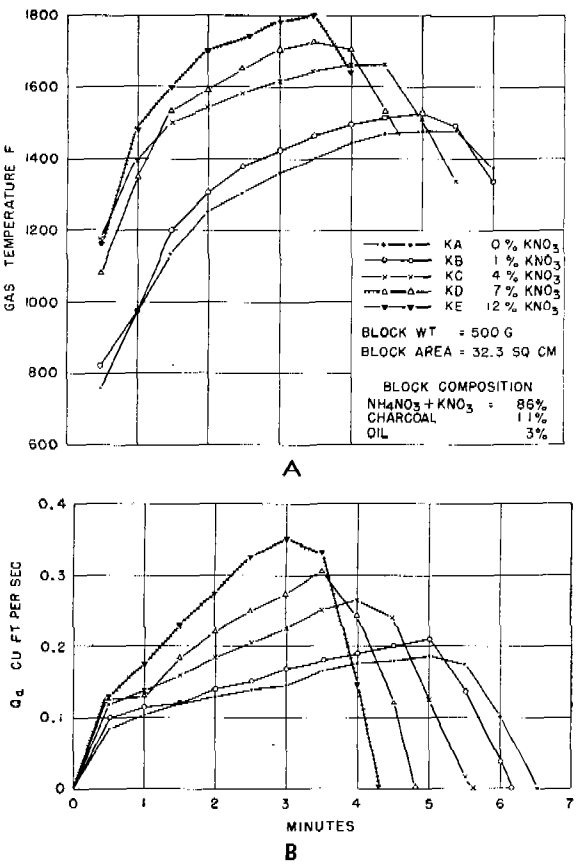


FIGURE 18. (A) Temperature of exit gases during burning of E29R1 fuel blocks containing different amounts KNO_3. (B) Gas flow rate under actual conditions for KNO_3 series.

the escape of air trapped in the block. In some cases double acting presses were used, thus applying pressure on both the top and the bottom of the pellet.

In this work, fuel blocks have been pressed in increments.

Lacquering. The exposed surfaces of all finished blocks are coated with a special pyroxylin base lacquer for protection against moisture. For best re-

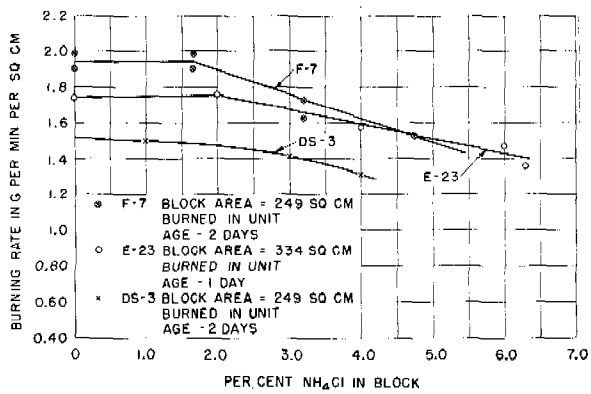


FIGURE 19. Burning rates of F7- and E23-type fuel blocks as functions of the NH_4Cl content of the block.

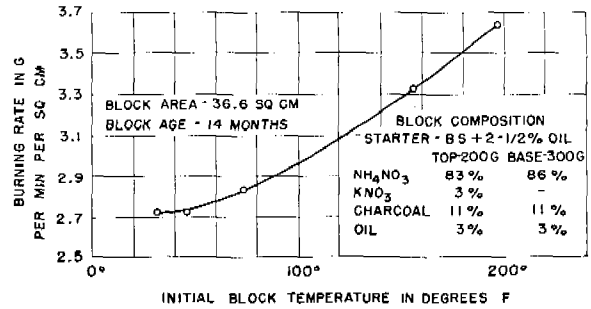


FIGURE 20. Burning rates of E29-type fuel blocks as a function of initial block temperature.

sults the lacquer should be restricted to the surface of the block. Penetration into the interior should be avoided for two reasons. (1) There are some indications that organic solvents promote surging with some charcoals. (2) An excess of lacquer tends to make the block ignite slowly. The best results and minimum penetration are achieved by spraying the lacquer at as high a viscosity as is practical. This is determined by the spray equipment available. Spraying is more satisfactory than brushing. The lacquer coat is less liable to crack at higher storage temperatures if the block is heated before the lacquer is applied.

FORMULA CHANGES

Required changes in block-burning rate have been achieved largely by formula variation. Ammonium nitrate has been the basic oxidizing agent in all mixtures, charcoal has been the basic reducing agent, and boiled linseed oil has been the basic binder. To these ingredients certain additives such as KNO_3 have been added to increase the burning rate and other additives such as NH_4Cl have been used to lower the burning rate.

Effect of Charcoal–Ammonium Nitrate Ratio on the Burning Rates of E29 Type Blocks. A series of E29R1 fuel blocks was made in which the charcoal-ammonium nitrate ratio was systematically varied. These were pressed into cans with 0.025-in. paper inner liners, aged twenty days, and burned in the open in triplicate. Data are presented in Figure 15. The greater change in burning rate occurred for charcoal percentages below 7%. Blocks containing 5% charcoal surged even when burned in the open. This is discussed in detail later under surging. All burning rates are computed using effective time, which is the arithmetical average of the total burning time and the time until the burning first begins to taper off.

Effect of Linseed Oil–Ammonium Nitrate Ratio on Burning Rates of E29R1-Type Blocks. In Figure 16, data showing the variation in burning rate of a single composition E29R1-type block as a function of per cent linseed oil binder are given. The increase in burning rate on curing is very pronounced in blocks containing 1 to 3% linseed oil. Paper liners in the fuel cans were not used in these tests nor in those reported below, unless specifically mentioned.

Effect of Potassium Nitrate-Ammonium Nitrate Ratio on Burning Rates of E29R1-Type Blocks. The effect of KNO_3 on block characteristics is shown in Figure 17 as burning rate vs per cent KNO_3. Temperature vs time curves and the gas flow rate vs time curves are given in Figures 18A and 18B respectively.

The volume of gas, corrected to 60 F and 1 atm, produced by blocks containing amounts of KNO_3 up to 12% was the same, within experimental error, as the volume produced by blocks containing no KNO_3.

Effect of Ammonium Chloride on the Burning Rates of E32- and F7-Type Blocks. Substitution of ammonium chloride for ammonium nitrate has been a satisfactory method for reducing the burning rate of fuel mixtures in the F7 and in the E23 units. In Figure 19, the burning rates of blocks for three different munitions are shown as a function of per cent NH_4Cl. All these blocks contain a top layer to give more rapid starting. NH_4Cl is added only to the base layer.

A number of other modifications were made in the composition of the mixture. For the details of these, reference should be made to the original report.[1]

VARIABLES DUE TO THE BURNING CONDITIONS

Block temperature, gas pressure on the block during burning, wall effects, etc., are of major significance

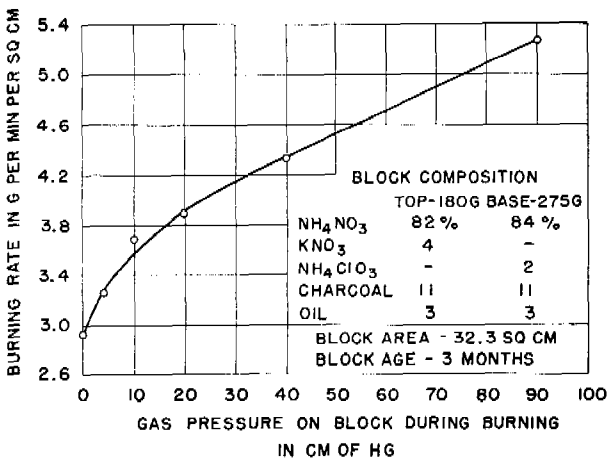


FIGURE 21. Burning rate of E29R1-type fuel block as a function of gas pressure on block during burning.

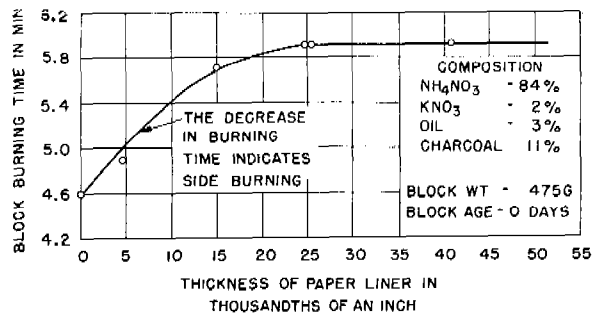


FIGURE 22. Effectiveness of paper liners in fuel can in retarding side burning in E29R1-type blocks.

in block performance. Not only do they influence the burning rate, but also temperature and pressure influence the surging of fuel blocks during burning.

Influence of Initial Block Temperature on Burning Rates of E29-Type Blocks. In Figure 20 the burning rate of E29 blocks is shown as a function of the initial block temperature. The blocks were in hexagonal E29 cans and had been stored for one year in a dry room at about 25 C before these tests were made.

Influence of Pressure During Burning. In Figure 21 the burning rate of standard E29R1 blocks is shown as a function of the gas pressure on the block during burning. The block temperature was initially about 25 C.

Effect of a Paper Liner in the Fuel Can. Inspection of the instantaneous flow rate vs time curves for standard one-layer E29R1 blocks reveals a gradual increase in gas flow rate with time of burning. The most likely cause[19] is an increase in the burning surface due to burning down the sides of the block.

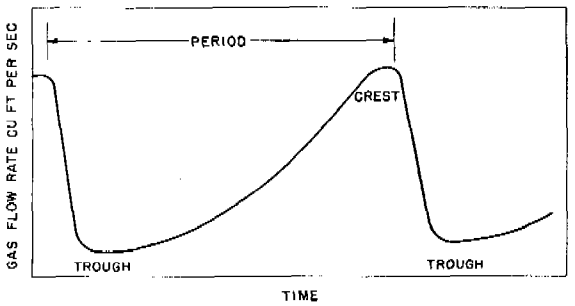


FIGURE 23. Typical flow rate - time curve for a fuel block while surging.

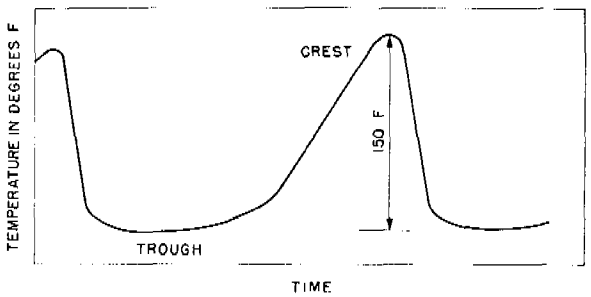


FIGURE 24. Typical temperature — time curve for a fuel block while surging.

Since side burning is due largely to heat conduction along the walls of the container, such burning can be decreased greatly by placing a nonconducting liner between the wall and the fuel mixture. In the E23 smoke generator, cardboard was used by the National Fireworks Co. as an insulator with good results. Such a liner aids in maintaining a more even gas flow rate and in decreasing the taper time.

The results of tests to determine the minimum thickness of paper insulator necessary to prevent side burning in the E29R1 block are given in Figure 22.

Since all blocks have the same composition, any decrease in burning time with a decrease in liner thickness indicates side burning. The minimum thickness of paper to prevent side burning completely is about 0.025 in. However, no center cone during burning was observed when paper 0.015 in. or over was used. A 0.015-in. liner of stencil board was used with good results in the E29R1.

31.3.5 Surging in Fuel Blocks

DESCRIPTION

Surging of fuel blocks is an irregular type of combustion characterized by a rapid evolution of gas

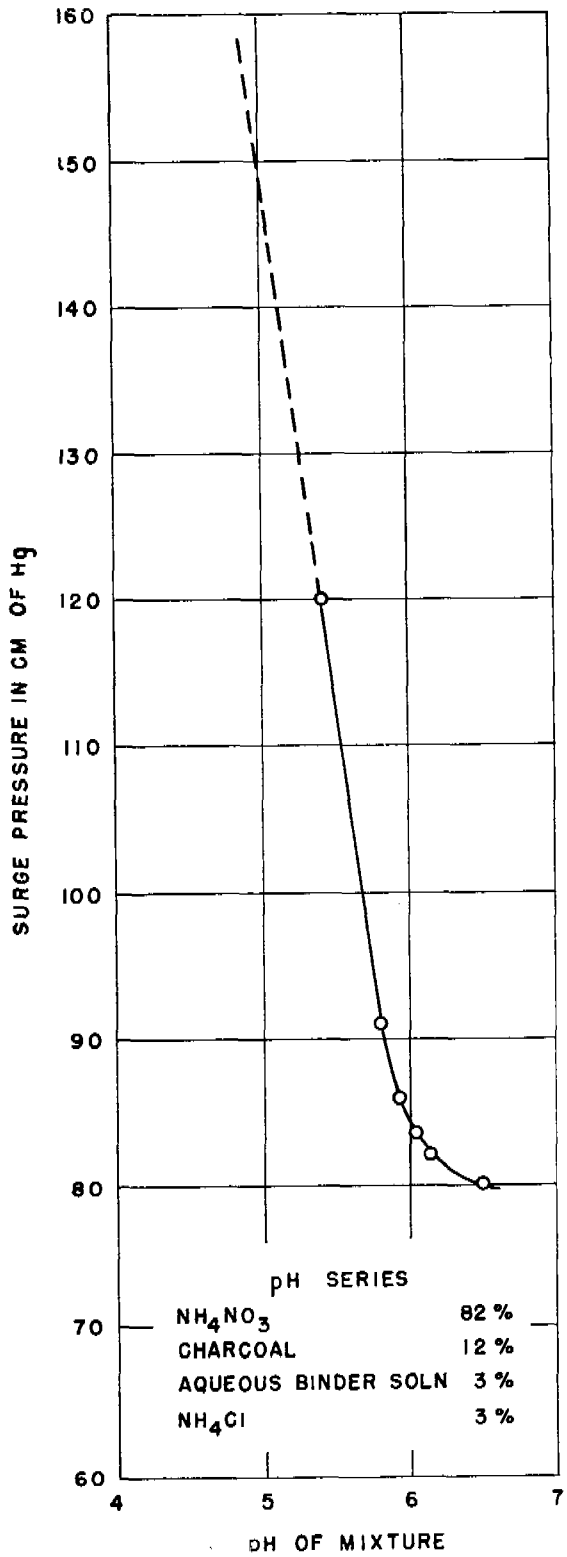


FIGURE 25. Effect of *p*H on surge pressure of fuel block. Block of *p*H 3.5 did not surge up to 220 cm Hg.

followed by a sharp decline in burning rate. This repeats itself many times in a regular cycle, giving a gas flow rate curve such as shown in Figure 23 and a temperature curve as in Figure 24. The length of time between successive crests (moments of maximum flow) is termed the *period* of the surge. This has ranged from 2 sec to 50 sec. Generally, an increase in the length of the period increases the violence of the surge.

The time of appearance of surging is unpredictable. It has been observed at the start, the middle, and the end of the burning time, as well as throughout the entire burning time. It has appeared in units of all sizes, ranging from the smallest grenade up to the 125-lb *B* model thermal generator, and appears to be very similar to "chuffing" in rockets.[10] Substitution of a boiled linseed oil binder for the cellulose nitrate-acetone binder decreased the frequency with which surging appeared in experimental fuel blocks. In fact, experimental work was conducted for several months before surging was observed with blocks containing an oil binder. On the other hand, cast blocks described later surged frequently in the early development. Hundreds of cast blocks and thousands of pressed blocks have been made which did not surge. Nevertheless, surging is not well understood. It causes the munition to malfunction and is occasionally dangerous to personnel, and should therefore be eliminated from the fuel blocks.

A series of blocks was made in which aqueous alkali solutions and acid solutions of different concentrations were used to replace the linseed oil as a binder in pressed compositions. The *p*H of each of these mixtures was determined, using a glass electrode. From this series a definite relationship between the pressure at which these blocks began to surge and the *p*H of the mixture was established. Data are given in Figure 25. The pressure at which surging began was quite characteristic and was taken as a semiquantitative measure of the surging tendencies.

During the development of the 50-lb colored smoke Mk 72 Mod 2 bomb, blocks were made from a new batch of charcoal and burned in a test munition. A very violent surging occurred soon after ignition and blew the unit apart. Subsequent blocks from this same lot of charcoal gave similar performance when burned in a dummy unit. Other blocks were then made using the same lots of ingredients except that another batch of charcoal was used. These blocks did not surge. The evidence indicated that, in this particular case, surging was related directly to the charcoal used.

Laboratory Analysis of Charcoal Which Caused Surging

The surge-producing and the smooth-burning charcoals were examined in some detail in the laboratory. Spectrographic analyses of the ash from both types showed no difference in their mineral composition. X-ray diffraction studies of the ash showed no difference between the charcoals.

Surface properties of the charcoals were next considered. Variations in the performance of charcoal have been attributed to the presence or absence of oxides on the charcoal surface.[16] Such oxides increase the ability of the charcoal to remove alkali from solution and decrease the ability to remove acid.[22] Charcoal, containing surface oxides, adsorbs polar molecules such as H_2O more rapidly than clean charcoal, and will thus settle much more rapidly in water.[22]

In order to establish the presence or absence of surface oxides, both the surge charcoal and good charcoal were floated on distilled water and the rate of settling of both samples was observed. The good charcoal wet easily and settled rapidly, thus indicating the presence of surface oxides. The surge charcoal failed to wet and was still floating after 24 hours. This indicated little surface oxide. Acid capacity was checked but differences in this test were too small to be significant. Thermal analysis of the two charcoals made according to the methods of Grim [23] showed no differences between the good and surge charcoals. Data on smooth-burning and surge charcoal are summarized in Table 4. The most significant difference is the evidence of surface oxides on the smooth-burning charcoal, and the lack of such oxides on the surging charcoal.

Table 4. Summary of tests on surging and nonsurging charcoals.

Test	No surge	Surge
% volatile matter	5.6	5.1
% ash	8.5	7.2
Mass median particle diameter (microns)	13.0	12.0
Charcoal surface area (sq m/g)	3.3	3.3
*p*H initial — 10 g C + 20 cc water	9.0	9.2
*p*H after adding 20 cc 0.22*N* HCl	6.0	5.9
*p*H as above after 24 hr	6.9	6.8
Ease of wetting	Very easy	Very difficult
Spectrographic analysis of ash	No difference	
X-ray diffraction analysis of ash	No difference	
Ignition temperature curves	No consistent difference	

Surging in Fuel Blocks Containing Only Five Per Cent Charcoal

Analysis of the Gases from a Surging Fuel Block Containing Only Five Per Cent Charcoal. Direct chemical evidence as to the reactions involved in surging was obtained by analyzing the gases. A block containing only 5% charcoal surged even when burned in the open. When burned under a pressure of 2 cm of mercury above atmospheric, surging was very pronounced, and it was possible to obtain gas samples at the trough of the surge (low rate of gas evolution) and the crest of the surge (high rate of gas evolution). These data are summarized in Table 5. The charcoal used in the production of fuel blocks has been analyzed for C, H, N, O, and ash. From the analysis, the formula for the charcoal may be written as C_6H_3O + 10% ash. The following reactions for the trough and crest of the surge fit the analytical data with considerable precision.

Charcoal	C_6H_3O + 10% ash
Linseed oil	$C_{57}H_{90}O_6$
Ammonium nitrate	NH_4NO_3

1. Reaction for crest:

$$17NH_4NO_3 + C_6H_3O + 0.03C_{57}H_{90}O_6 \longrightarrow 33H_2O + NO_2 + N_2O + 6.3CO_2 + 3.8H_2 + 15.5N_2 + O_2 + 1.5CO$$

Overall block composition		Composition of above reacting mixture	
NH_4NO_3	92%	NH_4NO_3	91.6%
Charcoal	5%	Charcoal	6.6%
Linseed oil	3%	Oil	1.8%
	100%		100.0%

2. Reaction for trough:

$$17NH_4NO_3 + 0.09C_6H_3O + 0.06C_{57}H_{90}O_6 \longrightarrow 36.8H_2O + 3NO_2 + 4CO_2 + 14.9N_2 + 0.6N_2O$$

Overall block composition		Composition of above reacting mixture	
NH_4NO_3	92%	NH_4NO_3	95.5%
Charcoal	5%	Charcoal	0.7%
Linseed oil	3%	Oil	3.6%

Discussion. From these data the course of the surge reaction *in this particular block* may be outlined. During the crest of the surge, NH_4NO_3 and the charcoal react according to reaction (1). It will be noticed, however, that the reacting mixture is richer in charcoal (6.6%) than the overall block composition (5%), and thus a layer of NH_4NO_3 containing some linseed oil but little charcoal is left on the immediate surface of the block. This layer burns

TABLE 5. Summary of gas analysis data for surging blocks containing 5% charcoal and 11% charcoal.

	5% charcoal				11% charcoal			
	Trough		Crest		Trough		Crest	
Gas	Observed	Calculated*	Observed	Calculated*	Observed	Calculated*	Observed†	Calculated*
H_2O	63.6	62.1	52.6	52.5	47.4	48.2	47.4	47.4
NH_3	0.4	0.0	0.05	0.0	0.0	0.0	0.0	0.0
NO_2	5.03	5.1	1.6	1.6	0.0	0.0	0.0	0.0
CO_2	6.4	6.7	10.4	10.0	11.5	11.9	13.7	13.9
CO	0.4	0.0	2.5	2.4	4.9	5.1	2.5	2.5
H_2	0.1	0.0	5.5	6.0	7.8	7.8	8.7	8.6
O_2	...	...	...	1.6	0.6	1.3	1.5	1.4
N_2 (residual)	24.9	25.1	27.3	24.6	28.1	25.7	26.0	26.2
N_2O	...	1.0	...	1.6	...	...	...	...
Mol wt	23.7	23.9	23.6	23.5	23.6	23.2	23.2	23.3

* Analysis calculated from equations given in the text.

† Observed analysis was corrected for an air leak.

through slowly according to the reaction given in the trough. The linseed oil is the chief reducing agent in the trough reaction, and it is known that linseed oil alone burns more slowly than charcoal. When the slow burning mixture has reacted, a normal surface is exposed and the charcoal again burns out rapidly in a crest reaction. Thus, the process is cyclic. It is probable that the linseed oil consumed in the crest reaction is present on the surface of the charcoal.

This mechanism of surging in a block containing 5% charcoal is supported by the following experimental data.

1. Analysis of gases from the trough, crest, and an intermediate point in the surge cycle, has given definite and consistent experimental support for the reactions outlined.

2. Blocks made at the same time with the same procedure from the same ingredients, but containing 7, 9, 11, and 13% charcoal, did not surge under any pressure, since only 6.6% charcoal is necessary to maintain the crest reaction outlined in the preceding paragraph.

3. Such a 5% charcoal block, when burned in the open, shows a mild form of surging which was amplified by any restriction to the high gas flow.

4. When the 5% block surges in the open, the crest of the surge and the crest *only* is marked by the evolution of a large number of sparks. The combustion of charcoal gives sparks while the combustion of linseed oil does not.

SURGING IN BLOCKS CONTAINING ELEVEN PER CENT CHARCOAL

Analysis of Gases From Surging Block Containing Eleven Per Cent Charcoal. Several E29-type blocks which surged had the following composition.

	Top — 200 g	Base — 300 g
NH_4NO_3	81%	85%
KNO_3	5%	1%
Charcoal	11%	11%
Linseed oil	3%	3%

They had been stored in a $CaCl_2$ dry box in an air-conditioned room for 14 months. Surging characteristics developed after about two or three weeks of storage. Gas samples were taken of a crest and trough. Analysis of the gas samples failed to show a large difference between trough and crest. This is in direct contrast to the block containing only 5% charcoal. Data are given in Table 5. The data for the crest fit the following equation with fair precision.

1. Surge crest of E29-type block.

$$17.0NH_4NO_3 + 0.8KNO_3 + 1.67C_6H_3O + 0.033C_{57}H_{90}O_6 \longrightarrow 32.7H_2O + 8.1CO_2 + 3.5CO + 5.3H_2 + 17.4N_2 + 0.9O_2 + 0.4K_2CO_3$$

The following equation fits the trough data.

2. Surge trough of E29-type block.

$$17.0NH_4NO_3 + 0.8KNO_3 + 1.6C_6H_3O + 0.03C_{57}H_{90}O_6 \longrightarrow 31.9H_2O + 9.2CO_2 + 1.7CO + 5.8H_2 + 17.4N_2 + 1.0O_2 + 0.4K_2CO_3$$

This reaction is very similar to the crest reaction.

The compositions of the reacting mixtures for the 11% block, as calculated from the above equations, are as follows.

	Crest	Trough	Actual as prepared
NH_4NO_3	83.1%	83.5%	81%
KNO_3	4.9%	5.0%	5%
Charcoal	10.2%	9.8%	11%
Oil	1.8%	1.7%	3%

[redacted]

Compositions for the crest and trough are very close to the prepared compositions of the block. Considerable carbonaceous material was left in the fuel container.

In summary, the following will be noted regarding the gas analysis of a surging block containing 11% charcoal.

1. A large difference in composition between trough and crest samples was *not* observed.

2. Somewhat more complete combustion occurs in the trough, producing more CO_2 and less CO.

3. The data indicate conclusively that large differences between trough and crest such as were observed in the 5% charcoal block do not exist in the 11% charcoal block.

Discussion. An explanation of surging in the 11% charcoal block is suggested by the results from the 5% charcoal block. If the charcoal in the 11% block were not of uniform activity, the more readily combustible material would burn out first to give the crest of the surge. The less active material would then burn more slowly in the trough. As soon as a fresh layer of the block was again exposed the more active charcoal would burn rapidly to give another crest, and this would be followed by a trough. Since charcoal would be burning in both cases (contrast with the block containing 5% charcoal), the reaction products should be the same in both cases except for somewhat more complete combustion where the charcoal is not as available. This is actually observed; the per cent CO_2 is slightly higher and CO is lower in the trough where charcoal is presumably less reactive. The more rapid combustion at the crest would explain the maximum temperature found there.

Mechanism of Surging

When two reducing agents are present in a mixture containing sufficient oxidizing agent for both and when the oxidizing agent reacts in the gas or vapor phase, these two reducing agents tend to be oxidized simultaneously. However, one will usually react faster than the other and become depleted from the reacting layer. The oxidation of the second agent then proceeds at a slower rate until the burning layer reaches more of the first agent. This results in periodic changes in the burning rate and has been observed as surging in thermal generator fuels or chuffing in rocket fuels. For example, if both charcoal and sulfur were included in the same block with sufficient oxidizing agent for both, the mixture could be expected to burn with periodic fluctuations in the burning rate and also in the relative percentage of CO or CO_2 and SO_2 in the reaction gases. In this case the course of the two reactions could be easily followed in the analyses of gas samples taken at several times during a surge period.

The results with 5% charcoal in the fuel represent a similar case with the linseed oil and charcoal serving as the two reducing agents. Here it is not so easy to trace the two reactions in the gas analysis, but it is possible, and this has been done. It is not necessary that the two reducing agents be different chemical compounds. If the same chemical compound is present in two different physical states such that one reacts more readily than the other, the same periodic burning will result. In this case it will not be possible to trace the slow and fast reaction by the analysis of the reaction gases, since both result in the same gaseous products. This was the case with 11% charcoal in the block.

It is not quite clear why the more reactive compound does not continue to react down through the block and leave the less reactive behind to burn later. It is an experimental fact, however, that this does not occur in these highly consolidated fuel blocks. The reaction proceeds regularly down through the block and completes itself in one layer before passing on to the next.

In the case of charcoal used as the reducing agent, it is understandable that one part could be more reactive than another or that latent tendencies in that direction could be further developed in the course of processing or burning. This has been apparent in several tests. Surging resulted from the addition of water or alkali solutions to the charcoal. The water would tend to develop differences in wetability, and the alkali in *alkali activation.* Surging in the intermediate pressure range has been observed, but not at high pressures (500 to 1,000 psi). This may be due to differences in the adsorption of the oxidizing vapors, which are critical in this range. Low temperatures often augment surging tendencies, whereas linseed oil as a binder diminishes them.

Charcoal oxidation is retarded by surface oxides and the catalytic action of alkali is due to its ability to remove those oxides and expose a clean reaction surface.[16] Clean charcoal without oxides on the surface would be more reactive than that heavily coated with the oxides. This clean charcoal burns very rapidly and produces a very violent and even explosive surge. This was observed in connection with a charcoal which surged and blew up. Examination

of this charcoal gave evidence of very little surface oxide. Smooth-burning charcoal gave evidence of considerable surface oxide.

Summary of Experiments on Surging

The following are experimental facts regarding surging.

1. Surging is related to the charcoal used in the block.
   a. Surging charcoals and nonsurging charcoals show no difference in ash composition.
   b. Surging charcoals give evidence of little surface oxide; nonsurging charcoals give evidence of surface oxides.
2. Water and aqueous alkali binders promote surging of charcoal fuels. Aqueous acid binders tend to retard surging.
3. Surging of thermal generator fuels is promoted by pressure in the range 0 to 100 psi. Surging of rocket fuels takes place at comparatively low rocket pressures (300 to 400 psi) which are high compared to thermal generator pressures. At high pressures (1,000 psi +) rocket fuels do not surge.
4. Surging of both rocket and thermal generator fuels is promoted by low initial fuel temperatures.
5. Surging tendencies increase with the age of charcoal blocks.
6. The simple geometry of the unit in which the block burns is apparently not related to the surging of a fuel block.
7. Surging was observed in a block containing a low percentage of charcoal (5%).
8. Analysis of the gases from a block containing 5% charcoal which surged indicates that more charcoal burns at the crest of the surge. More linseed oil burns at the trough of the surge.
9. Analysis of the gases from a block containing 11% charcoal shows no large difference in composition between gases from the trough and crest of a surge.
10. The temperature of fuel gases rises from a minimum at the trough to a maximum at the crest of the surge.
11. No relationship between particle size of the ingredients and surging tendencies has been detected.

Predictions Based on the Mechanism of Surging

Predictions (1) and (3) have not been checked by actual experiment. They are given here as a guide for further work.

1. The surging period is longer when small amounts of fast- or slow-burning charcoal are mixed with large amounts of slow or fast charcoal, respectively.
2. Two charcoals with different burning rates, but which do not surge when each is used alone, produce surging when used as a blend. (This has been experimentally verified in one case.)
3. Charcoal from a single retort batch may be free from surging tendencies. When batches are blended, the probability of surging increases.

It is to be noted that the nature and amount of binder used may introduce unexpected results in the NH_4NO_3-charcoal system.

31.3.6 Storage of Fuel Blocks

Two difficulties in particular are to be anticipated in surveillance of munitions containing NH_4NO_3 as an oxidizing agent. These are (1) moisture damage, and (2) powder breakup due to phase changes of NH_4NO_3. Of these, the first has been the most serious problem. In munitions burning at the low pressures of the thermal generator, the effect of slight surface cracks from phase changes has not been so significant as in high-pressure powders such as gunpowder or rocket fuels. No completely satisfactory method of waterproofing the block itself has been found, and the blocks must, therefore, be used in sealed munitions. The linseed oil binder and pyroxylin lacquer coating have increased the moisture resistance so that blocks in sealed units can undergo surveillance tests satisfactorily.

Change in Burning Properties of E29 Blocks with Age

In Figure 26, the burning time of the hexagonal E29-type blocks is shown as a function of the age of the block. The blocks were stored at the three temperatures 25 C, 40 C, and 60 C and cooled to room temperature before being burned.

The conclusions on curing E29-type blocks are summarized.

1. A pronounced acceleration in burning rate (decrease in burning time) occurs as the block cures, the most rapid change occurring during the first five days. This is followed by a more gradual change for 16 to 20 days. The burning rate is then virtually constant for a given temperature of storage.

In some cases equilibrium is reached before 20 days, but, in general, no change in burning rate occurs after 20 days. Data are available for blocks as old as 563 days.

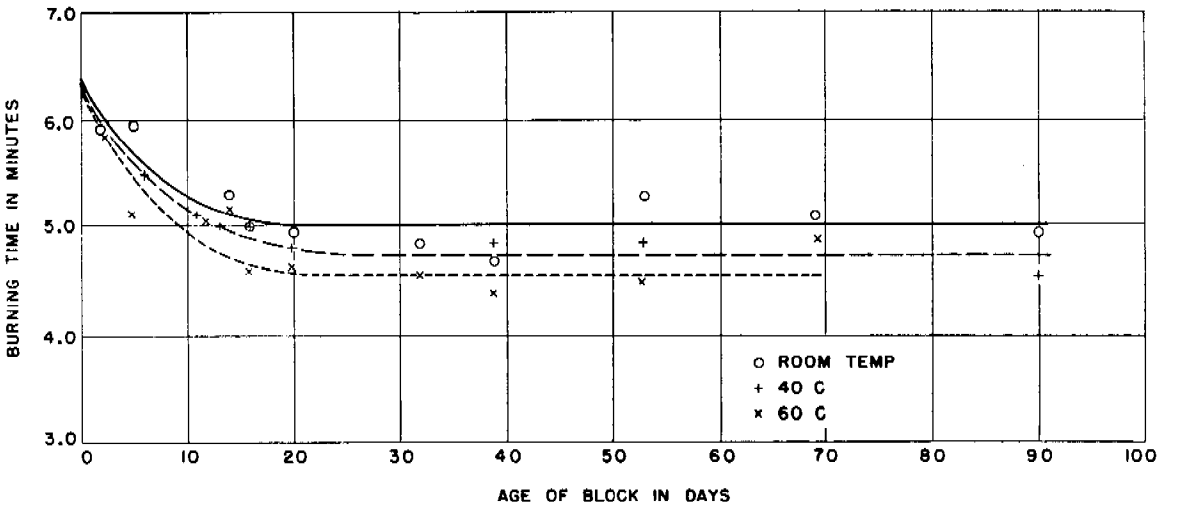


FIGURE 26. Effect of aging at different temperatures on the burning time of 500 g. Fuel blocks for E29 thermal generator.

2. The time required to reach equilibrium at high storage temperatures is not significantly different from that required at lower temperatures. The equilibrium burning *rate* for the high temperature is slightly higher than that for lower temperature. The initial rate of change of burning rate with time is, however, more rapid at the higher temperature than at the lower. (Figure 26.)

High-temperature storage at 60 C decreases the average burning time of E29 blocks by about 0.3 $\pm$ 0.1 min as compared with the average of blocks stored at room temperature. Figure 26 shows a difference of about 0.4 min, but the overall averages for a large number of blocks was less.

3. This behavior was general for all E29 mixtures.

These changes during curing were at first attributed to the polymerization or "drying" of the linseed oil used as a binder. If this were so, a commercial paint dryer in the formula should shorten the curing time. A paint dryer actually did not have any effect on the curing, although it did very markedly shorten the drying time of a thin film of linseed oil on glass.

An ammonium picrate–ammonium nitrate–ammonium dichromate–linseed oil mixture showed an excessive increase in burning rate on curing (136% increase). On the other hand, NH_4NO_3–$(NH_4)_2Cr_2O_7$–linseed oil mixtures showed no change on curing. Simple polymerization of linseed oil in the block apparently does not account for the changes. The reducing agent, such as charcoal, ammonium picrate, or guanidine nitrate, appears to have a far greater effect.

All NH_4NO_3 base blocks containing a linseed oil binder withstood cyclic surveillance and showed no breakup. Even blocks burned under 30 lb gas pressure after cyclic surveillance gave no evidence of increased burning rate due to internal cracking.

31.4 NONCARBON PRESSED FUEL MIXTURES

In view of the nonuniform properties of charcoal discussed in the preceding text, the preliminary development of a pressed fuel block which does not contain carbon was carried out, and excellent prospects of improved performance were obtained.[3] A survey of possible oxidizing and reducing agents for use in these fuels was made. Based on this survey, several promising mixtures were considered and these were given extensive preliminary tests in lined cans.

A mixture composed of guanidine nitrate, ammonium nitrate, linseed oil, and ammonium dichromate showed more promise as a thermal generator fuel than any of the other new mixtures tested.

31.4.1 Guanidine Nitrate–Ammonium Nitrate–Ammonium Dichromate–Linseed Oil

VARIATION OF BURNING RATE AND OTHER BLOCK PROPERTIES WITH $(NH_4)_2Cr_2O_7$ CONTENT

A basic mixture of NH_4NO_3 and guanidine nitrate was prepared in stoichiometric proportions for the reaction

$$(NH_2)_2CNH \cdot HNO_3 + 2NH_4NO_3 \longrightarrow 4N_2 + 7H_2O + CO_2.$$

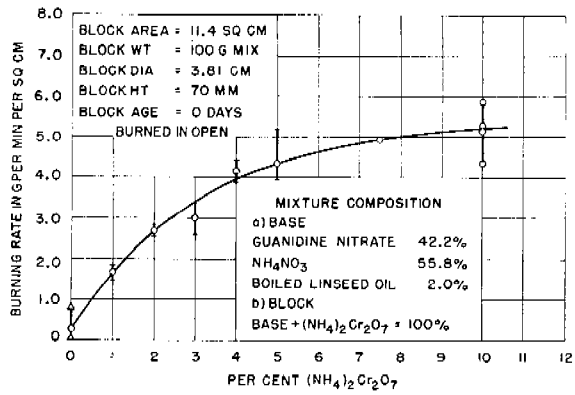


FIGURE 27. Burning rate of 100 g. Guanidine nitrate blocks as a function of per cent $(NH_4)_2Cr_2O_7$.

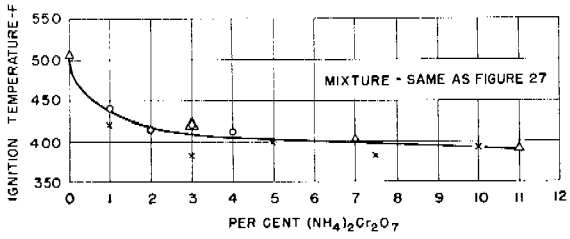


FIGURE 28. Ignition temperature for Guanidine nitrate — NH_4NO_3 mixture with increasing amounts of $(NH_4)_2Cr_2O_7$.

This mixture contained 55.8% NH_4NO_3, 42.2% guanidine nitrate and 2% linseed oil binder. To this mixture were added increasing amounts of ammonium dichromate catalyst. Small test blocks were prepared from each composition and burned in the open (740 mm pressure) two to four hours after pressing. The initial block temperature was 20 to 25 C. The burning rate is shown as a function of $(NH_4)_2Cr_2O_7$ content in Figure 27. The ignition point of each mixture is shown as a function of $(NH_4)_2Cr_2O_7$ content in Figure 28. The ignition point decreases and the burning rate increases as the per cent $(NH_4)_2Cr_2O_7$ is increased.

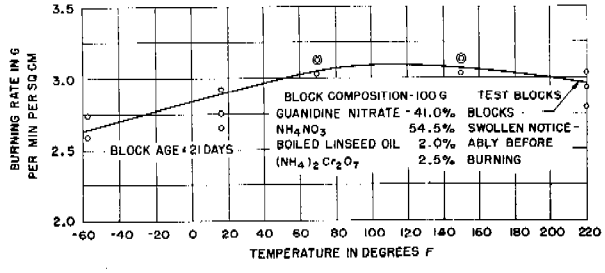


FIGURE 29. Burning rate of Guanidine nitrate - NH_4NO_3 mixture as a function of initial block temperature.

VARIATION OF BURNING RATE WITH INITIAL BLOCK TEMPERATURE

In Figure 29, the burning rates of blocks in the open are shown as a function of the initial block temperatures. The variation in burning rate with temperature for this mixture between 50 F and 220 F was small. Blocks held at 220 F swelled somewhat. This may account for the slight decrease in burning rate at the higher temperature.

VARIATION OF BURNING RATE WITH PRESSURE

In Figure 30, the burning rate is shown as a function of gas pressure during burning. The blocks had the same composition as those used in the temperature study.

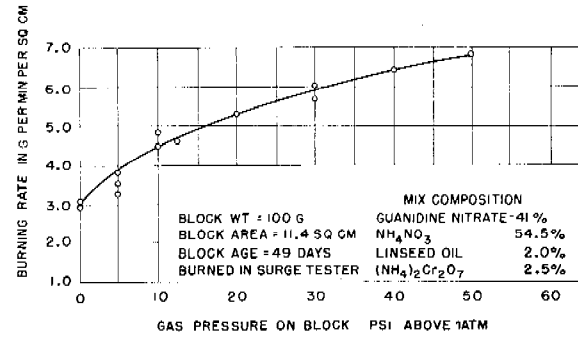


FIGURE 30. Burning rate of block as a function of gas pressure during operation.

VARIATION OF BURNING RATE WITH STORAGE TEMPERATURE

Representative blocks of the same composition as those used in the temperature study were stored for three weeks under the following conditions of temperature.

1. Room temperature (about 70 to 80 F), low humidity.
2. 150 F, low humidity (blocks were put in the oven after three days curing at room temperature).
3. Cyclic temperatures. Blocks were held 12 to 72 hr at low temperature (0 to 20 F); then transferred to 150 F storage and held for an equal period of time. This cycle was repeated eight to ten times. The temperature range includes two transition points for NH_4NO_3. Blocks were sealed against moisture.

Data showing burning rates of guanidine nitrate–ammonium nitrate–linseed oil–ammonium dichromate blocks after storage under each of these conditions are shown in Table 6. All blocks were brought to 70 F before burning.

TABLE 6. Burning rate of guanidine nitrate–NH_4NO_3–Oil-$(NH_4)_2Cr_2O_7$ blocks after storage at different temperatures.

Check immediately after pressing		Room temperature storage: 21 days at 70 F; low RH		150 F storage: 3 days 70 F; 18 days 150 F; 1 day 70 F			Cyclic 0–150 F, 8 cycles low RH		
Burning time min	Burning rate g/(min) sq cm	Burning time min	Burning rate g/(min) sq cm	Burning time min	Burning rate g/(min) sq cm	Remarks	Burning time min	Burning rate g/(min) sq cm	Remarks
3.4	2.58	2.8	3.13	3.3	2.65		3.15	2.78	
3.4	2.58	2.8	3.13	3.3	2.65		3.4	2.58	
3.5	2.50	2.9	3.02	3.1	2.82		3.15	2.78	No observable cracking. About 2% increase in block height.
		2.9	3.02	3.0	2.92	No	3.15	2.78	
		2.9	3.02	3.1	2.82	observable	3.1	2.82	
		3.0	2.92	3.1	2.82	swelling	3.1	2.82	
							3.3	2.65	
							3.3	2.65	
Avg 3.43	2.55	2.88	3.04	3.15	2.78		3.21	2.73	

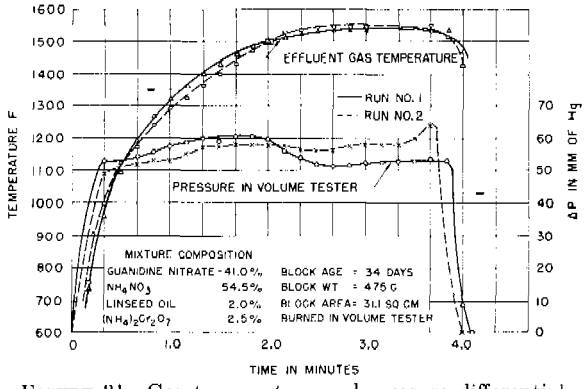


FIGURE 31. Gas temperature and pressure differential across exhaust orifice of volume tester during burning of block.

VOLUME TESTER DATA

E29R1-type blocks were burned in the volume tester. Pressure-time curves and temperature-time curves during operation of the block are shown in Figure 31. Flow rate vs time curves giving the gas volume under actual conditions are shown in Figure 32. Flow rate vs time curves for gas volume reduced to 60 F and 1 atm are shown in Figure 33. The rate of gas flow is remarkably uniform from this mixture.

TESTS IN E29R1

E29R1-type blocks were burned in E29R1 units. Guanidine nitrate blocks gave excellent performance in the unit.

31.4.2 Discussion of Noncarbon Mixtures

Since composite propellants of guanidine nitrate have never shown chuffing in rocket fuels, this mixture offers promise of more complete control of surging in thermal generator fuels. The most annoying feature of this mixture is the 19% increase in burning rate on curing. However, this increase is not excessive.

The importance of the reducing agent to the surging problem is further emphasized by these tests. In blocks containing excess $(NH_4)_2Cr_2O_7$ but no reducing

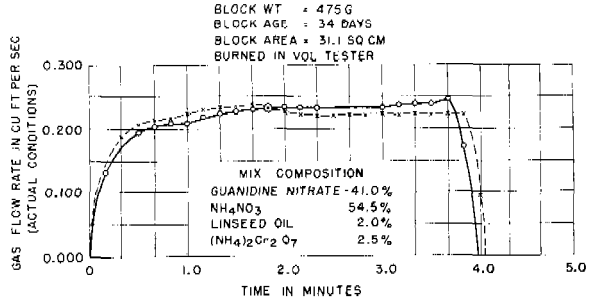


FIGURE 32. Gas flow rate — time curves for gas volume measured under actual conditions of temperature and pressure.

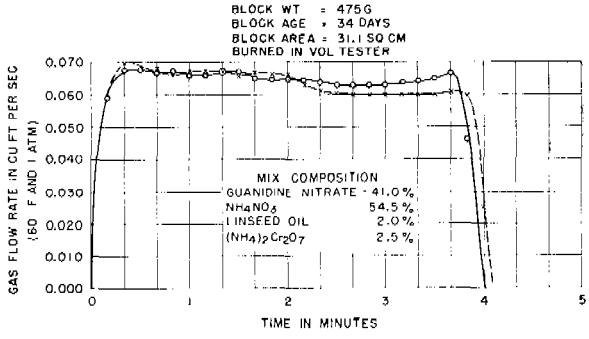


FIGURE 33. Gas flow rate - - time curves for gas volume reduced to 60 F and 1 atmosphere pressure.

agent, surging was severe in the unit, the volume tester and the pressure tester. Blocks containing sulfur showed somewhat less tendency to surge, while those containing guanidine nitrate or ammonium picrate showed no surging tendencies.

31.5 CAST FUEL COMPOSITIONS

31.5.1 Comparison of Cast and Pressed Mixtures

Cast fuel blocks differ from pressed blocks in that (1) the linseed oil binder of the pressed block is replaced by 1.0*M* or 0.75*M* H_3PO_4; (2) the burning rate of cast mixtures is controlled by variation in the relative amounts of starch and charcoal present in the mixture; (3) the cast mixture is poured into cans while molten and allowed to solidify, whereas the pressed mixture is compacted under pressure.

The basic chemistry in the combustion of the two blocks is very similar. A number of the basic principles, such as the effect of the particle size of the charcoal and alkali catalysis of the burning, can be applied to cast mixtures as well as to pressed.

31.5.2 Properties of Cast Mixtures

Cast mixtures are, in general, much slower burning than pressed mixtures. Burning rates range from 0.6 to 1.8 g per min per sq cm. The volume of gas produced per gram of mixture, measured at 60 F and 1 atm, is about the same in cast and pressed mixtures (0.84 l). The temperature of the gases from a burning cast block is somewhat lower than from a pressed block; thus, the overall capacity of cast blocks for evaporating other agents is less.

Cast blocks are more difficult to ignite and have presented a much more serious surging problem. The ignition temperature of the loose mixture is comparable to that of loose mixture for pressed blocks (200 to 240 C), but a *block* of cast mixture requires considerable hot slag from the starter to initiate combustion. Cast blocks ignited on the surface with a bunsen burner or blowtorch did not continue to burn after the torch was removed. Block density ranged from 1.41 to 1.52 g per cu cm.

Cast mixtures presented a rather serious corrosion problem in unprotected cans. A means for protecting the metal would have to be used or the composition of the mixture changed. The mechanical strength of the mixture was good. Units withstood transit and handling well. The cast mixture was never subjected to cyclic surveillance to check the action of NH_4NO_3 phase changes.

31.5.3 Manufacturing Procedure

Base Mixture

The base mixture consisting of NH_4NO_3, charcoal, phosphoric acid, NH_4Cl, and starch was mixed in a Simpson intensive mixer for about 10 min, then melted in a deep steam-jacketed kettle supplied with steam at 50 psi. The molten mixture flowed into the container placed on a balance pan below the outlet of the kettle. The formulas used are given in Table 2. Melting temperatures ranged from 110 to 120 C.

Top Mixture

While the base mixture was cooling, a faster mixture consisting of ammonium nitrate, ammonium chloride, charcoal, sodium nitrate, and phosphoric acid was mixed by hand and melted in a smaller steam-jacketed kettle. This mixture was poured onto the top of the base layer and allowed to cool.

Starter Mixture

The starter mixture was 54% KNO_3, 40% silicon, and 6% charcoal intimately mixed in the dry state and made into a slurry with a binder of 5% cellulose nitrate in acetone. This slurry was distributed over the surface of the block in a gridiron pattern.

Safety Rating of the Process

The product and process were examined by the Safety Section of the U.S. Bureau of Mines, and the process was classified as at least no more hazardous than the manufacture of black powder. The product is less hazardous than black powder.

31.5.4 Factors in the Control of Cast Block Characteristics

Variation of Ingredients

As in pressed blocks, charcoal was the least uniform ingredient. Conclusions concerning ingredients of pressed blocks are equally applicable to cast units.

Variations in the Manufacturing Procedures

A detailed study of the manufacturing procedure was not made. A standard procedure was established and followed as closely as possible. Mixing times, casting temperatures, and the like were maintained

TABLE 7

System	Melting point C	Mole % NH_4NO_3	Mole % $NaNO_3$	Mole % NH_4Cl	Mole % Other
a. *Melting points and compositions*[24] *for eutectic salt mixtures.*					
NH_4NO_3 — $NaNO_3$	120.8	80.27	19.73	....	....
NH_4NO_3 — NH_4Cl	140.9	82.92	....	17.08	....
NH_4NO_3 — $(NH_4)_2SO_4$	No eutectic				
NH_4NO_3 — $NaNO_3$ — NH_4Cl	112.5	74.76	17.71	7.53	....
NH_4NO_3 — NH_4Cl — KNO_3	134.5	76.54	13.92	....	KNO_3 9.54
NH_4NO_3 — NH_4Cl — $LiNO_3$	113.6	76.73	....	14.10	$LiNO_3$ 9.17

b. *Effect of water on freezing point of* NH_4NO_3.

Wt % H_2O	0	1.05	2.01	3.20	4.39	6.24	8.76	10.04
Freezing point, degrees C	169	157	146	133	122	112	99	95

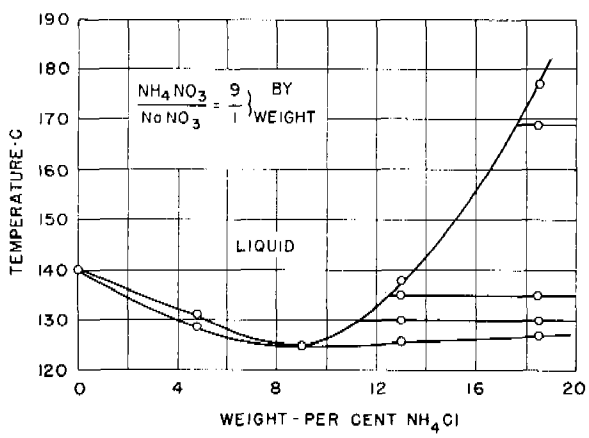


FIGURE 34. The system NH_4NO_3 — $NaNO_3$ — NH_4Cl.

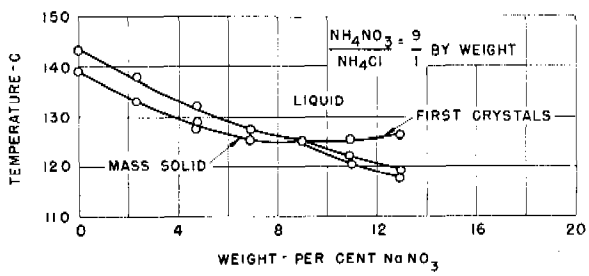


FIGURE 35. The system NH_4NO_3 — $NaNO_3$ — NH_4Cl.

fairly constant. Several problems appeared in the casting process which were troublesome.

Evolution of Gas. Some mixtures gave off NH_3 on heating. This caused swelling and produced holes in the block. NH_3 evolution was minimized by the addition of H_3PO_4 solution to the mixture.

Lowering of the Melting Point. This was accomplished by formula variation.

Corrosion of Casting Kettle. This was minimized by using H_3PO_4 instead of other acids to retard the NH_3 evolution.

FORMULA VARIATION

Burning rates and melting points of cast mixtures have been largely controlled by formula variation. Phase diagrams of NH_4NO_3 systems were studied to obtain a low melting mixture of oxidizing salts. Variation of the reducing agent was used to control the burning rate.

Phase Diagrams. Phase diagrams and melting point information for a number of pertinent systems [24] from the literature are summarized in Table 7.

Table 7b indicates that water is very effective in lowering the freezing point of NH_4NO_3.

These data were supplemented by additional phase investigations. Samples were melted in a small test tube suspended in an oil bath. Cooling curves were obtained for each mixture. Analytical or crystallographic studies were not made on any of the phases.

Data for a part of the ternary system NH_4NO_3–NH_4Cl–$NaNO_3$ are given in Figures 34 and 35. Data for the ternary system NH_4NO_3–NH_4Cl–H_2O are given in Figure 37, and for the quaternary system NH_4NO_3–NH_4Cl–$NaNO_3$–H_2O in Figure 36. The melting point of ammonium nitrate and the data in Figures 36 and 37 indicate that the NH_4NO_3 used in these experiments was not absolutely dry even after drying for 16 hr at 100 C. This nitrate apparently contains about 0.25% water, but this water is removed with great difficulty and is not detectable by heating at 70 C or by perchlorethylene extraction. Thus, this nitrate would be reported as 0% moisture if checked by the technique given in the specifications for NH_4NO_3, and would be considered "dry" in regular production work.

The eutectic mixture of NH_4NO_3–NH_4Cl–$NaNO_3$ appeared promising, but blocks made from this oxidizing mixture with charcoal as the reducing agent

CONFIDENTIAL

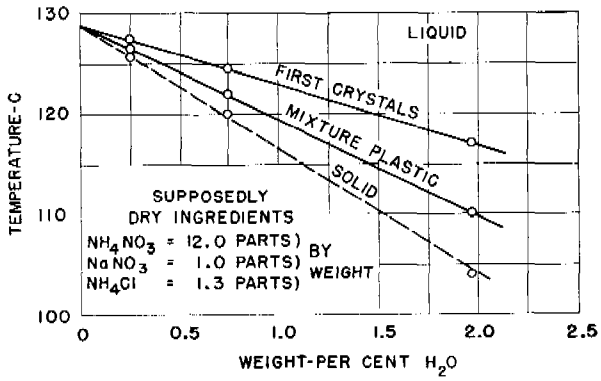


FIGURE 36. The system NH_4NO_3 — $NaNO_3$ — NH_4Cl — H_2O.

surged violently and burned too rapidly. It seemed desirable to eliminate the $NaNO_3$, and, since this resulted in a rise in the melting point, water was added as suggested by Figure 36. These blocks showed a tendency to swell on cooling and also surged when burned.

Addition of 1.0*M* H_3PO_4 minimized the evolution of NH_3 and also aided in the control of surging. From tests with a variety of compositions, the following formula was evolved.

NH_4NO_3	83%
1.0*M* H_3PO_4	3%
NH_4Cl	3%
Charcoal, Starch	11%

The burning rate was controlled by variation of the starch-charcoal ratio.

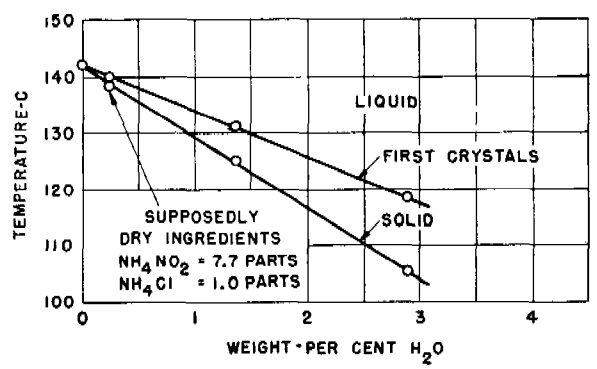


FIGURE 37. The system NH_4NO_3 — NH_4Cl — H_2O.

Effect of Starch on the Burning Rate. Variation of burning rate as a function of per cent starch in the block is shown in Figure 38. Percentages of starch up to 2.5% have little effect on the burning rate, but percentages in the range 2.7 to 4.0 influence the burning rate markedly.

Effect of pH of the Mixture. A series of cast blocks was made containing different concentrations of acid. The acid strength had a very marked influence on surging. Blocks containing 0.75*M* H_3PO_4 showed no tendency to surge, while blocks containing 0.25*M* H_3PO_4 surged so violently that seams of the fuel cans were split. Conditions other than acid concentration were identical in both sets of blocks. In a few later cases, increasing the acid concentration did not completely eliminate surging. Although the acid had a definite effect in controlling surging, it was not entirely satisfactory.

Storage of Cast Blocks

Cast blocks show no change in burning rate on curing; however, blocks with mild surging characteristics developed much more violent surging properties after storage. Storage at elevated temperatures appeared to cause a greater tendency to surge than storage at room temperature.

Cast blocks poured into noninsulated light gauge cans corroded through from the inside after about 50 to 75 days in either tropical or desert storage.

31.5.5 Suggestions for Improving Cast Mixtures

Casting a fuel block, rather than pressing it, should have a considerable advantage, especially for large-scale production. A number of the difficulties encountered with cast blocks might be overcome. Based on the present knowledge, certain principles now seem apparent which should serve as a guide for further development. First, a single reducing agent should be used to control surging. This agent could be charcoal, carefully prepared, and meeting rather exact specifications, or a pure compound such as guanidine nitrate or ammonium picrate. Second, the use of water or acid solutions should be avoided.

31.6 OTHER FUELS FOR THERMAL GENERATORS

The development work described in the preceding text was done on mixtures of two or more principal ingredients either pressed or cast into a solid block of fuel. At the time, these were believed to hold the best promise for satisfactory application in the thermal generator munitions. The results achieved apparently justify this belief. Nevertheless, it is recognized that other fuels have merit and deserve consideration. These may be classed as other solid fuels and liquid fuels.

31.6.1 Other Solid Fuels

Smokeless powder has been developed and used as a rocket propellant. Although rocket fuels burn under an entirely different set of conditions than do thermal generator fuels, a good many of the problems of production and operation are similar, and mixtures suitable for rockets can be modified in many cases to give satisfactory fuels for thermal generators. Smokeless powder is the most common rocket propellant, though during World War II a number of composite propellants such as intimate mixtures of ammonium picrate and sodium or potassium nitrate were developed. The advantages and disadvantages of smokeless powder and composite propellants for rockets have been compared [10] and the following advantages and disadvantages are pertinent to fuel block performance for thermal generators.

Advantages of Smokeless Powder Fuels

1. The composition and properties of smokeless powders are familiar through their use as gun propellants.
2. They can be manufactured with equipment on hand, by known processes. This is perhaps their greatest advantage.

Disadvantages of Smokeless Powder Fuels

1. The burning rate of smokeless powder is sensitive to changes in the gas pressure.
2. The burning rate is sensitive to changes in the initial powder temperature.
3. At very high and very low temperatures the mechanical properties of the powder show failure.
4. Chuffing, an irregular burning similar to surging in fuel blocks, is encountered at low temperatures.
5. Production of thick grains is difficult; the solventless process makes such grains possible, but equipment for the production of solventless powder is limited.

Advantages of Composite Fuels of Ammonium Picrate and Sodium Nitrate

Composite propellants vary with their composition. For a mixture of ammonium picrate and sodium or potassium nitrate compounded with a suitable binder, the following is pertinent.

1. The burning rate is much less sensitive to changes in equilibrium pressure or area of burning surfaces than are those of smokeless powders.

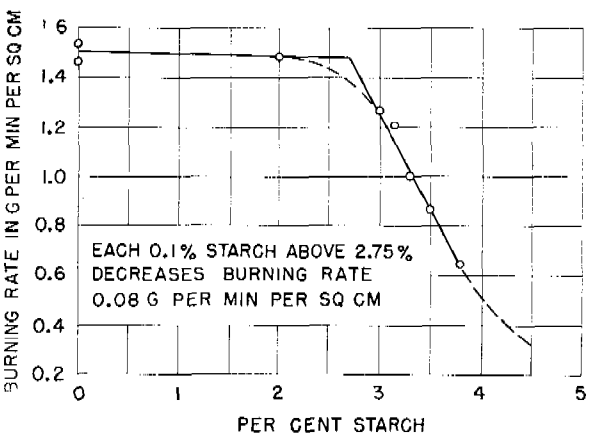


Figure 38. Burning rate of cast fuel blocks as a function of per cent starch in block.

2. The dependence of burning rate on the initial powder temperature is about one-fifth that of a typical smokeless powder.
3. No chuffing phenomena appear at any pressure.
4. Material can be produced in a wide range of block sizes.
5. A wide range of absolute burning rates is available due to the dependence of the burning rates on the particle size of the basic ingredients as well as the mixture composition.

Disadvantages of Composite Ammonium Picrate–Sodium Nitrate Fuels

1. Its preparation is not suited to conventional powder manufacturing equipment.
2. Mechanical strength is somewhat low.

Advantages of Charcoal–KNO_3 or $KClO_4$ and Binder Composite Fuels

For a mixture of charcoal, potassium nitrate or potassium perchlorate, and a cellulose nitrate binder, the following is pertinent.

1. The burning rate is much less pressure sensitive than that for smokeless powder.
2. The dependence of burning rate on initial powder temperature is one-sixth to one-half that of a typical smokeless powder.
3. Chuffing phenomena are encountered only at very low pressures (probably several hundred pounds per square inch in most rockets).
4. The powder shows increased mechanical strength

at high temperatures, as compared with double base powder.

5. There is a wide range of absolute burning rates.

6. Densities are 10 to 25% above conventional double base powders.

From this summary of the burning characteristics of rocket fuels it appears that composite propellants and related powders are more suited to the burning conditions and the wide range of burning rates required in the thermal generator than smokeless powders.

31.6.2 Liquid Fuels

Liquids such as hydrogen peroxide have been used successfully as a source of hot gas under pressure. They offer the desirable feature of a controlled rate of gas generation. The design of storage space and the means for controlling the rate of generation within the munition must be necessarily quite simple for these small munitions. It is questionable whether this restriction could be met with liquid fuels at the present time.

Chapter 32

NEW SCREENING SMOKE MIXTURES

By *E. W. Comings*

32.1 THE CHANGING REQUIREMENTS FOR SMOKE POTS

BOTH THE TACTICAL and production requirements for smoke pots varied considerably during World War II. At first, the available smoke munitions consisted of burning pots generating smoke of metal chlorides such as zinc chloride, bursting munitions containing white phosphorus or sulfur trioxide-chlorosulfonic acid mixture, and airplane spray tanks using the latter mixture or titanium tetrachloride. The need for screening large areas from attack from the air required greatly increased production of the smoke pots. This need was soon largely filled by the development of the continuous oil smoke generator. These were especially useful where smoke protection was required for an appreciable percentage of the time. However, there were not enough generators available nor could their use be justified in areas requiring very infrequent screens or hastily established screens. Smoke pots were well suited for these latter purposes as well as for some of the screens set up under fire both over land and over water. Somewhat unpredictable changes in the course of the war were reflected in large variations in the demand for the type and quantity of smoke pots.

32.1.1 Need for Substitute Smoke Mixture Specifications

These periods of large demand occurred at times when the supply of one or more of the ingredients in the mixture was short. Thus, at one time it was anticipated that sufficient chlorine could not be made available for the organic chlorides used in the mixture. Zinc and aluminum (early in the war) were possible limitations on the supply. Changes in the tactical use of the pots also revealed the need for revised specifications. When used for short periods of time the HC pots did not produce serious toxic effects, but where they were used for longer periods of time or when the concentration of smoke was high, objectionable toxic effects (from the zinc chloride smoke) were noticed.

The problem of eliminating the fire and explosion hazard from the HC-type mixture was ever present. This was apparently solved in the laboratory, but continued to recur with pots from the production line. All these problems indicated the need for improved smoke mixtures but especially for substitute mixtures or specifications which could be used to meet special production or tactical situations.

32.1.2 Use of Smoke Pots to Replace Continuous Smoke Generators

The continuous oil smoke generators developed during World War II must be supplied with both fog oil and fuel. If a simple expendable smoke generator could be built which would serve as the container for its own smoke agent and fuel, this might well be more advantageous than the continuous generators. The generator would then always be available with the smoke agent. This is essentially the description of a smoke pot, except that the smoke mixture has in the past been more expensive and less available than fog oil and gasoline. A plentiful and inexpensive smoke mixture for use in expendable pots would be preferable in many situations to the continuous oil smoke generators. Such pots could be emplaced in or around an area and fired selectively or in rotation from a central control. In an emergency, they could be ignited and rolled off the tail board of a truck. A single vehicle could thus supply many point sources over a line of considerable length.

32.1.3 Features Desired in a Smoke Mixture

The features especially desirable in a smoke mixture are: (1) all the ingredients should be available in sufficient quantities for large-scale production of the mixture; (2) a maximum of screening power should be obtained per unit weight of mixture; (3) the smoke should be nontoxic and also nonirritating to the eyes, throat, and skin, and noncorrosive to matériel; (4) the mixture should be suitable for large scale manufacture, storage, and transportation without hazard or deterioration.

No one mixture is likely to excel in all four of these features and some compromise must usually be made. These features will be discussed at greater length as a criterion for evaluating a smoke mixture.

Availability of Ingredients

Production of the mixture has been considered in terms of approximately 50,000 to 100,000 tons a year. If it had been necessary to protect large areas in continental United States from air attack, this figure would have been multiplied several fold. The availability of an ingredient is a relative term and depends upon many other often unpredictable factors, such as the demand for material necessary for its manufacture, the possible stoppage of raw material sources in wartime, and even the destruction of facilities for manufacture by enemy action or otherwise. Provision for substitute ingredients and substitute mixtures is a foresighted policy. The common materials generated by the smoke mixtures, and forming the basis of the actual smoke particles, and available in sufficient quantities to warrant consideration are: (1) metal chlorides of zinc, magnesium, aluminum, and iron, (2) phosphorus, (3) oleum, (4) sulfur trioxide and chlorosulfonic acid mixtures, (5) fog oil, (6) sulfur, and (7) possibly carbon.

In the mixtures based on the metal chlorides the metals were incorporated into the mixture either in the metallic form or as oxides, and the chlorine was supplied by organic chlorides such as hexachloroethane or carbon tetrachloride. Other oxidizing or reducing agents, such as perchlorates or calcium silicide, were used to supply heat or reduce the oxides. Substitute ingredients and mixtures for producing iron chloride smokes will be discussed below. Phosphorus, as used in the past, produced a large puff of smoke of short duration and was not suitable for use on friendly areas. A means of generating phosphorus smoke uniformly over a relatively long period of time, and of confining combustion within or near the smoke pot, would make this material more suitable for use in a smoke pot. The use of oleum or the sulfur trioxide-chlorosulfonic acid mixture both require a uniform rate of vaporization or generation throughout the functioning time of the pot. The development of smoke pots for generating fog oil and sulfur smokes will be described in this chapter.

Maximum Screening Power

The screening power per unit weight of mixture depends first on the weight of actual material available for forming the smoke particles, whether this is originally present in the mixture itself or is contributed from the air. Second, it depends on the efficiency with which this actual smoke material is used to form smoke particles with the greatest light scattering or obscuring ability. It is easily possible for a mixture to yield the largest amount of actual smoke material and yet produce a smoke cloud with a lower obscuring power, because the material is wasted in particles of a size which do not obscure efficiently.

Weight of Smoke Agent per Unit Weight of Smoke Mixture. The metal chlorides, phosphorus, oleum, and sulfur trioxide all have the advantage of removing water vapor from the air to augment the smoke material present in the mixture. The material, which actually forms the smoke particles, is a water solution of the salts or acid produced by the mixture. This advantage is greater in relatively humid atmospheres than it is in dry ones. Phosphorus has the added advantage that it increases the amount of smoke material by removing oxygen as well as water vapor from the air and yields an exceptionally high ratio of smoke material per unit weight of phosphorus. A comparison of the three metal chlorides and phosphorus is given in Table 1.[1]

Table 1. Smoke forming aqueous solution* produced by various agents in air at 75% relative humidity.

Agent	Oxygen from air g	Water vapor combining with the agent g	Water vapor absorbed as hygroscopic water g	Total g smoke-forming solution	Total g smoke solution per g chlorine in agent
Phosphorus	1.29	0.87	3.95	7.11	...
Aluminum chloride	0	0	4.0	5.0	18.8
Ferric chloride	0	0	2.1	3.1	14.2
Zinc chloride	0	0	1.5	2.5	9.6
Fog oil†	0	0	0	1.0	...
Sulfur†	0	0	0	1.0	...

* The figures are based on 1 g of agent shown in first column (except for the last column).

† These do not form aqueous solutions but are used in their original form.

It is evident from the table that for the agents compared, white phosphorus yields the greatest weight of aqueous solution in equilibrium with air at 75% relative humidity per unit weight of the agent. The smoke particles are composed of this aqueous solution. Aluminum chloride, ferric chloride, and zinc chloride yield decreasing amounts of solution in that order. This ratio of aqueous smoke-forming solution to smoke agent varies from 7.11 to 2.5 for these four agents. The same ratio for fog oil or sulfur is unity (1.0) since these agents are not hygroscopic and only

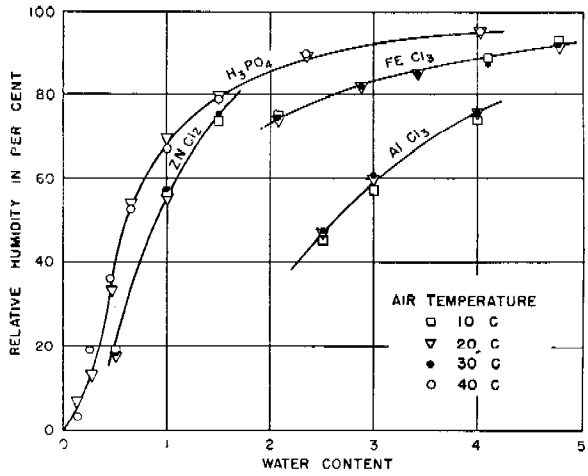


FIGURE 1. The variation in water content of smoke forming aqueous solutions with relative humidity.

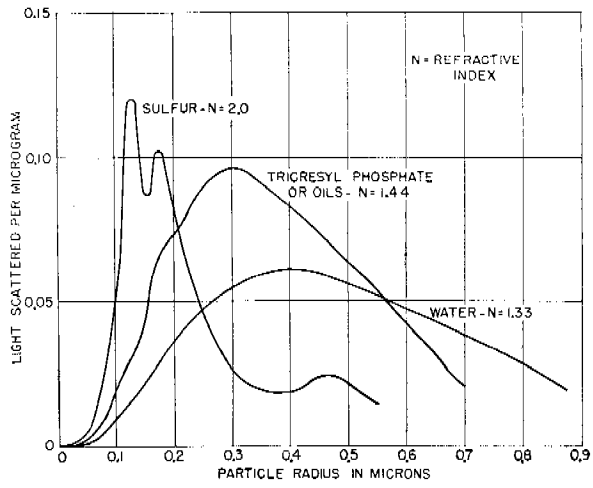


FIGURE 2. Scattering of light by smokes of sulfur, tricresyl phosphate (oils), and water. Watts of light scattered by one microgram of particles from a beam of one watt per cm^2 of wavelength. $\lambda = 0.55$ microns (green). (Based on calculations furnished by Dr. A. Lowan.)

the agent itself is available to form the smoke particles. The table does not take into account ingredients in the smoke mixture which remain behind as residue or otherwise contribute little to the obscuring power. This comparison will vary with the relative humidity of the air but changes very little with air temperature at any one value of the relative humidity. This is shown by Figure 1. These data have been taken from the literature except in the case of ferric chloride where the necessary measurements were made.[1] The re-examination of these data with additional experimental determinations is recommended.

Effect of Smoke Particle Size. Considerable information was developed during World War II on the effect of smoke particle size on obscuring power.[2, 3] The relative light-scattering effectiveness per unit weight of smoke agent as it varies with the smoke particle radius is shown in Figure 2. The hygroscopic agents forming aqueous solutions are represented approximately by the curve for water. This curve indicates a somewhat lower light-scattering power than for oil or sulfur with an optimum particle size of about 0.4 micron radius. The curve is quite flat, however, and the reduction in light-scattering power from the maximum is not great in the range from 0.25 to 0.6 or 0.7 micron radius. The screening power of a unit weight of water solution is roughly 60% of that of a unit weight of oil when both are compared near their optimum particle size. The optimum size (which was discussed in Chapter 22 of this volume) for oil particles is about 0.3 micron radius although the scattering power does not drop below 75% of the maximum in the range 0.2 to 0.45 micron radius. Sulfur shows an optimum at 0.13 micron that is 25% greater than oil, but this occurs in such a narrow particle size range and at such a small size that it is difficult to realize this advantage. The reduction in screening power due to variation from this optimum particle size is relatively great in the case of sulfur, a decrease of 0.03 micron in radius from the optimum resulting in about a 60% decrease in screening power. In general, all the agents show a more rapid decrease in screening power as the smoke particle size is reduced below the optimum than when it is made larger. This may not be so important from the practical point of view since it is doubtlessly easier to waste smoke agent in particles that are too large than in ones that are too small.

Volatility and Dilution. A screening smoke in the atmosphere eventually loses its obscuring power. The common mechanisms by which this occurs are by the evaporation of the particles or by dilution until the particle density is too low to obscure. The steam from a locomotive disappears by evaporation whereas a cloud of very small dust particles is eventually diluted since the particles are nonvolatile. The maximum area that can be obscured per unit weight of agent increases as the volatility of the agent decreases if the cloud disappears by evaporation. When the volatility of the agent is low enough that the smoke cloud loses its obscuring power by dilution, further decrease in the volatility will not increase the area obscured. There is not a clean cut distinction between the high and low volatility agents. Thus, both fog oil and sulfur smokes may disappear by evaporation,

but it is unlikely that the area obscured per unit weight of each would be increased by more than several per cent if they did not evaporate at all. A comparison of the weight of sulfur vapor and Diol 55 vapor required to saturate a cubic mile of air is of interest in this connection.

The vapor pressure curve for sulfur (solid) extrapolates to about 8×10^{-6} mm at 20 C. The calculated amount of sulfur vapor (S_8) required to saturate 1 cubic mile of air is as follows:

Degrees C	10	20	30
Pounds per cubic mile	330	1,000	3,100

A single figure at each temperature for Diol 55 cannot be given to compare with these since the Diol is not a pure compound. The amount of Diol 55 required to saturate 1 cubic mile varies depending on the initial amount of Diol introduced into the air.[2a] When this is from 70 to 7,000 lb per cubic mile, the weight required to saturate the air would range from 28 to 147 lb at 10 C, 56 to 390 lb at 20 C, and 70 to 1,060 lb at 30 C. Although these figures may not be very accurate, they indicate that, from the standpoint of vapor pressure, sulfur and Diol 55 are in the same class with a slight edge in favor of the Diol.

These figures may be compared with the estimated quantities of these agents required to screen a square mile of area. Under severe conditions 1,400 lb Diol 55 per square mile will give obscuration. The figure for sulfur is at least as large (possibly a little larger) and the required weight of HC mixture is of the same order.

The particles of aqueous solution formed by the hygroscopic agents are in equilibrium with the air surrounding them and will not evaporate even when the cloud is diluted. Such clouds lose their obscuring power by dilution.

Toxicity and Irritancy

Of all the smokes mentioned under "Availability of Ingredients," *zinc chloride* is probably the most toxic to personnel. When the dosage of this smoke is kept low, either by infrequent and short time exposure, or by keeping the clouds very dilute, no ill effects have been noted. However, when the screens are used for considerable periods of time or in high concentrations, personnel are adversely affected. None of the other smoke agents listed are toxic when in a smoke cloud. The hygroscopic agents are irritating while they are absorbing moisture from the air, but at a short distance from the smoke pot are quite innocuous. Fog oil is completely nonirritating. Some of the fuels used to vaporize it contain black powder or sawdust, and these produce fumes which are irritating to some extent. Sulfur smoke is slightly irritating to the eyes, but no health hazards have been observed among the workmen at the sulfur wells who are exposed continuously to sulfur fumes. Phosphorus in the elemental state is poisonous and it, as well as oleum and sulfur trioxide mixture, will produce serious burns if scattered about on personnel. The latter two are corrosive to matériel.

Stability in Manufacture, Transportation, and Storage

The HC mixture based on zinc chloride is, at best, on the border line between being safe and hazardous for handling. Rather serious consequences can ensue from a lack of close adherence to specifications. This may and has resulted in explosion or fire, either in manufacture, transportation, or storage. Nevertheless, large quantities of this mixture have been produced and handled satisfactorily. Other mixtures based on the metal chlorides are not hazardous but may possibly deteriorate on storage unless handled properly. The pots based on fog oil as a smoke agent are probably the least hazardous once the oil is incorporated in the mixture. The other components, essentially black powder or sawdust-chlorate mixture, are hazardous when dry. The latter is probably ruled out as far as practical use is concerned because of its extreme sensitivity. The sulfur nitrate mixtures have always been suspected of being hazardous especially in manufacture, but no evidence of this was found during extensive experimental work with them. Phosphorus, oleum, and the sulfur trioxide mixtures are not susceptible to spontaneous explosion, but leaky containers in storage or shipment or in tactical use must be avoided.

New screening smoke mixtures developed to meet some of these requirements better are described in the following text.

32.1.4 New Chlorine Carriers for Metal Chloride Screening Smoke Mixtures

Introduction

Aerosols of the hygroscopic metallic chlorides have been extensively used as screening smokes for a number of years. The hygroscopic nature of these aerosol particles permits them to pick up moisture

from the air immediately after discharge from the smoke pot, thus increasing the amount of material available for forming smoke.

One of the earliest of the metal chloride smokes was produced from the Berger mixture which consisted of Zn, CCl_4, ZnO, and kieselguhr, the last two constituents serving to absorb the CCl_4 and slow down the rate of reaction during smoke evolution. The smoke evolved was light gray in color and consisted largely of $ZnCl_2$ with some colloidal carbon. This pot had numerous limitations, chief among them being that the CCl_4 was a volatile liquid, thus making the pot subject to deterioration on storage and difficult to manufacture. Kendrick [6] at Edgewood Arsenal suggested solid hexachloroethane (C_2Cl_6) as a chlorine carrier to eliminate the inherent difficulties of liquid CCl_4. This compound has been used extensively since that time and is now the most widely used chlorine carrier for screening smokes.

Lawrence [7] reports the early work in the development of the hexachlorethane mixture, while Conkling [8] reviews the basic requirements of such a pot and summarizes the later developments. He suggested a mixture of

36% Zn
44% C_2Cl_6
10% NH_4ClO_4
10% NH_4Cl.

This was adopted and used with some modification until 1940. Limited supplies of NH_4ClO_4 led to attempts to substitute KNO_3 as the oxidizing agent. These mixtures ignited spontaneously during storage. Smith and Hormats [9] attributed the difficulty largely to heating due to water picked up during manufacture and to the low ignition temperature of the mixture containing KNO_3. They found that $KClO_4$ could be satisfactorily substituted for NH_4ClO_4 and the mixture had a higher ignition temperature than the nitrate mixture (249 to 269 C as compared with 110 to 140 C).

A mixture containing $CaSi_2$–ZnO–C_2Cl_6 has been widely used. The sensitivity of $CaSi_2$ to water and the difficulty of obtaining it led Finkelstein and Becker [10] and Barnard [11] to suggest a mixture of

5.50% Al
47.25% ZnO
47.25% C_2Cl_6.

This mixture is stable to water and has an ignition temperature of 775 to 800 C.[12] The smoke produced is excellent.

Hexachlorethane is made from acetylene and chlorine by a rather involved process. The supply is therefore limited by the amounts of chlorine and acetylene available as well as by the processing equipment on hand. A more readily available chlorine carrier is needed. To find such a compound a systematic survey of the periodic table has been made. The results are discussed in the following text.

Development of Mixtures

A large number of mixtures that produce a metal chloride screening smoke was investigated. The principal object was to find a mixture, comparable with the present HC mixture, that could be manufactured in large quantities in case the production of the HC mixture became limited by the supply of chlorine or acetylene, or by the processing equipment available for its manufacture. The mixtures tried were those based on:

1. The simple inorganic chlorides $FeCl_3$, $ZnCl_2$, and $PbCl_2$ reacting with Al.

2. The ferric chloride complexes, including those in which $FeCl_3$ is associated with KCl, NH_4Cl, NaCl, and $CaCl_2$, as well as the ammines in which it is associated with NH_3.

3. Mixtures of high efficiency containing $FeCl_3$, and also hexachloroethane in which all but about 5% of the mixture makes smoke.

4. A few mixtures in which Chlorpropane Wax (approximately octachloropropane) is substituted for hexachloroethane.

The following composition gives an excellent smoke comparable to the HC mixture.

A. 88% anhydrous $FeCl_3$
12% Al

This mixture is highly sensitive to moisture before it is pressed and is hazardous in manufacture unless special precautions are taken to handle it in a dry atmosphere. After pressing it is damaged by exposure to moist air or water but single units were not made dangerous by such exposure.

It is questionable whether a large production of anhydrous ferric chloride can be secured in a short time without using elemental chlorine to supply all three chlorine atoms. Several such processes have been suggested, but inquiries into each reveal technical difficulties that have not been satisfactorily overcome. Therefore, each is in the developmental stage with little certainty as to the time required to reach a satisfactory design. The chief difficulty is

that it is not practical to dehydrate ferric chloride from a solution made by the action of hydrochloric acid (and some chlorine) on iron or iron oxide. A hexahydrate is formed which breaks down when heated and gives off HCl rather than water.

This difficulty led to the investigation of ferric chloride complexes. If one mole of KCl is mixed with one mole of $FeCl_3 \cdot 6H_2O$ and heated, a complex is formed and the water can be driven off below 205 C without decomposition, giving a compound $KFeCl_4$. This complex in the mixture

B.	8.0%	Al
	30.0%	ZnO
	2.2%	$NaNO_3$
	59.8%	$KFeCl_4$,

gives a smoke of $ZnCl_2$, $KFeCl_4$, and $FeCl_3$ which is slightly inferior to and has a shorter burning time than the HC mixtures. It should be relatively easy to produce in quantity. It is less hygroscopic than the $FeCl_3$ and is much easier to handle in the mixing and pressing operations. The ignition temperature of the mixture is of the order of 335 to 350 C.

The efficiency of this mixture can be increased and the burning time lengthened by adding small percentages of hexachloroethane. A mixture of the following composition

C.	7.3%	Al
	27.2%	ZnO
	4.5%	$NaNO_3$
	52.0%	$KFeCl_4$
	9.0%	C_2Cl_6,

burned noticeably longer and gave a smoke slightly superior to the mixture with straight complex. This mixture is preferable to that with the complex alone if limited amounts of hexachloroethane are obtainable.

The use of the complex $KFeCl_4$ in smoke mixtures has the advantages that (1) it is easy to manufacture from available raw materials; (2) it is easy and safe to incorporate into a mixture, press, and store; and (3) it gives a good screening smoke, although not quite as good as the HC mixtures. It has the disadvantage of leaving a relatively high percentage of bulky residue in the pot.

It is recommended that the above two mixtures, *B* and *C*, be considered for the larger size smoke pots and floats in case the supply of organic chlorine carriers is not adequate. The choice between mixtures *B* and *C* will be dependent upon the supply of hexachloroethane available.

The high-efficiency mixture contains

D.	51.6%	$FeCl_3$
	38.3%	C_2Cl_6
	8.8%	Al
	1.3%	$NaNO_3$.

About 95% of the mixture is converted to smoke-forming products. It produces an excellent smoke with little residue, but contains both $FeCl_3$ and C_2Cl_6. It is sensitive to moisture in the same way as the $FeCl_3$–Al mixture.

Chlorpropane Wax, which was tested briefly, gives indication of having certain advantages over hexachloroethane as an organic chlorine carrier. It is manufactured by a relatively simple two-step process of chlorinating propane. Its vapor pressure is lower than C_2Cl_6. On the other hand, its chlorine efficiency from elemental chlorine to smoke is not so good.

A mixture similar to the HC mixture, in which hexachloroethane was replaced by octachloropropane, gave a smoke comparable to the present HC mixture. This mixture had the following composition:

E.	6.25%	Al
	46.15%	ZnO
	47.60%	C_3Cl_8.

If it is found that octachloropropane can be manufactured more readily than hexachloroethane, it is recommended that mixture *E* be tested to replace or supplement the present HC mixture using hexachloroethane.

Possible Chlorine Carriers

The physical properties of the more available simple chlorides were tabulated.[13] The chlorides of the metallic elements such as Ni, Cu, Cr, Hg, which are scarce during wartime, have not been considered.

The solid chlorides include $TiCl_3$, PCl_5, $BiCl_3$, $SbCl_3$, $SeCl_4$, $TeCl_4$, $ZnCl_2$, $FeCl_2$, $FeCl_3$, $CdCl_2$, $PbCl_2$, the chlorides of the alkaline earths (Be, Ca, Mg, Sr, Ba), and the chlorides of the alkali metals (Na, K, NH_4). With the exception of $CdCl_2$, $PbCl_2$, NaCl, and KCl, all these solids are deliquescent and give off considerable heat during hydration.

A comparison of the heats of reaction and free energies for reaction of these solid chlorides with Al is given in the original report.[13] Aluminum was chosen as the reducing metal since it stands high in the electromotive series, its chloride volatilizes at a comparatively low temperature, and secondary grades of powdered metal can be obtained in considerable

quantity.[11] The reduction of the alkali and alkaline earth chlorides is strongly endothermic (ΔH and ΔF are positive); therefore, the use of these simple chlorides is not practical. The reduction of both $ZnCl_2$ and $PbCl_2$ is slightly exothermic. The reduction of ferric chloride is more markedly exothermic. Since $FeCl_3$, $ZnCl_2$, and $PbCl_2$ are somewhat easier to obtain than the other chlorides, these were used in preliminary trials.

Smoke Mixtures from the Simple Chlorides

The Ferric Chloride and Aluminum Mixture. Theoretically, the reaction of Al with anhydrous $FeCl_3$ proceeds according to the equation:

$$Al + FeCl_3 \longrightarrow AlCl_3 + Fe + 36.6 \text{ kcal.} \quad (1)$$

The stoichiometric mixture for this reaction contains 14.7% Al and 83.3% $FeCl_3$. The smoke produced from such a mixture is excellent, being entirely comparable to that from the best of the HC mixtures. This mixture has several limitations, however, because of the extremely hygroscopic nature of the anhydrous $FeCl_3$. These limitations will be treated in more detail later.

The smoke from the mixture is red when it first leaves the pot, and gradually changes to buff, then to white. This suggested that $FeCl_3$ was being vaporized directly and the smoke was a mixture of iron and aluminum chlorides. Variation of the percentage of aluminum in the mixture and analysis of the resulting residues for aluminum and iron confirmed this observation. The most efficient mixture contains 12% Al and 88% $FeCl_3$. The percentage of aluminum can be varied over a wide range with little difference in performance.

Stability of Mixture. The hydration of $FeCl_3$ is accompanied by the evolution of considerable heat and HCl. The loose smoke mixture reacts vigorously with water to give HCl and sufficient heat to ignite the mixture. Under the low and moderate indoor humidities of winter and spring, it was found possible to mix and press successfully small batches of up to 5 lb. It was necessary to set the mixtures aside in airtight containers for as much as 24 hr after mixing and before pressing. This allowed the heat of hydration of the moisture picked up from the air during mixing to be dissipated before pressing. In two cases where pressing was carried out shortly after mixing, spontaneous ignition took place soon after pressing. In the high humidity of summer (70% humidity or higher) it was almost impossible to carry out the mixing and pressing operations in the laboratory. On one occasion about 20 lb of mixture were made up and set aside in screw-top glass bottles. One of these blew off the top and scattered hot mixture over the rest. They all ignited subsequently over a period of a few minutes and scattered glass and mixture over the laboratory. Another 10-lb mixture of the aluminum and $FeCl_3$ type was successfully mixed and stored but began to heat during pressing. The pressing operation was discontinued and some minutes later the mixture ignited. Apparently spontaneous ignition took place within the cake and blew it apart. Mixtures of $FeCl_3$ and aluminum are therefore quite sensitive to moisture and have to be handled in a dry atmosphere. If kept dry and then pressed, the cakes give every indication of being safe to store and handle.

After pressing, the mixture picked up moisture on top and could not be ignited until this hydrated layer was removed; however, no case of spontaneous ignition was ever observed after a mixture had been successfully pressed without overheating. Water can be poured directly on the pressed surface without vigorous reaction. Penetration of water into the pressed mass is sufficiently slow to allow dissipation of the heat of hydration of the $FeCl_3$.

Ignition Temperature of the Mixture. These values were obtained by slowly heating the loose mixture in a crucible and measuring the ignition temperature with a thermocouple in the mixture. Some smoking is first observed at 105 to 110 C. Ignition does not occur if the heat is removed at this point. Definite ignition occurs at 150 to 160 C.

Burning Time. The burning time for a 600-g pot is generally around 3 min. The 5-lb pots (can size — 5¼-in. diameter, 4 in. high) ranged in burning time from 3 min 45 sec to 5 min 15 sec. The amount of hydration during mixing may have some influence on the rate of burning.

Manufacture of Anhydrous Ferric Chloride. The successful commercial processes for the manufacture of anhydrous ferric chloride on a limited scale use elemental chlorine to supply the three chlorine atoms needed. This is done because it is not practical to dehydrate the ferric chloride formed in solution by the action of hydrochloric acid (and some chlorine) on iron or iron oxide. The ferric chloride forms a hexahydrate and, on heating, this gives up HCl rather than water. Elemental chlorine could be used for either increasing the production of hexachlorethane or ferric chloride. A large increase in demand for chlorine carriers would call for other sources of supply that do not depend on elemental chlorine. Work has

been done on several processes designed to avoid using elemental chlorine to supply two or all three of the chlorine atoms in anhydrous ferric chloride. Further developmental work is needed on all these processes. Some of them are outlined below and the engineering problems involved are pointed out.

1. Scrap iron or iron oxide can be treated with hydrochloric acid to produce ferrous chloride. The ferrous chloride is crystallized from solution, dehydrated probably under reduced pressure, and converted to the anhydrous ferric chloride. The latter step would probably be done with chlorine.

2. The reaction of sodium or calcium chloride, iron sulfide, and air has been suggested. Evidence exists [14] to indicate that the separation of anhydrous ferric chloride from the resulting mixture with sodium or calcium sulfate is difficult. It must be vaporized from the mixture, and its vapor pressure is very much less from the mixture than when pure. Possibly reduced pressure or an inert carrier gas and a high temperature would effect a separation.

3. The reaction of iron sulfate and calcium chloride is in the same class as paragraph 2.

4. Dehydration of the $FeCl_3 \cdot 6H_2O$ in a stream of hot dry HCl would require specially designed equipment.

5. The reaction between iron oxide (roasted pyrites) and dry HCl proceeds with the formation of three moles of water per mole of $FeCl_3$. By proper control of the temperature of the condensing surfaces it may be possible to condense anhydrous ferric chloride from the hot gas stream.

Chloride Complexes

Anhydrous ferric chloride has several disadvantages as a chlorine carrier, chief among which are its extreme hygroscopicity and the limitations in its manufacture which were discussed previously. Complex salts of ferric chloride have been investigated to avoid these difficulties.

Ammonium Ferric Chloride Complexes. Several complexes of NH_4Cl–$FeCl_3$–H_2O are reported in the literature [15, 16] including salts of the composition NH_4FeCl_4 and $(NH_4)_2FeCl_5 \cdot H_2O$. The former substance is obtained by fusion of equimolecular amounts of NH_4Cl and $FeCl_3 \cdot 6H_2O$. The water is removed by evaporation. A boiling point of 386 C has been reported. The $(NH_4)_2FeCl_5 \cdot H_2O$ is obtained by crystallization from a solution of the mixed chlorides. Because of its high percentage of NH_4Cl and its water of crystallization, this compound is of little interest here.

Theoretically the reduction of NH_4FeCl_4 with Al proceeds according to the equation

$$Al + NH_4FeCl_4 \longrightarrow AlCl_3\uparrow + NH_4Cl\uparrow + Fe. \quad (2)$$

The stoichiometric mixture for this equation burned very slowly, giving a poor smoke over a long period of time.

Various heating mixtures were tried with the above stoichiometric smoke mixture for the complex NH_4FeCl_4. No completely satisfactory heating mixture was found which could be used in connection with the above reaction. Complexes of KCl showed much less cooling action than complexes of NH_4Cl. For this reason KCl complexes were more desirable.

Potassium Ferric Chloride Complexes. The only salt of $FeCl_3$ and KCl found in the literature had the composition $K_2FeCl_5 \cdot H_2O$.[17]

1. $K_2FeCl_5 \cdot H_2O$, an orange-yellow complex, was prepared by evaporating water from a fused mixture of $FeCl_3 \cdot 6H_2O$ and 2KCl. The extra molecule of water was driven off to give a complex of the composition K_2FeCl_5. Mixtures made from this compound gave a very poor smoke with a high residue.

2. $KFeCl_4$. This complex was not found in the literature, but since ionic radii of NH_4^+ and K^+ are reasonably close to the same value, and salts of the two ions are isomorphous in many cases, the existence of this salt was suspected. The salt was prepared by evaporation of a mixture of $FeCl_3 \cdot 6H_2O$ and KCl. Two lots were prepared and analyzed. In making lot No. 1 the heat was removed as soon as the liquid water was gone. The massive product was a deep brownish-red but became bright yellow when ground. The color changed to reddish-orange when moisture was picked up. Lot No. 2 was fused after the liquid water was gone and the odor of chlorine could be detected coming from the mass. This massive product was a deeper brownish-red and remained red-brown after grinding. The analyses of the two products showed the following compositions.

	Observed % Cl	Theoretical % Cl	Observed % Fe	Theoretical % Fe
Lot 1	59.53	59.94	24.41	23.66
Lot 2	57.75	59.94	25.62	23.66

Excessive heating appears to have driven off chlorine to form some of the ferrous complex.

3. Mixtures from $KFeCl_4$. Mixtures of this complex combined with aluminum and zinc oxide to supply heat were made. A good smoke was produced which had a characteristic orange color as it left the pot. This color persisted longer than that with the

$FeCl_3$ mixture, gradually fading to white. The principal objections to this mixture were its comparatively short burning time and its relatively high percentage of residue (50%). The reaction

$$2Al + 3ZnO + 2KFeCl_4 \longrightarrow Al_2O_3 + 2ZnCl_2 + 2KCl + Fe$$

indicates a theoretical efficiency of 52.5% if no KCl is volatilized, and 71.5% if all of the KCl is volatilized. Analysis of the residues for potassium revealed that from 46 to 92% of the KCl was volatilized, dependent upon the amount of KNO_3 in the mixture.

The amount of residue was reduced by adding sufficient C_2Cl_6 to react with the Fe formed by the reaction. A mixture of

6.2% Al
23.2% ZnO
22.6% C_2Cl_6
43.5% $KFeCl_4$
4.5% KNO_3 or $NaNO_3$

gave a very good smoke, with about 30% residue. The smoke produced was tan, gradually fading to white. In volume and screening power it was not quite equal to the Al–ZnO–C_2Cl_6 mixture.

The hexachloroethane serves to improve the smoke but the quality is not markedly affected by considerable variation in the percentage. A mixture of the following composition is recommended if C_2Cl_6 is available.

52.0% $KFeCl_4$
27.2% ZnO
9.0% C_2Cl_6
7.3% Al
4.5% $NaNO_3$.

If C_2Cl_6 is not available, a mixture containing

8.0% Al
30.0% ZnO
2.2% $NaNO_3$
59.8% $KFeCl_4$

gives a good smoke for a shorter period of time.

The mixture is not nearly so sensitive to water as the $FeCl_3$ mixtures. However, if the loose mass is triturated with water, the $KFeCl_4$ will hydrate giving off HCl, evolving heat, and swelling markedly. The evolution of heat was never sufficient to ignite the mixture. The $KFeCl_4$ is definitely hygroscopic but less so than $FeCl_3$. The completed mixtures were very convenient to press and handle. The ignition temperature for this mixture was determined by the same technique as that used for the Al–$FeCl_3$ candle. Values of 335 to 350 C were obtained. $KFeCl_4$ appears very promising to supplement hexachloroethane. The complex should be easily manufactured from KCl and hydrated $FeCl_3$.

4. Manufacture of anhydrous $FeCl_3 \cdot KCl$ complex. It is evident that the manufacture of ferric chloride hexahydrate is much easier than that of the anhydrous material, especially if both products are made without the use of elemental chlorine. It should be possible to produce readily large quantities of the hexahydrate using hydrochloric acid and iron or iron oxide with no more than one atom of chlorine being supplied from elemental chlorine. The hexahydrate can be melted and mixed with an equal number of moles of KCl. The complex $KFeCl_4$ then forms and allows the dehydration to take place readily by heating to 205 C.

High-Efficiency Smoke Mixtures

In the reduction of ferric chloride by aluminum in the Al-$FeCl_3$ mixture, elemental iron is left as the principal constituent of the residue. Addition of enough C_2Cl_6 to remove the iron as $FeCl_3$ increases the theoretical efficiency of the mixture considerably, leaving the carbon of the hexachloroethane as the only element not used in smoke production. The reaction should proceed as follows:

$$2Al + 2FeCl_3 \longrightarrow 2AlCl_3 + 2Fe$$
$$2Fe + C_2Cl_6 \longrightarrow 2FeCl_3 + 2C$$

or in the following manner:

$$2Al + C_2Cl_6 \longrightarrow 2AlCl_3\uparrow + 2C + \text{heat}$$
$$FeCl_3\ (\text{solid}) + \text{heat} \longrightarrow FeCl_3\uparrow\ (\text{vapor}).$$

The end result is the same in both cases. Probably both reactions are involved.

The stoichiometric mixture for these reactions gives a theoretical efficiency of 96%. The mixture has the following composition:

8.8% Al
52.6% $FeCl_3$
38.6% C_2Cl_6.

The above mixture gave actual residues of from 3 to 5% of the original mixture, but the burning rate was too slow and the resulting rate of smoke evolution was correspondingly slow. Small amounts of $NaNO_3$ were added to increase the burning rate. This percentage is rather critical, very small differences having a marked effect upon the burning time.

A smoke cloud superior to that produced by the

HC mixture of Al–ZnO–C_2Cl_6 was produced by a mixture of the following composition:

8.8% Al
51.6% $FeCl_3$
38.3% C_2Cl_6
1.3% $NaNO_3$.

This mixture burned noticeably faster than the standard Al–ZnO–C_2Cl_6 mixture in M 1 pots.

Large percentages of both $FeCl_3$ and C_2Cl_6 are used in this type of mixture, but an extremely dense smoke cloud is produced. A mixture of this type may have application where a high-efficiency mixture is desired. Because of the $FeCl_3$ content it is sensitive to water before pressing, evolving HCl and heat. After pressing, the candle is damaged by water but the reaction is not vigorous. The mixture should be protected by a watertight container.

Chlorpropane Wax

Chlorpropane Wax produced on a pilot plant scale was investigated as a possible chlorine carrier. The product corresponded approximately to the formula C_3Cl_8. This material was substituted for hexachloroethane in the standard HC mixture of Al ZnO–C_2Cl_6.

The reactions are probably very similar to those for the standard HC candle.

$$2Al + 3ZnO \longrightarrow Al_2O_3 + 3Zn$$
$$4Zn + C_3Cl_8 \longrightarrow 4ZnCl_2\uparrow + 3C$$
$$C + ZnO \longrightarrow Zn + CO.$$

The reaction

$$8Al + 3C_3Cl_8 \longrightarrow 8AlCl_3\uparrow + 9C$$

undoubtedly occurs to some extent in conjunction with the above. The burning time was regulated by adjusting the per cent of Al.

A mixture with a smoke volume and burning time comparable to the standard HC mixture was produced. This had the composition:

Al = 6.25%
ZnO = 46.15%
C_3Cl_8 = 47.60%.

32.1.5 Sulfur-Nitrate Screening Smoke Mixtures

Summary

Mixtures containing essentially a nitrate, charcoal, and sulfur have been investigated as a source of screening smoke.[24] These mixtures are placed in a metal can with a perforated cover. The nitrate and charcoal and some of the sulfur react, giving off heat which vaporizes the remaining sulfur. The mixture of reaction gases and elemental sulfur vapor is emitted with some velocity through the perforations. Each jet entrains air and cools the sulfur vapor, condensing it to form minute smoke particles. This smoke is white and shows little of the yellow color of sulfur.

Sodium, potassium, or ammonium nitrate may be used. The former is available in the largest quantities while the latter gives a greater amount of diluting gases. The chief advantage of the mixture is that all the ingredients are available in large quantities. Weight for weight they are in the order of 50% as efficient as HC smoke mixtures.

The mixtures appear to be safe to handle and store. No evidence to the contrary has been found during the rather extensive experimental work. As a conservative precaution, however, it is recommended that adequate steps be taken to protect property and personnel from fire or explosion during the mixing and pressing operations.

Methods of Producing Sulfur Smoke

Sulfur smoke as discussed here refers to small particles of elemental sulfur suspended in the air. Such a smoke has been set up in a number of ways. A continuous sulfur boiler fired by a gasoline burner was described [19] in Chapter 30. This produced up to 500 lb per hr of sulfur smoke by forcing a mixture of sulfur vapor and superheated steam through nozzles under a pressure of several pounds per square inch.

A sulfur smoke was also produced on a small scale in three units housed in a greenhouse.[20] These produced sulfur smoke by (1) forcing a mixture of steam and sulfur vapor through nozzles, (2) using a steam-powered atomizer to spray liquid sulfur (containing 0.2% iodine) into a heated iron tube, (3) allowing molten sulfur to run into the exhaust of an automobile engine operating at 15 hp.

A stainless steel tubular sulfur boiler was built and operated.[21] This unit produced up to 275 lb per hr of sulfur smoke by forcing pure sulfur vapor through a nozzle at pressures up to 70 psi.

Sulfur smoke was also produced by a small two-compartment thermal generator pot.[22] A fuel block of ammonium nitrate and charcoal was placed in the lower compartment and lump sulfur in the upper. The hot gases from the fuel block passed to the upper compartment through a Venturi-shaped tube and the molten sulfur was drawn into the throat of the Ven-

turi through a hole. The mixture of sulfur vapor and fuel gases issuing from the top of the Venturi passed around a baffle and out through holes in the top of the upper compartment. Cooling of the vapor by air entrainment formed smoke.

A continuous portable sulfur smoke generator using the hot gases supplied by a gasoline burner and with molten sulfur sprayed into these through a hole in the throat of a Venturi tube was built and operated successfully.[23] The flow of hot gases through the Venturi and of the sulfur vapor-combustion gas mixture through the exit holes was induced by a steam entrainment jet.

The SN Mixture — Factors Affecting its Performance

This sulfur smoke mixture is composed of sulfur intimately mixed with a suitable fuel. When this mixture is ignited in a closed container with holes through which the resulting sulfur vapor-gas mixture can escape, a smoke of elemental sulfur particles is formed. The fuel used contained a nitrate as oxidizing agent and hence the mixtures have been designated sulfur-nitrate or SN mixtures.

Mixtures have been made which contain principally sulfur, sodium nitrate, and charcoal; sulfur, ammonium nitrate, and charcoal; and sulfur, potassium nitrate, and charcoal. The sulfur is present in considerable excess over that in black gunpowder and its latent heat of fusion and vaporization absorbs the heat of reaction and slows the burning rate. The rate of burning is influenced by the percentage of sulfur.

The mixtures can be made by blending and pressing the dry screened ingredients or by mixing the nitrate (except NH_4NO_3) and charcoal into the molten sulfur. Better results have been obtained by dry mixing and pressing since this method results in a greater percentage of the mixture being evolved as sulfur smoke. These dry mixtures must be pressed to insure a compact block and uniform burning. The minimum load to produce a satisfactory cake is of the order of 600 to 800 psi. Some of the sulfur reacts during the burning to form sulfides and sulfates which are left in the residue. This does not occur when ammonium nitrate is used, and apparently all the sulfur is then converted to smoke. In any case, the burning fuel does not produce SO_2 in the container. The percentage of sulfur which reacts during the burning, and the rate of burning depend to some extent on the particle size of the sulfur in the mixture. The ideal condition is an intimate mixture of nitrate and charcoal which transfers its heat of reaction to the sulfur without reacting with it. This situation can be approached by using a larger particle size for the sulfur than for the other ingredients. If the sulfur particle size is too large, however, some of the sulfur is not evaporated and the efficiency drops off. The rate of burning also increases because the sulfur is not so effective as a cooler. When the mixture is made by melting the sulfur, it is intimately mixed with the fuel and, on burning, a part is oxidized to SO_2 with the result that a thin smoke is produced.

The fuel gas-sulfur vapor mixture is hot as it comes from the burning block and will readily ignite and burn to form SO_2 if mixed with air. If, however, this mixing with air is carried out rapidly, the sulfur vapor is cooled below its ignition point before it ignites. Rapid dilution and cooling is also required to form the proper size sulfur particles (about 0.15 micron radius) for an effective screening smoke. This rapid cooling and dilution with air is accomplished by forcing the hot gases through a number of small orifices in the container out into the air. Orifices about $^3/_{32}$ in. in diameter have been used. The number of orifices must be balanced against the burning rate. If too few orifices are used, excessive pressure will develop and rupture the container. At low pressures the rate of flow through the orifices increases in proportion to the square root of the pressure in the container. This will adjust the flow rate automatically for small changes in the burning rate. At pressures above about 12 psi, the rate of flow increases much less with pressure. A sufficient number of orifices should be used to insure against the pressure rising higher than this. There will be no need then to build the containers to withstand a higher pressure. Inert gases, such as CO_2 or N_2, evolved by the fuel and mixed with the sulfur vapor, help to prevent flaming and give a smaller particle size in the smoke.

The amounts of heat and the volumes of gas generated by a number of possible fuel reactions are shown in Table 2. Of the possible reactions of charcoal with NH_4NO_3, $NaNO_3$, or KNO_3, the first gives the largest amount of heat and gas, and the others fall in the order named. This is based on the assumption that the carbon is oxidized to CO_2 [see equations (2), (4), (6), Table 2]. At 600 C the sodium nitrate produces 60% as much heat and 43% as much gas as the ammonium nitrate per unit weight of fuel mixture. If the sulfur enters the reaction [equation (9)] the amount of heat produced per unit weight of carbon plus nitrate is increased and in the case of

TABLE 2. The heat evolved and the volume of inert gases furnished by several fuel mixtures based on an assumed reaction is tabulated below.

	Reaction	kcal/g mix 20 C	kcal/g mix 600 C	Liters gas (STP, 0 C, 1 atm)
(1)	$C + NH_4NO_3 = CO + N_2 + 2H_2O$ (g)	0.588	0.384	0.975
(2)	$\frac{1}{2} C + NH_4NO_3 = \frac{1}{2} CO_2 + N_2 + 2H_2O$ (g)	0.87	0.667	0.910
(3)	$\frac{5}{2} C + NaNO_3 = \frac{5}{2} CO + \frac{1}{2} N_2 + \frac{1}{2} Na_2O$	0.029	....	0.578
(4)	$\frac{3}{4} C + NaNO_3 = \frac{3}{4} CO_2 + \frac{1}{2} N_2 + \frac{1}{2} Na_2O$	0.55	0.400	0.392
(5)	$\frac{5}{2} C + KNO_3 = \frac{5}{2} CO + \frac{1}{2} N_2 + \frac{1}{2} K_2O$	−0.065	....	0.515
(6)	$\frac{5}{4} C + KNO_3 = \frac{5}{4} CO_2 + \frac{1}{2} N_2 + \frac{1}{2} K_2O$	0.365	0.256	0.338
(7)	$\frac{2}{5} P + NH_4NO_3 = \frac{1}{5} P_2O_5 + N_2 + 2H_2O$ (g)	1.09	0.799	0.725
(8)	$P + NaNO_3 = \frac{1}{2} P_2O_5 + \frac{1}{2} N_2 + \frac{1}{2} Na_2O$	0.975	0.805	0.0963
(9)	$C + NaNO_3 + \frac{1}{2} S = \frac{3}{2} CO_2 + \frac{1}{2} N_2 + \frac{1}{2} Na_2S$	0.715	0.580	0.378
(10)	$2Al + C_2Cl_6 = C + 2AlCl_3$	0.838	0.679	0.000

(Note: The heat required to heat and vaporize sulfur (18 to 600 C) amounts to 0.216 kcal/g.)

sodium nitrate it is 87% of that with ammonium nitrate.

DESCRIPTION OF SN MIXTURES

The compositions of typical SN mixtures are shown in Table 3. These mixtures all produced excellent smoke in several tests although all gave somewhat variable performance.

SUGGESTIONS FOR IMPROVING THE MIXTURES

These mixtures were never completely developed to give reliable and reproducible results. The chief difficulty arose from nonuniform and nonreproducible rates of burning which resulted in flaming of the vapors in some cases. Work on these mixtures was discontinued in order to concentrate effort on the black powder-oil gel mixtures described below. The final results from the latter, however, were not entirely satisfactory. The two-compartment oil smoke generator (see Chapter 30) resulted in a satisfactory smoke pot, which meets the requirements for oil smoke pots in spite of its more complicated internal construction. The improvements developed for the fuel block for this latter pot and other thermal generators, and described in Chapter 31, could very likely be applied to the SN mixtures to give a satisfactory sulfur smoke pot of the intimate mixture type. Specifically the improvements suggested are:

1. The use of linseed oil binder instead of celluloid in acetone.
2. The use of a heavy paper liner for the cans to prevent burning down the sides of the mixture.
3. Pretreat the charcoal and develop specifications for its manufacture.
4. As an alternative for 3, the use of a noncarbon pyrotechnic fuel for mixing with the sulfur. All ingredients of such a fuel would be subject to rigid manufacturing control.

THE SCREENING POWER OF SULFUR SMOKE

The screening power of sulfur smoke has not been measured in tests on a relatively large scale in comparison with other types of smoke. In tests on a continuous sulfur smoke generator, producing as high as 275 lb per hr with an average particle size of 0.23 micron, it was estimated that in the order of 1,000 lb sulfur per square mile was required for a good screen in winds from 7 to 17 mph. This is approximately the same amount as for Diol and also HC mixture.

A visual comparison was made at Edgewood Arsenal of the M–1 HC smoke pots containing about 12 lb of HC mixture with SN pots containing about 5½ lb of mixture. The volume of smoke near the pots compared favorably, but the sulfur smoke was somewhat less persistent. The sulfur pots generate approximately 50% of the weight of the mixture as smoke, whereas the HC mixture gives in the order of 75% of its weight as $ZnCl_2$. The latter weight of smoke is augmented by taking water vapor from the air to hydrate the $ZnCl_2$.

A rough estimate of the cost of area screening by SN mixture can be made, although this is not based on adequate field tests and may be inaccurate. A figure of 1,400 lb per square mile required for screening is taken as a basis. In a 10-mph wind this would require 14,000 lb per hr of sulfur smoke or 28,000 lb per hr of SN mixture. With sodium nitrate at $1.35 per 100 lb, and sulfur about one cent per pound or less, the cost of the mixture prepared and loaded into containers should be in the order of 3 to 5 cents per lb. (*Note.* Diol itself costs from 3 to 4 cents per lb.) This would indicate a cost of $800 to $1,400 per hr per square mile for SN pots alone, exclusive of the labor to place and operate them.

SAFETY PRECAUTIONS

Mixtures of the type consisting essentially of

TABLE 3. Compositions of typical SN smoke mixtures.

Sulfur–$NaNO_3$–Charcoal

1,500 g mixture used with a surface area of 22.7 sq in.; binder, 5% celluloid in acetone; 75 g of starter, 32.0% $NaNO_3$, 8% charcoal, 60% sulfur.

$NaNO_3$, wt %	31.47	34.0
Charcoal, wt %	5.53	6.0
Sulfur, wt %	63.0	60.0
Binder, cc	140.0	150.0
Burning time, min	2–2½	4 4¾
Sulfur, mesh size	14–28	28 35
Per cent of mixture as smoke	47–50	46
Orifice size, in.	⅛ to 3/32	3/32
Number of orifices	12–14	14

Sulfur–NH_4NO_3–Charcoal

1,250 g mixture with a surface area of 38.5 sq in.; binder, 5% celluloid in acetone; sulfur, commercial flowers; 20 g British starter (40% Si, 54% KNO_3, 6% C) compressed into ½ x 2-in. diameter pellets; pressed in three layers.

	Bottom	*Middle*	*Top layer*
NH_4NO_3, wt %	45	55	86
Charcoal, wt %	9	11	14
Sulfur, wt %	46	34	..
Binder, cc	200	60	20
Weight of layers, g	1,000	200	50

NH_4NO_3–KNO_3–Charcoal–Sulfur

2,500 g mixture was used with a surface area of 50 sq in. The mixture was in three layers of 270 g, *A*; 1,750 g, *B*; then 270 g, *A*. A hard core of 270 g *A* compressed under 10 tons/sq in. was arranged to pass through the center of the other three layers; 20 g of *C* was used as starter and the whole pressed under 600 lb/sq in.

	A	*B*	*C*
Charcoal, wt %	6.3	3.1	15.0
NH_4NO_3, wt %	19.9	...	...
KNO_3, wt %	27.8	32.2	75.0
Sulfur, wt %	46.0	64.7	10.0
Binder, cc/100 g	30.5	14.2	25.0

sodium nitrate, charcoal, and sulfur have been mixed and pressed in amounts up to 3 lb and mixtures of potassium nitrate, charcoal, and sulfur in amounts up to 5½ lb. During this experimental work, there was no incident to indicate that these mixtures were sensitive or dangerous to handle by the methods of mixing and pressing employed. During burning of the completed experimental smoke pots in the field, there was a number of tests in which the mixture burned too rapidly for the gases to escape through the perforations in the cover; the cover was blown off and the contents scattered over a radius of several yards.

It was found possible to ignite small samples of the mixtures by impact. Samples fired on a type of machine that afforded some confinement for the mixture were found to give only a small amount of smoke upon the impact of a 2-kg weight dropped 70 to 75 cm. Under identical conditions, an explosive considered to be moderately sensitive gives complete detonations at 40 to 45 cm. On the other hand, TNT fails to fire at 100 cm. Under conditions which afforded very little confinement, samples gave a small amount of smoke, but no ignitions or detonations at 200 cm. The moderately sensitive explosive fires at approximately 25 cm. Therefore, the samples were apparently not very sensitive to impact. In all cases it was necessary for the operator to watch very closely for the small wisp of smoke which indicated that some decomposition had taken place.

A small pile of the mixture could not be ignited with an ordinary match. Black gunpowder is known as an unpredictable composition, and extreme care, practically amounting to distrust, should be exercised in processing it. Experience indicates that the cooling effect of the large excess of sulfur in these mixtures makes them much less sensitive to ignition by sparks and much slower burning when ignited than black powder. In view of the limited experience with the mixtures, however, it is advisable to handle them with the same precautions as black gunpowder.

32.1.6 Diol-Sawdust-Chlorate Smoke Mixtures

SUMMARY

An intimate mixture of Diol and a fuel was partially developed into a smoke pot of promising performance.[25, 23] The fuel consisted of a mixture of sawdust and charcoal, impregnated with a solution of potassium chlorate which was subsequently dried. The Diol was jelled with 2½ to 3% Ivory soap flakes. The chief drawback of this smoke mixture is the extreme hazard incurred in handling the impregnated sawdust, especially when dry, before the Diol is added. Once the Diol has been blended into the fuel the mixture is quite stable. This pot weighed about 45 lb, contained 39 lb of smoke mixture, and burned about 20 min.

THEORY OF OPERATION

The fuel used in this mixture is bulky. The oxidizing agent, which may be potassium chlorate or sodium nitrate, is deposited from solution in the pores and on the surface of the sawdust. It is very reactive in this condition and when the mixture is dry, combustion

will flash through the mixture very rapidly. If Diol is added and thoroughly mixed in so that the sawdust is oil soaked but not submerged in oil, the burning rate is slowed down considerably but the combustion may still pass throughout the mixture quickly and even fail to vaporize some of the oil. If the fuel is submerged in oil the combustion does not take place below the oil level, and burning takes place regularly and progressively down through the mixture volatilizing the oil as it goes. This latter is the principle on which the pot functions.

Description of the Smoke Pot

The arrangement of the smoke pot is shown in Figure 3.

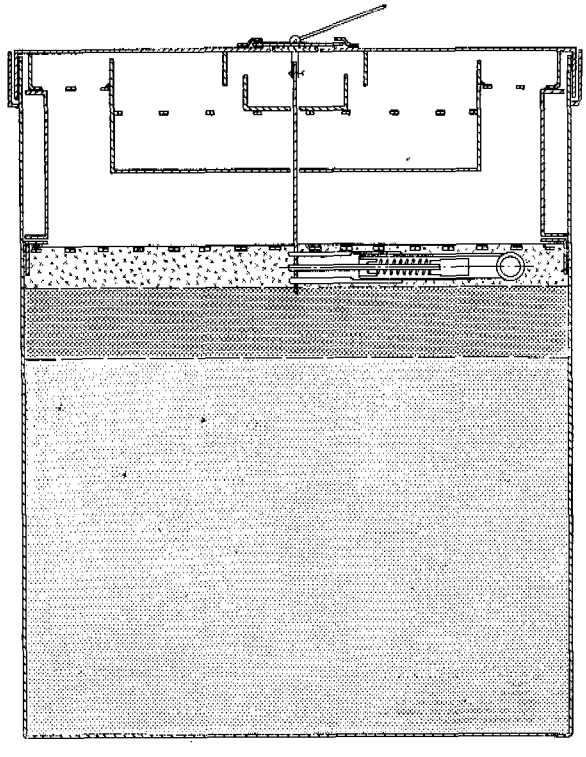


Figure 3. Experimental pot for Diol-sawdust-chlorate smoke mixture.

Smoke Mixture. A fairly satisfactory mixture consisted of 24.8% sodium chlorate, 10.1% charcoal, 10.1% sawdust, and 55% Diol. A mixture with a higher Diol content could probably be developed but the work did not continue far enough to establish the limits in this respect. The mixture was prepared by soaking the sawdust in a water solution of potassium chlorate and then drying this sawdust to remove the water. The treated dried sawdust was extremely hazardous to handle. The sawdust thus prepared was then mixed with a suspension of charcoal and additional chlorate in Diol. The Diol used was prepared by dissolving 2½ to 3% Ivory soap flakes in it at 230 F with continuous stirring during the cooling of the mixture. The cooling should take place at a moderate rate.

In addition to this main mixture, a transition mixture and a starting mixture were employed. About 35 lb of the main mixture with 3 lb of the transition mixture and 1½ lb of the starting mixture were used. The transition mixture contained 18% sodium chlorate, 5.6% charcoal, 21.9% sawdust, and 54.5% Diol and the starting mixture contained 13.5% sodium chlorate, 32.5% sawdust, and 54% Diol. In each case the ingredients were 24-mesh yellow pine sawdust, 150-mesh charcoal powder and Diol 55.

Container. The smoke mixture was placed in the bottom of a 12-in. diameter by 15-in. high steel can closed with a tight cover. The oil vapor and combustion gases issued from a single 1-in. diameter orifice in the center of the cover. A spark filter consisting of an arrangement of baffles was placed between the smoke mixture and the cover. The pot was well suited for use as a smoke float. The smoke mixture ignites when a strong acid comes in contact with it. This was the method used to ignite the pots. A glass vial of sulfuric acid was placed in a metal case and inserted in the starting layer of smoke mixture. The metal case contained a cocked firing pin actuated by a spring. The pin was held by a rod extending up through the cover of the pot. When the firing rod was pulled, the cocked pin was released and broke the acid vial igniting the smoke mixture.

The screening power of the smoke was entirely comparable to the oil smoke produced by the continuous oil smoke generators, except that the pot generated it at a much lower rate. The burned sawdust gave the smoke the acrid smell of burning wood which was somewhat irritating near the pot but was diluted sufficiently a short distance away.

Development

Smoke Mixture. Some of the salient features of the development work will be mentioned especially where they convey ideas for the improvement of this or similar mixtures.

The *charcoal* was added to increase the heat available to vaporize oil since charcoal has a significantly higher heat of combustion than wood. This resulted in complications due to a decreased burning rate.

The burning rate is affected by the ingredients used

in the mixture, their proportions, and method of preparation as well as the conditions of operation. The ideal mixture [26] will oxidize all the sawdust and charcoal and none of the oil. A theoretical mixture should be possible containing 17.5% sodium chlorate, 1.4% charcoal, 2.9% sawdust, and 78.2% Diol. Heat losses from the pot and incomplete combustion reduce the per cent Diol below this theoretical figure. It should be possible to incorporate a considerably larger percentage of Diol than the 55% used in the pots. The mixture was not very sensitive to the temperature of the mixture at the time of ignition. Two identical pots were prepared and stored, one at 110 F and the other at 10 F for 72 hr, and then burned immediately. The higher temperature pot burned in 18 min while the cold one burned in 21 min.

The oil was jelled to improve the performance at the higher temperatures (110 F). There was a tendency for a layer of oil to separate at these temperatures and interfere with the ignition. Various jelling agents were tested. These included aluminum stearate, oleate (titer number 10–12) flakes, amber flakes (titer number 42), and both Ivory and Swift soap flakes (both have a titer number of approximately 32). The oleate flakes were mainly sodium oleate; Ivory flakes are about half and half sodium oleate and sodium stearate; and the amber flakes, mainly sodium stearate. The oleate flakes formed a poor jell. The Ivory and amber flakes were about equal in jell-forming properties, with the Ivory flakes possibly a little superior. Of several greases tested, Nakta 8–F (Standard Oil Co. of Pennsylvania) gave the best results.

Sodium nitrate may possibly be substituted wholly or in part for the potassium chlorate. This may be found desirable due to a shortage of potassium chlorate or to the reduced hazard from sodium nitrate, although both chemicals are considered hazardous. Black gunpowder can be used for the fuel in place of the mixtures described. A smoke mixture with black gunpowder is described in the next section. The oil in the mixture depresses the burning rate and eliminates the hazards normally associated with black powder itself.

The Container. Several sizes of containers were tried in addition to the one described above. These were 12 in. in diameter by 8 in. high, 6 in. in diameter by 7 in. high, and 1¼ in. in diameter by 4 in. high. A 5-gal paint or oil can would no doubt be the most suitable. This would compare with the M4A2–HC smoke float.

The smoke exit orifice is of great importance since it controls the flaming tendency of the mixture, the particle size of the smoke, and hence its screening power, and the pressure within the pot. In the pot described, this orifice might well be reduced to a single ¾-in. diameter hole or several smaller orifices of the same total area.

The partially burned sawdust and charcoal showed a tendency to be blown from the pot in a shower of sparks. If the exit smoke velocity was low, these sparks ignited the oil vapors before they had time to condense to smoke particles, and flaming from the orifice resulted. Various forms of spark filters were tried over the smoke mixture. Those which consisted of an actual filtering material, such as a wire mesh or steel wool, were not satisfactory due to plugging of the filter. A baffle arranged as shown in Figure 3 was found to be quite satisfactory. The gases rose to the top of the pot around the periphery and then reversed their direction down into a centrally located ash trap and then reversed direction a second time to reach the exit orifice. This flow removed the ash and sparks without obstructing the flow of gases and vapors.

The trigger should be centrally located in the starting layer so that the flame will spread out radially in all directions equally.

32.1.7 Jelled Oil-Black Gunpowder Smoke Mixture

Requirements and Preliminary Work

The principle involved in these pots consists of vaporizing a high-boiling mineral oil by a fuel intimately mixed with the oil, followed by expulsion of the oil vapors and combustion gases from the fuel through an orifice or orifices and subsequent condensation of the oil vapor into oil droplets of about 0.3 micron radius. Oil droplets of this size have optimum screening powers.

Specifications called for the filling mixture (1) to be composed of noncritical materials; (2) to be chemically stable and capable of withstanding the effects of prolonged storage at temperatures up to 150 F; (3) to produce a thick, persistent, nontoxic smoke for 10 to 15 min; (4) to produce smoke at a maximum rate within a few seconds after ignition, the rate to be about the same at 0 F as at 150 F; and (5) the combined weight of filling and container to be 35 lb or less.

It was decided to develop a filling mixture similar

to the $KClO_3$–sawdust–oil mixtures. The use of chlorates was prohibited due to the great hazards involved in handling these salts. The possibility of utilizing black powder as fuel to vaporize the Diol was given primary consideration. Since a prerequisite of the fuel was its availability in large quantities, it was decided to confine the major portion of the work to sodium nitrate base (B) black powder. The A powder is more expensive and its base, potassium nitrate, is much more critical in supply than sodium nitrate. The A black powder is a trifle stronger, somewhat quicker, resists moisture better, and will keep in good condition longer than B blasting powder.

The best base charge developed was composed of 48% B black powder, $^{16}/_{24}$-mesh; 2% coarse sawdust; 8% treated AL wood pulp; and 42% Diol 55 jelled with 1½% sodium stearate. The best transition mixture was composed of 43% B black powder, $^{16}/_{24}$-mesh; 6% treated AL wood pulp; 21% coarse sodium nitrate; and 30% Diol 55 jelled with 1½% sodium stearate. Although both mixtures functioned reasonably well from −40 to 150 F and produced a good smoke cloud, neither was stable when stored at 150 F for prolonged periods. Syneresis of the Diol jell occurred at this temperature, resulting in the formation of a layer of free oil on top of the charge that destroyed the proper functioning of both mixtures. The manufacturing process for both mixtures was simple, short, and practical, and required no elaborate equipment.

A number of oils, greases, jells, and absorbents were tested in an effort to produce a mixture which would be stable at 150 F and would perform satisfactorily at all temperatures from −40 to 150 F. An outstanding characteristic of the oil-smoke mixture was the effect produced by varying the amount of jelling agent. When the amount of the latter was sufficient to stabilize the resultant jell at 150 F, a high percentage of fuel was required to maintain combustion. This resulted in a much higher temperature than was necessary to vaporize the unjelled oil. Consequently, the oil vapors were cracked and the smoke cloud was thin, nonpersistent, yellowish brown in color, and of very small particle size.

The various phases of the work will be described under separate headings.

General Experimental Tests

A total of 1590 oil-black gunpowder smoke mixtures were tested.[28] They were burned in containers ranging from 3 in. to 12 in. in diameter, and from 7¼ in. to 24 in. in height. The container used most effectively was a 5-gal, 24-gauge, lug-covered, straight-sided shipping container equipped with six $^{13}/_{32}$-in. diameter side orifices. The pot was ignited by an electric squib and primed with a mixture of Pb_3O_4, Al, and FeSi contained in a quick-melting zinc cup. The cup was soldered in a 3½-in. hole in a sheet metal diaphragm which was utilized to hold the charge securely in place. A cork gasket resting on a flat bead rolled in the side of the container formed a seal with the diaphragm. The filling mixture was composed of a fast-burning transition layer weighing 4 lb and a base charge weighing 24 lb. The entire unit weighed 35 lb.

The following conclusions were drawn:

1. A primer composed of red lead, aluminum, and ferrosilicon was entirely satisfactory.
2. From 2 to 4 lb of transition mixture were necessary to produce rapid, positive, and uniform ignition of the base charge.
3. Standard 5-gal paint pails were entirely suitable for use as containers.
4. No baffles or spark filters were required to prevent flaming when the smoke issued through small-diameter orifices.
5. No base charge was produced which proved satisfactory under all conditions to which smoke pots are exposed.
6. When sufficient jelling agent was added to oil to prevent separation of fuel from the oil and free oil from the jell at elevated temperatures, an excessive amount of black powder was required to maintain combustion.
7. Attempts to prevent separation of the fuel from the oil by the use of absorbent materials produced charges which burned at excessive rates due to the porosity of the charges.
8. Charges formulated with reduced amounts of jelling agent, supplemented by absorbent material, exhibited syneresis at elevated temperatures.
9. Potassium nitrate black powder was a much more efficient fuel than sodium nitrate black powder.

Experimental Development

Basic Mixture. The basic mixture which made up the major part of the charge to the smoke pot was compounded of a wide variety of ingredients consisting principally of various grades and types of black powder; oils such as Diol 55, Diol 55 with jelling agents, vaseline; bulky fillers such as wood pulp, ground newsprint, and sawdust; and sodium

nitrate. The Diol jell was prepared by heating Diol 55 with Ivory soap flakes to 240 C accompanied by considerable agitation and followed by cooling slowly in air without further agitation. Although a fair amount of smoke was produced by some of the initial filling mixture compositions, considerable trouble was encountered from flaming and uneven burning rates.

Decreasing the orifice diameter increased the velocity of the smoke vapors and decreased the particle size of the smoke. For example, smoke issuing from a $\frac{5}{8}$-in. diameter orifice was much finer and more persistent than if it had passed through a 1-in. diameter orifice. Subsequent tests were made in pots equipped with a medium-size single orifice, or a number of relatively small diameter orifices.

Numerous jelled-oil, vapor-producing materials were tested. Included in this group were: Diol 55 jelled with 3% sodium stearate; kerosene jelled with 3 and 5% sodium stearate; 969 oil jelled with 3, 8, and 23% sodium stearate and with 15% aluminum stearate. Base charges containing the relatively high stearate-content greases (15% aluminum stearate and 23% sodium stearate) and 4FB or 3FB black powder burned very slowly and produced very little smoke. In general, the charges containing the lower stearate-content jells burned faster, but still were slower and produced a thinner smoke than those containing unjelled oils. The extent to which the rate was retarded was proportional to the stearate content of the jell.

To circumvent the objectionable features of the jelled oils, and produce a filling mixture whose ingredients would not segregate at 150 F, a large number of base charges were formulated with B blasting powder, highly absorbent carbonaceous material, and either Diol 55 or vaseline. At least 7% of absorbent material was required to prevent the black powder from settling out of a 50–50 mixture of powder with vaseline or Diol 55 at 150 F. As a rule, these charges burned at a high nonuniform rate and produced a good volume of fairly white, persistent smoke.

A group of base charges, which contained a relatively fine granulation of KNO_3-base black powder, exhibited excellent smoke-producing properties. A charge which was representative of the group was composed of 37% 3FG sporting powder, 13% ammonia dope, and 50% Diol jell (1% sodium stearate). It was believed that the excellent properties possessed by this group of charges was due either to the fine granulation, the 4-hr milling time, or the KNO_3 base of the 3FG sporting powder. A supply of B blasting powder having the same granulation, i.e., $^{24}/_{46}$-mesh silk was procured. Charges containing this powder and having the same percentage composition as the one containing 3FG powder were very slow burning.

Charges containing 43% 3FG sporting powder, 5% T–14 wood pulp, 5% sawdust impregnated with 50% $NaNO_3$, and 47% Diol jell (1% sodium stearate) burned at a satisfactory uniform rate, and produced a good volume of fairly persistent smoke. The nitrate-impregnated sawdust, as well as the sporting powder fuel, apparently influenced the functioning of these charges. Charges in which a mechanical mixture of coarse sawdust and coarse sodium nitrate was substituted for the impregnated sawdust functioned practically as well as those just described. Substituting 3FG sporting powder which had been milled 1½ hr, instead of the usual 4 hr, in these formulations had very little effect on their performance. Sporting powder milled for 1½ hr would be a much cheaper product than the regular 4-hr milled powder.

B blasting powder, $^{24}/_{46}$-mesh, which had been milled for 3 or 4 hr did not improve the performance of charges similar in formulation to those containing B blasting powder, $^{24}/_{46}$-mesh which had been milled for 1½ hr. B blasting powder, which was manufactured with sporting powder pulverize (charcoal-sulfur mixture), possessed none of the desirable burning characteristics of sporting powder. Therefore, in view of the fact that B blasting powder of the same granulation as 3FG sporting powder, milled for the same period as sporting powder, or containing the same pulverize as the A powder did not equal the latter in performance, it is apparent that the excellent properties of sporting powder were due primarily to its base, potassium nitrate.

In order to secure more uniform distribution of the fuel in the filling mixture, B blasting powder, $^{16}/_{24}$-mesh (considerably finer than 4FB blasting powder) was tested in base charges having the following composition: 48% B blasting powder, $^{16}/_{24}$-mesh; 3% coarse sawdust; 5% T–14 wood pulp; and 44% Diol jell (1% sodium stearate). These charges burned at a fairly uniform rate and produced a good cloud of smoke. The $^{16}/_{24}$-mesh granulation of B powder was of normal composition. It was used in the majority of the charges tested during the latter part of the investigation. The 3% coarse sawdust in the above charges apparently maintained a thicker burning layer, thereby producing a uniform rate of smoke

production. The fact that these charges were dense, soft, and wet (oily) probably had a great effect on the burning. In practically all cases in which the charge was low in density, dry, and porous, the burning rate was uneven and uncontrollable.

The first few attempts to burn charges at initial temperatures greater than 120 F resulted in blowing the covers from the pots within a few moments after ignition. The fact that the charges were mixed at room temperature and then heated to 120 F or higher seemed significant. Mixing at 120 F under atmospheric pressure, or mixing at room temperature under 4 to 5 psia, resulted in charges which burned at a normal rate when ignited at 120 F. The excessive burning rates were evidently due to air entrapped during mixing at room temperature (sometimes as high as 22% of the volume occupied by the charge), which expanded when the charge was heated to 120 F and made the mixture porous. The viscosity of the Diol jell at 120 F was much less than at room temperature, and, consequently, less air was entrapped. Mixing under reduced pressure also reduced the amount of air entrapped. Although these two methods produced charges containing much less air than previously, a considerable amount of air still remained. An effective but impractical method of removing substantially all of the air, consisted of jouncing the pots at 150 F. This method was improved later by jouncing under reduced pressure. Subsequently, a simple, practical method was devised for removing most of the entrained air. It consisted of drawing the hot, freshly mixed charge into the smoke pot through a ⅝-in. diameter orifice under a fairly high vacuum.

When the last mentioned charge (48% B powder, 3% sawdust, 5% T–14 pulp, 44% Diol jell) was heated to 150 F and subjected to a test simulating the vibrations which might be encountered during shipping, the black powder settled to the bottom of the pot, leaving a 1½-in. top layer consisting only of oil and carbonaceous material. To prevent settling of the black powder under these conditions, the percentage of absorbent materials and the amount of sodium stearate in the Diol jell were increased, and more highly absorbent wood pulp was substituted for T–14 pulp. The resultant charge was composed of 48% B blasting powder, $^{16}\!/_{24}$-mesh; 2% coarse sawdust; 8% treated AL pulp; and 42% Diol jell (1½% sodium stearate). This charge performed very satisfactorily at all temperatures between 0 F and 150 F, and produced a good cloud of white, fairly persistent smoke for about 10 min. However, during hot storage at 150 F, the jell broke down to an extent depending on length of storage, causing the formation of an oil layer on top of the charge. Upon ignition of these pots after hot storage, the oil layer either quenched the primer or caused the charge to burn very slowly for several minutes. As soon as the oil layer was vaporized the remainder of the charge, which was now rich in fuel, burned at a high rate and in some cases the cover was blown from the pot.

Diol 55 in combination with Diol jelled with 6% sodium stearate resulted in charges which were quite stable at 150 F. This jell, when tested by itself at 150 F for one month, showed very little tendency to break. A typical charge was composed of 50% B blasting powder, $^{16}\!/_{24}$-mesh, 2% coarse sawdust, 8% treated AL pulp, 28% Diol 55, and 12% Diol jell (6% sodium stearate). This type of charge did not burn at a uniform rate, and its smoke was thin, yellowish white in color, and lacked persistency due to its high fuel-to-oil ratio. Although 1 part of black powder should vaporize 2 parts of oil, this charge required 2½ parts of fuel per 2 parts of oil.

Non-Jelled Mixture. A group of charges containing B blasting powder, shredded asbestos, and/or kieselguhr, Diol 55, and in some cases a few per cent of coarse sawdust were tested. A typical charge was composed of 40% B blasting powder, $^{16}\!/_{24}$-mesh, 14% shredded asbestos, and 46% Diol 55. This was the most efficient smoke charge tested. Only 1¾ parts of fuel were needed to vaporize 2 parts of oil. Since the oil contained no jelling agent, the problem of syneresis at 150 F did not exist. Another advantage of this type mixture was that very little air was entrained in it during mixing and, therefore, it required no de-airing. The smoke produced by this charge was very white, dense, and persistent, and possessed excellent screening qualities. The charge was very dense, soft, and oily. It surged considerably throughout its burning time. Much additional work would have to be done in order to perfect this particular type of mixture.

Other Tests. An oil-smoke mixture, composed of 48% B blasting powder, 8% AL pulp, 2% coarse sawdust, and 42% Diol jell (1½% sodium stearate), had no corrosive or other deleterious action on the various materials contained in a smoke pot such as the lacquer-coated steel container, the zinc primer cup, the galvanized sheet-metal diaphragm, and the cork gasket.

An 11¼-in. pot containing 25 lb of charge of this

composition performed very well when thrown in a pool of water.

Numerous tests on charges of various compositions at −40 F indicated that this temperature had a very considerable slowing effect on the burning rate.

Transition Mixtures. Transition mixtures were employed to produce rapid, uniform, and positive ignition of the base charge. It was also desirable (1) that they give off sufficient heat to warm the upper portion of the smoke pot in a relatively short time, thus minimizing the condensation of oil vapors on the inner walls of the container; (2) that they generate a good cloud of smoke themselves; (3) that they cause combustion to transfer smoothly to the base charge so that there would be no sag, in the production of smoke vapors, which would interrupt the continuity of the smoke cloud; (4) that they ignite over their entire surface within a few seconds; (5) that they perform the same at −40 F as at 150 F; and (6) that they have the same oil-to-absorbent ratio as the base charge, to prevent migration of the oil.

A layer ½ in. deep, weighing 1,000 g, was employed in a number of 12-in. pots. However, a 1-in. layer, weighing 2,000 g, proved much more effective in preheating the sides of the relatively heavy 12-in. pot, and in effecting more uniform ignition of the base charge. The formulation contained 10% of coarse $NaNO_3$ for the express purpose of securing a higher degree of oxidation, and thereby producing a greater amount of heat.

Some sag in smoke production between transition mixture and base charge occurred. In an effort to overcome this characteristic, annular rings, ⅞ in. deep and 1 in. wide, were formed in the surface of the base charge before adding the transition mixture. It was thought that the transition mixture in the depressions in the base charge would still be burning after the ridges of base charge had been ignited. The idea did not prove effective. A method for preventing sagging, which did prove satisfactory, consisted of blending about ⅛ of the transition mixture with the upper portion of the base charge. The remaining portion of the transition mixture was then added as a separate layer.

The transition mixtures developed contained:

B black powder, $^{16}/_{24}$-mesh	48	50
Treated AL pulp	8	8
Pellet $NaNO_3$	10	10
Diol 55	23	22
Diol jell (6% sodium stearate)	11	10

They were used together; 3 lb of the first mixture was placed on top of the base charge and then 1 lb of the second mixture, which was faster, was added. In actual operation, the top layer of transition mixture burned in a few seconds, igniting the second slower layer and, at the same time, blowing off the tapes which covered the orifices. Very little sagging occurred between the second transition mixture and the base charge. Both of these transition mixtures proved to be quite stable when stored at 150 F. In fact, the combination of Diol 55 jelled with 6% sodium stearate and Diol 55 absorbed by a carbonaceous material proved to be more stable at 150 F than any of the other vapor-producing materials tested in transition mixtures.

Containers. The container should be so designed that it could be manufactured easily and, if possible, be a currently manufactured, standard-size article. Tests were made in pots 6-in. diameter by 7¼ in., 12-in. diameter by 15 in., and in standard 5-gal round cans.

At first, the 6-in. pots were equipped with a single 1-in. diameter orifice. Later it was observed that a decrease in the diameter of the orifice changed the smoke particle size from coarse (blue sun's disk) to fine (magenta sun's disk).[a] A number of tests were then performed with pots equipped with a device which permitted the orifice diameter to be changed gradually from ⅞-in. to ⅜-in., while the pots were functioning.

Some of the first tests were made in pots which contained no baffles or spark filters. Even though glowing particles were carried out of the pot by the smoke stream, the tendency of the oil vapors to ignite from the sparks was only slight. Decreasing the orifice size and thereby increasing the velocity of the oil vapors minimized any tendency toward flaming. When the smoke velocity was greater than the rate of flame travel, flaming which did occur was only momentary.

A number of tests were made with 6-in. pots which contained a baffle arrangement to reduce the large number of sparks thrown out by certain types of charges. The baffle-type spark filter reduced the flaming tendencies of all base charges with which it was tried. Very coarse mesh screens, tested in an attempt to filter out sparks, quickly became clogged with residue, restricting the passage of the smoke

[a] The latter smoke particles were of 0.3 micron radius, which size is most desirable for maximum screening effect.

vapors. Consequently, very little work was done with screen-type spark filters.

Six-inch pots equipped with a number of equally spaced $^3/_{16}$-in. diameter orifices, drilled in the side of the lid, possessed numerous advantages over those with the single, large orifice in the top of the lid. The smoke from the multiple-side orifices was whiter, denser, of smaller particle size, and more persistent than smoke emitted through the single large orifice. Ejecting the smoke parallel to the ground through these small, side orifices also reduced the tendency of the smoke to rise, which was quite marked when the smoke issued in a column perpendicular to the ground. The smoke vapors from pots having a number of small orifices also showed little tendency to flame even when the pot was not equipped with a spark filter or baffles. Figure 4 shows a 6-in. pot equipped with fifteen $^3/_{16}$-in. side orifices. Twelve-inch pots equipped with fifty $^3/_{16}$-in. diameter side orifices were tested and found to have the same features as the multiple, side-orifice, 6-in. pots. The $^3/_{16}$-in. diameter orifices possessed one undesirable characteristic in that they frequently became clogged with residue. As a result, the pressure in the containers would rise and cause the filling mixture to burn unevenly. This condition was remedied by increasing the orifice diameter to $^3/_8$ in. and at the same time reducing the number of orifices to two for the 6-in. pot and to eight for the 12-in. pot.

Standard 5-gal containers similar to HC smoke floats were found to be quite satisfactory. These containers were equipped with eight $^3/_8$-in. side orifices for the first tests. The velocity of the smoke after passing through these orifices was lower than normal, and the number of orifices was reduced to seven. In order to have an even number of orifices and to obtain the advantages of slightly larger orifices, the number was decreased to six and their diameter was increased to $^{13}/_{32}$ in. This number and size of orifices was tested extensively. The pot is shown in Figure 5.

A fairly satisfactory method for sealing the charges in the pot was developed. An 18-gauge, flanged, sheet-metal diaphragm which fits tightly against the walls of the pot was forced down against a cork gasket $^1/_8$ in. thick, which in turn rested on a $^3/_8$-in. deep bead rolled into the side of the container. After the diaphragm was in place, it was secured by means of a second bead, $^1/_8$ in. deep, rolled immediately above the flange of the diaphragm. A better oil seal between the diaphragm and pot was secured by replacing the flanged diaphragm with a flat one and then rolling a

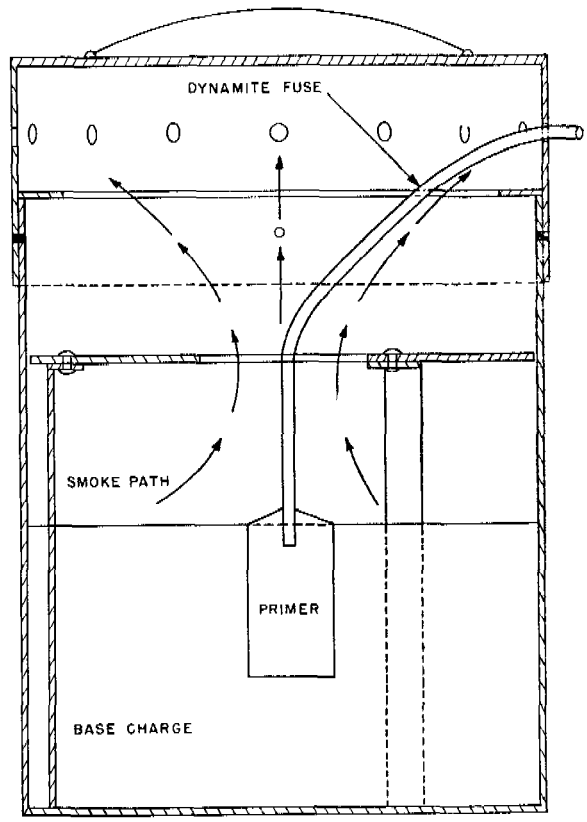


FIGURE 4. Six-inch diameter experimental smoke pot for jelled oil-black powder mixtures.

bead, similar to the lower bead, immediately above the diaphragm. As the bead was formed, a downward pressure was exerted against the diaphragm resulting in a positive oil seal.

The diaphragm shown in Figure 5 had a 3½-in. diameter hole in its center. A flanged 3-in. diameter x $^3/_4$-in. deep zinc primer cup was soldered to the edges of this hole. A zinc cover to confine the primer and to prevent moisture from coming in contact with it was soldered to the flange of the primer cup. Additional fittings containing an electric squib were attached to the lid of the primer cup. In operation, an electric current was applied to the Fahnestock clips on the pot cover which set off the squib. The primer was ignited by the squib, and, in turn, melted the zinc cup and its lid and ignited the transition mixture. The combustion gases and oil vapors escaped through the hole in the diaphragm, blew off the tapes, which covered the orifices, and then passed out into the atmosphere.

Two 5-gal pots were packed in separate wooden

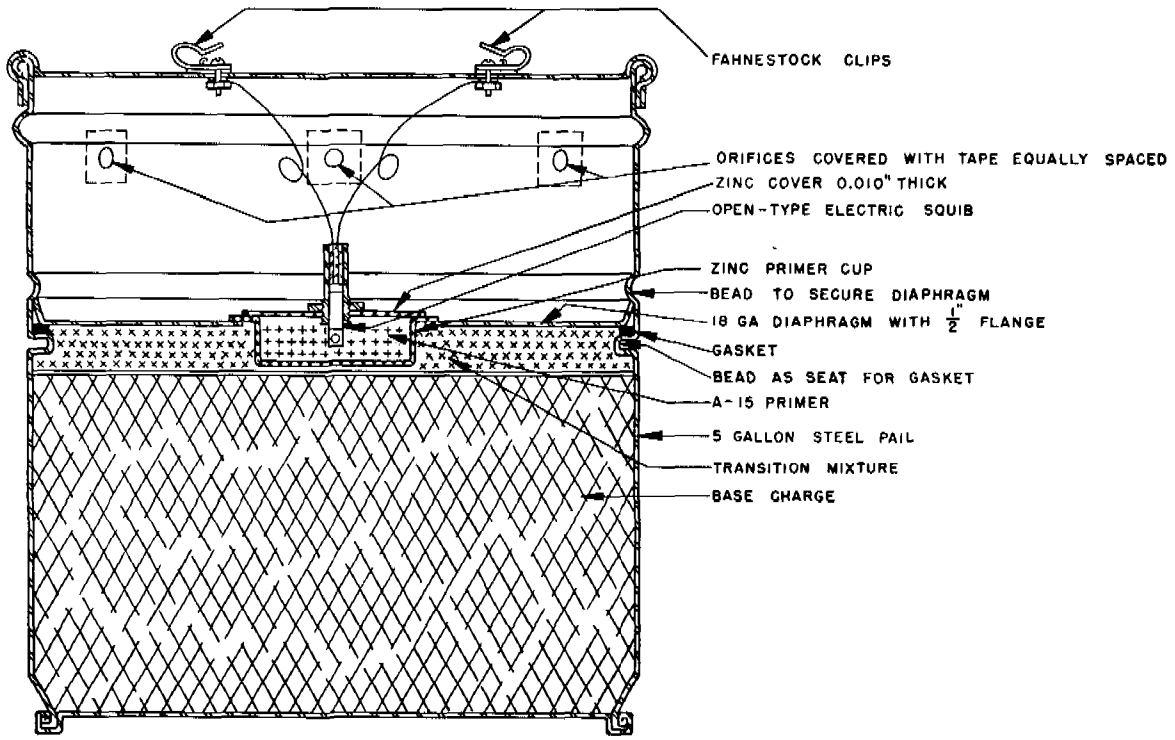


FIGURE 5. Experimental smoke pot in 5-gallon oil can. Jelled oil-black powder mixture.

boxes. Each box was subjected to rough usage tests which included vibrating on each face for 20 min, followed by dropping on each face and on two diametrically opposite corners from a height of 4 ft. The pots were then examined and found to be in excellent condition. Only a few minor dents were noted. Both pots functioned normally when burned.

Temperatures in the Smoke Pot. The maximum temperature of burning mixtures ranged from 560 to 1210 F. The maximum temperatures of smoke vapor ranged from 790 to 1010 F. Almost without exception, the charges in which the ratio of fuel to oil was greater than 1 exhibited the highest maximum temperatures.

The oil of charges whose maximum temperature was considerably greater than 800 F, evidently was cracked to a certain extent. The smoke from these charges was usually yellowish brown in color, thin, and lacking in persistency; whereas the smoke from charges whose maximum temperature was less than 800 F was fairly white, dense, and persistent.

Internal Pressure Measurements. The internal pressures of a number of 12-in. smoke pots were measured. All tests were performed with pots which were equipped with multiple side orifices. During one of the tests, the pressures at which the smoke particles produced a change in color of the sun's disk were noted. These pressures were as follows:

0 to 0.1 psi, blue sun's disk (coarse particles);
0.1 to 0.9 psi, permanganate sun's disk;
0.9 to 1.1 psi, magenta sun's disk (optimum particle size);
1.1+ psi, orange sun's disk (fine particles).

Note. This pressure, sun's disk relationship, is valid only during the first few minutes of the burning time. After this initial period, changes within the pot (temperatures, depth of residue, and so forth) and partial clogging of the orifices, produce entirely different relationships. For example, when the charge is practically consumed, the pressure might drop to 0.5 psi, yet the color of the sun's disk would be orange instead of permanganate.

Improvements in mixing and packing procedure and in composition resulted in charges whose average pressure was 0.75 psi, and whose maximum pressure was around 2 psi. Pots equipped with $\frac{3}{8}$-in. orifices developed lower pressures than those with $\frac{3}{16}$-in.

orifices (of equivalent total cross-sectional area). This was because the larger orifices did not become plugged with residue as readily as the smaller ones.

Since pressures no greater than 2 psi would be generated by an oil-smoke mixture which functioned satisfactorily, standard, lightweight shipping containers, such as 5-gal, 24-gauge, lug-cover, steel pails (used in the manufacture of HC floats), could be employed safely as oil-smoke pots.

Primers. In general, the method of priming consisted of placing the primer in a wax paper or zinc container imbedded centrally in the surface of the filling mixture, and igniting it by a black powder fuze or an electric squib. It was necessary to use an oil-proof container for the primer, as it would not ignite when wet with oil.

Twenty grams of primer were usually employed in 6-in. pots, and from 75 to 100 grams in 11¼-in. and 12-in. pots. The method of priming as finally developed for the 35-lb pot is shown in Figure 5.

Chapter 33

EXHAUST SMOKE GENERATOR FOR AIRPLANE ENGINES

By *H. F. Johnstone*

33.1 INTRODUCTION

The possibility of using the sensible heat of exhaust gases for the evaporation of oil for laying smoke was considered early in the war. In 1942, the DeVilbiss Company of Toledo, Ohio, undertook the design of exhaust-type smoke generators for small naval craft. A background existed of previous use of the principle in sky-writing, in the dissemination of fumigating chemicals, and (it is said) by rum runners off the Louisiana coast for screening purposes. The early efforts of DeVilbiss resulted in the production of prototype equipment for Hall-Scott gasoline marine engines and Grey diesel engines, both in the 175- to 250-hp class. The gasoline engine generator was the more satisfactory; it vaporized about 1½ lb of fog oil per hp-hour actual output. A few sets of this equipment were procured, but its adoption was not general.

An NDRC contract was later placed with the DeVilbiss Company for the development of large stationary smoke installations for protecting airfields and carriers. The completed prototype unit, in stationary mounting on a 550-hp Pratt and Whitney Wasp, Jr., aircraft engine, compared favorably in effectiveness of dispersal with the M–1 oil smoke generator.[1] No field of usefulness was envisaged for the device, however, and the last formal demonstration took place in November 1942.

Early in 1943, representatives of NDRC and the DeVilbiss Company conferred with the CWS Liaison Officer at Wright Field, and through him made arrangements for a joint AAF NDRC (DeVilbiss) attempt to develop exhaust smoke generating equipment for the B–26 bomber. The trial installation was fairly effective, and the plane was flown several times at Wright Field, at Edgewood Arsenal, and later before the AAF Board at Orlando, Florida. Evaporation rates of about 0.4 gal per hp-hour were obtained when diesel lubricating oil was dispersed. In September 1943, the Board decided to equip six single-engine planes with exhaust generators. The B–26 was returned to standard, and was not used for this purpose beyond that date.

After a delay of several months, during which time the DeVilbiss Company ceased to be active as an NDRC contractor, Division 10 attempted to renew the subject by means of a memorandum to the Navy Coordinator of Research and Development, giving a critical estimate of the possibilities of the development. The response was immediate, and at a meeting of the Navy Smoke Committee, in January 1944, the Bureau of Aeronautics was directed to equip three SB2A or SB2C aircraft with smoke generators, with assistance from Division 10. For this purpose, the Naval Aircraft Factory at the Philadelphia Navy Yard undertook the design and construction of six generators incorporating the B 26 experience. The units consisted of large cylindrical tanks into which the oil was injected through spray nozzles concurrent with the exhaust gases. The contact time was presumed to be sufficient to evaporate completely the droplets of oil. Two of these units were completed at NAF and installed on an SB2A. The plane was tested at the Amphibious Training Base, Fort Pierce, Florida, in June 1944. The smoke production compared favorably with that of the B–26, but the aerodynamic characteristics of the plane were adversely affected and mechanical failure of the units occurred.

In the meantime, the Munitions Development Laboratory [MDL] at the University of Illinois had been requested to analyze the entire smoke production process with a view to submitting an improved final design, since the earlier engineering had been on a strictly empirical basis. After the SB2A tests, MDL proposed a new design incorporating the Venturi atomization principle described in Chapter 29, and drastically reducing the diameter of the generator. Two of these generators were built under MDL direction by the Solar Aircraft Company of San Diego, California, between July 10 and July 17, 1944. These were installed on a TBM–1C plane at NAS, Patuxent, the following week, and the equipment was demonstrated at Fort Pierce on July 28. The performance and the further design modifications of this equipment will be described.

33.2 THEORETICAL CONSIDERATIONS

It has been shown that the maximum obscuration is obtained with an oil screening smoke when the

droplets are between 0.4 and 0.8 micron diameter. Since there is no practical means of subdividing a liquid into such small drops, it is necessary that the droplets be formed by condensation. The theory of oil smokes has been discussed in Chapter 27. It has been shown that the size of the droplets, which determines the amount of scattering of the light in the smoke cloud, depends, in part, on the rate of cooling of the saturated vapors.[3, 4] For practical reasons a spectrum of drop sizes is always obtained, and it is necessary only to chill the mixture of oil vapor and inert gases by emission into the cold air in order to obtain a screening smoke. The capacity of the smoke generator, therefore, is determined by the amount of heat available for evaporating the oil and by the size of the equipment used to effect the required heat transfer from the gases.

33.2.1 Evaporation Capacity of Exhaust Gases

The amount of oil that can be evaporated per pound of exhaust gas is determined by the initial temperature of the gas, the vapor pressure of the oil, and the specific and latent heats of the oil. The temperature of the mixture of oil vapor and exhaust gases that results, when the maximum amount of oil is evaporated, is called the *equilibrium saturation temperature.*

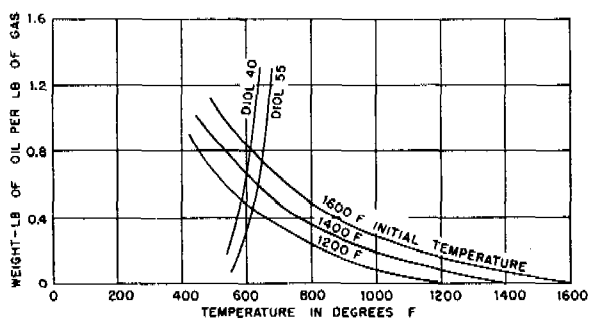


FIGURE 1. Determination of equilibrium saturation temperature.

The equilibrium saturation temperature and composition may be calculated from heat and material balances on the saturated gases. Either a graphical or trial-and-error calculation is necessary. The former is illustrated in Figure 1. The temperature and corresponding oil content of the saturated vapors are determined by the intersection of two curves, (1) a vapor composition-temperature curve showing the pounds of oil per pound of exhaust gases at saturation, and (2) a curve showing the temperature of the gas-oil vapor mixture as a function of the amount of oil evaporated per pound of gas. The latter curve depends, of course, on the initial temperature of the exhaust gases, whereas the former is independent of the initial temperature. It is evident from the shape of the curves that the initial gas temperature does not greatly affect the equilibrium saturation temperature, but a slight increase in the latter may greatly increase the amount of oil evaporated per pound of exhaust gases. Likewise, for any given initial temperature, the use of a slightly more volatile oil will lower the equilibrium saturation temperature somewhat, and will increase the amount of oil vapor present at equilibrium. Both of these points have a significant bearing on the present problem.

The saturation vapor concentration curve for the mixture of oil vapor and exhaust gases is determined from the vapor pressure of the oil by applying Dalton's law. The vapor pressure data for Diol 40 and Diol 55 were obtained from curves prepared by the Standard Oil Development Company.[5] The average molecular weights for these oils are 320 and 385, respectively. The latter corresponds to Navy Fog Oil No. 1 (also known in the Army as SGF No. 1). Diol 40 is a lighter, more volatile fog oil which corresponds to Navy Symbol 2075, which was recommended for use under cold weather conditions.

The weight of oil per pound of exhaust gases W_1 is given by the equation

$$W_1 = \frac{M_0}{M_g} \cdot \frac{p_0}{760 - p_0} \qquad (1)$$

where M_0 is the molecular weight of the oil;
M_g is the molecular weight of the gas (= 25.6);
p_0 is the saturation vapor pressure of the oil in mm mercury.

The following values were computed.

Temperature	p_0 mm Hg		W_1 lb oil/lb gas	
°F	Diol 40	Diol 55	Diol 40	Diol 55
550	14	5	0.235	0.088
600	40	20	0.694	0.360
650	100	45	1.90	0.835

The calculation of the heat balance for the mixture of oil vapor and gases requires a knowledge of the specific heat of the gases and of the oil, and the enthalpy of vaporization as a function of temperature.

The composition of the exhaust gases for an air-fuel ratio of 0.101 is as follows:

CO_2	4.96%
H_2	8.11
CO	13.50
CH_4	0.20
N_2	63.30
H_2O	9.91

The mean specific heat of the exhaust gases was calculated from the mean specific heats of the components. The enthalpy of the liquid oil and the enthalpy of vaporization are given by the equations: [6]

$$h_l = \frac{1}{\rho}(0.388t + 0.000225t^2 - 12.65), \quad (2)$$

$$h_{f_g} = \frac{1}{\rho}(110.9 - 0.09t), \quad (3)$$

where h_{f_g} = enthalpy of vaporization;
h_l = enthalpy of liquid oil in Btu per pound ($h = 0$ at 32 F);
ρ = specific gravity of oil at 60 F;
t = temperature in degrees F.

The heat balance on the basis of 1 lb of gas is given by the following equation:

$$W_2[(h_l - h_{70}) + h_{f_g}] = h'_{1400} - h'_l \quad (4)$$

where h' is the enthalpy of the gas above 32 F.

The calculations show that for an initial gas temperature of 1400 F and with Diol 55, the equilibrium saturation temperature is 630 F at which 0.61 lb of oil per lb of gas would be evaporated. This would require the transfer of 240 Btu per lb of gas. For the TBM–1 plane the maximum evaporation capacity is 1,070 gal of oil per hr, or a heat transfer of 3,168,000 Btu per hr, for the engine operating at 2,400 rpm and 42 in. manifold pressure. While complete equilibrium saturation cannot be reached, it is desirable to approach this condition as closely as possible in order to get the maximum capacity from the smoke generator.

33.2.2 Atomization and Rate of Heat Transfer

The most rapid transfer of heat from the gas to the oil is obtained when the largest amount of surface is available for the transfer, and when there is an intimate mixture of the oil and the hot gases. In order to make the evaporator as small as possible and to reduce the time of contact between the oil and gases to avoid decomposition or cracking, it is desirable to atomize the fog oil into the smallest droplets possible as it comes into contact with the gases.

As shown in Chapter 29, a convenient way for atomizing liquids into extremely small droplets by means of a low-pressure gas stream, is by injecting the liquid into a gas moving at high velocity through a Venturi throat. In this way, it is possible to atomize oil into droplets uniformly below 100 microns diameter and having an area of over 6,000 sq ft per gal. The conditions prevailing in the exhaust gases from an internal combustion engine are ideal for this type of atomization, especially since intimate contact and uniform dispersion of the droplets in the gas are desirable for the evaporation.

33.3 INSTALLATION OF VENTURI UNIT ON TBM PLANE [7]

Installation of the exhaust smoke generator was made first on two Grumman Avenger airplanes, types TBM–1C and TBM–3C. These planes differ only in the size of the engine used. The former has a Wright R2600–8 engine, with a normal rating of 1,500 hp when operating at 2,400 rpm and 39 in. mercury absolute manifold pressure [MAP]. The TBM–3C plane uses a Wright R2600–20 engine with a normal rating of 1,800 hp at 2,600 rpm and 47 in. MAP. The greater power and higher speed of this engine represents an increase of about 10% in the gasoline consumption and in the volume of exhaust gases over that of the R2600–8 engine under the conditions used during smoke generation. This, of course, provides a greater capacity for laying smoke. Both of these engines have 14 cylinders, with split exhaust collector rings, so that seven cylinders discharge the exhaust gases to ports on either side of the engine nacelle.

The design of the TBM-type airplane is quite suitable for adaptation of the exhaust smoke generator. The Venturi atomizer and a length of stack, sufficient to provide the necessary contact for evaporation of the oil, can be attached under the wing to the fuselage of the plane. Space is available between the fuselage and the landing gear wells for a stack about 8 in. in diameter. The length of the generator, however, is limited by the landing flaps to about 12 ft. In order to provide a contact time of approximately 0.05 sec, which was estimated to be the time required to supply the heat to evaporate the largest droplets, the size of the stacks was chosen as 6⅝ in. OD. This was a convenient diameter because it was the same as that of the original exhaust port on the engine.

33.3.1 Design of Venturi Section

The Venturi sections were designed in accordance with standard practice, with 30° convergent and 7° divergent sections. The throat diameter was found by calculation of the area to give the acoustic velocity of the exhaust gases when the engine was operating under takeoff power, assuming an allowable back-pressure of 6 to 8 in. mercury under these conditions.

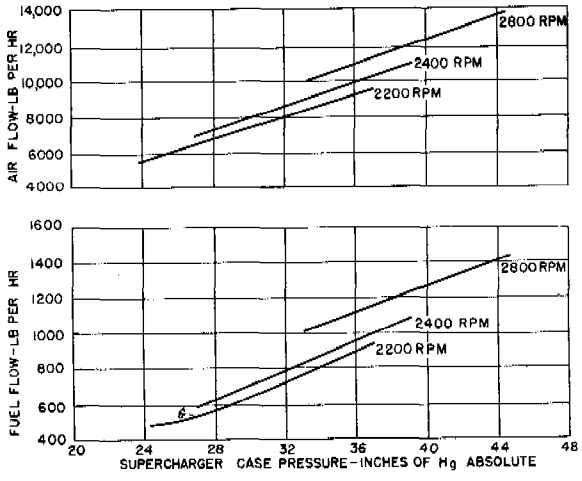


FIGURE 2. Air and fuel consumption data for R2600-8 engine part throttle — sea level.

Figure 2 shows the air and fuel consumption for R2600 8 engines. From these curves the amount of exhaust gas for any engine setting can be estimated. Assuming that the exhaust gas is equally divided between the two ports, it was estimated that at maximum power the flow of gas to each generator is approximately 6,600 lb per hr and that the temperature of the gas at the collector ring was 1400 F. Under these conditions, the perfect gas laws may be applied, so that the acoustic velocity is given by the equation

$$V_s = \sqrt{kg_c \frac{RT_t}{M_g}}, \tag{5}$$

where k = ratio of the specific heats, C_p/C_v, 1.36
g_c = dimensional constant, 32.2 (lb mass) (ft) per (lb force) (sec)^2
R = gas constant, 1,544 ft lb per (lb mole) (degrees R)
M_g = molecular weight of the gas, 25.6
T_t = absolute temperature at the throat

Assuming first that the flow of gases in the Venturi throat is frictionless and adiabatic, the relationship between the throat temperature and the temperature in the collector ring is given by the formula:

$$T_t = T_1\left(\frac{P_t}{P_1}\right)^{(k-1)/k}. \tag{6}$$

The subscript 1 refers to the conditions in the exhaust manifold. At the acoustic velocity

$$\left(\frac{P_t}{P_1}\right) = \left(\frac{2}{k+1}\right)^{k/(k-1)} = 0.536. \tag{7}$$

Thus

$$\left(\frac{P_t}{P_1}\right)^{(k-1)/k} = 0.848.$$

$$V_s = \sqrt{(1.36)(32.2)(63.1)(1860)(0.848)}$$
$$= 2{,}085 \text{ ft/sec}.$$

The specific volume of the gas at the throat is likewise related to the upstream pressure by the adiabatic formula:

$$v_t = v_1\left(\frac{P_1}{P_t}\right)^{1/k} = \frac{RT_1}{P_1M_g}\left(\frac{P_1}{P_t}\right)^{1/k}$$
$$= \frac{2.14 \times 10^5}{P_1} \text{ cu in./lb}. \tag{8}$$

The required area of the throat is then

$$A_t = \frac{6{,}600}{3{,}600} \times \frac{2.14 \times 10^5}{2{,}085\,P_1} = \frac{188}{P_1} \text{ sq in}. \tag{9}$$

A Venturi with a throat diameter of 3.34 in. corresponding to an area of 8.7 sq in. and a pressure of 21.7 psia was chosen for convenience in manufacture. The maximum back pressure on the exhaust manifold during takeoff was not expected to exceed 7 lb above atmospheric pressure at sea level, when no oil was being injected into the Venturi throat. Injection of oil into the Venturi throat would tend to increase the back pressure, but since this would not occur when the engine was operating under takeoff power the actual back pressure should never be as great as that calculated for the acoustic velocity.

33.3.2 Smoke Generators

The generators were constructed of stainless steel and consisted of an adapting elbow, a ball joint,[a] a Venturi throat, two lengths of 6⅝-in. OD tubing, 4 ft long, and a 45° elbow at the end. The entire equipment was constructed by the Solar Aircraft

[a] On later installations the ball joint was replaced with stainless steel flexible tubing.

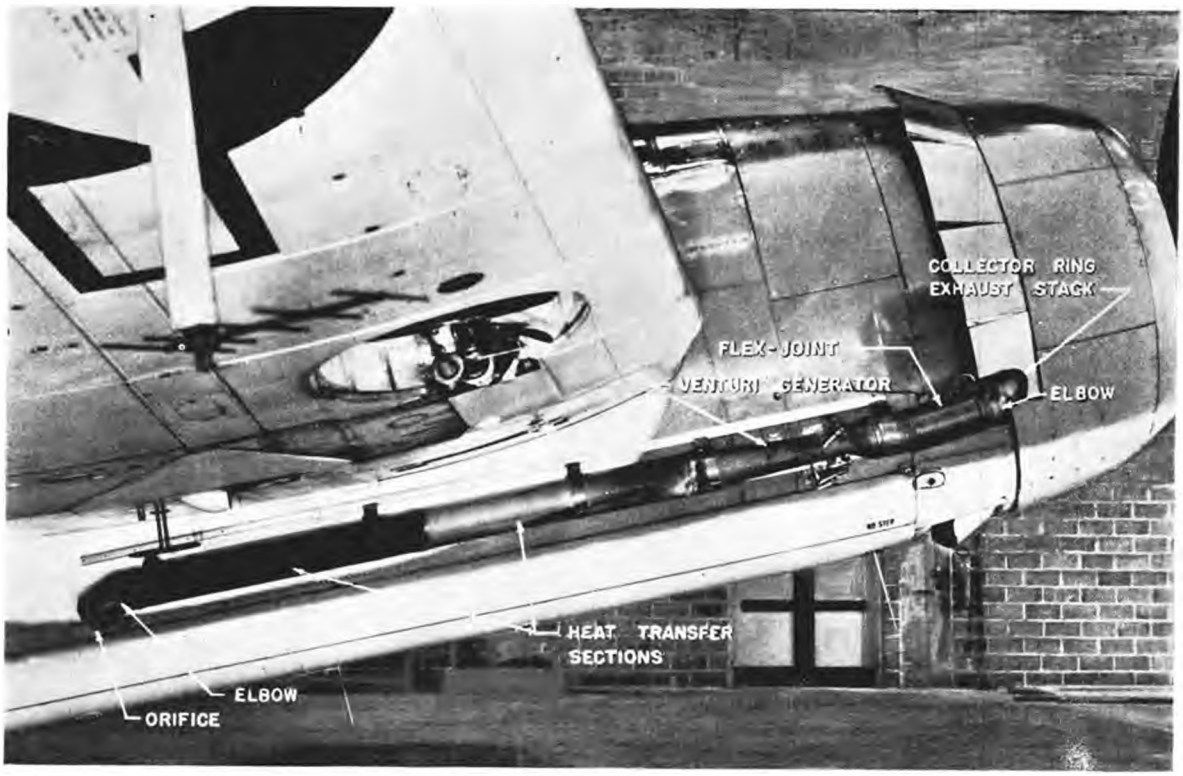


FIGURE 3. Exhaust smoke generator installed on TBM-3 plane. (Official Navy Photo.)

Company, San Diego, California. The adapting elbows replaced the exhaust port extensions, or flame dampeners, on the ship. The ball joints connected the elbow to the stack and permitted some movement of the engine without producing strain on the rest of the system attached to the fuselage. The short 45° elbow was installed at the end of the stack to divert the exhaust gases away from the fuselage. A 5-in. diameter orifice was attached to the end of the elbow to give an emission velocity of approximately 600 fps to the exhaust gases.

The generator was attached to the fuselage by means of clamps and hangers bolted to two aluminum angles which were in turn secured to the frame and skin in the ship. Figure 3 is a photograph of the first exhaust smoke generator installed on a TBM-3C plane.

33.3.3 The Hydraulic System

The fog oil was carried in the 270-gal bomb bay tank. In the original installation, two Pesco positive pressure fuel pumps, Model 1-E-754A, with capacities of about 17 gal per min at 160 psi, were used to pump the oil to the nozzle. One and one-quarter inch seamless flared aluminum tubing was used from the bottom of the tank to the suction side of the pumps, and 1-in. tubing was used from the pumps to the nozzles. By-pass lines with control valves in the radio operator's compartment were used to regulate the flow of oil to the two generators.

The nozzles used for injecting the oil into the Venturi throats were oil burner nozzles, made by the Todd Shipyards Corporation, with Mayflower plates size 28–10 and with 0.140-in. orifices. These nozzles produce a coarse hollow cone spray. They were connected to the oil supply manifold block with ½-in. aluminum tubing.

The Pesco pumps were motor-driven and were controlled by the pilot. Individual control switches were conveniently located in the cockpit, one for each pump. Since the power required by the motor exceeded that available from the standard 24-v 200-amp d-c generator, this was replaced by a 300-amp generator.

The total additional weight of the equipment on the plane, exclusive of the oil reservoir, was 210 lb.

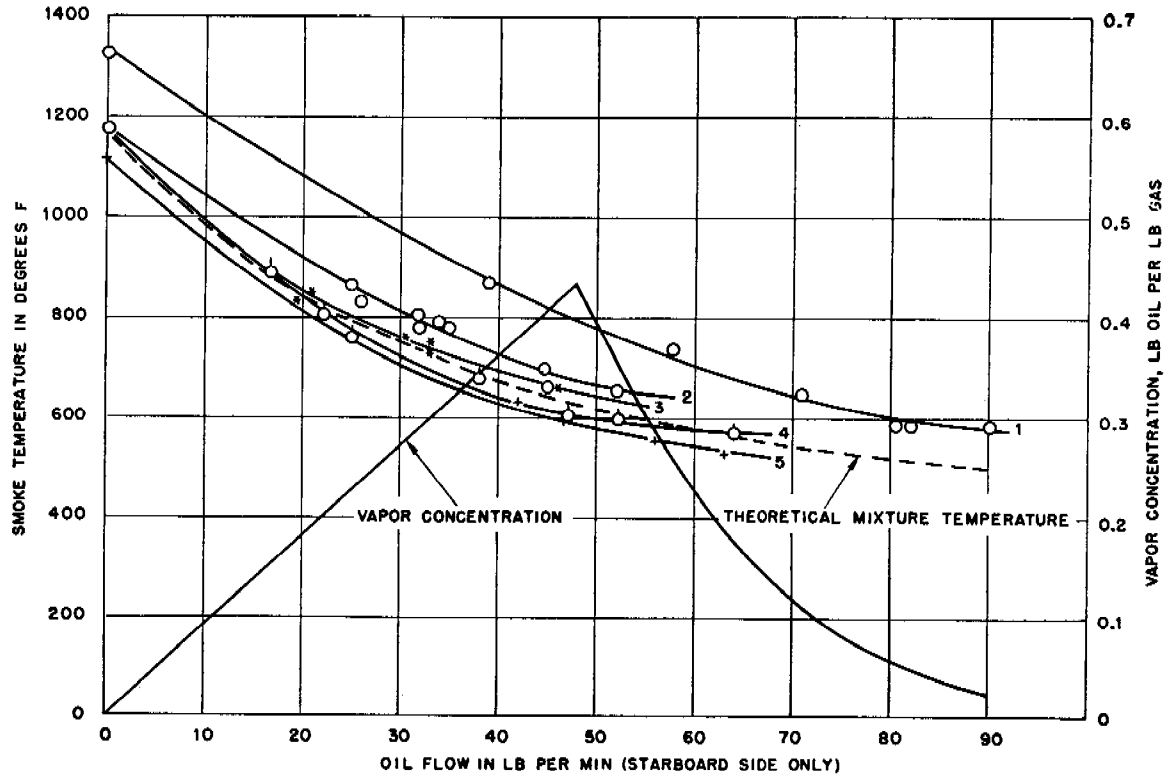


FIGURE 4. Smoke generator performance; oil flow, smoke temperature characteristic.

33.3.4 Performance of Equipment

A project was established by the Bureau of Aeronautics at the Tactical Test Unit, Patuxent River Naval Air Station, to determine the operating conditions of the equipment which gave the best smoke production, to evaluate the tactical usefulness of the Venturi smoke generator, and to determine the effect of the installation on the flight characteristics of the airplane. Personnel of the NDRC Munitions Development Laboratory participated in all of the tests and assisted in making modification of the equipment when necessary.[8, 9]

Evaporation Capacity

The capacity of the units for evaporating fog oil, as affected by various operating conditions, was determined by measuring the temperature of the exhaust gas-vapor mixture and by observing the wetness of the smoke as the oil flow was increased. If the evaporation of the oil was not complete because of insufficient time or area of contact, the gas temperatures for any given rate of oil flow would be higher than those calculated from the heat balance. Such temperature curves, supplemented by observation of the wetness of the smoke (determined by waving glass slides to determine if large droplets remain unevaporated), indicated the efficiency of the equipment and served as a basis of the comparison between operating variables.

Tests were run with the two fog oils, Diol 40 and Diol 55, and with two types of nozzles, the Todd nozzles described in the preceding section, and a nozzle designed by the Naval Aircraft Factory. The performance of the installations on the two TBM planes was also compared.

The temperature curves for the starboard generators are shown in Figure 4. It is evident that for the same operating conditions for the engine on the TBM–1 plane, the Todd nozzles and the Venturi give lower temperatures than the NAF nozzles. The use of the Todd nozzles without the Venturi, i.e., injecting the oil into a low-velocity gas stream, gives much higher temperatures. These results are interpreted as indicating that a combination of the Todd nozzles and the Venturi gives the best atomization of the oil, resulting in the most nearly complete evaporation in the time and contact available in the exhaust stack. The dotted curve in Figure 4 shows the theoretical

temperature when Diol 55 is injected into gases at 1188 F. It is evident that the actual temperature curve obtained when the Todd nozzles were used in the Venturi approached very closely to the ideal, thus indicating the high efficiency of the evaporation. The curve at the bottom of Figure 4 shows the calculated oil vapor content of the gas as a function of the rate of oil flow for ideal transfer. The sharp maximum at the equilibrium saturation is of interest since it indicates a decided decrease in smoke efficiency if too much oil is pumped. The lower temperature obtained with Diol 40, as compared with Diol 55, is consistent with that expected when using a more volatile oil. The higher temperatures obtained on the TBM–3C plane, as compared with those on the TBM–1C plane, are caused by the higher initial temperatures of the exhaust gases, and indicate the greater evaporation capacity of the generator on this plane.

It was concluded from these tests that approximately 54 lb per min of Diol 55 could be evaporated in each generator on the TBM–1C plane, corresponding to a total capacity of approximately 840 gal per hr when the engine is operated at 2,400 rpm and 42 in. manifold absolute pressure. About 10% more Diol 40 could be evaporated under the same engine conditions. For the TBM–3C plane, the corresponding figures were 67 lb, or 1,050 gal per hr. These represent an evaporation efficiency of approximately 85% of the theoretical, and indicate the extremely high rate of heat transfer in this type of equipment.

Effect of Equipment on Performance of Engine and Airplane

Flight tests were made to determine the drag created by the installation of the equipment on the plane. The results indicated that, at full speed under military power, the reduction in speed due to the drag was from 3 to 5 knots. The installation had no noticeable effect on the stability of the plane or on the stalling speed, nor did it affect the center of gravity of the plane. The back pressure on the engine under normal operating conditions, when the generator was not in use, was less than 1 psi. When the oil was being injected into the Venturi throat, however, the back pressure increased to about 5 psi (9 in. mercury). This caused no noticeable effect on the engine operation and performance, however, and apparently did not decrease the power output seriously or cause overheating or damage to the engine. After 55.6 hr of flight with the equipment on the TBM–3C plane, the engine was overhauled and examined and no excessive wear was found. Excepting the periodic cleaning of the nozzles which was necessary because of the collection of carbon after every few hours of operation, there was no failure or damage to any part of the smoke generating equipment.

Effectiveness of Smoke Screens

Visual evaluation of the smoke screens from the exhaust generator equipment was made in the course of tactical tests carried out with the Amphibious Research and Development Group at Fort Pierce, Florida. The observations were made by flying the planes between an amphibious vessel on which the observers were stationed and a landing craft LCM, which was stationed about 150 yd away. The smoke screens were laid with the planes flying into the wind and at an altitude of 50 to 75 ft. The screens were evaluated as to their density, uniformity, rapidity of contact with the water surface, persistence, length of time of obscuration, and the completeness with which the oil was evaporated.

It was concluded from these tests that the equipment was tactically suitable for the formation of smoke screens when used on a TBM–3 plane, provided the air was thermally stable and the wind not over 15 knots. Under these conditions the planes could be flown at 200 knots with flaps up and with the engine set at military power (2,600 rpm, 44.5 in. manifold absolute pressure). It was recommended that fog oil No. 1 be used when the oil temperatures were above 60 F and that the lighter oil, Navy Symbol 2075, should be used below 60 F and above 5 F.

In amphibious operations from ship to shore, this equipment was satisfactory for laying frontal screens under all wind conditions, except when there was an off-shore wind above 15 knots or a wind above 20 knots from any other direction. An example of the proposed use of the equipment for this type of operation is shown in Figure 5. Under calm conditions, a single plane could lay a satisfactory smoke screen which persisted for 3 to 4 min, but under less favorable conditions, it was necessary to reinforce the screen at much shorter intervals or, even better, to have another plane follow the lead plane so as to lay a denser smoke screen.

On the basis of the tests made by the Tactical Test Unit, the equipment for 12 planes was produced and sent to the Pacific Fleet for further evaluation. The units were installed on TBM–3C planes at Pearl Harbor NAS and tests were made for comparison



FIGURE 5. Aerial views of smoke screen from TBM–1 plane showing tactical use in amphibious operation. Airplane operation; 110 knots, flaps down, 2,400 rpm, 42 in. MAP; Diol 55 used at the rate of 840 gal per hr. (Official Navy Photo.)

between the oil exhaust smoke generator and the standard FS smoke tank. Consideration was given to the vulnerability of the plane laying the smoke screen over enemy positions, the number of planes required, the training of the crew, the ship stowage, the airplane installation and maintenance, and the reliability of the equipment.

It was concluded from these tests that the density of the smoke screen from the exhaust generator was not sufficient to compete with the smoke from the FS tank, in spite of the longer emission time and the advantages of handling a noncorrosive material. For satisfactory smoke screens under the atmospheric conditions likely to prevail, it was felt that three of the oil smoke planes would be required, and these would have to fly at a low elevation with flaps down in order to get the obscuration desired. This, of course, increased the vulnerability of the planes to a point where it was no longer practical to use the equipment. It was recommended that the equipment be improved to increase the evaporation capacity so as to put out a denser screen, and also that it be simplified in installation so that it could be attached to an airplane on board a combat carrier in less than one hour.

33.3.5 Methods of Increasing Smoke Output

Consideration had already been given to possible methods of increasing the output of the exhaust smoke generator so as to secure denser smoke screens. It was realized that the limitation to the capacity of the generator was the amount of heat available from the exhaust gases. Three ways of overcoming this were suggested.

1. *Use of more volatile fog oil.* Although this should lower the equilibrium saturation temperature and increase the rate of output, it had the disadvantage that the smoke was less persistent in hot weather, since a larger amount of oil would be required to saturate the air in the screen. No great advantage was found in using Diol 40 rather than Diol 55 in the tests at Fort Pierce. However, if an organic compound with a higher temperature coefficient of the vapor pressure were available, it might be more suitable than the hydrocarbon oils.

2. *Preheating the oil either before it is charged to the bomb bay tanks, or by means of a heat exchanger with the exhaust gases while the plane is in flight, before laying smoke.* This method seemed to have some possibilities and exhaust preheaters were obtained for one plane. It can be seen from equations (2) and (3) that, if the equilibrium saturation temperature is 600 F with exhaust gases at 1400 F, nearly 80% of the heat required to evaporate Diol 55 from 70 F goes to raising the temperature of the oil, while the other 20% is used for the latent heat of evaporation. Consequently, if it were possible to preheat the oil to 400 F, which is just below the flash point, nearly twice as much oil could be evaporated from the heat available in the exhaust gases. This method was abandoned when it appeared that it would complicate the equipment too much, and when the results on the third method gave assurance of success.

3. *Increase the heat content of the exhaust gases.* Several methods were considered by which, with reasonable adaptation to the limitations of the tail pipe, this might be accomplished.

   a. Burning the combustible constituents of the exhaust in the tail pipe.
   b. Burning a mixture of fuel and air in an external heater and combining the resulting gases with the exhaust gas in the tail pipe.
   c. Burning gasoline vapors led from the supercharger into the tail pipe.

The first method is the desirable one, since the gases are already available for combustion in large enough quantities to supply the necessary heat. Furthermore, the high gas temperatures and sea level pressures are factors favorable to good combustion. For an engine operating under military power at a fuel-air ratio of 0.10, the combustion efficiency is approximately 60%. With the R2600–20 engine this means that about 11,500,000 Btu per hr additional heat would be available, as compared to the 6,500,000 Btu per hr available before combustion.

The encouraging aspects of burning the exhaust gases, although not entirely free of difficulties, appeared to justify an investigation. Accordingly, the Solar Aircraft Company of San Diego, California, was engaged on a NDRC contract to develop the prototype unit.

33.4 DEVELOPMENT OF THE EXHAUST COMBUSTION SMOKE GENERATOR [10]

33.4.1 Theoretical Considerations

The composition of exhaust gases from internal combustion engines burning gasoline fuels depends on the fuel-air ratio.[11, 12] The average composition is

[redacted]

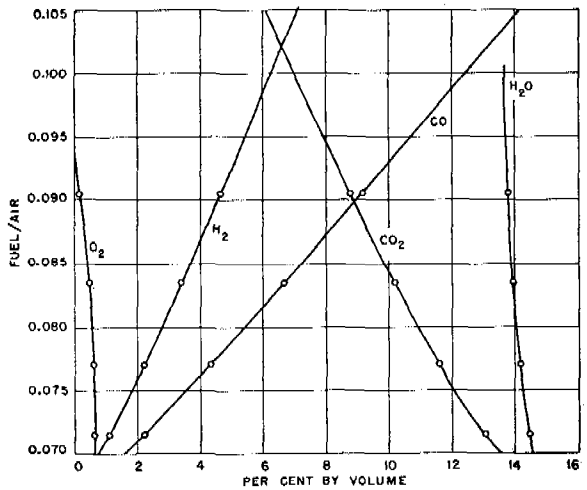


FIGURE 6. Average exhaust gas constituents vs fuel/air ratio of normal combustion processes. All percentages except for H_2O are based on dry volume. Methane (CH_4) is assumed to be 22% for all F/A.

shown in Figure 6. The specific heat was calculated from the average specific heat and the weight proportions of the constituents. It was assumed that 95% of the combustibles could be burned with no excess air. For the R2600–20 engine operating under military power, the following quantities were estimated for 100% combustion efficiency.

Initial exhaust temperature	1400 F
Initial exhaust flow	15,600 lb per hr
Heat in exhaust	6.51×10^6 Btu per hr
Heat from combustion	11.61×10^6 Btu per hr
Total heat available	18.12×10^6 Btu per hr
Smoke temperature	700 F
Oil evaporation	70 gpm

The primary problem in the development of the unit was to accomplish good combustion in the shortest possible distance, since only a limited length of tail pipe could be provided to evaporate the fog oil after the combustion process was completed. The factors contributing to the efficiency of the combustion within a short space are: moderate gas velocities, high initial gas temperatures, high static pressure, turbulence for rapid mixing, and good flame propagation. Since it is necessary to introduce the air for combustion by means of the ram effect, it was feared that the combustion efficiency might be affected by the attitude of the plane in flight, and that a diving attitude might disrupt the combustion or destroy the flame propagation if too high an air flow were provided. Another consideration, which subsequently proved to be unfounded, was the danger of burning of the oil during combustion of the gases, thus using

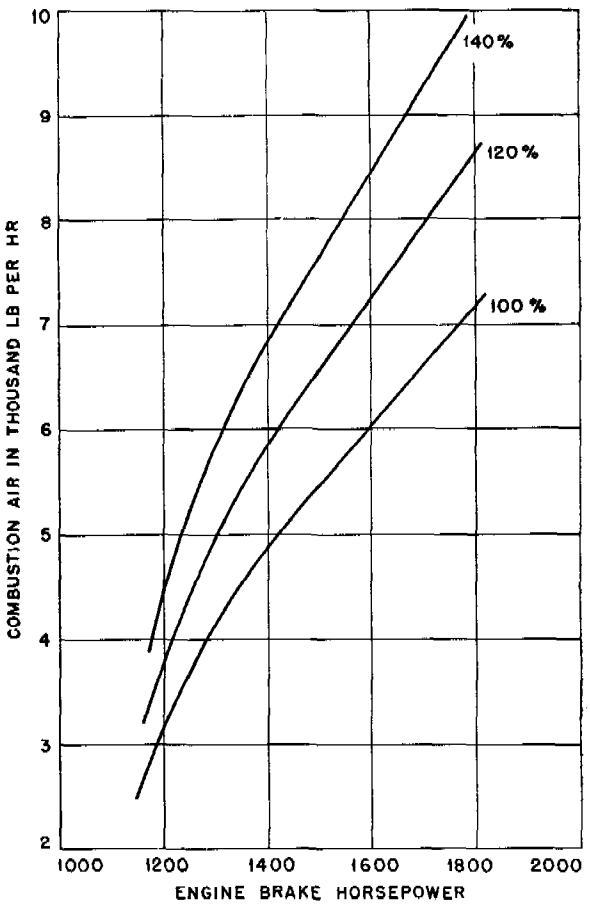


FIGURE 7. Secondary air required for combustion of exhaust gas constituents.

up the excess air. Previous experience with burning exhaust gas had indicated the difficulty in maintaining proper combustion within a small restricted area because of the unstable flame propagation and high ignition temperature of the hydrogen and methane. If sufficient air is mixed with exhaust gases at 1400 F to oxidize the combustibles, the gases in general will not ignite spontaneously since they are cooled below the ignition temperature. In order to assure dependable operation it was decided to use a pilot flame in a vapor-burning chamber. For this purpose, gasoline vapor was led from the supercharger case into a plenum chamber.

The calculated quantity of secondary air required for combustion is shown in Figure 7.

33.4.2 Development of Exhaust Combustion Units

The initial development of the combustion generator was carried out in an engine test cell in which

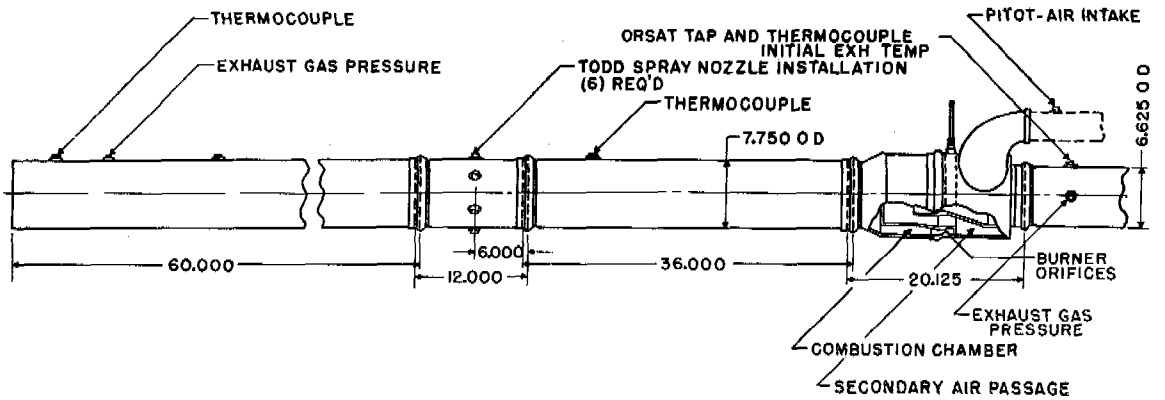


FIGURE 8. Diagram of test cell installation showing the tail pipe configuration and some of the instrumentation.

the units were operated with a Wright R2600 8 engine. This engine is essentially the same as the R2600–20 on the TBM–3C, except that the military power rating is 100 hp less. The test installation, which is shown in Figure 8, consisted of an exhaust duct leading from the right-hand collector ring to which was attached the combustion unit and a tail pipe comparable to that used on the airplane. Secondary air for combustion was furnished from a blower. Air flow measurements were taken with a calibrated Venturi, and the air flow was controlled with a butterfly-type valve. In most cases, high temperature measurements were made with quadruple-shielded thermocouples and potentiometer. Temperatures were taken of the initial exhaust gas upstream of the burner unit, at the point where the oil is sprayed into the tail pipe after combustion, and at the end of the tail pipe where the exhaust gas is ejected into the atmosphere. Since the gases were often in excess of 2200 F, and sometimes of a highly reducing or oxidizing nature, the temperature measurements did not have a high degree of accuracy. The installation in the test cell provided an accurate measurement of the air and fuel consumption from which exhaust flow data were obtained.

Several different designs of the combustion unit were built in order to improve the efficiency and stability of the combustion process. Typical of all designs was the introduction of the secondary air in such a manner as to cool the vapor plenum chamber and prevent overheating of the inter-air nozzle. These are shown in Figures 9A, B, C, D, and E.

Figure 9A shows the first combustion unit. In this design, the secondary air passages were too small to introduce sufficient air to support complete combustion. The gas temperature was approximately 1800 F and the exhaust heat was increased by a ratio of 1.38. Figure 9B incorporated such modified features as an exhaust nozzle to assist in the injection and mixing of combustion air, shortening of the combustion space of the pilot burner, and enlarging the tail pipe diameter from $6\frac{5}{8}$ to $7\frac{5}{8}$ in. The tests on the first unit had shown that the gas velocity in the tail pipe was too high for complete combustion within a short length. The larger burner gave an exhaust temperature in excess of 2000 F and an increase in the heat content of the gases by the ratio of 2.4. The flame front, however, was observed to be too close to the exhaust nozzle causing the inner surface of the plenum chamber to overheat to such an extent that the fuel vapor was ignited within the plenum chamber. Figure 9C represents an attempt to overcome this difficulty by eliminating the holes in the air shroud and extending the exhaust nozzle. With this arrangement, the heat ratio was brought up to 2.6 and the final exhaust temperature to about 2200 F. In this unit, ignition was obtained from a spark plug, which proved to be more reliable than a gas jet extending into the pilot burner.

Figure 9D represents a further improvement in preventing overheating of the plenum chamber by attaching a small collar to reduce the diameter of the air nozzle. This feature had the effect of reducing the static pressure on the pilot flame which assisted in relieving the blocking effect on the flame. This burner gave a temperature in excess of 2200 F and a heat ratio of about 2.6. Combustion was quite smooth for normal air flows but, with high rates of secondary air, violent intermittent explosions occurred in the tail pipe. Figure 9E represents an attempt to reduce the back pressures of the combustion generator by means of a diffuser shroud. It was believed that some

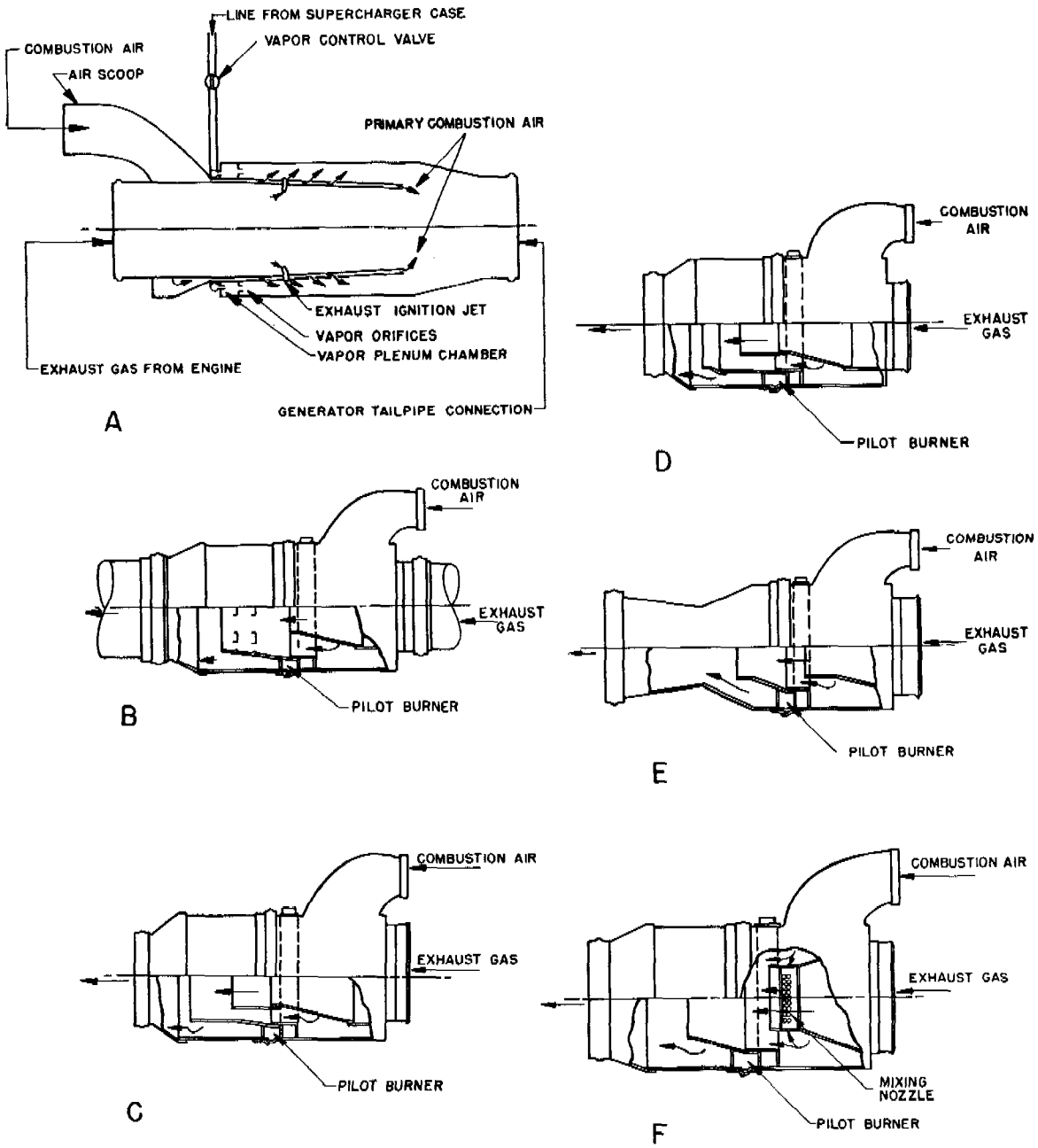


FIGURE 9. (A) First experimental combustion generator utilizing supercharger fuel/air vapors to stabilize combustion. (B) Experimental exhaust burner. (C) Exhaust burner with extended exhaust nozzle and large diameter air nozzle. (D) Exhaust burner with air nozzle reduced in diameter. (E) Exhaust burner with short exhaust nozzle and modified air nozzle using diffuser outlet. (F) Exhaust burner with mixer in exhaust nozzle.

pressure might be recovered without interfering with the combustion process. Tests proved, however, that this was not the case as the heat ratio dropped to below 2.1. It appeared that the turbulence was materially affected, resulting in poor mixing of the secondary air.

Figure 9F represents the final design of the combustion unit which was used as the prototype for the installations later made on the airplane. In this design, the hollow streamlined section was incorporated in the exhaust nozzle through which holes were drilled in the area of negative pressure. Air entrained

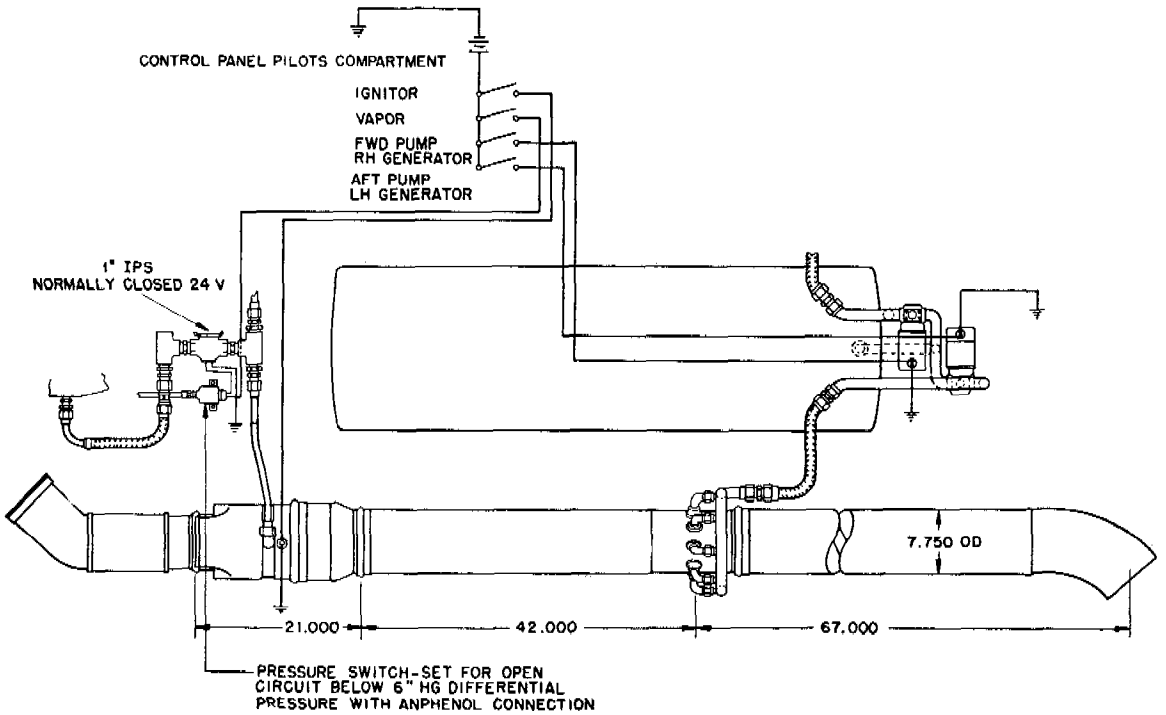


FIGURE 10. Schematic installation diagram smoke generator.

through the holes assured rapid diffusion into the center of the exhaust jet. There was evidence that this materially assisted in the combustion processes. The heat ratio was increased to between 2.6 and 2.7 and temperatures above 2200 F were obtained.

Data taken from the more advanced configurations of the combustion generator are shown in Tables 1 and 2. These indicate that it is possible to generate 2.6 to 2.7 times the original heat in the exhaust from the engine, which represents a combustion efficiency of about 90%, depending upon the air flow. All tests were conducted with a tail pipe of the length finally installed in the actual airplane. The heat values, as listed, were calculated from the gas temperatures taken at the spray nozzle section at a distance of about 38 in. from the combustion generator. It is probable that these temperatures were somewhat affected by local flame temperatures, but radiation losses tended to offset this effect.

The operation of the combustion generator is simple, necessitating only turning on the vapor and ignition switch, after which combustion immediately takes place and the gases come up to full heat in about 30 sec. No difficulty is experienced with flaming of the fog oil at the exhaust outlet unless the flow rate is extremely small, e.g., less than 1 gal per min at which time a yellow torching flame appears. An increase in oil flow rate extinguishes the flame immediately. When operated with the proper quantity of air (not more than 140%), combustion is smooth and virtually noiseless, with only a slight purr discernible above the noise of the engine. With excessive secondary air flow, intermittent backfiring occurs with loud reports. Combustion is easily extinguished with normal air flows by simply turning off the vapor switch; however, if the air flows are low (less than 100%), combustion may continue for a period of time. With still smaller air flows, combustion is sometimes spontaneous and can be maintained indefinitely, especially once the generator is heated.

While the burner is in operation, the surface of the tail pipe attains a high temperature. A temperature as high as 1450 F has been observed in the test cell. In order to investigate the possible effects of the hot tail pipe on the skin and structure of the airplane, an aluminum panel was placed approximately 4½ in. from the pipe surface. With the hottest conditions, the maximum temperature of the panel was 210 F. The actual airplane installation runs much cooler than that in the test cell because the air flow rate in the slip stream is much greater.

One of the interesting things that was noticed in

TABLE 1A. Test cell performance of exhaust burner with large exhaust nozzle.*

Run	Engine condition RPM	MAP Hg (in.)	HP	Spray section surface temp F	Carburetor air lb/hr	temp F	Fuel flow lb/hr	Initial exhaust condition lb/hr	temp F	Back pressure Hg (in.)
1	2,400	42.0	1,496	1345	10,745	75	1,099	5,922	1360	3.55
2	2,400	42.0	1,488	1350	10,633	75	1,090	5,808	1360	3.55
3	2,400	42.0	1,488	1390	10,633	75	1,090	5,808	1360	3.80
4	2,400	42.0	1,488	1395	10,633	75	1,090	5,808	1355	3.95
5	2,400	42.0	1,488	1370	10,633	75	1,090	5,808	1355	4.15
6	2,400	42.0	1,488	1370	10,633	75	1,090	5,808	1355	4.10
7	2,400	42.0	1,488	1375	10,633	75	1,090	5,808	1350	4.10
8	2,600	44.4	1,638	1360	12,248	80	1,270	6,699	1415	4.10
9	2,600	44.4	1,610	1370	12,192	80	1,270	6,671	1400	...
10	2,600	44.4	1,610	1370	12,192	80	1,270	6,671	1400	4.8
11	2,400	42.0	1,508	....	10,633	85	1,099	5,871	1360	2.65
12	2,400	42.0	1,508	....	10,633	85	1,099	5,871	1360	2.82
13	2,400	42.0	1,508	....	10,633	85	1,099	5,871	1360	2.95
14	2,400	42.0	1,508	....	10,633	85	1,099	5,871	1360	3.05
15	2,400	42.0	1,508	....	10,633	85	1,099	5,871	1360	3.10
16	2,400	42.0	1,508	....	10,633	85	1,099	5,871	1360	...
17	2,600	44.4	1,635	1355	12,164	85	1,270	6,657	1410	4.40
18	2,600	44.4	1,635	1385	12,164	85	1,270	6,657	1410	4.75
19	2,600	44.4	1,635	1395	12,164	85	1,270	6,657	1410	4.95

* Original unit with production exhaust nozzle and tail pipe assembly

TABLE 1B

Run	Fuel/air	Spray section temp F†	Tail pipe temp F‡	Secondary air Pressure H_2O (in.)	Flow lb/hr	Final exhaust gas condition lb/hr	temp F*	Heat content of exhaust Btu/hr Initial $\times 10^6$	Final $\times 10^6$
1	0.102	2150	2068	.92	2,280	8,202	2150	2.339	5.167
2	0.102	2140	2082	1.00	2,375	8,183	2135	2.294	5.114
3	0.102	2207	2150	1.65	3,095	8,903	2230	2.294	5.831
4	0.102	2195	2140	2.20	3,615	9,423	2230	2.283	6.172
5	0.102	2175	2155	2.80	4,125	9,933	2215	2.283	6.456
6	0.102	2155	2135	2.80	4,125	10,010	2215	2.283	6.507
7	0.102	2170	2170	2.80	4,125	10,002	2215	2.271	6.501
8	0.104	2058	2058	1.05	2,440	9,208	2032	2.760	5.451
9	0.104	2180	2165	1.90	3,335	10,071	2185	2.722	6.466
10	0.104	2210	2130	3.20	4,455	11,187	2232	2.722	7.327
11	0.103	....	....	.20	1,050	6,921	....	2.319	....
12	0.103	....	....	.95	2,305	8,176	....	2.319	....
13	0.103	....	....	2.33	3,730	9,601	....	2.319	....
14	0.103	....	....	3.75	4,860	10,731	....	2.319	....
15	0.103	....	....	5.00	5,660	11,531	....	2.319	....
16	0.103	....	....	...	....	....	....	2.319	....
17	0.104	2165	....	1.40	2,835	9,492	2160	2.736	6.008
18	0.104	2225	....	2.20	3,615	10,272	2240	2.736	6.749
19	0.104	2217	....	3.25	4,495	11,152	2240	2.736	7.327

* Shielded thermocouple at spray section.
† Nonshielded thermocouple at spray section.
‡ Nonshielded thermocouple at end of tail pipe.

these tests and which gave some difficulty in the later installations was that there was a considerable difference in the composition of the gases and performance of the unit when attached to the right- and left-hand exhaust ports on the engine. This discrepancy was attributed to the distribution of the fuel-air mixtures in the induction system of the engine. The manufacturers of the engines, Wright Aeronautical Corporation, stated that this phenomenon was characteristic of the R2600 series engines. It was also discovered during the test on the combustion generator that the condition of the spark plugs in the engine

had a considerable bearing on the quantitative relationship of the exhaust gas components. In several instances it was noted that the combustion was very poor, and that the flame did not fully propagate until it was some distance down the tail pipe from the burner. In every case, abnormally low initial exhaust temperatures were coincident with this condition. Low exhaust temperatures were almost always caused by dirty spark plugs. When these were replaced, the condition was immediately rectified and the burner operated normally.

33.5 INSTALLATION OF COMBUSTION UNIT ON TBM-3 PLANE

The general scheme of the combustion generator installation is illustrated in Figure 10. Two generators were installed, one on either side of the airplane, extending from the exhaust collector outlet parallel to the line of thrust below the wing, to a point approximately 3 ft from the trailing edge of the wing. The overall length of the tail pipe, including the combustion unit, was about 11 ft. The generators and tail pipe were held by brackets attached to an aluminum channel bolted to the side of the fuselage with a 4-in. space between the skin and the tail pipe. The generator assembly was connected to the manifold by means of a flexible hose and an elbow clamped to the manifold which was originally provided with a clamp attachment for flame dampeners. The position of the scoops on the experimental installation was above the generators, and was such that there was little or no air flow interference by the engine cowl flaps. Gasoline vapor was drawn from taps on either side of the supercharger to the common inlet of an electrically operated solenoid valve, from which it was again divided into a line for each generator. Automatic safety switches were provided to prevent the exhaust gas from being drawn into the supercharger case at negative pressures.

It should be noted that in this installation no Venturi section was used to atomize the oil, since this would have interfered with the operation of the burner which depended upon having little or no back pressure in order to permit the air for combustion to be introduced by the ram effect. Because of the additional volume of gas resulting from secondary air and the extremely high temperatures, the velocity through the 7⅝-in. tail pipe was approximately 600 fps. While this was less than the throat velocity in the first exhaust smoke generator and resulted in poorer atomization of the oil, it was in part compensated for by the higher temperatures which resulted in a faster rate of heat transfer. Nevertheless, the high heat efficiencies were never attained on this generator as they were on the first model and further improvements along this line should be sought. The spray nozzles which were used to inject the oil directly into the hot gases after combustion were the Todd nozzles with Mayflower 20-10 plates.

A preliminary program of flight testing was carried on at San Diego to regulate the combustion unit to give the maximum generation of heat. This was mainly accomplished by varying the scoop size to control the flow of secondary air. The position of the spray section was also altered, with respect to the burner, to give the optimum proportioning of combustion and evaporation space. The flight tests showed that the injection of secondary air by the exhaust nozzle was satisfactory at all flight altitudes or speeds of the plane.

It was again noticed that the port generator gave somewhat poorer performance than the starboard generator. The amount of oil evaporated in each generator was, respectively, 18.5 and 22.5 gal per min with the engine operating at 2,600 rpm and 47 in. MAP. Under these conditions a dense curtain of smoke could be laid, which had a duration of 4 to 5 min when the plane flew downwind and 2 min when the plane flew crosswind of a 12-knot wind. This performance was about 2½ times as good as that of the simple exhaust generator. Further tests were carried out on the plane by the Tactical Test Unit at Patuxent River Naval Air Station.[13] These verified the conclusions reached by the Solar Aircraft Company and demonstrated additional uses to which a squadron of planes equipped with the combustion exhaust smoke generator could be put for laying area screens.

On the basis of these tests the equipment was standardized as the Aircraft Oil Fog Generator, Mark 3. Procurement of 72 ship sets was immediately started with high priority. Actually, only 24 planes were equipped before the end of the war. In these, a simplified hydraulic system was used in order to eliminate the necessity of substituting the 300-amp generator for the standard 200-amp generator on the TBM-3C plane. The electric pump system was replaced with a hydraulic drive for pumping the fog oil.

The 24 planes equipped with the Mark 3 generator were delivered to the Fleet Operational Training Command, U. S. Atlantic Fleet, Norfolk, Virginia, just at the end of the war. During September and

October 1945, a series of operational and tactical tests were made on the equipment by Squadron VC–6 under the direction of the Research and Development Center. In order to improve and simplify the installation and to hasten procurement, several modifications were suggested in the hydraulic system and in the method of attaching the generators to the planes. These changes were accepted in the standardization of the modified equipment as the Aircraft Oil Fog Generator, Mark 4.[14]

During the course of the operational and tactical tests the 24 aircraft were operated for a total of 966.7 hr. The maximum time put on any single plane was 58.2 hr. A total of 77,500 gal of fog oil was used, and this amounted to approximately 33.3 plane hours of smoke generation with a maximum of 190 min for any individual plane. During these tests the planes were operated at military power (2,600 rpm, 47 in. MAP) for a total of approximately 66.7 hr with a maximum for a single plane of 5.1 hr. In some cases the planes flew continuously at this power for more than 10 min. In the course of these tests no engine trouble occurred on any of the planes that could be attributed to the smoke equipment.

33.6 TACTICAL USES OF AIRCRAFT OIL FOG GENERATOR [15]

The development of the oil fog generator for aircraft suggested several new tactical uses which could not be fulfilled by the older methods of dispersing smoke. It was now possible to lay a dense smoke curtain from a single plane flying at a speed of better than 200 knots and emitting smoke for a period of 6 min, or a swath 20 miles long and 100 yd wide in a single flight. It was estimated that a squadron of planes prepared for take-off could screen an anchorage of 8 square miles within 10 min from the receipt of the warning of the approach of enemy planes. In the tests carried out at Norfolk after the war, this tactical problem was worked out and demonstrated. Consideration was given also to the possibility of screening a task force under way and of screening an individual ship, especially when in a crippled condition.

33.6.1 Area Screening of an Anchorage

It was recommended that these screens be laid at an altitude of 400 ft since this would prevent any successful change in point of aim of an enemy plane that dived through the screen, and would take full advantage of a possible thermal inversion cap or existing air stability below 400 ft which would prevent the screen from falling to the surface of the water. With planes flying at 100-yd intervals, approximately 200 gal of fog oil will be emitted per square mile of screen. This appears to be adequate on the basis of the best information that can be obtained from experiments with surface equipment.

As the result of the Norfolk tests, it was concluded that area screens could be laid with the oil fog generator either in a dead calm or in a brisk breeze with turbulent air. The speed with which the screens could be laid is unaffected by the wind speed or direction, or by sea conditions. It was thought that the screens were as good as those laid by surface craft and usually better. The method has the advantage also of being more certain. On the other hand, the air screen cannot be laid at night without exceedingly hazardous operations. Furthermore, the presence of friendly airplanes over the ships means a loss of fire power to the ships which in some cases would be serious.

33.6.2 Screening a Task Force Under Way

While the tactics for this operation have not been tested at the time of writing of this report, it is believed that a squadron of TBM–3 planes, equipped with the smoke generator, could screen a task force covering an area approximately 5,000 yd x 5,000 yd by flying in formation with 200-yd spacing at an altitude of 300 to 400 ft along a course determined by the vector difference between the velocities of the moving task force and the wind. Complete coverage will be obtained within 4 to 5 min. The time for which the smoke will remain over the task force from a single maneuver is determined by the following equation:

$$t(\text{min}) = \frac{60d}{\mathbf{V}_{(TF-W)}},$$

where d is the distance the screen is laid beyond the ships (about 2 miles), and $\mathbf{V}_{(TF-W)}$ is the vector difference between the task force velocity and the wind velocity in knots. When the ships are moving with the wind, it may be necessary to renew the screen before it clears the task force since the smoke may have been weakened by diffusion. Table 2 is the estimated protection time obtainable for different wind and task force velocities. Shortly before the screen

TABLE 2. Protection of a task force by aircraft oil smoke screens.

Task force velocity		Wind velocity		Vector difference		Protection time (min)	
Speed (knots)	Direction	Speed (knots)	Direction	$V_{(TF-W)}$ (knots)	Plane course	Single maneuver	Total from 1 flight of aircraft
15	000°	10	000°	25	000°	5	15
15	000°	10	180°	5	000°	24*	72*
15	000°	10	90°	18	027°	8½	25

* The smoke may have been diffused prior to this time so that renewal would be required in 15 min thus giving a total time of only 45 min per flight.

becomes ineffective the planes should extend the screens by repeating the initial maneuver. Each plane should have sufficient fog oil to continue the screen in this manner at least twice in a single flight.

The total protection time will be at a minimum when the task force is proceeding upwind, and a maximum when proceeding downwind at the speed of the wind. Thus, when the task force is merely taking evasive action and its course is not predetermined by other factors, best results will be obtained if the ships steam downwind.

33.6.3 Screening of an Individual Ship

This appears to be one of the most useful applications of the aircraft oil fog generator, because surface methods of laying smoke screens are seldom available, especially to protect a crippled ship that has lost a portion of its fire power or maneuverability.

In one test at Norfolk, a blanket screen was maintained by means of three smoke planes over a destroyer under way, for approximately 30 min. This screen could have been maintained even longer. In this test, the wind conditions were quite unfavorable as the air was turbulent and the wind speed was 20 knots. It was necessary for the ship to vary its speed as well as its direction to stay under the cover. It was concluded that three smoke planes can protect a single ship which is able to move downwind with the smoke, but it would require more than three planes if the ship were moving crosswind at a speed relative to the wind greater than 5 knots.

33.7 DEVELOPMENT OF EXHAUST SMOKE GENERATOR FOR HIGH-SPEED PLANES

It is evident that if the aircraft oil smoke generator is to maintain a useful position in naval warfare, its development must be continued and extended to jet propulsion and rocket planes. Some thought was given to this, since it was contemplated that if the installation were successful on the TBM–3 plane, it would next be installed on the PV–2 plane. Some rough calculations showed that the quantity of heat available for evaporating the oil was approximately proportional to the speed of the planes. Although no consideration was given to the method of introducing the oil into the hot gas stream, it seemed apparent that higher pressures of the gas and, therefore, higher velocities would be available for atomizing the oil and evaporating the droplets.

It has been recommended that the Navy include in its fundamental research program, a study of the mixing of fluid streams, including atomization, momentum and energy balances, turbulence, nozzle design, high-speed combustion, and other aspects which underlie the development of the oil fog generator and other devices of military importance.

Chapter 34

MUNITIONS FOR THE DISPERSAL OF LIQUID DROPLETS

By *H. F. Johnstone*

34.1 INTRODUCTION

THE IMPORTANCE OF DISPERSING chemical warfare agents and insecticides as very small droplets to obtain maximum effectiveness was frequently demonstrated in field tests carried on during the war. This was not only true of the solid toxic agents which must penetrate to the lungs, but applied equally well to the liquid agents when it was desired to set up an immediate high concentration of vapor in the initial cloud in order to produce casualties before the gas mask could be adjusted. This concept of the use of liquid chemical agents was held by the Germans who designed many of their shells and bombs with extremely heavy bursters in order to convert the entire charging into aerosols. The American Army did not have any munition for setting up aerosols in this way, nor was there any completely successful method of dispersing small solid particulates.

The British and Canadians reported some work on HE chemical shells and bombs for the dispersion of liquids, including small-caliber armor-piercing shells and Bofors shells with RDX bursters. The results indicated that fragmentation of a liquid from heavy-wall projectiles is incomplete, and much of the charging remains as drops above 50 microns diameter. Thin-wall munitions, either projectiles or bombs, are suitable for dispersing a charging of a mobile liquid as small droplets. The violence of the explosion with the HE burster is often sufficient to give the cloud considerable vertical height.

34.2 LIGHT PLASTIC BOMB [1]

The work of the NDRC on munitions of this type was undertaken primarily to devise an aerial bomb for dispersing DDT solutions to exterminate mosquitoes in a region prior to a landing operation. The bomb was to be used for atomizing a liquid to give low concentrations of a finely divided aerosol, much in the same way that a chemical warfare agent might be used if it were highly toxic. It was desirable that the bomb provide uniform contamination of the vegetation by droplets in the range from 10 to 100 microns diameter. For this reason a small bomb was chosen so that wide dispersion from a single cluster could be obtained. Good ballistics of the bomb were not necessary since large areas would be treated at a single time. In order to make use of existing standard cluster adapters, it was decided to make the bomb the same size and shape as the AN–M50 4-lb magnesium incendiary bomb. The bomb was provided with an all-way fuze which would function on impact with soft ground, water, etc., when dropped from an airplane either at low or high altitudes.

The development work on the bomb was done in three parts, as follows:

1. A study of the atomization of liquids with high explosives to determine the limits of the drop size distribution.
2. A study of the effect of the shape and dimensions of the bomb and the thickness of the walls on the degree of atomization.
3. The development of a design suitable for production followed by procurement of sufficient quantities of the finished munition for testing.

34.2.1 Atomization of Liquids by Explosive Bursts

The first experiments were made by bursting various small containers, such as cans, flasks, and tubes, containing DDT solutions in a mobile solvent, by means of various types of bursters, such as blasting caps, Primacord, tetryl, and black powder. The containers were burst about 4 ft above the floor in a large room and the aerosol samples were collected by impactors located at a height of about 2 ft above the ground and along a radius from the burst. A paper was placed on the ground under the burst to show any ground loss. The slides from the impactors were examined under a microscope immediately after the burst. The results indicated that atomization of the mobile liquids to droplets below 50 microns diameter is quite possible. For best results, the solvents should be of low viscosity. The shape of the bomb is an important factor in fixing the optimum ratio of the explosive to charge and, apparently, limits the size of the munition.

In a second series of experiments, liquids of different viscosities were dispersed from containers of

TABLE 1. Droplet* spectra from plastic bombs with various chargings.

Bomb case Diameter (in.)	Bomb case Thickness (in.)	Burster diameter (in.)	Description of charging	Kinematic viscosity Stokes	Surface tension dynes/cm	Weight per cent of droplets below following diameters, μ 5	10	15	20	25	30	35	50	75
$1\frac{3}{4}$	$\frac{3}{32}$	$\frac{5}{16}$	10% DDT, 10% DBT in monochlorobenzene	0.0110	...	0.2	8	30	51	79	98	100		
$1\frac{3}{4}$	$\frac{3}{32}$	$\frac{5}{16}$	10% DDT, 10% DBT in monochlorobenzene	0.0110	...	0.1	6	21	50	70	77	99	100	
$1\frac{3}{4}$	$\frac{1}{16}$	$\frac{5}{16}$	20% oleic acid in CCl_4	0.0108	...	0.4	8	36	58	74	99	100		
$1\frac{3}{4}$	$\frac{1}{16}$	$\frac{5}{16}$	20% oleic acid, 1% *m*-cresol in CCl_4	0.0115	...	0.3	7	26	52	74	97	99.9	100	
$1\frac{3}{4}$	$\frac{1}{16}$	$\frac{5}{16}$	10% oleic acid in CCl_4	0.0084	...	3	34	76	97	100				
$1\frac{3}{4}$	$\frac{1}{16}$	$\frac{5}{16}$	5% oleic acid in CCl_4	0.0074	...	7	54	100						
$1\frac{3}{4}$	$\frac{1}{8}$	$\frac{5}{16}$	10% $FeCl_3 \cdot 6H_2O$ in acetone	0.0096	...	2	26	53	80	100				
3	$\frac{1}{8}$	$\frac{5}{16}$	10% $FeCl_3 \cdot 6H_2O$ in acetone	0.0096	...	0.1	2	7	11.5	15	30	43	72	100
$1\frac{3}{4}$	$\frac{1}{8}$	$\frac{1}{4}$	50% $FeCl_3 \cdot 6H_2O$ in water	0.0189	...	0	4	8.5	16	31	40	65	100	
$1\frac{3}{4}$	$\frac{1}{8}$	$\frac{5}{16}$	50% $FeCl_3 \cdot 6H_2O$ in water	0.0189	...	0	1.2	8	13	20	21	46	100	
3	$\frac{1}{8}$	$\frac{1}{4}$	50% $FeCl_3 \cdot 6H_2O$ in water	0.0189	...	0	1	5	9	14	23	42	91	100
3	$\frac{1}{8}$	$\frac{5}{16}$	50% $FeCl_3 \cdot 6H_2O$ in water	0.0189	...	0	0.4	2.5	6	9.5	13	31	64	100
$1\frac{3}{4}$	$\frac{1}{8}$	$\frac{5}{16}$	20% oleic acid in benzene, sp g 0.88	0.0125	30.4	0.1	0.7	17	34	66	95	100		
$1\frac{3}{4}$	$\frac{1}{8}$	$\frac{5}{16}$	20% oleic acid in CCl_4, sp g 1.43	0.0130	30.4	0.4	0.7	28	60	85	99	100		
$1\frac{3}{4}$	$\frac{1}{8}$	$\frac{5}{16}$	15% glycerine in water	0.0465	54.5	0.4	5	17	30	56	80	98	100	
$1\frac{3}{4}$	$\frac{1}{8}$	$\frac{5}{16}$	Same, plus wetting agent	0.0157	32.3	0.15	0.7	2.5	7	14	22	32	60	
$1\frac{3}{4}$	$\frac{1}{8}$	$\frac{5}{16}$	15% DBT in tetrachloroethane	0.0172	38.5	0.15	2	7	17	30	50	68	100	
$1\frac{3}{4}$	$\frac{1}{8}$	$\frac{5}{16}$	15% DBT in ethyl ether	0.0059	21.5	0.18	1.3	10	22	40	58	74	98	100
$1\frac{3}{4}$	$\frac{1}{8}$	$\frac{5}{16}$	15% DBT in carbonated CCl_4	.....	...	0.15	1.5	6	15	32	52	68	100	
$1\frac{3}{4}$	$\frac{1}{8}$	$\frac{5}{16}$	10% oleic acid in CS_2	0.0054	35.5	4	30	74	97	100				
$1\frac{3}{4}$	$\frac{1}{8}$	$\frac{5}{16}$	20% oleic acid in CS_2	0.0093	35.5	5	6	18	38	60	83	99.8	100	
$1\frac{3}{4}$	$\frac{1}{8}$	$\frac{5}{16}$	20% oleic acid in dioxane	0.0189	35	0.25	4.6	18	36	50	64	76	99.5	100
$1\frac{3}{4}$	$\frac{1}{8}$	$\frac{5}{16}$	20% Stanolind in CCl_4	0.0108	30	0.05	1.6	7	18	28	42	52	95	100
$1\frac{3}{4}$	$\frac{1}{8}$	$\frac{5}{16}$	50% Stanolind in CCl_4	0.0258	34	0	0.1	0.8	2.3	3.5	6	8	36	90
$1\frac{3}{4}$	$\frac{1}{8}$	$\frac{5}{16}$	10% DDT, 10% DBT in CS_2	0.0052	35.5	0.25	5	22	46	66	78	89	100	
$1\frac{3}{4}$	$\frac{1}{8}$	$\frac{5}{16}$	10% DDT, 10% oleic acid in CS_2	0.0056	36	7	12	40	78	96	100			
$1\frac{3}{4}$	$\frac{1}{8}$	$\frac{5}{16}$	10% naphthalene, 10% DBT in CCl_4	0.0086	31.5	1	12	44	70	100				
$1\frac{7}{16}$	$\frac{1}{8}$	$\frac{5}{16}$	10% DDT, 10% DBT in monochlorobenzene	0.0106	36.5	0.15	1.4	9	26	46	64	81	100	
$1\frac{7}{16}$	$\frac{1}{8}$	$\frac{5}{16}$	10% DDT, 10% DBT in CS_2	0.0056	35.5	0.3	6	30	66	90	99	100		

* The drop size data were obtained in chamber tests where the aerosol cloud was allowed to settle on glass slides for ½ hour.



FIGURE 1. Disassembled parts of plastic bomb.

different sizes and diameters. An axial burster in a bomb of small diameter with a thin wall gave a better break up of the solution than a bomb of larger diameter with the same amount of liquid. There is a minimum average drop size obtainable for any given solution regardless of the size of burster and the diameter of the container. The drop diameter increases rapidly as the viscosity of the liquid increases.

The results of a series of tests using plastic tubes made of bonded Kraft paper are shown in Table 1. Here the amount of explosive was not so critical in determining the drop size as in the case of the metal and glass tubes, nor was the diameter of the bomb so critical as with the other tubes. The thickness of the plastic case was not important since the case was completely pulverized by the explosion. Either plastic or metal tubes were used for the burster-well with equally good results. Best results were obtained using solvents of low viscosity, high surface tension, and high density. Dilute solutions were atomized more easily than concentrated solutions. For DDT, it was recommended that a 10% solution in carbon tetrachloride be used, and that the solution contain an equal percentage of a high-boiling oil, such as dibutyl phthalate or methyl naphthalene.

34.2.2 Design and Manufacture of the Plastic Bomb

On the basis of these results, a design was made of a bomb which could be fabricated from phenol formaldehyde bonded Kraft paper. This was selected because of its rigidity, strength, and frangibility. The parts of the bomb are shown in Figure 1. An all-way fuze of conventional design, provides the extreme sensitivity required for functioning the bomb on light surfaces, such as small branches, and on water. The axial burster consists of reconsolidated tetryl pellets in a $\frac{5}{16}$-in. brass tube. The fuze contains an M–26 primer cap which functions the M–17 detonator in the end of the tetryl tube. The fuze is armed by the removal of a pin which is held in place by the sealing cup. This, in turn, is maintained in position by a spring clip which flies off when the bomb leaves the cluster. An arming spring forces the sealing cup out of position and arms the fuze.

The bomb is not stabilized in flight and falls at random to give the maximum dispersion pattern. The capacity of the bomb is approximately 400 cc, corresponding in the case of the 10% carbon tetrachloride solution to approximately 68 g of DDT. It is estimated that, for the control of mosquitoes, about

2,400 of these bombs would be required per square mile. This should give a dosage of about 0.5 lb DDT per acre. Each bomb would have to contaminate an area about 35 yd square.

The plastic components for 3,500 bombs were obtained from the Formica Insulating Company of Cincinnati, Ohio. These were sent to the J. V. Pilcher Company, Louisville, Kentucky, where they were assembled. There was some difficulty in getting good seals before the proper gluing technique was developed. All parts were matched with a clearance of 0.003 in. The binding surfaces of the component parts were roughened by sanding, or by cutting helical or parallel 60° grooves 0.015 in. deep. The end plug and fuze holder were cut from laminated sheets with the laminations perpendicular to the axis of the pieces.

A number of cements for sealing the joints were tested. The best cement found was Chrysler Cycle-Weld, Code CB–2. This produced a bond stronger than the plastic itself and had a short curing time. It formed a satisfactory joint when cured at room temperature for 24 to 48 hr. The best reproducible results were obtained when the cement was applied to the parts before assembly rather than by forcing the glue into the joints under pressure. It was necessary that the cement be made up fresh, and never used after it was more than 2 hr old. It was also recommended that the grooving, or roughening of the surfaces be done within 24 hr prior to gluing.

After the assembly of the bombs and curing of the joints, each bomb was tested for leakage under water by applying air pressure at 30 psi. The percentage of failures in the later lots, after the gluing procedure had been worked out, was not more than 3%. After delivery, the bombs were again tested for leakage by filling with carbon tetrachloride containing a green dye. Here the percentage of failures amounted to 17%. Several of the bombs containing the carbon tetrachloride solution were placed in tropical surveillance for several weeks. No leaks developed during this time.

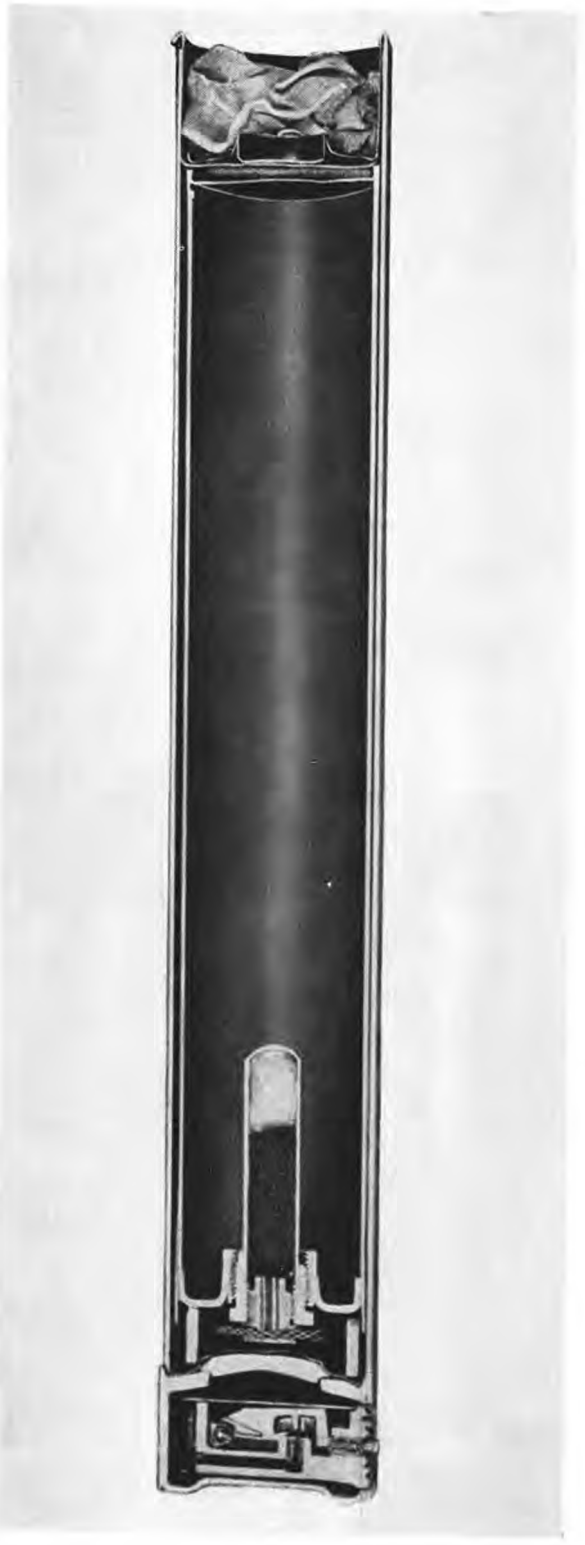


FIGURE 2. Cross section of EK–3 bomb.

34.3 EJECTION AIR-BURST BOMB [2]

Vesicant agents are effective when impinged as droplets on personnel. Contamination of terrain and buildings is another use. The common dispersal methods for these agents are by artillery shell, airplane sprays, and bombs. Shells are not always practical because of low-loading efficiency, high-

TABLE 2. Comparison of capacities and burster charges of ejection air-burst bombs.

	M-69*	EK-1	EK-3	EK-4
Maximum capacity, cc	1,650	1,350	1,270	1,125
Wt of HD filling, 10% void, g	1,870	1,530	1,440	1,275
Wt of empty bomb and parts, g	1,550	2,450	2,530	2,885
Grams of powder in burster†	0	6	6	9
Grams of powder for ejection‡	6	30	20	20
Total weight of bomb, g	3,426	4,016	3,996	4,189
Loading efficiency, %	54.6	38.2	36.0	30.4
Lb HD per 14- bomb cluster	57.6	47.2	44.4	39.3

* Oil incendiary bomb.
† Including ½ g of black powder; remainder is 37-mm smokeless ball powder.
‡ Grade A, No. 4 black powder.

crater loss, and nonuniformity of contamination. High-altitude airplane spray is difficult to aim and produces a light concentration over a large area. Low-altitude spray is effective, but such tactics are not always practical. The most effective bombs are those that are air-burst by means of a barometric, time, or proximity fuze. Such bombs disperse the filling more uniformly than ground-burst bombs and without crater loss. Inaccuracies and high costs of these fuzes, especially when used for small bombs, which are essential to obtain uniform coverage, are objections to this method. An equivalent to the bomb with proximity fuze is the base ejection air-burst bomb which, upon impact, ejects a canister containing the vesicant that bursts 100 to 300 ft above the ground.

Several attempts to develop an air-burst bomb of this type have been made in the past. A 30-lb bomb holding about 3 l of vesicant agent was tested at Edgewood Arsenal in 1930.[3] In this case, the explosive was contained in the nose section of the bomb and the entire tail section was blown into the air where it burst from 1 to 60 ft above the ground. During the war a modified version of the M-67 chemical bomb was proposed for the dispersion of mustard gas.[4] This consisted of a hexagonal canister of 1,350 cc capacity fitted into the standard hexagonal incendiary bomb, which was already provided with an impact fuze and powder chamber for ejecting the contents. The blast from the powder chamber simultaneously ignited a match train which initiated the powder burster in the inner canister so that it would burst in the air at an altitude of 100 to 250 ft. Tests on this bomb showed that the area, covered with drops larger than 1.5-mm diameter with a contamination greater than 0.5 g per sq m, was about four times that from the standard tail ejection chemical bomb, i.e., either the 10-lb M-69 or M-74 bomb.[5] With the bomb proposed, it was obvious that if impact occurred on rocks or hard surfaces, the case would be so badly deformed that the inner canister could not be ejected.

Further development of the munition was undertaken at the Munitions Development Laboratory. This resulted in two designs which were constructed for test purposes.

34.3.1 Hexagonal Bomb

In order to study the impact forces on the bomb, 25 units were assembled in M-69 incendiary bomb cases. These were fired from an inverted mortar to impact on clay, cinders, sand, and concrete at 240 fps. High-speed motion pictures of the bombs during impact were taken at 3,000 frames per sec. It was found that, on soft or hard soil, sand or cinders, the maximum rate of deceleration occurred just after the initial impact. When the bomb penetrated 20 in. into the soil, the maximum deceleration was about 1,550 times the acceleration of gravity. The average rate of deceleration was one-third to one-half of the maximum. When the bomb impacted on concrete at 240 fps, the tail section had an average rate of deceleration of more than 10,000 G, while the parts of the nose which collapsed averaged at least 10 times the deceleration rate of the tail section. The original design of the hexagonal bomb was known as the EK-1 bomb.

A new design, making use of the hexagonal incendiary bomb outer case and known as the EK-3 bomb, was produced. Changes were made to facilitate commercial manufacture and to strengthen the inner case. A stamped nose cup replaced the flat nose plate so that the assembly could be copper-brazed. The delay fuze was simplified by the use of a compressed powder delay train. A cross section of the EK-3 bomb is shown in Figure 2. One thousand of these bombs

were delivered to Edgewood Arsenal in September 1944. The inner cases were filled with 3.18 lb of mustard or thickened mustard and then were assembled into M-69 bomb cases. Some trouble was encountered as the result of leakage through the soft solder joints at the inner tail cup. Furthermore, the cases did not stand the pressure test of 60 psi without some leaks showing up. Field tests on this munition were scheduled for Dugway Proving Ground at the end of the war.

34.3.2 Round Bomb

The round bomb was designated EK-4. It had two obvious advantages, (1) greater ease of manufacture, and (2) greater strength and uniformity of deformation on severe impact. There was no standard round bomb in the 10-lb class and it was generally assumed that the hexagonal shape was necessary for clustering, although this was later proven to be untrue. The smaller agent capacity is a possible disadvantage of the round bomb, but this is not as great as it may appear at first. A comparison of the capacities of the models considered and the ejection and burster charges for each is shown in Table 2.

Considerable attention was given to the design of the inner case. Since it was impractical to prevent severe deformation when the bomb landed on concrete, a solution was found to the problem by controlling and directing the deformation so that it occurred at points which would not interfere with the ejection of the inner case. As a result of a series of firing tests, a bomb was finally designed which showed promise of proper functioning a large percentage of the time when striking concrete at a velocity of about 225 fps.

A cross section of this bomb, which was called the EK-4, is shown in Figure 3. The inner case is made from $2^{9}/_{16}$-in. OD 20-gauge steel tubing. The nose end and the middle section are corrugated so that deformation occurs inwardly, and the case is strengthened so that it does not bulge from the hydraulic pressure of the liquid. The nose and tail cups of the inner case are copper-brazed. The latter has a circular groove stamped in it so that the thickness of the remaining metal is slightly less than one-half of that of the wall. This insures that the agent is ejected through one end of the canister to provide large droplets. The outer case is made from $2^{13}/_{16}$-in. OD 18-gauge steel tubing, $19^{3}/_{8}$ in. long. A $9\frac{1}{2}$ in. long, 18-gauge sleeve was used to reinforce the nose end

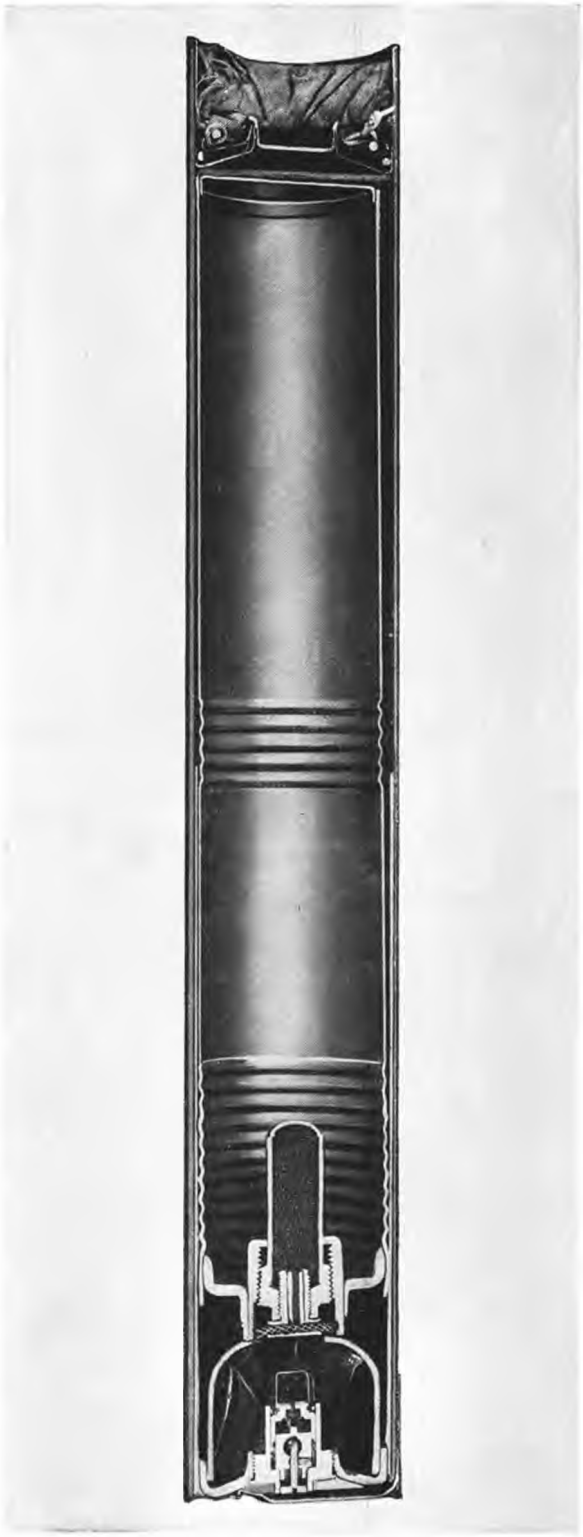


FIGURE 3. Cross section of EK-4 bomb.

of the bomb. A dome-shaped diaphragm is used to absorb some of the impact of the inner case and to provide a chamber for the powder bags. The delay element is a compressed black powder train, which is ignited by a length of Quickmatch. This train is set for a delay time of 4.2 sec and can be made reproducible to ± 0.2 sec. A new small inertia-type fuze was developed for the bomb. Cloth streamers similar to those used on the M–69 bomb are used to stabilize the bomb while falling. Good ballistics are obtained by attaching the streamers to a metal ring, which is fastened in turn to the bomb by means of nylon shroud lines 10 in. long.

One thousand complete EK 4 bombs were manufactured without difficulty and were delivered to Edgewood Arsenal in March 1945. The inner cases were filled with 2.8 lb of distilled mustard gas and thickened distilled mustard gas containing 0.5% oil red dye. The bombs were assembled, fuzed, and clustered, and sent to the Dugway Proving Ground Mobile Field Unit for field tests. The preliminary tests were started just before the end of the war. The static tests reported indicated that, when the bomb functioned properly, it distributed the filling fairly uniformly over a moderately large area which resulted in medium vapor dosages over that area.[6] The bomb did not show any great advantage over other available munitions for dispersing liquid agents. In open terrain, it gave results similar to those from low-altitude spray; in wooded terrain the results were similar to those from the M47A2 bomb. It was observed that many of the canisters were ejected too high before they burst, and the results could have been improved if all of the canisters had burst below the tops of the trees. A large percentage of the bombs did not function satisfactorily and further development is necessary before definite assessment of this type of munition can be made.

34.4 MUNITIONS CONTAINING LIQUIDS WITH DISSOLVED GASES UNDER PRESSURE

Several attempts were made to develop a munition for dispersing liquid agents as aerosols by means of a gas dissolved under high pressure in the liquid. It was shown in Chapter 29 that no advantage is to be gained in the atomization of the liquid by explosives when the bomb is pressurized with CO_2 at 500 psi. There are several other methods, however, by which the pressurized liquid might be atomized. Two of these were suggested by A. R. Olson of the University of California. Neither of these were found to produce the desired results and both appear to be impracticable for a munition for field use.[a] The test results will be described here briefly as they may be useful to others seeking information on this subject.

34.4.1 First Olson Bomb [8]

The first device proposed by Olson was a 100-lb bomb which was intended to impact and remain upright, and then disperse its liquid contents as an aerosol by spraying through a small hydraulic atomizing nozzle. The liquid was to be maintained in the bomb under high pressure of carbon dioxide, or other suitable gas which was relatively soluble in the agent. It was contemplated that the presence of a dissolved gas in the liquid under pressure would improve the atomization.

The solubilities of carbon dioxide in mustard gas and in butyl carbitol are shown in Tables 3 and 4. It was proposed that butyl carbitol be used as a simulant in the field tests because of the similarity of its properties to those of the vesicant agent.

TABLE 3. Solubility of CO_2 in mustard gas.[8]

Temperature degrees C	Press CO_2 psi	CO_2 g per 100 g H	$\frac{\Delta V}{V_0}$
20	200	3.4	...
	250	...	.062
	300	6.7	.082
	400	10.1	.130
	500	13.1	.190
	600	18.5	.285
	700	27.4	.475
12	200	3.5	...
	250	...	.090
	300	7.0	.120
	400	11.3	.165
	450	...	.215
	500	16.4	.260
	600	23.8	.520

The difficulty of insuring that the bomb performs in the prescribed manner when dropped from an air-

[a] It should be noted that this method of dispersing aerosols is indeed the basis of the *aerosol bomb* which was widely used for dispersing insecticides during the war. In this case, the gas used to pressurize the bomb was actually liquefied, and there was only a low concentration of the nonvolatile agent in the liquid vehicle. Furthermore, the rate of output of the bomb was much too low to be of use for field munitions. Particle size measurements on the aerosols generated from these bombs have been reported by LaMer.[7]

TABLE 4. Solubility of CO_2 in butyl carbitol.[8]

Temperature degrees C	Press CO_2 psi	CO_2 g per 100 g butyl carbitol	$\frac{\Delta V}{V_0}$
22	280	7.7	0.085
	470	18.1	0.180
	580	29.8	0.287
	670	42.2	0.409
	715	51.0	0.490
19	120	2.23	0.0189
	175	5.26	0.0396
	310	11.3	0.098
	530	27.0	0.226
	625	46.0	0.425
	775	95.0	0.91

plane was recognized, and several methods of stabilizing the bomb in flight and making it land upright were suggested. One of these even conceived of having a parachute and a tripod which would hold the bomb in an upright position a few feet off the ground while it was dispersing its contents. A test on this device at Dugway Proving Ground in April 1943 showed that, under the best conditions, the atomization in no way produced a true aerosol, and much of the charging was dispersed as large droplets which settled out within a few feet of the bomb.[9]

Further tests on this device were made at the Munitions Development Laboratory in order to determine if an improvement could be made by using different orifices or nozzles. Table 5 shows the results obtained in atomizing butyl carbitol saturated with CO_2 at pressures of 600 psi at room temperature. It is evident that all the nozzles tested produced droplets considerably above the range of stable aerosols. Further tests were run in a settling chamber with the Olson bomb itself with results consistent with those reported here.[10]

34.4.2 Second Olson Device [11]

Another device, which might have been developed into a practical munition if the results had been more favorable, consisted of a bomb or shell filled with spray tubes. These tubes were thin-wall cylinders filled with the liquid agent and saturated with carbon dioxide at a high pressure. The tubes were to have several orifices on opposite sides at each end, so that upon burst of the munition, the tubes would spin end-for-end due to the recoil of the liquid leaving the tube. The spinning was to accomplish the following: (1) the centrifugal force would keep the liquid at the end of the tube so that it would empty completely; (2) there would be an increased shearing force with the air to atomize the liquid in addition to the atomization effect of the dissolved CO_2; (3) the aerosol would be so rapidly diluted at the source that agglomeration of the droplets would not take place.

TABLE 5. Atomization of butyl carbitol pressurized with carbon dioxide under 600 psi at room temperature.

Nozzle No.	Nozzle	Drop diameter μ
1	No. 27 hypodermic needle, .075 in. long, and beveled as received	2 — 50
2	No. 27 hypodermic needle, .075 in. long, end ground square	2 — 50
3	.0313 in. ID tube, 3 in. long	5 — 75
4	Two tubes placed so that the streams would impinge on each other. Tubes were .0313 in. ID, .5000 in. long, and had an 0.014-in. diameter orifice in the end	5 — 75
5	1-in. length of .0313 in. ID tube, end square	5 — 90
6	1-in. length of .0313 in. ID tube, end flared to .1250 in. at 20°	5 — 90
7	Sharp-edged hole, .006-in. diameter, .0313 in. long	5 — 90
8	Slit, .001-in. wide and .25 in. long	5 — 90
9	Sharp-edged hole, .011-in. diameter, .0313 in. long	8 — 100
10	Fan-type spray with a .025-in. diameter hole	8 — 100
11	Sharp-edged hole, .016 in. diameter, .0313 in. long	10 — 125
12	Converging-diverging nozzle, divergence and size corresponding to a 5/0 dowel pin reamer	20 — 300

Preliminary tests [12] on this idea were made by ejecting a single tube $1\frac{3}{8}$ in. OD and 8 in. long from a bomb $1\frac{9}{16}$ in. ID and 16 in. long, filled with butyl carbitol under pressure of carbon dioxide. By means of a valve arrangement, the gas pressure could be increased until a frangible disk at the end of the bomb sheared at about 850 psi, releasing the tube and its contents. It was found that the tube actually spun end-for-end at a high velocity and was completely emptied in 3 to 5 sec.

Further tests were made with a larger multiple-unit ejection bomb, 48 in. long and $5\frac{1}{2}$ in. OD. This bomb had a capacity of 21 spray tubes similar to that described above. The entire bomb was charged with 14.3 lb of *o*-dichlorobenzene. Since the preliminary experiments showed that the bomb could not be used for setting up an aerosol, experiments were continued to determine if this device had any possibilities for dispersing mustard gas for antipersonnel purposes. Consequently, most of the tests were made with the simulant thickened with polymethyl methacrylate

TABLE 6. Dispersion and distribution of *o*-dichlorobenzene from spinning tubes.

Shoot No.	1	2	3	4	5	6
Wind velocity (mph)	7	8	10	8.5	2.5	5
Temperature (degrees C)	4	3	0	5	5.5	0
Viscosity of simulant (poises) at 0 C	1.25	1.25	1.25	1.25	1.70	1.70
CO_2 pressure, psia	130	110	0	...§	100	70
Wt of charging, g	6,500	6,500	6,500	6,500	6,850	6,500
"Recovery" %	79.2*	89	43.2‡	66.9‖	92	83.4**
% of tube contents discharged	100	100	0	0	100	90
Area contaminated >1.0 g/sq m and >1.0 mm diameter, sq yd	450	1,030	135	232	355	410
Concentrations (g/sq m)			Area contaminated sq yd			
>40	0	0	0	0	46	30
>30	25	19	2.5	15	72	39
>20	70	39	16	62	136	65
>10	160	160	70	130	205	175
>5	395*	295	170	215	260	320
>2	625*	1,140†	410	550	405	440
>1	750*	1,675	560	785	740	830
>0.5	860*	2,370	940	1,185	935	109
>0.25	...	...	...	...	1,150	...
Drop sizes (mm diameter)			Wt per cent			
0 — 0.50	22.7	23.7	37.7	44.9	24.2	22.7
0.50 — 0.75	14.6	15.2	23.1	23.8	15.1	14.3
0.75 — 1.00	22.9	16.4	22.3	15.8	16.5	12.1
1.00 — 1.20	14.4	12.1	9.1	6.4	14.8	16.4
1.20 — 1.40	10.4	8.0	4.8	3.9	5.3	8.3
1.40 — 1.60	9.2	7.6	1.8	2.6	5.0	10.9
1.60 — 1.80	2.1	3.5	0.6	0.4	7.8	4.3
1.80 — 2.00	2.0	5.1	0.3	0.1	4.4	1.9
2.00 — 2.20	0.6	2.4	0.3	0.4	2.2	1.2
2.20 — 2.38	0.3	3.4	...	0.7	2.6	3.2
2.38 — 2.53	0.3	1.4	...	0.4	1.0	1.0
>2.53	0.6	1.2	...	0.5	1.1	3.8

* These values are low since the contaminated area was not completely assessed.

** Plus 3.1% remaining in the tubes bring this value to 86.5%.

† Intermediate values were: 4 g per sq m 420 sq yd
3 g per sq m 685 sq yd

‡ Plus 29.6% remaining in the tubes bring this value to 72.8%.

§ In this shoot the CO_2 was bubbled through the liquid on the outside of the tubes after they were filled. The final CO_2 pressure was 200 psi and was in contact with the liquid for about 3½ min.

‖ Plus 29.6% remaining in the tubes bring this value to 96.5%.

and dyed red with duPont Rhodamine. The liquid was saturated with carbon dioxide in an auxiliary bomb and transferred to the ejection bomb under pressure. The pressure was increased until the shear disk ruptured and the entire contents were thrown in the air to an altitude of 150 to 300 ft. The spray tubes were mostly discharged by the time they reached the peak of their flight. They were scattered over an area of 50 yd wide by 70 yd long. Two tests were made that varied from the above procedure. In one test the simulant was not saturated with carbon dioxide and, in the other, the simulant on the outside of the tubes was saturated with the gas after the tubes were filled. In both cases the tubes did not discharge the liquid contents.

The multiple-tube ejection bomb produced a spray from 100 microns to 3 mm in diameter, 75% of which was above 0.5 mm. More than 90% of the liquid discharged from the spray tubes was above 0.5 mm. The liquid between the tubes was atomized somewhat more, thus lowering the overall antipersonnel efficiency of the munition. A change of the simulant viscosity from 1.25 to 1.75 poises appeared to produce no change in the drop size; however, the lower the CO_2 pressure, the larger the drops came from the bomb. Table 6 shows the results of six tests run on this device. The degree of ground contamination and the area contaminated depended largely upon the wind velocity. Using 14.3 lb of simulant, in a 2.5-mph wind, 936 sq yd were contaminated with a

concentration greater than 0.5 g per sq m, and 410 sq yd with a concentration greater than 1 g per sq m consisting of drops larger than 1.0 mm in diameter. In an 8-mph wind, the values were 1,675 sq yd and 1,030 sq yd, respectively. The lowest CO_2 pressure which would completely discharge the spray tubes was about 85 psi at 0 C.

It was concluded that the device is not effective for producing saturated aerosol clouds, but that it can be used to produce larger droplets that would have antipersonnel effects. The device is mechanically poor, and must be stored and transported while under high pressure. Once the munition is filled, the pressure varies greatly with the temperature. Therefore, the performance of a munition designed on this principle would also vary with the temperature. From a mechanical point of view, for antipersonnel effects and ground contamination, the airburst munition described in the previous section would have many advantages.

Chapter 35

MUNITIONS FOR THE DISPERSAL OF SOLID PARTICLES

By *H. F. Johnstone* and *H. C. Weingartner*

35.1 INTRODUCTION

THE EXISTENCE OF SEVERAL solid chemical and bacteriological agents of extremely high toxicity suggests the use of these materials as warfare agents. Since the toxicity of these agents is greatest through pulmonary action, they are most effective when dispersed as aerosols of particles sufficiently small to penetrate the nasal passages and reach and be retained by the alveoli of the lungs. These agents are, in general, odorless and difficult to detect in the dilute concentrations required to produce casualties. On the other hand, since the most effective particle sizes are easily removed by the gas mask filter, troops may have adequate protection by wearing the mask. The tactical use of these agents therefore requires instantaneous dispersion from a bomb or shell to set up an immediate dosage exceeding the lethal value before masks can be adjusted. The necessity for providing a new munition designed specifically for the dispersion of these agents became apparent when it was found that the standard munitions for dispersing chemical agents were quite unsuitable. The dispersal of powdered agents from bursting or tail-ejection bombs and shells was ineffective because of the formation of large compacted particles.[1, 2] Many of the agents are also subject to rapid detoxification even at moderate temperatures and, in some cases, it was found that an explosive shock would decrease or destroy the toxicity. These effects were present to a greater extent with aqueous solutions and suspensions than with dry powders.

Laboratory techniques for the dispersal of these agents were developed while toxicities were being studied and compared. Best results were obtained by dispersing dilute solutions by means of a Benesh air-atomizing nozzle containing a baffle for removing the large droplets.[3] It was shown also that the dry powders could be dispersed as essentially unitary particles by means of a pneumatic nozzle.[4, 5] Because of their complexity and the large quantities of air or gas required to effect the dispersion, these methods are unsuitable for incorporation into munitions for field use. From a practical standpoint, the objectives sought in the development of a suitable munition were:

1. Development of a bursting munition for dispersing dry powders by proper selection of the type and dimensions of the burster.
2. Development of a base or tail-ejection bomb or shell which would exert little or no mechanical action on the dry powders.
3. Development of a bursting munition for dispersing solutions or suspensions of the agent without detoxification.

The work in Division 10 NDRC was concerned mainly with the development of a munition for the dispersion of the protein agent designated as *W*. Early experiments indicated that this material was sensitive to heat and shock. Attention was given first, therefore, to a tail-ejection bomb using a compressed gas as propellant. In the field tests on this munition, comparisons were made with the dispersion obtained by high explosive. It was found that, with properly selected explosives, the detoxification of thick suspensions was not serious and that excellent dispersion could be obtained, suitable for field use because of the low concentration required at saturation.

35.2 FUNDAMENTAL PRINCIPLES

35.2.1 Impactability of Aerosol Particles

The solid particles in an aerosol are made up largely of aggregates of smaller primary particles. A relatively small fraction of the mass of the material exists as unitary particles. The tendency of a particle to deposit on a vertical surface depends on its diameter and density and the velocity with which it approaches the surface and on the size and shape of the surface. The measure of this tendency is called the *impactability*.

Sell [6] has calculated the impactability of small dust particles on objects of various shapes and has found it to be a function of the dimensionless group.

$$\frac{du\rho}{\mu} \cdot \frac{d}{D},$$

where d is the diameter of the dust particle, ρ is its density, u is the velocity with which it approaches the object, D is a characteristic length of the object and μ

is the viscosity of air. Figure 1 shows Sell's curves for the impactability of particles on surfaces of various shapes. For small dust particles, the impactability is roughly proportional to the product of the density of the particle and the square of its diameter. It may be expected, therefore, that a large, loosely knit aggregate of low density and large diameter will be deposited to the same extent as a smaller and denser aggregate under the same conditions, as long as $\rho_1 d_1^2 = \rho_2 d_2^2$. However, in passing through small channels or through filters such as exist in the nasal passages, the actual size of the particle is important in

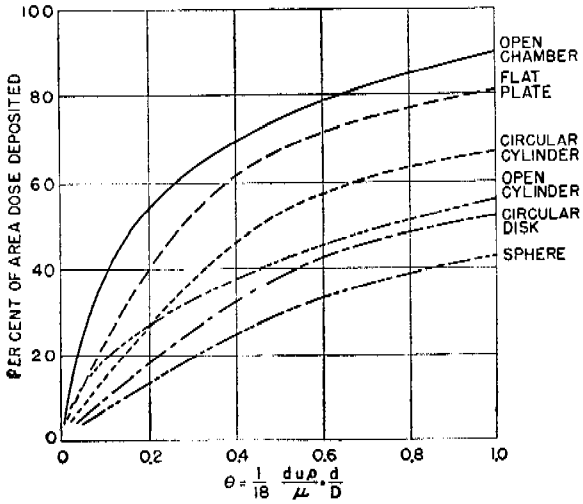


FIGURE 1. The deposition of airborne particles on vertical surfaces.

the removal and deposition from the air stream. Furthermore, the hygroscopicity of the particle must be a factor in the penetration of the nasal passages. Experiments at the University of Chicago Toxicity Laboratory show that approximately 50% of 6 microns diameter droplets of oil will pass through the nose into the lungs when the breathing rate is 17 lpm. The penetration is less for aerosols of calcium phosphate and sodium bicarbonate dust of the same size.[5] The effect of flow rate is shown by the decreased penetration at 63 lpm which corresponds to rapid breathing. In this case 50% transmission is achieved only by 2-micron liquid droplets and by particles of less than 1 micron diameter in the case of sodium bicarbonate dust. The penetration decreases with increasing particle size until at 10 to 12 microns diameter the screening is complete. The density of the aggregates in these tests was in the range 1.0 to 1.4 g per ml.

The retention of dust particles by the lungs is also a function of the particle size and, at a breathing rate of 17 lpm, half of the 1.5 micron calcium phosphate dust particles was retained. There is an optimum particle size, therefore, for penetration of the nasal passages and retention by the lungs. It appears from these measurements that the desired range is between 1.5 and 5 microns.

35.2.2 Effective Toxicity of an Aerosol

The effective toxicity of a particulate cloud depends upon the composition of the agent as well as upon the percentage of the material in the critical size range. The toxicity of the original charging is determined by the chemical and physical methods used in the preparation of the agent. The condition under which the agent is stored, the mode of functioning of the munition by which the agent is dispersed, and the behavior of the airborne particles from the point of burst are other important factors.

The protein agent W was prepared by the Procter and Gamble Company by precipitation or by spray drying from aqueous solutions. The spray-dried material consisted of particles about 10 microns in diameter, which could be reduced to below 5 microns without detoxification by air micronizing.[7]

For the purpose of carrying out field tests on munitions, it was desirable to have a simulant which possessed somewhat the same properties as the toxic protein. Egg albumin was most suitable, since it is also denatured by heating. Albumin powder with a mass median diameter [MMD] less than 4 microns was prepared by the duPont Company by ball-milling a suspension of the solid in organic liquids, or by micronizing in air. All of the ball-milled samples were seriously denatured as shown by the low solubility in water. Hammer-milling caused less denaturation, but was unsuccessful in reducing the particle size below 15 microns MMD.[8]

35.2.3 Dispersibility of Powders

It is well known that some powders are more easily dispersed than others. Experiments made at the Munitions Development Laboratory [MDL] using several types of very finely divided pigment powders showed that those materials, consisting of primary particles less than 0.1 micron diameter, could not be dispersed as unitary particles by any of the methods suggested above. The difficulty was apparently due

to the high contact surface area which required more energy for dispersion than was available from an air jet or from an explosive charge. Good dispersibility is often associated with powders having a high porosity or free state.[9] The most easily dispersed albumin sample tested contained nearly uniform particles of about 6 microns and had a low bulk density.[2] It is of interest to note that the "dustiness" of a powder of this sort apparently bears no relationship to its dispersibility.

Attempts were made to lower the cohesive forces between the particles by coating with surface active agents.[8] It was found that albumin and zinc oxide powders treated with diglycol laurate were more efficiently dispersed by small explosive munitions than the untreated powders. This treatment, however, did not improve the dispersion of albumin powder by gas-ejection bombs, but actually decreased the dispersibility. There was some indication that treatment of the powder with soya lecithin improved the dispersion of zinc oxide but not that of albumin. Other surface active agents which affected the dispersibilities were fatty acid esters, polyhydric alcohols, octadecylamine hydrochloride, and micro silica dust.

The dispersibilities of W and egg albumin powders were markedly influenced by their moisture contents. It appears necessary to maintain the moisture content less than 1% in order to get the best dispersion.[10] Since the protein material is hygroscopic, the humidity of the atmosphere in which it is prepared and into which it is dispersed is an important factor in determining the ultimate nature of the aerosol particles.

The existence of aggregates in the aerosol clouds depends upon the form of the agent in the munition as well as on the type of munition and, to some extent, on the concentration of the initial cloud. Aggregates from the dispersal of dry powders are, in general, large and fleecy, whereas those from the dispersal of thick suspensions of the powder in an inert liquid are apt to be smaller and more firmly bound. There is experimental evidence to show that aggregates exist due both to failure to separate the primary particles and to coagulation due to high initial concentrations.[2] The agent compartment of a gas-ejection bomb was divided into two compartments, one filled with dyed albumin and the other with undyed albumin powder. Examination of the airborne particles after the dispersion showed aggregates composed solely of dyed and solely of undyed particles, as well as aggregates of mixed color. Furthermore, densely aggregated single-colored nuclei with fringes of lightly held particles of both colors were found.

35.2.4 Concentration in Aerosol Clouds [11]

The travel of aerosol clouds in the air and the dosages downwind from the point of dispersion may be estimated by means of the British diffusion theory [12] corrected for losses by vertical and horizontal deposition. The concentration-time product F resulting from the passage of an aerosol cloud generated at a line source in open country is given by the equation

$$F = \frac{q - \int_0^x Fv\,dx}{Bux^{m/2}}, \tag{1}$$

where q is the source strength;
v is the settling velocity of the particles;
x is the distance downwind from the source;
B and m are meteorological constants;
u is the wind speed.

After differentiation with respect to x and separation of the variables this becomes

$$-\frac{dF}{F} = \left(\frac{v}{Bux^{m/2}} + \frac{m}{2x}\right)dx. \tag{2}$$

Upon integration, equation (2) becomes

$$F = \frac{K}{x^{m/2}} e^{-1/(Bux^{m/2}) \cdot (vx)/(1-m/2)}. \tag{3}$$

As $d \longrightarrow 0$, $v \longrightarrow 0$, and

$$e^{-1/(Bux^{m/2}) \cdot (vx)/(1-m/2)} \longrightarrow 1,$$

from which it is evident that

$$K = \frac{q}{Bu}.$$

Let the aerosol dosage F be expressed by

$$F = Ctf, \tag{4}$$

where Ct is the concentration-time product of a gas cloud of the same source emission as the aerosol cloud, and f is the fraction of the agent remaining airborne at any distance. Then f is given by

$$f = e^{-1/(Bux^{m/2}) \cdot (vx)/(1-m/2)}. \tag{5}$$

The term, $1/Bux^{m/2}$, is equal to the gas cloud Ct for an emission of 1 g per cm of line source. The settling velocity of small aerosol particles in still air by Stokes' law is

$$v = \frac{\rho d^2}{3.40 \times 10^{-6}}, \tag{6}$$

when all the quantities are in cgs units.

If the quantities are expressed in the more familiar units for use with the gas concentration slide rule,[12] equation (5) becomes

$$f = e^{-3.25/10^9 \cdot (\rho d^2)/(1 - m/2) \cdot Ct_g x}, \qquad (7)$$

where ρ = density of the aerosol material, g per cu m;
d = drop or particle diameter, microns;
x = distance downwind from the line source, yards;
Ct_g = gas cloud Ct for an emission from a line source of 1 lb per yd, mg-min per cu m;
$m = 2/[1 + (\log R)/(\log R + \log 2)]$;
R = (u at 2 m)/(u at 1 m);
u = wind speed.

In equation (4), Ct may be used in any convenient units and F will be given in the same units since f is dimensionless.

For aerosol particles larger than about 5 microns the evaluation of the constant K cannot be accomplished in this simple manner. In actuality, the conditions deviate from the theoretical at a point near the source. In equation (7), as $x \longrightarrow 0$, $Ct_g \longrightarrow \infty$. The result is that the deposition within a short distance from the source, according to the equation, is relatively large but actually the aerosol cloud may not touch the ground until it is several yards from the source. In this work it has been assumed that the value of f at 10 yd is unity, and that the value of f at any distance x is that calculated from equation (7) divided by the value at 10 yd. This is somewhat arbitrary and may have to be modified when more information becomes available.

The magnitude of the correction factor f has been determined for a liquid with a density of 1.0 g per cu m, drop diameters of 0.8, 8.0, 12.0, and 24 microns, and for the atmospheric conditions corresponding to a sunny day (R = 1.05) with a moderate wind (u = 5 mph), and a clear night (R = 1.25) with a low wind (u = 2 mph).[13] The values are given in Table 1.

35.3 TESTING OF MUNITIONS

35.3.1 Explosion Chamber

It is frequently convenient to carry out tests on small aerosol munitions by functioning them inside a large closed room. Animals may be exposed within the room, and samples taken of the aerosol at various points to determine the variation of concentration and particle size with time. The concentration-time relationship may be obtained by drawing the aerosol through a suitable filter and determining the half-life of the aerosol.

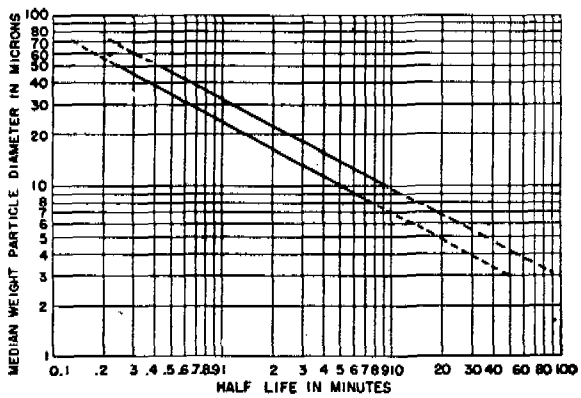


FIGURE 2. Limits of the half-life of a particulate cloud for settling in a closed room, in still air, and in turbulent air.

Another method of determining the settling rate, or the concentration-time relationship, is by means of pie plates exposed for fixed intervals of time during the settling. A differential pie plate settler was constructed for this purpose in testing the munitions developed at the MDL.[14]

The MMD of equivalent spherical particles may be determined directly from the half-life of the aerosol. It makes no difference whether the air is still or if there are drafts or thermal currents, provided there is no

TABLE 1. Value of the correction factor f for deposition of aerosol clouds under two atmospheric conditions. (ρ = 1.0 g/cm³)

Distance downwind yd	R = 1.05, u = 5 mph				R = 1.25, u = 2 mph			
	Drop diameter				Drop diameter			
	0.8μ	8μ	12μ	24μ	0.8μ	8μ	12μ	24μ
100	>0.99	0.98	0.96	0.85	>0.99	0.89	0.76	0.32
500	>0.99	0.96	0.94	0.78	>0.99	0.83	0.64	0.16
1,000	>0.99	0.96	0.93	0.74	>0.99	0.78	0.58	0.11
5,000	>0.99	0.95	0.90	0.65	>0.99	0.69	0.42	0.03
10,000	>0.99	0.95	0.88	0.59	>0.99	0.63	0.37	0.02

serious leakage of aerosol from the room. Figure 2 shows the limits of the half-life of particulate clouds in which the particles have a density of 2, and for a room height of 15 ft. This chart may be used for rooms of different heights and for materials of different densities by observing that the half-life of the cloud is proportional to the height of the room in which it is dispersed, and is inversely proportional to the density of the particles. The two lines show the variation in half-life caused by assuming both turbulent and quiescent settling and the extreme particle size distribution. Midway between the two lines lies the most probable case of normal particle distribution in turbulent settling. Although the density of the aggregates is often hard to evaluate to obtain an absolute answer, valid comparisons with the same filling dispersed in different ways are nevertheless possible.

For a cloud of uniform particles the settling data plotted as the logarithm of the fraction of the initial airborne charge against time is a straight line, of which the slope is proportional to the particle density and to the square of the particle diameter. It may be inferred, therefore, that a straight line settling curve implies the existence of particles of uniform deposition or impaction characteristics; whereas a curved line implies the existence of nonuniform particles. The smallest slope is associated with particles least likely to deposit by impaction.

The characterization of aerosols by optical methods has been extensively studied at Columbia University.[4] A statistical diameter suitable for comparison can be obtained from the scattering power of a deposit of the aerosol which has been allowed to settle upon a clean glass slide. For use in the laboratory, this method yields information on the rate of settling, particle density, refractive index, and size distribution of any aerosol.

Some further indication of the impactability of aerosol particles is obtained by the use of the cascade impactor, a sampling device in which air is drawn through a series of four orifices of decreasing cross-sectional area; after each orifice the air impinges upon coated slides.[15] The larger particles impact upon the slide in the low-velocity chamber. As the impinging velocity is increased by decreasing the orifice size, the smaller particles are collected. A representative diameter may be determined by comparing a chemical analysis of the mass of agent collected on each of the four slides with a calibration of the instrument. The calibration must be performed with a material having aggregate densities similar to those of the sample, otherwise the variation in aggregate density will obscure the true diameter determination.

The average equivalent diameters determined from relative impactability measurements must be supplemented by measurement of the actual dimensions of the airborne particles. This is done by microscopic examination of the cascade impactor slides, or sticky rods, slides, and other objects upon which the aerosol particles are collected.[2] The data are expressed as the distribution of mass within the limits of particle size. A sample may be characterized by its MMD. This diameter is usually approximated by the diameter corresponding to $\frac{1}{2} \Sigma nd^3$. Refinements in this approximation have been made at the University of Chicago Toxicity Laboratory in which corrections are made for nonsphericity and variations in density.[16] Since the particles and aggregates found on an impactor slide are not spherical and are of varying density, the mean diameter from the summation may be plotted against the cumulative per cent of the mass determined analytically on each slide and the value corresponding to 50% of the mass is determined. This is called the VMMD and is a closer approach to the true MMD.[17]

The size distribution of a sample of agent, as charged to the munition, is found by the microscopic examination of the agent dispersed in a fluid and spread upon a slide. A small sample of the powder is dispersed in a mobile liquid (butanol) by stirring mechanically at a high speed. The dispersion is stabilized by the addition of a thickening agent such as Canada balsam, and a small amount of the suspension is spread in a thin film between a clean slide and a cover glass. A representative area is then scanned to observe a sufficient number of particles (500 to 5,000) to evaluate properly the median diameter. Because the mass of a single large particle may be equivalent to thousands of smaller ones, care must be taken to observe a truly representative group of particles.[14]

35.3.2 Field Assessment of Munitions

In field trials, the relative impactability of the aerosol is determined from downwind total dosage samplers. These may be filters or impingers. The latter are samplers into which the aerosol is drawn through a horizontal tube facing upwind and trapped in a suitable inert liquid. The dosage is expressed as the concentration-time product $[Ct]$. The performance of munitions in dispersing solid agents may be

compared by the standard dispersal figure [SDF], which is the actual cross wind integrated Ct expressed as a percentage of the ideal gas cross wind integrated Ct as computed by means of the British gas slide rule. This figure is suitable only for similar field trials.

The field assessment of particle size distribution is performed, as described above, by using cascade impactors and impinging surfaces for microscopic examination. The sampling rates for cascade impactors, filters, and liquid impingers are adjusted as nearly as possible to provide isokinetic sampling conditions. The overall criterion in selecting an agent-munition combination is based upon the quantity of effectively dispersed active agent which can be applied by a single aircraft. This involves adjusting the dimensions of the munition to the munition performance and to the bomb-carrying equipment in the aircraft to get the maximum effective use of the aircraft as well as of the agent.

35.4 DEVELOPMENT OF MUNITIONS

35.4.1 British Work

Most of the early work on the dispersion of solid powders as particulate aerosols was done by the British.[18, 19] The bombs used were, for the most part, experimental modifications of the British 30-lb LC Mk 1 chemical bomb which had a 2-lb, 12-oz burster of 50/50 Amatol cast into the nose, and a capacity of 22 l. The modifications of this bomb, made for dispersing solutions and suspensions of the solid agents, were as follows.

1. The *Day* bomb which contained a small axial TNT burster of the type used in the standard 250-lb LC bomb. The case for the 30-lb bomb was cut off to about one-half the original length so as to fit the length of the burster. The chemical charging was thus entirely in the annular space.

2. The *Double-Day* bomb, for which the burster was twice the length of the standard burster for the 250-lb LC bomb and was approximately as long as the 30-lb bomb itself. The burster contained 917 g of TNT.

3. The *Whytlaw-Gray* bomb which contained a much heavier burster of 7 lb 12 oz TNT extending the full length of the 30-lb LC bomb, leaving only a small annular space for the chemical charging.

No attempt was made to disperse solid powders with these high-explosive bombs. A series of field trials, made at Porton Experimental Station in 1942 with aqueous solutions of W and suspensions in carbon tetrachloride, showed that lethal dosages could be set up by a single small bomb. The dispersion efficiency, however, was quite low, amounting to about 20% when the HE/chemical ratio was 0.2, falling to about 5% when the ratio was 0.5, and to 0.6% when the ratio was 1.5. The loss of activity with large amounts of explosives was partly due to the destruction of the poison. Since it was noted that the initial explosion was followed by a secondary flash, it was presumed that at least part of the destruction of the agent was due to inflammation.

35.4.2 Development of the Gas-Ejection Bomb [20, 21]

The possibility of dispersing the dry powder by means of gas ejection, in order to avoid the mechanical shock and thermal detoxification of the most sensitive agents, was explored at the MDL. The gas-ejection principle involved the introduction of the gas from a suitable reservoir under high pressure into a compartment containing the powdered agent until sufficient pressure was built up to rupture a shear diaphragm, thus releasing the gas-agent mixture. The dimensions of the initial cloud could be controlled by the use of a suitable deflector on the tail of the bomb. Without a deflector, the bomb formed a cloud 30 to 40 ft high, whereas, with a deflector, the initial cloud was not more than 12 to 15 ft high.

In the early experiments on this type of bomb, the gas was introduced slowly into the agent compartment with the expectation that the solid would become aerated and thus more easily dispersed. Release pressures below 400 to 500 psi gave poor dispersions, while pressures about 600 psi gave excellent dispersions of egg albumin suspensions.

This method of dispersing dry powders was also used for dispersing small quantities of toxic materials in the laboratory.[3, 4] Here it was found that increasing the release pressure up to 1,500 psi would improve the results, but for practical purposes the limitations of the weight of metal for the gas reservoir limited the pressure to 600 psi.

In later work at the MDL, the time of aeration of the solid was reduced until finally a double-compartment bomb was used in which the gas was released instantaneously into the agent compartment by the rupture of another shear disk, separating the two compartments. This disk ruptured at a higher

TABLE 2. Chamber tests on munitions for dispersing solid particles.

Run No.	Albumin sample SP	Weight of charge g	Modification of bomb: Diffuser tube	Modification of bomb: Ratio exit area to area of bomb	Modification of bomb: Deflector	Release pressure lb/sq in.	Cylinder pressure lb/sq in.	Per cent airborne* 5 min	11 min	28 min
					A CO_2 *Bomb*					
C-39	167DC	390	No	1	No	600	....	70	40	11
C-38		325	Yes	1	No	600	....	86	54	19
C-40	170B	255	No	1	No	600	....	40	30	14
C-42	170B	265	No	$\frac{1}{32}$	4 orifices	600	....	30	19	7
C-44	170C	265	No	1	No	600	....	53	35	13
C-45	170C	280	No	1	Conical	60	....	38	26	9
C-47	170C	295	No	1	No	600	....	50	34	11.5
C-48	170C	325	No	1	No	20	....	40	29	11.5
C-49	170C	345	No	$\frac{1}{8}$	Pointed conical	20	....	43	28	16
C-52	170C	355	No	$\frac{1}{8}$	Conical	20	....	26	19	6
C-53	170C	310	No	$\frac{1}{8}$	Flat	20	....	40	30	11
C-43	172 (yeast)	195	No	1	No	600	....	20	11	3
C-59	174A	342	No	1	No	600	....	41	20	5.5
C-60	174B	315	Yes	1	No	600	....	48	31	13
C-61	174B	325	No	1	No	600	....	29	15	2.5
C-62	174A	300	Yes	1	No	600	....	15	7.5	2.5
C-63	174A	330	No	1	No	600	....	25	18	6
C-64	174A	330	Yes	1	No	600	....	40	30	9
C-65	174B	300	Yes	1	No	600	....	50	35	14
C-66	174B	330	No	1	No	600	....	60	36	16
C-67†	174B	290	Yes‡	1	No	600	....	60	46	20
C-68	174B	290	Yes‡	1	No	600	....	65	50	21
C-69	174B	320	No	1	No	600	....	70	50	18
C-70	174B	320	No	1	No	600	....	70	52	20
C-71	174B	140	No	1	No	600	....	60	40	18
C-72	174B	213	No	1	No	600	....	75	52	23
C-73	175A	320	No	1	No	600	....	50	36	15
C-74	175B	300	No	1	No	600	....	30	19	12
					B *Air Bomb*					
CA-3	170A	210	....	1	No	405	4,100	35	11	2.5
CA-4	170A	210	....	$\frac{1}{8}$	No	270	2,100	41	14	2
CA-5	170A	210	....	$\frac{1}{8}$	No	135	1,200	17	7	2
CA-7	170A	240	....	1	4 orifices	280	2,100	28	18	5
CA-13	170C	215	....	$\frac{1}{16}$	Flat	60	3,000	16	12	6.5
CA-20	170C	268	....	$\frac{1}{16}$	Pointed	300	3,500	26	11	5
CA-21	170C	270	....	$\frac{1}{16}$	No	400	3,500	9.5	5	1
CA-22	170C	267	....	$\frac{1}{8}$	No	400	3,500	24	16	5
CA-23	170C	269	....	1	No	600	3,500	19	12	4
CA-24	170C	275	....	1	No	800	4,000	25	18	6.5
CA-30	170C	415	....	$\frac{1}{4}$	Flat	200	3,200	21	16	7
CA-33	174A	350	....	$\frac{1}{7}$	Perforated cap	400	4,000	10.5	14	5.4
CA-34	174A	310	....	$\frac{1}{7}$	Perforated cap	400	4,000	40	27	8.5
CA-35	174A	350	....	$\frac{1}{7}$	Perforated cap	400	4,000	18	12	4.8
CA-36	174A	310	....	$\frac{1}{7}$	Perforated cap	400	5,000	18	14	6.7
CA-37	174A	315	....	$\frac{1}{7}$	Perforated cap	400	5,000	25	21	11.5
CA-40	174A	325	....	$\frac{1}{7}$	Perforated cap	500	4,400	44	25	7.7
CA-41	174A	325	....	$\frac{1}{7}$	Perforated cap	500	4,400	16	8	2
CA-42	174A	320	....	$\frac{1}{7}$	Perforated cap	500	5,000	45	28	8
CA-43	174A	320	....	$\frac{1}{7}$	Perforated cap	500	5,000	25	14	5
CA-44	174A	330	....	$\frac{1}{7}$	Perforated cap	500	5,000	38	25	11
CA-45	174B	330	....	$\frac{1}{7}$	Perforated cap	500	5,000	37	23	8

* From best curves (on log C vs t plot) drawn through concentrations determined by filters at 4 to 8 min, 9 to 15 min, 16 to 24 min, and 25 to 35 min. Two samples were taken simultaneously at 8-ft level at two points in room, at 25 lpm. Uniform concentration of cloud in the room was assumed.

† Beginning with run C-67 leaks from the room were sealed. The percentage of the charge airborne at 28 min was noticeably increased. No CA runs were made after this time.

‡ Diffuser 8 in. long with 40 holes about $\frac{1}{32}$ in. in diameter.

TABLE 2 (*Continued*)

Run No.	Albumin sample SP	Weight of charge g	Modification of bomb: Diffuser tube	Modification of bomb: Ratio exit area to area of bomb	Modification of bomb: Deflector	Release pressure lb/sq in.	Cylinder pressure lb/sq in.	Per cent airborne: 5 min	Per cent airborne: 11 min	Per cent airborne: 28 min
			C *4-lb LC Canadian Bomb* §							
1	167DC	770	....	....	....	....	....	34	27	16
2	170A	645	....	....	....	....	....	30	24	15
			D *Tests in Firing Pit at Dugway Proving Ground*[10] *Cardox CO_2 unit*							
MW–3D	"W" 470–BM–199	298	....	1	No	600	....	10	6.5	3.5
			Experimental air bomb							
MW–3C	"W" 470–BM–199	508	....	1	No	800	....	12	7.5	3.5
			4-lb LC Canadian bomb							
W3	"W" 470–BM–199	...	....	....	....	....	....	18	10	4

§ Fired in room 30X100X15 ft with bomb suspended 6 ft off floor.

TABLE 3. Powdered egg albumins used in tests on dispersal efficiency of bombs at Munitions Development Laboratory supplied by the duPont Company.[3]

Designation of albumin	Preparation	Particle size distribution: Per cent by weight below diameter 2μ	5μ	10μ	20μ	Median dispersibility: Wt diameter	in gas-ejection bombs
SP–150	Pebble milled 48 hr in ASK,* untreated, micropulverized	3	27	56	100	8.7	Good
SP–152	Steel ball milled 48 hr in ASK, untreated, micropulverized	3	34	76	100	6.6	Good
SP–154	As above but treated 1% diglycol laurate	2	30	76	100	6.8	Bad
SP–156A	Steel ball milled 72 hr, untreated, micronized, cyclone collected	2	39	88	100	5.7	Poor
SP–158X	Steel ball milled 96 hr, treated ¾% soya lecithin, micronized 3 times, products combined	8	70	100	...	4.0	Bad
SP–167DC	Steel ball milled 48 hr, untreated, micronized for 4 times, cyclone collected	1	37	98	100	6.0	Excellent
SP–170A	Steel ball milled 96 hr in ASK and micronized	12	71	98	100	3.8	Very poor
SP–170B		50	100	...	...	2.0	Excellent
SP–170C		18	76	100	...	3.4	Good
SP–172	Yeast, micronized (one pass only)	50	100	...	...	2.0	Poor
SP–174A	Same as SP–167DC	30	100	...	...	2.5	Excellent
SP–174B	Same as SP–167DC	30	100	...	...	2.5	Excellent

* Atlantic Safety Kleen — naphtha and chlorinated hydrocarbons.

TABLE 4. Comparison of gas-ejection bombs and plastic bombs based on dispersion and stowage efficiency.

Bomb	Wt empty g	No. of bombs per 500-lb cluster	Wt filling g	Wt agent g	Per cent airborne at 50 min*	Weight (g) airborne at 50 min*	Wt agent / Total wt bomb g/g	Wt agent / 500-lb cluster g
Gas-ejection	2,400	38	350	350	4.12	14.4	0.128	13,400
Plastic 55% albumin in acetone	450	110	350	193	4.70	9.07	0.241	21,250
Plastic 35% albumin in CCl_4	450	110	483	170	3.2	5.43	0.183	18,700

* These two columns are comparisons based upon average tests using egg albumin in a static chamber.

pressure than the end disk so that the contents of the bomb were discharged immediately. Assessment of the resulting clouds from the two methods showed that they were essentially the same, and the later design was adopted as being more suitable for containing the agent.

The Cardox Bomb

A device operating on somewhat the same principle as the gas-ejection bomb has been used for mining coal for several years. This is produced by the Cardox Corporation of Chicago, Illinois. It consists essentially of a chamber containing liquid carbon dioxide, which is vaporized by means of an electrically ignited heater cartridge. The energy of the gas released by means of the shear disk is utilized for breaking down coal for mining. The heater element contains a mixture of potassium perchlorate and carbon.



Figure 3. Gas-ejection bomb with liquid CO_2 cylinder.

Through the cooperation of the Cardox Corporation, development was made of a gas-ejection bomb using liquid carbon dioxide. The prototype model is shown in Figure 3. The liquid carbon dioxide and the heater element are contained in the carbon dioxide cylinder (9) and secured by the shear disk (8) and the fluted screw plug (6). This was screwed into the nose assembly (3) containing the firing pin (4), the piston spring (5), and a direct-acting fuze (2). This entire assembly fitted into the nose of the outer case (1) containing tail vanes and a shear disk held in place by the deflecting surfaces shown. Upon functioning, the heater was ignited by a primer initiated by the action of the firing pin. The expanding gas flowed through the six holes in the nose assembly (3) into the agent compartment and finally issued from the bomb tail, dispersing the agent into a cloud shaped by the deflectors.

The optimum carbon dioxide charge to give proper functioning was found to be about 110 g. This required a 10-g heater cartridge and would disperse 300 to 400 g of the powdered agent.

The Air Bomb

A study was made of the thermodynamics involved in the operation of the bomb using various liquefied gases, such as NH_3, CO_2, SO_2, HCN, H_2S, Cl_2, CS_2, and CH_3Cl.[22] It was assumed that the bomb might be used at temperatures from −40 F to 150 F, and that it should provide a pressure of 600 psi at the release of the second shear disk. For such a temperature range, it was evident that any of these propellants would give a wide variation in pressure in the gas compartment. Furthermore, at the higher ambient temperatures, because of the excess heat available from the heater cartridge designed for functioning at low temperatures, the gas would enter the agent compartment with considerable superheat, and the particles might attain an instantaneous temperature of 500 F or more.

Calculations were also made to determine the feasibility of using compressed air for the propulsion gas. It was concluded that satisfactory operation could be obtained with a pressure of not more than 2,500 psi at −40 F and 4,500 psi at 150 F. The functioning of this bomb is similar to that of the CO_2 bomb, except that the firing pin merely punctures the retaining shear disk, permitting the escape of the compressed air. The outer case is the same for the two bombs and is similar in size to the M-69 and M-74 incendiary bombs so that the final munition can be clustered in the same cluster adapter as is used for these bombs.

35.4.3 Dispersion Tests with the Gas-Ejection Bomb

The results of several tests on the CO_2 bomb in a dispersion chamber are shown in Table 2. Data on the dispersion of the same material in the Canadian 4-lb light-case land mine are included for comparison. Table 3 shows the character of the egg albumin powder used in these tests. The airborne particles in every case consisted of large flaky aggregates and smaller three-dimensional aggregates formed by coagulation of primary particles at high concentration. It was found that the method of preparation of the powdered agent was quite important. In general, the most finely divided powders were the most difficult to disperse, but this was not always the case. The finely powdered albumin samples SP-170B gave

good dispersibility in the CO_2 unit, but yeast of equal fineness was much more difficult to disperse. The albumin SP–167DC was the easiest powder to disperse and had an MMD of 6 microns. This was a relatively homogeneous sample with the over- and undersize materials removed in a classifier.

Field trials at Dugway Proving Ground [23] showed that the coagulation of the particles at high concentration was most extensive in the center and more concentrated portion of the cloud, and that, when the cloud was produced from a group of bombs fired successively in a slow ripple manner, the coagulation was less than from a similar group of bombs fired simultaneously. The simultaneous functioning of two groups of five of the air units, each containing 350 g of dry albumin, is shown[21] in Figure 4. Ground loss in the immediate vicinity of the bombs was negligible, but some albumin was observed to have been deposited on the grass and on the vegetation as the cloud swept by.

The Dugway results showed that neither the air bomb nor the CO_2 bomb denatures W. The Canadian 4-lb LC bomb also gave little or no denaturation.[10] This bomb produced aerosol clouds similar to those from the gas-ejection bomb but gave a greater ground loss of the agent, due to the force of the explosion.

35.4.4 Development of the Plastic Bomb [24]

The possibility of using the lightweight plastic bomb, described in Chapter 34, for the dispersion of volatile suspensions of W was suggested when it was shown in field tests that dry W was not as easily denatured as had been expected. Preliminary tests at Dugway Proving Ground [10] showed that suspensions of W in carbon tetrachloride could be dispersed without denaturation, if a nitroguanidine burster was used. A laboratory study of the factors involved in the dispersion of powder suspensions in liquids was made, using egg albumin as a simulant. It was found that the more concentrated the suspension was, the better the dispersion obtained, up to a concentration just sufficient to wet each particle. Of a number of organic liquids used for the suspension, acetone and carbon tetrachloride gave the best results, and hexane and chloroform were somewhat poorer. The texture, fluidity, and appearance of these suspensions varied with the liquids used. For example, 40% albumin in carbon tetrachloride is much less fluid than 55% in acetone. The desirable physical properties of a liquid to give good dispersion are high volatility, low viscosity, low density, and, possibly, low surface tension.

The nitroguanidine bursters used in the plastic bomb varied from $\frac{3}{8}$ in. to $\frac{7}{8}$ in. diameter. Better dispersion efficiencies were obtained with the larger bursters. An attempt was made to increase the weight of the explosives in the burster by consolidating the nitroguanidine under pressure. This led to erratic initiation and low-order detonation of the bursters. When it was discovered that Pentolite bursters also did not seriously denature W, it was decided to use this explosive in the field tests on the bombs.

Table 4 shows a comparison between the plastic bomb and the gas-ejection bomb on the basis of weight, dispersion efficiency, and stowage. The best overall efficiency is given by the plastic bomb filled with a concentrated acetone suspension. The airborne particles dispersed from suspensions in the plastic bomb consisted of rather firmly bound aggregates, generally smaller than those from the gas-ejection bomb. Microscopic examination of the aerosol particles showed that there were many more unitary particles from a suspension than from the dry powders.

35.5 FIELD TESTS ON MUNITIONS

A series of field tests was made in the Spring of 1945 at the Canadian Field Experimental Station at Suffield, Alberta, to compare the dispersion of several dry agents and suspensions in the various munitions which have been described with those from British munitions developed for the same purpose.[17, 25]

Duplicate layout tests were performed to compare:

1. The dispersion of dry W from the gas-ejection bomb (air unit) with that from the Suffield 4-lb LC bomb, both fired statically.

2. The dispersion of 35% suspensions of W in CCl_4 from the plastic bomb with that from the SPD Mk 1 (Porton Type F) HE/chemical bomb, both fired statically.

3. The dispersion of spray-dried, air-ground W from the gas-ejection bomb (air unit) with that from the Suffield 4-lb LC bombs, both bombs being launched from inverted mortars at their estimated terminal velocities.

4. The dispersion of 35% suspensions of W in CCl_4 from the plastic bomb with that from the (Type-F) HE/chemical bomb, both bombs being launched from inverted mortars at their estimated terminal velocities.

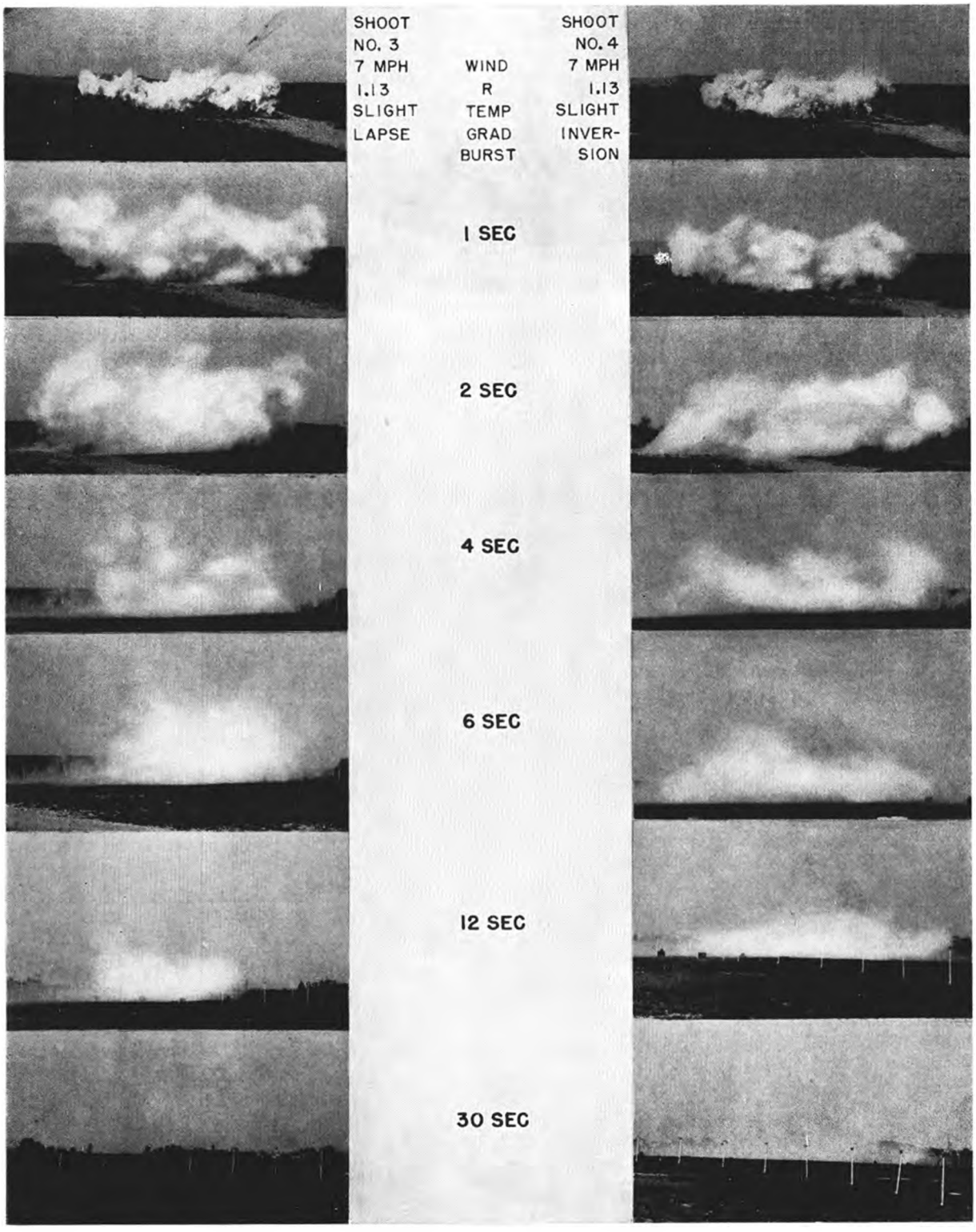


FIGURE 4. Clouds from simultaneous firing of five gas-ejection bombs charged with powdered egg albumin.

Total dosages were obtained by means of glass impingers as used at Porton. Particle size data were obtained from cascade impactors, sticky rods and coated slides. Bio-assays were made by exposing test animals to the clouds. All samplers were located on an arc 50 yd from the bombs. The bombs were compared on the basis of the standard dispersion figures and the volume-mass-median diameters [VMMD] of the particles in the clouds. These are shown in Table 5.

TABLE 5. Comparison of munitions for dispersing W.

Munition	SDF %	VMMD of clouds: Static bomb	VMMD of clouds: Launched bomb
Cardox CO_2 bomb — dry powder	28	19μ	38μ
Suffield LC — 4-lb bomb — dry powder	37	14μ	31μ
SPD Mk I (Type F) bomb — 35% suspension in CCl_4	57	9μ	7μ
Plastic bomb — 35% suspension in CCl_4	41	7μ	8μ

The dimensions of the initial clouds from all bombs were 10 to 15 ft high and 20 ft in diameter. At 50 yd, the clouds were 20 to 25 ft high and 60 to 65 ft wide. Ground contaminations were negligible for the suspensions and appreciable for the dry chargings. In all cases, the clouds contained unitary particles and aggregates. The munitions dispersing dry powders gave the coarsest aggregates, and those dispersing suspensions gave the largest numbers of unitary particles. About 19% of the dry agent and 30% of the suspended agent were dispersed as unitary particles. Little difference was noted in the structural characteristics of the aggregates from the two types of chargings except that the aggregates from suspensions were denser.

A test to compare the plastic and Type F bombs for the dispersion of the bacteriological agent U in a water slurry of micronized peat showed no measurable difference in performance. Heavy ground contamination was observed in the vicinity of both bombs. Other tests in which acetone suspensions of peat alone were dispersed gave negligible ground contamination.

The following conclusions regarding the dispersal of solid particulate agents were reached on the basis of these tests:

1. Solid particles may be dispersed more efficiently from suspensions in the proper liquid using high-explosive munitions than in the dry form from any available munition.

2. The plastic bomb is as efficient as the metal SPD Mk I bomb of similar size and shape, with regard to particle size, and is slightly less efficient than the metal bomb with regard to SDF. This difference, however, is within the experimental accuracy of the tests.

3. The 4-lb light-case bomb is somewhat better than the gas-ejection bomb with respect to both particle size and SDF.

4. The performance of the munitions is strongly influenced by the nature of the chargings.

Chapter 36

DISPERSION OF HERBICIDES

By *H. F. Johnstone* and *H. C. Weingartner*

IT IS WELL KNOWN that there are certain organic chemicals which, when present in the soil in extremely low concentrations, can destroy or prevent the maturing of plant life. The best known of these are 2,4 dichlorophenoxy-acetic acid and its sodium salt. The possible use of these materials, as a chemical warfare agent to destroy essential crops on the Japanese mainland and on the by-passed occupied islands, was given close consideration during the last year of World War II, and the development of methods of dispersing the agents was proceeding under high priority.

The nature of the agent permitted its application in the form of a solution or as a granulated solid. The methods of dispersion available were (1) spray of aqueous solution; (2) dusting of powdered solids; and (3) aimable airburst projectiles for either liquids or solids. Tactical restrictions required that the aircraft release the agent or munitions containing the agent below 500 ft or above 5,000 ft. Low-altitude attacks were considered for small targets to be treated with liquid agents released from existing available spray equipment. Dusting methods were not considered because of the lack of proper equipment in the combat areas, and because of the short time available for the development of equipment. For large target areas, i.e., rice paddies, emphasis was placed on the dispersal of the solid agent from aimable airburst projectiles.

This project was the responsibility of the Special Projects Division, ASF; the organization to which NDRC assistance was directly given was Camp Detrick, Technical Department, in whose files detailed reports covering this work are to be found.

36.1 PRINCIPLES

The problem in dispersing a solid agent is to apply, as uniformly as possible, the desired dosage of agent over the largest possible area in the proper physical condition and form to be effective.

The travel of solid particles released above the ground is similar to the travel of droplets of thickened liquid agents already studied.[1] It may be assumed that the granules quickly reach their terminal settling velocities relative to the air, and are accelerated to the horizontal wind velocity at every point in their paths to the ground. It follows then, that the distance D which a given particle falling in still air travels downwind before reaching the ground is proportional to the height of release above the ground h, and to the resultant wind velocity v, and is inversely proportional to the settling velocity of the particle u, or

$$D = \frac{kvh}{u}, \qquad (1)$$

where k = a constant.

The length of a pattern (parallel to the resultant wind) is proportional to the vh product and depends upon the relative settling velocities of the largest and the smallest particles released.

$$L = D_{\max} - D_{\min} = kvh\left(\frac{1}{u_{\min}} - \frac{1}{u_{\max}}\right), \qquad (2)$$

where $u_{\min}$, $u_{\max}$ = settling velocities of smallest and largest particles respectively.

The distribution of agent along the pattern length is determined by the particle size distribution in the agent charge. The width (crosswind dimension) of a pattern from an airburst munition depends upon the vh product, but, to a lesser degree than the downwind travel of a particle. It tends to approach a maximum as vh is increased, and within the limits of proposed tactics may be assumed to be between 100 and 250 yd.[1]

36.2 DESIRED PARTICLE SIZE DISTRIBUTION

The upper particle size limit was determined by a consideration of the relation between uniform gross contamination density and particle size in a given charging, for upon this relationship depends the rate of solution and concentration increase of agent in the water of the target rice paddies. On the basis of laboratory experiments, the upper size limit was established to be about that of a particle which just passes 6-mesh screen. The lower limit was chosen to include all particles falling in a predictable manner and not carried excessive distances by the wind. This

TABLE 1. Terminal velocities, particle densities, and desired size distribution of granules of agent — sample I.

Screen size U.S. Std	Size of opening mm	Average wt per particle mg	Settling velocity u ft/sec	Reciprocal settling velocity $1/u$ sec/ft	Desired cumulative weight per cent
2½	8.00	235.0	18.7	0.0535	...
3	6.73	157.0	17.5	0.0572	...
3½	5.66	100.0	16.0	0.0625	...
4	4.76	65.0	14.3	0.0700	...
5	4.00	41.0	13.7	0.0731	...
6	3.36	26.0	12.6	0.0794	0
7	2.83	16.6	11.8	0.0848	9.0
8	2.38	10.5	10.9	0.0917	19.0
10	2.00	6.7	10.0	0.1000	31.0
12	1.68	4.2	9.3	0.1075	42.0
14	1.41	2.6	8.5	0.1178	57.5
16	1.19	1.7	7.9	0.1266	70.0
18	1.00	1.1	7.3	0.1370	85.5
20	0.84	0.68	6.8	0.1470	100.0

limit was set arbitrarily at 20-mesh, since the difficulty of controlling particle size distribution increases as the size decreases.

The crosswind concentration gradient follows the normal distribution law. As the value of vh is increased, this gradient decreases and the concentration or dosages become more nearly uniform.

Assuming a constant average crosswind contamination, the particle size distribution, between set limits, to give a uniform downwind dosage may be determined. This relationship requires that the cumulative weight per cent of the agent must vary linearly along the length of a given pattern. If a graph of this relationship is plotted on rectangular coordinates, the line must pass through the points: cumulative weight per cent = 0, length = 0, and cumulative weight per cent = 100, $L = L$. For a given value of vh, the length is determined by the settling velocities of the extremes in particle size as shown in equation (2). The values of $1/u_{max}$ may be substituted for $L = 0$ and $1/u_{min}$ for $L = L$. The equation for the straight line relating the cumulative weight per cent to the settling velocity (and consequently the particle size) then is

$$\text{Cumulative weight per cent} = 100\frac{1/u - 1/u_{max}}{1/u_{min} - 1/u_{max}}, \quad (3)$$

where the cumulative weight per cent computed is that percentage of the agent, as charged, between sizes corresponding to settling velocities u_{max} and u.

The relationship between screen size and settling velocities must be determined experimentally for each type and form of agent to be used. Table 1 shows this relationship for a typical batch of granular agent together with the size distribution computed as described. The terminal velocity data are taken from a smooth curve correlating the experimentally measured terminal velocities of carefully screened fractions of agent falling through relatively still air against the average particle size.

36.2.1 Munitions

Munitions were devised and tested for the purpose of dispersing granular agents.

1. The Type A container consisted of a modified shell of an M–16 cluster adapter (Ordnance) containing four cylindrical cloth-bakelite molded agent containers, each about 13 in. in diameter and 7½ in. deep. On release from the cluster at a predetermined time, the four containers were opened by means of static lines secured to the adapter shell. This munition carried 125 lb of the granular agent shown in Table 1. The four containers were employed to provide several points of release to minimize the concentrating effect of a release from a point source.

2. The Type B container consisted of a single sheet metal container shaped to fit the curved contours of the M10A1 cluster adapter in which it was held. Upon release, the container was split into three longitudinal sections by the explosion of strands of Primacord. This container carried 200 lb of the granular agent.

It was observed that the dispersion from the Type B container occurred over a continuous finite distance. Since this device was simpler, cheaper, more easily obtainable, and since its agent capacity was

greater than that of the Type A containers, it was the only one used in subsequent field tests.

Field tests were conducted by the Granite Peak Installation at Dugway Proving Ground. The munitions were dropped from a Mitchell B–25 bomber flying parallel to the resultant wind and from an altitude sufficiently high to allow them to lose most of their horizontal velocity components before functioning. The munitions were functioned over a wide range of wind velocities and heights of burst. Meteorological data were taken at the control point and the necessary information was transmitted to the aircraft. The aiming point on the salt flat target area was identified by a black smoke signal. The heights of burst were determined by the use of theodolites. The resultant winds were measured as the munitions fell.

A reference point was established in the approximate center of the ground pattern. From this point by means of transit and stadia board, the pattern boundary, the vertical projection of the point of airburst to the ground, and the sampling points, were located.

Within the pattern, the concentrations were measured by determining the mass of agent in a given area. Where possible, the particles were picked up, counted, and weighed. Where the particles were too small to be picked up they were counted and their sizes estimated visually. An experimentally determined relationship between average particle sizes and weights permitted estimations of the mass of the small particles (see Table 1). Sampling points were selected to scan the entire pattern and to give representative estimations of the dosages. Depending upon the pattern size, from 30 to 60 samples were taken.

TABLE 2. Comparison of actual and desired particle size distribution for granular agent-sample A.

Screen No. U.S. Std	Cumulative weight per cent	
	Desired	Actual
4	0.0	0.0
6	12.0	17.5
8	28.0	48.0
10	39.0	76.0
12	49.0	77.0
14	62.0	85.0
16	73.0	89.0
20	100.0	93.0

The contamination densities and average particle sizes were plotted on a scaled diagram of the patterns, and constant dosage contours were drawn. The areas covered by various dosages, the overall pattern dimensions, and the distances from projected point of burst to the upwind edges of the patterns were measured. Material recoveries were determined, and the variations in granule sizes along the patterns were observed.

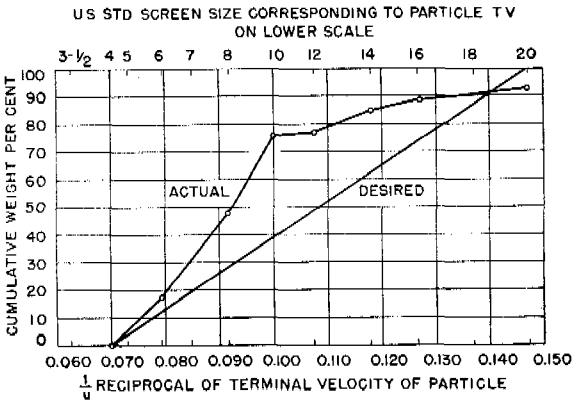


FIGURE 1. Desired and actual particle size distribution of agent. Sample A based upon experimental determination of terminal velocities of particles.

The granule size distribution in the charging used in the field trials was different from that calculated to give a uniform downwind contamination. The weight fraction of the larger size particles was too high, and that of the smaller size particles was too low. Seven per cent of the agent was below 20 mesh. The fraction between 10 and 12 mesh was extremely small. The differences are shown in Table 2 and Figure 1.

36.2.2 Results

The data in Table 3 show the pattern dimensions, contamination, downwind travel, wind velocities, and heights of burst for the trials.

Figures 2 and 3 show the approximate linear dependence of pattern length and downwind drift, respectively, on the *vh* product. This linear relationship cannot be expected to hold at low values of v or h because of the increased effect of the emission rate and track under those conditions.

It was observed that the areas of highest concentration were in the upwind half of the pattern, and that a gradual classification of particles occurred along the pattern. The largest particles were found at the upwind edge and progressively smaller ones were found further downwind until the subsize particles were so scattered that the definition of the downwind edge was uncertain. The upwind and side boundaries were well defined.

TABLE 3. Data for dispersion of granular agent (sample A) from aimable airburst projectile Type B.

Test No.	Resultant wind speed v mph	Height of burst h ft	vh ft × mph	Overall pattern length L yd	Overall pattern width W yd	Downwind distance from burst to upwind edge of pattern D yd	Recovery %	Area, in acres, contaminated with amounts in excess of 100 lb/acre	75	50	40	30	20	10	5	1	0+
3	8.5	1,398	11,890	490	183	130	55	0.03	0.25	0.61	0.80	1.05	1.35	2.32	4.02	7.35	15.34
4	17.0	1,648	28,000	1,203	107	300	63	..	..	..	..	..	1.40	3.62	7.35	12.10	23.50
5	11.0	2,240	24,640	973	150	10	82	..	..	..	0.47	0.90	2.21	4.75	7.09	14.95	26.70
6	11.0	4,060	44,660	1,454	106	400	100+	..	..	0.50	1.32	2.55	4.38	7.21	11.68	17.95	24.00
8	16.4	5,032	82,700	1,796	146	850	79	..	..	..	..	..	..	1.31	12.8	27.10	44.80
10	10.0	4,875	48,750	1,900	125	310	97	..	..	..	..	0.71	2.36	5.72	11.22	19.05	28.90
12	2.0	3,185	6,370	444	187	150	60	..	..	0.19	..	..	1.38	3.32	5.28	8.67	11.77
13	9.5	3,800	36,100	950	187	240	82	..	..	0.05	..	0.97	2.07	4.60	6.88	15.2	23.50

TABLE 4. Maximum areas covered by given dosages and corresponding (vh) product for charging used.

Desired contamination lb/acre	(vh)	Maximum area covered acres	Areas covered by other contaminations at same (vh) value (acres) 10 lb/a	5 lb/a	1 lb/a	0 + lb/a
10	50,000	6.3	...	10.8	20.5	31
5	77,000	12.5	4	...	26	42
1	80,000	27	0+	...	...	..

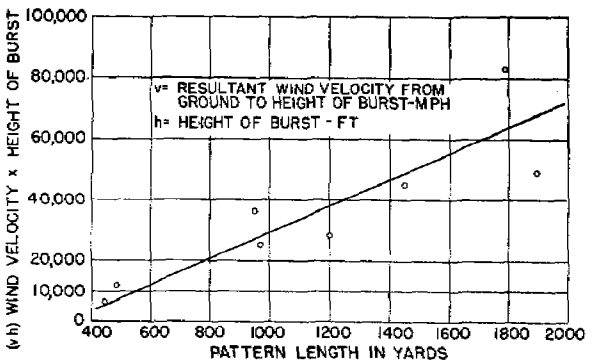


FIGURE 2. Relationship between pattern length and vh product.

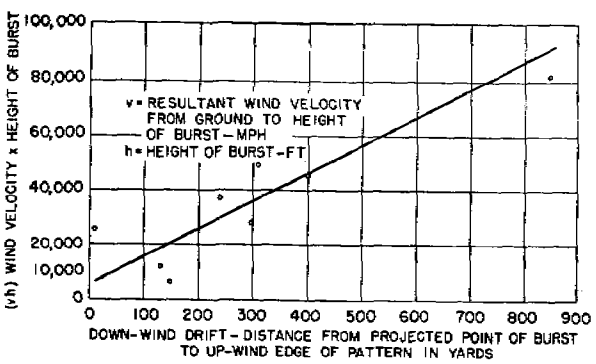


FIGURE 3. Relationship between downwind drift and vh product.

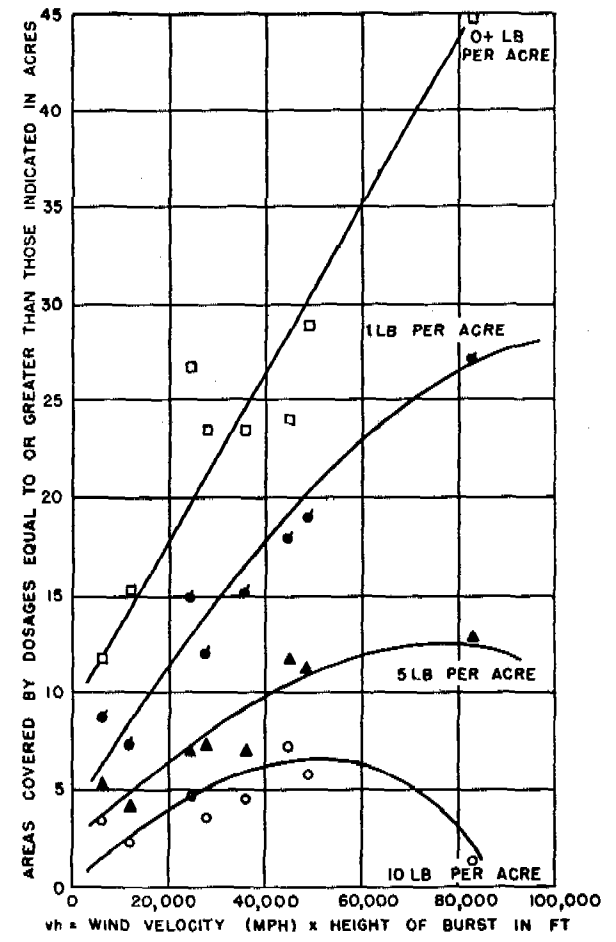


FIGURE 4. Area-Dosage; *vh* relationship for the charging used.

In several patterns, areas of low concentration between areas of higher concentration were observed in the portion of the pattern where the particle sizes were 10 to 12 mesh. These results are compatible with those which might be expected from a charge having the particle size distribution described.

Figure 4 shows the relationship between areas covered by various contaminations and the *vh* product. The total area can be expected to increase indefinitely with *vh*, for a given charging. The areas covered by higher contaminations can be expected to reach a maximum value. The highest contaminations will cover maximum areas at low *vh* values. Further increases will dissipate the material in an area of high contamination to increase the area of lower contamination. These relationships must be determined for each charging used. The maximum areas covered by a given contamination and the corresponding *vh* value for the charging used in these trials are given in Table 4. The data are insufficient to determine the maximum areas but show the approximate relationships.

The results imply that a more nearly uniform coverage with larger areas covered by contamination up to 5 lb per acre could have been achieved had the particle size been adjusted to contain fewer large particles and more small particles. Since the correction is in the direction indicated by the calculation described previously, the verification of that calculation is indicated, thus permitting size distributions to be specified between any limits of particle size for any granular agent.

Uniformly high concentrations probably could best be achieved by limiting the particle size to a narrow range, thus permitting the use of large *vh* products with decreased pattern lengths. Conversely, uniformly low dosages could be obtained with a charge containing particles between broad size limits, again employing high *vh* values for maximum uniformity.

Chapter 37

PLASTICIZED WHITE PHOSPHORUS

By *H. F. Johnstone*

37.1 INTRODUCTION

WHITE PHOSPHORUS WAS USED extensively during World War II for producing smoke screens in ground combat and in landing operations, and as an antipersonnel agent against enemy troops. In burster-type munitions the efficiency of WP as a smoke agent is small. Most of the charging burns within a few seconds after the burst, producing a cloud in which the smoke concentration is many times that required for effective screening. Moreover, the temperature rise in the concentrated cloud creates such a density gradient that it *pillars*, or rises rapidly from the ground, and becomes totally ineffective for ground screening. For this reason the burning-type smoke munitions, such as HC, were favored by the British Army almost to the exclusion of WP, and also found many tactical uses with the United States Forces. However, HC itself had certain limitations. For use in projectiles, it required a base ejection shell with low muzzle velocity and a low chemical efficiency. It was difficult to place by gunfire and was slow in developing a smoke screen. In high concentrations, and on prolonged exposure, its toxicity to troops was extremely hazardous. For these reasons, WP was much preferred by the American Army and Navy and was used extensively in the 4.2-in. chemical mortar supporting ground troops, in the 105 and 155-mm howitzers and guns, and in the 5-inch/38 caliber Navy guns for screening over water and on land.

Early in 1943, the NDRC was asked to investigate means of reducing the pillaring characteristic of WP smoke, and otherwise improving the smoke effectiveness of phosphorus munitions. Consideration of the problem indicated that the low effectiveness of solid phosphorus in bursting-type munitions is primarily attributable to the extensive fragmentation and the consequent high rate of combustion of the phosphorus. The temperature rise in the cloud immediately surrounding the burst is sufficient to produce a strong thermal updraft which rapidly lifts the cloud from the ground. On the other hand, the temperature rise in a cloud of effective, but not excessive, screening concentration would not be sufficient to develop thermal updrafts except under the most adverse atmospheric conditions.

From these considerations two methods of improving the smoke efficiency were suggested, (1) reduce the heat of combustion, and (2) control the rate of combustion. The former can be effected only by substituting for the phosphorus some compound with a lower heat of combustion. To this end, consideration was given to the use of phosphorus trioxide and other phosphorus compounds.[1] The second method is the more attractive because it would control not only pillaring, but also would realize the ultimate smoke efficiency of the phosphorus, and thus increase the total screening time several fold.

The following methods for controlling the rate of combustion by controlling the degree of fragmentation were suggested.

1. Mechanical reinforcement of the phosphorus with steel wool, asbestos, plastic tubes, wire screens or other devices, which would cause the ejection of the phosphorus in pieces of predetermined size.

2. Alteration of the physical properties of phosphorus, by addition of agents, to produce a plastic mass which would effectively resist shattering and be dispersed as pieces of moderate size.

Experiments were made on each of these methods. The reinforcing agents showed some improvement in the smoke efficiency, especially with mortar shells filled with longitudinal screen cylinders ½-in. diameter by 12 in. long.[2] It was also found that precast blocks of phosphorus could be used in some of the small bombs and these, on ejection as large masses, would burn for several minutes giving a nonpillaring smoke. Several types of plastic coatings were found suitable for keeping the blocks separated.

The most promising method of controlling the fragmentation of phosphorus and the pillaring of the smoke was found in the development of a new smoke agent, known as plasticized white phosphorus [PWP], consisting of an intimate mixture of granulated WP in a viscous rubber solution. This material burns more slowly, and the flying particles do not disintegrate by melting. Consequently, the pillaring is almost completely prevented and the screening time is greatly prolonged.

37.2 TEMPERATURE RISE IN PHOSPHORUS SMOKE CLOUDS

A rough estimate of the temperature rise in the smoke clouds from solid WP and PWP may be made from data obtained in field tests on fragmentation and particle dispersion.[3]

Data

Heat of combustion of WP	10,600 Btu per lb
Heat of combustion of PWP	12,000 Btu per lb
C_p of air	0.24 cal per g per degree C
Density of air	1.2×10^{-3} g per cc

Filling weights

4.2-in. mortar shell	
WP	7.6 lb
PWP	6.25 lb
M47A2 bomb	
WP	86 lb
PWP	72 lb

Approximate dimensions of burst (observed)

	Radius ft	Height ft	Volume cu ft
4.2-in. mortar shell			
WP	90	50	1.27×10^6
PWP	150	50	3.54×10^6
M47A2 bomb			
WP	150	90	6.37×10^6
PWP	300	90	25.3×10^6

Fraction of total filling weight burned in initial burst, and heat evolved

	Per cent burned (estimated)	Heat evolved Btu
4.2-in. mortar shell		
WP	90	72,500
PWP	60	45,000
M47A2 bomb		
WP	80	730,000
PWP	40	346,000

Calculated average temperature rise

Munition	Filling	Temperature rise degrees C
4.2-in. mortar shell	WP	1.75
	PWP	0.37
M47A2 bomb	WP	3.50
	PWP	0.50

The values shown are the average temperature rises in the initial clouds having the dimensions of the burst. Actually, the temperature rise at the center of the burst is much greater than shown and is zero at the assumed envelope.

37.3 MANUFACTURE OF PWP[4]

In the production of PWP, the phosphorus is reduced to an average particle diameter of about 0.5 mm by a process of granulation, in which a violently agitated mixture of molten phosphorus and hot water is cooled below the freezing point of phosphorus by the addition of cold water. The rubber solution is prepared as follows: GR–S rubber is reduced to pieces ⅛ in. to ¼ in. in diameter by shredding. The shredded rubber is mixed with the solvent and the mixture set aside for 6 to 24 hr until it becomes homogeneous by diffusion. The rubber solution is then mixed with the granulated phosphorus under water in a Cincinnatus-type mixer for 20 to 40 min. A flow sheet of the process designed for the Navy Bureau of Ordnance is shown in Figure 1.

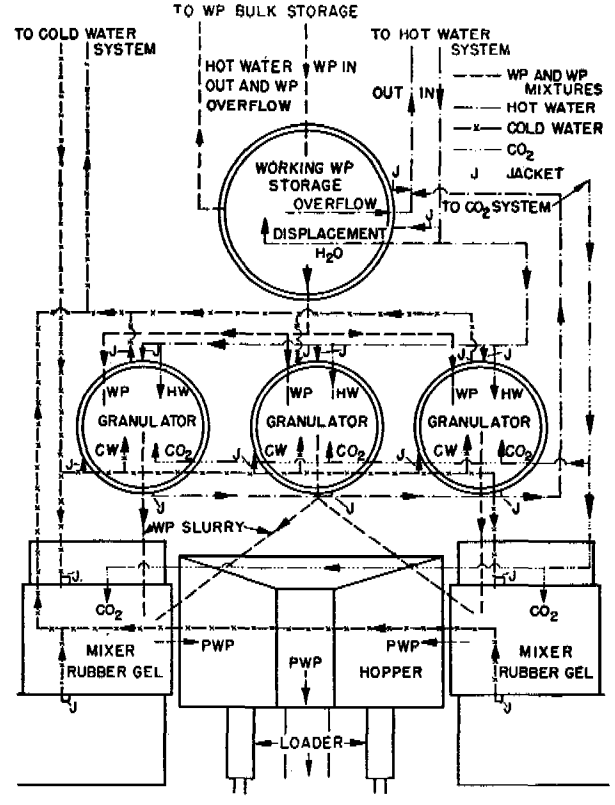


FIGURE 1. Flow sheet of PWP process (plan view of one unit).

Two types of PWP were developed to meet the ballistic requirements of the various smoke munitions. These differ mainly in their apparent viscosity, or consistency. The mixture designated as "75–35" PWP contains 75% phosphorus and 25% rubber solution which is 35% rubber and 65% xylene. This formula was satisfactory for bombs and rockets, which do not have critical ballistics. Rotating projectiles required PWP with a higher viscosity. Such a material is "75–40" PWP, which consists of 75% phosphorus and 25% rubber solution which is 40%

rubber and 60% solvent. PWP 75-40 was superseded by a type with a still higher viscosity, which is designated as "75–40–30LO." This formula contains 75% phosphorus and 25% rubber solution which is 40% GR S, 30% xylene and 30% linseed oil.

37.3.1 Granulation of Phosphorus

The phosphorus used in the manufacture of PWP is the standard technical grade. It is transported in the molten condition in steel tank cars and is usually stored in 10,000-gal horizontal steel tanks with internal steam coils to prevent solidification. In the PWP plant at Edgewood Arsenal,[5] the phosphorus was forced from these tanks by water displacement to a 500-gal vertical tank which served as a working storage. It was, in turn, transferred from this tank by water displacement to a 122-gal measuring tank from which it was sent to the granulators by displacement with a measured volume of water. All phosphorus lines were steam-jacketed and lagged. This method of handling phosphorus is safe and convenient, and it is easy to determine the amount of material transferred from one tank to another by means of hot-water meters and liquid-level gauges.

Batch Granulators

The batch granulators used in the pilot plant and in the large plant consisted of steam-jacketed vessels with high-speed agitators. The most convenient size for large scale production, as determined by the time cycle on the loading machine, was 165-gal capacity. Two of these granulators served one mixer. The charge placed in the granulator consisted of 400 lb of molten WP and an equal volume of water, or about 30 gal. The mixture was then agitated by means of two 3-bladed 7-in. impellers operated at 1,750 rpm by means of a 7½-hp motor. The agitation was continued for 5 min, and then cold water was run into the granulator to lower the temperature from 120 to 95 F. Within limits, the size of the particles could be altered either by varying the rate of agitation or the rate of cooling. Data taken in the pilot plants indicated that the desired rate of cooling should be about 4 F per minute in order to give a particle size within the specification limits, namely, 75% between 0.2 mm and 0.6 mm diameter, and not more than 5% in excess of 1.2 mm in diameter.

After cooling, the phosphorus slurry was discharged through a flush-type plug valve to the mixer which was located on a lower level. In order to prevent inflaming of the small particles of phosphorus which floated on the surface of the water, it was found desirable to keep the mixer closed and to maintain an atmosphere of carbon dioxide above the surface of the slurry during the transfer operation. For convenience, the line between the granulator and the mixer was steam-jacketed in case it became plugged by the freezing of the phosphorus resulting from leakage of the flush valve.

Continuous Granulator

Some work was done at the experimental plant at the University of Illinois on a continuous method of granulating phosphorus.[4] This had a number of advantages and probably would have been installed in the larger manufacturing plants if there had been time to work out the details. The process consisted of spraying molten phosphorus through a nozzle into a stream of hot water, as shown in Figure 2. The resulting mixture was cooled immediately by a merging stream of cold water, and the slurry was directed into the mixer. The particles of phosphorus from the jet granulator were smooth and round, in contrast with those from the batch granulator, which were rough and irregular in shape. The PWP made with the former had, on the average, a lower viscosity than that made using the batch granulator.

The following operating conditions for the jet granulator were found to give PWP of good thermal stability:

Pressure on phosphorus line: 18 to 20 psi
Orifice size: No. 44 drill
Rate of phosphorus flow: 7 to 7.7 lb per min
Hot water rate: 15 to 16 lb per min
Hot water temperature: 167 F
Cold water rate: 25 lb per min
Cold water temperature: 45 to 50 F

The particle size distribution for these conditions is:

Above 0.8 mm diameter: 5%
Between 0.2 and 0.8 mm diameter: 80%
Smaller than 0.2 mm diameter: 15%.

37.3.2 Preparation of Rubber Solution

The GR–S rubber used in the manufacture of PWP was the 80–20 butadiene-styrene polymer made in the government rubber plants. The nature of the material from different plants and even from different lots from the same plant varied widely. These variations affected the properties of the PWP to some extent, especially those of the higher viscosity type. There was a continued improvement in the product,

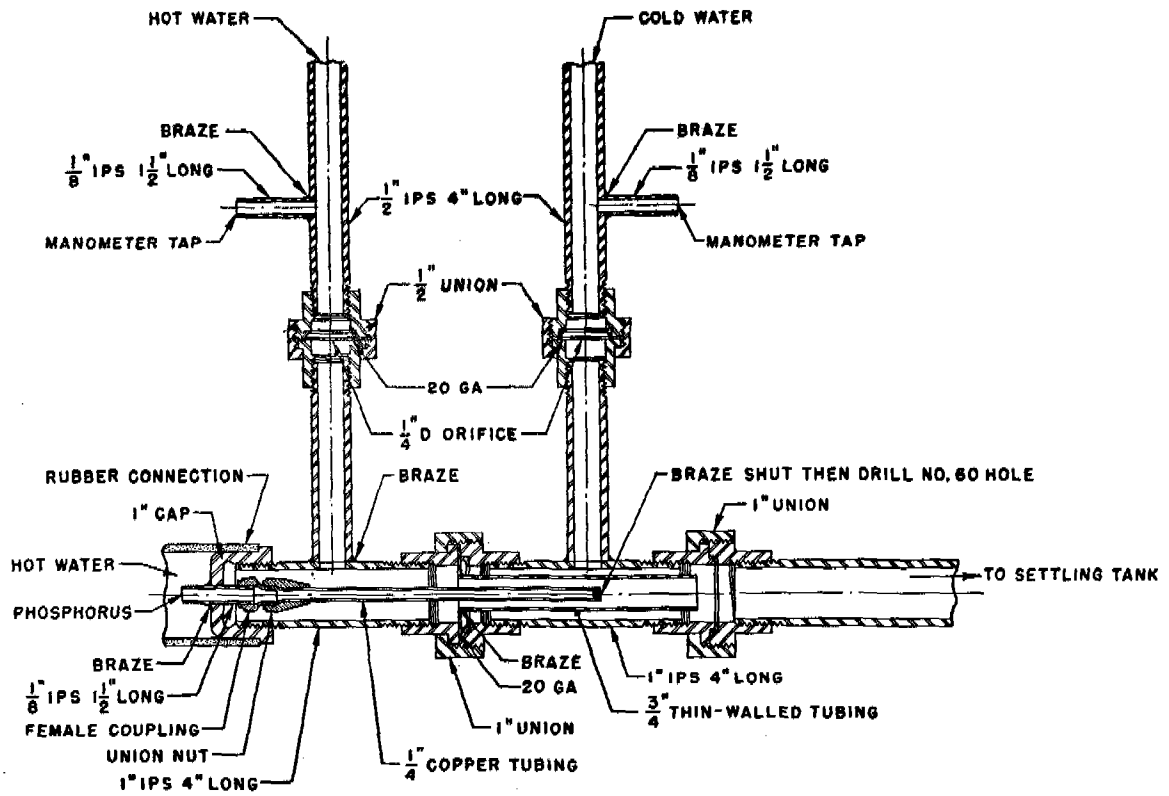


FIGURE 2. Continuous phosphorus granulator.

however, as the rubber plants came under better control.

Synthetic rubber is available either in bale or crumb form. The latter consists of irregular pieces ⅛- to ¼-in. diameter formed during the coagulation of the latex. This product is packaged after washing and drying. It is dusted sometimes with talc to prevent matting. In any case, unless the dusting is very thorough, compaction and cohesion of the particles occur in shipment and storage. The material must then be treated in the same way as the baled rubber which is made by pressing the crumb. The crumb form has the disadvantage that the dust is an unknown variable, and it is subject to more rapid deterioration because of the exposure of a large surface area to the oxygen of the atmosphere.

MILLING THE RUBBER

The particle size of the rubber determines the time required to obtain a homogeneous solution. In the manufacturing process, it was desirable to keep this time at a minimum. The preparation and use of finely divided rubber offered certain difficulties. If too much shredding was carried on in a single stage, the heat developed was excessive and the particles had a tendency to adhere to each other. Additional labor and equipment were required to cool the material and keep it in a free-flowing state, and power requirements were high. The best results were obtained with rubber reduced to an average of 3/16-in. to ¼-in. size. This was obtained by a single-stage reduction of 1-in. to 1½-in. cubes from a cutting machine in a Jeffrey Rigid Hammer Mill.

PREPARATION AND HANDLING OF THE RUBBER SOLUTION

In both the pilot plant and the large plant at Edgewood Arsenal, it was found convenient to prepare the rubber solutions in 5-gal buckets which were transported manually. For the Naval Ordnance Plant, special containers holding 60 lb of rubber and automatic handling equipment were designed and tested for serviceability.[6]

In practice, the milled rubber was poured into the required amount of solvent. This procedure was preferable to the reverse because it permitted better separation of the rubber particles and better wetting. The bucket was then closed tightly and tumbled by

mechanical means until the liquid was viscous enough to prevent the partially swollen particles from separating out. The time required for this step depended upon the particle size of the rubber and the type of solvent used, and varied from 5 to 15 min, or even longer. Some difficulty was experienced in getting good mixing when linseed oil was used in the formulas. The oil was mixed with the xylene before the rubber was added, but the two solvents diffused into the rubber at different rates and the composition of the remaining solution changed on standing. This difficulty could be largely avoided by prolonging the initial mixing time.

After the preliminary mixing, the rubber solution was poured into a special aging bucket. In order to prevent the thick rubber mix from adhering to the metal, the inside of the bucket was coated with a 20% starch paste made with Arabol Adhesive NLC–15, which was obtained from the Arabol Manufacturing Company of New York.

37.3.3 Mixing the Constituents

In the development work, several types of mixers were used for mixing the granulated phosphorus particles with the rubber gel solution. It was found that this operation was quite critical since, if the mixing operation was carried on for too long a time, it resulted in a break-down of the rubber, and if the mixing was poor, the phosphorus granules were not separated by films of rubber. Either of these conditions would result in a thermally unstable product which would allow the phosphorus to separate from the rubber matrix, when heated above the melting point of phosphorus. There was evidence that both a chemical and physical deterioration of the rubber takes place during the mixing operation, and therefore, there is an optimum time of mixing for each type of PWP in a given mixer. Not only does excessive working in the mixing and loading operations result in degradation of the rubber, but there is also evidence that the phosphorus itself causes an increase in the gel content of the rubber, especially if the temperature is allowed to rise due to the mechanical work on the viscous mixture.

The most satisfactory type of mixer found was the jacketed double-bladed Cincinnatus-type mixer with blades operating at the same speed in opposite directions. Mixers of 50-, 100-, and 300-gal capacity were used in the pilot plants and the large scale production. The 100-gal size was recommended because it had the proper capacity for coordination with the loading unit.

The mixers were provided with a split cover, one-half of which was permanently fastened, whereas the front half is removable for charging the rubber solution and discharging the product. Overhead sprays and an inlet pipe for CO_2 gas were also provided, as well as a drain hole near the top for removing the water.

The general method of operation of the mixers was to discharge the entire contents of the granulator as a slurry into the mixer, and then add the proper amount of the rubber solution while the mixer was being flushed with carbon dioxide. The excess water was then drained off and the mixer started. After the rubber solution had picked up the granulated phosphorus in 5 to 10 min, the water was run back into the mixer. The practice at this point was not always uniform but, in general, it was found better to have the water present during the mixing in order to aid in dissipating the heat. The mixing was continued for 15 to 20 min. The entire batch was then dumped into a hopper from which it was transferred by screws into the loading system.

37.4 LOADING PWP MUNITIONS

Since the amount of mechanical work to which the PWP may be subjected without damage must be kept at a minimum, it was found that extrusion of the material through a small-diameter tube by means of a screw could not be used for loading munitions with small filling holes. This was satisfactory, however, for the 100-lb bombs which could be filled directly from the 6-in. screw conveyor through a short nozzle. The bomb was weighed in place to control the net filling weight.

For small munitions, such as rockets and shells, the loading was done by means of hydraulic pistons operated by oil pressure. These consisted of two extrusion cylinders attached to a four-way valve on the 6-in. screw conveyor. While one cylinder was being filled, the contents of the other were being discharged into the munition by means of the piston. The cylinders were 4.5 in. ID and the pistons had a maximum stroke of 15 in. The stroke could be varied to control the delivery of the required amount of PWP for each munition. Both automatic and hand-operated controls were installed for operating the valve. It was found that a close weight tolerance could be maintained with the automatic equipment, and, in the

case of the 4.5-in. Navy rocket, the filling could be carried on at the rate of two heads a minute.

37.4.1 Control of Moisture Content

The moisture content of the product was determined by the consistency of the mixture, the *p*H of the slurry, and the amount of compression exerted on the product during the loading process. For the less viscous mixture used in bombs and rockets, it was desirable to increase the amount of compression by installing an orifice in the end of the 6-in. screw conveyor in order to squeeze out some of the water. The addition of sodium carbonate or sodium phosphate to the phosphorus slurry resulted in an increased moisture content of the product. In the pilot plant, the moisture content usually ran from 8 to 10%, but in the larger plant, it was found somewhat higher. There was no evidence, however, of an adverse effect of the high moisture content on the smoke quality of PWP in bombs, rockets, or other munitions.

37.4.2 Power and Services Required

An estimate of the material and power requirements in the manufacturing process was made on the basis of three months' operation of the pilot plant at Victor Chemical Works as follows.

Basis: 100 lb PWP

For 75–35 PWP	
Xylol	14.5 lb
Phosphorus	67.75
GR–S	7.75
Water	10.00
For 75–40 PWP	
Xylol	13.375 lb
Phosphorus	67.75
GR–S	8.875
Water	10.00
Gallons cooling water at 60 F	
Direct cooling	10.0 gal
Jacket cooling	55.5
Mixer cooling	90.0
	155.5
Estimated CO_2 usage	
Mixing	30 cu ft
Granulating	15

Power required = 4 hp hr

HP	Volts	Usage Service
¾	440	Continuous, hot water circulation
3	440	Intermittent, granulated Phosphorus pump
½	440	Intermittent, de-watering screw
¾	440	Continuous, loading screw
5.0	440	Intermittent, rubber mill
½	110	Intermittent, rubber gel mixer
10.0	440	Intermittent, mixer
¾	440	Intermittent, granulator

These figures agree approximately with those obtained in the larger plant at Edgewood Arsenal.

37.4.3 Labor Required in the Manufacturing Process

The estimate made by the Victor Chemical Works for the labor requirements were as follows.

Rubber, handling	0.12 man hr per 100 lb
Granulating	0.33
Mixing	0.33
Loading	0.33
Miscel. handling	0.33
Supervision	0.15

The Victor estimate does not include the labor required for handling of the empty munitions and loaded munitions, and the painting and boxing of the finished munition. In any Ordnance plant these items are always very large. The estimate made on basis of the operation of the Edgewood plant was as follows.

Labor required (for each shift)	
Phosphorus handling and granulation	3
Mixing	4
Loading	3
Empty munition, inspection	2
Empty munition, handling	2
Loaded munition, handling	15
Loaded munition, inspection	3
Preparing rubber gel	6
Laboratory inspection	2
Supervision	4
	44

About 60% of the labor performed in this plant was by women. The efficiency was not high, since it was the first large plant in operation and much of the production was of an educational nature. The plant had a manufacturing and loading capacity of 5,000 lb of PWP per 8-hr day.

37.5 PWP MUNITIONS

During the development of PWP a large number of munitions were filled and tested for comparison with other smoke munitions. These included the following:

Shell, 4.2-in. CM, M2
Shell, 4.2-in. RCM, E77
Shell, smoke, 75 mm, M64
Shell, smoke, 105 mm
Shell, smoke, 155 mm
Shell, smoke, 5-in./38 cal. Navy projectile
Shell, smoke, 60 mm, M302
Shell, smoke, 81 mm, M57
Rocket, smoke, 2.36-in., M10
Rocket, smoke, aircraft, 3.5-in., Mk 6
Rocket, smoke, 4.5-in., Mk 10, Mod 0
Rocket, smoke, 4.5-in., S.S., T-84
Rocket, smoke, 5-in., S.S.
Rocket, smoke, 7.2-in.
Bomb, 100-lb, M47A1, 2, 3
Grenade, smoke, M15

[redacted]

All these munitions were designed for use with WP and not PWP. They were used for test firing as a matter of convenience only, and it was realized that further improvements might be obtained with each munition if a new design could be made available which would allow for the lower density of the filling compared with that of WP.

37.5.1 Filling Weight

Since PWP contains substances which vaporize at elevated temperature, it is necessary to leave a void in the filled munition. The maximum loading weight for each type of munition can be calculated from a knowledge of the minimum volume tolerance of the munition, the composition and density of the PWP, and the pressure allowable at the maximum temperature to which the munition is subjected during storage. Actually, PWP has a density lower than that calculated from the densities of its constituents, because of numerous void spaces present in the mass of the material.

Assuming that the temperature of the munition will not exceed 65 C and that the pressure due to the expansion of the filling and the heating of the air in the void space from 25 C should not exceed 50 psi, the following calculation was made to determine the minimum void space required. [a]

Let u = volume of munition at 25 C;
u_1 = volume of munition at 65 C;
v = volume of total void space at 25 C;
v_1 = volume of total void space at 65 C;
k = fraction of total volume occupied by filling at 25 C;
$1 - k$ = fraction of void space at 25 C;
a = ratio of true density of filling at 25 C to that at 65 C;
α = coefficient of linear expansion for steel: 13.2×10^{-6};
w = water content of PWP, lb per lb dry PWP;
ρ = density, as indicated by the subscript.

The density of PWP may be calculated from the densities of its constituents as follows:

$$\rho_{PWP} = \frac{1 + w}{(.75/\rho_P) + (.25/\rho_R) + (w/\rho_W)}. \quad (1)$$

[a] The solubility of the air in the filling and the increase in vapor pressure of water and xylene are neglected.

The densities of the constituents are as follows:

	25 C	65 C
Phosphorus, ρ_P	1.824 g/cc	1.715
Rubber and xylene, ρ_R	0.8840	0.8145
Water, ρ_W	0.997	0.9806

The expansion of the munition shell is given by

$$\frac{u}{u_1} = \frac{1}{1 + 40 \times 3\alpha} = \frac{1}{1.0016}. \quad (2)$$

Assuming that the perfect gas law holds,

$$\frac{Pv}{P_1 v_1} = \frac{T}{T_1}, \quad (3)$$

$$v = u(1 - k), \quad (4)$$

$$v_1 = u_1 - aku = u(1.0016 - ak). \quad (5)$$

Then

$$P_1 = \frac{PT_1}{T}\left(\frac{1 - k}{1.0016 - ak}\right). \quad (6)$$

The values of k were calculated for several values of w, for $P_1 = 64.7$ psia, $P = 14.7$, $T_1 = 338$, and $T = 298$. These are shown in Table 1 with the corresponding values of a.

TABLE 1. Per cent void space required in any munition to give a maximum pressure of 50 psi at 65 C.

Water content of PWP lb/100 lb	Ratio of densities at 25 C and 65 C a	Fraction filled k	Per cent void $100\,(1-k)$
0	1.0725	0.9130	8.70
2	1.0710	0.9147	8.53
4	1.0694	0.9165	8.35
6	1.0679	0.9182	8.18
8	1.0663	0.9200	8.00
10	1.0648	0.9217	7.83
12	1.0633	0.9234	7.66
14	1.0619	0.9250	7.50
16	1.0604	0.9267	7.33

The loading tolerances for 75–35 and 75–40 PWP containing 12% and 16% water are shown for several munitions in Table 2. These are based on volume tolerances reported by the Chemical Warfare Service.

Figure 3 shows the relationship between the internal void (occluded air) and the density of PWP containing 12% and 16% water and also the variation of the external void space to be left in any munition if the pressure is not to exceed 50 psi at 65 C.

37.5.2 Ballistic Stability of PWP Munitions

As a result of firing tests on several different types of munitions, it was observed that (1) nonrotating

TABLE 2. Loading tolerances for PWP in various munitions (12% and 16% H_2O).

Munition	Per cent H_2O	Minimum loading volume of munition cc	Maximum weight of loading g	Load to
4.2-in. CM shell	12	2,310	2,914	6 lb 5 oz ± 2 oz
	16		2,878	6 lb 5 oz ± 2 oz
4.5-in. Mk 10 Navy rocket	12	3,486	4,402	9 lb 9 oz ± 2 oz
	16		4,343	9 lb 7 oz ± 2 oz
3.5-in. Mk 11 rocket	12	2,665	3,365	7 lb 5 oz ± 2 oz
	16		3,320	7 lb 3 oz ± 2 oz
4.5-in. T84 rocket	12	1,694	2,140	4 lb 10 oz ± 2 oz
	16		2,112	4 lb 9 oz ± 2 oz
3.5-in. Mk 6 Navy rocket	12	2,192	2,768	6 lb 0 oz ± 2 oz
	16		2,731	5 lb 14 oz ± 2 oz
81 mm T9 shell	12	1,135	1,433	3 lb 1 oz ± 2 oz
	16		1,414	3 lb 0 oz ± 2 oz
M47A2 bomb	12	26,219	33,100	72 lb 1 oz ± 1 lb
	16		32,660	71 lb 2 oz ± 1 lb

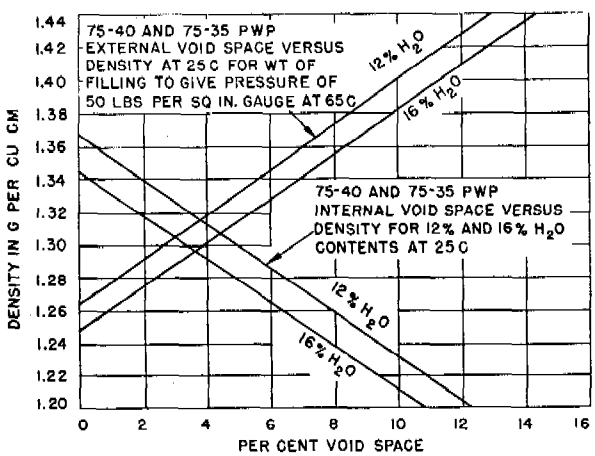


FIGURE 3. External void required in PWP munitions.

munitions (bombs and fin-stabilized projectiles) filled with any type of PWP are ballistically stable; (2) properly designed spin-stabilized rockets generally have stable flight with either 75–35, or 75–40, or stiffer mixes of PWP; (3) spin-stabilized shells with low-loading capacity (75 mm) are stable with both 75–35 and 75–40 PWP; (4) spin-stabilized shells with higher loading capacity (4.2-in. mortar, 105 mm and 155 mm) require a stiff thermally stable PWP if stable flight is to be obtained at maximum range or at elevated temperatures.

Much work was done on developing a satisfactory PWP for use in the 4.2-in. mortar shell. It was determined early in the program that mixes with low plasticity caused unstable flight when the shells were fired at long ranges (above 3,500 yd). Little is known about the behavior of gels and plastic solids in these shells. Set-back alone, caused by the forward acceleration of the shell from the gun, should not materially affect the balance. Instability, when it occurs, is perhaps caused by irregular flow of the filling as a result of the forward and spin accelerations. Suggested remedies are (1) to make the PWP stiffer and more resistant to flow, and (2) to make it less viscous and free to flow. To keep the advantages of the PWP as a smoke screening agent, all of the effort was directed toward making a stiff, thermally stable product.

Data from the firing of several hundred shells filled with PWP made of rubber from four different manufacturers and consisting of 75 35, 75–40, and 75–42 compositions gave the following conclusions:

1. Shells filled with 75–35 PWP with viscosity numbers (as measured on the standard plastometer) of 35 to 42 are not stable at maximum range.

2. Shells filled with PWP mixes with viscosity numbers greater than 57 are generally stable in flight at all ranges.

3. Heating the shell impairs the ballistic stability. This apparently is true only when thermal separation of the phosphorus takes place.

In all these tests, the shells were fired at ambient temperatures ranging from 40 to 95 F. Further tests showed that the flight stability is affected by heating the shells to 100 F, although the effects were noticeable only at extreme ranges. Shells fired at 120 F were unstable at all ranges, although previous firings had shown these shells to have good ballistics at all ranges when stored and fired at ambient temperatures. It was concluded, therefore, that projectiles having critical ballistic properties, such as the 4.2-in. mortar shell, require PWP of high viscosity.

TABLE 3. Summary of accelerated surveillance tests on 75–35 PWP made at pilot plant.

Rubber manufacturer	Shipment No.	Batch or series numbers	Number of batches	Results
Firestone Tire and Rubber Co	6	C and D series	81	"A" samples only. 66 batches showed no separation, 4 batches showed slight separation, 6 batches were unsatisfactory, 5 were not tested.
Firestone Tire and Rubber Co	18	E series	67	"A" samples only. All were satisfactory.
B. F. Goodrich	12	30E–32E, 42E–45E, 70E, 6F, 68F	10	All "A" samples were stable. Four "B" samples were unstable. All "C" samples were stable.
Goodyear Tire and Rubber Co	13	51E–53E, 60E, 4F, 19F, 21F, 77F, 78F	9	All "A" samples were stable. Four "B" samples were unstable. All "C" samples were essentially stable.
National Synthetic Co	14	59E, 64E–66E, 3F, 71F, 72F	7	Two "B" samples were unstable. All "A" and "C" samples were stable.
Copolymer Corporation	15	63E, 67E–69E, 1F, 18F	6	Four "B" samples were unstable. All "A" and "C" samples were stable.
Copolymer Corporation	19	23F, 69F, 70F	3	All "A," "B," and "C" samples were stable.
Copolymer Corporation	21	1H–4H	4	All "A," "B," and "C" samples were stable.

37.5.3 Thermal Stability of PWP

Phosphorus melts at 111 F and consequently PWP munitions in storage will often be subjected to temperatures above the melting point. While in this condition, complete separation of the phosphorus from the rubber matrix would result in pillaring of the smoke and would cause poor ballistics in critically balanced projectiles. Tests on the thermal stability of 75–35 PWP made in the experimental plant indicated that little or no separation of the phosphorus takes place even when the material was held at 150 F for as long as six months. In these tests, the samples were stored in glass bottles, and any separation of the phosphorus or growth of the droplets by coalescence was readily discernible. The same results were found for samples from the pilot plant when tested in this way. It was observed, however, that the material loaded in mortar shells often showed some separation of the phosphorus after heating for a few days. This could be noticed by slushing of the liquid from one end of the shell to the other when the munition was tipped, and was proved by opening the shell after cooling. At this time, a small-diameter loading screw was being used to extrude the PWP into the mortar shell. In order to have sufficient capacity, the screw was operated at a high speed and there was considerable slippage. Consequently, there was much mechanical working of the material as it was forced into the shell and flowed through the small openings in the longitudinal vane which partitions the shell into two parts. Because of the difference between the material in the glass bottles and in the shells, it appeared that the mechanical working was damaging the texture of the PWP so that it was no longer stable when heated. The screw extruder was then replaced with an extrusion cylinder of the type used at the experimental plant and the expected improvement was observed. It was also found at this time that many of the samples which were thermally unstable, because they had been overworked mechanically, would regain their thermal stability if allowed to stand for a few days before testing. Apparently, the network of rubber surrounding each phosphorus particle was repaired by aging. In some cases, however, the material appeared to be so badly damaged that it never regained the original thermal stability after loading. These observations were confirmed by tests made by the Chemical Warfare Service in which the stability of 75–35 PWP in M47A2 bombs was found to be satisfactory, but the same material in 4.2-in. mortar shells often showed separation.

Routine stability tests on the material produced in the pilot plant were made on three samples from each batch. One, designated "A," was taken from the mixer or hopper as soon as the mixing was completed and was placed in the oven immediately. A "B" sample was taken from the loading head and was also tested immediately. A third sample, "C," from the loading head was tested after aging for 24 hr. A summary of the results of these stability tests is shown in Table 3.

A further study of the cause of the occasional instability of batches of 75–35 PWP was made by the Plants Division at Edgewood Arsenal.[5] This revealed that, as the particle size of the granulated WP decreased so that more than 90% of the phosphorus was between 30 and 80 mesh, there was a greater number of unstable PWP batches. This result was consistent with the greater number of particles in the finer

TABLE 4. Summary of surveillance tests on 75–35 PWP in various munitions.

Rubber manufacturer and shipment number		Batch number	Number in surveillance	Thermal stability expressed as per cent phosphorus separating	Days in surveillance
		A *M47A2 (100-lb) bomb*			
Goodrich	12	68F	1	0	60
Goodyear	13	77F	1	0	30
National	14	72F	1	0	60
National	20	73F	1	0	30
Copolymer	19	70F	1	0	60
		B *4.5-in. naval rockets*			
Firestone	6	36D	4*	23, 30, 30, 36	....
Copolymer	15	18F	2	0, 2	....
Goodyear	13	19F	2	0, 2	....
Goodyear	13	21F	4	0, 0, 0, 0	90–180
Goodrich	12	68F	3	0, 4, 21	90–180
National	14	71F	3	0, 0, 1	90–180
National	14	72F	2	0, 1	90–180
Copolymer	19	23F	3	0, 0, 10	90–180
Copolymer	19	69F	2	0, 0	90–180
Copolymer	19	70F	2	0, 6	90–180
National	20	73F	3	0, 0, 11	90–180
		C *3.5-in. naval rockets*			
Firestone	6	30D	5	0, 0, 0, 1, 2	15–30
Copolymer	22	87L, 95L, 100L	4	0, 0, 8, 13.5	15–30
Copolymer	23	110L, 115L, 120L, 125L, 130L	5	0, 1, 3, 3, 4	15–30
		D *81-mm mortar shells*			
Copolymer	21	1H, 2H, 3H	9	All 0	60–90

* Loaded by screw extruder.

granulated material which presented more surface and decreased the film thickness of the rubber. Furthermore, it was found that many of the unstable batches had a higher density than the stable batches, indicating a higher phosphorus content. On the basis of several months' operation of the plant, it was possible to derive an *instability factor* represented by

$$u = [100(\text{apparent density} - 1.26)]^2 + (\%\ \text{WP between 30 mesh and 80 mesh standard screen} - 70).$$

These results led to the conclusion that, under the conditions existing at the Edgewood Arsenal plant, and using the rubber then available, it was advisable to maintain the particle size of the granulated phosphorus so that less than 60 to 70% passes a 30-mesh screen. Furthermore, careful control of the phosphorus content of the PWP must be exercised so that it will not exceed 75%, corresponding to an apparent density of 1.26.

A summary of the surveillance results on 75–35 PWP in bombs and rockets loaded at the NDRC pilot plant at Victor Chemical Works is shown in Table 4. The explanation of the occasional unstable batches might well be found in the lack of control of the degree of granulation and the composition of the material as was the case at Edgewood Arsenal.

When it became necessary to produce material of higher viscosity than 75–35 PWP in order to overcome the ballistic difficulties encountered with the critically balanced projectiles, the loading problem became more serious. PWP 75–40, which contains 2.5% more rubber in the mixture, has a viscosity number nearly twice that of the 75–35 PWP. Consequently, the amount of work done on the material in forcing it through a small filling tube frequently caused the material to become thermally unstable regardless of the method used for loading. Somewhat better results were obtained on PWP with high viscosity made with vegetable oil plasticizers, but even here the results were erratic.

Table 5 is a summary of the surveillance tests on 75–40 PWP in 4.2-in. mortar shells filled at the pilot plant. Table 6 contains the results on representative batches from 6,500 shells filled at the same plant with PWP containing vegetable oils.

Since the viscosity of PWP is an important prop-

TABLE 5. Summary of surveillance tests on 75–40 PWP in 4.2-in. mortar shells, M-2.

Rubber manufacturer and shipment number		Batch number	Number of shells in surveillance	Thermal stability as per cent of phosphorus separating
		A *Loaded with screw extruder*		
Firestone	6	34C, 25D	5	11, 14, 31, 36, 39
Firestone	18	19E, 25E	6	0, 0, 0, <1, <1, 3
Goodrich	12	33E	3	>30, >30, >30
Goodyear	13	49E	3	>30, >30, >30
National Copolymer	14	58E 61E	1	10
		B *Loaded with hydraulic ram extruder*		
Goodrich	12	7F	5	10, 13, 27, 33, >30
Goodrich	12	22F	7	3, 4, 8, 17, 20, 20, 24
Goodyear	13	5F	6	>30, 33, 38, 41, 44
Goodyear	13	20F	8	4, 11, 18, 23, 43, 44, 46, 49
Copolymer	15	2F	5	0.5, 0.5, 7, 7, 18
Copolymer	15	8F	3	28, 50, 70
Copolymer	15	9F	2	19, 31
Copolymer	15	10F	3	11, 41, 70
Copolymer	15	11F	3	6, 15, 36
Copolymer	15	12F	3	9, 11, 27
Copolymer	15	13F	3	7, 11, 36
Copolymer	15	14F	3	<1, 3, 26
Copolymer	15	15F	3	8, 13, 19
Copolymer	15	16F	1	0
Copolymer	19	24F	5	18, 25, 26, 28, 28
Copolymer	19	25F	2	13, 34
Copolymer	19	26F	2	10, 22
Copolymer	19	27F	2	1.5, 5
Copolymer	19	28F	2	2.5, 7
Copolymer	19	29F–34F	6 (1 each)	0, 2, 6, 7, 18, 41
Copolymer	19	35F–39F	6 (1 each)	2, 6, 11, 13, 20, 40
Copolymer	19	40F–45F	6 (1 each)	10, 17, 18, 19, 19, 37
Copolymer	19	46F–51F	6 (1 each)	1, 4, 6, 9, 11, 33
Copolymer	19	52F–57F	6 (1 each)	4, 13, 16, 23, 25, 27
Copolymer	19	58F–63F	7	0, 1.5, 3, 12, 20, 24, 43
Copolymer	19	64F–66F	4 (2 each)	40, 40, 48, 48
Copolymer	19	G1–G5	2 (1 each)	0, 0

erty affecting the ballistics, it was desirable to know the effect of prolonged aging on this property. Measurements were made on a large number of samples over a period of several months. The results are summarized in Table 7 and show that, in general, the viscosity increases slightly for a few days after manufacture and then remains essentially constant.

The cause of the thermal instability of high-viscosity PWP is not fully understood. Although it appears to be related to the physical structure of the mixture, there is also some evidence that the phosphorus itself exerts a chemical effect on some rubbers, causing an increase in the gel content in the film surrounding the particles, thereby destroying the strength and elasticity of the membranes. This effect is greater in some rubbers than in others. Furthermore, it is influenced by the acidity and oxygen content of the mixture. It is concluded that the 75–35 PWP, which is the filling to be used for bombs, rockets, and projectiles without critical ballistics, can be made thermally stable and otherwise satisfactory from a surveillance standpoint, but the manufacturing details of the more viscous filling for high-velocity, spin-stabilized shells have not yet been developed, and more information is necessary before a satisfactory product can be produced.

37.6 PWP AS A SCREENING AGENT

37.6.1 Tests on the 4.2-in. Chemical Mortar Shell and M47A2 Bomb at Dugway Proving Ground

After the preliminary tests on screening efficiency of PWP, 4.2-in. CM shells and M47A2 bombs were tested at Dugway Proving Ground in the spring of 1944. When compared with the same munitions filled

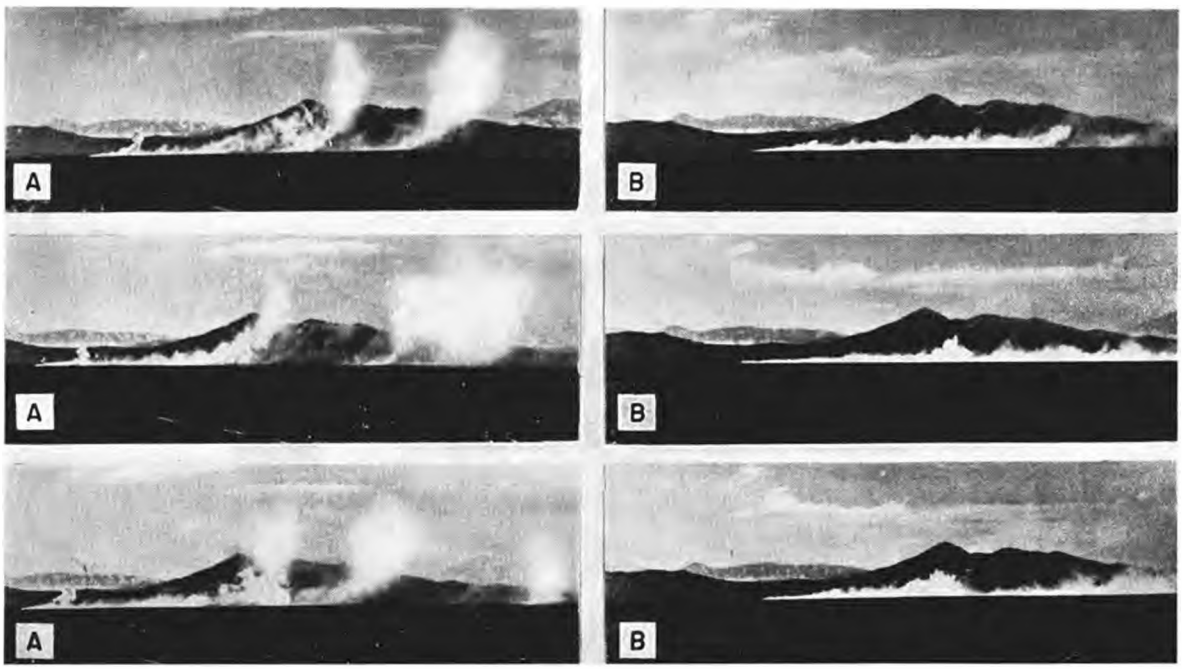


FIGURE 4. Comparison of 4.2-inch CM shells fired at 3,000 yards at about 1 minute intervals. (A) Standard WP. (B) Plasticized WP.

TABLE 6. Thermal stability of 75–40 PWP containing vegetable oil plasticizers in 4.2-in. mortar shells.

Rubber manufacturer and shipment	Batch number	Composition	Thermal stability			
			Sample from filling head tested in glass after 24 hr % separation	Age when placed in oven	Days in surveillance	% Separation of phosphorus
Copolymer 21	K–1	75–40–25LO	0	8	14	0
Copolymer 21	K–2	75–40–25LO	0	8	14	0
Copolymer 21	K–5	75–40–25LO	15	7	12	30
Copolymer 22	K–6	75–40–25LO	50	6	11	30
Copolymer 22	K–26	75–40–25LO	0	10	7	0
Copolymer 22	K–28	75–40–25LO	0	9	7	2
Copolymer 22	K–33	75–40–25LO	0	9	7	10
Copolymer 21	K–3	75–40–30LO	0	7	14	0
Copolymer 22	K–7	75–40–30LO	10	13	7	10
Copolymer 22	K–9	75–40–30LO	0	6	10	15
Copolymer 22	K–18	75–40–30LO	25	13	7	0
Copolymer 22	K–35	75–40–20SO	0	9	7	3
Copolymer 22	K–41	75–40–20SO	0	9	7	0
Copolymer 21	L–1	75–40–30LO	0	7	7	0
Copolymer 21	L–11	75–40–30LO	3	7	7	38
Copolymer 21	L–23	75–40–30LO	5	7	7	75
Copolymer 21	L–41	75–40–30LO	0	7	7	57
Nat Syn 20	L–27	75–40–30LO	20	7	7	75
Nat Syn 20	L–51	75–40–25LO	15	8	7	50
Nat Syn 20	L–61	75–40–25LO	0	7	7	3
Nat Syn 20	L–62	75–40–20SO	0	7	7	3
Nat Syn 20	L–70	75–40–25LO	0	9	7	8
Nat Syn 20	L–80	75–40–25LO	0	7	7	16
Nat Syn 20	L–81	75–40–25LO	0	7	7	16

TABLE 7. Effect of aging on apparent viscosity of PWP.

Rubber manufacturer and shipment		Batch number*	Composition	Viscosity number	Age days
Copolymer	15	E–61	75–40	62	18
				71	154
Goodrich	12	E–30	75–35	48	40
				48	58
Goodrich	12	E–33	75–40	52	11
				58	40
Goodrich	12	E–34	75–42	57	11
				58	40
Goodyear	13	E–51	75–35	52	34
				57	50
Goodyear	13	E–60	75–35	52	25
				41	156
National	14	E–64	75–35	49	15
				51	37
National	14	E–65	75–35	46	15
				55	37
National	14	E–71	75–42	75	13
				71	151
Copolymer	19	X–90	75–40–30LO†	91	37
				93	72
Copolymer	19	X–114	75–40–30LO	83	2
				76	5
				79	43
Copolymer	19	X–145	75–40–30LO	77	2
				73	28
Copolymer	19	X–130	75–40–10SO‡	62	1
				76	36
Copolymer	19	X–133	75–40–20SO	78	1
				97	35
Copolymer	19	X–135	75–40–30SO	130	1
				140	37
Copolymer	19	X–127	75–40–10CO§	48	1
				57	36
Copolymer	19	X–129	75–40–20CO	57	1
				71	36
Copolymer	19	X–134	75–40–30CO	77	1
				88	35
National	20	L–31	75–40–25LO	71	1
				78	37
National	20	L–27	75–40–30LO	78	1
				78	3
				84	38
National	20	L–62	75–40–20SO	63	1
				68	16
Copolymer	19	G–2	75–40–20SO	81	2
				104	29
Copolymer	19	G–4	75–40–30LO	74	2
				89	30
Copolymer	21	K–1	75–40–30LO	70	1
				88	5

* X-batches made at MDL, all others at Victor Chemical Works.

† Boiled linseed oil used as plasticizer. Percentage used in rubber mix indicated by number preceding LO.

‡ Refined soybean oil used as plasticizer.

§ Refined cottonseed oil used as plasticizer.

with WP, the PWP rounds produced markedly superior smoke screens. Figure 4 shows the difference in the smoke screens produced by mortar shells with the two types of filling. In contrast to those from WP, the screen from the PWP is continuous and the pillaring is negligible. In the case of the M47A2 bomb, the plasticized phosphorus produced about one-half as much a pillar as the solid phosphorus. The ground screen from the former, in contrast with that from the standard munition, had no tendency to lift. The duration of the screen near the source was at least 2.5 min compared with 1 min for the WP filling. Partial screening continued for several minutes longer. The area contaminated by the PWP was about 15,000 sq yd, whereas that contaminated by the solid WP was about 2,500 sq yd.

In May and June 1944, extensive tests were conducted at Dugway Proving Ground to compare M47A2 bombs filled with WP, WPT, and PWP. As a result of these, the following conclusions were reached relative to the M47A2 bomb with PWP.[7]

1. The M–4 burster is too powerful for use with PWP in the M47A2 bomb on hard ground.

2. The M–7 burster has insufficient brisance for the PWP-filled M47A2 bomb.

3. The $\frac{9}{16}$-in. TNT burster does not give sufficient distribution of the PWP when dropped in the M47A2 bomb. The smoke screening is excellent, but possible antipersonnel effects are reduced.

4. The $\frac{3}{4}$-in. tetryl burster gives satisfactory results on both hard and soft ground with M47A2 bomb filled with PWP.

5. The 75–40 PWP produced a slightly better smoke screen than either the 75–35 or the 75–42 mix, but has less effective antipersonnel distribution than the 75–35 mix.

6. The PWP filling in the M47A2 bomb produced a better smoke screen and better antipersonnel distribution than either the WP or WPT; the WPT ranks second in effectiveness. (WPT is a combination of WP and paper tubes, the latter adding mechanical strength and reducing the fragmentation of the phosphorus.)

Comparison tests were later made by the Chemical Warfare Board on the relative screening effectiveness of 4.2-in. chemical mortar shells filled with WP, SWP, and PWP. (SWP is a mechanical mixture of steel wool pellets and phosphorus.) The reports of these tests indicate that the PWP rounds were distinctly superior to the others, for either land or water impact.

37.6.2 PWP in the 4.2-in. Recoilless Mortar Shell

For use at low-angle fire, PWP proved very successful when used in the 4.2-in. recoilless mortar shell. In a large scale simulated combat problem at Camp Hood, Texas, in July 1945, this round was used for firing against cave installations with excellent results. During one test, five rounds of PWP-filled shell were fired into a small cave entrance and the smoke completely prevented observation from the inside of the cave for more than 15 min.[8]

37.6.3 PWP in Other Army Munitions

In addition to the munitions already mentioned, PWP was accepted for standardization in the following munitions used by the Army Ground Forces: 60-mm mortar shell,[9] 81-mm mortar shell,[9] 4.5-in. spin-stabilized rocket, and 2.36-in. rockets. It was shown to be superior to WP for laying smoke screens in the 75-mm, 105-mm, and 155-mm shells. Since these are seldom used to lay screens, however, but rather are used mainly as spotting rounds, WP has an advantage over PWP because of the pillaring effect of the smoke cloud. Therefore, it was not anticipated that these rounds will be filled with PWP.

37.6.4 PWP in Navy Munitions

PWP filling was first tested in Navy 4.5-in. barrage rockets in an extensive program on smoke tactics at the Amphibious Training Base, Fort Pierce, Florida, in June 1944. It was concluded that the new filling, because of its longer burning time, was superior to both FS and WP for land impact and about equal to FS and superior to WP for water impact.[10]

The superiority of the PWP over both FS and WP for screening landing operations was clearly demonstrated, in the tactical evaluation of the 4.5-in. rocket, the 7.2-in. chemical rocket and the 4.2-in. chemical mortar shells.[11] The munition requirements with PWP were appreciably less than those for the other fillings, and under some conditions, screens could be laid with PWP which were completely impractical with either FS or WP. These munitions were considered most effective in laying flank screens with offshore winds, and in screening enemy positions at some distance from the landing beach. Effective burning times up to 4 min were obtained. The 4.5-in. rockets functioned quite satisfactorily on both land and water impact. The chemical mortar shells filled with PWP functioned well on land, but on water the quantity of smoke was considerably reduced. Tumbling of the shells was not observed at the ranges used (500 to 2,000 yd). The 7.2-in. rockets functioned satisfactorily on land impact, but produced no smoke at all on the water. Therefore, the ½-in. tetryl burster and the Mk 137 Mod 1 fuze were considered unsatisfactory for the PWP filling. As a result of these tests, it was recommended that PWP-filled 4.2-in. mortar shells and 4.5-in. rockets be procured as quickly as PWP could be made available.

In the course of the work at Fort Pierce, M47A2 bombs filled with PWP were tested tactically in comparison with the standard WP filled munitions.[12] The PWP-filled bombs were again found more satisfactory for screening landing operations than the WP-filled munitions. The modified M–4 burster, consisting of 9/16-in. diameter TNT pellets with a tetryl pellet at each end, gave better results than the standard M–4. The bombs were considered particularly useful for laying flank screens with offshore winds, six being required for a screen of 8 min duration. In general, the bombs were considered most satisfactory in screening areas removed from the landing beach so that the antipersonnel effect of burning PWP could be exploited without interfering with friendly troops after the landing. The procurement of M47A2 PWP-filled bombs for the Navy was recommended in view of their general utility for screening landings.

A further demonstration of the effectiveness of PWP filling was carried out by the Amphibious Forces, U S Pacific Fleet, at Oahu in December 1944.[13] Both 4.5-in. rockets and M47A2 bombs were used. Figures 5, 6, and 7 show pictures of the screens in comparison with screens from WP bombs. It was concluded that effective screens could be maintained for from 2 to 5 times as long as with an equal quantity of bombs and rockets filled with WP or FS. It was recommended that delivery of munitions with this filling to the theaters of operation be expedited. Large-scale procurement was therefore initiated, but unfortunately no munitions reached the forward areas in time to be used in any operation.

As a result of the tests in Hawaii, a PWP filling for 3.5-in. aircraft rockets was developed and adopted. These were tested in June 1945 at the Naval Proving Ground, Dahlgren, Virginia. The 75-35 mixture was considered satisfactory and a 3/8-in. diameter tetryl

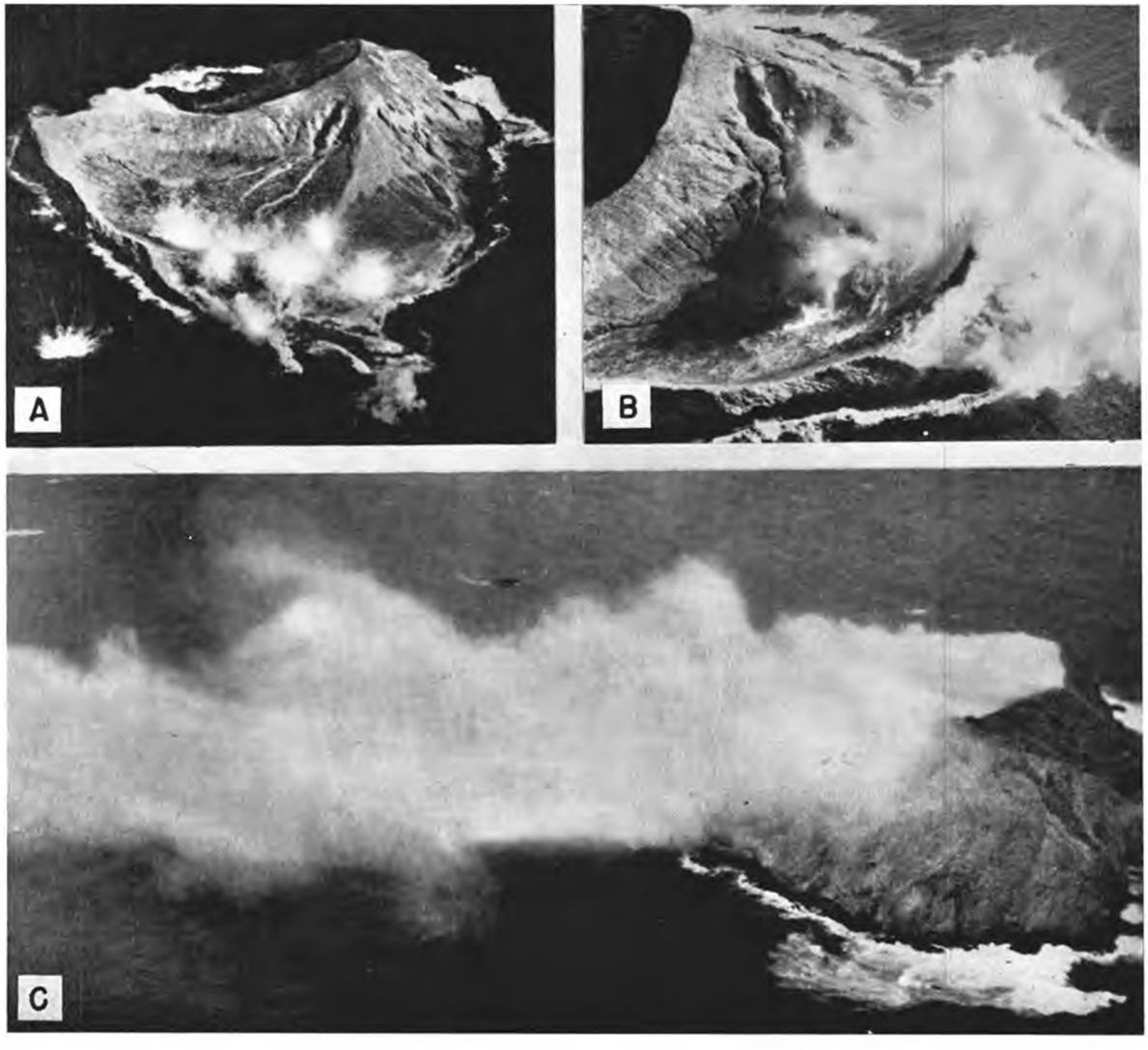


FIGURE 5. Smoke screen from ninety 4.5-inch Navy rockets, Mk10, PWP filled, fired from an LCI(G). Thirty-six rockets were fired in salvo after ranging in and then an additional 6 rockets were fired in salvo every 20 seconds. The screen was effective for about 9 minutes. (A) Aerial view of impact pattern of 36-round ripple. Streamers from individual rocket bursts show dispersion of large particles of PWP which have excellent antipersonnel effect. (B) Aerial view 1 minute after impact, showing PWP emitting smoke vigorously, and also the effect of eddy currents in spreading smoke over shoreward side and in crater of island. (C) Aerial view 4 minutes after initial impact showing very effective coverage of shoreward face of island and crater filled with smoke. (Official Navy Photo.)

burster gave best results. However, rockets with the standard ½-in. tetryl burster produced good smoke screens and were considered satisfactory until the smaller burster could be obtained.

In addition to the above, the development of a canister and burster for PWP filling for the ⅝-in. smoke shell was under way at the University of Illinois at the end of the war. Earlier experiments had shown that when the plastic filling was used in light munitions, a heavier burster was necessary than was used with WP filling.[14] A series of firing tests was carried out in June 1945, which showed that 30 g 81-mm powder, or 40–50 g tetryl is required to give satisfactory smoke screens.

37.6.5 Antipersonnel Effects of PWP

White phosphorus munitions were often used during the war for antipersonnel effects. The results ob-

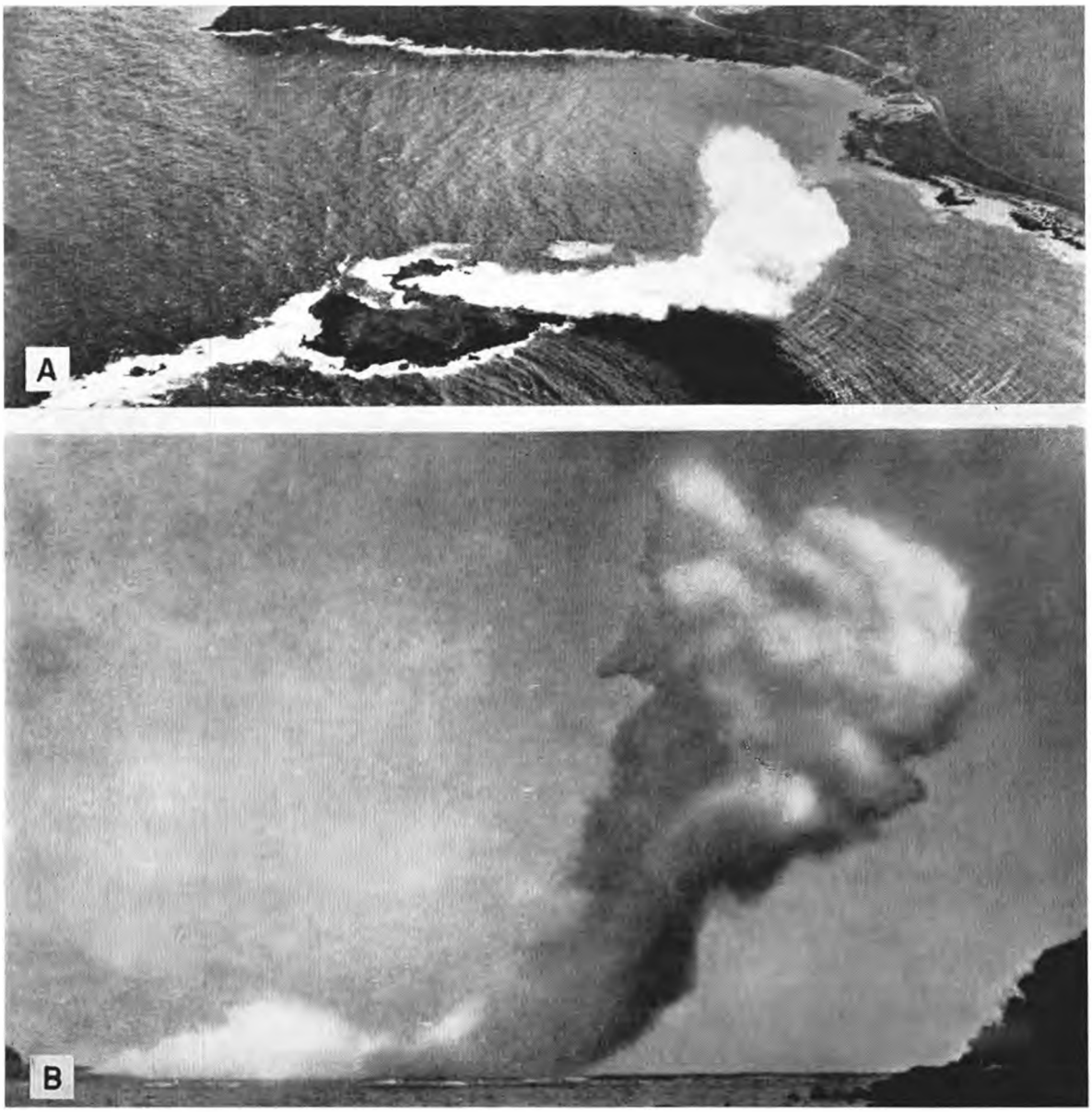


FIGURE 6. Smoke screen produced from four 100-lb M47A2 bombs, WP filled, with ½-charge M7 black powder bursters. A large proportion of the smoke has risen in a pillar and is not effective for screening at the surface. Compare with Figure 7. (A) Aerial view 1 minute, 30 seconds after initial bomb burst. (B) Surface view 1 minute, 30 seconds after initial burst. (Official Navy Photo.)

tained depended upon the disposition, discipline, and morale of the enemy. Combat reports often cited instances where the use of WP was more effective than HE. In some situations, a combination of the two was used with good results. In other cases, the use of WP as an antipersonnel agent was disappointing, especially when the enemy was well disciplined and made use of protective cover.

The first tests designed to compare the relative antipersonnel effectiveness of PWP and WP were made at Dugway Proving Ground in May 1944.[15] Chemical mortar shells filled with PWP and WP were fired at 2,200-yd range onto a target area contaminating straw-filled dummies, dressed in one layer of HBT cloth, located in shallow slit trenches. In addition, closely clipped goats were exposed to the fragments of PWP and WP at a distance of 15 yd from statically fired shells. The evaluation of the

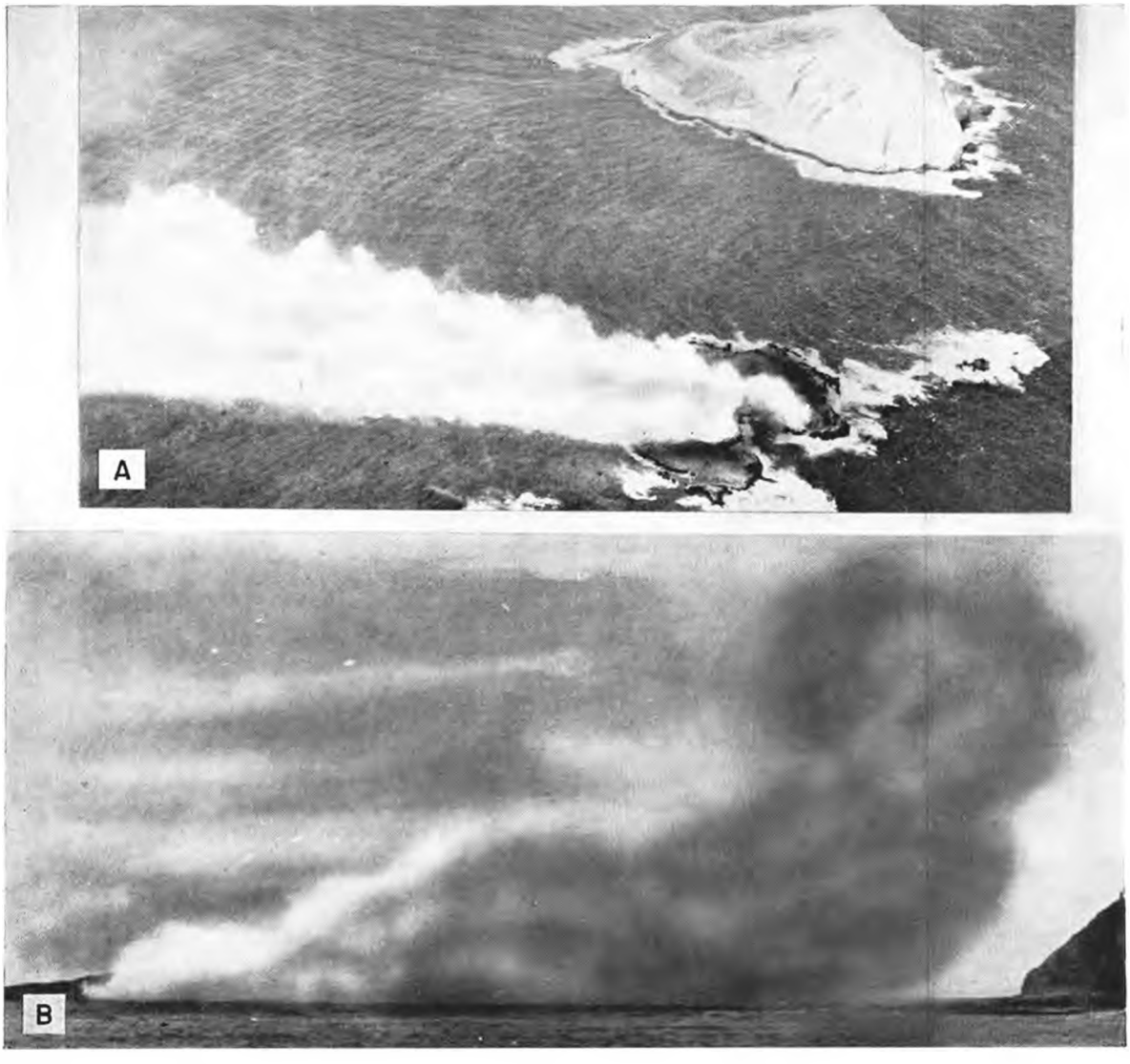


FIGURE 7. Smoke screen produced from four 100-lb M47A2 bombs, PWP filled, with ½-charge M-7 black powder bursters The screen was effective for a distance of 1,000 yards downwind from the source of a period of 8 minutes. (A) Aerial view of flank screen 1 minute, 8 seconds after burst. (B) Surface view 2 minutes, 25 seconds after burst. Note the small amount of smoke in the pillar from PWP as compared with the smoke in the pillar from WP in Figure 6. (Official Navy Photo.)

effectiveness of the phosphorus was based on the number, size, and location of hits on the dummies.[15] Burns obtained on goats were assessed according to number, size, and severity. Insufficient hits were obtained to give an evaluation of the casualty producing effects, but comparison of the burns from the two types of phosphorus was made. Test results showed:

1. There is no essential difference in the rate of healing of comparable burns from WP or PWP.

2. Because of the wider distribution of larger particles of PWP, a larger number of personnel will be hit with PWP than with WP.

3. No antipersonnel merits are lost through the use of PWP instead of WP.

Subsequent to these tests, the University of Illinois did considerable work on the fragmentation of PWP and WP in the burst of statically fired 4.2-in. chemical mortar shells, the effect of burning PWP and WP on cloth, and on the temperature of burning pieces of PWP and WP.[3] The conclusions reached were as

follows:

1. From a static burst of 4.2-in. chemical mortar shell charged PWP, as many as 4,900 burning particles larger than 0.025 g reached the ground. The maximum concentration of the particles occurred about 30 ft from the burst where there were about 35 particles per 100 sq ft. The amount of the filling reaching the ground was between 17 and 41%. For WP shells the amount of the filling available for antipersonnel purposes was less than 5%. The maximum concentration occurred within 15 ft of the burst, and the total number of particles greater than 0.0125 g varied from 100 to 2,650 for different bursts.

2. The burns produced on cloth by WP and PWP were of approximately the same size as these particles produced on noninflammable material. The size of burn from a piece of PWP was considerably smaller than a burn produced by an equal weight of WP.

3. Vaporized phosphorus from both WP and PWP was observed to diffuse through six layers of cloth.

4. The flame temperature of PWP is higher than that of WP, but the burning of PWP does not cause it to become hot enough to cause the rubber to flow. The phosphorus and xylene are given off in both liquid and gaseous form.

Additional work on the antipersonnel effects of WP, PWP, and SWP has been reported by the Medical Research Laboratory at Dugway Proving Ground in weekly reports from February through August, 1945. The comparative results may be summarized as follows:

1. Tests on the penetration of two layers of cloth separated from 0 to 19 mm by an air space with 100-mg pieces of WP and PWP showed the PWP to be inferior to the WP as measured by the time of penetration (3 sec vs 1 sec), size of burn on the cloth layers (18 mm diameter vs 28 mm diameter), and the thickness of air space they will penetrate (10 mm vs 19 mm).

2. The distribution of stain diameters on horizontal and vertical cards was determined for PWP, WP, and SWP from statically fired 4.2-in. chemical mortar shells. The ranges of stain diameters (in mm) used for classification were 60 to 100, 40 to 60, 25 to 40, 15 to 25, and 5 to 15. Compared with results from WP, the number of stains in the range 5 to 15 mm diameter is less for PWP. For other ranges, the number of stains near the point of burst is about the same for each agent, but with PWP the density does not decrease as rapidly with increasing distance from the shell as with WP. Similar tests showed that with SWP, the stain size distribution was essentially the same as for WP.

3. Tests were conducted to explore the effects of extremely heavy contaminations of WP in producing significant disability or death among closely clipped goats. In each test, four 4.2-in. chemical mortar shells were arranged symmetrically about the test animals placed on the ground surface and in slit trenches. The shell fillings were WP, PWP, and SWP. Goats were from 3.5 to 17.5 yd from the points of burst. Although in some cases, extensive second degree burns were obtained, none of the goats was more than mildly injured by the incendiary filling. It is concluded that, among closely clipped goats, neither death nor incapacitating injury may be achieved by means of 4.2-in. shells filled with WP, SWP, or PWP. There was little difference in the results obtained with the three types of fillings.

On the basis of all these tests it may be concluded that PWP compares favorably with WP as an antipersonnel agent. The value of each depends on the tactical situation, the weather, and the discipline, disposition, attire, and morale of the enemy troops.

37.7 SPECIFICATIONS AND CONTROLS USED IN THE MANUFACTURE OF PWP

37.7.1 Plant Inspection Methods

The following inspection procedures were used in the operation of the PWP plant at Edgewood Arsenal.

Particle Size

Specification. The white phosphorus shall be of such fineness that 75% shall be in the range of 0.2 mm to 0.6 mm in diameter, and not more than 5% shall be in excess of 1.2 mm in diameter.

The particle size of the phosphorus was measured by sieve analysis on each batch. A check was made between the results obtained by this method and those by microscopic examination. The sieve analysis proved more complete and accurate.

The analysis was run as follows:

1. A sample of one-half pint of the granules is used.

2. A series of three screens, 16-mesh, 30-mesh, and 80-mesh, is used and the weight of granules retained on each of these screens is determined.

The method of determining the weight of granules held on a given screen is as follows:

1. A graduate is filled with water to a given mark and the weight of graduate plus water is determined.

2. The sample of granules is transferred to the graduate and the graduate refilled to the same mark with water and reweighed.

3. The difference between the weights is determined.

4. The percentage in each range is calculated as follows:

Let G = weight of graduate in grams;
W = weight of water to fill graduate to mark;
X = volume of WP granules;
$1.8X$ = weight of WP granules.

Thus: Sp gr of water = 1.0; Sp gr of WP = 1.80.

(1) Wt of graduate plus water to mark = $G + W$

(2) Wt of graduate plus water plus WP to mark $= G + (W - X) + 1.8X = G + W + 0.8X$

Difference in wt, $[(2) - (1)] = 0.8X$,

where

X = difference in weight/0.8 = volume of WP

$1.8X$ = 2.25 × difference in weight = wt of WP

$$\% \text{ by wt} = 100 \times \frac{\text{difference in weight}}{\Sigma(\text{difference in weight})}.$$

The accuracy of the method depends upon the error in reading the level in the graduate, and thus, the graduate should be as small in diameter as possible.

Moisture

Specification. Moisture content was tentatively set at a maximum of 12% by weight.

In the early operation of the plant at Edgewood Arsenal the per cent moisture in the PWP was determined for each batch using samples from the mixer and from the extruder. The greatest source of error was in sampling. Because of the nature of the material and its tendency to exude water, it is doubtful that the results were accurate. Duplicate samples, however, gave fairly reproducible results. Later, the samples were taken from material extruded into a rocket body which was split and the halves clamped together. A 20- to 30-g sample was used. The water content was determined as prescribed in Federal Specification VV–L–791 (Method No. 300.14) using xylene as the solvent.

Thermal Stability

Specification. It was stipulated that not more than 2% by weight of white phosphorus should separate from the material when tested as prescribed.

A sample was taken from the mixer, and two samples were taken from the extruder for each batch. The mixer sample and one extruder sample were placed in the oven immediately. If the extruder sample showed less than 2% separation of the phosphorus after heating to 150 F for 24 hr, the other sample, which had aged 24 hr, was put in the oven for surveillance. Initially, the sample was extruded directly into a bottle, but later it was taken from the split rocket body.

The amount of separation was determined visually using the following code:

O.K.	no separation	0%
Fair	a few small droplets separation	0 to 2%
Poor	a pocket of separation covering less than half the bottom	2 to 5%
N.G.	anything from a layer covering the bottom to complete separation	5% or more

Specific Gravity

Specification. None.

The specific gravity was determined on the sample used for moisture determination.

The weighing vessel consisted of a wide-mouth container equipped with a sliding cover which closed the vessel without trapping air. Four weight determinations were necessary to determine the specific gravity: (1) the container filled with water, (2) the container partially filled with water, (3) the same plus the sample of PWP, and (4) the container with the PWP filled with water.

The difference between (2) and (3) gives the weight of the sample. The difference between (4) and (1) subtracted from the weight of the sample gives the weight of water displaced by the sample and is therefore equivalent to its volume. From the volume and weight of the sample the specific gravity was determined.

37.7.2 Plant Control Methods

Apparent Viscosity

Specification. None.

Apparatus. The extrusion plastometer used for measuring the viscosity of PWP is shown in Figure 8. It consisted of a cylinder having a cross-sectional area of 1.0 sq in., fitted with a piston, and with an orifice plug with an opening ¼-in. diameter and 3/16 in. long. The top of the orifice plug is tapered at a 45° angle to meet the diameter of the cylinder. Figure 9 shows the apparatus used to apply a known weight to the extrusion plastometer. The weights (25 and 50 lb each) are placed on a platform mounted

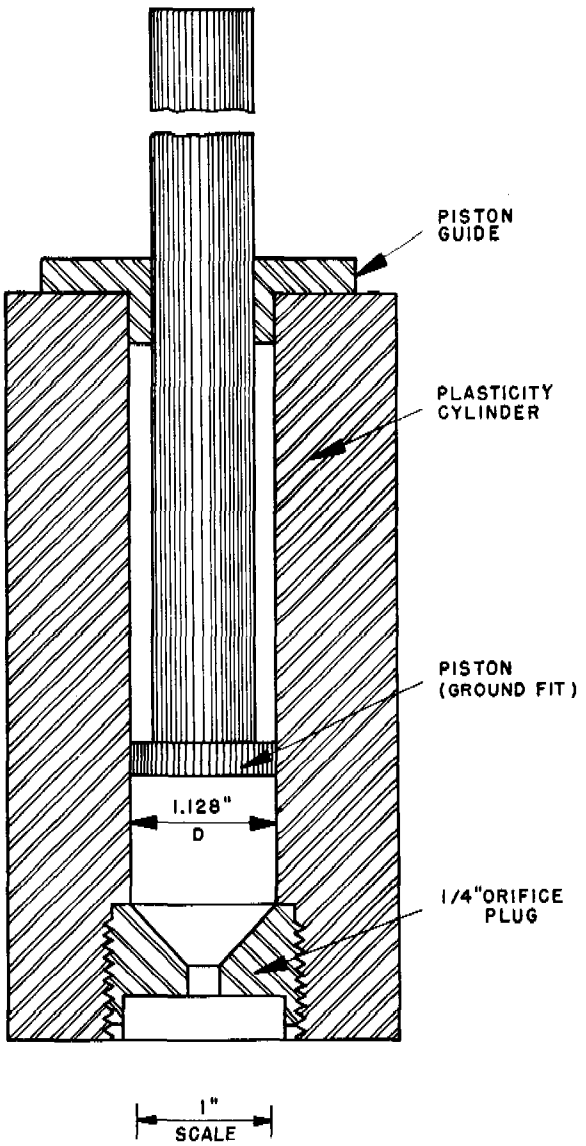


FIGURE 8. Extrusion plastometer.

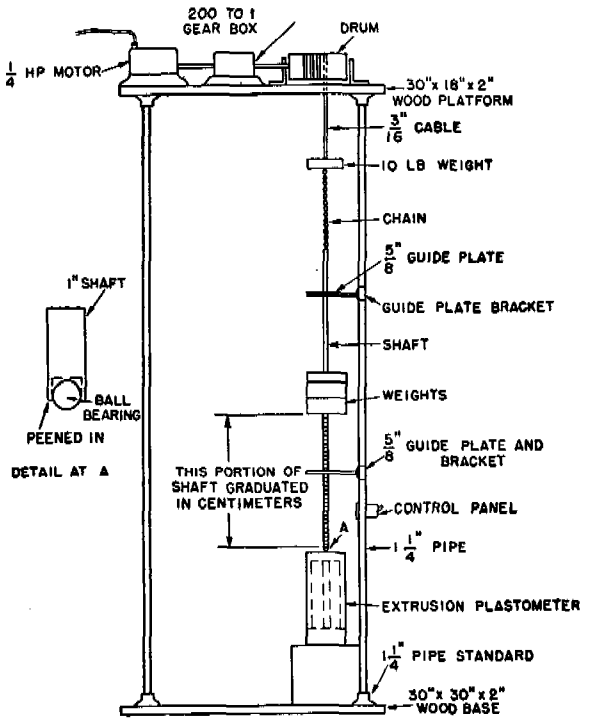


FIGURE 9. Loading mechanism for extrusion plastometer.

on the shaft which was raised and lowered by the reversible motor mounted on top. In addition, a hydraulic press capable of exerting a force of 3,000 lb and a thermostatic bath were required.

Method. The sample of PWP is brought to 25 C by storage in a water bath. The empty cylinder is fitted with a solid plug instead of the orifice and filled nearly to the top with the sample by tamping firmly with a rod. The sample is then compacted in the hydraulic press with a force of about 3,000 lb for a minute. This forces out the pockets of air and water and assures uniformity. The solid plug in the cylinder is then replaced by the orifice and the plastometer is mounted in its holder in a can filled with water at 25 C. The weighted shaft is lowered and the time required for the piston to move through a distance of 4 cm, after a preliminary 2 cm, is observed from calibration marks on the shaft. Generally two readings are obtained from the same sample by making a separate measurement of the time required to pass through a second 4 cm immediately following the first four. The time for the first 4 cm is referred to as t_1 and the time for the second 4 cm as t_2.

Calculation of Results. The shearing stress F and the indicated rate of shear S were calculated from the formulas:[17]

$$F = \frac{Pr}{2L} = \frac{W}{\pi R^2} \cdot \frac{r}{2L} = 0.333W$$

$$S = \frac{4q}{\pi r^3} = \frac{4 \times 6.45 \times V/60}{\pi(2.54/8)^3} = 4.28V = \frac{17.1}{t}$$

where P = pressure on sample in psi,
R = radius of cylinder in cm,
r = radius of capillary in cm,
L = length of capillary in cm,
q = rate of efflux in cc per sec,
F = stress in psi,
S = rate of shear in sec^{-1},

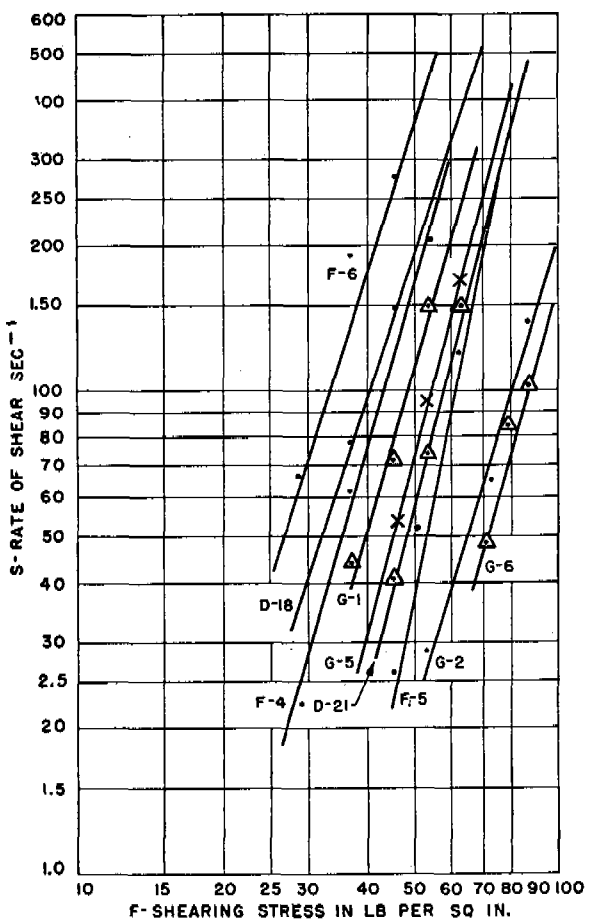


FIGURE 10. Rate of shear; shearing stress curves for PWP samples.

V = rate of movement of piston in cm per min,
W = weight in lb,
t = time in minutes required for piston to travel 4 cm.

In practice it was found that t_1 is usually larger than t_2. The average was used.

If the values of F and S obtained by using several different weights are plotted on log-log paper as in Figure 10, straight lines are obtained. The consistency, or apparent viscosity, of the material at any shearing rate is simply the ratio F/S. As an arbitrary value, the stress required to produce a shearing rate of 100 sec^{-1} was chosen to characterize PWP. Since the values were not absolute this was called the viscosity number.

Accuracy of the Method. Even though no absolute significance can be attached to the viscosity number determined with this instrument, the results were useful in comparing samples of PWP. The chief difficulty in getting reproducible data resulted from the variation in particle size of the phosphorus which occurred from one batch to another. If a sample contained a large number of phosphorus particles that were near the size of the orifice, a high value was obtained. Even in a single sample there was likely to be a noticeable variation in consistency. This was particularly true of samples that have been stored for some time, where the PWP on the surface was found to be stiffer than that underneath.

If a sample contained no particles larger than 1-mm diameter, and if care was taken in selecting a sample to fill the plastometer, the values obtained were generally reproducible to within 5%.

VISCOSITY OF CONCENTRATED RUBBER SOLUTION BY THE FALLING BALL METHOD

Specification. None.

Apparatus Used. 1. Test tubes, 150 x 16 mm, with marks etched or scratched 2 cm apart.

2. Soft iron hexagonal plungers 7/16 x 1¼ in.
3. Machine for homogenizing the rubber solutions.
4. Centrifuge.
5. Constant temperature bath.
6. Steel balls (1/16 in., or 0.1588 cm).
7. Cork fitted with small funnel, made by flanging the end of capillary tubing (2 mm), for introducing ball bearings into the center of the liquid surface.
8. Stop watch.

Method. The exact diameters of the ball bearings are measured with a micrometer and several are selected which are within 0.0005 cm of the same size. A known number of ball bearings is then weighed and their density calculated. Two marks, 2 cm apart, are scratched or etched on the walls of 150 x 16-mm test tubes. The internal diameters of the test tubes are measured with a micrometer.

The clean rubber sample is weighed to the nearest milligram and a 16.5% solution is made up by dissolving 1.700 ± 0.001 g of rubber in 10 ml of solvent. Ten milliliters of a solution of three parts of acetic acid to one thousand parts of CP xylene, by volume, is added from a pipet, and the test tube stoppered with a cork covered with tin foil. The rubber is allowed to swell and dissolve for at least 16 hr. Then a hexagonal plunger is placed in the test tube and the solution homogenized with the machine for 1 hr. See Figures 11 and 12.

The test tube is taken from the machine, and the air bubbles in the solution are removed by centrifuging. A cork fitted with a funnel prepared from

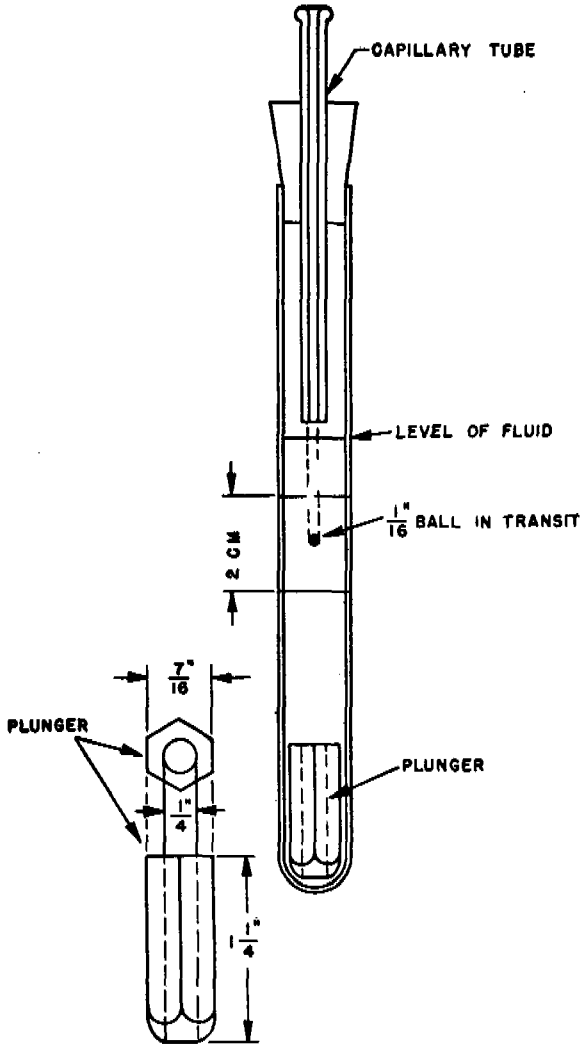


FIGURE 11. Apparatus for determining concentrated solution viscosity of rubber solutions.

2-mm capillary tubing is placed in the test tube, which is then placed upright in a constant temperature bath and equilibrated to 25 ± 0.1 C. The steel balls are dropped in, and the times of fall between the two marks on the test tube are measured with a stop watch. Measurements are made with three or four balls introduced one at a time.

The viscosity in poises was calculated using the equation:

$$\eta = \frac{gd^2(\sigma - \rho)}{18v} \cdot [1 - 2.104(d/D) + 2.09(d/D)^3 - 0.95(d/D)^5]$$

where η = viscosity (poises),
g = acceleration due to gravity (cm per sec^2),
σ = density of sphere (g per cubic cm),

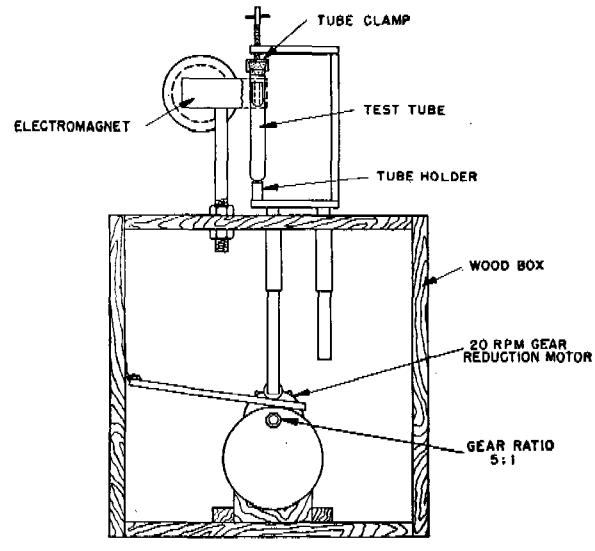


FIGURE 12. Magnetic stirrer.

ρ = density of fluid medium (g per cubic cm),
v = velocity of sphere relative to wall of tube (cm per sec),
d = diameter of sphere (cm),
D = internal diameter of test tube (cm).

Sample Data. Typical data include:

GR–S sample — Copolymer Rubber Corporation, Shipment No. 19 (Received 28 November 1944):

d = 0.1577 cm
D = 1.341 cm
σ = 7.96 g per cc
ρ = 0.90 g per cc
v = 2/43.5 cm per sec (times of fall, 43.6, 43.4 and 43.6 sec)
g = 980.6 cm per sec^2
η = 157 poises

Accuracy. The error of the measurements is from 1 to 1.5%. The times of fall of several balls through 2 cm of a particular rubber solution varied by about 1 part in 70. The values for the viscosities of several samples of the same rubber also vary by about 1 part in 70.

37.8 VARIATIONS IN THE MANUFACTURING PROCESS

37.8.1 Types of Rubbers and Solvents Used

All of the rubber used in the manufacture of PWP was the usual type of 80–20 butadiene-styrene polymer made by the emulsion process in the govern-

ment synthetic rubber plants. The specifications for this type of rubber call for a Mooney viscosity between 40 and 60. These rubbers contained approximately 5% fatty acid, 2% antioxidant, 0.5% soap and less than 2% water. The gel content of several of the early shipments was very high. As a matter of fact, it was thought at first that this was essential for making good PWP, because much of the early production at the pilot plant was with a product which ran from 16 to 46% gel. Later, it was found that such a high gel content was unusual, and before the production was started at the Edgewood Plant, the specifications for this type of rubber were set to require the gel content to be less than 3%. Nearly all of the later shipments had no gel whatever.

The swelling coefficients, intrinsic viscosity, and concentrated solution viscosity of the rubber also varied considerably in the early shipments. It was found that there could be a considerable range of these values without much affecting the plasticity of the product. In order to prevent too great a variation, however, it was finally recommended that the concentrated solution viscosity be held between 100 and 200 poises at 16.5% in xylene.

In order to determine if other rubbers might be available which would be more suitable than the GR–S, samples of several different compositions were obtained from rubber manufacturers. These included the 85–15, 65-35, and 50–50 butadiene-styrene polymers, acrylonitrile, polyisoprene, neoprene, and 75–25 isoprene-styrene polymer. None of these appeared to have any advantage over the usual GR–S, and most of them were definitely inferior for use in PWP.

In addition to varying the properties of the rubber, the possibility of modifying the composition by the addition of other agents was considered. Among those used were the tactifying resins, such as NXD-Galex (from the National Rosin Oil and Size Company), Staybellite Resin 10 (from the Hercules Powder Company), dibutyl phthalate, vegetable oil, zinc oxide, and reclaimed rubber. The most promising of these were the vegetable oils, such as linseed, soya bean, and cottonseed oil, which acted as plasticizers and greatly increased the viscosity of the product. Products having viscosity numbers above 60 could be made easily by substituting these oils for 40 to 50% of the xylene. Materials with higher viscosities could be made also by substituting a part or all of the xylene with lubricating oil, fuel oil, or turpentine. Those made with turpentine were more unstable than those made with xylene. Several batches were also made with light naphtha as a solvent. None of these solvents appeared to give products superior to those made with xylene, although further investigation along these lines may be warranted.

Higher viscosity products could be made by substituting a part or all of the xylene with monomeric methylmethacrylate, or styrene, which could be polymerized to give a very tough product, provided the GR–S had no antioxidant in it. The batches made in the laboratory had the antioxidant removed by extraction with acetone. A special rubber from which the antioxidant was omitted was later furnished by the Government Rubber Laboratory at the University of Akron. This material had entirely different properties and the PWP made with it was not thermally stable. It is possible that further work along these lines would produce a product which has low viscosity when made, thus improving the ease of shell filling, and then the viscosity could be increased in a curing process to give a stable material with the desired viscous properties.

37.8.2 Recommendations for Future Work

The variability in the thermal stability of the product that has been noted in the case of the high viscosity PWP, such as 75–40 and 75–40–30LO, indicates the necessity for further developmental work on this material. The fact that a thermally stable material has been made on many occasions, both in the experimental plant and in the pilot plant, shows that it is possible to make a satisfactory filling and that it is only necessary to get the manufacturing process under control and to specify the proper raw materials to produce a uniformly good material. This suggests that a fundamental investigation of the nature of PWP and the factors that control its thermal stability is necessary. Some work was done along this line but there was not sufficient time to carry it to a definite conclusion. The results indicated that some of the synthetic rubbers are much more affected chemically by the phosphorus than others, so that the gel content increased rapidly during the mixing process. There was no increase in the gel content for other rubbers but there was a pronounced decrease in the concentrated solution viscosity of the rubber. Rubbers from the same manufacturers sometimes behaved differently. There was no correlation between the effects of mixing and the original concentrated solution viscosity.

Other suggestions which have been made for

studies toward improving the quality of PWP are as follows.

1. The molecular size and distribution in the rubber, the percentage of sol and gel rubber, and the structure of these materials are all important factors in determining the strength and stability of the swelled polymer. The spread from 40 to 60 permitted in the Mooney number by the present GR–S specifications actually gives a very wide spread in the intrinsic rubber properties (especially in a process where the breakdown of the rubber is to be kept at a bare minimum) in distinction with ordinary rubber processing which introduces considerable breakdown followed by subsequent curing which tends to even out these variations. It is recommended that rubber be used with Mooney numbers between 50 and 55, and that the gel content be held between 2 and 5% rather than less than 3%. It is felt that these specifications will give a more reproducible product.

2. The tendency to form gel by chemical action of the phosphorus and phossy water is a typical characteristic of GR–S rubber. Other substances, such as copper, lead and manganese salts, peroxides, oxygen, and zinc oxide, produce the same results. The formation of gel around the phosphorus particles could easily be the cause of the thermal instability. This type of hardening has been prevented in the case of air and light by use of large quantities of antioxidant.

3. The effect of pigments and other occlusions, even small bubbles of air, should be studied. It is known that these have an important bearing on the physical properties of GR–S membranes.

4. The possibility of other polymers to replace GR–S should be included in this study. This field could not be explored during the war because of the lack of time and the inadvisability of trying to develop a new product needed in such large quantities as the demand for PWP indicated.

PART V

MISCELLANEOUS TOPICS

Chapter 38

INSECT CONTROL — THE DEVELOPMENT OF EQUIPMENT FOR THE DISPERSAL OF DDT

By *Herbert Scoville, Jr.*

38.1 INTRODUCTION

THE ADVENT of the war and the resultant rapid increase in personnel of the Armed Forces and their dispersal to many parts of the world, created a tremendous health problem whose importance was equalled by few other military considerations. One of the primary factors involved in this health problem was the control of insects, for, as an example, the number of casualties from malaria and other insect-borne diseases in the Pacific Theaters early in World War II, was equal to or greater than those from enemy action. From the point of view of morale of the fighting men, it was also important to reduce pest insects which often seriously hampered normal operations and reduced the efficiency of our forces. It was, therefore, incumbent upon the medical officers of both the Army and Navy to develop methods of controlling insects, particularly mosquitoes and flies, in all areas occupied by allied forces.

The necessity of placing men in localities that under ordinary circumstances would be considered uninhabitable increased the difficulty of obtaining adequate control measures. Almost inaccessible jungle areas were often the site of prolonged occupation by our forces. Since, in some cases, it was desirable to carry out insect control measures in places still occupied by appreciable numbers of the enemy, new complications were added to insect control work. Although many new and difficult problems arose in the forward areas, there also existed the tremendous task of controlling insects in numerous camps spread throughout this country and in many vital civilian areas.

Until the discovery of DDT, oil sprays containing pyrethrins were most generally used in controlling adult mosquitoes. However, the supply of this insecticide was extremely limited, particularly since the occupation by the Japanese of many localities in the southwest Pacific had eliminated the main sources of supply. When the insecticidal value of DDT [1-trichloro-2,2-bis-(*p*-chlorophenyl) ethane] in tests with the Colorado potato beetle was first discovered by the Geigy Company, and when it subsequently was found effective against a wide variety of insects by workers in England and this country, its possibilities in solving the insect control problems of the Services were considered. As additional test data became available to show its extreme toxicity to mosquitoes, flies, lice, etc., the production of DDT was expedited and, by the end of the war, was more than sufficient to satisfy the demands of all our Armed Forces.

Early tests with DDT, which proved to be both a contact and a stomach poison, showed that kills could be obtained in three ways: (1) *contact* kill, i.e., by collision of the airborne insecticide with the flying or resting adult, (2) *residual* kill, i.e., by pickup of the insecticide as a result of the insect moving over a contaminated surface, and (3) *larval* kill. Little was known, however, about the physical problems involved in obtaining efficient kills by any of these methods. It was particularly desirable to investigate the problem of optimum particle size for the dispersal of DDT insecticides under practical conditions. The concentrations of DDT, the best formulations and the dosages required, all needed study in order to obtain the maximum effectiveness from the DDT.

With the discovery of DDT, much of the previously used dispersal equipment and the methods of treatment had become obsolete. The high toxicity of DDT formulations greatly reduced the volume of material required to obtain control. Since the Armed Forces wished to carry out control measures throughout large areas, new techniques had to be evolved in order to keep the expenditure of manpower, material, and time within reasonable limits. Aircraft dispersal of insecticides took on a larger importance in view of this requirement. Although dusting with aircraft had been used in the past with some success under limited conditions, early tests with DDT showed that this technique was not too satisfactory, and was not the answer to the problem. Ground equipment that had been used previously was, in general, quite bulky, dispersed the insecticide solution at a rate too fast to be efficient with DDT, and produced only a coarse spray which was not completely satisfactory for many types

of insect control work. Development of new equipment designed primarily for the dispersal of DDT was, therefore, of primary importance.

38.2 CLARIFICATION OF THE PROBLEM OF PARTICLE SIZE AS RELATED TO INSECT CONTROL

38.2.1 Historical

In order to design equipment for dispersing DDT efficiently, information was first needed on the optimum particle size in which the insecticide should be distributed. Without such information it would be impossible to take full advantage of the toxic properties of DDT, material would be wasted, and control would frequently be impractical. The particle size required to obtain best results will depend not only on factors peculiar to the insecticide, such as susceptibility of the insect to the insecticide, its mode of action, and its chemical and physical properties, but also on such external conditions as meteorological factors, terrain, and method of treatment.

The problem of optimum particle size of insecticides has been the subject of investigation of a number of workers even before the discovery of DDT. Smith and Goodhue of the U.S. Department of Agriculture have summarized [1] some of this earlier work on the relation of particle size to insecticide efficiency, and concluded that the toxicity of solid insecticides increased with decrease in particle size. With oil sprays, the quantity of oil appears to be more important than the size of the droplets. In 1938, Burdette [2] described experiments in which honey bees were exposed to inhomogeneous oil aerosols of varying particle size, and he concluded that droplets of 1 to 10 microns in diameter had the greatest toxicity. From the point of view of practical application of insecticides, Searls and Snyder [3] concluded, as a result of work with cattle sprays, that very small droplets were unsatisfactory because of their failure to impact on the surface being treated. Druett [4] made some preliminary calculations of the pickup of spray droplets of different sizes by a mosquito. In order to obtain 100% collection by the antennae and legs, particles larger than 10 microns are required. This same efficiency can be attained by the head only when the diameter is greater than 25 microns. In an investigation of the drop size obtained from a number of different pyrethrum *aerosol bombs* which had given good entomological results,[5] it was found that most of the drops were less than 10 microns in diameter, but no attempt was made to correlate this information with the insecticidal efficiency of the different bombs.

38.2.2 Theoretical Relationship between Particle Size and Dosage Required for Contact Kill

As a part of the problem of determining optimum particle size for contact kill, it was considered desirable to make certain theoretical calculations [6] which could be used to check the laboratory and field tests, and which would provide a means for extrapolation to conditions not so susceptible to experimental confirmation. The derivation of any relationship between the dosage required to obtain insect kills and the particle size of the dispersed insecticide requires consideration of the probability of an insect being hit by a number of drops equal to or greater than that necessary to cause mortality.[7] This probability will, in turn, be dependent on the dose M of DDT necessary to kill a single insect, and the efficiency of a drop in contacting the insect. The lethal dose can only be obtained by experiment, but for the purpose of making calculations, a series of values in the proper range are assumed. The proper value can then be selected on the basis of laboratory tests. In the determination of the number of drops actually hitting an insect, two processes are recognized.

1. Pickup by settling of the drops according to Stokes' law:

$$u = \frac{d^2 \rho g}{18\eta} \tag{1}$$

where u = vertical velocity,
d = drop diameter,
ρ = drop density,
η = viscosity of the air,
g = acceleration due to gravity.

2. Impaction on the vertical surface of the insect: The fraction of drops which deposit on the frontal area of the mosquito is assumed to be given by the theory of Sell [8] and likewise increases with drop size.

For the case of the resting mosquito, the entire pickup occurs according to the first process, i.e., by settling on the insect's horizontal surface A. The airborne dosage Ct, which is required to have an average of ft drops hitting an area in time t, can be calculated by the following equation:

$$Ct = \frac{3\pi\eta d}{Ag} ft \tag{2}$$

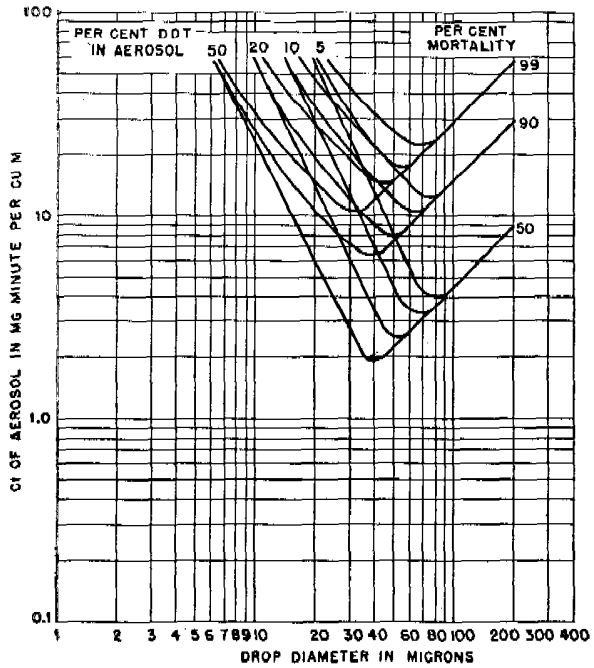


FIGURE 1. Ct of aerosol for various mosquito mortalities vs aerosol drop size. Resting mosquito. Computed for lethal dosage = 10^{-8} g.

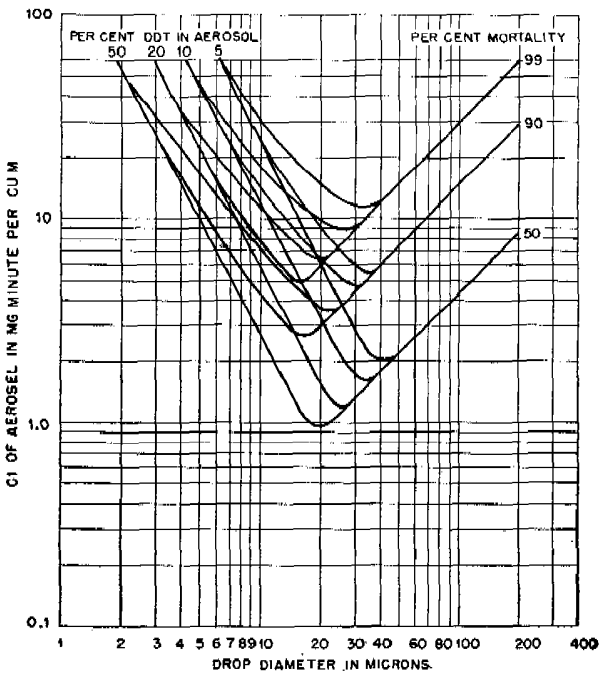


FIGURE 2. Ct of aerosol for various mosquito mortalities vs aerosol drop size. Resting mosquito. Computed for lethal dosage = 10^{-9} g.

where C = concentration of insecticide,
f = average number of drops hitting an area per unit time.

If one assumes a value of M, the lethal dose, the number of drops n which are necessary to kill an insect for any concentration of DDT in inert solvents can be immediately determined. Calculation is then required of the average number of drops ft hitting an area so that there is a certain probability W_{n+} that n or more drops hit any one area. Assuming that the drop distribution occurs at random, the following equation has been derived for the probability that n or more drops will strike the insect:

$$W_{n+} = 1 - e^{-ft} \sum_{K=0}^{K=n} \frac{(ft)^K}{K!} . \qquad (3)$$

This probability is the fraction of mosquitoes killed when n drops contain a weight M of DDT. If the average ft necessary is known, the Ct value is immediately obtained from equation (2).

In order to determine the effect of different variables on the dosage required to obtain certain percentage kills of mosquitoes, the above equations have been solved for three cases: 50%, 90%, and 99%; i.e., $W_{n+} = 0.50$, 0.90, and 0.99. Three values of M were assumed for the purpose of calculation: 10^{-8} (Figure 1), 10^{-9} (Figure 2), and 10^{-10} g (Figure 3), and the horizontal area of the mosquito was considered as 4.7×10^{-2} sq cm. The relationship between Ct of the aerosol and drop diameter derived, using these values, are shown graphically on a log-log scale in Figures 1, 2, and 3. A definite minimum in Ct necessary for a given mortality or an optimum particle size is clearly predicted. The initial steep linear decrease in Ct required for 50% kill has a slope of -2 and is due to the increase in settling velocity with the square of the drop size. It is interesting to note that there is a definite curvature with slopes less than -2 in the lower branch of the curve for higher percentage mortalities. The minimum is reached at approximately the size where one drop contains a lethal dose of DDT, and, since the number of drops necessary to kill can no longer decrease, the curve increases linearly as the diameter is further increased.

For the case of the flying mosquito, i.e., whenever the air is moving horizontally relative to the insect, the insecticide will be picked up both by settling and by impaction on the vertical surfaces. In horizontally moving air, a particle tends to move around any vertical surface unless there is a relative movement between the particle and the air. Inertial force, on the other hand, tends to keep the particle moving in a

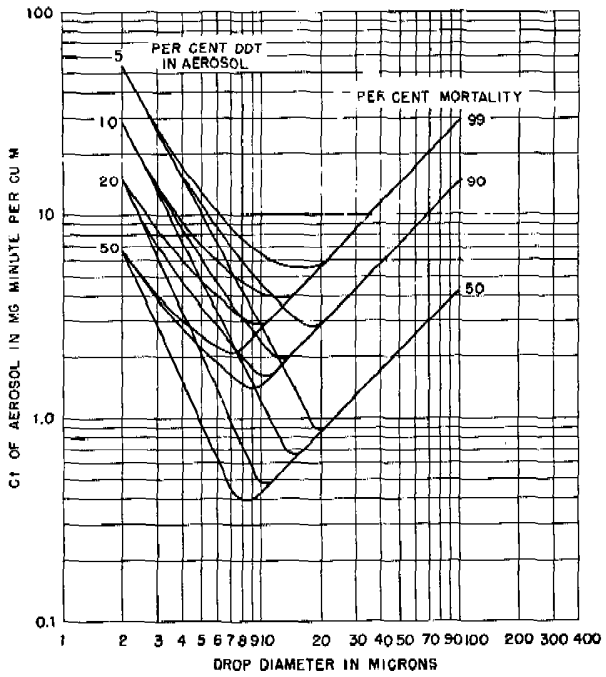


FIGURE 3. Ct of aerosol for various mosquito mortalities vs aerosol drop size. Resting mosquito. Computed for lethal dosage = 10^{-10} g.

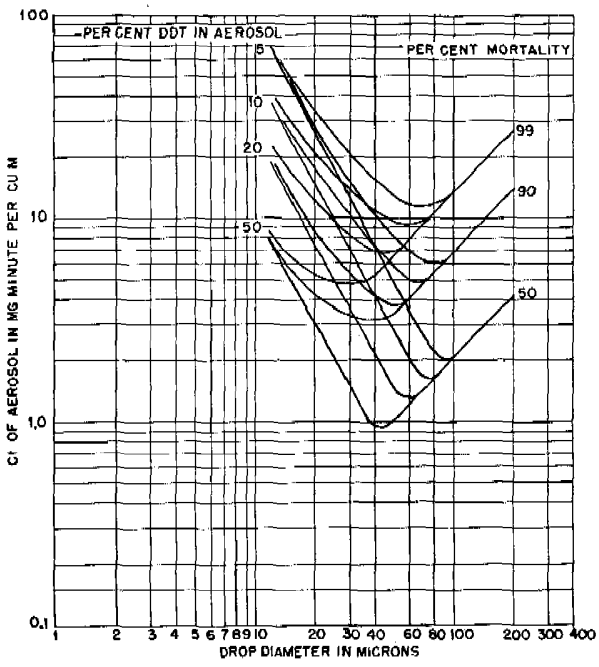


FIGURE 4. Ct of aerosol for various mosquito mortalities vs aerosol drop size. Flying mosquito. Computed for lethal dosage = 10^{-8} g.

straight line toward such a vertical surface instead of swinging laterally around it, and this force is likewise dependent on the square of the diameter of the particle. Sell's work on deposition of the particles [8] has been applied to the problem of insecticides.[9, 10] The deposition efficiency for different shaped objects is a function of the dimensionless parameter P.

$$P = 4.65 \times 10^{-6}\ \rho v \frac{d^2}{D}, \qquad (4)$$

where D = characteristic length of the object in ft,
v = velocity of insect relative to the air (mph). The viscosity of air (0.00018 poise) is included in the constant.

These calculations have been applied to the flying mosquito which was assumed to have a vertical projection similar to a flat plate with an area of 2.9×10^{-2} sq cm and a horizontal area of 9.9×10^{-2} sq cm. The equation for Ct taking into account both settling and impaction becomes as follows:

$$Ct = \frac{ft}{(9.9 \times 10^{-2} g)/(3\pi\eta d) + (6P \times 2.9 \times 10^{-2} u)/(\pi d^3 \rho)}. \qquad (5)$$

The values of ft are calculated from probability considerations in the same way as for the resting mosquito, and the relationships between Ct and d are plotted in Figures 4, 5, and 6. (M values are same as in Figures 1, 2, and 3 respectively.)

By comparing these curves with Figures 1, 2, and 3, it will be seen that the Ct necessary to obtain kills with flying mosquitoes is approximately one-half that required for the resting mosquito, and that this is principally due to the increased horizontal area of the flying insect. In addition, the minima have shifted to slightly higher drop sizes for the flying insect because P increases with the square of the drop size.

38.2.3 Experimental Determination of Relationship between Particle Size and Contact Kill

In addition to these theoretical studies, laboratory tests were undertaken to determine experimentally the optimum particle size for contact kill. This work was carried out with the cooperation of personnel from the Beltsville Laboratories of the US Department of Agriculture, working under contract with Division 5, Committee on Medical Research [CMR]. This group gave particular assistance in carrying out the entomological aspects of the work. The initial

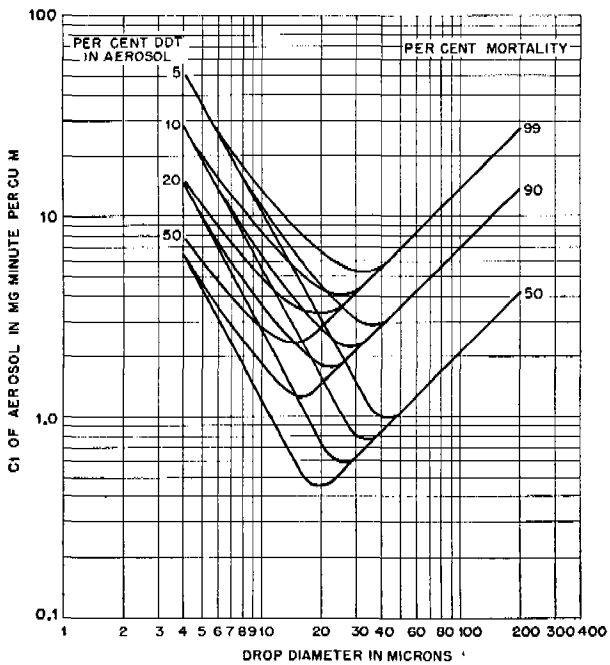


FIGURE 5. *Ct* of aerosol for various mosquito mortalities vs aerosol drop size. Flying mosquito. Computed for lethal dosage = 10^{-9} g.

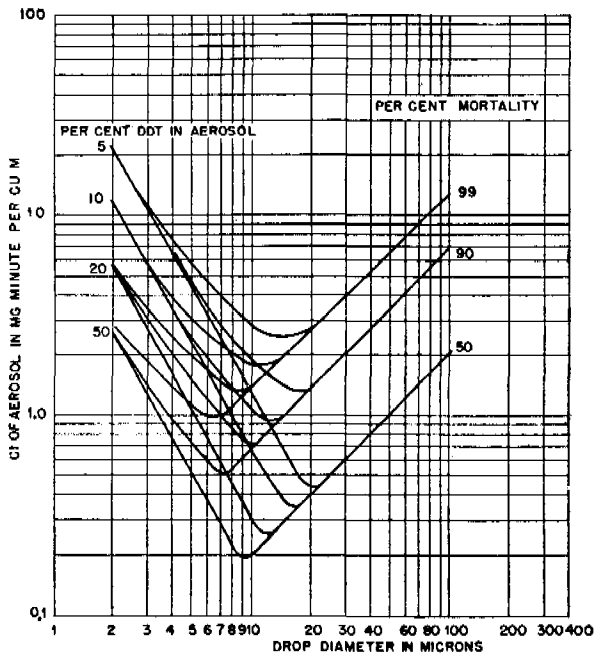


FIGURE 6. *Ct* of aerosol for various mosquito mortalities vs aerosol drop size. Flying mosquito. Computed for lethal dosage = 10^{-10} g.

experiments were done in a static chamber,[10] but, later, when the techniques had become further developed, the tests were carried out in a wind tunnel constructed for this purpose.[11]

In order to conduct rigorous experiments it was necessary to obtain an aerosol of very uniform particle size, since the inability to disperse the insecticide in this form had caused difficulty in interpretation of results of earlier investigators. In the course of the work on the development of screening smoke generators, a laboratory model was designed, capable of producing a homogeneous aerosol by carefully controlling the formation of nuclei for the aerosol particles.[12, 13] This generator had to be modified for use with insecticides,[10] since certain oxides of nitrogen, which were obtained with the earlier models, also exhibited toxic effects on insects. Therefore, for entomological experiments, the nuclei for the aerosol particles were produced by heating NaCl deposited on an electrically heated nichrome wire. Control experiments showed that neither the gases exhausted with the aerosol nor an aerosol of pure oil had toxic effects. In the early experiments, it was found possible to obtain homogeneous aerosol drops up to 15 microns diameter (90% of the mass falling in the range ± 10% from the average size), but, later,[11] the maximum particle size was increased to 20 microns. Automatic controls were used to maintain constancy of operation over a period of hours.

For most of the work both male and female *Aedes aegypti* mosquitoes were used as the test insects, but it was discovered that the males were much less resistant to DDT. Therefore, all quantitative results were based on kills of females. The insects were exposed for varying periods to different concentrations of aerosols, and the mortalities for a constant particle size were plotted against the amount of aerosol to which the insects were exposed. Some typical curves are shown in Figure 7. In some of the later work [14] the statistical method outlined by Bliss [15] was used in order to define more clearly the significance of the results. From the dosage-mortality graphs, the median lethal dosage for any given particle size could be read directly, and the values obtained for each drop size were plotted against the particle diameter on a log-log basis. Such an experimental curve is shown in Figure 8 in comparison with theoretical curves for toxicities of 10^{-9}, 5×10^{-10}, 2.3×10^{-10}, and 10^{-10} g of DDT per mosquito. The experimental curve has a slope very close to -2 for the descending portion, and thus the data are in close agreement with those predicted on the basis of Stokes' law, which require a

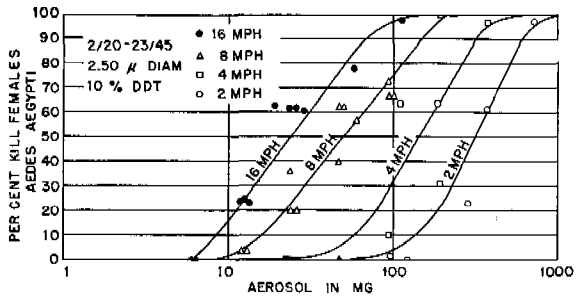


FIGURE 7. The effect of DDT dosage upon mortality for *Aedes aegypti* (mosquitoes).

proportionality to the square of the drop diameter for 50% mortality.

A minimum possible value for the lethal dose has been calculated, assuming that all the aerosol particles reached the insect by settling [10] and that the horizontal area is 0.03 sq cm for the mosquito. This value, 2.4×10^{-10} g of pure DDT, is slightly lower than the value estimated by comparison of the positions of the curves in Figure 8. In view of the experimental difficulties and the number of assumptions made, however, the agreement would seem quite good. The optimum particle size, as calculated theoretically, appears somewhat greater than that obtained by experiment, but it should be pointed out that the minimum in the experimental curve occurs at almost the largest particle size which could be used in the laboratory tests. Moreover, the differences are not great when considered from a practical point of view, since on an arithmetic scale the curves are quite flat. In practice, other factors will have greater influence on the optimum drop size for dispersal.

Further studies in the static chamber were made with fruit flies, *Drosophila melanogaster*.[16] The median lethal dosage of the aerosol for this insect was also found to be inversely proportional to the square of the drop diameter over the range studied (1 to 10 microns diameter), but the toxic dose for these insects was found to be approximately 30 times as great as that for *Aedes aegypti*.

Since it was recognized that, in practice, deposition on the insect will always occur, at least in part, as a result of the horizontal motion of the aerosol cloud, these laboratory studies were extended to a wind-tunnel investigation of the toxicity of DDT aerosols.[11] The theoretical treatment [6, 8] indicated the deposition upon the insect, and hence, the toxicity would be dependent upon the square of the drop diameter and the first power of the wind velocity relative to the insect. Adult *Aedes aegypti* were exposed in cages to

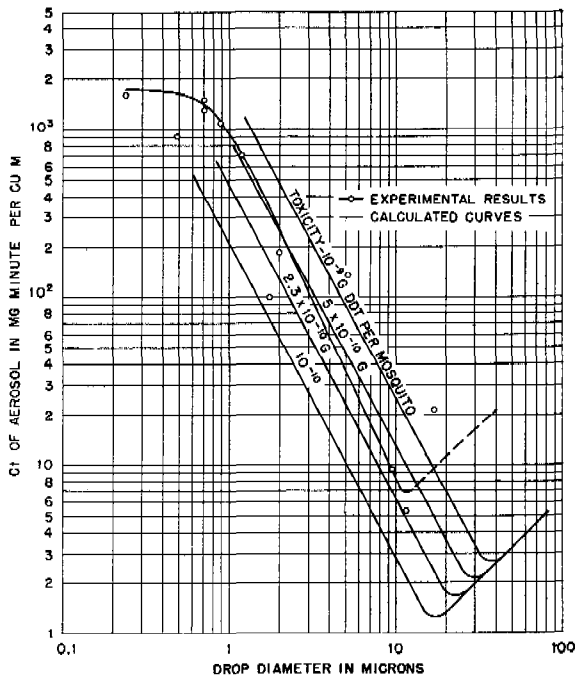


FIGURE 8. Comparison of experimental and calculated dosages required for 50 per cent kill. Eight per cent DDT solution.

homogeneous aerosols of particles up to 20 microns diameter in wind velocities of 2, 4, 8, and 16 mph. Although the mosquitoes flew about the cage in the absence of wind, there was little or no activity during the exposure period, and the insects remained quietly on the wire screen. At low velocities they tended to congregate on the front screen of the cage, but at 16 mph they were almost all blown against the rear screen and held there by the air flow. The control experiments showed that the insects were not injured at 16 mph. Since the results obtained under the different conditions showed no discontinuities, it was assumed that the different insect behavior did not affect the validity of the results. As a result of these experiments, the theoretical calculations were confirmed. The dosage for 50% mortality was found to be inversely proportional to d^2v (d = drop diameter in microns, and v = wind velocity in miles per hour) for low values of this product. However, for high values ($d^2v > 1{,}000$), when the deposition is essentially complete, the dosage becomes independent of wind velocity and particle size (see Figure 9). On the basis of the data obtained in the wind tunnel, the median lethal dose for the female *Aedes aegypti* was determined as 3×10^{-8} g DDT. This figure is in close agreement with that reported by a number of in-

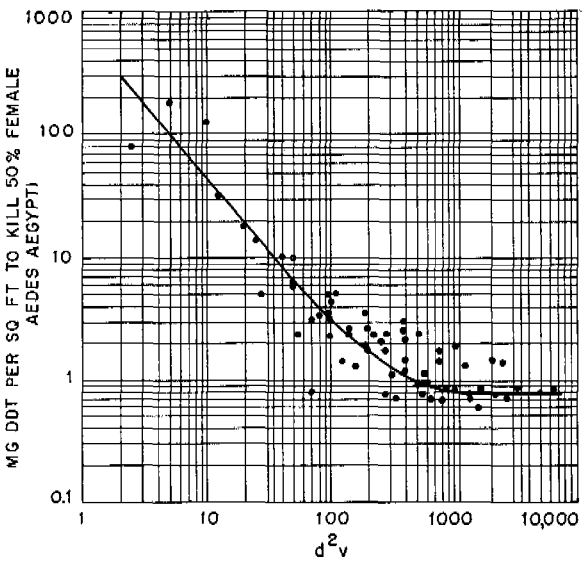


FIGURE 9. DDT in mg/sq ft required to kill 50 per cent females *Aedes aegypti* (as function of drop diameter, *d*, and wind velocity, *v*).

vestigators using bio-assay as a method of analysis for DDT.

It will be seen from the experimental results obtained both in the static chamber and in the wind tunnel, as well as from the theoretical calculations, that as the particle size is decreased below 10 microns in diameter, the dosage required to obtain kill of mosquitoes by direct contact with the aerosol increases rapidly. These observations are of extreme practical importance and proved very helpful in designing dispersal equipment. When DDT first came into use, many investigators had thought that dispersal as a smoke, i.e., drops 0.4 to 0.7 micron in diameter, might give excellent results. However, it was now apparent that drops of this size would be relatively ineffective in obtaining kill, and it was realized that equipment would have to be designed so as to obtain larger particles. The maximum drop size which can be used efficiently could not, however, be determined as easily since somewhat different results were obtained with different test conditions. According to the static chamber tests, the optimum drop diameter was in the neighborhood of 10 microns, but results in the wind tunnel did not give any indication of the optimum size. They did, however, show that under most conditions, increasing particle diameter above 20 microns did not greatly increase the deposition on the insect. However, calculations of the median lethal dose, 3×10^{-8} g DDT, showed that an 83-micron drop containing 10% DDT would be required for one drop to contain a lethal dose. Therefore the drop diameter above which the toxicity must start decreasing must lie somewhere between 20 and 80 microns, the exact value being determined by probability considerations. This is in agreement with the theoretical calculations.

An indirect confirmation of the relationship between particle size and toxic dose was obtained from data taken in field tests of the exhaust generator on the TBM–1C plane.[17] The dosages obtained during the test were calculated from horizontal slides. The Ct_d, i.e., the dosage for each drop size increment, was multiplied by the factor W_d which is the computed relative efficiency of the drop size d for killing mosquitoes as computed from the theoretical curve for the conditions of the test. The actual kills in the areas 2 hr after treatment were 86% and 88% while the corrected dosages predicted a kill of 99%. In view of the inevitable roughness of such field measurements, this agreement would appear quite good.

38.2.4 Experimental Measurement of Factors Involved in Residual Kills

Since it was recognized that the residual kill of insects, as well as contact kill, was an important factor in obtaining control, laboratory tests were carried out to assess this effect.[18] A knowledge of the contamination required for kill, the duration of the toxicity, the effect of external conditions on the toxicity of the deposit, the effect of varying the method of application, and the type of surface were all considered of utmost practical importance. To assist in the analysis of the deposits, a radioactive tracer of triphenyl phosphate was added to the DDT solutions, and the contamination was determined by exposing a measured area of the treated surface to a Geiger-Muller counter. A number of experiments were carried out, using cages which were dipped in the DDT solutions, but since the DDT was found to decompose rapidly on the iron wire, it was found necessary to coat the screens with a layer of glyptal resin.

As a result of these tests, it was shown that the rate of knockdown was proportional to the contamination density, and for doses above 5 μg DDT per sq cm of screen (these doses should be multiplied by a factor 1.6 to obtain the contamination on the basis of wire area), complete knockdown occurred within 1

hr. Decrease in the concentration of DDT in the solvent oil increased the rate of knockdown for a given contamination density, and a maximum effectiveness was obtained with 1% solution DDT in Prorex D, a paraffinic oil. Certain methylated naphthalene solvents, such as Velsicol NR 70 and Velsicol 70 Special (a fraction obtained from the distillation of the NR–70) were found to be excellent solvents for DDT, and, in addition, to have some residual toxicity by themselves. The screen tests also showed that the rate of paralysis in mosquitoes, female *Anopheles quadrimaculatus*, was considerably more rapid than that in houseflies; 1 μg per sq cm screen gave nearly 100% kill of mosquitoes in 2 hr while 5 hr were required with flies. Tests were also made using leaves in place of wire surfaces. In this case, a deposition of 1 μg per sq cm of surface was required to obtain 50% mortality with 2-hr exposure periods. No decrease in toxicity was observed over a period of 48 hr. When leaves were used, the 5% solution of DDT was more toxic than a 2% solution, this result being in contrast to the data obtained on screen surfaces. This was attributed to failure to obtain a continuous film on the hairy leaf surfaces when such low dosages were used.

These results were extended to a study of the effects of surface on the residual kills of female *Drosophila*.[19] These results showed that DDT, whether sprayed in a volatile or nonvolatile solvent, was only about one-fifth as effective when deposited on leaf surfaces as when deposited on glass. The time required for 100% kill was used as a criterion, and approximately 1 μg per sq cm was used to obtain 100% kills. There was some evidence that certain leaf surfaces were more satisfactory for obtaining residual kill than others.

38.2.5 Relationship between Particle Size and Dosage Obtained in the Field

Although the relationship between particle size and dosage required to obtain toxic effects is of fundamental importance to the solution of the problem of proper particle size for dispersal, consideration must also be given to ability to obtain a toxic dose under field conditions with any given particle size. A number of factors must be considered in any attempt to set up a given dosage in the field. First, the meteorological conditions, which exist at the time treatment is carried out, will determine the dosage obtained. Since the dosage Ct is directly proportional to the time at which the insecticide remains at any one given position, the dosage obtained from a given source strength will be inversely proportional to the speed of the wind. With thermally stable air, aerosol clouds will settle and remain close to the surface, but when the air is unstable even relatively large particles may be carried to high altitudes, and the treatment be rendered completely ineffective. Second, the density of the foliage in both horizontal and vertical planes will also determine the dosage which can be obtained from particles of any given size. Large particles will deposit readily on all surfaces and settle rapidly to the ground, so that an insecticide dispersed in such form will penetrate a relatively short distance through thick foliage. However, small particles whose impaction efficiency is low may travel far and remain airborne for a long time even in dense undergrowth. In addition to its effect on deposition, the density of the foliage will determine the wind speed and, consequently, the travel of the insecticide cloud.

Since it was recognized that these factors might completely outweigh toxicity considerations, attempts were made to study this problem both theoretically and experimentally. A considerable amount of work on the travel of gas clouds had been carried out by both Americans and British. The British equations for gas diffusion in the air were extended to include aerosol clouds by taking into account finite settling velocity of the particles.[6, 9, 20] The fundamental equation for a line source in this case is:

$$CtF = \frac{Q - \int_0^x CtF u dx}{Bvx^{m/2}}, \qquad (6)$$

where Q is the product of the source strength and the time of emission, u is the settling velocity, v is the wind speed, x is the distance from the source, and B and m are meteorological constants,

$$m = \frac{2}{1 + (\log R)/(\log R + \log 2)},$$

$$R = \frac{v \text{ at 2 meters}}{v \text{ at 1 meter}}.$$

By solving equation (6), it has been possible to determine F, the fraction of the agent remaining airborne at any distance, as a function of the meteorological conditions and the particle size. Results of these calculations are shown in Table 1.

From these calculations it is evident that drops smaller than 10 microns in diameter will travel long distances downwind even at low wind velocities, as-

TABLE 1. The fraction F of agent remaining airborne of aerosol clouds under two different atmospheric conditions.

Distance downwind (yards)	R = 1.05 (lapse), v = 5 mph Drop diameter (microns) 0.8	8	12	24	R = 1.25 (inversion), v = 2 mph Drop diameter (microns) 0.8	8	12	24
100	0.99	0.98	0.96	0.85	0.99	0.89	0.76	0.32
500	0.99	0.96	0.94	0.78	0.99	0.83	0.64	0.16
1,000	0.99	0.96	0.93	0.74	0.99	0.78	0.58	0.11
5,000	0.99	0.95	0.90	0.65	0.99	0.69	0.42	0.03
10,000	0.99	0.95	0.88	0.59	0.99	0.63	0.37	0.02

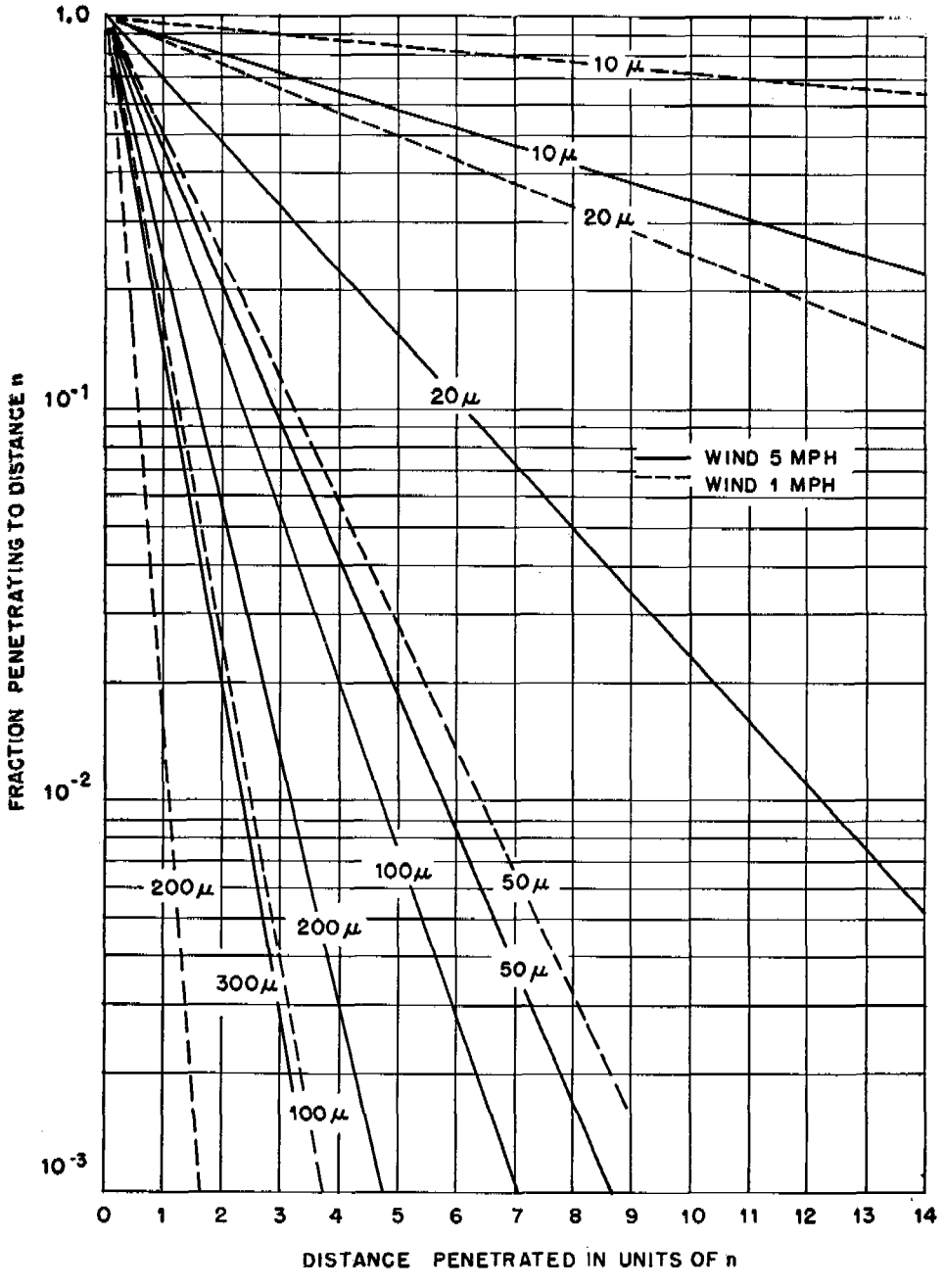


FIGURE 10. Horizontal penetration of an aerosol through a forest.

suming that the only force driving the particles to the ground is gravity. With aircraft dispersal the downdraft from the plane will, however, frequently supply an added force.

These calculations of aerosol cloud-travel in the open have been extended to wooded areas where deposition on the horizontal and vertical surfaces of the foliage is also a factor.[9] In order to characterize the density of the foliage, two lengths δ and γ have been defined. The length δ is the horizontal distance for which the sum of the vertical foliage surfaces in any cross section is equal to the cross section, and γ is a similar distance in a vertical direction. For the purposes of calculation, it has been assumed that the foliage is twice as dense in a vertical direction as in a horizontal direction, i.e., $\delta/\gamma = 2$. The fraction, $\Delta Q/Q$, lost in traveling a horizontal distance, Δx, is given by

$$-\frac{\Delta Q}{Q} = \Lambda\frac{\Delta x}{\delta} + \frac{\Delta \gamma}{\gamma} \qquad (7)$$

where $\Delta\gamma$ is the distance fallen in a vertical direction and Λ is the impaction efficiency of the particle on the vertical surface as given by Sell.[8] Impaction

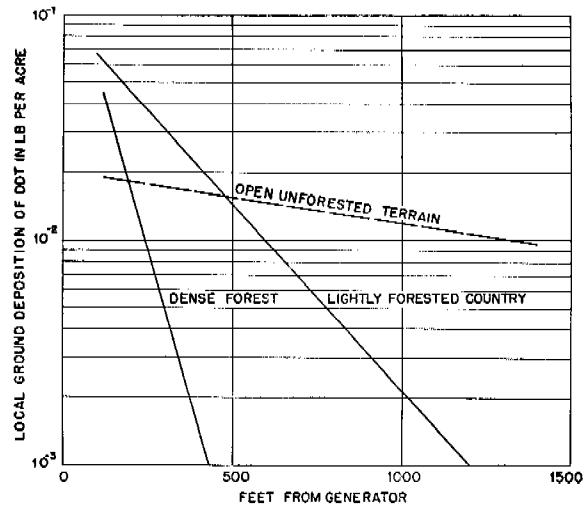


FIGURE 11. Local ground deposition vs distance from generator.

efficiency Λ was assumed to lie between Sell's values for a flat plate and a circular cylinder and is a function of $\rho v d^2/D$ (D is a characteristic dimension of the foliage). From this relationship, F, the fraction penetrating to a distance x downwind, has been calculated for various size drops and wind speeds of 1 and 5 mph (see Figure 10).

These calculations have been checked experimentally by measuring the variation in local ground deposition in various types of terrain, using the Hochberg-LaMer aerosol generator dispersing droplets under 15 microns in diameter.[21] These results are shown in Figure 11. In addition, tests have been made using coarse sprays in a 7 mph wind.[22] The ground deposition in the open was also measured with the CWS E-12 (Hochberg-LaMer) generator with DNOC (dinitro-ortho-cresol) and DDT.[23] The pickup by various types of foliage was measured by exposing leaves in a wind tunnel at 4 mph to particles less than 3 microns in diameter containing a radioactive tracer.[18] The efficiency for drops of this size was very low and in good agreement with the calculated values, although the pickup was apparently greater by some of the hairy leaves.

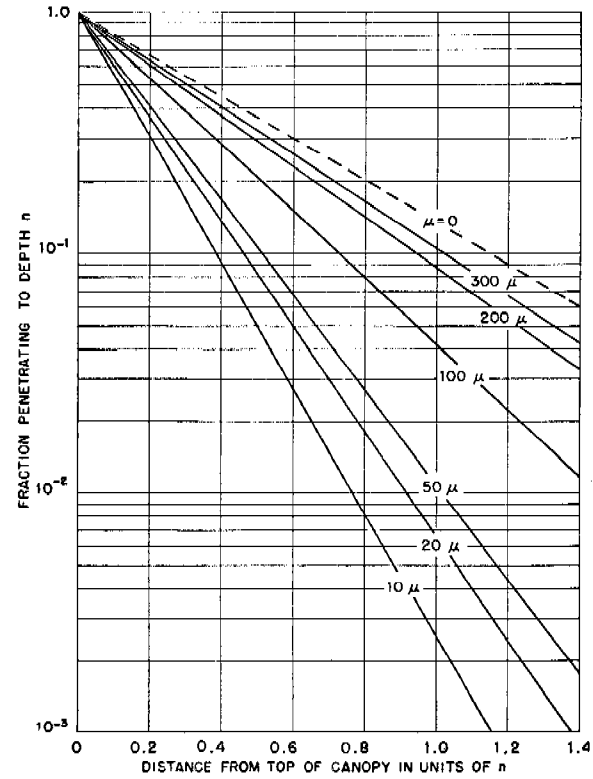


FIGURE 12. Vertical penetration of an aerosol through foliage. Crosswind velocity, 1 mph; no downdraft.

Similar theoretical treatment has been made for the vertical penetration into foliage of an aerosol dispersed by aircraft.[6] The fraction penetrating to a depth y has been calculated for several particle sizes for a crosswind velocity of 1 mph and no downdraft from the aircraft (Figure 12). Under these conditions, it would appear that the larger drops will penetrate downward through the canopy more efficiently than smaller ones. The physical explana-

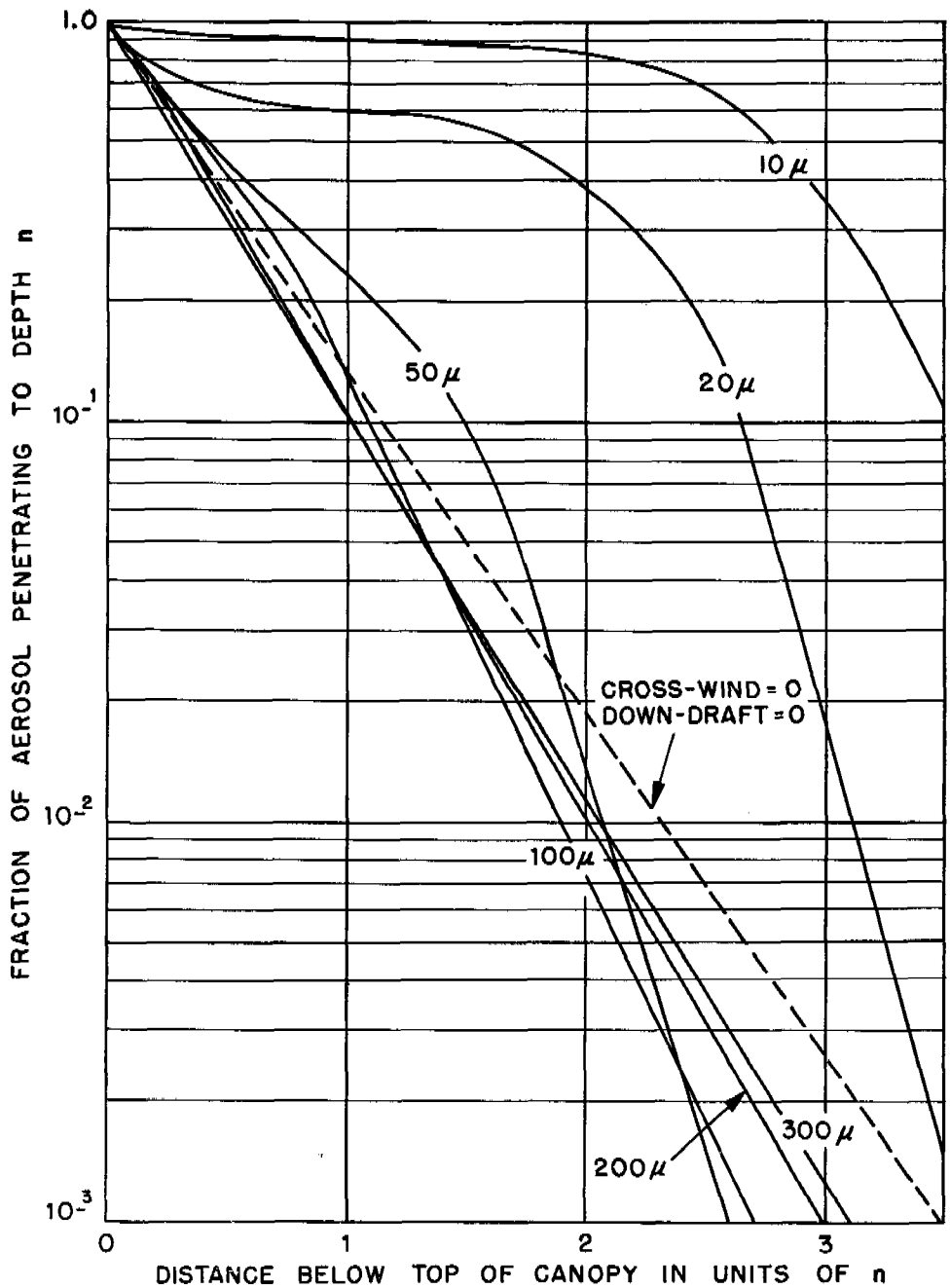


FIGURE 13. Vertical penetration of an aerosol through foliage in presence of downdraft. μ, wind velocity — 1 mph; v_0, downdraft — 5 mph.

tion for this effect is essentially that the larger drops fall faster and have less opportunity to impinge horizontally on the foliage than do the smaller ones. For no crosswind, $u = 0$, all sizes of drops penetrate the foliage to the same extent.

If, on the other hand, the aerosol is dispersed by an airplane which is flying only a short distance above the forest canopy, the downwash of the plane will push the aerosol downward through the layers of the forest. The penetration efficiency of all size drops will be increased, but since the impingement on the foliage is a function of the square of the drop size, this downward component will increase the relative penetration efficiency of the smaller drops. Since the down-

wash velocity will decrease with distance under the canopy, its effect will decrease as the height of the canopy becomes greater. Calculations of the penetration efficiency of different drop sizes with initial downdraft of 5 mph have been made (Figure 13). It should be remembered that these calculations do not take into consideration inhomogeneities which are always present in a natural forest. Meteorological turbulence has also been neglected.

Some confirmation for these calculations has been obtained from the results of aircraft dispersal tests carried out in Panama. Two types of equipment used were a simple vertical discharge sprayer, dispersing particles with a mass median diameter [MMD] of 200 to 300 microns, and a TBM exhaust generator dispersing particles of 25 microns diameter. Although the entomological results from these two types of equipment were almost identical, it was observed that the penetration efficiency of the larger drops as obtained from the sprayer was greater than that of the smaller drops obtained from the exhaust generator.

Because of the apparent importance of the downwash on aircraft dispersal, an investigation was made of the factors which affected this velocity in order that the spray outlets could be positioned to take best advantage of this effect.[6] The optimum position would presumably be where the downdraft is utilized to best advantage and where none of the droplets are carried into the turbulent wake. This position would be ahead and below the forward edge of the wing at the point where the flow lines around the wing have maximum divergence. If the spray is too close to the trailing edge or lower surface of the airfoil, it may come out in the wake and be dissipated in turbulent motion. If the spray is too far below the airfoil, the downward component of the velocity may be quite small.

38.3 GROUND DISPERSAL EQUIPMENT

38.3.1 Historical

Before DDT had come into general use, a large number of different types of equipment had been developed for dispersing insecticides. For the treatment of large areas, power sprayers requiring large quantities of compressed air to achieve liquid breakup had been widely used. Since the insecticide solution was dispersed in relatively large drops, the spread of the insecticide occurred almost entirely as a result of impetus provided by the compressed air. This seriously limited the area which could be treated in a single traverse, and increased the time and personnel required to cover an area. Moreover, most of these sprayers were bulky and therefore impractical to use in the war theaters. Since the laboratory experiments and theoretical calculations, as described in Section 38.2, had shown that droplets in the range of 5 to 50 microns diameter were not only the most toxic but also would remain airborne for appreciable periods, the development of new equipment to disperse DDT in this form appeared desirable for treatment of large areas.

Screening smoke generators had been developed by the NDRC and the Armed Services, but the particle size of the droplets produced ranged from 0.4 to 0.7 micron in diameter, which was too small for insecticide work. Attempts were made to modify the Hession generator, a combustion gas-type oil fog generator designed for screening smokes, in order to produce larger sizes by adding a large chimney in which condensation would proceed more slowly than in open air. Although theoretically sound, preliminary experiments on this development were unsatisfactory, even when a 6-ft chimney was attached to the outlet.

Dr. Goodhue of the U.S. Department of Agriculture had developed a Freon bomb which has been successfully used for the dispersal of pyrethrum and later DDT.[24] This bomb disperses the insecticide in droplets less than 10 microns in diameter, the atomization being obtained by expelling a mixture of the oil solution and gaseous Freon 12 through a capillary at a pressure of about 75 psi. Although these bombs have great insecticidal effectiveness, their small size limits their use to enclosed spaces, and larger units would be impractical for treating extensive areas because of their weight and expense.

38.3.2 The Hochberg–LaMer Type Generators

This same principle of atomization, i.e., the mixing of the insecticide solution with a gas under pressure, has, however, been adapted to a generator which can be used for treating large areas.[25] Steam is used in place of Freon to break up the DDT-oil solution into small drops and eject them into the atmosphere. The mixture of steam and oil is obtained by pumping a 50–50 DDT-oil-water emulsion through a heater coil where the water but not the oil is vaporized. The DDT-oil solution is broken up into small droplets by

the shearing action of the steam under pressure, and the drops are then discharged through nozzles into the air. The particle size of the insecticide solution which is dispersed depends on the composition of the emulsion, particularly the ratio of volatile to nonvolatile material, the pressure and temperature at the input to the nozzle, and the characteristics of the nozzle. An increase in temperature results in a decrease in particle size. Tests with one of the later models showed that a coil temperature of 450 F and a pressure of 80 psi gave an aerosol of particles with an MMD of 10 microns. Reduction of the temperature to 350 F produced particles with an MMD of 32 microns. Even under optimum operating conditions, a small amount of smoke is produced by partial evaporation of the oil and subsequent condensation into very small drops. The production of these small smoke particles, however, does not decrease the effectiveness of the dispersal, since the nonvolatile DDT does not vaporize and is consequently not wasted in the very small drops which are insecticidally ineffective. Since DDT decomposes at elevated temperatures, care was required to avoid loss of DDT in this type of equipment. However, chemical and entomological tests have shown such decomposition to be negligible as long as proper operating conditions are observed.

The first, or inventor's model, of the generators, known as the Hochberg-LaMer type, had a capacity of 20 gal of DDT emulsion per hr.[25] This was pumped through the coil by means of a gear pump with a suitable flow control system. When tested in the field, the inventor's model generator gave excellent insecticidal results, but the capacity of only 20 gal emulsion per hr was considered insufficient for obtaining practical control over large areas. Therefore, the manufacture of Hochberg-LaMer type generators of greater capacity was undertaken,[26, 27] and a model dispersing as high as 90 gal per hr was eventually designed. After these generators were tested in the field, the development of more rugged and practical models was considered desirable.

Since screening smoke generators which were sufficiently durable for use in the field had already been designed, the modification of this type of equipment, in order to disperse the DDT in drops of greater insecticidal effectiveness than would be obtained with smoke, appeared very desirable. This was accomplished on both the Besler 374 (Navy screening smoke generator) and the Army M2.[28] The primary changes required were the substitution of a new pump, capable of handling the required volume of emulsion, the alteration of a thermostatic control to permit operation at temperatures near 450 F instead of 900 F, the insertion of a filter capable of removing the sediment present in DDT solution, and the inclusion of a more satisfactory flow control system. These models have found considerable practical use and gave good results in tests in the war theaters.

In all the generators, considerable difficulty has been observed in obtaining satisfactory pumps. The gear pumps have an inherent weakness in that there is no way of taking up the wear. This is particularly serious when emulsions are being used instead of oil solutions. To avoid this difficulty, pumps with capacities in excess of those required were employed, and a certain amount of the liquid was continually by-passed back to the container. On the various models a number of different flow control systems have been used in order to maintain constant flow during operation.[28] By reduction of the quantity of liquid by-passed, the same flow was maintained through the generator even when the pump capacity had dropped off. However, this method of handling the wear is inherently unsatisfactory, and the design was changed to substitute a double plunger pump. With this method an emulsion was not required, since the oil-DDT mixture and water could be pumped separately and mixed directly in the heat coils. This greatly simplified the use of the generator because the problem of preparing suitable emulsions was eliminated. These pumps were employed successfully on both the Army M2 generator, which became known as the Disperser, Insecticide, Aerosol, Mechanical, E–12 [29] (see Figure 14), and on the Besler 374.

Various models of Hochberg-LaMer insecticide generators have been tested in many parts of the world in cooperation with the Navy, Army, U.S. Department of Agriculture, Tennessee Valley Authority, and British Commonwealth Scientific Office under a wide variety of conditions against a number of different species of mosquitoes and flies.[22, 30–32] As a result of these tests, it has been possible to suggest methods of use of these generators for the control of these insects in the field.[21, 29] In order to obtain control over large areas with an aerosol, the wind is used to distribute the insecticide, thus reducing the manpower and time required for treatment. As a consequence, aerosol dispersal is dependent on the wind to obtain results. The effect of the wind on the deposition of DDT from a Hochberg-LaMer generator has been determined in the field, and the results are

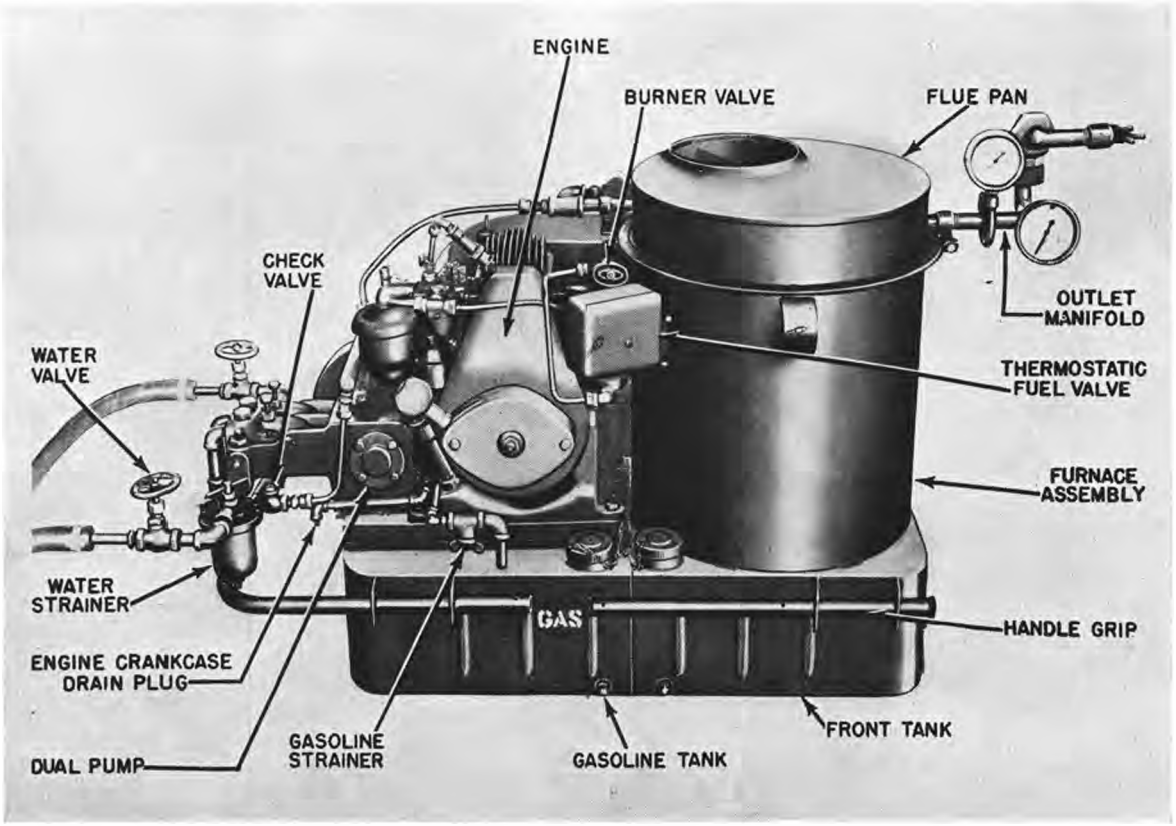


FIGURE 14. Hochberg-LaMer-type generator, CWS model, E-12.

shown in Figure 11. These can be compared with values in Figure 10, which were calculated theoretically. The deposition will also be dependent on the thermal gradient in the lower air, for with inversion conditions, all sizes of drops will remain close to the ground, whereas, with lapse conditions, even relatively large drops may be carried high in the air where they will be ineffective in obtaining insect kills. The airborne dosage of insecticide at any point, neglecting loss due to deposition, will be inversely proportional to wind speed, for a constant source strength. Consequently the source strength will have to be increased in high winds to obtain sufficiently high dosages. However, this will not necessarily mean increased output per unit area, since the distance between swaths, which should be made crosswind, can be greater under these conditions. For example, in low winds frequent passes at short intervals downwind will be required to cover an area, and this will often be a serious obstacle in jungle terrain where even relatively small drops may penetrate only a few hundred feet.

Therefore, keeping these factors in mind, procedures for the use of these generators have been evolved.[29] When possible, all treatment should be carried out under thermally stable atmospheric conditions and in moderate winds. When feasible, the distance between swaths should be kept small, 500 yd being a good swath width, for with wide swaths excessive dosages will be required near the generator in order to obtain a sufficiently high dosage far downwind. In low winds, the swath width should be even narrower. Within certain limits the particle size of the aerosol from these generators can be altered by changing the coil temperature so that when deposition is desirable, operating conditions giving the larger drops should be used. Thus, when treatment in high winds or unstable thermal conditions is required, the larger particles (40 microns) are desirable. Similarly, when larval control, which requires deposition on the water, is the primary objective, operational conditions producing the larger drops should also be used. However, in low winds the smaller diameters, 5 to 10 microns, are better since this will permit

the insecticide to remain airborne for longer periods and cover a larger area. For contact kills of adults and larval control with the Hochberg-LaMer generator, doses of 0.1–0.3 lb DDT per acre have, in general, been found satisfactory. Little or no residual effect is obtained with these amounts, but when dealing with insects of short flight range, retreatment will be required only at 7- to 10-day intervals because of the time required for infiltration of new populations.

In addition to these tests on mosquitoes and flies, the generators were tried out against several other forms of insects with varying results. These tests have shown that the aerosol generators have considerable promise for controlling cankerworms and black flies.[33, 34] When used with DNOC (dinitro-ortho-cresol), the Hochberg-LaMer generators gave promising results against grasshoppers at a dosage of approximately 4 lb per acre, but with DDT, negligible kills were obtained.[23] This test is particularly significant since it demonstrates the feasibility of using these generators with insecticides other than DDT, Tests with DDT against the spruce budworm showed that kills could be obtained, but the aerosol method appeared less efficient than aircraft sprays.[34, 35]

38.3.3 Exhaust Generators for Motor Vehicles

Although excellent results have been obtained with the Hochberg-LaMer type generators, this type of equipment is essentially complicated, and a simpler type of disperser is very desirable for many situations in the field. Therefore, work was undertaken to develop a light, portable piece of equipment which could be rapidly installed near the area to be treated. For this purpose, an exhaust generator for motor vehicles has been designed.[36] This consists of a Venturi atomizer which employs the exhaust gases from the internal combustion engine to break up the insecticidal solution, and uses gravity to inject the liquid into the Venturi. In this way the necessity for pumps, for supplementary heating systems, and for other mechanical items, which could get out of order, is completely eliminated.

The atomization is obtained by the shearing forces on the liquid caused by the relative velocity between the solution and the gas. The gas velocity, upon which the degree of atomization will depend, is limited in the exhaust of an engine by the back-pressure which can be practically used with the engine. Because of this, the Venturi principle has been adopted in order to achieve high gas velocity with low back-pressure. The throat diameter of the Venturi is chosen to give a velocity of 1,500 fps at the highest power setting which would be used for spraying, this setting being low enough so that almost continuous operation is possible without excessive overheating. Early tests showed that a certain amount of drooling was obtained out of the end of the Venturi, due to the impingement of the droplets against the wall of the divergent section. This difficulty was eliminated by cutting off the Venturi at a point where the exit diameter was less than twice the throat diameter, i.e., where the gas velocity was still greater than 300 fps. For the injection of the solution into the Venturi, several systems were tested, but a simple coaxial tube was found to give as good results as the more complicated arrangements. By using a tube of sufficiently large diameter, the liquid could be injected under the force of gravity with the aid of suction due to the Venturi. The use of the simple tube has the additional advantage that small particles of rust or sediment passed freely through it, and do not cause difficulty from clogging

This principle has been successfully applied to the design of exhaust generators for the quarter-ton, 4x4 truck, *Jeep* [36] (Figure 15), and the cargo carrier, M29C, *Weasel*.[37] Venturis of $\frac{7}{16}$ in. or $\frac{3}{8}$ in. have been found best for the former, depending on whether the engine is in good condition or not, while a $\frac{5}{8}$-in. Venturi has been selected for the Weasel. When these generators were used on passenger or other civilian vehicles, the results have not been too successful because of over-heating due to the inadequate cooling system of the engines. However, in practice, it should be possible to design generators which will give satisfactory results with these vehicles, but some sacrifice in capacity may be required.

Tests have shown that this type of equipment has a great many practical uses. Alteration of the solution flow rate by means of a simple gate valve makes it possible to disperse the insecticide in droplets ranging in diameter all the way from smoke ($<$ 1 micron) to a coarse spray ($>$ 150 microns). With the Jeep engine, which is rated at 40 to 60 hp, an aerosol with droplets from 10 to 50 microns in diameter can be dispersed at a rate of 5 to 10 gal per hr, and a coarse spray can be dispersed at 30 to 50 gal per hr. The operating conditions of the engine will also affect the particle size, and when possible, a speed of 6 mph in low gear is recommended. Because of the ability to change the drop size at will, the generator has great practical

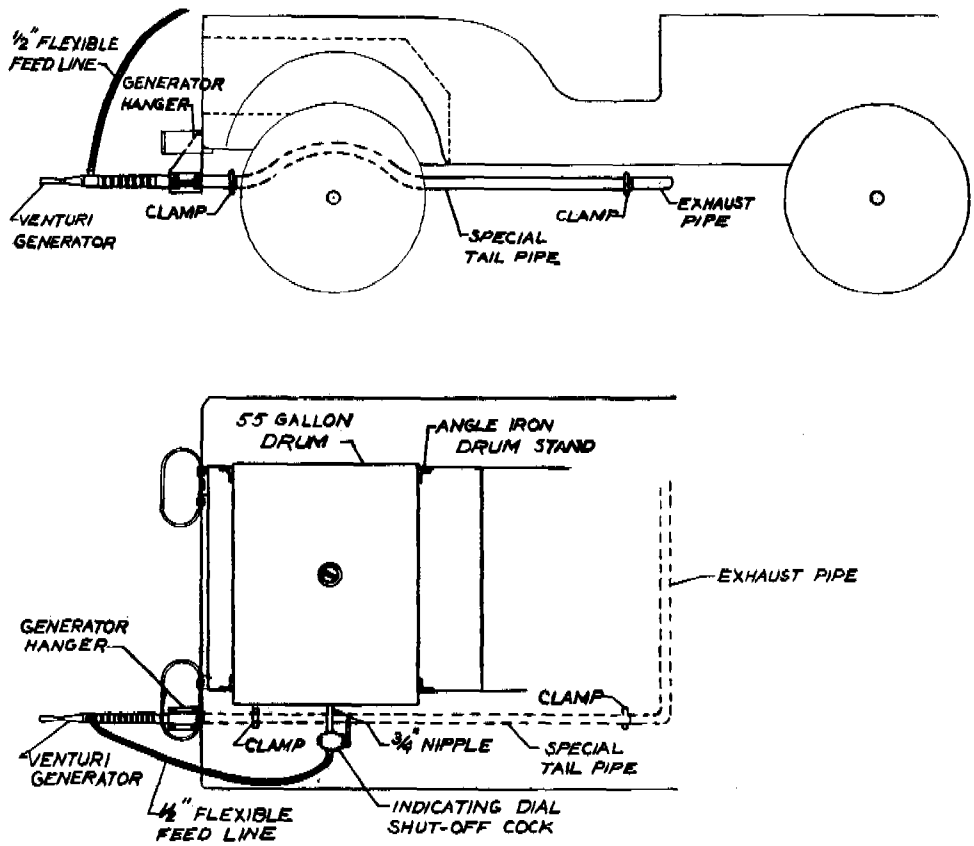


FIGURE 15. Installation of generator at rear of Jeep.

value for obtaining adult and larval control over small areas and for residual treatment of heavily infested localities. Several DDT formulations have been used successfully with these generators, but for general use a 5% solution in fuel oil is considered the most satisfactory. A 20% solution in Velsicol NR–70 or other methylated naphthalene solvents, and the Army and Navy DDT emulsion concentrates can also be employed. Decomposition of DDT in these generators was found to be negligible due to the short contact time of the DDT with the hot gases. When volatile solvents, such as xylene, are used, evaporation is appreciable, and for this reason, these solvents are not considered so satisfactory as relatively nonvolatile ones.

These generators have been tested in numerous localities, and the results have been very promising.[36] They are particularly useful for the treatment of camp areas, air fields, recreation centers, etc. For the treatment of larger areas, other equipment with greater output can frequently be used more efficiently.

38.3.4 Thermal Candles

During the war a requirement was voiced for the development of a smudge pot or a grenade for dispersing an insecticidal aerosol. The British believed such a device would be useful for obtaining control by troops in forward areas. Since the thermal generator candle, F–7, had been developed for the dispersal of acrosols,[38] attempts were made to adapt this munition directly for insecticidal purposes.[39] This device employs the hot gases from a fuel block to atomize the agent in a Venturi. These generators were filled with 2,300 g of a 20% DDT solution in Velsicol NR–70 and burned from 3 to 3½ min. In a single performance test, 30 of these were functioned so as to obtain a nominal dosage of about 2½ lb DDT per acre. Seventy-five per cent of the charge was dispersed in droplets less than 5 microns in diameter, and as a consequence, this fraction was probably relatively ineffective in obtaining insect kills. However, the entomological results were excellent throughout

the area treated. Despite the promise shown by this single test, no further work was done on this development, since it was considered that the method was too involved and relatively inefficient. The development of grenades was continued by the Chemical Warfare Service, who worked on the manufacture of a pyrotechnic mixture containing DDT.[40] They were able to develop a munition which gave good entomological results, but the usefulness and economy of this method of dispersal has not been proven. The number of sources which would be required per unit length of front, in order that the separate aerosol clouds will merge within a reasonable distance downwind, necessitates the use of high dosages of insecticide.

38.4 AIRCRAFT DISPERSAL EQUIPMENT

38.4.1 Historical

Prior to the discovery of DDT, no insecticide which could be produced economically in large quantities was sufficiently toxic to warrant the dispersal on a large scale of aircraft sprays. Aircraft dispersal with dusts had been used quite extensively, but its application was quite limited. However, with the production of DDT on a tremendous scale, the possibility of covering large areas by the dissemination of solutions or emulsions had opened a new field for dispersal of insecticides. The value of aircraft dispersal was particularly great as a control measure in the war theaters, for it made possible the covering of inaccessible areas with a minimum of personnel and equipment. Moreover, a definite requirement existed for methods for obtaining control in areas where the danger from enemy action was still great, and the use of aircraft offered the only feasible method of accomplishing this objective.

First attempts at dispersing DDT from the air were made with standard Chemical Warfare Service spray tanks such as the M 10, M–33, or British SCI tanks. Even when these were modified by the addition of restrictions to the outlet, the flow rates were irregular, and the liquid breakup poor. As a consequence, high doses of DDT were required, and the coverage was frequently spotty. The Orlando Laboratory of the U.S. Department of Agriculture first designed a DDT sprayer for the Cub airplane (Husman-Longcoy apparatus).[41] Although the liquid breakup was not remarkably good, this equipment gave reasonably good entomological results. Since it required a wind-driven pump, a large Venturi, and nozzles, it was complicated for such a small plane and was not readily adaptable to larger and fast military aircraft which would frequently be required in many areas for control purposes. Therefore, the initiation of extensive research into the development of new equipment for the dispersal of DDT from both light and heavy planes was desirable. Such equipment should give good liquid breakup, distribute the insecticide evenly over an area, and should, at the same time, be as simple and adaptable as possible. In attempts to accomplish these objectives, two lines of attack were followed: (1) the production of an exhaust DDT generator, and (2) the development of efficient spray equipment which would employ the slipstream of the plane to atomize the liquid.

38.4.2 Aircraft Exhaust Generators [17]

With an exhaust generator, the atomization of the insecticide solution is obtained by injection of the solution into the high-velocity exhaust gas stream. Since the gases are sufficiently hot to evaporate the solvent and eventually decompose the DDT, it is essential to reduce time of contact between the solution and the hot gases to a minimum. This is accomplished by injection of the solution near the exit of the exhaust stack, so that the droplets are emitted into the cold air immediately after the atomization is effected. Since it is essential to keep the back-pressure in the exhaust stack to a minimum in order not to affect the performance of the aircraft engine, use is made of the Venturi principle in order to increase the velocity of the gases with a minimum of back-pressure.

In an investigation of the theory of atomization of liquids, a study was made of the empirical equations developed by Nukiyama and Tanasawa as a result of several hundred runs with small gas atomizing nozzles.[42] The first equation is as follows.

$$d_0 = \frac{585\sqrt{\sigma}}{v\sqrt{\rho}} + 597\left(\frac{\mu}{\sqrt{\sigma\rho}}\right)^{0.45}\left(\frac{1{,}000Q_L}{Q_a}\right)^{1.5}, \quad (8)$$

where d_0 = diameter, in microns, of a single drop with the same ratio of surface to volume as a representative sample of the drops in the spray;

v = difference in velocity between air and liquid at the *vena contracta*, in m per sec;

Q_L/Q_a = volume flow rate of liquid/volume flow rate of air;

ρ = liquid density, g per cc;

μ = liquid viscosity, poises;

σ = liquid surface tension, dynes per cm.

The second empirical equation which expresses the data on distribution of drop sizes in liquid sprays is as follows:

$$\frac{dn}{dd} = ad^p e^{-bd^q}, \tag{9}$$

where d = drop diameter, in microns;
n = total number of drops, in the sample chosen as a basis, which have diameters between zero and d microns.
a, b, p, and q are constants.

Nukiyama and Tanasawa found that, with their small atomizing nozzles, $p = 2$ and $q = 1$ over a wide range of conditions. At high values of d_0, i.e., for poorly atomized sprays, q dropped to a value of ½. The relationship between q, a, b, v, and d_0 when $p = 2$ has been calculated. The constant q is a measure of the flatness of the drop distribution curve; a high value of q means that most of the drops are in a narrow range of sizes, whereas a low value corresponds to the spreading of drops over a considerable range of sizes. Experimental results indicate that q is constant for any given nozzle over a wide range of operating conditions, but that it is affected markedly by the type and size of the atomizing device used. Since it is frequently more useful to know the MMD of the spray than the value of d_0, the relationship between these two diameters has been calculated for different values of q (for q equal to 1; $\mathrm{MMD}/d_0 = 1.14$).

Experimental work was undertaken to confirm these equations, and apply them to data obtained by other investigators in the field. While this work was preliminary and served primarily to point out the experimental difficulties involved in such an investigation, it indicated that the relationships implicit in the equations were sound and could be used as an aid in designing equipment for the atomization of liquids. The following tentative conclusions were reached as a result of these studies.

1. It is better to use relatively large diameter liquid jets than relatively small diameter jets with higher liquid velocities, since small jets have the disadvantage of high-pressure drop and do not give much better atomization.

2. As long as the liquid jet discharges into the neighborhood of the *vena contracta* of the orifice or nozzle, the angle from which it comes, the point in the region in the *vena contracta* at which it discharges, and the shape of the convergent part of the constriction that produces the high-velocity gas stream at the *vena contracta*, have little effect on the atomization. Consequently, the style of orifice or nozzle can be chosen on the basis of other factors, such as ease of manufacture, installation, and cleaning.

3. In a Venturi atomizer, a decrease in gas density and an increase in gas viscosity reduce the degree of atomization.

The throat diameter of a Venturi of an aircraft exhaust generator must be designed [42, 51] to obtain at normal engine operating conditions, a throat velocity sufficient to give the desired liquid breakup. On the other hand, the diameter must be sufficiently large to avoid excessive back-pressure on the engine. These factors can be determined by use of the gas laws and the equation for throat velocity in a Venturi according to the following equations.

$$V_2 = \sqrt{2g_c \frac{K}{K-1} \frac{RT_1}{M} \frac{1 - (P_2/P_1)^{(K-1)/K}}{1 - (D_2/D_1)^4} (P_2/P_1)^{2/K}}, \tag{10}$$

$$\frac{W}{A_2} = \frac{M}{RT_1} V_2 P_1 \left(\frac{P_2}{P_1}\right)^{1/K}. \tag{11}$$

Subscripts 1 and 2 refer to upstream and throat conditions respectively.

V_2 = throat velocity (fps). This can be estimated for a desired mass median diameter from equation (8). In general, it will range from 500–750 fps depending on the degree of liquid breakup desired.
g_c = dimensional constant, 32.2 (lb mass) (ft per sq sec) per lb force.
K = C_p/C_v.
R/M = specific gas constant in consistent units.
T_1 = absolute upstream temperature (degrees R).
P_1, P_2 = static pressures (lb force per sq ft).
A_2 = throat area (sq in.).
D_1, D_2 = diameters (in.).
W = exhaust gas flow (lb mass per sec).

The first actual attempt to obtain an aerosol of DDT by injecting a solution into the exhaust of an airplane engine was made in 1944 by the Orlando Laboratory of the Bureau of Entomology and Plant Quarantine of the U.S. Department of Agriculture. A Cub plane was used, and with the injection rates used (120 gal per hr), both large droplets and smoke were obtained. Later in cooperation with the Tennessee Valley Authority, exhaust equipment was installed on a 4–DX Stearman airplane which carries a 450-hp engine.[39] In the earlier models, the solution was injected directly into a simple extension of the

exhaust manifold. However, the back-pressure was too great when the diameter of the stack extension was sufficiently small to obtain satisfactory atomization. Therefore, instead of a straight stack, a Venturi which combined low back-pressure and high gas velocity was installed. A 2⅜-in. diameter throat proved most satisfactory with this plane, and the solution flow rate and engine power setting was selected so as to obtain an aerosol with an MMD of about 50 microns. The equipment was used to disperse a 20% DDT-Velsicol NR–70 solution for routine anopheline larviciding in the Tennessee Valley Authority during the past year, and a dosage of only 0.1 lb DDT per acre gave excellent results. As in the case of the Jeep generator, it was found that a more satisfactory drop spectrum and uniform distribution of insecticide is obtained by reducing the length of the divergent section of the Venturi to a point where the diameter is approximately 2.5 times the throat diameter.[43] When an aerosol of MMD of 35 microns was used, the DDT was uniformly distributed over a swath greater than 200 ft so that excellent control was obtained with low doses without endangering other forms of wildlife. The good results obtained with the 450-hp Stearman prompted the design of a generator for the PT-17, a Stearman with a 220-hp engine. A 2-in. diameter Venturi is used on this plane, and results of normal control operations were excellent. Twelve of these generators were produced by the Tennessee Valley Authority for use in Greece by the United Nations Relief and Rehabilitation Association.

The promise shown by the exhaust generators on the Stearman planes warranted the development of similar equipment for use on large military aircraft. Exhaust screening smoke generators had been previously designed for a Navy TBM-type aircraft.[44] Since the general principles involved in the development of the smoke generator and the insecticide generator are very similar, it seemed desirable to try to design equipment for this type of aircraft which, with slight modification, could be used either for screening smokes or for insecticide work.[17] With the smoke generator, the fog oil is injected 8 to 10 ft from the exit of the exhaust stack in order to allow sufficient contact time for complete evaporation of the oil. Since a minimum contact time is required with insecticides, the smoke generator had to be modified so as to inject the DDT-oil solution near the end of the stack. Thus, by mere alteration of the point of injection of the solution, it proved possible to obtain either smoke or insecticide equipment. With this type of aircraft, which contained a Curtiss-Wright R2600-10 engine rated at 1,510 hp at 2,400 rpm and 42 in. Hg absolute manifold pressure, a Venturi with a 3⅜-in. throat gave good results. The oil was pumped from a 270 gal bomb bay tank at 20 to 30 gal per min into the Venturi throat through Todd 28–10 Mayflower nozzles. Some difficulty was obtained with the clogging of these nozzles due to coking of the DDT solution, and frequent cleaning of the nozzle plates was recommended. However, in exhaust generators developed later it was found that the nozzles were not required to obtain atomization, so that the plates could be dispensed with entirely. This observation was in agreement with the predictions implicit in the empirical equations of Nukiyama and Tanasawa.

By suitable alteration of the engine power setting and the solution flow rate, aerosol clouds can be obtained with a MMD varying all the way from 10 microns to greater than 100 microns. Thus, with the engine operating at 2,400 rpm and 42 in. Hg manifold pressure and with a delivery rate of 25 gal of 20% DDT in Velsicol NR-70 per minute, a cloud with an MMD around 20 microns is obtained. At 30 in. Hg manifold pressure and 30 gal per min flow rate, an MMD diameter in the neighborhood of 100 microns is generated.[45] The evaporation of the Velsicol NR–70 solvent increases as the power setting is raised and the flow rate lowered. At 2,400 rpm, 42 in. Hg, and a flow rate of 24 gal per min, the evaporation was about 30%. Analysis indicated that no decomposition of the DDT was occurring.

This equipment was given entomological evaluation in Florida and Panama, and the results were excellent.[45] Doses of 0.3 to 0.4 lb DDT per acre, obtained by flying the aircraft in 100-yd swaths, gave virtually complete control of all adults and anopheline larvae. Observation indicated that the aerosol plume was pushed down by the slipstream of the plane at a rate of approximately 10 mph, the plume reaching the ground at all points when the plane flew at altitudes below 200 ft. Penetration of the aerosol into the foliage was excellent although the jungle canopy extended 100 to 125 ft above the ground. In a test carried out under thermally unstable conditions and in a high wind, the ground deposition was negligible, but the reduction of mosquitoes was nevertheless between 80% and 90%.

The promise shown by this generator on the TBM prompted the design of similar equipment for use with other military aircraft such as the SB2C-4,



FIGURE 16. Installation of exhaust aerosol generator of SB2C–4 plane.

PBJ–1H (B–25), and C–47 planes.[47–49] Since the combination of a smoke generator and an insect disperser no longer appeared tactically desirable, simplification of the design was attempted. Instead of extending the exhaust pipe down the fuselage of the plane, a short stack, comprising only a Venturi, was attached directly to the exhaust manifold of the engine.[47] (See Figure 16.) This model gave good results, and in most flight attitudes, contamination of the plane by the insecticide solution was negligible. The PBJ–1H airplane did not contain exhaust collector rings, but rings from a TBM aircraft could be installed without serious modification to the plane. Since this plane contains two engines, it was possible to double the output per unit time in cases where particularly high dosages were desirable. Since pumps are required to inject the insecticide solution into the Venturi at the flow rates needed with fast military aircraft, the original installation of the exhaust equipment could not be accomplished too rapidly. With the SB2C–4 an estimate of 24 man-hours was made for the time required.

The principle of the exhaust generator was also applied to small aircraft as a substitute for the Husman-Longcoy sprayers and breaker bar equipment designed for the L–5. These sprayers were complicated and had the disadvantage of requiring small orifices which gave frequent trouble from clogging. In order to make the exhaust equipment as simple as possible the use of pumps was dispensed with in a model installed on a Taylorcraft, and the insecticide solution fed by gravity into the Venturi.[50] This generator was very similar in design to the exhaust equipment for the Jeep [36] and was capable of dispersing a 20% DDT solution in Velsicol NR–70 at 45 to 100 gal per hr depending on the particle size desired. In order to insure getting the insecticide to the ground, it was considered desirable to use larger drops with this generator, since the downward push of the slipstream from these small planes is not as great as from the larger military aircraft. Preliminary design of an exhaust generator was also made from an L–5, but no installation has been made on this aircraft.[51]

38.4.3 DDT Spray Devices

The initial spraying of DDT from aircraft was carried out with equipment designed for the dispersal

of chemical warfare agents, but since in most cases these were designed to produce large drops rather than small ones they did not prove entirely satisfactory. Moreover, the flow rates were very irregular, and this led to spotty coverage. Modification of this equipment by placing restrictions in the outlets improved the situation somewhat, but they were still not very satisfactory.

Laboratory tests with pneumatic sprays indicated that when larger amounts of air were available, satisfactory fragmentation of liquids could be obtained.[52] This observation suggested spraying the insecticide solution into the slipstream of an airplane in such a manner as to take best advantage of the air flow for achieving liquid breakup. Tests with air velocities of 220 and 400 fps showed that volatile solutions of low viscosity were much more readily broken up than the nonvolatile ones. In order to make best use of the slipstream, a spray apparatus which would employ a Venturi effect to increase the velocity of the air was suggested. Several models, which according to calculations should give a velocity of up to about 800 fps at the point where the liquid is sprayed, were designed in cooperation with the Army Air Forces. Among these were a rectangular Venturi, a round Venturi, a streamlined pipe, a streamlined grid, and a simple vertical discharge pipe.[53] Measurements of particle size from the different devices in tests at Wright Field indicated that drops in the range of 150 to 300 microns diameter were being obtained with all types when 5% DDT in fuel oil was being dispersed. Little improvement was obtained by using the more complicated Venturi systems. Although time did not permit extensive measurements, there was some indication that the Venturis were not giving the calculated air flow rates, probably because of the back pressure resulting when the solution was injected. Two of these devices, the vertical discharge pipe (see Figure 17) and the streamlined grid consisting of a series of Venturis arranged in a grid shape, were selected for extensive insecticide tests in Florida and Panama.[54] In order to keep the equipment as simple as possible, the solution is fed entirely by gravity from large bomb bay tanks, the rate being controlled with a 4-in. gate valve. Both B-25 and C-47 aircraft were used with these devices, and each contains two tanks with a total capacity of 550 and 800 gal for the B-25 and C-47, respectively. The flow rate is quite uniform for both types of sprayers until the tanks are nearly empty; the suction from the Venturis in the grid tends to improve this property.

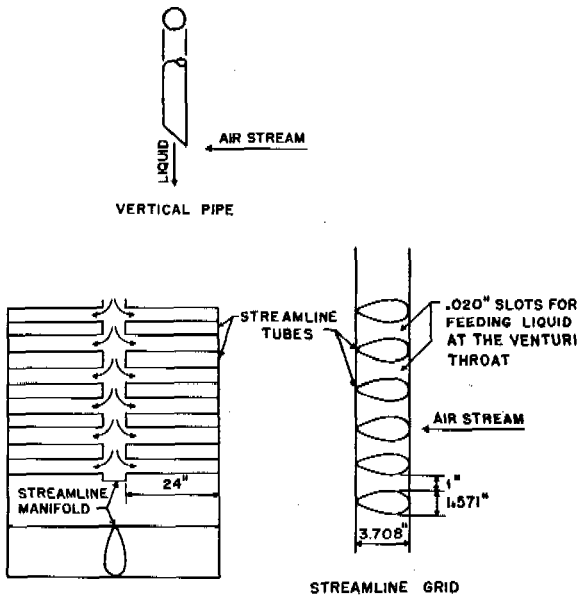


FIGURE 17. Vertical discharge pipe and streamlined grid.

In Panama, several tests were run over dense tropical jungle. With doses of 0.3 and 0.6 lb per acre, nearly 100% reduction of adults and anopheline larvae were obtained with both devices. Many drops, 100 to 200 microns in diameter, penetrated through the 100-ft canopy to the jungle floor. In view of the simplicity of the straight vertical discharge tube, this device was chosen as standard for dispersal of DDT by the Army Air Forces. This equipment would give satisfactory results on all large, fast military aircraft, but the air stream from small planes is inadequate to achieve satisfactory breakup.

Later tests were carried out in Florida to compare the effectiveness of this straight discharge pipe with the C-47 exhaust generator.[49] Although more rapid kills were obtained with the exhaust equipment, the control by both types was about identical after 24 hr. Therefore, in view of its extreme simplicity and adaptability, the spray equipment is considered more feasible for routine control by the Army. The larger drops obtained with this device may be relatively less toxic to the insects, but they insure a greater dosage on and near the surface under all meteorological conditions. In these tests, 20% DDT in methylated naphthalene solvents was used with the straight discharge tube as well as the exhaust generator. The results indicated that the more concentrated solutions were just as good when the same dosage of DDT was used per acre. Since the concentrates in-

crease the payload of a single flight of the airplane, their use is considered desirable whenever they can be made available in the field.

38.4.4 Aircraft Bombs for Dispersing Insecticides

The possibility of using insecticide bombs to be dropped from aircraft was considered. In order to obtain good control throughout an area such bombs should be small and capable of fitting in a standard cluster in order to get wide dispersion. As a solution to this problem, attempts were made to use a plastic bomb which was being developed for other purposes.[55] One hundred and ten of these bombs which contain 390 cc of agent fit into the M–17 cluster adapter. These bombs contain a tetryl burster to disperse the solution. Tests were made to determine the drop size of the dispersed insecticide in the area over which deposition occurred. When filled with 10% DDT, 10% Velsicol NR–70, and 80% CCl_4, the MMD of the droplets was below 10 microns. As the per cent volatile material is decreased, the drop size increases. The area of burst from a single bomb covered about 390 sq yd. With the cessation of hostilities, the requirement for this type of device has ceased to exist, although more extensive tests are pending.

38.5 DDT FORMULATIONS

When DDT first came into general use, two formulations were developed which could be generally used with the existent dispersal equipment. These were a 5% solution in fuel oil or kerosene and an emulsion concentrate (the Army concentrate contained 25% DDT, 65% xylene, and 10% Triton X–100 and the Navy formulation contained 55% xylene and 20% Triton X–100). Although these formulations were satisfactory for many purposes, it seemed desirable to obtain another solvent to replace the kerosene or fuel oil in order that more concentrated nonvolatile solutions could be prepared. This would allow the shipment of concentrates to the field for subsequent dilution with readily available oils. Such a concentrate should be stable at low temperatures in order to prevent separation of the DDT during storage or shipment. In order to be satisfactory for dispersal purposes, the solvent should be nontoxic and relatively nonvolatile, the viscosity should be low and the flash point high.

In the search for such a solvent, an investigation was made of the polymethylated naphthalenes which are marketed by a number of companies under such trade names as Velsicol NR–70, AR 60, AR–50, and AR–40, Koppers K–327, Aro-Sol 151B, APS–202, and Culicide oils.[56, 57] These solvents are capable of dissolving more than 33% DDT at room temperature, and 25% solutions may be diluted to any concentration with kerosene or fuel oil without separation of DDT crystals even at 32 F. The physical properties vary somewhat from solvent to solvent, but they are generally satisfactory for most dispersal uses. However, they attack rubber and, to a lesser extent, synthetics, so that metal gaskets and tubing are recommended in all equipment being used with these solvents. The Velsicol NR 70 has been used extensively in aircraft dispersal work and been shown to have some insecticidal potency of its own.

For the Hochberg-LaMer-type generators, certain special problems had to be solved in developing satisfactory formulations. In addition to the ability to dissolve the requisite amount of DDT, it is necessary to obtain a solution with a volatility which would give the desired drop sizes with the normal operating conditions with the generator. If volatile solvents are employed, evaporation is excessive and the drops too small. Decomposition of the DDT might take place. For the earlier generators which used emulsions, the following formula, which contained approximately 5% DDT, has been developed.[25, 58]

10 cc lube oil
20 cc xylene
9 g DDT
2 g Atlas Tween 85
100 cc water

Other emulsifiers such as Triton X–100 and a mixture of Span 80 and Tween 80 were used successfully in place of Tween 85. Where more concentrated solutions are desired, 35% DDT in Aro-Sol 151B, a polymethylated naphthalene, is used in place of the lube oil-xylene mixture.[57]

Since the Army and Navy had xylene emulsion concentrates already available in the war theaters, formulations for the use of the concentrate in the Hochberg-LaMer generator were developed.[59] The addition of diesel and lube oil gives a formula, which under normal operating conditions for the Besler 374 and E–12 generators, produces an aerosol of proper drop size. However, the coils on the E 12 generator are not made from stainless steel so that the emulsifier in the concentrate corrodes and reduces their life. Therefore, since this model does not require an

emulsion because of its double plunger pump, the use of the concentrate with this generator is not recommended.

In order to insure that all formulations had good insecticidal properties, tests were made in a wind tunnel to determine the relative effectiveness of DDT aerosols from different solvents in obtaining contact kill of adult mosquitoes.[14] As long as the solvent was sufficiently nonvolatile to prevent complete evaporation, no difference could be noted within the limits of experimental error. The relative value of the different formulations in obtaining residual kills has not been thoroughly investigated, but there is some evidence that emulsions or suspensions give a more effective deposit than some of the oil formulations.[60]

38.6 PHYSICAL METHODS FOR FIELD ASSESSMENT

In the course of the development of new equipment for the dispersal of DDT, it became apparent that methods of assessing the value of the new devices must be found. Final evaluation of the usefulness of any equipment has of necessity to be made on the basis of its entomological effectiveness under different field conditions. However, since entomological tests require a great deal of effort, can be carried out only in certain places and under certain conditions, and frequently do not offer a clear-cut answer as to the relative value of different treatments, it is very desirable to evaluate new devices by physical methods which can be correlated with entomological results. Two physical properties which are considered important in this type of work are the particle size of the dispersed material and the insecticide dosage at any point. This latter measurement should include not only the airborne dosage, but also the deposit on the ground and other surfaces.

In the work on screening smokes, a number of different optical devices, such as the Owl [13] and Slope-o-Meter,[61] had been developed for the measurement of particle size, but none of these could be used satisfactorily for drops larger than 1 or 2 microns in diameter. Since such small drops have been shown to be relatively ineffective for insecticidal work, this type of apparatus is not of much use in this field. For measuring larger drops, it was found necessary to collect samples on slides and to measure and count the drops with a microscope.

Two methods of collecting the drops have been used successfully under different conditions. One method of collection involved taking of a sample in a wide-mouth container and allowing the drops to settle on the slide which is placed on the bottom. This method picks up all sizes of drops equally efficiently, but requires some care in collecting the sample to insure that the larger sizes are not selectively deposited on the walls of the container.

By a second method, a slide is waved through the insecticide cloud, and the particles collected by impingement. A fairly representative sample is obtained as long as the drops are larger than about 25 microns in diameter. However, for smaller particles, the impaction efficiency is appreciably less than 100%, and a correction must be made for the failure of the waved slides to pick up the smaller drops. The relative efficiency for the different sizes can be calculated according to data of Sell for a flat plate,[8] but for all practical purposes, an approximation (which is sufficiently accurate for most work), is obtained if it is assumed that the per cent of particles picked up is proportional to the square of the particle radius.

A number of special devices have also been developed which collect samples by impaction and give more accurate results than the manual waving of the slides. The cascade impactor,[62] in which the sample is drawn through a series of orifices so as to allow the particles to impact on slides, has been used quite extensively. The orifices are chosen so as to impact selectively different particle size ranges on the various slides, and, in this way, it is possible to separate the drops into four size groups. When a properly calibrated instrument is used, counting the drops is unnecessary, and analysis of the quantity of material on the successive slides is sufficient to characterize the drop size distribution of the cloud. The largest drop size range which can be measured on this device is from 15 to 50 microns in diameter, and the smallest, 1 to 5. However, since this instrument requires a source of suction to pull the sample through the impactor, it is somewhat cumbersome to use on a large scale in the field, and for most practical purposes, the simple waved slides give satisfactory results.

Under various conditions, a number of different types of slides have been used successfully. Originally oleophobic slides coated with four monomolecular layers of copper barium stearate were used, but since these slides were difficult to prepare, another coating, NNO (mannitan monolaurate), was substituted by workers from the Department of Agriculture. Recently, it has been found quite satisfactory to use carefully cleaned plain glass slides, and calculate the

actual diameter of drops on a basis of an experimentally determined spread factor. For most solutions this spread factor is in the neighborhood of 0.4. These types of slides give good results for drops as small as 1 to 2 microns in diameter as long as the solvent is sufficiently nonvolatile. However, when volatile solvents are used, they are unsatisfactory since the drop will spread and evaporate before the counting can be completed. A photographic method of counting the drops has been developed by the Chemical Warfare Service,[63] and its use reduces the time required to obtain a record, but even with this apparatus, the plain glass and oleophobic slides are not too satisfactory. Another coating which has been found particularly useful when volatile solvents are used is magnesium oxide.[62, 64] With this material a crater is left when the drop impacts on the slide, and a more or less permanent record of the drop size is obtained. Since the crater is a direct measurement of the diameter of the original drop, no spread factor is required with these slides. However, it is important that the thickness of the magnesium oxide layer be greater than the diameter of the drop in order to get accurate results. This method can be used for drops as small as 20 microns in diameter, but particles smaller than this do not leave a crater which can be accurately measured. A carbon coating has been suggested as a replacement for magnesium oxide, but the results with it have been found less reproducible.[64]

For the measurement of airborne dosage, the ordinary methods which had been useful for sampling toxic gas clouds are not completely satisfactory for correlation of physical data with entomological effectiveness. Experimental data and theoretical calculations have shown that the particle size of the cloud has a great effect on the dosage required for the kill of adult insects on the wing. Therefore, for adequate physical assessment it is necessary to know the airborne dosage of each particle size or particle size increment. Since simple mass analysis does not provide any breakdown into particle size ranges, it is unsatisfactory for this type of work.

A new method has therefore been suggested for determining airborne dosage by the use of horizontal slides,[6] since the deposition of particles of a given drop size is related to the dosage, Ct, of those particles in the air at that point. The relationship between Ct and the area deposit may be expressed as follows:

$$Ct_d = \frac{N_d M_d}{u_d},$$

where Ct_d = concentration-time product of drops having a diameter of d;
N_d = average number of drops of diameter d deposited per unit area of horizontal surface;
M_d = weight of drop having a diameter d;
u_d = settling velocity of drops having diameter d.

Since both M_d and u_d are proportional to the drop density, the above expression is independent of the drop density. If it is assumed that laminar flow occurs at a small distance above the plate, then Stokes' law may be used for determining u_d for drops smaller than 80 microns. For larger drops, this law no longer holds for the terminal velocity, and the Ct's are higher than those obtained using this law. In Figure 18 a plot of Ct (mg min per cu m) per unit deposition density (drops per square centimeter) versus the drop diameter in microns is given. In using this method of determining dosage, the number of drops in each size increment is counted microscopically for a unit area. The dosage of each increment can be determined directly from the product of this number and the proper factor from Figure 18. In order to obtain the total Ct at any point, a summation must be made over all the drop

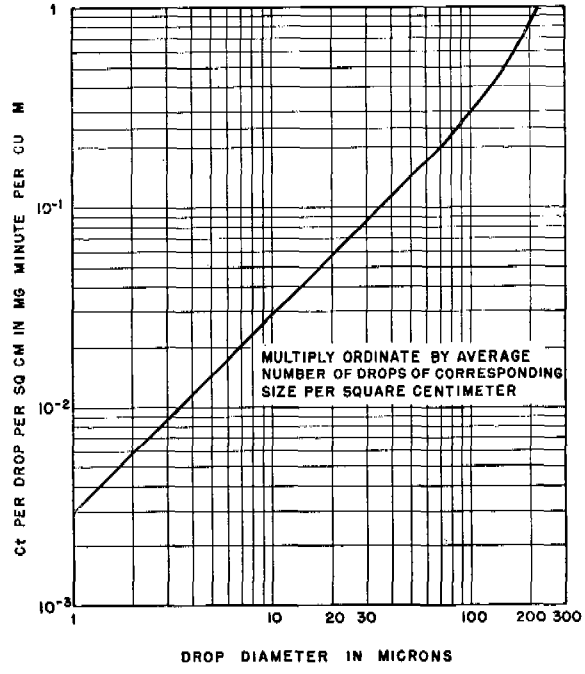


FIGURE 18. Aerosol Ct as a function of horizontal area dosage.

sizes. With these horizontal slides, it has been found advisable to use a holder or plate so that the top of the slide is flush with the sides of the plate. This is necessary in order to avoid edge effects which would tend to give spurious results. With this method a considerable amount of microscopic counting is required in order to obtain statistically significant results.

Another method for measuring airborne dosage has been suggested by workers at Chicago Toxicity Laboratory.[65] This method collects the sample on two or three vertical wires of different diameters and relies on the relative collection efficiency of the different wires for different particle diameters in order to obtain the dosage. From the ratio of the pickup on different wires, the MMD of an aerosol cloud and the true area dose can be calculated from previously prepared graphs giving the correction factors. The Ct can be calculated from the area dose by dividing by the wind speed. With this method it is only necessary to determine analytically the amount of material collected on the different wires, so that no counting or measuring of the particles is required.

A number of tests both in the wind tunnel and in the field have been carried out in an attempt to determine the practicability of using either of these two methods for measurement of airborne dosage of insecticides.[66] For comparison, Cascade impactors, filters, and electrostatic precipitators were used. The results of the horizontal slides were about as reproducible as those obtained by other methods, but the dosages were appreciably lower than those obtained with filters or electrostatic precipitators. The method involving the wires suffered from inability to obtain a good analytical method which was sufficiently sensitive to measure the small doses which are entomologically important in the field. The necessity of knowing the wind speed in order to calculate the dosage is also a disadvantage. No correlation between either of these methods and entomological results has yet been attempted, and until such data are available, it is difficult to draw any conclusions as to their merits. It must be emphasized again that the final evaluation of any dispersal device must depend on the entomological results obtained on treatment under a variety of field conditions.

38.7 SUMMARY AND CONCLUSIONS

As a result of the research carried out on the development of equipment for dispersing DDT, a number of conclusions have been reached which should prove of lasting value, with respect to the dispersal of DDT as well as insecticides in general. The optimum particle size for obtaining contact kills of adult insects on the wing has been experimentally determined within certain limits, and a theoretical basis for these observations has been worked out. It has been shown quite conclusively that as the particle diameter is decreased below 10 microns, the dosage required for contact kills increases rapidly. This significant observation demonstrates conclusively the inadvisability of using droplets of screening smoke size, 0.4 to 0.7 micron, in insecticidal work. Since it has been shown that the ineffectiveness of the small drops is due to their failure to impinge on the insect rather than to any toxicity consideration peculiar to DDT, it is indicated that these small drops will be less effective regardless of the insecticide used or the type of insect being treated.

While no exact limit has been determined for the point where the drop size becomes too large to be insecticidally effective, it has been shown that the toxicity of drops between 10 and 60 microns does not vary widely. The theoretical calculations have shown that the point at which the effectiveness starts to decrease as the particle size increases is dependent on the number of drops which must actually hit the insect to produce mortality. Since this will, in turn, depend on the concentration of insecticide in the solution and its toxicity to the particular insect, any new insecticide or insect will have to be examined with these factors in mind.

In addition to these laboratory studies on the toxicity of the different particle sizes, sufficient field work backed by theoretical calculations has been carried out so that recommendations can be made of the best manner of dispersing DDT under a variety of practical conditions. This information can be applied to all types of insect control work.

The experimental work on the residual effect of DDT has been much more limited. However, the studies that have been made were sufficient to point the way toward future research. The type of solution dispersed, the type of surface treated, the conditions of exposure, and the manner in which treatment was made, have all been shown to have a profound effect on the residual action. Fundamental studies correlating the physical character of the deposit and the type of surface with the insecticidal effectiveness should be made. The relative importance of residual kill and contact kill should also be investigated. These studies

would be of great help in developing insecticide formulations and methods of treatment.

Two new devices have been developed for the ground dispersal of insecticides. Thermal generators of the Hochberg-LaMer type have been produced to disperse a relatively homogeneous aerosol whose effectiveness in killing adults and larvae has been clearly demonstrated in many regions of the world. The general principles involved in such devices have been clarified so that new equipment can now be designed without excessive experimentation. Further simplification is undoubtedly still possible and greater adaptability to different conditions should be attempted. Work is now under way on a generator which injects the DDT solution after the heating coil. If successful, this will eliminate a lot of the trouble due to coking and corroding and should simplify the use of new insecticide formulations. Although Hochberg-LaMer-type generators are large and complex, they can be operated easily after brief instruction. The controlled particle size should prove even more valuable for insecticide operations in civilian areas than in the war theaters because of the care which must be exercised under such conditions. Further work with this type of generator against agricultural pests should be carried on.

The exhaust generator for motor vehicles has been enthusiastically received because of its extreme simplicity and should have wide use in the future. Although the dispersal is not as carefully controlled as with the more complicated Hochberg-LaMer generators, this device should be extremely valuable for controlling a number of insect pests in small areas. The ability to vary at will the drop size from an aerosol to a coarse spray is an excellent feature. Further work is required to adapt this type of equipment to ordinary commercial vehicles such as trucks and tractors.

In the field of aircraft dispersal, two methods have been developed, both having their respective advantages. The simple sprays have proven very useful in the war theaters where simplicity and ease of installation and maintenance are prime requisites. The ability to use these sprays under a wide variety of meteorological conditions was an important factor in their use. Moreover, in these areas, the effects of the insecticide treatment on other forms of life do not have to be given serious consideration. The straight discharge pipe gives satisfactory results on fast military aircraft, but would not be satisfactory for slow light planes. Work on the development of the Venturi-type sprayers for military planes might be warranted.

For civilian purposes, dispersal has to be carried out under more carefully controlled conditions in order to avoid damage to other forms of wild life and crops. Moreover, in civilian work, the complexity of the apparatus is not such an important factor since the equipment can be permanently installed. For these reasons, the aircraft exhaust generators should be of particular value in this type of work. The small aerosol droplets produced permit uniform deposition of the insecticide over the entire area, and the dosage used can be more carefully controlled. The ability to alter the drop size from a fine aerosol to a spray makes this type of equipment extremely useful under a wide variety of conditions. Design of Venturis for use on new types of aircraft should be continued.

In addition to the design and development of actual devices for dispersal of DDT, research on the theory of atomization has been inaugurated. These studies are of prime importance in the design of any equipment for the dispersal of insecticides, and warrant continuation. The fundamentals involved in atomization have never been clearly resolved, and results of research in this line should prove of value in many other fields as well as in the dispersal of insecticides.

38.8 LIST OF MATHEMATICAL SYMBOLS USED

M = dose DDT for kill.
u = vertical velocity of drops.
d = diameter of drop.
ρ = density.
g = acceleration due to gravity.
η = viscosity air.
A = horizontal surface of insect.
C = concentration.
t = time.
Ct = dosage.
f = average number of drops hitting area per unit time.
n = number of drops.
D = characteristic length of object (insect, foliage).
v = horizontal velocity.
P = dimensionless parameter (Sell).
Ct_d = dosage for drop size increment.
W_d = relative efficiency of drop size in killing an insect.
W_{n+} = probability n or more drops hit any one area.
Q = source strength × time of emission.
x = horizontal distance.
m = meteorological constant.
R = meteorological constant (v_{2m}/v_{1m}).
F = fraction of material remaining airborne.
δ = horizontal distance for which the sum of the vertical foliage surfaces in any cross section is equal to the cross section.

γ = vertical distance for which the sum of the horizontal foliage surfaces in any cross section is equal to the cross section.
$\Delta Q/Q$ = fraction lost travel horizontal.
y = vertical distance.
Λ = impaction efficiency on vertical surface (Sell).
d_0 = diameter of single drop with the same ratio of surface to volume as a representative sample of the drop in the spray.
σ = liquid surface tension.
μ = liquid viscosity.
Q_a = volume flow rate of gas.
Q_L = volume flow rate of liquid.
u_d = settling velocity of drops of diameter d.
M_d = weight of drop of diameter d.
N_d = average number of drops of diameter d deposited per unit area.
q = constant in empirical equation of Nukiyama and Tanasawa.
p = constant in empirical equation of Nukiyama and Tanasawa.
a = constant in empirical equation of Nukiyama and Tanasawa.
b = constant in empirical equation of Nukiyama and Tanasawa.
V_2 = gas velocity in Venturi throat.
gc = dimensional constant in equation for throat velocity in a Venturi.
K = C_p/C_v (specific heat at constant pressure/specific heat at constant volume).
R/M = specific gas constant.
T = temperature.
D_2 = diameter of Venturi throat.
D_1 = diameter of exhaust stack.
P_1 = exhaust stack pressure.
P_2 = Venturi throat pressure.
A_2 = Venturi throat area.
W = exhaust gas flow.

Chapter 39

INORGANIC TOXIC GASES

By *John C. Bailar, Jr.*

39.1 INTRODUCTION

Among the many toxic gases suggested or investigated during the war were several that are entirely, or in part, inorganic in nature. These include some well-known substances such as iron carbonyl, cyanogen, hydrogen cyanide, cyanogen chloride, and arsine. None of these, except cyanogen chloride, received a great amount of study, as their use had been previously investigated and found impractical. Of the newly discovered gases, those containing fluorine proved to be of particular interest because some of them show great stability and high toxicity. It was hoped also that their high volatility would correlate with penetration of canisters. The most important members of this group which were studied by OSRD are disulfur decafluoride (S_2F_{10}, 1120, F5, Z) and the fluophosphate esters.

39.2 DISULFUR DECAFLUORIDE

39.2.1 Preparation

This substance was discovered by Denbigh and Whytlaw-Gray [1] as a by-product in the uncontrolled reaction of fluorine and sulfur. The yields in their experiments were less than 1%. The toxicity and stability of the substance, and its complete lack of odor or lacrimatory properties, suggested that it might be an ideal war gas. A great amount of effort was expended in studying its properties and in seeking a satisfactory method of preparation. The latter result was not achieved, and the effort was finally abandoned in the United States. It has been calculated [2] that the cost of the fluorine used in making 1120 would run between $21.00 and $140.00 per lb. The material used for tests on toxicity and other properties amounted to about 3 kg, the preparation of which required the work of four men for about a year. However, further study of the nature of the material and of fluorination reactions may yet yield a suitable method.

Methods Studied

The Controlled Reaction of Fluorine and Sulfur. This has been the most successful method yet studied, giving yields approaching 30% (based on sulfur) in some cases. For best results, the fluorine must be diluted with an inert gas, and the temperature must be carefully controlled. Nitrogen has commonly been used as the inert gas.[3] The use of sulfur hexafluoride in place of nitrogen did not improve the result.[4]

In the most successful procedure,[3] purified fluorine is mixed with pure nitrogen in the ratio of 1/10 and passed over solid sulfur in a copper boat contained in a copper reaction tube, which is kept at room temperature by artificial cooling. The products of the reaction are caught in suitable traps. If the fluorine-nitrogen ratio is too low, the lower fluorides of sulfur (SF_2 and S_2F_2) are formed in considerable amount; if the ratio is too high, SF_6 is almost the only product. Attempts to adapt this procedure to large-scale apparatus were not entirely successful, as the yield obtained was much decreased. The difference is probably due to insufficient control of operating conditions, and could doubtless be overcome by further study.[5]

The fluorine used must be extremely dry. A fresh fluorine generator usually gives a poor yield because the issuing gas is slightly moist or contains OF_2, which seems to exert a harmful effect. Best results are obtained only after the generator has run for several days; fair results can be obtained usually after the generator has operated for 24 hr.

Many variants of this plan were studied.[4, 6] The sulfur was finely divided and suspended in the nitrogen; melted, vaporized in a stream of nitrogen, dissolved in sulfur monochloride or carbon disulfide, or suspended in liquid hydrogen fluoride.

It is probable that the reaction of sulfur with fluorine liberates enough heat to give a high temperature at the point of reaction. This seems to be essential to the formation of 1120; on the other hand, the 1120 must be removed from the hot zone immediately or it is decomposed or further fluorinated. If this view is correct, the successful preparation of 1120 from the elements depends upon the maintenance of proper conditions of temperature, rate of flow, and other physical conditions. Attempts to prepare 1120 by allowing very hot sulfur vapor (700 C) to react with fluorine close to a cold condensing surface were

unsuccessful. The reaction gave only sulfur tetrafluoride and sulfur hexafluoride.

The Action of Fluorine on Sulfur Compounds. Mercuric sulfide, sulfur monochloride, sodium disulfide, potassium pentasulfide, antimony trisulfide, and sulfur tetrafluoride were studied, but with little success. These studies yielded excellent methods of preparation of other sulfur fluorides, however. It was observed that the action of fluorine on mercuric sulfide gives pure sulfur hexafluoride, and it reacts with the vapor of sulfur monochloride to give sulfur tetrafluoride of high purity in good yield.

The Fluorination of Sulfur Chlorides by Heavy Metal Fluorides.[7] This method seemed attractive in that it does not involve the use of elemental fluorine. Attempts were made to fluorinate sulfur monochloride by means of the fluorides of several heavy metals. Evidently sulfur monofluoride (S_2F_2) was formed, but it was quickly destroyed, either by reaction with the glass, or through its own instability. Whether S_2F_2 could be further fluorinated to S_2F_{10} was, therefore, not determined. A valuable by-product of this research was the development of a method of making anhydrous fluorides of the heavy metals. According to this method, a mixture of dry hydrogen fluoride gas and an inert gas is passed countercurrent over the heated metal oxide in a rotary kiln. The water which is formed is swept away by the gas stream. For each of the metal oxides certain conditions of temperature, temperature gradient, and rate of flow of gases must be maintained.

The Action of "Higher" Inorganic Fluorides upon Sulfur. This study amounted, for the most part, to a search for a nonelectrolytic method of preparing fluorine. Fluorides, such as $3KF \cdot HF \cdot PbF_4$, K_2MnF_5, K_2MnF_6, $3KF \cdot 2CeF_4 \cdot 2H_2O$, $CeF_4 \cdot H_2O$, IF_5, and $ZrOF_2$, are said to be formed without the use of elementary fluorine, and to yield fluorine upon heating. They might thus be used as regenerable sources of fluorine. Mixed with sulfur and heated, they might give the desired compound. It was found,[8] however, that the compounds were difficult to prepare and were poor sources of fluorine.

The Action of Fluorinating Agents on Sulfur Compounds.[9] Sulfur chloride and the tetrafluoride were treated with such fluorinators as iodine pentafluoride, bromine trifluoride, and hydrogen fluoride. In the main, these methods give mixtures of the tetrafluoride and hexafluoride of sulfur.

The Defluorination and Coupling of Sulfur Hexafluoride. It has been reported[10] that sulfur will react with sulfur hexafluoride at 400 C, but this could not be confirmed. Sulfur hexafluoride does react readily with many anhydrous salts, however.[4] Sodium and calcium iodides, sodium and barium bromides, and calcium sulfide were studied. In every case, free sulfur and the metallic fluoride were formed.

The Electrolysis of Fuming Sulfuric Acid in Liquid Hydrogen Fluoride. This gave no sulfur-fluorine compounds.[6, 11]

The Action of Hydrogen Fluoride upon Sodium and Barium Dithionates. This method was attempted because the dithionate ion contains a sulfur-sulfur link. No sulfur fluorides were formed.

Reaction of Fluorine Oxide with Sulfur and with Sulfur Dissolved in Sulfur Monochloride. The products were sulfur tetrafluoride and the oxyfluorides of sulfur.[11]

39.2.2 Properties

Disulfur decafluoride is a volatile, heavy liquid (density 2.08 at 0 C)[1] with a slight odor. When pure it melts at −53 C, but the melting point is very sensitive to traces of impurities. Burg[12] has calculated the boiling point to be 30.1 C from the vapor pressure equation

$$\log_{10} p_{mm} = -\frac{1856.8}{T} + 1.75 \log_{10} T - 0.008166 + 7.1348.$$

Below the melting point, the solid follows the equation

$$\log_{10} p_{mm} = 8.32 - \frac{1607}{T}.$$

The substance is practically insoluble in water (less than 0.005% by weight).

Disulfur decafluoride is inert to many chemical reagents, such as caustic alkalies and strong acids, and does not attack steel. It is unreactive toward glass, paraffins, and Apiezon L stopcock grease, and can be dried over phosphorus pentoxide or potassium hydroxide. Although it does not react with the common organic solvents, it dissolves in olive oil (with which it reacts slightly) to the extent of 4%. It is not attacked by fluorine, but reacts with chlorine with the formation of a slightly volatile liquid. Ethylene reacts slowly with 1120.

The thermal stability of 1120 is truly remarkable, as decomposition proceeds very slowly below 200 C, and becomes marked only above 250 C. The reaction seems to give a mixture of sulfur tetrafluoride and sulfur hexafluoride. The same decomposition is

brought about by contact with animal tissues, vegetable oils, or charcoal. Since in each case the reaction proceeds to only a slight extent, it is supposed that it is catalytic and that the catalyst is readily poisoned. Early in the investigation it was hoped that the decomposition on charcoal in the gas mask canister might prove to be valuable in warfare, as the resulting gases are extremely irritating and might cause the removal of the mask during a gas attack. However, the reaction products other than SF_6 (which is harmless) are retained by absorbents.

The thermodynamic properties of 1120 have been investigated thoroughly,[13] and numerous reactions of the sulfur fluorides have been predicted.

39.2.3 Chemical Detection of S_2F_{10}

The fact that S_2F_{10} liberates iodine from a solution of potassium iodide or sodium iodide in acetone has been made the basis of a quantitative test for determining S_2F_{10} in air.[14] The liberated iodine can be determined colorimetrically or by titration with thiosulfate, and the fluoride can be determined gravimetrically by precipitation with triphenyl tin chloride.[15] Obviously, any other oxidizing agents which may be present in the gas under analysis will also liberate iodine. It was shown, however, that the other substances, which might logically be present in S_2F_{10} from shell explosions, either do not interfere in this analysis or can be removed readily before analysis. These substances include NO_2, N_2O, SO_2F_2, SF_6, and SF_4. The reaction of 1120 with iodide is evidently complex, and conditions must be controlled carefully if consistent results are to be obtained. For example, if the iodide-acetone solution contains water, the amount of iodine liberated is low. At the same time, however, a roughly equivalent quantity of acid is formed. Apparently, there are competing reactions, one of which liberates iodine, while another liberates hydrogen ion.

S_2F_{10} can be detected qualitatively through its reaction with *p*-phenylenediamine. A piece of paper, wet with a solution of the amine in acetone, is exposed to the atmosphere under investigation. A pink color indicates the presence of S_2F_{10}. As little as 0.1 μg of 1120 can be detected.

39.3 DIALKYLMONOFLUOROPHOSPHATES

Dialkylmonofluorophosphates were first prepared by Lange[16] who reported that inhalation of even minute quantities produces severe headache, followed by visual trouble. These effects last for several hours. These observations indicate that substances of this class might be of military value, and investigations were started independently in the United States, in England, and (as found out later) in Germany. New methods of preparation were developed, and several esters were prepared and studied. The work of the American investigators was finally set aside in favor of more pressing investigations. The fluorophosphates show such sufficient promise, however, that they should be investigated further. It is quite possible that esters not yet prepared will be found to be more toxic than any which have been studied.

39.3.1 Preparation

Lange's method of preparation consisted of:

1. The preparation of ammonium fluorophosphate by fusion of phosphorus pentoxide with ammonium fluoride;

$$P_2O_5 + 3NH_4F \longrightarrow NH_4HPO_3F + NH_4PO_2F_2 + NH_3.$$

2. Conversion of the ammonium salt to the silver salt by metathesis with silver nitrate.

3. Alkylation of the silver salt with an alkyl iodide. He reported an overall yield of about 12%.

Several more direct methods at once suggest themselves:

1. Reaction of alcohol with phosphorus oxychloride

$$2ROH + POCl_3 \longrightarrow (RO)_2POCl + 2HCl$$

followed by fluorination of the product.

2. Partial fluorination of phosphorus oxychloride, followed by alkylation with the appropriate alcohol,

$$POCl_3 + HF \longrightarrow POCl_2F + HCl,$$
$$POCl_2F + 2ROH \longrightarrow (RO)_2POF + 2HCl.$$

3. Preparation of alkyl phosphites, followed by oxidation and fluorination,

$$PCl_3 + 3ROH \longrightarrow P(OR)_3 + 3HCl$$
$$P(OR)_3 + Cl_2 \longrightarrow (RO)_2POCl + RCl.$$

4. Preparation of monofluorophosphoric acid, followed by esterification with olefines, alcohols, or ethers,

$$P_2O_5 + 3HF \longrightarrow H_2PO_3F + HPO_2F_2.$$

Method 1 proved to be a successful process for the preparation of the lower homologs.[17] For example, phosphorus oxychloride reacts practically quantitatively with two moles of methyl alcohol, yielding a

mixture of CH_3OPOCl_2, $(CH_3O)_2POCl$ and $(CH_3O)_3P$. After removal of the hydrogen chloride, the mixture can be fluorinated, and $(CH_3O)_2POF$ can be isolated from the final mixture, the yield being about 30%.

The reaction between phosphorus oxychloride and ethyl alcohol does not proceed to complete esterification so readily, so that better yields (about 45%) of the fluorinated product can be obtained.

The preparation of the isopropyl ester by the same process, however, involves peculiar difficulties, for the reaction of isopropyl alcohol with phosphorus oxychloride yields several unidentified by-products, and the intermediate diisopropylmonochlorophosphate decomposes when heated in the presence of the hydrogen chloride by-product.[18] Neutralization of the hydrogen chloride with dry ammonia gas made the method workable, however, and some diisopropylmonofluorophosphate was obtained in this way. McCombie's method of preparing this ester[19] is much more satisfactory, however. This involves the esterification of phosphorus trichloride, followed by oxidation with chlorine:

$$3iC_3H_7OH + PCl_3 \longrightarrow (iC_3H_7O)_2POH + iC_3H_7Cl + 2HCl.$$

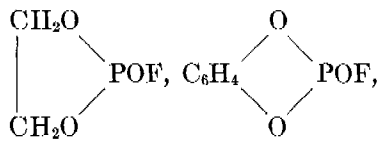
$$(iC_3H_7O)_2POH + Cl_2 \longrightarrow (iC_3H_7O)_2POCl + HCl.$$

The first of these reactions gives about a 70% yield, while the second is apparently quantitative. Most of the hydrogen chloride escapes, and the remainder may be destroyed by bubbling ammonia into the solution. Introduction of hydrogen fluoride gives an overall yield of 60% of the monofluorophosphate. (If the hydrogen chloride is not completely destroyed, none of the fluorophosphate is obtained.) It is not necessary to isolate any of the intermediate products.

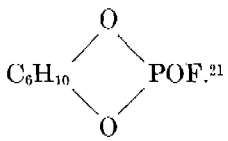
Some of the difficulties encountered in the preparation of the isopropyl ester are evidently due to the branching of the chain, for the *n*-propyl and *n*-butyl esters can be prepared in the same manner as the methyl and ethyl compounds, though the yield in the case of the *n*-butyl ester is somewhat lower than in the other cases.

In attempts to increase the toxicity of the fluorophosphates, chlorine substituted compounds were prepared.[20] Ethyl-β-chloroethyl monofluorophosphate was prepared by the successive reactions of chlorohydrin and ethyl alcohol with phosphorus oxychloride, followed by fluorination with sodium fluoride. All of these reactions proceed smoothly, and give good yields. Di-β-chloroethyl monofluorophosphate was obtained in good yield in a similar manner.

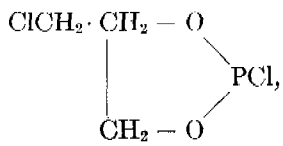
Toxicity tests indicated that ethyl fluorophosphate is more valuable from a military point of view than is the methyl ester. Since it is desirable to have the molecular weight of the ester as low as possible, attempts were made to prepare cyclic esters such as



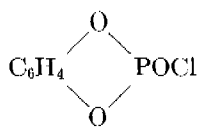
and



None of the experiments attempted were successful and the project had to be abandoned before its completion. Further work would probably lead to successful syntheses. Ethylene glycol reacts with phosphorus oxychloride, but under all conditions tried, the products obtained were polymers. Carre[22] has reported that glycerine α-monochlorohydrin reacts with phosphorus trichloride to give



so it is probable that cyclic esters of pentavalent phosphorus may be obtained. Moreover, the compound



has been obtained.[23] Hydrogenation and fluorination of this compound would give the interesting cyclohexane monofluorophosphate.

Reports from England indicated that cyclohexyl monofluorophosphate had very desirable properties, and the American military authorities began to request samples of it before directions for its preparation had been received from England. Accordingly, the preparative methods that had proved successful in the formation of the simpler esters were employed in attempts to prepare it.[24] Attempts were also made to reduce the phenyl ester catalytically. None of these methods gave the desired product; the only successful method devised is apparently that developed by McCombie and his co-workers in England.[25] This method involves the reaction of cyclohexyl alcohol

with phosphorus oxydichlorofluoride to give the desired product directly. However, the partial fluorination of phosphorus oxychloride to $POCl_2F$ is difficult, for once the fluorination of the phosphorus oxychloride starts, it is difficult to stop it short of complete replacement of chlorine by fluorine. Fortunately, the boiling point falls as fluorination becomes more complete, so that if the fluorination is carried out at the boiling point of phosphorus oxychloride, the phosphorus oxydichlorofluoride can be drawn off as it is formed, and some of the desired product obtained. Booth and Dutton [26] have obtained 40% yields of $POCl_2F$ by the reaction of phosphorus oxychloride with calcium fluoride. Under the best conditions, the reaction of boiling phosphorus oxychloride and hydrogen fluoride has been made to give yields of 60% of the dichlorofluoride.[27]

39.3.2 Properties

The fluorophosphates are colorless liquids, the vapor pressures of which are only a few millimeters of mercury at room temperature. They are almost insoluble in water, and are attacked by it only very slowly, remaining unhydrolyzed when left in contact with water for many days. They do not attack glass or steel.[18] Their odor is faint and not unpleasant. Inhaling them in minute quantities produces a constriction of the pupils resulting in partial blindness which lasts for several hours. In larger quantities, they produce headache, convulsions, and death.

39.4 ALKYLDIFLUOROPHOSPHATES

These compounds were prepared by fluorination of the corresponding chlorophosphates.[28] Although the yields are not good, sufficient quantities of material were obtained for investigation. The ethyl ester is a colorless liquid having a density of about 1.25 and boiling at 85 C. It decomposes slowly above 50 C, but this may be due to reaction with the walls of the (glass) vessel rather than straight thermal decomposition. It is soluble in organic solvents and reacts vigorously with water. This is surprising in view of the great stability of the monofluoro esters.

39.5 ALKYLMONOFLUOROTHIOPHOSPHATES

These esters cannot be prepared in an analogous manner to the oxy compounds as the reaction of thiophosphoryl chloride and alcohol does not proceed in the desired manner. With ethyl alcohol, ethyl chloride is produced quantitatively. However, in the presence of pyridine, a small yield of the monochlorothiophosphate is obtained. This is readily fluorinated.[18] The diethyl ester is a colorless liquid, heavier than water, and boiling at 55 C under 10 mm pressure. It is extremely stable toward hydrolysis.

39.6 FLUOROSULFONATES

Because of the interest in fluorophosphates, some fluorosulfonates were prepared and their properties noted.[29] Fluorosulfonic acid was first prepared by Thorpe and Kermann [30] who obtained it from the action of liquid hydrogen fluoride upon liquid sulfur trioxide. Ruff and Braun [31] reported an almost theoretical yield of the acid by the reaction of 60% oleum and fluorspar. The acid can also be made in theoretical yields by the reaction of anhydrous hydrogen fluoride and chlorosulfonic acid.

Meyer and Schramm [32] prepared esters of fluorosulfonic acid by the reaction of the acid with absolute diethyl ether, ethylene, and diazomethane. The first two of these methods were repeated and found to give good results. Ethyl fluorosulfonate is a clear liquid having a density of 1.29 at 27 C, and boiling at 112 C at atmospheric pressure (42.5 at 55 mm). It decomposes upon boiling but is remarkably stable toward hydrolytic decomposition, as it is not destroyed by refluxing with 20% sodium hydroxide for 2 hr. It does not fume in air and does not etch glass noticeably even on standing for several weeks. It is destroyed, however, by nitric and sulfuric acids. It is soluble in the usual organic solvents. It has the typical ester odor, but is a lachrymator.

The methyl ester (from the acid and absolute dimethyl ether) is similar, but is not so effective a lachrymator. Attempts to prepare the isopropyl ester were unsuccessful; this ester seems to be unstable, decomposing upon boiling, even in vacuo.

39.7 OTHER GASES

Many other inorganic gases were investigated, but none of great military interest was found. A few of the more interesting will be mentioned.

Phosphorus trifluoride was prepared by the $SbCl_5$ catalyzed reaction of phosphorus trichloride and antimony trifluoride.[33] It forms an unstable complex, $(CH_3)_3N \cdot PF_3$, through which it can be purified, since SiF_4 and other impurities do not react with trimethylamine. The phosphorus trifluoride can be simply distilled with the complex, or the complex can be sublimed, and then decomposed to yield pure

phosphorus trifluoride. The material is probably too volatile to become a useful war gas. (The vapor pressure is 376 mm at −111.9 C and 181 mm at −120.8 C.) By combination with trimethylamine, PF_3 can be given an effective boiling point of about 0 C.[34]

Dimethylamino phosphorus difluoride was prepared in accordance with the equation

$$2(CH_3)_2NH + PF_3 \longrightarrow (CH_3)_2NPF_2 + (CH_3)_2NH_2F.$$[33]

It is a liquid at ordinary temperatures, boiling at 50 C

$$(\log_{10} P_{mm} = 7.863 - 1610/T).$$

The compound is not entirely stable, but at room temperature, it comes to equilibrium with its decomposition products when only 4% decomposition has taken place.

$$2(CH_3)_2NPF_2 \rightleftarrows PF_3 + [(CH_3)_2N]_2PF.$$

This latter compound, bisdimethylamino phosphorus fluoride, can be prepared also by the action of dimethylamine upon $(CH_3)_2NPF_2$. It was found to be relatively nontoxic.

Dimethylamino phosphorus difluoride hydrolyzes very slowly, so it was thought that it might penetrate into the lungs more deeply than phosphorus trifluoride itself. Whether this is true was not determined; the material is not strongly toxic.

The closely related compound $(CH_3)_2NPOF_2$ was prepared in an analogous manner and also by the reactions

$$POCl_3 + 2(CH_3)_2NH \longrightarrow (CH_3)_2NPOCl_2 + (CH_3)_2NH_2F$$

followed by

$$3(CH_3)_2NPOCl_2 + 2SbF_3 \longrightarrow 2SbCl_3 + 3(CH_3)_2NPOF_2 \quad (SbCl_5 \text{ catalyzed}).$$

This compound is not strikingly toxic.

Action of dimethylamine on dimethylamine phosphoryl difluoride yields bisdimethylamine phosphoryl fluoride $[(CH_3)_2N]_2POF$, which is an analogue of the very toxic aliphatic fluorophosphates, and which is also toxic (median lethal concentration of 0.095 mg per l on mice exposed for 10 min). This compound can also be prepared directly from phosphoryl fluoride and dimethylamine or from phosphoryl chloride and dimethylamine followed by fluorination with antimony fluoride. It is a liquid boiling at 50 C under a pressure of 2 mm. It is not readily hydrolyzed by pure water, but is quickly attacked by alkalis. It would seem that this compound, like the analogous fluorophosphates, deserves further study.

Substitution of arsenic for phosphorus in the compound $(CH_3)_2NPF_2$ did not produce a toxic compound.[33] This substance was prepared by the interaction of dimethylamine and arsenic trifluoride.

A small yield of 2, 2′, 2″ trifluoro triethylamine, $(FC_2H_5)_3N$, was prepared by a very tedious fluorination of the corresponding chloro compound with anhydrous silver fluoride. The substance was tested for vesicant action, but the results were negative.[35]

Nitrogen trifluoride, which was reported by Ruff to be highly toxic, was obtained from the electrolysis of molten ammonium bifluoride. After careful purification, it was found to be relatively nontoxic. The substances NHF_2 and NH_2F, which have been reported by Ruff to be even more toxic than NF_3, could not be obtained at all.

Acyl chlorides are known to be toxic, and some of them have found wide use as war gases. The corresponding fluorides would be expected to be more volatile (and hence less readily adsorbed in a gas mask), less readily destroyed by hydrolysis, and more toxic. Unfortunately, they have been difficult to prepare. During the course of this work, however, a satisfactory method was developed.[36] This involves the conversion of acyl chlorides to the corresponding fluorides by the action of anhydrous hydrogen fluoride at suitable temperatures and pressures. Thus, phosgene can be converted to COFCl or COF_2 and oxalyl chloride to oxalyl fluoride. In the former case, complete fluorination can be avoided by drawing off the partially fluorinated product as it is formed. Carbonyl chlorofluoride has an odor resembling that of phosgene, but the two can easily be distinguished. It is readily absorbed by bases.

Arsine has often been suggested as a war gas, but it is too volatile to be persistent and too unstable to be kept for more than a few days. An attempt was made to find a solvent in which arsine would be stabilized and in which it would have a reasonably low vapor pressure.[37] The solvents used were thionyl chloride, *p*-ethylnitrobenzene, 1-nitropropane, triethyl borate, and tributyl borate. In thionyl chloride, arsine decomposes in a few minutes, and in the other solvents, within a few hours. In triethyl and tributyl borate, the vapor pressure is lowered by as much as 30%, so if a stabilizer can be found, these solutions may be of value. It should be borne in mind, however, that arsine is an endothermic compound; if it is to be stabilized, it will probably have to be mixed with some compound with which it forms a stable bond.

Chapter 40

THE PREPARATION OF FLUORINE

By *John C. Bailar, Jr.*

40.1 INTRODUCTION

THE ELEMENT FLUORINE was first prepared by Moissan by the electrolysis of a solution of potassium fluoride in anhydrous hydrofluoric acid at about −20 C in a platinum-iridium U tube. Corrosion was severe, and the yield of fluorine was small. Nevertheless, modifications of this method have always constituted the only practical method of making fluorine. It has frequently been suggested that fluorides of metals in their higher valence states might be thermally decomposed to liberate fluorine, but no practical method based upon this principle has been discovered. It is true that some metallic fluorides can be decomposed with the liberation of fluorine (AgF_2, for example), but such fluorides can be prepared only by the use of elemental fluorine. The element is such a powerful oxidizing agent that metals in union with it are not readily reduced by heat alone.

Electrolysis of anhydrous fluorides always employs mixtures of hydrogen fluoride and alkali metal or other metal fluorides. As the proportion of metal fluoride is increased, the melting point of the mixture rises, necessitating changes in the design and operation of the cell. Low-temperature operation has obvious advantages, but the low-temperature baths are so rich in hydrogen fluoride that the vapor pressure of this constituent is high. Moreover, corrosion of the anodes and the electrolytic cell is often more troublesome in these baths than in those operating on molten salt mixtures. The best bath will contain a low-melting eutectic salt mixture with a small concentration of hydrogen fluoride, the supply of which will be replenished at frequent intervals or continuously. Recent discoveries [1] at Massachusetts Institute of Technology have shown that a bath of the composition RF·1.5HF (where R is K containing a small percentage of Li) melts at about 70 C and serves as an excellent electrolyte for the preparation of fluorine. This is perhaps the best method discovered to date. In order to show why this is so, and to give a basis for further work, the use of several baths will be described.

40.2 BATHS OPERATING AT ROOM TEMPERATURE

A cell using a bath rich in hydrogen fluoride and liquid at room temperature was patented in 1936, and was restudied under OSRD.[1, 3, 4] It was found to be unsuited for large-scale production of fluorine. At the low temperature employed, hydrogen and fluorine dissolve in the electrolyte, so that each of the effluent gases contains an admixture of the other in a mixture sometimes rich enough to be explosive.[3] Moreover, corrosion of the nickel anodes and the walls of the vessel is serious. In one run, for example, 1 g of nickel was devoured for each 2.07 ± .02 g of fluorine produced. Attempts to decrease the corrosion by varying the current density and other operating factors were without effect.[5] Other metals were tried as anodes in place of nickel, but the results were even less promising. Graphite anodes are rapidly disintegrated by the bath. Some iron from the walls of the vessel is also dissolved, and a heavy sludge of ferrous and nickel fluorides gradually forms in the electrolyte, so that the run eventually has to be stopped to allow cleaning of the cell.[1] These low-temperature cells sometimes give a current efficiency of 80% when the run is first started, but this soon falls to about 50% (based on fluorine delivered) and then remains constant.[7] The yield based on hydrogen, however, is always about 80%,[1] the difference indicating the loss of fluorine due to corrosion. The cells operate at 7 to 9 v and 30 amp. Anhydrous hydrogen fluoride is added slowly while the cell is in operation. Since the vapor pressure of hydrogen fluoride over this bath is high, reflux condensers cooled by solid carbon dioxide or some other refrigerant must be provided.

40.3 BATHS OPERATING AT MEDIUM TEMPERATURES

Baths approximating the composition KF·2HF and KF·3HF have been used for many years. The former are operated at 100 to 110 C and the latter at 70 to 100 C. The cells are heated by a steam jacket

or electrically, though external heating is often unnecessary after electrolysis is begun. Here again, much hydrogen fluoride escapes as vapor and must be refluxed back into the cell or trapped out and replenished. Corrosion is severe, but not so severe as in the bath which operates at room temperature. From 7 to 8 lb of fluorine can be produced for each pound of nickel lost from the anode. Current efficiency based on fluorine often goes as high as 70 to 75%. Certain types of carbon and graphite can be used as anode materials, though it is difficult to predict how well a given sample of carbon will withstand the attack of the bath. Ungraphitized carbon is ordinarily better than graphite.[6] Corrosion of the vessel is also much less marked than with the more acid baths. While low-silicon steel can be used, and usually is, copper or copper-plated steel is superior. This method of preparing fluorine has been fairly satisfactory in commercial use. With good carbon anodes, current efficiencies are much higher than with nickel anodes, sometimes being better than 90%. The major problem in the operation of this method is the swelling and disintegration of the carbon anodes at their point of union with the anode holders. A careful study of this has been made,[8] and it has been shown that corrosion is minimized if the carbon-metal bond is below the surface of the bath. Magnesium, brass, and copper are the best metals to use for electrode holders, whereas aluminum, nickel, and Monel are badly attacked. The destruction of the union between the carbon and the metal can be minimized by the use of colloidal graphite (*Aquadag*) as a *joint compound* between the metal and carbon surfaces.[6] Another method of handling the problem is to run the carbon anode through the cover of the cell, making the carbon-metal connection outside of the cell.

The addition of a few per cent of lithium fluoride tends to lower the melting point of the bath, so that the hydrogen fluoride content can be cut without having to raise the operating temperature. Such a bath might have the composition 82.7% KHF_2, 3% LiF, 14.3% HF, which approximates the formula $RF \cdot 1.5HF$. This composition is maintained by direct addition of hydrogen fluoride while the cell is in operation. Because of its lower hydrogen fluoride content, this bath corrodes the vessel less than the low-temperature bath, so that steel vessels are quite acceptable. With copper-lined cells, the bath remains nearly free of corrosion products. This bath also has the advantages of being nonhygroscopic and of showing a much lower vapor pressure than the low-temperature bath. Nickel electrodes cannot be used, however, as the metal is destroyed rapidly and little fluorine is formed.[7] Carbon, on the other hand, is attacked hardly at all. At high-current densities, *polarization* sets in, seriously interfering with the production of fluorine. This phenomenon will be discussed later. When the cell is operating properly, current efficiencies of 95 to 98% can be obtained. Two such cells ran unattended (on a reduced amperage) for 72 hr without any trouble.[9]

Cells operating at 130 to 150 C, but still using a bath of the general composition $RF \cdot 1.5HF$, can be prepared by using 66.8% KHF_2, 14.4% NaF, and 18.7% HF. This seems to offer no advantage over the bath containing lithium fluoride, and the cell corrosion is much worse.[6]

40.4 BATHS OPERATING AT HIGH TEMPERATURES

Baths of the composition $MF \cdot HF$ can be electrolyzed at 250 C or higher, and have been widely used. This method of making fluorine is nearly as successful as that operating in the neighborhood of 100 C.[6] The cell must be heated to the required temperature by gas or electricity, but additional heating is not required while electrolysis is under way. The cell must be of copper or Monel rather than of steel, and the anodes are of graphite or graphitized carbon. Sludge formation is slight, and current efficiencies are over 90%. However, the composition of the bath must be carefully controlled.

Baths containing no hydrogen fluoride have received some attention, but none have been found which can be electrolyzed to give fluorine at temperatures as low as 300 C, which seems to be the upper limit for operation with carbon in contact with fluorine.[6] Mixtures of potassium fluoride and lithium fluoride with the fluorides of antimony, zinc, lead, and cadmium have been studied.[5, 7] This method holds promise, and further study of it should be made.

40.5 POLARIZATION AND THE ANODE EFFECT

When a cell with a carbon anode is operated at a high current density, *polarization* sometimes takes place. The voltage rises, often to 50 or 100 v, and the amount of current passing through the cell falls.

While the cell is operating at the higher voltage, no fluorine is formed, but the anode is attacked with the formation of carbon fluorides. This phenomenon of polarization is not clearly understood, and it cannot be produced at will.[10] Sometimes, but not always, it disappears spontaneously. If it does not, it can usually be overcome by resorting to certain practical and empirical remedies. These include breaking the current, short circuiting the cell, or reversing the current momentarily. Sometimes the polarization disappears if the anode is connected to the cell wall for an instant, or if alternating current is superimposed upon the direct current being used for electrolysis. The use of direct current from a rectifier is helpful. While the cell is polarized, the anode is enveloped in a multitude of tiny sparks.[10] It has often been suggested that polarization is due to impurities in the electrolyte, but it has been demonstrated that small quantities of sulfuric acid and of water do not produce severe polarization.[8] Samples of anodes which have undergone polarization have not been demonstrated to contain any impurities that are not found in anodes which have functioned without polarization. Yet the phenomenon seems to be inherent in the nature of the anode used. One example has been reported [11] of a carbon rod which became polarized repeatedly. None of the usual methods of breaking the polarization was effective for more than a few minutes. Even baking, scraping, and washing had no effect in decreasing the tendency of this sample to polarize.

Carbon anodes do not seem to be wet by the fluoride electrolyte. As electrolysis proceeds, the surface of the anode often becomes glossy and increases in hardness. The nature of this glaze is not known, but it does not seem to be the cause of the anode effect, for highly glazed electrodes sometimes function perfectly. The most logical explanation of the polarization effect is that the electrode is surrounded by a thin but impervious gas film, which adheres tightly.[10] There is some evidence that the presence of lithium fluoride in the electrolyte causes the liquid to wet the anode and also prevents polarization.[12]

Although the problems of corrosion and of polarization of the cell remain as troublesome problems, it may now be said safely that the preparation of fluorine on a fairly large scale is feasible and practical. Several companies are producing fluorine commercially, and as its use increases, the price may fall to as little as $0.25 to $0.50 a pound.[12]

Chapter 41

THE STABILIZATION OF CYANOGEN CHLORIDE

By *Anton B. Burg*

41.1 INTRODUCTION

CYANOGEN CHLORIDE is one of the promising nonpersistent gases because it penetrates humidified canisters unless they are given special impregnation to protect against this agent. Other advantages of cyanogen chloride are its relatively high boiling point (13 C), which makes it easier to load into munitions than either cyanogen or phosgene, and its noninflammability, a great advantage over hydrogen cyanide. It also persists longer in the neighborhood of wet surfaces (e.g., vegetation) than does hydrogen cyanide or phosgene.

The one great disadvantage of cyanogen chloride has been its instability. It may have a pronounced tendency to polymerize, often very suddenly and with little warning, yielding cyanuric chloride and a variety of other solid or liquid polymers as well as degradation products. Large bombs containing this agent have been known to detonate in normal storage, amply demonstrating the danger of storing the raw commercial product in contact with steel. Even if deterioration occurred without explosions, the loss of the cyanogen chloride could not be tolerated. It, therefore, was necessary to learn as much as possible of the conditions under which cyanogen chloride would become unstable, and to devise methods of preventing troubles arising from its instability, preferably without serious alteration of specifications for the munitions destined to contain the material.

Previous to World War II, very little was known of such matters. The only definitely recognized catalyst for the degradation process was hydrogen chloride, and by inference, other acids also were regarded as harmful. No very effective stabilizer had been recognized. It was known to Wurtz [1] that chlorine causes polymerization of cyanogen chloride to the trimer, cyanuric chloride, provided that water and HCN are present as impurities. According to Jennings and Scott,[2] this effect could be understood as due to the formation of HCl, which Chattaway and Wadmore had recognized as a more direct catalyst for the polymerization process.[3] Various authors differ on the question of whether HCl would cause explosions, but it can be argued that it will do so often if the sample is large enough so that the heats of hydrolysis and polymerization are not rapidly dissipated. Price and Green [4] found that the HCl-catalyzed hydrolysis of cyanogen chloride (to form NH_4Cl and CO_2) proceeds far more rapidly than the HCl-catalyzed polymerization. There was general agreement that purification of cyanogen chloride improves its stability.

NDRC work on this problem began in 1942 as a supplement to the investigation of absorbents.[5] The preliminary study checked much of the earlier knowledge and indicated that the bad effect of HCl or of chlorine could be largely overcome by addition of magnesium oxide. Sodium cyanide was found to be harmful, yielding dark *azulmic* materials. Most of the tests with common materials were not carried on long enough to detect their bad effects, but the main inference, that munition storage of cyanogen chloride could be made feasible, was later shown to be sound.

More detailed studies were attempted next by research personnel of the American Cyanamid Company.[6] Although most of the experiments were somewhat lacking in precision, it could be recognized that crude cyanogen chloride was far less stable in steel containers than in contact only with glass, that alkene oxides were not dependable stabilizers, that primary or secondary alcohols and other hydroxyl compounds were seriously harmful, and that crude cyanogen chloride from the pilot plant would meet the preliminary specification of freedom from deterioration during 30 days, even in a steel container at 65 C. Other conclusions were overthrown by the more precise and extensive work which became possible after the main production began in the plant at Azusa, California.[7]

It was evident that the safe production, handling, and long-term storage of militarily useful quantities of cyanogen chloride would require far more detailed knowledge of its behavior under various conditions than the preliminary researches could give. A considerably expanded program of laboratory research therefore was undertaken under a new NDRC contract [7] in addition to the large-scale testing project at Dugway Proving Ground. The new program in-

cluded nearly 2,000 tests of the stability of cyanogen chloride, varying greatly in purity, with or without various artificial impurities, and in contact with numerous metals or other solids. Most of this work was directed toward recognition of harmful classes of substances, toward evaluation of various proposed stabilizers, toward understanding the process of deterioration, and toward the prediction of normal-storage stability from the results of thermally accelerated tests.

For such purposes, it was necessary to develop and use a standardized *surveillance* test technique, such that all comparable samples would be tested in a similar manner, simulating munition storage as closely as feasible. Also, it was necessary to develop and use a number of new analytical methods for determining water, acidity, soluble and insoluble residues, and numerous deterioration products and intermediates. The techniques ranged in difficulty from simple titrations to the use of high-vacuum manifolds and low-temperature fractionating columns. Precise measurements of physical properties also were involved. The various results and conclusions are summarized in this chapter.

41.2 CONDITIONS AFFECTING STABILITY OF CYANOGEN CHLORIDE

The stability of cyanogen chloride depends markedly upon the presence or absence of other substances, such as it may meet in munitions or retain as impurities in manufacture, or which may be added for definite reasons. Some foreign substances strongly influence the effects of others, either increasing a bad effect, or protecting against it.

41.2.1 Substances Specifically Harmful toward Cyanogen Chloride [7]

The following classes of substances proved so destructive toward cyanogen chloride that they must be definitely avoided or counteracted in munitions in which they might occur with it in long-term storage.

1. All acids, especially in the presence of water or iron, or both, must be avoided. Addition of a 3% to 5% proportion of concentrated hydrochloric acid usually causes explosion.

2. All hydrogen compounds are dangerous, including hydrocarbons, greases, mineral or vegetable oils, alcohols, alkene oxides, water, and HCN, which sooner or later will react with cyanogen chloride to form HCl, leading to a rapidly accelerating process of destruction. Chlorine greatly increases the rate of this destruction, but is nearly harmless toward pure cyanogen chloride. Were it not too expensive, the removal of both HCN and water from crude cyanogen chloride would be recommended.

3. Iron, especially as rust or iron salts, accelerates the conversion by CNCl of HCN or water to HCl. Oxidized, sulfidized, or nitridized coatings proved very bad, but with variable rate of effect. Ferric chloride proved to be about as harmful as metallic iron, and it is believed that some other iron compound is the real catalyst. Iron first removes free HCl, which returns after the iron is well coated.

4. Certain other metals, such as copper, zinc, or their alloys, are especially destructive toward cyanogen chloride containing either HCN or water, but they have no bad effect upon pure cyanogen chloride. Aluminum is about as destructive as iron, and Dural is even more so, causing explosion of samples as small as 35 g. Tin is mildly harmful.

5. Cyanides are harmful when water is present, and this means that any strong-base stabilizers (CaO, BaO) may be used only when the cyanogen chloride is low in HCN, or in water, or both. HCN in 10% proportion has led to detonation in munition tests at 65 C. On the other hand, HCN has some protective effect against HCl, through formation of the solid $H_2C_2N_2 \cdot 3HCl$.

6. Cyanuric chloride and such higher polymers as $C_4N_4Cl_4$ are harmful toward crude cyanogen chloride through reaction with water to form HCl, or through oxidation of iron to form a catalyst activating the HCN. Another reaction product, C_2HNCl_4 (always formed if there is a source of hydrogen), reacts directly with water or HCN to form HCl, or even yields HCl by itself through Fe-catalyzed decomposition.

7. Ammonium chloride, which results from the destruction of water by the quantitative reaction $ClCN + 2H_2O = NH_4Cl + CO_2$, becomes disproportionately harmful at temperatures above 100 C. At any temperature, it is a source of the very harmful C_2HNCl_4, but this effect is very slow at normal temperatures.

41.2.2 Substances Inert toward Cyanogen Chloride [7]

Of the various substances produced by CK, related to it, or likely to meet it in munitions, the following are not harmful.

[redacted]

1. Carbon monoxide, carbon dioxide, cyanogen, traces of air.

2. Carbon tetrachloride (a fairly important by-product of degradation).

3. Dry cyanuric chloride, cyanuric acid, or alkali cyanates (all in absence of iron or HCN).

4. Neutral salts (NaCl, $CaCl_2$) become harmless as soon as the water is gone (by ClCN hydrolysis). In solution they promote corrosion of iron, introducing a catalyst for deterioration.

5. Silver solder, Monel, and stainless steel become harmless when the cyanogen chloride is dry. Lead, magnesium, and manganese are quite harmless and cadmium actually has a stabilizing effect. Platinum and gold are inert.

6. Pyrex glass, which was used as the container material in all tests, was recognized as inert toward cyanogen chloride in that variation of the wall-liquid ratio did not affect test results.

7. Potassium dichromate (used to induce passivity of iron munition walls) is not seriously harmful toward cyanogen chloride. The same is true of small proportions of vapor-phase corrosion inhibitors furnished by the Shell Development Company (VPI 220 and 260).

41.2.3 Substances Acting as Stabilizers for Cyanogen Chloride

Many different substances have been proposed as stabilizers for cyanogen chloride and most of these have been tested.

The alkene oxides were favored at one time [8] because they absorb HCl and water without converting HCN to cyanide, but they proved useful only for especially unstable lots.[7] A normal lot of crude cyanogen chloride, which will survive surveillance for 60 days with iron at 65 C, can only be harmed by alkene oxides, which ultimately yield far more HCl than they absorb.

The dialkyl cyanamides also seemed very favorable at one time, for they doubled, tripled, or quadrupled the stability of ordinary crude cyanogen chloride and were effective at 0.1% concentration.[7] On the other hand, they ultimately permitted acid to develop, and better stabilizers were considered desirable.

During the early stages of this work, it was assumed that no solid stabilizer would be acceptable, on account of the inconvenience of putting such material into munitions. In the absence of any really good liquid stabilizer, however, tests of solids were initiated at the University of Chicago.[9] Numerous metal salts or oxides were tried, and the most effective seemed to be those which would be expected to remove soluble iron, thus preventing the very start of the series of reactions whereby HCN, NH_4Cl, or other sources of hydrogen, yield HCl. Thus, fluorides form FeF_6^{---}, a very stable complex ion, and phosphates also hold ferric iron very firmly. Of all such substances tried, sodium pyrophosphate ($Na_4P_2O_7$, dry) seemed most spectacularly effective, and, in fact, a 5% addition of this substance to crude cyanogen chloride preserves it in contact with iron even at 100 C for almost indefinitely long periods of time.

Experiments with solid stabilizers were carried on also at the University of Southern California [7] and at Dugway Proving Ground.[8] Calcium and barium oxides were rejected as too likely to cause dangerous heat effects on contact with wet cyanogen chloride. Sodium hexametaphosphate and disodium hydrogen phosphate proved to be very good stabilizers but not so good as sodium pyrophosphate. Potassium pyrophosphate was definitely inferior. A 2% proportion of $Na_4P_2O_7$ proved useful but inadequate. A badly (e.g., 20%) deteriorated sample can be saved by addition of 5% of $Na_4P_2O_7$. This stabilizer has not yet failed to improve a sample of cyanogen chloride, although hundreds of varied tests have been done.

Tests of sodium fluoride in proportions up to 2% indicated that this stabilizer might be nearly as effective as similar proportions of $Na_4P_2O_7$, but tests with 5% of either stabilizer at 100 C showed NaF to be far inferior; especially for saving bad samples.[7]

41.3 MECHANISM OF DETERIORATION [7]

It now seems probable that the actual catalyst, in all instances of normal deterioration of cyanogen chloride, is hydrogen chloride. This acid is always found among the degradation products, and its concentration reaches a maximum when the polymerization is happening most rapidly. Its action can be understood on the basis of an addition compound, $ClCN \cdot HCl$, in which the carbon atom is activated toward attraction of the nitrogen atom of a second ClCN molecule. The 1/1 addition compound actually has been made (at low partial pressure) and observed to decompose into ClCN, HCl, and polymer. The stability of such an addition compound may be expected to decrease with rising temperature, counteracting the usual increase of reaction rate with tem-

perature. This balance of factors explains an observed slightly negative effect of temperature upon the rate of the HCl-catalyzed polymerization.

The specific mechanisms, whereby HCl is formed from other hydrogen-containing impurities, are complex and often obscure, but in general terms, one can recognize that cyanogen chloride behaves much like chlorine, having a similar oxidation potential, but less rapid reactions. Such a chlorinating effect must be responsible for the formation of C_2HNCl_4, a slightly volatile liquid which invariably is found whenever the deterioration process has occurred with the typical sudden acceleration. This substance evidently is not easily formed except by the effect of a catalyst, such as iron salts. Conversely, C_2HNCl_4 oxidizes iron more rapidly than ClCN does, and more of the iron catalyst thus becomes available. The C_2HNCl_4 can break down in two ways: by HCl catalysis to form CCl_4 and HCN, or by iron-catalysis to form HCl and a nonvolatile solid. It also reacts with either HCN or water to form HCl, and is formed, at least indirectly, from either HCN or water by reaction with cyanogen chloride. Thus, it is possible that C_2HNCl_4 is formed and destroyed several times during the degradation of cyanogen chloride.

Another strong oxidizing agent, resulting from the self-chlorinating effect of cyanogen chloride, is the nearly nonvolatile liquid $C_4N_4Cl_4$ (in early reports regarded as an isomer of trimeric cyanuric chloride). This *tetramer* apparently has an open-chain structure with a $=CCl_2$ unit at one end and $-CN$ at the other. It is very stable, but has enough chlorinating power to convert HCN to HCl in the presence of an iron catalyst. Thus, it is another of the intermediates responsible for the rapid formation of HCl toward the end of a long period of storage of cyanogen chloride. Others may be the less volatile liquids, gums, and solids which probably represent longer chains of similar structure.

None of these intermediates seems effective against cyanogen chloride unless HCN, water, or some breakdown catalyst also is present. The most important is C_2HNCl_4, which alone could account for the usual rapid acceleration of the polymerization of crude cyanogen chloride. When pure ClCN is polymerized by heating with only a little dry HCl, the reaction occurs very smoothly, without the usual acceleration.

Since iron plays an important part in both the formation and the harmful effect of the reaction intermediates, the preventive effect of substances which hold ferric ion in harmless combination, such as fluorides or phosphates, is easily understood.

41.4 EFFECT OF TEMPERATURE UPON RATE OF DESTRUCTION [7]

It appears that the various slow reactions in crude cyanogen chloride, leading ultimately to the formation of catalytically important proportions of HCl (and consequent rapid destruction), are governed by the usual rule that the rate doubles with each temperature rise of 10 degrees C. This rule was verified by the results of comparative stability tests at 65 and 100 C, using 122 lots of cyanogen chloride from the plant at Azusa. Other comparative tests at 35, 45, 55, and 65 C also verified the rule. Extensive analyses at different points in the degradation process showed that the reaction mechanisms are essentially the same at all temperatures below 100 C. On the other hand, tests at 125 C deviated completely from the usual temperature coefficient, for reasons which are not evident. It is also worthy of note that the HCl catalysis is nearly independent of temperature; this reaction is fast, however, and involves no important part of the total *surveillance* time.

Thus it is possible to predict, within about 20%, the time when a given lot of crude cyanogen chloride will develop enough acidity for rapid (perhaps explosive) deterioration, provided one has the results of a 65 or 100 C iron-contact surveillance test on the same lot. All but the first 40 lots produced at Azusa were fairly uniform, and most of this material should remain in good condition without stabilizers for about three years at normal temperatures (25 C). With sodium pyrophosphate it should be stable for more than a hundred years.

41.5 ANALYTICAL METHODS FOR CYANOGEN CHLORIDE

41.5.1 Acidity

Determination of acid in cyanogen chloride by titration in aqueous solution is not very satisfactory because HCl-catalyzed hydrolysis increases the acidity. Rapid withdrawal of the cyanogen chloride from the water by CCl_4 extraction, followed by titration of the aqueous layer, gives far more dependable results. If polymer is present, it is well to eliminate it by distillation, preferably in vacuo.[7]

41.5.2 Water

Three methods are suitable for determination of water in cyanogen chloride: observation of the temperature of cloud disappearance in a well-dried solvent (correcting for the effect of HCl),[7] distillation through a weighed P_2O_5 tube and observing the gain in weight,[10] and measurement of the acetylene produced by reaction of the sample with calcium carbide.[7] The first two methods are suitable only for fairly fresh material containing no polymer, whereas the last method remains accurate until carbon tetrachloride appears, when water would be absent in any case. These methods are dependable only if the operating personnel is especially trained in their use.

41.5.3 Degradation Products

Specific methods for determining the several products of deterioration of cyanogen chloride are lacking. One can distinguish roughly between soluble and insoluble residues,[10] and the former are well indicated by an increase in the density of liquid cyanogen chloride.[7] The absorption spectra of the soluble products are too similar for easy distinction in mixtures. Volatile products, such as CCl_4, C_2HNCl_4, $(CN)_2$, HCl, CO_2, and CO, can be separated in the high-vacuum manifold and recognized by their physical properties.[7]

41.6 SUMMARY

The chief objection to the use of cyanogen chloride as a CW agent has been its tendency toward explosive polymerization. This reaction is now well understood as due chiefly to acid catalysis, and the substances which cause this are known. Since it is not economical to eliminate the three most common sources of trouble, namely, hydrogen cyanide, water, and iron, it is well to stabilize the crude product by addition of a substance which works against both iron and acidity. Organic liquid stabilizers have not proved adequate, but cyanogen chloride stabilized by sodium pyrophosphate seems to be permanently dependable. The stability of the cyanogen chloride produced at Azusa is predicted to be maintained for about three or four years, without stabilizers.

Chapter 42

STABILIZATION AND FLAME INHIBITION OF HYDROGEN CYANIDE

By *Anton B. Burg*

42.1 INTRODUCTION

HYDROGEN CYANIDE has long been known as a very fast-acting and efficient toxic gas, sufficiently cheap, easy enough to handle in munitions, and having adequate volatility, for satisfactory use as a nonpersistent chemical warfare agent. It offers the further advantage of fairly easy penetration of many gas mask canisters, without any very strong warning odor. In spite of such favorable properties, this agent has two major disadvantages in that it is occasionally unstable and it is frequently destroyed by flame during dispersal from bursting bombs. The problem of stability seems to have been fairly well solved, but inflammability remains a major difficulty, not wholly avoidable by present methods except under certain special conditions.

42.2 STABILIZATION

The question of the stability of high-purity hydrogen cyanide was quite serious at one time, for storage of this substance as a liquid in steel containers usually resulted in a brown discoloration followed by powerful explosions, destructive of personnel and matériel. This trouble has nearly disappeared as a result of investigations of stabilizers during the period between world wars. Both the du Pont Company and American Cyanamid Company were active in such research, and more than three thousand compounds were tested as stabilizers. As a result, du Pont chose phosphoric acid, which works against a destructive accumulation of basic catalysts for decomposition, while Cyanamid preferred sulfur dioxide for its action as both antibase and antioxidant. The Chemical Warfare Service now specifies addition of 0.07% H_3PO_4 and 0.25% SO_2 for combined action. Accelerated tests at 65 C, in munitions at Dugway Proving Ground, and on the laboratory scale in Pyrex tubes with steel inserts (by NDRC), have shown that it is quite safe to store the doubly stabilized HCN during long periods of time at ordinary temperatures. Tests in Pyrex tubes further indicate that it will be safe to use containers made of or lined with aluminum or copper (but not magnesium) for HCN containing the stabilizers.

The glass tube experiments have shown that the combination of two stabilizers for HCN really is better than either stabilizer alone. One reason may well be that due to the protective action of SO_2, the steel walls of the container tend less to deplete the supply of phosphoric acid. With phosphoric acid alone, this depletion may be serious, although occasional renewal of the phosphoric acid by direct addition will save even very discolored hydrogen cyanide.

As a result of such studies, personnel at Dugway Proving Ground developed a technique for forcing phosphoric acid into large (M78 and M79) bombs, as an effective means of saving off-color HCN in such bombs.

In relation to the use of hydrocarbons in HCN (in order to inhibit ignition of the expanding cloud from a bomb) the effects of 70-octane gasoline, pentanes, and hexanes, upon the stability of HCN, were studied.[1–3] In glass tubes with steel inserts, HCN stabilized by SO_2 and H_3PO_4 survived over a year at 65 C, with or without the hydrocarbons.

Further NDRC studies on the stability of HCN included investigation of the effects of various materials likely to be met in munitions. Lead carbonate luting pastes have long been recognized as damaging to stability, but a special TiO_2-base luting paste proved quite harmless. Solvents such as CCl_4 or C_2Cl_4 also have no ill effects. Tests in Pyrex tubes indicated that powdered copper (found in captured Japanese frangible glass HCN grenades) is a very effective stabilizer. Cyanogen chloride (5%) is an even more effective stabilizer for HCN in contact with iron in Pyrex tubes, but becomes quite destructive in proportions above 20%. It is to be reiterated that these tests were done in Pyrex containers, which may not perfectly duplicate actual steel munitions. Thus, it is possible that stabilizers having only an antibase action will work well against the alkaline effect of glass, but have far less effect against oxidizing agents, or that a stabilizer which works well in a steel container will be far less effective in the presence of glass. On the whole, however, it is believed that a

stabilizer may safely be trusted if it works well in a glass tube test, whereas the rejection of a stabilizer on the basis of such tests may not always be final.

42.3 INFLAMMABILITY OF HYDROGEN CYANIDE

Inflammability was recognized as a major problem when field experiments on hydrogen cyanide were attempted at Dugway Proving Ground, at Bushnell, Florida, and in Panama. The exact conditions which will lead to *flashing*, or ignition, during the bursting of the HCN-filled munition, are not known with any high degree of certainty; it is known only that some HCN munitions are less likely to flash than others, but that some which are presumed safe from flashing, ultimately may perform badly under new circumstances.

The actual manner of ignition during a bomb-burst is fairly clear: during the first phase of the burst, no ignition can occur because there is too little air to support combustion; then as the HCN becomes diluted with air the small flame of the burster spreads through the expanding cloud. Thus, three general approaches to the problem are recognizable: (1) the use of *cold* burster charges, which will not ignite any inflammable gas cloud; (2) increasing the power of the burster to such an extent that the agent flies outward at a rate faster than the flame can follow; or (3) adding some substance to the HCN which will either wholly suppress its inflammability or so slow the rate of flame propagation that the burster flame cannot follow the expanding cloud. The first two approaches would have required new specifications on bursters, and a great deal of field work which could hardly be accomplished during the relatively short period of our war effort. The third approach was the subject of much laboratory and field work, leading to some improvement over the original situation.

42.4 LABORATORY STUDY OF FLAME INHIBITORS

The laboratory work was started on the assumption that the burning of HCN in air might involve a free-radical chain mechanism, which might be suppressed by addition of some other substance capable of capturing the radicals and breaking the chain reaction. A number of additives actually do lower the upper concentration limit of inflammability, and some quite specifically decrease the rate at which the flame travels through the HCN-air mixture. Such effects, however, seem not to be correlated with any tendency of the additives to capture free radicals. Thus CCl_4, C_2Cl_4, C_2HCl_3, ClCN, $AsCl_3$, SO_2, $SOCl_2$, water, CH_3Br, propylene oxide, cyclohexane, tetramethyl lead, methyl formate, acetaldehyde, and methanol, used in proportions of 0.1 to 12 mole per cent, either have no noticeable effect, or actually increase the violence of HCN explosions. Some hydrocarbons compete with HCN for reaction with oxygen, thereby lowering the upper limit of inflammability. Many of these also decrease the rate of flame travel even at medium concentrations of HCN in air.

The failure of several typical chain-breaking substances to inhibit the HCN-air explosion leads to doubt of the free-radical hypothesis. This doubt seems entirely justified in view of other experiments designed to test the free-radical mechanism. Unlike most chain reactions, the HCN-air flash shows but little dependence upon pressure or upon surface area. Photochemical activation, at temperatures just below the flash point, also seems to be ineffective; apparently such free radicals as may be formed are not able to initiate any chain reaction.

In default of the free-radical hypothesis, or any other evident source of understanding of the flame reaction, further laboratory work becomes empirical. Mild inhibiting effects were observed after addition of acetone, ethyl ether, methyl cyclopentane, ethylene, 1,2-dibromoethane, methyl chloride, methyl iodide, carbon disulfide, benzene, cyclopentane, or propane. Much more effective were hydrogen selenide and mixtures or single isomers of amylene, pentane, hexane, or heptane. These usually lowered the upper limit of inflammability far more than in proportion to the amount added. Instead of the usual sharp explosion of HCN in air, the reaction was slowed down to an observable flame front, moving as slowly as 2 fps in some cases.

42.5 FIELD STUDY OF ANTIFLASH AGENTS

As a result of the visual evidence that hydrocarbons in the light-gasoline range serve both to lower the upper limit of inflammability of HCN in air and to decrease the rate of travel of the flame through the HCN-air mixture, field tests of the effects of such hydrocarbons in actual bombs were undertaken at Dugway Proving Ground. M47A2 bombs were chosen for these tests because of the earlier experience that

SECRET

about 35% of all such bombs would flash the HCN during dispersal. The tests were quite successful, in that 39 M47A2 bombs, which were filled with ordinary stabilized HCN and 3 or 5% of isopentane, neohexane, 2-methylbutene-2, mixed amylenes, or 70-octane gasoline, were exploded without flash, while three of the eight control-test bombs (without hydrocarbon) ignited the HCN in a great blaze. One hydrocarbon-treated bomb did flash, but this was a case of low-order bursting, in which only the upper half of the bomb was opened. A pool of liquid HCN remained in the lower half and was ignited. This case serves to emphasize that hydrocarbons are useful flash inhibitors only for normally bursting bombs. They will not prevent ignition of a stationary pool or slowly expanding cloud of HCN.

The extent to which hydrocarbons will inhibit flashing of HCN in larger bombs remains uncertain after tests by the Dugway Mobile Unit at Bushnell, Florida. Some M79 bombs flashed in spite of added gasoline, but adequate control comparisons were lacking. Another difficulty was that the miscibility of the gasoline in HCN was limited to 3%, and this small proportion might not be very effective. Hexane is far more miscible (4 to 7%, depending upon temperature), but pentane is preferred because it is still more so (6 to 11%). Proper field testing of the effect of 5 to 10% pentane in large HCN bombs is a matter for further recommendation. This could not be done at Dugway Proving Ground, because the large bombs seldom flash at that altitude, but such tests, with proper controls, should be feasible at sea level.

Chapter 43

WIND-TUNNEL STUDIES OF FOG DISPERSAL, GAS DIFFUSION, AND FLOW OVER MOUNTAINOUS TERRAIN

By *Hunter Rouse*

43.1 INTRODUCTION

PROBLEMS OF FLUID MOTION which are too complex for analytical solution and too extensive for full-scale investigation are, in such fields as aeronautics and hydraulics, generally handled by means of tests on scale models. Once the conditions essential to dynamic similarity between model and prototype have been established, such model tests are certain to result in a tremendous saving in time and expense, for the variables may be controlled with laboratory precision over as great a range as desired, and exploratory measurements convertible to full-scale conditions may rapidly be made for any arbitrary combination of variables.

Three types of problem in fluid motion posed by the Armed Services of World War II were of a nature which recommended use of the model technique yet differed sufficiently from standard practice to require the development of new facilities and new methods of testing. Preparation of a low-velocity wind tunnel for this purpose is described herein, and details are given of the experimental apparatus and the general methods of measurement and evaluation of results. Use of the test facilities in determining heat requirements for the burner method of fog dispersal, as requested by the Navy Bureau of Aeronautics, is discussed, and a generalized analysis of heat-diffusion measurements is presented and applied to a specific installation in the Aleutians. The development of high-capacity burners for either gasoline or fuel oil is explained. Attention is given to the use of both heated wind curtains and wind-curtain-and-burner combinations as means of reducing the waste of fuel characteristic of the burner method. A detailed analysis is also made of the relative costs of burner and wind-curtain systems.

Application of the model technique to problems of gas and smoke diffusion for the Chemical Warfare Service is next described. Through use of schematic structural forms, it is shown that the eddy patterns and the corresponding rates of diffusion in urban districts are controlled by the boundary geometry, regardless of scale or wind speed, and that the model results may therefore be generalized. The results of tests for steady gas release in models of schematic urban districts and typical Japanese cities are then presented in generalized form. Thereafter, a means of evaluating the concentrations that would be caused by full-scale bursts is indicated from model measurements of continuous gas release. Correlation of model tests with field measurements completes the discussion of gas diffusion.

A brief description follows of the model study of terrain effects upon wind structure, as undertaken for the Army Air Forces. The results of exploratory measurements of velocity and turbulence distribution over a model of the Tokyo region are described. Preliminary tests upon the influence of vertical distortion of the boundary, preparatory to studies of wind patterns over models of Puerto Rico under direct contract with the AAF, are finally interpreted.

43.2 MODEL TECHNIQUE IN THE LOW-VELOCITY WIND TUNNEL

Despite the great advancements which were made in the science of fluid motion between World Wars I and II, only a few flow problems of technical importance became subject to complete analytical solution. On the other hand, application of similitude principles known long before World War I progressed to such an extent that every new airplane, projectile, and battleship was finally designed on the basis of scale-model investigations in the wind tunnel, water tunnel, or towing tank.

The similitude principles in question stem from three fundamental relationships of fluid mechanics. For a given geometrical form of the flow boundary, the pattern of motion (and hence the distribution of pressure, velocity, and turbulence) is known to be a unique function of three dimensionless parameters called the Froude number, the Reynolds number, and the Mach number. The Froude number is a measure of gravitational influence upon the flow; it has the form $V/\sqrt{L\Delta\gamma/\rho}$, in which V is a velocity, L a length,

$\Delta\gamma$ a difference in specific weight, and ρ a density. The Reynolds number is a measure of viscous influence upon the flow; it has the form $VL\rho/\mu$, in which μ is a viscosity and V, L, and ρ have the same significance as before. The Mach number is a measure of elastic effects; it has the form $V/\sqrt{E/\rho}$, E being the bulk modulus of elasticity.

As a first approximation, any flow problem may be regarded as predominantly gravitational, viscous, or elastic. The flow characteristic under study should then be obtainable analytically or experimentally as a function of the corresponding dimensionless parameter. Since a dimensionless plot of this function is not restricted to any one scale or fluid, it should be equally applicable to model conditions in the laboratory and prototype conditions in the field. In a word, determination of the function by model tests at once makes available the required characteristics of full-scale design.

Under many circumstances it is not necessary to establish the entire trend of such a functional relationship, particularly if only one specific set of prototype requirements is to be determined. Since this set of requirements automatically establishes a particular value of the Froude, Reynolds, or Mach number, it is merely necessary to conduct a model test at the same value of this number to yield the desired information.

Inasmuch as gravitational, viscous, and elastic effects in actuality seldom occur singly, such approximations sometimes require further refinement if considerable accuracy is to be obtained. This is particularly true if gravitational and viscous influences are of the same order of magnitude. Unfortunately, as inspection of the Froude and Reynolds numbers will show, it is impossible to secure both viscous and gravitational similitude between model and prototype if the same fluid is used, since one requires an increase in velocity, and the other a decrease, as the linear scale is reduced.

In spite of these limitations, the model method of analysis provides manifold advantages in the approximate solution of such complex phenomena of flow as the majority of technical problems involve. Since the time and expense of a test program vary nearly as the cube of the linear scale, the economy of small-scale tests in comparison with full-scale investigations is obviously tremendous. In the laboratory, moreover, the essential variables may be controlled at will, with the twofold result that exploratory studies may be made over a range that would be prohibitive in the field, and yet any set of conditions may be duplicated at any time. To offset the very pertinent disadvantage that it is impossible to reproduce in a model every single factor that may influence the prototype phenomenon, one need only note that the possible combinations of such factors are usually so vast in number that their systematic field investigation would likewise be out of the question.

With the greatly increased complexity of present-day warfare, it is not surprising that new problems of fluid motion, never before studied at model scale, should arise. Three of these in turn were proposed to the Iowa Institute of Hydraulic Research of the State University of Iowa: (1) the characteristics of gas diffusion in urban districts; (2) the characteristics of heat diffusion in fog-dispersal installations; and (3) the characteristics of eddy diffusion in winds over mountainous terrain. For the first of these experimental projects a special low-velocity wind tunnel was constructed, together with the necessary measuring apparatus. The basic similarity of the second and third projects, however, permitted much of the same equipment and experimental technique to be used. In fact, the first and third, though differing considerably in ultimate goals, were almost identical in fundamental nature; the second differed only to the extent that gravitational effects played the fundamental role.

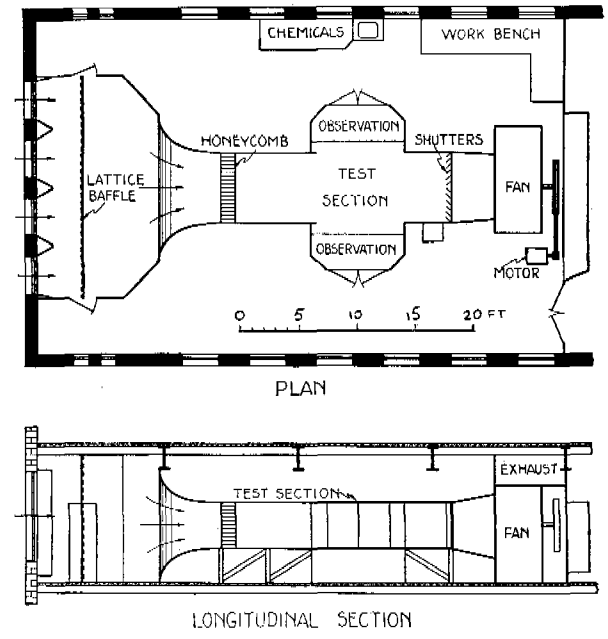


FIGURE 1. Wind-tunnel details.

The wind tunnel constructed for these studies [1] consisted of a 20-ft duct of uniform rectangular cross section 6 ft wide and 4 ft high. At the inlet end (see Figure 1) was a large stilling chamber provided with baffles to eliminate disturbances in the air drawn from outside the laboratory structure, a bell entrance and honeycomb yielding an even velocity distribution and low degree of turbulence in the tunnel test section. The outlet of the duct was connected to the suction side of a 35,000-cfm fan, which exhausted outside the building. Adjustable louvers between the tunnel and blower permitted a fine control of the wind speed from 1 to 25 fps. Along the ceiling of the tunnel was a four-rail track providing longitudinal travel of a gauge carriage, which in turn provided lateral and vertical motion of any instruments mounted thereon. Scales and verniers yielded coordinate locations of the instruments to 0.001 ft. These instruments, as well as the wind speed, were controlled from closed observation chambers on either side of the test section.

Instruments used in flow measurements were the following: (1) a direct-reading generator anemometer, for approximate observation of the mean wind speed; (2) a sensitive anemometer (Figure 2) with revolution

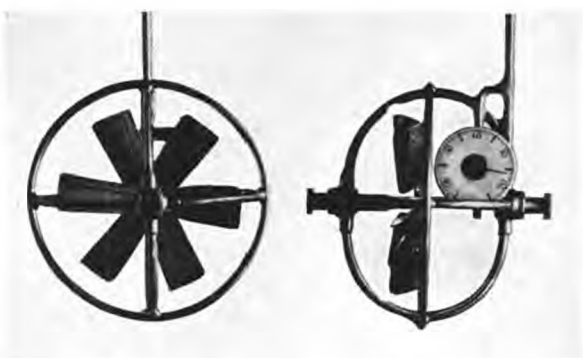


FIGURE 2. Anemometer; runner diameter 1¼ inches.

indicator for local wind speeds from 0.75 to 10 fps; (3) a Prandtl-Pitot tube and Wahlen gauge, for wind speeds above 5 fps; (4) a 6-tube direction-indicating instrument (Figure 3) which, in combination with the Wahlen gauge, provided readings of the magnitude of the velocity vector and its horizontal and vertical deviations from the longitudinal direction; (5) a Dickinson meter for determining gas concentrations, the intake and cell of which were mounted on the gauge carriage for point sampling; and (6) a series of copper-constantan thermocouples, and a portable precision potentiometer for temperature traverses.

Jet manifolds for propane gas were located in the stilling chamber, or could be inserted in the tunnel floor at desired locations, to produce thermal stratification of the wind stream. Dry ice was also used for this purpose. SO_2 could be introduced through the same manifolds, or from suitably located point sources. For visual or photographic study of flow patterns by means of smoke filaments, air which passed over titanium tetrachloride could be injected through similar point sources. The large-scale generation of smoke for observational purposes was accomplished by vaporizing oil in the exhaust duct of a small gasoline engine.

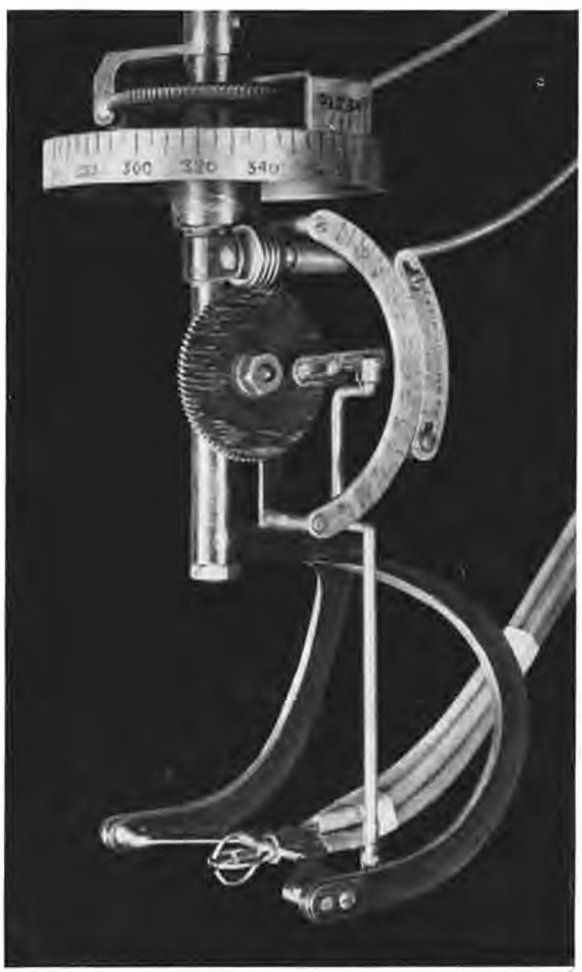


FIGURE 3. Directional velocity indicator.

In general, the technique of experimentation was as follows. On the basis of existing theory and experience, the essential variables of the problem in question were combined through the II theorem of

SECRET

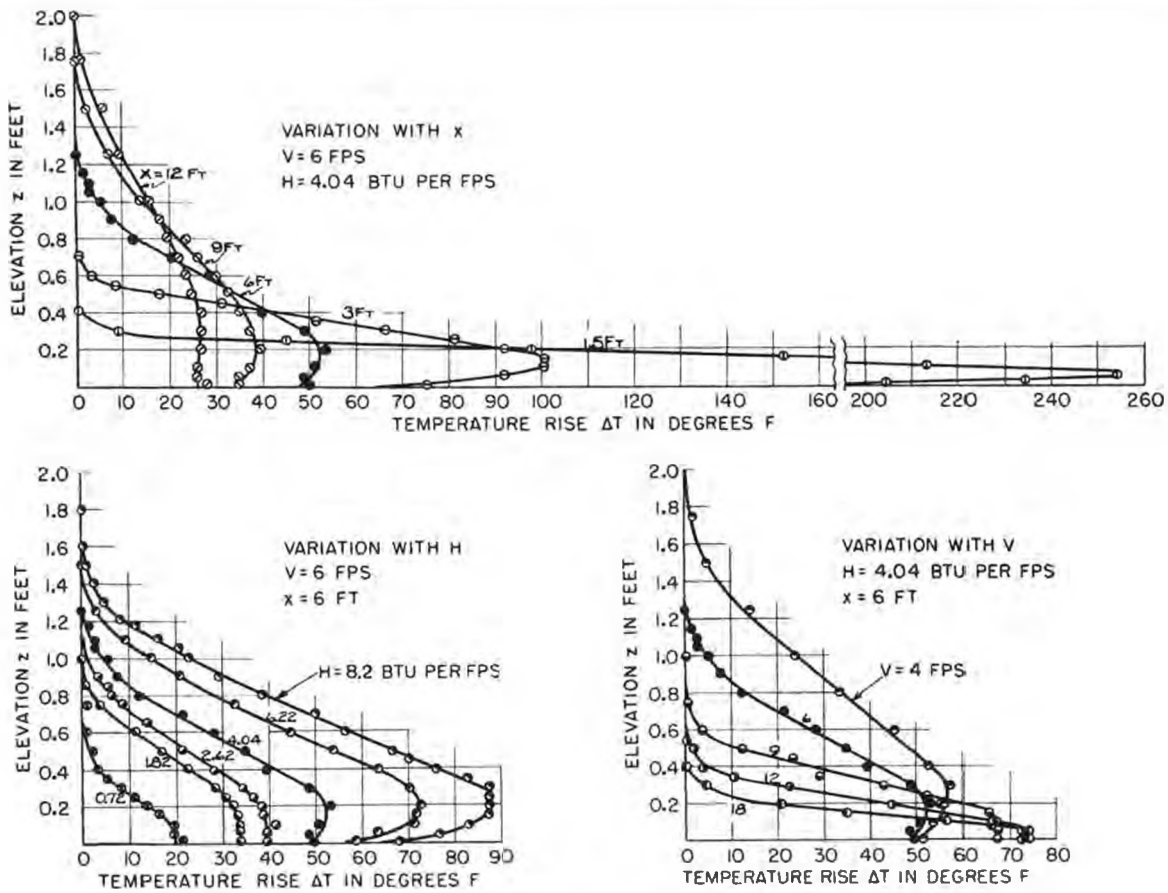


FIGURE 4. Variation in vertical temperature traverse with x, H, and V.

dimensional analysis into a series of dimensionless parameters, one of which was expressed as a function of the others. Since these parameters formed the basis of the required similarity of model and prototype conditions, whenever possible the validity of the parametric grouping was checked experimentally at different magnitudes of the individual variables (such as scale or velocity). Once such a check was at hand, the detailed model tests were conducted, the dimensionless form of the results making them immediately applicable to prototype scale. In most cases, known field conditions were simply duplicated at specific values of the dimensionless parameters. Sometimes, however, it was desirable to determine, or at least approximate, the form of the functional relationship. This was accomplished by judicious selection of the flow variables, so that the desired range of variation could be covered systematically without wasting time in haphazard measurements. The function was then evaluated graphically in terms of the pertinent parameters as coordinates.

43.3 EXPERIMENTS ON FOG DISPERSAL

Soon after the beginning of the mass bombing of Axis countries by planes based in England, it became apparent that more planes were being lost through crash landings in English fog than through flak and fighter attack over the continent. For this reason the problem of freeing landing fields from fog was given very high priority, and all possible methods of improving visibility were tested by British and American scientists and engineers.

Such methods may, in brief, be grouped into three classes: (1) the induced coalescence of fog droplets to form drops of sufficient size to fall as rain, (2) the removal of excess moisture from the air by chemical drying, and (3) the evaporation of the fog by raising the air temperature. Of the first class, the possibility of spraying water into the air to combine with the fog droplets was suggested but never tried, while the use of low-frequency sirens to produce coalescence by vibratory means received but one inconclusive field

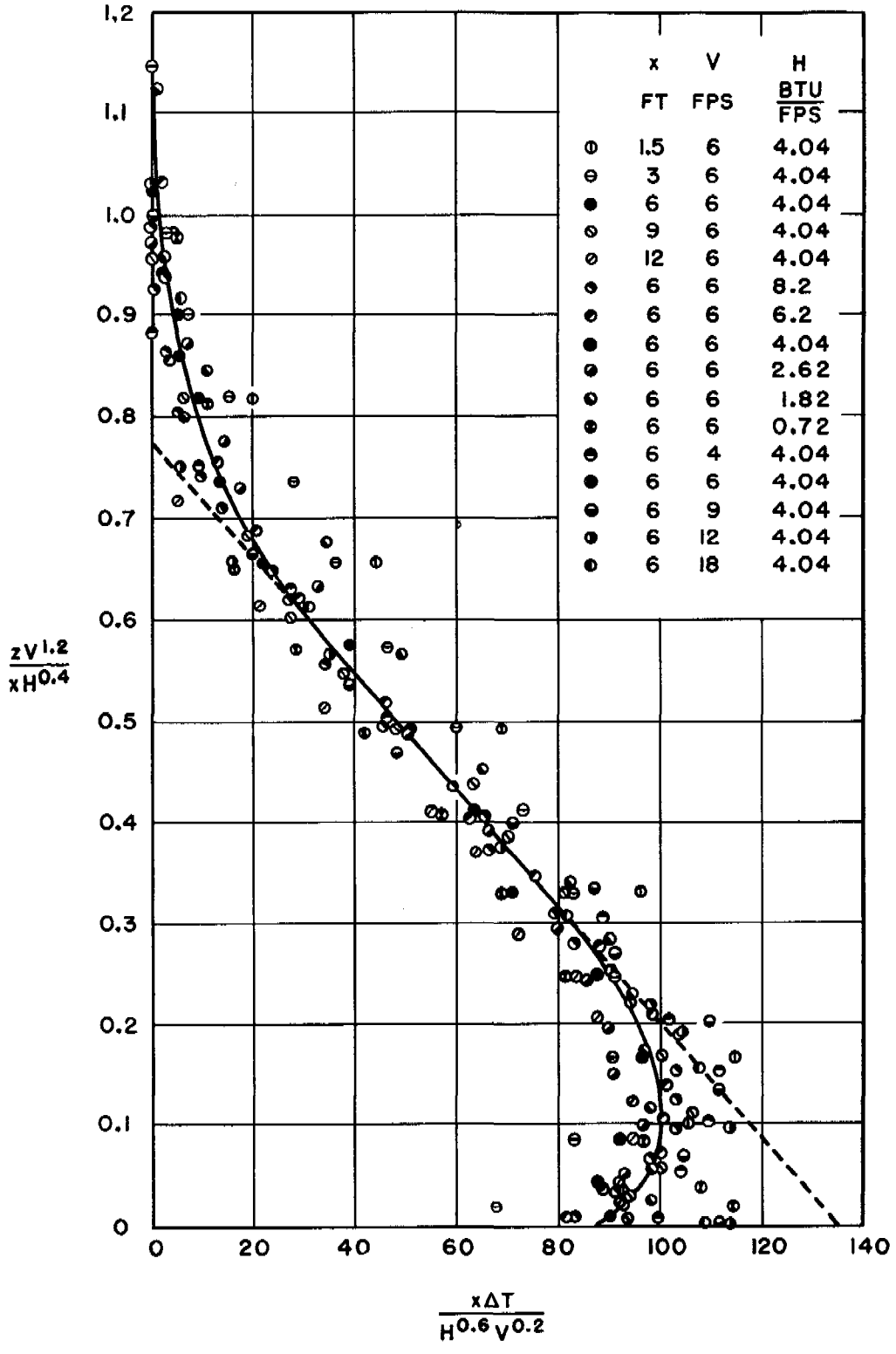


FIGURE 5. Composite plot of vertical temperature traverses for all values of x, H, and V.

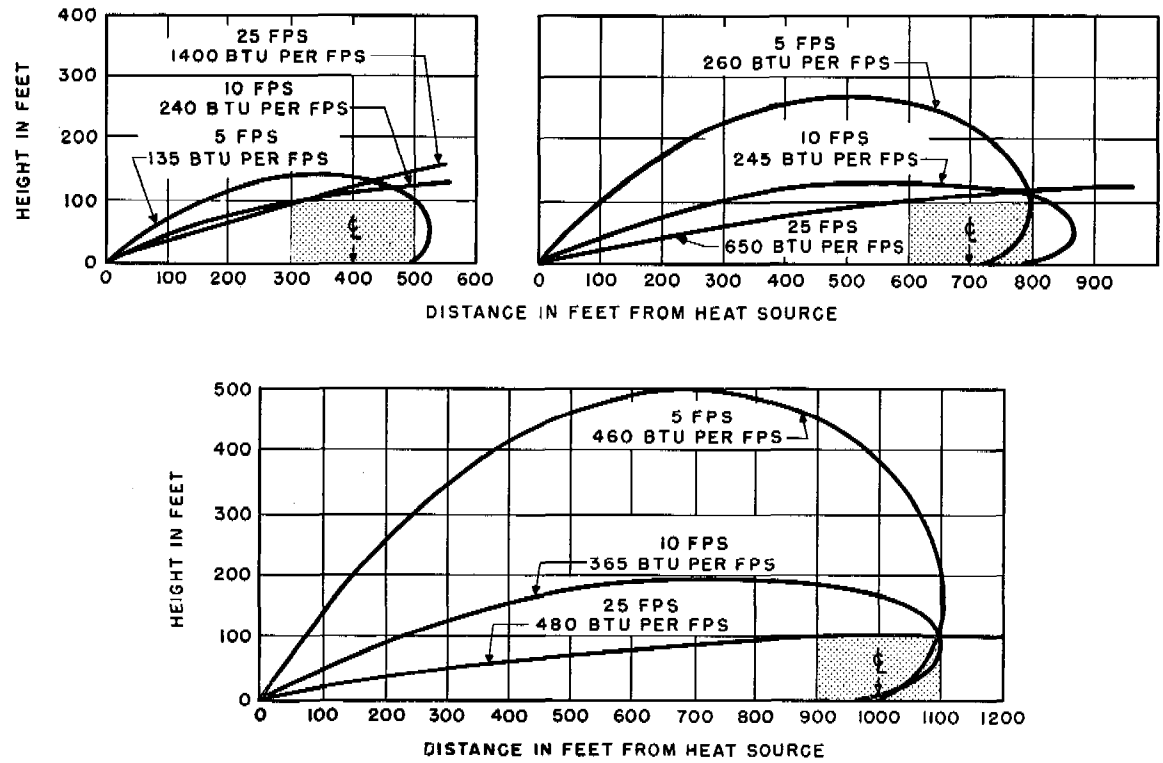


FIGURE 6. Typical 5 F isotherms for various crosswind velocities and distances of heat source from centerline of runway.

test. Of the second class, the injection of calcium chloride into the air with portable blowers was tested extensively [2] but not brought into practical application. The third class of dispersal method, however, received steadily increasing attention from the British, after it was determined that a temperature rise of 5 to 7 degrees Fahrenheit would effectively dispel the radiation type of fog prevalent in England. Early tests were made of burning coke in long trenches bordering the landing strips, but too much time was required to ignite and control the fires. Fuel oil, in turn, proved to yield too smoky a blanket of heated air to improve visibility. Ultimately, gasoline was found to give the desired results, and very extensive systems of preheaters and burners surrounding the field were devised, which would clear a satisfactory zone over the runway in the radiation type of fog without undue loss of time. These were described in a long series of British reports.

Such English fogs are characterized by relatively small thickness and near-stagnant air conditions. In fact, the heated clearance zone frequently extended entirely through the fog blanket, while the air flow induced by the thermal currents often resulted in local winds of greater magnitude than those accompanying the fog formation. On the other hand, if natural winds of appreciable speed prevailed during the clearance operation, the zone of clearance tended to be shifted off the runway in the downwind direction. Since fog formation in the United States and its possessions is generally not of the radiation type and may be accompanied by winds of considerable speed, the British experience with clearance methods was not considered a sufficient basis for the design of American fog-dispersal installations.

43.3.1 Burner Studies

At the request of the Navy Bureau of Aeronautics, the Iowa Institute undertook in the fall of 1943 the determination of heat requirements and proper burner location for securing clearance conditions over runways at various wind speeds. Instead of assuming a particular model scale for wind-tunnel measurements, an effort was made to analyze experimentally the general problem of heat diffusion from a line source at right angles to the direction of flow.[3]

The floor of the tunnel test section was suitably fireproofed, and a manifold containing a series of closely spaced jets for burning propane gas was built

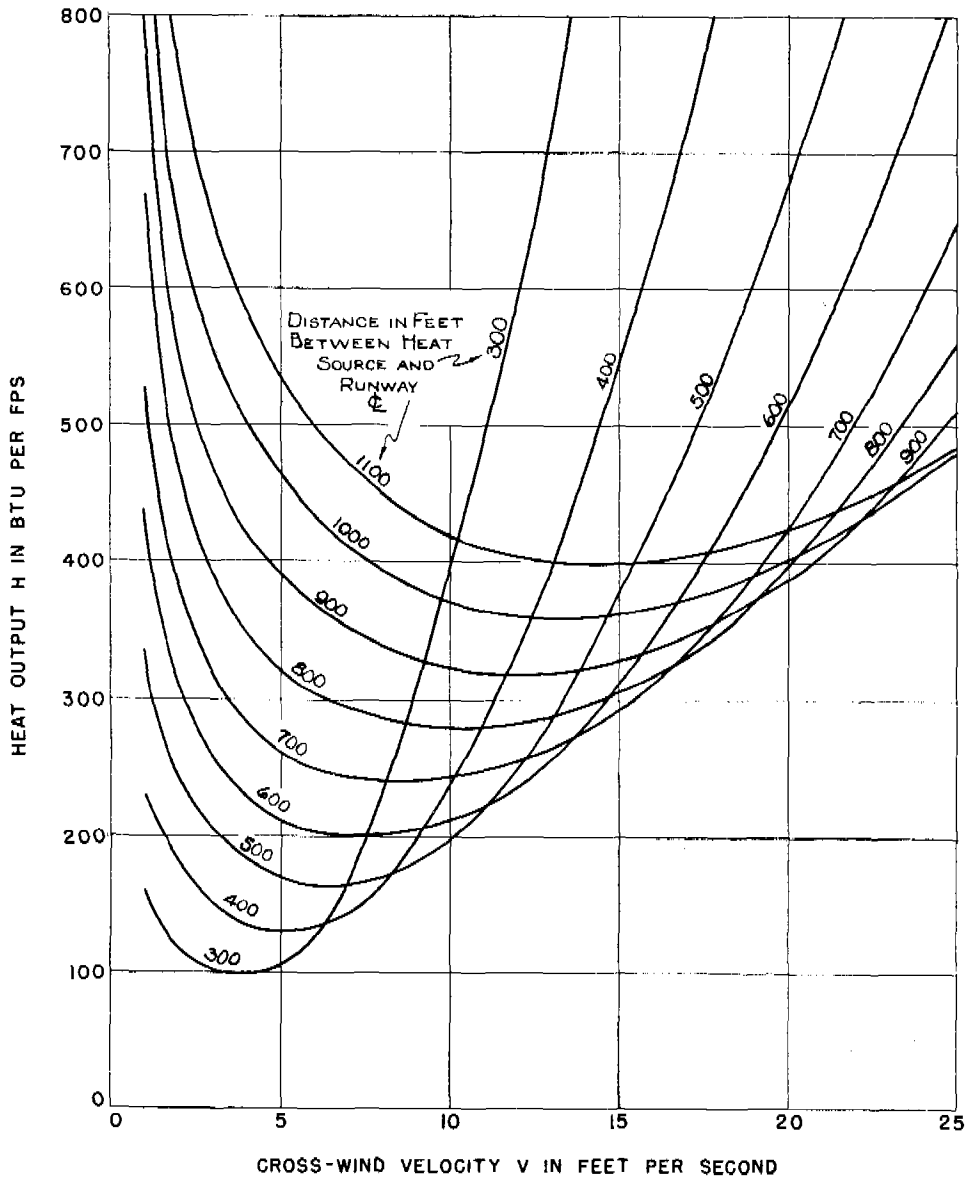


FIGURE 7. Curves of H vs V for various distances of heat source from runway centerline (ΔT = 5 F).

in across the tunnel. Means were at hand of varying the wind speed, the rate of combustion, and the elevation and longitudinal position of a thermocouple carriage. Preliminary vertical temperature traverses at various distances from the heat source (Figure 4) showed that the heated zone expanded essentially linearly with distance downwind, the rate of expansion increasing with increasing rate of heat output and decreasing with increasing wind speed. A series of vertical temperature traverses was then made, systematically covering the available range of wind speed, heat output, and distance downwind.

Analysis of the experimental results indicated that all temperature traverses, could, as a close approximation, be superposed to yield a single generalized distribution curve (Figure 5) if the ordinate and abscissa scales, respectively, had the form $zV^{1.2}/xH^{0.4}$ and $x\Delta T/H^{0.6}V^{0.2}$, in which

x = distance downwind, in feet;
z = elevation, in feet;
V = wind speed, in feet per second;
H = rate of heat output in Btu per foot per second;
ΔT = temperature rise, in degrees Fahrenheit.

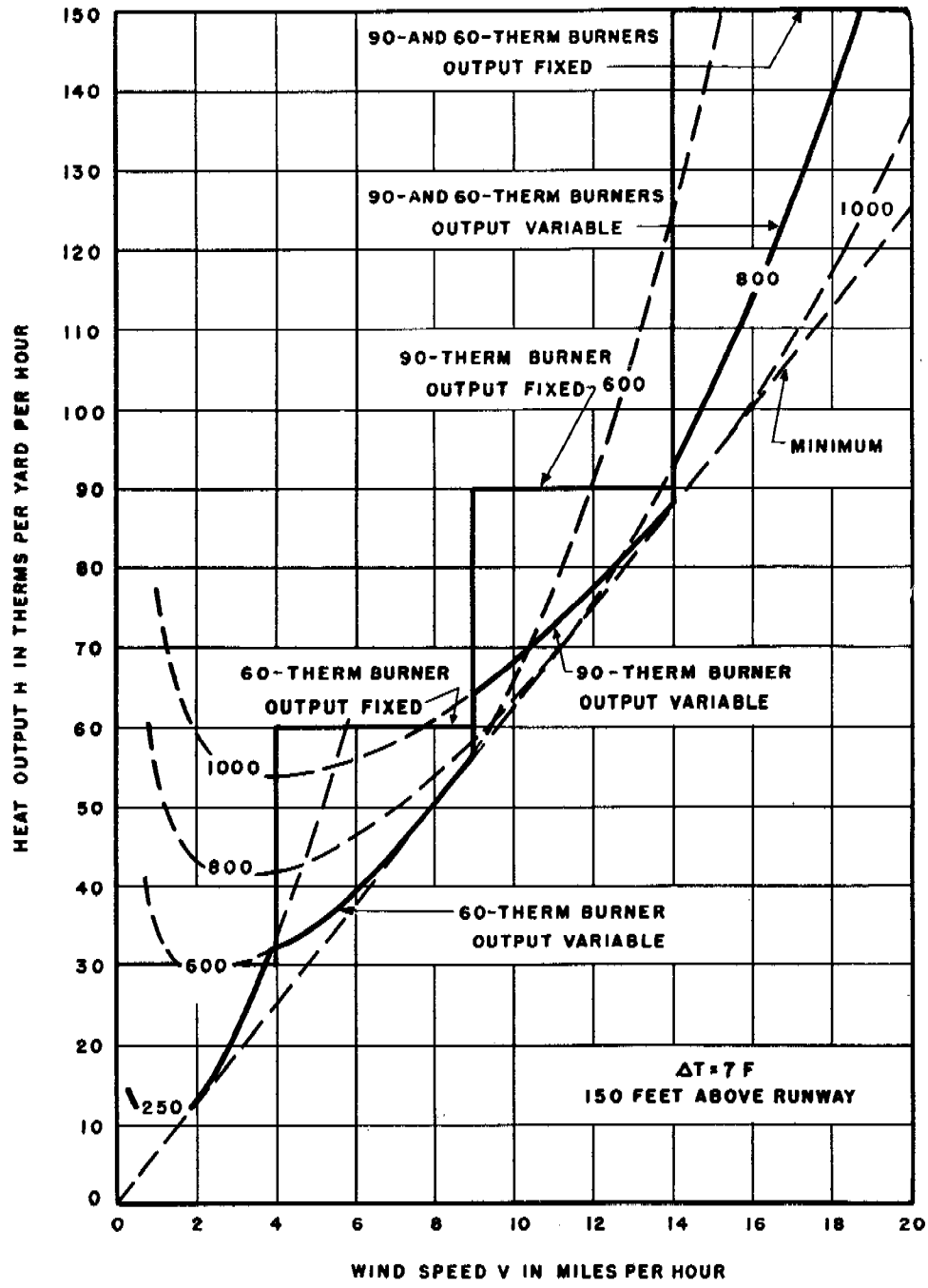


FIGURE 8. Recommended burner characteristics for Shemya installation. Plotted points and temperatures are typical data from recommended 10-ft burner with 36 jets.

Although these coordinate parameters are not dimensionless, it is to be noted that their product, when multiplied by γ and c_p (the unit weight and specific heat of the air), is truly a dimensionless quantity. The area of the surface bounded by the experimental curve, when multiplied by γc_p, therefore represents a numerical value embodying the approximate solution of the problem in question. That is,

$$\frac{\gamma c_p V}{H}\int \Delta T dz = 0.94.$$

Since the process of thermal convection is es-

sentially independent of viscous effects at the relatively high temperature differences studied in the wind tunnel, there appears no reason to doubt the validity of the function at prototype as well as model scales. In fact, the Froude criterion for similarity ($V^2 \sim L\Delta T$) is perforce embodied in the general functional relationship. That is, since for geometrical similarity z/x must be constant, the ordinate parameter indicates that $H \sim V^3$, substitution of which in the abscissa parameter yields $V^2 \sim x\Delta T$.

Interpretation of the generalized function is as follows: Let it be assumed that in a wind of speed V, a given rise in temperature ΔT is to be produced to a height z over a runway Δx wide by a burner located a distance x upwind from the runway centerline. If, for simplicity, the actual function of Figure 5 is approximated by the straight line

$$1.3\frac{zV^{1.2}}{xH^{0.4}} + 0.0074\frac{x\Delta T}{H^{0.6}V^{0.2}} = 1,$$

solution thereof will yield the required heat output H; moreover, the curve $z = f(x)$ for the corresponding values of V, ΔT, and H will enclose the zone throughout which ΔT is at least as great as that required (see Figure 6). If it is further assumed that the burner location is the most economical for the given wind speed (i.e., that H is as low as possible), the high point of the curve $z = f(x)$ will correspond to the top of the clearance zone. It follows that a change in either wind speed for the given burner location or in location for the given wind will result in asymmetry of the curve if ΔT is to remain constant. As a matter of fact, a burner properly located for a given wind will be inefficiently placed for a wind of any other speed, owing to the required increase in heat output to produce the necessary coverage in lower or higher winds.

If the temperature rise for clearance is specified, it is possible from the generalized diagram or simplified equation to plot a family of curves of heat requirements versus wind speed for a series of distances from burner to runway, as shown in Figure 7. Such a diagram will then permit rapid determination of most efficient burner location for most frequent operating conditions, and the heat requirements for all other wind speeds will be immediately at hand. However, even cursory inspection of the individual curves for a given burner-runway spacing will indicate the tremendous waste of fuel which must occur at all wind speeds which differ appreciably from that for which the design is made.

At the request of the Army Air Forces, the Bureau of Aeronautics of the Navy in 1943–44 installed on the island of Amchitka in the Aleutians a burner system based essentially upon the British methods. This installation was found to provide satisfactory clearance at low-wind speeds, but at moderate to high speeds the clearance zone was shifted off the runway in the downwind direction. When a similar request was made for an installation on the island of Shemya in 1944, the Iowa Institute was asked to make recommendations for burner locations and capacities based upon its previous findings, and upon further studies on relief models of the island.

After careful statistical evaluation of available weather data,[4, 5] it was decided to adopt the value $V = 20$ mph as the maximum for design purposes. Since investigation of existing terrain effects upon the rate of heat diffusion failed to reveal any appreciable change in the basic function, this function was then used to prepare the accompanying diagram (Figure 8) of heat requirements vs wind speed. In order to eliminate the considerable waste of fuel caused by use of a single burner line at other than the designed wind speed, it was recommended that the following three lines of burners be installed on the prevailing windward side: first, a line having an output of 30 therms per yd per hr at a distance of 250 ft from the runway centerline; second, a 60-therm line 600 ft from the centerline; third, a 90-therm line 1,000 ft from the centerline. For stagnant or near-stagnant conditions, similar 30-therm burners on opposite sides of the runway would provide the necessary circulation of heated air over the landing zone, as in the British installations. At wind speeds up to 9 mph the windward 60-therm line would be sufficient, and from 9 to 14 mph the 90-therm line would be used. For speeds as high as 20 mph, the 60- and 90-therm lines could be used in parallel.

As may be seen from the diagram, fixed-output burners would still result in an appreciable waste of fuel. This could be greatly reduced, however, through proper control of the heat output in approximate accordance with the magnitude of the actual wind speed. In other words, the series of abrupt steps on the diagram would then be replaced by the lower series of curves, which more nearly approach the minimum line.

Since the capacity of the larger burners required for this installation was well above that of the normal British burner systems, and since the Bureau of Aeronautics was desirous of having a burner which

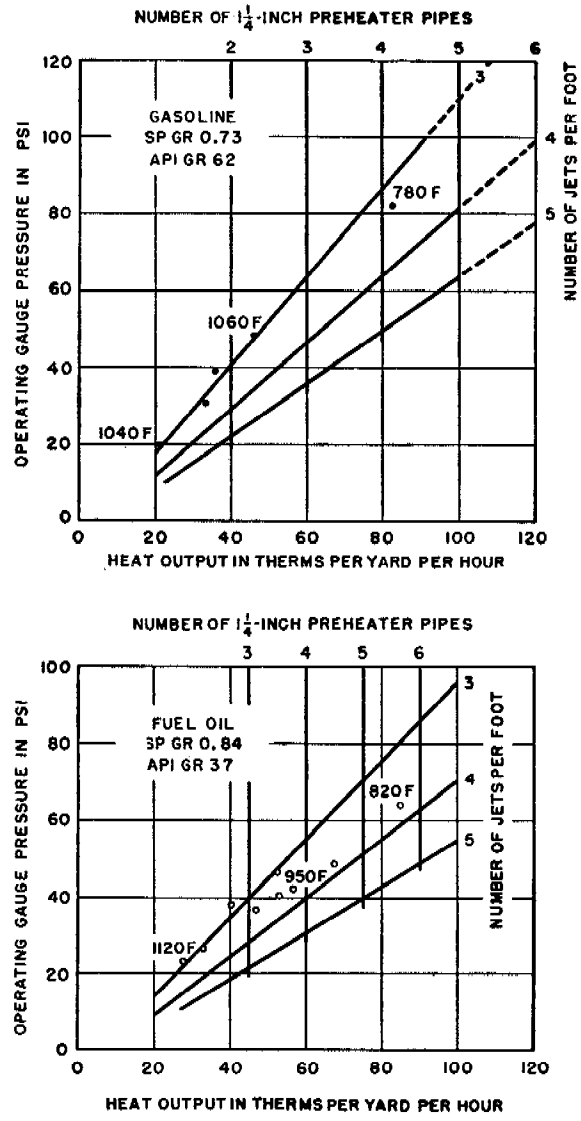


FIGURE 9. Design curves of pressure vs heat output for various jet and preheater-pipe arrangements.

would operate on fuel oil as well as gasoline, the Iowa Institute undertook the development of two types of large-capacity burner for this purpose. One of these, produced by the Department of Mechanical Engineering of the University of Iowa,[6] consisted of a rectangular preheater coil and central jet manifold in 6-ft units placed in shallow trenches. Twelve preheating jets in the bottom of the manifold continuously vaporized th incoming fuel, which burned with a luminous flame from eight main jets along the top. The capacity of this fuel-oil burner varied from 20 therms per yd per hr at 20 psi line pressure to 100 therms at 40 psi.

The burner developed by the Institute [7] consisted of a series of horizontal preheater pipes feeding a single jet manifold in the path of the horizontal flames from the jets. This burner had a capacity of 25 to 90 therms when using fuel oil, and 25 to 120 therms with gasoline, utilizing adjustable line pressures varying from 30 to 80 psi. In connection with its development, empirical diagrams (Figure 9) relating line pressure, thermal output, jet spacing, and number of preheater pipes were prepared.

Although the Shemya installation was never undertaken, owing to the unexpectedly rapid progress of the war with Japan, the several forms of burner were tested under field conditions at the Landing Aids Experiment Station [LAES] of the Bureau of Aeronautics at Arcata, California. Financed by the Iowa contract, but not supervised by the Institute, was the development [8] of a spring-loaded, high-pressure jet which would vary in outlet area as well as in velocity with change in line pressure. LAES reports on the performance of these burners were not available at the time of writing this report.

43.3.2 Wind-Curtain Studies

In view of the necessarily low efficiency of the burner method of fog dispersal, both British and American agencies experimented for several years with the general scheme of directing preheated air over the landing strip by means of blowers. Early attempts to mount heaters and blowers upon trucks proved impractical, because the great weight of the units deprived them of necessary maneuverability except on dry ground. Thereafter, the University of Illinois investigated, by means of model experiments,[9] the feasibility of forcing heated air through ducts terminating in long slots on each side of the landing strip. The vertical curtains of hot air formed by these slots induced a downward return flow over the landing strip at low to moderate crosswinds, the mixing of the heated air in the zone of circulation effectively raising the temperature in the clearance zone by the desired amount.

In order to determine the possibility of using a single wind curtain over a considerable range of wind speed, the Iowa Institute followed its burner studies with a series of wind-tunnel tests of wind-curtain characteristics.[10] Exploratory observations indicated that a vertical curtain of air in a crosswind would be deflected downwind in such manner (Figure 10) as to form a large ground eddy with axis parallel to the

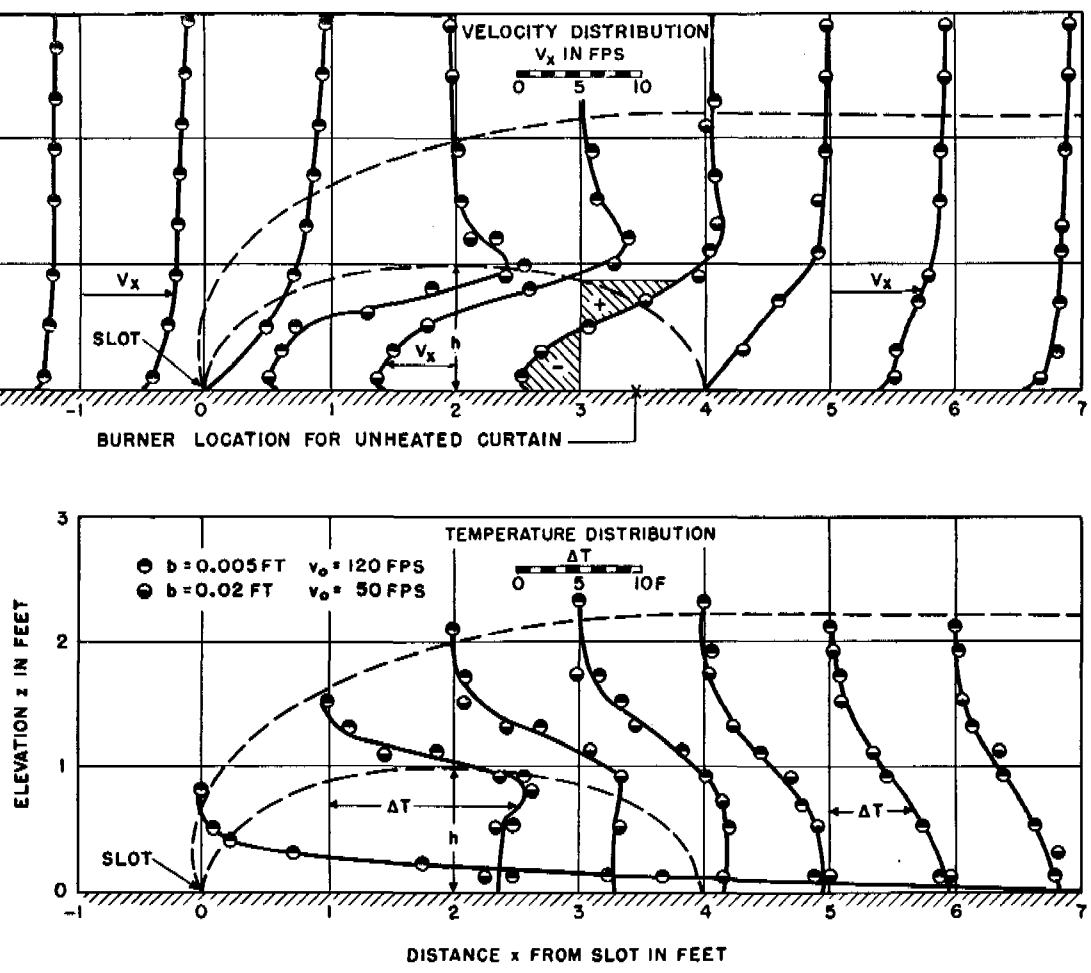


FIGURE 10. Velocity and temperature characteristics of a heated wind curtain.

slot and having a height approximately one-fourth as great as its width. The height h of this eddy evidently depended upon the wind speed V, the slot width b, and the efflux velocity v_0. The general relationship of these variables was then determined through systematic variation of all three, the data falling upon the empirical curve

$$\frac{h}{b} = 5\left(\frac{v_0}{V}\right)^{1.5}$$

over the maximum available range of variation. Since the phenomenon of air entrainment by jets is one of turbulent rather than viscous flow, the relationship determined in the wind tunnel is probably sufficiently free from scale effects as to be applicable to field as well as laboratory conditions.

If heated air is forced through such slots, on the other hand, one must assume that a Froude number $V/\sqrt{L\Delta T}$ should have the same magnitude in both model and prototype if the conditions are to be truly similar. However, subsequent wind-tunnel tests with heated air failed completely to disclose any effect of buoyancy upon the eddy form; thermal phenomena, in other words, appeared to be entirely secondary to the inertial reaction between the jet and the oncoming air. Moreover, the process of diffusion between the deflected curtain and the underlying eddy invariably resulted in a relatively uniform distribution of heat from the curtain throughout the underlying eddy, with the result that the heated wind curtain gave promise of being a far more efficient method of fog dispersal than the burner.

Evaluation of the heat requirements for a specific temperature rise, $\Delta T = 5$ F, over a 100-ft zone above a runway as a function of wind speed resulted in the linear relationship for power vs speed shown in Figure 11. The wind-curtain slot is assumed to be located $100 \times 4/2 = 200$ ft upwind from the runway

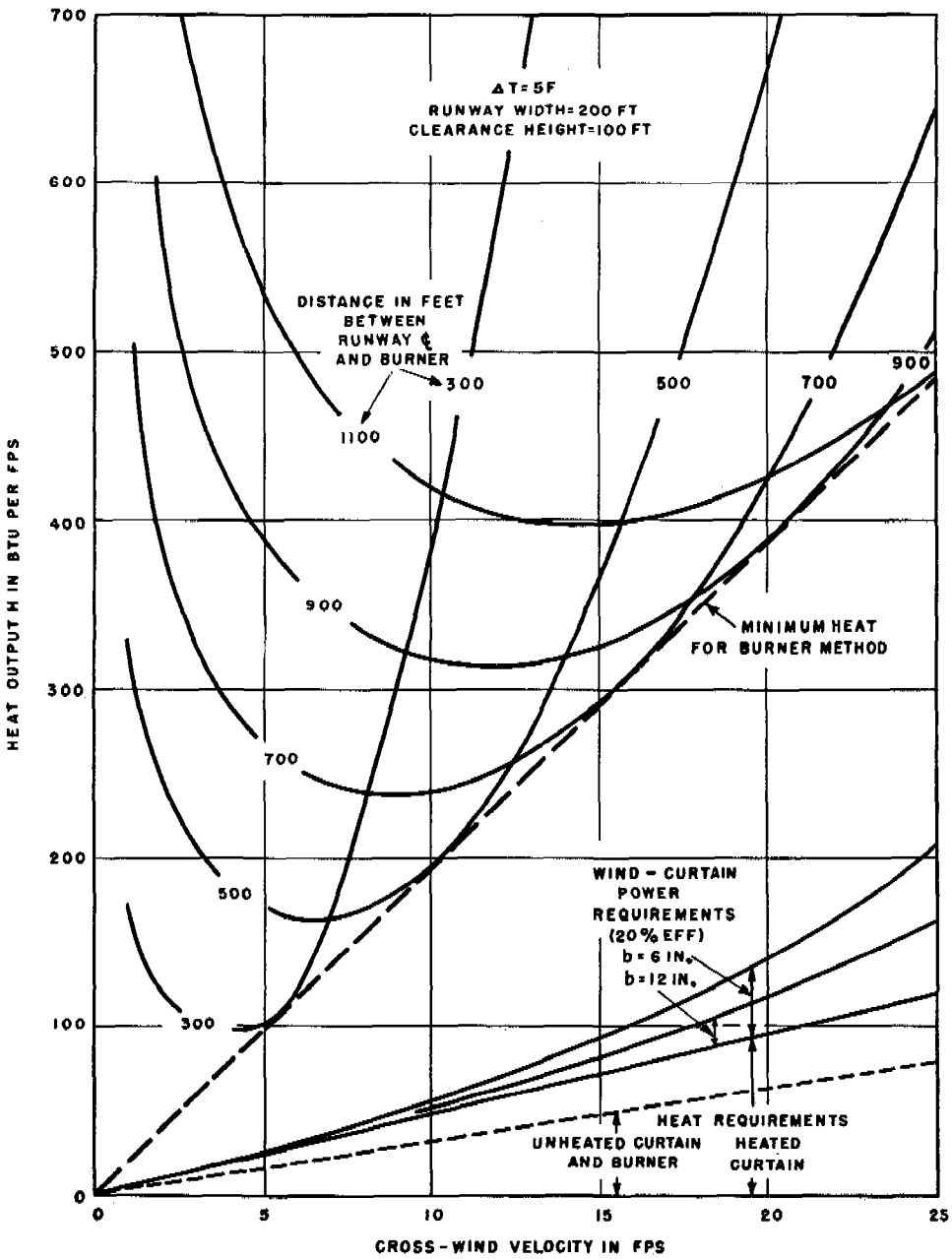


FIGURE 11. Fuel requirements of wind curtain vs burner.

centerline, and the power requirements include the cost of fuel for both the heaters and the engines for the blowers. Although the heat required remains the same, the power requirement is seen to vary with the width of curtain slots. In any event, the cost of operation of the wind curtain is found to be only 35% of the very minimum for the burner under identical wind conditions.

Owing to the fact that an appreciable portion of the heated air discharged from the curtain slot passes downwind without being entrained in the ground eddy, the possibility of increasing efficiency and reducing installation costs through combination of a nonheated wind curtain with a surface burner was investigated. A burner line was placed on the downwind side of the runway, but within the zone of reverse flow of the ground eddy (see Figure 10). The heat from the burner was diffused throughout the

eddy to a desirably uniform degree, and evaluation of temperature traverses yielded the line of heat requirements shown as a broken line in Figure 11. Evidently, a further saving of some 10% of burner costs can be expected from such an arrangement.

Since the foregoing tests were restricted to winds at right angles to runway and wind curtain, supplementary studies were made for other wind orientations. It was found that while use of the wind speed itself yielded computed values of the eddy width (measured normal to the runway) which were smaller than those measured, use of the normal component of the velocity vector gave results which were as much too large. Therefore, evaluation of the curtain velocities for required eddy widths could safely be based upon the actual magnitude of the wind speed for angles as low as 30° between wind direction and runway centerline. For winds down the runway, an end curtain extending perhaps 4 times the runway width and having twice the capacity of the longitudinal curtains should, in combination with both longitudinal curtains, provide ample distribution of heat for clearance. Since a curtain would be required along each side of the runway to counter winds from any direction, a double curtain would thus be available for wind speeds approaching zero.

The primary disadvantage of the wind-curtain in comparison with the burner method is the relatively great initial cost of the engines, blowers, and ducts which it requires. In the belief that its greater economy of operation might nevertheless offset this disadvantage, the Iowa Institute undertook the compilation of estimated costs of constructing and operating the two types of fog dispersal under identical conditions.[11]

From information obtained at Wright Field, the cost of installing burners along the two sides of a runway would be approximately $40,000 per 1,000 ft of runway. Based upon current cost of labor and materials, construction of a similar double length of the wind-curtain system would require some $1,500,000. Minimum operating costs of the burner in a 15-mph wind would amount to about $4,000 per hr, and for the wind curtain about $1,000 per hr, i.e., an hourly saving of $3,000. If it is assumed that fog and landing frequencies require perhaps 200 hr of clearance per year, little more than two years would evidently be needed to retire the increased initial cost of the wind-curtain system through its relative economy of fuel consumption.

Under the Iowa contract, but independently of Institute supervision, an analytical investigation [12] was made of the probable increase in efficiency of the wind-curtain system through adaptation of the so-called *thrust augmentor* used effectively in jet propulsion. Although tests were not made to verify the assumed conversion factors, it was estimated by the investigator that the gain in jet efficiency (and hence the reduction in cost of installation and operation) would be some 33%. This would obviously represent a considerable lowering of the time required to offset the initial cost through relative economy of operation.

At the time of writing this report, tentative plans have been laid for testing a section of a wind-curtain installation at Arcata under fog conditions. It is not known whether such plans will actually be carried to completion.

43.4 EXPERIMENTS ON GAS DIFFUSION

Tests made in England and in this country on the rate of gas diffusion and dissipation in specific open streets, courts, and buildings, led the University of Illinois in 1942 to propose a more general series of exploratory measurements upon schematic structures from which conclusions could be drawn which would not be restricted to the particular boundary forms already investigated. Although it was originally intended to perform these tests in the field at full scale, in the spring of 1943 a subcontract was written with the Iowa Institute to prepare a special wind tunnel for laboratory tests on model structures, which was expected to result in a great saving of time and expense. The tunnel constructed for this purpose [1] was almost immediately requisitioned for the fog-dispersal tests already described, but the measurements on gas diffusion discussed in the following pages were conducted intermittently whenever the higher priority investigation would permit.

In order to formulate and check the scale relationships which would be used to convert model results to prototype values, a series of hollow cubes was first constructed having dimensions of 24, 12, 6, 3, and 1½ in. These were placed, in turn, at the midpoint of the test section with open side up, and carefully filled with a known quantity of SO_2. The rate of dissipation of the SO_2 in winds of constant speed was then measured against time with a standard Dickinson meter. It was soon noted that the diffusion of the gas from even the largest cube in the lowest wind was

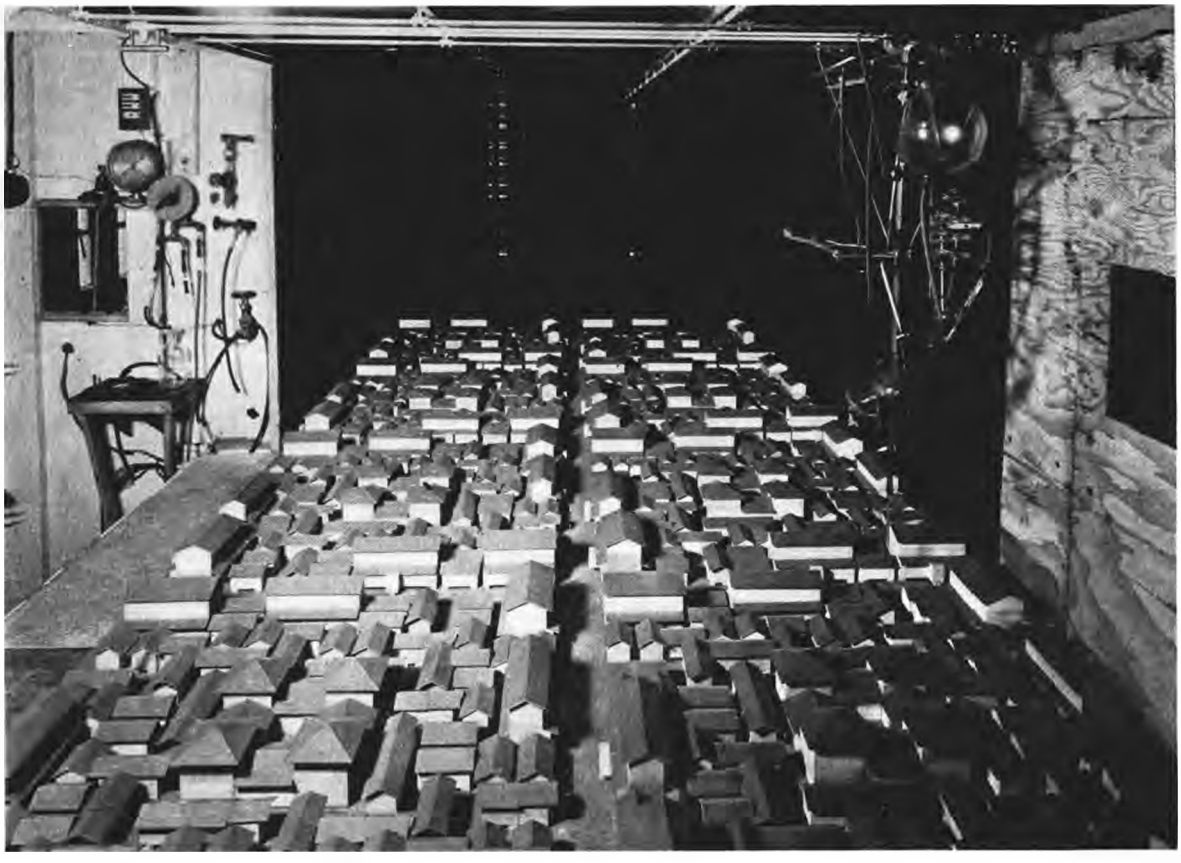


FIGURE 12. Model buildings in Japanese urban district.

so rapid that the Dickinson-meter indication represented its own rate of clearing rather than the rate at which the gas was removed from the cube. Search for a concentration meter with a response of the required rapidity proved fruitless. Since small-scale experiments are characterized by a reduction in time intervals roughly comparable to the reduction in the length dimension, it was concluded therefore that further efforts to investigate gas diffusion in the wind tunnel as a function of time should not be made.

The preliminary studies with the cubes of various sizes were then revised to include only the spatial variation of concentration under conditions of steady gas release. Each cube in turn was placed in the tunnel with its open side downwind, gas was released at a controlled rate within the cube, and concentration traverses were made in the downwind direction at various wind speeds and various rates of gas release. Owing to the angularity of the cubic form of body under study, the scale and intensity of the downwind eddies which produced the diffusion of the gas proved to be independent of the Reynolds number except at very low wind speeds or very small dimensions of the cube. It was, therefore, possible to reduce the variation in gas concentration in the downwind direction to a single dimensionless function [13] by measuring longitudinal distances in terms of the dimension h of the cubes and by referring the point concentration c to the quantity Q/v_0h^2, in which Q is the volume rate of gas release and v_0 the wind speed. The resulting function should, therefore, be independent of scale and wind speed, provided only that the diffusion was the result of eddies produced by a structure of the specified geometry under neutral conditions.

In a subsequent study to determine the effect of multiple cubic structures regularly spaced, some 72 6-in. cubes were placed at regular 12-in. intervals over the entire floor of the tunnel, and concentration traverses were made at three levels with various locations of the point of injection, various rates of gas release, various wind speeds, and several different

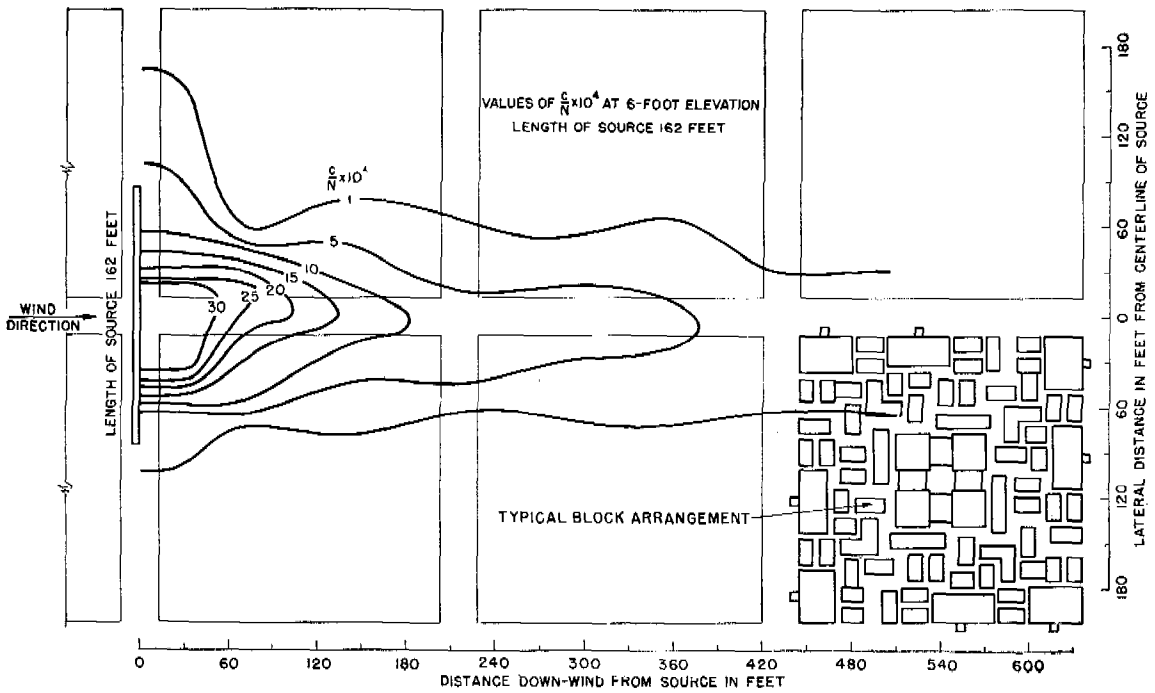


FIGURE 13. Concentration contours for gas diffusion in a Japanese urban district.

orientations of wind direction. It was found possible to reduce all such measurements to a series of relative concentration contours superposed upon the plan view of the block arrangement, the contours having geometrically progressive values of the dimensionless parameter cv_0h^2/Q. The fact that these contours were independent of wind speed and rate of gas release indicated that they should also be independent of scale as in the case of the earlier experiments with single structures. Although the schematic nature and arrangement of the structures limited the direct usefulness of the test results in foretelling field conditions for specific urban districts, nevertheless they revealed a very pronounced rate of vertical diffusion with distance downwind which should rapidly reduce the gas concentration at street level in any urban area.

In order to apply the foregoing method to the investigation of diffusion under urban conditions of specific interest, photographs of a series of Japanese cities were carefully studied, and a series of typical building proportions were formulated therefrom.[14] These building types were then reproduced at a scale of 1/72 in multiple units of such number (some 1,000 in all) as to pave the entire tunnel floor with the series of repeating city blocks shown in Figure 12. Instead of releasing the gas from a point source as in the foregoing tests, lateral manifolds were prepared which would simulate the initial *pancake* widths of bursts from 500- and 1,000-lb bombs at street level, either centered on one of the intersections or midway between two intersections. Concentration traverses, made in the same manner as in the case of the cubes, resulted in dimensionless contour plots such as that reproduced in Figure 13, the length L of the model and prototype foot being used instead of a building height h as the characteristic linear dimension in the quantity $N = Q/v_0L^2$.

As shown by this plot, the vertical diffusion is relatively great, while the lateral spread is quite limited. In other words, bursts would have to be closely spaced both laterally and longitudinally to result in a reasonably high concentration. To check the principle of contour superposition for the determination of the required spacing, the results obtained from runs with the two release manifolds placed approximately end to end, and then individually in the same positions, were compared. As may be seen from Figure 14 for a typical lateral section, the sum of the concentrations for the individual runs is very nearly identical with the distribution for the combined run, indicating that simple addition of superposed contour values will permit determination of the required bomb spacing for any desired minimum concentration.

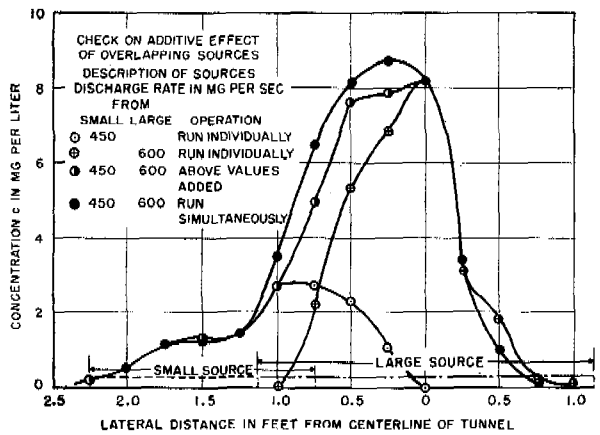


FIGURE 14. Test of superposition principle.

Since such small-scale experiments are perforce restricted to steady-state conditions until better means of measuring rapidly changing concentrations are available, means were next sought of foretelling from steady-state measurements the diffusion which would occur following bursts of the same pancake proportions. An analytical investigation of the diffusion process [14] indicated that the unsteady rate of diffusion would follow a different spatial variation, so that the steady-state contours would not yield directly even the relation between the peak concentrations C_m to be expected downwind from bursts. Nevertheless, the mathematical forms of the two diffusion functions appeared to provide a means of converting results from one to the other in a quantitative manner, once the numerical constants had been determined from wind-tunnel and field measurements of steady and burst conditions, respectively, for the same boundary conditions.

At the Dugway Proving Ground of the Chemical Warfare Service, a so-called Japanese Village, already in use for incendiary studies, appeared suitable for field tests of the type required. With the cooperation of the CWS, 500- and 1,000-lb bombs of NO_2 were exploded upwind from this village, and the concentrations at 27 points within the village were measured against time by means of Dickinson meters. Evaluation of the C_{max} and Ct values from these measurements [15] yielded contour patterns of the type shown

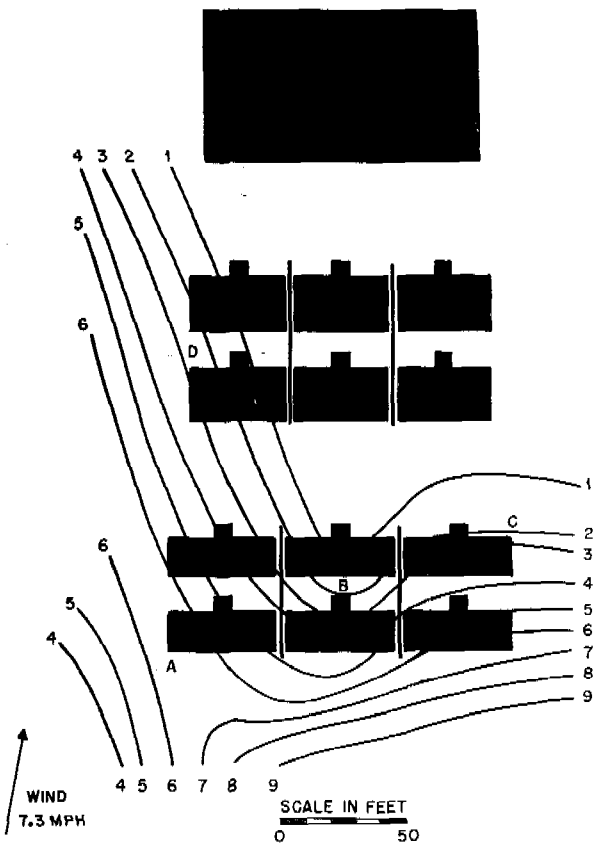


FIGURE 15. Contours of $\frac{C_m}{M} \times 10^7$ for 500-pound bomb.

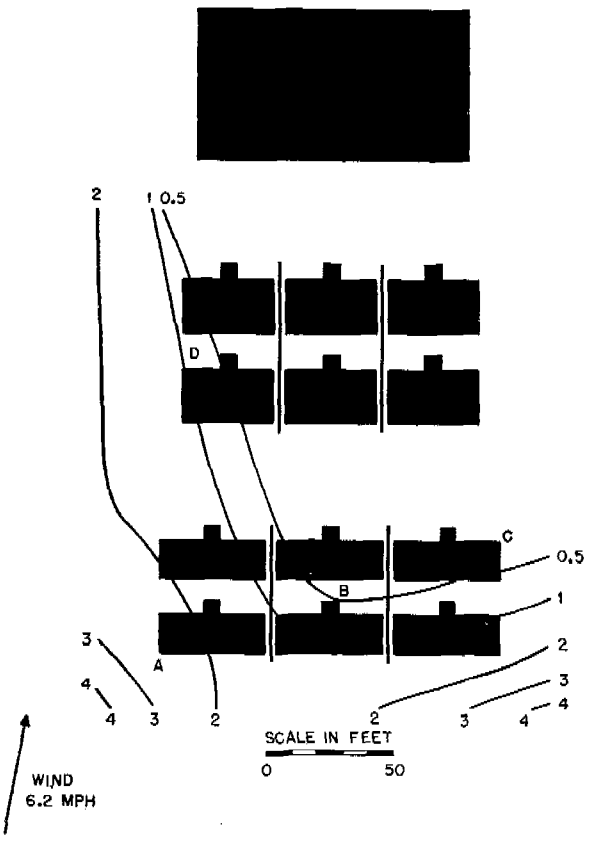


FIGURE 16. Contours of $\frac{Ct}{P} \times 10^4$ for 1,000-pound bomb.

TABLE 1. Field measurement and wind-tunnel predictions.

Point	C_m/M Computed	C_m/M Measured	Ct/P Computed	Ct/P Measured
		500-lb bomb		
A	7.4×10^{-7}	6.5×10^{-7}	1.6×10^{-1}	4.5×10^{-1}
B	1.5×10^{-7}	2.0×10^{-7}	0.3×10^{-1}	$<1.0 \times 10^{-1}$
C	0.7×10^{-7}	2.5×10^{-7}	0.2×10^{-1}	2.5×10^{-1}
D	5.8×10^{-7}	2.5×10^{-7}	1.3×10^{-1}	1.5×10^{-1}
		1,000-lb bomb		
A	4.1×10^{-7}	3.0×10^{-7}	1.3×10^{-1}	2.5×10^{-1}
B	7.3×10^{-7}	0.7×10^{-7}	1.3×10^{-1}	0.5×10^{-1}
C	2.4×10^{-7}	0.7×10^{-7}	0.8×10^{-1}	$<0.5 \times 10^{-1}$
D	3.5×10^{-7}	1.0×10^{-7}	1.1×10^{-1}	1.0×10^{-1}

in Figures 15 and 16, the contour parameters $C_m/M = C_m L^3/q$ and $Ct/P = CtL^2V/q$ involving the volume of gas released q in place of the steady release rate Q. Immediately following these field tests, wind-tunnel measurements were made with steady release of SO_2 at similar upwind points for a 1/72 scale reduction of the village structures (see Figure 17). As may be seen from the resulting contours shown in Figure 18, the laboratory measurements were necessarily far more detailed and reproducible; the field tests, in fact, showed the usual difficulty of variable wind speed and direction and proper meter placing. Nevertheless, evaluation of the numerical constants involved in the conversion from the steady to the burst diffusion function resulted in the comparison between field measurement and wind-tunnel predictions shown in Table 1.

Although considerable scatter is apparent, the accuracy of the predictions will be found to be as great as the reproducibility of the field measurements.

To the extent that the diffusion pattern of gas is controlled by the eddies shed by structural irregularities, small-scale studies of urban districts should yield quite as dependable results as field tests, with a vast saving in time and expense. If, however, bombing is to occur under the most advantageous conditions (i.e., very low wind speed and stable temperature gradient), then the present impossibility of reproducing viscous and thermal effects at small scale makes the wind-tunnel prediction of such phenomena out of the question. It is nevertheless believed that many situations in which wind plays the predominant role may be studied profitably in the manner outlined herein.

As an outgrowth of certain photographic studies of eddy patterns conducted in the wind tunnel of the Iowa Institute, a portion of the contract involved the



FIGURE 17. Model of Japanese village.

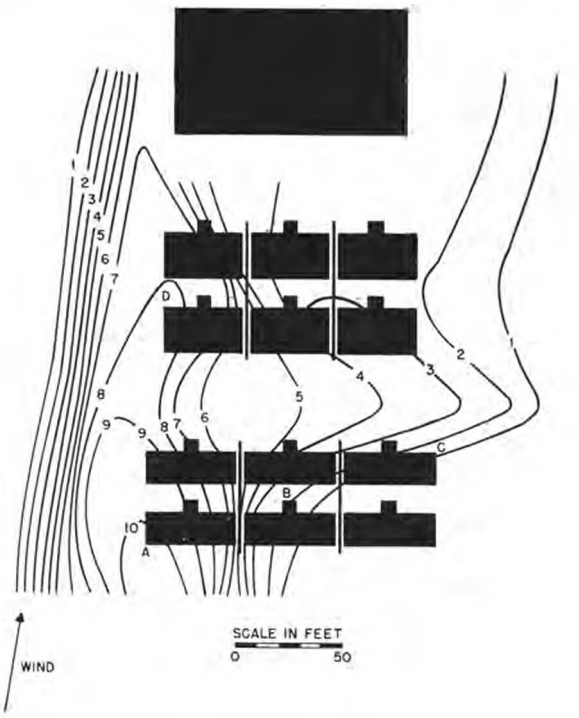


FIGURE 18. Contours of $\frac{C}{N} \times 10^4$ from model simulating field test with 500-pound bomb.

preparation of a 400-ft reel of 16-mm motion pictures [16] intended for training purposes by the CWS. This film illustrated the following phenomena by means of smoke and specially prepared models: the relative rates of smoke or gas diffusion under neutral, lapse, and inversion conditions; the effect upon diffusion of boundary roughness such as rocks or shrubbery; the effect of orchard and forest growth upon smoke or gas released upwind from and within the wooded section; eddy forms produced by screens, walls, and individual buildings; and, finally, the influence of building clusters. The film was originally submitted with descriptive titles, with the understanding that a sound film with running comments was to be prepared therefrom by the CWS.

43.5 EXPERIMENTS ON WIND FLOW OVER TERRAIN MODELS

At the request of the Weather Division of the Army Air Forces, the Iowa Institute undertook in the spring of 1945 a series of preliminary measurements of the distribution of velocity and turbulence over a relief model of the Tokyo Bay region. At that time American bombers were experiencing unexpected gustiness of the atmosphere during westerly winds which made precision bombing of Tokyo difficult, and all possible clues to the cause of the difficulty were desired. Although it was fully realized that model tests in the Iowa wind tunnel could clarify at best only a portion of the problem (that resulting from eddies shed by the mountainous region to the west) it was hoped that such information might be correlated with such other effects as those due to thermal instability.

The rubber relief model supplied by the Navy had a horizontal scale of 1/50,000 and a vertical distortion of 1.6/1. Though certain sections of the model were missing, those at hand were placed upon the floor of the wind-tunnel test section, and vertical velocity traverses were made at typical points between the mountains and the city. Thereafter, corresponding turbulence traverses were made at the same points, using the method of gas diffusion for the evaluation of the relative velocity of fluctuation and the coefficient of eddy diffusion. Such measurements clearly demonstrated the change in wind structure caused by the mountainous terrain, and permitted a qualitative evaluation of the height to which the disturbance extended.[17]

Specific use of such information was prevented by two unrelated circumstances. On the one hand, the fact that it was impossible to perform the model tests at the same Reynolds number as that of the prototype precluded accurate quantitative conversion of the test results to full-scale conditions; in other words, boundary-layer growth in the model was not necessarily the same as that to be expected in the actual atmosphere over Tokyo, although the pronounced roughness of the model tended toward minimum rather than maximum viscous effects. On the other hand, it was found impossible during war conditions to obtain sufficient weather information for the Tokyo region to permit correlation of the model indications with actual occurrences.

In view of the fact that such model studies would permit considerable simplification of wind-structure analysis, once small-scale results had been proved dependable, it was believed advisable to conduct experiments of a similar nature over models of regions for which extensive weather data were at hand. A model of the island of Guam was provided for this purpose, but the model scale was too small and the available weather reports too incomplete to warrant further tests. Since the island of Puerto Rico appeared more suitable for the investigation, it was decided to have relief models of this island made at several different vertical distortion ratios.

During the preparation of these models by the Army Air Forces, the Iowa Institute conducted tests of the effect of distortion [18] upon three series of boundary forms: semi-ellipsoids, cones, and parallelepipeds of similar base dimensions but having heights varying in geometric progression. Theoretical analysis of the flow pattern around ellipsoids of various axis ratios showed at once that in no simple way could measurements of the flow pattern around any ellipsoid be converted to yield usable results for any other ellipsoid, indicating that the distortion of a boundary and the resulting distortion of the flow pattern are not geometrically comparable. The measurements over the several series of schematic boundary irregularities (made with the specially constructed three-dimensional velocity meter shown in Figure 3) checked both the theoretical distribution for the semi-ellipsoids and the conclusions derived therefrom. In some instances it was found possible to approximate the velocity distribution for one of the boundaries from that obtained from its "distorted" counterpart, but in practically every instance the error was essentially the same order as the effect which it was desired to measure.

The OSRD contract under which these studies were conducted terminated before the foregoing tests had been completed, and they were continued under direct contract with the Army Air Forces, together with measurements over the Puerto Rico models. It must be concluded from these tests that measurements over small-scale terrain models are unlikely to yield useful quantitative information, unless the boundary configuration is so extreme as to require no vertical distortion for the required precision of indication. As an example of desirable terrain characteristics for wind-tunnel study, reference may be made to successful observations made over a model of Gibraltar, which has sufficient relative height to yield a pronounced eddy pattern that is essentially independent of Reynolds number effects.

[redacted]

Chapter 44

RADIOACTIVE TRACERS

By *W. D. Walters*

44.1 INTRODUCTION

IN A NUMBER of studies undertaken by investigators in Division 10, radioactive materials were employed as tracers. The various types of investigations that were performed in connection with the charcoal and smoke filter problems will be described briefly in the pages which follow. In the present summary the results of the radioactive tracer experiments will not be discussed in detail, since the significance of the results with respect to the general problems of the behavior of absorbents and filters has been considered in earlier chapters.

44.2 PREPARATION OF WAR GASES CONTAINING RADIOACTIVE ELEMENTS

For the utilization of the radioactive tracer technique, it was necessary to have a source of the desired radioactive elements and rapid methods of preparation of small quantities of radioactive toxic agents. Although some investigators obtained radioactive elements in small quantities without charge or by direct purchase order, a large fraction of the radioactive starting materials needed in the Division 10 program was supplied through contracts with the University of California and with Harvard University.

The methods (shown in Table 1) for preparing the radioactive compounds, such as phosgene and arsine, from available radioactive starting materials were usually developed by the groups which subsequently used the radioactive compounds for studies of adsorbents or filters. However, at the Pennsylvania State College a study was made to determine the most feasible methods for synthesizing various radioactive war gases. In this study the methods were actually investigated by the use of nonradioactive substances, but consideration was given to the state of combination in which the radio-element would be obtained. In Table 1, in order to indicate that the method was developed for the incorporation of a given radioactive element, but not used for a radioactive sample of the element, the element is marked with an asterisk.

It is evident that in most cases the methods of preparation given in Table 1 were not new reactions but were adaptations of known methods to the preparation of radioactive toxic agents. The references to the earlier studies reported in the open literature are given in the reports cited, but they have not been included here on account of the shortage of space.

44.3 APPARATUS

As in the case of the preparation of materials, general methods for the detection of radioactive substances had been developed prior to the NDRC investigations and various types of apparatus were available. Therefore, the apparatus employed in any Division 10 investigation usually represented a modification of existing apparatus to fit the needs of the particular problem being studied plus new items of apparatus designed on the project.

One of the pieces of apparatus used quite extensively was a Geiger counter tube which had mica windows of thickness 2 to 3 mg per sq cm, and which was used for the determination of the activity of compounds of radio-sulfur or any other beta emitter with energy of radiation 100,000 volts or greater.[3] When the tube was shielded by 2 in. of lead, the background amounted to only 20 counts per minute. The tube was developed at the California Institute of Technology, and on the same project a counting rate meter circuit of the Evans-Alder-Kip type was constructed. This circuit was found to be very useful in combination with a recording milliammeter. In addition, a scale of 32 circuit was built and used for the determination of radioactivities.

In the early NDRC work it appeared that, under favorable conditions, radioactive H^3 might be employed for the measurement of small concentrations of hydrogen-containing compounds.[4] Therefore, a Geiger-Muller counter suitable for the measurement of the activity of H^3 in very low concentrations was developed at the Radiation Laboratory of the University of California. To measure the activity of H^3, the hydrogen must be converted into elementary hydrogen before it is introduced into the counter, and

TABLE 1. War gases or simulated war gases containing radioactive elements.

Compound	Radio-element (half-life)[a]	Method of producing radio-element	Process for preparation of compound	Reference
$COCl_2$	C^{11} (20.5 min)	B, *d-n*	$CO \xrightarrow[h\nu]{Cl_2} COCl_2$	8
$COCl_2$	Cl^{38} (37 min)	Cl, *d-p*	$LiCl–Cl_2$ exchange $Cl_2 \xrightarrow[h\nu]{CO} COCl_2$	8
$COCl_2$	Cl*		$AgCl \xrightarrow[350°]{CO} COCl_2$	2
$COCl_2$	Cl*, O*, or C*		$CO + Cl_2 \xrightarrow[\text{act C}]{\Delta} COCl_2$	2, 9
AsH_3	As^{74} (16 days)	Ge, *d-n*	[b] $T(GeO_2) \xrightarrow[\text{aq reg}]{Na_3AsO_4} As^{V} \xrightarrow[HBr]{HCl} As^{III} \xrightarrow{Zn\,H^+} AsH_3$	5
AsH_3	As^{74} (17 days)	Ge, *d-n*	[c] $T(GeO_2) \longrightarrow As^{V} \xrightarrow[H^+]{Zn} AsH_3$	6, 10, 9
H_2S	S^{35} (88 days)		$BaSO_4 \xrightarrow[\Delta]{H_2} BaS \xrightarrow{H^+} H_2S$	3
SF_6	S^{35} (88 days)		$H_2S \xrightarrow{KIs} S \xrightarrow{F_2} SF_6$	3
CNCl	N*		(i) $N_2 \xrightarrow[\Delta]{Ca} Ca_3N_2 \xrightarrow[\Delta]{H_2O} NH_3$ (ii) $NH_3 + CO_2 \xrightarrow[\Delta]{K} KCN$ (iii) $KCN \xrightarrow{Cl_2} CNCl$	12, 9
CNCl	C*		As in (ii) and (iii) above	12, 9
CNCl	Cl*		$Cl_2 \xrightarrow{NaCN} CNCl$	12, 9
HCN	N* or C*		KCN prepared as in (i) and (ii) $KCN \xrightarrow[FeSO_4]{H_2SO_4} HCN$	15, 9
SeF_6	Se*		$Se \xrightarrow{F_2} SeF_6$	17, 9
CCl_3NO_2	Cl*		$(CH_3)_2CO + HNO_3 + HCl \longrightarrow CCl_3NO_2$	9
$(C_6H_5O)_3PO$	P^{32}?		Rad $PO_4^- \xrightarrow[\Delta]{P} P \longrightarrow PCl_5$ $PCl_5 \xrightarrow{C_6H_5OH} (C_6H_5O)_3PO$	1

[a] Reported value not always in agreement with the value accepted at the present time.
[b] $T(GeO_2)$ denotes target material, GeO_2, was subjected to the treatment indicated.
[c] For details of separation and preparation see reference (6).

for this reason, as well as others, the method found little use in the Division 10 program.

44.4 STUDIES OF CHARCOALS AND WHETLERITES

44.4.1 Concentration of Agent in the Effluent Gas Stream

By the use of toxic gas-air streams containing molecules of radioactive agent as well as molecules of nonradioactive agent, it was found that the total concentration of the agent in the gas stream before and after passage over a charcoal bed could be determined readily and accurately by the measurement of radioactivity. In this work, calibration experiments were, of course, necessary. Concentrations of arsine,[5] phosgene,[8] hydrogen sulfide,[3] and sulfur hexafluoride [3] were determined by passing the gas stream through glass vessels covered with a thin film of aluminum which was placed next to the mica-covered Geiger counter tube. Although a number of factors may influence the sensitivity of the method, it was observed that with the apparatus and activity of radio-samples available at the time of these investigations, the radioactive tracer technique could be used to obtain concentrations as low as the following:

Substance	Concentration	Accuracy
H_2S	0.32 mg per cu m	30 to 40%
SF_6	0.3 mg of S per cu m	10%
AsH_3	10 mg per cu m	25%

SECRET

As would be expected, the accuracy was better for the determination of higher concentrations.

Another method of obtaining a sample of a gas mixture from a static system or from a flowing stream was also devised.[3] A glass hypodermic needle was used to remove a few cubic centimeters of the gas mixture, and this sample was then injected into a closed vessel through a small hole covered with a rubber band. By locating the aluminum or cellophane window of the vessel near a Geiger counter, the activity of the sample could be measured. Concentrations as low as 0.1 mg S per cu m in a 5- to 10-cc sample of an air-H_2S mixture or an air-SF_6 mixture could be measured by this method.

The flow method mentioned above was of considerable value in the measurement of effluent concentration as a function of time during adsorption and desorption experiments. In general, the results of the radioactive tracer technique proved useful in (1) measuring the performance of charcoals and whetlerites,[5, 8, 13] (2) determining the sensitivity and the efficiency of certain chemical breakpoint indicators, such as the silver nitrate indicator for arsine,[5, 14] and (3) testing various theoretical adsorption equations.[5, 8]

44.4.2 Reaction Products in the Effluent Gas Stream

In a consideration of the application of the radioactive tracer method to the study of the removal of toxic agents by charcoal, it is apparent that the radioactivity of the effluent stream represents the radioactivity not only from the unremoved toxic gas, but also from any radioactive reaction products appearing in the effluent gas stream. In the case of arsine containing radioactive arsenic, the reaction products containing arsenic are essentially nonvolatile compounds readily retained by the charcoal. However, with phosgene containing radioactive carbon, and under certain conditions with phosgene containing radioactive chlorine, an appreciable fraction of the radioactivity in the effluent stream may be due to radioactive reaction products. By carrying out experiments first with phosgene containing C^{11} and then with phosgene containing Cl^{38}, the group on project OEMsr-28 at the California Institute of Technology obtained results which were useful in the identification of the reaction products and the determination of the concentration under different experimental conditions.[8,16]

44.4.3 Distribution of Toxic Agent or Reaction Product in the Charcoal Bed

By means of radioactive war gases it was possible to observe the accumulation of the adsorbed toxic agent or of radioactive reaction products in the charcoal bed. Experiments with radio-arsine were performed to measure the accumulation of arsenic at a single position in the charcoal bed as a function of time and also to determine the distribution of arsenic along the charcoal bed. At the California Institute of Technology the change in the radioactivity of the top layer of the charcoal bed with time was obtained by the use of the previously described counting apparatus when a lead slit 3 mm wide and 100 mm thick was placed adjacent to the top of the charcoal bed.[5] For the investigation of the distribution of the radioactive arsenic along the charcoal bed, a 3-mm lead slit was used to scan the bed after radio-arsine had been passed through the bed for a definite time. Another method employed in the distribution experiments was the use of fine brass screens to divide the charcoal bed into sections which could be removed after passage of the gas and their separate activities determined.

At the University of Rochester, on Project NDCrc-76, the distribution of As^{74} (from radio-arsine) in the charcoal bed was also studied.[6] Experiments were performed in order to determine how the distribution depended upon the time of passage of the gas, initial concentration of arsine, moisture content of the charcoal, and humidity of the gas stream. The distribution of arsenic along the bed was obtained by separating the charcoal bed into sections and measuring the activity of a definite weight of charcoal from each section. The separation into sections was accomplished by means of a screw arrangement for lifting the entire bed so that successive layers of charcoal of the desired size could be removed (without the use of screens).

One of the significant results revealed by the experiments at Pasadena and at Rochester was that the top layer of the charcoal bed is not completely saturated when the silver nitrate breakpoint is reached.

In the case of phosgene containing radioactive chlorine, the accumulation of *labeled* chlorine in the charcoal layer on the influent side of the bed was measured at the California Institute of Technology. It was found that the amount of chlorine increased rapidly with time until the breakpoint was reached

(activity of effluent 1% of influent), but after the breakpoint the accumulation in the top layer practically ceased.[8]

44.4.4 Location of the Reaction Product in the Individual Particles of Whetlerite

Another application of the radioactive technique to the study of the removal of war gases was an investigation at the University of Illinois (Project NDCrc-152) to ascertain the location of the reaction product (probably As_2O_3) from arsine in a single particle of charcoal or whetlerite.[7] Various charcoals were treated with arsine containing radioactive arsenic. A thin section could be prepared by grinding down a single particle, and when the section was placed in contact with a photographic plate, the radioactivity produced an image showing the location of arsenic in the particle. Radioactive ash skeletons were also prepared by carefully ashing a few particles of the exposed whetlerite. Radiographic images of these ash skeletons could be obtained upon a photographic plate. In this work the treatment of the particles with radio-arsine was carried out at Rochester and at Pasadena. The results of these radiographic studies were of considerable interest and showed among other things that the reaction product from arsine lies near the surface of the whetlerite particle. This layer of reaction product was quite thin in the case of extruded charcoals, particularly along the smooth, cylindrical sides of the particle.

44.4.5 Distribution of the Catalyst in the Individual Particles of Whetlerite

In addition to the study of the location of the reaction product, the radioactive tracer method was employed at the University of Illinois to determine the location of the catalyst in the whetlerite particles.[7, 18] Impregnating solutions containing radioactive elements, such as cobalt, phosphorus, and thorium, were used to treat blocks of charcoal, and the sides of the dried blocks scraped off so that the activity of the layers could be measured. In the later work, thin sections of impregnated charcoal particles containing Cu^{64}, $NaS^{35}CN$, or Ag^{106} were prepared, and radiographs obtained as mentioned above. The charcoals impregnated with $NaS^{35}CN$ had been prepared at the University of California, and those with Ag^{106} at the Northwestern Technological Institute. Radiographs of the ash skeletons were also prepared. In this study it was observed that, in general, the *soaking* method of silver impregnation distributed the catalyst throughout the particle, but the *spraying* procedure tended to produce a thin outer layer of catalyst.

44.5 STUDY OF SMOKE FILTERS

One of the earliest uses of radioactive tracers in the program of Division 10 (or its predecessors, Sections B–5 and B–6) was in connection with the testing of filter materials.[1] The problem of determining the performance of smoke filters, especially against liquid smokes, was quite important, and on Project NDCrc-49 at the University of Illinois a method was developed for testing filter materials by the use of aerosols produced from radioactive triphenyl phosphate. An aerosol of triphenyl phosphate containing radioactive phosphorus was passed through a series of circular pads prepared from the filter material being tested. These pads were in contact under a definite pressure. After passage of the smoke for the desired period of time, the pads were separated and each pad counted on a Geiger counter. The results obtained by this method contributed to the development of a theory of filtration. Moreover, the results showed that the existing method of testing gas-mask filters was objectionable from several standpoints and that immediate steps should be taken to produce better smoke filters.

44.6 FIELD USE OF RADIOACTIVE TRACERS

As an extension of the use of the radioactive tracer procedures employed in laboratory work, it might be expected that, under certain conditions, radioactive tracers might be used to determine ground contamination, aerosol concentration, or vapor concentration of toxic agents during field tests. In this connection it is interesting to note that the radioactive method for measuring the ground contamination from mustard-filled munitions was investigated by the Chemical Warfare Service at the Dugway Proving Ground.

GLOSSARY

A. Angstrom.

AC. Symbol for hydrogen cyanide.

AD. Apparent density; the weight of 1 ml, not the true density because of the free space between particles.

AL. Woodpulp.

AR-50. Designation for relative humidity of charcoal and air in test; charcoal as received, air at 50 per cent RH.

ASC. Designation for impregnated charcoal which contains copper, silver and chromium.

ASM. Impregnant for whetlerite made with molybdenum in place of chromium.

ASV. Impregnant for whetlerite made with vanadium (same as above).

BC CHARCOAL. Barnebey-Cheney, prepared from nut shells or peach pits.

BW. Biological warfare.

C. Critical bed depth.

CFI CHARCOALS. Colorado Fuel and Iron Company. Experimental gas mask charcoal made from coal.

CG. Symbol for phosgene.

CK. Symbol for cyanogen chloride.

Ct. Concentration-time; product for gas exposure. Units are either mg min per liter or mg min per cubic meter. The former is often used for non-persistent gases and the latter for persistent.

CtA. Product of gas dosage by area covered. See Chapter 16.

CWSC. Designation for charcoal prepared by the Carlisle Company, using the Prest-o-log process. See Chapter 3. Also referred to as Seattle or Crown-Zellerbach charcoal.

CWSE1-TE1. Designation for a sample of Type A whetlerite prepared from coconut charcoal at Edgewood Arsenal.

CWSN. Designation for charcoal manufactured by National Carbon Company, by zinc chloride process. A number indicates the particular batch, e.g., CWSN5, CWSN44, etc.

CYAN DA. CWS symbol for Diphenylchloroarsine.

DBT. Dibutylphthalate.

DC. Symbol for diphenylcyanoarsine.

DIOL. Trade name of oil used for screening smoke.

DM. Symbol for Adamsite.

DOP. Dioctylphthalate.

E6. Designation for thiocyanates impregnated whetlerite. This was never put into production.

EN. Symbol for ethylenimine.

FPM. Foot per minute.

FPS. Foot per second.

FS. Fuming sulfuric acid. Used to produce smoke.

GPH. Gallons per hour.

GPL. Grams per liter.

H. Symbol for mustard gas. Also designated as HS prior to 1942.

HBT. Herringbone twill cloth used in clothing.

HC. Symbol for hexachlorethane, used for producing smoke. HC pot is a smoke pot employing this chemical.

HCE. British for hexachlorethane.

HD. Distilled mustard.

HE. High explosive.

HN-3. Nitrogen mustard $N(ClCH_2CH_2)_3$.

HTU. Height of a transfer unit.

IAS. Indicated air speed.

IR. Voltage drop.

IT. Index of turbulence.

LPM. Liters per minute.

LST. Local standard time.

MB. Methylene blue.

MCE. German war gas Tabun.

MDL. Abbreviation for Munitions Development Laboratory at University of Illinois.

MMD. Mass median diameter.

MMG. Microgram or 10^{-3} mg.

MSV. Moisture saturation valve.

μG. Microgram.

NATIONAL. National Carbon Company. Charcoal prepared by the N. C. Co. is frequently referred to a "National" Charcoal. It is made by the zinc chloride process. Designated as CWSN.

N. Gas capacity of absorbent at saturation. See Chapter 2.

NRL. Naval Research Laboratory.

PCC. Pittsburgh Coke & Chemical Company.

PCI. Pittsburgh Coke and Iron Company now known as PCC Company.

PPM. Parts per million.

PS. Symbol for chloropicrin.

PSI. Pounds per sq inch.

PWP. Plasticized white phosphorus.

R. Symbol for ratio of wind velocities at two different levels. See Chapter 14.

RH. Relative humidity.

RETENTIVITY. A term used to describe the ability of charcoal to retain an adsorbed gas.

SA. Symbol for arsine.

SEATTLE CHARCOAL. Charcoal prepared by carbonization and activation of Prest-o-logs from wood sawdust. Designated as CWSC. Sometimes called "Carlisle" since made by the Carlisle Company.

SDF. Standard dispersion figure. See Chapter 35.

SIP INDICATOR. Indicator used for CK tests. See Chapter 2.

SN. Sulfur-citrate mixture used for smoke production. See Chapter 32.

STP. Standard temperature and pressure.

SPACE VELOCITY (HR). "In quantitative work on heterogeneous catalysis, it is customary to express rates in terms of the volume of feed gases introduced to the catalyst in unit time. Specifically, the term 'space velocity' (hr) is equal to the volume of feed gases in liters per hour (measured at standard temperature and pressure) divided by the apparent volume of the catalyst measured in liters." (Definition by Dr. Pease.)

SWP. Mechanical mixture of steel wool and white phosphorus. See Chapter 37.

TABUN. German war gas.

TCP. Tricresyl phosphate.

TPP. Triphenyl phosphate.

TYPE A WHETLERITE. Charcoal impregnated by copper oxide.

See Chapter 4. Type ASC whetlerite contains copper, silver, and chromium.

TYPE D MIXTURE. Gas mask absorbent containing 20 per cent soda lime and 80 per cent Type A whetlerite by volume.

VMMD. Volume mass median diameter. See Chapter 35.

WHETLERITE. All impregnated gas mask charcoals which contain copper are known as whetlerites. The usage dates back to 1918 when copper impregnated charcoal was prepared by Whetzel and Fuller.

WP. White phosphorus used as smoke munition.

WPT. White phosphorus loaded into bombs in paper tubes. See Chapter 37.

XEROGEL. A granular ion-exchange resin prepared as gas absorbent. See Chapter 4.

Z. Symbol by British for S2F10.

BIBLIOGRAPHY

Abbreviations for Official Titles of Reports

DPGSR	Dugway Proving Ground Special Report
DPGMR	Dugway Proving Ground Memorandum Report
EATR	Edgewood Arsenal Technical Report
FM	Field Manual. War Department publication
FMTR-MIT	Foreign Material Technical Report from MIT laboratory
MIT-MR	Massachusetts Institute of Technology Memorandum Report
MSR	Monthly Summary Report Sections 10.1 and 10.5, NDRC
NDRC	Informal Reports from Division 10 or Section B-6. The latter have Roman serial numbers
OSRD	Formal reports from OSRD
SJPR	San José Project Report
TCIF	Technical Command Informal Report
TDMR	Technical Division Memorandum Report
TM	Technical Manual. War Department publication

Numbers such as Div. 10-200-M5 indicate that the document listed has been microfilmed and that its title appears in the microfilm index printed in a separate volume. For access to the index volume and to the microfilm, consult the Army or Navy agency listed on the reverse of the half-title page.

Chapter 1

1. *Chemicals in War*, A. M. Prentiss, McGraw-Hill Book Co., 1937.
2. *War Department Basic Field Manual*, FM-21-40, September, 1942.
3. *War Department Technical Manual*, TM-3-205, October, 1941.
4. *Summary of Results in Section B-6, December 1941 to August 1942* (Final Report), W. A. Noyes, Jr., OSRD 1182, OEMsr-660, Service Projects CWS-7, NL-B26, and others, University of Rochester, Feb. 6, 1943. Div. 10-200-M5
5. Bimonthly Reports of Division 10, NDRC.
6. *Standard U. S. Army Gas Masks and Components*, S. H. Katz, TDMR 878, Aug. 2, 1944.

Chapter 2

1. *Some Aspects of the Physical Chemistry of the Respirator*, C. J. Danby, J. G. Davoud, et al, Oxford University extra-mural report, not dated.
2. *Standard Methods of Test (Chemical and Physical) Employed in CW Investigations*, S. A. Mumford, Porton Memorandum No. 17, Mar. 7, 1942.
3. *Correlation Between the British Volume Activity and the United States Chloropicrin Tube Life*, J. C. Arnell, Chemical Warfare Laboratories, Ottawa, Proofing Section Report No. 10, Oct. 25, 1943.
4. *An Intermittent Flow Canister Test Machine*, J. W. Zabor, W. C. Pierce, R. K. Brinton, et al, OSRD 1193, OEMsr-282, Service Project CWS-7, Jan. 28, 1943. Div. 10-201.1-M12
5. *The Effect of Tube Diameter and Type of Air Flow on Charcoal Breakdown Times*, J. R. Arthur, E. J. Brockless, et al, Oxford University Research Report No. 43.20.
6. *A Critical Examination of the Correlation of Tube and Container Gas Test Results*, K. D. Wadsworth, Porton 2001 (U. 138).
7. *Chemical Warfare Service Pamphlet No. 2. Part I. Canister Test Methods. Part II. Absorbent Test Methods. Part III. Collective Protector Test Methods.*
8. *A Comparison of Tube and Container Gas Tests for Various Charcoals*, Oxford University Research Report No. 44.16, July 10, 1944.
9. *A Study of Charcoal Adsorption and Methods of Testing Charcoals for Use in Gas Mask Canisters*, R. Macy, EATR 52, May 10, 1942.
10. *Correlation of Tube and Canister Tests for Service Life of ASC Impregnated Charcoal*, G. B. Wilson, TDMR 764, Nov. 3, 1943.
11. *Canister Test Methods and Apparatus. Tube Test Efficiencies at Break Points*, G. B. Wilson, TDMR 321, Nov. 10, 1941.
12. *Canister Test Methods and Apparatus. Tube Tests — A Concentration Time Study*, G. B. Wilson, TDMR 324, Nov. 15, 1941.
13. *Comparison of Gas Penetration Concentrations on U. S. German and Japanese Gas Mask Canisters*, L. A. Jonas, TDMR 770, Nov. 29, 1943.
    Preliminary Report on the CC Penetration Through and Desorption From Japanese Army Service Canisters, L. A. Jonas, TCIR 146, June 23, 1944.
14. *Performance of the M-10 Canister Against HS Under Humid Tropical Conditions*, W. C. Pierce and J. W. Zabor, OSRD 1194, OEMsr-282, Service Project CWS-7, Feb. 3, 1943. Div. 10-201.1-M13
15. *Fundamental Factors in the Design of Protective Respiratory Equipment. Inspiratory Air Flow Measurements of Human Subjects With and Without Resistance*, L. Silverman et al, OSRD 1222, Mar. 4, 1943. Div. 11-204.2-M1

Chapter 3

1. *Kimberley-Clark Process for Production of Activated Carbon From Lignin-Wood Flour Mixtures*, Final Report, CWS Contract W-266-CWS-238, undated.
2. *Manufacture of Activated Charcoal in New Zealand from Coconut Shell Charcoal*, Coal Survey Division, Dominion Laboratory, Wellington, New Zealand, A. C. L. 31, Jan. 6, 1943.
3. *Activation of Charcoal by Chlorine*, M. E. Barker, Memorandum, CWS-334.8/149, Nov. 26, 1941.
4. *The Effect of Treating Activated Charcoal with Air or Air-Steam Mixtures at Elevated Temperatures*, C. R. Bierman, G. L. Pratt, and B. A. White, OSRD 5240, OEMsr-282, Service Projects CWS-7 and NS-338, June 21, 1945. Div. 10-202.13-M25
5. *Changes in Properties of PCI Charcoal and Whetlerite During Activation*, F. E. Blacet and T. Skei, OSRD 1349, OEMsr-282, Service Project CWS-7, Apr. 20, 1943. Div. 10-202.13-M12
6. *G. L. Cabot Carbon Black Charcoals*, F. E. Blacet and T. Skei, OEMsr-282, Service Project CWS-7, NDRC Report 10.1-15, Northwestern University, June 3, 1943. Div. 10-202.1-M12
7. *The Non-Uniform Activation of Charcoal*, F. E. Blacet and T. Skei, OEMsr-282, Service Project CWS-7, NDRC Report 10.1-18, Northwestern University, June 15, 1943. Div. 10-202.13-M14
8. *Effect of Activation Time on Properties of PCI Charcoal and Corresponding Whetlerites (Second Report)*, F. E. Blacet, W. Conway Pierce, and T. Skei, OSRD 1746, OEMsr-282, Service Project CWS-7, Northwestern University, Aug. 10, 1943. Div. 10-202.11-M6
9. *Ultra Fine Structure of Coals and Cokes*, H. K. Lewis and Company Ltd., p. 224.
10. *A Study of the Carbonization of Coal Materials*, B. A. White, L. Byman, et al, OEMsr-282, Service Project CWS-7, NDRC Informal Report 10.5-49, Northwestern University, Nov. 24, 1944. Div. 10-202.12-M15
11. *Whetlerization of Apricot Pit Charcoals*, E. Conroy, Central Laboratory Job Report W-7, Dec. 11, 1943.
12. *A Study of the Effect of Uniformity of Activation of Sieve Fractions on CC Canister Performance for Mixtures of PCI Charcoal*, J. C. Cooper and R. J. Kunz, NDRC 10.5-21, Mar. 14, 1944. Div. 10-201.1-M23
13. *Nitrogen Surface Area Measurements on a Series of PCI Samples Subjected to Steam Activation for Various Periods of Time*, P. H. Emmett and J. T. Kummer, NDRC 10.5-20, Mar. 1, 1944. Div. 10-202.13-M19
14. *The Production by Messrs. Sutcliffe, Speakman & Co., Ltd., of Briquetted Coal Charcoal on the Semi-bulk Scale*, Porton Report No. 2453, Nov. 26, 1942.
15. *Zinc Chloride Activated Wood Charcoal*, G. W. Heise et al, OSRD 4324, Sept. 30, 1944. Div. 10-202.13-M24
16. *The Manufacture of Activated Carbon*, S. Hormats, TDMR 1083, July 4, 1945.
17. *Studies of Impregnated Charcoals*, H. F. Johnstone and G. L. Clark, OSRD 172, Nov. 8, 1941. Div. 10-202.14-M4
18. *A Study of Impregnated Charcoal*, H. F. Johnstone and G. L. Clark, OSRD 1143, Dec. 9, 1942. Div. 10-202.143-M4
19. *Atlas Charcoal Plant*, H. F. Johnstone, Memorandum to W. A. Noyes, Jr., Jan. 29, 1943.
20. *A Study of Pore Development and ASC Whetlerite Performance of Charcoals Prepared from Briquetted Coal*, A. Juhola and T. Skei, NDRC 10.1-46, June 28, 1944. Div. 10-202.111-M3
21. *Determination of Pore Diameters in Charcoal*, A. Juhola, NDRC 10.1-58, Jan. 24, 1945. Div. 10-202.111-M4
22. *Memorandum of Conference of Representatives of G. L. Cabot Company and Division 10*, R. J. Kunz, Aug. 3, 1942.
23. *The ASC Whetlerization of Barnebey-Cheney Coquito Nuts, Peach Pits and English Walnut Shell Activated Charcoals*, R. J. Kunz, Central Laboratory Job Report ECL-3, Nov. 19, 1943.
24. *Whetlerization of Atlas Apricot Pit Charcoals*, R. J. Kunz, Central Laboratory Job Report W-7, Dec. 11, 1943.
25. R. J. Kunz, MSR, June 15, 1944. Div. 10-200-M7
26. R. J. Kunz, MSR, July 15, 1944.
27. *Activation of Charcoal*, W. L. McCabe, NDRC LVIII, Carnegie Institute of Technology, Dec. 29, 1941. Div. 10-202.13-M2
28. *Activation of Charcoal. Effect of Varying Gas Mixture and Gas Temperatures*, W. L. McCabe, NDRC LXXIII, Feb. 15, 1942. Div. 10-202.13-M4
29. *Preparation of Wood Charcoal*, W. L. McCabe, OSRD 1002, Oct. 21, 1942. Div. 10-202.12-M6
30. *Memorandum on Visit to Carlisle Lumber Company*, W. L. McCabe, Mar. 8, 1943.
31. *Preparation of Wood Charcoal Suitable for Activation*, W. L. McCabe et al, OSRD 1856, Sept. 29, 1943. Div. 10-202.12-M11
32. *Activation of Charcoal and of Anthracite*, W. L. McCabe and R. York, Jr., NDRC LXXXVI, Carnegie Institute of Technology, Mar. 15, 1942. Div. 10-202.13-M5
33. *Activation of Charcoals by the Jiggler Process*, R. J. Kunz and R. B. Rogge, OSRD 4283, Oct. 23, 1944. Div. 10-202.131-M13
34. *Properties of Gas Coke Samples*, T. Skei, Central Laboratory Job Report 58, Oct. 16, 1942.
35. *Properties of NRL-MP-60 Wood Char*, T. Skei, Central Laboratory Job Report 61, Oct. 28, 1942.
36. *Properties of Kimberley Clark Carbons*, T. Skei, Central Laboratory Job Report 74, Dec. 7, 1942.
37. *Whetlerizability of Saran Samples*, T. Skei, Central Laboratory Job Report 89, Jan. 26, 1943.
38. *Cliffs-Dow Char*, T. Skei, Central Laboratory Job Report 87, Jan. 26, 1943; *ibid*, No. 116, Apr. 24, 1943.
39. *Whetlerization and Surveillance Studies on PCI Charcoal at Various Stages of Activation*, T. Skei, OSRD 4112, Sept. 9, 1944. Div. 10-202.13-M23
40. *Carbonization of Peach Pits and Their Preparation into ASC Whetlerite*, B. A. White and R. J. Kunz, NDRC 10.5-39, July 15, 1944. Div. 10-202.134-M4
41. *The Effect of Air Carbonization in the PCC Charcoal Process*

Upon the Whetlerite Qualities of the Adsorbent, B. A. White et al, OSRD 5115, May 24, 1945. Div. 10-202.14-M31
42. *Studies of the Preparation of Activated Charcoal Suitable for Whetlerization from Coconut Shells*, B. A. White et al, OSRD 5116, May 24, 1945. Div. 10-202.134-M5
43. *The Effect of Primary Particle Size in the Processing of PCC Type Charcoal*, B. A. White et al, OSRD 5234, June 21, 1945. Div. 10-202.18-M4
44. *The Reactivation in Oxygen of CWS Charcoals*, T. F. Young, OSRD 4104, Sept. 7, 1944. Div. 10-202.132-M2
45. *A Laboratory Study of Activation*, R. York, Jr., NDRC CXXXVI, June 15, 1942. Div. 10-202.13-M6
46. *Activation of Charcoal*, R. York, Jr., NDRC CLXIV, July 15, 1942. Div. 10-202.13-M8
47. *Activation of Gas Charcoal by a New Jiggler Process*, R. York, Jr., OSRD 956, July 31, 1942. Div. 10-202.131-M3
48. *Activation of Charcoal*, R. York, Jr., Informal Progress Report Contract NDCrc-124, Aug. 15, 1942.
49. *Activation of Charcoal*, R. York, Jr., Informal Progress Report Contract NDCrc-124, Oct. 15, 1942.
50. *Activation of Charcoal*, R. York, Jr., Informal Progress Report Contract NDCrc-124, Nov. 15, 1942.
51. *Further Development of a Laboratory Type Jiggler for Activating Gas Charcoal*, R. York, Jr., OSRD 1521, Carnegie Institute of Technology, June 17, 1943. Div. 10-202.131-M4
52. *Composition of Gases Evolved During Activation*, R. York, Jr. et al, NDRC 10.4-30, Aug. 1, 1943. Div. 10-202.13-M16
53. *Activation of Carbonized Peach Pits and Black Walnut Shells in PCI Reports*, R. York, Jr., NDRC 10.5-9, Dec. 15, 1943. Div. 10-202.134-M3
54. *Activation of Charcoal in a Boiling Bed Furnace*, R. York, Jr., OSRD 4011, Aug. 12, 1944. Div. 10-202.13-M21
55. *Gas and Chemical Activation of Charcoal*, R. York, Jr. et al, OSRD 5278, June 29, 1945. Div. 10-202.13-M26
56. *Effect of Pore Size and Pore Size Distribution on Performance of ASC Whetlerite at High Humidities*, J. W. Zabor and A. Juhola, NDRC 10.1-40, Feb. 11, 1944. Div. 10-202.111-M2

Chapter 4

1. *Cyanogen Chloride II*, W. M. Latimer, OSRD 363, Report 168, University of California, Jan. 21, 1942. Div. 10-202.152-M3
2. *Progress Report on L-11 Project 54*, J. C. Elgin, Apr. 15, 1941.
3. *A Search for New Reactants*, F. E. Blacet and W. G. Young, OSRD 472, Mar. 12, 1942. Div. 10-202.141-M7
4. *A Study of the Physical Variables in the Production of Whetlerite and Silvered Whetlerite*, F. E. Blacet, D. H. Volman, and R. P. Connor, OSRD 621, June 9, 1942. Div. 10-202.12-M3
5. *Miscellaneous Experiments with National Charcoals. The Minimum Requirements of CWSNC-1 Charcoal*, F. E. Blacet, D. H. Volman, and G. J. Doyle, NDRC CCXXIV, Nov. 10, 1942. Div. 10-202.14-M17
6. *Adsorption of Constituents from a Standard Whetlerizing Solution*, F. E. Blacet, D. H. Volman, and G. J. Doyle, NDRC CCXXIII, Nov. 5, 1942. Div. 10-202.14-M16
7. *The Adsorption of Silver on Charcoal from Whetlerizing Solution*, F. E. Blacet, D. H. Volman, and G. J. Doyle, NDRC CXX, May 18, 1942. Div. 10-202.14-M9
8. *The Minimum Silver Requirements for Different Activated Charcoals*, F. E. Blacet and D. H. Volman, NDRC CLXVIII, July 28, 1942. Div. 10-202.14-M13
9. *Experiments with Type AS Whetlerites at Fostoria, Columbus, and Zanesville, Ohio*, F. E. Blacet, OSRD 1126, Dec. 9, 1942. Div. 10-202.1-M7
10. *An Investigation of the Possible Explosion Hazard Presented by Silver Whetlerizing Solutions and Residues*, F. E. Blacet and D. H. Volman, OSRD 1527, June 21, 1943. Div. 10-202.14-M26
11. *A Study of Impregnated Charcoal by X-Ray Diffraction Methods*, H. F. Johnstone and G. L. Clark, OSRD 1143, Dec. 9, 1942. Div. 10-202.143-M4
12. *Composition of Gases Evolved from Drying Whetlerites*, F. E. Blacet and D. H. Volman, OSRD 1201, NDRC 10.1-4, Jan. 4, 1943. Div. 10-202.14-M20
13. *A Study of the Partial Vapor Pressures of the Volatile Constituents in Whetlerizing Solutions*, F. E. Blacet and D. H. Volman, OSRD 1351, Apr. 20, 1943. Div. 10-202.19-M3
14. *An Additional Study of the Partial Vapor Pressures of the Volatile Constituents in Whetlerizing Solutions*, F. E. Blacet and D. H. Volman, OSRD 1626, July 3, 1943. Div. 10-202.14-M27
15. *C. G. Aging of Type AS and ASC Whetlerites*, F. E. Blacet, W. C. Pierce, T. Skei, R. K. Brinton, OSRD 1691, Aug. 6, 1943. Div. 10-202.16-M12
16. *The Absorption of HCN by Whetlerites and Other Absorbents*, E. O. Wiig, L. V. M'Carty, H. Scoville, N. L. Morse, F. Zimer, NDRC CLXXXIV, Sept. 15, 1942. Div. 10-202.154-M26
17. *The Removal of HCN and C_2N_2 by Absorbents*, E. O. Wiig, L. V. M'Carty, H. Scoville, N. L. Morse, F. Zimor, NDRC CCXVIII, Nov. 23, 1942. Div. 10-202.154-M29
18. *Absorption of AC, C_2H_2 and SA by Whetlerites and Other Absorbents*, E. O. Wiig, L. V. M'Carty, H. Scoville, N. L. Morse, F. Zimor, NDRC CCIII, Oct. 15, 1942. Div. 10-202.154-M28
19. *The Effect of Impregnation on the Removal of Ethylene Imine. Break Times for Di-, Tri-, and Penta Methylene Imines*, P. A. Leighton, NDRC LXX. Div. 10-202.14-M33
20. *Behavior of Sulfur Dioxide and Several Other Gases on Whetlerite*, P. A. Leighton, NDRC CXXXVII, June 15, 1942. Div. 10-202.156-M14
21. *A Summary of Tests on Soda Lime*, W. C. Pierce, OSRD 970, Oct. 21, 1942. Div. 10-202.2-M4
22. *Preliminary Study of Hexamine Impregnation*, F. E. Blacet and J. G. Roof, NDRC CXXII, May 22, 1942. Div. 10-202.141-M9
23. *The Preparation and Surveillance of Hexamethylene Tetramine Impregnated Charcoals*, F. E. Blacet and J. G. Roof, OSRD 1352, Apr. 20, 1943. Div. 10-202.14-M23

24. *The Deterioration of Thiocyanate Whetlerites*, W. M. Latimer, OSRD 132, Sept. 8, 1941. Div. 10-202.16-M2
25. *I. Solubility of AgSCN in Whetlerizing Solutions; II. The Adsorption of Ag^+ and SCN^- by Charcoals from Solutions*, F. E. Blacet and D. H. Volman, NDRC CLXXVII, Aug. 3, 1942. Div. 10-202.14-M14
26. *A Study of Thiocyanate Treated Whetlerites*, F. E. Blacet and T. Skei, NDRC CCX, Sept. 17, 1942. Div. 10-202.14-M15
27. *Summary of Test Data on E-6 Whetlerite*, W. C. Pierce and J. W. Zabor, NDRC CIX, May 9, 1942. Div. 10-202.16-M5
28. *Catalysis*, Berkmann, Morrell, Egloff, Reinhold Pub. Co. 1940.
29. *Cyanogen Chloride*, W. M. Latimer, OSRD 102, June 16, 1941. Div. 10-202.152-M1
30. *Behavior of Hopcalite, Whetlerites, etc. toward CK*, W. M. Latimer, H. W. Anderson, and H. Kerlinger, NDRC LXVI, Jan. 15, 1942. Div. 10-202.152-M2
31. *Stability of CK. Constants for Various Charcoals*, W. M. Latimer, H. W. Anderson, and H. Kerlinger, NDRC CII, Apr. 14, 1942. Div. 10-202.152-M4
32. *The Use of Mercury Compounds in the Impregnation of Activated Charcoal*, F. E. Blacet, R. J. Grabenstetter, and C. H. Simonson, OSRD 629, May 25, 1942. Div. 10-202.141-M10
33. *Iodine, Halogen Acids, and Their Salts as Charcoal Impregnants*, F. E. Blacet, R. J. Grabenstetter, and C. H. Simonson, NDRC CLXIII, July 27, 1942. Div. 10-202.141-M11
34. *Analytical Chemistry of Industrial Poisons*, M. B. Jacobs, Reinhold Publishing Co.
35. *A Study of the Poisoning of Various Absorbents toward Arsine by HCN*, E. O. Wiig, OSRD 628, June 6, 1942. Div. 10-202.154-M22
36. *The Effect of Impregnation on the Absorption of Ethylene Imine and Other Basic Materials*, P. A. Leighton, NDRC LXX. Div. 10-202.14-M33
37. *Summary of Protection Data on Ethylene Imine*, P. A. Leighton, NDRC LXXII, Jan. 23, 1942. Div. 10-202.156-M7
38. *Studies of Absorbents*, P. A. Leighton, NDRC LXXXVIII, Mar. 15, 1942. Div. 10-202.151-M3
39. *Ethylene Imine; Polymerization; Thermal Effects, etc.*, P. A. Leighton, NDRC CVI, Apr. 15, 1942. Div. 10-202.156-M10
40. *One-Step Impregnation with Whetlerizing Solutions Containing Copper, Silver, and Either Molybdenum, Vanadium or Tungsten*, F. E. Blacet and R. J. Grabenstetter, NDRC CLXXVI, Aug. 5, 1942. Div. 10-202.141-M12
41. *One-Step Impregnation with Copper, Silver, and Either Molybdenum, Vanadium, or Zinc*, F. E. Blacet, R. J. Grabenstetter, and C. H. Simonson, NDRC CCXXV, Nov. 10, 1942. Div. 10-202.141-M15
42. *Progress Report on ASM Whetlerite*, E. O. Wiig, OSRD 1455, May 25, 1943. Div. 10-202.12-M9
43. *Type ASMT Whetlerite Prepared in Rotary Driers, Laboratory Scale*, E. O. Wiig, F. E. Blacet, et al, OSRD 1693, Aug. 6, 1943. Div. 10-202.12-M10
44. *An Investigation of the Applicability of ASC Type Whetlerizing Equipment to the Preparation of ASM Whetlerite*, R. J. Kunz, NDRC 10.5-28, Mar. 15, 1944. Div. 10-202.12-M13
45. *Progress Report on ASCM Whetlerite*, E. O. Wiig, H. Scoville, et al, OSRD 1454, May 25, 1943. Div. 10-202.1-M11
46. *Preparation and Properties of ASV Whetlerites*, E. O. Wiig, H. Scoville, et al, OSRD 1912, Oct. 13, 1943. Div. 10-202.12-M12
47. *Picoline as Impregnant for Gas Mask Absorbents*, E. O. Wiig, OSRD 3130, Jan. 15, 1944. Div. 10-202.141-M17
48. *One-Step Impregnation with Whetlerizing Solutions Containing Copper, Silver and Chromium*, F. E. Blacet, R. J. Grabenstetter, and C. H. Simonson, NDRC CXCVI, Oct. 15, 1942. Div. 10-202.141-M14
49. *Determination of Pore Diameters in Charcoals*, F. E. Blacet and A. Jubola, NDRC 10.1-58, Jan. 24, 1945. Div. 10-202.111-M4
50. *Second Report on the Use of Copper, Silver and Chromium Solutions as Charcoal Impregnants*, F. E. Blacet et al, NDRC CCXXII, Dec. 21, 1942. Div. 10-202.141-M16
51. *Study of Zinc Chloride Carbon I*, G. W. Heise and J. A. Slyh, NDRC 10.5-11, Dec. 10, 1943. See also NDRC 10.5-15, -17, -22, -29, -32, -38, -39, -43, -46 for more data on zinc chloride carbons. Div. 10-202.133-M1 Div. 10-202.13-M18 Div. 10-202.134-M4
52. *Preliminary Report on the Aging of ASC Whetlerite under Various Atmospheres in Sealed Systems*, F. E. Blacet, J. G. Roof, J. N. Pitts, NDRC 10.1-29, Sept. 22, 1943. Div. 10-202.16-M14
53. *The State of Impregnants on ASC Charcoal. Magnetic Susceptibility Studies*, I. M. Klotz and R. J. Grabenstetter, NDRC 10.1-39, Jan. 28, 1944. Div. 10-202.141-M18
54. *Optimum Operating Conditions for a Laboratory Size Rotary Batch ASC Whetlerite Drier*, L. C. Weiss and G. L. Pratt, Central Laboratory Job Report ECL-7, Dec. 28, 1943.
55. *Additional Study of the Partial Vapor Pressure of the Volatile Constituents in Whetlerizing Solutions*, F. E. Blacet and D. H. Volman, NDRC 10.1-16, July 3, 1943. Div. 10-202.14-M27
56. *Reactions Involving Chromium which Occur when ASC Whetlerizing Solution is in Contact with Charcoal*, F. E. Blacet, D. H. Volman, G. J. Doyle, NDRC 10.1-17, June 11, 1943. Div. 10-202.14-M25
57. *Effect of Moisture on SA, AC, and CK Tube Lives for Two Type ASC Whetlerites*, F. E. Blacet and T. Skei, NDRC CCXXI, Dec. 10, 1942. Div. 10-202.17-M6
58. *Second Report on the Aging of ASC and ASCP Whetlerite Containing Various Amounts of Water in Sealed Systems*, F. E. Blacet, J. G. Roof, J. N. Pitts, NDRC 10.1-36, Nov. 12, 1943. Div. 10-202.17-M8
59. *Surveillance of Base Charcoals*, F. E. Blacet, R. J. Grabenstetter, C. H. Simonson, NDRC 10.1-25, Aug. 10, 1943. Div. 10-202.16-M13
60. *The Reactivation in Oxygen of CWS Charcoals*, T. F. Young, S. W. Weller, S. L. Simon, M. G. Buck, OSRD 4104, Aug. 4, 1944. Div. 10-202.132-M2

61. *Surveillance Studies on Whetlerites at Northwestern University. A Summary of Work from 1942 to 1944*, T. Skei, OSRD 4346, Nov. 15, 1944. Div. 10-202.16-M20
62. *Adsorption of Cyanogen by Charcoal. Amine Impregnated Charcoals*, W. M. Latimer, H. W. Anderson, H. Kerlinger, NDRC CXLIX, June 15, 1942. Div. 10-202.152-M5
63. *Impregnated Charcoal. Specific Impregnants for Increasing CC Protection*, F. E. Dolian and S. Hormats, TDMR 767, Nov. 12, 1943.
64. *The Use of Pyridine and Picoline in Gas Mask Charcoals*, L. C. Weiss, G. L. Pratt, et al, NDRC 10.1-56, Nov. 16, 1944. Div. 10-201.1-M32
65. *Summary of Pilot Plant Studies of the Preparation of ASC Whetlerite*, R. J. Kunz, E. H. Conroy, et al, OSRD 4129, Sept. 14, 1944. Div. 10-202.12-M14
66. *Design and Construction of the Whetlerization Pilot Plant at the NDRC Division 10 Central Laboratory*, R. J. Kunz, OSRD 1778, Sept. 6, 1943. Div. 10-202.14-M29
67. *The Effect of Backfeeding on the Quality of ASC Whetlerite*, R. J. Kunz and E. H. Conroy, NDRC 10.5-30, May 6, 1944. Div. 10-202.19-M5
68. *Reclamation of Type A Whetlerite*, R. J. Kunz and E. H. Conroy, NDRC 10.5-23, Mar. 9, 1944. Div. 10-202.19-M4
69. *Leaching and Rewhetlerization: Their Effect on Whetlerite Quality*, L. C. Weiss, H. Waggoner, and M. Bierman, NDRC 10.1-54, Sept. 18, 1944. Div. 10-202.16-M18
70. *Use of Aminated Phenol-Formaldehyde Xerogels as Gas Adsorbents*, G. F. Mills, OSRD 1771, Sept. 4, 1943. Div. 10-202.21-M6
71. *Further Studies on the Characteristics and Impregnation of Aminated Phenol-Formaldehyde Xerogels*, P. A. Leighton and S. W. Grinnell, NDRC CCXI, Nov. 15, 1942. Div. 10-202.21-M2
72. *Use of Amine Resins as Gas Adsorbents*, G. F. Mills, NDRC 10.4-46, Jan. 20, 1944. Div. 10-202.21-M7
73. *Catalysts for the Oxidation of Carbon Monoxide in Air*, R. N. Pease, OSRD 3071, Jan. 4, 1944. Div. 10-202.2-M6
74. *Journal of Industrial and Engineering Chemistry*, Bray and Fraser, 1920.
75. *X-Ray Studies in Whetlerites*, H. F. Johnstone and G. L. Clark, NDRC CLXXVIII, Aug. 15, 1942. Div. 10-202.143-M3
76. *Charcalite, a Calcium Chloride Impregnated Charcoal Drying Agent*, R. N. Pease and J. H. McLean, OSRD 3776, June 15, 1944. Div. 10-202.142-M2
77. *An Exploratory Study of Carbon Monoxide Protection on Charcoal and Other Carriers*, D. H. Volman and G. J. Doyle, NDRC 10.1-41, Feb. 7, 1944. Div. 10-202.153-M1
78. *Factors in Canister Design*, I. M. Klotz and H. Cutforth, OSRD 5239, June 7, 1945. Div. 10-202.156-M20
79. *Conversion of Types A and AS Impregnated Charcoals to Type ASC Impregnated Charcoal*, S. Hormats and B. M. Zeffert, TDMR 824, Apr. 18, 1944.
80. *Conversion of Types A and AS Impregnated Charcoals to Type ASC Impregnated Charcoals in Laboratory Pilot Plant*, R. A. Fisher and E. Croft, Jr., TDMR 833, Apr. 22, 1944.
81. *Relative Ignition Temperatures of Impregnated Charcoals*, F. E. Dolian, TDMR 897, Sept. 22, 1944.
82. *Reworking Impregnated Charcoals*, R. A. Fisher, J. Y. G. Walker, Jr., and E. Croft, Jr., TDMR 976, Jan. 30, 1945.
83. *The Protection Afforded by Respirators Against Cyanogen Chloride, and the Improvement Effected by Pyridine Impregnation of the Charcoal Filling*, Ptn. 4221 (T. 10533A), Aug. 10, 1943.
84. *Impregnated Charcoal. Pyridine as an Impregnant*, F. E. Dolian, B. Zeffert, and S. Hormats, TDMR 727, Aug. 23, 1943.
85. *Use of Pyridine in the Preparation of a Whetlerite with Increased CC Protection*, S. N. Naldrett, Chemical Warfare Laboratories, Ottawa, Research Section Report No. 30, Sept. 15, 1943.
86. *Impregnation of Charcoal with Amines to Improve Cyanogen Chloride Protection*. S. N. Naldrett, Chemical Laboratories, Ottawa, Research Section Report No. 29, Oct. 15, 1943.
87. *Type ASCP Impregnated Charcoal*, S. Hormats and B. M. Zeffert, TDMR 803, Feb. 19, 1944.
88. *Whetlerite Process Development. Experimental Production of Type E11 Impregnated Charcoal at Zanesville CWS Plant*, F. E. Dolian and B. M. Zeffert, TDMR 818, Mar. 27, 1944.
89. *Reactants for CC*, R. P. Graham and R. G. Davis, McMaster University, C. E. 160, June 15, 1944.
90. *The Properties of Coppered Coal Charcoals Containing (a) Molybdenum (b) Pyridine*, Oxford University, Research Report No. 44.19 (Z. 12697), Sept. 22, 1944.
91. *Protection Against Cyanogen Chloride. Charcoal Impregnated with Pyridine*, Ptn. 4221 (T. 4868), (Y. 3228), Apr. 12, 1943.
92. *Improved Impregnated Charcoal. Preparation and Test of Whetlerites Containing Sodium Hydroxide and Amines*, J. C. Goshorn and P. O. Rockwell, EATR 153, May 29, 1934.
93. *Service Canister (10). Development of a Manufacturing Process for Impregnated Charcoal E6*, P. A. Hartman, EATR 326, Aug. 2, 1940.
94. *Impregnated Charcoal Type A and E-6. Effect of Impurities in Base Charcoal*, S. Hormats, TDMR 295, Sept. 5, 1941.
95. *Adsorption Characteristics of Charcoal Impregnated with Thiocyanate*, R. S. Brown, C. E. 87, Dec. 15, 1941.
96. Chemical Warfare Monograph, Vol. 47, June 1919.
97. H. V. Wright, EACD 438, November 1927.
98. Anti-Gas Dept. Weekly Reports for Project D 1.1-14, 1927–28.
99. R. S. Brown and J. G. Hartnett, EATR 200, December 1935.
100. R. S. Brown and J. B. Hartnett, EATR 220, April 1936.
101. *Compilation of N_0 and λ_c Values for Miscellaneous Whetlerites before and After Aging*, D. B. Ehrlinger, L. C. Weiss, G. L. Pratt, J. B. Fehrenbacher, J. W. Zabor, and T. Skei, NDRC 10.1-48, Aug. 12, 1944. Div. 10-202.16-M17
102. *Manufacture of Whetlerite in the Experimental Plants*, H. V. Wright and F. Bellinger, EACD 510, Apr. 8, 1929.
103. *Impregnated Charcoal Type A, Improved. Copper Ammonium Carbonate Impregnating Solution*, S. Hormats, F. C. Whitney, and S. C. Malkiewicz, TDMR 275, Apr. 15, 1941.

SECRET

104. *Studies on Arsine Protection*, W. C. Pierce, B. M. Abraham, and H. G. Monteith, NDRC XL, Oct. 25, 1941.
105. *Performance of Canisters after Wearing Tests at Camp Sibert, Alabama*, W. C. Pierce, J. W. Zabor, and H. S. Joseph, OSRD 3058, Dec. 31, 1943. Div. 10-201.1-M22
106. *Nickel Impregnated Charcoal*, L. Williams, C. E. 21, Dec. 15, 1941.
107. *Study of Impregnation*, J. C. Elgin, OSRD 586, Apr. 9, 1942. Div. 10-202.14-M7
108. *Impregnation of Activated Charcoals to Obtain High SA Lives*, A. P. Colburn, OSRD 853, Sept. 1, 1942. Div. 10-202.141-M13

Chapter 5

1. *Surveillance Studies on Whetlerites at Northwestern University — A Summary of Work from 1942–1944*, T. Skei, OSRD 4346, Nov. 15, 1944. Div. 10-202.16-M20
2. *Preliminary Report on the Aging of ASC Whetlerite under Various Atmospheres in Sealed Systems*, J. G. Roof, F. E. Blacet, et al, NDRC 10.1-29, Sept. 22, 1943. Div. 10-202.16-M14
3. *Second Report on the Aging of ASC and ASCP Whetlerite Containing Various Amounts of Water in Sealed Systems*, J. G. Roof, F. E. Blacet, et al, NDRC 10.1-36, Nov. 12, 1943. Div. 10-202.17-M8
4. *Performance of Canisters After Wearing Tests at Camp Sibert*, W. C. Pierce, J. W. Zabor, and H. S. Joseph, OSRD 3058, Dec. 31, 1943. Div. 10-201.1-M22
5. *Additional Surveillance Tests on Canisters Used in the First Sibert Surveillance Study*, T. Skei, OSRD 4015, July 1944. Div. 10-201.1-M29
6. *Performance of M10 and M9A2 Canisters After Regular Use at Camp Sibert, Alabama*, T. Skei, J. W. Fehrenbacher, and H. S. Joseph, OSRD 4014, July 1944. Div. 10-201.1-M28
7. *Canister Surveillance Studies, I*, T. Skei, R. K. Brinton, and W. C. Pierce, NDRC 10.1-32, October 1943. Div. 10-201.1-M17
8. *Whetlerization and Surveillance Studies on PCI Charcoal at Varying Stages of Activation*, T. Skei, OSRD 4112, Sept. 9, 1944. Div. 10-202.13-M23
9. *Surveillance of Types ASC and ASCM Whetlerites*, E. O. Wiig, et al, OSRD 1873, Oct. 1, 1943. Div. 10-202.16-M15
10. *Picoline as Impregnant for Gas Mask Absorbents*, E. O. Wiig, et al, OSRD 3130, Jan. 15, 1944. Div. 10-202.141-M17
11. *Impregnated Charcoal. Pyridine as an Impregnant*, F. E. Dolian, B. Zeffert, and S. Hormats, TDMR 727, Aug. 23, 1943.
12. *Impregnated Charcoal. Stability of Type ASC Impregnated Charcoal*, F. E. Dolian, B. Zeffert, and S. Hormats, TDMR 714, Aug. 7, 1943.
13. *Comparative Evaluation of Types ASC, ASM, and ASV Impregnated Charcoals*, B. M. Zeffert and S. Hormats, TDMR 765, Nov. 10, 1943.
14. *Impregnated Charcoal. Specific Impregnants for Increasing CC Protection*, F. E. Dolian and S. Hormats, TDMR 767, Nov. 12, 1943.
15. *Surveillance of ASC Impregnated Charcoal, Series 1, P. C. 1. Base Charcoal Impregnated at Edgewood Arsenal in April 1943*, H. J. Allison, Jr., TDMR 799, Jan. 28, 1944.
16. *Type ASCP Impregnated Charcoal*, S. Hormats and B. M. Zeffert, TDMR 803, Feb. 19, 1944.
17. *Whetlerite Process Development. Experimental Production of Type E11 Impregnated Charcoal at Zanesville C. W. S. Plant*, F. E. Dolian and B. M. Zeffert, TDMR 818, Mar. 27, 1944.
18. *Compilation of N_0 and λ_c Values for Miscellaneous Whetlerites Before and After Aging*, T. Skei, et al, OSRD 4013, Aug. 12, 1944. Div. 10-202.16-M17
19. *Surveillance Tests on ASC, E11, and E13 Whetlerites*, T. Skei, OSRD 4232, Oct. 12, 1944. Div. 10-202.16-M19
20. *Performance of M10, M10A1, and M1A1 Canisters After Use in the Southwest Pacific Area*, J. B. Fehrenbacher, F. E. Blacet, et al, OSRD 4928, Apr. 12, 1945. Div. 10-201.1-M35
21. *The Preparation and Surveillance of Hexamethylenetetramine-Impregnated Charcoals*, J. G. Roof and F. E. Blacet, OSRD 1352, Apr. 20, 1943. Div. 10-202.14-M23
22. *The Use of Pyridine and Picoline in Gas Mask Charcoal*, L. C. Weiss, et al, NDRC 10.1-56, Nov. 16, 1944. Div. 10-201.1-M32

Chapter 6

1. Brunauer and P. H. Emmett, *J. Am. Chem. Soc.*, **57**, 1935, p. 1754.
2. P. H. Emmett and Brunauer, *ibid.*, **59**, 1937, p. 1553.
3. Brunauer, P. H. Emmett, and Teller, *ibid.*, **60**, 1938, p. 309.
4. Harkins and Jura, *ibid.*, **66**, 1944, pp. 919, 1362.
5. Harkins and Jura, *ibid.*, **66**, 1944, p. 1366.
6. P. H. Emmett, *ibid.*, **68**, 1946, p. 1784.
7. P. H. Emmett and DeWitt, *Ind. Eng. Chem., Anal. Ed.*, **13**, 1941, p. 28.
8. P. H. Emmett in Kraemer's *Advances in Colloid Science*, Interscience Publishers, New York, 1942, pp. 1–36.
9. "Symposium in New Methods for Particle Size Determination," P. H. Emmett, *Am. Soc. for Testing Materials*, 1941, p. 95.
10. Cassie, *Trans. Faraday Soc.*, **41**, 1945, p. 450.
11. Hill, *J. Chem. Physics* (to be published).
12. P. H. Emmett, *Ind. Eng. Chem.*, **37**, 1945, p. 639.
13. Deitz and Gleysteen, *J. Research Natl. Bur. Standards*, **29**, 1942, p. 191.
14. Joyner, Weinberger, and Montgomery, *J. Am. Chem. Soc.*, **67**, 1945, p. 2182.
15. Pickett, *J. Am. Chem. Soc.*, **67**, 1943, p. 1938.
16. Hill, *ibid.*, **68**, 1946, p. 535.



17. *Survey of Pore Structure in Charcoal*, A. Juhola, OSRD 5500, June 1945. Div. 10-202.111-M5
a. E. O. Wiig, Madison, and A. Juhola, Monthly Progress Report to CWS Feb. 1, 1946.
18. Beebe, Beckwith, and Honig, *J. Am. Chem. Soc.*, **67**, 1943, p. 1554.
19. Schmidt, *Z. physik. Chem.*, **133**, 1928, p. 280.
20. P. H. Emmett and DeWitt, *J. Am. Chem. Soc.*, **65**, 1943, p. 1253.
21. Barrer, *J. Soc. Chem. Ind.*, **64**, 1945, p. 130.
22. Barrer and Ibbitson, *Trans. Faraday Soc.*, **40**, 1944, pp. 195, 206.
23. *Absorption and Surface Area Measurements on Whetlerites and Charcoal Samples*, P. H. Emmett, H. A. Pohl, J. Holmes, and J. T. Kummer, OSRD 1777, Sept. 6, 1943. Div. 10-202.15-M18
a. *Physical Adsorption*, Brunauer, Princeton Press, 1941, p. 444.
24. *Physical Chemistry of Activation of Charcoal*, T. F. Young, OSRD 5354, July 21, 1945. Div. 10-202.13-M27
25. Lemieux and Morrison, Canadian Report C. E. 151, Sept. 20, 1943.
a. P. H. Emmett, J. Holmes, and J. T. Kummer, NDRC 10.1-1, Dec. 15, 1942. Div. 10-202.15-M11
b. P. H. Emmett, J. Holmes, H. A. Pohl, and J. T. Kummer, NDRC 10.4-26, May 27, 1943. Div. 10-202.15-M16
26. *Absorption of Nitrogen on CWSN Base Charcoals*, P. H. Emmett, J. Holmes, J. T. Kummer, and Mace, NDRC 10.5-3, Sept. 11, 1943. Div. 10-202.11-M8
27. P. H. Emmett, J. Holmes, H. W. Anderson, J. T. Kummer, Mace, and Jenkins, OSRD 5065, May 30, 1945. Div. 10-202.15-M19
28. *Determination of Pore Diameters in Charcoal*, A. Juhola and F. E. Blacet, NDRC 10.1-58, Jan. 24, 1945. Div. 10-202.111-M4
29. A. Juhola and T. Skei, NDRC 10.1-46, June 28, 1944. Div. 10-202.111-M3
30. P. H. Emmett, J. Holmes, and J. T. Kummer, NDRC CLXXIX, Aug. 15, 1942. Div. 10-202.15-M11
32. P. H. Emmett, J. Holmes, J. T. Kummer, Mace, and H. W. Anderson, OSRD 4959, Apr. 20, 1945. Div. 10-202.17-M9
33. Lawson, *Trans. Faraday Soc.*, **32**, 1936, p. 473.
34. Polanyi and Goldman, *Z. physik. Chem.*, **132**, 1928, p. 321.
35. *Rate of Sorption of Water Vapor from Humid Air Streams by Activated Carbons*, A. P. Colburn, OSRD 849, Sept. 1, 1942.
36. A. P. Colburn, NDRC CI, Apr. 15, 1942. Div. 10-202.17-M3
37. A. P. Colburn, NDRC CXXXIII, June 17, 1942. Div. 10-202.17-M5
38. Lowry, *J. Am. Chem. Soc.*, **46**, 1929, p. 824.
39. Coolidge, *ibid.*, **48**, 1926, p. 1795.
40. McBain, Porter, and Sessions, *ibid.*, **55**, 1933, p. 2294.
41. *Sorption of Gases and Vapors by Solids*, McBain, G. Routledge & Sons, London, 1932.
42. P. H. Emmett and H. W. Anderson, *J. Am. Chem. Soc.*, **67**, 1945, p. 1492.
43. Fineman, Guest, and McIntosh, Canadian Report C. E. 147, Nov. 20, 1943. See also *Can. J. Research*, **24B**, 1946, p. 109.
44. *A Treatise on Physical Chemistry*, edited by H. S. Taylor, D. Van Nostrand Co., Kraemer, Chapter XX, p. 1661.
45. Cohan, *J. Am. Chem. Soc.*, **60**, 1938, p. 433.
46. Morrison and McIntosh, Canadian Report C. E. 147, Aug. 8, 1944. See also *Can. J. Research*, **24B**, 1946, p. 137.
47. H. F. Johnstone and G. L. Clark, NDRC LXXXIX, Apr. 9, 1942. Div. 10-202.17-M2
50. Washburn, *Proc. Nat. Acad. Sci.*, **7**, 1921, p. 115.
51. Lamb and Woodhouse, *J. Am. Chem. Soc.*, **58**, 1930, p. 2637.
52. P. H. Emmett, H. A. Pohl, and J. T. Kummer, NDRC CXXIII, May 15, 1942. Div. 10-202.15-M11
53. Brunauer, Deming, Deming, and Teller, *J. Am. Chem. Soc.*, **62**, 1940, p. 1723.
54. Beeck, *Reviews of Modern Physics*, **17**, 1945, p. 61.
55. Anderson, *Z. phys. Chem.*, **88**, 1914, p. 191.
56. Foster, *Trans. Faraday Soc.*, **28**, 1932, p. 645.
57. National Carbon Co., NDRC 10.5-34, June 10, 1942. Div. 10-202.13-M18
58. National Carbon Co., NDRC 10.5-43, Aug. 10, 1944. Div. 10-202.13-M18
59. National Carbon Co., MSR, Sept. 15, 1944.
61. Ritter and Drake, *Ind. Eng. Chem.*, Anal. Ed., **17**, 1945, p. 782.
62. Drake and Ritter, *ibid.*, p. 787.
63. P. H. Emmett, MSR, Mar. 15, 1944. Div. 10-202.1-M8
64. J. W. Zabor and A. Juhola, NDRC 10.1-40, Feb. 11, 1944. Div. 10-202.111-M2
65. P. H. Emmett, NDRC LII, Dec. 22, 1941. Div. 10-202.13-M3
66. P. H. Emmett, NDRC CLXXIX, Aug. 15, 1942. Div. 10-202.15-M11
68. F. E. Blacet and T. Skei, NDRC 10.1-8, Mar. 12, 1943. Div. 10-202.13-M10
69. P. H. Emmett and J. Holmes, NDRC 10.5-12, Nov. 12, 1943. Div. 10-202.111-M1
70. Dewey and Lefforge, *Ind. Eng. Chem.*, **24**, 1932, p. 1045.
71. Lowry and Hulett, *J. Am. Chem. Soc.*, **42**, 1920, p. 1393.
72. Lowry and Hulett, *ibid.*, p. 1408.
73. T. F. Young, OSRD 4104, Sept. 7, 1944. Div. 10-202.132-M2
74. Lambert, *Trans. Faraday Soc.*, **32**, 1926, p. 452.
75. Rhead and Wheeler, *J. Chem. Soc.*, **103**, 1913, p. 461.
76. Lepin, *Physik. Z. Sowjetunion*, **4**, 1933, p. 282.
77. Schilow, Schatanowskaja, and Tschmutow, *Z. physik. Chem.*, **150**, 1930, p. 31.
78. Schilow, Schatanowskaja, and Tschmutow, *Z. physik. Chem.*, **A 149**, 1930, p. 211.
79. King, *J. Chem. Soc.*, **1937**, p. 1489.
a. Shah, *J. Chem. Soc.*, **1929**, pp. 2661, 2676.
80. Barrer, *J. Chem. Soc.*, **1936**, p. 1261.
a. Stock, *Z. Anorg. Chem.*, **195**, 1931, p. 158.
81. P. H. Emmett, NDRC 10.1-1, Jan. 13, 1943. Div. 10-202.15-M11
82. Keyes and Marshall, *J. Am. Chem. Soc.*, **44**, 1927, p. 152.
83. Blench and Garner, *J. Chem. Soc.*, **1924**, p. 1288.
84. Marshall and MacInnes, *Can. J. of Res.*, **15B**, 1937, p. 75.
85. Aharoni and Simon, *Z. physik. Chem.*, **B4**, 1929, p. 175.
86. Juza and Langheiss, *Z. Elektrochemie*, **45**, 1939, p. 689.
87. *Analysis of Base Charcoals*, E. O. Wiig and J. F. Flagg, NDRC 10.1-26, June 1943. Div. 10-202.11-M7

88. Brunner, *Z. Elektrochemie*, **38**, 1932, p. 58.
89. *Surveillance of Base Charcoals*, F. E. Blacet et al, NDRC 10.1-25, Aug. 10, 1943. Div. 10-202.16-M13
90. Allmand, *J. Phys. Chem.*, **33**, 1929, p. 1682 a.
91. Allmand, *Proc. Roy. Soc.* (London), **129A**, 1930, p. 235.
92. Allmand, *Proc. Roy. Soc.* (London), **130A**, 1930, p. 193.
93. Allmand, *Proc. Roy. Soc.* (London), **134A**, 1932, p. 554.
94. Allmand, *Proc. Roy. Soc.* (London), **169A**, 1938, p. 25.
95. Allmand, *Trans. Faraday Soc.*, **28**, 1932, p. 225.
96. Muller and Cobb, *J. Chem. Soc.*, **1940**, p. 177.
97. Stenhouse, *Ann. der chem. Pharm.*, **101**, 1897, p. 243.
98. Vander Ley and Wibaut, *Rev. trav. chim.*, **51**, 1932, p. 1143.
99. Bente and Walton, *J. Phys. Chem.*, **47**, 1943, p. 329.
100. Ruff, *Kolloid Z.*, **37**, 1935, p. 270.
104. Stratton and Winkler, *Ind. Eng. Chem.*, **34**, 1942, p. 603.
105. J. T. Kummer, Thesis, The Johns Hopkins University, Dept. Chem. Eng. (1946).
109. London, *Z. physik. Chem.*, **B11**, 1930, p. 222.
110. Denbigh, *Trans. Faraday Soc.*, **36**, 1940, p. 936.
111. *Studies on Activated Charcoals and Whetlerite*, P. H. Emmett, NDRC LII, Dec. 22, 1941. Div. 10-202.13-M3
112. Ferguson, Sheffer, and Waldock, Canadian Report, C. E. 107-20, Apr. 10, 1942.
113. Ferguson and Barnartt, Canadian Report C. E. 107, Report No. 3, III-1-763, Apr. 12, 1943.
114. Ferguson and Barnartt, Canadian Report, C. E. 107, III-1-1519, Mar. 6, 1944.
a. Stevens, Canadian Report, C. E. 161, Report No. 2, III-1-1625, May 16, 1944.
115. *Study of Zinc Chloride Carbon*, G. W. Heise and J. A. Slyh, NDRC 10.5-11, Dec. 10, 1943. Div. 10-202.133-M1
116. Trost and Morrison, Canadian Report, C. E. 151, III-1-1815, Aug. 25, 1944.
117. *Absorbents for Gas Masks*, E. O. Wiig, MSR, Dec. 15, 1944. Div. 10-202.1-M8
118. *Retentivity of Charcoals*, D. H. Volman, G. J. Doyle, and F. E. Blacet, OSRD 5236, Apr. 23, 1945. Div. 10-202.15-M20
119. Stevens, Canadian Report C. E. 161, III-1-1806, Sept. 9, 1944.
120. Mackenzie and Stevens, Canadian Report, C. E. 161, III-1-1852, Oct. 20, 1944.
121. *Chemisorption of Gases on Charcoals and Type A Whetlerites*, P. H. Emmett, H. A. Pohl, and J. T. Kummer, NDRC 10.4-29, July 8, 1943. Div. 10-202.15-M17
122. *X-Ray Studies*, H. F. Johnstone and G. L. Clark, NDRC CLXXVIII, Aug. 31, 1942. Div. 10-202.143-M3
123. *Study of Impregnated Charcoal by X-Ray Diffraction*, H. F. Johnstone and G. L. Clark, OSRD 1143, Dec. 9, 1942. Div. 10-202.143-M4
124. Lamb, *Ind. Eng. Chem.*, **11**, 1919, p. 429.
a. Garner and Kingman, *Trans. Faraday Soc.*, **25**, 1929, p. 24.
125. *Application of the Electron Microscope to the Study of Charcoal*, H. F. Johnstone and G. L. Clark, OSRD 1686, Aug. 3, 1943. Div. 10-202.143-M5
126. T. F. Young, NDRC V, June 18, 1941. Div. 10-202.11-M1
127. Kobe, *J. Ch. Ed.*, **8**, 1931, p. 236.
128. Bangham, *Proc. Roy. Soc.*, **147A**, 1934, p. 175; *Trans. Faraday Soc.*, **33**, 1937, pp. 1459, 1463.
129. Hendricks, Melson, and Alexander, *J. Am. Chem. Soc.*, **62**, 1940, p. 1457.
130. Cornet, *J. Chem. Phys.*, **11**, 1943, pp. 5, 217.

Chapter 7

1. *The Nature of the Product Desorbed from Charcoal Brought Halfway to the Break Point with PS*, G. P. Baxter and H. W. Anderson, Informal Report C.
2. *The Increase in Weight of Charcoal at the Break Point*, M. Dole, NDRC XXVI, Aug. 29, 1941. Div. 10-202.11-M2
3. *A Study of the Penetration of Charcoal by Chloropicrin by Means of an Ultraviolet Photometer*, M. Dole and I. M. Klotz, NDRC LXIV. Div. 10-202.155-M1
4. *Effect of Activation Time on Properties of PCI Charcoal and Corresponding ASC Whetlerite (Second Report)*, T. Skei, F. E. Blacet, and W. C. Pierce, NDRC 10.1-23, OSRD No. 1746, Aug. 10, 1943. Div. 10-202.11-M6
5. *Performance of the M10 Canister Against HS under Humid Tropical Conditions*, W. C. Pierce, OSRD 1194, Feb. 3, 1943. Div. 10-201.1-M13
6. *Unpublished Work on the Performance of the M10 Canister Against HN3 Under Humid Tropical Conditions*, J. W. Zabor and W. C. Pierce.
7. "The Behavior of Gas Mask Charcoal Towards Phosgene and Chlorine," J. B. Nielsen, *Zeitschrift Fur das gesamte Schiess- und Springstoffwesen mit der Sonderabteilung Gasschutz*, **27**, 1932, pp. 136–139, 170–173, 208–211, 244–248, 280–284.
8. *Adsorption Studies on Chloropicrin and Phosgene*, M. Dole, I. M. Klotz, and S. W. Weller, NDRC CLXXII, July 15, 1942.
9. *An Investigation of the Mechanism of Removal of Phosgene, etc.*, D. M. Yost, R. W. Dodson, D. S. Martin, and W. P. Nies, OSRD 903, Sept. 25, 1942. Div. 10-202.155-M5
10. *Unpublished Work on the Mechanism of Removal of CG*, J. W. Zabor and W. C. Pierce.
11. *An Intermittent Flow Canister Test Machine*, W. C. Pierce, NDRC 10.1-3, OSRD No. 1193, Jan. 28, 1943. Div. 10-201.1-M12
12. *Variation of the CG Life of Various Humidified Adsorbents with Decreasing Temperature*, J. W. Zabor and W. C. Pierce, NDRC CC, Nov. 4, 1942.
13. *Preliminary Tests with COClF*, J. W. Otvos and R. G. Dickinson, NDRC CCVI, Oct. 21, 1942. Div. 10-202.156-M16
14. *Tube Tests with HF*, J. W. Otvos, H. F. Johnstone, and R. G. Dickinson, NDRC CXLVIII, June 29, 1943. Div. 10-402.2-M3
15. *Retentivity Tests with HF*, H. F. Johnstone and R. G. Dickinson, NDRC CCVII, Oct. 10, 1942. Div. 10-202.15-M14
16. *Chemisorption of Gases on Charcoals and Type A Whetler-*

ites, R. A. Pohl, J. T. Kummer, and P. H. Emmett, NDRC 10.4-29, July 8, 1943. Div. 10-202.15-M17
17. *Retention of HCl by the MIXA1 Canister*, R. K. Brinton and W. C. Pierce, NDRC CLXVII, July 29, 1942. Div. 10-201.1-M7
18. *Removal of H_2S*, D. M. Yost, NDRC XXIV. Div. 10-202.15-M3
19. *Action of Nitrogen Dioxide on Activated Charcoals, Whetlerites and Other Substances*, W. B. Lewis, R. K. Brinton, W. J. Blaedel, and F. E. Blacet, NDRC 10.1-20, June 25, 1943. Div. 10-202.156-M18
20. *Toxicity of Nitrogen Oxides and Container Penetration Tests*, S. F. Penny and J. F. Leib, Chemical Warfare Laboratories, Ottawa, Physiological Section Report No. 29, Dec. 28, 1943.
21. *Behavior of SO_2 and of Several Other Gases on Whetlerite*, P. A. Leighton, NDRC CXXXVII, June 15, 1942. Div. 10-202.156-M14
22. *Phosphorus Trifluoride Removal by Whetlerite and by Soda Lime-Whetlerite Mixtures*, A. J. Stosick, J. W. Otvos, and R. G. Dickinson, NDRC XCI, Apr. 6, 1942. Div. 10-202.156-M8
23. *Selenium Hexafluoride. Break Times at Various Temperatures and Water Contents*, R. G. Dickinson, NDRC XXXII. Div. 10-202.15-M23
24. *Comparative Retentivities of Whetlerites and Type D Mixtures for SeF_6 and for 1120*, A. J. Stosick, J. W. Otvos, C. W. Gould, Jr., and R. G. Dickinson, OSRD 616, May 9, 1942. Div. 10-202.156-M12
25. *Preliminary Tube Tests with COClF*, J. W. Otvos, H. F. Johnstone, A. J. Stosick, and R. G. Dickinson, NDRC CCVI, Oct. 21, 1942. Div. 10-202.156-M16
26. *Toxicity, Pathological and Charcoal Penetration Studies of Sulfur Pentafluoride*, E. M. K. Geiling, OSRD 3030.
27. *Preliminary Examination of 1120 Removal*, A. J. Stosick, J. W. Otvos, C. W. Gould, Jr., and R. G. Dickinson, OSRD 300, Dec. 18, 1941. Div. 10-202.156-M4
28. *Summary of a Review on Hydrogen Cyanide, Cyanogen, and Cyanogen Chloride Removal by Gas Mask Absorbents*, H. Scoville, C. Wagner, and E. O. Wiig, OSRD 1268, Mar. 17, 1943. Div. 10-202.154-M31
29. *The Hydrogen Cyanide-Cyanogen Reaction on Type A Whetlerite and the Absorption of Cyanogen by Charcoals*, L. V. M'Carty — Ph.D. thesis, University of Rochester, 1945.
30. *HCN and C_2N_2 Absorption*, CWS Report.
31. *Animal and Chemical Tests on Cyanogen in the Effluent Air Stream After Adsorption of HCN*, J. W. Zabor and W. C. Pierce, NDRC CCIX, OSRD 1090, Dec. 7, 1942. Div. 10-202.152-M8
32. *Mechanism Studies on the Removal of Cyanogen Chloride from an Air Stream by Charcoal*, F. Zimer — Part I, Ph.D. thesis, University of Rochester, 1945.
33. I. M. Klotz, MSR, Dec. 15, 1943.
34. *The Use of Pyridine Bases as Specific Impregnants for Increasing the Protection of Charcoal Adsorbents Against Cyanogen Chloride*, F. J. Ball, — Ph.D. thesis, University of Rochester, 1945.
35. *Compilation of N_0 and λ_c Values for Miscellaneous Whetlerites Before and After Aging*, T. Skei and J. W. Zabor, OSRD 4013, Aug. 12, 1944. Div. 10-202.16-M17
36. *Unpublished Work on the Sorption of Ammonia by Gas Mask Adsorbents*, J. W. Zabor and W. C. Pierce.
37. *Ammonia Protection Afforded by the Service Canister*, J. H. Dinius, S. M. Jessop, and J. W. Thomas, TDMR 377, May 25, 1942.
38. *A Study of the Distribution of Arsine in Impregnated Charcoal by Means of Radioactive Tracers*, J. W. Hickey, Ph.D. thesis, University of Rochester, 1942.
39. *The Effect of Water on the Adsorption of Arsine and Hydrogen Cyanide by Impregnated Charcoals*, H. Scoville, Jr., Ph.D. thesis, University of Rochester, 1942.
40. *Temperatures in Canisters and Tubes During SA Removal*, I. M. Klotz, R. K. Brinton, and M. Dole, NDRC CLXII, July 25, 1942. Div. 10-201.1-M6
41. *The Location and Identification of Reaction Products in Whetlerite Treated with Arsine*, H. F. Johnstone, OSRD 704. Div. 10-202.14-M10
42. *Calorimetric Studies on the Removal of Arsine*, J. B. Hatcher, G. B. Guthrie, and H. M. Huffman, NDRC CXCVIII, Oct. 15, 1942. Div. 10-202.156-M15

Chapter 8

1. "Rates of Water Vapor Adsorption from Air by Silica Gel," J. E. Ahlberg, *Ind. Eng. Chem.*, **31**, 1939, p. 988.
2. *The Effect of Tube Diameter and Type of Air Flow on Charcoal Breakdown Times*, J. R. Arthur, E. J. Brockless, and J. W. Linnett, Oxford University, Research Report No. 43.20, (Y. 9896).
3. "Concentration of Dilute Solutions of Electrolytes by Base-Exchange Materials," R. H. Beaton and C. C. Furnas, *Ind. Eng. Chem.*, **33**, 1941, p. 1500.
4. "Some Aspects of the Behavior of Charcoal with Respect to Chlorine," G. S. Bohart and E. Q. Adams, *J. Am. Chem. Soc.*, **42**, 1920, p. 523.
5. *Rate of Sorption of Water Vapor from Humid Air Streams by Activated Carbons*, A. P. Colburn, E. O. Kraemer, and L. W. Schmidt, OSRD 849, Aug. 1, 1942.
6. G. Damkohler, *Z. Elektrochem.*, **42**, 1936, p. 846; **43**,1937, p. 1.
7. *Some Aspects of the Physical Chemistry of the Respirator*, C. J. Danby, J. G. Davoud, D. H. Everett, C. N. Hinshelwood, and R. M. Lodge, Oxford University.
8. "The Theory of Chromatography," D. De Vault, *J. Am. Chem. Soc.*, **65**, 1943, p. 532.
9. *Adsorption Studies on Chloropicrin and Phosgene*, M. Dole, I. M. Klotz, and S. Weller, OSRD 972, July 15, 1942. Div. 10-202.155-M4
10. *The Adsorption Wave*, T. B. Drew, F. M. Spooner, and J. Douglas, NDRC 10.5-48, Nov. 17, 1944. Div. 10-202.157-M8
11. *Design of Collective Protectors*, T. B. Drew, OSRD 993, Oct. 15, 1942. Div. 9-212.11-M3
12. "Cation-Exchange Water Softening Rates," J. du Domaine, R. L. Swain, and O. A. Hougen, *Ind. Eng. Chem.*, **35**, 1943, p. 546.
13. "Adsorption Studies of Vapors in Carbon Packed Tow-

ers," H. C. Engel and J. Coull, *Trans. Am. Inst. Chem. Eng.*, **38**, 1942, p. 947.
14. "Heat Transfer from a Gas Stream to a Bed of Broken Solids," C. C. Furnas, *Trans. Am. Inst. Chem. Eng.*, **24**, 1930, p. 1942.
15. "Heat, Mass and Momentum Transfer in the Flow of Gases Through Granular Solids," B. W. Gamson, G. Thodos, and O. A. Hougen, *Trans. Am. Inst. Chem. Engrs.*, **39**, 1943, p. 1.
16. "Fluid Flow Through Porous Carbon," M. R. Hatfield, *Ind. Eng. Chem.*, **31**, 1939, p. 1419.
17. *Drying of Gases*, O. A. Hougen and F. W. Dodge, OSRD 123.
18. "Solid Catalysts and Reaction Rates," O. A. Hougen and K. M. Watson, *Ind. Eng. Chem.*, **35**, 1943, p. 529.
19. "Principles of Reactor Design. Gas-Solid Interface Reactions," D. H. Hurt, *Ind. Eng. Chem.*, **35**, 1943, p. 522.
20. *The Nature of Air Flow Through Granular Charcoal Beds*, B. N. P. Hutchesson and K. D. Wadsworth, Porton Report No. 2607, Mar. 17, 1944.
21. *Problem of Gas Removal*, L. S. Kassel, NDRC XV, (n.d.). Div. 10-202.15-M22
22. *Factors in Canister Design and Tube Testing: Critical Bed Depth and the Nature of Gas Flow Through Charcoal*, I. M. Klotz, OSRD 3774, June 23, 1944. Div. 10-201.1-M26
23. *Critical Bed Depths in Removal of CC by the E3 Canister*, I. M. Klotz, J. B. Fehrenbacher, and V. Johnson; *Critical Bed Depths and Mechanism of Removal of Six Gases*, W. L. McCabe, I. M. Klotz, W. E. Roake, H. G. Cutforth, and J. W. Thomas, OSRD 5239, June 7, 1945. Div. 10-202.156-M20
24. *A Systematic Study of Pressure Drop in Beds of Charcoal*, R. J. Kunz, and D. G. Anderson, NDRC 10.5-26, Apr. 24, 1944. Div. 10-202.11-M10
25. *Calculation of the Effect of Reversible Absorption on the Charcoal on Respirator Characteristics*, M. W. Lister, Report on Canadian Project C. E. 4, May 29, 1941. (See also summary by J. F. Kincaid, NDRC XII.) Div. 10-202.15-M21
26. *A Study of Charcoal Adsorption and Methods of Testing Charcoals for Use in Gas Mask Canisters*, R. Macy, EATR 52, Report completed July 1, 1930; issued May 10, 1942.
27. *Gas Mask Canister Design and Charcoal Testing*, D. MacRae, TDMR 942, Dec. 15, 1944.
28. "Layer Filtration, a Contribution to the Theory of Gas Masks," W. Mecklenburg, *Z. Elektrochemie*, **31**, 1925, p. 488; *Kolloid* **52**, 1930, p. 88.
29. *Considerations of the Adsorption Wave in Canister Design*, F. G. Pearce, MIT-MR 132, Apr. 2, 1945.
30. *Variation of the CG Life of Various Humidified Adsorbents with Decreasing Temperature*, W. C. Pierce, OSRD 1055, Nov. 26, 1942. Div. 10-202.16-M10
31. *Studies of Canister Performance at High Humidities and Flow Rates*, W. C. Pierce, OSRD 1081, Dec. 7, 1942. Div. 10-201.1-M11
32. *Mesh Size Studies*, W. C. Pierce, J. W. Zabor, D. R. Ehrlinger, J. Fehrenbacher, A. L. Hart, and A. Juhola, NDRC 10.1-11, Apr. 12, 1943. Div. 10-201.21-M1
33. *Design Methods for Adsorbent Section of Canisters*, O. A. Short and F. G. Pearce, MIT-MR 114, Nov. 25, 1944.
34. *A Study of Humidification and Dehumidification of Charcoal in Collective Protector Canisters*, O. A. Short, F. G. Pearce, and K. R. Nickolls, MIT-MR 97, Aug. 25, 1944.
35. "Heterogeneous Ion Exchange in a Flowing System," H. C. Thomas, *J. Am. Chem. Soc.*, **66**, 1944, p. 1664.
36. *A Critical Examination of the Correlation of Tube and Container Gas Test Results*, K. D. Wadsworth, Ptn. 2001 (U. 138), 1943, (Y. 23256).
37. "Studies on Adsorption and Desorption in Beds of Granular Adsorbents," E. Wicke, *Kolloid Zeitschrift*, **93**, 1940, p. 129. Translated by M. Dole NDRC XLVI, 1941; also translated by C. A. MacConkey, National Research Council of Canada, Ottawa, 1942.
38. *Adsorption Studies of PS on CWSN-19 and CWSC-11*, R. H. Wilhelm, J. C. Whitwell, and S. F. Williams, Final Report, Contract No. NDC-rc 108, Dec. 15, 1943.
39. *A Brief Investigation of Removal of Arsine in Air-Arsine Mixtures by Charcoal Using the Radioactive Tracer Method*, D. M. Yost, OSRD 361, Jan. 7, 1942. Div. 10-202.154-M12
40. *An Investigation of the Mechanism of Removal of Phosgene from Phosgene-Air Mixtures by Charcoal, Using the Radioactive Tracer Method*, D. M. Yost, OSRD 903, Sept. 25, 1942. Div. 10-202.155-M5
41. *Some Mathematical Theories for Charcoal Tube Testing*, D. M. Yost and D. S. Martin, NDRC 10.1-12, Apr. 30, 1943. Div. 10-202.1-M9

Chapter 10

1. *Report on Aerosols*, W. H. Rodebush, OSRD 77, Mar. 12, 1941. Div. 10-500-M1
2. *Report on Aerosol Filter Materials*, W. H. Rodebush, OSRD 58, July 24, 1941. Div. 10-201.22-M1
3. *Report on Filter Materials*, W. H. Rodebush, OSRD 101, June 12, 1941. Div. 10-201.2-M1
4. *Report on Aerosol Filter Materials*, W. H. Rodebush, OSRD 168, Nov. 7, 1941. Div. 10-201.22-M3
5. *Report on Filtration of Aerosols and the Development of Filter Materials*, W. H. Rodebush, I. Langmuir, and V. K. LaMer, OSRD 865, Sept. 4, 1942. Div. 10-201.22-M5
6. *Smokes and Filters*, I. Langmuir and K. Blodgett, OSRD 3460, Apr. 12, 1944. Div. 10-201.22-M14
7. *Preparation of Superfine Organic Fibers from Cellulose Esters*, Tennessee Eastman Corporation, OSRD 1048, Nov. 26, 1942. Div. 10-201.22-M7
8. *Reports on Asbestos Bearing Filter Paper*, A. D. Little, Inc., OSRD 336, OSRD 431, OSRD 962, OSRD 4378. Div. 10-201.22-M2 Div. 10-201.22-M4 Div. 10-201.22-M6 Div. 10-201.22-M15

Chapter 11

1. *Status Summary on the Protection Against Non-Persistent Agents by Allied and Enemy Canisters Under Tropical Conditions*, Project Coordination Staff, Edgewood Arsenal, Report No. 2, July 19, 1944.
2. *Gas Protection Afforded by Japanese Canisters*, J. B. Fehrenbacher and F. E. Blacet, OSRD 5238, May 30, 1945. Div. 10-201.31-M4
3. *Gas Protection Afforded by German Canisters*, J. B. Fehrenbacher and F. E. Blacet, OSRD 4929, Apr. 12, 1945. Div. 10-201.31-M3
4. NDRC MSR for period ending Nov. 15, 1944.
5. *German VM 40 Civilian Gas Masks*, R. Munro and J. E. Kaufman, FMTR-MIT 45, Mar. 17, 1945.
6. *German Civilian Air Defense Gas Masks*, P. Gilmont and J. E. Kaufman, FMTR-MIT 44, Mar. 17, 1945.
7. *Evaluation of British Mk II/L Respirator Containers*, J. E. Kaufman, FMTR-MIT 48, Apr. 26, 1945.
8. *The Protection of United States and Enemy Canisters Against Nitrogen Dioxide*, W. B. Lewis, J. W. Thomas, and F. E. Blacet, OSRD 5343, July 18, 1945. Div. 10-201.32-M3

Chapter 12

1. *Charcalite: A Calcium Chloride Impregnated Charcoal Drying Agent*, R. N. Pease, OSRD 3776, June 15, 1944. Div. 10-202.142-M2
2. *Catalysts for the Oxidation of Carbon Monoxide in Air*, R. N. Pease et al, OSRD 3071, Jan. 4, 1944. Div. 10-202.2-M6
3. *Volume Requirements for a Carbon Monoxide Canister for Use with Diluter-Demand Regulator Equipment*, R. N. Pease, NDRC 10.1-47, June 15, 1944. Div. 10-201.1-M27
4. *Carbon Monoxide Asphyxia*, C. K. Drinker, Oxford University Press, 1938, p. 89.
5. Lamb, Bray, and Frazier, *Ind. Eng. Chem.*, **12**, 1920, p. 213.

Chapter 14

1. "Recording Nocturnal Radiation," A. Angstrom, *Medell. Stat. Meteor. Hydrogr. Anst. Stockholm*, **6**, No. 8, 1936.
2. "Transfer of Heat and Momentum in the Lowest Layers of the Atmosphere," A. C. Best, *Geophysical Memoirs*, **7**, No. 65, 1935.
3. "Notes on Radiation in the Atmosphere," D. Brunt, *Quart. J. Roy. Met. Soc.*, **58**, 1932, p. 389.
4. *Physical and Dynamical Meteorology*, D. Brunt, MacMillan Co., London, 1939.
5. "Professional Note No. 6," E. H. Chapman, M. O. 232, 1919.
6. *Special Report to General Kabrich for Revision of TM 3-240*, R. G. Dickinson, T. S. Gilman, and H. S. Johnston, October 1944.
7. "The Climate of the Layer of Air Near the Ground," R. Geiger, *Die Wissenschaft*, **78**, Braunschweig, 1927.
8. *Physics of the Air*, W. J. Humphreys, McGraw-Hill Book Co., 1940.
9. Jelinek, *Beit. z. Phys. der f. Atm.*, **24**, 1937, p. 3.
10. *Micrometeorology of Woods and Open Areas Within the Withlacoochee Land Use Project, Florida*, H. Johnston assisted by A. Pardee, A. Englander, and W. Ironside, DPGSR 35, Sept. 11, 1944.
11. *Correlation of Gas Concentrations with Meteorological Data*, W. M. Latimer, S. Ruben, K. S. Pitzer, and W. D. Gwinn, OSRD 2086, Dec. 29, 1943. Div. 10-302.1-M18
12. *Weather Analysis and Forecasting*, S. Petterssen, McGraw-Hill Book Co., 1940, p. 99.
13. "Strahlungsstudien," M. Robitzsch, *Arb. Obs. Lindenberg*, **15**, 1926, p. 194.
14. *Phys. Ocean. and Met.*, C. G. Rossby, MIT, 1935.
15. "Das Massenaustausch bei der ungeordneten Stromung in freier Luft und seine Folgen," Wilh. Schmidt, *Wiener Ber.*, **126**, 1917, p. 757.
16. "Temperatures of the Soil and Air in a Desert," J. G. Sinclair, *M. W. Rev.*, 1922, S. 142.
17. O. G. Sutton, *Proc. Roy. Soc.*, **146**, 1934, p. 701.
18. "Theory of Diffusion," G. I. Taylor, *Proc. Math. Soc.*, **20**, 1929, p. 196.
19. M. D. Thomas, NDRC 10.3A-17, Apr. 17, 1943. Div. 10-302-M1
20. *Evaluation of Meteorological Data of the Lowest Atmosphere, Salt Lake City, Utah*, Mrs. R. Wexler.
21. *Meteorology of Ground Layer*, R. Wexler, Special Report, Dugway Proving Grounds, November 1943.
22. *Résumé of Recent Knowledge on the Technical Aspects of Chemical Warfare in the Field*, Project Coordination Staff, Edgewood Arsenal, Report No. 9, May 17, 1945.
23. SJPR 22, October 1944.

Chapter 15

1. "Transfer of Heat and Momentum in the Lowest Layer of the Atmosphere," A. C. Best, *Geophysical Memoirs*, No. 65, 1935.
2. *A Comparison of Three Types of Cup Anemometers at Low Velocities*, R. G. Dickinson and H. S. Johnston, NDRC 10.3A-38, Oct. 26, 1943. Div. 10-301.1-M1
3. *A Remote Indicating Cup Anemometer with Magnetic Coupling*, R. G. Dickinson and D. L. Kraus, NDRC 10.3A-44, May 30, 1944. Div. 10-301.1-M2
4. *An Apparatus for Temperature Profile Measurement*, R. G. Dickinson, R. L. Mills, and H. S. Johnston, NDRC 10.3A-45, Apr. 11, 1944. Div. 10-301.2-M3

5. *Dugway Recording Instruments*, S. W. Grinnell, Special Dugway Report.
6. *Micrometeorology of Woods and Open Areas Within the Withlacoochee Land Use Project, Florida*, H. Johnston assisted by A. Pardee, A. Englander, and W. Ironside, DPGSR 35, Sept. 11, 1944.
7. *Meteorological Instruments*, W. M. Latimer, S. Ruben, K. S. Pitzer, and W. D. Gwinn, NDRC 10.3A-6, Feb. 15, 1943. Div. 10-301-M1
8. *Investigation of the Micrometeorology of a Medium Dense, High Canopy Jungle on a Small Tropical Island*, W. W. Stone, R. G. Dickinson, D. L. Kraus, T. S. Gilman, and R. D. Mills, SJPR 22, Oct. 9, 1944.
9. *I. Meteorological Instruments; II. Observations in the Field*, W. M. Latimer, S. Ruben, K. S. Pitzer, and W. D. Gwinn, NDRC 10.3A-14, Apr. 15, 1943. Div. 10-301-M2
10. *Meteorological Instruments; Wind Velocity Measurements*, D. M. Yost, and R. Dodson, NDRC 10.3A-1, Dec. 15, 1942. Div. 10-301.11-M1
11. *Graphically Recording Bi-Directional Vanes*, D. M. Yost and R. W. Dodson, NDRC 10.3A-40, Nov. 1, 1943. Div. 10-301.11-M3
12. *Experiments on the Measurement of Air Temperatures with Thermocouples*, D. M. Yost, J. B. Hatcher, and R. Scott, NDRC 3A-26, July 20, 1943. Div. 10-301.2-M1
13. *Thermocouple Experiments*, D. M. Yost, J. B. Hatcher, R. Scott, NDRC 10.3A-32, Aug. 27, 1943. Div. 10-301.2-M2
14. *Meteorological Instruments* (second edition), W. E. K. Middleton, University of Toronto Press, 1943.

Chapter 16

1. *The Meteorology of Chemical Warfare*, Porton Memorandum No. 6, 1939.
2. *Radius of Pan-Cake Cloud*, Dugway Proving Ground Report No. 18.
3. *Comparison of Experimental Data and British Theory*, Dugway NDRC Weekly Report No. 37.
4. *The Behavior of Non-Persistent Gas Clouds Released from Bombs in the Targhee National Forest*, M. Dole and F. X. Webster, DPGMR 12, Dec. 4, 1943.
5. *Large-Scale Field Tests with 4.2-Inch Mortar Using Non-Persistent Agent. Part A. Factual*, W. S. Guthmann and J. T. Nolen, Apr. 25, 1944, *Part B. Evaluation*, W. S. Guthmann and J. W. Zabor, DPGMR 13, June 13, 1944.
6. *Florida Forest Field Trials of Non-Persistent and Persistent Agents, I. Non-Persistent Agents*, M. Dole and J. T. Nolen, DPGMR 15, May 19, 1944.
7. *500-lb, 1000-lb, 2000-lb, and 4000-lb Bombs Filled With Non-Persistent Agents*, DPGMR 18, June 2, 1944.
8. *Meteorology for Chemical Warfare and Smoke*, 2nd edition, Meteorological Office, Air Ministry, Great Britain, S. D. No. 216, 1942.
9. *Wind-Tunnel Studies of the Diffusion of Gas in Schematic Urban Districts*, NDRC 10.3A-46, OSRD 3859, July 5, 1944. Div. 10-401.121-M2
10. *Correlation of Gas Concentrations with Meteorological Data*, OSRD 2086, Dec. 29, 1943. Div. 10-302.1-M18
11. *Gas Concentration from Line Sources in a Forested Area*, OSRD 3049, Dec. 29, 1943. Div. 10-302.2-M3
12. *Gas Concentration from Line Sources and C. W. Bombs on a Beach Area*, OSRD 3059, Dec. 31, 1943. Div. 10-302.2-M4
13. *Résumé of Recent Knowledge on the Technical Aspects of Chemical Warfare in the Field*, Project Coordination Staff, Edgewood Arsenal, Report No. 9, May 17, 1945.
14. *Determination of the Burst Radii and Pancake Radii of CC- and CG-Filled 1000-lb Bombs Functioned Statically in Jungle*, W. D. Gwinn, J. G. Roof, and R. J. Grabenstetter, SJPR 2, June 15, 1944.
15. *Behavior of CC and CG Clouds Released by Simultaneous Functioning of Eight 1000-lb Bombs in Tropical Forest*, W. D. Gwinn, J. G. Roof, and J. W. Otvos, SJPR 6, July 15, 1944.
16. *Factors Influencing the Behavior of Nonpersistent Agents in Tropical Forests*, W. D. Gwinn, J. G. Roof, and J. W. Otvos, SJPR 7, July 15, 1944.
17. *Relative Effects of Ground Slope and Wind Direction and Velocity on Movement of Gas Clouds*, J. G. Roof and W. D. Gwinn, SJPR 12, Sept. 10, 1944.
18. *Dropping Trials of 1000-lb M79 Bombs in Jungle*, E. Nelson and J. G. Roof, SJPR 14, Sept. 29, 1944.
19. *Static and Drop Trial of 500-lb M78, CC Filled Bombs in Jungle*, E. Nelson, SJPR 15.
20. *Behavior of Gas Clouds of CC and CG Formed by Dropping of 96 1000-lb Bombs on Rough Jungle Terrain*, J. G. Roof and T. J. Hogan, SJPR 16.
21. *Large Scale Field Tests with the 4.2-Inch Chemical Mortar Firing CC-Filled Shells in the Jungle*, F. J. Zalesak and T. J. Hogan, SJPR 17, Oct. 11, 1944.
22. *The Assessment in Open Country of 4000-lb A/C Bombs Charged Non-Persistent Gas*, B. A. Griffith, Suffield Report No. 110-A, Apr. 25, 1944.
23. *The Diffusive Properties of the Lower Atmosphere. An Account of Investigations at the Chemical Defence Experimental Station, Porton, Wilts, 1921–1942*, O. G. Sutton, Issued by Meteorological Research Committee, Air Ministry, Great Britain, M. R. P. 59, Dec. 29, 1942.
24. Evans and Levy, OSRD 1176. Div. 10-401.123-M1

Chapter 17

1. *An Ultraviolet Photometer for the Detection and Quantitative Estimation of Very Small Concentrations of Noxious Gases in Air*, M. Dole, OSRD 170, Nov. 7, 1941. Div. 10-402.21-M1
2. *Sampling Methods for Field Experiments*, W. M. Latimer, NDRC CLXXXVI, Sept. 15, 1942. Div. 10-402.2-M4
3. *Determination of Ammonia Concentrations in Field Tests*, F. E. Blacet, NDRC 10.1-5, Jan. 16, 1943. Div. 10-402.2-M7

4. *A Portable Continuous Gas Concentration Meter*, R. G. Dickinson, NDRC 10.3A-9, Feb. 24, 1943. Div. 10-401.111-M1
5. *Measurement of CC with the Portable Continuous Gas Concentration Meter*, R. G. Dickinson, NDRC 10.3A-12, Mar. 15, 1943. Div. 10-401.111-M2
6. *Measurements of AC, CC and Mixtures of the Two with the Portable Continuous Gas Concentration Meter*, R. G. Dickinson, NDRC 10.3A-13, Apr. 15, 1943. Div. 10-401.111-M3
7. *The Hot Wire Analyzer for Gas Concentrations*, W. M. Latimer, OSRD 3048, Dec. 3, 1943. Div. 10-401.11-M1
8. *Operation Manual for Dickinson Field Conductivity Meter*, R. K. Brinton and J. W. Otvos, OSRD 5344, July 18, 1945. Div. 10-402.3-M1
9. *Dugway Proving Ground Field Sampling Methods for Non-Persistent Gases*, M. Dole and C. W. Huffman, DPGSR 19, Sept. 14, 1944.

Chapter 18

1. *Colloid Chemistry*, A. W. Thomas, McGraw-Hill Book Co., 1934, p. 15.
2. *Report on Aerosols*, W. H. Rodebush, OSRD 77, Mar. 12, 1941. Div. 10-500-M1

Chapter 19

1. *Filter Penetration by Aerosols of Very Small Particle Size*, W. H. Rodebush et al, OSRD 2050, Nov. 24, 1943. Div. 10-201.22-M13
2. *Smoke*, Whytlaw-Gray and Patterson, Edward Arnold & Co., London, 1932, p. 184.
3. *The Preparation of Solid Materials for Dispersion as Aerosols*, F. C. McGrew, OSRD 3902, July 17, 1944. Div. 10-504.3-M2
4. "The Removal of Mist by Centrifugal Methods," C. F. Goodeve, *Trans. Faraday Society*, 1936, p. 1218.
5. *Clouds and Smokes*, Wm. E. Gibbs, J. and A. Churchill, 1924, p. 43. *See also* Ref. 1, p. 96.
6. *Hydrodynamics*, H. Lamb, Fifth Edition, p. 567.
7. Reference 1, p. 72.
8. *Micromeritics*, J. M. Dalla Valle, Pitman, New York, 1943.
9. Hatch and Choate, *J. Franklin Institute*, **207**, 1929, p. 371.
10. T. Hatch, *J. Franklin Institute*, **215**, 1933, p. 27.
11. *The Kinetic Theory of Gases*, L. B. Loeb, McGraw-Hill, 1934, p. 402. *See also* Reference 5, p. 48.
12. *Ibid.*, p. 394.
13. See Reference 2, p. 57.
14. Unpublished Report, D. E. Goldman.
15. See Reference 2, p. 67.
16. *Applied Math. Panel, Memo 100.1 M*, NDRC, 1944.
17. "The Motion of a Sphere in a Viscous Fluid," H. S. Allen, *Phil-Mag. (5)*, **50**, 1900, p. 323.
18. *E. A. Progress Report to Col. Fleming*, H. A. Abramson, July 7, 1942.
19. *Unipolar Smoke and Filter Penetration*, V. K. LaMer et al, NDRC 10.2-2, August 1943. Div. 10-201.22-M12
20. Paranjpe, *Proc. Ind. Acad. Sci.*, **4a**, 1936, p. 423.
21. *Thermal Forces as a Means of Determining Size and Size Distribution in Aerosols*, V. K. LaMer et al, NDRC 10.2-5, Sept. 23, 1943. Div. 10-501.11-M8
22. *Analysis of Inhomogeneous Smoke*, V. K. LaMer and D. Sinclair, OSRD 155, Nov. 5, 1941. Div. 10-501.11-M1
23. "The Coagulation of Smoke by Supersonic Vibrations," E. N. deC. Andrade, *Trans. Faraday Soc.*, **42**, 1936, p. 1111.
24. "Experiments on Coagulation by Supersonic Vibrations," R. C. Parker, *Trans. Faraday Soc.*, **42**, 1936, p. 1115.
25. "The Aggregation of Suspended Particles in Gases by Sonic and Supersonic Waves," O. Brandt and E. Hiedemann, *Trans. Faraday Soc.*, **42**, 1936, p. 1101.
26. *Sonic Flocculator as a Fume Settler: Theory and Practice*, H. W. St. Clair, U. S. Bureau of Mines, R. I. 3400, 1936, p. 51.
27. "Hydrodynamisch-Akustische Untersuchung," Walter Koenig, *Ann. Physik*, **42**, 1891, pp. 353 and 549.
28. *Fog Types, etc.*, Meteorological Office, Air Ministry, S. D. T. M. 45.
29. *Electricity and Magnetism*, J. H. Jeans.
30. Georg Thomas, *Ann. d. Physik*, **42**, 1913, p. 1079.
31. "On the Circulations Caused by the Vibration of Air in a Tube," E. N. deC. Andrade, *Proc. Roy. Soc.*, **134**, 1931, p. 445; also "On the Groupings and General Behavior of Solid Particles Under Influences of Air Vibrations in Tubes," *Phil. Trans. Roy. Soc.*, **A230**, 1932, p. 413.
32. J. Robinson, *Proc. Lond. Phys. Soc.*, **25**, 1913, p. 256.
33. "The Action of Sound Waves Upon Droplets of Fog," S. V. Gorbatchev, *Russian Journal Physical Chemistry*, **7**, 1936, p. 536.
34. a. *Dissipation of Water Fog by Intense Sound of Audible Frequency*, V. K. LaMer and D. Sinclair, OSRD 1667, Aug. 17, 1943. Div. 10-503.2-M1
b. *Report of Tests of Sonic Dissipation of Fog in California*, V. K. LaMer, NDRC 10.2-13, Apr. 13, 1944. Div. 10-503.2-M3
35. E. F. Burton et al, Toronto Report, C. E. 42, November 1942, also Reference 6, Chap. 21.

Chapter 20

1. *Production of Smokes of Homogeneous Particle Size for Screening Tests and Development of Dyes from Thermally Dispersed Smokes*, V. K. LaMer et al, OSRD 364, Jan. 29, 1942. Div. 10-501.11-M3
a. *Portable Optical Instrument for the Measurement of the Particle Size in Smokes, the "Owl", an Improved Homogeneous Aerosol Generator*, V. K. LaMer and D. Sinclair, OSRD 1668, Aug. 3, 1943. Div. 10-501.11-M6

2. *Dispersal and Persistence Properties of Solid Aerosols*, V. K. LaMer et al, NDRC 10.2-9, Nov. 12, 1943. Div. 10-504.3-M1
3. *The Optical Characterization of Any Aerosol in the Laboratory or Field. The Production of Aerosols from Powdered Solid Materials*, V. K. LaMer, J. Q. Umberger, D. Sinclair, F. E. Buchwalter, OSRD 4904, Oct. 31, 1944. Div. 10-601.2-M1

Chapter 21

1. G. Mie, *Ann. der Phys.*, **25**, 1908, p. 377.
2. Hans Blumer, *Zeits. f. Phys.*, **32**, 1925, p. 119; **38**, 1926, pp. 304, 920; **39**, 1926, p. 195.
Engelhard and Friess, *Koll. Zeits*, **81**, 1937, p. 129.
R. Ruedy, *Canadian Journal of Research*, **19A**, 1941, p. 117.
3. *Electromagnetic Theory*, J. A. Stratton, McGraw-Hill Book Co., Stratton and Houghton, *Physical Review*, **38**, 1931, p. 159.
4. *Verification of the Mie Theory*, V. K. LaMer, D. Sinclair, et al, OSRD 1857, Sept. 29, 1943. Div. 10-501.1-M2
5. *Scientific Papers*, Lord Rayleigh, Cambridge University Press, 1899, Vol. I, pp. 92–93.
Lord Rayleigh, *Loc. Cit.*, **4**, 1903, p. 400, eq. 13.
6. a. *Production, Analysis, and Use of Aerosols of Uniform Particle Size*, V. K. LaMer and D. Sinclair, OSRD 119, Aug. 8, 1941. Div. 10-501-M1
b. *Measurement of Particle Size in Smokes, the Owl*, V. K. LaMer and D. Sinclair, OSRD 1668, Aug. 24, 1943. Div. 10-501.11-M6
7. *Screening Smokes*, W. H. Rodebush, et al, OSRD 940, Part II, Sec. 2, Oct. 5, 1942. Div. 10-502-M5
8. W. S. Stiles, *Phil. Mag.*, **7**, 1929, p. 204.
9. G. Wolfson, *Handbuch der Physik*, **XX**, 314.
10. Reference 7, Part II, Sec. 1.
11. L. Brillouin, NDRC Applied Math. Panel Report, Nos. 87.1 and 87.2.
12. *Determination of Particle Size Distribution in Smokes by Analysis of Scattered Light*, V. K. LaMer and D. E. Goldman, NDRC 10.2-4, July 28, 1943. Div. 10-501.11-M5
13. *"Owl" Settings for DOP Smokes*, F. T. Gucker, Jr., et al, NDRC 10.1-27, Sept. 7, 1943. Div. 10-501.11-M7
14. *Tests of the Owl*, V. K. LaMer et al, NDRC 10.2-3, July 23, 1943. Div. 10-501.11-M4
15. W. Lotmar, *Helv. Chim. Acta.*, **21**, 1938, p. 792.
16. R. S. Krishnan, *Proc. Ind. Acad. Sci.*, **7A**, 1938, p. 21.
17. Private communication from E. I. DuPont de Nemours Experimental Station, E. D. Bailey.
18. *Testing of Daytime Distress Signals*, V. K. LaMer et al, OSRD 4539, Jan. 5, 1945. Div. 10-501.23-M3
19. *Total Scattering Function for Complex Indices of Refraction*, A. N. Lowan et al, Math. Tables Project, National Bureau of Standards.

Chapter 22

1. K. R. May, Porton Report No. 2463; see also Monthly Progress Reports NDRC Munitions Development Laboratory, 1944–45.
2. V. J. Schaefer, private communication.
3. *Dissipation of Water Fog by Intense Sound of Audible Frequency*, V. K. LaMer et al, OSRD 1667, Aug. 17, 1943. Div. 10-503.2-M1
4. *Smoke*, Whytlaw-Gray and Patterson, Edward Arnold and Co., London, 1932.
5. K. E. Stumpf, *Koll. Zeits*, **86**, 1939, p. 339.
6. *Studies of Particle Size in Smokes*, H. Eyring, OSRD 292, Dec. 8, 1941. Div. 10-501.11-M2
7. *Preparation of Solid Materials for Dispersion as Aerosols*, F. C. McGrew, OSRD 3902, July 17, 1944. Div. 10-504.3-M2
8. *Chemical Engineers Handbook*, J. H. Perry, McGraw-Hill Book Co., 1934, p. 709.
9. E. L. Anderson, *Journal Industrial Hygiene*, **21**, 1939, p. 39.
10. H. H. Watson, *Trans. Faraday Soc.*, **32**, 1936, p. 1073.
11. Porton Report No. 2521.
12. W. H. Rodebush et al, OSRD 865, Sept. 4, 1942. Div. 10-201.22-M5
13. *Production, Analysis, and Use of Aerosols of Uniform Particle Size*, V. K. LaMer and D. Sinclair, OSRD 119, Aug. 8, 1941. Div. 10-501-M1
14. *Analysis of Inhomogeneous Smoke*, V. K. LaMer and D. Sinclair, OSRD 155, Nov. 5, 1941. Div. 10-501.11-M1
15. *Dispersal and Persistence Properties of Solid Aerosols*, V. K. LaMer et al, NDRC 10.2-9, Nov. 12, 1943. Div. 10.504.3-M1
16. *Optical Characterization of Any Aerosol*, V. K. LaMer et al, OSRD 4904, Oct. 31, 1945. Div. 10-601.2-M1
17. a. *Measurement of Particle Size in Smoke, the Owl*, V. K. LaMer and D. Sinclair, OSRD 1668, Aug. 24, 1943. Div. 10-501.11-M6
b. *Characteristics of Different Models of the Owl*, V. K. LaMer and D. Sinclair, NDRC 10.2-3, July 23, 1943. Div. 10-501.11-M4
c. *Concentration of Sound for Use in Fog Dissipation*, V. K. LaMer and D. Sinclair, NDRC 10.2-6, Oct. 15, 1943. Div. 10-503.2-M2
18. *Physics of the Air*, W. J. Humphreys, McGraw-Hill Book Co., 1940, p. 551.
19. Hilding Kohler, *Trans. Faraday Soc.*, **32**, 1936, p. 1153.
20. Wilson, *Cambridge Philos. Soc.*, **32**, 1936, p. 493.
21. *The Slope-O-Meter*, V. K. LaMer and S. Hochberg, NDRC 10.2-15, June 19, 1944. Div. 10-501.11-M9

Chapter 23

1. *Report on Aerosols*, W. H. Rodebush, OSRD 77, Mar. 12, 1941. Div. 10-500-M1
2. *Filtration of Aerosols and the Development of Filter Materials*, W. H. Rodebush, I. Langmuir, and V. K. LaMer, OSRD 865, Sept. 4, 1942. Div. 10-201.22-M5

3. *Smokes and Filters. Supplement to Section I.*, I. Langmuir and K. Blodgett, OSRD 3460, Apr. 12, 1944. Div. 10-201.22-M14
4. *Filter Penetration of Aerosols of Very Small Particle Size*, W. H. Rodebush, C. E. Holley, Jr., and B. A. Lloyd, OSRD 2050, Nov. 24, 1943. Div. 10-201.22-M13
5. *Final Report on Filtration Efficiency and Particle Size. III-I-2000*, C. E. 42, University of Toronto, November 1944.
6. *Filter Material*, W. H. Rodebush, OSRD 101, June 12, 1941. Div. 10-201.2-M1
7. *Preparation of Asbestos Fibers of Small Diameter and Dispersion of Solids*, OSRD 431, A. D. Little, Inc. Mar. **2**, 1942. Div. 10-201.22-M4
8. *Asbestos Bearing Filter Paper*, T. L. Wheeler and E. Stafford, OSRD 4378, Nov. 23, 1944. Div. 10-201.22-M15
9. *Aerosol Filter Materials*, W. H. Rodebush, OSRD 168, Nov. 7, 1941. Div. 10-201.22-M3
10. *Aerosol Filter Materials*, W. H. Rodebush, OSRD 120, July 24, 1941. Div. 10-201.22-M1
11. *Preparation of Superfine Organic Fibers from Cellulose Esters*, OSRD 1048, Tennessee Eastman Corporation, Nov. 26, 1942. Div. 10-201.22-M7

Chapter 24

1. *Test Methods Conference, CWS Development Laboratory, MIT. Group VI-Filter Tests*, Sept. 2, 1942, pp. 1–2 and 45–63 deal with general recommendations on smoke testing.
2. Reference 1, pp. 8 and 50–51.
3. *Production, Analysis, and Use of Aerosols of Uniform Particle Size*, V. K. LaMer and D. Sinclair, OSRD 119, Aug. 8, 1941. Div. 10-501-M1
Also *Measurement of Particle Size in Smoke*, V. K. LaMer and D. Sinclair, OSRD 1668, Aug. 24, 1943. Div. 10-501.11-M6
4. *Development of the DOP Smoke Penetration Test for Filter Materials*, J. H. Dinius and A. W. Plummer, MIT-MR-52, Jan. 8, 1944.
5. *Development of Smoke Penetration Meters*, H. W. Knudson and L. White, Naval Research Laboratory Report No. P-2642, Sept. 14, 1945.
6. Reference 1, pp. 12–16 and 41–43.
7. *Canister and Charcoal Test Methods*, CWS Pamphlet No. 2, Part 1, Section C, DM, Apr. 3, 1943.
8. *Gas Mask Filters and Filter Materials, DM Tests January 1934 to September 1941*, P. A. Hartman and E. K. Long, EATR 362, Feb. 24, 1942.
9. Reference 6, Section D, DA.
10. Reference 12, pp. 17–18 and 43–45.
11. *Canister Test Methods Section H — Methylene Blue*, CWS Pamphlet No. 2, Part 1, Jan. 4, 1943.
12. *Methylene Blue Penetration Tester MIT-E2*, A. W. Plummer, MIT-MR-5, May 6, 1942.
13. *Evaluation of the Methylene Blue Penetration Tester MIT-E2*, H. J. Allison, Jr., and E. K. Long, TDMR 440, Sept. 23, 1942.
14. *Report on Aerosols*, W. H. Rodebush, OSRD 14, Sept. 12, 1941.
15. *Design of Apparatus, MIT-E1R1, for Filter Testing Using Radioactive Triphenyl Phosphate Smoke*, B. Vonnegut, MIT-MR-6, July 18, 1942.
16. Reference 1, pp. 40–41.
17. Reference 1, pp. 26 39.
18. *Optical Smoke Penetration Meter*, B. Vonnegut, MIT-MR-2, Mar. 16, 1942.
19. *Optical Smoke Penetration Meter, E1R1*, D. W. Beaumont, MIT-MR-27, Mar. 6, 1943.
20. *Ionization Penetrometer*, A. R. Hogg and A. J. Roennfeldt, C. D. Note No. 14 from Munitions Supply Laboratories, Maribyrong, Australia, Nov. 18, 1943.
21. "A Photoelectric Smoke Penetrometer," A. S. G. Hill, *J. Sci. Inst.*, **14**, 1937, p. 296.
22. Reference 1, pp. 8–11.
23. *Carbon Smoke Penetration*, L. Yaffe, R. L. McIntosh and W. Boyd Campbell, McGill University and the Pulp and Paper Research Institute of Canada, Progress Reports Nos. 1–4, Montreal, 1942.
24. *Canister Development Studies*, W. K. Lewis, OSRD 850.
25. *Filtration of Aerosols and the Development of Filter Materials*, W. H. Rodebush, I. Langmuir, and V. K. LaMer, OSRD 865, Sept. 4, 1942. This report contains *The Balanced Photoelectric Smoke Penetrometer* by S. Hochberg. Div. 10-201.22-M5
26. *A Sensitive Photoelectric Smoke Penetrometer*, F. T. Gucker, Jr., H. B. Pickard, and C. T. O'Konski, OSRD 5499, Aug. 28, 1945. Div. 10-201.22-M16
27. *Photoelectric Smoke Penetration Meter MIT-E2*, W. B. Nottingham, D. W. Beaumont, and J. H. Dinius, MIT-MR-203, Oct. 11, 1945.
28. *A Particle-Counting Smoke Penetrometer*, F. T. Gucker, Jr., H. B. Pickard, C. T. O'Konski, and J. N. Pitts, Jr., OSRD 5501, Aug. 31, 1945.
29. *Development of Stable Thallous Sulfide Photoconductive Cells for Detection of Near Infrared Radiation*, R. J. Cashman, OSRD 5997, Oct. 31, 1945.
30. *Smoke Penetration Meter E3, Engineering Tests*, H. Scherr, EATR 237, Feb. 7, 1938.
31. *Smoke Penetration Meter E3, Final Report on Project D 1.3-1a1*, L. Finkelstein and H. Scherr, EATR 331, Aug. 28, 1940.
32. *Operation of Smoke Penetration Meter E3 for Production Testing of MIXA1 Canister Filters*, CWS Directive No. 40A, June 6, 1942.
33. *Canister Test Methods, Section K — Smoke Penetration*, CWS Pamphlet No. 2, Part I.
34. *Smoke Penetration Tests of Canadian and U. S. Army Canisters*, P. A. Hartmann and E. K. Long, TDMR 332, Nov. 10, 1941.
35. *Effect of Oil Smokes from Esso Jr. and Oil-O-Matic Screening Smoke Generators on Filters as Determined by Field Tests*, MIT-MR-14, Sept. 28, 1942.
36. *The Effect of Oil Smokes and Amyl Stearate Smokes on Filters*, P. A. Hartmann and J. E. Kaufman, TDMR 364, Apr. 28, 1942.
37. *Tests of British Light-Type Respirator Canisters*, J. H. Dinius, TDMR 556, Jan. 31, 1943.

[redacted]

38. *A Note on the Effect of Oil Screening Smokes on Resin-Impregnated Filters and the Stability of These Filters Under Tropical Conditions*, Chemical Defence Experimental Station, Porton, England, May 12, 1943.
39. Reference 1, p. 17.
40. *Development of MIT-E1 Canister Tester*, W. B. Nottingham, F. F. Diwoky, and D. W. Beaumont, MIT-MR-32, May 8, 1943.
41. *Canister and Charcoal Test Methods, Part I, Section M, Installation Operation, and Maintenance of Meter, Smoke Penetration, MIT-E1R1*, CWS Pamphlet No. 2, Jan. 17, 1944.
42. Reference 1, pp. 31–32.
43. Reference 1, pp. 11–12 and 39–40.
44. Porton Report No. 2161; Porton Specification 1206.
45. *Evaluation of the British Sodium Flame Apparatus as a Filter Tester*, C. A. Rinehart and J. H. Dinius, TDMR 578, Feb. 26, 1943.
46. *Performance of Sodium Flame Penetrometer*, M. W. Lister, Chemical Warfare Laboratories, Ottawa, Canada, Sept. 26, 1944.
47. *Standard Methods of Test (Chemical and Physical) Employed in C. W. Investigations. I(3) Tests on Particulate Filters*, Porton Memorandum No. 17, Mar. 7, 1942.
48. *Aerosols, A Survey and Bibliography of Recent Literature*, D. F. Jurgensen, MIT-MR-8, July 17, 1942.

Chapter 25

1. *Screening Smokes*, T. K. Sherwood, OSRD 436, Mar. 15, 1942. Div. 10-502-M2
2. *Production of Smokes of Controlled Size by the Use of Induction Nozzles*, H. C. Hottel, OSRD 468, Jan. 12, 1942. Div. 10-501.2-M1
3. *Smoke Generator*, I. Langmuir and V. J. Schaefer, OSRD 487, Mar. 31, 1942. Div. 10-501.201-M1
4. *Screening Smokes*, W. H. Rodebush, V. K. LaMer, I. Langmuir, T. K. Sherwood, OSRD 940, Oct. 5, 1942. Div. 10-502-M5
5. *Practical Considerations Involved in the Use of Screening Smokes*, W. H. Rodebush, OSRD 1321, Apr. 9, 1943. Div. 10-502-M7
6. *Use of a Sulfur Boiler for Smoke Generation*, W. K. Lewis, OSRD 1692, Aug. 9, 1943. Div. 10-501.2-M3
7. *Large Scale Screening Tests, Camp Sibert, Alabama*, W. H. Rodebush and H. F. Johnstone, OSRD 1687, Aug. 10, 1943. Div. 10-302.1-M10
8. *Study of Oil Smoke Plumes by Motion Pictures*, H. F. Johnstone, OSRD 1697, Aug. 6, 1943. Div. 10-502-M8
9. *Smoke Experiments Carried Out At Camp Sibert, Alabama*, T. S. Gilman and P. Hayward, OSRD 1712, Aug. 14, 1943. Div. 10-302.1-M11
10. *Reports on Special Smoke Project Amphibious Training Command*, U. S. Atlantic Fleet, N. O. B. Norfolk, Va., 1944–45.
11. *Cominch P-04 Smoke Screens for Amphibious Operations*, Headquarters of the Commander-in-Chief, U. S. Fleet.

Chapter 26

1. *Screening Smokes*, T. K. Sherwood, OSRD 436, Mar. 15, 1942. Div. 10-502-M2
2. *Production of Smokes of Controlled Size by the Use of Induction Nozzles*, H. C. Hottel, OSRD 468, Jan. 12, 1942. Div. 10-501.2-M1
3. *Smoke Generator*, I. Langmuir and V. J. Schaefer, OSRD 487, Mar. 31, 1942. Div. 10-501.201-M1
4. *Screening Smoke*, W. H. Rodebush, V. K. LaMer, and I. Langmuir, OSRD 940, Oct. 5, 1942. Div. 10-502-M5
5. *The Pancake Effect in Gas Clouds*, W. M. Latimer, OSRD 1176, Feb. 3, 1943. Div. 10-401.123-M1
6. *Practical Considerations Involved in the Use of Screening Smokes*, W. H. Rodebush, OSRD 1321, Apr. 9, 1943. Div. 10-502-M7
7. *Use of a Sulfur Boiler for Smoke Generation*, W. K. Lewis, OSRD 1692, Aug. 9, 1943. Div. 10-501.2-M3
8. *Study of Oil Smoke Plumes by Motion Pictures*, H. F. Johnstone, OSRD 1697, Aug. 6, 1943. Div. 10-502-M8
9. *Smoke Experiments Carried Out at Camp Sibert, Alabama*, T. S. Gilman and P. Hayward, OSRD 1712, Aug. 14, 1943. Div. 10-302.1-M11
10. *Concentrations in Gas Clouds Under High Inversion Conditions*, W. M. Latimer and S. Ruben, OSRD 1749, Aug. 31, 1943. Div. 10-302.1-M14
11. *The Evaporation of Small Drops of Thiodiglycol and Levinstein Mustard*, H. F. Johnstone, R. W. Parry, OSRD 2002, Nov. 9, 1943. Div. 10-501.12-M1
12. *The Concentration of Vapor in H Aerosol Clouds*, H. F. Johnstone and W. E. Winsche, OSRD 3284, Feb. 22, 1944. Div. 10-504-M1
13. *Statistical Considerations in the Use of DDT Aerosols*, W. H. Rodebush, OSRD 4757, Mar. 5, 1945. Div. 10-602.21-M2

Chapter 27

Project C. E. 128

Department of Physics, University of Manitoba

1. III-1-789, *Visual Aspects of the Screening Problem.*
2. III-1-997, *I. Determination of the Extinction Coefficient of Smoke.*
II. The Contrast Limen in Smoke Chamber Experiments.
III. Further Results on the Mechanism of Obscuration.
3. III-1-1048, *I. The Dependence of Cloud Brightness on the*



Amount of Smoke and on the Direction of Observation in the Field.
II. Brightness Meters.
4. III-1-1230, *Visibility of Targets in Relation to Night Screening.*
5. III-1-1298, *The Brightness of HCE Clouds Under Different Viewing Conditions in Sunlight and Moonlight.*
6. III-1-1481, *Smoke Screen Estimates. Part I. Flank Screening Under Overcast Day Conditions.*
7. III-1-1851, *Smoke Screen Estimates. V. Area Screening Under a Full Moon and a Cloudless Sky: Comparison with Observed Data of C. D. Reports 1098 and 1099, and Comments on Inferences Drawn in Those Reports.*
8. III-1-1893, *Smoke Screen Estimates. Part VI. Area Screening Under Cloudless Day Conditions Against Observation and Against Aimed Bombing Attack.*
9. III-1-1939, *A Survey of Visibility Limen Data.*
10. III-1-2001, *The Probability of Detection and Recognition of Targets of Low Apparent Contrast which Varies with Time.*
11. III-1-2036, *A Field Attenuation Meter for the Study of Flank Screening Problems.*

Chapter 29

1. R. A. Castleman, Jr., Bur. Standards, *J. Research*, **6**, 1931, p. 369.
2. J. Sauter, *Forsch. Gebiete Ingenieurw.*, 1928, p. 312.
3. Guy Littaye, *Comptes rendus*, **219**, 1943, pp. 99, 340.
4. S. Nukiyama and Y. Tanasawa, *Trans. Soc. Mech. Engrs.* (Japan), **4**, 1938, pp. 14, 86; **4**, 1938, pp. 15, 138; **5**, 1939, pp. 18, 63; **5**, 1939, pp. 18, 68; **6**, 1940, pp. 22, II-7; **6**, 1940, pp. 23, II-18.
5. *A Study of the Atomization of Liquids*, H. C. Lewis, D. G. Edwards, M. J. Goglia, R. I. Rice, and L. W. Smith, OSRD 6345, November 1945. Div. 10-501.2-M6
6. *Chemical Engineers Handbook*, 2nd Edition, McGraw-Hill Book Co., 1941, p. 842.
7. Monthly Progress Reports of the Munitions Development Laboratory, Contract OEMsr-102, April to August 1945.
8. *Chemical Engineers Handbook*, 2nd Edition, McGraw-Hill Book Co., 1941, p. 1984.
9. *National Advisory Committee for Aeronautics, Report No. 425*, D. W. Lee, 1932.
10. *Mechanical Formation of Fogs*, W. G. Brown, OSRD 325, Feb. 7, 1942. Div. 10-503.1-M2
11. *Use of Aqueous Solutions for Producing Screening Fogs or Smokes by Pneumatic Spray Nozzles*, A. R. Olson and G. D. Gould, OSRD 537, Apr. 29, 1942. Div. 10-502-M4
12. *I, Toxic Smoke Candle, and II, Screening Smoke Units*, E. W. Comings, OSRD 1076, Dec. 1, 1942. Div. 10-504.12-M3
13. *Mechanical Formation of Smokes*, G. G. Brown, OSRD 153, Oct. 18, 1941. Div. 10-501-M2
14. *The Mechanical Formation of Screening Smokes Using Salt Solutions*, G. G. Brown, OSRD 980, October, 1942. Div. 10-502-M6
15. *The Formation of Screening Smokes*, G. G. Brown, OSRD 414, Feb. 26, 1942. Div. 10-502-M1
16. *The Assessment of Aerosols*, H. F. Johnstone, NDRC 10.4-48, Dec. 31, 1943; and Munitions Development Laboratory Biweekly Reports of November 10 and 24, 1943. Div. 10-504.2-M3
17. *Memorandum on Airplane Vesicant Spray*, T. K. Sherwood, OSRD 2093, Dec. 2, 1943. Div. 11-203.522-M1
18. *The Break-Up of a Liquid Jet and Its Application to Aircraft*, Porton Departmental Report No. 146.
19. *The Fragmentation of Liquid C. W. Agents*, Porton Report No. 2215, Serial No. 11, May 14, 1941.
20. Munitions Development Laboratory Monthly Progress Report for October 1944.
21. Munitions Development Laboratory Monthly Progress Report for December 1944.
22. *Supplementary Test of Improved Equipment and Techniques for Dissemination of DDT by Aircraft (Phase I and II)*: AAF Board, Orlando, Florida, Mar. 1, 1945; *Development and Test of Spray Equipment for L-5 Aircraft for Dissemination of Insecticide DDT*, AAF Tactical Center and U. S. Department of Agriculture, Orlando, Florida, June 5, 1945.
23. *Final Test Report for DDT Insecticide Disseminator Units, Item 3*, Navy Contract NOa(s) 7065, Cornell Aeronautical Laboratory (formerly Curtiss-Wright Corporation) June 19, 1945.
24. *Chemical and Physical Methods for the Assessment of Insecticide Dispersal*, C. W. Huffman, C. R. Naeser, and J. G. Hartnett, TDMR 1241, Mar. 29, 1946.
25. *The Mechanism of Dispersal of Liquids by Pressure Explosion*, R. Whytlaw-Gray, Extramural Research Item No. 21, V. 727, University of Leeds, Dec. 20, 1940 to Mar. 17, 1941.
26. *Dispersal Under Various Conditions of a Mobile Liquid Filling by 20 mm SAP.CW Projectiles (20 mm Hispano HE Shell)*, B. A. Toms, Porton Report No. 2514, June 29, 1943.
27. *The Break-Up of Liquids by Explosion, Part I*, C. N. Davies, Porton Report No. 2425, Sept. 30, 1942.
28. *The Dispersal of Liquid Chargings from Bursting Weapons*, A. W. Birnie, Technical Minute No. 37, Suffield Experimental Station, Oct. 4, 1943.

Chapter 30

1. *Screening Smokes*, W. H. Rodebush, V. K. LaMer, I. Langmuir, T. K. Sherwood, OSRD 940, Oct. 5, 1942. Div. 10-502-M5
2. *Large Scale Screening Tests, Camp Sibert, Alabama, May 4–7, 1943, Part I* — W. H. Rodebush, *Part II* — H. F. Johnstone, P. G. Roach, H. C. Weingartner, OSRD 1687, Aug. 10, 1943. Div. 10-302.1-M10

3. *The Concentration of Vapor in H Aerosol Clouds*, H. F. Johnstone, W. E. Winsche, OSRD 3284, Feb. 22, 1944. Div. 10-504-M1
4. *The Evaporation of Small Drops of Thiodiglycol and Levinstein Mustard*, H. F. Johnstone and R. W. Parry, OSRD 2002, Nov. 12, 1943. Div. 10-501.12-M1
5. *The Generation and Use of Concentrated Mustard Vapor Clouds*, H. F. Johnstone and E. W. Comings, OSRD 3012, Dec. 14, 1943. Div. 10-504.1-M1
6. *Development of an Experimental Thermal Generator Pot for Dispersing Mustard Gas as an Aerosol*, C. H. Adams, M. H. Raila, and E. W. Comings, OSRD 6431, Dec. 29, 1945. Div. 10-504.1-M2
7. *Development of a Smoke Unit*, E. W. Comings, OSRD 518, Apr. 23, 1942. Div. 10-504.12-M2
8. *The Development of the Thermal Generator Candle*, E. W. Comings, E. D. Shippee, M. Forester, OSRD 3150, Jan. 18, 1944. Div. 10-504.12-M5
9. *I. Toxic Smoke Candle, and II. Screening Smoke Units*, E. W. Comings, OSRD 1076, Dec. 1, 1942. Div. 10-504.12-M3
10. *Smoke Production*, E. W. Comings and E. D. Shippee, OSRD 109, June 27, 1941. Div. 10-504.4-M1
11. *Development of a Smoke Unit*, E. W. Comings, OSRD 167, Nov. 5, 1941. Div. 10-504.4-M2
12. *Agent Decomposition in Toxic Smoke Candle*, H. A. Fiess and E. W. Comings, Unpublished Report from OSRD Contract OEMsr-102, Aug. 26, 1942.
13. *Florida Trials with the Experimental H Generator*, DPGSR 34, Aug. 29, 1944.
14. *Development of a Thermal Generator Bomb for Dispersing Concentrated Mustard Aerosol*, E. D. Shippee and E. W. Comings, OSRD 6574, Feb. 4, 1946. Div. 10-504.3-M3
15. *The Physiological Activity of the Cloud Produced by the Comings Thermal Generator*, Suffield Report No. 98, Nov. 25, 1943.
16. *The Diffusive Properties of the Lower Atmosphere, an Account of Investigations at Chemical Defense Experimental Station, Porton, Wilts, 1921–42*, O. G. Sutton.
17. Frossling Gerlands, *Beitrage fur Geophysik*, **52**, 1938, p. 170.
18. *Estimating the Value of the Wind Gradient Parameter, "R,"* A. Bleasdale, Porton Report No. 2408, Aug. 27, 1942.
19. *A Study of the Atomization of Liquids*, H. C. Lewis, D. G. Edwards, M. Goglia, R. I. Rice, and L. W. Smith, OSRD 6345, Nov. 23, 1945. Div. 10-501.2-M6
20. *The Dispersal of Liquid Chargings from Bursting Weapons*, A. W. Birnie, Suffield Technical Minute No. 37, Oct. 4, 1945.
21. Dugway Proving Ground Report for Week Ending December 6, 1944, Report No. 85, Series 2.
22. Dugway Proving Ground Report for Week Ending June 26, 1945, Report No. 114.
23. Dugway Proving Ground Report for Week Ending August 28, 1945, Report No. 123.
24. Dugway Proving Ground Report for Week Ending April 17, 1945, Report No. 104.
25. Dugway Proving Ground Report for Week Ending April 24, 1945, Report No. 105.
26. *Fuel Blocks for Thermal Generators*, R. W. Parry, M. H. Raila, R. C. Johnson, D. B. Ehrlinger, P. N. Rylander, C. H. Simonson, R. P. Connor, and E. W. Comings, OSRD 6636, Mar. 11, 1946. Div. 10-504.11-M3
27. *Telescoping Metal Tails for a Small Cluster Bomb (Thermal Generator, 10-lb-E29R1)*, E. C. Manthei and J. A. Peck, OSRD 6121, Oct. 17, 1945. Div. 10-504.2-M9
28. *Development of a Colored Smoke Target Identification Bomb (Bomb, Target Identification, Smoke, Mk 72, Mod 2)*, C. H. Adams, E. H. Conroy, and E. W. Comings, OSRD 6432, Dec. 29, 1945. Div. 10-504.2-M11
29. TCIF 303.
30. Letter (EW21/S77) from the Chief of the Bureau of Ordnance to the Chief, CWS, Apr. 7, 1945.
31. *Development of Oil Thermal Generator Floating Smoke Pot, E-23*, M. F. Nathan, R. W. Davis, E. C. Manthei, and E. W. Comings, OSRD 6428. Dec. 29, 1945, Div. 10-501.21-M5
32. Chicago Toxicity Laboratory Report, OSRD 4639.
33. Letter from Commanding General, CWS Technical Command to Chief, Technical Division, CWS, SPCVD 470.6 (Smoke Candles) June 14, 1945.
34. Letter from Commander Amphibious Training Command, U. S. Atlantic Fleet, to Chief of the Bureau of Ordnance (Serial No. 0815), Feb. 9, 1945.
35. *Development of Training Oil Smoke Pot, E-21*, M. F. Nathan, R. W. Davis, and E. W. Comings, OSRD 6211, Oct. 24, 1945. Div. 10-501.21-M4
36. Letter from Chief, CWS Technical Division to Director, Munitions Development Laboratory (SPCVD 470.6 University of Illinois, October 25, 1944).
37. *Explosive Hazards of Oil Smokes in Confined Places*, Test made at the Bureau of Mines, Pittsburgh, Pennsylvania, and reported by Lt. S. R. Purcell, CWS Pyrotechnics Division, in a trip report, July 11, 1945.
38. Letter from Commanding Officer, CWS Technical Command, Edgewood Arsenal to Chief, Technical Division, CWS, SPCVD 470.6 — *Non-Toxic Oil Smoke Training Candle E-21*, Dec. 21, 1945.
39. *Use of Sulfur Boiler for Smoke Generation*, W. K. Lewis, OSRD 1692, Aug. 9, 1943. Div. 10-501.2-M3
40. *Sulfur Smoke Generator*, designed by I. Bencowitz, Texas Gulf Sulphur Company — sketch dated Oct. 14, 1942.
41. *A Continuous Sulfur Smoke Generator*, E. W. Comings and W. L. Lundy, OSRD 3213, Feb. 4, 1944. Div. 10-501.2-M4
42. *A Floating Colored Smoke Signal (DS-4)*, D. G. Edwards, C. H. Adams, E. H. Conroy, and E. W. Comings, OSRD 6375, Dec. 10, 1945. Div. 10-501.23-M1
43. *Testing of Daytime Distress Signals*, V. K. LaMer, J. Q. Umberger, D. Sinclair, F. Buchwalter, and I. Johnson, OSRD 4539, Jan. 5, 1945. Div. 10-501.23-M3
44. *A New Daytime Distress Signal*, I. Johnson and V. K. LaMer, NDRC 10.2-16, Oct. 23, 1944. Div. 10-501.23-M2
46. Letter from Chief, Technical Command (SPCVD 412.41) May 16, 1945.
47. Chemical Warfare Pocket Book (British), 1942, p. 45.
48. Dugway Proving Ground Report No. 126, for two-week period ending Sept. 25, 1945.
49. *Cold Weather Trial of Comings H Thermal Generator*, Suffield Report No. 136, A. W. Birnie, June 24, 1945.

SECRET

50. *Final Report of CWS Contract W-18-035-CWS-1232*, E. W. Comings, Jan. 31, 1946.
51. Monthly Progress Reports of the NDRC Munitions Development Laboratory, University of Illinois, for March, April, and May 1944.
52. Monthly Progress Report of the NDRC Munitions Development Laboratory, November 1944.

Chapter 31

1. *Fuel Blocks for Thermal Generators*, R. W. Parry, M. H. Raila, R. C. Johnson, D. Ehrlinger, C. H. Simonson, R. P. Connor, and E. W. Comings, OSRD 6636, Mar. 11, 1946. Div. 10-504.11-M3
3. Final Report of the Munitions Development Laboratory, CWS Contract W-18-035-CWS-1232, Jan. 31, 1946. An excerpt from this report covering the work on fuel blocks is included in OSRD 6636. Div. 10-504.11-M3
4. *Development of the British Type "M" Candle*, CWD 206A and 207A. Reported in Reference 5.
5. *The Nine-Pound DM Candle*, EACD 241, Weaver, 1924.
6. *Low Temperature Fuels for Toxic Smokes*, Finkelstein, TDMR 214, 1940.
7. *Laboratory Development of Nine-Pound HS-Sulfone Candle*, TDMR 272, Finkelstein and Magram, 1941.
8. *Development of a New Fuel for the DM Candle*, MacIntire, TDMR 479, 1942.
10. *Rocket Fundamentals*, Allegheny Ballistics Laboratory SR-4, OSRD 3992, 1944. Div. 3-210-M3
11. *The 32°C Transition of NH_4NO_3*, Kincaid and St. George, OSRD 1577, 1943. Div. 8-110.3-M1
12. "Symposium on Gas Temperature Measurement," Ribaud, Laure, and Goudry, *J. Inst. Fuel*, **12**, S18.
14. Taylor and Neville, *J. Amer. Chem. Soc.*, **43**, 1921, p. 2055.
15. "A Study of Carbon Combustibility by a Semi-Micro Method," Blayden, Riley, and Shaw, *Fuel in Science and Practice*, **22**, 1943, p. 2.
16. Blayden, Riley, and Shaw, *ibid.*, **22**, 1943, p. 64.
17. Blayden, Noble, and Riley, *J. Inst. Fuel*, **7**, 1934, p. 139.
18. *Comprehensive Treatise on Inorganic and Theoretical Chemistry*, Mellor, **2**, 1922, p. 829.
19. McCullough, R., and Long, Informal Conference at Dayton, Ohio, July 26, 1945.
21. *Explosibility and Fire Hazard of NH_4NO_3*, Davis, Circular No. 719, U. S. D. A., 1945.
22. *The Reactivation in Oxygen of CWS Charcoals*, T. F. Young, S. W. Weller, S. L. Simon, and M. G. Buck, OSRD 4104, Sept. 7, 1944. Div. 10-202.132-M2
23. Grim and Roland, *American Mineralogist*, **27**, 1942, pp. 746–760, 801–818.
24. International Critical Tables, Vol. III and IV.

Chapter 32

1. *The Vapor Pressure of $FeCl_3$-H_2O Solutions and Its Relation to Smoke Production*, E. W. Comings and C. H. Adams, Report from OSRD Contract OEMsr-102, Jan. 6, 1943 (unpublished).
2. *Screening Smokes*, W. H. Rodebush, V. K. LaMer, I. Langmuir, and T. K. Sherwood, OSRD 940, Oct. 5, 1942. Div. 10-502-M5
   a. *Ibid., Part V*, T. K. Sherwood.
3. *Verification of Mie Theory — Calculations and Measurements of Light Scattering by Dielectric Spherical Particles*, V. K. LaMer, OSRD 1857, Nov. 11, 1943. Div. 10-501.1-M2
6. Kendrick, EACD No. 30, CWS.
7. *Development of the HC Smoke Mixtures*, E. T. Lawrence, 1925.
8. *Development of the Universal Type HS Smoke Candle*, E2R3, L. J. Conkling.
9. *Investigation of Causes of Ignition of HC Smoke Pot*, Smith and Hormats, TDMR No. 307, 1941.
10. L. Finkelstein and Becker, TDMR 472, CWS.
11. *A1-ZnO-Hexachloroethane Filling*, Barnard, TDMR 489, CWS, 1942.
12. J. H. Ladd and Barnard, TDMR 544, CWS, 1943.
13. *New Chlorine Carriers for Metal Chloride Screening Smoke Mixtures*, E. W. Comings, R. W. Parry, C. H. Adams, E. D. Shippee, and M. Forester, OSRD 3011, Dec. 14, 1943. Div. 10-502-M9
14. H. F. Johnstone, H. C. Weingartner, and W. E. Winsche, *Am. Chem. Soc.*, **64**, 1942, p. 241.
15. *Textbook of Inorganic Chemistry*, J. A. N. Friend, Charles Griffin and Company, 1925, **9**, *Part II*, p. 102.
16. F. W. J. Clendinnen, *Jour. Chem. Soc. Trans.*, **123**, 1923, p. 1340.
17. G. Malquori, *Gazz. Chim. Ital.*, **57**, 1927, p. 665; **58**, 1928, p. 891.
19. Unpublished report by I. Bencowitz of the Texas Gulf Sulphur Co., 1942.
20. *Sulfur as a Screening Smoke*, V. K. LaMer and S. Hochberg, OSRD Contract OEMsr-148, Jan. 5, 1943 (unpublished).
21. *Use of Sulfur Boiler for Smoke Generation*, W. K. Lewis, OSRD 1692, Aug. 9, 1943. Div. 10-501.2-M3
22. *Development of the Thermal Generator Candle*, E. W. Comings, OSRD 3150, Jan. 18, 1944, p. 18. Div. 10-504.12-M5 see also *Part I, Toxic Smoke Candle*, E. W. Comings, OSRD 1076, Dec. 1, 1942, p. 39. Div. 10-504.12-M3
23. *A Continuous Sulfur Smoke Generator*, E. W. Comings and W. L. Lundy, OSRD 3213, Feb. 4, 1944. Div. 10-501.2-M4
24. *Development of the SN Screening Smoke Mixture*, E. W. Comings, C. H. Adams, E. D. Shippee, and M. Forester, OSRD 1772, Sept. 4, 1943. Div. 10-501.21-M2
25. *The Aerosol Smoke Pot*, W. D. Pye, Report No. 6 for period February 1–28, 1943 on OSRD Contract OEMsr-142, Apr. 16, 1943 (unpublished).
26. *The Aerosol Smoke Pot*, W. D. Pye, Report No. 7 for period March 1–April 3, 1943 on OSRD Contract OEMsr-142, Apr. 16, 1943 (unpublished).
28. *The Development of a Portable Aerosol Smoke Pot*, H. H. Champney, L. B. Counterman, R. Kamrath, J. G. Wisler, and R. M. Adams, OSRD 4565, Jan. 9, 1945. Div. 10-501.21-M3

CONFIDENTIAL

Chapter 33

1. *Exhaust Type Airplane Unit*, J. E. Cook and H. A. Roselund, Final Report of Contract OEMsr-578, covering period March 1942 to September 1943.
3. *Screening Smokes*, W. H. Rodebush, V. K. LaMer, I. Langmuir, and T. K. Sherwood, OSRD 940, Oct. 5, 1942. Div. 10-502-M5
4. *Verification of Mie Theory — Calculations and Measurements of Light Scattering by Dielectric Spherical Particles*, V. K. LaMer, OSRD 1857, Nov. 11, 1943. Div. 10-501.1-M2
5. *Graphical Method for Evaluating Relative Permanency of Fog Oils* (SGF), Standard Oil Development Company, Feb. 23, 1943.
6. *Chemical Technology of Petroleum*, Gruse and Stevens, McGraw-Hill Book Co., 1942.
7. *The Development of an Exhaust Smoke Generator for Military Aircraft*, M. J. Goglia and H. F. Johnstone, OSRD 5488, Aug. 25, 1945. Div. 10-501.203-M2
8. NDRC Munitions Development Laboratory Monthly Progress Reports, August 1944 to April 1945.
9. *Tactical Evaluation of Exhaust Manifold Generated Oil Type, Smoke Screen Equipment*, Naval Air Station, Patuxent River, Maryland, for January 29, 1945, February 28, 1945, and March 15, 1945.
10. *Development of Exhaust Combustion Smoke Generator for the TBM-3 Airplane*, Final Report on Contract OEMsr-1446, OSRD 6343, Nov. 23, 1945. Div. 10-501.203-M3
11. *Interrelation of Exhaust Gas Constituents*, H. C. Gerish and F. Voss, N. A. C. A. Report No. 616, 1937.
12. "Relation of Exhaust Composition to Air/Fuel Ratio," B. A. D'Alleua and W. A. Lovell, *S. A. E. Trans.*, 31, 1936.
13. NATC, Patuxent River, Maryland, confidential letter and report, Serial C-718 of July 9, 1945.
14. *Aircraft Oil Fog Generator, Mk. 4, Tests*, Report of COTCLant/S77/(RD 214) Serial 03774 of October 29, 1945.
15. *Use of Aircraft Oil Fog Generator, Mk. 4, for Laying Large Blanket Type Smoke Screens*, COTCLant confidential letter, COTCLant/S77/(RD214) Serial 03815 of November 10, 1945.

Chapter 34

1. *The Development of a Light High Explosive Bomb for Dispersing Toxic and Insecticidal Aerosols*, H. F. Johnstone, R. L. LeTourneau, and H. C. Weingartner, OSRD 6565, Jan. 28, 1946. Div. 10-504.2-M12
2. *Development of a Small Base Ejection Air-Burst Bomb for Dispersing Liquid Agents*, R. J. Kallal and R. W. Davis, OSRD 6300, Nov. 7, 1945. Div. 10-504.2-M10
3. M. H. Davis and D. L. Woodbury, EATR 37, Edgewood Arsenal, Sept. 15, 1930. Div. 10-504.2-M10
4. *M-67 Bomb Modified for Improved Dispersion of H*, E. K. Carver and G. Broughton, OSRD 2058.
5. Weekly Report on the Research and Development Program, Dugway Proving Ground, week ending April 12, 1944.
6. Dugway Proving Ground Weekly Reports, Series 2, Nos. 116, 117, and 118; July 10, 17, and 24, 1945.
7. *Particle Size Measurements on Certain "Aerosol" Bombs for the Department of Agriculture*, V. K. LaMer, NDRC 10.2-14, Apr. 24, 1944. Div. 10-504.2-M4
8. *Special Summary on the Dispersal of Liquids by Gases*, A. R. Olson, Progress Report Contract OEMsr-538, Mar. 16, 1943.
9. *Test of Bomb Developed by Professor A. R. Olson*, W. S. Guthmann and T. M. North, DPGSR No. 6, June 1, 1943.
10. *A Study of Aerosols Produced by the Olson Bomb*, F. T. Gucker, Jr., NDRC 10.1-14, May 15, 1943. Div. 10-504.2-M1
11. *Field Methods of Dispersing Chemical Warfare Agents*, A. R. Olson and K. J. Tong, OSRD 3578, May 4, 1944. Div. 10-504.2-M5
12. *Tests on CO_2 Spraying Devices*, F. G. Straub and R. J. Kallal, OSRD 3577, May 4, 1944. Div. 10-501.2-M5

Chapter 35

1. *Preliminary Field Tests on Powdered "W" Dispersed with the E-5 Tail Ejection Bomb*, Mangun, Skipper and Karel, TDMR 699, July 21, 1943.
2. Biweekly and Monthly Progress Reports of the Munitions Development Laboratory, 1943 and 1944.
3. NDRC, Division 9, University of Chicago Toxicity Laboratory Monthly Reports, 1943 and 1944. Div. 9-125-M2
4. *The Optical Characterization of Any Aerosol in the Laboratory or Field. The Production of Aerosols from Powdered Solid Materials*, V. K. LaMer, NDRC Division 10 Final Report, Oct. 31, 1944.
5. Informal Monthly Progress Report on Toxicity and Irritancy of Chemical Agents, University of Chicago Toxicity Laboratory, Feb. 15, 1946.
6. W. Sell, *Forschungsheft*, 1931, p. 347.
7. *Final Report on Preparation of W*, Procter and Gamble Company, NDRC Division 9.
8. *The Preparation of Solid Materials for Dispersion as Aerosols*, F. C. McGrew, OSRD 3902, July 17, 1944. Div. 10-504.3-M2
9. *Micromentics, The Technology of Fine Particles*, J. M. Dallavalle, Pitman Co., 1943, p. 118.
10. Dugway Proving Ground Medical Research Laboratory, Weekly Reports for 1944.
11. *The Deposition of Non-Volatile Aerosol Clouds in Open and Forested Areas*, W. E. Winsche, NDRC 10.4-55, Mar. 1, 1944. Div. 10-501.12-M3
12. *Meteorological Aspects of Chemical Warfare*, O. G. Sutton, H. Garnett, and P. A. Sheppard, Porton Report No. 2070, Jan. 16, 1939;

A Generalization of the Theory of Turbulent Atmospheric Diffusion, Porton Departmental Report No. 88, Aug. 31, 1939;
The Meteorology of Chemical Warfare, Porton Memorandum No. 6;
The Diffusive Properties of the Lower Atmosphere (An Account of Investigations at the Chemical Defence Experimental Station, Porton, Wilts, 1921–1942), O. G. Sutton.

13. *Some Theoretical Aspects of the Behavior of DDT Aerosols Dispersed from Aircraft*, W. E. Winsche, R. L. Le Tourneau, L. W. Smith, and H. F. Johnstone, OSRD 5710, Sept. 19, 1945. Div. 10-602.121-M5
14. *The Assessment of Aerosols*, H. F. Johnstone, NDRC 10.4-48, Dec. 31, 1943. Div. 10-504.2-M3
15. *The Cascade Impactor*, K. R. May, Porton Report No. 2463, Dec. 8, 1942.
16. *Memorandum to Suffield Experimental Station*, W. L. Doyle, University of Chicago Toxicity Laboratory, Published as Appendix II of Suffield Report No. 137.
17. *The Efficiency of Dispersal of Agent W as a Dry Powder and from Suspension by Different Munitions*, Suffield Report No. 137, June 30, 1945.
18. *The Production of Particulate Clouds from Bombs — Part I. Comparison of Different Bursting Systems in 30-lb LC Bombs*, E. Boyland, J. H. Gaddum, G. S. Hartley, and W. R. Lane, Porton Report 2391, Aug. 11, 1942;
Experiments on Particulate Clouds, J. H. Gaddum, Ptn. 1708 (S. 2507), Feb. 28, 1943;
The Production of Particulate Clouds from Bombs, Part II. Comparison of Different Thicknesses of Burster and Case, J. H. Gaddum and R. W. Pittman, Porton Report No. 2397, July 18, 1942.
19. *Field Trials with W in Bombs*, J. H. Gaddum, Porton.
20. *Gas Ejection Bombs for the Dispersal of Finely Divided Powders*, C. A. Getz, J. C. Hesson, H. C. Weingartner, and H. F. Johnstone, OSRD 5489, Aug. 25, 1945. Div. 10-504.2-M8
21. *Development of Munitions for Dispersing Solid Particulates*, H. F. Johnstone, OSRD 4166, Sept. 25, 1944. Div. 10-504.2-M6
22. *Munitions for Gas Dispersal*, Munitions Development Laboratory Monthly Progress Report Contract OEMsr-102, March 1944. Div. 10-504-M2
23. *Studies of the Toxicity and Dispersibility of W in Munitions*, Franklin, Lephin, Weingartner and Graef, MRL (DPG) Report No. 2, Project A1.12 and A10.3, July 19, 1945.
24. *The Development of a Light High Explosive Bomb for Dispersing Toxic and Insecticidal Aerosols*, H. F. Johnstone, R. L. LeTourneau, and H. C. Weingartner, OSRD 6565, Jan. 28, 1946. Div. 10-504.2-M12
25. *Comparison of the Type F Bomb vs Plastic Bomb Both Charged "U" Slurry*, H. Wolochow, Suffield Field Report No. 1011, May 18, 1945.

Chapter 36

1. *Memorandum on Airplane Vesicant Spray*, T. K. Sherwood, OSRD 2093, Dec. 2, 1943. Div. 11-203.522-M1

Chapter 37

1. Munitions Development Laboratory Monthly Reports, October, November, and December 1943.
2. Reports on Contract OEMsr-949 as follows:
Tests on the Reinforced Phosphorus Fillings for Mortar Shells, Monthly Reports for July and August 1943;
The Use of Carbon Black in WP Shells, NDRC 10.4-10, Nov. 11, 1943. Div. 10-504.21-M1
1. Static Firing Tests on Tail-Ejection (E-5) Bombs, NDRC 10.4-42, Dec. 7, 1943; Div. 10-504.21-M2
Tests on M-69 Bombs Charged with Coated Precast Blocks of WP, NDRC 10.4-56, Mar. 30, 1944. Div. 10-504.21-M4
3. *The Burning Properties and Anti-Personnel Effect of PWP*, H. F. Johnstone, D. G. Edwards, M. F. Nathan, F. A. Orr, and M. M. Woyski, OSRD 4733, Mar. 3, 1945. Div. 10-504.21-M11
4. *The Development of Plasticized White Phosphorus (PWP)*, M. M. Woyski, E. A. Ford, C. E. Shoemaker, F. A. Orr, J. A. Mattern, R. D. Emmick, P. G. Roach, H. F. Johnstone, and J. C. Bailar, Jr., OSRD 6566, Jan. 28, 1946. Div. 10-504.21-M13
5. *Plasticized White Phosphorus Process and Development*, TDMR 1130, Nov. 26, 1945.
6. *Design of a Plant for Manufacturing and Loading Plasticized White Phosphorus*, E. A. Ford, OSRD 6122, Oct. 17, 1945. Div. 10-504.21-M12
7. *Functioning and Comparison Tests of Smoke Bombs, M47A2, WP, WPT, and PWP Filled; HC Filled*, J. P. Clay, E. H. Lewis, E. W. Marshall, and P. G. Roach, DPGMR No. 19.
8. *Report of CWS Participation in Combined Arms Test — Tactical Employment of 4.2-inch RCM*, Camp Hood, Texas, July 15, 1945.
9. Conf. letter 0.0.471.381/222(c) SPOTM — Art Amm Br of Feb. 27, 1945, *Firing Tests of Shell, Smoke, PWP, 60 mm M302(T6) and Shell, Smoke, PWP, 81 mm M57.*
10. ComPhibTraLant conf. ltr. FE25/S70-1/A9 Serial 02310 of June 29, 1944: *4.5-inch Plasticized WP Smoke Rockets; Progress Report of Service Test.*
11. ComPhibTraLant conf. ltr. FE25/S77/L5/(RD30) Serial 03528 of Sept. 18, 1944: *4.5-inch and 7.2-inch Smoke Rockets and 4.2-inch Chemical Mortar Smoke Shells; Service Tests and Tactical Use in Screening Landing Operations.*
12. ComPhibTraLant conf. ltr. FE25/S70-1(RD30) Serial 03417 of Sept. 9, 1944: *Bombs M47A2, WP and PWP Filled, for Screening Landing Operations.*
13. ComPhibsPac conf. ltr. CAF/S76 Serial 059 of Jan. 22, 1945: *Demonstration of Smoke Munitions for Use in Amphibious Operations.*
14. *Plasticized White Phosphorus in Small Munitions*, OSRD 4700, R. I. Rice et al, Feb. 16, 1945. Div. 10-504.21-M9
15. *Part I — Comparison of Anti-Personnel Effects of Plasticized WP and Solid WP in 4.2-inch CM Shells. Part II —*

Evaluation of Flight Characteristics of 4.2-inch CM Shell, M2, Filled with Plasticized WP, — Dugway Proving Ground Special Report No. 30.

16. *Burning Power and Harassing Effects of White Phosphorus,* Porton Report No. 2604.
17. *Physics,* Dillon and Johnson, **4,** 1933, p. 225.

Chapter 38

1. "Particle Size in Relation to Insecticide Efficiency," C. M. Smith and L. D. Goodhue, *Industrial and Engineering Chemistry,* **34,** 1942, p. 490.
2. *Some Principles Governing the Production of Air Floated Oil Particles and Their Relation to the Toxicity of Contact Oil Sprays to Insects,* R. C. Burdette, Bull. 632, New Jersey Agriculture Experimental Station, January 1938.
3. "Relation of Viscosity to Drop Size and the Application of Oils by Atomization," E. M. Searls and F. M. Snyder, *Journal of Economic Entomology,* **29,** 1936, p. 1167.
4. *The Deposition of Spray Droplets on a Mosquito in Flight,* H. A. Druett, H. L. Green, and R. M. A. Welchman, Porton 1641, June 1944.
5. *Particle Size Measurements on Certain Aerosol Bombs for the Department of Agriculture,* V. K. LaMer, S. Hochberg, B. Zimm, and B. Williamson, NDRC 10.2-14, Apr. 24, 1944. Div. 10-504.2-M4
6. *Some Theoretical Aspects of the Behavior of DDT Aerosols Dispersed from Aircraft,* H. F. Johnstone, W. E. Winsche, R. L. LeTourneau, and L. W. Smith, OSRD 5710, National Research Council Insect Control Committee 116, Sept. 19, 1945. Div. 10-602.121-M5
7. *Statistical Considerations in the Use of DDT Aerosols,* W. H. Rodebush, OSRD 4757, OSRD Insect Control Committee Report 13, Mar. 5, 1945. Div. 10-602.21-M2
8. *Forschungsarbeiten Verein deutschen Ingenieuren,* W. Sell, Verlag, Berlin, 1931.
9. *Deposition of Non-Volatile Aerosol Clouds in Open and Forested Areas,* W. E. Winsche and H. F. Johnstone, NDRC 10.4-55, Mar. 1, 1944. Div. 10-501.12-M3
10. *Toxicity of DDT to Mosquitoes. Effect of Particle Size on the Efficiency of Oil Aerosols Bearing DDT,* V. K. LaMer, S. Hochberg, K. Hodges, I. Wilson, and J. Adamo, OSRD 4447, Dec. 11, 1944. Div. 10-602.21-M1
11. *The Effect of Particle Size and Speed of Motion of DDT Aerosols of Uniform Particle Size in a Wind Tunnel on the Mortality of Mosquitoes,* R. Latta, L. D. Anderson, E. E. Rogers, V. K. LaMer, S. Hochberg, H. K. Hodges, J. C. Rowell, and I. Johnson, OSRD 5566, National Research Council Insect Control Committee Report 119, Sept. 7, 1945. Div. 10-602.21-M4
12. *Production, Analysis, and Use of Aerosols of Uniform Particle Size,* V. K. LaMer and D. Sinclair, OSRD 119, Aug. 8, 1941. Div. 10-501-M1
13. *A Portable Optical Instrument for the Measurement of Particle Size in Smokes, the "Owl," and the Improved Homogeneous Aerosol Generator,* V. K. LaMer and D. Sinclair, OSRD 1668, Aug. 1943. Div. 10-501.11-M6
14. *Effect of Solvents on the Toxicity of DDT Aerosols,* V. K. LaMer, S. Hochberg, H. Lauterbach, I. Johnson, R. Latta, L. D. Anderson, E. E. Rogers, OSRD 5936, National Research Council Insect Control Committee Report 123, Aug. 31, 1945. Div. 10-601.1-M3
15. "The Calculation of the Dosage Mortality Curve," C. I. Bliss, *Annals of Applied Biology,* **22,** 1935, p. 134.
16. *Toxicity to Drosophila (Fruit Flies) of Aerosols of DDT of Uniform Droplet Size in Oil of High Boiling Point,* V. K. LaMer, S. Hochberg, B. H. Zimm, B. Williamson, OSRD 4796, Mar. 15, 1945. Div. 10-602.22-M2
17. *The Development of an Aerosol Generator for Dispersing DDT Solutions from the Exhaust of an Aircraft Engine,* H. F. Johnstone, R. J. Kallal, and H. Adams, OSRD 5309, OSRD Insect Control Committee Report 95, July 5, 1945. Div. 10-602.121-M2
18. *The Toxicity of DDT Films and Aerosol Deposits,* H. F. Johnstone, W. H. Rodebush, R. L. LeTourneau, C. W. Kearns, J. S. Laughlin, and F. McKee, NDRC 10.4-74, Oct. 1, 1944. Div. 10-602.2-M1
19. *Toxicity to Drosophila (Fruit Flies) of DDT Deposited from Aerosols on the Surface of Certain Leaves and Grass,* V. K. LaMer, S. Hochberg, B. Zimm, B. Williamson, and J. Betheil, NDRC 10.2-18, Dec. 7, 1944. Div. 10-602.22-M1
20. *The Deposition of Drops of a Non-Volatile Liquid Vesicant on Vertical and Horizontal Surfaces,* W. E. Winsche and H. F. Johnstone, NDRC 10.4-49, Jan. 15, 1944. Div. 10-501.12-M2
21. *Mosquito Control by Ground Dispersal of DDT as Aerosol from Large Scale Generators,* R. Ellis and V. K. LaMer, NDRC 10.2-19, OSRD Insect Control Committee Report 9, Dec., 1944. Div. 10-602.11-M1
22. *Salt Marsh and Anopheline Mosquito Control by Ground Dispersal of DDT Aerosols,* V. K. LaMer, F. Brescia, I. Wilson, K. C. Hodges, J. C. Rowell, OSRD 5731, National Research Council Insect Control Committee Report 122, Sept. 18, 1945. Div. 10-602.21-M5
23. *Efficacy of DDT and DNOC as Insecticides for Grasshoppers when Dispersed by a Hochberg-LaMer Type Aerosol Generator,* V. K. LaMer, NDRC 10.2-25, National Research Council Insect Control Committee Report 137, Oct. 25, 1945. Div. 10-602.23-M3
24. "Insecticidal Aerosol Production. Spraying Solutions in Liquefied Gases," L. D. Goodhue, *Industrial and Engineering Chemistry,* **34,** 1942, pp. 1456–1459.
25. *Hochberg-LaMer Aerosol Generator Inventor's Model,* V. K. LaMer and S. Hochberg, OSRD 4901, OSRD Insect Control Committee Report 15, Apr. 15, 1945. Div. 10-602.11-M3
26. *Aerosol Generator for DDT Dispersal,* Stewart-Warner Corp., December 1944.
27. *Visit to Stewart-Warner Corp.,* K. C. Hodges, and V. K. LaMer, Memorandum Report, Division 10, NDRC, November 1944.
28. *Conversion of Besler No. 374 Screening Smoke Generator to a Hochberg-LaMer Aerosol Generator for Insecticidal Purposes with Supplement on Conversion of Besler M-2 Generator,* V. K. LaMer, S. Hochberg, R. Ellis, F. E. Buch-

walter, and J. C. Rowell, OSRD 4894, OSRD Insect Control Committee Report 53, Apr. 5, 1945. Div. 10-602.11-M2

29. *Disperser, Insecticide, Aerosol, Mechanical, E-12,* TB CW 32 War Department, November 1945.
30. *Test of Large Area Mosquito Control with Hochberg-LaMer Aerosol Generator in Lodge Village, British Guiana,* K. C. Hodges and J. C. Rowell, OSRD 5310, OSRD Insect Control Committee Report 96, July 5, 1945. Div. 10-602.21-M3
31. *Reports on the Use in the South Pacific of the Navy Screening Smoke Generator (M374) Converted to an Insecticidal Aerosol Generator According to the Hochberg-LaMer Principle,* F. Brescia and I. Wilson, OSRD 5730, National Research Council Insect Control Committee 121, May 7, 1945. Div. 10-602.11-M4
32. *Field Tests of Hochberg-LaMer Aerosol Insecticide Generator Against Salt Marsh Mosquitoes at Mantoloking, N. J.,* V. K. LaMer, S. Hochberg, J. Q. Umberger, I. Wilson, J. C. Rowell, J. Bethell, NDRC 10.2-23, National Research Council Insect Control Committee Report 134, Oct. 23, 1945. Div. 10-602.21-M6
33. *Cankerworms as Test Insects for DDT Field Tests of Models of the Hochberg-LaMer Insecticidal Aerosol Generator at Hempstead Lake State Park, Long Island, New York,* V. K. LaMer, S. Hochberg, J. Q. Umberger, J. Bethell, OSRD 6004, National Research Council Insect Control Committee Report 124, Sept. 28, 1945. Div. 10-602.23-M1
34. *Black Fly Control with DDT-Oil Aerosol Using the Hochberg-LaMer Generator with Notes on Spruce Bud Worm and Larch Case Bearer Control at Lake Placid, New York,* V. K. LaMer, NDRC 10.2-26, National Research Council Insect Control Committee Report 140, Nov. 8, 1945. Div. 10-602.23-M4
35. *Report of the Use of Hochberg-LaMer Aerosol Generator for Dispersing DDT to Control the Spruce Budworm,* G. L. Osberg and B. W. Flaherty, Chemical Warfare Laboratories, Ottawa, Research Section Report No. 59, November 1945.
36. *Development of an Exhaust DDT Aerosol Generator for the 1/4-Ton 4 x 4 Truck ("Jeep"),* H. F. Johnstone, R. L. LeTourneau, R. J. Rice, and H. F. Hrubecky, OSRD 6301, National Research Council Insect Control Committee 139, Nov. 7, 1945. Div. 10-602.122-M3
37. *Installation of an Exhaust DDT Aerosol Generator on the Cargo Carrier M29C (Weasel),* H. F. Johnstone and R. J. Rice, NDRC 10.4-84, National Research Council Insect Control Committee Report 102, July 20, 1945. Div. 10-602.122-M2
38. *Development of an Experimental Thermal Generator Pot for Dispersing Mustard Gas as an Aerosol,* E. W. Comings, C. H. Adams, and M. H. Raila, OSRD 6431, Dec. 29, 1945. Div. 10-504.1-M2
39. *Tests with an Exhaust Aerosol DDT Generator on a 450 H.P. Stearman Aircraft,* H. F. Johnstone, R. L. LeTourneau, C. W. Kearns, R. J. Kallal, C. H. Adams, and R. L. Metcalf, OSRD 4399, OSRD Insect Control Committee Report 51, Nov. 29, 1944. Div. 10-602.121-M1
40. CWS Monthly Progress Report on Insect and Rodent Control, April to September 1945.
41. *Application of Sprays by Means of Portable Spray Unit from Cub Planes,* Bureau of Entomology and Plant Quarantine, U. S. Department of Agriculture, CC-2-421, April 1944.
42. *A Study of the Atomization of Liquids,* H. F. Johnstone, H. C. Lewis, D. G. Edwards, M. J. Goglia, R. I. Rice, and L. W. Smith, OSRD 6345, National Research Council Insect Control Committee Report 148, Nov. 23, 1945. Div. 10-501.2-M6
43. Progress Report for Month of August 1945, Biology Section, Health and Safety Department, Tennessee Valley Authority, A. D. Hess, September 1945.
44. *The Development of an Exhaust Smoke Generator for Military Aircraft,* H. F. Johnstone and M. J. Goglia, OSRD 5488, Aug. 25, 1945. Div. 10-501.203-M2
45. *Operational Procedures for Airplane Dispersal of DDT Aerosol by Type TBM-3 Aircraft,* B. Commoner, J. C. Early, and M. H. Tuttle, U. S. Naval Air Test Center, Patuxent No. NA83/A16-3/C-760, BC/egd(TT), June 1945.
46. *Development and Test of Airplane Dispersal of DDT Aerosol,* B. Commoner, L. E. McDonald, and M. H. Tuttle, U. S. Naval Air Station, Patuxent River, Maryland, NA83(TT), BC/egd, A16-3, January 1945.
47. *Exhaust Aerosol Generator for Dispersal of DDT Solution with SB2C-4 Airplane,* J. H. Clark, OSRD 5487, National Research Council Insect Control Committee 114, Aug. 25, 1945. Div. 10-602.121-M3
48. *Exhaust Aerosol Generator on the PBJ-1H for the Dispersal of DDT and Oil Smoke,* J. H. Clark, OSRD 5510, National Research Council Insect Control Committee Report 115, Aug. 30, 1945. Div. 10-602.121-M4
49. *Tests of Exhaust Generator Spray Equipment on C-47 Aircraft,* Army Air Force Board Project J4670.
50. *The Development of an Exhaust DDT Aerosol Generator for the Taylorcraft Light Airplane,* R. I. Rice, OSRD 6344, National Research Council Insect Control Committee Report 144, Nov. 23, 1945. Div. 10-602.121-M6
51. *Considerations on the Design of a DDT Exhaust Generator for L-5 Aircraft,* H. F. Johnstone and R. J. Kallal, NDRC 10.4-85, National Research Council Insect Control Committee Report 165, December 1945.
52. *The Production of Aerosol Droplets Below 25 Microns Diameter for the Dispersal of Insecticides and CW Agents,* H. F. Johnstone, R. L. LeTourneau, R. J. Kallal, and D. R. Powell, NDRC 10.4-60, Apr. 20, 1944. Div. 10-602-M1
53. Monthly Progress Report from NDRC Munitions Development Laboratory, University of Illinois, December 1944.
54. *Test to Determine Suitability of Especially Designed Spray Equipment for the Dissemination of DDT from B-25 and C-47 Aircraft,* Army Air Forces Board, Orlando, Florida, Project No. 4095BG725, April 1945.
55. *The Development of a Light High Explosive Bomb for Dispersing Toxic and Insecticidal Aerosols,* H. F. Johnstone, R. L. LeTourneau, H. C. Weingartner, D. R. Powell, P. N. Rylander, R. C. Johnson, and C. H. Simonson, OSRD 6565, Jan. 28, 1946. Div. 10-504.2-M12
56. Monthly Progress Report from NDRC Munitions De-

velopment Laboratory, University of Illinois, H. F. Johnstone and R. L. LeTourneau, May 1945.

57. *Sun Oil Company Solvent Aro-Sol (151B) as a Practical Solvent for DDT*, V. K. LaMer, S. Hochberg, and J. Bethell, NDRC 10.2-22, OSRD Insect Control Committee Report 60, Apr. 30, 1945. Div. 10-601.1-M2
58. *The Solubility of DDT in Mixtures of Xylene and Lubricating Oil (10W), The Density of These Solutions when Saturated with DDT*, V. K. LaMer, S. Hochberg, and J. Bethell, NDRC 10.2-20, National Research Council Insect Control Committee Report 112, April 1945. Div. 10-601.1-M1
59. *Formulas Utilizing DDT Concentrate*, V. K. LaMer, F. Brescia, I. Wilson, K. C. Hodges, J. C. Rowell, I. Johnson, J. Bethell, OSRD 5729, National Research Council Insect Control Committee Report 120, Aug. 18, 1945. Div. 10-601.2-M2
60. "Efficiency of DDT as a Residual-Type Spray Against Adult Disease-Carrying Mosquitoes Laboratory Tests," J. B. Gahan, B. V. Travis, and A. W. Lindquist, *J. Economic Entomology*, **38**, 1945, pp. 236–240.
61. *Slope-o-Meter; an Instrument for the Rapid Determination of Particle Radius and Concentration in the Laboratory and Field*, NDRC 10.2-15, V. K. LaMer, June 19, 1944. Div. 10-501.11-M9
62. *The Cascade Impactor, an Apparatus for Sampling Solid and Liquid Particulate Clouds*, K. R. May, Ptn. Report No. 2463, December 1942.
63. CWS Monthly Progress Report on Insect and Rodent Control, September 1945.
64. *Particulate Program — Comparison of Carbon Coated and Magnesium Oxide Coated Slides*, D. Benedict, S. Black, K. P. DuBois, R. G. Herrmann, A. McGinnis, H. E. Landahl, J. Savit, and W. R. Schmitz, The University of Chicago Toxicity Laboratory Informal Progress Report NS-1, April 1945.
65. Informal Progress Reports from University of Chicago Toxicity Laboratory NS-1 to NS-5, W. L. Doyle et al, April to August 1945.
66. *Comparison of Sample Methods for Measuring Aerosols Cts*, Captain Charles R. Naeser, Report of Conference at Edgewood Arsenal, Maryland, CWS Technical Command, June 26, 27, 28, 1945, July 1945.

Chapter 39

1. "The Preparation and Properties of Disulfur Decafluoride," Kenneth G. Denbigh and Robert Whytlaw-Gray, *J. Chem. Soc.*, 1934, p. 1346.
2. *Agent F5*, C. B. Griffine, Jr., A Memorandum Report TDMR 971, Feb. 3, 1945.
3. *Report on Improved Methods of Preparation and Preliminary Study of Physical and Chemical Properties of Compound 1120*, A. B. Burg, OSRD 179, Nov. 15, 1941. Div. 10-402.32-M1
4. *The Fluorides of Sulfur, Part III*, J. H. Simons, OSRD Report, May 13, 1942. Div. 10-402.311-M2
5. *The Preparation and Properties of 1120 — II*, A. B. Burg, OSRD 294, Serial No. 149, Dec. 30, 1941. Div. 10-402.32-M1
6. *The Fluorides of Sulfur, Part I*, J. H. Simons, The Pennsylvania State College, Contract Report, Jan. 24, 1942. Div. 10-402.311-M2
7. *Final Report on Contract OEMsr-299*, L. F. Audrieth and John C. Bailar, Jr., Aug. 1, 1945.
8. *A Study of the Preparation of Compound 1120 Through the Use of a Regenerative Chemical*, G. L. Clark and P. M. Bernays, University of Illinois, Contract Report, Feb. 15, 1942. Div. 10-402.32-M3
9. *The Fluorides of Sulfur, Part II*, J. H. Simons, The Pennsylvania State College, Contract Report, Mar. 13, 1942. Div. 10-402.311-M2
10. "The Fluorides and Oxyfluorides of Sulfur," M. Trautz and K. Ehrmann, *J. prakt. Chem.*, **142**, 1935, p. 79.
11. *The Chemistry of the Sulfur Fluorides*, J. H. Simons, OSRD 1036, Oct. 21, 1942. Div. 10-402.2-M5
12. *Final Summary Report, Contract NDCrc-113*, A. B. Burg, June 5, 1944. Div. 10-402.36-M8
13. *Heat of Formation of S_2F_{10}*, H. M. Huffman, J. B. Hatcher, and E. L. Ellis, OSRD 776, July 29, 1942. Div. 10-402.36-M3

    Calorimetric Studies II. The Entropy and Free Energy of S_2F_{10}, H. M. Huffman, J. B. Hatcher, and G. B. Guthrie, OSRD 934, Oct. 10, 1942. Div. 10-402.36-M4

    Thermodynamic Data on S_2F_{10}, H. M. Huffman, OSRD 1055, Nov. 21, 1942. Div. 10-402.36-M5
14. *The Chemical Detection of 1120*, D. S. Tarbell, OSRD 879, July 1, 1942. Div. 9-422.121-M3
15. "The Determination of Fluorine by Precipitation as Triphenyltin Fluoride," N. Allen and N. Howell Furman, *J. Am. Chem. Soc.*, **54**, 1932, p. 4625.
16. "Esters of Monofluophosphoric Acid," W. Lange and G. v. Krueger, *Ber.* **65B**, 1932, p. 1598.
17. *Progress Reports*, L. F. Audrieth and J. C. Bailar, Jr. University of Illinois, June 16, 1942 and July 15, 1942. Div. 10-402.311-M4 Div. 10-402.311-M5
18. *A Report on Fluophosphates and Related Compounds*, L. F. Audrieth and J. C. Bailar, Jr., University of Illinois Contract Reports, Oct. 15, 1942 and Nov. 15, 1942. Div. 10-402.311-M13
19. *Report No. 5 on Fluophosphates*, H. McCombie, British Report W-8285.
20. *A Report on Fluophosphates and Related Compounds*, J. C. Bailar, Jr., M. M. Woyski, C. D. Wagner, and J. E. Husted, University of Illinois Contract Reports, Jan. 15, 1943 and Feb. 15, 1943. Div. 10-402.311-M14
21. *A Report on Fluophosphates and Related Compounds*, J. C. Bailar, Jr., M. M. Woyski, and J. E. Husted, University of Illinois Contract Reports, Mar. 15, 1943. Div. 10-402.311-M14
22. "Action of Phosphorus Trichloride on Glycerine and Glycol," *Bull. soc. Chim.* (3), **27**, 1902, p. 268.
23. "Brenzcatechyl-phosphorus Oxychloride and *o*-Phenylene Phosphate," L. Anschutz and W. Brocker, *J. prakt. Chem.*, **223**, 1926–27, p. 379.

24. *A Report on Fluophosphates and Related Compounds*, J. C. Bailar, Jr., M. M. Woyski, and J. E. Husted, University of Illinois Contract Report, Apr. 15, 1943. Div. 10-402.311-M14
25. *Report No. 9 on Fluophosphates*, H. McCombie, Y-3043, WA.579-5, B-2929.
A Report on Fluophosphates and Related Compounds, J. C. Bailar, Jr., J. B. Ziegler, Jr., and M. M. Woyski, University of Illinois Contract Report, October 1943. Div. 10-402.311-M13
26. "The Fluorination of Phosphorus Trichloride," H. S. Booth and F. B. Dutton, *J. Am. Chem. Soc.*, **61**, 1939, p. 2937.
27. *Final Report on Contract OEMsr-299*, J. C. Bailar, Jr. and L. F. Audrieth, University of Illinois, Aug. 1, 1945.
28. *The Alkyl Difluophosphates and the Mono- and Difluothiophosphates*, L. F. Audrieth and J. C. Bailar, Jr., University of Illinois Contract Report, Sept. 15, 1942. Div. 10-402.311-M12
29. *Fluosulfonic Acid and Its Alkyl Esters*, L. F. Audrieth and J. C. Bailar, Jr., University of Illinois Contract Report, July 15, 1942. Div. 10-402.311-M6
30. "Fluosulfonic Acid," T. E. Thorpe and Walter Kirman, *J. Am. Chem. Soc.*, **61**, 1892, p. 921.
31. "Hydrofluoric Acid and Fluosulfonic Acid," O. Ruff and H. J. Braun, *Ber.*, **47**, 1914, p. 646.
32. "Esters of Fluosulfonic Acid," J. Meyer and G. Schramm, *Z. anorg. allgem. Chem.*, **206**, 1932, p. 24.
33. *The Preparation of New Toxic Gases*, A. B. Burg, OSRD 4012, June 5, 1944. Div. 10-402.36-M8
34. *Studies Relating to Phosphorus Trifluoride*, A. B. Burg, NDRC CLIX, July 27, 1942. Div. 10-402.311-M7
35. *New Toxic Gases IX*, A. B. Burg, D. L. Armstrong, and R. N. Doescher, University of Southern California Contract Report, Apr. 15, 1943. Div. 10-402.311-M15
36. *The Preparation of Acyl Fluorides*, J. H. Simons, NDRC LIV, Dec. 16, 1941. Div. 10-402.311-M1
37. *Vapor Pressure of Arsine in Various Solvents*, L. F. Audrieth and J. C. Bailar, Jr., University of Illinois Contract Report, June 17, 1942.

Chapter 40

1. *The Generation of Fluorine*, W. C. Schumb, E. L. Gamble, H. H. Anderson, and A. J. Stevens, NDRC CXCV, Oct. 17, 1942.
The Generation of Fluorine, W. C. Schumb, OSRD 984, Nov. 3, 1942. Div. 10-402.31-M1
2. *Electrolytic Cell for Producing Fluorine*, W. S. Calcott and A. F. Benning, E. I. duPont de Nemours and Co., United States Patent 2,034,458, Mar. 17, 1936.
3. *An Electrolytic Cell Designed for Fluorine Production*, J. H. Simons, OSRD 4199, July 24, 1942. Div. 9-252-M1
4. *The Production of Fluorine by Electrolysis*, R. C. McHarness, R. G. Benner, et al, E. I. duPont de Nemours and Company, OSRD 1114, Dec. 9, 1942. Div. 10-402.31-M3
5. *The Generation of Fluorine*, W. C. Schumb, E. L. Gamble, H. H. Anderson, and A. J. Stevens, NDRC 10.3B-4, Jan. 15, 1943. Div. 10-402.31-M2
6. *The Generation of Fluorine*, W. C. Schumb, E. L. Gamble, H. H. Anderson, and A. J. Stevens, NDRC 10.3B-24, June 15, 1943; OSRD 1690, June 15, 1943. Div. 10-402.31-M4
7. *The Generation of Fluorine*, W. C. Schumb, Massachusetts Institute of Technology Contract Report, Nov. 15, 1942. Div. 10-402.31-M2
8. *The Generation of Fluorine*, W. C. Schumb, E. L. Gamble, H. H. Anderson, and A. J. Stevens, NDRC 10.3B-18, Apr. 15, 1943. Div. 10-402.31-M2
9. *The Generation of Fluorine*, W. C. Schumb, E. L. Gamble, and A. J. Stevens, NDRC 10.3B-28, July 15, 1943. Div. 10-402.31-M2
10. *The Generation of Fluorine*, W. C. Schumb, E. L. Gamble, H. H. Anderson, and A. J. Stevens, NDRC 10.3B-15, Mar. 15, 1943. Div. 10-402.31-M2
11. *The Generation of Fluorine*, W. C. Schumb, E. L. Gamble, H. H. Anderson, and A. J. Stevens, NDRC 10.3B-22, May 15, 1943. Div. 10-402.31-M2
12. *The Generation of Fluorine*, W. C. Schumb, OSRD 3227, Feb. 9, 1944. Div. 10-402.31-M4

Chapter 41

1. C. A. Wurtz, *Ann. Chem.* (Liebig), **79**, 1851, p. 285.
2. W. L. Jennings and W. B. Scott, *J. Am. Chem. Soc.*, **41**, 1919, p. 1241.
3. F. D. Chattaway and J. M. Wadmore, *J. Am. Chem. Soc.*, **81**, 1902, p. 191.
4. T. S. Price and S. J. Green, *J. Soc. Chem. Ind.*, **39**, 1920, p. 98T.
5. W. M. Latimer, NDRC reports dated April 14 and August 14, 1942.
6. Reports Under Contract No. W-285-CWS-4782, American Cyanamid Co., October 1942 to December 1943.
7. Monthly and Final Reports under Contracts OEMsr-1004, W-18-035-CWS-883, and W-18-035-CWS-1257, August 1943 through December 1946; A. B. Burg et al.
8. Weekly Reports of Dugway Proving Ground, 1943–46.
9. M. S. Kharasch, Reports under Contract No. OEMsr-394.
10. J. H. Yoe, Reports under Contract No. OEMsr-139.

Chapter 42

1. *Final Summary Report under Contract OEMsr-1004, Part (a)*, A. B. Burg.
2. Weekly Reports of Dugway Proving Ground.
3. Monthly Reports under Contract No. W-18-035-CWS-883, A. B. Burg et al.

Chapter 43

1. *Scale Model Studies of the Movement of Smoke and Gas Clouds*, H. Rouse, NDRC 10.3A-36, Oct. 10, 1943. Div. 10-302.1-M15
2. *Local Dissipation of Natural Fog*, H. G. Houghton and W. H. Radford, Massachusetts Institute of Technology, 1938.
3. *Wind-Tunnel Studies of the Diffusion of Heat from a Line Source*, H. Rouse, M. L. Albertson, R. A. Jensen, and C. F. Schadt, NDRC 10.2-12, Mar. 18, 1944. Div. 10-401.121-M1
4. *Fog-Dispersal Recommendations for the Island of Shemya*, H. Rouse, M. L. Albertson, R. A. Jensen, and C. F. Schadt, Informal Report to Division 10, NDRC, Dec. 26, 1944.
5. *Fog-Dispersal Recommendations for the Island of Shemya*, Supplementary letter of Jan. 15, 1945, from H. Rouse to W. A. Noyes, Jr.
6. *The Iowa Radiant Burner*, H. O. Croft and J. M. Trummel, Informal Report to Division 10, NDRC, Apr. 30, 1945.
7. *Development of a Fog-Dispersal Burner for Gasoline and Fuel Oil*, M. L. Albertson, Informal Report to Division 10, NDRC, June 15, 1945.
8. *Fuel Nozzle for Fog Dispersal Equipment*, J. B. Hoffman, Informal Report to Division 10, NDRC, Oct. 1, 1945.
9. *Study of the Use of Air Curtains for Fog Dissipation*, A. P. Kratz, E. C. Manthei, and C. F. Holley, Jr., OSRD 3775, June 13, 1944. Div. 10-503.2-M4
10. *Wind-Tunnel Studies of the Diffusion of Heat by Single Wind Curtains and Baffles*, H. Rouse, M. L. Albertson, R. A. Jensen, and D. F. Schadt, OSRD 4334, Nov. 11, 1944. Div. 10-401.121-M3
11. *Wind-Curtain Installations for Fog Dispersal*, R. A. Jensen, Informal Report to Division 10 NDRC, July 16, 1945.
12. *Report on a Design Adapting the Principles of the Aerofoil Ring to the Wind Curtain Installation at Arcata, California*, T. D. Gregg, Informal Report to Division 10, NDRC, Oct. 27, 1945.
13. *Wind-Tunnel Studies of the Diffusion of Gas in Schematic Urban Districts*, H. Rouse, M. L. Albertson, R. A. Jensen, and C. F. Schadt, NDRC 10.3A-46, May 9, 1944.
14. *Wind-Tunnel Studies of Gas Diffusion in a Typical Japanese Urban District*, A. A. Kalinske, R. A. Jensen, and C. F. Schadt, NDRC 10.3A-48, June 8, 1945. Div. 10-401.121-M4
15. *Correlation of Wind-Tunnel Studies with Field Measurements of Gas Diffusion*, A. A. Kalinske, R. A. Jensen, and C. F. Schadt, NDRC 10.3A-48a, Sept. 29, 1945. Div. 10-401.121-M5
16. *Diffusion of Smoke and Gas by Wind*, (motion picture prepared for the Chemical Warfare Service by the Iowa Institute of Hydraulic Research through Division 10, NDRC).
17. *Preliminary Wind-Tunnel Studies on Air Flow Over Mountainous Terrain*, A. A. Kalinske, R. A. Jensen, and C. F. Schadt, Informal Report to Division 10, NDRC, July 25, 1945.
18. *Wind-Tunnel Studies on Effects of Vertical Distortion of Terrain Models*, report by the Iowa Institute of Hydraulic Research for the Weather Service of the Army Air Forces, Jan. 14, 1946.

Chapter 44

1. *Report on Aerosols*, W. H. Rodebush, OSRD 77, Mar. 12, 1941. Div. 10-500-M1
2. *Rapid Methods of Preparing Phosgene*, J. H. Simons, OSRD 88, Apr. 21, 1941. Div. 10-402.36-M1
3. *The Development of Laboratory Methods of Detecting and Analyzing Gases Containing Radioactive Sulfur*, D. M. Yost, OSRD 127, Aug. 25, 1941. Div. 10-402.35-M3
4. *The Measurement of Radioactive Hydrogen*, E. O. Lawrence, OSRD 128, Aug. 26, 1941. Div. 10-402.35-M4
5. *A Brief Investigation of Removal of Arsine in Air-Arsine Mixtures by Charcoal Using the Radioactive Tracer Method*, D. M. Yost, OSRD 361, Jan. 9, 1942. Div. 10-202.154-M12
6. *A Study of the Removal of Arsine by Whetlerite*, E. O. Wiig, OSRD 462, Mar. 23, 1942. Div. 10-202.154-M15
7. *The Distribution of the Catalyst in Whetlerite; The Location and the Identification of the Reaction Products in Whetlerite Treated with Arsine*, H. F. Johnstone and G. L. Clark, OSRD 704, June 1, 1942. Div. 10-202.14-M10
8. *Investigation of the Mechanism of Removal of Phosgene from Phosgene-Air Mixtures, Using the Radioactive Tracer Method*, D. M. Yost, OSRD 903, Sept. 25, 1942. Div. 10-202.155-M5
9. *I. Rapid Methods for Synthesizing War Gases; II. The Chemistry of the Sulfur Fluorides*, J. H. Simons, OSRD 1036, Oct. 21, 1942. Div. 10-402.2-M5
10. *A Study of the Removal of Arsine and of Poisoning by Hydrogen Cyanide; Preparation of Phosgene from Materials which Could Contain Radio-Chlorine*, Parts 2 and 3 of a Joint Report, B6-1, Mar. 25, 1941.
11. *The Preparation of Radioactive Chlorpicrin*, J. H. Simons, NDRC IV, May 28, 1941. Div. 10-402.35-M1
12. *Preparation of Radioactive Cyanogen Chloride*, J. H. Simons, NDRC VIII, July 22, 1941. Div. 10-402.35-M2
13. *Use of Radioactive Tracer Technique for Arsine Removal*, D. M. Yost, NDRC XXXIII, Sept. 30, 1941. Div. 10-202.154-M7
14. *Conclusions from Investigations on the Adsorption of SA and the Distribution of the Arsenic on the Charcoal Bed*, E. O. Wiig, NDRC XXXVI, Oct. 14, 1941. Div. 10-202.15-M5
15. *Preparation of Radioactive Hydrocyanic Acid*, J. H. Simons, NDRC LIII, December, 1941. Div. 10-402.35-M5
16. *Phosgene and Mustard Gas Removal*, D. M. Yost, NDRC LXXI, Jan. 26, 1942. Div. 10-202.155-M2
17. *Preparation of Radioactive Selenium Hexafluoride*, J. H. Simons, NDRC LXXXI, Feb. 12, 1942. Div. 10-402.35-M6
18. *Location of Silver on Silvered Whetlerite and Charcoals*, H. F. Johnstone and G. L. Clark, NDRC CXIII, May 11, 1942. Div. 10-202.143-M2

MICROFILMED REPORTS

DIVISION 10

Other reports which have been microfilmed are included in the following listing.

Progress Report for Division 10, [Informal Report No.] I, (n.a.), [1941 (?)] Div. 10-101-M1

Monthly Summary Report of Projects 10.1 and 10.4, Division 10, NDRC, for the period of June 15 to July 15, 1943, (n.a.), [July 1943.] Div. 10-101-M3

Division 10 Meeting, Dumbarton Oaks, D. C. October 26 and October 27, 1943, (n.a.), [October 1943.] Div. 10-101-M4

Division 10 Meeting, Evanston, Illinois, January 28 and January 29, 1944, (n.a.), [January 1944.] Div. 10-101-M5

Division 10 Meeting, Edgewood Arsenal, June 14, 1944, (n.a.), [June 1944.] Div. 10-101-M6

Monthly Summary Reports of Section 10.1 of Division 10, NDRC, (n.a.), Feb. 15 and Mar. 15, 1945. Div. 10-101-M7

Report on Trip to England, W. A. Noyes, Jr., NDRC VI, [June 1941.] Div. 10-102-M1

Monthly Summary Report of Section 10.1 and 10.4 of Division 10, NDRC, for the period of August 15 to September 15, 1943, (n.a.), Sept. 15, 1943. Div. 10-200-M6

Monthly Summary Report of the Central Laboratory, Division 10, NDRC, (n.a.), Northwestern University, Apr. 15, 1945. Div. 10-200-M8

Canister Protection for Gases — A Survey, W. Conway Pierce and J. W. Zabor, Nov. 16, 1943. Div. 10-201.1-M21

Accelerated Aging Studies, ([*Part*] *IX, Supplement to Monthly Summary Report* [*of*] *August 15, 1944*), T. Skei, C. Palmer, et al, Northwestern University, [Aug. 15, 1944.] Div. 10-201.1-M30

Surveillance of Type ASC Whetlerite in M-10 5/8" Service Canisters, T. Skei, OEMsr-282, Service Project CWS-7, OSRD 4231, Northwestern University, Oct. 3, 1944. Div. 10-201.1-M31

Summary of Investigations by the Engineering Pilot Group, ([*Parts*] *VII, IX, and XI to XVIII. Informal Reports 10.4-23 and -31; 10.5-4, -5, -8, -13, -16, -19, -27, and -31, for the period May 10 to August 10, 1943, and September 10, 1943 to May 10, 1944*), R. J. Kunz, J. C. Cooper, et al, OEMsr-282, Service Project CWS-7, Northwestern University. Div. 10-202.1-M10

Accelerated Aging Studies, ([*Study No.*] *III to IX for December 15, 1943; January 15, February 15, March 15, April 15, June 15, August 15, 1944*), T. Skei, C. Palmer, et al, Northwestern University. Div. 10-202.16-M16

Carbon Monoxide Removal, (*Monthly Reports for the Period from July 15, 1943 to January 15, 1944*), R. N. Pease, J. H. McLean, et al, NDCrc-131, Princeton University. Div. 10-202.2-M5

Carbon Monoxide Removal and Drying Agents (*Monthly Reports for March 15, June 15*(?), *July 15, and August 15, 1944*), R. N. Pease, G. M. Brown, et al, NDCrc-131, Princeton University. Div. 10-202.2-M8

Division 10 Meeting Northwestern Technological Institute, April 20 and April 21, 1943, Part I — Conference on Meteorology and Chemical Warfare, Part II — Protection Problems, Smoke Generators, and Development Problems, W. D. Walters and M. T. O'Shaughnessy, April 1943. Div. 10-300-M1

Division 10 Meeting at National Academy of Sciences June 28 and June 29, 1943, Part I — Conference on Practical Aspects of Division 10 Work in Relation to Chemical Warfare, Part II — Review of the Recent Work of Division 10, (n.a.), June 1943. Div. 10-300-M2

Bibliography on Micrometeorology, 1927 to 1943 (as a supplement to the bibliography in Geiger's *Kima der bodennahen luftschicht*), I. Klotz, J. Colbert, G. J. Doyle, OEMsr-282, Northwestern University, Nov. 15, 1943. Div. 10-300-M3

Progress Report for May, L. F. Audrieth and J. C. Bailar, Jr., letter to Dr. Noyes, University of Illinois, May 14, 1942. Div. 10-402.311-M3

Preliminary Tube Tests with Various Substances, R. G. Dickinson, NDCrc-137, California Institute of Technology, Aug. 5, 1942. Div. 10-402.11-M8

The Preparation and Properties of 1120, ([Parts] IV, V, and VII), A. B. Burg, D. L. Armstrong, et al, [NDCrc-113,] University of Southern California, February 15, March 20, and May 15, 1942. Div. 10-402.32-M4

Calorimetric Studies of Compound 1120, H. B. Huffman, J. B. Hatcher, and E. L. Ellis, Cal. Inst. of Tech., Mar. 15, 1942. Div. 10-402.32-M5

Progress Report re 1120, J. H. Simons, letter to Dr. W. A. Noyes, Jr., Apr. 19, 1942. Div. 10-402.32-M6

A Study of the Preparation of Compound 1120 Through the Use of a Regenerative Chemical, G. L. Clark, May 25, 1942. Div. 10-402.32-M7

New Toxic Agents: Compound 1120, (*Parts I to V, Progress Reports for the period* [*July 15*] *to December 21, 1942*), A. B. Burg, D. L. Armstrong, and R. N. Doescher, NDCrc-113, Service Project CWS-26, University of California. Div. 10-402.32-M8

Proceedings of Conference on Aerosols [*at*] *Evanston, Illinois* [*from*] *February 25 to 27, 1943,* (n.a.), February 1943. Div. 10-500-M2

[*Aerosols,*] (*Monthly Progress Reports for the months of January 1944, and September 1944 to June 1945*), (n.a.), OEMsr-102, Service Project CWS-27, AC-108, and others, University of Illinois. Div. 10-500-M3

OSRD FORMAL REPORTS

OSRD No.

73 *Production of Artificial Fog by Spraying Salt Solutions*, W. G. Brown (W. K. Lewis), Jan. 17, 1941. Div. 10-503.1-M1

77 *Report on Aerosols*, W. H. Rodebush, Mar. 12, 1941. Div. 10-500-M1

80 *Report on the Theory of Coagulation of Smokes in Closed Vessels*, I. Langmuir, Mar. 27, 1941. Div. 10-501.1-M1

84 *A Preliminary Study of Adsorbents, Part I*, H. F. Johnstone and G. L. Clark; *Part II*, E. O. Wiig; *Part III*, F. T. Gucker, Jr.; *Part IV*, W. C. Pierce; *Part V*, T. F. Young; *Part VI*, P. H. Emmett, Apr. 24, 1941. Div. 10-202.151-M1

88 *Rapid Methods of Preparing Phosgene*, J. H. Simons, Apr. 21, 1941. Div. 10-402.36-M1

101 *Filter Material*, W. H. Rodebush, June 12, 1941. Div. 10-201.2-M1

102 *Cyanogen Chloride*, W. M. Latimer, June 16, 1941. Div. 10-202.151-M1

103 *Investigations on the Adsorption of Hydrogen Cyanide and Arsine by Charcoals*, E. O. Wiig, June 22, 1941. Div. 10-202.154-M1

104 *Methods of Studying the Removal of Selenium Hexafluoride*, R. G. Dickinson, June 27, 1941. Div. 10-202.156-M2

109 *Smoke Production*, E. W. Comings, June 27, 1941. Div. 10-504.4-M1

111 *The Removal of Ethylene Imine*, P. A. Leighton, June 27, 1941. Div. 10-402.2-M1

119 *Production, Analysis, and the Use of Aerosols of Uniform Particle Size*, V. K. LaMer, Aug. 6, 1941. Div. 10-501-M1

120 *Aerosol Filter Materials*, W. H. Rodebush, July 24, 1941. Div. 10-201.22-M1

125 *Studies on War Gas Detection and Analysis*, J. H. Yoe, Aug. 24, 1941. Div. 10-402.2-M2

127 *The Development of Laboratory Methods of Detecting and Analyzing Gases Containing Radioactive Sulfur*, D. M. Yost, Aug. 25, 1941. Div. 10-402.35-M3

128 *The Measurement of Radioactive Hydrogen*, E. O. Lawrence, Aug. 26, 1941. Div. 10-402.35-M4

132 *The Deterioration of Thiocyanate Whetlerites*, W. M. Latimer, Sept. 8, 1941. Div. 10-202.16-M2

137 *A Study of the Dispersion of Solids in Gases*, R. Stevenson, Sept. 10, 1941. Div. 10-504.12-M1

153 *Mechanical Formation of Smokes*, G. G. Brown, Oct. 18, 1941. Div. 10-501-M2

155 *Analysis of Inhomogeneous Smoke*, V. K. LaMer, Nov. 5, 1941. Div. 10-501.11-M1

167 *Development of a Smoke Unit*, E. W. Comings, Nov. 5, 1941. Div. 10-504.4-M2

168 *Aerosol Filter Materials*, W. H. Rodebush, Nov. 7, 1941. Div. 10-201.22-M3

170 *An Ultraviolet Photometer for the Detection and Quantitative Estimation of Very Small Concentrations of Noxious Gases in Air*, M. Dole, Nov. 7, 1941. Div. 10-402.21-M1

OSRD No.

172 *Studies on Impregnated Charcoal*, H. F. Johnstone and G. L. Clark, Nov. 8, 1941. Div. 10-202.14-M4

179 *Improved Methods of Preparation and Preliminary Study of Physical and Chemical Properties of Compound 1120*, A. B. Burg, Nov. 15, 1941. Div. 10-402.32-M1

180 *Arsine Removal by Adsorbents*, W. C. Pierce, Nov. 15, 1941. Div. 10-202.154-M8

181 *The Effect of Particle Size on SA and A C Lives and on the Resistance of the Charcoal Bed*, E. O. Wiig, Nov. 17, 1941. Div. 10-202.18-M2

283 *The Use of Gold Chloride and Potassium Permanganate as Arsine Breakpoint Indicators*, E. O. Wiig, Dec. 18, 1941. Div. 10-202.154-M10

292 *Studies of Particle Size in Smokes*, H. Eyring, Dec. 8, 1941. Div. 10-501.11-M2

294 *The Preparation and Properties of 1120 — II*. A. B. Burg, Dec. 30, 1941. Div. 10-402.32-M2

300 *Preliminary Examination of 1120 Removal*, R. G. Dickinson, Dec. 18, 1941. Div. 10-202.156-M4

304 *The Removal of Hexamethylene Diamine*, P. A. Leighton, Jan. 7, 1942. Div. 10-202.156-M6

336 *Sources of Mineral Fiber and Dispersion of Asbestos*, Arthur D. Little, Inc., Nov. 3, 1942. Div. 10-201.22-M2

361 *A Brief Investigation of Removal of Arsine in Air-Arsine Mixtures by Charcoal Using the Radioactive Tracer Method*, D. M. Yost, Jan. 7, 1942. Div. 10-202.154-M12

362 *Secondary Impregnation of Whetlerites with Mercury Compounds for the Production of Moisture-Resistant SA Catalysts*, A. P. Colburn, Jan. 21, 1942. Div. 10-202.141-M5

363 *Cyanogen Chloride, II*, W. M. Latimer, Jan. 21, 1942. Div. 10-202.152-M3

364 *Production of Smokes of Homogeneous Particle Size for Screening Tests and Development of Dyes from Thermally Dispersed Smokes*, V. K. LaMer, Jan. 29, 1942. Div. 10-501.11-M3

375 *Mechanical Formation of Fogs*, W. G. Brown, Feb. 26, 1942. Div. 10-503.1-M2

414 *The Formation of Screening Smokes*, G. G. Brown, Feb. 26, 1942. Div. 10-502-M1

431 *Asbestos Fibers of Small Diameter and Dispersion of Solids*, A. D. Little, Inc., Mar. 2, 1942. Div. 10-201.22-M4

436 *Screening Smokes*, T. K. Sherwood, Mar. 3, 1942. Div. 10-502-M2

437 *The Value of Soda Lime in Gas Adsorbents*, W. C. Pierce, E. O. Wiig, P. A. Leighton, R. G. Dickinson, W. M. Latimer, M. Dole, and W. A. Noyes, Jr., Mar. 6, 1942. Div. 10-202.2-M2

448 *The Effect of Concentration and Temperature on the AC Life of Standard Whetlerite*, E. O. Wiig, Feb. 29, 1942. Div. 10-202.16-M3

449 *Electrical Resistance and Temperature of Charcoals*, M. Dole, Dec. 13, 1941. Div. 10-202.15-M7

OSRD No.

462 *A Study of the Removal of Arsine by Whetlerite*, E. O. Wiig, Mar. 23, 1942. Div. 10-202.154-M15

468 *Production of Smokes of Controlled Size by the Use of Induction Nozzles*, H. C. Hottel, Jan. 21, 1942. Div. 10-501.2-M1

472 *A Search for New Reactants*, F. E. Blacet, Mar. 12, 1942. Div. 10-202.141-M7

487 *Smoke Generator*, I. Langmuir, Mar. 31, 1942. Div. 10-501.201-M1

496 *Studies of the Preparation and Evaluation of Gas Mask Adsorbents, A Summary of the Activities of Section B-6 to March 13, 1942*, W. L. McCabe, R. York, P. H. Emmett, T. F. Young, H. F. Johnstone, J. C. Elgin, W. M. Latimer, W. C. Pierce, M. Dole, Mar. 13, 1942. Div. 10-202.1-M2

518 *Development of a Smoke Unit*, E. W. Comings, Apr. 23, 1942. Div. 10-504.12-M2

533 *Phosphorus Trifluoride Removal by Whetlerite and by Soda Lime — Whetlerite Admixtures*, R. G. Dickinson, Apr. 6, 1942. Div. 10-202.156-M8

537 *Use of Aqueous Solutions for Producing Screening Fogs or Smokes by Pneumatic Spray Nozzles*, A. R. Olson and G. D. Gould, Apr. 29, 1942. Div. 10-502-M4

561 *Hydrogen Cyanide Removal by Gas Mask Absorbent*, E. O. Wiig, Apr. 6, 1942. Div. 10-202.154-M16

571 *Stability of Cyanogen Chloride. Constants for Various Charcoals With Cyanogen Chloride*, Preparation of Cyanogen and Nitrosyl Chloride, W. M. Latimer, Apr. 14, 1942. Div. 10-202.152-M4

586 *Studies on Impregnation*, J. C. Elgin, Apr. 9, 1942. Div. 10-202.14-M7

594 *Effect of Water Upon the Removal of Arsine by Whetlerite*, E. O. Wiig, May 20, 1942. Div. 10-202.154-M21

616 *Comparative Retentivities of Whetlerites and Type D Mixture for SeF_6 and for 1120*, R. G. Dickinson, June 9, 1942. Div. 10-202.156-M12

621 *A Study of the Physical Variables in the Production of Whetlerite and Silvered Whetlerite*, F. E. Blacet, June 9, 1942. Div. 10-202.12-M3

628 *A Study of the Poisoning of Various Absorbents Toward Arsine by Hydrogen Cyanide*, E. O. Wiig, June 6, 1942. Div. 10-202.154-M22

629 *The Use of Mercury Compounds in the Impregnation of Activated Charcoal*, F. E. Blacet, May 25, 1942. Div. 10-202.141-M10

703 *Removal of Chloropicrin and the Nature of its Desorption Product. The Removal of Chloracetophenone as a Smoke at Low Temperature*, G. P. Baxter, July 1, 1942. Div. 10-202.155-M3

704 *Part I. The Distribution of the Catalyst in Whetlerite; Part II. The Location and Identification of Reaction Products in Whetlerite Treated with Arsine*, H. F. Johnstone, June 1, 1942. Div. 10-202.14-M10

710 *Arsine and Hydrogen Cyanide*, E. O. Wiig, July 1, 1942. Div. 10-202.154-M23

720 *I. Correlation of Canister Test Life with Human Tolerance for Cyanogen Chloride. II. The Cyanogen Chloride Protection Afforded by Humidified Adsorbents*, W. C. Pierce, June 29, 1942. Div. 10-201.1-M4

OSRD No.

759 *The Effect of Organic Vapors on Service Lives of Whetlerites and Type D. Mixtures*, R. G. Dickinson, D. N. Yost, E. O. Wiig, W. M. Latimer, P. A. Leighton, July 29, 1942. Div. 10-202.16-M9

776 *Heat of Formation of S_2F_{10}*, Hugh M. Huffman, July 29, 1942. Div. 10-402.36-M3

849 *Rate of Sorption of Water Vapor from Humid Air Streams by Activated Carbons*, A. P. Colburn, Sept. 1, 1942.

851 *Temperature in Canister and Tubes During SA Removal*, M. Dole, I. Klotz, R. K. Brinton, Strodtz, J. B. Fehrenbacher, July 25, 1942. Div. 10-202.1-M5

853 *Impregnation of Activated Charcoals to Obtain High SA Lives*, A. P. Colburn, September 1942. Div. 10-202.141-M13

865 *Filtration of Aerosols and the Development of Filter Materials*, W. H. Rodebush, I. Langmuir, V. K. LaMer, Sept. 4, 1942. Div. 10-201.22-M5

903 *An Investigation of the Mechanism of Removal of Phosgene From Phosgene-Air Mixtures by Charcoal, Using the Radioactive Tracer Method*, D. M. Yost, Sept. 25, 1942. Div. 10-202.155-M5

934 *Calorimetric Studies II, The Entropy and Free Energy of S_2F_{10}*, H. M. Huffman, Oct. 10, 1942. Div. 10-402.36-M4

940 *Screening Smokes*, W. H. Rodebush, V. K. LaMer, I. Langmuir, T. K. Sherwood, Oct. 5, 1942. Div. 10-502-M5

956 *Activation of Gas Charcoal by a New Jiggler Process*, R. York, Jr., July 31, 1942. Div. 10-202.131-M3

962 *Studies and Investigations in Connection With the Dispersion of Solids*, A. D. Little, Inc., Oct. 31, 1942. Div. 10-201.22-M6

970 *A Summary of Tests on Soda Lime*, W. C. Pierce, Oct. 21, 1942. Div. 10-202.2-M3

972 *Adsorption Studies on Chloropicrin and Phosgene*, Dole and Klotz, July 15, 1942. Div. 10-202.155-M4

974 *Interaction of Hydrogen Cyanide with Various Adsorbents*, R. N. Pease, Oct. 21, 1942. Div. 10-202.151-M5

980 *The Mechanical Formation of Screening Smokes Using Salt Solutions*, G. G. Brown, Oct. 29, 1942. Div. 10-502-M6

984 *The Generation of Fluorine*, W. C. Schumb, Nov. 3, 1942. Div. 10-402.31-M1

993 *Studies on the Design of Collective Protectors*, T. B. Drew, Oct. 15, 1942. Div. 9-212.11-M3

998 *The Penetration and Persistence of Carbon Dioxide when Released in an Enclosed Court*, F. E. Blacet, H. F. Johnstone, Oct. 30, 1942. Div. 10-401.122-M1

1002 *Preparation of Wood Charcoal*, W. L. McCabe, Oct. 21, 1942. Div. 10-202.12-M6

1028 *Studies on the Preparation and Evaluation of Gas Mask Adsorbent — A Summary of the Activities of Section B-6 August 7, 1942*, F. E. Blacet, M. Dole, H. F. Johnstone, Kunz, W. M. Latimer, W. C. Pierce, T. F. Young, Aug. 8, 1942. Div. 10-202-M1

1036 *I. Rapid Methods for Synthesizing Certain War Gases. II. The Chemistry of the Sulfur Fluorides*, J. H. Simons, Oct. 21, 1942. Div. 10-402.2-M5

OSRD No.

1048 *Preparation of Superfine Organic Fibers from Cellulose Esters*, Tennessee Eastman Corporation, Oct. 26, 1942. Div. 10-201.22-M7

1053 *Thermodynamic Data on S_2F_{10}*, H. M. Huffman, Oct. 21, 1942. Div. 10-402.36-M5

1055 *Variation of the CG Life of Various Humidified Adsorbents with Decreasing Temperature*, W. C. Pierce, Oct. 26, 1942. Div. 10-202.16-M10

1072 *Retentivity Tests with Hydrogen Fluoride*, R. G. Dickinson, Dec. 8, 1942. Div. 10-202.156-M17

1076 *I, Toxic Smoke Candle and II, Screening Smoke Units*, E. W. Comings, Dec. 1, 1942. Div. 10-504.12-M3

1081 *Studies of Canister Performance at High Humidities and Flow Rates*, W. C. Pierce, Dec. 7, 1942. Div. 10-201.1-M11

1090 *Animal and Chemical Tests on Cyanogen in Effluent Air Stream After Adsorption of HCN*, W. C. Pierce, Dec. 7, 1942. Div. 10-202.152-M8

1106 *Preliminary Tube Tests with COClF*, R. G. Dickinson, Dec. 8, 1942. Div. 10-202.152-M9

1114 *The Production of Fluorine by Electrolysis*, E. I. duPont de Nemours & Co., Dec. 9, 1942. Div. 10-402.31-M3

1125 *Third Report on the Comparison of Impregnated Charcoals*, F. E. Blacet, Dec. 9, 1942. Div. 10-202.14-M18

1126 *Experiments with Type AS Whetlerites at Fostoria, Columbus, and Zanesville, Ohio*, F. E. Blacet, Dec. 9, 1942. Div. 10-202.1-M7

1133 *Studies of the Adsorption Wave for PS on Carbon*, J. E. Elgin, Dec. 9, 1942. Div. 10-202.157-M6

1143 *A Study of the Impregnated Charcoal by X-Ray Diffraction Methods*, H. F. Johnstone and G. L. Clark, Dec. 9, 1942. Div. 10-202.143-M4

1144 *Determination of the Vapor Pressure of HS*, W. C. Pierce, Dec. 9, 1942. Div. 10-402.2-M6

1169 *Summary of the Work on Division 10 Projects During the Period from November 16 to December 15, 1942*, W. C. Pierce, W. H. Rodebush, D. M. Yost, H. F. Johnstone. Div. 10-101-M2

1175 *Analytical Methods for Whetlerites and Whetlerizing Solutions*, F. E. Blacet, Feb. 3, 1943. Div. 10-202.14-M21

1176 *The "Pancake" Effect in Gas Clouds*, W. M. Latimer, Feb. 3, 1943. Div. 10-401.123-M1

1182 *Summary of Results in Section B-6, December 1941 to August 1942*, W. A. Noyes, Jr., Feb. 6, 1943. Div. 10-200-M5

1193 *An Intermittent Flow Canister Test Machine*, W. C. Pierce, Jan. 28, 1943. Div. 10-201.1-M12

1194 *Performance of the M10 Canister Against HS Under Humid Tropical Conditions*, W. C. Pierce, Feb. 3, 1943. Div. 10-201.1-M13

1201 *Composition of Gas Evolved from Drying Whetlerites*, F. E. Blacet, Jan. 4, 1943.

1268 *Summary of a Review on Hydrogen Cyanide, Cyanogen, Cyanogen Chloride Removal by Gas Mask Absorbents*, E. O. Wiig, Mar. 22, 1943. Div. 10-202.154-M31

1280 *The Preparation of Wood Charcoal Suitable for Activation*, W. L. McCabe, Mar. 24, 1943. Div. 10-202.12-M8

OSRD No.

1321 *Practical Consideration Involved in the Use of Screening Smokes*, W. H. Rodebush, Apr. 24, 1943. Div. 10-502-M7

1349 *Changes in Properties of PCI Charcoal and Whetlerite During Activation*, F. E. Blacet, Apr. 24, 1943. Div. 10-202.13-M12

1350 *The Vulnerability of United States, Canadian and British Canisters Toward CC at High Humidities*, W. C. Pierce, Apr. 28, 1943. Div. 10-201.32-M1

1351 *Study of the Partial Vapor Pressures of the Volatile Constituents in Whetlerizing Solutions*, F. E. Blacet, Apr. 20, 1943. Div. 10-202.19-M3

1352 *The Preparation and Surveillance of Hexamethylenetetramine-impregnated Charcoals*, F. E. Blacet, Apr. 28, 1943. Div. 10-202.14-M23

1447 *I. Nitrobenzene as a Compound to Simulate HS. II. Distribution of Nitrobenzene Vapors in a Closed Room*, M. Dole, July 5, 1943. Div. 10-402.2-M9

1453 *The Gas Protection of the M10 Canister*, W. C. Pierce, June 3, 1943. Div. 10-201.1-M14

1454 *ASCM Whetlerite*, E. O. Wiig, June 7, 1943. Div. 10-202.1-M11

1455 *ASM Whetlerite*, E. O. Wiig, May 25, 1943. Div. 10-202.12-M9

1456 *A Comparison of Canadian and American Light-Type Canisters*, W. C. Pierce, June 7, 1943. Div. 10-201.32-M2

1477 *Thermal Data on KB-14 and KB-16*, H. F. Huffman, June 8, 1943. Div. 10-402.36-M7

1521 *Further Development of a Laboratory Type Jiggler for Activating Gas Charcoal, and Tentative Results of Gasification Rate Studies*, R. York, Jr., June 25, 1943. Div. 10-202.131-M4

1526 *Micrometeorological Observations at U. S. Army Smoke Tests in the Los Angeles Area, March 17–18–19, and April 20, 1943*, R. G. Dickinson, June 19, 1943. Div. 10-302.1-M8

1527 *An Investigation of the Possible Explosion Hazard Presented by Silver Whetlerizing Solutions and Residues*, F. E. Blacet, June 26, 1943. Div. 10-202.14-M26

1569 *Persistence Experiments with Sulfur Dioxide in a Wooded Area*, F. E. Blacet, July 13, 1943. Div. 10-302.2-M1

1626 *Additional Study of the Partial Vapor Pressures of the Volatile Constituents in Whetlerizing Solutions*, F. E. Blacet, June 21, 1943. Div. 10-202.14-M27

1667 *Dissipation of Water Fog by Intense Sound of Audible Frequency*, V. K. LaMer and D. Sinclair, Aug. 17, 1943. Div. 10-503.2-M1

1668 *A Portable Optical Instrument for the Measurement for the Particle Size in Smokes, the "Owl", and an Improved Homogeneous Aerosol Generator*, V. K. LaMer, D. Sinclair, Aug. 24, 1943. Div. 10-501.11-M6

1686 *Application of the Electron Microscope to the Study of Charcoal*, H. F. Johnstone and G. L. Clark, Aug. 7, 1943. Div. 10-202.143-M5

1687 *Large Scale Screening Tests, Camp Sibert, Alabama, May 4–7, 1943, Part I* — Rodebush, *Part II*, Johnstone, Roach, Weingartner, Aug. 26, 1943. Div. 10-302.1-M10

1690 *The Generation of Fluorine*, W. C. Schumb, Aug. 17, 1943. Div. 10-402.31-M4

OSRD No.

1691 *CG Aging for Type AS and ASC Whetlerites; Fourth Comparison Chart*, F. E. Blacet, W. C. Pierce, Aug. 17, 1943. Div. 10-202.16-M12

1692 *Use of Sulfur Boiler for Smoke Generation*, W. K. Lewis, Aug. 31, 1943. Div. 10-501.2-M2

1693 *Type ASM Whetlerite Prepared in Rotary Drier*, E. O. Wiig, Aug. 6, 1943. Div. 10-202.12-M10

1697 *A Study of Oil Smoke Plumes by Motion Pictures*, H. F. Johnstone, Aug. 19, 1943. Div. 10-502-M8

1712 *Smoke Experiments Carried out at Camp Sibert, Alabama*, T. S. Gilman, P. Hayward, Aug. 25, 1943. Div. 10-302.1-M11

1746 *Effect of Activation Time on Properties of PCI Charcoal and Corresponding Whetlerites (Second Report)*, F. E. Blacet, W. C. Pierce, T. Skei, Sept. 9, 1943. Div. 10-202.11-M6

1747 *Penetration and Persistence of Gases in an Enclosed Court*, F. E. Blacet, M. Dole, H. F. Johnstone, Sept. 6, 1943. Div. 10-401.122-M3

1748 *The Persistence and Penetration of Gas in a House*, F. E. Blacet, Sept. 13, 1943. Div. 10-401.124-M1

1749 *Concentrations in Gas Clouds Under High Inversion Conditions*, W. M. Latimer, Sept. 6, 1943. Div. 10-302.1-M14

1771 *Use of Aminated Phenol-Formaldehyde Xerogels as Gas Adsorbents*, G. F. Mills, Sept. 4, 1943. Div. 10-202.21-M6

1772 *Development of the SN Screening Smoke Mixture*, E. W. Comings, C. H. Adams, E. D. Shippee, M. Forester, Sept. 20, 1943. Div. 10-501.21-M2

1777 *Adsorption and Surface Area Measurements on Whetlerites and Charcoal Samples*, P. H. Emmett, Sept. 14, 1943. Div. 10-202.15-M18

1778 *Design and Construction of the Whetlerization Pilot Plant at the NDRC Division 10 Central Laboratory*, R. J. Kunz, Sept. 14, 1943. Div. 10-202.14-M29

1780 *Analyses of Base Charcoals*, E. O. Wiig, J. F. Flagg, Sept. 22, 1943. Div. 10-202.11-M7

1856 *The Preparation of Wood Charcoal Suitable for Activation*, W. L. McCabe, L. Byman, F. P. Williams, J. E. Jenkins, Oct. 9, 1943. Div. 10-202.12-M11

1857 *Verification of Mie Theory — Calculations and Measurements of Light Scattering by Dielectric Spherical Particles*, V. K. LaMer, Nov. 11, 1943. Div. 10-501.1-M2

1872 *A Meter for the Calibration of Breather Pumps*, W. C. Pierce, J. W. Zabor, D. P. Smith, Oct. 12, 1943. Div. 10-201.1-M16

1873 *Surveillance of Types ASC and ASCM Whetlerites*, E. O. Wiig, Nov. 12, 1943. Div. 10-202.16-M15

1912 *Preparation and Properties of ASV Whetlerites*, E. O. Wiig, Oct. 24, 1943. Div. 10-202.12-M12

1982 *Apparatus for Evaluating the Maximum Inspiratory and Expiratory Resistances of Gas Masks During Wearing*, W. C. Pierce, J. W. Zabor, D. P. Smith, Nov. 11, 1943. Div. 10-201.1-M20

1983 *A Study of Smoke Clouds in a Coastal Area; Field Experiments Near Brownsville, Texas*, D. M. Yost, C. Croneis, T. S. Gilman, Nov. 12, 1943. Div. 10-302.1-M16

OSRD No.

1984 *Apparatus and Method for Determining Gas Mask Outlet Valve Leakage Under Conditions of Use*, D. P. Smith, J. W. Zabor, Nov. 11, 1943. Div. 10-201.1-M19

2002 *The Evaporation of Small Drops of Thiodiglycol and Levinstein Mustard*, H. F. Johnstone, R. W. Parry, Nov. 12, 1943. Div. 10-501.12-M1

2050 *Filter Penetration by Aerosols of Very Small Particle Size*, W. H. Rodebush, C. E. Holley, Jr., B. A. Lloyd, Jan. 4, 1944. Div. 10-201.22-M13

2086 *Correlation of Gas Concentrations With Meteorological Data*, W. M. Latimer, K. S. Pitzer, S. Ruben, W. D. Gwinn, T. W. Norris, Jan. 3, 1944. Div. 10-302.1-M18

2088 *Present Status of Development of Toxic Gases*, W. A. Noyes, Jr., Dec. 10, 1943. Div. 10-402.2-M14

3011 *New Chlorine Carriers for Metal Chloride Screening Smoke Mixtures*, E. W. Comings, Dec. 31, 1943. Div. 10-502-M9

3012 *The Generation and Use of Concentrated Mustard Vapor Clouds*, H. F. Johnstone, E. W. Comings, Dec. 12, 1943. Div. 10-504.1-M1

3048 *The Hot Wire Analyser for Gas Concentrations*, W. M. Latimer, S. Ruben, T. H. Norris, W. D. Gwinn, Dec. 3, 1943. Div. 10-401.11-M1

3049 *Concentrations From Gas Bombs in the Mt. Shasta Forest Region*, W. M. Latimer, S. Ruben, W. D. Gwinn, T. H. Norris, Jan. 3, 1944. Div. 10-302.2-M3

3058 *Performance of Canisters After Wearing Tests at Camp Sibert, Alabama*, W. C. Pierce, J. W. Zabor, H. S. Joseph, Jan. 8, 1944. Div. 10-201.1-M22

3059 *Gas Concentrations from Line Sources and CW Bombs on a Beach Area*, W. M. Latimer, W. D. Gwinn, Dodson, Houston, Leininger, Winklemen, Jan. 10, 1943. Div. 10-302.2-M4

3071 *Catalysts for the Oxidation of Carbon Monoxide in Air*, R. N. Pease, N. C. Robertson, W. J. Shelburne, Jr., Jan. 12, 1944. Div. 10-202.2-M6

3130 *Picoline as Impregnant for Gas Mask Absorbent*, E. O. Wiig, H. Scoville, Jr., Jan. 21, 1944. Div. 10-202.141-M17

3150 *The Development of the Thermal Generator Candle*, E. W. Comings, Jan. 22, 1944. Div. 10-504.12-M5

3213 *A Continuous Sulfur Smoke Generator*, E. W. Comings, W. L. Lundy, Feb. 11, 1944. Div. 10-501.2-M3

3227 *The Generation of Fluorine*, W. C. Schumb, Feb. 10, 1944. Div. 10-402.31-M5

3284 *The Concentration of Vapor in H Aerosol Clouds*, H. F. Johnstone, W. E. Winsche, Feb. 26, 1944. Div. 10-504-M1

3320 *Studies of the Adsorption Wave on Two Types of Charcoal*, R. H. Wilhelm, S. F. Williams, J. C. Whitwell, Mar. 10, 1944. Div. 10-202.157-M7

3460 *Smokes and Filters — Supplement to Section I*, I. Langmuir, K. B. Blodgett, Apr. 25, 1944. Div. 10-201.22-M14

3461 *Aqueous Hydrolysis of CNCl*, I. M. Klotz, Apr. 25, 1944. Div. 10-202.152-M10

3463 *Development and Testing of a Pump-type Autovent for Nitrogen Elimination in Navy High Altitude Rebreather*, D. S. Martin, J. E. Seegmiller, Apr. 25, 1944. Div. 10-203-M3

OSRD No.

3577 *Tests on CO_2 Spraying Devices*, F. G. Straub, R. J. Kallal, May 20, 1944. Div. 10-501.2-M5

3578 *Field Methods of Dispersing Chemical Warfare Agents*, A. R. Olson, Karl Jan Tong, May 20, 1944. Div. 10-504.2-M5

3714 *A Remote Indicating Cup Anemometer with Magnetic Coupling*, R. G. Dickinson, D. L. Kraus, July 7, 1944. Div. 10-301.1-M2

3774 *Factors in Canisters Design and Tube Testing; Critical Bed Depth and the Nature of Gas Flow Through Charcoal*, I. M. Klotz, June 23, 1944. Div. 10-201.1-M26

3775 *Study of the Use of Air Curtains for Fog Dissipation*, A. P. Kratz, E. C. Manthei, C. E. Holley, June 13, 1944. Div. 10-503.2-M4

3776 *Charcolite: A Calcium Chloride Impregnated Charcoal Drying Agent*, R. N. Pease, June 15, 1944. Div. 10-202.142-M2

3859 *Wind-Tunnel Studies of the Diffusion of Gas in Schematic Urban Districts*, H. Rouse, July 5, 1944. Div. 10-401.121-M2

3902 *The Preparation of Solid Materials for Dispersion as Aerosols*, F. C. McGrew, July 17, 1944. Div. 10-504.3-M2

3975 *Use of Aminated Phenol-Formaldehyde Xerogels as Gas Adsorbents*, G. F. Mills, Aug. 4, 1944. Div. 10-202.21-M8

4011 *Activation of Charcoal in a Boiling-Bed Furnace*, R. York, Jr., Aug. 12, 1944. Div. 10-202.13-M21

4012 *The Preparation of New Toxic Gases*, A. B. Burg, Aug. 12, 1944. Div. 10-402.36-M8

4013 *Compilation of N_0 and λ_c Values for Miscellaneous Whetlerites Before and After Aging*, T. Skei et al, Aug. 12, 1944. Div. 10-202.16-M17

4014 *Performance of M10 and M1XA2 Canisters After Regular Use at Camp Sibert, Ala.*, T. Skei et al, Aug. 12, 1944. Div. 10-201.1-M28

4015 *Additional Surveillance Tests on Canisters Used in the First Sibert Surveillance Study*, T. Skei, Aug. 12, 1944. Div. 10-201.1-M29

4104 *The Reactivation in Oxygen of CWS Charcoals*, T. F. Young, Sept. 7, 1944. Div. 10-202.132-M2

4112 *Whetlerization and Surveillance Studies on PCI Charcoal at Varying Stages of Activation (Third Report)*, T. Skei, Sept. 9, 1944. Div. 10-202.13-M23

4129 *Summary of Pilot Studies on the Preparation of ASC Whetlerite*, R. J. Kunz, Sept. 14, 1944. Div. 10-202.12-M14

4157 *Pilot Plant Study of the Processing of Plasticized White Phosphorus*, H. Adler, Sept. 21, 1944. Div. 10-504.21-M8

4166 *Development of Munitions for Dispersing Solid Particulates*, H. F. Johnstone, Sept. 25, 1944. Div. 10-504.2-M6

4231 *Surveillance of Type ASC Whetlerite in M10-5/8" Service Canisters*, T. Skei, Oct. 3, 1944. Div. 10-201.1-M31

4232 *Surveillance Tests on ASC, E11, and E13 Whetlerites*, T. Skei, Oct. 12, 1944. Div. 10-202.16-M19

4283 *Activation of Charcoal by the Jiggler Process. A Summary of Results Obtained in the Fourth (Metal Tube) Pilot Mode*, R. J. Kunz, Oct. 23, 1944. Div. 10-202.131-M13

OSRD No.

4324 *Zinc Chloride Activated Wood Charcoal*, G. W. Heise, J. A. Slyh, et al, Sept. 30, 1944. Div. 10-202.13-M24

4334 *Wind-Tunnel Studies of the Diffusion of Heat by Single Wind Curtains and Baffles*, H. Rouse, Nov. 11, 1944. Div. 10-401.121-M3

4346 *Surveillance Studies on Whetlerites at Northwestern University — A Summary of Work from 1942–1944*, T. Skei, Nov. 15, 1944. Div. 10-202.16-M20

4377 *Combustion Gas Type Fog Generator for Shipboard Installation 400–500 GPH Capacity Machine No. H-202*, J. W. Hession, V. K. LaMer, Nov. 30, 1944. Div. 10-501.202-M2

4378 *Asbestos Bearing Filter Paper*, T. L. Wheeler, E. Stafford, Nov. 23, 1944. Div. 10-201.22-M15

4399 *Tests with an Exhaust Aerosol DDT Generator on a 450 H. P. Stearman Aircraft*, R. L. LeTourneau, C. W. Kearns, R. J. Kallal, C. H. Adams, R. L. Metcalf, Nov. 20, 1944. Div. 10-602.121-M1

4447 *Toxicity of DDT to Mosquitoes. Effect of Particle Size on the Efficiency of Oil Aerosols Bearing DDT*, V. K. LaMer, S. Hochberg, K. Hodges, Dec. 11, 1944. Div. 10-602.21-M1

4539 *Testing of Daytime Distress Signals*, V. K. LaMer, J. Q. Umberger, D. Sinclair, et al, Jan. 5, 1945. Div. 10-501.23-M3

4565 *The Development of a Portable Aerosol Smoke Pot*, H. H. Champney, L. B. Counterman et al, Jan. 9, 1945. Div. 10-501.21-M3

4700 *Plasticized White Phosphorus in Small Smoke Munitions*, H. F. Johnstone, R. I. Rice, M. F. Nathan, F. A. Orr, C. E. Shoemaker, Feb. 16, 1945. Div. 10-504.21-M9

4733 *The Burning Properties and Anti-Personnel Effect of PWP*, H. F. Johnstone, D. D. Edwards, M. F. Nathan, F. A. Orr, M. M. Woyski, Sept. 15, 1944. Div. 10-504.21-M11

4757 *Statistical Considerations in the Use of DDT Aerosols*, W. H. Rodebush, Jan. 1, 1945. Div. 10-602.21-M2

4796 *Toxicity of Drosophila (Fruit Flies) of Aerosols of DDT of Uniform Droplet Size in Oil of High Boiling Point*, V. K. LaMer, Seymore Hochberg, Bruno H. Zimm, Byron Williamson, Oct. 31, 1944. Div. 10-602.22-M2

4848 *The Temperature of the Liquid Contents of Munitions Exposed to Sunlight*, G. C. Gross, D. L. Armstrong, A. B. Burg, Jan. 2, 1945. Div. 10-504.2-M7

4894 *Conversion of Besler No. 374 Screening-Smoke Generator to a Hochberg-LaMer Aerosol Generator for Insecticidal Purposes — with Supplement on Conversion of Besler M-2 Generator*, V. K. LaMer, S. Hochberg, R. Ellis, F. Buchwalter, J. C. Rowell, Apr. 2, 1945. Div. 10-602.11-M2

4895 *Gel-Type Hopcalite and Some Granular Reagents for Carbon Monoxide*, R. N. Pease, Apr. 5, 1945. Div. 10-202.151-M6

4896 *Results of Canister Tests Against Carbon Monoxide*, R. N. Pease, C. Orenyo, Apr. 5, 1945. Div. 10-201.1-M34

4897 *Further Investigation of Drying Agents*, R. N. Pease, J. H. McLean, Apr. 5, 1945. Div. 10-202.142-M3

4898 *Protection Against Carbon Monoxide*, R. N. Pease, Apr. 5, 1945. Div. 10-202.2-M8

OSRD No.

4901 *The Hochberg-LaMer Aerosol Generator*, V. K. LaMer, S. Hochberg, Oct. 31, 1944. Div. 10-602.11-M3

4904 *The Optical Characterization of Any Aerosol in the Laboratory or Field. The Production of Aerosols from Powdered Solid Materials*, V. K. LaMer, J. Q. Umberger, D. Sinclair, F. E. Buchwalter, Oct. 31, 1944. Div. 10-601.2-M1

4928 *Performance of M10, M10A1, and M1A1 Canisters After Use in the Southwest Pacific Area*, J. B. Fehrenbacher, Betty Roake, Marion Walker, Betty Mortenson, Mar. 3, 1945. Div. 10-201.1-M35

4929 *Gas Protection Afforded by German Canisters*, J. B. Fehrenbacher, Mar. 7, 1945. Div. 10-201.31-M3

4930 *Gas Protection of Australian Coconut Charcoal*, J. B. Fehrenbacher, Mar. 12, 1945. Div. 10-202.01-M2

4959 *Part I: Water Isotherms and Rates of Adsorption and Desorption: Part II: Macro Pore Measurements*, P. H. Emmett et al, Apr. 20, 1945. Div. 10-202.17-M9

5065 *Adsorption and Surface Area Measurements on Whetlerites and Charcoal Samples*, P. H. Emmett et al, May 30, 1945. Div. 10-202.15-M19

5114 *Surveillance of ASC-Ni Whetlerites With CK*, R. J. Grabenstetter, May 9, 1945. Div. 10-202.16-M21

5115 *The Effect of Air Carbonization in the PCC Charcoal Process Upon the Whetlerite Qualities of the Adsorbent*, B. A. White, C. R. Bierman, G. L. Pratt, May 24, 1945. Div. 10-202.14-M30

5116 *Studies of the Preparation of Activated Charcoal Suitable for Whetlerization from Coconut Shells*, B. A. White, C. R. Bierman, G. L. Pratt, May 1, 1945. Div. 10-202.134-M5

5117 *Magnetic Studies on Impregnated Charcoal*, H. G. Cutforth, I. M. Klotz, Apr. 27, 1945. Div. 10-202.14-M32

5139 *A Summary of Work by the University of California Group*, W. M. Latimer, June 20, 1945. Div. 10-302.1-M21

5234 *Effect of Preliminary Particle Size in the Processing of Pittsburgh Coke and Chemical Company Type Charcoal*, B. A. White et al, May 22, 1945. Div. 10-202.18-M4

5235 *Determination of Ammonia in Low Concentration Evolved from Canisters*, W. B. Lewis, May 21, 1945. Div. 10-201.1-M36

5236 *Relentivity of Charcoals A Study with Methyl Ethyl Ether, Neopentane and Methanol*, D. H. Volman, G. J. Doyle, Apr. 23, 1945. Div. 10-202.15-M20

5237 *Leaching and Rewhetlerization of Impregnated Charcoals*, R. J. Grabenstetter, L. C. Weiss, Apr. 26, 1945. Div. 10-202.1-M13

5238 *Gas Protection Afforded by Japanese Canisters*, J. B. Fehrenbacher, May 30, 1945. Div. 10-201.31-M4

5239 *Factors in Canister Design and Tube Testing: II and III. Critical Bed Depths and Mechanisms of Removal of Six Gases*, W. L. McCabe, I. Klotz, W. E. Roake, H. G. Cutforth, B. White, Nov. 28, 1944 to June 7, 1945. Div. 10-202.156-M20

5240 *The Effect of Treating Activated Charcoal with Air or Air-Steam Mixtures at Elevated Temperatures*, C. R. Bierman, G. L. Pratt, B. White, June 14, 1945. Div. 10-202.13-M25

OSRD No.

5241 *Preparation and Properties of Aerosols*, F. T. Wall, June 21, 1945. Div. 10-500-M4

5277 *Miscellaneous Impregnants*, R. J. Grabenstetter, May 31, 1945. Div. 10-202.141-M19

5278 *Gas and Chemical Activation of Charcoal*, R. York, Jr., July 30, 1945. Div. 10-202.13-M26

5309 *The Development of an Aerosol Generator for Dispersing DDT Solutions from the Exhaust of an Aircraft Engine*, H. F. Johnstone, R. J. Kallal, C. H. Adams, June 1, 1945. Div. 10-602.121-M2

5310 *Mosquito Control With Hochberg-LaMer Aerosol Generator in British Guiana*, K. C. Hodges, J. C. Rowell, July 5, 1945. Div. 10-602.21-M3

5343 *The Protection of United States and Enemy Canisters against Nitrogen Dioxide*, W. B. Lewis, J. W. Thomas, May 22, 1945. Div. 10-201.32-M3

5344 *Operational Manual for Dickinson Field Conductivity Meter*, R. K. Brinton, J. W. Otvos, June 25, 1945. Div. 10-402.3-M1

5354 *Summary of Investigations of the Physical Chemistry of the Activation of Charcoal*, T. F. Young, July 21, 1945. Div. 10-202.13-M27

5487 *Exhaust Aerosol Generator for Dispersal of DDT Solutions With SB2C-4 Airplane*, Solar Aircraft Co., Aug. 3, 1945. Div. 10-602.121-M3

5488 *The Development of an Exhaust Smoke Generator for Military Aircraft*, H. F. Johnstone, M. J. Goglia, July 20, 1945. Div. 10-501.203-M2

5489 *Gas Ejection Bombs for the Dispersal of Finely Divided Powders*, C. A. Getz and J. C. Hesson, Aug. 25, 1945. Div. 10-504.2-M8

5499 *A Sensitive Photoelectric Smoke Penetrometer*, F. T. Gucker, Jr., H. B. Pickard, C. T. O'Konski, July 30, 1945. Div. 10-201.22-M16

5500 *Survey of Pore Structure in Charcoal*, A. Juhola, June 20, 1945. Div. 10-202.111-M5

5501 *A Particle-Counting Smoke Penetrometer*, F. T. Gucker, Jr., Aug. 31, 1945.

5510 *Exhaust Aerosol Generator on the PBJ-1H for the Dispersal of DDT and Oil Smoke*, J. H. Clark, Aug. 30, 1945. Div. 10-602.121-M4

5563 *Final Report on Contract OEMsr-282*, F. E. Blacet, Aug. 20, 1945. Div. 10-101-M8

5566 *The Effect of Particle Size and Speed of Motion of DDT Aerosols of Uniform Particle Size in a Wind Tunnel on the Mortality of Mosquitoes*, V. K. LaMer, R. Latta, July 30, 1945. Div. 10-602.21-M4

5710 *Some Theoretical Aspects of the Behavior of DDT Aerosols Dispersed from Aircraft*, H. F. Johnstone, W. E. Winsche, R. L. LeTourneau, L. W. Smith, Sept. 19, 1945. Div. 10-602.121-M5

5729 *Formulas Utilizing DDT Concentrate*, V. K. LaMer, Sept. 18, 1945. Div. 10-601.2-M2

5730 *Reports on the Use in the South Pacific of the Navy Screening Smoke Generator (M374) Converted to an Insecticidal Aerosol Generator According to the Hochberg-LaMer Principle*, F. Brescia, I. Wilson, Sept. 18, 1945. Div. 10-602.11-M4

5731 *Salt Marsh and Anopheline Mosquito Field Control Tests with the Hochberg-LaMer Insecticidal Generator Using*

OSRD No.

Oil-DDT Aerosols, V. K. LaMer, R. Latta, F. Brescia, I. Wilson, K. Hodges, J. Rowell, Sept. 18, 1945. Div. 10-602.21-M5

5936 *Effect of Solvents on the Toxicity of DDT Aerosols*, V. K. LaMer, R. Latta, Aug. 31, 1945. Div. 10-601.1-M3

6004 *Cankerworms as Test Insects*, V. K. LaMer, S. Hochberg, J. Q. Umberger, J. Bethell, Sept. 28, 1945. Div. 10-602.23-M1

6088 *Meteorological Instruments*, S. W. Grinnell, Oct. 15, 1945. Div. 10-301-M3

6121 *Telescoping Metal Tails for a Small Cluster Bomb (Thermal Generator, 10-lb-E29R1)*, E. C. Manthei, J. A. Peck, Sept. 1, 1945. Div. 10-504.2-M9

6122 *Design of a Plant for Manufacture and Loading Plasticized White Phosphorus*, E. A. Ford, Sept. 15, 1945. Div. 10-504.21-M12

6172 *An Alternative Circuit for the Portable Continuous Gas Concentration Meter*, J. W. Otvos, R. G. Dickinson, Dec. 31, 1944. Div. 10-401.111-M5

6173 *A Mercury Contact Wind Direction Vane*, R. G. Dickinson, R. L. Mills, H. S. Johnston, Dec. 31, 1944. Div. 10-301.11-M4

6174 *Portable Instruments for Use in the Study of Micrometeorology and Microclimatology of the Southwest Pacific Area*, R. L. Mills, R. G. Dickinson, Aug. 1, 1945. Div. 10-301-M4

6211 *Development of a Training Oil Smoke Pot, E21*, M. F. Nathan, R. W. Davis, E. W. Comings, Oct. 1, 1945. Div. 10-501.21-M4

6300 *Development of a Small Base Ejection Air-Burst Bomb for Dispersing Liquid Agents*, R. J. Kallal, R. W. Davis, Sept. 30, 1945. Div. 10-504.2-M10

6301 *Development of an Exhaust DDT Aerosol Generator for the ¼ Ton, 4 x 4 Truck (Jeep)*, R. L. LeTourneau, R. I. Rice, H. F. Hrubecky, Oct. 1, 1945. Div. 10-602.122-M3

6341 *I. Wind-Tunnel Studies of Fog-Dispersal Methods, II. Wind-Tunnel Studies of Gas Diffusion in Urban Districts, III. Wind-Tunnel Studies of Air Flow Over Mountainous Terrain*, H. Rouse, Nov. 19, 1945. Div. 10-401.121-M6

OSRD No.

6343 *Development of Exhaust Combustion Smoke Generator for the TBM-3 Airplane*, Solar Aircraft Company, Nov. 23, 1945. Div. 10-501.203-M3

6344 *The Development of an Exhaust DDT Aerosol Generator for the Taylorcraft Light Airplane*, R. I. Rice, Oct. 20, 1945. Div. 10-602.121-M6

6345 *A Study of the Atomization of Liquids*, H. C. Lewis, D. G. Edwards, M. J. Goglio, R. I. Rice, L. W. Smith, Oct. 10, 1945. Div. 10-501.2-M6

6373 *Final Report on Contract OEMsr-102 (Including Contract OEMsr-599)*, H. F. Johnstone, E. W. Comings, Oct. 30, 1945. Div. 10-500-M5

6375 *Development of a Floating Colored Smoke Signal (DS-4)*, D. G. Edwards, C. H. Adams, E. H. Conroy, Oct. 20, 1945. Div. 10-501.23-M4

6428 *Development of Oil Thermal Generator Floating Smoke Pot, E23*, M. F. Nathan, R. W. Davis, E. C. Manthei, E. W. Comings, Nov. 15, 1945. Div. 10-501.21-M5

6431 *Development of an Experimental Thermal Generator Pot for Dispersing Mustard Gas as an Aerosol*, C. H. Adams, M. H. Raila, E. W. Comings, Oct. 15, 1945. Div. 10-504.1-M2

6432 *Development of a Colored Smoke Target Identification Bomb (Bomb, Target Identification, Smoke, Mk 72, Mod. 2)*, C. H. Adams, E. H. Conroy, E. W. Comings, Oct. 20, 1945. Div. 10-504.2-M11

6565 *The Development of a Light High Explosive Bomb for Dispersing Toxic and Insecticidal Aerosols*, H. F. Johnstone, R. L. LeTourneau, H. C. Weingartner, Jan. 28, 1946. Div. 10-504.2-M12

6566 *The Development of Plasticized White Phosphorus (PWP)*, M. M. Woyski, P. G. Roach, H. F. Johnstone, J. C. Bailar, Jr., Jan. 28, 1946. Div. 10-504.21-M13

6574 *Development of a Thermal Generator Bomb for Dispersing Concentrated Mustard Aerosol*, E. D. Shippee, M. H. Raila, E. W. Comings, Feb. 4, 1946. Div. 10-504.3-M3

6636 *Fuel Blocks for Thermal Generators*, R. W. Parry, M. H. Raila, R. C. Johnson, D. Ehrlinger, C. H. Simonson, R. P. Connor, E. W. Comings, J. C. Bailar, Jr., Mar. 11, 1946. Div. 10-504.11-M3

SECTION B-6[a]

I. *Heats of Wetting and Surface Areas; A Study of the Removal of Arsine and of Poisoning by Hydrogen Cyanide; The Preparation of Phosgene from Materials which Could Contain Radio Chlorine; Preliminary Investigations of Variation of Electrical Resistance of Charcoal Due to Adsorption; Progress Report on Project No. 50*, Mar. 25, 1941. Div. 10-101-M1

II. *Summary of English Report*, J. F. Kincaid, (n.d.). Div. 10-102-M2

III. *Report on Activities of Section L-11*, W. A. Noyes, Jr., Apr. 25, 1941. Div. 10-202.156-M1

IV. *The Preparation of Radioactive Chlorpicrin*, J. H. Simons, May 28, 1941. Div. 10-402.35-M1

V. *On the Structure of Charcoal*, T. F. Young, June 18, 1941. Div. 10-202.11-M1

VI. *Report on Trip to England*, W. A. Noyes, Jr., July, 1941. Div. 10-102-M1

VII. *Study of the Preparation of Whetlerite and of Promoted Whetlerites*, J. C. Elgin, July 16, 1941. Div. 10-202.12-M1

VIII. *Preparation of Radioactive Cyanogen Chloride*, J. H. Simons, July 22, 1941. Div. 10-402.35-M2

IX. Memorandum from H. F. Johnstone, Aug. 8, 1941. Div. 10-202.16-M1

X. *Comments on Report by F. N. Matthews' Diffraction of X-rays by Impregnated Charcoal*, H. F. Johnstone, Aug. 12, 1941. Div. 10-202.143-M1

XI. *Outline of the Problem of Canister Design*, W. A. Noyes, Jr., Aug. 15, 1941. Div. 10-201-M1

XII. *Summary of Lister's Report*, J. F. Kincaid, (n.d.). Div. 10-202.15-M21

XIII. *Report on Adsorption of HCN by Various Materials*, R. N. Pease, Aug. 28, 1941. Div. 10-202.154-M4

XIV. *Report on Research Performed in Section B-6, NDRC*, W. A. Noyes, Jr., Sept. 3, 1941. Div. 10-200-M1

XV. *Problem of Gas Removal*, L. S. Kassel, (n.d.). Div. 10-202.15-M22

XVI. *Notes on the Kassel Report*, J. F. Kincaid, Sept. 16, 1941. Div. 10-202.157-M2

XVII. *Agenda for Meeting, Pittsburgh*, (SECRET), W. A. Noyes, Jr., Sept. 19, 1941. Div. 10-201-M2

XVIII. *Report on Impregnation*, A. P. Colburn, E. O. Kraemer, Aug. 25, 1941. Div. 10-202.15-M1

XIX. *Removal of EN*, P. A. Leighton, Aug. 26, 1941. Div. 10-202.156-M3

XX. *Effect of Osmium in Whetlerites*, F. E. Blacet, Aug. 26, 1941. Div. 10-202.154-M2

XXI. *Impregnation of Charcoals with Liquid Ammonia Solutions*, F. E. Blacet, Aug. 26, 1941. Div. 10-202.154-M3

XXII. *Summary of Work*, W. C. Pierce, Aug. 26, 1941. Div. 10-202.15-M2

XXIII. *Summary of Work* (Location of Cu in whetlerite, Nature of Red Coating, Attempts to increase Cu content and arsine life of whetlerites by means of vacuum and pressure, note on ash determination), T. F. Young, Aug. 28, 1941. Div. 10-202.141-M1

XXIV. *Removal of H_2S; Project for Studying the Removal of $CoCl_2$*, D. M. Yost, Aug. 28, 1941. Div. 10-202.15-M3

XXV. *Conclusions from Results of Investigations on the Adsorption of Hydrogen Cyanide and Arsine by Impregnated Charcoals*, E. O. Wiig, Aug. 29, 1941. Div. 10-202.154-M5

XXVI. *The Increase in Weight of Charcoal at the Break-Point. Summary of work on* (a) *electrical resistance of charcoal*, (b) *rise of temperature of charcoal on adsorption of PS*, (c) *ultraviolet absorption apparatus*, M. Dole, Aug. 29, 1941. Div. 10-202.11-M2

XXVII. *Study of Impregnation*, J. C. Elgin, Aug. 30, 1941. Div. 10-202.14-M1

XXVIII. *Study of Adsorption Wave*, J. C. Elgin, Aug. 30, 1941. Div. 10-202.157-M1

XXIX. *The Efficiency of Charcoal toward Chloracetophenone at Low Temperatures, The Removal of Chlorpicrin*, G. P. Baxter, September 1941. Div. 10-202.15-M4

XXX. *Hydrogen Cyanide and Arsine Lives of Equilibrated Charcoals*, E. O. Wiig, Sept. 10, 1941. Div. 10-202.154-M6

XXXI. *Brief Summary of Information Relative to the Mechanisms of Removal of Various War Gases*, W. A. Noyes, Jr., Oct. 6, 1941. Div. 10-202.156-M21

XXXII. *Work on Contract B-71, Selenium Hexafluoride*, R. G. Dickinson, Oct. 15, 1941. Div. 10-202.15-M23

XXXIII. *Use of Radioactive Tracer Technique for Arsine Removal*, D. M. Yost, Sept. 30, 1941. Div. 10-202.154-M7

XXXIV. *Report on Activities of Section B-6*, (SECRET), W. A. Noyes, Jr., Oct. 29, 1941. Div. 10-202.12-M2

XXXV. *Informal Progress Report on Project B-6, 54, Impregnation*, (SECRET), J. C. Elgin, Oct. 22, 1941. Div. 10-202.14-M2

XXXVI. *Conclusions from Investigations on the Adsorption of SA and the Distribution of the Arsenic on the Charcoal Bed*, E. O. Wiig, Oct. 14, 1941. Div. 10-202.15-M5

XXXVII. *Studies on Impregnation*, A. P. Colburn, Oct. 31, 1941. Div. 10-202.14-M3

XXXVIII. *Hydrogen Cyanide and Carbon Monoxide*, R. N. Pease, Oct. 16, 1941. Div. 10-202.15-M6

XXXIX. *The Effect of Particle Size on the SA and AC Lives and on the Resistance of the Charcoal Bed*, E. O. Wiig, Nov. 9, 1941.

XL. *Studies on Arsine Protection*, W. C. Pierce, Oct. 25, 1941.

XLI. *Mesh Size and Arsine Saturation Values*, W. C. Pierce, Nov. 10, 1941. Div. 10-202.18-M1

XLII. *Effect of Intermittent versus Continuous Running on the SA Life of Copper Whetlerite*, J. C. Elgin, Nov. 19, 1941. Div. 10-202.154-M9

XLIII. *Substitutes for Gas Mask Absorbents. The Use of Wyolite as an Inert Carrier for Absorbents*, G. F. Smith, Nov. 27, 1941. Div. 10-202.2-M1

XLIV. *Ultraviolet Photometer for War Gases*, M. Dole, Nov. 19, 1941. Div. 10-402.21-M2

[a] This series was discontinued in August 1942 when Division 10 was organized.

XLV. *A Study of the Penetration of Charcoal by Chloropicrin by Means of the Ultraviolet Photometer*, M. Dole, Dec. 3, 1941.

XLVI. *Investigations on Ad- and Desorption Processes in Granular Stream-Penetrated Beds of Adsorbents*, E. Wicke (translated by M. Dole), (n.d.). Div. 10-202.15-M24

XLVII. *Nature of the Impregnant and New Absorbents*, H. F. Johnstone and G. L. Clark, Dec. 5, 1941. Div. 10-202.141-M2

XLVIII. *The Use of Gold Chloride and Potassium Permanganate as Arsine Breakpoint Indicators*, E. O. Wiig, Dec. 6, 1941.

XLIX. *Removal of HCN by Whetlerite*, R. N. Pease, Dec. 29, 1941. Div. 10-202.154-M11

L. *Nature of Impregnant and New Absorbents*, H. F. Johnstone and G. L. Clark, Dec. 26, 1941. Div. 10-202.01-M1

LI. *The Effect of Particle Size on the SA Lives of Equilibrated Charcoals*, E. O. Wiig, Dec. 17, 1941. Div. 10-202.18-M3

LII. *Adsorption, Surface Area and Pore Size Studies on Activated Charcoals and Whetlerite*, P. H. Emmett, Dec. 22, 1941. Div. 10-202.13-M3

LIII. *Preparation of Radioactive HCN*, J. H. Simons, Dec. 11, 1941. Div. 10-402.35-M5

LIV. *Preparation of Acyl Fluoride*, J. H. Simons, Dec. 16, 1941. Div. 10-402.311-M1

LV. *Study of Impregnation*, J. C. Elgin, Dec. 22, 1941. Div.10-202.14-M19

LVI. *Adsorption Wave Studies*, J. C. Elgin, Dec. 22, 1941. Div. 10-202.157-M3

LVII. *Distribution of Copper in Whetlerites, Mechanism of Whetlerization*, T. F. Young, Dec. 26, 1941. Div. 10-202.14-M5

LVIII. *Activation of Charcoal*, W. L. McCabe, Dec. 23, 1941. Div. 10-202.13-M2

LIX. *Removal of Chloracetophenone at Low Temperatures*, G. P. Baxter, Dec. 29, 1941. Div. 10-202.156-M5

LX. *The Removal of EN*, P. A. Leighton, Dec. 23, 1941. Div. 10-202.156-M22

LXI. *A Search for Promoter Activity in Whetlerites*, F. E. Blacet, Dec. 26, 1941. Div. 10-202.141-M3

LXII. *Impregnations from Liquid Ammonia from the Liquid Phase and with Cupric Acetyl Acetonate*, F. E. Blacet, Dec. 22, 1941. Div. 10-202.13-M1

LXIII. *Substitutes for Gas Mask Canister Soda Lime*, G. F. Smith, Dec. 20, 1941. Div. 10-202.15-M25

LXIV. *A Study of the Penetration of Charcoal by Chlorpicrin by Means of the Ultraviolet Photometer*, M. Dole, Dec. 13, 1941. Div. 10-202.155-M1

LXV. *Summary of Data on Protection toward Various Gases*, W. A. Noyes, Jr., Feb. 4, 1942. Div. 10-202.151-M2

LXVI. *Behavior of Hopcalite, Certain Whetlerites, Some Resins, and Whetlerite-Soda Lime Mixtures toward Cyanogen Chloride*, W. M. Latimer, Jan. 15, 1942. Div. 10-202.152-M2

LXVII. *Activation of Charcoal: Comparison of Jiggler and Pilot Plant Operation*, W. L. McCabe, Jan. 15, 1942. Div. 10-202.131-M1

LXVIII. *Adsorptions and Surface Areas of Certain Charcoals and Whetlerites*, P. H. Emmett, Jan. 18, 1942. Div. 10-202.15-M8

LXIX. *Study of Impregnation: Iodic Acid*, J. C. Elgin, Jan. 15, 1942. Div. 10-202.141-M4

LXX. *The Effect of Impregnation on the Removal of Ethylene Imine. Break times for di-, tri-, and pentamethylene imines*, P. A. Leighton, Jan. 15, 1942. Div. 10-202.14-M33

LXXI. *Phosgene and Mustard Gas Vapor Removal*, D. M. Yost, Jan. 26, 1942. Div. 10-202.155-M2

LXXII. *Summary of Protection Data on Ethylene Imine*, P. A. Leighton, Jan. 23, 1942. Div. 10-202.156-M7

LXXIII. *Steam Activation on Samples from Various Sources*, W. L. McCabe, Jan. 20, 1942. Div. 10-202.13-M4

LXXIV. *Nature of Reaction Product of SA on Whetlerite*, H. F. Johnstone, Feb. 3, 1942. Div. 10-202.1-M1

LXXV. *Heat of Wetting and Apparent Density*, T. F. Young, Feb. 4, 1942. Div. 10-202.15-M9

LXXVI. *Part I. Summary of Present Knowledge Concerning the Value of Soda Lime for a Canister Filling*, W. C. Pierce, Feb. 4, 1942. *Part II. The Effect of Soda Lime on Protection*, W. A. Noyes, Jr., Feb. 19, 1942.

LXXVII. *The Effect of Concentration and Temperature on the AC Life of Standard Whetlerite*, E. O. Wiig, Feb. 19, 1942.

LXXVIII. *Performance Data on Some Recent Samples*, W. A. Noyes, Jr., Feb. 17, 1942. Div. 10-202.14-M6

LXXIX. *Studies of CC and CNBr*, W. L. Latimer, Feb. 15, 1942. Div. 10-202.15-M10

LXXX. *Removal of HCN by Whetlerite; Substitute Absorbents; Pyrolysis of Cotton Cellulose; and Protection Against Carbon Monoxide*, R. N. Pease, Feb. 15, 1942. Div. 10-202.154-M13

LXXXI. *Preparation of Radioactive Selenium Hexafluoride*, J. H. Simons, Feb. 12, 1942. Div. 10-402.35-M6

LXXXII. *Substitutes for Gas Mask Absorbents*, G. F. Smith, Feb. 10, 1942. Div. 10-202.2-M1

LXXXIII. *Variation of SA Life with Temperature and Poisoning of AC toward SA Lives*, E. O. Wiig, Mar. 15, 1942. Div. 10-202.16-M4

LXXXIV. *Removal of HCN by Whetlerite; Pyrolysis of Cotton Cellulose; Protection against Carbon Monoxide*, R. N. Pease, Mar. 15, 1942. Div. 10-202.154-M14

LXXXV. *Adsorption and Surface Area Measurements on Whetlerite and Charcoal Samples*, P. H. Emmett, Mar. 15, 1942. Div. 10-202.15-M11

LXXXVI. *Activation of Charcoal and of Anthracite*, R. York, (W. L. McCabe), Mar. 15, 1942. Div. 10-202.13-M5

LXXXVII. *Sorption Time Data for Water Vapor on Whetlerite*, A. P. Colburn, Mar. 16, 1942. Div. 10-202.17-M5

LXXXVIII. *Studies of Adsorbents*, P. A. Leighton, Mar. 15, 1942. Div. 10-202.151-M3

LXXXIX. *X-Ray Studies: (1) Humidified Charcoals at Low Temperature, (2) Silvered and E6 Whetlerites*, H. F. Johnstone and G. L. Clark, Apr. 2, 1942. Div. 10-202.17-M2

XC. *Résumé of Data on World War Work*, A. Patterson, June 1919. Div. 10-202.141-M6

XCI. *Phosphorus Trifluoride Removal by Whetlerite and by Soda Lime — Whetlerite Mixtures*, R. G. Dickinson, Apr. 6, 1942.

XCII. *Protection against Carbon Monoxide at Low Concentrations; Removal of Hydrogen Cyanide by Whetlerite*, R. N. Pease, Apr. 15, 1942. Div. 10-202.156-M9

XCIII. *The Adsorption of PS and CG*, M. Dole, Apr. 15, 1942. Div. 10-202.156-M11

XCIV. *Adsorption and Surface Area Measurements on Whetlerite and Charcoal Samples*, P. H. Emmett, Apr. 15, 1942. Div. 10-202.15-M11

XCV. *Comparative AC Retentivities of Whetlerite and Type D Mixture*, E. O. Wiig, Apr. 22, 1942. Div. 10-202.15-M13

XCVI. *The Effect of Initial Concentration on the Arsine Life (I); SA Testing (II)*, E. O. Wiig, Apr. 15, 1942. Div. 10-202.154-M17

XCVII. *Substitutes for Gas Mask Absorbents. The Use of Wyolite as an Inert Carrier for Absorbent*, G. F. Smith, Apr. 15, 1942. Div. 10-202.2-M1

XCVIII. *Summary. Protection Against Two Gases*, prepared by W. D. Walters, April, 1942. Div. 10-202.151-M7

XCIX. *The Behavior of Mixtures of Charcoal and Inert Material*, W. C. Pierce, Apr. 10, 1942. Div. 10-201.2-M2

C. *The Nature of the Product Desorbed from Charcoal Brought Half Way to the Breakpoint with Chlorpicrin*, G. P. Baxter, Apr. 14, 1942. Div. 10-202.15-M12

CI. *The Rate of Water Absorption of Charcoals and Whetlerites*, A. P. Colburn, Apr. 23, 1942. Div. 10-202.17-M3

CII. *Stability of Cyanogen Chloride; Constants for Various Charcoals with Cyanogen Chloride; Preparation of Cyanogen and Nitrosyl Chloride*, W. M. Latimer, Apr. 14, 1942.

CIII. *Studies on the Reaction Product of Arsine on Charcoal and Whetlerite*, H. F. Johnstone and G. L. Clark, Apr. 10, 1942. Div. 10-202.154-M18

CIV. *Flow Rate Studies on the E20R48 Miniature Canister*, W. C. Pierce, Apr. 22, 1942. Div. 10-201.1-M1

CV. *Absorbent Performance Data for Use in Canister Designing*, W. C. Pierce, Apr. 23, 1942. Div. 10-201.1-M2

CVI. *EN: Polymerization, Thermal Effects, Effect of Oxygen, Effect of Drying, Miscellaneous Gases, Especially Amines*, P. A. Leighton, Apr. 15, 1942. Div. 10-202.156-M10

CVII. *Variation of SA Life with Relative Humidity for Equilibrated Charcoals*, E. O. Wiig, May 15, 1942. Div. 10-202.17-M4

CVIII. *Italian Canister (large size) D.z.g.c. 3-1934*, E. O. Wiig, May 15, 1942. Div. 10-201.31-M1

CIX. *Summary of Test Data on E-6 Whetlerite*, W. C. Pierce, May 9, 1942. Div. 10-202.16-M5

CX. *Central Laboratory Report of May 16, 1942*, W. C. Pierce et al. Div. 10-200-M2

CXI. *The Adsorption of CG*, M. Dole, May 15, 1942. Div. 10-202.157-M4

CXII. *Efficiency of Whetlerite Containing Considerable Proportions of Water Against Chlorpicrin*, G. P. Baxter, May 15, 1942. Div. 10-202.16-M6

CXIII. *I. X-Ray Studies of Various Materials, II. Carbonization of Resins, III. Electron Microscope Studies, IV. Location of Silver on Silvered Whetlerites and Charcoals, V. The Irreversible Adsorption of As_2O_3 from Alcohol by Whetlerite*, H. F. Johnstone and G. L. Clark, May 11, 1942. Div. 10-202.143-M2

CXIV. *Protection against Carbon Monoxide*, R. N. Pease, May 15, 1942.

CXV. *Mechanism of Removal of HCN by Whetlerite*, R. N. Pease, May 15, 1942. Div. 10-202.154-M20

CXVI. *Calorimetric Studies on Arsine Removal*, H. M. Huffman, May 14, 1942. Div. 10-202.154-M19

CXVII. *Problems Relating to CC*, W. M. Latimer, May 15, 1942. Div. 10-202.141-M8

CXVIII. *The Design of a Pilot Plant Jiggler for Charcoal Activation*, R. York, May 15, 1942. Div. 10-202.131-M2

CXIX. *A Comparison of Impregnated Charcoals*, F. E. Blacet and T. Skei, May 5, 1942. Div. 10-202.14-M8

CXX. *The Adsorption of Silver on Charcoal from Whetlerizing Solutions*, F. E. Blacet and D. Volman, May 18, 1942. Div. 10-202.14-M9

CXXI. *The Use of Mercury Compounds in the Impregnation of Activated Charcoal*, F. E. Blacet and R. J. Grabenstetter.

CXXII. *Preliminary Study of Hexamine Impregnation*, F. E. Blacet and J. G. Roof, May 22, 1942. Div. 10-202.141-M9

CXXIII. *Adsorption and Surface Area Measurements on Whetlerite and Charcoal Samples*, P. H. Emmett, May 15, 1942. Div. 10-202.15-M11

CXXIV. *Flow Resistance of Axial and Radial Canisters*, W. C. Pierce, May 15, 1942. Div. 10-201.1-M3

CXXV. *Substitutes for Gas Mask Absorbents. The Use of Wyolite as an Inert Carrier for Absorbents*, G. F. Smith, May 15, 1942. Div. 10-202.2-M1

CXXVI. *The Effect of Preliminary Passage of Air-Hexane Mixtures on the SA and AC Life of CWSE-1 TE-1 and Type D Mixture*, E. O. Wiig, May 28, 1942. Div. 10-202.156-M13

CXXVII. *Study of the Adsorption Wave*, J. C. Elgin, May 15, 1942. Div. 10-202.157-M5

CXXVIII. *I. The Effect of Various Vapors on the SA Life of Absorbents; II. A Continuation of the Study of the Effect of AC on the SA Life and the Effect of SA on the AC Life of Absorbents; III. Variation of SA Life with Relative Humidity for Dry and Equilibrated Whetlerites*, E. O. Wiig, June 15, 1942. Div. 10-202.16-M7

CXXIX. *Design of a Lightweight Canister*, W. C. Pierce, July 18, 1942. Div. 10-201-M3

CXXX. *I. Correlation of Canister Test Life with Human Tolerance for Cyanogen Chloride; II. The Cyanogen Chloride Protection Afforded by Humidified Adsorbents*, W. C. Pierce, May 29, 1942.

CXXXI. *I. Carbonization of Resins and Other Plastics; II. Nature of Reaction Product from Arsine on Whetlerite; III. X-Ray Studies*, H. F. Johnstone and G. L. Clark, June 11, 1942. Div. 10-202.1-M3

CXXXII. *Calorimetric Studies on Arsine Removal*, H. M. Huffman, June 15, 1942. Div. 10-202.154-M19

CXXXIII. *Rate of Humidification of Charcoals and Whetlerites*, A. P. Colburn, June 17, 1942. Div. 10-202.17-M5

CXXXIV. *Adsorption and Surface Area Measurements on Whetlerite and Charcoal Samples*, P. H. Emmett, June 15, 1942. Div. 10-202.15-M11

CXXXV. *Production of Primary Charcoal by the Carlisle Process*, W. L. McCabe, June 16, 1942. Div. 10-202.12-M4

CXXXVI. *A Laboratory Study of Activation*, R. York, Jr., June 15, 1942. Div. 10-202.13-M6

CXXXVII. *Behavior of Sulfur Dioxide and of Several Other Gases on Whetlerite*, P. A. Leighton, June 15, 1942. Div. 10-202.156-M14

CXXXVIII. *Part I. Summary to Date on Resins; Part II. Aminated Phenol-Formaldehyde Xerogels as Absorbents*, P. A. Leighton, June 15, 1942. Div. 10-202.21-M1

CXXXIX. *Substitutes for Gas Mask Absorbents. The Use of Wyolite as an Inert Carrier for Absorbents*, G. F. Smith, June 15, 1942. Div. 10-202.2-M1

CXL. *Vapor Pressure of Arsine Dissolved in Thionyl Chloride, etc.*, L. F. Audrieth and J. C. Bailar, Jr., June 17, 1942. Div. 10-401.1-M1

CXLI. *The Dialkylmonofluophosphates*, L. F. Audrieth and J. C. Bailar, Jr., June 16, 1942. Div. 10-402.311-M4

CXLII. *Protection against Carbon Monoxide*, R. N. Pease, June 15, 1942. Div. 10-202.2-M3

CXLIII. *Optimum Concentrations of Copper, Ammonia, and Carbon Dioxide for Whetlerizing Solutions*, F. E. Blacet and D. Volman, June 22, 1942. Div. 10-202.14-M11

CXLIV. *Preliminary Study of Whetlerites from: I. Different Size Extruded Charcoals; II. Charcoals Activated at Different Temperatures*, F. E. Blacet and D. Volman, June 23, 1942. Div. 10-202.1-M4

CXLV. *Diffusion of the Limiting Factor for Critical Bed Length*, M. Dole, June 25, 1942. Div. 10-202.19-M1

CXLVI. *Final Report on Arsine and Hydrogen Cyanide*, E. O. Wiig, July 1, 1942.

CXLVII. *Second Report on the Comparison of Impregnated Charcoals*, F. E. Blacet, T. Skei, June 29, 1942. Div. 10-202.14-M12

CXLVIII. *Tube Tests with Hydrogen Fluoride*, R. G. Dickinson, June 29, 1942. Div. 10-402.2-M3

CXLIX. *Adsorption of Cyanogen by Charcoal. Amine-Impregnated Charcoals*, W. M. Latimer, June 15, 1942. Div. 10-202.152-M5

CL. *Cyanogen in Effluent Air Stream after the Absorption of HCN by Whetlerites*, E. O. Wiig, July 15, 1942. Div. 10-202.154-M24

CLI. *Comparison of the Effect of Water, AC, and Other Poisons on the SA Lives of Silvered and Unsilvered Whetlerites*, E. O. Wiig, July 15, 1942. Div. 10-202.16-M8

CLII. *The Use of Non-Persistent Gases*, W. A. Noyes, Jr., July 17, 1942. Div. 10-402.1-M1

CLIII. *I. Study of Foreign Canister Materials. II. X-Ray Results from Various Materials. III. Preparation of Charcoals from Resins and Other Materials. IV. Adsorption of AsO_3 from Alcohol by Charcoal and Whetlerites*, H. F. Johnstone and G. L. Clark, July 15, 1942. Div. 10-200-M3

CLIV. *Studies of CC on Absorbents; Stability of Cyanogen; Cyanogen in the Effluent from AC Tube Tests*, W. M. Latimer, July 14, 1942. Div. 10-202.152-M6

CLV. *Leakage of Facepieces*, D. M. Yost, July 31, 1942. Div. 10-201.1-M5

CLVI. *Adsorption and Surface Area Measurements on Whetlerites and Charcoal Samples*, P. H. Emmett, July 15, 1942. Div. 10-202.15-M11

CLVII. *Fluophosphates and Related Compounds*, L. F. Audrieth and J. C. Bailar, Jr., July 15, 1942. Div. 10-402.311-M5

CLVIII. *Fluorosulfonic Acid and Its Alkyl Esters*, L. F. Audrieth and J. C. Bailar, Jr., July 15, 1942. Div. 10-402.311-M6

CLIX. *Studies Relating to Phosphorus Trifluoride*, A. B. Burg, July 15, 1942. Div. 10-402.311-M7

CLX. *Oxygen Treatment of Charcoal. Heats of Combustion of Charcoals*, T. F. Young, June 15 to July 15, 1942. Div. 10-202.13-M7

CLXI. *The Preparation and Preliminary Study of $(CH_3)_2NPF_2$*, A. B. Burg, July 24, 1942. Div. 10-402.36-M2

CLXII. *Temperatures in Canisters and Tubes during SA Removal*, M. Dole, July 25, 1942. Div. 10-201.1-M6

CLXIII. *Iodine, Halogen Acids and their Salts as Charcoal Impregnants*, F. E. Blacet, July 27, 1942. Div. 10-202.141-M11

CLXIV. *Activation of Charcoal*, R. York, Jr., July 15, 1942. Div. 10-202.13-M8

CLXV. *The Preparation of Crude Char*, W. L. McCabe, July 16, 1942. Div. 10-202.12-M5

CLXVI. *The Protection of M1 and MIXA1 Canisters against Sulfur Dioxide*, W. C. Pierce, July 29, 1942. Div. 10-201.1-M8

CLXVII. *Retention of HCl by the MIXA1 Canister*, W. C. Pierce, July 29, 1942. Div. 10-201.1-M7

CLXVIII. *I. The Effects of Cuprous Copper and Nitrate Ions in Whetlerizing Solutions; II. The Minimum Silver Requirement for Different Activated Charcoals*, F. E. Blacet, July 15, 1942. Div. 10-202.14-M13

CLXIX. *Study of the Adsorption Wave*, J. C. Elgin, July 16, 1942. Div. 10-202.157-M5

CLXX. *Relative Protection of Dewey and Almy Super Soda Limes and High Copper Whetlerite in the M10 Canister*, R. K. Brinton and W. C. Pierce, Aug. 5, 1942. Div. 10-201.1-M9

CLXXI. *Foreign Canisters and Canister Fillings*, F. T. Gucker, Jr., Aug. 1, 1942. Div. 10-201.31-M2

CLXXII. *Adsorption Studies on Chloropicrin and Phosgene*, M. Dole, July 15, 1942.

CLXXIII. *Further Experiments with Cyanogen. Stability of CC*, W. M. Latimer, Aug. 14, 1942. Div. 10-402.34-M1

CLXXIV. *A Preliminary Study of the Performance of Double Layer Absorbents*, W. C. Pierce, J. W. Zabor, and T. Skei, Aug. 17, 1942. Div. 10-202.151-M4

CLXXV. *A Study of HCN and $(CN)_2$ Concentrations in the Effluent from Various Absorbents Exposed to HCN under Several Conditions. Lowering the Vapor Pressure of Arsine*, E. O. Wiig, Aug. 15, 1942. Div. 10-202.154-M25

CLXXVI. *One-Step Impregnation with Whetlerizing Solutions Containing Copper, Silver, and either Molybdenum, Vanadium, or Tungsten*, F. E. Blacet and R. J. Grabenstetter, Aug. 5, 1942. Div. 10-202.141-M12

CLXXVII. *I. The Solubility of Silver Thiocyanate in Whetlerizing Solution. II. The Adsorption of Silver Ions and Thiocyanate Ions by Charcoal from Solutions*, F. E. Blacet and D. Volman, Aug. 3, 1942. Div. 10-202.14-M14

CLXXVIII. *I. X-Ray Studies of Basic Copper Carbonate in Whetlerites. II. X-Ray Studies of some Hopcalites. III. X-Ray Studies on Hexamethylene Tetramine and NaOH-treated Charcoals and Whetlerites. IV. Preparation of Charcoals from Resins*, H. F. Johnstone and G. L. Clark, Aug. 15, 1942. Div. 10-202.143-M3

CLXXIX. *Adsorption and Surface Area Measurements on Whetlerite and Charcoal Samples*, P. H. Emmett, Aug. 15, 1942. Div. 10-202.15-M11

CLXXX. *Vapor Pressures of Diethyl Fluophosphate, Ethyl Difluophosphate, Dimethyl Fluophosphate, Ethyl Fluo-*

sulfonate, and Trimeric Phosphonitrilic Chloride, L. F. Audrieth and J. C. Bailar, Jr., Aug. 15, 1942. Div. 10-402.311-M9

CLXXXI. *I. Alkyl Fluosulfonates; II. Phosphonitrilic Fluoride*, L. F. Audrieth and J. C. Bailar, Jr., Aug. 15, 1942. Div. 10-402.311-M10

CLXXXII. *Tube and Canister Test Methods Used at the B6 Central Laboratory*, W. C. Pierce, Aug. 30, 1942. Div. 10-201.1-M10

CLXXXIII. *The Carbonization of Pres-to-logs*, W. L. McCabe Aug. 13, 1942. Div. 10-202.134-M1

CLXXXIV. *The Absorption of HCN by Whetlerite and Other Absorbents*, E. O. Wiig, Sept. 15, 1942. Div. 10-202.154-M26

CLXXXV. *Interaction of Hydrogen Cyanide with Various Adsorbents*, R. N. Pease, Aug. 28, 1942.

CLXXXVI. *Sampling Methods for Field Experiments*, W. M. Latimer, Sept. 15, 1942. Div. 10-402.2-M4

CLXXXVII. *Protection against Cyanogen*, W. M. Latimer, Sept. 15, 1942. Div. 10-202.154-M27

CLXXXVIII. *The Alkyl Difluophosphates and the Mono- and Difluothiophosphates*, L. F. Audrieth and J. C. Bailar, Jr., Sept. 15, 1942. Div. 10-402.311-M12

CLXXXIX. *Phosphonitrilic Fluoride; Diethyl Sulfamyl Fluoride*, L. F. Audrieth and J. C. Bailar, Jr., Sept. 14, 1942. Div. 10-402.311-M11

CXC. *Calorimetric Studies on the Removal of Arsine*, H. M. Huffman, Sept. 15, 1942. Div. 10-202.154-M19

CXCI. *Respirators for Civilian Use*, W. C. Pierce, Sept. 9, 1942. Div. 10-200-M4

CXCII. *Drying Agents for Use with Hopcalite*, R. N. Pease, Sept. 15, 1942. Div. 10-202.142-M1

CXCIII. *The Penetration and Persistence of Carbon Dioxide when Released in an Enclosed Court*, F. E. Blacet and H. F. Johnstone, Aug. 28, 1942.

CXCIV. *Prevention of Wall Leakage in Axial Canisters*, W. C. Pierce, Oct. 14, 1942. Div. 10-201-M4

CXCV. *The Generation of Fluorine*, W. C. Schumb, Oct. 17, 1942.

CXCVI. *One-Step Impregnation with Whetlerizing Solutions Containing Copper, Silver, and Chromium*, F. E. Blacet, Oct. 15, 1942. Div. 10-202.141-M14

CXCVII. *Summary of Results in Section B-6, December 1940 to August 1942*, W. A. Noyes, Jr., Aug. 31, 1942.

CXCVIII. *Calorimetric Studies on the Removal of SA*, H. M. Huffman, Oct. 15, 1942. Div. 10-202.156-M15

CXCIX. *Adsorption and Surface Area Measurements on Whetlerite and Charcoal Samples*, P. H. Emmett, Oct. 16, 1942. Div. 10-202.15-M11

CC. *Variation of the CG Life of Various Humidified Adsorbents with Decreasing Temperature*, W. C. Pierce, Nov. 4, 1942.

CCI. *An Ultraviolet Photometer for Routine Analysis*, M. Dole, Nov. 5, 1942. Div. 10-402.21-M3

CCII. *I. Study of Commercial Whetlerite; II. Work on Charcoal*, H. F. Johnstone and G. L. Clark, Oct. 15, 1942. Div. 10-202.1-M6

CCIII. *I. The Adsorption of HCN, C_2N_2, and SA by Whetlerite and Other Adsorbents; II. The Effect of Temperature on the HCN Life of Whetlerite; III. Desorption and Recovery of Adsorbents after Adsorption of HCN on C_2N_2*, E. O. Wiig, Oct. 15, 1942. Div. 10-202.154-M28

CCIV. *The Effects of Reactivation on the Properties of Certain Activated Charcoals*, T. F. Young, Oct. 21, 1942. Div. 10-202.132-M1

CCV. *Studies on Canister Performance at High Humidities and Flow Rates*, W. C. Pierce, Nov. 16, 1942.

CCVI. *Preliminary Tube Tests with COCl$_2$*, R. G. Dickinson, Oct. 21, 1942. Div. 10-202.156-M16

CCVII. *Retentivity Tests with Hydrogen Fluoride*, R. G. Dickinson, Oct. 10, 1942. Div. 10-202.15-M14

CCVIII. *Properties of Cyanogen: Toxicity, Adsorption by Charcoal, Detection and Estimation*, D. M. Yost, Sept. 15, 1942. Div. 10-202.152-M7

CCIX. *Animal and Chemical Tests on Cyanogen in Effluent Air Stream after Adsorption of HCN*, W. C. Pierce, Nov. 1, 1942.

CCX. *A Study of Thiocyanate-Treated Whetlerites*, F. E. Blacet, Sept. 17, 1942. Div. 10-202.14-M15

CCXI. *Further Studies on the Characteristics and Impregnation of Aminated Phenol-Formaldehyde Xerogels*, P. A. Leighton, Nov. 15, 1942. Div. 10-202.21-M2

CCXII. *Wind Velocities and Gustiness*, D. M. Yost, Nov. 15, 1942. Div. 10-302.1-M1

CCXIII. *The Preparation from Wood of Charcoal Suitable for Activation*, W. L. McCabe, Nov. 15, 1942.

CCXIV. *Experiments with CC and C_2N_2*, W. M. Latimer, Nov. 15, 1942. Div. 10-402.34-M2

CCXV. *The Fixed Oxygen Content of Charcoal*, R. N. Pease, Nov. 20, 1942. Div. 10-202.11-M4

CCXVI. *Adsorption and Surface Area Measurements on Whetlerite and Charcoal Samples*, P. H. Emmett, Nov. 16, 1942. Div. 10-202.15-M11

CCXVII. *The "Pan-Cake" Effect in Gas Clouds*, W. M. Latimer, Dec. 15, 1942.

CCXVIII. *The Removal of HCN and C_2N_2 by Absorbents*, E. O. Wiig, Nov. 23, 1942. Div. 10-202.154-M29

CCXIX. *Analytical Methods for Whetlerites and Whetlerizing Solutions*, F. E. Blacet, Dec. 8, 1942. Div. 10-202.14-M28

CCXX. *Third Report on the Comparison of Impregnated Charcoals*, F. E. Blacet, Dec. 10, 1942.

CCXXI. *Effect of Moisture on SA, AC, and CC Tube Lives for Two Type ASC Whetlerites*, F. E. Blacet, Dec. 10, 1942.

CCXXII. *Second Report on the Use of Copper, Silver, and Chromium Solutions as Charcoal Impregnants*, F. E. Blacet, Dec. 21, 1942. Div. 10-202.141-M16

CCXXIII. *Adsorption of Constituents from a Standard Whetlerizing Solution*, F. E. Blacet, Nov. 5, 1942. Div. 10-202.12-M7

CCXXIV. *Miscellaneous Experiments with National Charcoals; The Minimum Silver Requirements of CWSN-Cl Charcoal*, F. E. Blacet, Nov. 10, 1942. Div. 10-202.14-M17

CCXXV. *One-Step Impregnation with Copper, Silver, and Either Molybdenum, Vanadium, or Zinc*, F. E. Blacet, Nov. 10, 1942. Div. 10-202.141-M15

CCXXVI. *A Study of the Physical Variables in the Production of Type A and Type AS Whetlerites from CWSN-44, CWSNC-1, and CWSPCI-1 Charcoals*, F. E. Blacet, Nov. 5, 1942. Div. 10-202.11-M3

CCXXVII. *A Study of Impregnated Charcoal by X-Ray Diffraction Methods*, H. F. Johnstone and G. L. Clark, Aug. 31, 1942. (Also published as a formal report identified as Division B Serial No. 468, OSRD No. 1143.) Div. 10-202.143-M4

DIVISION 10 NDRC INFORMAL REPORTS

Report[a] *No.*	*Date*	*Investigator*	*Title*
10.1-1	12/15/42	P. H. Emmett	Adsorption and Surface Area Measurements on Whetlerite and Charcoal Samples Div. 10-202.15-M11
10.1-2	12/21/42	E. O. Wiig	I. Variation of HCN Life with Layer Depth for Type ASC Whetlerite; II. The Effect of Particle Size on the C_2N_2 Life Div. 10-202.154-M30
10.1-3*	1/28/43	W. C. Pierce	An Intermittant Flow Canister Test Machine Div. 10-201.1-M12
10.1-4*	1/4/43	F. E. Blacet	Composition of Gas Evolved from Drying Whetlerites
10.1-5	1/16/43	F. E. Blacet	Determination of Ammonia Concentrations in Field Tests Div. 10-402.2-M7
10.1-6	2/24/43	F. T. Gucker, Jr.	A Colorimetric Method of Determining the Mass Concentration of Triphenyl Phosphate Smokes Div. 10-201.22-M11
10.1-7*	3/19/43	F. E. Blacet	A Study of the Partial Vapor Pressures of the Volatile Constituents in Whetlerizing Solutions Div. 10-202.14-M22
10.1-8*	3/12/43	F. E. Blacet	Changes in Properties of PCI Charcoal and Whetlerite During Activation Div. 10-202.13-M10
10.1-9	4/3/43	W. C. Pierce	An Accelerated Flow Method for Humidifying Small Samples of Adsorbents for Plant Control Tests Div. 10-202.17-M7
10.1-10	4/5/43	F. E. Blacet	Surveillance of Whetlerites Div. 10-202.16-M11
10.1-11	4/12/43	W. C. Pierce	Mesh Size Studies, I Div. 10-201.21-M1
10.1-12	4/30/43	D. M. Yost	Some Mathematical Theories for Charcoal Tube Testing Div. 10-202.1-M9
10.1-13	5/14/43	F. E. Blacet	Methods of Analysis for the Freons in Air Div. 10-401.1-M2
10.1-14	5/15/43	F. T. Gucker, Jr.	A Study of Acrosols Produced by the Olson Bomb Div. 10-504.2-M1
10.1-15	6/3/43	F. E. Blacet	G. L. Cabot Carbon Black Charcoals Div. 10-202.1-M12
10.1-16*	6/9/43	F. E. Blacet	Additional Study of the Partial Vapor Pressures of the Volatile Constituents in Whetlerizing Solutions Div. 10-202.14-M27
10.1-17	6/11/43	F. E. Blacet	Reactions Involving Chromium which Occur when ASC Whetlerizing Solution Is in Contact with Charcoal Div. 10-202.14-M25
10.1-18	6/15/43	F. E. Blacet	The Non-Uniform Activation of Charcoals Div. 10-202.13-M14
10.1-19	6/10/43	F. E. Blacet and W. C. Pierce	I. Protection afforded by ASC Whetlerites of Varying Copper Content; II. Surveillance of ASC Whetlerites of Varying Copper Content Div. 10-202.14-M24
10.1-20	6/25/43	F. E. Blacet	Action of Nitrogen Dioxide on Activated Charcoals, Whetlerites, and other Substances Div. 10-202.156-M18
10.1-21[b]	8/2/43	F. E. Blacet	Analytical Methods for Whetlerites and Whetlerizing Solutions Div. 10-202.14-M28
10.1-22	7/27/43	F. E. Blacet	Changes in Properties of Barnebey-Cheney Company Pecan Charcoal and Whetlerite During Activation Div. 10-202.11-M5
10.1-23*	8/10/43	F. E. Blacet and W. C. Pierce	Effect of Activation Time on Properties of PCI Charcoal and Corresponding ASC Whetlerites (Second Report) Div. 10-202.11-M6
10.1-24	8/12/43	W. C. Pierce	Preparation and Properties of a New Modification of the Starch-Pyridine-Iodine CC Indicator for Canister Testing Div. 10-201.1-M15
10.1-25	8/10/43	F. E. Blacet	The Surveillance of Base Charcoals Div. 10-202.16-M13
10.1-26*	6/11/43	E. O. Wiig	Analyses of Base Charcoals Div. 10-202.11-M7
10.1-27	9/7/43	F. T. Gucker, Jr.	Polarization Relationships in Homogeneous and Inhomogeneous Smokes; "Owl" Settings for DOP Smokes Div. 10-501.11-M7
10.1-28*	9/2/43	E. O. Wiig	Preparation and Properties of ASV Whetlerite Div. 10-202.12-M12
10.1-29	9/22/43	F. E. Blacet	Preliminary Report on the Aging of ASC Whetlerite under Various Atmospheres in Sealed Systems
10.1-30	9/15/43	D. M. Yost	Nitrogen Elimination in the Navy High Altitude Rebreather Div. 10-203-M2

[a] Asterisk indicates that the NDRC informal report has also been published as an OSRD (Div. 10, NDRC) formal report.
[b] This report supersedes B-6 Report CCXIX as revised May 10, 1943.

Report No.	*Date*	*Investigator*	*Title*
10.1-31	9/15/43	W. C. Schumb	The Generation of Fluorine Div. 10-402.31-M2
10.1-32	10/14/43	W. C. Pierce	Canister Surveillance Studies, I Div. 10-201.1-M17, M18
10.1-33	10/15/43	D. M. Yost	Nitrogen Elimination in the Navy High Altitude Rebreather Div. 10-203-M2
10.1-34	10/15/43	W. C. Schumb	The Generation of Fluorine Div. 10-402.31-M2
10.1-35	11/15/43	D. M. Yost	Nitrogen Elimination in the Navy High Altitude Rebreather Div. 10-203-M2
10.1-36	11/12/43	F. E. Blacet	Second Report on the Aging of ASC and ASCP Whetlerite Containing Various Amounts of Water in Sealed Systems Div. 10.202.17-M8
10.1-37	11/15/43	W. C. Schumb	The Generation of Fluorine Div. 10-402.31-M2
10.1-38*	12/21/43	E. O. Wiig	Picoline as Impregnant for Gas Mask Absorbents Div. 10-202.141-M17
10.1-39	1/28/44	W. C. Pierce	The State of Impregnants on ASC Charcoal: Magnetic Susceptibility Studies Div. 10-202.141-M18
10.1-40	2/11/44	W. C. Pierce	The Effect of Pore Size and Pore-Size Distribution on the Performance of ASC Whetlerites at High Humidities Div. 10-202.111-M2
10.1-41	2/7/44	F. E. Blacet	An Exploratory Study of Carbon Monoxide Protection on Charcoal and Other Carriers Div. 10-202.153-M1
10.1-42	3/30/44	W. C. Pierce	Canister Protection at High Concentrations Div. 10-201.1-M25
10.1-43	3/29/44	W. C. Pierce	Canister Efficiency of CC Removal at Varied Breathing Rates Div. 10-201.1-M24
10.1-44	5/12/44	W. C. Pierce	Determination of Pyridine and Ammonia in Whetlerite and Whetlerizing Solutions Div. 10-202.14-M30
10.1-45*	5/18/44	I. M. Klotz (Central Lab.)	Factors in Canister Design and Tube Testing: Critical Bed Depth and the Nature of Gas Flow Through Charcoal Div. 10-201.1-M26
10.1-46	6/28/44	T. Skei et al (Central Lab.)	A Study of Pore Development and ASC Whetlerite Performance of Charcoals Prepared from Briquetted Coal Div. 10-202.1-M3
10.1-47	6/15/44	R. N. Pease	Volume Requirements for a Carbon Monoxide Canister for Use with Diluter-demand Regulator Equipment Div. 10-201.1-M27
10.1-48*	7/10/44	T. Skei et al (Central Lab.)	Compilation of N_0 and λ_c Values for Miscellaneous Whetlerites before and after Aging Div. 10-202.16-M17
10.1-49*	7/24/44	T. Skei (Central Lab.)	Additional Surveillance Tests on Canisters Used in the First Sibert Surveillance Study Div. 10-201.1-M29
10.1-50*	7/22/44	T. Skei et al (Central Lab.)	Performance of M10 and MIXA2 Canisters after Regular Use at Camp Sibert, Ala. Div. 10-201.1-M28
10.1-51*	8/12/44	T. Skei et al (Central Lab.)	Whetlerization and Surveillance Studies on PCI Charcoal at Varying Stages of Activation (Third Report) Div. 10-202.13-M23
10.1-52*	9/6/44	T. Skei et al (Central Lab.)	Surveillance of Type ASC Whetlerite in M10-5/8" Service Canisters Div. 10-201.1-M31
10.1-53*	9/12/44	T. Skei et al (Central Lab.)	Surveillance Tests on ASC, E11, and E13 Whetlerites Div. 10-202.16-M19
10.1-54	9/18/44	L. C. Weiss	Leaching and Rewhetlerization: Their Effect on Whetlerite Quality Div. 10-202.16-M18
10.1-55	10/14/44	I. M. Klotz with F. E. Blacet	Diffusion Coefficients and Molecular Radii of PS, CG, AC and CC Div. 10-202.156-M19
10.1-56	11/16/44	L. C. Weiss	The Use of Pyridine and Picoline in Gas Mask Charcoal Div. 10-201.1-M32
10.1-57	11/28/44	I. M. Klotz	I. Factors in Canister Design and Tube Testing, II. Critical Bed Depths in Removal of CC by the E3 (or M11) Canister Div. 10-201.1-M33
10.1-58	1/24/45	A. J. Juhola with F. E. Blacet	Determination of Pore Diameters in Charcoal Div. 10-202.111-M4
10.2-1	3/28/43	V. K. LaMer	The Efficient Generation of Chlorosulphonic Acid Smokes for Screening Purposes Div. 10-502-M3
10.2-2	8/26/42 (pub. 8/43)	V. K. LaMer	Unipolar Smoke and Filter Penetration Div. 10-201.22-M12
10.2-3	7/23/43	V. K. LaMer	Characteristics of Different Models of the "Owl" Div. 10-501.11-M4

Report No.	*Date*	*Investigator*	*Title*
10.2-4	7/28/43	V. K. LaMer	Determination of the Particle Size Distribution in Smokes by Analysis of the Scattered Light Div. 10-501.11-M5
10.2-5	9/23/43	V. K. LaMer	Thermal Forces as a Means of Determining Particle Size and Size Distribution of Aerosols Div. 10-501.11-M8
10.2-6	10/15/43	V. K. LaMer	Large Horn for the Concentration of Sound from a "Victory" Siren for Use in Fog Dissipation Div. 10-503.2-M2
10.2-7	10/18/43	V. K. LaMer	Properties of Oils with Special Reference to Their Use in Smoke Generators Div. 10-501.22-M1
10.2-8	10/18/43	V. K. LaMer	Comparison of S.G.F. No. 1 Oil (Texas Company) with Other Oils for Use in Oil Fog Generators Div. 10-501.22-M2
10.2-9	11/12/43	V. K. LaMer	Dispersal and Persistance Properties of Solid Aerosols Div. 10-504.3-M1
10.2-10	12/10/43	E. I. duPont de Nemours & Co.	A Method for Determining Dispersibility of Powdered Solids by High Explosive Bursts Div. 10-504.2-M2
10.2-11	1/20/44	V. K. LaMer	"Wetness" in Screening Smokes and a Comparison of the Quality of Smoke from the Hession and Besler Units at Edgewood Arsenal, Nov. 9 and 10, 1943 Div. 10-501.201-M2
10.2-12	3/18/44	H. Rouse	Wind-tunnel Studies of the Diffusion of Heat from a Line Source Div. 10-401.121-M1
10.2-13	4/13/44	V. K. LaMer	Report of Tests of Sonic Dissipation of Fog in California Div. 10-503.2-M3
10.2-14	4/24/44	V. K. LaMer	Particle Size Measurements on Certain "Aerosol" Bombs for the Department of Agriculture Div. 10-504.2-M4
10.2-15	6/19/44	V. K. LaMer	The Slope-O-Meter: An Instrument for the Rapid Determination of Particle Radius and Concentration in the Laboratory and Field Div. 10-501.11-M9
10.2-16	10/23/44	V. K. LaMer	A New Daytime Distress Signal Div. 10-501.23-M2
10.2-17	9/19/44	V. K. LaMer	Field and Laboratory Testing of Smoke Signals with Special Reference to Floating Distress Signals for Air-Sea Rescue Div. 10-501.23-M1
10.2-18	12/7/44	V. K. LaMer	Toxicity to Drosophila (Fruit Flies) of DDT Deposited from Aerosols on the Surface of Certain Leaves and Glass Div. 10-602.22-M1
10.2-19	Dec. 1944	V. K. LaMer	Mosquito Control by Ground Dispersal of DDT as Aerosol from Large Scale Generator Div. 10-602.11-M1
10.2-20	Apr. 1944	V. K. LaMer	The Solubility of DDT in Mixtures of Xylene and Lubricating Oil (10W); The Density of These Solutions when Saturated with DDT Div. 10-601.1-M1
10.2-21	Aug. 1945	V. K. LaMer	The Suitability of Vertical Slides as a Particle Size Measurement Method Div. 10-501.11-M10
10.2-22	Apr. 1945	V. K. LaMer	Sun Oil Company Solvent Aro-Sol (151B) as a Practical Solvent for DDT Div. 10-601.1-M2
10.2-23	8/24/45	V. K. LaMer	Field Tests of Hochberg-LaMer Aerosol Insecticide Generator Against Salt Marsh Mosquitoes at Mantoloking, New Jersey Div. 10-602.21-M6
10.2-24	10/23/45	V. K. LaMer	Laboratory Experiments Testing Effects of DDT on Wood Tick Dermacentor Variabilis Div. 10-602.23-M2
10.2-25	10/25/45	V. K. LaMer	Efficacy of DDT and DNOC as Insecticides for Grasshoppers when Dispersed by a Hochberg-LaMer Type Aerosol Generator Div. 10-602.23-M3
10.2-26	11/8/45	V. K. LaMer	Black Fly Control with DDT-Oil Aerosols Using the Hochberg-LaMer Generator with Notes on Spruce Bud Worms and Larch Case Bearer Control at Lake Placid, New York Div. 10-602.23-M4
10.3A-1	12/15/42	D. M. Yost	Meteorological Instruments; Wind Velocity Measurements Div. 10-301.11-M1
10.3A-2	1/14/43	F. T. Wall	Movement of Smoke in the Atmosphere Div. 10-302.1-M2
10.3A-3	1/15/43	D. M. Yost	Report of Meteorological Observations Made During U. S. Army Smoke Tests at Sault Ste. Marie, Michigan, December 28–30, 1942. Div. 10-302.1-M3



Report No.	*Date*	*Investigator*	*Title*
10.3A-4	1/15/43	D. M. Yost	Testing Charcoal Fines by the "Spotted Dick" Test Div. 10-202.15-M15
10.3A-5	1/15/43	D. M. Yost	Suggested Field Laboratory Method of Testing Permeable Fabrics for Resistance to Penetration by Mustard Vapor Div. 10-202.19-M2
10.3A-6	2/15/43	W. M. Latimer	Meteorological Instruments Div. 10-301-M1
10.3A-7	2/10/43	H. F. Johnstone	Dispersion of Gases in a Closed Court and the Design of Wind Obstacles Div. 10-401.122-M2
10.3A-8	2/8/43	R. G. Dickinson	Determination of CG in Air, using Silica Gel Div. 10-402.2-M8
10.3A-9	2/24/43	R. G. Dickinson	A Portable Continuous Gas Concentration Meter Div. 10-401.111-M1
10.3A-10	2/15/43	D. M. Yost	Micro-Meteorological Measurements Made During the Smoke Screening Tests at the Portsmouth (Va.) Navy Yard on February 3 and 8, 1943 Div. 10-302.1-M4
10.3A-11*	2/15/43	M. Dole	I. Nitrobenzene as a Compound to Simulate HS; II. Distribution of Nitrobenzene Vapors in a Closed Room Div. 10-402.2-M9
10.3A-12	3/15/43	R. G. Dickinson	Measurement of CC with the Portable Continuous Gas Concentration Meter Div. 10-401.111-M2
10.3A-13	4/15/43	R. G. Dickinson	Measurements on AC, CC and Mixtures of the Two with the Portable Continuous Gas Concentration Meter Div. 10-401.111-M3
10.3A-14	4/15/43	W. M. Latimer and S. Ruben; K. Pitzer	I. Meteorological Instruments; II. Observations in the Field Div. 10-301-M1
10.3A-15	4/16/43	H. F. Johnstone	Meteorological Observations in Connection with the Study of Smokes and Gases Div. 10-302.1-M5
10.3A-16*	5/3/43	R. G. Dickinson	Micrometeorological Observations at United States Army Smoke Tests in the Los Angeles Area, March 17, 18, and 19 and April 20, 1943 Div. 10-302.1-M8
10.3A-17	4/17/43	M. D. Thomas Amer. Smelting & Refining Co.	Temperature Gradients and R Values in Relation to the Smoke Conditions in the Salt Lake Valley Div. 10-302-M1
10.3A-18*	6/15/43	F. E. Blacet, M. Dole, and H. F. Johnstone	The Penetration and Persistence of Gases in an Enclosed Court Div. 10-401.122-M3
10.3A-19	6/21/43	R. G. Dickinson	Some Observations at Rosamond Dry Lake on Parameters Used in the Treatment of Gas and Smoke Clouds Div. 10-302.1-M9
10.3A-20	6/10/43	W. M. Latimer	Tabulations of Data on Concentrations in Gas Clouds under Various Meteorological Conditions Div. 10-302.1-M6
10.3A-21	5/26/43	H. F. Johnstone	Large-Scale Screening Tests with Esso Smoke Generators Div. 10-501.201-M2
10.3A-22*	6/15/43	H. F. Johnstone	A Study of Oil Smoke Plumes by Motion Pictures Div. 10-502-M8
10.3A-23*	7/10/43	F. E. Blacet	The Persistence and Penetration of Gas in a House Div. 10-401.124-M1
10.3A-24*	7/14/43	W. M. Latimer and S. Ruben; K. Pitzer	Concentrations in Gas Clouds under High Inversion Conditions Div. 10-302.1-M14
10.3A-25	6/20/43	D. M. Yost and R. G. Dickinson	Experiments on the Accumulation of Sulfur Dioxide in Fox Holes Div. 10-402.2-M11
10.3A-26	7/20/43	D. M. Yost	Experiments on the Measurement of Air Temperatures with Thermocouples Div. 10-301.2-M1
10.3A-27	6/18/43	D. M. Yost	Report on the Preliminary Investigation of the Micrometeorological Conditions at Rancho Grande, Calif. Div. 10-302.1-M7
10.3A-28	8/22/43	D. M. Yost	Experiments at the Rancho Grande, July 28 and 29, 1943, on (1) the "Doughnut" Effect, and (2) the Influence of Terrain on the Flow of Gas Clouds Div. 10-302.1-M12
10.3A-29	8/12/43	D. M. Yost	A Short Photographic Record of the Motion of a Bidirectional Vane Div. 10-301.11-M2
10.3A-30	8/25/43	D. M. Yost	Measurements on the Widths of Smoke Clouds Div. 10-302.1-M13
10.3A-31	8/27/43	D. M. Yost	Further Experiments on the Accumulation of Sulfur Dioxide in Fox Holes Div. 10-402.2-M12

Report No.	*Date*	*Investigator*	*Title*
10.3A-32	8/27/43	D. M. Yost	Thermocouple Experiments Div. 10-301.2-M2
10.3A-33	8/31/43	D. M. Yost	Measurements on SO_2 and NH_3 with the Portable Continuous Gas Concentration Meter Div. 10-401.111-M4
10.3A-34	8/31/43	D. M. Yost	Chemical Analysis of Mixtures of NH_3 and Air and SO_2 and Air Div. 10-402.2-M13
10.3A-35	9/14/43	W. M. Latimer and S. Ruben	Gas Concentrations from Line Sources in a Forested Area Div. 10-302.2-M2
10.3A-36	10/10/43	H. Rouse	Scale Model Studies of the Movement of Smoke and Gas Clouds Div. 10-302.1-M15
10.3A-37*	9/1/43	D. M. Yost	A Study of Smoke Clouds in a Coastal Area; Field Experiments near Brownsville, Texas Div. 10-302.1-M16
10.3A-38	10/26/43	R. G. Dickinson	A Comparison of Three Types of Cup Anemometers at Low Velocities Div. 10-301.1-M1
10.3A-39	12/10/43	W. M. Latimer	Dugway Trials with the Hot Wire Meter Div. 10-302.1-M17
10.3A-40	11/1/43	D. M. Yost	Graphically Recording Bi-Directional Vanes Div. 10-301.11-M3
10.3A-41	1/25/44	R. G. Dickinson	Micro-meteorological Conditions at Prisoner's Harbor on Santa Cruz Island, California (June 24–July 13, 1943) Div. 10-302.1-M19
10.3A-42	4/1/44	F. E. Blacet	Determination of CC and CG Concentrations in Field Tests Div. 10-402.2-M15
10.3A-43	4/1/44	F. E. Blacet	Determination of SO_2 Concentrations in Field Tests Div. 10-402.2-M16
10.3A-44*	4/10/44	R. G. Dickinson	A Remote Indicating Cup Anemometer with Magnetic Coupling Div. 10-301.1-M2
10.3A-45	4/11/44	R. G. Dickinson	An Apparatus for Temperature Profile Measurement Div. 10-301.2-M3
10.3A-46*	5/9/44	H. Rouse	Wind-Tunnel Studies of the Diffusion of Gas in Schematic Urban Districts Div. 10-401.121-M2
10.3A-47	1/3/45	R. G. Dickinson	Micrometeorological Observations in Connection with DDT Operations in Panama Div. 10-302.1-M20
10.3A-48	6/8/45	A. A. Kalinske	Wind-Tunnel Studies of Gas Diffusion in a Typical Japanese Urban District Div. 10-401.121-M4
10.3A-48a	9/29/45	A. A. Kalinske	Correlation of Wind-Tunnel Studies With Field Measurements of Gas Diffusion Div. 10-401.121-M5
10.3B-1	12/15/42	W. C. Schumb	The Generation of Fluorine Div. 10-402.31-M2
10.3B-2	12/15/42	J. C. Bailar, Jr.	Fluophosphates and Related Compounds, VI Div. 10-402.311-M14
10.3B-3	12/21/42	A. B. Burg	New Toxic Gases, V
10.3B-4	1/15/43	W. C. Schumb	The Generation of Fluorine Div. 10-402.31-M2
10.3B-5	1/15/43	J. C. Bailar, Jr.	A Report on Fluophosphates and Related Compounds, VII Div. 10-402.311-M14
10.3B-6	1/15/43	D. M. Yost	Nitrogen Elimination in High Altitude Rebreather Div. 10-203-M1
10.3B-7	2/15/43	W. C. Schumb	The Generation of Fluorine Div. 10-402.31-M2
10.3B-8	2/19/43	A. B. Burg	New Toxic Gases, VII Div. 10-402.311-M15
10.3B-9	2/16/43	H. M. Huffman	Thermal Data on KB-16
10.3B-10	2/15/43	D. M. Yost	Nitrogen Elimination in High Altitude Rebreather Div. 10-203-M1
10.3B-11	3/15/43	H. M. Huffman	Thermal Data on KB-16
10.3B-12	2/15/43	J. C. Bailar, Jr.	Fluophosphates and Related Compounds, VIII Div. 10-402.311-M14
10.3B-13	3/15/43	J. C. Bailar, Jr.	Fluophosphates and Related Compounds, IX Div. 10-402.311-M14
10.3B-14	3/15/43	A. B. Burg	New Toxic Gases, VIII Div. 10-402.311-M15
10.3B-15	3/15/43	W. C. Schumb	The Generation of Fluorine Div. 10-402.31-M2
10.3B-16*	4/15/43	H. M. Huffman	Thermal Data on KB-14 and KB-16 Div. 10-402.36-M7
10.3B-17	4/15/43	A. B. Burg	New Toxic Gases, IX Div. 10-402.311-M15
10.3B-18	4/15/43	W. C. Schumb	The Generation of Fluorine Div. 10-402.31-M2
10.3B-19	4/15/43	D. M. Yost	Nitrogen Elimination in High Altitude Rebreather Div. 10-203-M1

Report No.	*Date*	*Investigator*	*Title*
10.3B-20	5/5/43	D. M. Yost	Nitrogen Elimination in High Altitude Rebreather Div. 10-203-M1
10.3B-21	4/15/43	J. C. Bailar, Jr.	Fluophosphates and Related Compounds, X Div. 10-402.311-M14
10.3B-22	5/15/43	W. C. Schumb	The Generation of Fluorine Div. 10-402.31-M2
10.3B-23	6/15/43	D. M. Yost	Nitrogen Eliminator for High Altitude Oxygen Rebreather Div. 10-203-M1
10.3B-24*	6/15/43	W. C. Schumb	The Generation of Fluorine Div. 10-402.31-M4
10.3B-25	7/15/43	A. B. Burg	I. Flame-Damping of Hydrogen Cyanide; II. Stabilization of Cyanogen Chloride Div. 10-402.33-M1
10.3B-26	6/17/43	G. P. Baxter	Preparation of Certain Extremely Pure Strontium Salt Div. 10-402.2-M10
10.3B-27	7/15/43	D. M. Yost	Nitrogen Elimination in High Altitude Rebreather Div. 10-203-M1
10.3B-28	7/15/43	W. C. Schumb	The Generation of Fluorine Div. 10-402.31-M2
10.3B-29	8/15/43	D. M. Yost	Nitrogen Elimination in Navy High Altitude Rebreather Div. 10-203-M2
10.3B-30	8/15/43	A. B. Burg	Flame-Damping of Hydrogen Cyanide, II; Stabilization of Cyanogen Chloride, III. Div. 10-402.33-M1
10.3B-31	8/15/43	W. C. Schumb	The Generation of Fluorine
10.4-1	12/17/42	Chemical Process Co.	Preparation and Use of Amine Resins for Gas Adsorption Div. 10-202.21-M3
10.4-2	12/18/42	A. D. Little, Inc.	Dispersion of Fine Fibers and Solids Div. 10-201.22-M8
10.4-3	12/15/42	R. J. Kunz	Summary of Investigations at the Activation Laboratory, I Div. 10-202.13-M9
10.4-4	1/15/43	R. J. Kunz	Summary of Investigations at the Activation Laboratory, II Div. 10-202.13-M9
10.4-5	1/15/43	Chemical Process Co.	Studies of Adsorbent Resins Div. 10-202.21-M4
10.4-6	1/15/43	A. D. Little, Inc.	Asbestos Impregnated Filter Papers Div. 10-201.22-M9
10.4-7*	1/15/43	W. L. McCabe	The Preparation of Wood Charcoal Suitable for Activation Div. 10-202.12-M8
10.4-8	2/10/43	R. J. Kunz	Summary of Investigations at the Activation Laboratory, III Div. 10-202.13-M9
10.4-9	2/10/43	A. D. Little, Inc.	Dispersion of Asbestos Fibers (Filter Paper Products) Div. 10-201.22-M10
10.4-10	2/10/43	Chemical Process Co.	Preparation and Use of Amine Resins for Gas Adsorption Div. 10-202.21-M3
10.4-11	3/12/43	R. J. Kunz	Summary of Investigations of Activation Laboratory, IV Div. 10-202.13-M9
10.4-12	3/11/43	Chemical Process Co.	Development of Amine Resin Adsorbents for Gas Adsorption and other Purposes Div. 10-202.21-M5
10.4-13	3/10/43	A. D. Little, Inc.	Dispersion of Asbestos Fibers (Filter Paper Products) Div. 10-201.22-M10
10.4-14	4/1/43	R. York, Jr.	Weight and Size Losses During Laboratory Activation of PCI Char Div. 10-202.13-M11
10.4-15	4/15/43	R. J. Kunz	Summary of Investigations at the Activation Laboratory, V Div. 10-202.13-M9
10.4-16	4/9/43	A. D. Little, Inc.	Dispersion of Asbestos Fibers (Filter Paper Products) Div. 10-201.22-M10
10.4-17	4/13/43	G. F. Mills Chemical Process Co.	Development of Amine Resin Adsorbents for Gas Adsorption and Other Purposes Div. 10-202.21-M5
10.4-18	5/1/43	R. York, Jr.	Activation of Charcoal in a "Boiling Bed" Furnace Div. 10-202.13-M13
10.4-19	5/10/43	R. J. Kunz	Summary of Investigations at the Activation Laboratory, VI Div. 10-202.13-M9
10.4-20*	4/1/43	R. York, Jr.	Further Development of a Laboratory Jiggler for Activating Gas Charcoal, and Tentative Results on Gasification Rate Studies Div. 10-202.131-M4
10.4-21	5/15/43	E. W. Comings	Smoke Investigations Div. 10-501.2-M2
10.4-22*	6/1/43	H. F. Johnstone and G. L. Clark	Application of the Electron Microscope to the Study of Charcoal Div. 10-202.143-M5

Report No.	*Date*	*Investigator*	*Title*
10.4-23	6/10/43	R. J. Kunz	Summary of Investigations by the Engineering Pilot Group, VII Div. 10-202.1-M10
10.4-24	6/15/43	E. W. Comings	Smoke Investigations
10.4-25*	6/24/43	G. F. Mills Chemical Process Co.	Use of Aminated Phenol-Formaldehyde Xerogels as Gas Adsorbents Div. 10-202.21-M6
10.4-26	5/27/43	P. H. Emmett	Adsorption and Surface Area Measurements on Whetlerite and Charcoal Samples Div. 10-202.15-M16
10.4-27	7/10/43	R. J. Kunz	Summary of Investigations by the Engineering Pilot Group, VIII Div. 10-202.13-M15
10.4-28	7/5/43	L. B. Counterman Hercules Powder Co.	The Development of a Filling Mixture for Smoke Pots, Grenades, and Floats Div. 10-501.21-M1
10.4-29	7/8/43	P. H. Emmett	Chemisorption of Gases on Charcoals and Type A Whetlerites Div. 10-202.15-M17
10.4-30	8/1/43	R. York, Jr.	Composition of Gases Evolved during Activation Div. 10-202.13-M16
10.4-31	8/10/43	R. J. Kunz	Summary of Investigations by the Engineering Pilot Group, IX Div. 10-202.1-M10
10.4-32	8/2/43	Hercules Powder Co.	The Development of a Filling Mixture for Smoke Pots, Grenades, and Floats Div. 10-501.21-M1
10.4-33	9/6/43	Hercules Powder Co.	The Development of a Filling Mixture for Smoke Pots, Grenades, and Floats Div. 10-501.21-M1
10.4-34	9/15/43	A. B. Burg	Flame-Damping of Hydrogen Cyanide III; Stabilization of Cyanogen Chloride IV Div. 10-402.33-M1
10.4-35*	8/1/43	H. F. Johnstone	The Evaporation of Small Drops of Thiodiglycol and Levinstein Mustard Div. 10-501.12-M1
10.4-36	10/4/43	Hercules Powder Co.	The Development of a Filling Mixture for Smoke Pots, Grenades, and Floats Div. 10-501.21-M1
10.4-37	10/14/43	A. B. Burg	Flame-Damping of Hydrogen Cyanide IV; Stabilization of Cyanogen Chloride V Div. 10-402.33-M1
10.4-38*	10/20/43	H. F. Johnstone E. W. Comings	The Generation and Use of Concentrated Mustard Vapor Clouds Div. 10-504.1-M1
10.4-39	11/15/43	A. B. Burg	Flame-Damping of Hydrogen Cyanide V; Stabilization of Cyanogen Chloride VI Div. 10-402.33-M1
10.4-40	11/11/43	Victor Chemical Works	The Use of Carbon Black in WP Shells Div. 10-504.21-M1
10.4-41	11/8/43	Hercules Powder Co.	The Development of a Filling Mixture for Smoke Pots, Grenades, and Floats Div. 10-501.21-M1
10.4-42	12/7/43	Victor Chemical Works	I. Static Firing Tests on Tail-ejector (E-5) Bombs; II. Notes on WP in Anti-personnel Role Div. 10-504.21-M2
10.4-43	12/3/43	E. W. Comings	Improvements in the Fuel Block for the Thermal Vapor Generator Div. 10-504.11-M1
10.4-44	12/14/43	A. B. Burg	Flame-Damping of Hydrogen Cyanide VI; Stabilization of Cyanogen Chloride, VII Div. 10-402.33-M1
10.4-45	1/3/44	Hercules Powder Co.	The Development of a Filling Mixture for Smoke Pots, Grenades, and Floats Div. 10-501.21-M1
10.4-46	1/20/44	Chemical Process Co.	Use of Amine Resins as Gas Adsorbents Div. 10-202.21-M7
10.4-47	1/15/44	A. B. Burg	Stabilization of Cyanogen Chloride, VIII Div. 10-402.34-M3
10.4-48	12/31/43	H. F. Johnstone	The Assessment of Aerosols Div. 10-504.2-M3
10.4-49	1/15/44	H. F. Johnstone	The Deposition of Drops of a Non-volatile Liquid Vesicant on Vertical and Horizontal Surfaces Div. 10-501.12-M2
10.4-50	2/14/44	A. B. Burg	Stabilization of Cyanogen Chloride, IX Div. 10-402.34-M3
10.4-51	2/7/44	Hercules Powder Co.	The Development of a Filling Mixture for Smoke Pots, Grenades, and Floats Div. 10-501.21-M1
10.4-52	3/13/44	A. B. Burg	Stabilization of Cyanogen Chloride, X Div. 10-402.34-M3
10.4-53	2/1/44	J. C. Bailar, Jr. and H. F. Johnstone	Preparation of Plasticized Phosphorus Mixtures Div. 10-504.21-M3
10.4-54	3/6/44	Hercules Powder Co.	The Development of a Filling Mixture for Smoke Pots, Grenades, and Floats Div. 10-501.21-M1
10.4-55	3/1/44	H. F. Johnstone	The Deposition of Non-volatile Aerosol Clouds in Open and Forested Areas Div. 10-501.12-M3
10.4-56	3/30/44	Victor Chemical Works	Tests on M-69 Bombs Charged with Coated Precast Blocks of WP Div. 10-504.21-M4

[redacted]

Report No.	*Date*	*Investigator*	*Title*
10.4-57	4/10/44	J. C. Bailar, Jr.	Plasticized White Phosphorus (PWP) Div. 10-504.21-M5
10.4-58	4/15/44	A. B. Burg	Stabilization of Cyanogen Chloride and Hydrogen Cyanide, XI Div. 10-402.34-M3
10.4-59	4/3/44	Hercules Powder Co.	The Development of a Filling Mixture for Smoke Pots, Grenades, and Floats Div. 10-501.21-M1
10.4-60	4/20/44	H. F. Johnstone R. L. LeTourneau	The Production of Aerosol Droplets below Twenty-five Micron Diameter for the Dispersal of Insecticides and CW Agents Div. 10-602-M1
10.4-61	5/14/44	A. B. Burg	Flame-Damping of Hydrogen Cyanide, VII; Stabilization of Cyanogen Chloride XII Div. 10-402.33-M1
10.4-62	5/8/44	Hercules Powder Co.	The Development of a Filling Mixture for Smoke Pots, Grenades, and Floats Div. 10-501.21-M1
10.4-63	5/1/44	H. F. Johnstone E. W. Comings	Fuel Blocks for the Model G-8 Thermal Generator Bomb Div. 10-504.11-M2
10.4-64	6/5/44	Hercules Powder Co.	The Development of a Filling Mixture for Smoke Pots, Grenades, and Floats Div. 10-501.21-M1
10.4-65	6/30/44	J. C. Bailar, Jr.	Factors Affecting the Thermal Stability of Plasticized Phosphorus Div. 10-504.21-M6
10.4-66	6/15/44	A. B. Burg	Stabilization of Cyanogen Chloride, XIII Div. 10-402.34-M3
10.4-67	7/4/44	Hercules Powder Co.	The Development of a Filling Mixture for Smoke Pots, Grenades, and Floats Div. 10-501.21-M1
10.4-68	7/15/44	A. B. Burg	Stabilization of Cyanogen Chloride, XIV Div. 10-402.34-M3
10.4-69	8/7/44	Hercules Powder Co.	The Development of a Filling Mixture for Smoke Pots, Grenades, and Floats Div. 10-501.21-M1
10.4-70	8/14/44	A. B. Burg	Stabilization of Cyanogen Chloride, XV Div. 10-402.34-M3
10.4-71	9/4/44	Hercules Powder Co.	The Development of a Filling Mixture for Smoke Pots, Grenades, and Floats Div. 10-501.21-M1
10.4-72	9/15/44	A. B. Burg	Stabilization of Cyanogen Chloride, XVI Div. 10-402.34-M3
10.4-73	9/1/44	J. C. Bailar, Jr.	The Development of Plasticized White Phosphorus, IV Div. 10-504.21-M7
10.4-74	10/1/44	H. F. Johnstone W. H. Rodebush	The Toxicity of DDT Films and Aerosol Deposits Div. 10-602.2-M1
10.4-75	9/15/44	H. F. Johnstone	The Burning Properties and Anti-Personnel Effect of PWP
10.4-76	10/14/44	A. B. Burg	Stabilization of Cyanogen Chloride, XVII Div. 10-402.34-M3
10.4-77	9/25/44	Munitions Dev. Lab. & TVA Health and Safety Department	Tests with an Exhaust Aerosol DDT Generator on a 450 H. P. Stearman Aircraft
10.4-78	11/15/44	A. B. Burg	Stabilization of Cyanogen Chloride, XVIII Div. 10-402.34-M3
10.4-79	12/14/44	A. B. Burg	Stabilization of Cyanogen Chloride, XIX Div. 10-402.34-M3
10.4-80	1/13/45	A. B. Burg	Stabilization of Cyanogen Chloride, XX Div. 10-402.34-M3
10.4-81	2/20/45	H. F. Johnstone E. A. Ford	The Apparent Viscosity of PWP Div. 10-504.21-M10
10.4-82	6/15/45	P. A. Pitt	The Tailpipe Combustion Unit to Increase the Rate of Smoke Production of TBM-3 Exhaust Generator Div. 10-501.203-M1
10.4-83	5/1/45	R. I. Rice H. F. Hrubecky	Directions for Installation and Operation of Exhaust-Type Aerosol Generator on "Jeep" Div. 10-602.122-M1
10.4-84	7/20/45	R. I. Rice	Installation of an Exhaust DDT Aerosol Generator on the Cargo Carrier M29C (Weasel) Div. 10-602.122-M2
10.5-1	9/1/43	R. York, Jr.	Activation of Carbonized Pres-to-Logs Div. 10-202.134-M2
10.5-2	9/10/43	R. J. Kunz	Summary of Investigations by the Engineering Pilot Group, X Div. 10-202.131-M5
10.5-3	9/11/43	P. H. Emmett	Adsorption of Nitrogen on CWSN Base Charcoals Div. 10-202.11-M8
10.5-4	10/15/43	R. J. Kunz	Summary of Investigations by the Engineering Pilot Group, XI Div. 10-202.1-M10
10.5-5	11/15/43	R. J. Kunz	Summary of Investigations by the Engineering Pilot Group, XII Div. 10-202.1-M10
10.5-6	11/12/43	R. York, Jr.	Activation of Charcoal in a Boiling-Bed Furnace (second report) Div. 10-202.13-M13

[redacted]

Report No.	*Date*	*Investigator*	*Title*
10.5-7	12/1/43	R. York, Jr.	The Effect of the Activation Process on the Nitrogen Adsorption and Whetlerite Properties of PCI and Carlisle Chars Div. 10-202.11-M9
10.5-8	12/10/43	R. J. Kunz	Summary of Investigations by the Engineering Pilot Group, XIII Div. 10-202.1-M10
10.5-9	12/15/43	R. York, Jr.	Activation of Carbonized Peach Pits and Black Walnut Shells in PCI Retorts Div. 10-202.134-M3
10.5-10	1/15/44 (written 7/1/43)	R. J. Kunz	Preliminary Design and Cost Estimate for Five-Ton-per-Day Activation Plant Based on Jiggler Process Div. 10-202.131-M6
10.5-11	12/10/43	National Carbon Co., Inc.	Study of Zinc Chloride Carbon, I Div. 10-202.133-M1
10.5-12	11/12/43	P. H. Emmett	Pore Size Alteration of Charcoal Div. 10-202.111-M1
10.5-13	1/10/44	R. J. Kunz	Summary of Investigations by the Engineering Pilot Group on Carbonization, Activation, and Whetlerization, XIV Div. 10-202.1-M10
10.5-14	2/1/44	R. York, Jr.	An Hypothesis of the Activation Mechanism in Charcoal Div. 10-202.13-M17
10.5-15	1/10/44	National Carbon Co.	Study of Zinc Chloride Carbon, II Div. 10-202.133-M1
10.5-16	2/10/44	R. J. Kunz	Summary of Investigations by the Engineering Pilot Group on Carbonization, Activation, and Whetlerization, XV Div. 10-202.1-M10
10.5-17	2/10/44	National Carbon Co.	Zinc Chloride-Activated Wood Charcoal, III Div. 10-202.13-M18
10.5-18	3/1/44	R. York, Jr.	A Modified Boiling-bed Furnace for Charcoal Activation by Steam, III Div. 10-202.13-M20
10.5-19	3/10/44	R. J. Kunz	Summary of Investigations by the Engineering Pilot Group on Carbonization, Activation, and Whetlerization, XVI Div. 10-202.1-M10
10.5-20	3/1/44	P. H. Emmett	Nitrogen Surface Area Measurements on a Series of PCI Samples Subjected to Steam Activation for Various Periods of Time (to Nov. 11, 1943) Div. 10-202.13-M19
10.5-21	3/14/44	R. J. Kunz	A Study of the Effect of Uniformity of Activation of Sieve Fractions on CC Canister Performance for Mixtures of PCI Charcoals
10.5-22	3/10/44	National Carbon Co.	Zinc Chloride-Activated Wood Charcoal, IV Div. 10-202.13-M18
10.5-23	3/9/44	R. J. Kunz	Reclamation of Type A Whetlerite Div. 10-202.19-M4
10.5-24	3/25/44	R. J. Kunz	The Effect of Time and Temperature of Activation on the Properties of PCI Charcoal Activated in the Jiggler Pilot Plant Div. 10-202.131-M8
10.5-25	3/20/44	R. J. Kunz	Activation of Charcoal by the Jiggler Process. A Summary of the Results Obtained in the First Two Pilot Models Div. 10-202.131-M7
10.5-26	4/24/44	R. J. Kunz and D. G. Anderson	A Systematic Study of Pressure Drop in Beds of Charcoal Div. 10-202.11-M10
10.5-27	4/10/44	R. J. Kunz	Summary of Investigations by the Engineering Pilot Group on Carbonization, Activation, and Whetlerization, XVII Div. 10-202.1-M10
10.5-28	3/15/44	R. J. Kunz	An Investigation of the Applicability of ASC-type Whetlerizing Equipment to the Preparation of ASM Whetlerite Div. 10-202.12-M13
10.5-29	4/10/44	National Carbon Co.	Zinc Chloride-Activated Wood Charcoal, V Div. 10-202.13-M18
10.5-30	5/6/44	R. J. Kunz	The Effect of Backfeeding on the Quality of ASC Whetlerite Div. 10-202.19-M5
10.5-31	5/10/44	R. J. Kunz	Summary of Investigations by the Engineering Pilot Group on Carbonization, Activation, and Whetlerization, XVIII Div. 10-202.1-M10
10.5-32	5/10/44	National Carbon Co.	Zinc Chloride-Activated Wood Charcoal, VI Div. 10-202.13-M18
10.5-33	5/23/44	R. York, Jr.	A Modified Boiling-bed Furnace for Charcoal Activation by Steam, IV
10.5-34	6/10/44	National Carbon Co.	Zinc Chloride-Activated Wood Charcoal, VII Div. 10-202.13-M18

[redacted]

Report No.	*Date*	*Investigator*	*Title*
10.5-35	7/14/44	R. J. Kunz	Activation of Charcoal by the Jiggler Process. Factors other than Time-Temperature Affecting Product Quality and Yield Div. 10-202.131-M11
10.5-36	7/10/44	R. J. Kunz	Design, Construction, and Operating Characteristics of the Third Pilot Jiggler Activator Div. 10-202.131-M10
10.5-37	6/30/44	R. J. Kunz	The Effect of Time and Temperature of Activation upon the Properties of Barnebey-Cheney and Carlisle Charcoals Processed in the Jiggler Pilot Activator Div. 10-202.131-M9
10.5-38	7/10/44	National Carbon Co.	Zinc Chloride-Activated Wood Charcoal, VIII Div. 10-202.13-M18
10.5-39	7/15/44	R. J. Kunz	Carbonization of Peach Pits and Their Preparation into ASC Whetlerite Div. 10-202.134-M4
10.5-40*	8/4/44	T. F. Young	The Reactivation in Oxygen of CWS Charcoals Div. 10-202.132-M2
10.5-41*	8/15/44	R. J. Kunz	Summary of Pilot Studies of the Preparation of ASC Whetlerite Div. 10-202.12-M14
10.5-42	8/14/44	R. J. Kunz	A Study of the Steam Activation of Various Charcoals in a Small Horizontal Rotary Retort Div. 10-202.13-M22
10.5-43	8/10/44	National Carbon Co.	Zinc Chloride Activated Wood Charcoal, IX Div. 10-202.13-M18
10.5-44*	8/15/44	R. J. Kunz	Activation of Charcoal by the Jiggler Process. A Summary of Results Obtained in the Fourth (Metal Tube) Pilot Model Div. 10-202.131-M13
10.5-45*	8/15/44	R. J. Kunz	Final Design and Cost Estimate for a Two-Ton-per-Day Activator Using the "Jiggler" Process Div. 10-202.131-M12
10.5-46	9/10/44	National Carbon Co.	Zinc Chloride-Activated Wood Charcoal, X Div. 10-202.13-M18
10.5-47*	9/30/44	National Carbon Co.	Zinc Chloride-Activated Wood Charcoal, Final Report Div. 10-202.13-M24
10.5-48	11/20/44	T. B. Drew et al	I. The Adsorption Wave. II. Study of the Adsorption Wave. III. Plotting of the Schumann-Furnas Graphs for Low Values of the Concentration Div. 10-202.157-M8
10.5-49	11/24/44	B. White et al	A Study of the Carbonization of Coal Materials Div. 10-202.12-M15

DIVISION 10

Chief

W. A. NOYES, JR.

Members

F. E. BLACET
H. F. JOHNSTONE
V. K. LAMER
W. M. LATIMER
W. L. MCCABE
W. C. PIERCE
W. H. RODEBUSH
D. M. YOST

Technical Aides

M. T. O'SHAUGHNESSY
W. C. PIERCE
C. D. WAGNER
W. D. WALTERS

W. J. WYATT

Special Advisors

L. M. K. BOELTER
M. K. FAHNESTOCK
E. P. HECKEL
I. M. JOHNSTON
R. D. MADISON
A. C. WILLARD

Consultants

F. E. BARTELL
A. F. BENTON
W. D. BONNER
W. E. BRINKER, JR.
L. O. BORCKWAY
W. G. BROWN
G. L. CLARK
A. P. COLBURN
E. W. COMINGS
C. CRONEIS
M. DOLE
T. B. DREW
J. C. ELGIN
H. W. ELLEY
P. H. EMMETT
F. T. GUCKER, JR.
W. D. HARKINS
L. F. HAWLEY
J. H. HILLMAN, III
H. G. HOUGHTON
W. C. JOHNSON
L. S. KASSEL
C. A. KRAUS
F. J. KUNZ
A. B. LAMB
V. K. LAMER
I. LANGMUIR
P. A. LEIGHTON
G. N. LEWIS
H. H. LOWRY
W. L. MCCABE
R. B. MONTGOMERY
A. R. OLSON
M. T. O'SHAUGHNESSY
K. S. PITZER
A. B. RAY
H. A. ROSELUND
P. W. SCHUTZ
T. K. SHERWOOD
D. SINCLAIR
A. F. SPILHAUS
M. D. THOMAS
F. T. WALL
E. O. WIIG
R. E. WILSON
W. P. YANT
T. F. YOUNG
F. W. H. ZACHARIASEN

SECTION L-1

Chairman

W. H. RODEBUSH

Members

H. EYRING
V. K. LAMER
L. PAULING
R. STEVENSON

I. LANGMUIR

Consultants

W. G. BROWN
E. W. COMINGS

[redacted]

SECTION L-11

Chairman

W. A. NOYES, JR.

Vice-Chairmen

W. M. LATIMER

W. L. MCCABE

Members

A. F. BENTON
A. B. BURG
A. P. COLBURN
T. B. DREW
P. H. EMMETT

F. T. GUCKER, JR.
H. F. JOHNSTONE
R. N. PEASE
W. C. PIERCE
E. O. WIIG

T. F. YOUNG

Consultants

F. E. BARTELL
S. BRUNAUER
T. H. CHILTON
G. L. CLARK
R. G. DICKINSON

W. D. HARKINS
L. S. KASSEL
A. R. OLSON
A. B. RAY
T. D. STEWART

W. P. YANT

Technical Aide

W. D. WALTERS

SECTION B-5

Chairman

W. H. RODEBUSH

Members

H. EYRING
V. K. LAMER

I. LANGMUIR
L. PAULING

Technical Aides

F. T. GUCKER, JR.

M. T. O'SHAUGHNESSY

W. D. WALTERS

Special Advisors

W. W. DUECKER

M. T. O'SHAUGHNESSY

Consultant

N. K. CHANEY

SECTION B-6

Chairman

W. A. NOYES, JR.

D. M. YOST

Vice-Chairmen

H. F. JOHNSTONE
W. M. LATIMER

W. L. MCCABE
W. C. PIERCE

Members

F. E. BLACET
M. DOLE
J. C. ELGIN
P. H. EMMETT

F. T. GUCKER, JR.
H. F. JOHNSTONE
P. A. LEIGHTON
W. C. PIERCE

T. F. YOUNG

Special Advisors

R. B. MONTGOMERY

A. F. SPILHAUS

Consultants

F. E. BARTELL
A. F. BENTON
W. D. BONNER
W. E. BRINKER, JR.
S. BRUNAUER
R. J. CASHMAN
T. H. CHILTON
T. B. DREW

W. D. HARKINS
L. F. HAWLEY
L. S. KASSEL
H. H. LOWRY
A. B. RAY
C. E. REED
T. D. STEWART
J. TURKEVICH

W. P. YANT

Technical Aide

W. D. WALTERS

Contract No.	*Contractor*	*Subject*
NDCrc-13	Massachusetts Institute of Technology	Special fuels for jet propulsion, colored smokes and related pyrotechnic problems.
NDCrc-18	The College of the City of New York	The study of dispersion of solids in gases.
NDCrc-28	Princeton University	The preparation of smokes of predetermined particle size and determination of particle size.
NDCrc-33	Columbia University	The study of physical properties of smokes.
NDCrc-47	University of Illinois	The formation of smokes. *Supplement 1:* To conduct large scale tests of the smokes developed.
NDCrc-49	University of Illinois	The study of dispersion of solids in gases.
NDCrc-65	University of Chicago	Gas absorbents. A study of the structure of gas absorbents.
NDCrc-70	University of Delaware	Impregnating agents for gas adsorbents.
NDCrc-71	University of Chicago	The mechanical formation of fogs and smokes.
NDCrc-76	University of Rochester	Mechanism of adsorption of gases.
NDCrc-104	General Electric Company	The preparation of smokes and experimental study of their properties.
NDCrc-106	Princeton University	Impregnating agents for gas adsorbents.
NDCrc-108	Princeton University	The absorption wave in gas adsorbents.
NDCrc-109	Northwestern University	Gas absorbents. *Supplement 1:* To conduct studies and experimental investigations in connection with thermal effects in gas absorbents.
NDCrc-112	Harvard University	The removal of chloropicrin and phosgene.
NDCrc-113	University of Southern California	The preparation of new toxic gases.
NDCrc-115	California Institute of Technology	The development of laboratory methods of gas detection, using radioactive elements as tracers.
NDCrc-119	Johns Hopkins University	The determination of pore size and surface adsorbents. *Supplement 1:* The determination of pore size and surface adsorbents, and the specific absorption capacity of active charcoal. *Supplements 2, 3, 4:* Extension of time and addition of funds.
NDCrc-122	Stanford University	The removal of ethylene imine. *Supplement 1:* The removal of ethylene imine, and investigations of certain synthetic resins as possible gas absorbents. *Supplement 2:* Extension of time and addition of funds. *Supplement 3:* (i) The removal of ethylene imine, (ii) investigations of certain synthetic resins as possible gas absorbents, and (iii) the meteorological conditions effecting the use of chemical warfare agents.
NDCrc-124	Carnegie Institute of Technology	Production and activation of gas charcoal. *Supplement 1:* Conduct studies and investigations in connection with (i) the production and activation of charcoal, (ii) the pre-impregnation of charcoal with metallic compounds prior to activation, and (iii) the activation of such pre-impregnated charcoal.
NDCrc-126	University of California	The removal of cyanogen chloride and its action as an adsorbent poison. *Supplement 1:* Extension of time. *Supplement 2:* The removal of cyanogen chloride and its action as an adsorbent poison, and a study of the form and effectiveness of gas clouds. *Supplements 3, 4, 5, 6, 7:* Extension of time and addition of funds.
NDCrc-131	Princeton University	Protection against carbon monoxide; absorbent properties of synthetic resins. *Supplement 1:* The study and experimental investigations in connection with synthetic gases, and removal of carbon monoxide. *Supplement 2:* (i) Protection against carbon monoxide, (ii) adsorbent properties of syntheticresins, and (iii) the removal of carbon monoxide at low partial pressures.
NDCrc-133	University of California	New solid reactants.
NDCrc-135	University of California	Development of apparatus and method for using radioactive hydrogen as a tracer.
NDCrc-137	California Institute of Technology	The adsorption of selenium hexafluoride by charcoal. *Supplement 1:* The adsorption of selenium hexafluoride by charcoal and the use of halogen compounds and certain inorganic substances as chemical warfare agents. *Supplement 2:* (i) The adsorption of selenium hexafluoride by charcoal and the use of halogen compounds and certain inorganic substances as chemical warfare agents, and (ii) the factors affecting the travel of gas clouds and the development of devices for the analysis of gas clouds.

Contract No.	*Contractor*	*Subject*
		Supplements 3, 4, 5: Extension of time and addition of funds. *Supplement 6:* Delivery of models of such devices as may be developed.
NDCrc–138	University of California	To maintain and operate a cyclotron. *Supplement 1:* To prepare, by the use of the cyclotron, radioactive materials, and to furnish artificially radioactive substances.
NDCrc 152	University of Illinois	Development of X-ray or other techniques for studying reactive agents in adsorbents, and the development of new adsorbents. *Supplement 1:* Development of X-ray or other techniques for studying reactive agents in adsorbents, and the development of new adsorbents, and the X-ray of metallic catalysts and the reaction products on the surface of these catalysts or other adsorbents.
NDCrc–154	University of Illinois	The development of substitutes for activated carbon.
NDCrc–166	University of Virginia	Methods of detection of gases.
NDCrc–167	Pennsylvania State College	Rapid methods of making war gases for tests of adsorbents.
NDCrc 171	Harvard University	To furnish artificially radioactive substances produced by means of the cyclotron.
NDCrc–208	University of Michigan	Experimental investigations of screening smokes.
OEMsr–16	University of California	New solid reactants, new impregnants, and new methods of impregnation.
OEMsr–22	Northwestern University	The development of an ultra-violet absorption apparatus for the analysis of war gases in a gas stream.
OEMsr–28	California Institute of Technology	Adsorption of war gases by means of radioactive tracers.
OEMsr–59	Harvard University	Use of cyclotron for the preparation of radioactive sulfur and arsenic.
OEMsr–83	Arthur D. Little, Inc.	Sources of mineral fibers and the dispersion of asbestos.
OEMsr–102	University of Illinois	Development of equipment for the formation of smokes. *Supplement 1:* Studies and experimental investigations in connection with the development of equipment for the formation of smokes and methods of generating toxic smokes in the field. *Supplements 2, 3:* Extension of time. *Supplement 4:* (i) The design of munitions for chemical warfare, (ii) the construction and testing of models which are developed hereunder, (iii) the reproduction of developed munitions in sufficient quantity for testing by the Services, (iv) investigation of new physical and chemical combination as fillings for chemical warfare munitions existing or developed under this contract, (v) the behavior of gas and smoke clouds in built-up city areas and woods. *Supplements 5, 6, 7:* Extension of time. *Supplement 8:* (i) The design of munitions for chemical warfare, for screening and signal smokes, for the dissemination of insecticides, and for related purposes, (ii) the construction and testing of models which are developed hereunder, (iii) the reproduction of developed munitions in sufficient quantity for testing by the Services, (iv) investigation of new physical and chemical combination as fillings for chemical warfare munitions existing or developed under this contract, and (v) the development of equipment for the generation of aerosols from airplanes, for screening, insecticidal and other purposes. *Supplements 9, 10, 11, 12, 13, 14, 15:* Extension of time and addition of funds.
OEMsr–103	California Institute of Technology	Development of an instrument for the rapid determination of particle size distribution of smokes. *Supplement 1:* Extension of time and addition of funds.
OEMsr–108	University of Illinois	Dispersion of solids in gases and of smoke filtration. *Supplement 1:* Extension of time. *Supplement 2:* Dispersion of solids and liquids in gases and removal of suspended solid or liquid particles from gases by filtration or by other means. *Supplement 3:* (i) Properties of aerosols and filter materials for aerosols, particularly with the radioactive tracer technique, and (ii) the behavior and use of screening smokes, with reference to weather and terrain. *Supplement 4:* (i) Properties of aerosols and filter materials for aerosols, particularly with the radioactive tracer technique, and (ii) the behavior and use of screening smokes, and the rendering of assistance to the Services in the study thereof, and (iii) the use of aerosols for special purposes, including insect control. *Supplement 5:* (i) Properties of aerosols and filter materials for aerosols, particularly with the radioactive tracer technique, and (ii) the behavior and use of screening smokes, and the rendering of assistance to the Services in the study thereof, and (iii) the use of aerosols for special purposes, including insect control, and (iv) the dispersal of DDT as an aerosol and on the effectiveness of aerosols of DDT as insecticide. *Supplement 6:* Extension of time.

Contract No.	*Contractor*	*Subject*
OEMsr–116	Carnegie Institute of Technology	Preparation of wood charcoal suitable for activation. *Supplement 1:* Extension of time.
OEMsr–131	General Electric Company	The preparation of smokes and experimental study of their properties. *Supplement 1:* The preparation of smokes and experimental study of their properties, and to produce field units for production of screen smokes, and to carry out related field tests. *Supplement 2:* (i) The preparation of smokes and experimental study of their properties, (ii) to produce field units for production of screen smokes and to carry out related field tests, and (iii) study in connection with the determination of the screening power of certain smokes under moonlight and starlight illumination and the investigation of the ability of the normal eye to detect contrast under such conditions. *Supplement 3:* Extension of time and addition of funds. *Supplement 4:* The removal of aerosols from air by filtration. *Supplements 5, 6:* Extension of time.
OEMsr–142	Servel, Inc.	Development of a practical device for the production of screening smokes. *Supplement 1:* Development of a practical device for the production of screening smokes, this development to be based on a laboratory device now in existence. *Supplement 2:* Development of a practical device for the production of screening smokes, this development to be based on a laboratory device now in existence, and also the development of a smoke bomb. *Supplement 3:* Extension of time.
OEMsr–148	Columbia University	Measurement of particle size and particle size distribution in aerosols and the production of screening smokes. *Supplement 1:* (i) Measurement of particle size and particle size distribution in aerosols, (ii) the production of screening smokes, and (iii) the production of suitable smokes for special screening purposes. *Supplement 2:* (i) Measurement of particle size and particle size distribution in aerosols, (ii) the production of screening smokes, and (iii) the production of suitable smokes for special screening purposes, and (iv) the development of devices for the production of screening smokes. *Supplement 3:* (i) Further studies on aerosols, and studies and experimental investigations in connection with, (ii) the evaluation of screening smokes and the development of instruments for their evaluation, (iii) the dispersion of toxic solids as aerosols and the evaluation of the aerosols so produced, and (iv) the development of screening smoke generators. *Supplement 4:* Extension of time. *Supplement 5:* Investigations in connection with (i) aerosols, (ii) the evaluation of screening smokes and the development of instruments for their evaluation in the field, (iii) the dispersion of toxic solids as aerosols and the evaluation of the aerosols so produced, (iv) the development of screening smoke generators, (v) the evaluation and improvement of colored smoke signals, (vi) the application of aerosols to insecticidal uses and other miscellaneous uses of military importance.
OEMsr–199	California Institute of Technology	Heats of removal of war gases on adsorbents. *Supplements 1, 2:* Extension of time and addition of funds.
OEMsr–219	Arthur D. Little, Inc.	The dispersion of solids. *Supplement 1:* Addition of funds. *Supplement 2:* The dispersion of asbestos in paper or other materials. *Supplement 3:* The dispersion of asbestos in paper and other materials, and the fabrication of particulate filters from sheet materials thus produced. *Supplements 4, 5, 6:* Extension of time and addition of funds.
OEMsr–221	United Gas Improvement Company	Inorganic fibers suitable for filters.
OEMsr–226	University of Illinois	A study of the preparation of compound 1120, particularly through the use of a regenerative chemical.
OEMsr–236	University of California	The production and stabilization of smokes and fogs.
OEMsr–251	University of Michigan	Mechanical formation of smokes, including the formation of toxic smokes and screening smokes by means of large-scale, high-pressure sprays.
OEMsr–272	Tennessee Eastman Corporation	Preparation of superfine organic fibers of 1 or 2 microns diameter.
OEMsr–282	Northwestern University	The study of properties of absorbents for certain toxic gases and of the behavior of absorbents, and other studies, and to equip, staff, and operate a laboratory for these purposes. *Supplement 1:* Conducting studies and experimental investigations in connection with (i) the properties of absorbents for certain toxic gases and the behavior

Contract No.	*Contractor*	*Subject*
		of absorbents, (ii) the preparation of certain toxic gases, (iii) the development of oxygen-breathing equipment and carbon impregnated clothing, (iv) the assembly and operation of a small pilot jiggler activation unit, (v) the operation of a small-scale pilot plant for the experimental production of crude char from domestic raw materials, with special emphasis on color as part or all of the raw material, (vi) the determination of factors affecting the field use of chemical warfare agents, and (vii) the behavior, productive value, and design of canisters. *Supplement 2:* Extension of time. *Supplement 3:* (viii) Method of impregnation of charcoal on a pilot plant scale. *Supplement 4:* Extension of time. *Supplement 5:* (i) The properties and preparation of activated charcoals and whetlerites, (ii) rebreathers, and (iii) the field use of chemical warfare agents. *Supplement 6:* (i) The preparation and properties of charcoals and whetlerites, (ii) canister testing and design, (iii) field use of chemical warfare agents. *Supplement 7:* Extension of time. *Supplement 8:* (i) The preparation and properties of charcoals and whetlerites, (ii) canister testing and design, (iii) field use of chemical warfare agents, and delivery of models of such equipment as may be developed and samples of such absorbents as may be produced. *Supplements 9, and 10:* Extension of time.
OEMsr-299	University of Illinois	A study of the preparation of compound 1120, particularly through the use of a regenerative chemical. *Supplements 1, 2:* Extension of time. *Supplement 3:* (i) The preparation of a certain compound and derivatives for use as war gas, and (ii) modified fillings for smoke munitions. *Supplement 4:* Extension of time.
OEMsr 345	Owens-Corning Fiberglas Corp.	Electrical dispersion of oil, clay, and other materials to produce a screening smoke.
OEMsr 349	Columbia University	Analysis of adsorption wave in gas adsorbents. *Supplement 1:* Extension of time.
OEMsr–376	American Viscose Corporation	The development of very fine filaments for use as gas mask filters. *Supplement 1:* Extension of time and addition of funds.
OEMsr–405	Massachusetts Institute of Technology	Methods of formation of toxic smokes. *Supplement 1:* Extension of time.
OEMsr–414	E. I. Du Pont de Nemours	Development of an electrolytic fluorine generator that will produce one pound of fluorine per hour. *Supplement 1:* Addition of funds.
OEMsr 539	University of California	The production of screening smokes and fogs without the use of large compressors, and the stabilization of such smokes and fogs under field conditions. *Supplement 1:* The production of screening smokes and fogs without the use of large compressors, and the stabilization of such smokes and fogs under field conditions, and the stability and persistence of toxic smokes or simulated agents. *Supplements 2, 3:* Extension of time. *Supplement 4:* (i) The production of screening smokes and fogs without the use of large compressors, (ii) the stabilization of such smokes and fogs under field conditions, (iii) the stability and persistence of toxic smokes or simulated agents, and (iv) field methods of dispersing chemical warfare agents. *Supplement 5:* Extension of time.
OEMsr–548	University of Rochester	The use of two gases simultaneously or in sequence in chemical warfare. *Supplement 1:* The use of two gases simultaneously or in sequence in chemical warfare, (ii) the performance of whetlerite against cyanogen chloride. *Supplement 2:* (i) The use of two gases simultaneously or in sequence in chemical warfare, (ii) the performance of whetlerite against cyanogen chloride, and (iii) new methods of impregnation of charcoal.
OEMsr–578	DeVilbiss Company	Development of stationary oil smoke generators. *Supplement 1:* (i) Development of stationary oil smoke generators, (ii) the development of motor truck smoke generators. *Supplement 2:* Extension of time. *Supplement 3:* (i) Stationary oil smoke generators, (ii) small portable oil smoke generators, (iii) exhaust-type oil smoke generators for aircraft, and (iv) modification of the color of the smoke produced by oil smoke generators of any type. *Supplement 4:* (i) Stationary oil smoke generators, (ii) small portable oil smoke generators, (iii) exhaust-type oil smoke generators for aircraft, (iv) modifica-

Contract No.	*Contractor*	*Subject*
		tion of the color of the smoke produced by oil smoke generators of any type, and (v) smoke generators operated by steam. *Supplement 5:* Extension of time.
OEMsr–580	Carnegie Institute of Technology	Methods of production and activation of gas charcoal. *Supplement 1:* (i) Methods of production and activation of gas charcoal, (ii) the pre-impregnation of charcoal with metallic compounds prior to activation, and (iii) the activation of such pre-impregnated charcoal. *Supplement 2:* Extension of time and addition of funds.
OEMsr–586	University of Chicago	The physical chemistry of the activation of charcoal. *Supplements 1, 2, 3, 4, 5:* Extension of time.
OEMsr–587	Massachusetts Institute of Technology	The use of sulfur to produce screening smokes. *Supplements 1, 2:* Extension of time.
OEMsr–588	Massachusetts Institute of Technology	The development of fluorine generators and their use in the preparation of certain mechanical compounds. *Supplement 1:* Extension of time.
OEMsr–599	University of Illinois	The physical form of activated charcoal and whetlerite with the use of the X-ray and the electron microscope. *Supplement 1:* (i) The physical form of activated charcoal and whetlerite with the use of the X-ray and the electron microscope, and (ii) the behavior of smoke and gas clouds in built-up sections of cities. *Supplement 2:* (i) The physical activated charcoal and whetlerite with the use of X-ray and electron microscope, (ii) the determination of factors affecting the preparation and performance of whetlerite, and (iii) the behavior of smoke and gas clouds in built-up city areas and woods.
OEMsr–603	Distillation Products, Inc.	(i) The design of generators for production of screening smokes, (ii) vapor pressures of oils suitable for liquid smokes, and (iii) additives to increase the persistence of liquid smokes.
OEMsr–660	University of Rochester	The interpretation of data on absorbents.
OEMsr–676	Chemical Process Company	The preparation of resins as gas absorbents. *Supplements 1, 2:* Extension of time.
OEMsr–713	Gaertner Scientific Corporation	Construction of 4 models of an instrument to determine the particle size of smoke. *Supplements 1, 2:* Extension of time.
OEMsr–861	California Institute of Technology	To conduct field studies of agents and weapons for chemical warfare including meteorological investigations to determine the conditions for the use of chemical warfare agents, and to develop such instruments as may be necessary for conducting such studies. *Supplements 1, 2, 3, 4, 5:* Extension of time.
OEMsr–889	Williams Oil-O-Matic Company	The development of smoke generator using a minimum amount of strategic materials, and such oils as are available to produce a smoke which may be darkened for use in night screening operations. *Supplements 1, 2:* Extension of time.
OEMsr–917	Harvard University	The preparation of certain extremely pure inorganic chemicals.
OEMsr–948	Victor Chemical Works	The improvement of the performance of WP munitions. *Supplements 1, 2:* The improvement of WP munitions by physical and chemical modification of the WP loadings. Construction and operation of a pilot plant for preparing 1200 pounds to 1500 pounds per day of PWP shell filling (as developed under Contract OEMsr–102, University of Illinois) and for loading munitions with this material.
OEMsr–963	E. I. du Pont de Nemours and Company	The dispersion of finely powdered solid materials, especially surface treated materials as aerosols, both by jet dispersion and explosion, and the evaluation by physical and physical-chemical tests of the properties of the aerosols produced. *Supplement 1:* The preparation of aerosols of solid materials, and the reduction of solid organic materials to suitable particle size for aerosol formation. *Supplements 2, 3, 4:* Extension of time.
OEMsr–1004	University of California	The methods of (i) lowering the inflammability of hydrogen cyanide, (ii) stabilizing cyanogen chloride, and (iii) preparing special inorganic compounds. *Supplement 1:* Addition of funds. *Supplement 2:* The methods of (i) lowering the inflammability of hydrogen cyanide, (ii) stabilizing cyanogen chloride and hydrogen cyanide, and (iii) preparing special inorganic compounds.
OEMsr–1021	Hercules Powder Company	(i) The development of a filling for smoke pots, grenades, floats, etc., consisting of a combustible mixture such as black powder intimately mixed with either high-boiling oil or granulated sulfur, (ii) the development of containers in which this mixture can be burned efficiently, and (iii) the development of a process for manufacture of the mixture in quantity.

Contract No.	*Contractor*	*Subject*
		Supplements 1, 2, 3, 4, 5: Extension of time.
OEMsr–1150	The Heil Company	(i) Improvement in design and performance of the DeVilbiss model SCE smoke generator, and (ii) engineering development work on other smoke generators.
OEMsr–1200	National Carbon Company, Inc.	The improvement of activated charcoals (particularly the zinc chloride type) and whetlerite. *Supplement 1:* Extension of time.
OEMsr–1243	Iowa Institute of Hydraulic Research	Studies and experimental investigations in connection with the circulation of air in situations such as would be encountered (i) in the application of certain methods for the dissipation of fog over airfields, and (ii) in the use of gas warfare. *Supplement 1:* Extension of time and addition of funds. *Supplement 2:* (i) Circulation of air in situations such as would be encountered in the application of certain methods for the dissipation of fog over airfields, and in the use of gas warfare, (ii) the improvement of equipment used in the dissipation of fog over airfields. *Supplement 3:* Extension of time. *Supplement 4:* (i) Circulation of air in situations such as would be encountered in the application of certain methods for the dissipation of fog over airfields, and in the use of gas warfare, (ii) the improvement of equipment used in the dissipation of fog over airfields, and (iii) local winds and cloud cover over selected Japanese target areas using small-scale models in a wind tunnel. *Supplement 5:* Extension of time and addition of funds.
OEMsr–1277	Delco Appliance, Division of General Motors Corporation	(i) Development of, from partially completed models supplied by Columbia University under Contract OEMsr–148, one or more finished designs of light-weight, combustion-type oil smoke generators of approximately 50 gal/hr capacity, eliminating if possible the use of water as an operating fluid, (ii) fabricate 3 or more replicas of the preferred design for tests by the Armed Services, and (iii) conduct research on further smoke generators or other related equipment. *Supplements 1, 2, 3, 4, 5, 6, 7:* Extension of time.
OEMsr–1334	E. I. du Pont de Nemours and Company	Ultra fine cellulose acetate fiber-batt and the production of 100 sq ft thereof.
OEMsr–1388	Columbia University	(i) The production and evaluation of aerosols for killing insects, (ii) a method of evaluating smoke generated by smoke signals, and (iii) the production of colored smokes. *Supplements 1, 2, 3, 4, 5, 6, 7:* Extension of time and addition of funds.
OEMsr–1446	Solar Aircraft	The development of devices for the generation and dispersion of screening smoke and insecticidal aerosols on the service-type airplanes. *Supplements 1, 2, 3:* Extension of time.

SERVICE PROJECT NUMBERS

The projects listed below were transmitted to the Executive Secretary, National Defense Research Committee, NDRC, from the War or Navy Department through either the War Department Liaison Office for the NDRC or the Office of Research and Inventions (formerly the Coordinator of Research and Development), Navy Department.

Service Project No.	*Subject*
AC–108	Spraying Equipment for DDT.
AC–125	Japanese Weather Model Studies.
CWS–1	Aerosols, Generation, and Precipitation. Collection of fundamental scientific information on the dissemination of particulate clouds from solid materials, and carrying out of experimental work upon which to base further improvement of munitions employed to generate smokes and the development of improved protective devices used for the removal of smoke particles from the air. Extended to include dispersion of fogs. Extended to include Dispersal of Insecticides and Rodenticides. Extended to include Development of a Smoke Generator incorporating either a preheating system for the oil or a secondary combustion system for the exhaust gases.
CWS–7	Fundamental Study of Gas Mask Absorbents. The collection, evaluation, and testing of all available information influencing the design of gas mask canisters. The formulation of rules from the data collected with a view to simplifying the manufacture of such equipment.
CWS–8	The Generation of Colored Smokes. The study and development of more efficient means of disseminating colored smoke clouds, particularly black and orange, for certain marking purposes.
CWS–15	Improved Filter Materials. To devise detailed methods of improving the manufacture of existing types of filter materials, especially with the view of reducing the effect of high humidity upon the filter and for increasing the filtration of liquid smoke particles.
CWS–16	Improved Filter Design. To redesign the filter of the gas mask canister so as to provide for the maximum filter surface with the best filter material.
CWS–17	Production and Stabilization of a Fog. Part *a:* Extended to include a project to color the smoke produced by the unit developed by Dr. I. Langmuir. Part *a:* Transferred to NS–123.
CWS–24	Development of Protective Cloth. To develop a charcoal impregnating cloth with a binding agent other than rubber or synthetic rubber which will give better protection against chemical agents for which the present clothing does not give good protection of the present clothing against the agents for which there is now ample protection.
CWS–26	Meteorology Applied to Chemical Warfare. The accumulation and evaluation of micrometeorological data and the determination of the behavior of chemical warfare agents under various climatological and terrain conditions and the development of suitable instruments.
CWS–27	Simple and Unusual Munitions for Setting up Field Concentrations of Chemical Warfare Agents.
NA–106	Oxygen Breathing Apparatus. Development of oxygen breathing apparatus for use with liquid oxygen. Studies and experimental investigations in connection with the development of indicating instruments for determining low concentrations of noxious gases in air.
NA–164	Dissipation of Fog Over Airfield Runways, Development of Means of.
NE–104	Development of an Accurate Method of Evaluating Smoke Generated by Smoke Signals.
NL–B1	Problems Related to the Manufacture and Use of Potassium Peroxide in Oxygen Breathing Equipment. a. The production of K_2O_4 from Potassium compounds, avoiding the use of metallic potassium or sodium. b. Sources of cheap metallic potassium. c. Vapor-liquid equilibrium data for sodium-potassium. d. Development of an alloy to withstand liquid alkalies at 600–800°. e. Nitrogen fixation at −30°C for elimination of nitrogen from oxygen breathing equipment at high altitudes. f. Development of an instrument for the measurement of oxygen partial pressures. g. Reactant to remove carbon dioxide and water vapor from air at −30°C.

Service Project No.	*Subject*
	h. Reactant evolving heat on contact with carbon dioxide or water vapor at low temperatures by Trigger reactant for K_2O_4.
	i. Physiological performance tests of oxygen rebreather equipment development of improved masks.
NL–B11	Colored Smokes.
NL–B26	Analytical Methods and Technique for Determining the Protective Properties of Gas Mask Canisters Against Mustard Gas, Phosgene, Chloropicrin, Hydrogen Cyanide, Arsin, and such other Gases as may possibly be used in Chemical Attack.
	Replaced by NS–338.
NL–B28	Development of a Better Chemical than "Whetlerite" for Filtering of Neutralizing Toxic War Gases Particularly Under Conditions of High Temperature and Humidity Combined with Salt Spray.
	Replaced by NS 338.
NL–B29	Check the Efficiency of the New Charcoal Developed by the Chemical Warfare Service in Comparison with Coconut Shell Charcoal with Particular Consideration of Conditions of High Temperature and Humidity Combined with Salt Spray.
	Replaced by NS–338.
NL–B34	Improved Methods of Measurement for Study of Protection Given by Filters Against Smokes at High Humidities.
	Replaced by NS–338.
NM–100	Dispersal of DDT.
NO–276	Colored Smokes for Target Identification and Sea Markers.
NO–292	Consulting Service on Design and Construction of PWP Loading Plant.
NS–123	The Coloring of Smoke from a Langmuir Unit.
NS–150	Combustion Gas Type Smoke Generator. Desired to fulfill the following requirements: 1. Burn as fuel a liquid which is in common use by the Navy. 2. Make optimum smoke at a combustion rate of about 300 to 400 gallons per hour.
NS–338	Investigation of Respiratory Protection. To cover work not only on gas absorbents, but also on canisters, facepieces, speech diaphragms, outlet valves, filters, and methods of protection against any new type of agent.
SG 6	Investigation of the Chemistry of Insecticides and Repellants. Devise analytical procedures for determining the constituents present in DDT, to isolate, characterize and synthesize these constituents so that their relative toxicity can be determined and to study practical methods of purification. Other insecticides and repellants will be included in the scope of the investigation.

INDEX

The subject indexes of all STR volumes are combined in a master index printed in a separate volume. For access to the index volume consult the Army or Navy Agency listed on the reverse of the half-title page.

Absorption properties of colored particles, 332
Absorption vs. adsorption, 9
Acids as war gases, 152–165
Acoustical forces as precipitation factors
  see Aerosol coagulation by sound vibration
Activated charcoal
  hydrogen and oxygen content, 36
  packet structure, 35
  pore structure, 35
  substitutes, 84–87
Activated charcoal, manufacture, 23–39
  Cabot Co. carbon black processes, 29–30
  coconut charcoal, 31
  commercial manufacture, 31–32
  history, 23
  Jiggler method of activation, 37
  Kimberly-Clark Co., 30–31
  Pittsburgh Coke and Chemical Co., 27–28
  Prest-o-log process, 28–29
  Saran charcoal, 31
  summary, 23–24
Activated charcoal, properties
  see Charcoal characteristics, measurement; Charcoal structure
Activated charcoal, raw ingredients, 24–26
  bituminous coal, 25
  coconut, 25
  esoteric materials not needed, 26
  lignin, 25
  nut shells, 25
  requirements for materials, 24
  sawdust, 25
  synthetic materials, 25
  tests for raw material, 26
Activation of charcoal by chemicals, 38–39
  chemical method requirements, 38
  mechanism of activation, 39
  zinc chloride process, 38–39
Activation of charcoal by steam, 31–37
  activation rate, 37
  carbonization, 33–34
  crushing and briquetting, 32–33
  final step, 34
  process variables, 34–35
  summary, 23–24
  surface complex formed during activation, 131–132
  temperature control, 35
  weight loss, internal vs. external, 36
Acyl chlorides as war gases, 609
Adamsite smoke, 362
Adiabatic lapse rate
  effect on stability, 383
  influenced by convection, 219
  normal rate, 213
  saturated rate, 214
  super-lapse, 215
Adsorption, relation to molecular structure, 134–140
  adsorption data for gases, 135
  entropy term estimated, 136–137
  experimental data, 138–139
  integral heat of adsorption, calculation, 137–140
  molecular size, 108–109
  pressure of adsorbate, 135–136
  temperature of adsorption, 135
  thermodynamic equation, adsorption of gas on solid, 136
Adsorption heat, acid on charcoal surface, 142
Adsorption isotherms, surface area measurements, 97–99
  adsorption as function of relative pressure, 98–99
  adsorption data equation, 97
  applications of method, 98–99
  Harkins and Jura's work, 98
Adsorption method, porous area measurements, 97–99
Adsorption of vapors by charcoal, 140–142
  carbon tetrachloride adsorption, 141–142
  chloropicrin adsorption, 140
  isopiestic technique in adsorption studies, 141
  4-picoline adsorption, 141
  pyridine adsorption, 141
Adsorption of water vapor from charcoal, 102–108
  adsorption vs. capillary condensation, 105–107
  density of water in charcoal, 107
  equilibration, charcoal with water vapor, 105
  freezing method studies of adsorbed water, 107
  hysteresis, 103, 106
  nature of water adsorption, 105–108
  nature of water in capillaries, 107–108
  nitrogen adsorption studies, 107–108
  oxygen surface complexes, 128
  rate of adsorption, 104–105
  water adsorption isotherms, 102–104
Adsorption vs. absorption, 9
Adsorption wave, 169–182
  canister life equations, 181–182
  curvature, adsorption isotherm, 173
  factors affecting break time, 174–180
  reasons for study of wave, 169–170
  speed of adsorption, 170
  steps in removal of toxic gas from air, 169–170
  summary, 182
  symbols used in study, 182
Adsorption wave theories, 170–174
  diffusion as rate-controlling step, 171–173
  effluent concentration curve, 170
  general differential equation, 170–171
  removal rate determined by more than one step, 173
  surface reaction as rate-controlling step, 172–173
  theories compared with experiment, 173–174
  variables effecting removal rate, 171
Aedes aegypti, DDT test mosquitoes, 581–583
Aerograms (thermodynamic graphs) 214
Aerosol cloud evaporation, 412–419
  boundary curves of concentration in cloud, 417
  effect of nonvolatile impurities, 414–415, 418–419
  effect of temperature on vapor concentration, 413
  evaporation equations, 415–417
  maximum drop size for saturation maintenance, 413–414, 417–418
  nomenclature, 418–419
  persistence dependent on saturation, 412–413
  smoke cloud evaporation, 386–387
Aerosol coagulation, 305–308
  see also; Aerosol settling
  Brownian motion, 305–306
  concentration gradient, 305–306
  homogeneous aerosol coagulation, 306
  law of atmosphere, 305–306
  stirred settling and coagulation combined, 306–308
  summary, 297
Aerosol coagulation by sound vibration, 309–313
  attraction of particles due to air motion, 311–312
  laboratory experiments, 312

Carbon monoxide reaction with aminated resins, 86
Carbon tetrachloride adsorption by charcoal, 141
Carbons for gas mask filters
see Activated charcoal
Carbon-smoke penetrometer, 373
Cardox gas-ejection bomb, 542
Cascade impactor, collection of insecticide samples, 599
Catalytic actions of activated charcoal, 52–53
Centrifugal forces, aerosol coagulation, 302
Centrifugal separation, 335–336
Charcalite drier, 203–204
Charcoal, activated
see Activated charcoal
Charcoal as thermal generator fuel
see Thermal generator fuel blocks
Charcoal characteristics, measurement, 97–149
adsorption and molecular structure, 134–140
adsorption of vapors, 140–142
adsorption of water vapor, 102–108
chemisorption of gases by whetlerites, 144
heats of adsorption and immersion, 142–143
influence of pore size on performance, 117–121
oxygen surface complexes, 125–132
pore size alteration, 121–125
pore size and distribution, 108–117
retentivity, 143–144
summary, 147–149
surface coatings, 132–134
Charcoal impregnation, 40–87
absorbent resins as activated charcoal substitutes, 84–87
catalytic reactions, 52–53
compounds used as impregnants, 53–55
copper-silver-chromium impregnants, 64–81
hexamine impregnation, 48–50
iodic acid impregnation, 56
mercury impregnation, 56
molybdenum and vanadium impregnation, 57–64
organic base impregnations, 81–84
reactions during adsorption process, 53
thiocyanate impregnations, 50–52
vapor phase impregnation, 56
whetlerites, 40–41
Charcoal pore size, alteration, 121–125
chromium oxide treatment, 124–125
hydrogenation without impregnation, 123
influence of impregnants on alteration, 124–125
iron oxide treatment, 124–125
nickelous oxide treatment, 125
partial oxidation without impregnation, 124
steaming without impregnation, 123
Charcoal pore size, influence on performance, 117–121
free volume of pore as efficiency criterion, 118–119
macropore volume and cyanogen chloride activity, 119
pore measurements and cyanogen chloride lives, 118–119
pore measurements and noxious gases, 120–121
terminology, 117
Charcoal pore size, measurement, 108–117
Kelvin equation, 109–112
mercury forced into charcoal, pressure measured, 114–117
molecular size as criterion, 108–109
surface area changes from water take-up, 113–114
water adsorption and desorption isotherms, 112–113
Charcoal structure, 145–147
chemical behavior, 146
cylindrical capillaries, 146
electron microscope observations, 146
expansion during adsorption, 146
microscopic study, 145
platelet arrangement of carbon in charcoal, 145
pore shape, 145
speculative nature of studies, 145
true density of carbon in charcoal, 146–147
X-ray study, 145
Charcoal surface area measurement, 97–102
adsorption method of measurement, 97–99
methods, 99–101
performance predictions from measurements, 101–102
Chemical activation of charcoal, 38–39
Chemical behavior of charcoal, 146
Chemical bombs, 424–441
see also E29R1 chemical bomb
basic dosage equation, 430
choice of size and dosage, 430
dosage distribution, 430–432
effect of meteorological conditions, 430–431
integrated crosswind dosage, 430
munitions' effectiveness, 431–432
target area covered by given dosage, 429–430
Chemical removal of gases, 150–168
acid-forming gases, 152–165
base-forming gases, 165–166
gases retained by physical adsorption, 151–152
purpose of investigation, 150
readily oxidizable gases, 166–168
readily reducible gases, 168
steps in removal process, 169–170
Chemisorption of gases by whetlerites, 144
Chloride smoke screen mixtures, 488–494
anhydrous ferric chloride manufacture, 491–492
chloride complexes, 492–493
chlorine carriers, 490–491
chloropropane, 494
development of mixtures, 488–490
ferric chloride and aluminum mixture, 491–492
high efficiency mixtures, 493–494
stability of mixtures, 491
Chlorine surface complexes on charcoal, 133
Chloropicrin
adsorption on charcoal, 140
canister protection against chloropicrin, 200
effect of gas mixture's humidity, 151
nature of desorbed product, 151
rate of removal, 179
reaction with base charcoal and whetlerites, 151
Chloropicrin gas test
disadvantages, 19
operation, 18
use, 13
Chloropropane, smoke screen use, 494
Chromium adsorption from whetlerite solutions, 73–74
copper chromate removal of cyanogen chloride, 73–74
precipitate formation, 73
valence state of impregnant, 73–74
Chromium impregnated charcoal, 62
Chromium oxide as charcoal impregnant, 124–125
Clausius-Clapeyron equation, applied to whetlerite solutions, 68
Clouds of smoke
see Smoke clouds
Clouds of toxic gases
see Gas clouds
Coal, use in manufacture of activated charcoal, 25
Coconuts, gas mask charcoal material
deficiencies, 23

improvement process, 31
performance, 25
Color of light transmitted through fog, 350
Colored particles as light scatterers, 332–333
absorption characteristics, 332
calculation tables, 333
color distribution, 321–322
color of transmitted light, 333
dye smoke particle size, 333
multiple scattering, 333
optical density of pure dye smoke, 333
Colored smoke identification bomb, 455–458
components, 456–457
dyes, 458
flaming control, 457–458
fuel block formulas, 461
nylon parachute, 457
operation, 456
Colored smoke signal, 451–455
construction, 453–454
development, 451–452
dye chamber, 454–455
fuel block formulas, 461
operation, 454
proposed design, 454
specifications, 451
theory, 452
Contrast limen, smoke screens, 389–392
conditions approaching extinction, 390
light extinction by fog, 389–390
light extinction by screening smoke, 390
visibility dependent on concentration, 390
visibility formula, 390–392
visibility in natural fog, 389
Convection, vertical air movement, 219–220, 385–386
Convection currents in aerosol settling process, 303
Convective ceiling, smoke clouds, 385
Copper Carbonite, 41
Copper compounds, effect of dehydration and evaporation, 41
Copper impregnated charcoal
see Whetlerites
Copper-silver-chromium whetlerites, 64–81
ammonia evolution, 78
compared with molybdenum whetlerites, 61–62, 64
conversion, one whetlerite to another, 81
effect of base charcoal, 74
leaching and rewhetlerization, 79–80
metallic constituents, 67
removal of gases, mechanism of, 74–76
Copper-silver-chromium whetlerites, aging, 75–76
aging under field conditions, 76
canister design, effect on aging, 76
charcoal surface, effect on aging, 75–76
nature of aging process, 75–76
organic base additions, 82–84
*p*H factor, effect on aging, 75
storage in closed containers, 75
Copper-silver-chromium whetlerites, production, 76–78
air flow, 77
back feeding, 78
charge temperature, 77
drier, 68, 77
flue gas, 78
impregnator, 76
temperature schedule, 77
Copper-silver-chromium whetlerites, solutions, 64–74
ammonia and carbon dioxide concentration, 66
chromium adsorption, 73–74
copper and chromium concentrations, 64–66
heats of solution, 71
laboratory impregnation, 68
metallic constituents, 66–67
preparation, 67
vapor pressure, 68
volatile constituents, 71
Coronae measurements, light beam in fog, 347–348
"Critical bed depth," gas, 177–182
approximation methods of determination, 181–182
depth due to diffusion, 177–178
depth due to granular processes, 178
mechanism of removal, 179–180
nature of adsorbent, 180
variation with velocity of flow, 178
Cunningham correction coagulation equation, 306
CWS-MIT-E1 canister tester, 372
CWS-MIT-E2 photoelectric smoke penetrometer, 367
Cyanogen chloride
canister protection, 198–199
conductimetric analysis, 285
lives of gas masks, 92, 118–121
properties and reactions, 55–56
protection of hexamine impregnated adsorbents, 50
protection of thiocyanate impregnated whetlerites, 51
reaction with organic bases, 81–82
surveillance, 91
Cyanogen chloride removal mechanism, 161–164
complexity of mechanism, 161
copper oxide role in reaction, 161
hydrolysis, 163–164
metal oxides, 162
oxidation, 163–164
physical adsorption process, 161
removal from whetlerites, 74
whetlerites for cyanogen chloride protection, 162–163
Cyanogen chloride stabilization, 613–617
acidity determination, 616
deterioration mechanism, 615–616
deterioration products, 617
polymerization tendency, 613
research history, 613–614
substances harmful to cyanogen chloride, 614
substances inert to cyanogen chloride, 614–615
substances stabilizing cyanogen chloride, 615
summary, 617
temperature, effect on deterioration, 616
water content determination, 617
Cyclohexyl monofluorophosphate, 607

DDT dispersal, 577–603
atomization by sprays, 407–408
conclusions and summary, 601–603
formulations, 598–599
mathematical symbols, 602–603
nonvolatile solvent required, 598
recommendations for use, 601–603
research recommendations, 601
DDT dispersal, aircraft equipment, 593–598
airplane exhaust generators, 593–596
historical summary, 593
insecticide bombs, 598
plane's downwash, effect on dispersal, 587–588
spray devices, 596–598
summary, 602
DDT dispersal, assessment methods, 599–601
airborne dosage of particle size, 600–601
entomological results as final evaluation, 601
samples collected by impaction, 599–600
samples collected on slides, 599–600
samples collected on vertical wires, 601
DDT dispersal, ground equipment, 588–593

exhaust generators for motor vehicles, 591–592
Freon bomb, 588
Hochberg-LaMer type generators, 588–591
thermal candles, 592
DDT dispersal, optimum particle size, 578–588
contact-kill particle size, 578–583
deposition on insect, wind tunnel studies, 582–583
dosage-mortality graphs, 581
foliage density as dosage determinant, 586–588
meteorological conditions as dosage determinant, 584–586
pre DDT research, 578
residual kills, 583–584
resting vs. flying mosquito, 578–580
summary, 601
uniform particle size aerosols, 581
DDT dispersing bomb, 524–527
atomization of liquids by explosive bursts, 524–526
design and manufacture, 526–527
droplet spectra from chargings, 525
Desorption isotherms, charcoal pore size measurements, 109–113
adsorption vs. desorption on nitrogen, 109–112
Kelvin equation, 112–113
Desorption tests, gas masks, 19
Dialkylmonofluorophosphates, 606–608
cyclic esters, 607
isopropyl ester, 607
preparation, 606–608
properties, 608
toxicity tests, 607
Diaphragm pump sampler, gases, 286–287
Dichlorobenzene, Olsen bomb use, 532
Differential settler, smoke measuring instrument, 341–343
Diffraction rings, light beam through fog, 347–348
Diffusion
as rate-controlling step in toxic gas removal, 171–172
atmospheric diffusion, 380, 384
control of "critical bed depth" of gases, 177–178
eddy diffusion, 380
gas diffusion, 173, 633–638
kinetic vs. thermal diffusion, 297
Dimethylaminophosphorusdifluoride, 609
1,2-dinitro-tetrafluoro-ethane, 157
Dioctylphthalate, smoke material, 361
Diol fog, light beam observations, 326
Diol-sawdust-chlorate smoke mixtures, 497–499
Diphenylchloro arsine tests, 362
Disulfur decafluoride, 604–606
action of fluorides on sulfur compounds, 605
chemical detection, 606
controlled reaction of fluorine and sulfur, 604–605
fluorination of sulfur chlorides, 605
preparation, 604–605
properties, 605–606
thermal stability, 605
Droplet dispersing bombs, 524–533
bombs containing dissolved gas in liquids, 530–533
DDT dispersing, plastic bomb, 524–527
drop size distribution, 399–402
ejection-airburst bomb, 527–530
Droplet formation by nozzles, 398
Drosophila melanogaster, DDT test flies, 582–583
DS-4 colored smoke signal, 451–455
Dugway recording instruments, 255–259
Dust
particle size, 301
properties; *see* Aerosol
retention in lungs, 535
Dye smokes
colored smoke screens, 392
floating, smoke signals, 454–455
optical density, pure dye smoke, 333
particle size, 333
requirements for colored smoke munition, 458

E-20 nonfloating oil smoke pot, 445–446
E-21 training oil smoke pot, 446–447
E-23 floating oil smoke pot, 441–445
E29R1 chemical bomb, 424–441
bomb size choice, 429–432
chemical efficiency, 428–429
feeding of agent to gas stream, 433
field test, 440
50-lb nonclustering bomb, 432
fuel block formulas, 461
high-velocity vaporizer, 433–435
recommendations for improvement, 440
thermal generator characteristics, 424–425
thermal generator cluster, 432
E29R1 chemical bomb, construction, 425–428, 435–439
agent feed system, 436
bomb body, 425–426
bomb tail, 427
booster tube powder, 435–436
centrifugal arming fuze, 428
cloth streamer tail, 436
clustering bands, 436
coating on agent compartment, 436–437
folding metal tail, 437
fuel block, 426–427
metal telescoping tail, 427–428, 438–439
sealing of fuel and ignition system, 439
streamer tail with shroud line, 437–438
Earth temperature, 216–218
albedo effect, 218–219
black-body temperature, 217
diurnal variation, 218
ocean temperature, 218
radiation of solar energy, 216–217
soil below earth's surface, 218
surface moisture effect, 218
Eddy currents, 637–638
Eddy diffusion, 380
Eddy velocity, 220
Edgewood Arsenal, E3 canister tester, 371–372
"Effective scattering area" of drop, 390
Egg albumen, toxic agent simulant, 535–536
suitability for testing, 535
treatments to improve dispersibility, 536
use in bomb dispersal efficiency tests, 541
Ejection-airburst vesicant bomb, 527–530
advantages, 527
hexagonal bomb, 528–529
round bomb, 529–530
EK-1 vesicant dispersing bomb, 528–529
EK-4 vesicant dispersing bomb, 529–530
Electrical properties of aerosols
effect of filtration, 313
homogeneous smoke charge, 308
summary, 299
unipolar smoke charge, 309
Electron microscope, 335
Entropy term, gas adsorption, 136–137
Esterline-Angus meters, wind recorders, 256–257
Ethylenimine, mechanism of removal, 166
Evaporation capacity of exhaust gases, 507–509
enthalpy of oil and vaporization, 509
equilibrium saturation temperature, 508
weight of oil per exhaust gases, 508
Evaporation of aerosols
see Aerosol cloud evaporation

Evaporation of vapor drops, 386–387
Exhaust generator for airplanes
see Airplane exhaust generator
Exhaust generators for motor vehicles, 591–592
Explosions, atomization of liquids, 408–410
atomization mechanism, 408–409
drop size distribution, 409–410
explosive bursts, 524–526
German bursters, 408

F-7 thermal generator candle, insecticide use, 592
F7A mustard generator pot, 419–425
condensate composition, 422–423
experimental models, 421–422
field tests, 423–424
fuel block formulas, 461
operation, 420–421
Ferric chloride mixtures, smoke screen use, 491–493
Fibers used in aerosol filters, 191–193
asbestos, 192–193
glass wool, 191
organic fibers, 192
rock wool, 191
summary, 5
Field canister tester, 292–293
Field conductivity analyzer, gases, 289–291
Filtration of aerosols, 190–193, 354–359
clogging, 358
diffusion mechanism vs. inertial effects, 356–357
direct interception, 354
effect of aerosol electrical properties, 313
effect of particle size, 313
electrostatic filters, 191, 358–359
force resisting motion of particle, 355
foreign filters, 190
impingement of small particles, 356
Stokes' law deposition, 355
summary, 299–300
theory, 356–357
velocity effect, 357
Filtration of aerosols, materials
asbestos, 192–193
fiber content, 191
fiber diameters, 354–355
glass wool, 191, 357
organic fibers, 192
rock wool, 191, 357–358
synthetic fibers, 358
Flies, DDT test subjects, 582–584
Flow of fluids through granular solids, 174–175
Flow rate in gas mask testing, 14–15
breather pumps, 15
British vs. U. S. tests, 15
human breathing, 14–15
intermittent flow testing, 14–15
tube tests, 15
Fluid motion studies
see Wind tunnel studies
Fluorides, mechanism of removal, 156–158
arsenic trifluoride, 157
boron trifluoride acetonitrile, 157
1,2-dinitro-tetrafluoro-ethane, 157
phosphorous trifluoride, 156
phosphoryl trifluoride, 157–158
sulfur pentafluoride, 157
sulfuryl chloro-fluoride, 156–157
Fluorine and sulfur reactions, 604–605
action of fluorine on sulfur compounds, 605
controlled reaction, 604–605
nonelectrolytic method, fluorine preparation, 605
sulfur chlorides, fluorination by heavy metal fluorides, 605
sulfur hexafluoride reactions, 605
Fluorine preparation, 610–612
baths at high temperatures, 611
baths at medium temperatures, 610–611
baths at room temperature, 610
hydrogen fluoride-less baths, 611
metal fluorides, decomposition, 610
polarization and anode effect, 611–612
Fluorophosphates, 606–608
alkyldifluorophosphates, 608
alkylmonofluorothiophosphates, 608
cyclohexyl monofluorophosphate, 607
dialkylmonofluorophosphates, 606–608
Fluorosulfonates, 608
Fog
defined, 301
Diol fog, 350
effect on light, 389–390
English fogs, 626
naturally-occurring fogs, 298
oleic acid fogs, 321–322
particle size, 298, 301
production by mechanical atomization, 405–406
properties; *see* Aerosol
stearic acid fogs, 321–322
Fog dispersal, wind tunnel studies, 624–633
burner construction, 629–630
burner studies, 626–630
dispersal methods, 624
heat diffusion analysis, 627–629
relative cost, burners vs. wind curtains, 633
wind-curtains, 630–633
Forest
foliage, DDT lethal dosage determinant, 586–588
temperatures, 234–236
thermal turbulence, 236
"Free volume," charcoal pore volume, 117
Freon insecticide bomb, 588
Frossling's measurements, vaporization rate of droplets, 416
Froude number, measure of gravitational influence, 621–622
Fuch's evaporation equation, 386–387
Fuel blocks for thermal generators, 459–484
ammonium picrate-sodium nitrate fuels, 483–484
cast fuel mixtures, 479–482
fuel mixture formulas, 461
liquid fuels, 484
pressed charcoal fuel mixtures, 462–477
pressed fuel mixtures without carbon, 477–480
smokeless powder fuels, 482–483
surge tester, 464
volume tester, 463–464

Gas adsorption process
see Adsorption wave
Gas clouds, 260–283
atmospheric stability, effect on efficiency of cloud, 260
gravity effects, 268–269
munition efficiency, 260
toxic dosage for given munition, 260
wind speed effect on efficiency, 260
Gas clouds, in urban areas, 281–283
cul-de-sacs, danger from, 283
flow of air in sewers, 282
wind circulation in courtyards, 282
wind circulation in streets, 281–282
Gas clouds, release, 260–264
beach area behavior, 264
cloud travel data, 263
forest area behavior, 263
"line source" release, 260–264
open terrain release, 260–263
Gas clouds, travel theory, 264–268
application to bombs, 266–267
basic formulas, 264–266
disadvantages, 267–268
gas concentration slide rule, 266
Gas clouds from bombs, 269–281
500 lb bombs, 270
1,000 lb bombs, 269–270
2,000 and 4,000 lb bombs, 271
ammunition expenditure, 273–276
casualty production, 272–273
dosage variation with height, 271
multiple bombs, area coverage, 271

multiple bombs in line, 271
munition requirements for desired casualty effects, 272–273
munition requirements for surprise effects, 276
munition requirements for wooded areas, 281
surprise areas, 272
surprise attack objectives, 272–273
uniform coverage of target area, 273
Gas clouds from mortar shells, 277–281
atmospheric stability, 277–278
dosage effect, 278
wind velocity effect, 277
wooded area performance, 279–281
Gas concentration slide rule, 266
Gas diffusion, wind tunnel studies, 633–638
comparison of field measurement and wind tunnel predictions, 636–638
contour patterns of gas released over Japanese village, 637
diffusion after pancake bursts, 637
diffusion as time function, 633
motion pictures of eddy currents, 637–638
relative concentration contours, 634
urban districts, schematic models, 634–636
Gas ejection bomb, 539–543
air bomb, 542
ammunition expenditures, 273–276
Cardox bomb, 542
compared with plastic bomb, 541
development, 539–542
dispersion test, 542
line distribution vs. upwind distribution, 274–276
Gas evolution from charcoals during heating, 128–132
Gas mask canister lives, 175–177, 181–182
break time equation, 181
"critical bed depth", 177–182
effected by moisture, 88–89
life-thickness curves, 175–177
Mecklenburg equation, 176
Gas mask canister tests, 18–22
see also Gas mask canisters, aging programs; Smoke filter testing
desorption tests, 19
field tests, 20
flow rate tests, 18
human tests, 19–20
minican tests, 20
tester simulating breathing cycle, 292–293
types of tests, 18–19
Gas mask canisters, aging programs, 89–90
canisters aged in carriers, 95
cyclic chamber simulation of temperature changes, 89–90
field tests, 90
simulation of climatic conditions at Edgewood Arsenal, 89
Gas mask canisters, design, 183–189
amount of protection, 183–184
breathing resistance, 186–189
effect on whetlerite deterioration, 76
lack of ruggedness, 189
mesh size, effect on resistance and protection, 188–189
radial-flow design, 185
relation of resistance to canister size, 188
relation of weight and protection, 185–186
Gas mask canisters, filters
see Aerosol filtration; Aerosol filtration, materials
Gas mask canisters of World War II, 9–10, 184–185
CBI theater use, 93–94
facepiece canisters, 185
hosetube canisters, 184–185
M1; 10
M1XA1; 9, 10
M9A2; 9
M10; 9–10
M11; 10
New Guinea use, 92–93
radial flow canisters, 9
relative merits of canister types, 184
Gas mask carbon
see Activated charcoal
Gas mask filters
see Aerosol filtration; Aerosol filtration, materials
Gas mask protection, 194–206
carbon monoxide, 203–206
chloropicrin, 200
cyanogen chloride, 198–199
foreign canisters, 194
gas penetration theory, 12–13
hydrogen cyanide, 199
nitrogen dioxide, 201
phosgene, 196–198
Gas mask tests, 12–22
canister tests, 18–22
chloropicrin test, 18
concentration of test gas, 16–17
deficiencies of test methods, 21–22
field testing, necessity for, 208
flow rate, 14–15
hardness test, 20
heat of wetting, 20
humidity, 13–14
indicators, 15–16
layer depth studies, 20
rough handling resistance, 21
screen analysis, 21
temperature, 17
test gases, 13
tube tests, 17–18
Gas masks, 7–22, 194–209
chin type combat mask, 9
combat mask requirements, 8
development during World War II, summary, 207–208
diaphragm masks, 8
face pieces, 8
M2A1, service mask, 8
M2-1-1 training mask, 8
M3-light, service mask, 8
M5-combat mask, 8
Navy mask, 9
optical masks, 8
pre-World War II development, 7
recommendations for future research, 208–209
status in 1945; 11

Gas penetration theory, 12–13
Gases, war
see War gases
Geiger counter, measurement of radioactive elements, 640–642
Generators, thermal
see Thermal generator
German bursters, 408
German gas mask filter research, 190
Glass wool, aerosol filter, 191, 357
Graphs, thermodynamic, 214
Gravity effects on gas clouds, 268–269
Gravity winds, 222–223
Guanidine nitrate, thermal generator fuel, 477–480
Gunpowder smoke pot mixtures
see Smoke pot mixtures, oil and gunpowder
Gustiness, air motion, 220
Gustiness, vanes for measuring, 253–254

Harkins and Jura's work on surface area measurements, 98
Heat conductivity of earth's surface, 217–218
Heat diffusion, 627–629
Heat of immersion, charcoals, 142–143
Heat of wetting, charcoals, 20, 143
Herbicide dispersal, 546–550
areas of high concentration, 548
maximum areas covered by given dosage, 549
munitions for dispersal, 547–548
particle densities, 547
particle size distribution, 546–547
terminal velocities, 547
travel of solid particles, 546

Hexachlorethane, smoke screen use, 488–490
Hexamine impregnation of whetlerites, 48–50
  application process, 49
  cyanogen chloride, 50
  disadvantages, 49
  *p*H factor, effect on impregnants, 49
  salt additions, 49–50
  X-ray studies, 50
Hill's photoelectric smoke penetrometer, 363
Hochberg-LaMer DDT generators, 588–591
  formulas for DDT concentrates, 598–599
  meteorological factors affecting use, 589
  operation principle, 588
  procedures for use, 590
  pumps, 589
  summary, 602
Hopcalite, catalyst, 203–205
  gel type, 204–205
  pre-drying by charcalite, 203–204
  thermal activity, 205
Humidity
  detrimental to canister performance, 88–89
  in gas mask testing, 13–14
  micrometeorological measurements, 255
Hydrocarbons, as antiflash agents, 619–620
Hydrogen chloride, catalyst in cyanogen chloride deterioration, 615–616
Hydrogen cyanide, 618–620
  adsorption by whetlerites, 46–47
  canister protection, 199
  conductimetric analysis, 285
  flame inhibitors, 619
  hydrocarbons as antiflash agents, 619–620
  inflammability, 619
  removal mechanism, 74–75, 158–161
  stabilization, 618–619
Hydrostatic head pump, gas sampler, 284–285
  advantages, 285
  concentration vs. time curve, 285
  construction, 284
  cyanogen chloride analysis, 285
  hydrogen cyanide analysis, 285
  operation, 284
  phosgene analysis, 285

Impregnated charcoal
  see Charcoal impregnation
Indicators for gas mask testing, 15–16
  break point conditions, 16
  choice of test indicator, 15
  physical vs. chemical indicators, 16
Insecticides
  see DDT dispersal
Integral heat of adsorption for gases, 137–140
Iodic acid impregnated charcoal, 56
Ionization penetrometer, Australian, 363
Iowa Institute fog dispersal studies, 626–633
Iron oxide as charcoal impregnant, 124–125

Japanese gas mask filters, 190
Jiggler method of charcoal activation, 37

Katabatic wind, 222
Kelvin equation, pore size measurement, 109–113
  adsorption vs. desorption isotherms, 112
  applied to adsorbates other than water, 109–112
  applied to desorption isotherms, 112–113
  capillary condensation vs. multimolecular adsorption, 109
  drawbacks of method, 109–111
  nitrogen adsorption near saturation, 111–112
Kimberly-Clark Co.
  activated charcoal manufacture, 30–31
  nephelometer, 364–365
  sulfur smoke generator, 449–450
Koenig's equation, force components in sound field, 311–312

Land breezes, 223–224, 383
Larsonite, ammonia impregnated charcoal, 40
Leaching of whetlerites, 78–80
Life-thickness curves of canisters, 175–177
Light beam through fog, 347–348
Light extinction by fog and smoke, 389–390
Light scattered by aerosols
  see Scattering of light
Lignin, raw material for activated charcoal, 25
"Line source" release of gas clouds, 260–264
  beach area release, 264
  forest area release, 263
  open terrain release, 260–263
Liquid droplet dispersing bombs, 524–533
  bombs containing gases dissolved in liquid, 530–533
  DDT dispersing, plastic bomb, 524–527
  ejection-airburst bomb, 527–530
Logarithmic-probability distribution, aerosol size, 304–305
Lungs, retention of dust particles, 535

M2-1-1 gas mask, 8
M2A1 gas mask, 8
M3 gas mask, 8
M5 gas mask, 8
M1XA1 gas mask canister, 9
M9A2 gas mask canister, 9
M10 gas mask canister, 9
M11 gas mask canister, 10
M47A2 bomb filled with plasticized white phosphorus, 561–564
Mach number, measure of elastic effects, 621–622
Macropores, definition, 117
Mass median diameter (MMD)
  aerosol powders, 535, 537–538
  droplets, 401
Mass-concentration meter, 338–339, 362–363
"Mechanical goat," canister tester, 292–293
Mecklenburg equations for canisters, 176
Mercury cup anemometer, 244
Mercury impregnated charcoal, 56, 114–115
Mesh size of canisters, 188–189
Meteorological principles, 213–238, 382–386
  see also Micrometeorology in wooded areas
  air motions, 219
  air-mass effects, 224–225
  atmospheric stability, 213–214
  breezes, land and sea, 223–224, 383–384
  convection, 219–220, 385–386
  DDT lethal dosage, 584–586
  ground layer of air, 214
  ground temperatures, 217–218
  gustiness, 219–220
  radiation effects, 215–217
  stability conditions over water, 382
  stability relations at land-water boundaries, 383–384
  thermal gradient as stability determinant, 383
  thermal stability, 382
  turbulence, 219–220, 382
  wind fluctuations, 220–224
Methylene blue smoke filter tests, 362

Micrometeorological instruments, 239–259
anemometers, 239–246
circuits used in field, 259
for assessment of munition samples, 255–256
frequency meter, relay-type, 256–257
humidity measurements, 255
instruments for field use, 255–259
keep-alive circuit, 257–259
photocell illumination recorder, 255
recording instruments, 256
selection of instruments, 255–256
smoke puffer, 254
temperature apparatus, 247–253
use in continuous observations, 225–229
vanes for gustiness, 253–254
wind direction recorders, 246–247, 259
Micrometeorology in wooded areas, 230–238
forest temperatures, 234–236
low canopy jungle conditions, 237–238
turbulence in forest, 236
wind direction, 232–233
wind speed, 230–232
Micropores defined, 117
Microscopic examination of aerosol particles, 334–335
electron microscope, 335
light microscope, 334
suspension of water droplet in castor oil, 334
Mie theory of light scattering by particles, 318–321
angular distribution of intensity, 321
intensity of scattered light, 318
plane-polarized components, 321
scattering coefficient, 318–320
total scattering by one particle, 318
MIT-E1 canister tester, 372
MIT-E1R1 optical mass-concentration meter, 363
MIT-E1R7 smoke generator, 361
MIT-E2 smoke penetrometer, 367
MIT-Freeport Sulfur Co. generator, 448
MMD (mass median diameter)
aerosol powders, 535, 537–538
droplets, 401
Molybdenum whetlerites, 57–64
aging characteristics, 61
compared with copper-silver-chromium whetlerites, 61–62, 64
drying process, 59–60
heat treatment temperature, 57–58
mixed impregnations, 58
optimum concentrations of components, 59
organic acid additions, 58
pilot plant experiments, 61–62
rotary vs. static oven driers, 60
simultaneous impregnation, molybdenum and chromium, 62
surveillance quality, 95–96
zinc impregnations, 57
Mortar shells for gas cloud dispersal, 277–281
atmospheric stability, 277–278
dosage effect, 278
wind velocity effect, 277
wooded area performance, 279–281
Mosquito exterminating bomb, 524–527
atomization of liquid by explosive bursts, 524–526
design and manufacture, 526–527
droplet spectra from chargings, 525
Mosquitoes, DDT test subjects, 578–588
aedes aegypti, 581–583
anopheles quadrimaculatus, 583–584
males less resistant than females, 581
rate of paralysis, mosquitoes vs. flies, 584
research history, 578
resting vs. flying mosquitoes, 578–580
toxic dosage, mosquitoes vs. flies, 582
Motion, fluid
see Wind tunnel studies
Munitions
see also Bombs
airplane exhaust generator, 507–523, 593–596
atomization of liquids by explosions, 408–410
atomization of liquids by nozzles, 398–406
atomization of liquids in airplane sprays, 406–408
herbicide dispersing, 547–548
mustard gas generator pot, 419–425
PWP (plasticized white phosphorus) munitions, 555–565
smoke munitions, 395–396
smoke pots, 441–448, 485–506
thermal generators, 411–484
Munitions for dispersing liquid aerosols, 524–530
Munitions for dispersing solid aerosols, 537–545
British developmental work, 539
Cardox bomb, 542
chamber tests, 540–541
compressed air bomb, 542
conclusions, 545
DDT dispersing plastic bomb, 524–527
dissolved gases under pressure in liquids, 530–533
ejection-airburst bomb, 527–530
field tests, 543–545
gas-ejection bomb, 539–542
particle size distribution assessment, 538–539
plastic bomb, 543
tests, 537–538
Mustard gas as toxic agent, 151
Mustard gas generator pot, 419–425
condensate composition, 422–423
experimental models, 421–422
field tests, 423–424
fuel block formulas, 461
operation, 420–421

Nasal penetration by aerosols, 534
NDRC balanced smoke filter, 365
NDRC optical mass-concentration meter, 362
NDRC photoelectric smoke filter penetrometer, 365
NDRC-E1R2 smoke penetrometer, 365–367
Nephelometer, filter tester, 364–365
Newton's law, bodies in turbulent motion, 308
Nickelous oxide as charcoal impregnant, 125
Nitrate and sulfur smoke screen mixtures
see Sulfur-nitrate smoke screen mixtures
Nitrogen adsorption isotherms, 121–122
Nitrogen adsorption on charcoal, 107–108, 111–112
Nitrogen dioxide
canister protection, 201
mechanism of removal, 155
Nitrogen surface complex on charcoal 132–133
Nitrogen trifluoride as war gases, 609
Nonpersistent gases, sampling methods, 284–294
air injector, 293
diaphragm pump sampler, 286–287
field canister tester, 292–293
field conductivity analyzer, 289–291
hot wire analyzer, 287–289
hydrostatic head pump sampler, 284–285
radio control of samplers, 293
rotary distributor sampler, 291–292
snap sampler, 293
suggestions, selection of methods, 294
summary, 294
tape recorder, 293
ultraviolet photometer, 293

Nozzle atomization of liquids, 398, 406
hydraulic nozzle performance, 405
pneumatic nozzle performance, 399–402
smoke screen production, 405–406
types of nozzles, 399
Venturi atomizer, 402–405
NRL smoke generator, 361
NRL-E2 smoke penetration meter, 367
NRL-E3 smoke penetration meter, 372 373
Nukiyama and Tanasawa studies
atomizing nozzle equations, 593–594
pneumatic nozzle, 399–402
Nut shells, activated charcoal raw materials, 25
Nylon parachute for target identification bomb, 457

Ocean temperature, diurnal variations, 218
Oil smoke generation by airplane exhaust, 507 523
Oil smoke pots, 441–448
floating pot, 441–445
fuel block formula, 461
nonfloating pot, 445–446
training pot, 446–447
Oil vapor smoke generators, 377–378
Oil-gunpowder smoke mixtures
see Smoke pot mixtures, oil and gunpowder
Oleic acid fogs, illuminated for color studies, 321–322
Olsen bomb, pressurized liquid dispersal, 530–533
atomization of butyl carbitol, 531
dichlorobenzene dispersal from spinning tubes, 532
impracticality, 530–531
ineffective for saturated aerosol production, 531–533
multiple tube ejection bomb, 531–533
solubility of carbon dioxide in butyl carbitol, 531
solubility of carbon dioxide in mustard gas, 530
spinning tubes, 531
Optical measurements of particle size, 343–353
color of transmitted light, 350 353
coronae, 347-348
Owl instrument, 343–347
Slope-o-meter, 348-350
Orchard heater, British smoke screen layer, 375
Organic base impregnations of charcoals, 81 84
pyridine and picoline impregnations, 82–84, 96
reactions of bases with cyanogen chloride, 81 82
Owl, smoke observation instrument, 343–347
Oxygen surface complexes on charcoals, 125–132
complex formed during steam activation, 131–132
complexes present on charcoal, 126
degassing experiments, 129, 131
displacement of complex by adsorption of vapors, 131
effect of exposure to air, 130
gas evolution from charcoals during heating, 128 132
heat of binding, oxygen and carbon, 128
influence on adsorption of ammonia, 128
influence on adsorption of water vapor, 128
influence on base and acid adsorptive properties, 127
oxygen pickup by charcoals, 126
wettelerizability, 131

Paper as aerosol filter material, 357
PCC activated charcoal manufacture, 27 28
Penetrometers for smoking testing
see Smoke penetrometers
*p*H factor
effect on copper-silver-chromium wettlerites, 75
effect on hexamine impregnants, 49
Phenol-formaldehyde resins, 84 87
Phosgene
canister protection, 196 198
conductimetric analysis, 285
reaction with unimpregnated charcoal, 152 153
reaction with wettlerites, 152–154
removal mechanism, 152–154
Phosphorus, plasticized white
see PWP (plasticized white phosphorus)
Phosphorus trifluoride, 156, 608
Phosphoryl trifluoride, 157 158
Photocell illumination recorder, 255
Photoelectric smoke penetrometers
see Smoke penetrometers, photoelectric
Photometer for gas sampling, 293
Picoline impregnated charcoals, 82 84, 96
Pittsburgh Coke and Chemical Co., activated charcoal manufacture, 27 28
Plastic bomb, aerosol dispersal, 524–527
atomization of liquids by explosive bursts, 524 526
compared with gas-ejection bomb, 541
design and manufacture, 526–527
droplet spectra from various chargings, 525
liquid droplet dispersal, 524–527
solid particulate dispersal, 543
Polanyi relationship, adsorption temperature and adsorbate, 135
Polarization
in fluorine preparation, 611–612
photometer, 345
solid particles illumined by polarized light, 330
uniform size particles, 322–323
Pore size, charcoal
see Charcoal pore size
Pore structure, activated charcoal, 32
Porous materials, measurement of surface, 97–99
adsorption as function of pressure, 98–99
adsorption data equation, 97 98
small pore structures, 98–99
Powder dispersion, 535–536
aggregates in aerosol cloud, 536
British bombs for solid powder dispersal, 539
dispersibility of various powders, 535–536
egg albumen, 535, 541
gas-ejection bomb, 539–543
Precipitation of aerosols, 297
Prest-o-log process, activated charcoal manufacture, 28–29
PS (chloropicrin)gas test
disadvantages, 19
operation, 18
use, 13
PWP (plasticized white phosphorus), 551–574
antipersonnel effects, 565–568
recommendations for future work, 573–574
temperature rise, 552
white phosphorus, 551
PWP (plasticized white phosphorus), manufacture, 552–555, 572–573
granulators, batch, 553
granulators, continuous, 553
labor, 556
mixing of constituents, 555
phosphorus granulation, 553
power and services, 556
rubber, variations in types, 572–573
rubber solution preparation, 553–555
solvents, variant types, 573
PWP (plasticized white phosphorus), manufacturing specifications, 568 572
apparent viscosity, 569–571

moisture, 569
particle size, 568-569
specific gravity, 569
thermal stability, 569
viscosity of rubber solution, 571–572
PWP (plasticized white phosphorus), munitions, 555–565
ballistic stability, 557–558
comparison with white phosphorus munitions, 561–564
filling weight, 557
loading, 555
moisture control, 556
screening efficiency, Army bombs, 561–564
screening efficiency, Navy munitions, 564–566
PWP (plasticized white phosphorus), stability, 557–561
ballistic stability, 557–558
effect of aging on viscosity, 563
effect of particle size, 559–560
"instability factor", 559
stability, PWP containing vegetable oil, 562
summary, surveillance tests, 559–561
thermal stability, 569
Pyridine adsorption on charcoal, 141
Pyridine impregnated charcoals, 82–84, 96

Radiation and atmospheric effects, 216–217
absorption of water vapor, 215
atmospheric counterradiation, 217
black-body temperature of earth, 216–217
radiation, clear vs. cloudy sky, 217
reflected radiation, 215
sky radiation, 216–218
Radioactive smoke test, 362
Radioactive tracer technique in gas studies, 640–643
apparatus, 641
concentration of agent in gas stream, 641
distribution, toxic agent in charcoal bed, 642–643
location of catalyst in whetlerite, 643
location of reaction product in whetlerite, 643
reaction products in gas stream, 642
smoke filter study, 643
war gases containing radioactive elements, 640–641
Rankinites, copper impregnated charcoals, 41
Rayleigh theory of scattered light, 318
Reflection of solar radiation by atmosphere, 215–217
Research recommendations
atomization theory, 602
DDT dispersal, 601
E29R1 chemical bomb, 440
gas masks, 208–209
physiological effects of canister breathing resistance, 187
PWP (plasticized white phosphorus), 573–574
Resins, absorbent, 84–87
aminated resins, 84
chemical absorption vs. physical adsorption, 85
effect of impregnants, 86–87
evolution of ammonia, 87
impregnation, 86
preparation, 85–86
volume changes with humidity, 85–86
Reynolds number
flow of fluids measurement, 174–175
viscous influence upon flow, measurement of, 621–622
wind tunnel studies, 638–639
Richardson number, relation to gas cloud travel, 263
Rock wool as aerosol filter, 191, 357–358
Rockets for smoke screen laying, 564–565
"Rotary distributor sampler," gases, 291–292
Rubber, PWP (plasticized white phosphorus) constituent, 553–555

St. Clair's aerosol coagulation work, 310–312
Sampling methods for nonpersistent gases
see Nonpersistent gases, sampling methods
Saran charcoal
characteristics, 25
of theoretical interest, 31
preparation process, 31
Sawdust, activated charcoal raw material, 25
Sawdust-chloride smoke pot mixtures, 497–499
Scattering of light by colored particles, 332–333
absorption characteristics, 332
calculation tables, 333
color of transmitted light, 333
dye smoke particle size, 333
multiple scattering, effect on color, 333
optical density, pure dye smoke, 333
Scattering of light by nonuniform size particles, 327–330
heterogeneous aerosol without coagulation, 328–329
scattered intensity vs. particle radius, 328
scattering analysis, 329–330
transmission in settling, 328–329
Scattering of light by single particles, 318–321
angular distribution of intensity, 321
intensity of scattered light, 318
Mie theory, 318–321
plane-polarized components, 321
scattering coefficient, 318–320
total scattering, one particle per unit intensity, 318
Scattering of light by solid particles, 330–332
effective density, 331–332
effective refractive index, 331–332
polarization, 330
scintillating particles, 330–331
transmission in settling, 331–332
Scattering of light by uniform size particles, 321–327
angular color distribution, 321–322
polarization, 322–323
scattering by large particles, 327
total scattering, 323–326
transmission, 326
Screening by smoke
see Smoke screens
Sea breezes
effect on gas cloud travel, 264
meteorological characteristics, 223, 383–384
on islands, 224
Selenium hexafluoride, 156
Sell's calculations of particle impactability, 534–535
Settling of aerosols under gravity
see Aerosol settling
Shemya installations, fog dispersal studies, 629
Silver adsorption by whetlerizing solutions, 44
Silver permanganate, carbon monoxide catalyst, 205
Silver peroxide, carbon monoxide catalyst, 205
Slide rule for gas concentration calculation, 266
Slope-o-meter, 348–350
construction, 348–350
light transmission as wavelength function, 348
limitations, 350
operation, 350
Smoke
coverage for stated area, 376
defined, 301

electrical charge, homogeneous smoke, 308
general properties; *see* Aerosol
particle size, 301
production by combustion, 299
production by condensation, 315
stability, 297
unipolar charged smoke, 309
Smoke clouds, behavior under meteorological conditions, 384–386
see also Smoke clouds, travel
angle of rise, 386
convective pattern, 385–386
stable conditions, 384–385
unstable conditions, 385
Smoke clouds, disappearance, 386–388
see also Aerosol cloud evaporation
concentration of cloud, 386
deposition rate, 387
evaporation, 386–387
inertial effects, 388
Smoke clouds, travel, 380–384
atmospheric diffusion, 380
atmospheric diffusion theory, 384
effect of temperature on density, 380
formation, 380
land-water boundary conditions, 383–384
thermal gradient, 383
thermal stability, 382
turbulence, 382
wind speed and direction, 381–382
Smoke filter testing, 360–374
apparatus required, 360
chemical test-smoke generators, 361
flow rate selection, 360
materials for test smoke, 361
smoke generators, 361
Smoke filter testing during production, 371–374
carbon-smoke penetrometer, 373
Edgewood Arsenal E3 canister tester, 371–372
MIT-E1 canister tester, 372
NRL-E3 smoke penetrometer, 372–373
particle-counting canister tester, 373
sodium-flame penetrometer, 373
Smoke filter testing in laboratory, 361–371
adamsite tests, 361
Australian ionization penetrometer, 363
diphenylchloro arsine tests, 362
methylene blue tests, 362
optical smoke penetrometers, 362–363
penetrometers, comparative tests, 368–371
photoelectric smoke penetrometers, 363–368
radioactive smoke test, 362
Smoke formation
see Aerosol formation
Smoke from color dyes, 332–333
absorption properties, 332
color of transmitted light, 333
colored smoke clouds, 392
optical density, 332–333
particle sizes, 333
Smoke generators for airplanes
see Airplane exhaust generator
Smoke observation instrument, Owl, 343–347
Smoke particle sampler, 336–337
advantages, 336
construction, 336
lithopone and zinc oxide deposits on slides, 337
method of sampling, 336–337
variety of particle shapes, 337
Smoke penetrometers, 362–371
comparative tests, 368–371
MIT-E1R1 mass-concentration meter, 363
NDRC mass-concentration meter, 362
optical, 362–363
particle-counting smoke penetrometer, 368–371
Smoke penetrometers, photoelectric, 363–368
British carbon-smoke penetrometers, 364
CWS-MIT-E2 penetrometer, 367
Hill penetrometer, 363
Kimberly-Clark nephelometer, 364–365
NDRC balanced smoke filter, 365
NDRC-E1R2 penetrometer, 365–367
NRL-E2 penetrometer, 367
Smoke pot, floating, 441–448
control of oil feed rate, 443
design and construction, 442–443
floating stability, 445
fuel block formula, 461
operational principles, 441–442
specifications, 441
toxicity, 444–445
Smoke pot mixtures, 485–506
applications, 485
availability of ingredients, 486
continuous smoke generators, 485
diol-sawdust-chloride mixtures, 497–499
metal chloride mixtures, 488–494
stability, 488
substitute specifications, need for, 485
sulfur-nitrate mixtures, 494–497
toxicity, 488
Smoke pot mixtures, oil and gunpowder, 499–506
blasting powder, 501
composition of charges, 501–503
conclusions from experiments, 500
containers, 503–505
internal pressure measurements, 505–506
jellied oil, vapor producing materials, 501
non-jellied mixtures, 502
primers, 506
requirements, 499–500
temperatures in pots, 505
transition mixtures, 503
Smoke pot mixtures, screening power, 486–488
effect of smoke particle size, 487
hygroscopic nature of mixtures, 486
volatility and dilution, 487–488
Smoke protection
see Gas mask protection
Smoke puffer, wind detector, 254
Smoke screens, 375–379
blanket vs. curtain screens, 375
colored smoke screens, 392
coverage, 376
laid by airplane exhaust smoke generators, 513–515
laid by airplane rockets, 564–565
laying methods, 378
mechanical atomization production, 405–406
meteorological conditions, effect of, 375
obscuring power, 300
oil vapor smoke generators, 377–378
Smoke screens, materials, 376–377
see also Smoke pot mixtures
coagulation period, 376–377
inflammability, 377
particle size, oil smokes, 376–377
requirements, 376
sulfur, 376
Smoke screens, tactical uses, 522–523
area screening of an anchorage, 522–523
defensive screens, 379
individual ship screen, 523
offensive screens, 379
task force under way, screening of, 522–523
Smoke screens, visibility, 389–392
amount of smoke required for observation, 391–392
conditions approaching extinction, 390
contrast limen, 389
dependence on concentration, 390
light extinction by fog, 389–390
light extinction by screening smoke, 390
visibility formula, 390–392

UNCLASSIFIED

visibility in natural fog, 389
Smoke settler, differential, 341–343
Smoke settler, homogeneous, 339
Smoke signals, floating, 451–455
colored signals, proposed design, 454
construction, 453–454
development, 451–452
dye chamber, 454–455
fuel block formulas, 461
specification, 450
theory, 452
Smokeless powder, thermal generator fuel, 482–483
Smoluchowski expression, collisions between particles, 307
"Snap sampler," gases, 293
Soda lime, whetlerite component, 48
Sodium-flame penetrometer, 373
Soil, 217–218
albedo effect, 218–219
diurnal variations in temperature, 218
heat conductivity, 218
temperature below earth's surface, 217–218
temperature on earth's surface, 217–218
thermometer, 250
Solar radiation, 215–217
albedo effect, 218–219
atmospheric counterradiation, 217
influence on earth temperature, 215–216
reflection, 215
water vapor absorption, 215
Solenoid production, 214
Sound vibrations causing aerosol coagulation, 309–313
attraction of particles due to air motion, 311–312
laboratory experiments, 312
motion of particles relative to each other, 310–311
theory summarized, 312
vortex motion, air around particles, 312
Stability of aerosols, 301–305
acoustical forces, 302
adhesion vs. separation, 302
Brownian movement, effect on stability, 301
centrifugal forces, 302
density variations with height, 305–306
diffusion and evaporation, 297
precipitation, 297
settling of heterogeneous aerosols, 303–305
settling of homogeneous aerosols, 302–303
summary, 297
thermal and electrical forces, 302
Steam activation of charcoal
see Activation of charcoal by steam
Stearic acid fogs, illuminated for color studies, 321–322
Stearman planes, DDT dispersing equipment, 594
Stokes' law, fall of small spheres, 303
Stokes' law deposition, rate of fall of particle during filtration, 355
Stokes-Cunningham velocity of fall of a particle, 307
Sulfite processed into gas mask charcoal, 30–31
Sulfur and fluorine reactions, 604–605
action of fluorine on sulfur compounds, 605
controlled reaction, 604–605
fluorination by heavy metal fluorides, 605
nonelectric method of fluorine preparation, 605
sulfur hexafluoride, defluorination, 605
Sulfur as smoke screen material, 376
Sulfur dioxide, mechanism of removal, 155–156
Sulfur pentafluoride, 157
Sulfur smoke generators, 448–450
Kimberly-Clark generator, 449–450
MIT-Freeport Sulfur Co. generator, 448
Texas Gulf Sulphur Co. generator, 448
Sulfur surface coatings on charcoal, 134
Sulfur-nitrate smoke screen mixtures, 494–497
composition, 497
fuel gas-sulfur vapor mixture, 495
safety precautions, 497
screening power, 496
suggestions for improvement, 496
sulfur smoke production, 494–495
summary, 494
Sulfuryl chloro-fluoride, 156–157
Summary, NDRC, Division 10 activities, 5, 7
Surface area measurements, charcoals, 97–102
adsorption method of measurement, 97–99
methods applicable to charcoals, 99–101
Surface coatings on charcoal, 132–134
chlorine coatings, 133
nitrogen coatings, 132–133
sulfur coatings, 134
Surging in fuel blocks, 471–476
description, 471–472
laboratory analysis, surge-producing charcoal, 473–475
mechanism of surging, 475–476
summary, surging experiments, 476

Tanasawa's pneumatic nozzle studies, 399–402
Tape recorder, gas sampler, 293
Target identification bomb of colored smoke, 455–458
components, 456–457
dyes, 458
flaming control, 457–458
fuel block formulas, 461
nylon parachute, 457
operation, 456
Task force under way, screening of, 522–523
TBM-3 exhaust smoke generator, 509, 521–522
combustion generator installation, 521
DDT dispersal use, 595
plane design suited for generator, 509
standardization of equipment, 521–522
test results, 522
Telescoping tail, E29R1 bomb, 438–439
Temperature gradient measurement, 383
Temperature in forests, 234–236
Temperature measurers, 247–253
aspirated thermocouple systems, 247–251
recording resistance thermometers, 251–252
surface thermometers, 252
Temperature of ground, 216–218
albedo effect, 218–219
as solar energy radiator, 216–217
black-body temperature, 217
diurnal variation, 218
heat conductivity, surface materials, 217–218
ocean temperature, 218
soil below earth's surface, 217
surface moisture effect, 218
Texas Gulf Sulphur Co. generator, 448
Thermal generator
aerosol cloud evaporation, 415–419
aerosol persistence, 412–415
carrier gas from fuel, 412
design requirements, 411–412
heat from fuel gases, 411–412
heat transfer, 412
thermal stability of agent, 411
vapor transfer, 412
Thermal generator fuel blocks, 459–484
alkali activation of charcoal, 466–467
ammonium nitrate variables, 466–468

[redacted]

UNCLASSIFIED

UNCLASSIFIED

burning characteristics, 460
burning condition variables, 470–471
effect of charcoal particle size, 465–466
factors influencing reactivity, 467
formula variations, effect on burning rate, 470
lacquering variables, 469–470
mixing variables, 468
physical characteristics, 460
pressing variable, 468–469
testing of blocks, 463–464
Thermal generator fuel blocks, surging, 471–476
description, 471–472
gas analysis of surging blocks, 474–475
mechanism of surging, 475–476
summary, surging experiments, 476
surging vs. nonsurging charcoals, 472–474
Thermal generator fuels
ammonium picrate-sodium nitrate fuels, 483–484
liquid fuels, 484
smokeless powder fuels, 482–483
Thermal generator fuels, cast mixtures, 479–482
cast vs. pressed mixtures, 479–480
formula variations, 481–482
manufacturing process, 480
mixture formulas, 461
*p*H of mixture, 482
properties, 480
storage, 482
suggestions for improvement, 482
Thermal generator fuels, pressed mixtures, 462–480
block properties, 462–463
cast vs. pressed mixtures, 479–480
control of block characteristics, 464–471
manufacturing procedure, 463
mixture formulas, 461
noncarbon mixtures, 477–480
storage difficulties, 476–477
Thermal generator mustard pot, 419–425
conclusions, 424–425
condensate composition, 422–423
experimental models, 421–422
field tests, 423–424
fuel block formulas, 461
operation, 420–421
Thermal generator types 411–484
colored smoke munitions, 451–458
E29R1 bomb, 424–441
F7A mustard pot, 419–425
oil smoke pots, 441–448
sulfur smoke generators, 448–450
"Thermal precipitator," smoke particle sampler, 336–337
advantages, 336
construction, 336
lithopone and zinc oxide deposits on slides, 337
method of sampling, 336–337
variety of particle shapes, 337
Thermal stability of atmosphere, 382
Thermal turbulence in forest, 236
Thermocouple systems, aspirated, 247–251
aspirator, 249–250
electrical system, 250–251
mast, 248
observational procedure, 251
radiation shields, 247
Thermodynamic atmosphere graphs, 214
Thermometer, earth surface temperature measurements, 252
Thermometer, recording resistance, 251–252
Thiocyanate impregnations of whetlerites, 50–52
ammonia odor evolved, 51
cyanogen chloride life, 51
disadvantages, 49
storage effect, 51
Tobacco smoke, illustration of Rayleigh's theory, 322
Tokyo Bay wind velocity and turbulence studies, 638
Toxic gas adsorption
see Adsorption wave theories
Toxic gas clouds
see Gas clouds
Toxic gases, inorganic, 604–609
alkyldifluorophosphates, 608
alkylmonofluorothiophosphates, 608
dialkylmonofluorophosphates, 606–608
disulfur decafluoride, 604–606
fluorosulfonates, 608
miscellaneous gases, 608–609
Tricresyl phosphate smoke material, 361
Triphenyl phosphate smoke material, 361
Turbulence
caused by irregular air motion, 219–220
caused by wind speed, 382
in forest, 236
thermal instability, turbulence cause, 382

Ultraviolet photometer, gas sampler, 293

Vanadium whetlerites, 62–64
cyanogen chloride life increase, 57
heat treatment temperature, 57
impregnating solution, 62–63
preparation, 63–64
storage lines, 63
surveillance quality, 95–96
Vapor condensation during aerosol formation, 299
Vapors adsorbed by charcoals
see Adsorption of vapors by charcoal
Venturi
air scoop for atomization, 406–409
airplane exhaust generator, 510
atomizer, 402–405, 594
vaporizer, modifications for E29R1 bomb, 433–435
Vesicant dispersing air-burst bomb, 527–530
advantages, 527
hexagonal bomb, 528–529
round bomb, 529–530
Visibility through fog and smoke, 389–392
conditions approaching extinction, 390
contrast limen, 389
dependence on particle size, 390
formulae, 390–392
light extinction by fog, 389–390
light extinction by smoke, 390
natural fog, 389

War gases
acid forming, 152–165
acyl chlorides, 609
amines, 166
ammonia, 165
arsine, 166–168, 609
base-forming, 165–166
carbon monoxide, 203–206
chloropicrin, 151
cyanogen chloride, 161–164
fluorides, 156–158
fluorophosphates, 606–608
general conclusions, 164–166
hydrogen cyanide, 158–161, 618–620
inorganic gases, 604–609
mustard gas, 419–425
nitrogen dioxide, 155, 201
nonpersistent gases, 284–294
phosgene, 152–154, 196–198
readily oxidizable, 166–168
retained by physical adsorption, 151–152
sulfur dioxide, 155–156
Water adsorption from charcoal
see Adsorption of water vapor from charcoal
Whetlerite type A, 40–44
canister performance, 41
copper impregnant analyzed, 41
distinct from "whetlerite A," 40

UNCLASSIFIED

UNCLASSIFIED

preparation conditions, 44
preparation process, 41
Whetlerite type AS
plant production, 43
preparation conditions, 44
preparation process, 43–44
Whetlerites, 40–48
catalyst located by radioactive tracers, 643
chemisorption of gases, 144
definition, 40
early development, 40–41
reaction product located by radioactive tracers, 643
type D mixture, 48
Whetlerites, aging studies, 91–95
accelerated aging data, 92
canisters field use, 92–95
cyanogen chloride protection, 91
dry storage, 91
moist storage, 91
rate of aging, 91
Whetlerites, gas adsorption, 46–48
arsine adsorption, 46–47
basic vapors adsorption, 47
hydrogen cyanide adsorption, 46–47
"poisoning effect", 47
various vapors adsorption, 47–48
Whetlerites, hexamine impregnated, 48–50
cyanogen chloride protection, 50
disadvantages, 49
hexamine application process, 49
*p*H factor, effect on impregnants, 49
salts added to impregnant, 49–50
X-ray studies, 50
Whetlerites, molybdenum impregnated
see Molybdenum whetlerites
Whetlerites, surveillance, 88–96
see also Whetlerites, aging studies
canister aging programs, 89–90
early studies, whetlerite stability, 89
effect of moisture on canister lives, 88–89
molybdenum whetlerites, 95–96
picoline impregnants, 96
pyridine impregnants, 96
vanadium whetlerites, 95–96
Whetlerites, thiocyanate impregnated, 50–52
ammonia odor evolved, 51
application to whetlerite type A, 50
application to whetlerite type AS, 51
cyanogen chloride life, 51
disadvantages, 49
effect of storage, 51
Whetlerizing solutions, 44–46
adsorption of constituents from solution, 44
concentrations, 44
gases evolved during drying, 46
heat of solution, 46
silver adsorption, 44
vapor pressure, 45
X-ray studies, 45
Whytlaw-Gray powder dispersing bomb, 539
Wind curtains, 630–633
Wind direction
effect on smoke cloud travel, 381–382
in wooded area, 232–233
Wind direction recorders, 246–247
CIT type vane, 246
8-point commercial vane, 247
field use, 259
relay-type frequency meter, 256–257
Wind fluctuations, 219–224
anabatic winds, 223
convection, 219–220
eddy velocity, 220
gradient wind, 220
gravity winds, 222–223
gustiness, 220
katabatic wind, 222
land and sea breezes, 223–224
surface wind, 220
thermal belts, 223
turbulence, 219–220
Wind speed
at various heights, 222
effect on area covered by gas clouds, 277
effect on efficiency of gas cloud, 260
effect on gustiness, 220
effect on 1,000 lb gas bombs, 269–270
effect on smoke cloud travel, 381–382
in wooded areas, 230–232
measurements, 221–222
turbulence cause, 382
Wind tunnel studies, 621–639
experimentation technique, 623–624
flow measurement instruments, 623
flow over terrain models, 638–639
flow pattern around irregular boundaries, 638
fluid mechanics, fundamental relationships, 621–622
fog dispersal, 624–633
gas diffusion, 633–638
model method of study, 622
wind tunnel construction, 623–624
Wooded areas, micrometeorology, 230–238
forest temperatures, 234–236
low canopy jungle conditions, 237–238
turbulence in forest, 236
wind direction, 232–233
wind speed, 230–232

X-ray studies
charcoal structural characteristics, 145
copper content of whetlerites, 45
hexamine impregnated whetlerites, 50

Zinc chloride process, charcoal activation, 38–39
calcination, primary and secondary, 39
development, 38
manufacturing process, 38–39
mechanism of activation, 39
reaction of mixer, 39
Zinc impregnated charcoals, 57–58

UNCLASSIFIED